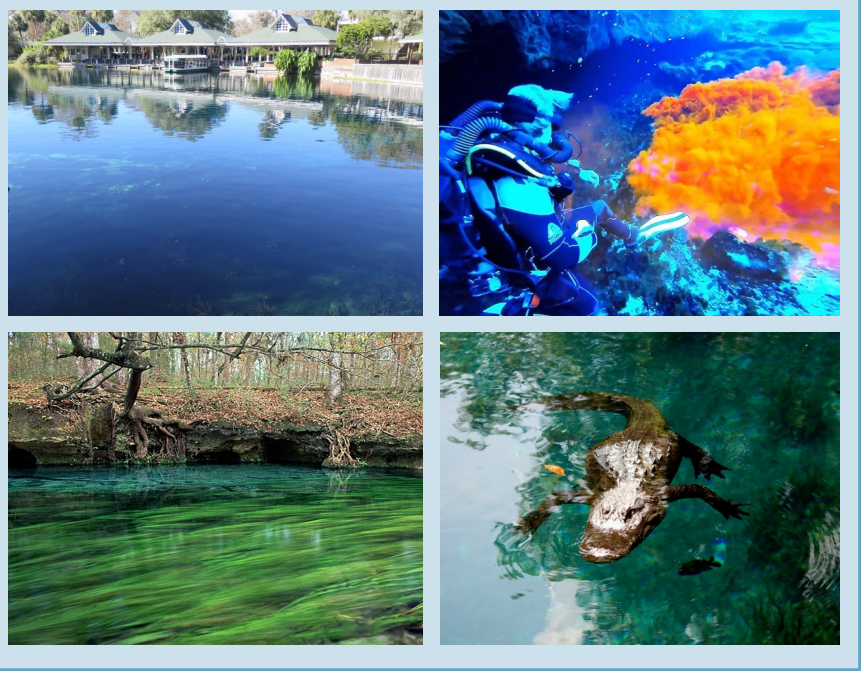

Collaborative Research Initiative on Sustainability and Protection of Springs

CRISPS

ANNUAL REPORT

July 2015

submitted to:

St. Johns River Water Management District
Springs Protection Initiative [SPI], UF Contract # 27789

UF | UNIVERSITY of FLORIDA
Water Institute

C R I S P S

COLLABORATIVE RESEARCH INITIATIVE ON SPRINGS PROTECTION AND SUSTAINABILITY [CRISPS]

Annual Report
July 2015

Principal Investigators

K. Ramesh Reddy, University of Florida
Ed Lowe, St. Johns River Water Management District

University of Florida Investigators
Mike Annable; Matt Cohen; Tom Frazer; Wendy Graham; James Jawitz;
David Kaplan; Marc Kramer; Patrick Inglett; Jon Martin; and Todd Osborne

St. Johns River Water Management District Investigators
Patrick Burger; Mike Coveney; Dean Dobberfuhl;
Rob Mattson; Dale Smith; and Peter Sucsy

This is the first annual report of a 3-year project in compliance with Agreement between University of Florida (UF) and St. Johns River Water Management District (SJRWMD), UF Contract #27789.

TABLE OF CONTENTS

HYDRAULICS AND HYDRODYNAMICS

LIST OF TABLES

Page

SURFACE WATER HYDROLOGY

GROUNDWATER HYDROLOGY

NITROGEN BIOGEOCHEMISTRY

Page

HYDRAULICS AND HYDRODYNAMICS

PHYSICOCHEMISTRY

BIOLOGY

LIST OF FIGURES

Page

NITROGEN BIOGEOCHEMISTRY

Page

Page

Page

HYDRAULICS AND HYDRODYNAMICS

Page

Page

Page

PHYSICOCHEMISTRY

Page

Page

Page

Page

Page

Page

Page

Page

BIOLOGY

Page

EXECUTIVE SUMMARY: PROGRAM OVERVIEW AND YEAR 1 OUTCOMES

ES.1 INTRODUCTION

The Floridan aquifer is arguably Florida's most significant water resource, and one of the best indicators of its' health is the quantity and quality of water emanating from the ground as spring discharge. Florida's springs not only reflect the status of the aquifer, but also influence the ecological health and integrity of many of the State's most significant surface water ecosystems.

There has been substantial ecological degradation of many of Florida's springs, indicated by reduced flow, increased nitrate, increased biomass and cover of benthic algae and invasive aquatic plants, decreased abundance of native submerged aquatic vegetation (SAV), and changes in fish and invertebrate communities (Scott et al. 2004; Munch et al. 2006). Such changes threaten the ecologic and economic value of the springs and of the surface waters into which they flow.

Recognizing the ecological and economic significance of the Floridan aquifer and its springs, the St. Johns River Water Management District (SJRWMD) developed a Springs Protection Initiative (SPI) in 2013, with three major components: projects, regulation, and scientific research. In support of the Initiative's scientific research component, University of Florida (UF) and the SJRWMD formed a program in 2014 called Collaborative Research Initiative on Springs Protection and Sustainability (CRISPS). The overarching goal of this program is to understand the relative influence and manageability of natural and anthropogenic factors that affect a key indicator of spring ecosystem health – the primary producer community (i.e., vascular plants and benthic algae) [Box ES.1]. This understanding can then inform effective management of the Floridan aquifer and its associated springs. This summary presents outcomes to date of projects being conducted by UF in close collaboration with SJRWMD.

There are three major objectives for the CRISPS program:

1. Improve the scientific foundation for management of nitrate loading to springs. Delineate spatial variation in the Silver Springs springshed of hydrologic conveyance rate to the springs; identify sources of nitrogen to the springs; and quantify nitrogen loss rates (primarily through nitrate reductive pathways including denitrification) in soils and the aquifer.

2. Evaluate whether reduction of nitrate concentrations/loads alone will be sufficient to restore the balance between benthic filamentous algae and native aquatic vegetation. Develop a predictive model or suite of models that elucidate the influence of nitrate concentration on benthic algal abundance and other aspects of primary producer community structure and function.

3. Assess the relative influence and manageability of non-nitrate drivers controlling primary producers. Determine if there are drivers, other than nitrate, that influence significantly the structure and function of the primary producer community.

Box ES.1. Collaborative Research Initiative on Springs Protection and Sustainability [CRISPS] Program Organization and Research Team.

CRISPS Program Organization and Research Team

The SJRWMD Springs Protection Initiative Leader is Casey Fitzgerald and the project manager is Mary Brabham. The research program managers for CRISPS are K. Ramesh Reddy for UF and Ed Lowe for SJRMWD. The UF project manager for CRISPS is Lisette Staal. The field data collection program for SJRWMD is led by David Hornsby.

Two supergroups - the Springshed Supergroup and the Springs Protection Supergroup - each contain smaller work groups with specific research objectives. The lead for the Springshed Supergroup is Mike Cullum with SJRWMD and the lead for the Springs Ecosystem Supergroup is Ed Lowe with SJRWMD.

Springshed Supergroup Projects
This supergroup is quantifying inputs, transformations and transport of nitrogen to and through the Floridan aquifer to the Silver Springs system.

1) **Surface Water Hydrology** SJRWMD - Dale Smith: Rainfall, evapotranspiration, recharge, runoff quantity and quality. UF - Marc Kramer and James Jawitz: Nitrogen and phosphorous loading and flux from soils in the Silver Spring springshed; HSPF modeling.
2) **Groundwater Hydrology:** SJRWMD - Patrick Burger: Groundwater modeling of aquifer levels, transmissivity, conduit flow, spring discharge. UF - Wendy Graham: Conduit and fracture flow modeling. UF - James Jawitz: Transport and loss of nitrogen within the Upper Floridan aquifer in the Silver Springs springshed.
3) **Nitrogen Biogeochemistry** – SJRWMD - Dean Dobberfuhl: N sources, N transformation, uptake, and loss. UF - Patrick Inglett: Nitrogen sources, transformations and loss from land surface to springs.

Springs Ecosystem Supergroup Projects
This supergroup is examining effects of physicochemical and biological drivers on primary producer community structure and function in the spring run.

1) **Hydraulics and Hydrodynamics** – SJRWMD - Peter Sucsy: Hydrodynamic and hydraulic attributes and drivers of the spring system. UF - David Kaplan: Velocity validation transects and methodology; flow-way development.
2) **Physicochemistry** – SJRWMD - Mike Coveney: Interrelationships between hydrologic and hydrodynamic drivers and physicochemical attributes; effects of physicochemical drivers on benthic algal. UF - Matt Cohen, , Todd Osborne, Jon Martin: Benthic sources and sinks of nutrients and nitrogen dynamics and metabolism.
3) **Biology** – SJRWMD - Rob Mattson: Biological drivers of primary producers with emphasis on benthic algal abundance. UF - Tom Frazer: Trophic interactions.

ES.2 GENERAL APPROACH

The physical, chemical, and biological status of springs is affected by surface water hydrology, groundwater hydrology, land use, soils, geology, nutrient transformations and transport in the groundwater system, and biological interactions. Unraveling this complexity rests upon multidisciplinary research. CRISPS includes applied and foundational science, spanning various environmental drivers influencing spring hydrology, hydrodynamics, biogeochemical cycling of elements, water quality, and primary producer community structure and function. To study these complex interactions, we are using the Silver Springs ecosystem in Marion County as a case example. Other springs, such as the Alexander Springs, will be examined in a less comprehensive fashion. Under the SPI, SJRWMD will, in addition, conduct a cross-system analysis for a suite of springs with sufficient data to explore the interrelationships among environmental drivers and ecosystem attributes.

The Springshed Supergroup is cooperatively developing a suite of models of surface and groundwater and for nitrogen biogeochemistry - input rates and forms, transformations, losses, and transport (Figure ES.1). Model outputs will be spatial and temporal variation in hydrologic and nutrient loading forcings to the Floridan aquifer and springs. Springshed forcings are expected to be related to variation in rainfall, temperature, season, nitrogen input rates and forms,

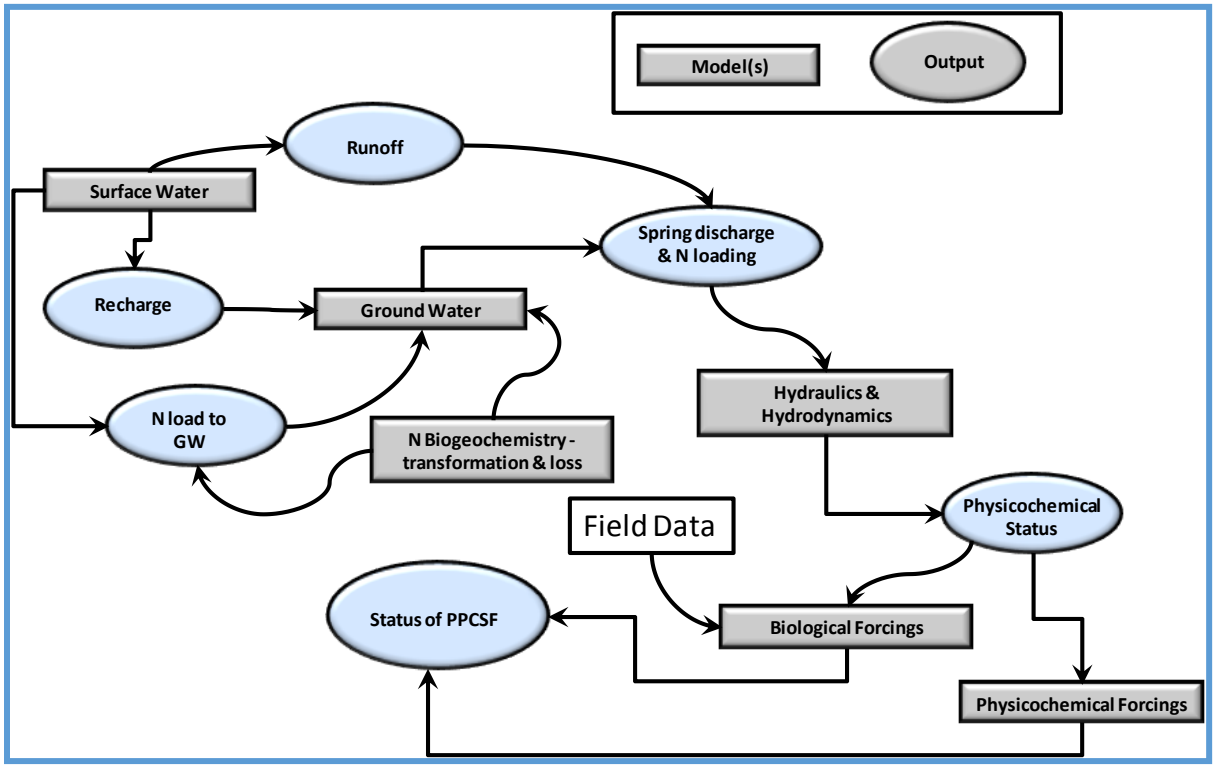

Figure ES.1. Schematic illustrating multidisciplinary frame work for the CRISPS program. A suite of models will be developed to link rainfall and nitrogen inputs, transformation, and transport in the springshed and aquifer to the status of primary producers. Springshed models will include effects of land use and land cover, soils, geology, and other relevant factors. Springs ecosystem models will include forcings from concentrations of nitrate and other nutrients, physical drivers, and biological drivers on primary producers.

soil types, and land use and land cover. Importantly, improved understanding of the significance of conduit/fracture flows and of nitrogen transformations, loss, and transport through the groundwater system will be incorporated into the groundwater model.

The Springs Ecosystem Supergroup is developing a set of related hydrodynamic, biogeochemical, and biological models of the Silver Springs ecosystem. These springs models will receive forcings from the groundwater and watershed models to simulate their effects on various attributes of the physicochemistry of the springs such as flow rate and velocities, depths, nutrient concentrations, photosynthetically active radiation, and dissolved oxygen concentrations. We will be using the spatial and temporal variation in these physicochemical attributes as forcings on primary producers in mechanistic, empirical, or mixed models. Potential forcings from variation in biological drivers, such as density of benthic algal grazers, are also being considered. Based on physicochemical and biological forcings, we will assess the relative potential influences of the various drivers on primary producers.

Prior to development and calibration of the models to be employed by both supergroups, a considerable amount of data needs to be collected in the Silver Springs springshed and the Silver Springs ecosystem. Experimental data are needed also to clarify influences of the various drivers of primary producers in the Silver Springs ecosystem.

ES.3 SPRINGSHED PROCESSES

ES.3.1 Surface Water Hydrology

The purpose of this project is to quantify nitrogen and phosphorus loading and flux from soils in the Silver Springs springshed through development of an HSPF model. In this first year of work we focused our efforts on methods development, laboratory techniques, verification and validation of field deployment methods and field testing instrumentation and retrieval capabilities. Activities included participation in in-person meetings, field testing and field visitation of select sites, site identification, field equipment testing as well as fertilizer application and recovery experiments.

Analytical and preliminary field methods have been evaluated including selection of anion/cation resin, exploration of a range of fertilizer types, experimentation with irrigation and fertilizer trials, and testing elution methods. A preliminary throughflow collector has been designed with 50-90% collection efficiency, which is capable of being rapidly deployed at 2 sites/day with up to 12 instruments/site. A radio-frequency identification (RFID) retrieval technology has been developed using a semi-passive RFID reader/tag technique. The timeline for the project was extended by a full year, enabling outcomes developed during this first year to ensure success during the next two years. (For details, see Section 1 of this report-Kramer et al.)

ES.3.2 Groundwater Hydrology

Karst aquifers are highly heterogeneous due to discrete conduits embedded in the porous limestone matrix. This heterogeneity influences hydrologic processes, controls travel paths and travel times of water and solute flux through the system, and dictates “hot-spot” regions within the springshed where surface-applied nitrate may be transported rapidly to springs. The purpose

of this project is to develop conduit and fracture flow models to determine transport and loss of nitrogen within the Upper Floridan aquifer in the Silver Springs springshed.

ES.3.3 Conduit and Fracture Flow Modeling

In this first year of work, we made refinements to an existing discrete continuum model for coupling conduit-matrix flow to include solute transport and kinetic calcite dissolution algorithms. The resulting hydro-chemical model simulates conduit evolution over geologic time and predicts flow and solute flux in the resulting coupled conduit-matrix system that comprises the karst aquifer. The enhanced model is now being applied to the Silver Springs springshed to generate an ensemble of possible conduit networks that incorporate what is known about the local geology. Preliminary results of these simulations suggest that conduit geometry is influenced by topography, presence/absence of a confining layer overlying the karst aquifer, sinkhole density and location, and porous matrix hydraulic conductivity.

In the next phase of the project the ensemble conduit networks will be used to quantify the influence of conduits on flow and nitrate transport to Silver Springs, and the uncertainty of flow and transport predictions resulting from uncertainty about the conduit geometry. Results of this effort will determine whether it is important for the SJRWMD to incorporate conduits into their models of the Silver Springshed in order to make management decisions. (For details see Section 2 of this report- Graham et al.)

ES.3.4 Nitrogen Transport and Loss

In this first year of work field measurements were collected to identify portions of the aquifer that contribute most significantly to water flow and solute flux to Silver Springs. Groundwater velocities and solute fluxes are being measured *in situ* using passive flux meters. These measurements will be used to determine flow characteristics and natural attenuation of solute loads with special emphasis on nitrate.

We are testing different deployment durations to maximize sensitivity of measurements. Thus far, instruments have been deployed for approximately 2 months at a time. We have monitored 14 locations to date. Groundwater fluxes range from 2.6 to 10.9 cm d^{-1} with a mean value of 6.2 cm day^{-1} - relatively low, indicative of matrix flow through the limestone. Nitrate fluxes were found to be below detection limit of this technique. However, phosphate fluxes measured were in the range of 0 to 0.8 mg PO_4-P m^{-2} d^{-1} and sulfate fluxes ranged from 1.3 to 31 mg SO_4-S m^{-2} d^{-1}. We are identifying locations of higher flux that contribute disproportionately to spring discharge. Age dating of groundwater collected from different locations in the aquifer will also provide support for the identification of high-vulnerability land uses in the springshed. We are currently identifying well locations for age-dating sampling. In the well with the highest nitrate concentration so far, we measured high nitrate flux consistent with the groundwater sampling data. In other wells that had lower, yet measurable, nitrate concentrations, we have not detected nitrate flux. This result is not final because there are some internal inconsistencies, such as non-zero fluxes of other solutes. We are currently conducting field and laboratory assessments to identify whether nitrate is being transformed in the well. (For details, see Section 3 of this report- Jawitz et al.)

ES.3.5 Nitrogen Biogeochemistry

In addition to water delivery, biogeochemical transformation of N species in soils and shallow aquifers determine how much nitrate enters the Floridan aquifer. The overall goal of this component of the CRISPS effort is to determine the capacity for natural attenuation of land surface N load in the soil profile, vadose zone and shallow aquifer.

In this first year of work we measured physico-chemical characteristics of soil profiles in select land uses in the Silver Springs springshed. Results to date indicate potential for denitrification during transit from surface soils to spring vents, with a high degree of spatial heterogeneity among sites sampled. Surface soils are the most significant sink for nitrate, however, buried layers of relic peat and marine deposits demonstrate potential for high rates of denitrification in surficial aquifers and areas where deep marine-based groundwater mixes with the surficial aquifer. In the soil profiles sampled, denitrification was largely restricted to 0 –10 ft soil depth, or in buried marine/peat layers where organic carbon was found in adequate supply. Results also showed that in many cases denitrification was limited by the availability of nitrate.

Stable isotopic signatures of nitrogen and oxygen in nitrate showed potential movement of nitrate throughout the soil profile and locations of denitrification in surface soils. Stable isotope ratios and dissolved gases such as methane, nitrous oxide, dinitrogen, and argon showed significant denitrification activity in spatially distributed wells and the head spring vent of the Silver Springs springshed. Stable isotopic signatures of nitrate in wells indicated that fertilizer was the major source of nitrate in the headspring. (For details, see Section 4 of this report- Inglett et al.)

ES.4 SPRINGS ECOSYSTEM PROCESSES

ES.4.1 Hydraulics and Hydrodynamics

The purpose of this project is to develop a more thorough understanding of the velocity and residence time distributions in the channel of Silver River, to quantify location and magnitude of transient storage and exchange, identify critical shear stresses for the entrainment and detachment of algae; and link study findings to ongoing 3-D modeling with a focus on impacts of submerged aquatic vegetation on velocities, residence times, and stage-discharge relationships.

Preliminary observations of the reach-scale hydraulic characterization indicate the presence of three upstream flow paths and is supported by initial EFDC modeling, providing support for that model and the utility of tracer experiments to inform modeling efforts. Tracer data show complete spring bowl flushing within approximately 6 hours and estimated mean travel times of 6 and 12 hours for the two back-channel flow paths. Reach-scale mean velocity in the upper reach was slower than that in the lower reach, and lower-reach velocity was faster in this study when compared to a 2009 study. Mean residence time for the whole river was 6.6 hours.

We obtained point-scale velocity data that allowed for comparison with District velocity measurements made using an acoustic Doppler current profilers. In general, velocities measured by each method agreed and indicated sharp velocity gradients from above to below the vegetation canopy, however, point-based measurements captured velocities near the benthic

surface in some locations where the acoustic Doppler current profilers did not provide data. These data provide a set of reference measurements for calibration and validation of modeled 1-D velocity profiles. Initial parameterization of these profiles show general agreement with measured velocities and are useful for selecting and parameterizing the correct EFDC turbulence closure model.

We conducted biologically active tracer experiments which showed that Silver River sediments have higher total adsorption capacity and relative microbial concentrations compared with a sandy-bottomed reference creek, providing an estimate of the overall biogeochemical activity. However, reach-scale studies using this tracer may be impractical.

Initial results from our algal cover characterization show promise for high-resolution, spatially distributed mapping of algal cover with high correlations observed between image colors and algal cover, and corresponding correlation with flow velocity. This suggests that the blue-green color of algae-covered submerged aquatic vegetation may serve as a proxy for algal cover, perhaps providing a more accurate measure than quadrat methods. This process can be automated to map large areas of submerged aquatic vegetation and provides additional support for the hypothesis that velocity exerts some level of control on periphytic algal communities.

We demonstrated that flow resistance in Silver River is dominated by vegetative drag. We successfully implemented and tested a three-dimensional hydrodynamic model that accounts for vegetative drag and turbulence in Silver River. The model provides a methodology for estimating velocity profiles, shear stresses, and dispersion throughout the river, especially for conditions outside of present day observations, and provides a means to test the efficacy of proposed management scenarios. (For details, see Section 5 of this report- Kaplan et al.)

ES.4.2 Springs Ecosystem Physicochemistry

The purpose of this project is to quantify benthic sources and sinks of nutrients and nitrogen dynamics and metabolism. This is being accomplished through three sub-projects

ES.4.2.1 Nitrogen dynamics and metabolism

We used synoptic spatial sampling of algal and submerged aquatic vegetation cover along the length of Silver River, along with a suite of hydraulic, edaphic and ecological variables, to explore patterns of, and controls on, variation in primary producer community structure. Submerged aquatic vegetation cover was generally high while algal cover was more variable. Spatial variation in algal cover was best explained by SAV cover, distance downstream, and surface water velocity. While none of the water chemistry parameters provided significant explanation of algal cover, some sediment properties were positively associated with algal cover. Submerged aquatic vegetation cover declined with increasing water column calcium, chloride and sediment clay content. Surveys of Alexander Springs Creek are underway, and will provide useful chemical contrast, and also be used to inform the location of subsequent measurements of SAV growth and benthic metabolism.

We have begun quantitative interpretation of high-resolution time series of pH, dissolved oxygen, nitrate, and phosphate to estimate open-channel ecosystem metabolism and autotroph

nutrient use in 4 reaches along the Silver River and 2 reaches along Alexander Springs Creek. Data analysis protocols have been established, and formal analysis of these time series is scheduled to commence in the next phase of the project.

We have initiated benthic chamber measurements of ecosystem metabolism to investigate nutrient use kinetics at below-ambient concentrations, which is integral for predicting ecosystem behavior as nitrate concentration are reduced. The study consists of 4 co-deployed roving chambers with *in situ* dissolved oxygen sensors for measuring metabolism during week-long deployments. We have also initiated submerged aquatic vegetation growth monitoring at 16 sites in Silver and Alexander spanning the range of benthic conditions observed during our survey. At each location, we are monitoring submerged aquatic vegetation growth, morphometric properties and water and soil chemistry. (For details, see Section 6 of this report-Cohen et al.)

ES.4.2.2 Nitrate Inhibition of Submerged Aquatic Vegetation

In response to observations of declining production of SAV in several Florida springs, an investigation has been initiated to determine the potential role of nitrate/ nitrite (NOx) concentrations in the inhibition of SAV growth. The proposed mechanism of inhibition stems from the hypothesis that two dominant species of SAV, *Vallisneria americana* and *Sagittaria kurziana* have not yet evolved a metabolic mechanism to turn off nitrate reductase, an enzyme that converts readily available nitrate into ammonia. Because ammonia is phyto-toxic at elevated concentrations, it must be utilized rapidly, predominantly in protein synthesis. This process requires energy from photosynthate and under elevated NO_3-N availability, could produce a significant energetic burden on SAV. To date, a multiple tank recirculating mesocosm array has been constructed and both species of SAV have been established and are growing under a range of NO_3-N concentrations. At the cessation of the growing season, plants will be harvested and biometry and chemical analyses completed. Further investigations include role of hypoxia on survivorship and proliferation of SAV. Algae shear stress tests will also be performed on plants during the harvest phase of year 1 and 2 to determine the velocity required to remove periphytic algal growth from both species. (For details, see Section 7 of this report-Osborne et al.)

ES.4.2.3 Benthic Sources and Sinks of Nutrients

We conducted a detailed survey of benthic sediment depth and chemical composition in Silver River to evaluate the role of benthic sediments as sources or sinks for nutrients and trace elements as related to primary producers. Preliminary results indicate that bottom sediments are ubiquitous and in certain locations over 6 m thick. The sediments contain interbedded shell hash layers and organic, carbon–rich, fine grain sediments. Soil erosion in the springshed west of Silver River may be the source of sediment in the river. Low C:N ratios of the sediments suggests that the organic matter deposited is well humified. Sediment carbon is tightly coupled with total nitrogen, suggesting the source of most nitrogen is organic matter. Total C and P is poorly coupled, suggesting that the sediments are rich in inorganic P associated with Ca and Mg (apatite P) and Fe and Al (non-apatite P). Organic matter decomposition and dissolution of minerals under aerobic and anaerobic conditions is the primary source of dissolved nutrients and trace elements in the porewaters. Elevated porewater concentrations of dissolved nutrients indicate that benthic sediments are a diffusive source of NH_4^+, Fe(II), Mn(II), and soluble reactive phosphorus. For details, see Section 8 of this report-Martin et al.)

ES.4.3 Springs System Biology - Trophic Interactions

The purpose of this project is to investigate trophic interactions, specifically, to identify the role of macroalgae in the Silver River food web.

In this first year of work, we conducted analyses of stable carbon and nitrogen isotopes that indicate a functional and diverse food web in Silver River. With regard to primary producers in the Silver River, $\delta^{13}C$ and $\delta^{15}N$ values indicate clearly that rooted macrophytes and their epiphytes fuel much of the secondary production that, in turn, supports a diverse assemblage of organisms that occupy higher trophic levels. Of particular importance is our finding that benthic algae (mostly nuisance filamentous species) do not contribute substantially to the diet of key consumers such as snails. Instead, it appears that only herbivorous insects heavily exploit these algae as a food source. Because algal production is consumed by chironomids and trichopterans (emergent insects), it is likely that much of this algal production is exported to the terrestrial environment. In essence, benthic algal mats in Silver River, and likely other spring systems, may be largely decoupled from the broader aquatic food web. This is a dynamic that may fundamentally impact energy flow and material transport at the watershed scale. Our stable isotope analyses coupled with other diet information indicate also that redear sunfish and kinosternid turtles are primary predators on gastropods, which have the potential to exert control on the production of nuisance algae.

We examined stomach contents of alligators in the Silver River, revealing that they feed heavily on gastropods and crustaceans. This finding has profound implications for any effort to model the Silver River food web because previous food web models have considered alligators to be top/apex predators that mainly consume fish and other vertebrates occupying higher trophic levels. In other ecosystems alligators are known to both directly and indirectly affect key ecosystem processes through their interactions with prey and the environment. Integration of this novel data into spring food webs will help to refine our understanding of predation and top-down pressures in influencing community dynamics within these complex ecosystems. (For details, see Section 9 of this report-Frazer et al.)

ES.5 GENERAL CONCLUSIONS

The physical, chemical, and biological status of springs is affected by surface water hydrology, groundwater hydrology, land use, soils, geology, nutrient transformations and transport in both groundwater and surface water systems, and other ecological processes and biotic interactions. Unraveling this complexity hinges heavily on a highly integrated research effort. CRISPS is inherently multidisciplinary and provides the framework necessary to do so.

The preliminary results and outcomes to date for both springshed and spring ecosystem supergroups indicate that substantial progress has been made in the first year of the CRISPS program. Field methods have been established, experiments performed, and suite of models are being developed to characterize and quantify key processes. The progress made thus far suggest clearly that the program is well positioned to achieve the three broad objectives identified at the outset of the CRISPS program.

Details of results and outcomes to date are presented in the reports listed in Box ES.2.

Box ES.2. List of work order annual reports (FY2015)

CRISPS: Work Orders- FY1- 2015

Springshed Supergroup

Work Order #4: Groundwater Hydrology: Conduit and Fracture Flow Modeling (PI, Wendy Graham)

Work Order #6: Groundwater Hydrology: Transport and Loss of Nitrogen within the Upper Floridan Aquifer in the Silver Springs Springshed (PI, James Jawitz)

Work Order #7: Surface Water Hydrology: Nitrogen and Phosphorous Loading and Flux from Soils in the Silver Spring Springshed: HSPF Modeling (PI, Marc Kramer)

Spring Ecosystem Supergroup

Work Order #2: Hydraulics and Hydrodynamics: Velocity Validation Transects and Methodology; Flow-way Development (PI, David Kaplan)

Work Order #3: Physicochemistry: Benthic Sources and Sinks of Nutrients and Nitrogen Dynamics and Metabolism (PI, Matt Cohen, Co-PIs Jon Martin and Todd Osborne)

Work Order #5: Biology: Trophic Interactions (PI, Tom Frazer)

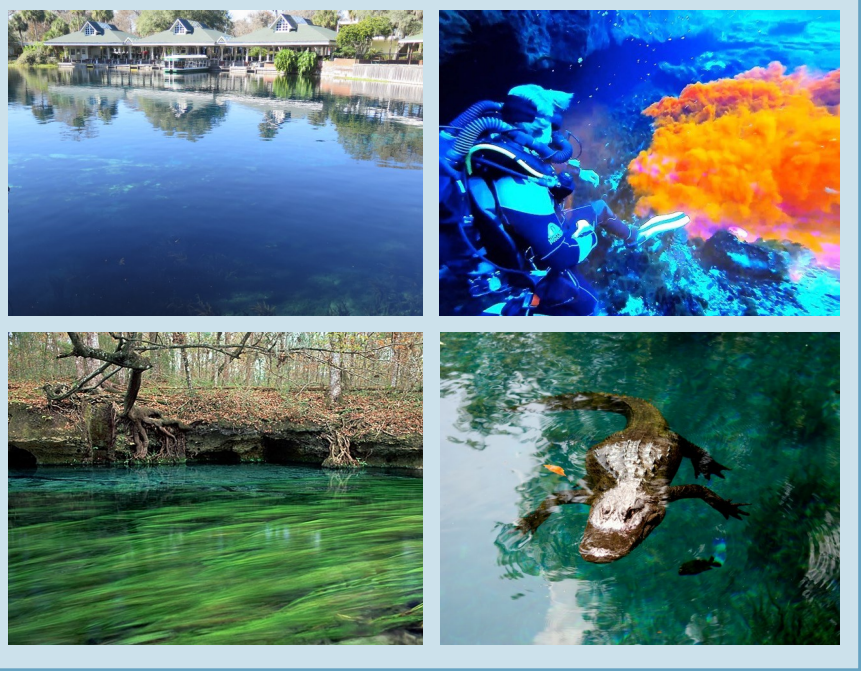

Collaborative Research Initiative on
Sustainability and Protection of Springs [**CRISPS]**

Section 1

[Work Order No: 7]

ANNUAL REPORT

July 2015

submitted to:

St. Johns River Water Management District
Springs Protection Initiative [SPI], UF Contract # 27789

UF | UNIVERSITY of FLORIDA
Water Institute

C R I S P S

Section 1

SURFACE WATER HYDROLOGY

Nitrogen and Phosphorous Loading and Flux from Soils in the Silver Springs Springshed

Annual Report 2015
Work Order No. 7

Principal Investigators:
M.G. Kramer, University of Florida
D. Smith, St. Johns River Water Management District
T. Cera, St. Johns River Water Management District

Project Team:
M.G. Kramer, Soil and Water Science Department
A. Desormeaux, Soil and Water Science Department
J.W. Jawitz, Soil and Water Science Department
M.D. Annable, Engineering School of Sustainable Infrastructure and Environment
University of Florida, Gainesville FL 32611

This document reports interim progress of a work order in the first year of a 3-year project in compliance with Agreement between University of Florida (UF) and St. Johns River Water Management District (SJRWMD) UF Contract #27789. It is part of the *UF Collaborative Research Initiative on Springs Protection and Sustainability (CRISPS)* and supports the science component of *the SJRWMD Springs Protection Initiative (SPI).*

1.1 ABSTRACT

An overview of accomplishments in the first nine months is provided below. Overall, the initial 9 month period provided ample time for student training on analytical and preliminary field methods, selection of anion/cation resin, exploration of a range of fertilizer types, experimentation with irrigation and fertilizer trials, and testing elution methods. A preliminary throughflow collector was designed with 50-90% collection efficiency, which is capable of being rapidly deployed (up to 12 instruments/site at two sites/day). An RFID retrieval technology was developed using a semi-passive RFID reader/tag technique. A PhD dissertation is being developed to address this task order in June – August 2015. Furthermore, the timeline for the project was extended by a full year. Therefore, the preliminary outcomes developed during this initial project period will ensure success during the subsequent two years.

Table 1.1. Summary of preliminary (9 month) accomplishments/outcomes on this task.

Outcome	September	October	November	December	January	February	March	April	May	June
1.2.1										
1.2.2										
1.2.3										
1.2.4										
1.2.5										
1.2.6										
1.2.7										
1.2.8										
1.2.9										

1.2 OUTCOMES

1.2.1 Equipment Checks

Serviced, tested, and verified analytic equipment for project (November): This included student training on Seal AQ1 with technician, mixing reagents, troubleshooting instrument and developing maintenance schedule and spare parts protocols and implementing EPA procedures for nitrate and total phosphorous. Used independent check and calibration methods to verify results.

1.2.1.1 Results

The Seal AQ1 is fully functional and dedicated to this project. All protocols and procedures for mixing reagents, performing QA/QC runs, servicing and maintaining the instrument are in place.

1.2.2 Method Development

KCl extraction and testing of a variety of anion and cation resins (October, November, December): Students developed streamlined KCl extraction procedures to batch process resin, including testing a variety of KCl, testing for purity, new filtration techniques, and evaluating efficacy of dissolution of KCl on a range of particle sizes. This was later (May 2015) extended to test for subsampling of resin extraction (after homogenization of resin) method.

1.2.2.1 Selection of Ion-Exchange Resin and Determination of Functional NO_3-N Capacity

Breakthrough curves were performed on a variety of resins, which allowed for the determination of the functional NO_3-N capacity and resin weight necessary for expected N loadings. Breakthrough curves were performed by loading 42 g (mL) moist resin with an ammonium-nitrate solution at the rate of 2 mL s^{-1} (Figure 1.1). An aliquot was taken every 100 mL and analyzed for NO_3-N concentration. Resin adsorption was calculated by subtracting effluent concentration from the load water concentration for each effluent volume (100 mL).

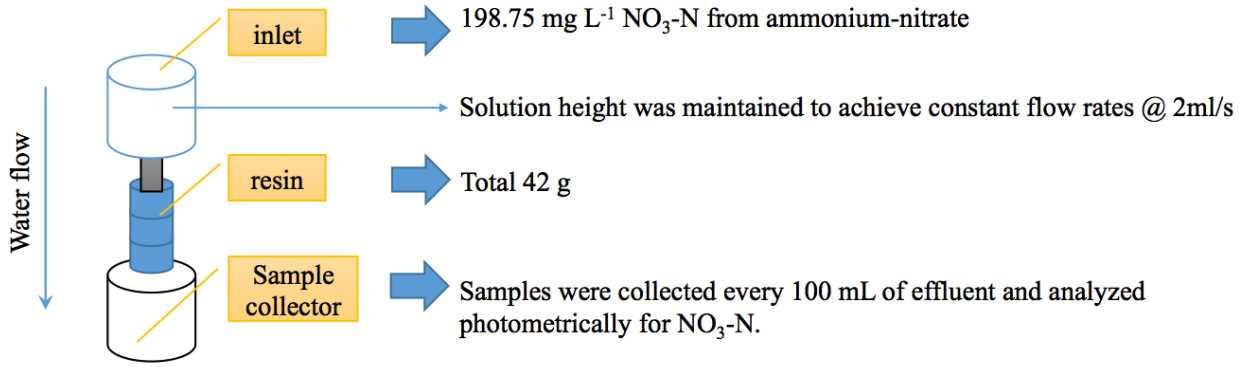

Figure 1.1. Diagram showing set up of breakthrough curve experiment. Resin was loaded with an ammonium nitrate solution at the rate of 2 mL s^{-1}. An aliquot was taken every 100 mL and analyzed for NO_3-N.

ResinTech MD-30 is a mixed-bed (anion/cation) resin that was able to adsorb 8.3 mg g^{-1} resin before NO_3-N breakthrough at 8.9 mg g^{-1} resin (Figure 1.2). Based on the 104 cm^2 surface area of the resin columns, this functional capacity corresponds to a leaching rate of 1,400 kg ha^{-1} NO_3-N. ResinTech MD-30 mixed-bed (anion/cation) resin had the greatest functional nitrate capacity, with the additional ability to measure soil cations (e.g. NH_4-N).

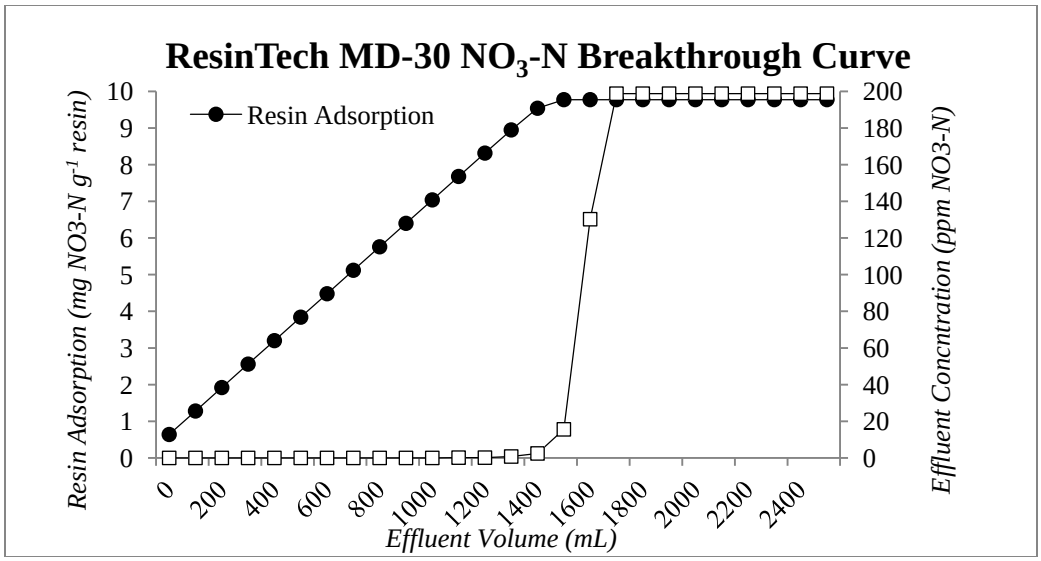

Figure 1.2. NO_3-N breakthrough curve for ResinTech MD-30 mixed-bed exchange resin, showing breakthrough at 8.9 mg NO_3-N g^{-1} resin.

1.2.2.2 Resin Extraction Methods

In addition to resin capacity, resin extraction was also tested. The conventional resin extraction method requires shaking the resin in 2M KCl for 1 hr, with 90% recovery efficiency after two extractions. Resin must be filtered after shaking to collect effluent, so resin must be scraped from the filter and placed back into the bottle for subsequent extractions. This procedure is time consuming and can potentially result in resin loss. This conventional method ('shake') was compared to a more efficient method of placing the resin in filter paper and pouring the 2M KCl extractant through the resin ('pour'). The N recovery efficiencies were measured for both methods after two extractions, as well as an additional measurement of the recovery efficiency of the new 'pour' method after a third extraction.

For each sample, 5 kg ha^{-1} N was loaded onto 25 g resin from KNO_3 and load water effluent was measured to determine actual N loading. Both treatments were extracted using 250 mL of 2M KCl and a 20 mL sample of the extraction effluent was analyzed. The 'pour' method was extracted one additional time to determine number of extractions required to meet the recovery efficiency of the conventional method.

Table 1.2. Recovery efficiencies ± standard error for the conventional and new resin extraction method.

Treatment	Extractions	Recovery Efficiency (%)
Pour	2	88 ± 2
Pour	3	92 ± 2
Shake	2	89 ± 2

Both methods resulted in almost identical recovery in two extractions and were not significantly different (P = 0.64). The new method performs as well as the traditional method, allows for faster sample turnaround (saves 1.5 hrs per sample), and eliminates resin loss from filter to bottle transfer. The resin extraction protocol was updated to use the pour through method was used for all further resin extractions.

1.2.2.3 Results

An optimal, cost effective anion/cation resin was selected and N and P retention estimates were obtained. The KCl extraction method verified 90% recovery rates. Furthermore, the amount of resin necessary for 3, 6, 9 and 12 month N and P loading were ascertained.

1.2.3. Initial Laboratory Irrigation/Fertilizer Experiment (November, December)

An initial fertilization experiment using ammonium nitrate in resin columns. A range of experiments were conducted on the UF Ag Teaching Farm, including testing fertilizer loading using zero tension lysimeters placed at the surface, as well as buried to a depth of 30 cm. The protocols and procedures were further modified to include zero tension water collectors above the soil surface to quantify irrigation and rainfall inputs.

1.2.3.1 Greenhouse Resin Column Recovery Experiment

A greenhouse experiment was conducted using 20 cm soil cores taken from the UF Ag Teaching Farm (Figure 1.3). Resin columns were attached below the soil columns and ammonium-nitrate was surface applied to the soil columns at the rates of 0, 96, 190, and 480 kg ha^{-1} NO_3-N to cover a range of fertilizer application rates. Columns were irrigated with 17 cm DI water, corresponding to three soil pore volumes. Resin columns were taken back to the lab, extracted with 2M KCl, and extractant was analyzed for NO_3-N (EPA method 353.2). NO_3-N recovered is the sum of three extractions (Table 1.3). The lowest fertilizer rate (33 kg ha^{-1} NO_3-N) resulted in a recovery greater than 100%, while the higher rates showed recovery efficiencies around 80%. Two potential causes were insufficient irrigation rates or the transformation of NO_3-N; additional experiments used 6-7 pore volumes to ensure adequate leaching of fertilizer N.

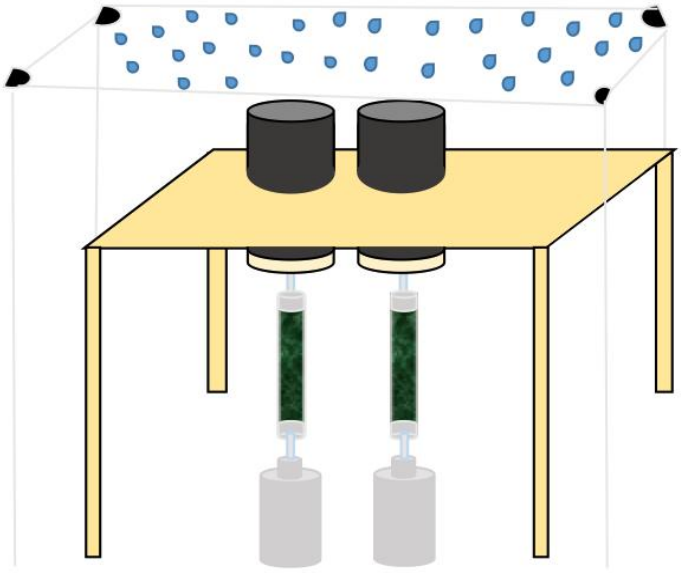

Figure 1.3. Diagram of column setup for greenhouse resin column recovery experiment. Soil cores were taken from the UF Ag Teaching Farm and placed in 20 cm PVC columns. Resin columns were attached to the base of the soil cores, irrigation water was allowed to flow freely through the cores and resin columns, and leachate was collected in 1L bottles.

Table 1.3. NO_3-N recovery for greenhouse soil core experiment.

NO_3-N Added (kg ha^{-1} NO_3-N)	NO_3-N Recovered (kg ha^{-1} NO_3-N)	Recovery Efficiency (%)
0	0.44	n/a
33	34	102
99	80	80
199	165	83

1.2.3.2 Low Rate Recovery Efficiency Experiment

Many of the experiments were performed at high N loading rates, to test the upper limits of the resin capacity. However, it is equally critical to determine the loading rate at which the extracted resin can be differentiated from a control. A lab experiment was conducted to determine background NO_3-N levels on the selected resin and to test the recovery efficiency of the resin at low N loading rates. It was hypothesized that resin loaded with low rates of a fertilizer N solution could be differentiated from no-N controls, despite background NO_3-N levels on the resin

Potassium nitrate was dissolved in DI water was poured through a column containing 25 g moist ResinTech MD-30 mixed-bed ion exchange resin at a constant rate of 2 mL s^{-1}. Three replications were used for each N application level and resin was extracted by shaking in 2M KCl for 1h. N recovered was the sum of two extractions (Table 1.4).

Table 1.4. Low-rate resin NO_3-N recovery.

N Applied (kg ha^{-1} NO_3-N)	N Recovered (kg ha^{-1} NO_3-N)	
0 (control)	0.1 ± 0.006	a
1	1.2 ± 0.06	b
2.7	2.1 ± 0.3	c
5	3.7 ± 0.3	d
10	8.0 ± 0.5	e

The N recovery for the lowest N rate (1 kg ha^{-1} NO_3-N) was significantly different than that of the 0 kg ha^{-1} NO_3-N control ($P < 0.001$); however, recovery efficiencies were poor and suggest that two extractions is not sufficient for complete N recovery. The background NO_3-N levels of the 25 g resin (0.1 kg ha^{-1} NO_3-N) correspond to a signal of 0.7 kg ha^{-1} for 175 g of resin used in the resin column.

1.2.3.3 Results

A range of fertilizer types (ammonium nitrate, calcium nitrate) confirmed >90% recovery efficiency of the resin.

1.2.4 Evaluated N Attenuation Maps Developed by SJWRMD (January)

1.2.4.1 Results

It was determined that the N attenuation maps developed by SJWRMD staff addressed task 1 and could be used to estimated initial N attenuation across the select sites.

1.2.5 Prototyped Field Deployable Resin Collectors (February, March, April, May)

Tested a suite of configurations that would allow for low impact, rapid deployment and retrieval capability.

While lab and greenhouse experiments showed adequate adsorption capacity of the resin, experiments at the University of Florida Ag Teaching Farm did not confirm NO_3-N adsorption in a field setting. Field experiments where NO_3-N fertilizer was applied to the land surface at various rates and leached through the soil were showing no NO_3-N adsorption, despite irrigation volumes in excess of 8 pore volumes. Using a water-budget approach, where water collectors were placed in the soil below the resin columns, it was determined that no water was flowing through the resin columns. Initial column designs restricted flow from an area of 104 cm^{-2} to an area of 4 cm^{-2}, which artificially increased soil moisture in the upper part of the column and soil pore water preferentially flowed around the column in unsaturated flow conditions. A new configuration extended the height of the column, but field testing suggested this extension was not enough to avoid preferential flow around the column. Saturated flow rates were measured for a variety of configurations hypothesized to encourage drainage, which included adding gravel to the base of the column (0.78 ± 0.03 mL min^{-1}), adding a sponge below the gravel (1.83 ± 0.07 mL min^{-1}), and glass beads overlying a sponge (2.83 ± 0.18 mL min^{-1}). While placing a sponge at the base of the column and adding glass beads encouraged drainage

under saturated conditions in the lab, field-tests were still unable to show water flow through the columns.

After various stages of design modifications, an open resin column was constructed that could contain the resin without restricting water flow. However, the textural discontinuity of the soil, drain cloth, and resin was still hypothesized to affect water movement through the column. A new set of field tests were designed to test the recovery efficiency of the new design in the field and set a benchmark recovery efficiency to judge further design changes against.

Resin columns were constructed by stretching French drain cloth over the top of a 10 cm length of 10 cm inner diameter ABS. A 10 cm ABS coupling was tightened over top to secure the cloth and the column was turned over and filled with ResinTech MD-30 color changing mixed-bed exchange resin. A second drain cloth was stretched over top and another 10 cm ABS coupling was tightened to secure the cloth. The resin was thus trapped securely in the center of the column between french drain cloth on either end.

Plots (1 m^2) were arranged in a completely randomized design, with three replications. Three NO_3-N rates were used (0, 100, and 500 kg ha^{-1} NO_3-N), to measure the recovery at multiple application rates. Columns were installed to a depth of 30 cm using a 10 cm soil auger, ensuring the bottom drain cloth was placed in contact with the soil. Soil was excavated in 10 cm increments and then replaced over the column in the original order. Calcium nitrate was applied to the surface and plots were irrigated using sprinkler irrigation at a rate of 5 cm d^{-1} for a total of 9 days (7 pore volumes). Figure 1.5 shows a diagram of the experimental set up.

Soil samples were taken above the resin column to confirm complete leaching of NO_3-N and the resin columns were excavated. Soil samples were extracted with 2 M KCl and none of the extracts were above the detection limit of the instrument. The resin was also extracted with 2 M KCl and recovery efficiencies ranged from 48 to 57% (Table 1.5).

An alternate design was tested, which eliminated the drain cloth at the topsoil/resin interface in order to increase hydraulic conductivity (Figure 1.5). The experiment was repeated exactly, using the new design (Table 1.6). No soil sample extracts were above the detection limit, confirming adequate irrigation application, and recovery efficiencies surpassed those of the initial design.

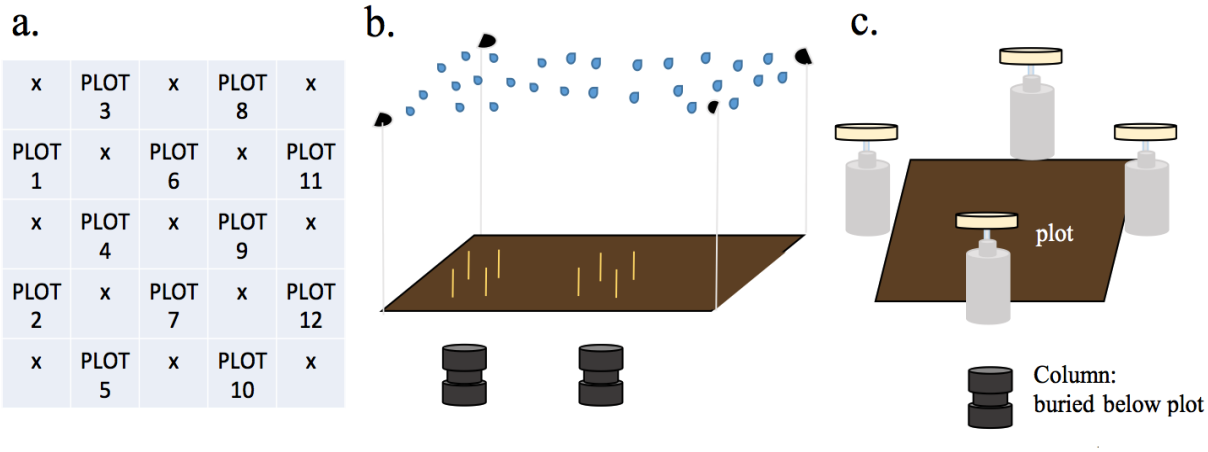

Figure 1.4. Diagrams of the field experiment set-up showing a) 1 m^2 plots with x indicating irrigation collectors between each plot, b) a side view showing the irrigation system, plots outlined with wooden stakes, and resin columns buried 30 cm below the soil surface, and c) a close of up a single plot, with each plot being surrounded by four irrigation collectors.

Table 1.5. NO_3-N recoveries for initial open column design.

Treatment	NO_3-N Added (mg NO_3-N)	NO_3-N Recovered (mg NO_3-N ± standard error)
0 kg ha^{-1} NO_3-N	0	8.2 ± 1.3
100 kg ha^{-1} NO_3-N	205	120 ± 7.8
500 kg ha^{-1} NO_3-N	1036	500 ± 130

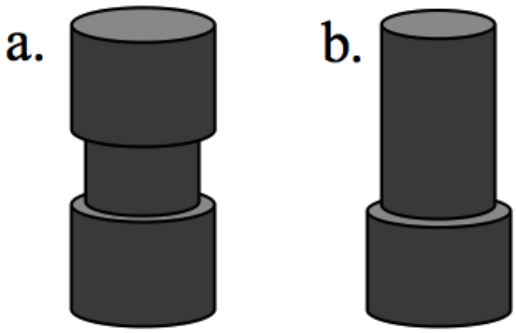

Figure 1.5. Initial resin column design (a), with a coupling on each side of a PVC column that tightly secured a piece of drain cloth, and final design (b) with top coupling and drain cloth removed.

Table 1.6. Nitrate N recoveries for modified open column design.

Treatment	NO_3-N Added (mg NO_3-N)	NO_3-N Recovered (mg NO_3-N ± stdev)
0 kg ha^{-1} NO_3-N	0	12 ± 9.3
100 kg ha^{-1} NO_3-N	205	115 ± 38
500 kg ha^{-1} NO_3-N	1036	930 ± 84

1.2.5.1 Results

The initial design used a sealed resin design, while subsequent designs embedded the resin matrix directly into the ABS core. Benchmark recovery of 48 to 57% was established with first column design and surpassed by the second column design (56 to 89%) although variability was high. Field-testing on the resin columns indicated that instrumenting 12 throughflow cores per site on up to two sites per day is achievable.

1.2.6 Tested and Verified RFID Technology Retrieval Capability (February, March)

1.2.6.1 Results

An indoor RFID reader and large antenna were 1) modified to operate on a 12v battery system in lieu of A/C adaptor, 2) developed into a field deployable RFID payload, which included laptop, RFID reader, modified field ready antenna mount system and mounting hardware, 3) tested with a range of passive and semi active RFID tags (buried at various depths). The RFID retrieval capability of buried resin columns was verified for 30 cm depths (Table 1.7).

1.2.7 Extended the Timeframe to Three Years Instead of Two (May)

1.2.7.1 Results

Extended the time to select sites, deploy and retrieve throughflow resin collectors to allow for better synchrony with other working groups and site selection logistics. To date, only two sites (of the initial 30) were selected.

1.2.8 Initiated a PhD Study Plan (June).

1.2.8.1 Results

A PhD plan of work is expected to be completed by August 2015.

1.2.9 Routine Meetings with UF team, SJWRMD Staff and Other UF Groups (Sept – May).

1.2.9.1 Results

Weekly UF project meeting, monthly or bimonthly in person meetings with SJWRMD staff and other UF working groups on site selection, progress to date, new opportunities and coordination with other on-going activities, provided critical input on direction, timeline, and feasibility of task implementation. It was concluded that extending the

timeline (without modification of the budget) would allow all tasks identified to be completed.

Table 1.7. RFID signal at 75cm from the soil surface.

RFID Tag		Received Signal Strength Indicator-RSSI						
Depth	Orientation	Antenna distance from Tag (meter)						
cm	Degree	0	0.5	1	1.5	2	2.5	3
0	0	-41		-51		-61	-65	
	90	-46		-55		-65		
7.5	0	-42		-48		-58		
	90	-44		-51	-55			
15	0	-50		-58				
	90	-54	-59					

Antenna distance from soil surface = 0cm

RFID Tag		Received Signal Strength Indicator-RSSI						
Depth	Orientation	Antenna distance from Tag (meter)						
cm	Degree	0	0.2	0.4	0.6	0.8	1	1.2
0	0	-28						
	90	-26						
7.5	0	-30	-47	-53				
	90	-26	-44	-47	-60			
15	0	-39	-57	-59				
	90	-38	-48	-55				

signal is detected
signal is undetected

1.3 FUTURE OPPORTUNITIES AND CHALLENGES

The modified throughflow collector demonstrated 50-90% N recovery rates based on a calcium nitrate fertilizer addition experiment. This configuration will be further modified, depending on the rainfall/irrigation intensity and rate of fertilizer addition. Higher rates of fertilizer inputs and sufficiently high irrigation inputs generally resulted in greater efficiency of throughflow collectors. Future plans include 1) developing a final optimal particles size, matrix flow of the throughflow collector 2) quantifying efficiency of the optimized throughflow collector, 3) applying an adjustment factor based on throughflow collector efficiency to estimate N and P loading across the various field sites. Site access remains a major limitation in this project. The UF team is working closely with SJWRMD staff to select sites and obtain necessary permissions.

1.4 9 MONTH PROGRESS IN 2014-2015

This project was initially proposed to end in 2016. Instead, the timeline (and task implementation) has been extended to 2017. The problem of budgeting and tracing N within a springshed like that of Silver Springs is daunting. In this process, the use of models, estimates, and assumptions can result in gross errors and erroneous conclusions unless direct measures of flow and flux are used wherever possible. Resin-based *in-situ* methods offer a direct measurement of N flux out of the rooting zone and are the best and most cost-effective approach. The "costs" of validating the resin column method are far outweighed by the benefits of this low-cost, low-maintenance instrument. The subsurface ion-exchange resins (SIERs) adsorb and accumulate ions from the soil solution and allow for cumulative N flux (temporal integration) with a single measurement. As they are small in size, SIER approaches require minimal site disturbance so they can be positioned directly in the land use being studied. Thus, the primary advantages of the *in-situ* resin approach is that it is a direct (not estimated) measure of N flux that can integrate windows of time and can be applied in far greater numbers to more completely capture more land uses and soil conditions than conventional buried lysimeters.

The initial 9-month effort in 2014-2015 were focused on methods development, laboratory techniques, verification and validation of field deployment methods and field testing instrumentation and retrieval capabilities. Activities included participation in in person meetings, field testing and field visitation of select sites, site identification, field equipment testing and fertilizer application and recovery experiments. Although we have conducted several laboratory experiments and limited field evaluation, additional work is needed prior to watershed scale deployment of SIER, as described below.

- Field deployment of SIERs in the springshed is anticipated for 2016 spring and summer growing seasons.
- Prior to watershed-scale field deployment, SIER techniques must be adapted to site-specific conditions. Therefore, additional work is needed to make specific adaptations include matching the resin pore size distribution with local soils for hydraulic flow through (Physics), matching the resin adsorptive capacity with local soil solution ionic strength (Chemistry), and measuring correction factors to account for biogeochemical transformations (Biology).
- Previous SIER deployments by other investigators have measured solute fluxes, but not water flux. Measuring water flux with ion exchange resins requires considerations of additional solute interactions. We have extensive experience with sorbent-based flux meters for measuring both water and solute fluxes in aquifer and streams. It would be a unique advancement if we could develop the SIER method to simultaneously quantify solute flux and water flux (recharge).

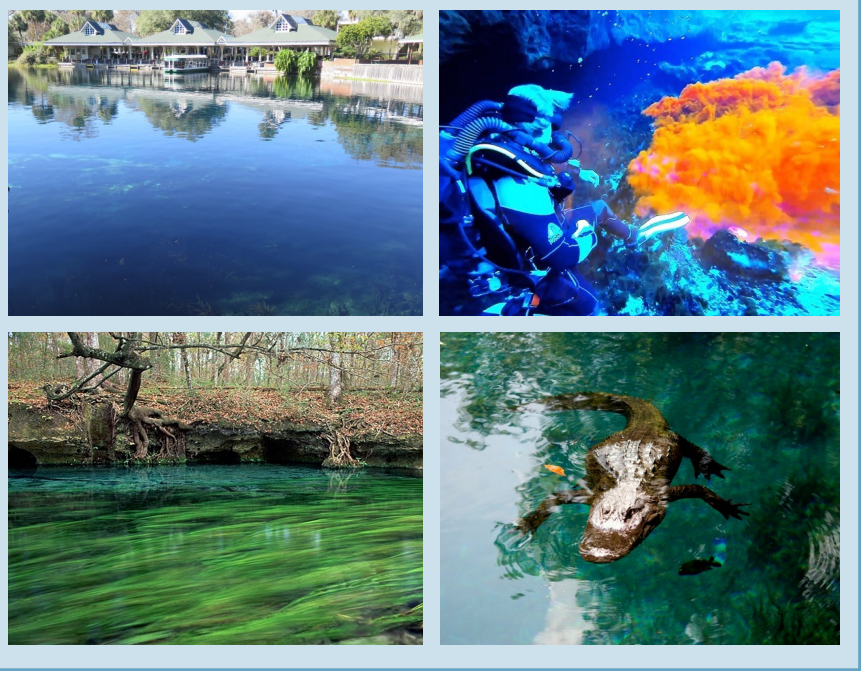

Collaborative Research Initiative on
Sustainability and Protection of Springs [**CRISPS]**

Section 2

[Work Order No: 4]

ANNUAL REPORT

July 2015

submitted to:

St. Johns River Water Management District
Springs Protection Initiative [SPI], UF Contract # 27789

UF | UNIVERSITY of FLORIDA
Water Institute

C R I S P S

Section 2

GROUNDWATER HYDROLOGY

Conduit and Fracture Flow Modeling

Annual Report 2015
Work Order No.4

Principal Investigators:

Wendy Graham, University of Florida
Patrick Burger, St. Johns River Water Management District

Project Team

Wendy Graham
Rob de Rooij
Wes Henson
Agricultural and Biological Engineering
Water Institute,
University of Florida,

Patrick Burger
St. Johns River Water Management District

This document reports interim progress of a work order in the first year of a 3-year project in compliance with Agreement between University of Florida (UF) and St. Johns River Water Management District (SJRWMD) UF Contract #27789. It is part of the *UF Collaborative Research Initiative on Springs Protection and Sustainability (CRISPS)* and supports the science component of *the SJRWMD Springs Protection Initiative (SPI).*

2.i PROLOGUE

The objective of the Springs Protection Initiative Work Order #4 is to answer the following questions: 1) How much do piezometric heads, the magnitude and timing of springflow, and the magnitude and timing of solute delivery to the Silver Springs change when a representative system of conduits is incorporated into Silver Springshed model using MODFLOW-CLN? 2) What characteristics of the conduit network and porous media properties contribute most uncertainty to the prediction of piezometric heads, the magnitude and timing of springflow, and the magnitude and timing of solute delivery to Silver Springs? and 3) Is the actual spatial configuration of conduits important to predicting springflow and solute breakthrough, or is behavior consistent among aquifer realizations generated using the same statistics for conduit and porous matrix properties? Answering these questions will help the SJRWMD determine whether incorporating conduits into its existing Silver Springs groundwater models will improve management decisions in the Silver Springshed.

To answer these questions three tasks were proposed: 1) Develop a conduit generation algorithm capable of generating ensembles of possible conduit networks for the Silver Springshed and evaluate the processes and parameters that have strong influence on conduit evolution; 2) Conduct unconditional Monte Carlo flow experiments for the Silver Springshed and evaluate parameters that contribute most uncertainty to the prediction of heads and springflow; and 3) Conduct unconditional Monte Carlo transport experiments for the Silver Springshed and evaluate parameters that contribute most uncertainty to the prediction of solute fluxes, flow paths and travel times to the Silver Springs.

This annual report covers the period July 1, 2014 to June 30 2015 and summarizes progress made on Task 1: Development of a conduit generation algorithm capable of generating ensembles of possible conduit networks for the Silver Springshed and evaluate the processes and parameters that have strong influence on conduit evolution.

2.1 ABSTRACT

Physics-based distributed models for simulating flow and solute transport in karst aquifers are generally based on the discrete-continuum approach in which flow in the three-dimensional porous limestone matrix is coupled with flow in discrete one-dimensional conduits. In general, however, little is known about the geometry of conduit networks. To quantify and analyze the reliability of discrete-continuum models it is important to explore flow and transport behavior over an ensemble of possible karst conduit networks within a stochastic framework. Thus there is a need for stochastic generation of realistic karst conduit networks. This report documents a new methodology to generate a stochastic ensemble of possible karst conduit networks. Starting from an existing discrete-continuum model for coupling conduit-matrix flow (1), we added solute transport and kinetic dissolution algorithms. The resulting hydrochemical model can be used to simulate the widening of conduits over geological timescales, and subsequently to simulate flow and solute transport within the evolved karst aquifer. In this report we present example simulations of head, spring flow, and solute transport for a variety of conduit networks generated within the Silver Springshed.

2.2 INTRODUCTION

Karst aquifers are highly heterogeneous due to the presence of conduits that have a higher permeability than the surrounding porous limestone matrix. This heterogeneity influences the hydrodynamic functioning of karst aquifers and therefore conduit networks should ideally be incorporated into numerical models that simulate flow and transport in these systems. Indeed, there exists a variety of discrete-continuum models in which conduits are explicitly represented as discrete one-dimensional features embedded in a porous limestone continuum (de Rooij 2013; Kiraly 1985; Kiraly 1998; Shoemaker et al. 2008). However, the applicability and validity of discrete-continuum models is limited because, in general, little is known about the geometry of conduit networks. As a result, discrete-continuum modeling studies are often restricted to hypothetical karst systems (de Rooij 2013; Kiraly 1985). Modeling studies of hypothetical karst systems have proven to be useful for gaining insights into the hydrodynamic functioning of the epikarst (Kiraly et al. 1995; Eisenlohr 1997a) and for testing classical methods for spring hydrograph analysis (Eisenlohr 1997a; Eisenlohr 1997b).

A rigorous statistical analysis of model uncertainty, originating from lack of knowledge about conduit network geometry, requires multiple model runs using an ensemble of possible karst conduit networks. Thus, there is a need for methodologies to generate realistic karst conduit networks. These methodologies may be based on process-imitating or structure-imitating approaches (Pardo-Iguzquiza 2012). Process-imitating or speleogenetic approaches are based on models that simulate the evolution of conduits due to dissolution kinetics. To date, the main objective of speleogenetic models has been to study the evolution of the conduits (Kaufmann et al. 2010; Kaufmann 2009; Kaufmann 2003a; Kaufmann 2003b; Kaufmann and Braun 2000; Dreybrodt et al. 2010; Gabrovsek and Dreybrodt 2010) and not to generate an ensemble of possible conduit networks. Structure-imitating approaches aim to reproduce the structure of the conduit network by empirical means without accounting for physical and chemical processes. For example the structure-imitating approach proposed by Pardo-Iguzquiza et al. (2012) is based on resampling from templates to generate individual conduit sections, and a diffusion-limited

aggregation method to join the conduit segments and generate the network topology. Ronayne (2003) used a non-looping invasion percolation model, proposed by Stark (1991), to generate conduit networks.

Structure-imitating approaches have the disadvantage that the empirical models require statistical information about the conduit network geometry that is often unavailable. Moreover, a drawback of many empirical models is that it is difficult to predict, a priori, overall topology of the resulting conduit network in terms of connectivity. For example, Pardo-Iguzquiza et al. (2012) simulate connectivity using a diffusion-limited aggregation method and information about the resulting network connectivity is only available after the simulation.

Pseudo-genetic approaches, that mimic speleogenetic processes without simulating actual dissolution processes, have been developed to generate conduit networks more efficiently by avoiding computations needed to simulate dissolution kinetics (Borghi 2012). Pseudo-genetic approaches define a heuristic erosion potential along preferential flow paths and an iterative process over which conduits are progressively widened. The pseudo-genetic approach proposed by Jaquet et al. (2004) is based on a modified lattice-gas automaton in which walkers with a certain erosion potential travel through the medium. Borghi et al. (2012), use a pseudo-genetic approach in which conduits are eroded iteratively along minimum effort pathways computed by a fast-marching algorithm. The methodology of Lafare (2012) generates conduits using a heuristic erosion potential function depending on the flow velocities and mean water ages.

Pseudo-genetic and pure speleogenetic approaches have a disadvantage in that they depend on boundary conditions that govern the evolution process. These boundary conditions ideally require the reconstruction of geological conditions during the formation of conduits, which is not always feasible. A related problem is that it is not clear when to stop the conduit generation process. Moreover, many pseudo-genetic and genetic models are not be capable of reproducing actual locations of known geologic features. However, considering that the topology of a conduit network is the result of dissolution processes, pseudo-genetic and genetic approaches are well-suited to reproduce realistic conduit networks in terms of connectivity. In particular, these approaches account for the positive feedbacks between flow and dissolution (NDGFM 2013; Siemers and Dreybrodt 1998) as the conduits are being generated.

In this report, we present an efficient and versatile process-imitating speleogenetic methodology to generate conduit networks, adapted from the pseudo-genetic procedure presented by Borghi et al (2012). A schematic describing the methodology is shown in Figure 2.1. Contrary to existing models that simulate karst genesis, our hydrochemical model is not intended to only study karst genesis. Instead we aim to generate conduit networks, with minimal computational effort on a relatively large regional scale, that honor known field conditions such as springs, sinkholes, fracture planes and bedding planes. Our ultimate goal is to use the model to generate an ensemble of realistic conduit networks in a Monte Carlo framework to evaluate the uncertainty of discrete-continuum model predictions of flow and solute transport in real-world systems when conduit geometries are imperfectly known.

The proposed methodology is sufficiently general to be applied to different hydrogeological settings. In this report, we apply the model to the Silver Springshed in North Central Florida

(Figure 2.2). Silver Springs is a first-order magnitude spring that discharges from the Upper Floridian Aquifer. Previous efforts have modeled groundwater flow in the Silver Springshed using the equivalent porous medium MODFLOW model (Gabrovsek and Dreybrodt 2000). While these equivalent porous media models reproduce reliable steady-state springflow rates and regional hydraulic head

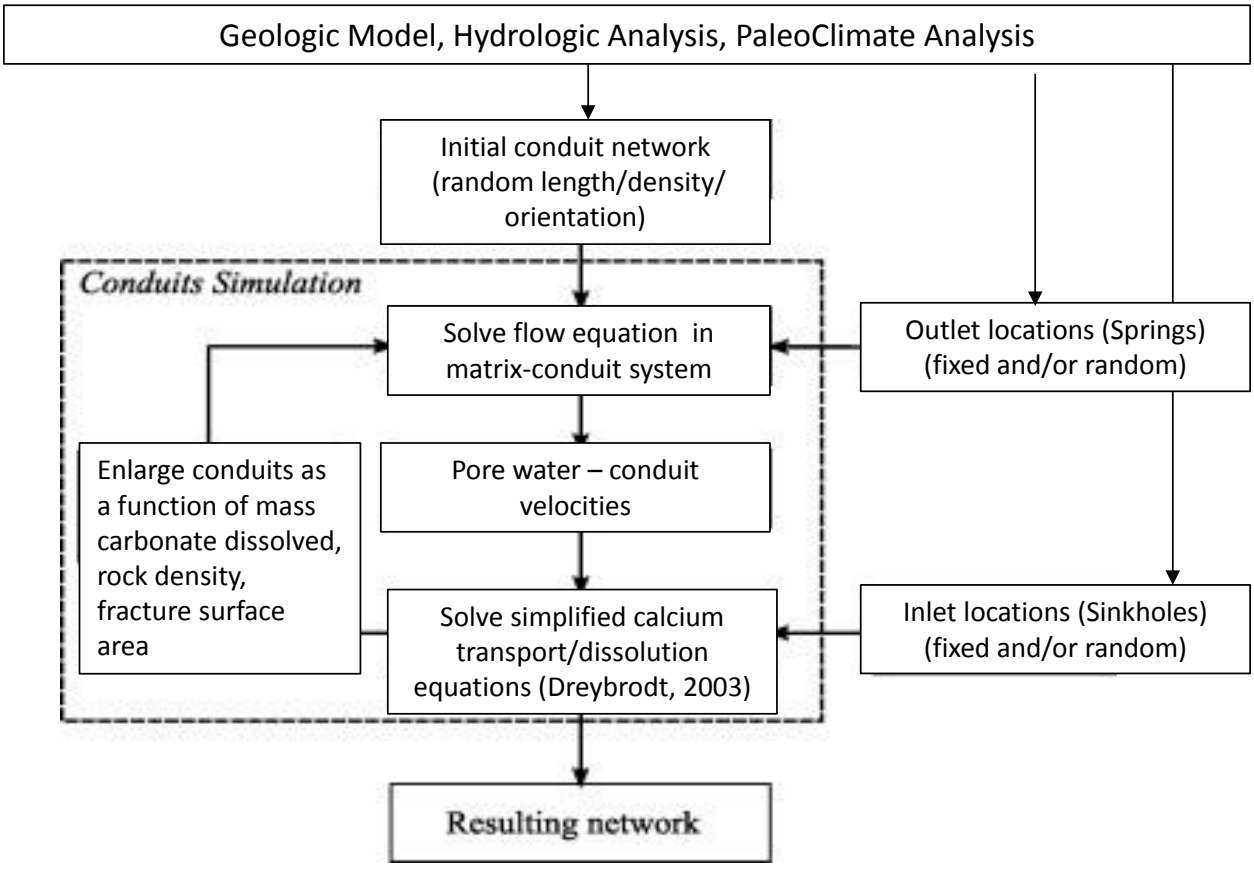

Figure 2.1. Conduit Evolution Algorithm, adapted from Borghi et al. 2012.

contours, they likely underestimate maximum flow velocities and may not accurately reproduce water and solute flowpaths because they do not account for the presence of conduits. To illustrate the methodology and the influence of conduit networks on flow and solute transport we simulate head, spring flow, and solute transport for a variety of conduit networks generated within the Silver Springshed.

2.2.1 Theory

We assume that karst aquifers can be represented by one-dimensional conduits with a circular cross-section embedded in a porous limestone matrix. We consider physical and chemical processes within the conduits and the matrix. Some previous studies karst evolution studies have represented conduits as ducts having a rectangular cross-section. In these studies the conduits are often referred to as fractures even when the fractures are represented by one-dimensional discrete features. Other studies have considered karst dissolution in a single two-dimensional fracture

(Hanna and Rajaram 1998; Szymczak and Ladd 2011; Szymczak and Ladd 2009; Detwiler and Rajaram 2007; Pandey et al. 2014; Chaudhuri et al. 2013;Andre and Rajaram 2005).

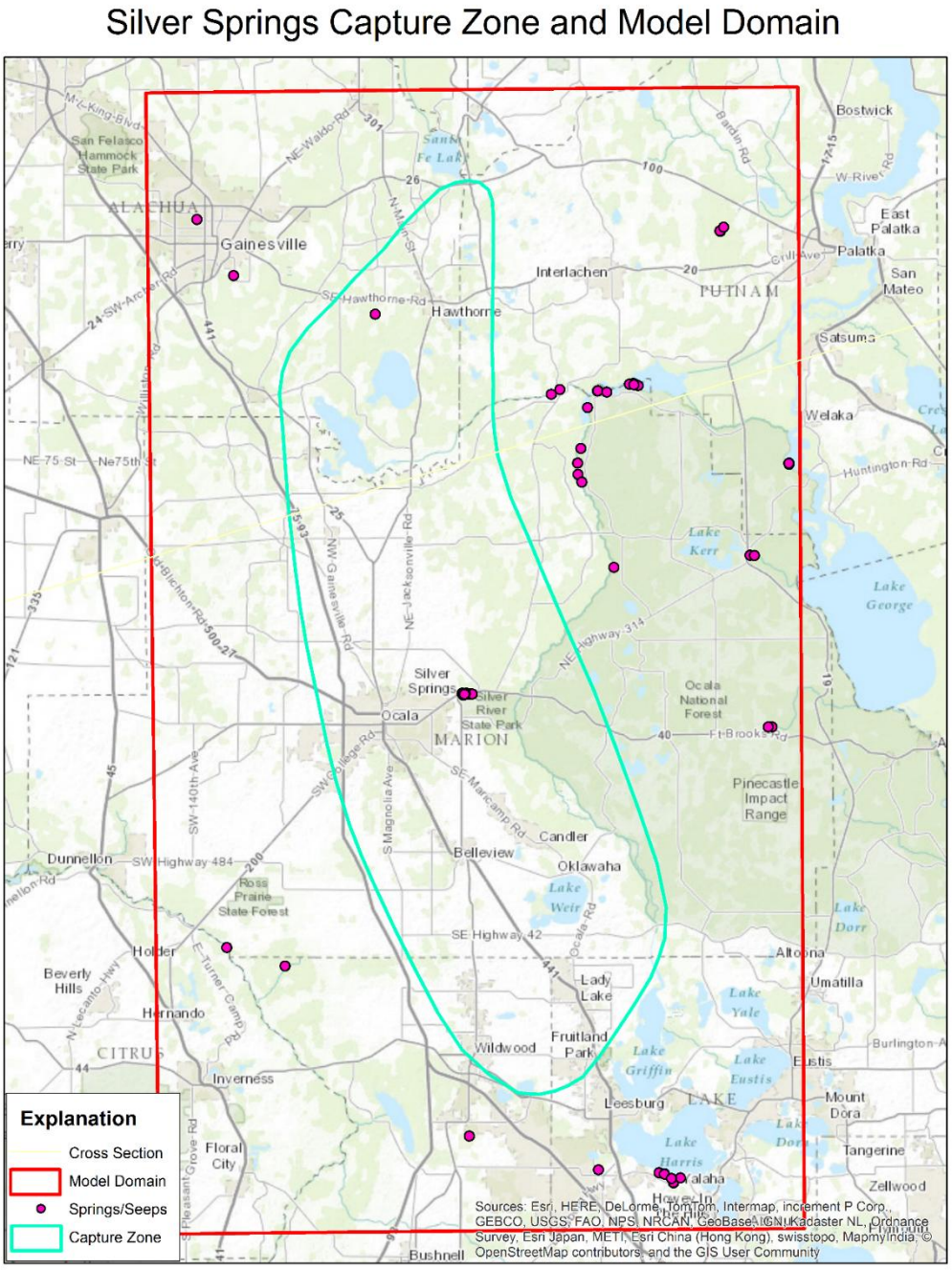

Figure 2.2. Location map for Silver Springs in North Central Florida. Red outline is SJRWMD MODFLOW model domain boundary. Turquoise outline is estimated 1,000 year capture zone for Silver Springs.

2.2.2 Flow and reactive solute transport

Conduit flow is governed by the following mass-balance equation:

$$C_c \frac{\partial p}{\partial t} + \frac{\partial (vA)}{\partial s} + q_{c,O} - q_{c,I} + q_{c \to m} = 0 \quad (1)$$

where C_c is capacity term for conduit flow [m], p the pressure head [m], v the velocity [m s^{-1}], A the cross-sectional area of flow [m^2], s the spatial coordinate in the direction parallel to the conduit [m], $q_{c \to m}$ a sink term associated with exchange from the conduit to the matrix [m^2 s^{-1}] and $q_{c,O}$ and $q_{c,I}$ are conduit sink and source terms [m^2 s^{-1}], respectively. The flow velocity v in the conduit equals Q/A. The mass balance equation for matrix flow is given by:

$$C \frac{\partial p}{\partial t} - \nabla \cdot \mathbf{q} + q_{m,O} - q_{m,I} + q_{m \to c} = 0 \quad (2)$$

where C is a capacity term for matrix flow [L^{-1}], p the pressure head, $\mathbf{q}$ the darcy flux [m s^{-1}], $q_{m \to c}$ a sink term associated with exchange from the matrix to the conduit [1 s^{-1}] and $q_{m,O}$ and $q_{m,I}$ are matrix sink and source terms, respectively [1 s^{-1}].

Reactive solute transport of calcium in the conduits is governed by the following advection-dispersion-reaction equation:

$$\frac{\partial (Ac)}{\partial t} + \frac{\partial (vAc)}{\partial s} - \frac{\partial}{\partial s}\left(DA \frac{\partial c}{\partial s} \right) + c q_{c,O} - c_I q_{c,I} + c q_{c \to m} - P_c = 0 \quad (3)$$

where c is the concentration [mol m^{-3}], D is the hydrodynamic dispersion coefficient for conduit flow [m^2 s^{-1}], c_I the concentration at inflow boundaries and P_c a calcium production term [mol m^{-1} s^{-1}] . Reactive transport in the matrix is governed by the following advection-dispersion-reaction equation:

$$\frac{\partial (\theta c)}{\partial t} + \nabla (\mathbf{q} c) - \nabla (\theta \mathbf{D} \nabla c) + c q_{m,O} - c_I q_{m,I} + c q_{m \to c} - P_m = 0 \quad (4)$$

where θ is the water content [-], $\mathbf{D}$ the hydrodynamic dispersion tensor [m s^{-1}] and P_m a calcium production term [mol m^{-3} s^{-1}]. Equations (3) and (4) are based on the assumption that solute transport between the conduits and the matrix is solely governed by advection.

2.2.3 Calcite dissolution

The change in conduit radius r[m] due to a dissolution rate R[mol m^{-2} s^{-1}] follows from a mass balance at the conduit wall:

$$\frac{\partial r}{\partial t} = \frac{R}{\omega \rho} \quad (5)$$

where ω is the number of moles of calcite per unit mass of calcite [mol kg^{-1}] and ρ the density of calcite [kg m^{-3}]. Similarly, within the porous matrix, change of porosity φ [–] due to a dissolution rate R [mol m^{-2} s^{-1}] is given by:

$$\frac{\partial \varphi}{\partial t} = \frac{\theta R S}{\omega \rho} \tag{6}$$

where S is the specific reaction surface [1 m^{-1}] of porous limestone. Typically, the reaction surface per unit volume of porous material is very large and aggressive water (i.e., undersaturated with calcium) entering the porous matrix quickly becomes saturated with respect to calcite. As a result, dissolution of the porous matrix is effectively limited to a small region with a sharp reaction front where the aggressive water is introduced. Within the bulk of the matrix continuum the calcium concentration simply equals the saturation equilibrium concentration for calcium c_{eq}:

$$c = c_{eq} \tag{7}$$

The dissolution of limestone at the conduit-matrix interface is governed by surface-controlled and transport controlled-reaction rates. The first-order surface-controlled dissolution rate R_s [mol m^{-2} s^{-1}] is given by (Perne et al. 2014):

$$R_s = k_s \left(1 - c_s / c_{eq}\right) \tag{8}$$

where k_s is the surface-controlled rate coefficient [mol m^{-2} s^{-1}], c_s the calcium concentration at the interface [mol m^{-3}] and c_{eq} the calcium saturation equilibrium concentration [mol m^{-3}]. The transport-controlled dissolution rate accounts for transport through the diffusion boundary layer and is given by:

$$R_t = k_t \left(1 - c_s / c\right) \tag{9}$$

where k_t is the transport-controlled rate coefficient and c the bulk calcium concentration within the water. Equating equation (8) and equation (9) gives an expression for c_s which can be inserted in either one of these two equations to find the following expression for the effective first-order dissolution rate R (Szymczak and Ladd 2009; Perne et al. 2014):

$$R_1 = k_1 \left(1 - c / c_{eq}\right) \tag{10}$$

with:

$$k_1 = \frac{k_t k_s}{k_t + k_s} \tag{11}$$

The transport-controlled rate coefficient k_t is given by:

$$k_t = \frac{D_m}{\varepsilon c_{eq}} \tag{12}$$

where D_m is the diffusion coefficient [m^2 s^{-1}] and ε the thickness of the boundary layer. The thickness of the boundary layer is defined by the Sherwood number:

$$N_{Sh} = \frac{2r}{\varepsilon} \tag{13}$$

The Sherwood number for laminar conduit flow is 3.66 (Goode 1996). For turbulent flow the Sherwood number is derived using (Goode 1996):

$$N_{Sh} = 0.027 N_{Re}^{4/5} N_{Sc}^{1/3} \tag{14}$$

where N_{Re} and N_{sc} are the Reynolds number and the Schmidt number, respectively. The Reynolds number is given by:

$$N_{Re} = \frac{2vr\rho_w}{\mu} \tag{15}$$

with v the velocity [m s^{-1}], ρ_w the density of water [kg m^{-3}] and μ the dynamic viscosity of water [kg m^{-1} s^{-1}]. The Schmidt number is given by:

$$N_{Sc} = \frac{\mu}{\rho_w D_m} \tag{16}$$

It has been observed that as calcium concentrations approach saturation the reaction rate decreases due to impurities within the limestone which inhibit dissolution (Svensson and Dreybrodt 1992; Cornaton and Perrochat 2006). This phenomenon is known as the kinetic trigger effect (White 1977) and has been modeled by switching dissolution from first-order to higher order kinetics when the calcium concentration exceeds a certain value c^*. The higher order effective rate is typically given by (Lichtner 1988):

$$R_n = k_n \left(1 - c/c_{eq}\right)^n \tag{17}$$

with k_n defined as:

$$k_n = k_1 \left(1 - c^*/c_{eq}\right)^{1-n} \tag{18}$$

such that $R_1 = R_n$ at $c = c^*$. A general expression for the reaction rate be written as:

$$R = \begin{cases} R_1 & \text{if} \quad c \le c^* \\ R_n & \text{if} \quad c > c^* \end{cases} \tag{19}$$

Figure 2.3 illustrates the effect of the kinetic trigger on reaction rate *R*. The decrease in dissolution rates close to saturation allows aggressive water to penetrate further into the aquifer than would otherwise be possible.

2.3 MODEL DESIGN

2.3.1 The quasi-steady state approximation

Combining equation (3) and (5) and using $P_c = 2\pi rR$ results in the following reactive transport equation:

$$\frac{\partial c}{\partial t} + \frac{\partial (vc)}{\partial s} - \frac{\partial}{\partial s}\left(D \frac{\partial c}{\partial s} \right) + cq_{\mathrm{c,O}} - c_I q_{\mathrm{c,I}} + cq_{\mathrm{c}\to m} = \frac{2\omega\rho}{r}\frac{\partial r}{\partial t} \tag{20}$$

Hanna and Rajaram (1998) and Lichtner (1988) have shown that because the density of the limestone rock is much larger than the maximum calcium concentration, the rate of change in conduit radius is much slower than the rate of change in concentration and the rate of change in the flow field. Thus, the flow and reactive transport equations in the conduits can be simplified with a "quasi-stationary state approximation" using the steady-state equations:

$$\begin{aligned} \frac{\partial (vA)}{\partial s} + q_{\mathrm{c,O}} - q_{\mathrm{c,I}} + q_{\mathrm{c}\to\mathrm{m}} &= 0 \\ \frac{\partial (vc)}{\partial s} - \frac{\partial}{\partial s}\left(D \frac{\partial c}{\partial s} \right) + cq_{\mathrm{c,O}} - c_I q_{\mathrm{c,I}} + cq_{\mathrm{c}\to m} &= 2\pi rR \end{aligned} \tag{21}$$

Within the matrix, we assume that the porosity remains constant and that the concentration of calcium equals the equilibrium concentration. Therefore, the flow and reactive transport equations in the matrix are simplified:

$$\begin{aligned} \nabla \cdot \mathbf{q} + q_{\mathrm{m,O}} - q_{\mathrm{m,I}} + q_{m\to c} &= 0 \\ c &= c_{\mathrm{eq}} \end{aligned} \tag{22}$$

Equations (21) and (22) allow simulation of conduit generation processes through a sequence of steady states (Hanna and Rajaram 1998; Lichtner 1988). To begin, steady state flow and concentrations fields and corresponding dissolution rates are computed based on initial conduit diameters. The dissolution rate, in turn, determines the rate of conduit radius enlargement. The quasi-steady rate of conduit radius enlargement is applied over a "dissolution time step" to

modify the conduit diameters. The process is then repeated using the modified conduit diameters. A sequence of these dissolution time steps can be applied to simulate the dissolution process over the desired geologic timescale.

Equations (21) and (22) constitute a speleogenesis model that solves advective-dispersive-reactive transport within the conduits. This is different from many other speleogenesis models in which advective-reactive transport is solved within the conduits and fractures (Kaufmann and Braun 2000; Siemers and Dreybrodt 1998; Perne et al. 2014). The advection-reaction equation is independent of downstream conditions and may be solved from upstream to downstream. Equations are solved for each conduit cell separately with complete mixing assumed at conduit junctions. The strength of our scheme lies in the fact that it can be easily implemented in any model code capable of handling advective-dispersive transport.

2.3.2 Numerical Solution of Flow

The numerical solution of flow in the conduits and the porous limestone matrix follows the approach described by De Rooij et al. (2013). This solution is based on a discrete-continuum approach and a finite difference scheme. The coupling of conduit-matrix flow is governed by a Peaceman well-index which depends on the conduit radius. Thus, after each dissolution timestep the Peaceman well-indices are updated. To permit efficient steady-state flow computations for large regional domains, instead of using Richards equation to simulate variably saturated flow in the porous matrix, an option was added to solve for flow using the 3-D saturated flow equation. The height of the model domain is adjusted in accordance with the change in height of the water table at each time step, using an approach similar to that used in MODFLOW. Contrary to MODFLOW, however, net recharge is applied to the topmost model cells even if the water table drops below the cell. The vertical hydraulic conductivity is assumed to remain constant, at its saturated value, to transmit recharge to the water table.

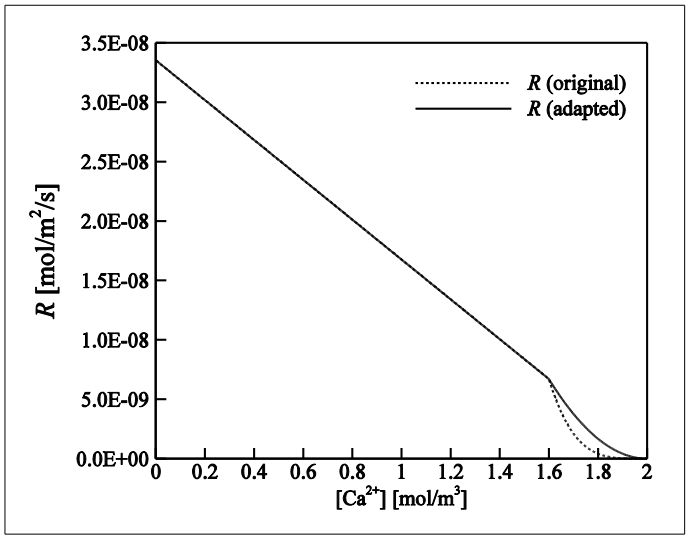

Figure 2.3. Effect of the kinetic trigger on reaction rate as calcium concentration approaches saturation (c*=1.6 mol m^{-2})). Solid line corresponds to equations (10) and (17). Dashed line corresponds to equations (26) and (27).

Within the conduits the pipe flow equation proposed by Swamee and Swamee (2007) is implemented, assuming the conduits always remain full. This equation provides for a smooth transition between laminar and turbulent flow. For laminar flow the equation approximates the Poiseuille equation. For turbulent flow, the equation approximates the Darcy-Weisbach equation. The Swamee and Swamee (2007) equation allows conduit flow to automatically switch from laminar to turbulent conditions during conduit evolution (Figure 2.4).

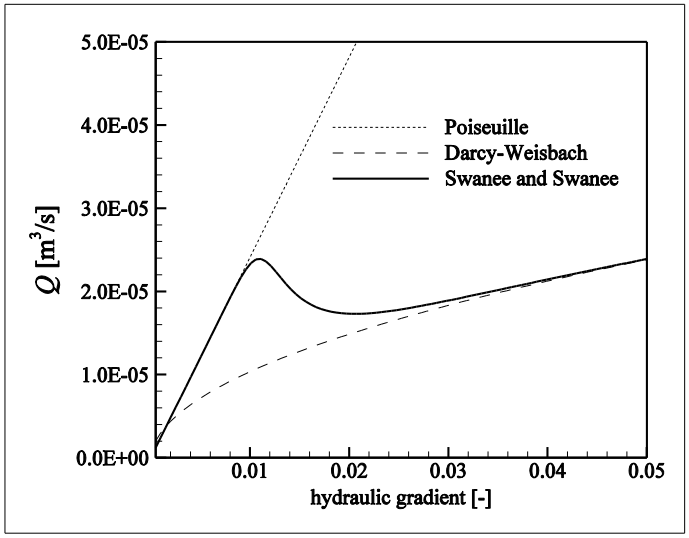

Figure 2.4. Swamee and Swamee (2007) pipe flow equation showing smooth transition between laminar and turbulent flow as hydraulic gradient in pipe increases (solid line). Poiseuille equation for laminar flow (dotted line) and Darcy-Weisbach equation for turbulent flow (dashed line) are also shown for comparison.

2.3.3 Numerical Solution of Reactive Transport

Reactive transport is also simulated using finite differences. Accurate numerical solution of advection-dispersion equations is subject to criteria for spatial as well as temporal discretization, which are typically given in terms of Courant and Peclet numbers. To avoid small space and time discretization that would result in extremely long computation times for large regional models, we use an upwind scheme that is unconditionally stable regardless of discretization. The drawback of upwinding is that it introduces numerical dispersion.

In the numerical solution of reactive transport the reaction term must be handled carefully to avoid numerical instability and time stepping restrictions. Reaction rates defined by equations (10) and (17) can result in numerical instability, with reaction rates jumping between first and higher order during non-linear iterations. This behavior is likely the due to the fact that the derivative of the reaction rate is highly discontinuous at $c = c^*$ (Figure 2.3). Therefore the following expression for the higher-order effective rate, which has a continuous derivative at c^*, was adopted (Pandey 2014; Andre and Rejaram 2005; Svensson and Dreybrodt 1992):

$$R_n = fR_1 \tag{26}$$

with:

$$f = 1 - \frac{c - c^*}{c_{eq} - c^*} \tag{27}$$

Computations with this relationship were found to be more efficient. Figure 2.3 illustrates that the adapted expression compares reasonably well to the original expression.

2.3.4 Initial Conduit Network

The simulation of conduit evolution requires an initial conduit network, albeit with vanishingly small diameters, in order for dissolution to begin. This requirement constrains conduits to only evolve within a predefined network, which is a limitation of the methodology. However, specification of the initial conduit work does provide a means to force the generation of conduits in certain locations (i.e., known inception horizons, Filipponi et al. 2009).

In our work the initial conduit network is generated using an approach similar to that typically used to generate stochastic fracture networks (Bauer and Sauter 2005). The main difference is that we generate line segments instead of planes. From a conceptual point of view the line segments may be viewed as the intersections of fracture planes with a bedding plane or inception horizon. To reflect that sets of fractures may exist in various orientations, the segments are subdivided into a number of subsets, each with a different orientation. For each subset a number of fractures and probability distribution functions for the location, length and orientation of fractures within the subset must be specified. It is assumed that the initial radius of the conduit segments scales with their length (L):

$$r = \bar{r}L / \bar{L} \tag{28}$$

where L is the randomly generated conduit length, $\bar{r}$ is the mean radius and $\bar{L}$ is the mean length as determined by the probability distribution function. If necessary geometrical restrictions may be imposed on the segment generator. For example, a minimum distance between segments of the same subset can be specified to avoid multiple segments with similar orientations within a small region. Between two intersecting segments a minimum distance between the intersection point and the end points of the segments may be provided to avoid very small conduit cells in the final spatial discretization.

2.3.5 Boundary Conditions for Regional Scale Modeling

The flow boundary conditions during the conduit evolution process are generally unknown and may be varied to obtain different conduit configurations. However the land surface boundary condition must be handled carefully to avoid unrealistic flow scenarios. For example, if the presence of surface water is not accounted for, then the effective rainfall rate (precipitation – evapotranspiration) into the subsurface may be overestimated, resulting in unrealistically high hydraulic heads (i.e., above the land surface). Moreover, forcing all effective rainfall to be transmitted by the subsurface can result in unrealistically steep hydraulic gradients. Simulating surface water flow using rigorous mass balance and flux equations over large regional domains can be computationally demanding, therefore an alternative computationally efficient

methodology was developed. This methodology limits the hydraulic heads in the topmost matrix cells to a spill elevation by applying drains to these cells. The flux rate associated with these drains is:

$$q = \begin{cases} \gamma\left(h_c - z_s\right) & \text{if } h_c > h_s \\ 0 & \text{if } h_c \le z_s \end{cases} \tag{29}$$

where h_c is the hydraulic head in a topmost cell, z_s the spill elevation associated with the drain and γ the drain conductance term [1 s^{-1}]. Spill elevations are computed from topography using a procedure adapted from Wang and Liu (2006). The original purpose of the Wang and Liu procedure was to increase the topography in digital elevation models to the spill elevation such that local depressions were removed. Here we use the spill elevation to approximate the maximum depth of water that can be stored in local depressions. Thus within local depressions the spill height is above the land surface and water can pond on the surface up to the spill height. Outside local depressions the spill elevation equals land surface elevation. Water drained from the land surface using this method is permanently removed from the domain.

As discussed by Bauer et al. (2005) and Clemens et al. (1999) the epikarst, a zone of enhanced weathering near the surface, plays a significant role in speleogenesis by distributing the effective rainfall within the subsurface. In the absence of an evolved conduit network, this distribution will generally be diffuse. Once a conduit network starts to form and the first sinkholes appear the epikarst layer will focus flow towards the sinkholes. This flow focusing mechanism enhances dissolution in the conduit network. As the conduit network evolves, the water table may be lowered causing sinkholes at higher elevations to become inactive.

To account for the flow focusing mechanism of sinkholes we place a number of sinkholes randomly along the initial conduit network. These sinkholes are connected to the conduit layer by a vertical stack of matrix cells with a relatively high vertical hydraulic conductivity. A column of high hydraulic conductivity porous media is used, rather than a vertical conduit, in order to avoid computational difficulties associated with variably saturated vertical conduits in the vadose zone. The topmost matrix cells are assigned the same high horizontal hydraulic conductivity throughout the domain. Using this set up, as conduits begin to form and lower the local water table the high conductivity cells focus flow from the top layer toward the sinkhole and conduit mimicking the natural process. Although this is a highly simplified representation of sinkholes, flow into the sinkhole is computed implicitly. Thus, the method does not require specification of additional boundary conditions at sinkhole locations as is the case in other methods (Bauer et al. 2005). This methodology proposed here is reasonable if the main interest is to generate a conduit network of large lateral extent.

2.4 MODEL APPLICATION

The conduit generation algorithm described above was applied to the Silver Springshed in North Central Florida, with the long term goal of generating an ensemble of realistic conduit networks that can be incorporated into the existing regional MODFLOW model (Gabrovsek and Dreybrodt 2000) using MODFLOW-CLN. To generate conduits within the springshed the regional

MODFLOW model was clipped to the 1,000 year capture zone (Figure 2.2). The spatial discretization of the porous matrix was taken directly from the original MODFLOW model which consists of seven layers and uses a horizontal discretization of 762 m (2,500ft). Layer 1 represents the surficial aquifer and Layer 2 is a relatively low permeability unit that underlies the surficial aquifer in the eastern portion of the domain. Layers 3, 4 and 5 represent the Upper Floridian Aquifer. Layer 7 represents the Lower Floridian Aquifer that is separated from the Upper Floridian Aquifer by the lower permeability layer 6. The existing conduit network is thought to have evolved primarily within the Upper Floridan aquifer at the interface between the Ocala and Avon Park limestone. Thus, for this example, the conduit network was evolved in layer 4, which coincides with the Ocala Limestone Formation.

To generate conduits for the Silver Springshed an initial random conduit network, consisting of sets of intersecting segments within a horizontal plane, was generated and mapped to the middle of layer 4. Subsequently, a specified number of sinkholes was located randomly at the land surface overlying the initial conduit network. As described above, these sinkholes are represented by a stack of relatively high permeability cells that occupy layers 1-4. In the original equivalent porous media MODFLOW model, the calibrated effective hydraulic conductivity for the Upper Floridan aquifer was relatively high, reflecting the influence of karstification. It is reasonable to assume a significantly lower Upper Floridan matrix hydraulic conductivity in the conduit evolution model, since the conduits are represented as discrete features. For the examples presented here the hydraulic conductivity for the matrix blocks in layers that make up the Floridian Aquifer was approximated to be $0.1E^{-3}$ m s^{-1}, a value representative of karst limestone rock (Freeze and Cherry 1979). The top epikarst layer and "sinkholes" were assigned a higher hydraulic conductivity of $0.1E^{-3}$ m s^{-1}. A constant effective rainfall of $1.2E^{-8}$ m s^{-1} was applied to the land surface and no lateral flux boundary conditions were applied everywhere.

Figure 2.5 shows a series of conduit networks that evolved over a simulation time of 120,000 years using two different segment densities, two different segment orientations, and two sinkhole densities. Figures 2.6 through 2.8 illustrate the head fields that result from the evolved conduit networks at the end of the simulation time. Also shown in Figures 2.6 through 2.8 are springflows from domain as the conduit networks evolve. These figures indicate that for some of the example conduit networks (e.g., 103 and 110) Silver Springs fails to form because the conduit networks do not develop enough to capture significant flow. Thus for these cases surface outflow from topographic low points in the domain, rather than spring outflow, dominates over the entire simulation time.

Figure 2.9 shows the solute breakthrough curve at the spring for a unit solute pulse applied to the land surface for one conduit network (Case 101). Figure 2.10 shows snapshots of solute distribution, in layer 1 and layer 4 porous media and in layer 4 conduits, at three points along the rising limb of the breakthrough curve. Figure 2.11 shows snapshots of solute distribution in layer 1 and layer 4 porous media and in layer 4 conduits, at three times after a reverse solute pulse was injected into the spring for the same conduit network. Hot colors in Figure 2.11 correspond to regions of the conduit network and porous matrix that transmit solute rapidly to the spring. It should be noted that Figures 2.10 and 2.11 are provided to illustrate the solute transport capabilities of the DisCo model for a hypothetical conduit system, and do not, at this point, show actual vulnerable locations in the springshed.

2.5 CONCLUSIONS AND FUTURE DIRECTIONS

Task 1 of the Work Order 4, developing a conduit generation algorithm capable of generating ensembles of possible conduit networks for the Silver Springshed, is complete. Experimentation with the algorithm on synthetic aquifer systems, as well as the Silver Springshed domain, indicates that flow boundary conditions specified during the conduit evolution process have an extremely strong effect on the pattern of conduit evolution. After boundary conditions, the presence of an overlying confining layer and sinkhole density and location appear to be the most influential factors affecting conduit evolution. Fracture density and orientation are also influential, but this influence seems to decline above a threshold fracture density. Lower porous media hydraulic conductivity values were found to enhance the formation of conduits.

Modern-day lake, river and lateral boundary conditions in the SJRWMD local Silver Springs Model were found to generate unrealistic conduit networks surrounding the entire Oklawaha River (Figure 2.12). As a result, we recommend that the simplified model domain used to generate examples shown in Figures 2.5-2.9 be adopted to generate the ensemble of conduits for the Monte Carlo experiments. The generated conduits can then be inserted into either the original SJRWMD local Silver Springs model (Figure 2.12), or into 1,000 year capture zone domain model (Figures 2.5-2.11) to conduct the Monte Carlo experiments.

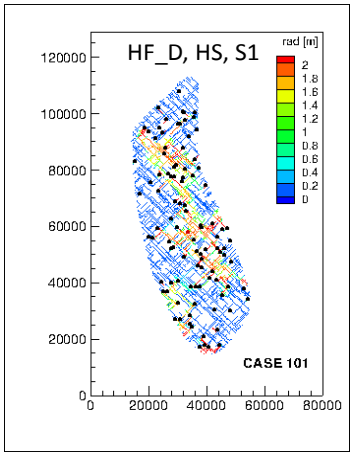

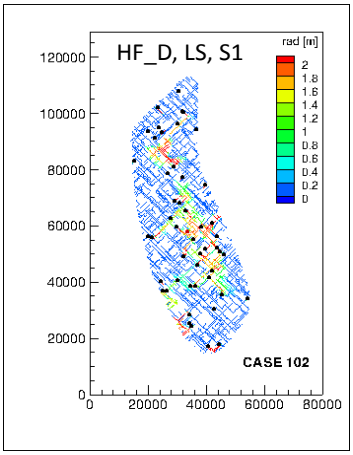

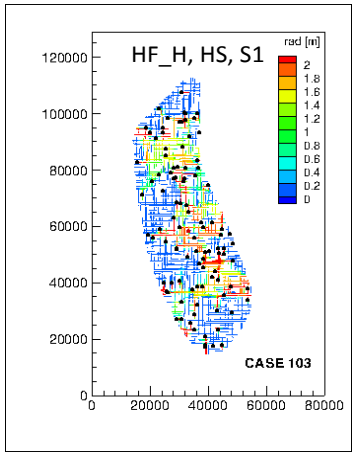

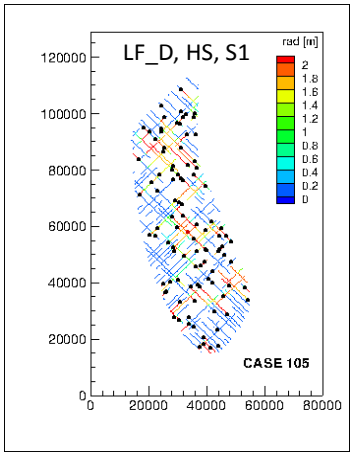

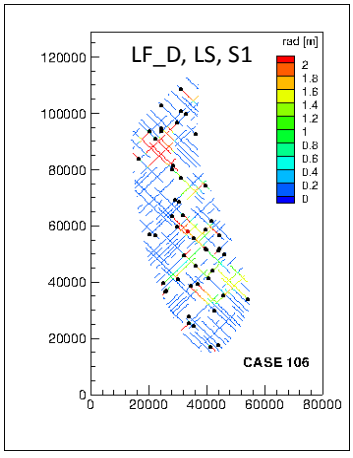

HF_D: High density diagonal fractures
LF_D: Low density diagonal fractures
HF_H: High density horizontal fractures

HS High density sinkholes
LS Low density sinkholes

S1 – random seed 1

Figure 2.5. Example random conduit networks resulting from high and low density diagonal initial fractures, high density horizontal fractures, and high and low density sinkholes.

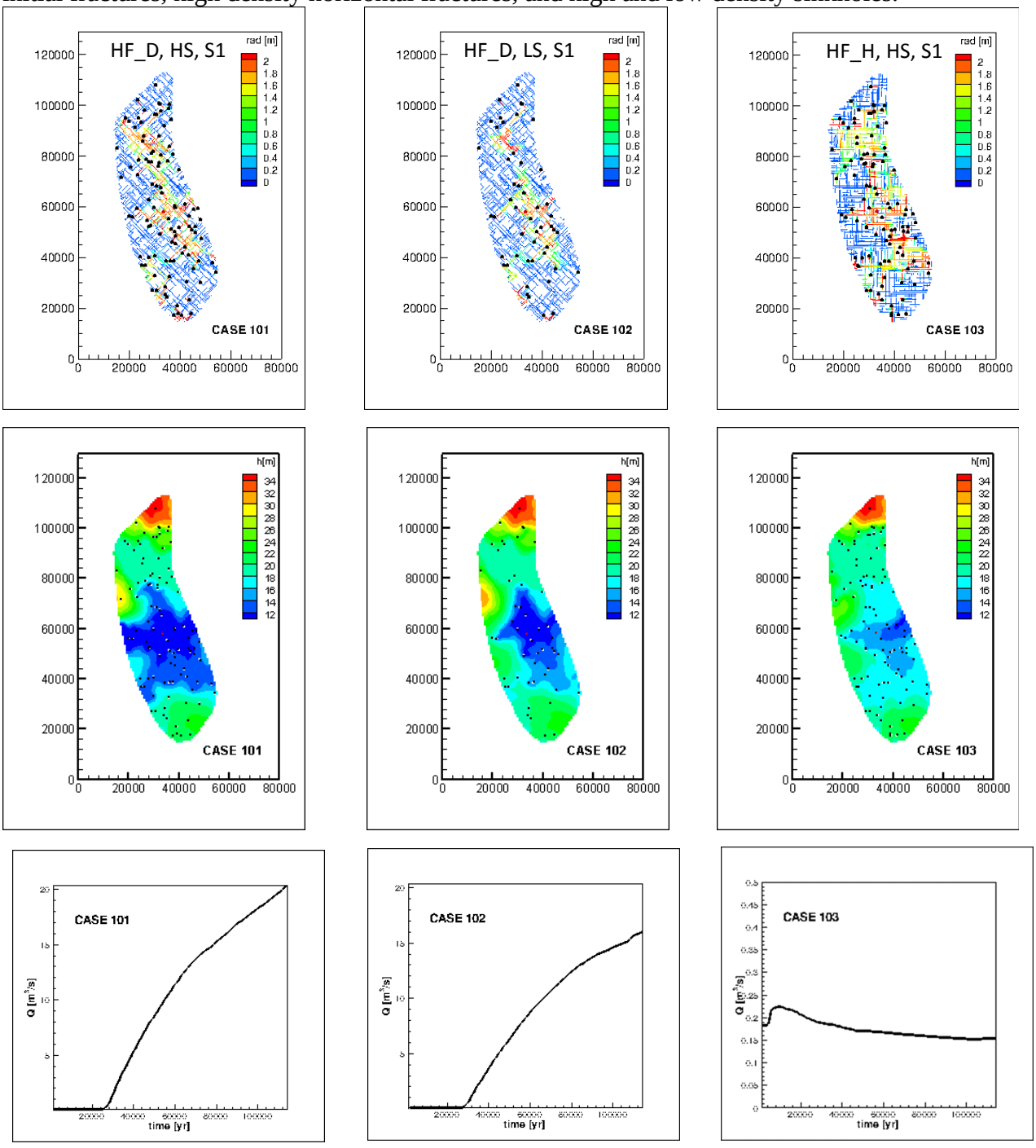

Figure 2.6. Example random conduit networks (top row), resulting head fields (middle row) and resulting spring discharge (bottom row).

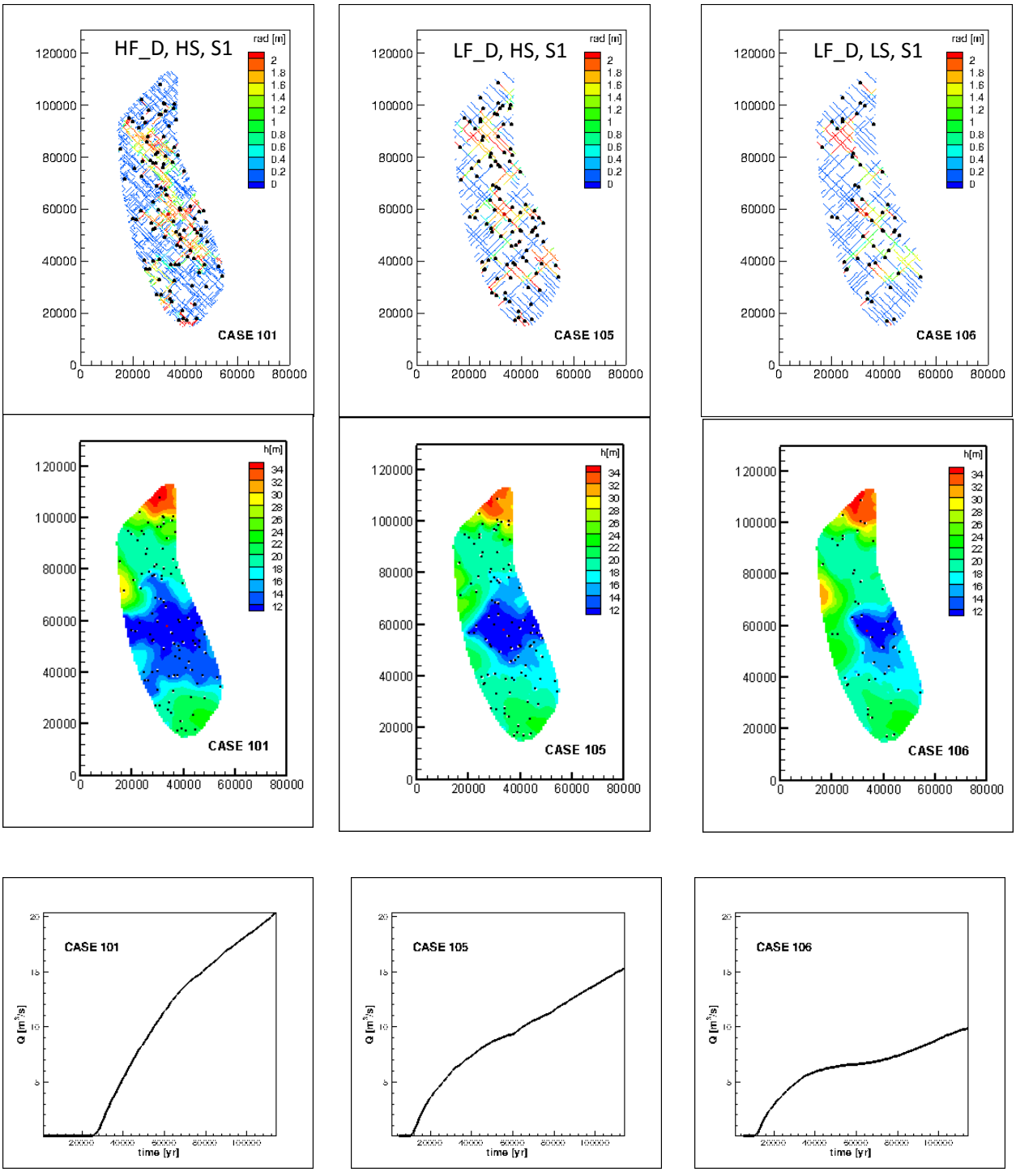

Figure 2.7. Example random conduit networks (top row) resulting head fields (middle row) and resulting spring discharge (bottom row).

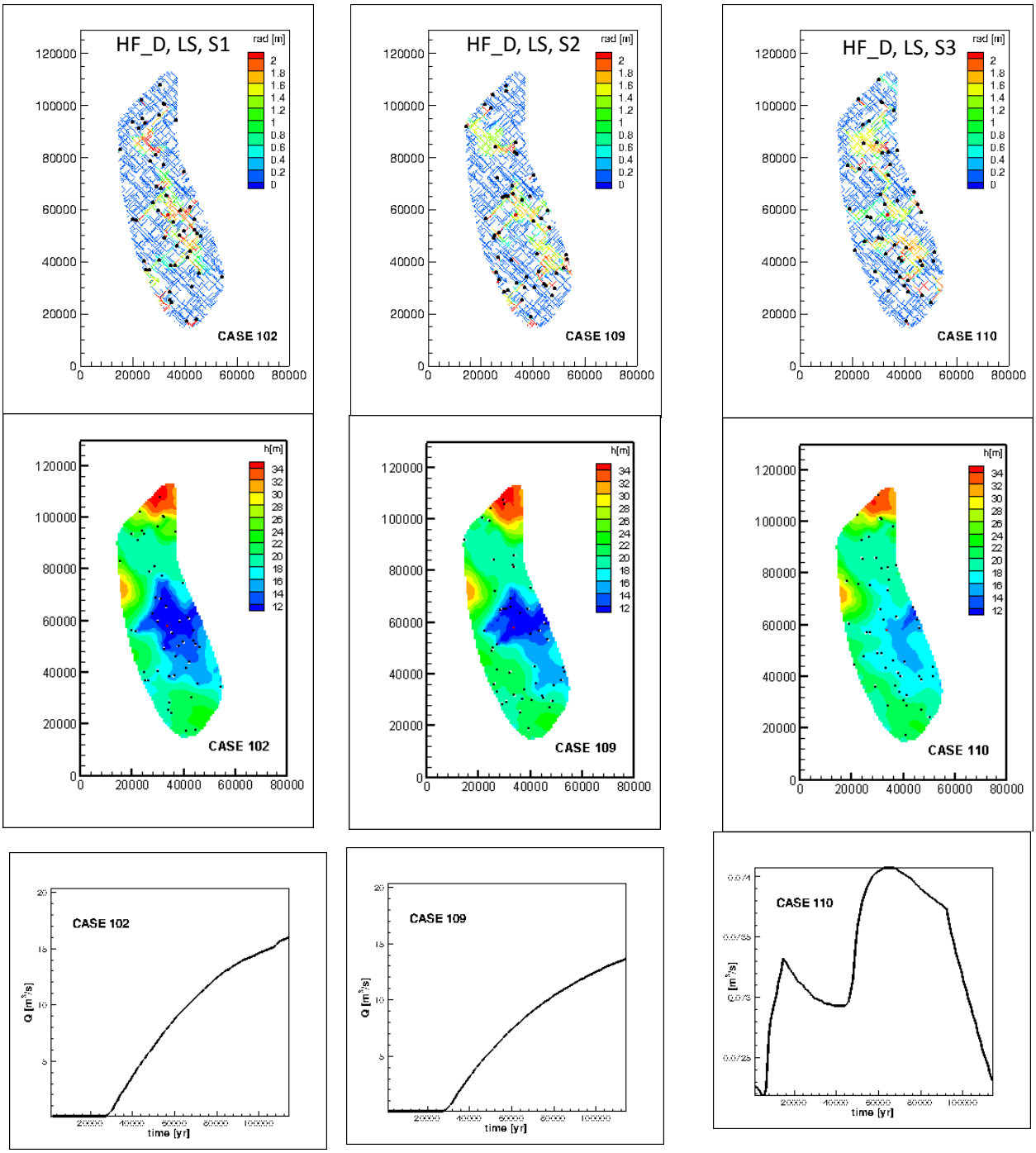

Figure 2.8. Example random conduit networks (top row) resulting head fields (middle row) and resulting spring discharge (bottom row).

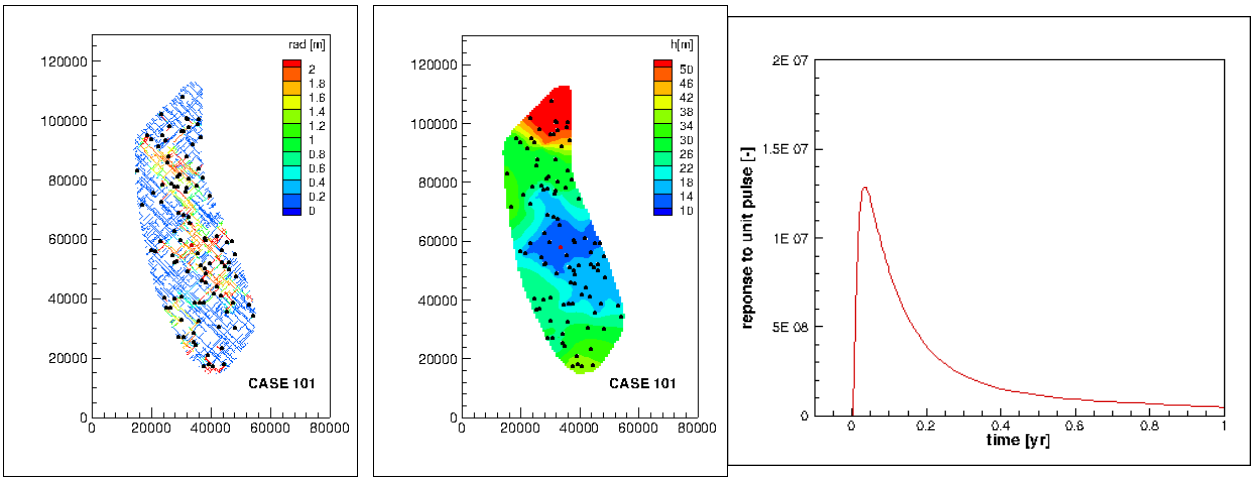

Figure 2.9. Example random conduit network (right), head field (center), solute breakthrough curve (left) at spring resulting from unit solute pulse at the land surface (right).

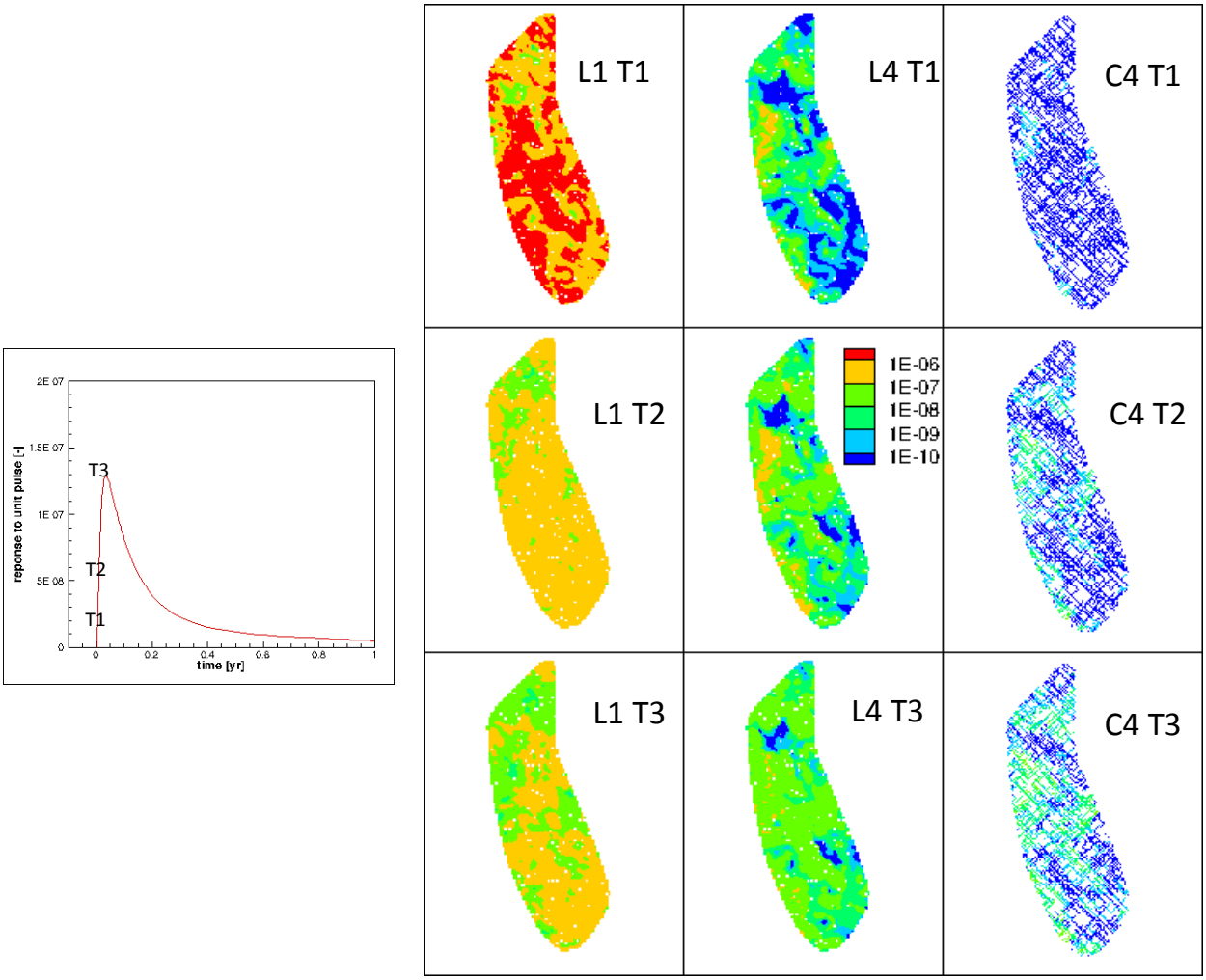

Figure 2.10. Plots of solute distribution in layer 1 (left column), layer 4 (center column) and layer 4 conduits (right column) for three points on the rising limb of the spring solute breakthrough curve (left) resulting from a unit pulse applied to the land surface (Case 101).

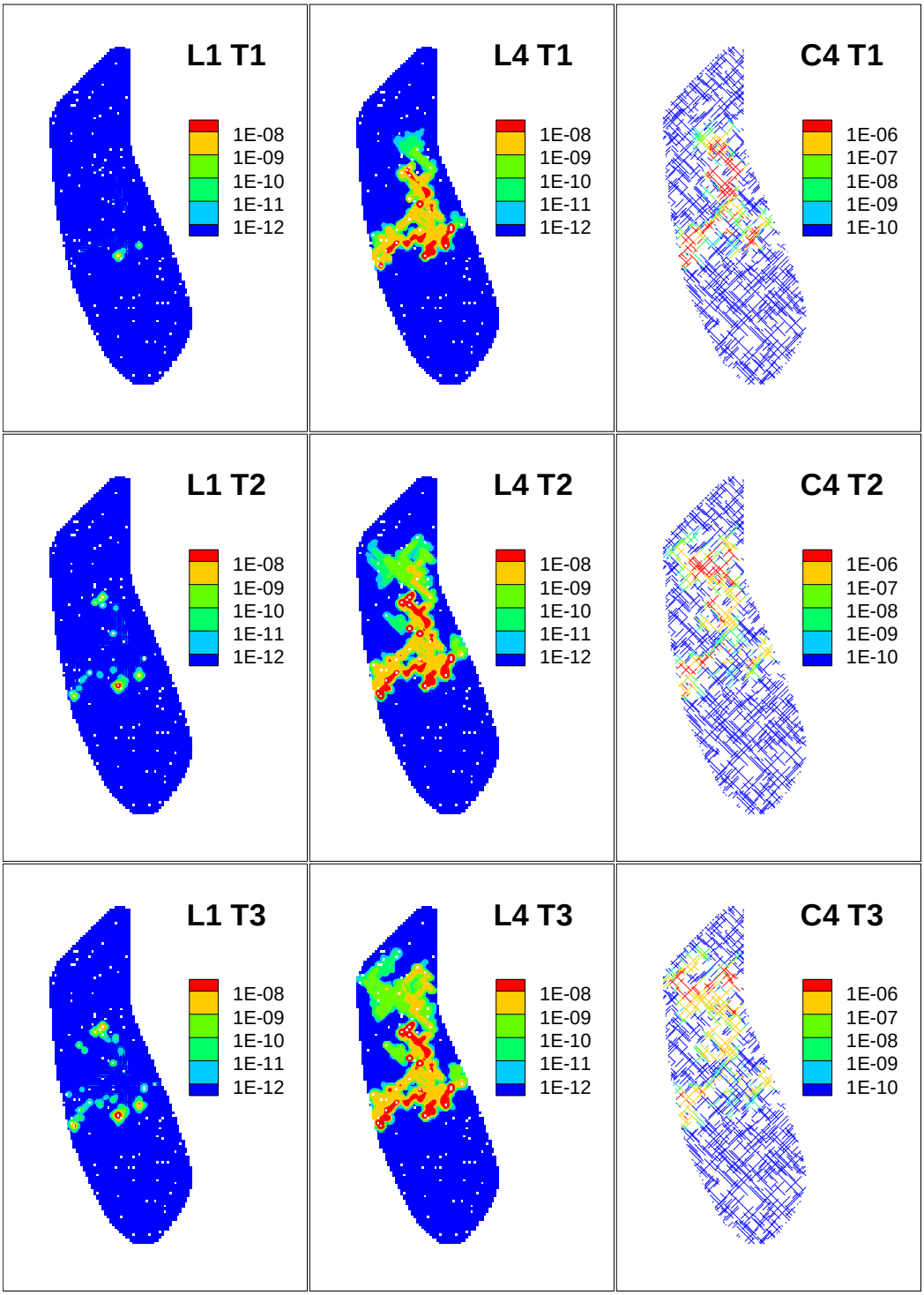

Figure 2.11. Plots of solute distribution in layer 1 (left column), layer 4 (center column) and layer 4 conduits (right column) for three times after reverse injection of a unit pulse at the Spring (Case 101).

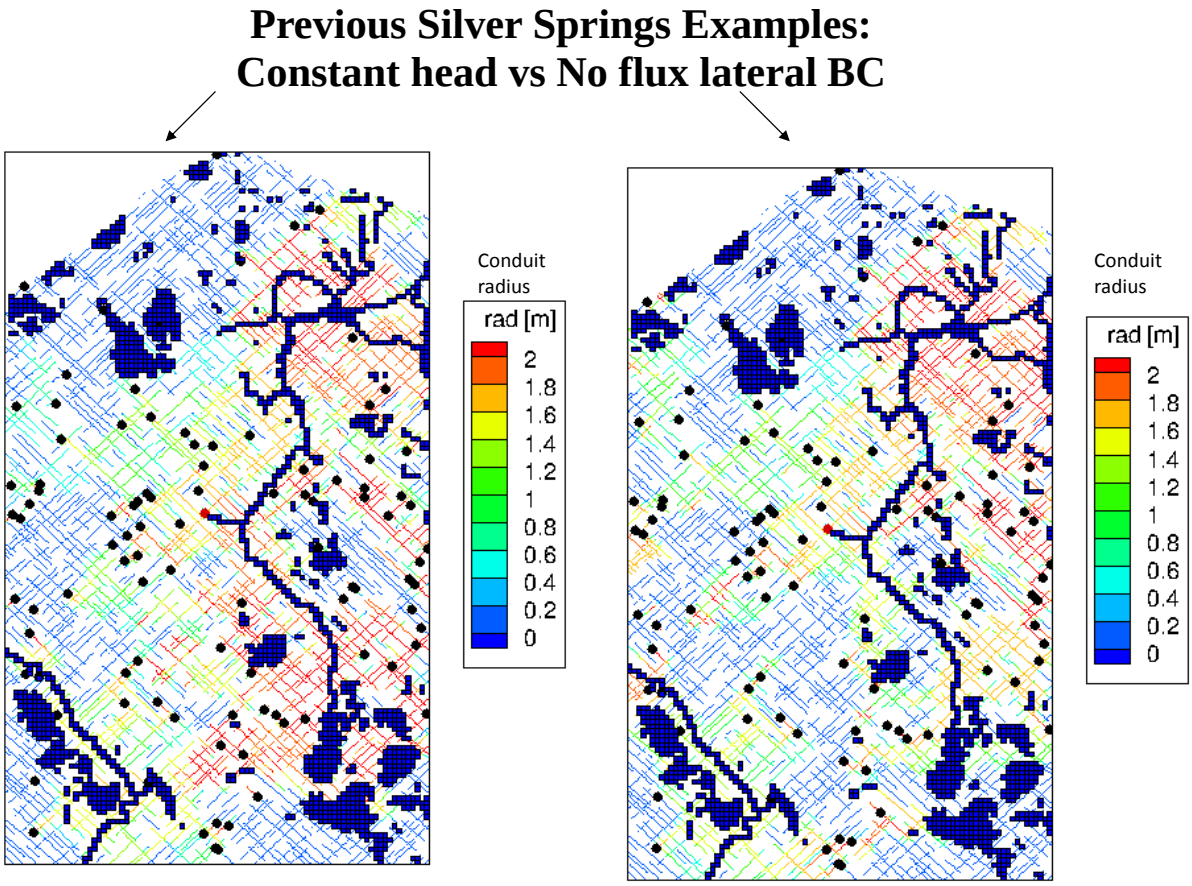

Figure 2.12. Example random conduits generated using the SJRWMD Silver Springs local model assuming constant head lateral boundary conditions (left) and no flux lateral boundary conditions (right). Unrealistic conduit networks surrounding the Oklawaha River are generated, likely as a result of within domain lake and river boundary conditions.

2.6 REFERENCES

de Rooij R; Perrochet P; Graham W. From rainfall to spring discharge: Coupling conduit flow, subsurface matrix flow and surface flow in karst systems using a discrete-continuum model. Advances in Water Resources. 2013;61:29-41.

Kiraly L. FEM-301 – A three dimensional model for groundwater flow simulation, NAGRA Technical Report 84-49. NAGRA Technical Report 84-491985.

Kiraly L. Modelling karst aquifers by the combined discrete channel and continuum approach. Bulletin du Centre d'Hydrogéologie. 1998;16:77-98.

Shoemaker WB; Kuniansky EL; Birk S; Bauer S; Swain ED. Documentation of a Conduit Flow Process (CFP) for MODFLOW-2005.Techniques and Methods, Book 6, Chapter A24. 2008.

Kiraly L; Perrochet P; Rossier Y. Effect of epikarst on the hydrograph of karst springs: a numerical approach. Bulletin du Centre d'Hydrogéologie. 1995;14:199-220.

Eisenlohr L; Bouzelboudjen M; Kiraly L; Rossier Y. Numerical versus statistical modelling of natural response of a karst hydrogeological system. Journal of Hydrology. 1997a;202(1-4):244-62.

Eisenlohr L; Kiraly L; Bouzelboudjen M; Rossier Y. Numerical simulation as a tool for checking the interpretation of karst spring hydrographs. Journal of Hydrology. 1997;193(1-4):306-15.

Pardo-Iguzquiza E; Dowd PA; Xu C; Jose Duran-Valsero J. Stochastic simulation of karst conduit networks. Advances in Water Resources. 2012;35:141-50.

Kaufmann G; Romanov D; Hiller T. Modeling three-dimensional karst aquifer evolution using different matrix-flow contributions. Journal of Hydrology. 2010;388(3-4):241-50.

Kaufmann G. Modelling karst geomorphology on different time scales. Geomorphology. 2009;106(1-2):62-77.

Kaufmann G. Numerical models for mixing corrosion in natural and artificial karst environments. Water Resources Research. 2003a;39(6).

Kaufmann G. A model comparison of karst aquifer evolution for different matrix-flow formulations. Journal of Hydrology. 2003b;283(1-4):281-9.

Kaufmann G; Braun J. Karst aquifer evolution in fractured, porous rocks. Water Resources Research. 2000;36(6):1381-91.

Dreybrodt W; Romanov D; Kaufmann G. Evolution of caves in porous limestone by mixing corrosion: A model approach. Geologia Croatica. 2010;63(2):129-35.

Gabrovsek F; Dreybrodt W. Karstification in unconfined limestone aquifers by mixing of phreatic water with surface water from a local input: A model. Journal of Hydrology. 2010;386(1-4):130-41.

Ronayne MJ. Influence of conduit network geometry on solute transport in karst aquifers with a permeable matrix. Advances in Water Resources. 2013;56:27-34.

Stark CP. AN INVASION PERCOLATION MODEL OF DRAINAGE NETWORK EVOLUTION. Nature. 1991;352(6334):423-5.

Borghi A; Renard P; Jenni S. A pseudo-genetic stochastic model to generate karst networks. Journal of Hydrology. 2012;414:516-29.

Jaquet O; Siegel P; Klubertanz G; Benabderrhamane H. Stochastic discrete model of karst networks. Advances in Water Resources. 2004;27(7):751-60.

Lafare A. Modelisation mathematique de la speleogenese : une approche hybride a partir de reseaux de fractures discrets et de simulations hydrogeologiques Universite Montpellier II. 2012.

Northern District Groundwater Flow Model (NDCFM) Version 4.0. HydroGeoLogic, 2013.

Siemers J; Dreybrodt W. Early development of karst aquifers on percolation networks of fractures in limestone. Water Resources Research. 1998;34(3):409-19.

Gabrovsek F; Dreybrodt W. Role of mixing corrosion in calcite-aggressive H_2O-CO_2-$CaCO_3$ solutions in the early evolution of karst aquifers in limestone. Water Resources Research. 2000;36(5):1179-88.

Hanna RB; Rajaram H. Influence of aperture variability on dissolutional growth of fissures in karst formations. Water Resources Research. 1998;34(11):2843-53.

Szymczak P; Ladd AJC. The initial stages of cave formation: Beyond the one-dimensional paradigm. Earth and Planetary Science Letters. 2011;301(3-4):424-32.

Szymczak P; Ladd AJC. Wormhole formation in dissolving fractures. Journal of Geophysical Research-Solid Earth. 2009;114.

Detwiler RL; Rajaram H. Predicting dissolution patterns in variable aperture fractures: Evaluation of an enhanced depth-averaged computational model. Water Resources Research. 2007;43(4).

Pandey SN; Chaudhuri A; Kelkar S; Sandeep VR; Rajaram H. Investigation of permeability alteration of fractured limestone reservoir due to geothermal heat extraction using three-dimensional thermo-hydrochemical (THC) model. Geothermics. 2014;51:46-62.

Chaudhuri A; Rajaram H; Viswanathan H. Early-stage hypogene karstification in a mountain hydrologic system: A coupled thermohydrochemical model incorporating buoyant convection. Water Resources Research. 2013;49(9):5880-99.

Andre BJ; Rajaram H. Dissolution of limestone fractures by cooling waters: Early development of hypogene karst systems. Water Resources Research. 2005;41(1).

Perne M; Covington M; Gabrovsek F. Evolution of karst conduit networks in transition from pressurized flow to free-surface flow. Hydrology and Earth System Sciences. 2014;18(11):4617-33.

Svensson U; Dreybrodt W. Dissolution kinetics of naturalcalcite minerals in CO_2-water systems approaching calcite equilibrium. Chemical Geology. 1992;100(1-2):129-45.

Goode DJ. Direct simulation of groundwater age. Water Resources Research. 1996;32(2):289-96.

Cornaton F; Perrochet P. Groundwater age, life expectancy and transit time distributions in advective-dispersive systems: 1. Generalized reservoir theory. Advances in Water Resources. 2006;29(9):1267-91.

Lichtner PC. The quasi-stationary state approximation to coupled mass-transport and fluid-rock interaction in a porous medium. Geochimica Et Cosmochimica Acta. 1988;52(1):143-65.

Swamee PK; Swamee N. Full-range pipe-flow equations. Journal of Hydraulic Research. 2007;45(6):841-3.

Xu CS; Dowd P. A new computer code for discrete fracture network modelling. Computers & Geosciences. 2010;36(3):292-301.

Wang L; Liu H. An efficient method for identifying and filling surface depressions in digital elevation models for hydrologic analysis and modelling. International Journal of Geographical Information Science. 2006; 20(2):193-213.

Bauer S; Liedl R; Sauter M. Modeling the influence of epikarst evolution on karst aquifer genesis: A time-variant recharge boundary condition for joint karst-epikarst development. Water Resources Research. 2005;41(9).

Clemens T; Huckinghaus D; Liedl R; Sauter M. Simulation of the development of karst aquifers: role of the epikarst. International Journal of Earth Sciences. 1999;88(1):157-62.

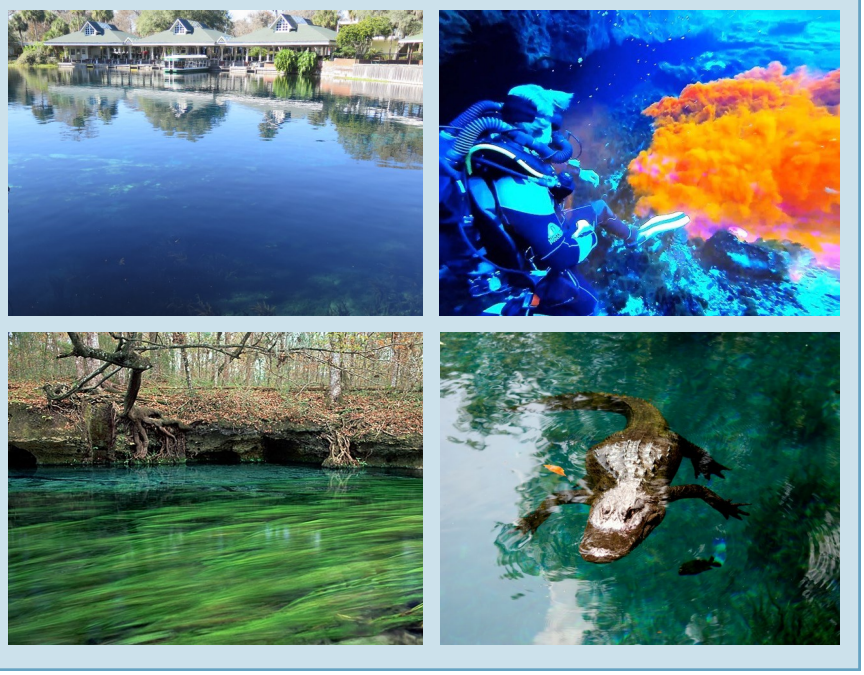

Collaborative Research Initiative on
Sustainability and Protection of Springs [**CRISPS]**

Section 3

[Work Order No: 6]

ANNUAL REPORT

July 2015

submitted to:

St. Johns River Water Management District
Springs Protection Initiative [SPI], UF Contract # 27789

UF | UNIVERSITY of FLORIDA
Water Institute

C R I S P S

Section 3

GROUNDWATER HYDROLOGY

Transport and Loss of Nitrogen within the Upper Floridan Aquifer in the Silver Springs Springshed

Annual Report 2015
Work Order No. 6

Principal Investigators:

James W. Jawitz, University of Florida
Patrick Burger, St Johns River Water Management District

Project Team

James W. Jawitz, Soil and Water Science Department
Michael D. Annable, Engineering School of Sustainable Infrastructure and Environment
Antonio Yaquian, Soil and Water Science Department
University of Florida

This document reports interim progress of a work order in the first year of a 3-year project in compliance with Agreement between University of Florida (UF) and St. Johns River Water Management District (SJRWMD) UF Contract #27789. It is part of the *UF Collaborative Research Initiative on Springs Protection and Sustainability (CRISPS)* and supports the science component of *the SJRWMD Springs Protection Initiative (SPI).*

3.1 ABSTRACT

The goals of this work are to provide field-measured hydrogeologic data that can be used for active resource management in the Silver Springs springshed. *In situ* measurements are being conducted to identify portions of the aquifer that contribute most significantly to water flow to the spring, and also solute flux to the spring. Groundwater velocities and solute fluxes are being measured in situ using passive flux meters (PFMs). We are testing different deployment durations to maximize sensitivity of our measurements. So far, instruments have been deployed for approximately 2 months at a time. Approximately 30 measurements will be conducted for the project; we have monitored in 14 locations so far. Groundwater fluxes measured to date range from 2.6 to 10.9 cm d^{-1} with mean 6.2 cm d^{-1}. In ongoing work, we seek to identify locations of higher flux that contribute disproportionately to spring discharge. Age dating of groundwater collected from different locations in the aquifer will also provide support for the identification of high-vulnerability land uses in the springshed. We are currently identifying well locations for age-dating sampling.

3.2 INTRODUCTION

This document provides a compilation of our activities investigating the movement of water and solutes through the Silver Springs groundwater system. The focus to date has been on measuring the spatial distribution of water flow and solute flux.

The goals of this work are to provide field-measured hydrogeologic data that can be used for active resource management in the Silver Springs springshed. Specific management questions to be addressed include: What portions of the springshed are most directly linked to the spring outlet? Which portions of the springshed have the shortest-circuit connections of water flow and solute pathways from the land surface to the spring outlet? Which areas are more likely to have little connection to the spring outlet? If management interventions are desired, such as land use modification or restriction, then which portions of the springshed should be targeted? The types of information needed to answer these questions are as follows:

- Recharge of water and solutes (such as nitrate) within the springshed,
- Attenuation of solute leaching through soil and vadose zones, and
- Aquifer flow path lengths, velocities, and solute attenuation through the aquifer.

Each of these processes is heterogeneous and thus must be understood in terms of the spatial distribution throughout the springshed. This work is intended to provide new data about these processes within the Silver Springs springshed to be integrated within a management-decision framework.

The goal of this project is to determine groundwater flow characteristics and natural attenuation rates of N loads in the upper Floridan Aquifer System. Groundwater velocities, ages, nitrate fluxes, and denitrification rates will be measured at a network of wells using a suite of monitoring techniques. The data from this project will be used directly in springshed models.

3.3 SITE DESCRIPTION

Silver Springs with an approximate discharge of 25 m^3 s^{-1} is one of Florida's first magnitude springs and among the largest springs worldwide. Its 2,500 km^2 springshed overlies the mostly unconfined Upper Floridan Aquifer. The aquifer is approximately 100 m thick and predominantly consists of porous, fractured and cavernous limestone, which leads to excellent surface drainage properties (no major stream network other than Silver Springs run) and complex groundwater flow patterns through both rock matrix and fast conduits. Over the past few decades, discharge from Silver Springs has been observed to slowly but continuously decline, while nitrate concentrations in the spring water have enormously increased from a background level of 0.05 mg L^{-1} to over 1 mg L^{-1}. In combination with concurrent increases in algae growth and turbidity, for example, and despite an otherwise relatively stable water quality, this has given rise to concerns about the ecological equilibrium in and near the spring run as well as possible impacts on tourism.

Among the largest remaining uncertainties are the largely unknown geometry and properties of the karst conduit network as well as perhaps the exact shape and size of the springshed. In the case of the karstified Silver Springs aquifer the interplay of slow matrix flow and fast fracture / conduit flow creates highly complex flow and transport conditions.

Groundwater travel times to a stream network are usually exponentially distributed, independent of size, shape and conductivity of the watershed and independent of the stream network geometry. This assumption for karst appears reasonable, since the conduits are so much more conductive as the matrix and travel time along them are so much shorter (as reported from tracer tests). Overall, tracer results (directly injected into fast flow zones) give travel times at the order of months, while the porous models range over several decades. The groundwater age analyses are in the middle, which may again be indicative of the importance of mixing between fast conduit and slow matrix water. So travel time may be exponential in the porous matrix and then something else, but much quicker, in the conduits, which in total would give a bimodal (dual domain) travel time distribution. If we can come up with a travel time model that can accommodate tracer, age dating and porous model results, that would be a first large step forward.

3.4 METHODS

3.4.1 Groundwater Velocity and Nitrate Flux Measurements

In the case of the karstified Silver Springs aquifer the interplay of slow matrix flow and fast fracture / conduit flow creates highly complex flow and transport conditions. Borehole dilution tests were first considered to characterize the groundwater velocity distribution vertically in selected wells. This method is subject to considerable constraints in open-rock boreholes, however. Thus, we preferred to use Passive flux meters (PFMs) for local flux measurements of groundwater, nitrate and its degradation products.

The passive flux meter (Hatfield et al. 2004) simultaneously measures time-averaged water flux, q, and solute mass flux, J, with depth in a flow field in a porous medium. The interior composition consists of a permeable sorbent that can intercept and retain nutrients (or

contaminants) from up-gradient groundwater flow. An appropriate sorbent (e.g., activated carbon, activated alumina, anionic/cationic resin, etc.) can be selected according to the target solute. The sorbent is pre-loaded with known amounts of water-soluble tracers. When the PFM is exposed to groundwater flow, the resident tracers are desorbed and eluted from the sorbent matrix at rates proportional to groundwater flow through the PFM. Since the magnitude of groundwater flow is unknown in the actual application, multiple resident tracers, which have different elution rates, are used. The degree of tracer elution is related to the retardation factor, which can be measured by laboratory column elution or batch sorption/desorption tests (Hatfield et al., 2004). After sufficient exposure to groundwater flow, the PFM is removed from the well and the sorbent is extracted to quantify the nutrients (or contaminants) intercepted and resident tracers remaining. The extracted nutrients and residual tracer mass are used to estimate time-averaged nutrient and water flux, respectively.

Using PFMs, karst flux data becomes available as depth profiles along monitoring wells, which allows a characterization several important features: (1) Vertical heterogeneity of flow and transport as produced by spatial heterogeneity in input sources and aquifer characteristics. This type of information is fundamental for assessing the internal dispersion and mixing behavior of the aquifer as well as for the interpretation of any kind of point measurements. (2) Vertical trends in flow and transport as produced by the large scale boundary conditions of the aquifer. This may help delimiting the hydraulically active upper portion of the aquifer from a possibly stagnant lower part. The size of the active aquifer is directly related to the mean nitrate travel time towards the spring and stagnant parts of the aquifer may act as additional nitrate reservoirs, with nitrate uptake and release by diffusion from / into the active aquifer. (3) The spatial distribution of well averaged groundwater and nitrate fluxes may contribute to identifying larger scale flow, transport and reaction patterns between recharge locations and the spring. Comparing depth averaged fluxes of nitrate and its degradation products, for example, at different distances from the spring allows conclusions about nitrate reaction behavior at the transport scale. (4) Temporal variations in measured fluxes (e.g., between rainy and dry seasons) indicates the temporal variability of aquifer behavior.

In open-rock boreholes we used a modified PFM enclosed in PVC screened pipe. To maximize the nitrate detection capabilities, PFMs were deployed in the wells for approximately 56 days.
Groundwater flux measurements collected in a plane (Figure 3.1) encircling the spring outlet will enable mass balance confirmation of the total groundwater and solute fluxes. The sum of the measured fluxes should equal the discharge from the spring. The heterogeneous measured groundwater fluxes will indicate which parts of the aquifer are contributing more significantly to water and solute discharge.

3.4.2 Groundwater Age

The age of groundwater at the Silver Springs vents and in wells throughout the springshed can provide critical information on spatial contributions of N loads. Groundwater velocity and flow path lengths combine to control travel times.

Once we have a map of travel times (i.e., mean travel time perhaps in combination with another map of travel time variance due to dispersion and / or mean travel time uncertainty), we can combine it with maps of all other relevant information (e.g., land-use / N input) and discretize

the system spatially in one way or another (e.g., group by similar travel time, similar land-use, or both). For example, for simple implementation, we can use matrices of travel time versus land-use for different moments in time and then convolute in space and time to see what comes out of the spring. Capturing the overall tendencies over the past decades is the best that we can do to gain some confidence in future predictions.

Wells are currently being identified for sampling for tritium and chlorofluorocarbon (CFC) analysis. This work is being conducted in close coordination with SJRWMD staff. The samples will be submitted for laboratory analysis externally.

3.5 RESULTS

3.5.1 Borehole Dilution

On August 20, 2015, a borehole dilution test was performed on well M0764 at 48-52 feet depth. Later that day, a second test was initiated in well M0762 at 122-126 feet depth. A third test was performed on September 12, 2015, in well M0762 at 148-152 feet. After this test the BHD device was lost at 173 feet. The data collected from these tests are incomplete but in general they show velocities that are relatively low in the confined aquifer (< 20 cm d^{-1}, Table 3.1). These values are a bit higher than the range measured so far using PFMs. In general, the agreement within a factor of 2 between the two methods is considered reasonable at this stage in the investigations.

3.5.2 Flux Meters

We have deployed PFMs in 14 wells (Figure 3.2) and we have data from nine wells where we have performed PFM measurements. Additionally we are currently analyzing data from another five wells. So far, we have found water flux in all wells to be 4-11 cm d^{-1}. Nitrate flux (mg m^{-2} d^{-1}) was below detection limit in most wells, at low levels (<5) in two wells, M0775 and M0777, and considerably higher in well M0771 (Tables 3.1 to 3.4).

Note that non-detect of nitrate in selected wells is accompanied by non-zero fluxes of other solutes (e.g., phosphate and sulfate). Nitrate flux detection limit estimated mean concentration ~ 0.6 mg L^{-1}.

In the case of the last set of wells (M0771, 72, 73, 78 and 85) we know from SJRWMD monitoring records and our own water samples that these wells have nitrate concentration above 1 mg L^{-1}. We reached consensus on the fact that PFM detection limits was not the problem. We are currently investigating resin sorption/desorption, nitrate transformations in situ, and other analytical issues.

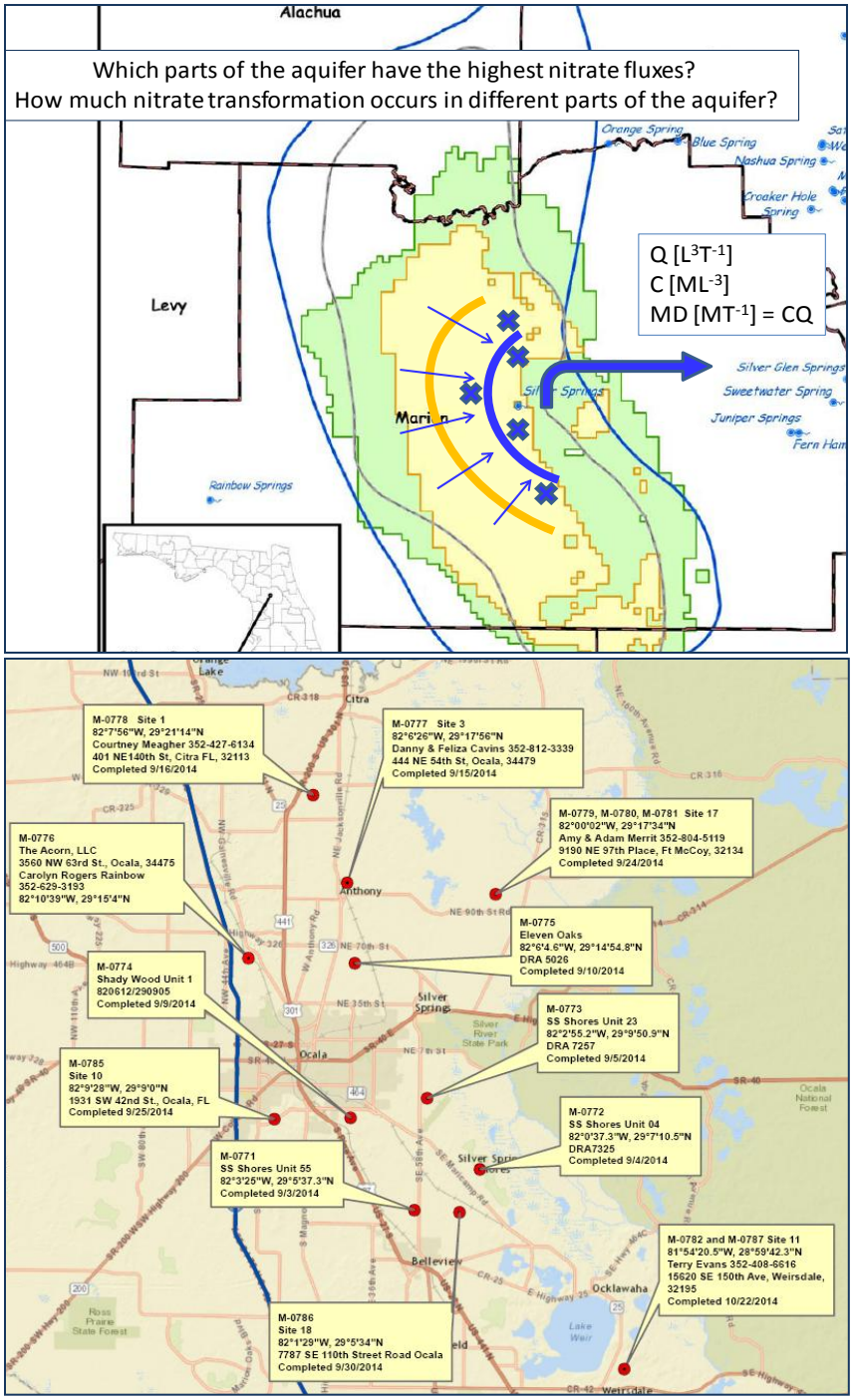

Figure 3.1. (top) Illustration of groundwater flux plane in the Silver Springs springshed, (bottom) selected well locations for flux measurements.

Table 3.1. Borehole dilution test results from Sharpes Ferry wells. Insufficient data were collected from this method for definitive conclusions, but the measured water fluxes were reasonably consistent with values determined from passive flux meters.

Well Name	Date	Depth	Data collection	Collected data points	Data points used in calculations	q (cm d^{-1})
M-0764	20-Aug	48-52	Manual	12	7	29.8
M-0762	20-Aug	122-126	Manual	4	2	18.6
M-0762	12-Sep	148-152	Logged	749	413	13.6

Figure 3.2. Passive flux meter (left) deployment in a well, (middle) sampling, and (right) compact design. Darker sections are activated carbon, lighter section is ion-exchange resin for measuring solute fluxes.

Table 3.2. PFM data from Wells 777 and 775, indicating non-zero sulfate and phosphate fluxes and water fluxes (Darcy velocities) in the range 2.6 – 8.5 cm d^{-1}.

Well_ID	Depth (ft)	Darcy Velocity (cm/day)	NO3 Flux (mg/m^2/day)	PO4 Flux (mg/m^2/day)	SO4 Flux (mg/m^2/day)
M-777	46.5	8.5	0.0	2.8	1.5
M-777	47.9	9.1	0.0	2.4	2.1
M-777	49.1	9.8	0.0	1.3	9.2
M-775	46.5	6.2	0.0	2.8	3.7
M-775	47.9	4.9	0.0	2.9	1.2
M-775	49.1	2.6	0.0	3.2	1.6

Table 3.3. PFM data from Wells 764 and 762, indicating non-zero sulfate and phosphate fluxes and water fluxes (Darcy velocities) in the range 4.7 – 8.7 cm d^{-1}.

Well_ID	Depth (ft)	Darcy Velocity (cm/day)	Br Flux mg/m^2/day	NO3 Flux mg/m^2/day	PO4 Flux mg/m^2/day	SO4 Flux mg/m^2/day
M-764	47.1	5.5	1.0	0	2.3	27
M-764	48.4	6.8	2.0	0	1.6	53
M-764	49.4	8.7	3.8	0	0.8	79
M-762	121.5	5.8	0	0	0	7
M-762	122.9	5.6	0	0	0	8
M-762	124.0	5.9	0	0	0	14
M-762	146.1	5.6	0	0	0	6
M-762	147.3	5.3	0	0	0	6
M-762	148.7	5.0	0	0	0	9
M-762	168.3	6.0	0	0	2.4	5
M-762	169.4	4.8	0	0	1.5	4
M-762	170.7	4.7	0	0	0.8	4

On July 2, 2015, we installed PFMs of compact design in wells M-771,M-073 and M-0785. These will be sampled after 10 day residence time, and two subsequent times 20 and 30 days after. These measurements will provide support for the consistency of our measured water flux values. Also, these will assess whether nitrate shows evidence of *in situ* transformation following sorption on the resins.

Table 3.4. PFM data from Wells 771, 772, 773, 778, 785. PFMs were sub-sampled as top (T), middle (M), and bottom (B). Nitrate flux was detected in 771 at all depths. Water fluxes (Darcy velocities) were found in the range 4.1 – 10.9 cm d^{-1}.

Well_ID	Depth (ft)	Darcy Velocity (cm/day)	NO3 (mg/L as NO3)
771T	67.6	4.8	
771M	68.8	5.0	
771B	70.3	5.0	
771T	68.4		53
771M	69.5		78
771B	71.0		91
772T	44.6	5.8	
772M	45.8	5.3	
772B	47.3	5.7	
772T	45.4		0
772M	46.5		0
772B	48.0		0
773T	42.6	5.3	
773M	43.8	5.5	
773B	45.3	5.6	
773T	43.4		0
773M	44.5		0
773B	46.0		0
778T	50.6	4.9	
778M	51.8	10.9	
778B	53.3	10.6	
778T	51.4		0
778M	52.5		0
778B	54.0		0
785T	85.6	9.5	
785M	86.8	4.8	
785B	88.3	4.1	
785T	86.4		0
785M	87.5		0
785B	89.0		0

3.6 CONCLUSIONS AND RECOMMENDATIONS

Our preliminary conclusions, including brief discussions of future plans are listed below. These conclusions address the primary goals of the project, but we emphasize again here that these conclusions may change as additional information becomes available.

Fewer well sites are available for in situ characterization than was initially believed. Some wells are no longer functional. Some are instrumented for continuous water level recording and thus not accessible. We have identified a suite of candidate wells for our investigations, but the task of well selection has been iterative and continuous.

Groundwater flux (Darcy velocities) measured to date are relatively low. This are indicative of matrix flow through the limestone. The relative contribution of conduit flow to the spring discharge is not known, but is thought to be significant, perhaps dominant. Thus, our next phase will focus on locating and identifying high-flux fractures and conduits in existing wells. Down-hole videos and flowmeters will be used extensively in this phase. Subsequent flux meter deployments will be targeted to these higher-flow zones.

In the well with the highest nitrate concentration that we have found so far, we measured high nitrate flux consistent with the groundwater sampling data. However, in other wells that had lower, but measurable nitrate concentrations, we have not detected nitrate flux. This result is not final because there are some internal inconsistencies, such as non-zero fluxes of other solutes. We are currently conducting field and laboratory assessments to identify whether nitrate is being transformed in the well.

3.7 FUTURE RESEARCH NEEDS

For the next sites for flux measurement, we will use three circular transects around SS for PFM deployment: 2-5 km, 5-8 km, and 8-15 km (Figure 3.3). We will prioritize PFM deployment in wells closer to SS (inner most transect) as we hypothesize that nitrate and water fluxes will increase with proximity to the spring.

The age of groundwater at the Silver Springs vents and in wells throughout the springshed can provide critical information on spatial contributions of N loads. The data acquired through deployment of passive flux meters will identify regions of the aquifer where groundwater age data would provide high value information. The results will provide a measure of local groundwater age distribution with area and groundwater depth to refine our understanding of the travel time from areas of the springshed to the Silver Springs discharge.

Wells are currently being identified for sampling for tritium and CFC analysis. This work is being conducted in close coordination with SJRWMD staff. The samples will be submitted for laboratory analysis externally.

A priority is to locate high-flux zones for both water and nitrate. We are investigating this through existing wells. However, if another recharge area tracer test is conducted, we suggest using flux meters to passively monitor multiple wells between the injection point and the spring. Sequential deployment of approximately 6 PFMs in each well will enable construction of breakthrough curves at multiple locations this will enable quantification of travel time mean and variance, and the spatial distribution of these properties.

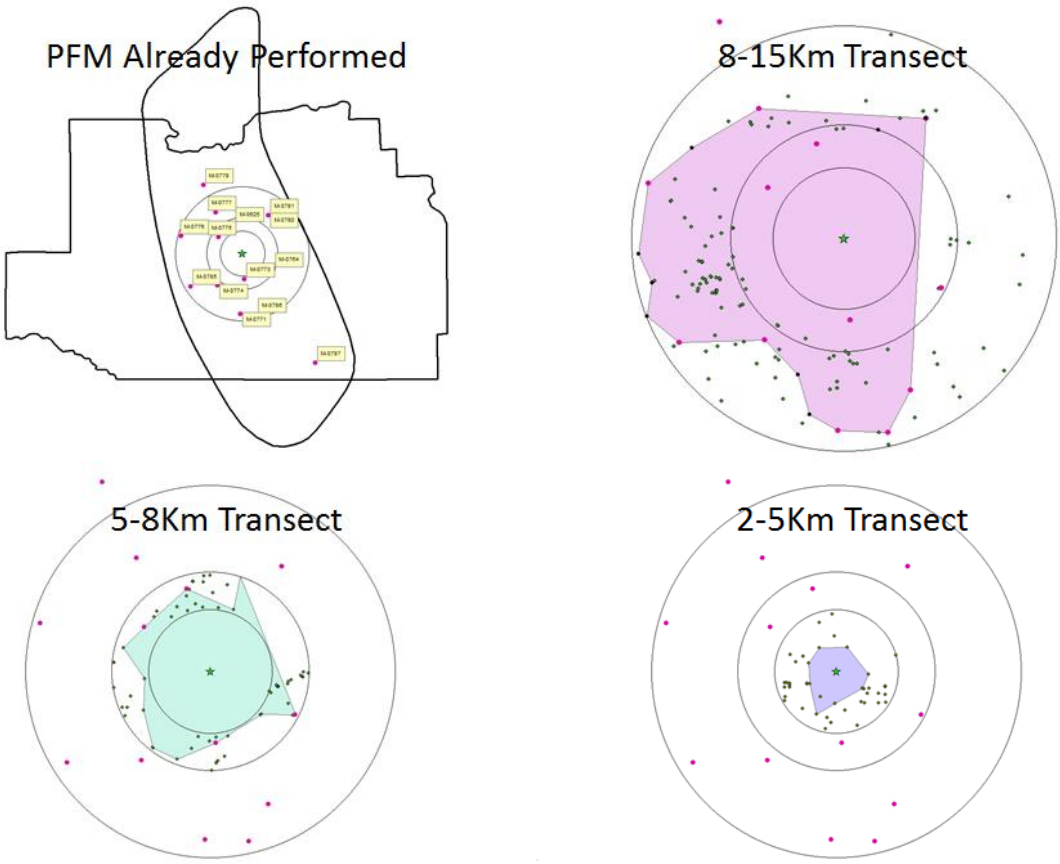

Figure 3.3. Potential well locations for forming transect planes at different distances from the spring.

3.8 REFERENCES

Annable, M.D. et al., 2005. Field-scale evaluation of the passive flux meter for simultaneous measurement of groundwater and contaminant fluxes. *Environmental science & technology*, 39(18): 7194-7201.

Hatfield, K., Annable, M., Cho, J., Rao, P.S.C. and Klammler, H., 2004. A direct passive method for measuring water and contaminant fluxes in porous media. *Journal of Contaminant Hydrology*, 75(3): 155-181.

Kim, Y., J.H. Kim, B.H. Son, S.W. Oa. 2005. A single well push-pull test method for in situ determination of denitrification rates in a nitrate-contaminated groundwater aquifer. *Water Science and Technology*, 52(8), 77-86.

Klammler, H., M.A. Newman, E. Szilágyi, J.C. Padowski, K. Hatfield, J.W. Jawitz, M.D. Annable. 2007. Initial Test Results for a Passive Surface Water Fluxmeter to Measure Cumulative Water and Solute Mass Fluxes. *Environmental Science & Technology*, 41:2485-2490.

Padowski, J.C., E.A. Rothfus, J.W. Jawitz, H. Klammler, K. Hatfield, M.D. Annable. Effect of Passive Surface Water Flux Meter Design on Water and Solute Mass Flux Estimates. *Journal of Hydrologic Engineering*, 2009, 14(12), 1334-1342.

SJRWMD, 2006. Fifty-Year Retrospective Study of the Ecology of Silver Springs, Florida. Special Publication SJ2007-SP4, SJRWMD.

SJRWMD, 2011. Silver Springs Nutrient Pathway Characterization Project. Final Report, Florida Department of Environmental Protection.

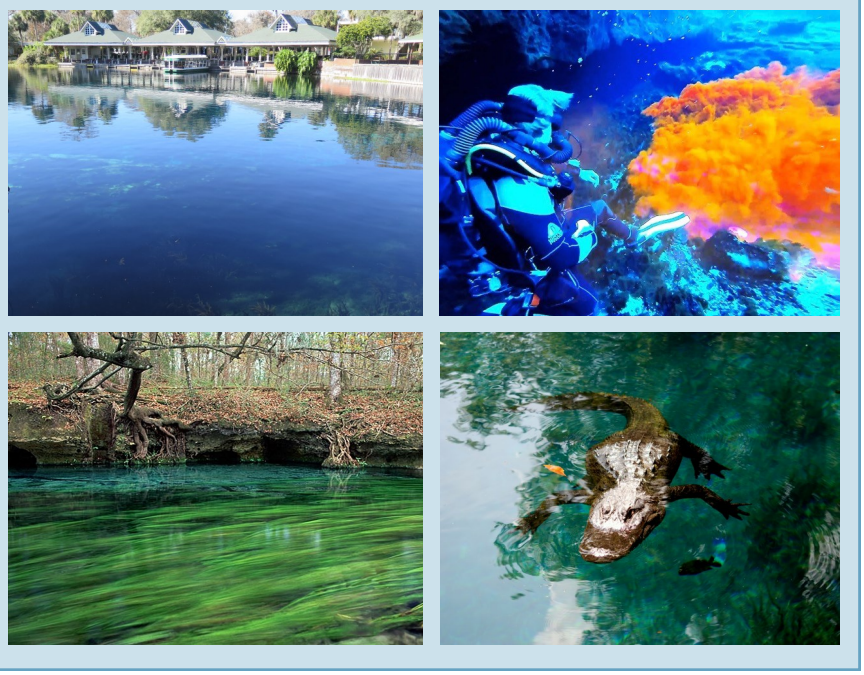

Collaborative Research Initiative on
Sustainability and Protection of Springs [**CRISPS]**

Section 4

[Work Order No: 1]

ANNUAL REPORT

July 2015

submitted to:

St. Johns River Water Management District
Springs Protection Initiative [SPI], UF Contract # 27789

UF | UNIVERSITY of FLORIDA
Water Institute

C R I S P S

Section 4

NITROGEN BIOGEOCHEMISTRY

Sources, Transformations and Loss of Nitrogen from Land Surface to Springs

Annual Report 2015
Work Order No. 1

Principal Investigators:

Patrick W. Inglett, University of Florida
Dean Dobberfuhl, St. Johns River Water Management District

Project Team:
Patrick Inglett
Xiaolin Liao, Post Doc. Associate
Katelyn Foster, Graduate Student
Soil and Water Science Department
University of Florida

Dean Dobberfuhl
Andy Canion
Philip Benson
St. Johns River Water Management District

This document reports interim progress of a work order in the first year of a 3-year project in compliance with Agreement between University of Florida (UF) and St. Johns River Water Management District (SJRWMD) UF Contract #27789. It is part of the *UF Collaborative Research Initiative on Springs Protection and Sustainability (CRISPS)* and supports the science component of *the SJRWMD Springs Protection Initiative (SPI).*

4-i PROLOGUE

This portion of the project is tasked with tracing nitrogen from sources within the springshed through the vadose zone and aquifer to discharge at the spring vent. Three main approaches are used to reach this objective. First nitrogen sources and attenuation in the surface system is assessed through analysis of nutrient composition and rates of denitrification in soil and vadose zone profiles. Second, groundwater composition of nutrients, stable isotopes of nitrate, and dissolved gases are monitored in wells throughout the springshed to assess large-scale patterns of denitrification within the aquifer and determine the potential pathways involved. Lastly, stable isotopes of nitrate and dissolved gases are monitored seasonally at the spring vents to determine the overall potential for denitrification within the aquifer as well as any seasonality which may be taking place.

Results from the first year of work indicate that there is potential for denitrification during transit from surface soils to spring vents. Surface soils are the most significant sink for nitrate, however buried layers of relic peat and marine deposits demonstrate the potential for high rates of denitrification in surficial aquifers and areas where deep, more marine-based ground water mixes with surficial aquifers. Patterns of stable isotopes as well as dissolved gases show promise as potential indicators of denitrification in the subsurface. Patterns of stable isotopes of nitrate observed in soil/vadose zone profiles thus far indicate that caution must be used before attributing groundwater isotopic signatures to surface land use nitrogen inputs.

Future work will continue monitoring for seasonal patterns and better establishment of spatial processes within the springshed. Statistical analysis of dissolved gases and denitrification indicators with groundwater geochemistry will better identify specific zones in the springshed with high potential for denitrification. Additional soil-based work will derive a relationship for surface nitrogen attenuation through denitrification based on nitrogen loading level, moisture content, and temperature. Measurements of boron isotopes will be applied to help identify and disentangle nitrate isotopic signatures in groundwater where manure and sewage inputs are likely. Noble gas composition as well as age dating of ground waters will also assist in determining the proportion of nitrogen exiting the spring vent that has been denitrified, as well as facilitate understanding of hydrologic flow path for calculation of nitrate transport in the aquifer and identification of denitrification hotspots, particularly those involving mixing of deep, older groundwater.

Section 4.1 Characterization of N Sources and Denitrification in Soils of Various Land Uses

4.1.1 ABSTRACT

This report summarizes progress to date of an integrated UF/SJRWMD project. Broadly, the workgroup is tasked with estimating terrestrial nutrient loading, attenuation through the soil and subsoil profile, and the potential for attenuation in the Upper Floridan Aquifer. Profiles of the soil/subsoil of several key land uses were obtained while drilling 12 experimental wells in the Silver Springs spring shed. The samples have been characterized using a range of parameters including total and extractable nutrients (carbon, nitrogen, phosphorus, and selected metals), redox potential, denitrification enzyme assay (DEA), and stable isotopic patterns of soil nitrogen and extractable nitrate. For most of the profiles obtained, there are three main layers or strata including a surface sand overlying clays (sometimes mixed with sand and potentially calcareous and mottled with iron) which is then over the bedrock limestone. Surficial aquifers or situations where the water table is above the clay confining unit were observed at two locations, and at one location buried peat and relic marine horizons were observed. Nitrogen distributions consisted primarily of two main patterns with one group (likely soils with low nitrogen loading) exhibiting high extractable nitrogen in the surface layers (where organic matter was concentrated), and another group (likely soils with higher nitrogen status) exhibiting the lowest rates of extractable nitrogen in the upper surface and increasing nitrogen levels at depth.

In general, significant DEA activity was only observed in the surface 0 to 3 m with occasional but very low rates observed in deeper profile layers. One notable exception to this rule was the site with buried peat and relic marine horizons which exhibited strong denitrification potential at depths of over 12 m. Denitrification activity was occasionally limited by carbon, but most often was limited by nitrate concentrations. Correlations were thus observed with nitrogen parameters, and the most variability explained by total extractable nitrogen. Stable isotopic profiles support the patterns of denitrification and indicate a potential for using isotopic ratios to track nitrogen sources in the spring shed. However, in many cases surface isotopic ratios were not reflected in the groundwater indicating transport of other nitrogen sources or physical processes affecting nitrate transport through the profile.

4.1.2 INTRODUCTION

4.1.2.1 Project Overview and Background

Florida's springs ecosystems are economically and culturally valuable resources. The majority of Florida's springs are surface expressions of the underlying Floridan aquifer, and therefore serve as recorders of changes in groundwater recharge and quality. Water quality and ecosystem health in springs is tightly linked to point source and diffuse inputs of mobile pollutants to the land surface and, eventually, the groundwater within the watershed of the spring system. This link between land use and spring water quality is especially critical in karst areas where there is little overburden to separate the land surface and aquifer.

The Silver Springs System (Marion County, FL) is the largest spring system in the St. Johns River Water Management District (SJRWMD). Elevated nitrate concentration in the spring discharge is considered a primary factor that has contributed to an increase in algal mat cover and ecosystem degradation in the Silver River (Quinlan et al. 2008). The concentration of nitrate in Silver Springs has increased from less than 0.05 mg L^{-1} NO_3-N in the early 1900s to the present day concentration of 1.2 mg L^{-1} (Figure 4.1.1). Nitrate concentrations currently exceed the numeric nutrient criteria of 0.35 mg L^{-1} (F.A.C., 2013) set for Silver Springs. This observed increase in nitrate concentration is linked to intensified land use activities that contribute nitrogen to the groundwater within the watershed, or springshed, of the spring system (Figure 4.1.2, Munch et al. 2007).

Naturally occurring attenuation processes retain or remove a considerable portion of the nitrogen that is loaded on the land surface in the springshed. Attenuation in the soil may include plant uptake and immobilization, or N may be removed completely by the conversion of nitrate into gaseous N through denitrification. Further removal of nitrogen may be accomplished by denitrification within the Floridan Aquifer System (FAS) after it has passed through the unsaturated zone (Heffernan et al. 2012).

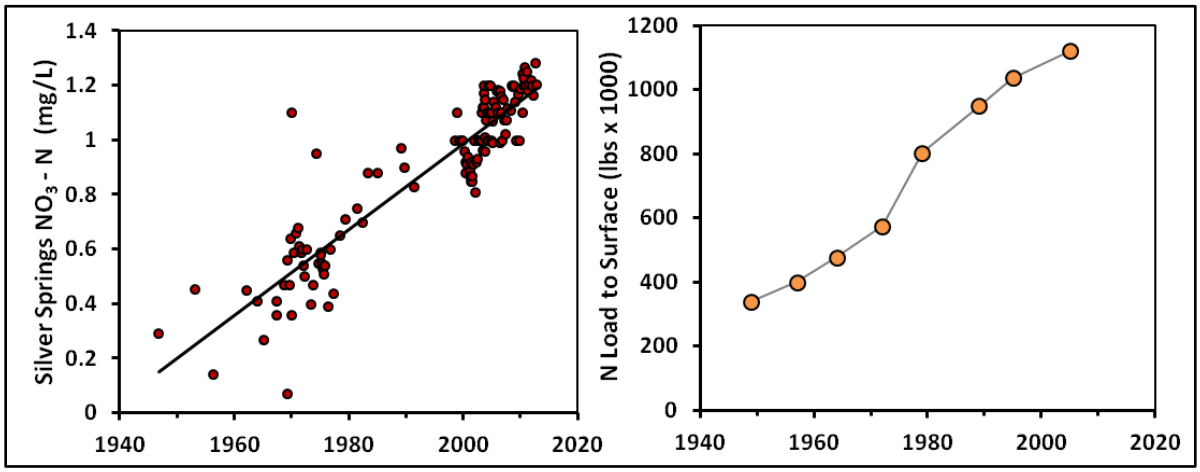

Figure 4.1.1 Trends in nitrate concentration and nitrogen loading in the Silver Springs springshed. Nitrogen loads were estimated for the 2-year capture zone of the spring. Data are reproduced from the report of Munch et al. 2007.

The extent to which nitrogen sources are attenuated between land surface and the aquifer depends on the nitrogen source, transit time to the groundwater, and soil processes. Attenuation can be estimated as a simple coefficient using literature values of attenuation for similar nitrogen sources (Katz et al. 2009). However, spatial variability in groundwater recharge, soil processes, and hydrostratigraphic features (e.g., presence of a confining unit) are not accounted for using this approach and may exert a stronger control on nitrogen attenuation than the source of nitrogen. Intrinsic aquifer vulnerability models do take into account recharge and soil processes, but do not account for surface loads or fate and transport (Aller et al. 1987; Arthur et al. 2007). Specific groundwater vulnerability assessments account for nitrogen loading in addition to

intrinsic vulnerability parameters and are a more informative approach for prudent management decisions.

In addition to assessing the vulnerability of the aquifer to land surface loads, determining the potential for denitrification in the Floridan aquifer will be informative with respect to the timescale of recovery of nitrate concentrations in Silver Springs. Legacy nitrogen that remains in the aquifer from previous land use activities may continue to impact the spring for many years after loads have been mitigated. However, if this legacy nitrogen takes long enough to reach the spring, then even slow denitrification rates have the potential to remove a considerable portion of the legacy nitrogen.

4.1.2.2 Workgroup Objectives and Deliverables

Planning of restoration projects in the Silver Springs springshed requires a detailed understanding of the spatial patterns on nitrogen loading, the potential for nitrogen attenuation, and current groundwater impacts. Integration of these components will allow for the identification of both where there are groundwater impacts and where there is potential for remediation of the impacts. The overall goal of the workgroup at SJRWMD is to identify these areas of the springshed where high nitrogen loading and low nitrogen attenuation overlap. The following objectives are defined to accomplish this goal:

1. Identify nitrogen sources and rates of loading within the springshed boundary.

2. Estimate attenuation of nitrogen between the land surface and the Upper Floridan Aquifer.

3. Verify that areas of the springshed with high N loads and low attenuation show elevated N concentrations in groundwater.

Deliverables for these objectives are outlined below. This report contains deliverables 5 and 6.

1. A springshed nitrogen inventory, in the form of a GIS layer, that will show the cumulative N load to land surface from diffuse and point source N inputs. (SJR)

2. An analysis of status and trends of N concentrations from all available groundwater monitoring data. (SJR)

3. A spatial statistical analysis to identify the environmental parameters that are the best predictors of elevated N in groundwater wells. (SJR)

4. A model for estimating attenuation between the land surface and Upper Floridan Aquifer. The model output will be used in the groundwater fate and transport model. (SJR)

5. Measure denitrification potential in surficial soils and vadose matrix. (UF)

6. Analyze solid phase materials for biogeochemically relevant constituents and stable isotopes. (UF)

7. Sample selected wells for stable isotopes and gasses to investigate contaminant sources and potential for denitrification in the FAS. (UF).

4.1.2.2 Background – UF Contribution

Springs protection and restoration requires an interagency effort to implement practices for managing N loads, and central to this effort is an understanding of the transport and transformation of N from land surface to aquifer. The rate of N (primarily nitrate) leaching from the soil layer may be slowed by plant uptake and immobilization, or N may be removed completely by the conversion of nitrate into gaseous N through denitrification. The attenuation of N by these processes can be estimated by land-use specific attenuation coefficients in order to more accurately predict N loading to the aquifer at the springshed scale (Katz et al. 2009). However, there is still considerable uncertainty in this approach because it does not account for spatial and temporal variability in local surface hydrology, soil processes, and hydrostratigraphic features (e.g., presence of confining units). Constructing models that account for these aforementioned landscape features to estimate the attenuation of N in a spatially explicit manner will improve targeting of mitigation efforts in areas that experience high N loading and low natural attenuation.

Sources of nitrogen in groundwater systems are frequently inferred based on the isotopic composition of nitrate (Fogg et al. 1998) where various N sources have distinct isotopic composition ranges in $\delta^{15}N$ and $\delta^{18}O$ (Kendall and McDonnel 1999). Based on changes in groundwater nitrate isotopic composition, it is also possible to infer and calculate denitrification and other N loss processes, but with the caveat that isotopic composition of nitrate sources is known (Xue et al. 2009). For this reason, accurate spatial measurements of nitrate isotopic composition within the watershed are required to adequately separate transformation and mixing processes of nitrogen in groundwater systems.

In addition to N source (e.g., organic N, fertilizer), soil processes (such as nitrification and denitrification) can directly affect the isotopic composition of leached NO_3-N. Therefore, it is required that signatures of surface N from various land uses be accurately related to the isotopic signature of N leaching from various systems in the Silver Spring springshed. Soil processes and conditions are thus a key to understanding the identification of sources and attenuation of nitrogen prior to input into the FAS.

The ability of a soil to support denitrification largely depends on soil conditions such as moisture content affecting oxygen status, availability of carbon fuel denitrifying microbial populations, and levels of nitrate (Smith and Tiedje 1979). Many of these parameters are highly temporal or seasonal in nature depending on rainfall levels and management practices (fertilizer applications, etc.). For this reason, models of N attenuation in the soil zone should be effectively parameterized to capture the diversity of N levels and the soil conditions affecting denitrification-based N attenuation in the Silver Springs springshed.

In support of the St. John's River Water Management District's efforts in Springs Protection, the overall goal of this project is to determine the capacity for natural attenuation of land surface N loads in the soil, vadose zone, and upper FAS and identify potential sources of other nutrient/geochemical constituents which may influence biota in springs. The approach of this work is to characterize patterns of N forms and other nutrients in relation to microbial composition and denitrification activity in vertical profiles of soil and geologic strata in the major land uses of the Silver Springs springshed.

4.1.3 Materials and Methods

4.1.3.1 Site Description and Sampling

The Silver Springs springshed covers more than 230,000 ha in north-central Florida, occurring primarily in the counties of Alachua and Marion (Phelps 2004). The climate of the region (measured at Ocala, FL) is humid sub-tropical with a warm wet season (June-October) and a cool dry season (November-May). Approximately 51 inches of rainfall occurs annually and the mean annual temperature is approximately 22°C (http://www.usclimatedata.com/).

Twelve sites were selected representing the major land uses within the springshed (Figure 4.1.1). Soils and geologic strata were sampled from each of these locations with the installation of water sampling wells during the period of September and October 2014. Well drilling was conducted using a standard geotechnical rig by Huss Drilling, Inc. (Dade City, FL). The approach utilized a 6 inch auger to develop the main borehole with subsequent sampling at defined intervals using a 2 inch diameter, 2 feet in length split-spoon core sampler. Photographs were recorded for each spoon section, and as unique soils indicators or geologic features were encountered (based on color and textural discontinuities), samples were collected from the split spoon sampler for further analysis of nutrients and microbial activity.

Samples for analysis of denitrifying enzyme activity (DEA) and extractable and total nutrients were collected into polyethylene bags and stored on ice, while separate samples for microbial community analysis were collected into sterile whirl Pak sampling bags using sterile techniques (sterilizing with ethanol between samples and collecting sample from only the central portion of the core) and placed on dry ice. Samples for DEA and nutrients were stored inside airtight containers at 4°C until analyzed while frozen samples for molecular analysis were stored on dry ice until they could be shipped for analysis.

Fresh soils were used to measure redox potential, water extractable nutrients and DEA. A portion of soil samples was oven dried at 105°C for 3 days to determine moisture content and ground using a mortar and pestle and total nutrient determinations. Another subsample of sieved soil was air dried and ground using a mortar and pestle for Mehlich-3 extractable P, Fe, Al, Ca, and Mg.

4.1.3.2 Redox and Nutrient Parameters

Redox potential was measured using a commercial platinum wire redox electrode (Thermo Fisher Scientific #1363982) relative to a Calomel reference electrode (Thermo Fisher Scientific accumet #13620258) both electrodes were calibrated using standardized solution (Ricca Chemical, R5464500-550C) and results expressed as millivolts relative to standard hydrogen electrode.

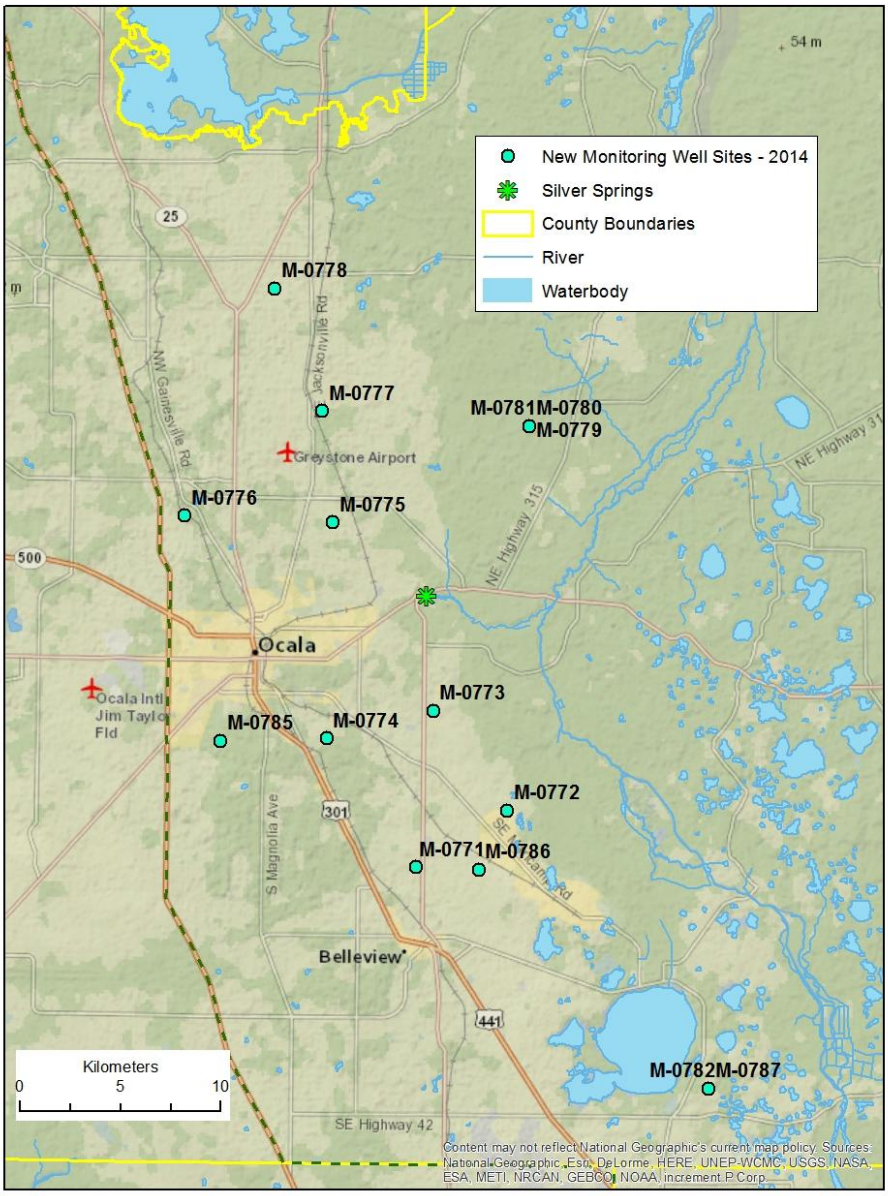

Figure 4.1.2. Locations, IDs, and drilling dates of the wells installed for the project and used for collection of soil and vadose zone profile materials.

Table 4.1.1. Land use description and well depth for the project wells in the Silver Springs springshed.

Well ID	Depth (feet)	Depth (m)	Major Land use
M-0771	56	17	Retention pond, golf course, septic
M-0772	35	11	Retention pond, medium density residential
M-0773	42	13	Septic
M-0774	95	29	Septic
M-0775	52	16	Hay, low density residential, septic
M-0776	50	15	Hay, horse farm
M-0777	60	18	Agriculture, hay, horse farm
M-0778	60	18	Agriculture, improved pasture
M-0779	145	44	Pine plantation
M-0780	69	21	
M-0781	35	11	
M-0785	90	27	
M-0786	42	13	Spray field, sewage treatment
M-0782	195	59	Improved pasture, nursery
M-0787	102	31	

Field moist materials were extracted with DI water (1:10, soil: water ratio) for determination of water extractable NO_3, NH_4^+, TN, and TOC. Mehlich-3 extraction of P, Ca, Mg, Fe, and Al was performed by the Analytical research Laboratory of the Soil and water Science Department at UF.

Loss on ignition (LOI) was obtained by combusting 0.2 g dry soil at 550°C for 4 h. Soil total C and N (TC and TN) content were measured using Thermo Flash EA 1112 elemental analyzer (CE Elantech, Inc.). Soil total P (TP) was measured colorimetrically using a Shimadzu UV-160 spectrometer (method 365.1 U.S. EPA 1993) following ashing and dissolution in 6N HCl (Anderson, 1976). Extractable ammonium (Ext. NH_4-N) and nitrate (Ext. NO_3-N) were determined in DDI extracts using methods 350.1 and 353.2, respectively (USEPA, 1993) by a discrete analyzer (AQ2, Seal Analytical, Mequon, WI, USA). Soil extracts were also measured for soluble reactive P directly and for total dissolved P following autoclave persulfate digestion using Shimadzu UV-160 spectrophotometer (method 365.1 U.S. EPA 1993).

4.1.3.3 Denitrification Enzyme Activity

Soil profiles materials covering the range of depths and textures were selected to measure denitrification enzyme activities in profiles. The method was modified from Smith and Tiedje (1979), using the acetylene block technique. Samples were amended with NO_3-N, chloramphenicol, and acetylene, and were incubated under anaerobic conditions at room

temperature (~23°C) with or without glucose added. Headspace gas was collected at 6, 24, 48, and 72 hours. The potential denitrification rate was calculated from the steepest portion of curve produced when cumulative N_2O evolution was plotted against time.

Concentration of N_2O in the headspace gas was determined with a Shimadzu GC-14A gas chromatograph equipped with an electron capture detector (ECD) and Porapak Q column. The operation temperatures for the column, injection port, and detector were 70, 120, and 230°C, respectively. A 10 ppm standard N_2O gas (Scott Specialty Gases, Inc., Plumsteadville, PA) was used to calibrate the measurement, and results were reported as nmols N_2O per gram dry weight per hour (nmols $N_2O\ g^{-1}\ dw\ h^{-1}$).

4.1.3.4 Statistical Analysis

Data were analyzed with JMP v.8© statistical software (SAS Institute Inc., Cary, NC). Spearman rank correlation coefficients were computed to evaluate the relationship between different N parameters and moisture content. Spearman rank correlation does not assume variables are normally distributed (Sokal and Rohlf, 1995).

4.1.4 Results and Discussion

4.1.4.1 Profile Characteristics

Table 4.1.1 shows the land use based on Florida Land Cover Classification System (FLUCCS) for the well sites used in the study. The collection of samples during installation of the wells in these land uses revealed a wide diversity of soil and geologic materials in the vadose zone of the springshed (Figures 4.1.3-4.1.4). The layers were typical of the widely established geologic profiles of the region with sands overlying various thicknesses of undifferentiated sediments and units of the Hawthorn layer overlying Ocala limestone (Scott 1988; Scott et al. 2001).

Where present, clay layers were generally thin (2-3 m) with one exception being the almost continuous clay layer (> 40 m) encountered at the site of M-0782/0787 (Figures 4.1.4 and 4.1.5l). It is difficult to distinguish whether these clay layers represent the Hawthorn layer, but several of these heavy clay samples exhibited greenish or pale gray colors commonly attributed to this unit (Scott 1988). Apart from texture (clay vs sand), the most prominent feature of the samples was reddish colors indicating the presence of extensive amounts of oxidized iron (Figures 4.1.5a-l).

In general, lowest redox potentials were encountered in the surface soils (0-1.8 m) or deep in the profile, while highest redox potentials were measured in intermediate layers with high clay content (Figure 4.1.6). In the site M-0779/0780/0781, the redox potential reached as low as -186 mV at the depth of 9.1-9.8 m (Figure 4.1.6). For most of the soil profile redox potential should indicate the dominant electron acceptor being used by microbial respiration, where highly

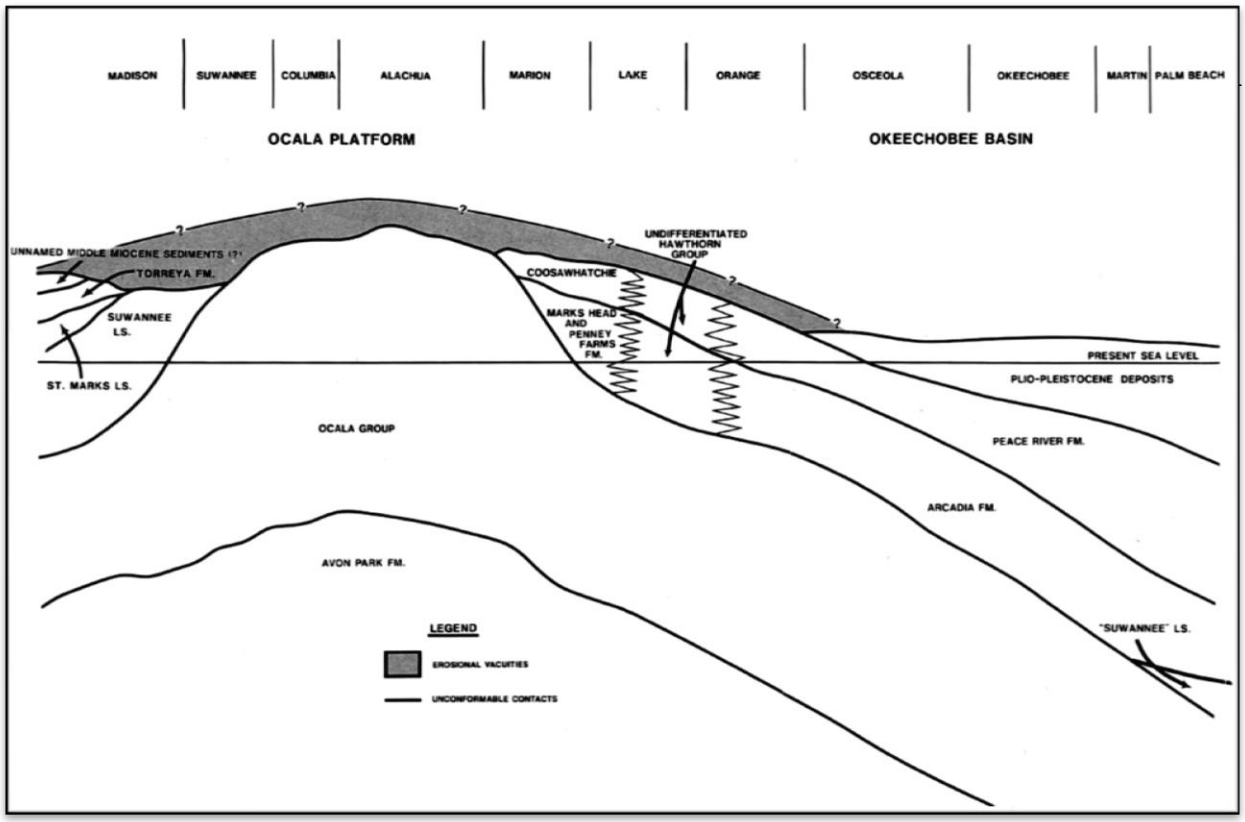

Figure 4.1.3. Vertical cross section of lithographic units encountered in the study area crossing Alachua, Marion, and Lake countries (from Scott 1988).

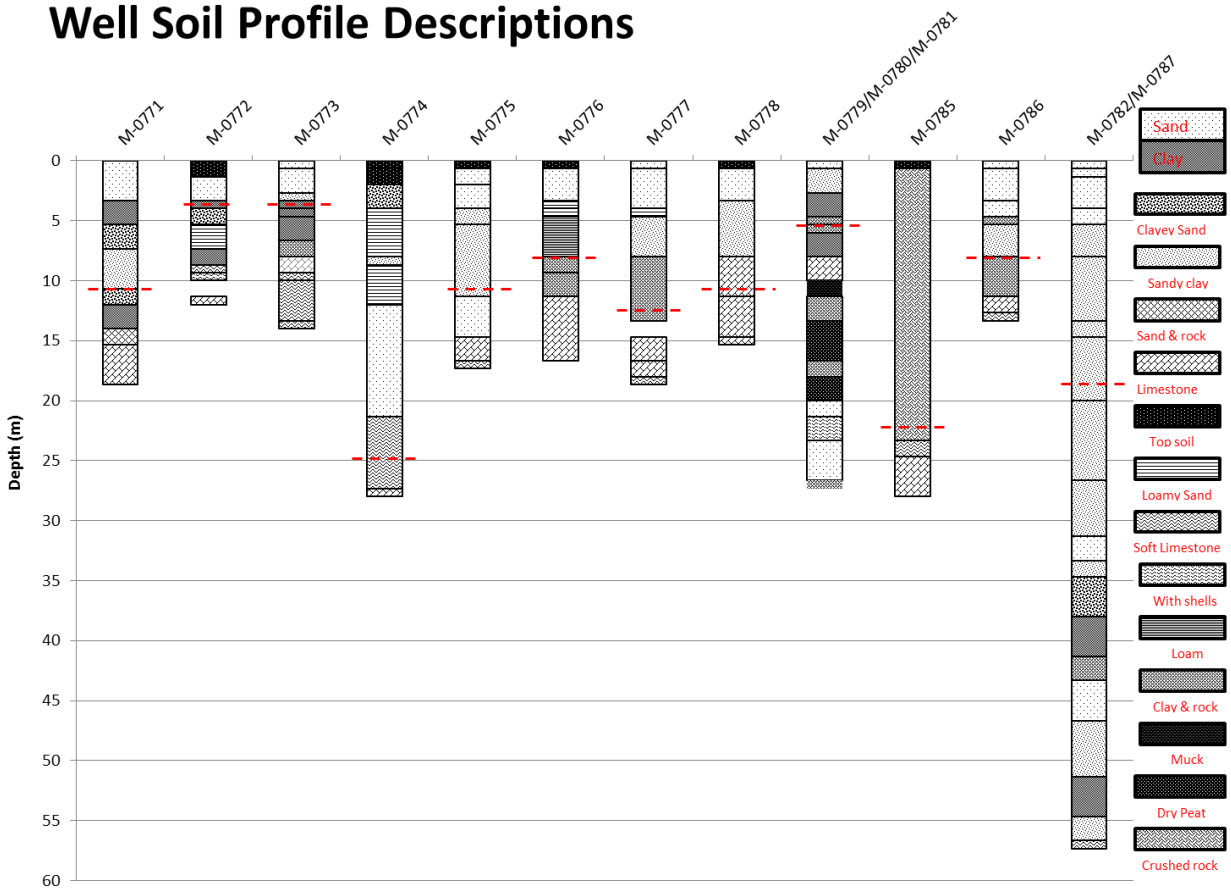

Figure 4.1.4. Vertical patterns of soil and vadose zone materials encountered during installation of study wells in the Silver Springs springshed.

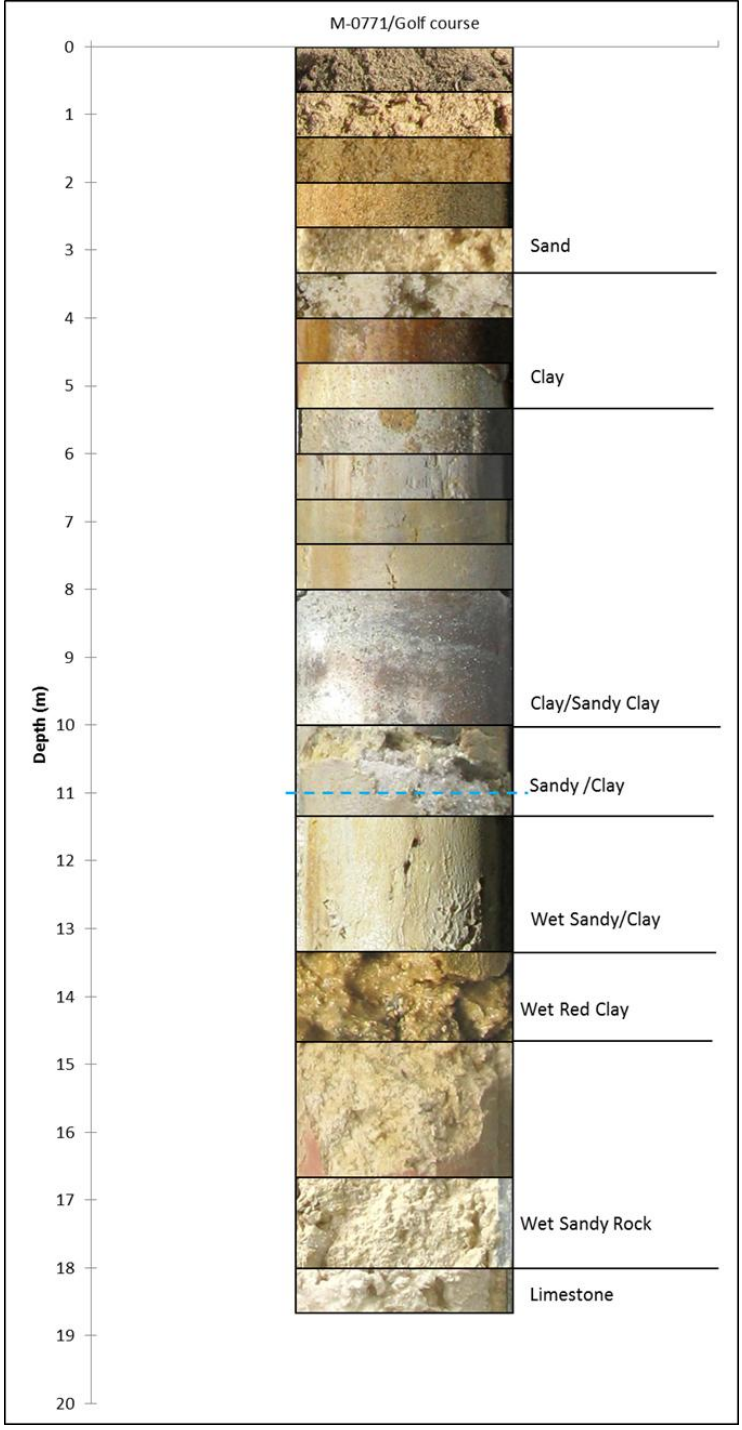

Figure 4.1.5a. Composited images of soil and vadose zone materials encountered during installation of study well M-0771 in the Silver Springs springshed.

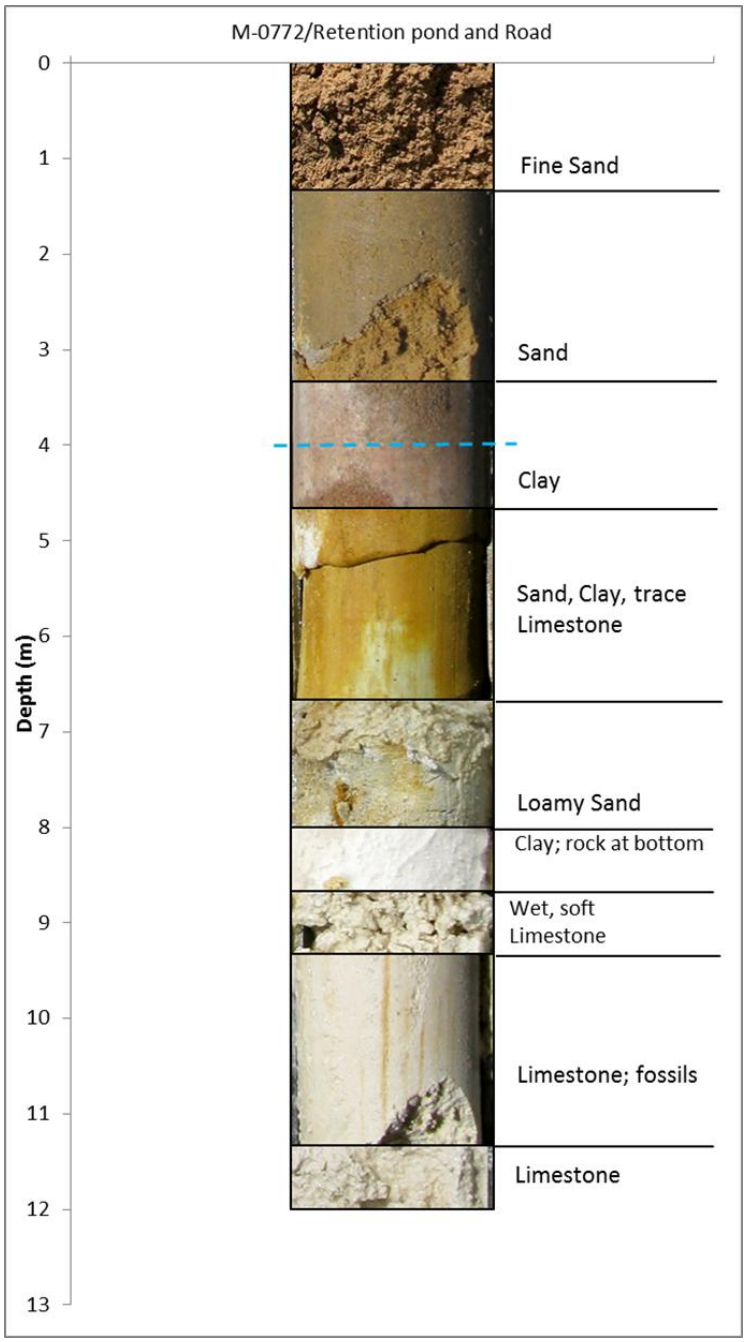

Figure 4.1.5b. Composited images of soil and vadose zone materials encountered during installation of study well M-0772 in the Silver Springs springshed.

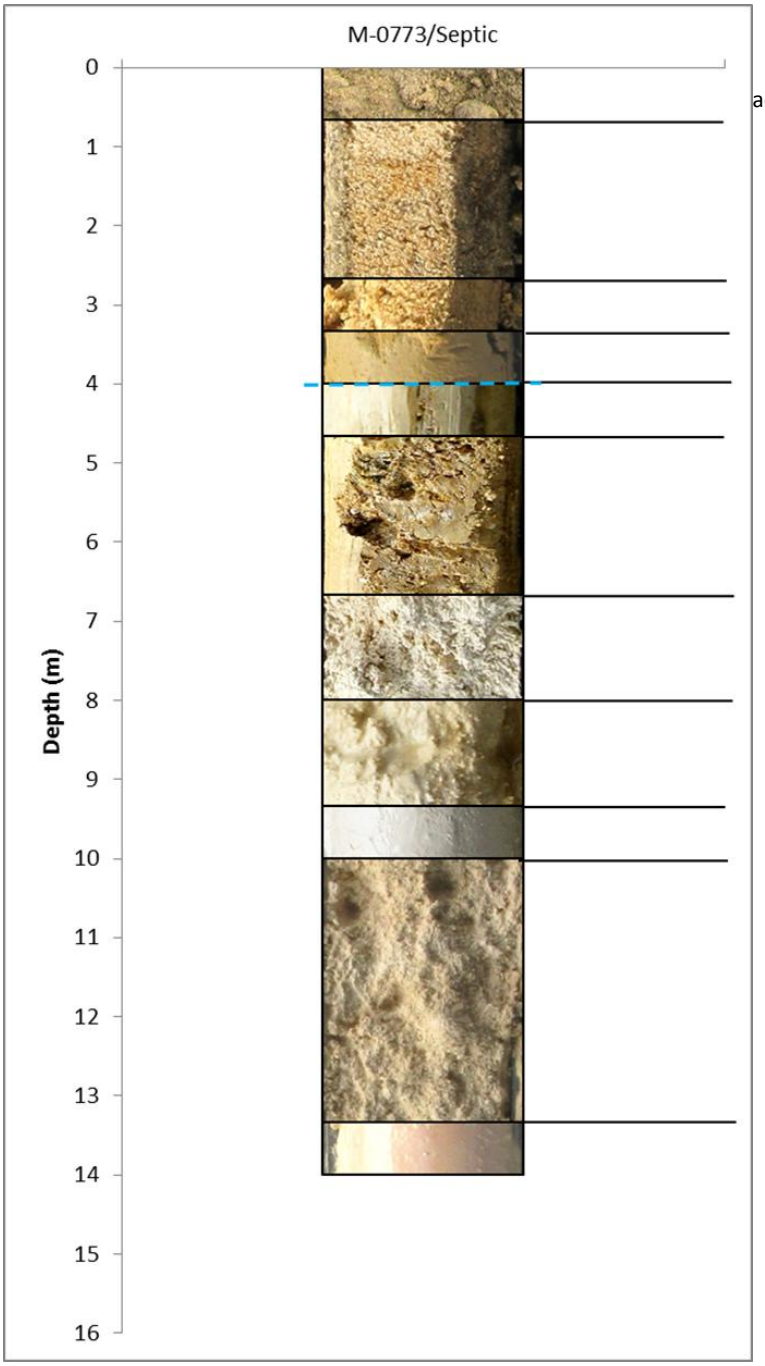

Figure 4.1.5c. Composited images of soil and vadose zone materials encountered during installation of study well at the well M-0773 in the Silver Springs springshed.

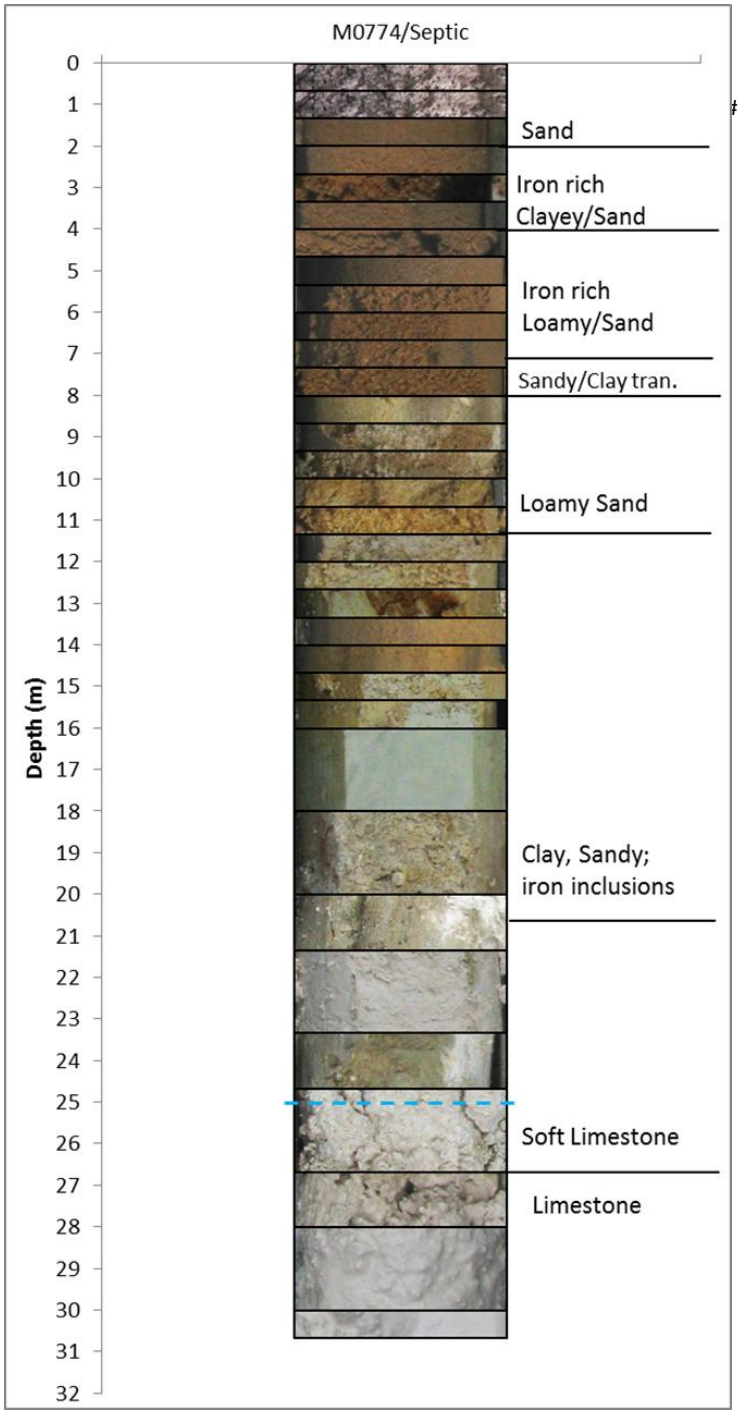

Figure 4.1.5d. Composited images of soil and vadose zone materials encountered during installation of study well M-0774 in the Silver Springs springshed.

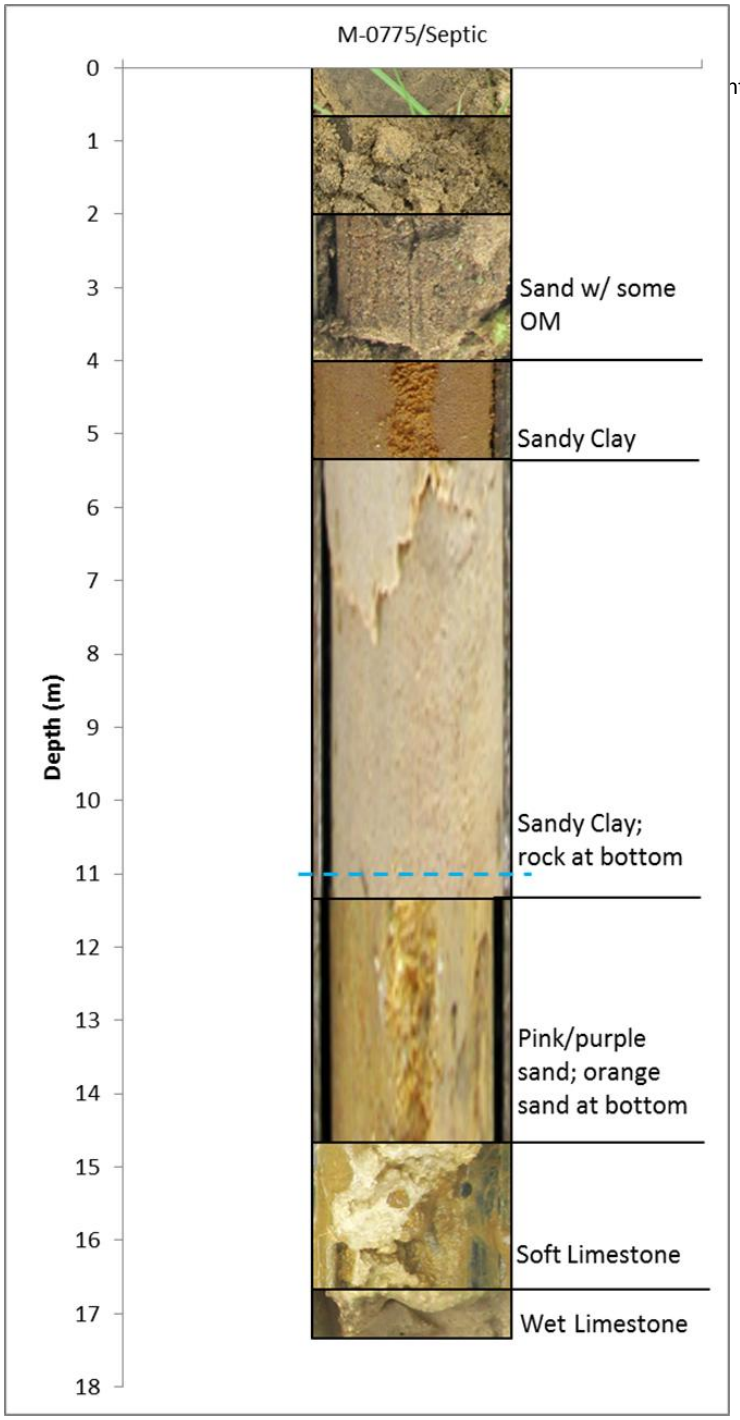

Figure 4.1.5e. Composited images of soil and vadose zone materials encountered during installation of study well M-0775 in the Silver Springs springshed.

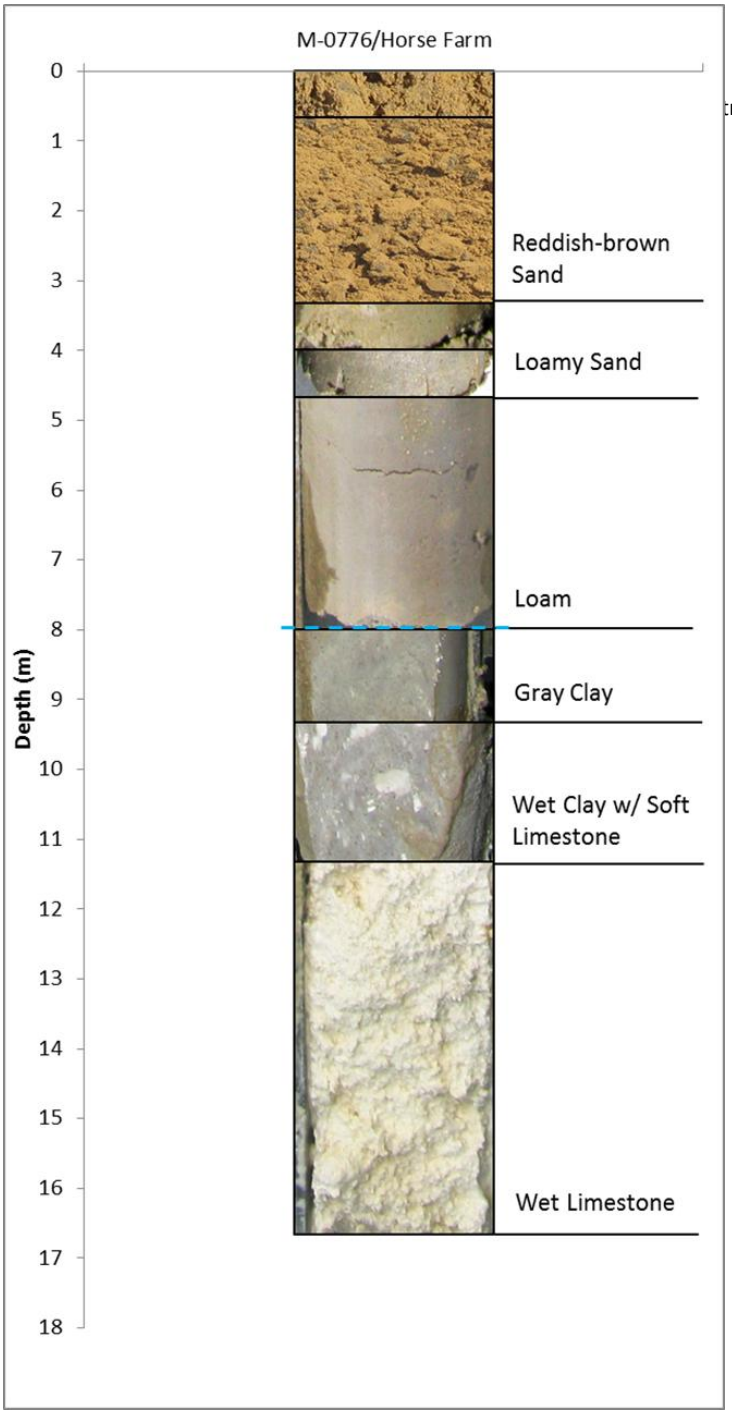

Figure 4.1.5f. Composited images of soil and vadose zone materials encountered during installation of study well M-0776 in the Silver Springs springshed.

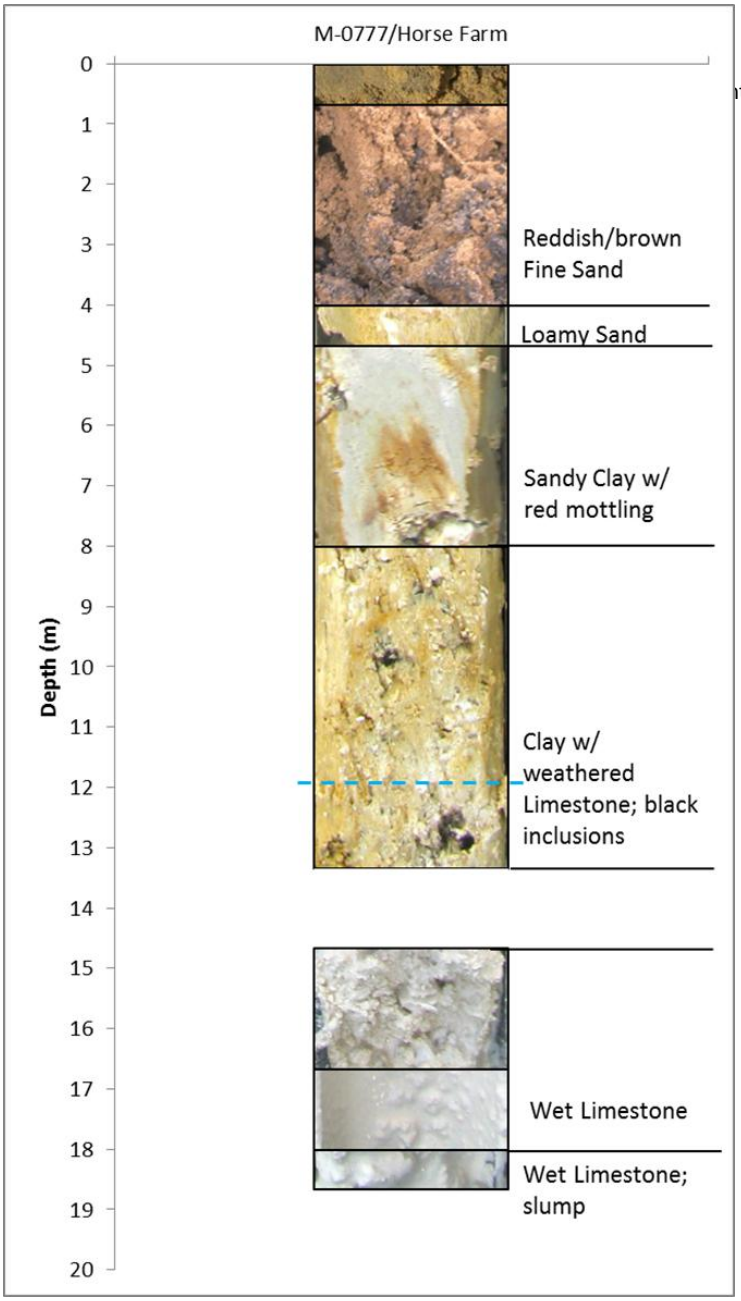

Figure 4.1.5g. Composited images of soil and vadose zone materials encountered during installation of study well M-0777 in the Silver Springs springshed.

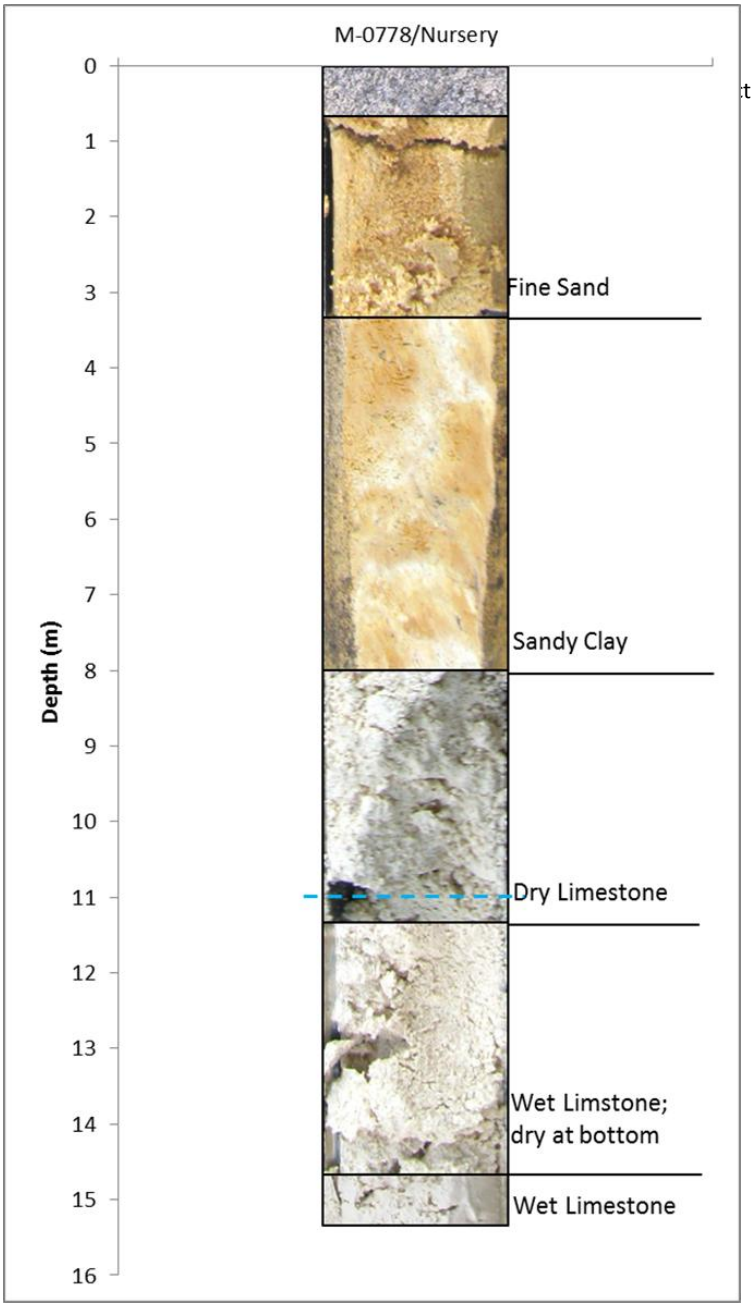

Figure 4.1.5h. Composited images of soil and vadose zone materials encountered during installation of study well M-0778 in the Silver Springs springshed.

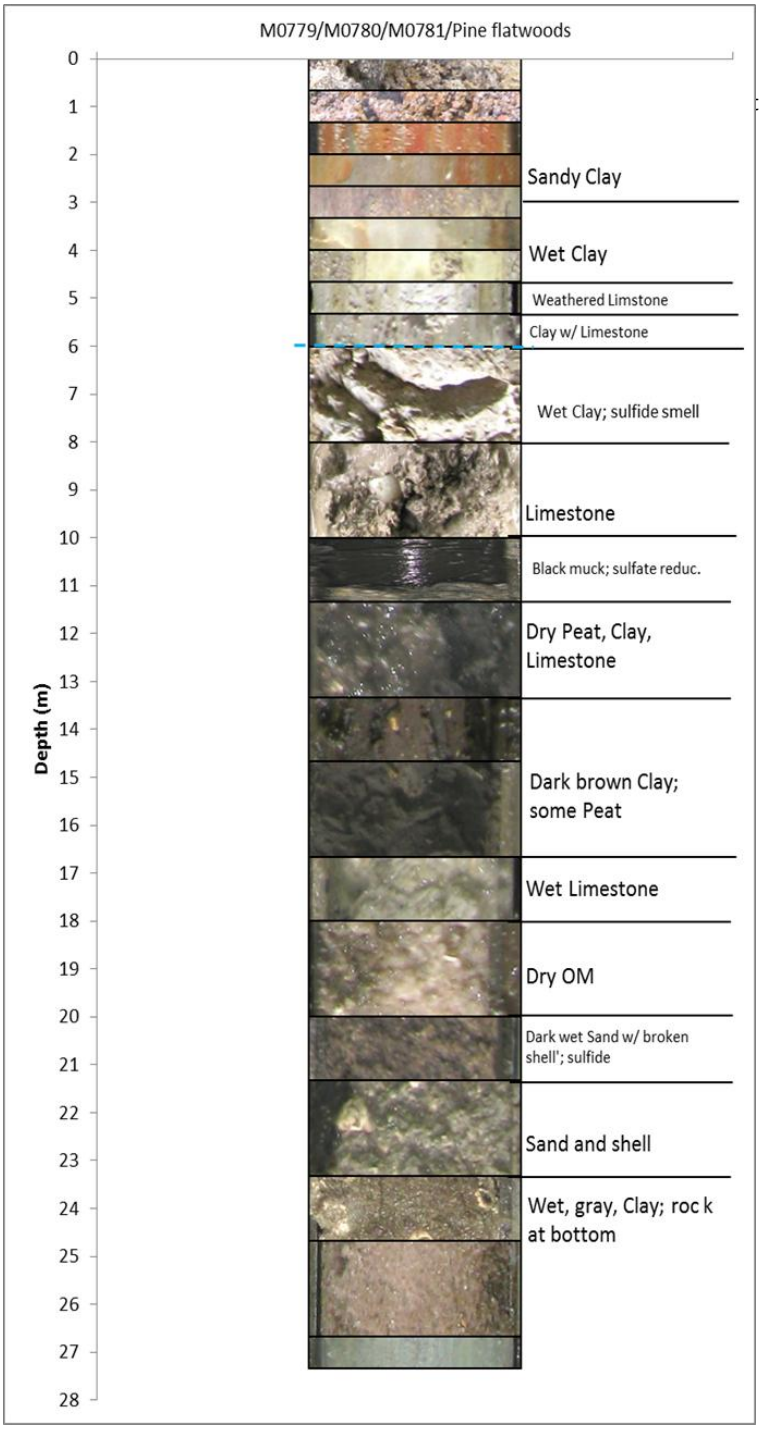

Figure 4.1.5i. Composited images of soil and vadose zone materials encountered during installation of study wells M-0779/0780/0781 in the Silver Springs springshed.

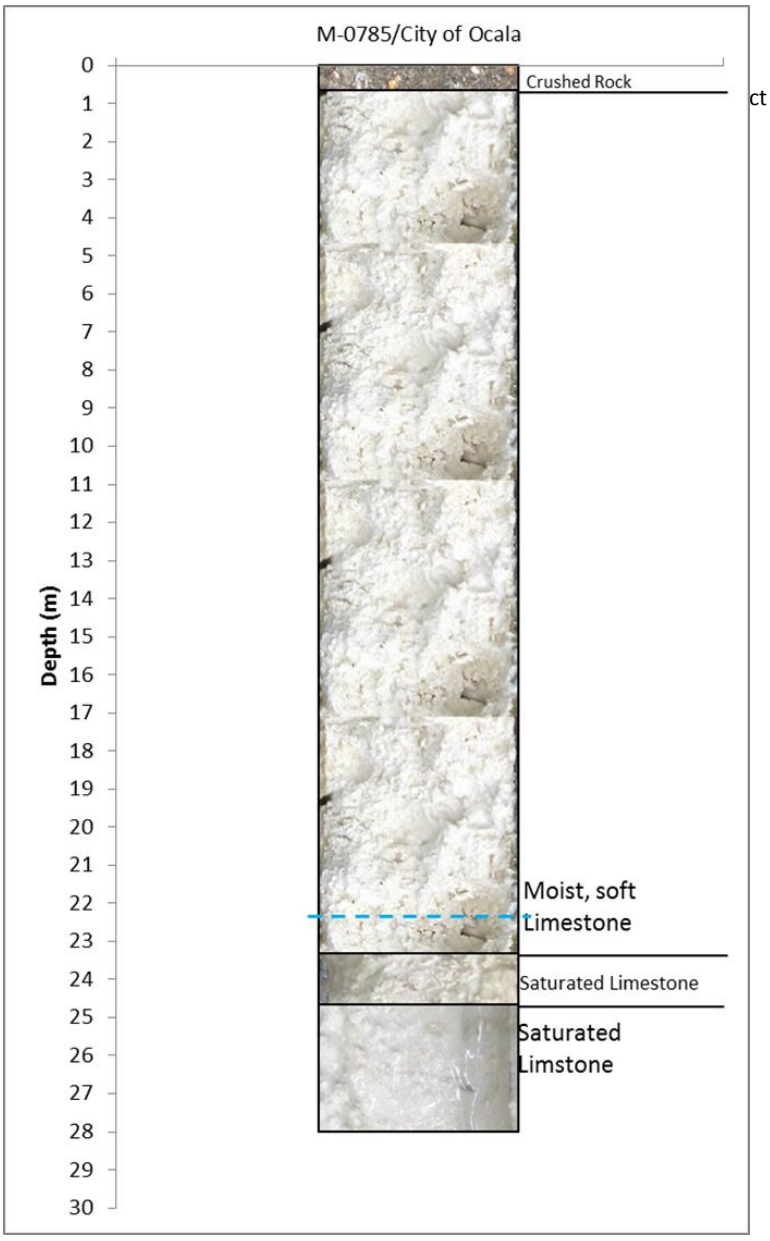

Figure 4.1.5j. Composited images of soil and vadose zone materials encountered during installation of study well M-0785 in the Silver Springs springshed.

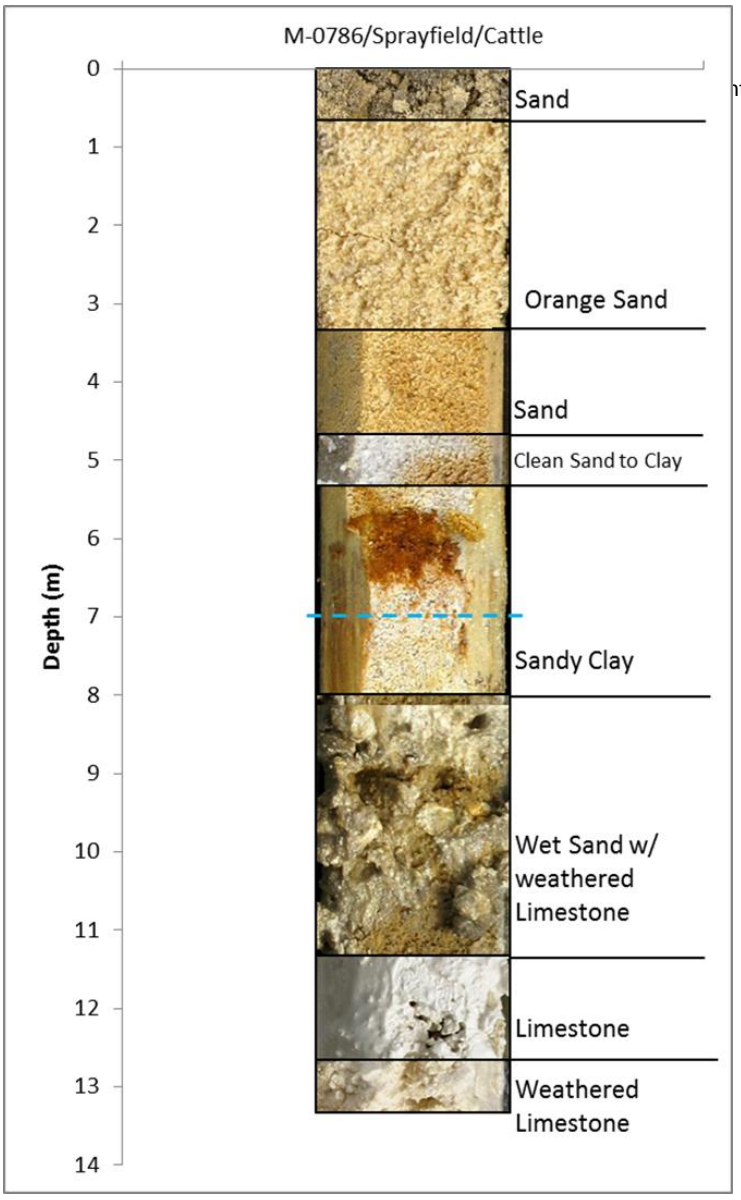

Figure 4.1.5k. Composited images of soil and vadose zone materials encountered during installation of study well M-0786 in the Silver Springs springshed.

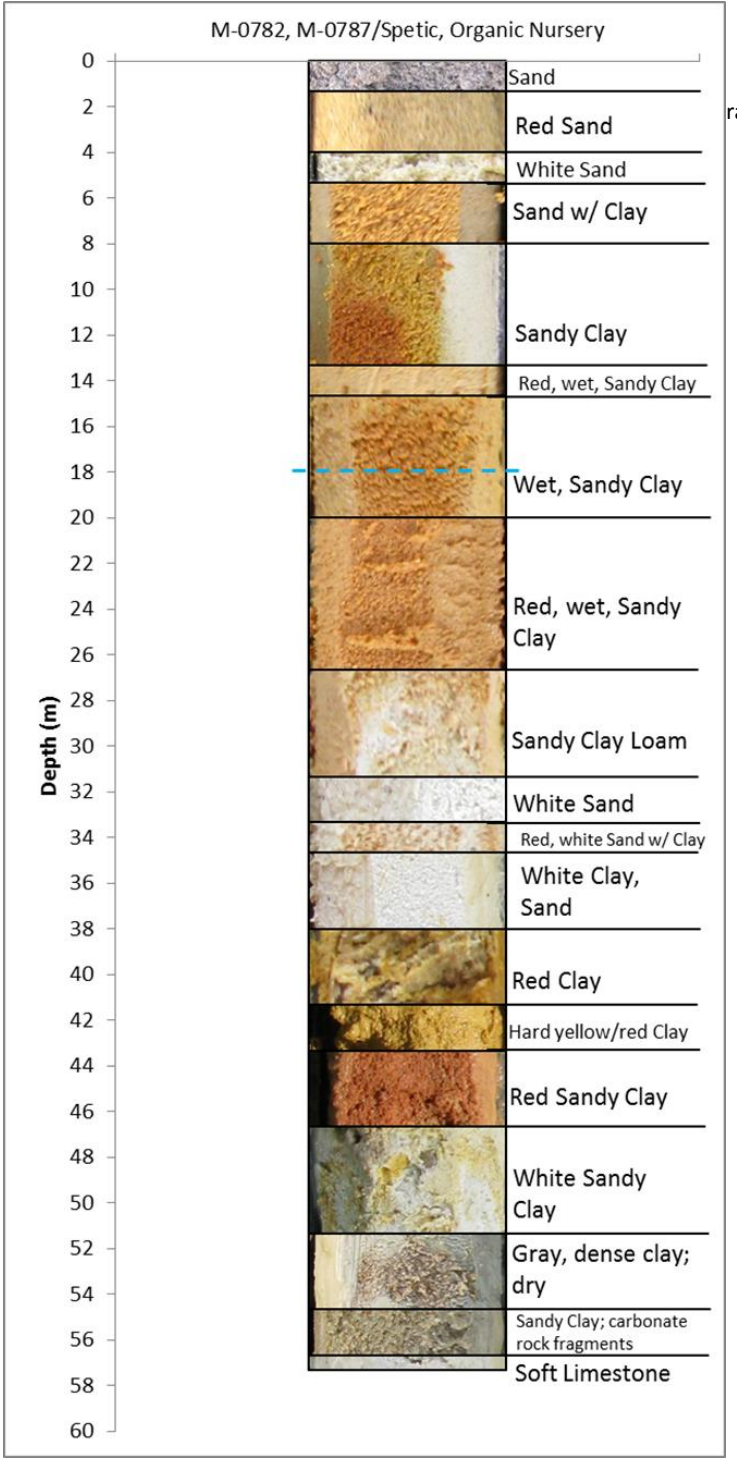

Figure 4.1.5l. Composited images of soil and vadose zone materials encountered during installation of study wells M-0782, M-0787 in the Silver Springs springshed.

positive values (+400-700 millivolts) are indicative of aerobic respiration. For most of the profile samples, the redox potential was positive, but within ranges where denitrification is possible (Feast et al. 1998; Wlodarczyk et al. 2003).

The loss on ignition (LOI) also showed high numbers in the clay layer, and then decreased with the soil depth (Figure 4.1.7). For most of the sites, the LOI fell in the range of 0-10%, however, in the site M-0779/0780/0781, LOI reached as high as 53.1% at the depth of 10.4-11.0 m (Figure

4.1.7). Typically, LOI is used to infer organic matter content. This is likely true in the surface soil layers, however the high porosity in the tight clays may have resulted in weight changes due to loss of tightly held interstitial water.

More indicative of organic matter content in the surface layers, total carbon (TC) contents were below 10% in the sand and clay layers, and exceeded 10% in the deep limestone layers which reflected C as $CaCO_3$ and $MgCO_3$ (12% -14% TC content) (Figure 4.1.8). Above the limestone, TC content likely reflected organic matter with accumulations only in the surface soils zone. This was not the case for the 10-12 m depth at the site M-0779/0780/0781, where a buried layer of t peat was encountered with TC contents reaching >30% (Figure 4.1.8). As a confirmation of suspected patterns of organic matter, water extractable total organic carbon (Ext. TOC) immediately decreased below the top 1.2 m soil profiles for most of the sites (Figure 4.1.10). For wells M-0779/0780/0781, however, Ext. TOC has a sharp increase in the 9.1-9.8 m and 10.4-11.0 m clay layers with the values of 186 and 165 mg kg^{-1}, respectively.

Generally, the TN showed a decreasing tread with increasing soil depth, and sometimes had a peak in the clay layers. For most of sites, the total nitrogen contents (TN) were very low (<1%) compared to other terrestrial soils (Figure 4.1.9). The TN in the site M-0779/0780/0781was higher and reached a peak of approximately 1.4% in the buried peat layers. The patterns of water extractable ammonia and nitrate (Ext. NH_4-N and Ext. NO_3-N) varied between different sites (Figure 4.1.11). In the sites of M-0777, M-0778, M-0775, and M-0785, there was a decreasing trend of Ext. NH_4-N and Ext. NO_3-N with soil depth though the values did not change significantly. High Ext. NH_4-/NO_3-N values were observed in the clay layers for other sites. In the sites of M-0771, M-0772, and M-0776, the soil Ext. NH_4-N values were similar with or higher than the Ext. NO_3-N values above the water level, but below the water table, the Ext. NO_3-N levels exceeded the Ext. NH_4-N. In the sites of M-0773, M-0786, M-0774, and M-0782/0787, the dominant

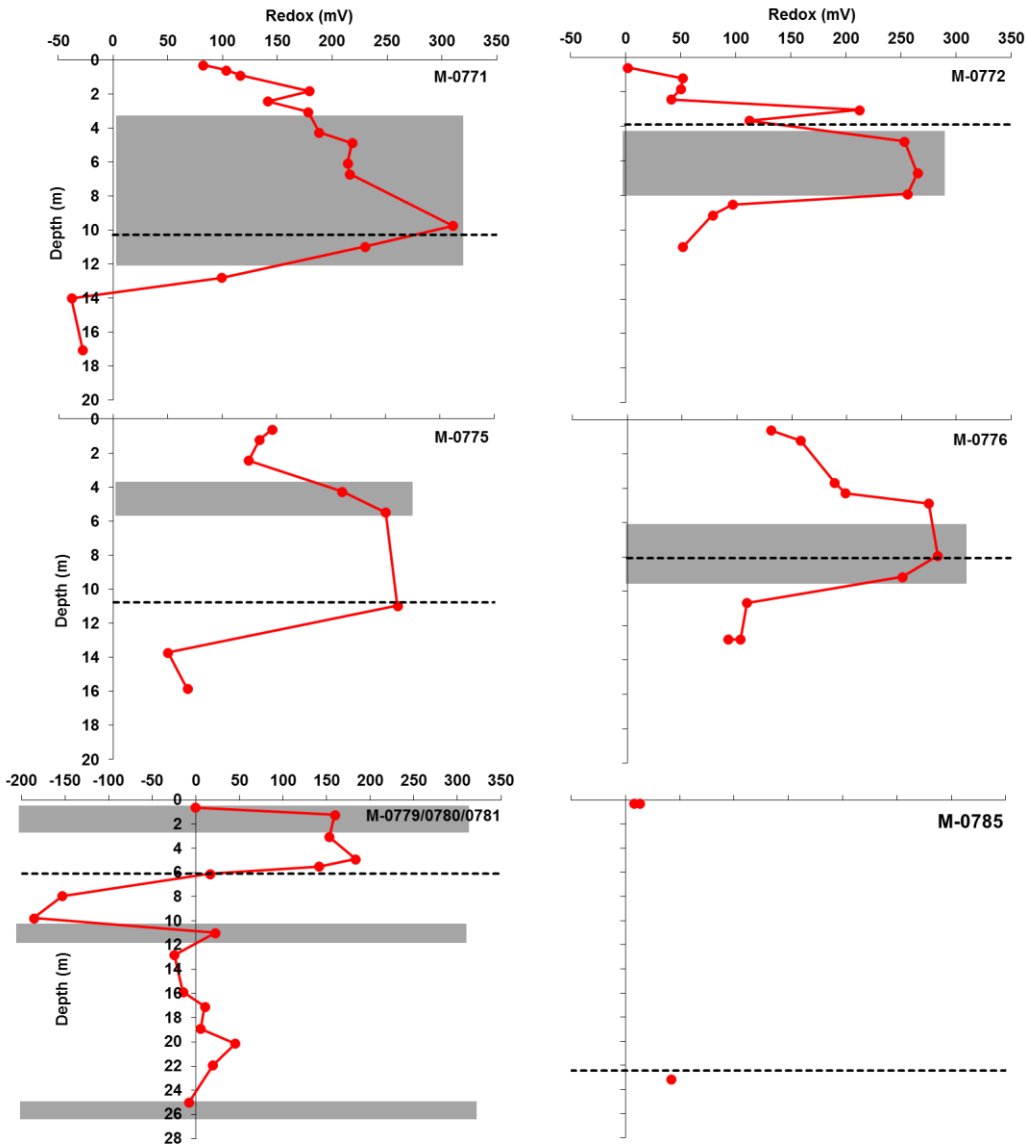

Figure 4.1.6. Vertical profiles of redox potential (mV) in soil and vadose zone profiles for the 12 study wells. The gray areas and the dash lines represent the clay layers and the water table, respectively.

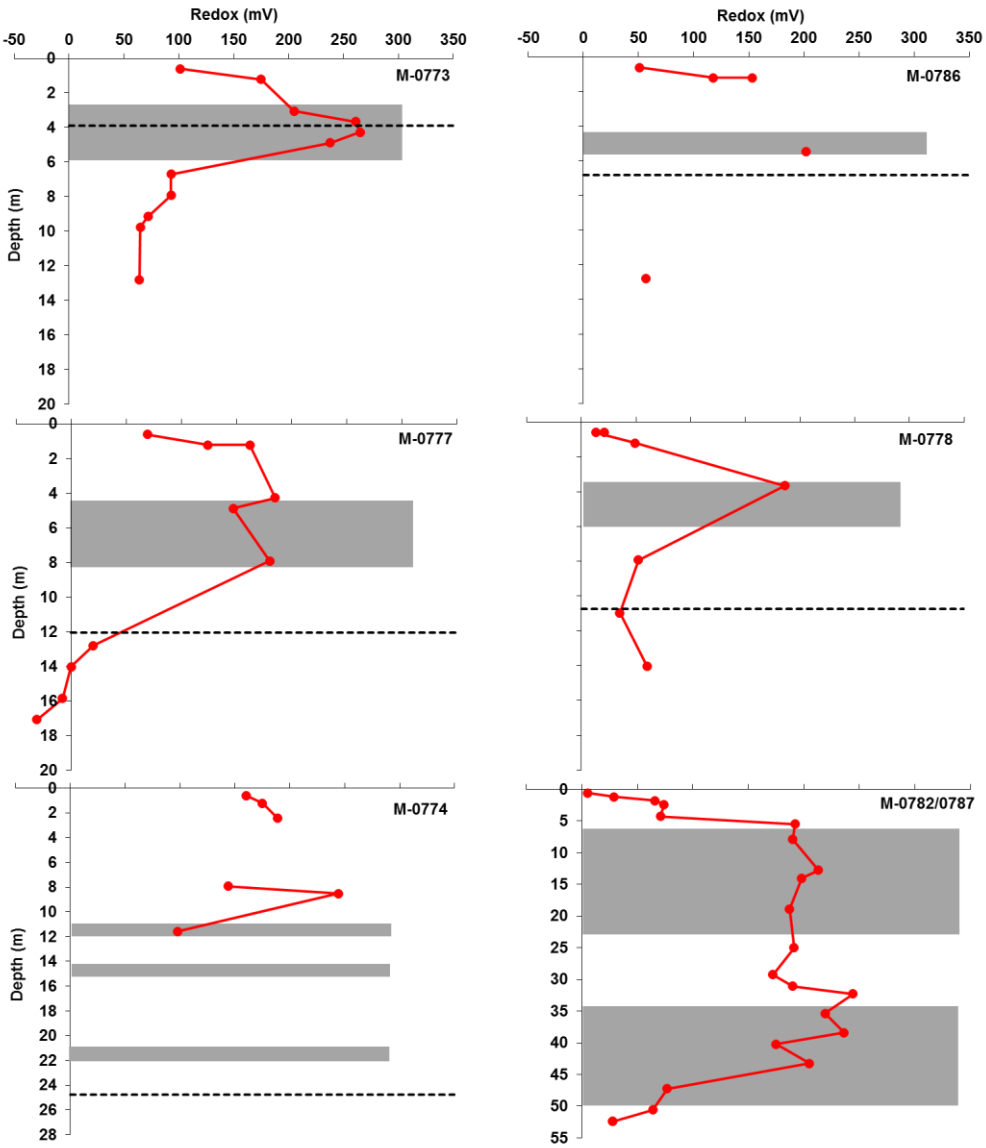

Figure 4.1.6 (cont.). Vertical profiles of redox potential (mV) in soil and vadose zone profiles for the 12 study wells. The gray areas and the dash lines represent the clay layers and the water table, respectively.

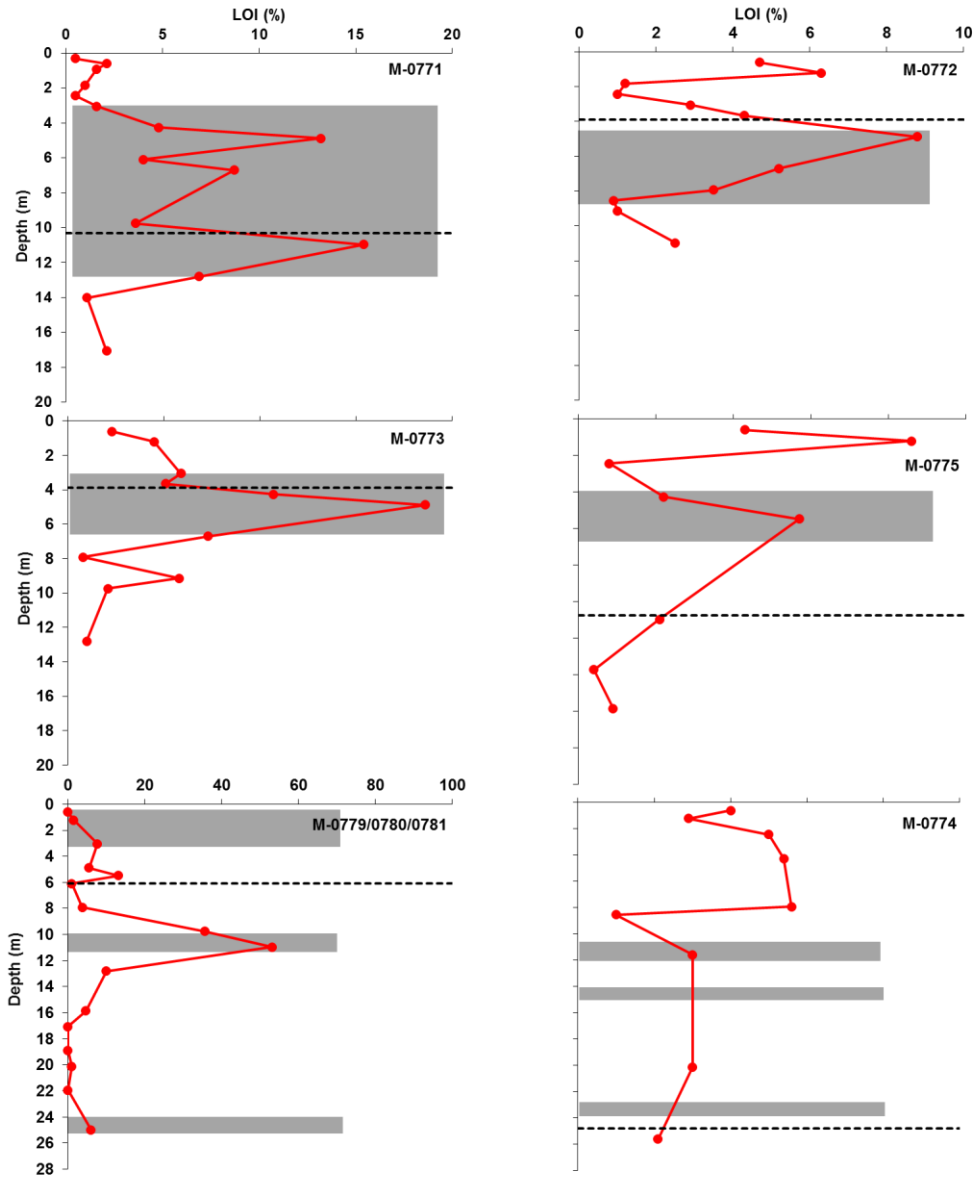

Figure 4.1.7. Vertical profiles of loss on ignition (LOI) in soil and vadose zone profiles for the 12 study wells. The gray areas and the dash lines represent the clay layers and the water table, respectively.

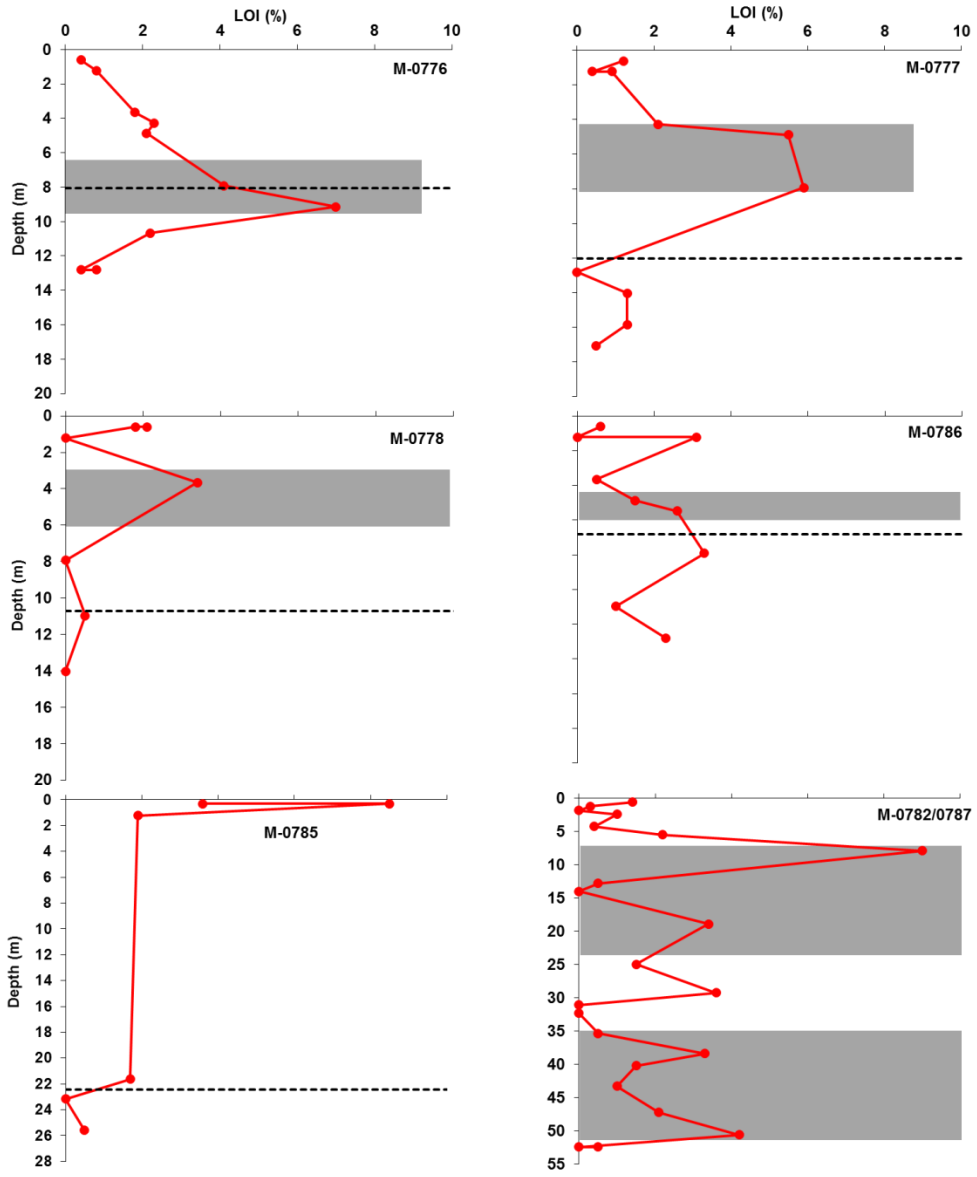

Figure 4.1.7 (cont.). Vertical profiles of loss on ignition (LOI) in soil and vadose zone profiles for the 12 study wells. The gray areas and the dash lines represent the clay layers and the water table, respectively.

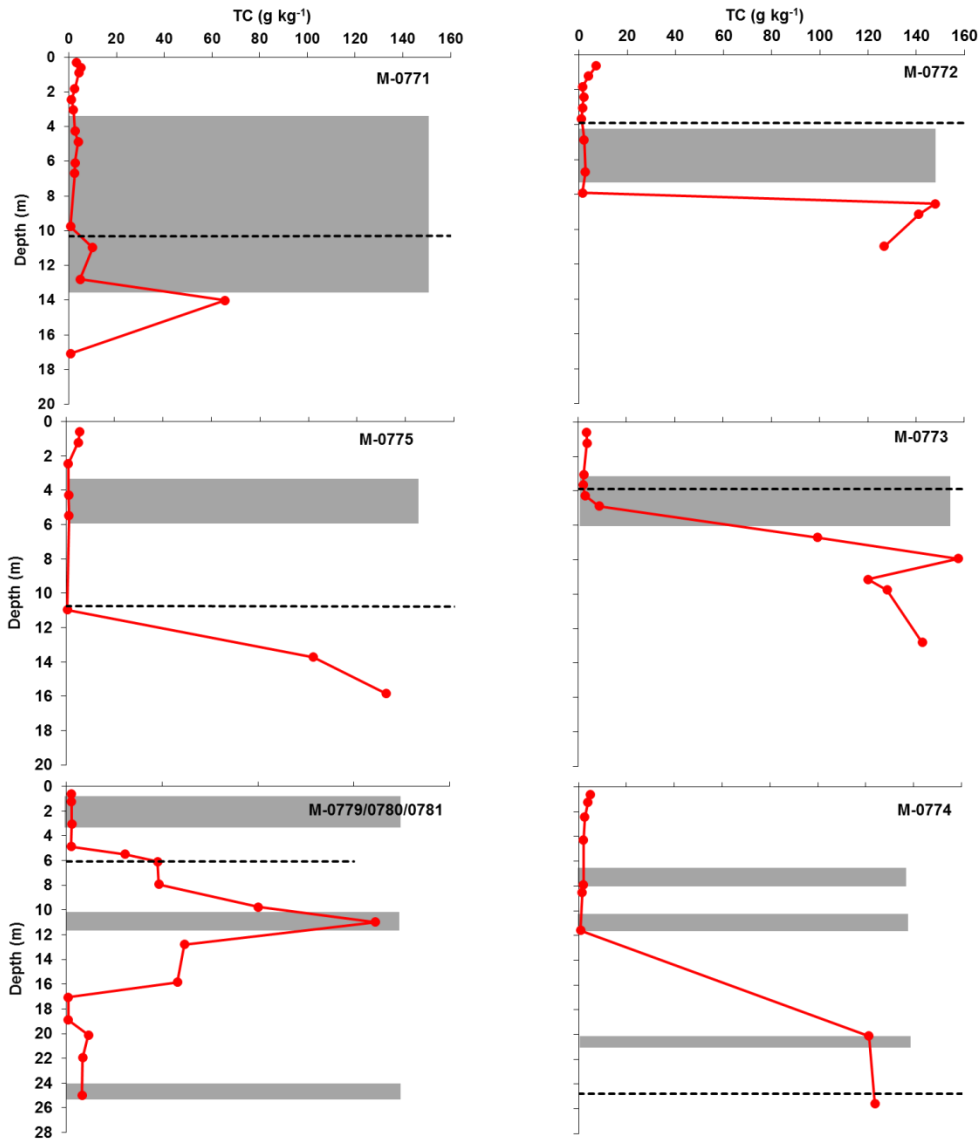

Figure 4.1.8. Vertical profiles of total carbon (TC) in soil and vadose zone profiles for the 12 study wells. The gray areas and the dash lines represent the clay layers and the water table, respectively.

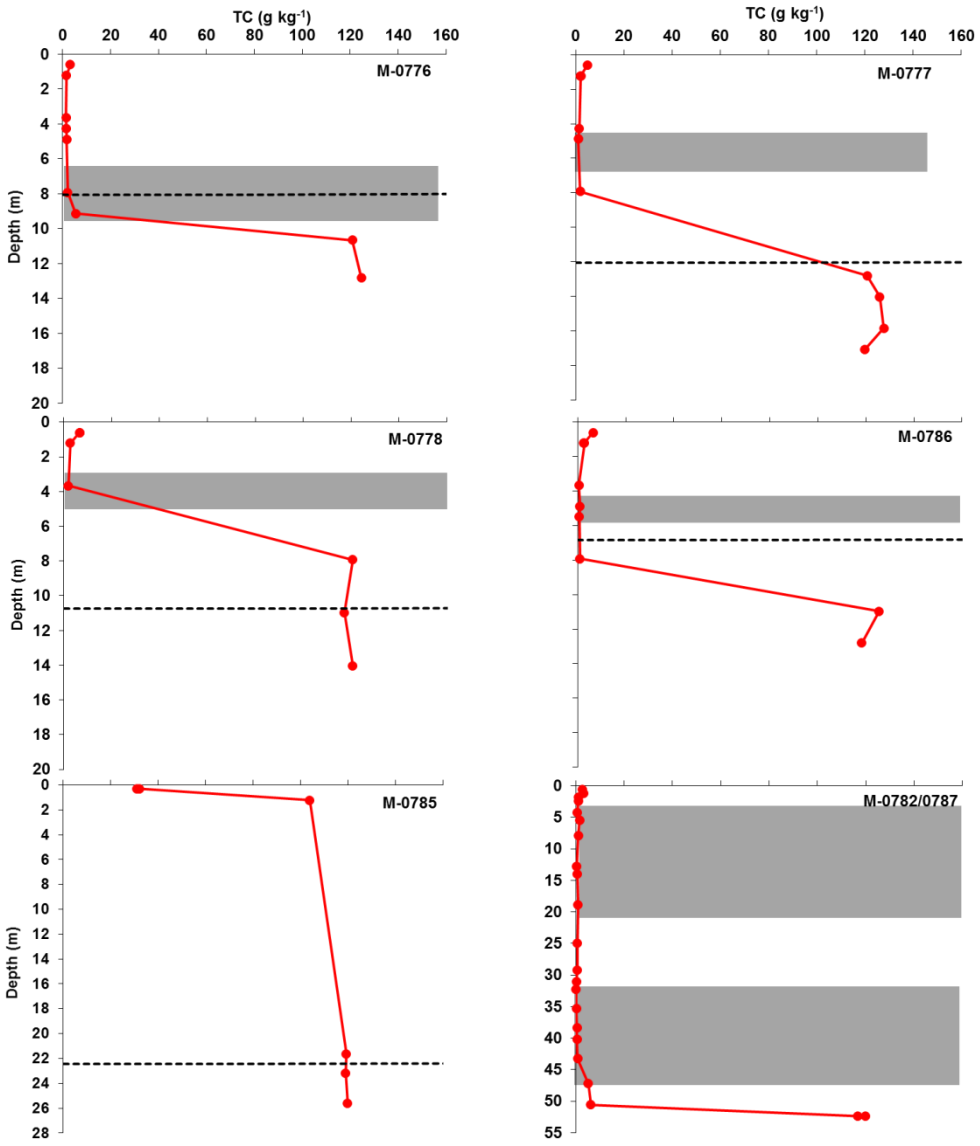

Figure 4.1.8 (cont.). Vertical profiles of total carbon (TC) in soil and vadose zone profiles for the 12 study wells. The gray areas and the dash lines represent the clay layers and the water table, respectively.

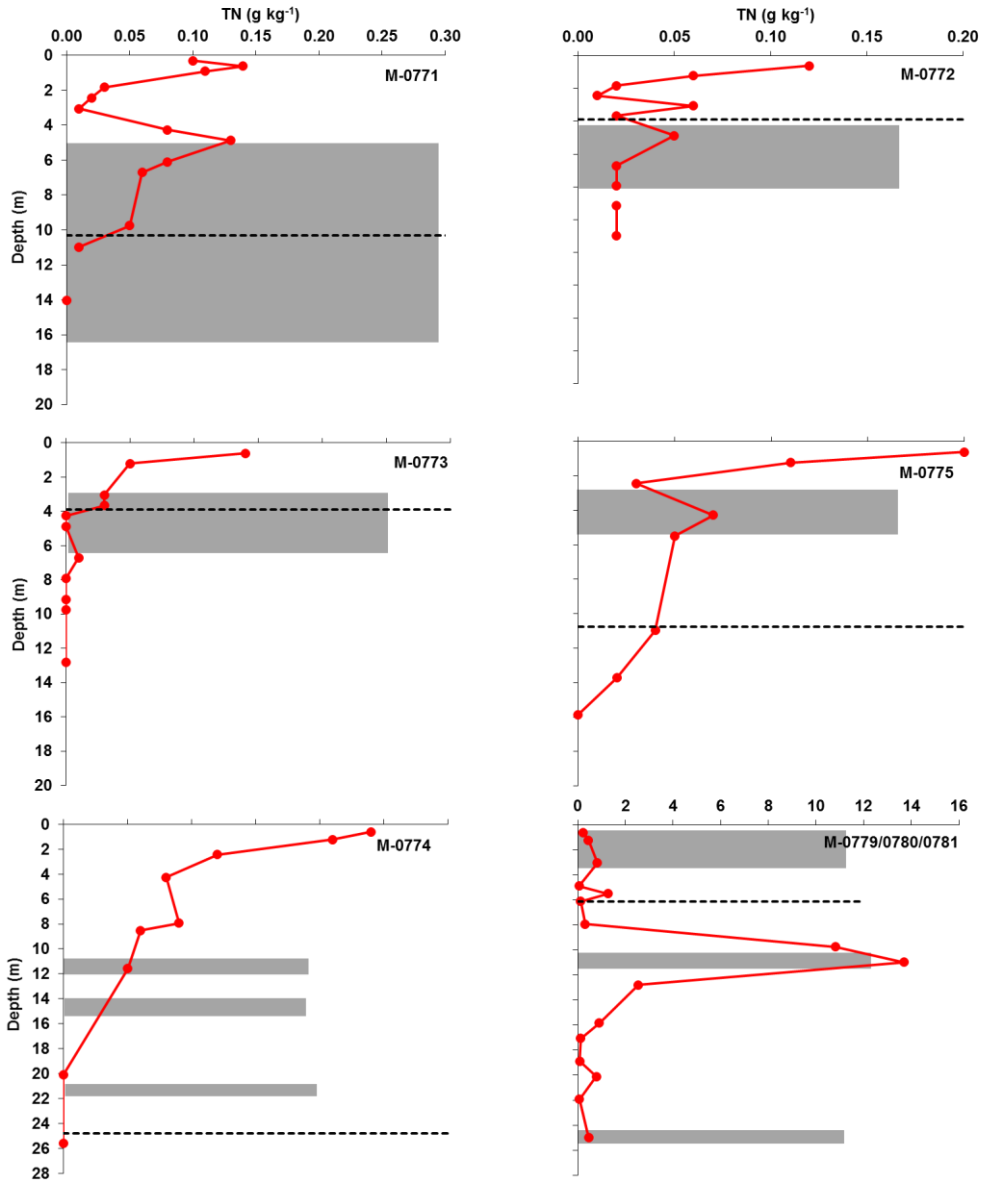

Figure 4.1.9. Vertical profiles of total nitrogen (TN) in soil and vadose zone profiles for the 12 study wells. The gray areas and the dash lines represent the clay layers and the water table, respectively.

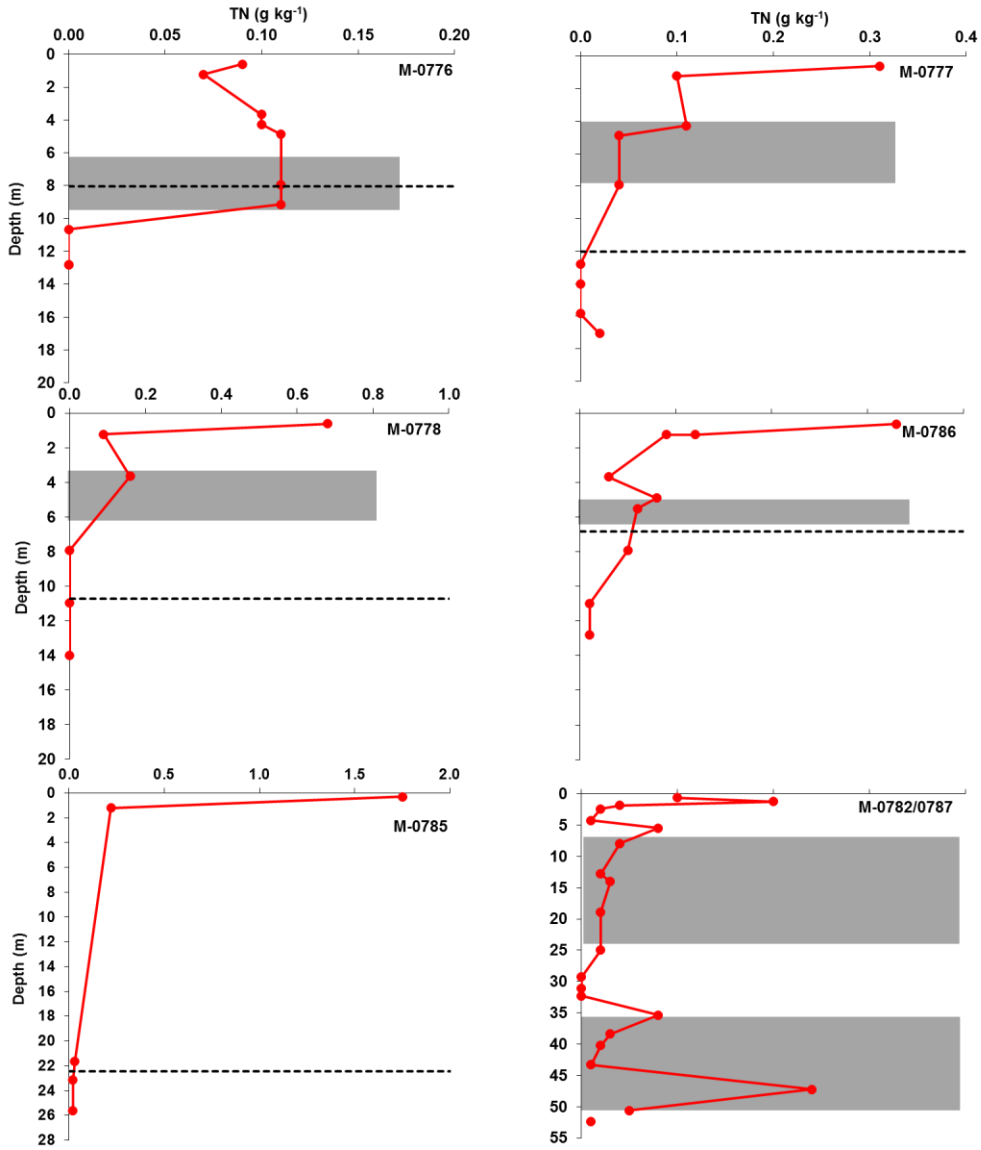

Figure 4.1.9 (cont.). Vertical profiles of total nitrogen (TN) in soil and vadose zone profiles for the 12 study wells. The gray areas and the dash lines represent the clay layers and the water table, respectively.

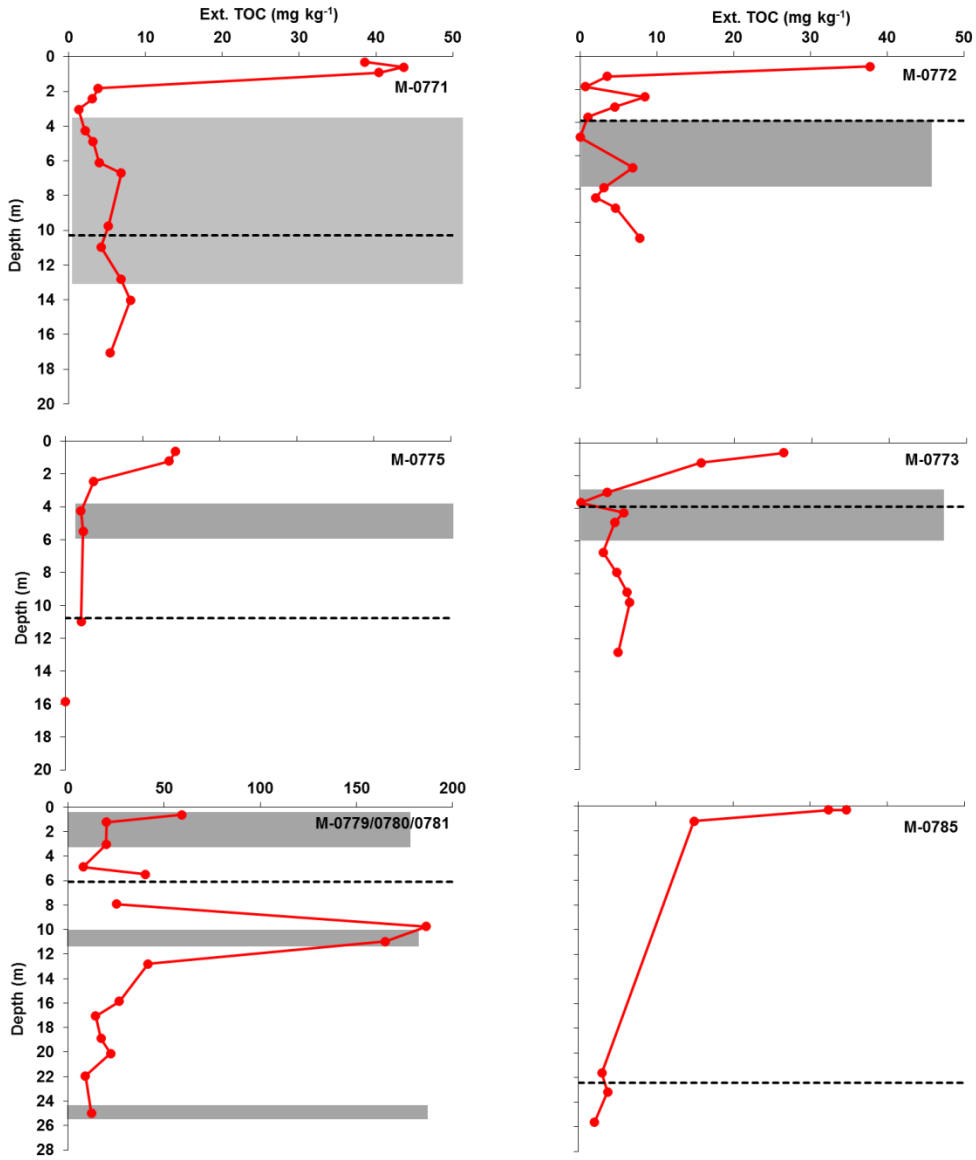

Figure 4.1.10. Vertical profiles of water extractable total organic carbon (Ext.TOC) in soil and vadose zone profiles for the 12 study wells. The gray areas and the dash lines represent the clay layers and the water table, respectively.

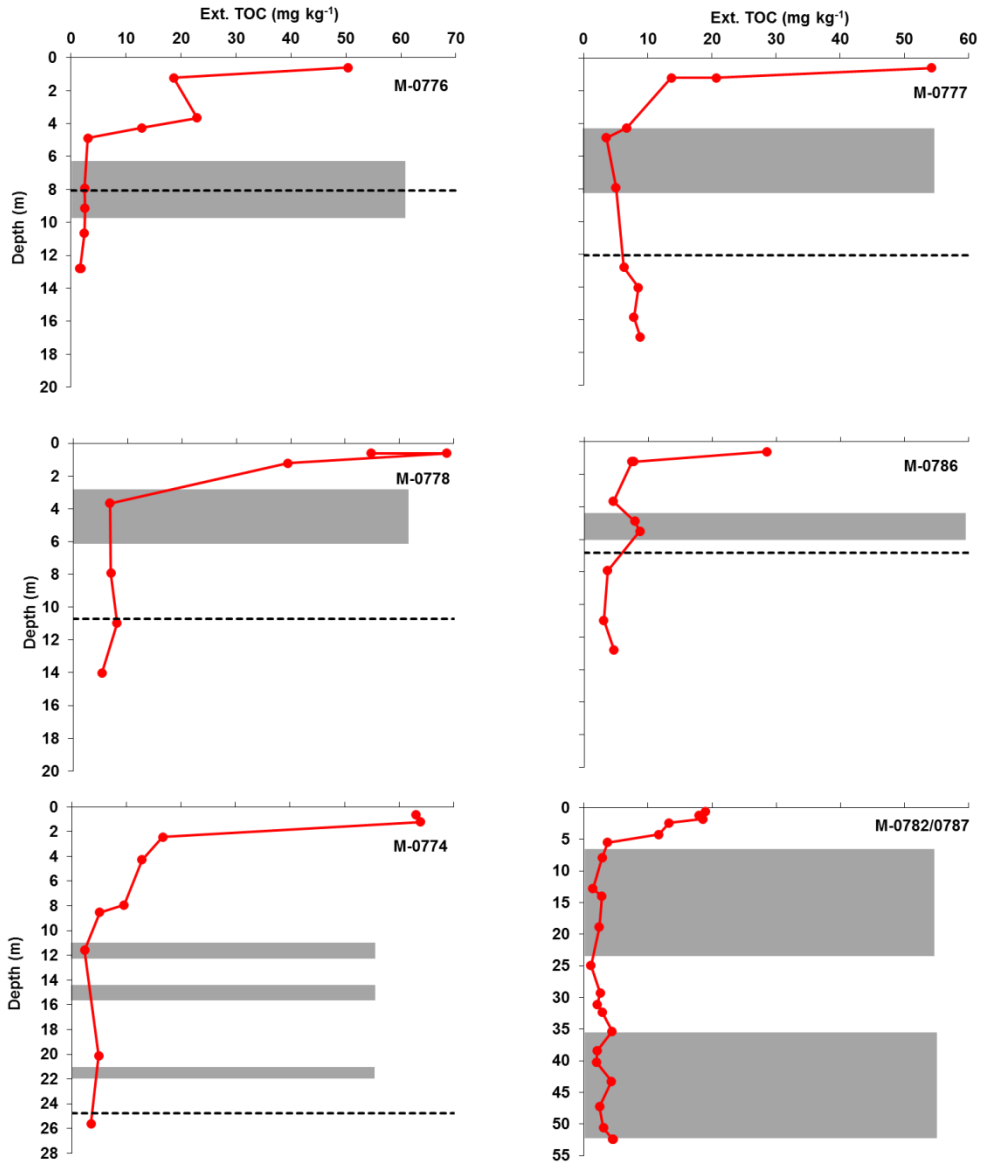

Figure 4.1.10 (cont.). Vertical profiles of water extractable total organic carbon (Ext.TOC) in soil and vadose zone profiles for the 12 study wells. The gray areas and the dash lines represent the clay layers and the water table, respectively

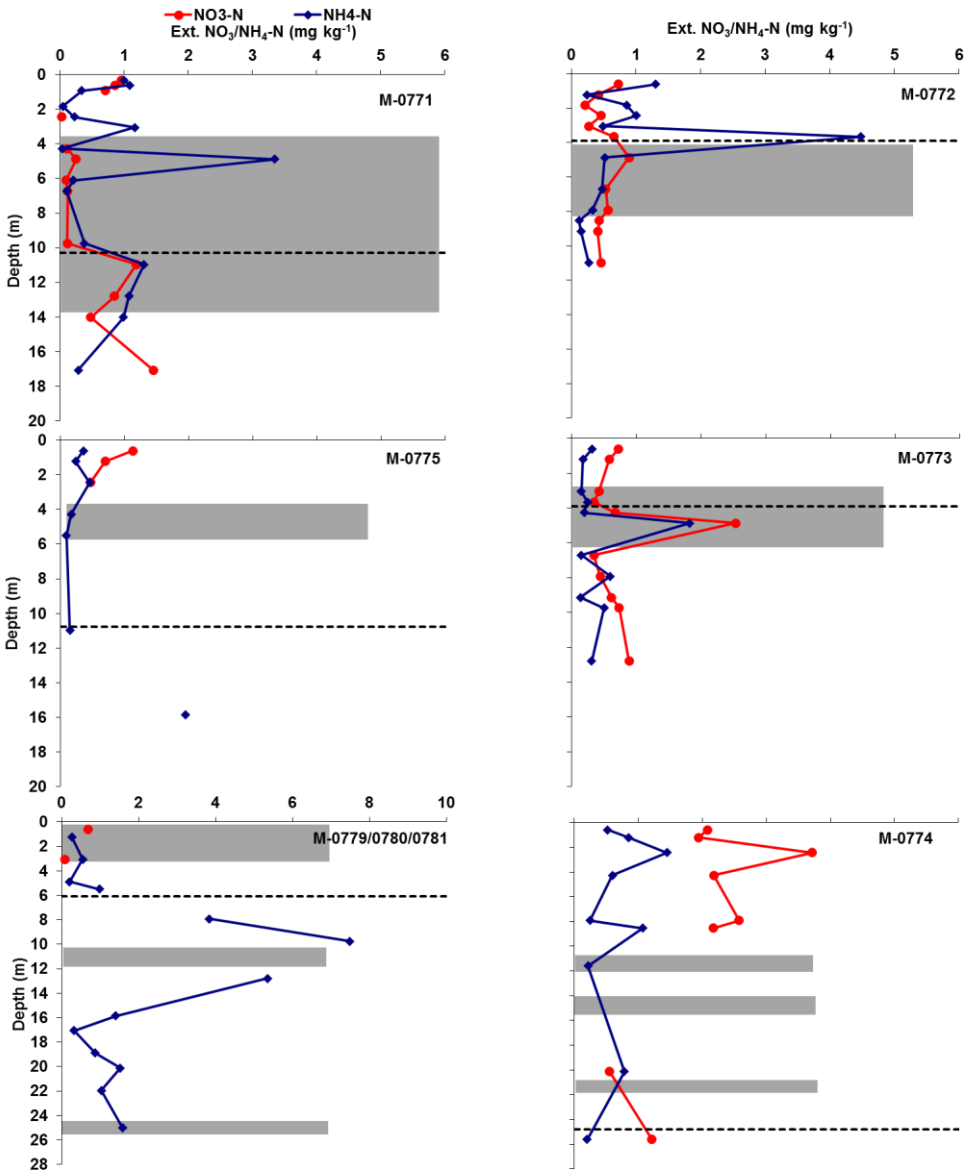

Figure 4.1.11. Vertical profiles of water extractable nitrate and ammonium (Ext.NO_3/NH_4) in soil and vadose zone profiles for the 12 study wells. The gray areas and the dash lines represent the clay layers and the water table, respectively.

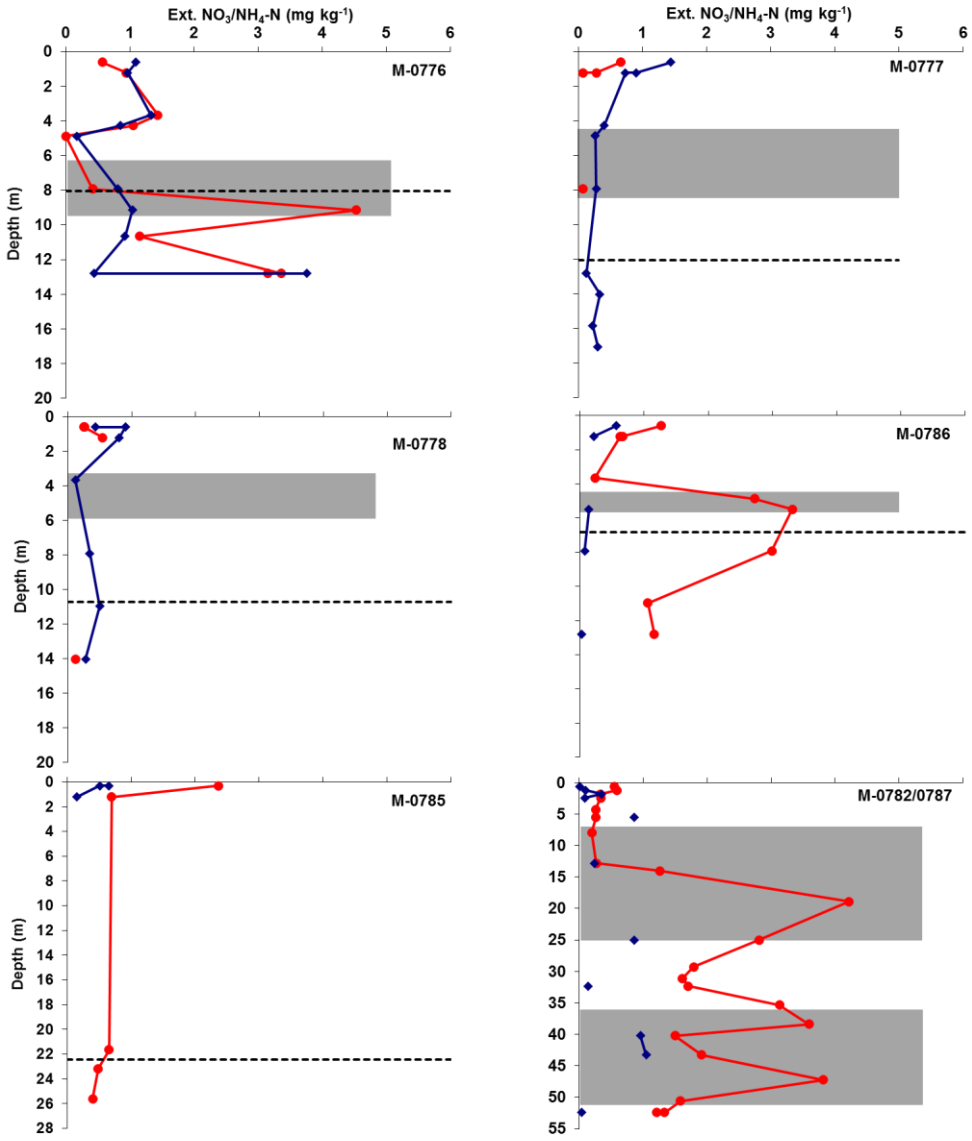

Figure 4.1.11 (cont.). Vertical profiles of water extractable nitrate and ammonium ($Ext.NO_3/NH_4$) in soil and vadose zone profiles for the 12 study wells. The gray areas and the dash lines represent the clay layers and the water table, respectively.

inorganic nitrogen form was Ext. NO_3-N which were much higher than the concentration of Ext. NH_4-N. In contrast, Ext. NH_4-N was the dominant inorganic nitrogen form throughout the profile at the sites of M-0779/0780/0781.

4.1.4.2 Subsoil Phosphorus Storage and Leaching Potential

Total P showed a distinctive vertical pattern with low accumulations of P in the surface soil which increased dramatically with depth. This increase in TP was particular indicative of clay layers in all soils (except the site of M-0785) and characteristically was elevated in the lowest

clay layers such as those of sites M-0779/0780/0781, M-0782/0787, M-0771, M-0772, and M-0773. This elevated TP likely represents the true Hawthorn unit composition which is identified as a Miocene phosphatic sediments (Scott 1988).

It makes sense that the water extractable total phosphorus (WSTP) was higher than the water extractable inorganic phosphorus (WSP) (Figure 4.1.13). For most of the sites, the WSTP and WSP dropped when reaching the clay layer and then increased at the low boundary of the clay layer. For most of the sites, Mehlich 3-P (M3-P) showed a decreasing pattern before entering the clay layer where M3-P started to increase (Figure 4.1.14).

Leaching of P to groundwater is generally considered less of an issue for calcareous soils due to their considerable capacity to adsorb P (Pizzeghello et al. 2014). Several researchers, however, have pointed out the importance of the subsoil for P leaching (e.g., Djodjic et al. 2004; Peltovuori 2007; van Beek et al. 2009). Also, most of the P leaching studies on subsoil assess only down to 1 m soil depth (Andersson et al. 2013; Pizzeghello et al. 2014). In our study, we measured the extractable P down to 20 to 55 m deep in the vadose zone.

Based on the results for total phosphorus and extractable forms and metals in the soil/subsoil profiles, we will be able to assess patterns of phosphorus storage and attenuation in the spring shed. It is unclear how important this will be for ecological changes in the Springs, but given current and potential land use changes, the issue of phosphorus storage and mobility will likely be a significant future issue four aquatic systems in the region.

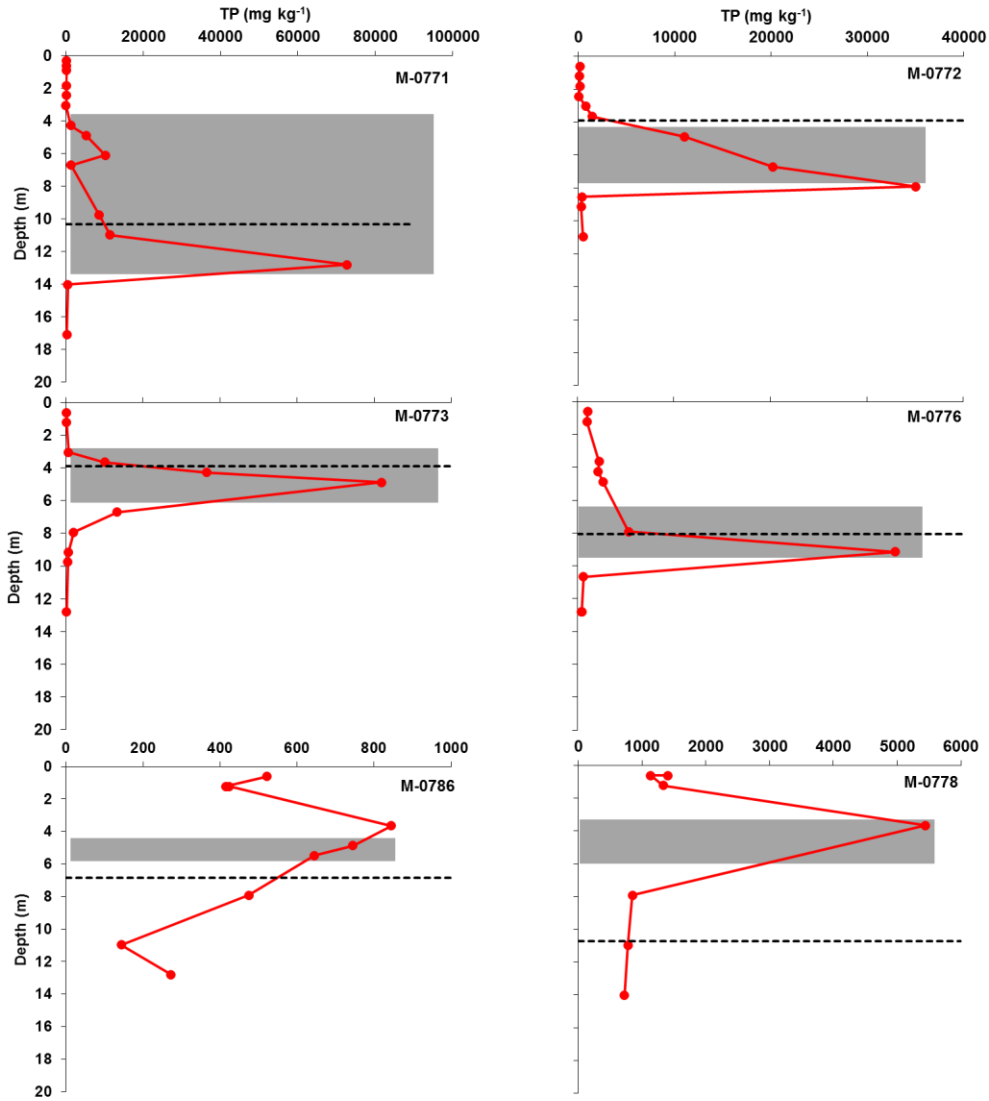

Figure 4.1.12. Vertical profiles of total phosphorus (TP) in soil and vadose zone profiles for the 12 study wells. The gray areas and the dash lines represent the clay layers and the water table, respectively.

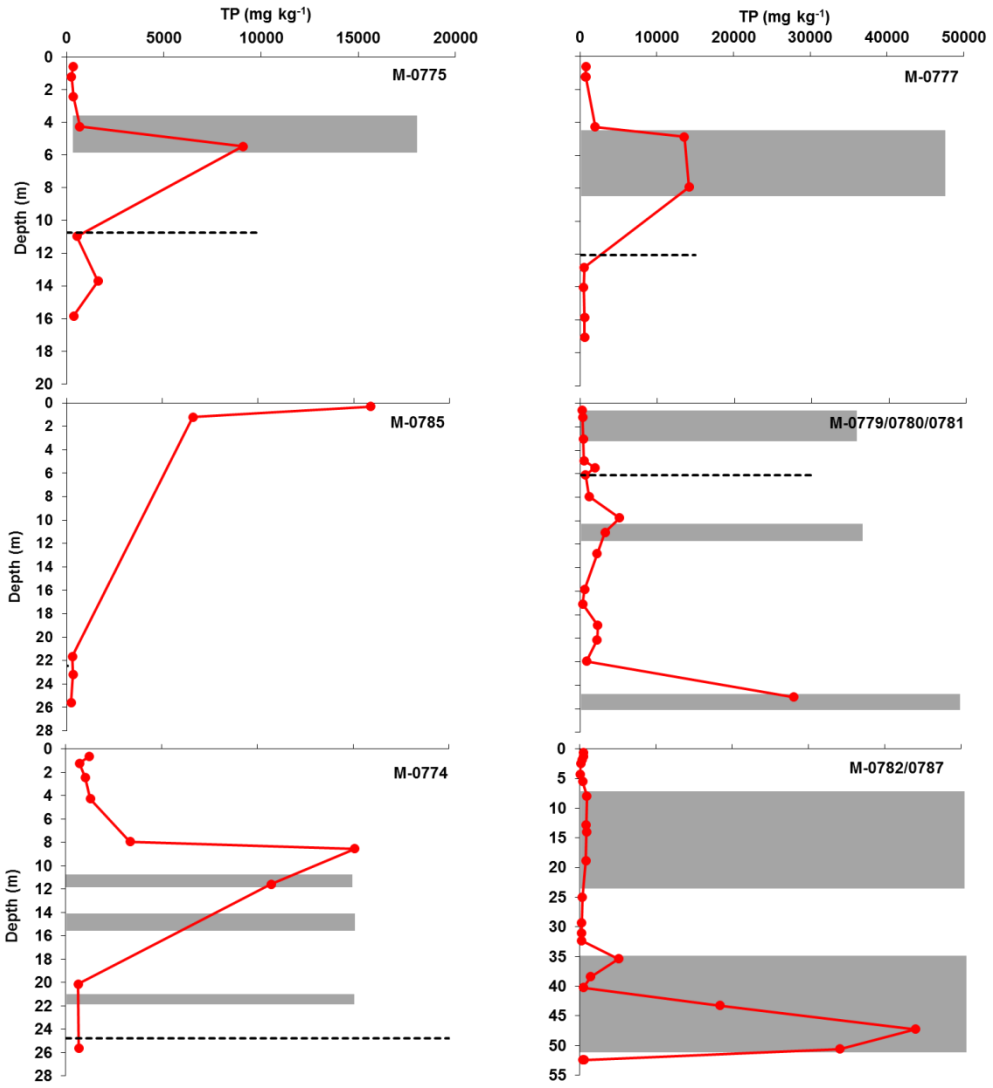

Figure 4.1.12 (cont.). Vertical profiles of total phosphorus (TP) in soil and vadose zone profiles for the 12 study wells. The gray areas and the dash lines represent the clay layers and the water table, respectively.

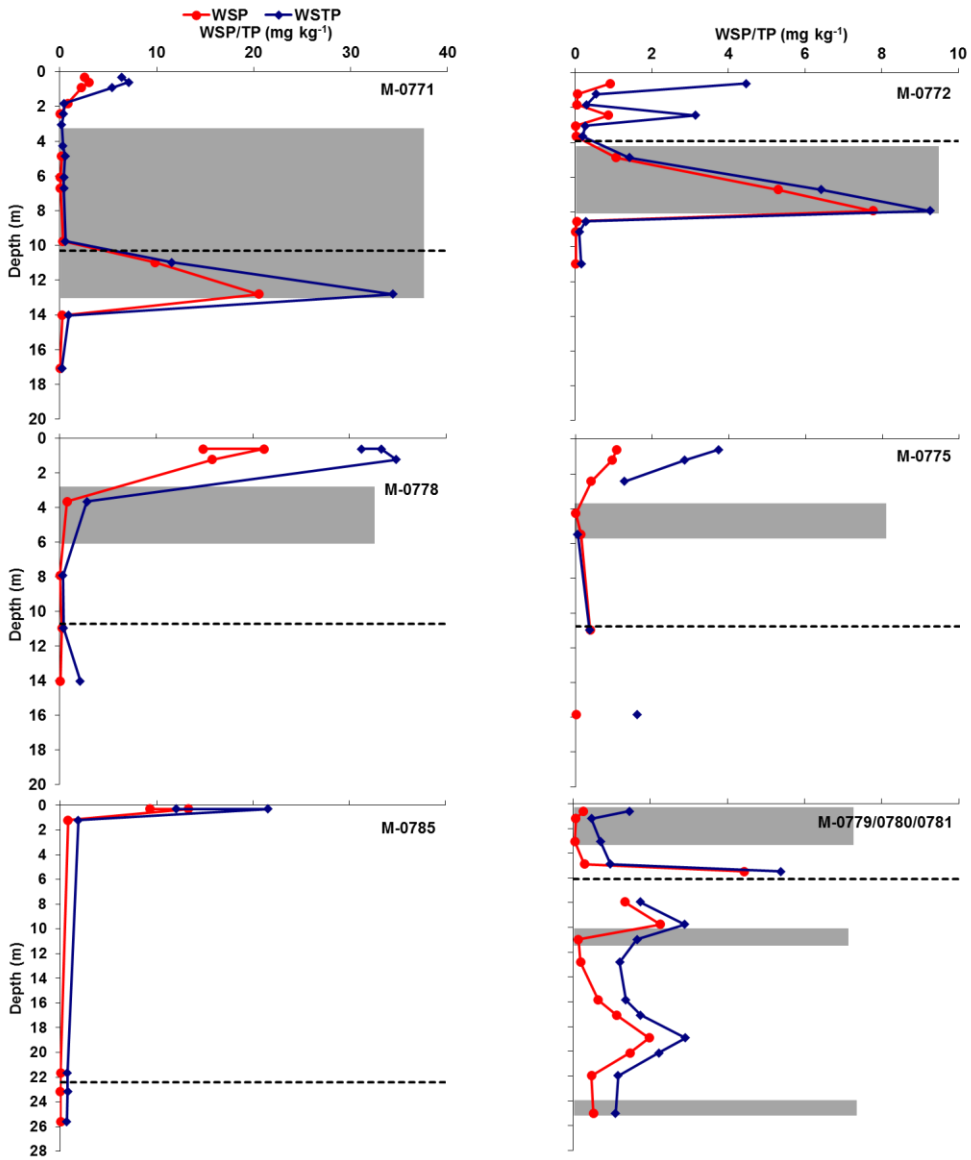

Figure 4.1.13. Vertical profiles of water soluble reactive P (WSP) and water soluble total P (TP) in soil and vadose zone profiles for the 12 study wells. The gray areas and the dash lines represent the clay layers and the water table, respectively.

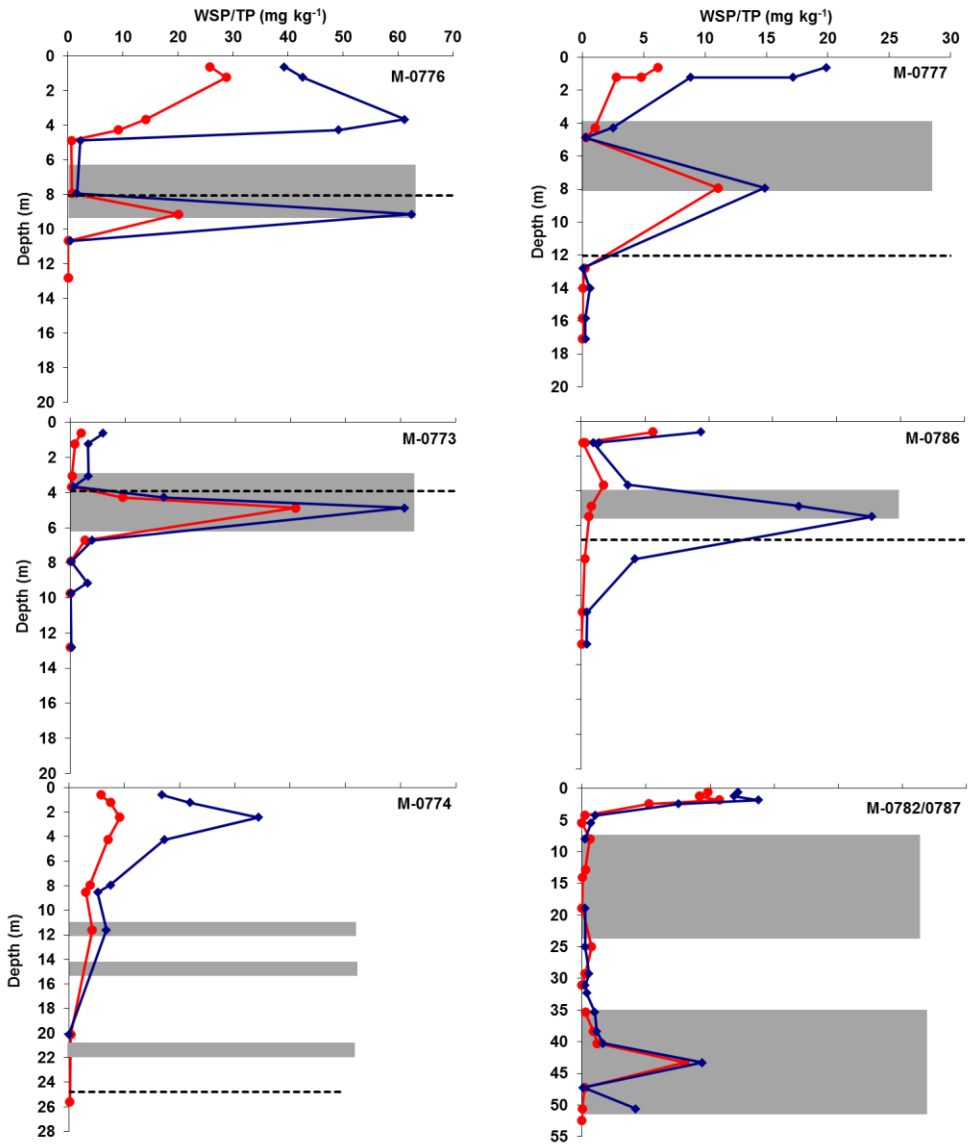

Figure 4.1.13 (cont.). Vertical profiles of water soluble reactive P (WSP) and water soluble total P (TP) in soil and vadose zone profiles for the 12 study wells. The gray areas and the dash lines represent the clay layers and the water table, respectively.

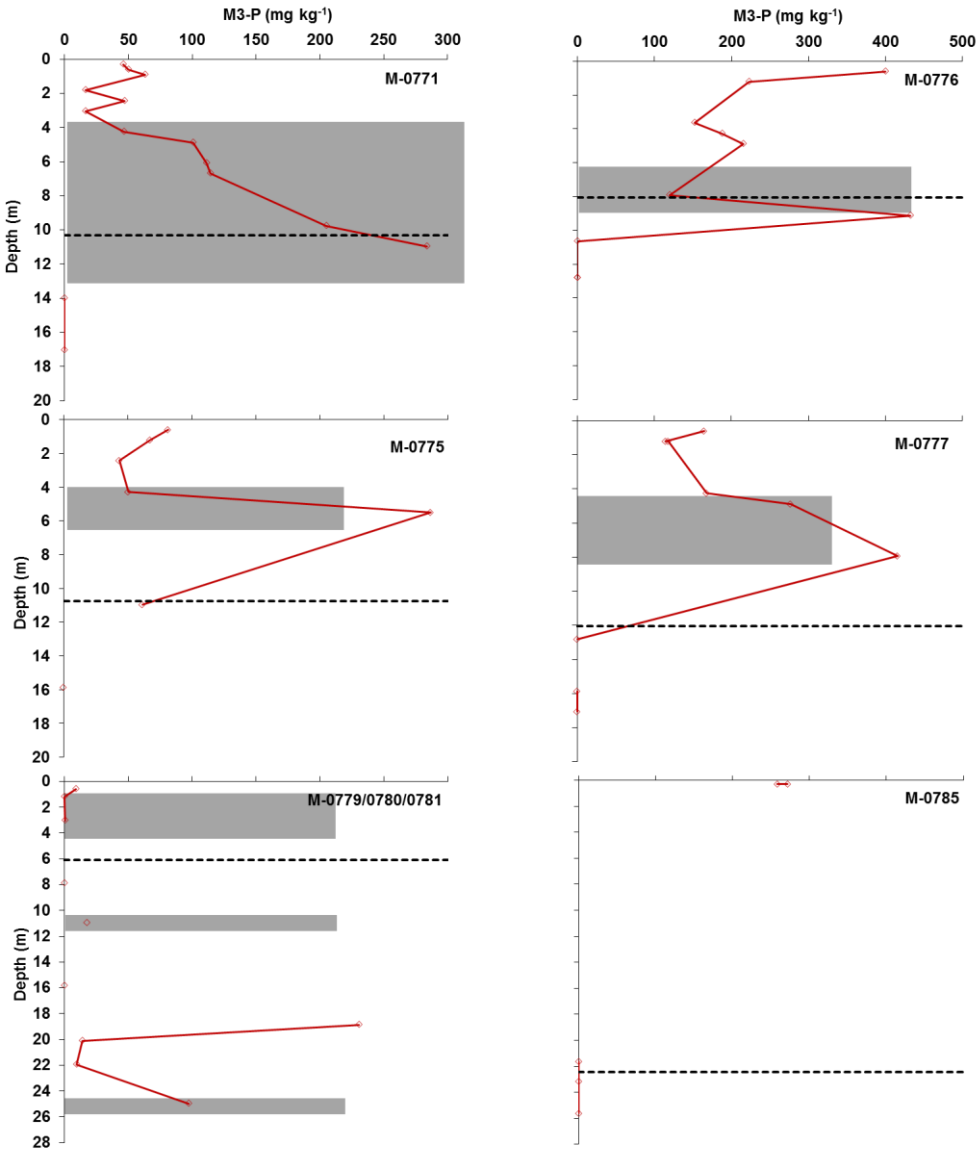

Figure 4.1.14 Vertical profiles of Mehlich 3-P in soil and vadose zone profiles for the 12 study wells. The gray areas and the dash lines represent the clay layers and the water table, respectively.

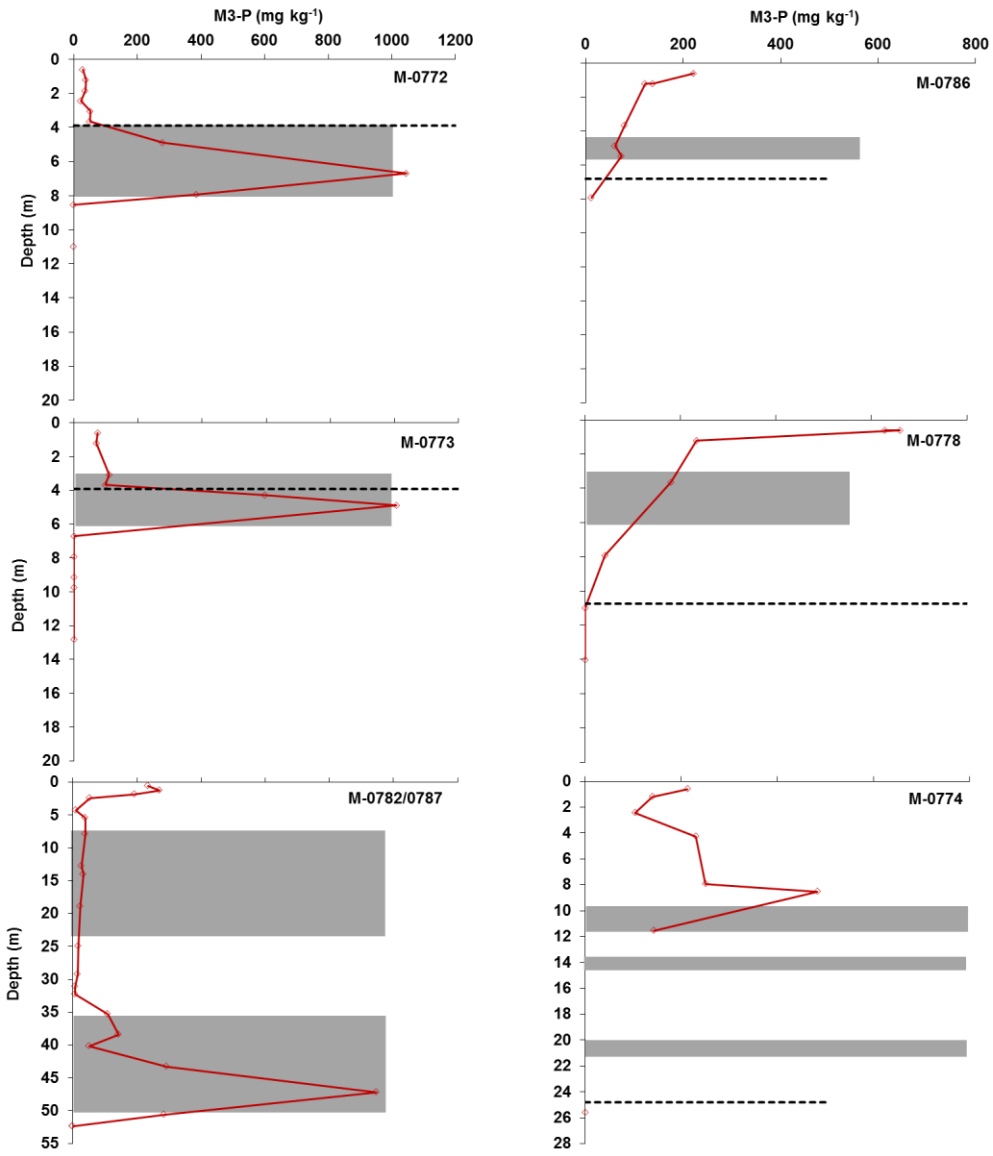

Figure 4.1.14 (cont.). Vertical profiles of Mehlich 3-P in soil and vadose zone profiles for the 12 study wells. The gray areas and the dash lines represent the clay layers and the water table, respectively.

4.1.4.3 Denitrification Enzyme Activities

Denitrification enzyme activities (DEA) with the addition of glucose and nitrate showed a decreasing trend with the soil depth in all the sites (Figure 4.1.15). Significant DEA activities were observed only in the top 1.2 m soils. For the top 0-0.6 m, soils in the wells of M-0786 (0.55 ± 0.002 nmols N_2O g^{-1} dw h^{-1}), M-0779/0780/0781 (0.47 ± 0.15 nmols N_2O g^{-1} dw h^{-1}), M-0785 (0.49 ± 0.18 nmols N_2O g^{-1} dw h^{-1}), and M-0774 (0.48 ± 0.04 nmols N_2O g^{-1} dw h^{-1}) had the highest DEA values, followed with M-0773 (0.32 ± 0. 21 nmols N_2O g^{-1} dw h^{-1}), and M-0778 (0.24 ± 0.06 nmols N_2O g^{-1} dw h^{-1}). The 0.6-1.2 m deep soil in the well of M-0779/0780/0781 still showed high DEA values with the average of 0.18 ± 0.05 nmols N_2O g^{-1} dw h^{-1}.

These results document the potential of surface soils in this region to denitrify, however the observed rates were very low compared with agricultural soils, or manure loaded systems (Barton et al. 1999).

Only in one case did we observe significant DEA activity at depth in the profile (Figure 4.1.15), with that being the 20 m layer at the M-0779/0780/0781 site. The high detected presence of sulfide at this site may indicate the potential for autotrophic denitrification with H_2S as an electron donor. Sulfur-based autotrophic denitrification is of special interest for environmental engineers due to its simultaneous removal of nitrate and reduced sulfur (Shao et al. 2010). This process is mostly found in hydrothermal vents, marine sediments, oil field, and wastewater treatment plants (Jannasch and Mott 1985; Brettar 1991; Vaiopoulou et al. 2005; Manconi et al. 2007). Its importance in freshwater systems, however, is also been indicated (Burgin and Hamilton 2007). For example, Böttcher et al. (1990) found that much of the nitrate uptake in a groundwater aquifer was ascribed to *Thiobacillus denitrificans* which is one of the most commonly reported autotrophic denitrifiers.

$$5H_2S + 8NO_3^- \rightarrow 5SO_4^{2-} + 4N_2 + 4H_2O + 2H^+ \quad (1)$$

$$14NO_3^- + 5FeS_2 + 4H^+ \rightarrow 7N_2 + 10SO_4^{2-} + 5Fe^{2+} + 2H_2O \quad (2)$$

$$H_2S + NO_3^- + H_2O \rightarrow SO_4^{2-} + NH_4^+ \quad (3)$$

$$NH_4^+ + NO_2^- \rightarrow N_2 + 2H_2O \quad (4)$$

Also, given that NH_4-N concentration was higher than NO_3-N at depth of 20 m in the M-0779/0780/0781 site, there is also potential for either anaerobic mineralization of buried peat N or dissimilatory nitrate reduction to ammonium (DNRA). Though most studies on the pathway of DNRA have been done in marine ecosystems, evidence has also been found in aquifers (Burgin and Hamilton 2007).

The presence of ammonium in the layers for some other sites in this study also indicates the potential for anaerobic ammonia oxidation (Anammox). Burgin and Hamilton (2007) hypothesized that Anammox would be expected to be limited to areas that relatively low in labile carbon. Apart from the M-0779/0780/0781 site, we saw the coexistence of both NO_3^- and NH_4^+ (Figure 4.1.11), and the decreasing ext. TOC (Figure 4.1.10) in the deep soil.

Additionally, iron can be used as an energy source/electron donor by ferrous oxidation bacteria to reduce nitrate autotrophically in reduced iron environments (Lowrance and Pionke, 1989; Straub et al. 1996; Hauck et al. 2001). We did see iron-rich layers in some wells (e.g., M-0772, M-0773, M-0774, M-0777, M-0779/0780/0781, and M-0786). Thus, though we did not measure any significant DEA rates, it is possible that other nitrate removal pathways could happen.

Comparison of the DEA rates with and without the addition of glucose tests whether carbon is a limiting factor for denitrification (Figure 4.1.16). This analysis showed that only the soils in the sites of M-0773 and M-0774 would be limited by carbon for denitrification. We did not find a highly significant correlation between any of the measured nutrient parameters and rates of DEA, but the DEA rates were more likely to be controlled by extractable nitrate and carbon (Figure

4.1.17). For this reason we constructed the following stepwise regression model as a potential predictor of DEA in soils of the springshed. In this analysis, total nitrogen was the most influential variable followed by extractable nitrate, with minimal contributions from extractable organic carbon, phosphorus or moisture content.

$$DEA=-0.06-0.03*MC+0.0002*TP+0.99*TN+0.21*Ext.\ NO_3\text{-}N-0.004*Ext.\ TOC,\ R^2 = 0.67$$

4.1.4.4 Stable Isotope Profiles

Sources of nitrogen in groundwater systems are frequently inferred based on the isotopic composition of nitrate (Fogg et al. 1998) where various N sources have distinct isotopic composition ranges in $\delta^{15}N$ and $\delta^{18}O$ (Figure 4.1.17, Kendall and McDonnel 1999). Based on changes in groundwater nitrate isotopic composition, it is also possible to infer and calculate denitrification and other N loss processes, but with the caveat that isotopic composition of nitrate sources is known (Xue et al. 2009).

Patterns of stable isotopes of nitrate ($\delta^{15}N$, $\delta^{18}O$) measured in selected profiles of this study indicate a potential confirmation of movements of nitrate throughout profiles as well as location of major denitrification rates in the surface (Figure 4.1.18). The lowest isotopic values of both nitrogen and oxygen were observed at M-0774 indicating the predominance of other ammonium fertilizer or soil organic N sources. In contrast, much higher $\delta^{18}O$ values indicate an increased source of nitrate fertilizer at both M-0776 and M-0782/0787 sites (Figures 4.1.18 and 4.1.19). The patterns observed at the M-0786 are puzzling as they tend to indicate a significant nitrification effect (e.g., lower $\delta^{15}N$ of nitrate than soil total nitrogen and low $\delta^{18}O$) and do not exhibit the high $\delta^{15}N$ characteristic of wastewater which is the suspected dominant matter to source at this site (Figures 4.1.18 and 4.1.19).

Complicating the interpretation of these isotopic patterns is the fact that in most cases the observed signature likely represents a mixture of nitrogen sources which may vary seasonally. Also, interaction between nitrate in the soil particles may also result in fractionation of isotopic signals during infiltration (Ledgard et al. 1984). Because this study assessed extractable nitrate, this type of isotopic interaction could appear as an isotopic enrichment in our measured value when nitrate is preferentially held by the soil particles. As the extractant used in this study was water, this effect should be minimal and the observed isotopic signatures should reflect the "leachable" nitrate. Further, in the sandy soils of this region, interaction between nitrate and the soil should be minimal; however, iron oxide coatings observed in these profiles have shown potential to interact with nitrogen forms (Huang et al. 2003; Jones et al. 2015).

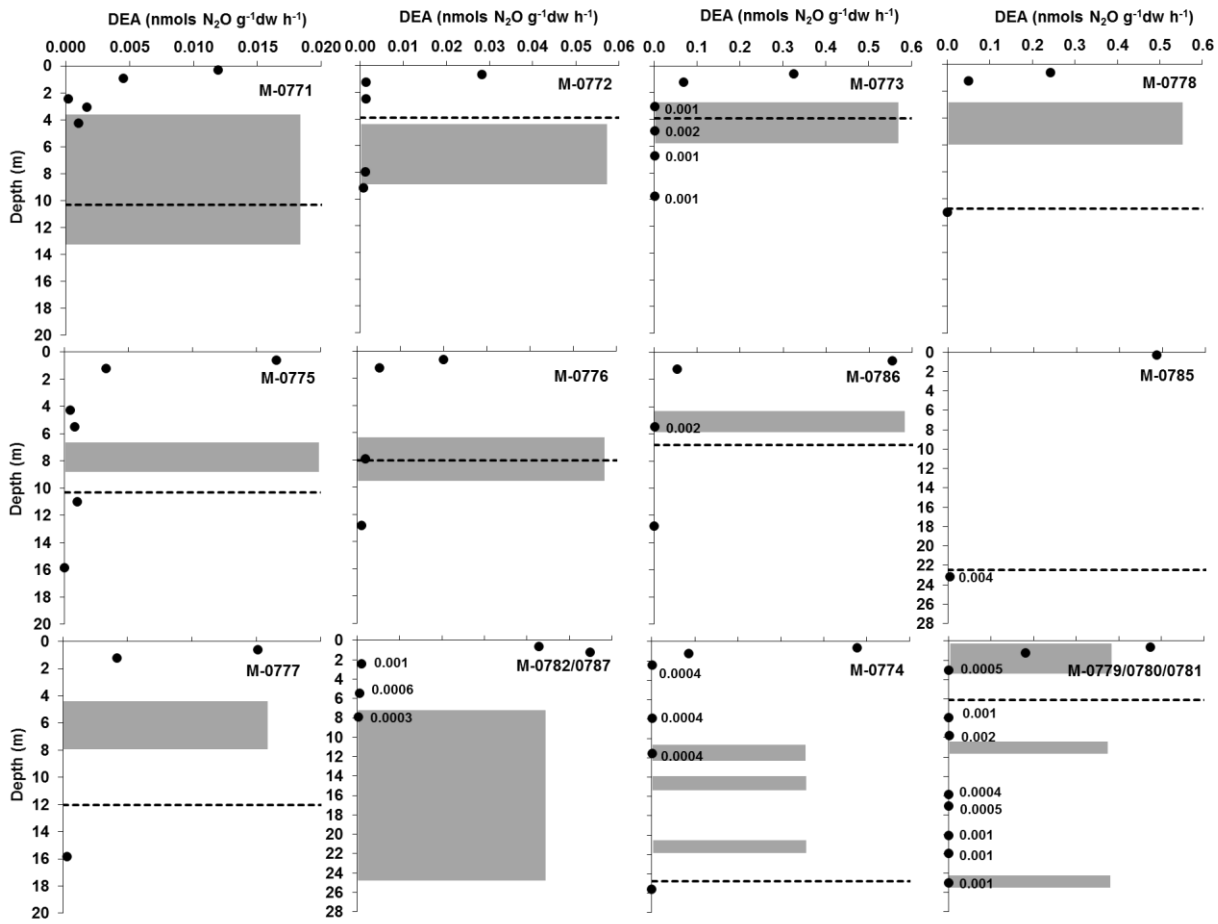

Figure 4.1.15. Vertical profiles of denitrfication enzyme activity (DEA) in soil and vadose zone profiles for the 12 study wells. The gray areas and the dash lines represent the clay layers and the water table, respectively.

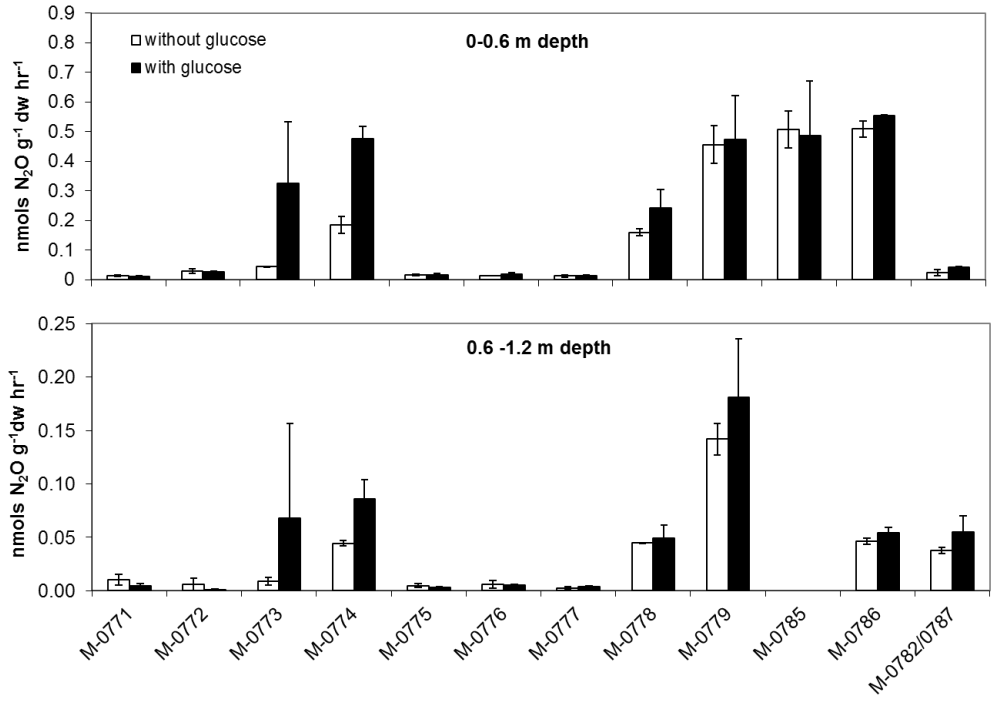

Figure 4.1.16. Comparison of denitrfication enzyme activity (as production of N_2O) with and without added glucose in soil and vadose zone profiles for the 12 study wells.

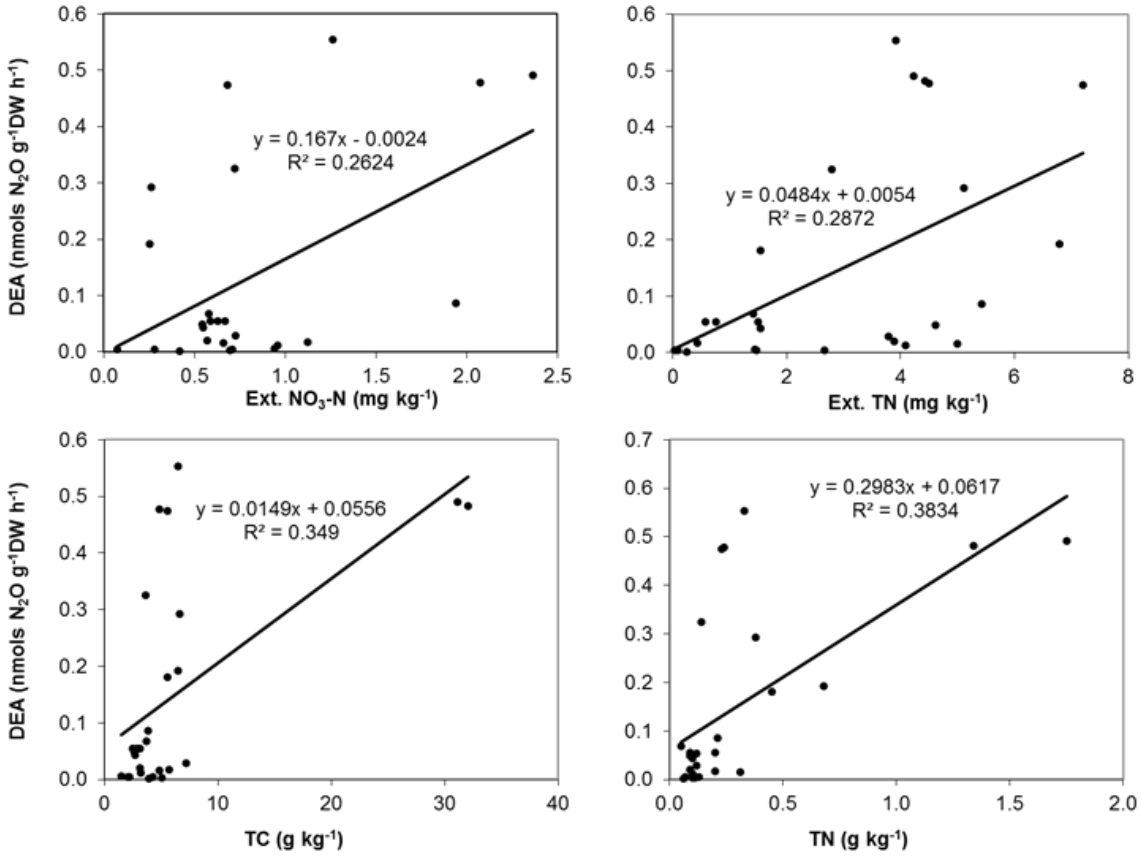

Figure 4.1.17. Correlations of denitrfication enzyme activity (DEA) with with total and extractable carbon and nitrogen parameters in soil and vadose zone profiles for the 12 study wells.

Steady enrichment of both oxygen and nitrogen isotopes in the upper 2 m of the profile at M-0774 and M-0782/0787, as well as at depths up to 4-5 m in the M-0786 and M-0776 sites indicate active denitrification in all of the profiles. In M-0774, continued enrichment of both ^{15}N and ^{18}O of nitrate with depth may indicate continued denitrification throughout the soil and vadose zone. This continued enrichment may also indicate that the surface nitrogen is also the source of nitrogen to the groundwater in this area. In contrast, at the M-0782/0787, M-0776, M-0786 sites, isotopic values for nitrate in the surface appeared decoupled from those observed in groundwater. At the M-0782/0787 site there appeared to be three regions of isotopic patterns including the surface extending down to the first clay layer at 7 m, an intermediate region from the water table at 18 m down to 35 m, and a third distinct isotopic signal from the clay layer encountered at 35 m to the bottom of the profile. It is unclear what is driving these observed differences, however these observations highlight the difficulty in potentially ascribing isotopic signals in wells to the land use in the immediate vicinity.

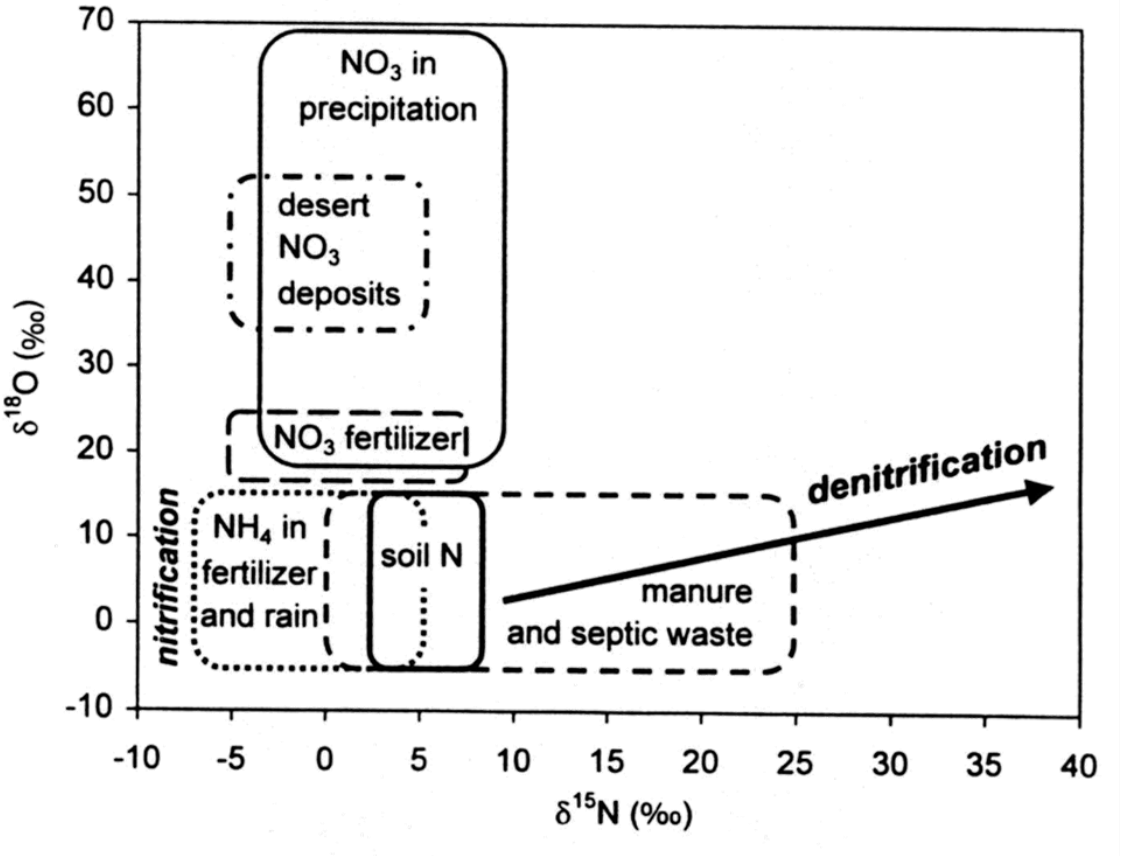

Figure 4.1.18. Schematic of typical ranges of $\delta^{18}O$ and $\delta^{15}N$ of nitrate from various sources as well as the isotopic effect of denitrification. (Adapted from http://wwwrcamnl.wr.usgs.gov/isoig/isopubs/Fig16-9.jpg)

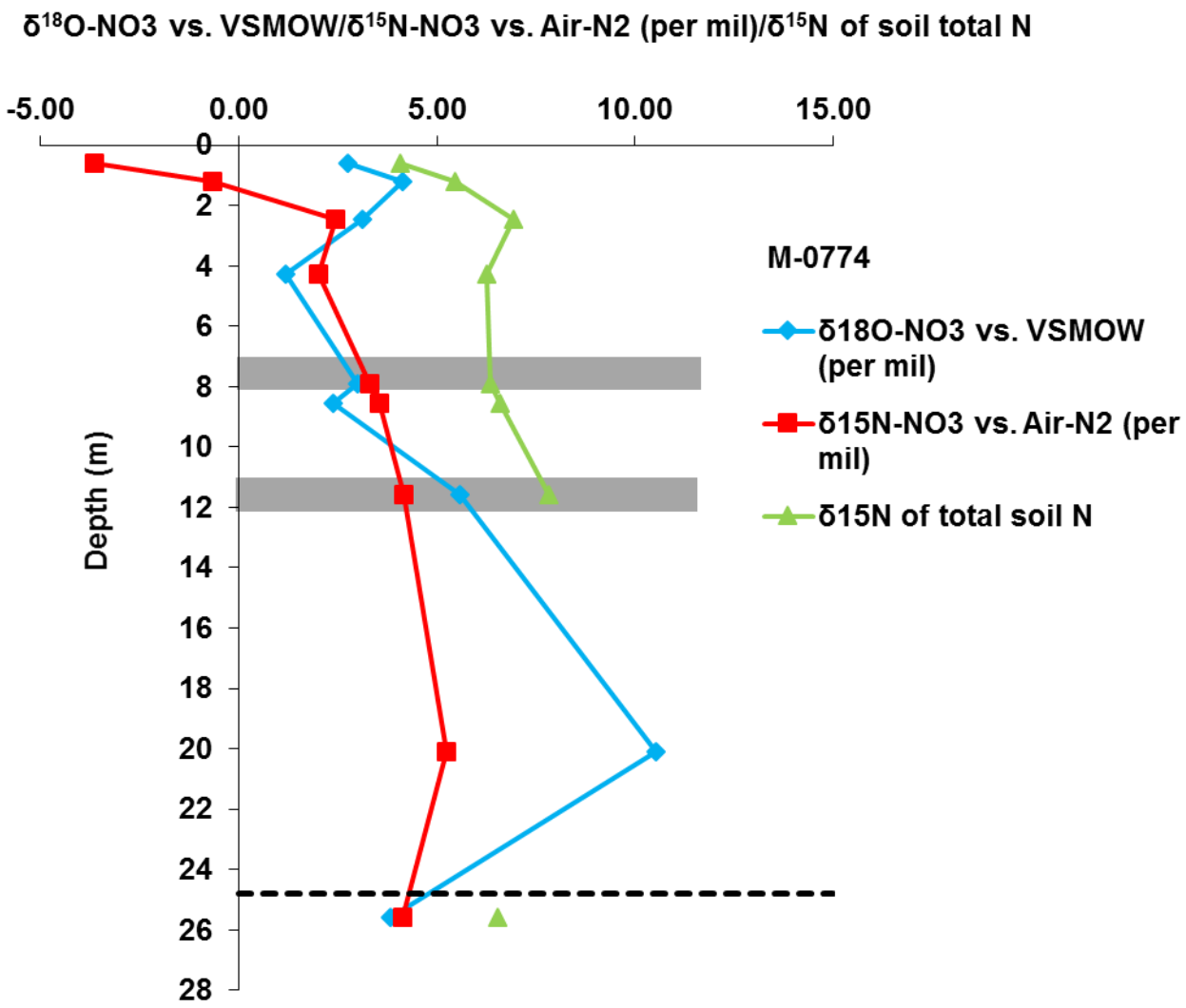

Figure 4.1.19. Vertical profiles of $\delta^{18}O$ and $\delta^{15}N$ of nitrate and $\delta^{15}N$ of total bulk N in soil and vadose zone profiles for the M-0774 site. The gray areas and the dash lines represent the clay layers and the water table, respectively.

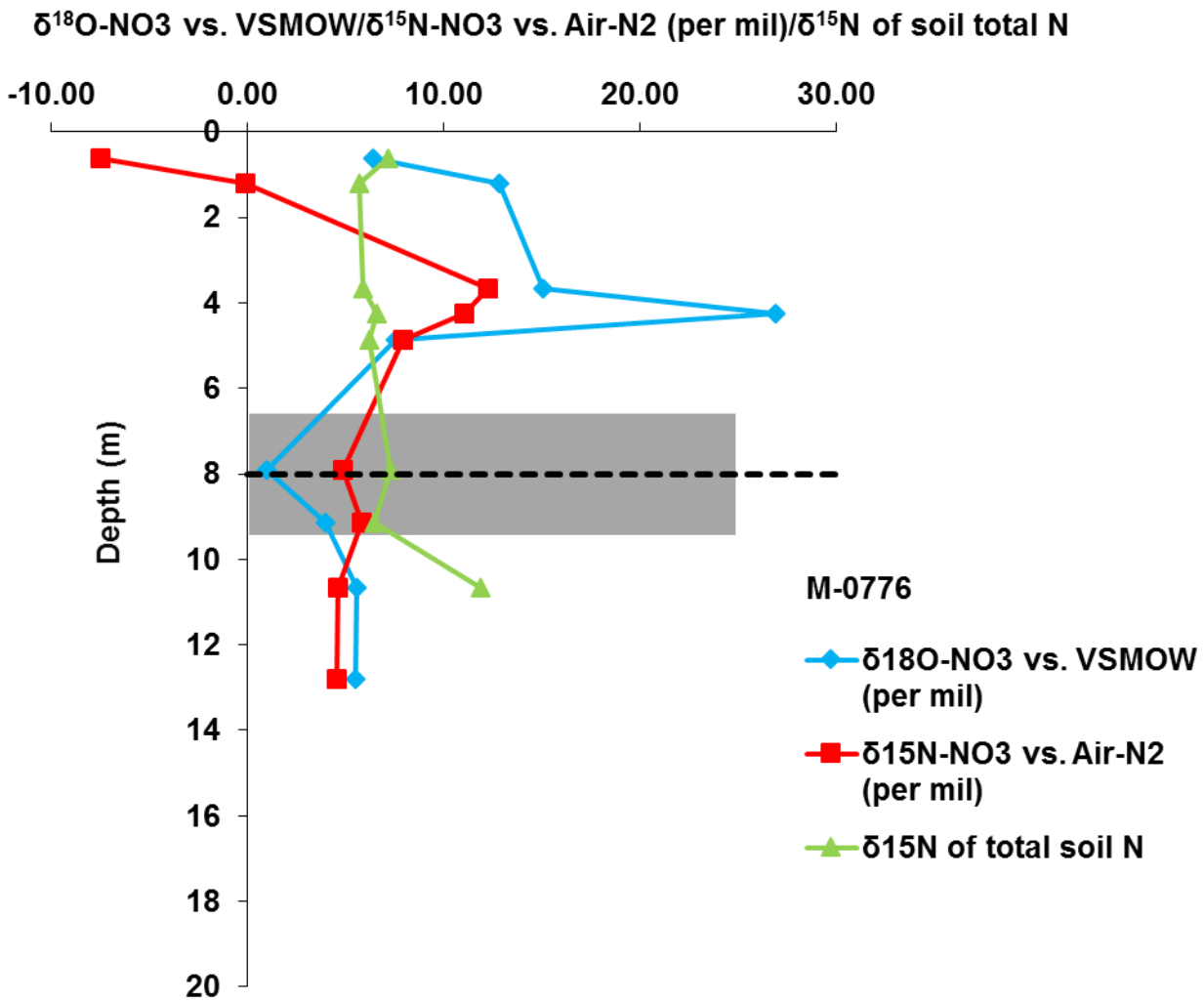

Figure 4.1.19 (cont.). Vertical profiles of $\delta^{18}O$ and $\delta^{15}N$ of nitrate and $\delta^{15}N$ of total bulk N in soil and vadose zone profiles for the M-0776 site. The gray areas and the dash lines represent the clay layers and the water table, respectively.

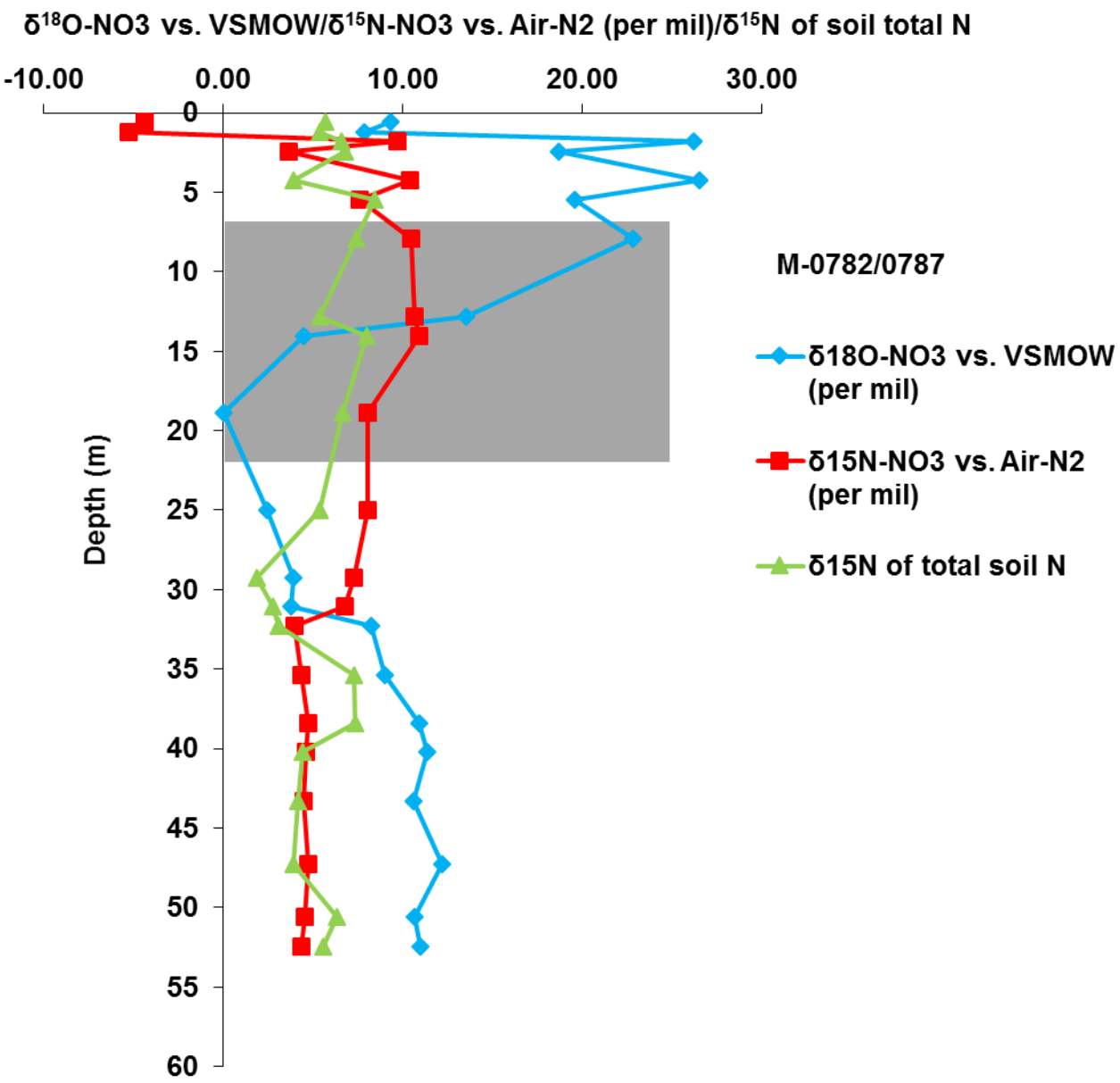

Figure 4.1.19 (cont.). Vertical profiles of $\delta^{18}O$ and $\delta^{15}N$ of nitrate and $\delta^{15}N$ of total bulk N in soil and vadose zone profiles for the M-0782/0787 site. The gray areas and the dash lines represent the clay layers and the water table, respectively.

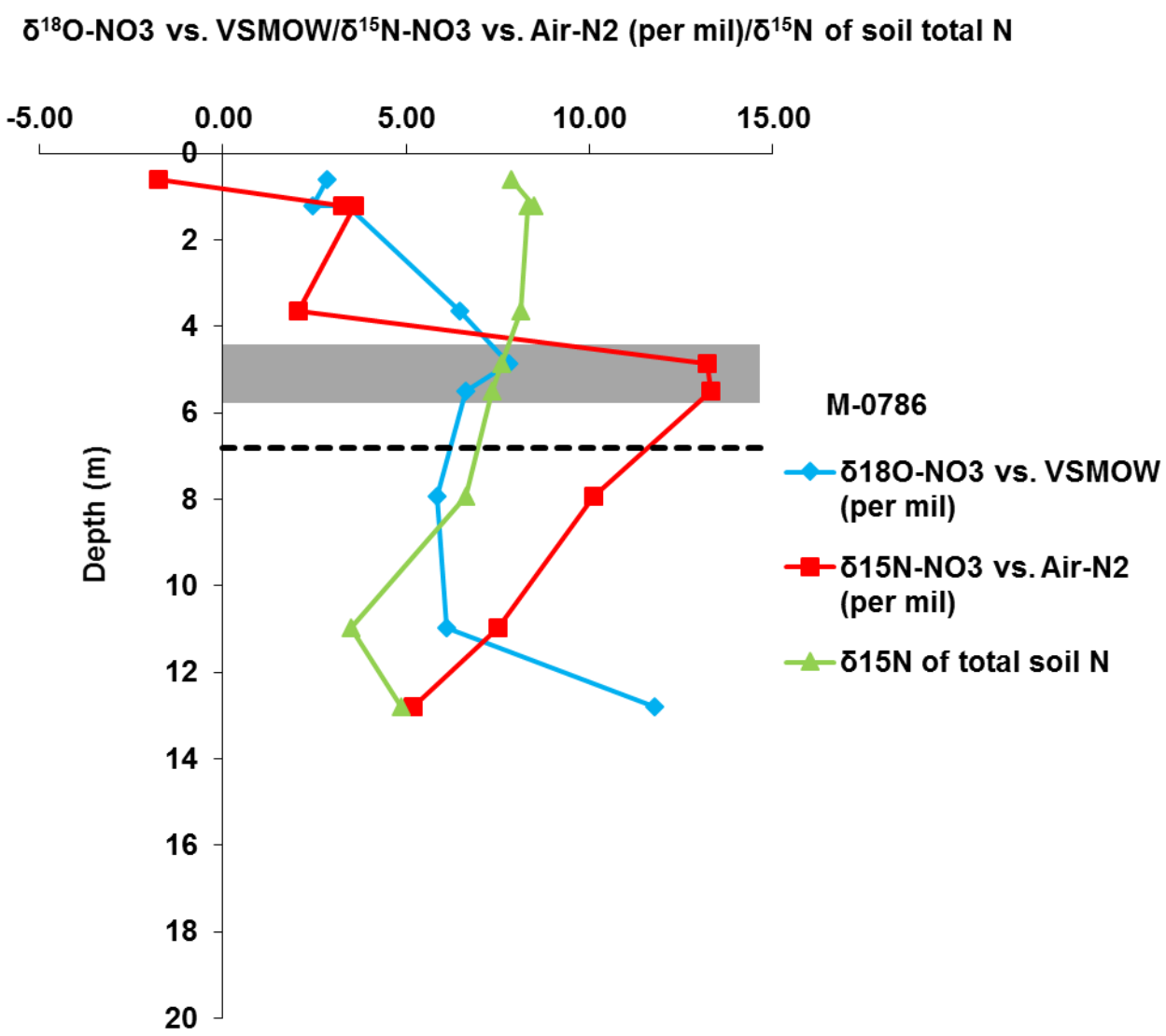

Figure 4.1.19 (cont.). Vertical profiles of $\delta^{18}O$ and $\delta^{15}N$ of nitrate and $\delta^{15}N$ of total bulk N in soil and vadose zone profiles for the M-0786 site. The gray areas and the dash lines represent the clay layers and the water table, respectively.

4.1.5 CONCLUSIONS AND RECOMMENDATIONS

Except where deeper layers contain appreciable organic C or S, most denitrification occurs in the topsoil and down to a depth of 3 m. During the timescale of the experiments used in this study, aquifer materials of carbonate show very little if any denitrification ability. This does not imply that there is no denitrification in the aquifer, but current techniques may not facilitate its direct measurement. This highlights the importance of other indirect measures of denitrification, such as dissolved gases and stable isotope measurements.

The surface materials of this study poorly represented their intended land use, particularly those where heavy nitrogen loads were expected. In these types of soils, N content is the most limiting factor affecting denitrification. Stable isotopic patterns in the soil/vadose zone profiles indicate the potential for isotopic tracing (unique surface source characteristics), but alteration of these signals with denitrification and possible physical interaction with clays for other reactive surfaces warrant the use of extreme caution in interpreting groundwater signatures as indications of land use/loading.

4.1.5.1 Future Research Needs

It is clear from the results obtained thus far that there is a strong need better relationship for N/C control of denitrification. We are currently conducting incubations of soils with various N loading levels to derive more accurate relationships between denitrification, moisture content, and temperature. The observed patterns of stable isotopic ratios of nitrate indicate promise for using this measurement to indicate N potential to calculate denitrification rates in the soil and vadose zone. Before this technique can be utilized, a comparison of these measured values with actual nitrate leaching from soil cores or profiles should be conducted.

Use of the stable isotopic ratios as nitrogen source tracking will also be improved with a better geochemical analysis of groundwater (e.g., elemental and ion ratios) as well as the use of boron concentration and isotopic ratios. We are currently preparing samples for boron isotope analyses. We are also awaiting results of the molecular analyses of microbial communities in the soil and vadose materials collected in this study. When obtained, these results should shed light on some of the observed denitrification patterns which may be associated with given soil types and land use combinations.

4.1.6 REFERENCES

Anderson JM, 1976. An ignition method for determination of total phosphorus in lake sediments. Water Research, 10: 329–331.

Andersson H, Bergström L, Djodjic F, Ulén B, Kirchmann H, 2013. Topsoil and subsoil properties influence phosphorus leaching from four agricultural soils. Journal of Environmental Quality, 42: 455-463.

Barton L, McLAY CDA, Schipper LA, Smith CT, 1999. Annual denitrification rates in agricultural and forest soils: a review. Australian Journal of Soil Research, 37(6): 1073-1094.

Böttcher J, Strebel O, Voerkelius S, Schmidt HL. 1990. Using isotope fractionation of nitrate nitrogen and nitrate oxygen for evaluation of microbial denitrification in a sandy aquifer. Journal of Hydrology, 114: 413–24.

Brettar I, Rheinheimer G, 1991 Denitrification in the Central Baltic: evidence for H2S-oxidation as motor of denitrification at the oxic–anoxic interface. Marine Ecology Progress Series 77:157–169.

Burgin AJ, Hamilton SK, 2007. Have we overemphasized the role of denitrification in aquatic ecosystems? A review of nitrate removal pathways. Frontiers in Ecology and the Environment, 5: 89–96.

Djodjic F, Börling K, Bergström L, 2004. Phosphorus leaching in relation to soil type and soil phosphorus content. Journal of Environmental Quality, 33:678–684. doi:10.2134/jeq2004.0678.

Feast NA, Hiscock KM, Dennis PF, Andrews JN, 1998. Nitrogen isotope hydrochemistry and denitrification within the chalk aquifer system of north Norfolk, UK. Journal of Hydrology, 211(1-4): 233-252.

Fogg G E, Rolston DE, Decker DL, Louie DT, Grismer ME, 1998. Spatial variation in nitrogen isotope values beneath nitrate contamination sources. Groundwater, 36(3): 418-426.

Hauck S, Benz M, Brune A, Schink B, 2001. Ferrous iron oxidation by denitrifying bacteria in profundal sediments of a deep lake (Lake Constance), FEMS Microbiology Ecology, 37(2): 127-134.

Huang YH, Zhang TC, Shea PJ, Comfort SD, 2003. Effects of Oxide Coating and Selected Cations on Nitrate Reduction by Iron Metal. Journal of Environmental Quality, 32(4): 1306-1315.

Jannasch HW, Mott MJ, 1985. Geomicrobiology of deep-sea hydrothermal vents. Science, 229(4715): 717-725 .

Jones LC, Peters B, Pacheco JSL, Casciotti KL, Fendorf S, 2015. Stable Isotopes and Iron Oxide Mineral Products as Markers of Chemodenitrification. Environmental Science & Technology, 49(6): 3444-3452.

Katz BG, Sepulveda AA, Verdi RJ, 2009. Estimating Nitrogen Loading to Ground Water and Assessing Vulnerability to Nitrate Contamination in a Large Karstic Springs Basin, Florida. Journal of the American Water Resources Association, 45: 607-627.

Kendall C, McDonnell JJ, eds. *Isotope tracers in catchment hydrology*. Elsevier, 1999.

Ledgard SF, Freney JR, Simpson JR, 1984. Variations in natural enrichment of ^{15}N in the profiles of some Australian pasture soils. Australian Journal of Soil Research, 22: 155-164.

Lowrance RR, Pionke HB, 1989. Transformations and movement of nitrate in aquifer systems. In: Follett (Ed.) 1989. Nitrogen management and ground water protection. pp. 373-392.

Manconi I, Carucci A, Lens P, 2007. Combined removal of sulfur compounds and nitrate by autotrophic denitrification in bioaugmented activated sludge system. Biotechnology and Bioengineering, 98(3): 551-560.

Peltovuori T, 2007. Sorption of phosphorus in fi eld-moist and air-dried samples from four weakly developed cultivated soil profi les. Eur. J. Soil Sci. 58:8– 17. doi:10.1111/j.1365-2389.2006.00789.x.

Phelps GG (2004). Chemistry of Ground Water in the Silver Springs Basin, Florida, with an emphasis on Nitrate. USGS.

Pizzeghello D, Berti A, Nardi S, Morari F, 2014. Phosphorus-related properties in the profiles of three Italian soils after long-term mineral and manure applications. Agriculture, Ecosystems & Environment, 189: 216-228.

Scott TM, 1988. The lithostratigraphy of the Hawthorn Group (Miocene) of Florida: Florida Geological Survey Bulletin 59, 148 p.

Scott TM, Campbell KM, Rupert FR, Arthur JD, Missimer TM, Lloyd JM, Yon JW, Duncan JG, 2001, Geologic map of the State of Florida: Florida Geological Survey Map Series 146, 1 map sheet, [accessed 12/16/2003] http://www.dep.state.fl.us/geology/gisdatamaps/index.htm.

Shao MF, Zhang T, Fang HHP, 2010. Sulfur-driven autotrophic denitrification: diversity, biochemistry, and engineering applications. Applied microbiology and biotechnology, 88: 1027-1042.

Smith MS, Tiedje JM, 1979. Phases of denitrification following oxygen depletion in soil. Soil Biology and Biochemistry, 11(3): 261-267.

Sokal RR, Rohlf FJ, 1995. Biometry. W.H. Freeman, New York.

Straub KL, Benz M, Schink B, Widdel F, 1996. Anaerobic, nitrate-dependent microbial oxidation of ferrous iron. Applied Environmental Microbiology 62: 1458–1460.

Wlodarczyk T, Stepniewska Z, Brzezinska M, 2003. Denitrification, organic matter, and re- dox potential transformations in Cambisols. International Agrophysics, 17: 219-227.

Vaiopoulou E, Melidis P, Aivasidis A, 2005. Sulfide removal in wastewater from petrochemical industries by autotrophic denitrification. Water Research, 39(17): 4101-4109.

van Beek CL, van der Salm C, Plette ACC, van de Weerd H, 2009. Nutrient loss pathways from grazed grasslands and the effect of decreasing inputs: Experimental results for three soil types. Nutrient Cycling Agroecosystem, 83:99–110. doi:10.1007/s10705-008-9205-z.

Xue D, Botte J, De Baets B, Frederik Accoe, Angelika Nestler, Philip Taylor, Oswald Van Cleemput, Michael Berglund, Pascal Boeckx, 2009. Present limitations and future prospects of stable isotope methods for nitrate source identification in surface-and groundwater. Water research 43(5): 1159-1170.

Section 4.2 Dissolved Gases and Stable Isotopes of Nitrate in Silver Springs Vents

4.2.1 ABSTRACT

Dissolved gases and stable isotopic ratios are useful indicators of groundwater conditions and processes such as denitrification. This study focuses on measurements of dissolved gases (methane, nitrous oxide, N_2, and argon) and stable isotopic ratios ($\delta^{18}O$ and $\delta^{15}N$) of nitrate in spatially distributed wells and the headspring vent of the Silver Springs springshed. Concentrations of dissolved methane and nitrous oxide showed a wide range in wells of the springshed. Methane was correlated with several chemical parameters including concentrations of both nitrate and ammonium, while nitrous oxide was only significantly correlated with chloride content. Patterns of stable isotopic ratios of nitrate in well samples indicated the potential dominance of fertilizer nitrate sources and enrichments due to denitrification. Similar findings were observed in the east and west vents of Mammoth headspring. Differences were observed between the vents as well as with sampling date, with larger amounts of N_2 gas being found in the west vent. Seasonal variability coincided with similar variability in nitrate stable isotopic ratios indicating variable amounts of denitrification in the Floridan Aquifer System.

4.2.2 INTRODUCTION

In addition to understanding N attenuation in the soil and vadose zone, denitrification within the Floridan Aquifer System (FAS) may also remove nitrate after it has passed through the unsaturated zone. It was recently estimated that 32% of the N load to the FAS in North and Central Florida is removed by denitrification in the aquifer prior to emergence at springs (Heffernan et al. 2012). This loss of N in the aquifer may be underestimated in groundwater models, which generally assume negligible denitrification rates in the FAS. Measurements of excess N_2 (the end product of denitrification) and stable isotopes of nitrate ($\delta^{15}N$ and $\delta^{18}O$) from the Silver Springs main vent has not provided clear evidence for denitrification within the FAS (Phelps 2004). However, multiple sources of nitrate and a varying contribution of young and old groundwater may obscure any denitrification signal at the spring vent.

It has been demonstrated that the different vents of the Silver Springs group represent a variety of potentially different groundwaters from the springshed (Osmond et al. 1974; Phelps 2004). Likewise, there is also high potential for these different groundwaters to reflect different N sources and potential for attenuation of N loading to the Silver River. The sources and attenuation processes are also likely to be seasonal in nature varying with both intensity of groundwater discharge and changes in landuse activities.

Heffernan et al. (2012) demonstrated that analysis of dissolved gases and stable isotopic composition of nitrate can be used to indicate the percentage of nitrogen present in samples of spring water that has been removed by the process of denitrification during transit to the spring

vent. Thus, seasonal changes in these indicators of denitrification could serve as a powerful tool to identify covarying springshed or climate-related processes which contribute to the observed nitrogen attenuation within the FAS.

4.2.3 MATERIALS AND METHODS

4.2.3.1 Site Description

The Silver Springs springshed covers more than 300,000 ha in north-central Florida, occurring primarily in the counties of Alachua and Marion (Phelps 2004). The climate of the region (measured at Ocala, FL) is humid sub-tropical with a warm wet season (June-October) and a cool dry season (November-May). Approximately 51 inches of rainfall occurs annually and the mean annual temperature is approximately 22°C (http://www.usclimatedata.com/).

Silver Springs, the largest of Florida's first magnitude springs, (Scott et al.2004; Rosenau et al.1977) discharges approximately >500 million gallons per day [mgd]) from the Floridan Aquifer (Osburn et al. 2002) and is also likely the largest limestone spring in the United States (Rosenau et al.1977). Silver 'head' spring consists of 2 primary vents (East and West) which represent on average, about 45% of flow in the Silver River is from Silver Main Spring.

4.2.3.2 Sampling

Twelve wells installed in the first phase of this project were used to sample groundwaters throughout the springshed. These wells locations were chosen to represent various land uses and to approximately capture the geologic hydrostratigraphy and travel times of water within the spring shed. Water samples were collected from these wells in the spring of 2015 for determination of chemical constituents (nutrients and metals), dissolved gas composition (N_2, Ar, CH_4, and N_2O), and stable isotopic composition of nitrate. In addition to these wells, the Water Management District routinely samples a suite of groundwater wells in the area. Water samples were collected from all wells for chemical analyses and determination of isotopic composition of nitrate.

Well water samples were collected using a Grundfos Redi-flo II submersible well pump. Water samples for nutrients and isotopes were collected into rinsed polyethylene bottles and stored either at 4°C (nutrients and metals) or frozen (nitrate stable isotopes). Water samples for dissolved gases were collected by adjusting be pump flow rate to approximately 4 L per minute and eliminating bubbles from all tubing. Samples were collected underwater with no gaseous headspace into either 160 mL serum bottle (dissolved methane and nitrous oxide) or 22 mL glass tubes with polyseal caps (N_2/Ar).

Water samples were collected from the Silver Spring vents (East and West) quarterly in 2014 and every other month beginning in January 2015. Samples for nutrients, metals, and stable isotope of nitrate were collected by the water management district in their routine sampling. Samples for dissolved gases (CH_4, N_2O, N_2, and Ar) were collected inside the vents by divers using double ended glass tubes sealed at both ends with septa caps.

4.2.3.3 Sample Analysis-

Analyses for nutrients and metals were conducted by the St. John's River Water Management District certified analytical laboratory while the samples for stable isotopic composition of nitrate were shipped on ice to the Facility for Isotope Ratio Mass Spectrometry at the University of California, Riverside.

The determination of dissolved methane and nitrous oxide followed the EPA method (Kampbell and Vandegrift 1998). Briefly, a headspace was prepared by displacing 10% of the water with high purity helium (He). The bottles were shaken for five minutes and specific volumes of headspace samples were injected onto gas chromatographic (GC) columns. For our purposes, 1,000 μL headspace gas samples were measured for methane (CH_4) on a Shimadzu GC-14-A gas chromatograph equipped with a flame ionized detector (FID) with column and detector/injector port temperatures of 110^{o}C and 160^{o}C, respectively. Similarly, 500 μL from the bottle headspace was analyzed for nitrous oxide (N_2O) using a GC-ECD with column, injection port, and detector temperatures of 70, 120, and 230°C, respectively.

Analysis of dissolved N_2 and Ar was conducted using a membrane mass spectrometer (Inglett et al. 2013) using water standards at 20 and 30°C to calibrate the measurement.

4.2.4 RESULTS AND DISCUSSION

4.2.4.1 Ground Water Patterns of Dissolved Gases and Stable Isotopes

The underground water in the well M-0774 had high dissolved N_2O concentration with the average of 32.5 ± 0.4 μg L^{-1}, followed with that in the wells of M-0776 (23.4 ± 0.1 μg L^{-1}), and the well M-0771 (21.0 ± 0.4 μg L^{-1}). For the cluster of wells of M-0779/0780/0781, the dissolved N_2O concentration in the shallow well M-0781 (10.7 m depth) was higher (14.4 ± 1.0 μg L^{-1}) compared to the other two wells with the average of 4.9 ± 0.4 μg L^{-1} for the 21 m-deep well (M-0780) and 5.2 ± 0.2 μg L^{-1} for the 44 m-deep well (M-0779) (Figure 4.2.1). Those values fell in the range of the same land use reported by others (Table 4.2.2, Hiscock et al. 2003).

Formation of nitrous oxide in the groundwater is predominately controlled by incomplete nitrification and denitrification reactions, and therefore could potentially be associated with various indicators of denitrification including low oxygen, or the presence of potential electron donors (e.g., organic carbon, sulfide, or methane) (Jahangir et al. 2013). If this is indeed the case, nitrous oxide levels (which are stable under most groundwater conditions) could be used as a sensitive indicator of potential nitrification and denitrification within the groundwater system.

In the limited data set of this study, we did not observe a significant correlation of nitrous oxide levels in groundwater with any of these potential indicators of denitrification. We did observe a significant correlation between dissolved N_2O and water Cl^- (r = 0.82, P <0.01, Table 4.2.2), indicating a possible interaction (through denitrification or DNRA) of nitrate- containing waters with a deeper anoxic, marine derived aquifer (Molofsky et al. 2013). Alternatively, of nitrous oxide with chloride could indicate dominance of nitrogen sources from wastewater treatment or septic systems which are also enriched in chloride (McQuillan 2004).

Based on the dissolved oxygen levels in the groundwater, the high N_2O in the wells of M-0779/0780/0781 was likely controlled by incomplete denitrification because of the low DO (0.12-0.32 mg L^{-1}) and low nitrate (1.78-2.49 µM). In contrast, for other wells, the N_2O may be more likely to correlate with nitrification because of the comparatively high DO (>1 mg L^{-1}) and nitrate (>10 µM). For example, Hiscock et al. (2013) observed a positive correlation between NO_3^- and N_2O for Chalk groundwater samples indicating that nitrification was the principal production mechanism for N_2O.

Overall, dissolved methane levels were low in most of the study wells with the exception of the M-0779/0780/0781 site where methane levels averaged 60.8 ± 13.8 µg L^{-1}, 472.8 ± 21 µg L^{-1}, 84.8 ± 6.1 µg L^{-1} for the depths of 44 m, 21 m, and 10.7 m, respectively (Figure 4.2.1). The high level of dissolved methane in these wells, especially for the 21 m depth well, would be related to the hydrogen sulfide and low oxygen level (0.12-0.32 mg L^{-1}). Heisig and Scott (2013), for example, reported that in south-central New York states, in the wells with methane concentration of 0.5 mg L^{-1} or greater, the concentration of dissolved oxygen was 0.2 mg L^{-1} or less and hydrogen sulfide was detected. We did not measure the hydrogen sulfide concentration but did see the significantly negative correlation between dissolved methane and dissolved oxygen (Table 4.2.2). The significant negative correlation between dissolved CH_4 and NO_X-N and NH_4-N indicate the possibility of alternate nitrate reduction pathways coupled to anaerobic methane oxidation (Ettwig et al. 2010; Haroon et al. 2013).

$$CH_4 + 4NO_3^- \rightarrow CO_2 + 4NO_2^- + 2H_2O$$
$$3CH_4 + 8NO_2^- + 8H^+ \rightarrow 3CO_2 + 4N_2 + 10H_2O$$
$$CH_4 + NO_3^- + 2H^+ \rightarrow CO_2 + NH_4^+ + H_2O$$

Stable isotopes of nitrate in water samples collected from the wells in this study showed similar ranges of enrichment in $\delta^{15}N$ (1.4-18.4 ‰) and $\delta^{18}O$ (-0.5-21.9 ‰) (Table 4.2.3). According to traditional isotopic values of nitrogen sources, these ranges tend to indicate a predominance of ammonium fertilizer and soil nitrogen followed by nitrate fertilizer sources in the wells of this study (Figure 4.1.18). With the assumption that denitrification proceeds in an approximate 1:1 (Granger et al. 2008) to 2:1 (Aravena and Robertson 1998; Lehmann et al. 2003) enrichment ratio, most of the isotopic values for nitrate in these aquifer samples can be explained by denitrification of the original nitrogen sources indicated above (Figure 4.2.2).

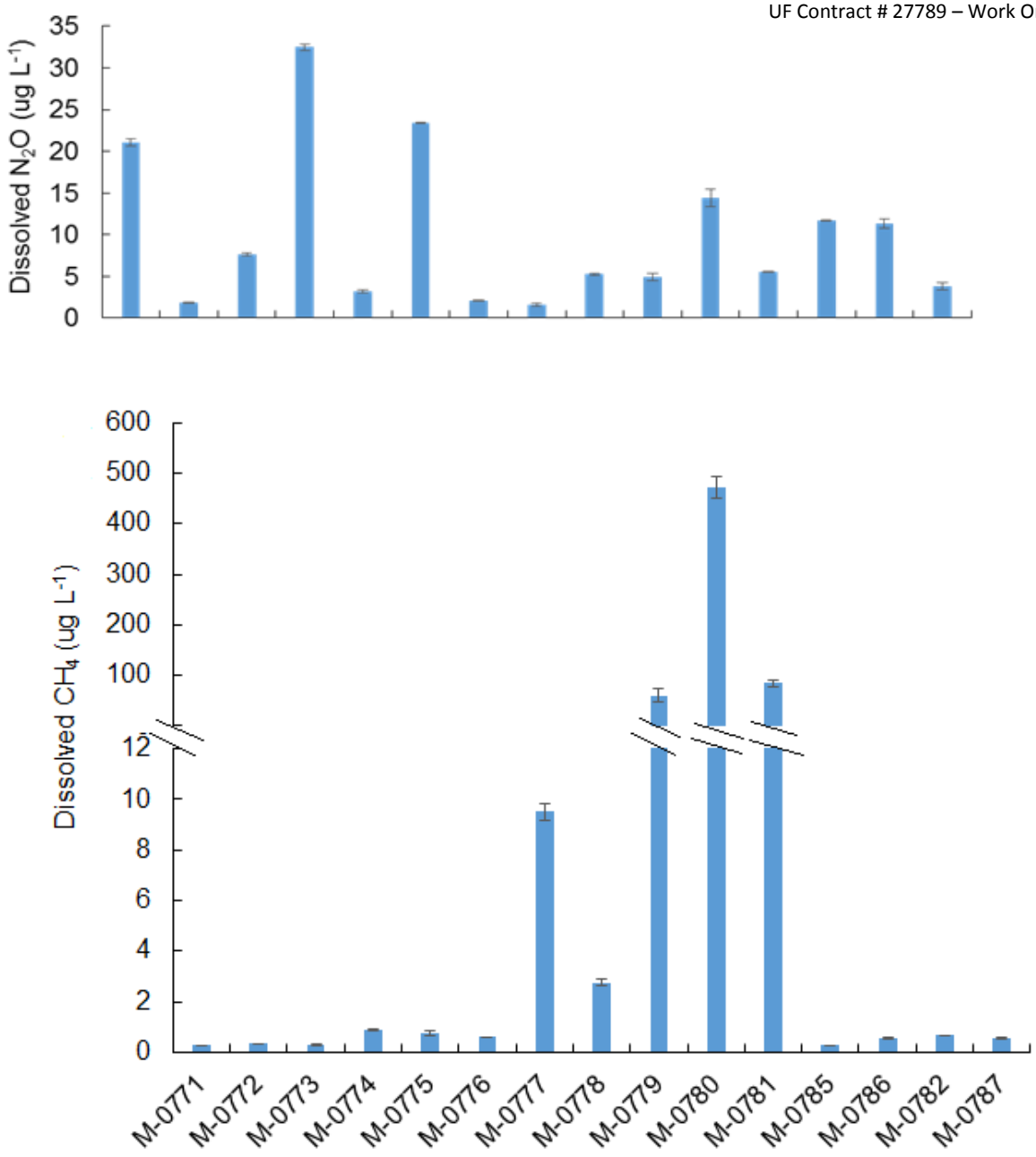

Figure 4.2.1. Measured concentrations of dissolved gases (CH_4 and N_2O) in water samples collected from the 12 study wells installed for this project.

Table 4.2.1. Significant correlation of dissolved CH_4 and N_2O with selected properties of groundwaters sampled in the study wells (based on incomplete dataset).

Parameter, y	**Parameter, x**	**Spearman ρ**	**Prob>|ρ|**
Dissolved N_2O	Cl^-	0.8182	**
Dissolved CH_4	DO	-0.5827	*
	TOC	0.7133	**
	NH_4-T	0.7321	**
	NOx-T	-0.6857	**
	Water Temp	-0.6679	**
	Alkalinity	0.5214	*

**-$P < 0.01$, *-$P < 0.05$

Table 4.2.2. Comparison of N_2O concentrations for subsurface waters from aquifers and agricultural drainage (adopted from Hiscock et al. 2003).

aquifer (unconfined)	land use	N_2O (µg L^{-1})
Chalk, Cambs, and Norfolk	arable	6.6-84.8 (26.5)
Chalk, Cambridgeshire	arable	6.9-169.7 (52.3)
weathered bedrock, England and Scotland	uncultivated upland	0.5-2.1 (1.2)
poorly consolidated clay, silt, sand, and gravel	rangeland, arable and cattle	0.04-41.4 (1.3)
alluvium, sands, and gravels	urban, forest, and cropped field soils	0.7-310.6 (30.4)
sand	woodland with manure disposal	11-22
karstic limestone	sewage effluent disposal	4.0-13.2
sand	sewage effluent disposal	83.6-396
clay soils, agricultural drains	arable	0.5-15689 (96.8)
alluvial riparian zone underlain by clay aquiclude	maize, riparian forest	(756.8)
clay and loess soils, agricultural drains	grassland	<6.292
	mixed arable and grass	<94.3
hydromorphic silty clay loam soils, shallow water table	arable and pasture	9.4-957.9

4.2.4.2 Seasonal Patterns of Dissolved Gas and Stable Isotopes in the Spring Vents

The concentrations of dissolved N_2O gas for the spring vents were in the range of 4 to 9 µg L^{-1} (Figure 4.2.3). The values in the east vent were significantly higher than those in the west vent for March and April samplings, which would attribute to the higher NO_3-N concentration typically observed in the east vent (Butt and Aly 2008). The dissolved CH_4 in the spring vents fell in the range of 0.4-1.6 µg L^{-1}, with higher values in the east vents (Figure 4.2.3). Concentrations of both methane and nitrous oxide were variable with sampling date, but it is difficult to draw any conclusions regarding a seasonal pattern with such a limited dataset.

Table 4.2.3. Values of $\delta^{18}O$ and $\delta^{15}N$ of nitrate in samples collected from the monitoring wells in the Silver Springs springshed.

Well ID	Sampling date	NO_3 (µM)	$\delta^{18}O$-NO_3 vs. SMOW (‰)	$\delta^{15}N$-NO_3 vs. Air-N_2 (‰)
M0419	1/20/2015	36.71	4.1	3.8
M0205	1/20/2015	15.23	9.1	12.3
A0421	1/20/2015	2.44	10.7	9.5
M-0766	1/20/2015	49.73	14.3	18.4
M-0443	1/21/2015	1.74	18.1	15.0
A-0725	1/21/2015	3.82	-0.5	3.0
M-0779	1/21/2015	1.89	14.7	7.4
M-0780	1/22/2015	2.49	14.3	7.7
M-0781	1/22/2015	1.78	9.5	6.4
M-0036	1/22/2015	1.86	14.0	6.8
M-0044	1/26/2015	1.85	21.9	6.1
M-0239	1/26/2015	49.56	5.9	6.7
M-0045	1/26/2015	1.99	9.9	5.2
A-0436	1/27/2015	11.67	5.4	7.9
A-0420	1/27/2015	2.27	7.7	6.8
A-0071	1/27/2015	32.44	9.2	10.7
M-0063	1/27/2015	111.89	4.6	4.4
M-0052	1/28/2015	4.95	6.8	6.3
M-0527	1/28/2015	310.40	8.0	7.6
M-0778	1/28/2015	33.81	15.1	17.1
M-0777	2/9/2015	10.49	0.9	3.7
M-0785	2/9/2015	82.29	6.1	6.6
M-0217	2/9/2015	66.24	3.7	2.8
M-0040	2/10/2015	13.54	5.3	2.3
M-0026	2/10/2015	1.74	10.1	3.8
M-0762	2/10/2015	1.93	16.4	7.9
M-0764	2/11/2015	3.01	7.0	1.4
M-0773	2/11/2015	190.31	4.7	7.2
M-0771	2/12/2015	760.59	5.7	6.0
M-0772	2/12/2015	27.64	2.9	4.9

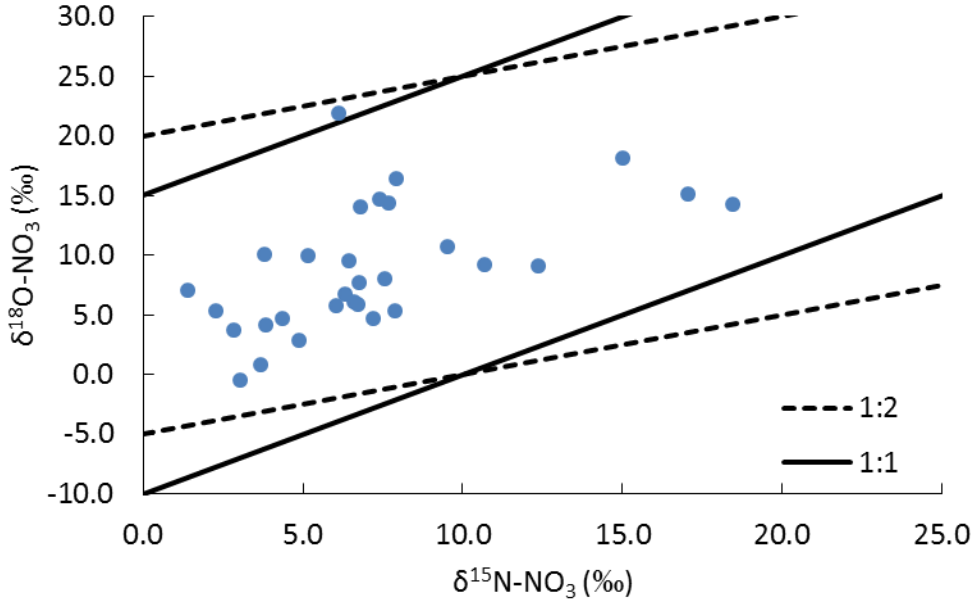

Figure 4.2.2. The $\delta^{18}O$ and $\delta^{15}N$ of nitrate from the 15 wells and other 46 old wells (* currently data not completed). Solid and dotted lines represent theoretical upper and lower bounds for enrichment due to denitrification based on the $\delta^{18}O$-NO_3: $\delta^{15}N$-NO_3 fractionation ratio of 1:1 and 1:2, respectively.

Since denitrification results in the final production of dissolved N_2, increase in N_2 concentration in the water has been used to estimate microbial denitrification (Blicher-Mathiesen et al. 1998). However, due to the relatively high background concentration of dissolved N_2, its dependence on the recharge temperature, and degassing problems, dissolved Ar is measured in addition of N_2 to estimate the excess of N_2 produced by denitrification (Kendall 1998). Measurements of dissolved N_2 and Ar in the Silver Spring Mammoth vents are similar to, but slightly higher than those reported by Phelps (2004) (Figure 4.2.4). Based on the presence of dissolved methane and nitrous oxide, we would infer the East vent to be more anaerobic and favorable for denitrification. Despite this observation, however, there is apparently more denitrification (excess N_2) present in the West Mammoth vent (Figure 4.2.4).

Analysis of the patterns of dissolved N_2 and the N_2:Ar can be used to indicate the potential for seasonality in the amount of excess N_2 derived from denitrification (Figure 4.2.5). Small but measurable changes are present in these values in the water discharging in the Mammoth vents. Similar patterns are also present in the $\delta^{15}N$ and $\delta^{18}O$ of nitrate with the west vent being more isotopically-enriched (Figure 4.2.6). Again, with such a small dataset, it is premature to infer seasonal trends or causes, but the observed correlation of N_2:Ar with stable isotopic values of nitrate support the conclusion that these signals represent variable amounts of denitrification in the Floridan Aquifer System of the Silver Spring springshed (Figure 4.2.7).

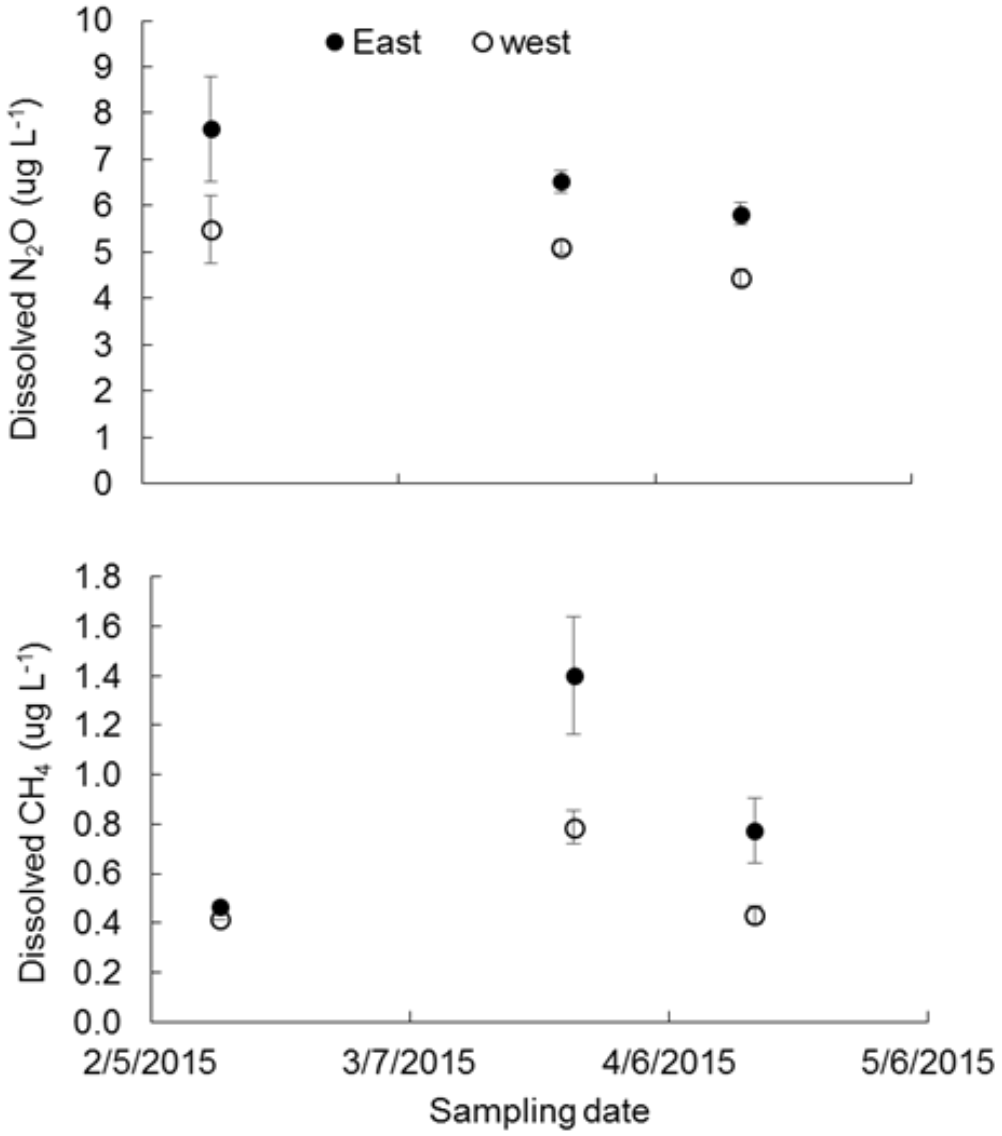

Figure 4.2.3. Seasonal patterns of dissolved N_2O and CH_4 from July 2014 through April 2015 in the east and west vents of the Silver Spring mammoth head spring.

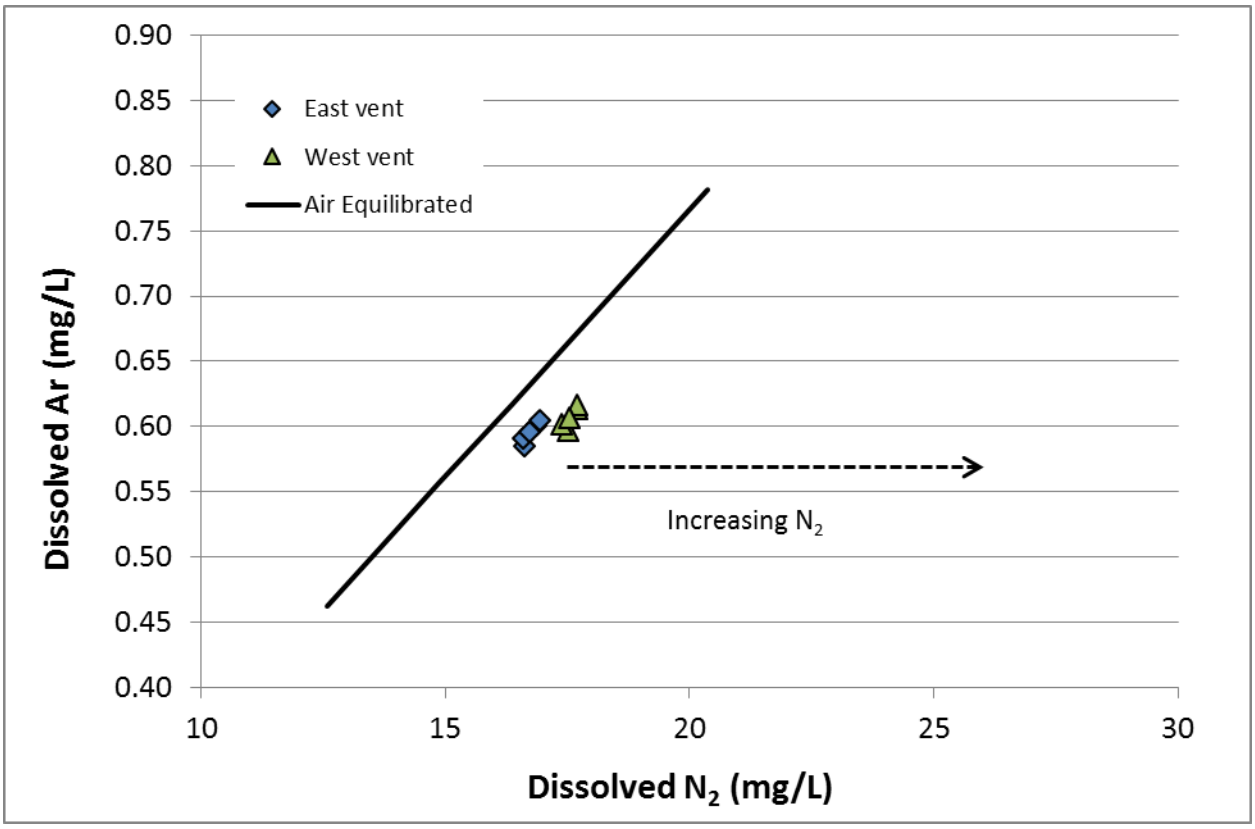

Figure 4.2.4. Concentrations of dissolved N_2 and Ar observed from July 2014 through April 2015 in the east and west vent of the Silver Spring mammoth head spring.

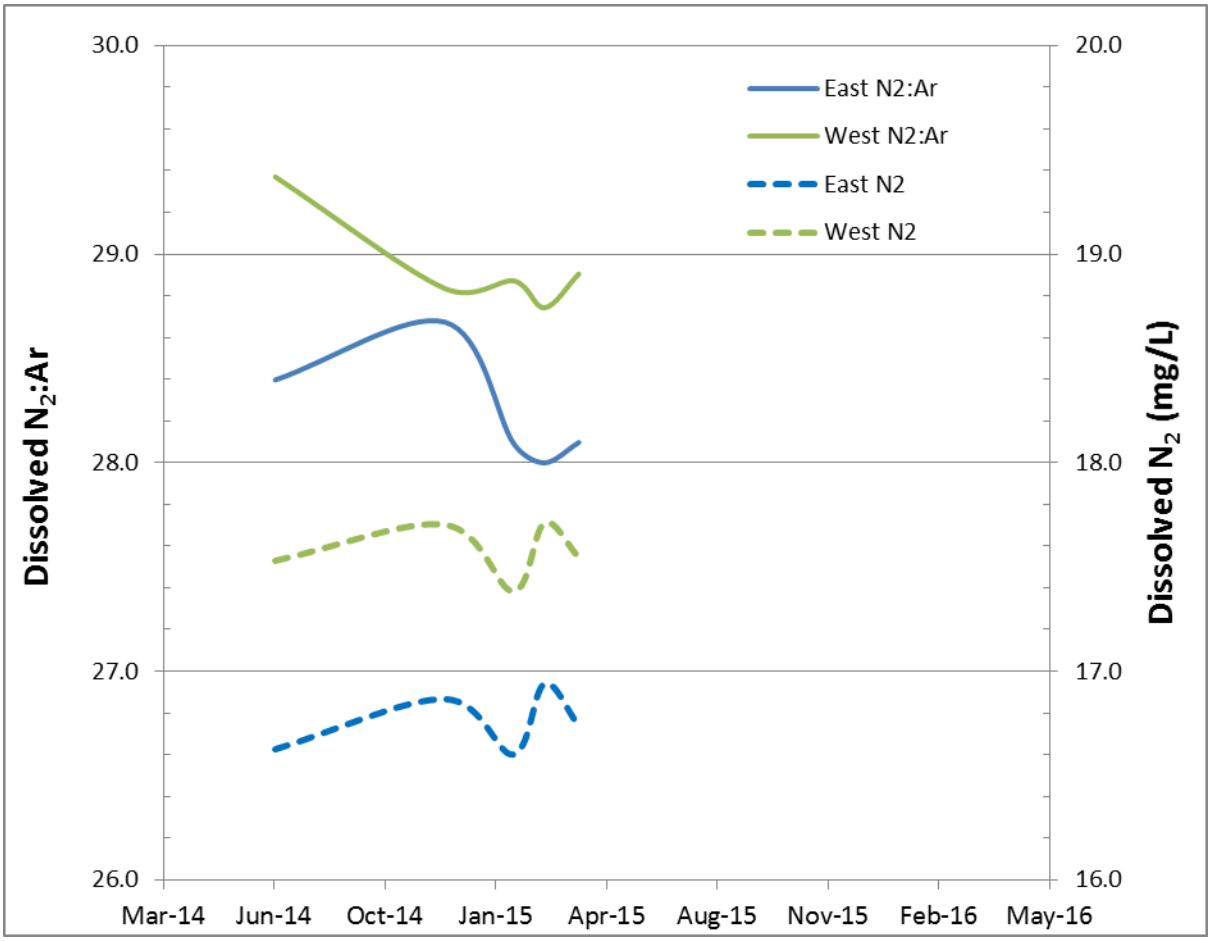

Figure 4.2.5. Seasonal patterns of dissolved N_2 and N_2:Ar observed from July 2014 through April 2015 in the east and west vents of the Silver Spring mammoth head spring.

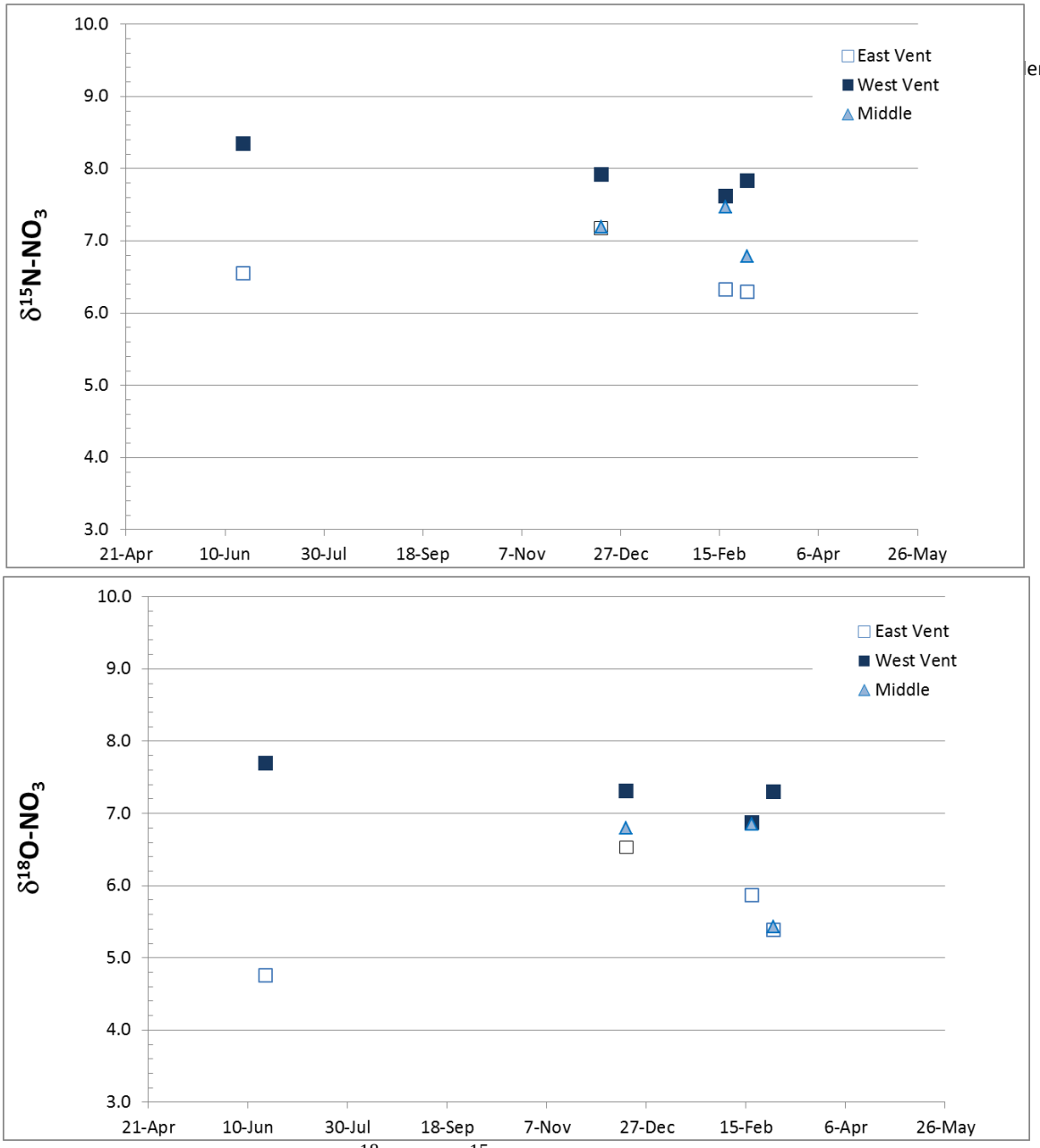

Figure 4.2.6. Seasonal patterns of $\delta^{18}O$ and $\delta^{15}N$ of nitrate observed from July 2014 through April 2015 in the east and west vents of the Silver Spring mammoth head spring.

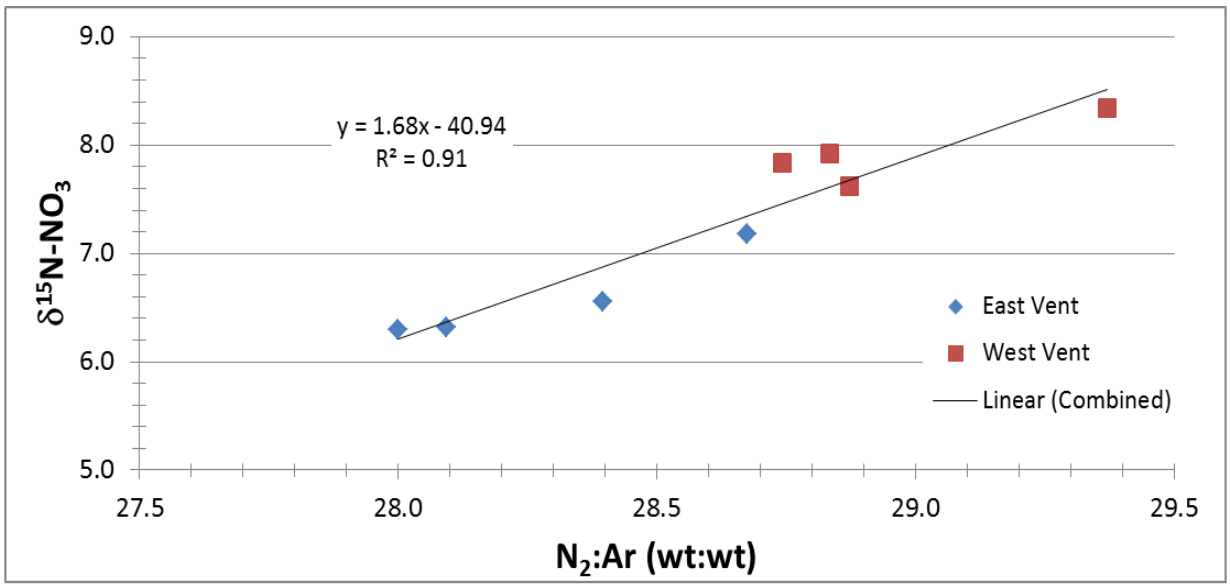

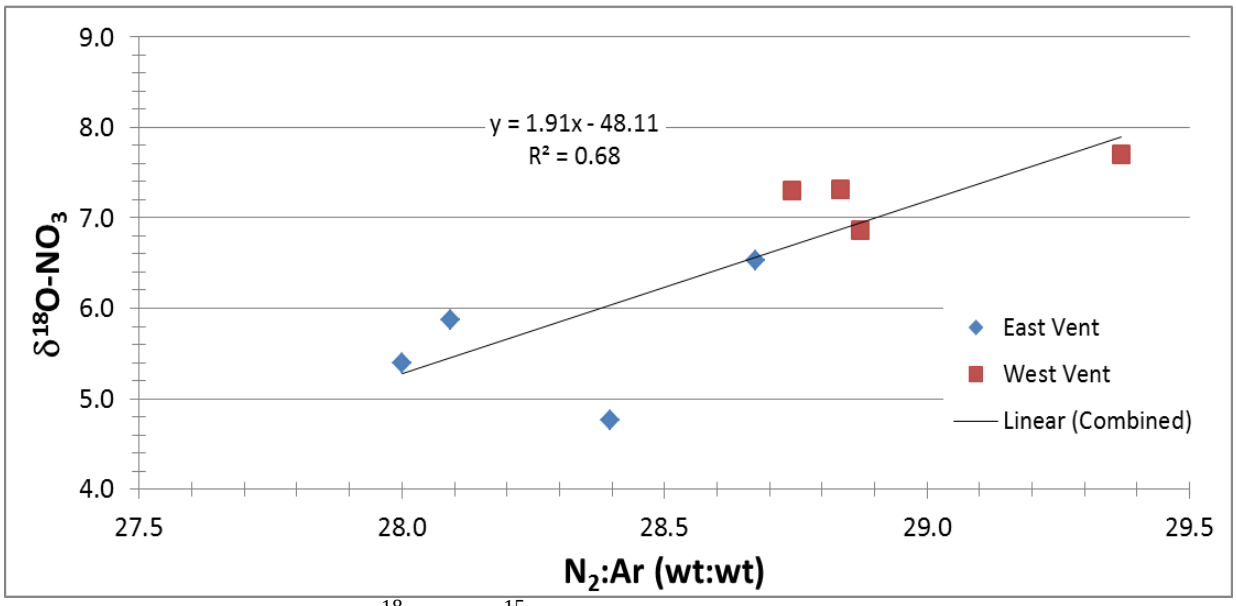

Figure 4.2.7. Correlations of $\delta^{18}O$ and $\delta^{15}N$ of nitrate and N_2:Ar for samples collected from July 2014 through April 2015 in the east and west vents of the Silver Spring mammoth head spring.

4.2.5 CONCLUSIONS AND RECOMMENDATIONS

This study targets the spatial and temporal patterns of denitrification indicators in the Floridan Aquifer System of the Silver Springs springshed. The results thus far are inconclusive, but a number of important findings have been made. For example, stable isotopic ratios of nitrate seem to indicate common and consistent nitrate sources with enrichments consistent with isotopic theory during denitrification. Dissolved concentrations of methane and nitrous oxide also show potential association with nitrogen cycling processes as they have in other systems.

Though the exact process(es) responsible for the concentrations of measured dissolved gases (methane and nitrous oxide) is currently unknown, the patterns of the correlations of these gases with other water quality parameters suggest a promising use of these to better identify zones of potential denitrification. Dissolved gas concentrations, gas ratios (N_2:Ar), and stable isotopic ratios of nitrate in the spring vents demonstrate there is a significant amount of seasonal variability, and that this variability is likely related to recharge patterns, age of water exiting the vents, and patterns of denitrification in the aquifer.

4.2.5.1 Future Research Needs

Based on the apparent utility of the dissolved gas and stable isotopic ratios of nitrate, there is a continued need for monitoring of seasonal patterns in dissolved gases and isotopes in vents and wells. Furthermore, there is a need for more measurements of dissolved gases to link with in conjunction with these measurements, analysis of dissolved noble gas concentrations are also needed to better constrain recharge temperatures for excess air calculation (allowing more accurate excess N_2 determination). Samples for this analysis have been collected and submitted for analysis.

Age dating of aquifer samples will allow estimation of residence and travel times of wells in the springhsed, as well as facilitating the development of water age/total denitrification relationships and more constrained rates of aquifer denitrification. Collection of microbial community samples (particulates in well samples) will commence in the next round of well sampling. Molecular analysis of community diversity and expression of genes related to denitrification will further corroborate inferred patterns of dissolved gases and isotopic signals of denitrification hotspots.

4.2.6 REFERENCES

Aravena R, Robertson WD, 1998. Use of multiple isotope tracers to evaluate denitrification in ground water: study of nitrate from a large-flux septic system plume. Groundwater, 36(6): 975-982.

Blicher-Mathiesen G, McCarty GW, Nielsen LP, 1998. Denitrification and degassing in groundwater estimated from dissolved dinitrogen and argon. Journal of Hydrology, 208: 16-24.

Butt P, Aly A, 2008. Silver springs spring vent documentation and geochemical characterization. Technical report, special publication SJ2008-SP6. http://floridaswater.com/technicalreports/pdfs/SP/SJ2008-SP6.pdf.

Ettwig KF, Butler MK, Paslier DL, Pelletier E, Mangenot S, Kuypers MMM, Schreiber F, Dutilh BE, Zedelius J, de Beer D, Gloerich J, Wessels HJCT, van Alen T, Luesken F, Wu ML, van de Pas-Schoonen KT, den Camp HJMOp, Janssen-Megens EM, Francoijs K-J, Stunnenberg H, Weissenbach J, Jetten MSM, Strous M, 2010. Nitrite-driven anaerobic methane oxidation by oxygenic bacteria. Nature, 464: 543-548.

Granger J, Sigman DM, Lehmann MF, Tortell PD, 2008. Nitrogen and oxygen isotope fractionation during dissimilatory nitrate reduction by denitrifying bacteria. Limnology and Oceanography, 53(6): 2533-2545.

Haroon MF, Hu S, Shi Y, Imelfort M, Keller J, Hugenholtz P, Yuan Z, Tyson GW, 2013. Anaeroubic oxidation of methane coupled to nitrate reduction in a novel archaeal lineage. Nature, 500: 567-570.

Heffernan JB, Albertin AR, Fork ML, Katz BG, Cohen MJ (2012). Denitrification and inference of nitrogen sources in the karstic Floridan Aquifer. Biogeosciences 9: 1671-1690.

Heisig P, Scott T-M, 2013. Occurrence of methane in groundwater of south-central New York State, 2012 – systematic evaluation of a glaciated region by hydrogeologic setting U.S. Geological Survey Scientific Investigations Report. 2013-5190.

Hiscock KM, Bateman AS, Muehlherr IH, Fukada T, Dennis PF, 2003. Indirect emissions of nitrous oxide from regional aquifers in the United Kingdom, Environment Science & Technology, 37: 3507–3512.

Inglett PW, Kana T, An S. 2013. Membrane inlet mass spectrometry approaches for measuring denitrification. Chapter 27, pp. 503-518. In: DeLaune, Reddy, Richardson, and Megonigal, eds. Methods in Biogeochemistry of Wetlands, Soil Science Society of America. Madison, WI. 1024 pp.

Jahangir MMR, Johnston P, Barrett M, Khalil MI, Groffman P, Boeckx P,Fenton O, Murphy J, Richards KG, 2013. Denitrification and indirect N_2O emissions in groundwater: Hydrologic and biogeochemical influences. Journal of Contamination Hydrology 152: 70-81.

Kampbell D, Vandegrift S, 1998. Analysis of dissolved methane, ethane, and ethylene in ground water by a standard gas chromatographic technique. Journal of Chromatography Science, 36: 253 - 256.

Lehmann MF, Reichert P, Bernasconi SM, Barbieri A, McKenzie JA, 2003. Modelling nitrogen and oxygen isotope fractionation during denitrification in a lacustrine redox-transition zone. Geochimica et Cosmochimica Acta, 67(14): 2529-2542.

McQuillan D, 2004. Ground-water quality impacts from on site septic system. Proceedings, National Onsite Wastewater Recycling Association, 13th Annual Conference, Albuquerque, NM, November 7–10, pp. 6–18.

Molofsky LJ, Connor JA, Wylie AS, Wagner T, Farhat SK, 2013. Evaluation of methane sources in groundwater in northeastern Pennsylvania. Groundwater, 51(3): 333–349.

Munch DA, Toth DJ, Huang C, Davis JB, Fortich CM, Osburn WL, Phlips EJ, Quinlan EL, Allen MS, Woods MJ, Cooney P, 2007. Fifty-year retrospective study of the ecology of Silver Springs, Florida. *Special Publication SJ2007-SP4*. St. Johns River Water Managmeent District: Palatka.

Osburn W, Toth DJ, Boniol D, 2002. Springs of the St. Johns River Water Management District. Technical Report SJ2002-5. Palatka, FL: St. Johns River Water Management District.

Osmond JK, Kaufman MI, Cowart JB, 1974, Mixing volume calculations, sources, and aging trends of Floridian Aquifer water by Uranium isotopic methods: Geochimica et Cosmochimica Acta, v. 38, p.1083-1100.

Phelps GG, 2004. Chemistry of ground water in the Silver Springs Basin, Florida, with an emphasis on nitrate. Scientific Investigations Report 2004-5144. Denver, CO: USGS.

Rosenau JC, Faulkner GL, Hendry Jr. CW, Hull RW, 1977. Springs of Florida. Geological Bulletin No. 31, revised. Tallahassee, FL: Florida Geological Survey.

Scott TM, Means GH, Meegan RP, Means RC, Upchurch SB, Copeland RE, Jones J, Roberts T, Willet A, 2004. Springs of Florida. Bulletin No. 66. Tallahassee, FL: Florida Geological Survey.

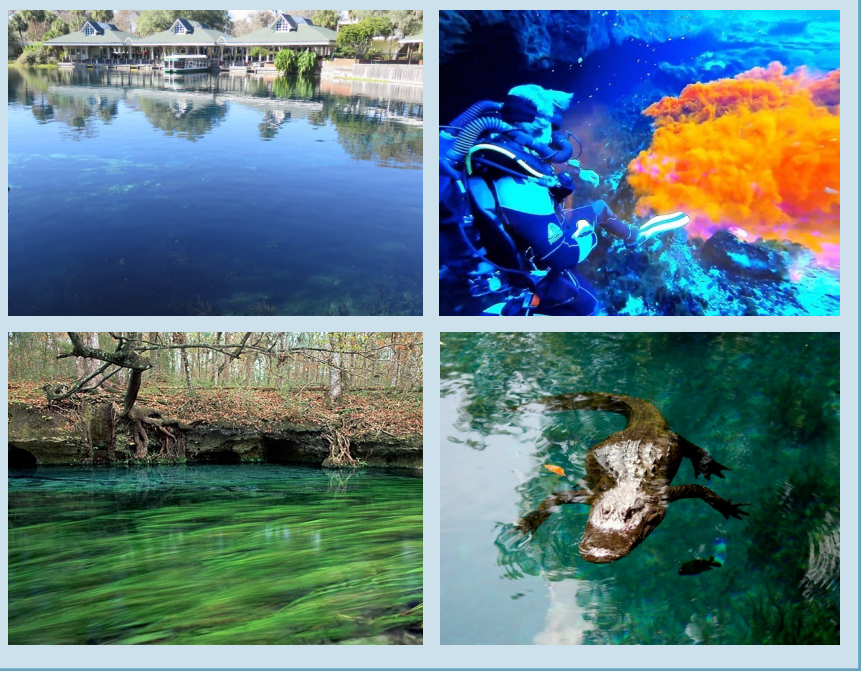

Collaborative Research Initiative on
Sustainability and Protection of Springs [**CRISPS]**

Section 5

[Work Order No: 2]

ANNUAL REPORT

July 2015

submitted to:

St. Johns River Water Management District
Springs Protection Initiative [SPI], UF Contract # 27789

UF | UNIVERSITY of FLORIDA
Water Institute

C R I S P S

Section 5

HYDRAULICS AND HYDRODYNAMICS

Velocity and Residence Time Distributions and Transient Storage

Annual Report 2015
Work Order No. 2

Principal Investigators:

David Kaplan, University of Florida
Pete Sucsy, St Johns River Water Management District

Project Team

David Kaplan
Alexis Johnson
Nathan Reaver
Engineering School of Sustainable Infrastructure and Environment
University of Florida

Pete Sucsy
Ed Carter
Joseph Stewart
Yanfeng Zhang
St Johns River Water Management District

This document reports interim progress of a work order in the first year of a 3-year project in compliance with Agreement between University of Florida (UF) and St. Johns River Water Management District (SJRWMD) UF Contract #27789. It is part of the *UF Collaborative Research Initiative on Springs Protection and Sustainability (CRISPS)* and supports the science component of *the SJRWMD Springs Protection Initiative (SPI).*

Section 5.1 Velocity and Residence Time Distributions and Transient Storage

5.1.1 ABSTRACT

The St. Johns River Water Management District (SJRWMD), in partnership with the University of Florida (UF), has initiated the SJRWMD-UF *Springs Protection Initiative-Science (SPIS)/Collaborative Research Initiative on Sustainability and Protection of Springs (CRISPS)* via RFQ 27789. A detailed background and set of major objectives and questions related to Silver River hydraulics and hydrodynamics are presented in Section 4 of that RFQ, with a primary goal of predicting unsteady water level profiles and velocity profiles using a suite of models (EFDC and HEC-RAS). The objectives of the University of Florida Spring System Hydrodynamics/Hydraulics work order is to: 1) yield a more thorough understanding of the velocity and residence time distributions in the channel of the Silver River and to quantify the location and magnitude of transient storage and exchange; 2) identify critical shear stresses for the entrainment and detachment of algae; and 3) link study findings to ongoing 3-D modeling with a focus on SAV impacts on velocity, residence times, and effects on stage-discharge relationship. These goals are being pursued over a three-year timeline; this report summarizes progress made towards these goals in the first project year.

5.1.2 INTRODUCTION

Velocity and residence time distributions (RTDs) are sentinel hydraulic characteristics that describe solute transport in riverine systems and are critical for understanding the potential for biogeochemical transformations in the advective and transient storage pools. In particular, the primary in-stream controls on NO_3-N concentration in springs are uptake and storage by autotrophs (i.e., submerged aquatic vegetation and benthic and epiphytic algae) and denitrification in biofilms and sediments. Several microcosm studies suggest that NO_3-N removal in a wetland system is accomplished primarily by macrophyte uptake rather than denitrification (e.g., Veraart et al. 2011), however a number of field studies show wide variation in the relative proportion of NO_3-N uptake via denitrification versus autotrophic uptake (Table 5.1.1).

Literature suggests the region beneath a stream bed where surface water and groundwater interact—known as the hyporheic zone—is a biogeochemical hotspot, however the hydraulic interactions between flow, velocity, hyporheic exchange, and water column autotrophic uptake of NO_3-N in springs are not well understood (e.g., Chapman et al., 1995; Heffernan and Cohen, 2010). Given the importance of flow, velocity, and mixing in dictating spring chemistry and biology, the objectives of this effort are to use pulse injection of a conservative solute to perform in-stream tracer studies. Experimental results allow us to estimate reach-scale hydraulic properties of the Silver River by fitting observed breakthrough curves (BTCs) via non-linear regression fitting of 1-D transport and mixing models (e.g., OTIS [Runkel 2007]) and provide valuable data for EFDC model testing and calibration. These results are also compared with the one previous tracer available for the Silver (Hensley 2010).

Table 5.1.1. Estimated proportion of NO_3-N removal via denitrification vs. autotrophic uptake.

Denitrification (%)	Autotrophic Uptake (%)	Notes	Source
16 +/-10	-	NO_3-N removal, tracer study in TN	Mulholland et al., 2004
16-43	-	Over 43% in 25% of streams studied (probably more because study disregarded time delay)	Mulholland et al., 2008
-	34-40	NH_4 and NO_3-N removal in wastewater treatment wetland, greater in submerged plants than cattails because of roots/leaves	Reddy, 1983
6	77	77% value based on Cedergreen and Madsen, 2002	Veraart et al., 2011
50-59	-	NO_3- removal with groundwater input	Hanson et al., 1994
72	-	Under N fertilization	Hamersley, 2002 (thesis)
75	25	Seasonal discrepancy in percentages of root uptake	Caffrey & Kemp, 1992
89-96	4-11	In microcosms with emergent and free floating plants	Lin et al., 2002
80	-	In spring and fall in the Ichetucknee Springs	Heffernan & Cohen, 2010

While the tracer injections described above allow us to estimate hyporheic exchange volumes by fitting hydraulic parameters to BTC data, novel hydraulic tracer methods have recently been introduced to directly quantify the role of microbial metabolism in nutrient processing. One such "smart tracer" (Haggerty et al. 2008) is the resazurin-resorufin system. Resazurin (Raz) is a redox-sensitive phenoxazine compound that reduces to resorufin (Rru) in the presence of metabolic activity by aerobes and facultative anaerobes; thus the Raz-Rru system can be used to assess the relative proportion of spring vent discharge water that is directly affected by microbial metabolism (and is therefore likely to be undergoing denitrification). While unlikely to be feasible for reach-scale use on large rivers due to cost, we present initial results of lab studies using the Raz-Rru system with Silver River sediments that are useful for predicting Raz transformations under varying hydrologic conditions and may be useful for identifying the presence of transient storage zones with high rates of biogeochemical activity.

5.1.2.1 Site Description

All experiments described in this section were undertaken in the Silver River in Ocala, FL. Additional information about the site can be found in the document introduction.

5.1.3 MATERIALS AND METHODS

5.1.3.1 Dye Tracer Experiments

5.1.3.1.1 Field and Laboratory Methods

With the assistance of over 20 volunteers, UF implemented the first of four proposed dye tracer experiments on March 8th. Divers assisted in the release of 18.9 L (5 gallons) of 20% Rhodamine WT directly in the flow stream of the Mammoth (Main) Spring vent at approximately 18:00 (Figure 5.1.1). The flow of dye downstream was tracked at nine fixed stations (Figure 5.1.2). Three in-stream, submersible fluorometers (two Turner Designs CS3 and one Turner Designs SCUFA, Turner Designs, Inc., Sunnyvale, CA) were calibrated in the lab prior to deployment and collected data at 1-minute intervals. Six ISCO automated samplers collected 250-500 mL grab samples at one-hour intervals, with the exception of the unit in the main spring bowl, which collected samples every 30 minutes. 3 ISCO samplers were located adjacent to in-stream fluorometers, but sampled within vegetation beds to explore the potential for differential mixing and transient storage in these zones.

Additionally, three boats ("rovers") collected 318 grab samples to characterize differential mixing (if present) along three gradients: 1) across the channel reach; 2) with depth; and 3) within five eco-geomorphological features (SAV beds, debris jams, emergent beds, and benthic depressions). Samples were collected using weighted tubing connected to a hand pump (Figure 5.1.3). Rover sampling continued overnight through the next morning. Rover samplers noted time, GPS location, sample depth, distance from bank, and eco-geomorphological feature. Analysis of rover data is ongoing, and is not presented in this report.

All ISCO and grab samples were refrigerated within 24 hours of collection and analyzed within one week. Rhodamine calibration curve development and concentration measurements used a 30 ppb stock solution of Rhodamine to produce the standard concentrations (30, 27, 21, 18, 15, 12, 9, 6, 3, 1.5, 0.3, 0.15, and 0 ppb, each with 7 replicates. Florescence of each of the 7 replicates was measured using an excitation filter of 530/25 nm and an emission filter of 590/35 nm with a detector sensitivity of 75. Replicate measurements for each concentration were averaged and a linear calibration model was fit to the averaged values (R^2 = 0.9972). The calibration equation was then used to calculate Rhodamine concentrations of collected samples based on their florescence measurements under the same excitation and emission settings.

Figure 5.1.1. Clockwise from top left: diver just after releasing injection vessel cap, research vessels in main spring bowl after dye release, injection vessel suspended from research vessel with dye release, underwater view of diver after dye release.

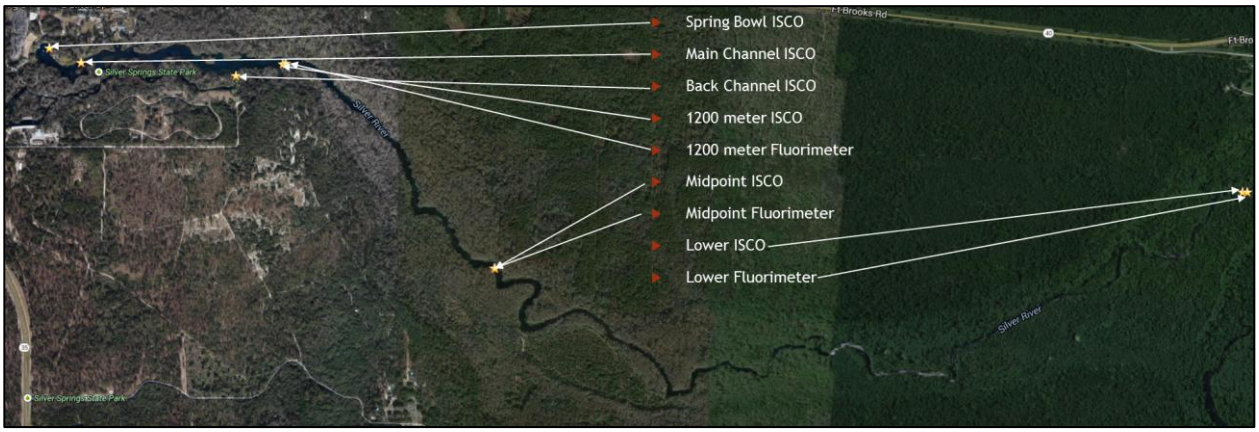

Figure 5.1.2. Fixed-location dye sampling sites on the Silver River for Match 4th, 2015 injection.

Figure 5.1.3. Clockwise from top: hand pump device, sampling tube and weight deployed for sample collection, "rover" boat sample collection.

5.1.3.1.2 Tracer Data Analysis

5.1.3.1.2.1 Solute Transport Model

Hydraulic transport parameters were estimated from BTC data using the **O**ne-dimensional **T**ransport with **I**nflow and **S**torage (OTIS) model (Runkel, 1998). OTIS is a solute transport model for streams and rivers that models one-dimensional flow and transport along river longitudinal distance, but assumes spatial homogeneity of solute concentration in other two dimensions (width and depth). The model is based on the advection-dispersion equation, which relates changes in solute concentration with respect to time and space to advection, dispersion, and transient storage in the stream system and is given by a set of coupled differential equations:

$$\frac{\partial C}{\partial t} = -\frac{Q}{A}\frac{\partial C}{\partial x} + D\frac{\partial^2 C}{\partial x^2} + \frac{q_{LIN}}{A}(C_L - C) + \alpha(C_s - C)$$

$$\frac{\partial C_s}{\partial t} = \alpha\frac{A}{A_s}(C - C_s)$$

where C is concentration (ppb), t is time (s), Q is discharge ($m^3\ s^{-1}$), A is channel cross-sectional area (m^2), D is the dispersion coefficient ($m^2\ s^{-1}$), q_{LIN} is the sum of inflows to the system ($m^3\ s^{-1}$), C_L is solute concentration in inflows (ppb), α is the storage exchange coefficient ($1\ s^{-1}$), and C_s is solute concentration in transient storage (ppb). The second equation describes the rate of concentration change in the transient storage zone as a function of the effective stream and storage zone areas and concentrations, where A_s is storage zone cross-sectional area (m^2) and C_s is storage zone concentration (ppb) (Stream Solute Workshop, 1990). OTIS is solved numerically using various finite difference approaches (each with pros and cons regarding solution stability and accuracy, see below), but it also has an analytic solution for a pulse injection and no lateral inflow, which allows for numerical solution benchmarking:

$$C(x,t|A,As,D,\alpha,Q) = e^{-\alpha t}\left[\frac{\frac{M}{A}}{2\sqrt{\pi D t}}e^{\frac{-\left(x-\frac{Q}{A}t\right)^2}{4Dt}}\right] + \alpha\int_0^t\left[\frac{\tau I_1\left(\frac{2\alpha A}{As}\sqrt{\frac{As}{A}(t-\tau)\tau}\right)}{\sqrt{\frac{As}{A}(t-\tau)\tau}}e^{-\frac{\alpha A}{As}(t-\tau)-\alpha\tau}\frac{\frac{M}{A}}{2\sqrt{\pi D\tau}}e^{\frac{-\left(x-\frac{Q}{A}\tau\right)^2}{4D\tau}}\right]d\tau$$

5.1.3.1.2.2 Model Fitting Approaches

Conventional model fitting techniques seek the "best" fit of a model to observed data via optimization of an objective function (e.g., minimizing sum of square errors, maximizing R^2, etc.). While widely used, this approach has limitations for some applications. Optimization with an objective function requires a search procedure of parameter space. If the objective function has many features (i.e. local minima or maxima) in parameter space, it is possible for the searching algorithm to become trapped in a region that does not contain the "true" best fit parameters of the model to the data. In addition, the objective function may not be very sensitive to changes in certain parameters of the model. This could potentially cause certain parameters in the model to be non-identifiable, meaning that many different values of that parameter would give a similar value to the objective function.

Various methods have been proposed to address these issues, such as weighting data or using only portions of a dataset to fit models. However, these methods add a subjective component to the analysis that then has to be justified. In addition, it is more difficult to determine the uncertainty in the parameter estimates resulting from the optimization process. There has been discussion in the literature about whether all of the parameters in the OTIS model are identifiable when fitting to breakthrough curve data (Kelleher et al. 2013). Identifiability of model parameters is important when trying to understand reach-scale properties of streams, as each parameter has a physical interpretation.

To identify and address some of these issues of identifiability, we used a Bayesian method to estimate OTIS model parameters in addition to a standard objective function optimization using OTIS-P software, which uses non-linear regression routines from STARPAC (Donaldson and Tryon 1990). The Bayesian method does not depend on searching an objective function in parameter space; instead, it involves drawing samples from a parameter probability distribution defined by the model, data, and any prior knowledge about the parameters. The Bayesian method allows to us determine the most likely parameter values of the model for the data, much like the objective function optimization, but also provides a probability distribution for each parameter, giving a quantitative measure of the uncertainty for each parameter. Additionally, by sampling probability distributions of model parameters, the Bayesian approach allows us to develop

parameter uncertainty estimates vs. a single deterministic number for each parameter (Figure 5.1.4). We expect this method to allow us to better understand the uncertainty in OTIS model parameters estimated from our dye tracing experimental data.

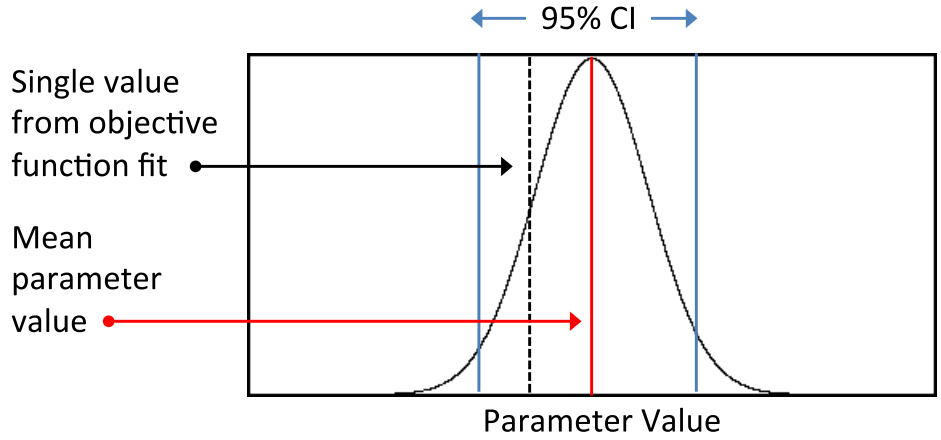

Figure5.1.4. Example fitted parameter distribution (solid black line) and 95% credible interval resulting from Bayesian model fitting vs. a single parameter value derived from traditional techniques (black dashed line).

Bayesian model fitting is based on Bayes theorem:

$$p(Hypothesis|Data) = \frac{p(Data|Hypothesis)p(Hypothesis)}{p(Data)}$$

or the commonly used form:

$$p(Hypothesis|D) \propto p(Data|Hypothesis)p(Hypothesis)$$

The components of this proportionality are generally referred to in the following manner:

$$posterior\ distribution \propto likelihood\ distribution \times prior\ distribution$$

The prior distribution reflects the knowledge of the model parameters before including experimental data, the likelihood distribution is the distribution from which the data is thought to be generated (i.e. the model under consideration), and the posterior distribution reflects the knowledge of the model after including experimental data.

For our specific case, the data are the measured breakthrough curves, and the hypothesis is that the data is generated from the OTIS model. Since the OTIS model is solved numerically, rather than with an analytic expression, it can be represented with the following notation:

$$OTIS(A, As, D, \alpha, x, t)$$

where A is the channel cross sectional area, As storage zone cross section area, D is the aggregate dispersion coefficient, α is the exchange rate between the channel and storage zone, x is the longitudinal position from the dye release point, and t is the time elapsed since the dye release. The measured breakthrough curve data have three coordinates, concentration $\{C_i\}$, longitudinal position from the dye release point $\{x_i\}$, and time elapsed since the dye release $\{t_i\}$.

For our analysis, we are interested in the probability distribution of the parameters of the OTIS model given the measured breakthrough curves. For a single measured breakthrough curve observation, *i*, Bayes theorem can be written as:

$$p(A, As, D, \alpha | C_i, x_i, t_i) \propto Normal(C_i | mean = OTIS(A, As, D, \alpha, x_i, t_i), variance = \sigma^2) p(A) p(As) p(D) p(\alpha) p(\sigma^2)$$

where:

$$p(A) = Normal(A | mean = 0, variance = 100^2)$$
$$p(As) = Normal(As | mean = 0, variance = 100^2)$$
$$p(D) = Normal(D | mean = 0, variance = 100^2)$$
$$p(\alpha) = Normal(\alpha | mean = 0, variance = 100^2)$$
$$p(\sigma^2) = Gamma\left(\frac{1}{\sigma^2}, a = 0.001, b = 0.001\right)$$

In these expressions the observed concentration, C_i, is thought to come from a normal distribution (likelihood distribution) with a mean equal to the OTIS model evaluated at the corresponding longitudinal position and time, and variance representing deviations from the OTIS model due to experimental error. The remaining distributions are the prior distributions for the OTIS model parameters and variance parameter. These prior shave been chosen to be very vague for all of the parameters, reflecting little knowledge about the value of the parameter before the experiment. This reflected in the choice of mean (0) and variance (100^2) for these distributions, giving a very wide, nearly flat distribution centered on zero. This effectively means before our experiment we think almost any parameter values are equally likely. These weakly informative priors allow the data to dominate the shape of the posterior distribution.

If we take into all of the experimental data Bayes theorem becomes:

$$p(A, As, D, \alpha | \{C_i\}, \{x_i\}, \{t_i\}) \propto \left[\prod_i Normal(C_i | mean = OTIS(A, As, D, \alpha, x_i, t_i), variance = \sigma^2)\right] p(A) p(As) p(D) p(\alpha) p(\sigma^2)$$

where:

$$p(A) = Normal(A | mean = 0, variance = 100^2)$$
$$p(As) = Normal(As | mean = 0, variance = 100^2)$$
$$p(D) = Normal(D | mean = 0, variance = 100^2)$$
$$p(\alpha) = Normal(\alpha | mean = 0, variance = 100^2)$$
$$p(\sigma^2) = Gamma\left(\frac{1}{\sigma^2}, a = 0.001, b = 0.001\right)$$

All observed data points are independent and therefore their likelihood functions are multiplied together. The posterior distribution for the model parameters given the data is explicitly expressed in the above proportionality. To find the most likely parameter values we can calculate the mean of each of the parameters from the posterior distribution. Since the posterior distribution does not have an easily obtained analytic expression we use a Monte Carlo approach to draw enough samples from the distribution to characterize it. This is the main difference

between the optimization of objective functions and Bayesian inference: in Bayesian inference we sample from a "known" probability distribution, while in optimization we search a parameter space. The method we use to sample from the posterior distribution is a Markov chain Monte Carlo (MCMC) random walk using the Metropolis-Hasting within a Gibbs sampling algorithm.

5.1.3.2 Raz-Rru Experiments

This section describes batch experiment methods used to determine kinetic transformation and sorption rates for Raz and Rru in sediments from the Silver River. These rates were compared with those derived using sediments from a sandy-bottom river in order to quantify the general effectiveness of Raz as an indicator of microbial metabolism and biogeochemical potential in Florida streams.

5.1.3.2.1 Raz and Rru Detection Wavelengths

Standard solutions of Raz and Rru were prepared in concentrations ranging from 0 to 200 µg L^{-1} (ppb) and for each, fluorescence was measured for a range of excitation and emission wavelengths on a bench-top fluorometer. As Rru exhibits greater fluorescence than Raz, there is a degree of error introduced in separating mixed signals and signal saturation can be an issue above 150 ppb. For both compounds, the strongest fluorescence signals were produced with excitation at 530 nm and emission at 645 nm (530/645 nm) and 480/590 nm, respectively. The best fit calibration equations for each compound are shown below:

$$Raz_{590} = 3.8144Z + 136.31$$
$$Raz_{645} = 17.238Z + 88.833$$
$$Rru_{590} = 99.206U + 86.351$$
$$Rru_{645} = 134.41U + 36.564$$

where Z is the Raz concentration in ppb and U is the Rru concentration in ppb. The total signals for each wavelength were set equal to the sum of the Raz and Rru signals, and the resulting set of equations was solved for Z and U in all subsequent measurements:

$$S_{590} = Raz_{590} + Rru_{590}$$
$$S_{645} = Raz_{645} + Rru_{645}$$

5.1.3.2.2 Field Sites

Sediment was collected from two systems in Florida with significant differences in soil composition and hydrologic regime. The first was the Silver River near Ocala, FL, a well preserved state park area where the river is driven by first magnitude spring flows of approximately 650 cubic feet per second (cfs). The collection point was located on a vegetated slope where hyporheic exchange was likely forced by the direction of flow. The sediment was highly organic with a high water content and loamy texture. For comparison purposes, sediment was also collected from Jennings Creek, a 1.41 cfs urban stream in Gainesville, FL that is impacted heavily by runoff from surrounding roadways. The sediment was characterized primarily by sand and small gravel. The sample site was located on a similarly sloped area of the reach downstream of a small riffle-pool sequence where hyporheic exchange may be expected.

5.1.3.2.3 Batch Experiments

Batch culture experiments were performed according to methods adapted from González-Pinzón et al (2012). A total of 20 samples were prepared where 50 g of sediment from the Silver River were added to each of nine 200 mL sample bottles. Another nine were filled with sediment from Jennings Creek. The final two samples contained deionized water only. Sediment samples were filled to a final volume of 60 mL using collected stream water. The water samples and 6 sediment samples from each site were autoclaved at 121°C for 20 minutes to eliminate the presence of microbial activity. Half of the autoclaved samples were then filled with the requisite volume of Raz for a final concentration of 100 ppb and the other half were treated with Rru to a concentration of 100 ppb. The 6 live samples were treated with Raz only. The samples were then placed on a shaker table and incubated at room temperature for a period of 6 hours. 250 µL samples were taken from each bottle at approximately 30 min intervals over the incubation period. Samples were buffered to a pH above 8 with 10 µL of 1 M NaOH to avoid the need for signal corrections and then centrifuged to remove residual sediment. 200 µL samples were pipetted to 96-well plates and total fluorescence was measured at 480/590 nm and 530/645 nm. Laboratory lights were kept off throughout the experiment to avoid photodegradation.

5.1.3.2.4 Kinetics and Advection-Dispersion Modeling

The rates of Raz and Rru transformation and adsorption to sediment particles were modeled by fitting measured concentrations from the batch experiments to the following equations:

$$\partial Raz = -k_{fRaz} \cdot Raz \cdot Bac + k_{rRaz} \cdot Bac_{total} - k_{rRaz} \cdot Bac - k_{fsRaz} \cdot Raz \cdot S + k_{rsRaz} \cdot S_{total} - k_{rsRaz} \cdot S$$

$$\partial Rru = k_U \cdot Bac_{total} - k_u \cdot Bac - k_{fsRru} \cdot Rru \cdot S_u + k_{rsRru} \cdot S_{utotal} - k_{rsRru} \cdot S_u$$

$$\partial Bac = -k_{fRaz} \cdot Raz \cdot Bac + k_{rRaz} \cdot Bac_{total} - k_{rRaz} \cdot Bac + k_u \cdot Bac_{total} - k_u \cdot Bac$$

$$\partial S = -k_{fsRaz} \cdot Raz \cdot S + k_{rsRaz} \cdot S_{total} - k_{rsRaz} \cdot S$$

$$\partial S_u = k_{fsRru} \cdot Rru \cdot S_u + k_{rsRru} \cdot S_{utotal} - k_{rsRru} \cdot S_u$$

where k_f represents forward absorption by bacteria, k_{fs} represents forward sorption to sediment, and k_r represents reverse reactions. Bac_{total} is the total microbial concentration, Bac is number of bacteria occupied by Raz, k_u is the conversion of Raz to Rru, and S is the number of sorption sites available for Raz, while S_u represents sorption sites for Rru, and S_{total} is the total sorption sites. The conversion of Raz to Rru is assumed to be irreversible; however, Raz absorption by microbial cells does not necessarily indicate transformation. Sorption of both compounds to sediment is reversible.

Hydraulic transport parameters were estimated for two hypothetical reaches with sediments exhibiting the sorption and decay parameters fitted for Jennings Creek and the Silver River and applied to a modified version of the OTIS model presented above that includes decay terms (Runkel, 1998; Hensley & Cohen, 2012):

$$\frac{\partial C}{\partial t} = -\frac{Q}{A}\frac{\partial C}{\partial x} + D\frac{\partial^2 C}{\partial x^2} + \frac{q_{LIN}}{A}(C_L - C) + \alpha(C_s - C) - kC$$

$$\frac{\partial C_s}{\partial t} = \alpha \frac{A}{A_s}(C - C_s) - kC$$

When reduction and adsorption of Raz (or Rru) is observed, a - kC term is included in the model to account for the combined predicted first order conversion of resazurin to resorufin in the hyporheic zone as well as adsorption to sediments (Lemke et al, 2013). In this equation, α is mathematically equivalent to the parameter q_{he} developed by Lemke et al. (2013), which quantifies the discharge subject to hyporheic exchange per volume of stream water. Breakthrough curves of Raz and Rru in the two simulated systems were compared from the standpoints of adsorption capacity and microbial activity.

5.1.4 RESULTS AND DISCUSSION

5.1.4.1 Dye Tracer Experiments

5.1.4.1.1 Breakthrough Curve Data

Dye was released at approximately 18:00 on March 4, 2015 and was complete within approximately 5 minutes, with the majority of dye injected within the first 90 seconds. Visual inspection of the dye plume suggested three primary flow paths after injection: downstream, towards the back channel, and recirculation into the spring bowl (Figure 5.1.5). The following three figures show BTCs measured *in-situ* (3 fluorometers) and via ISCO grab samples (6 locations).

Figure 5.1.5. Visual interpretation of dye flows after injection. Figure by Ed Carter.

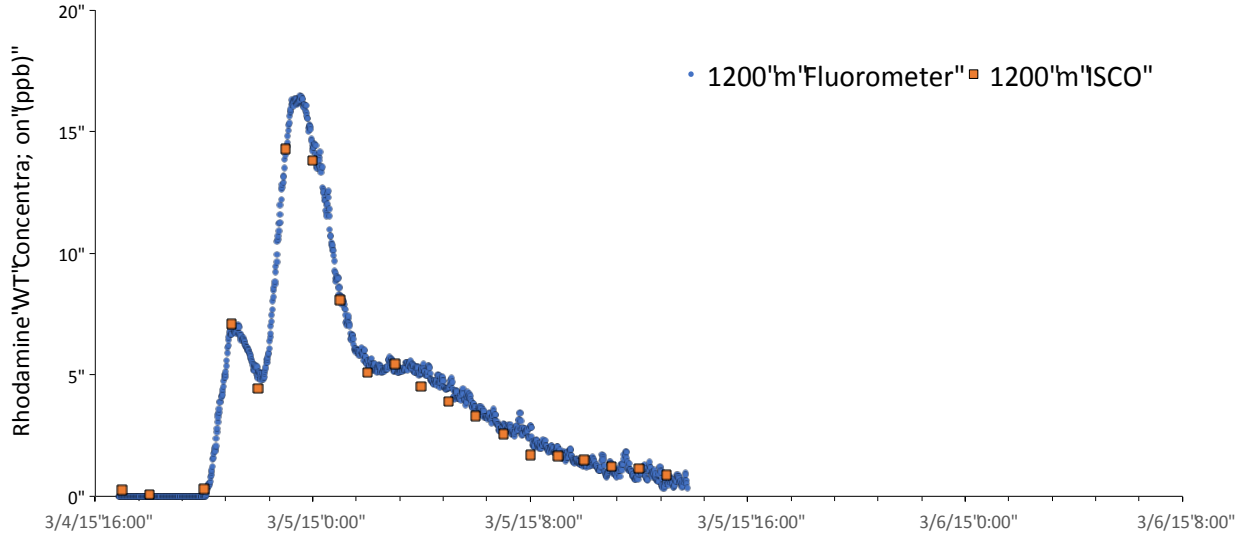

Figure 5.1.6. BTC at the 1,200-m station measured continuously (blue dots) and with ISCO grab samples (orange squares), which agree closely. Note three distinct concentration peaks. See Figure 5.1.2 for measurement locations.

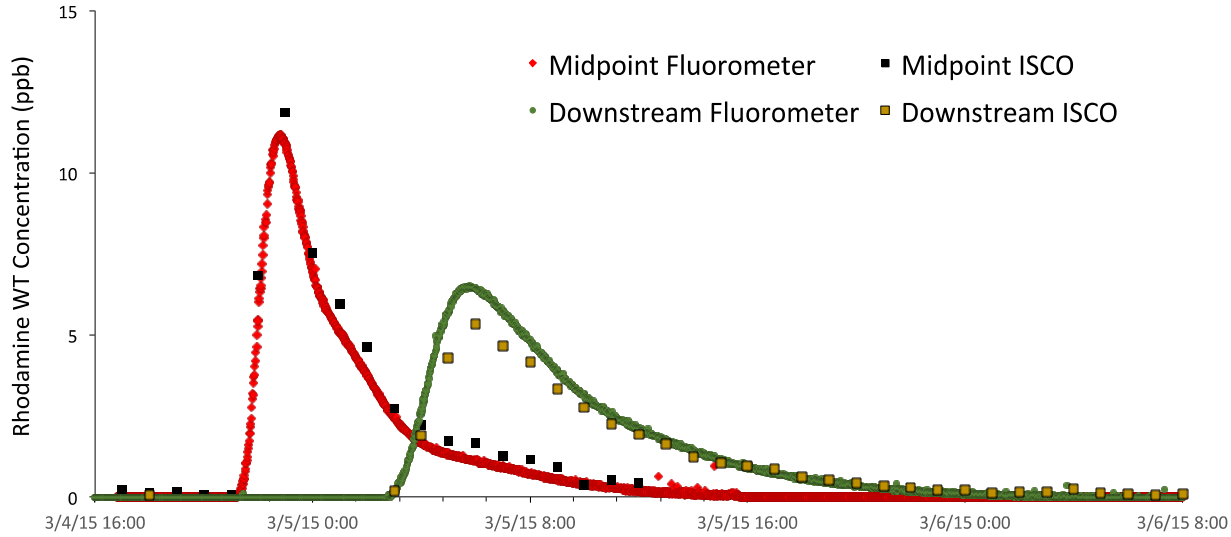

Figure 5.1.7. Rhodamine BTCs at the midpoint and downstream stations measured continuously (red and green dots) and with ISCO grab samples (black and orange squares). See Figure 5.1.2 for measurement locations.

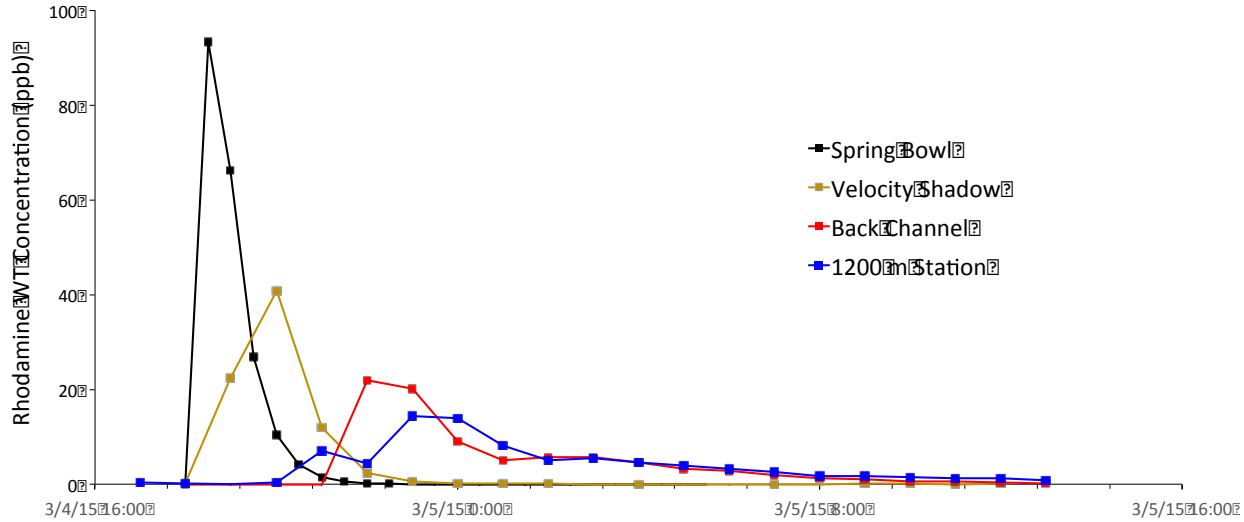

Figure 5.1.8. Rhodamine BTCs at four ISCO monitoring stations. See Figure 5.1.2 for measurement locations.

Analysis of these data is ongoing, however we can draw a number of initial conclusions about flow and transport in the Silver River during the time of the injection. First, multiple peaks in the BTCs at the 1,200 m station (Figure 5.1.6) indicate the presence of three upstream flowpaths: one via the main river channel and two through the "back channel". While it is counterintuitive that the concentration of the first peak (characterizing main channel flow and the bulk of tracer mass) is lower than the second peak (characterizing the faster of the two back channel flow paths.), this occurs due to the placement of both the fluorometer and ISCO sampler intake close to the right (southern) bank in this location (to take advantage of the 1,200 m USGS station as a mounting platform). Despite large flows out of the main spring bowl, complete transverse (and presumably vertical) mixing is not achieved within 1,200 m, resulting in the highest concentration dye plume bypassing the station in the channel center. Additional spring flows along the main channel also serve to dilute concentrations relative to the pulse delivered from the spring bowl into the back channel. The higher-concentration second peak occurs when that pulse arrives out of the back channel and hugs the right bank as it enters the main channel. These interpretations are well supported by initial EFDC modeling (see below), providing support for that model and the utility of using tracer experiments to inform modeling efforts, however transport parameters cannot be derived from the OTIS model for this BTC.

BTCs at the midpoint and downstream stations (Figure 5.1.7) illustrate delayed arrival and attenuated peak concentration from advection, dispersion, and any transient storage. Triple peaks observed at the upstream station are smoothed at both stations, allowing is to fit the OTIS model to estimate reach-scale parameters advection and dispersion parameters (see below). At both stations, fat tails on the distribution of ISCO samples (i.e., slow concentration declines late in the BTC) suggest potential transient storage, which is also quantified via the model fitting process. In general, ISCO and fluorometer samples matched well at the midpoint station, but were divergent at the downstream station, where the Rhodamine concentration peak measured in the vegetation bed was lower than that in the main channel (and showed delayed attenuation), suggesting that vegetation beds can serve as a partial barrier to mixing.

Data from the four additional ISCOs (Figure 5.1.8) provide additional insight into flowpaths and residence times in the upper reach of the Silver River. In particular, data from the spring bowl ISCO suggest a complete flushing time of approximately 6 hours and data from the back channel ISCO captures the two back channel dye pulses, allowing us to qualitatively estimate mean travel times of water following those two paths (approximately 6 and 12 hours for the faster and slower flow paths, respectively). All BTC data are included in Appendix 5.1.1.

5.1.4.1.2 Model Fitting and Comparisons

Observed BTC data were fitted to the OTIS model using both conventional and Bayesian techniques, however we continue to refine our numerical methods for both fitting procedures and the *results presented here should be considered provisional*. Fitting was applied for upstream and downstream reaches separately as well as for the entire river. Figure 5.1.9 characterizes the upper stream reach from the main vent to the midpoint station, Figure 5.1.10 characterizes the entire river to the downstream station, and a separate analysis of just the downstream reach (and comparison to a previous tracer injection experiment) appears below.

Figures 5.1.9 and 5.1.10 illustrate the generally good agreement of fitted models with observed data, as well as between the parameter estimates from both fitting techniques. While BTC peaks are fitted fairly well in both locations, the models underestimate Rhodamine concentration in the falling limb of the pulse, reflecting an underestimation of the role of transient storage. This finding has been noted by several authors, and is likely due to the assumption of exponentially distributed residence times (Gooseff et al. 2003), which may be better represented by a power-law distribution (Haggertey et al. 2002). Indeed the magnitude of disagreement between the fitted OTIS and observed BTCs may be an indicator of longer and/or slower transient flowpaths (e.g., through the hyporheic zone) and alternate modeling approaches will be explored with these and future data in the future. Also apparent in Figures 5.1.9 and 5.1.10 is the close agreement between parameter estimates from conventional fitting and the mean parameter estimate using the Bayesian estimate (Table 5.1.2). While not unexpected, this gives us confidence in the Bayesian results, while the parameter estimate distributions provide a measure of relative parameter uncertainty.

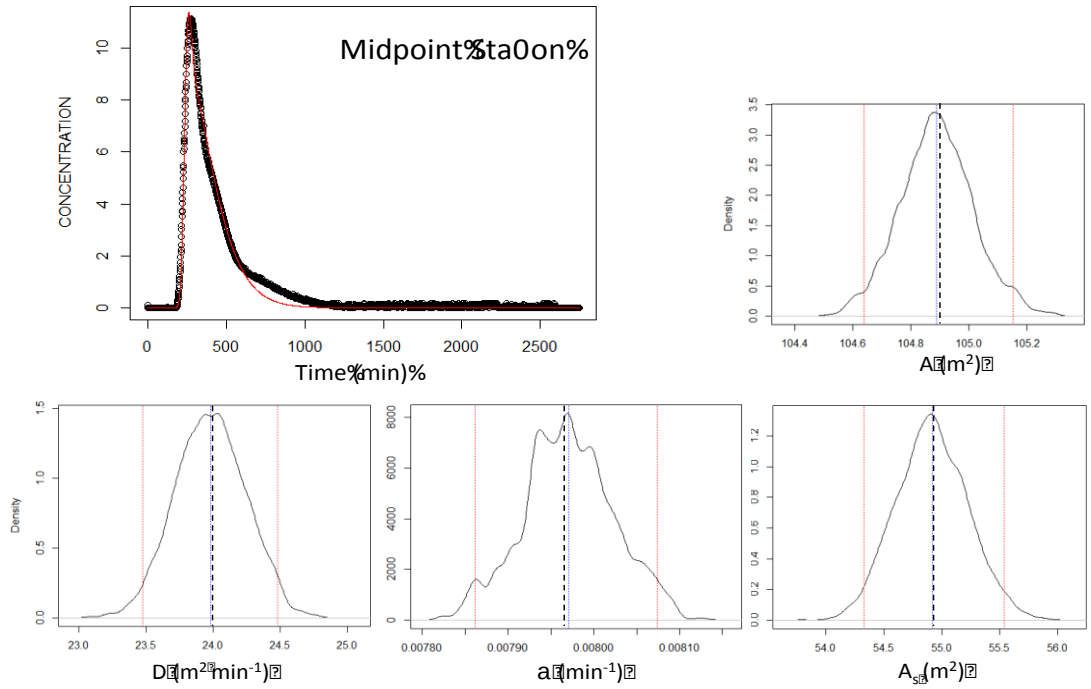

Figure 5.1.9. OTIS model (red line) fitted to BTC data (black circles) from the midpoint station (upper left). Parameter estimates from standard model fitting (black dashed lines) are compared with Bayesian parameter distributions (solid black line) and the mean/95% credible parameter intervals (blue/red lines, respectively).

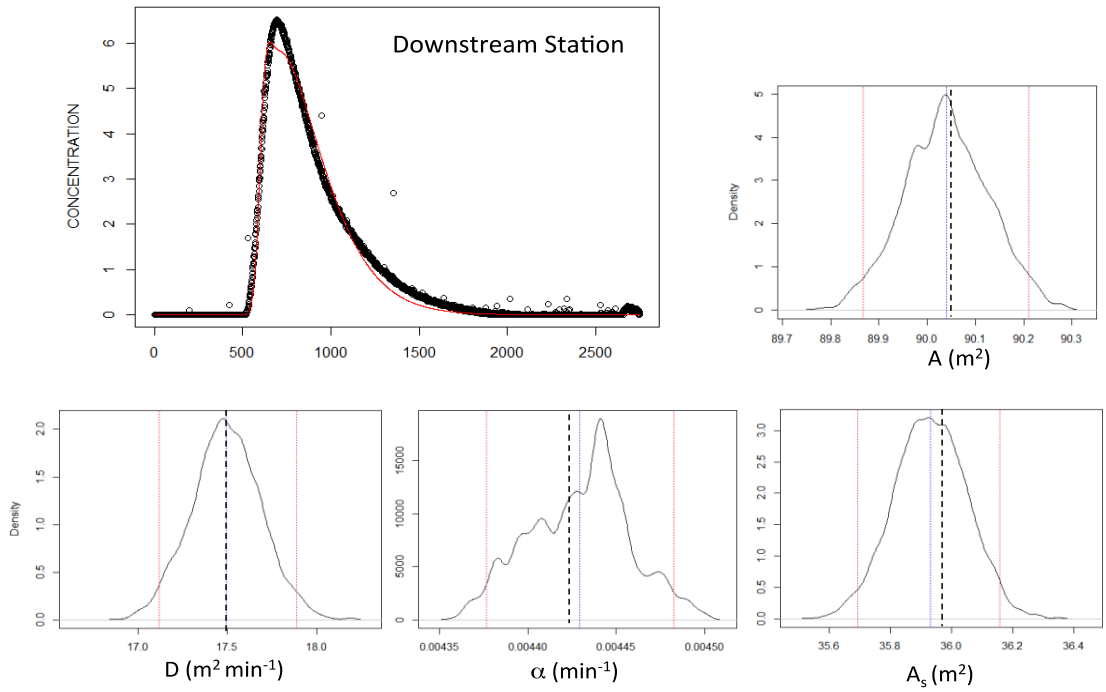

Figure 5.1.10. OTIS model (red line) fitted to BTC data (black circles) from the downstream station (upper left). Parameter estimates from standard model fitting (black dashed lines) are compared with Bayesian parameter distributions (solid black line) and the mean/95% credible parameter intervals (blue/red lines, respectively).

The population of model parameters derived with the Bayesian method can also be used to assess potential model identifiably issues by looking for relationships between model parameters. We would expect no correlation between truly unique model parameters, while parameters with interchangeable (i.e., non-unique) parameterizations might be expected to show strong correlation. Figure 5.1.11 presents these relationships based on our initial analyses, and though results may be refined with future work, we expect the general finding to remain: correlation between a subset of model parameters (D and A_s, A and α; Figure 5.1.11) indicates parameter non-uniqueness, which can make interpretation and comparison of optimized model parameters difficult. We will continue our research to better quantify and, if possible, avoid issues of non-uniqueness using these and subsequent data sets collected in project years 2 and 3.

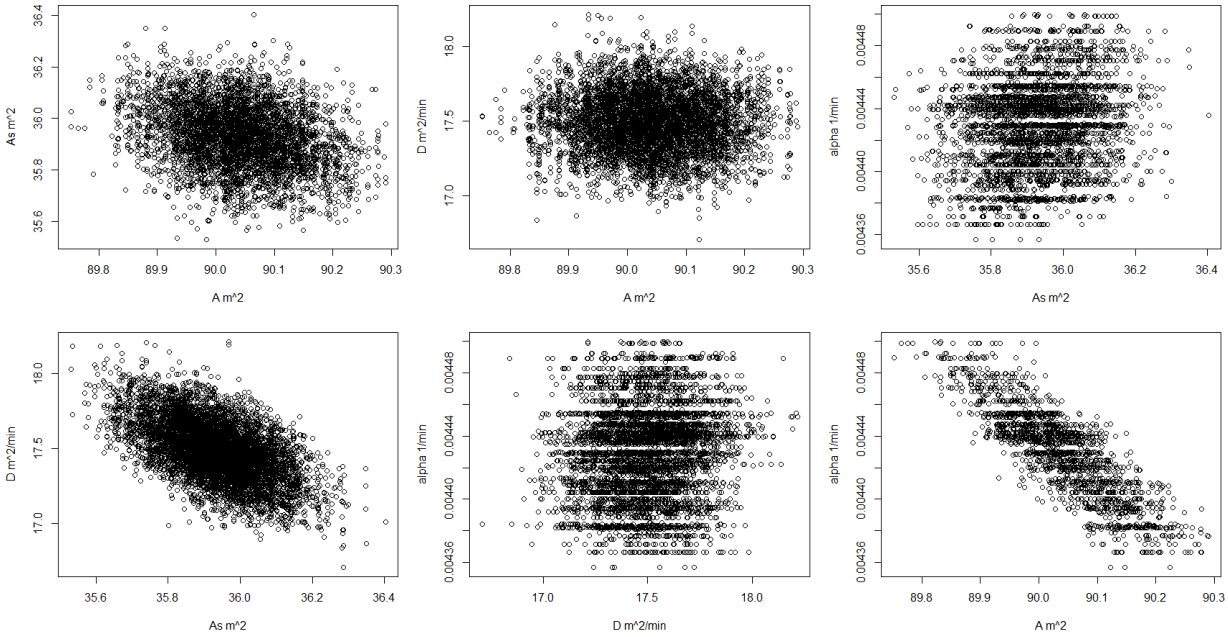

Figure 5.1.11. Relationships between parameter pairs across the entire population of Bayesian model fits.

Several steps were required to estimate the hydraulic properties of just the downstream reach (between the midpoint and downstream stations), and to compare these results to a previous experiment (Hensley, 2010). While midpoint and downstream measurement locations used in the two studies were identical, the 2009 study injected the dye as a line released at the 1,200 m station, while this study injected the dye as a "point" in the main spring vent. To circumvent this issue, for both studies we used the measured BTC at the midstream reach as un upstream flow and concentration boundary condition and then fit the OTIS model to the BTC at the downstream station. Fitted OTIS model parameters were then used to compare simulated 2009 and 2015 BTCs at the downstream station based on the fitted hydraulic properties of those two times.

Figures 5.1.12a and 5.1.12b present measured BTCs at the midpoint and downstream locations in 2009 and 2015, respectively. Fitted OTIS model parameters for these observed data were then used to simulate the BTC shown in Figure 5.1.12c, assuming an upstream dye injection based on Hensley (2010). Visual inspection reveals substantial differences in the BTC simulated for the

two experiments. Notably, the peak arrives sooner in 2015 (indicating higher velocities) and the BTC tail has a much longer decay (likely indicating increased transient storage). These interpretations are supported by the fitted OTIS model parameters, which are summarized for these and all other BTCs (and solution methods) in Table 5.1.2.

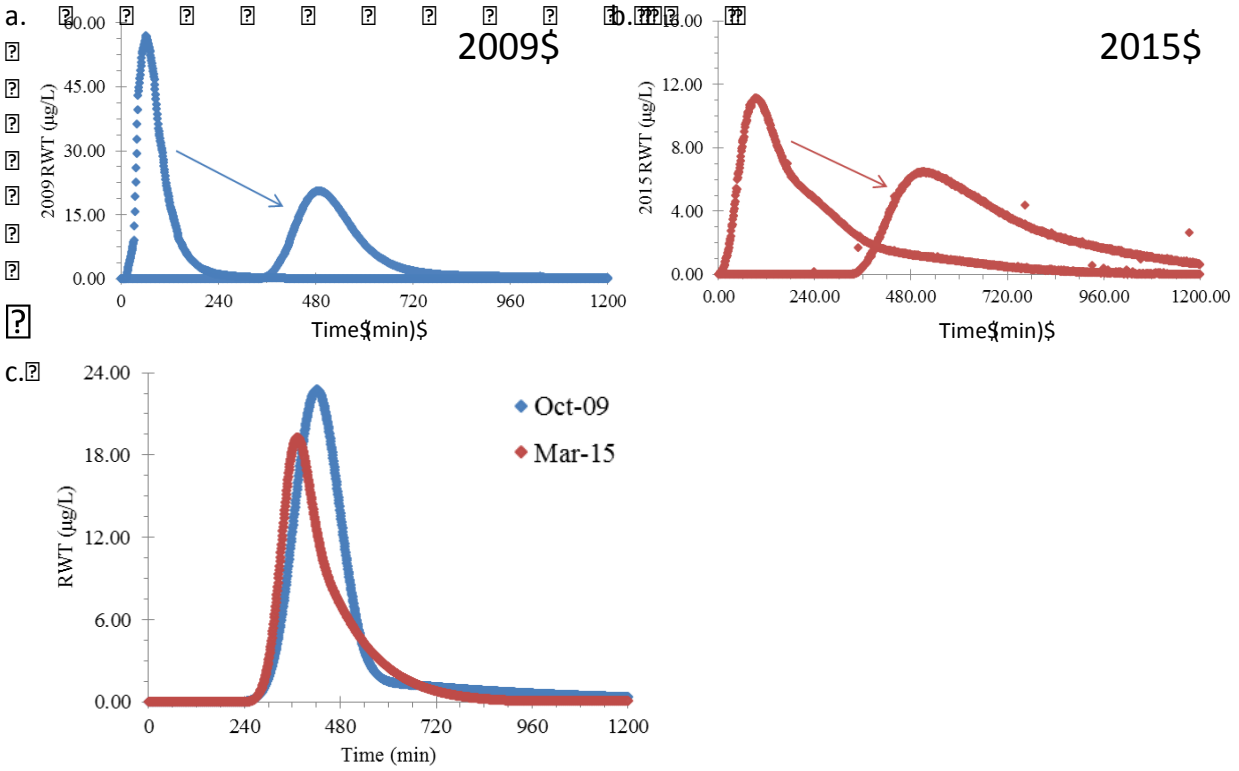

Figure 5.1.12. Comparison of 2009 and 2015 tracer experiments for the downstream portion of the Silver River. See text for details.

Table 5.1.2. Fitted OTIS model parameters for all BTCs presented above.

	Upstream (both 4/2015)		Downstream (both SSE)		Whole River (both 4/2015)	
Parameter	SSE	Bayes	10/2009	4/2015	SSE	Bayes
Q (m^3s^{-1})	20.0	20.0	15.5	20.0	20.0	20.0
L (m)	2,700	2,700	5,300	5,300	5,300	5,300
A (m^2)	104.9	104.9	73.4	80.8	90.1	90.1
A_s (m^2)	54.9	54.9	18.1	17.3	35.9	35.9
D (m^2 s^{-1})	24.0	23.9	10.7	5.8	17.5	17.5
α (L s^{-1})	7.96 x 10^{-3}	7.967x 10^{-3}	1 x 10^{-5}	5 x 10^{-5}	4.42 x 10^{-3}	4.43 x 10^{-3}
τ (min)	236	236	418	357	398	398
u (m s^{-1})	0.19	0.19	0.21	0.25	0.22	0.22

5.1.4.1.3 Breakthrough Curve Data vs. EFDC Model

District scientists have been developing a hydrodynamic EFDC model for the Silver River with a primary goal of predicting unsteady water level profiles and velocity profiles. The BTC data presented above provide an opportunity to calibrate and validate EFDC model performance using measured data. Model development is ongoing, however an initial, uncalibrated version of the model was used to simulate the 2015 dye release for comparison with observed BTCs (Figure

5.1.13). We note that *these comparisons should be considered provisional*, as model development is ongoing.

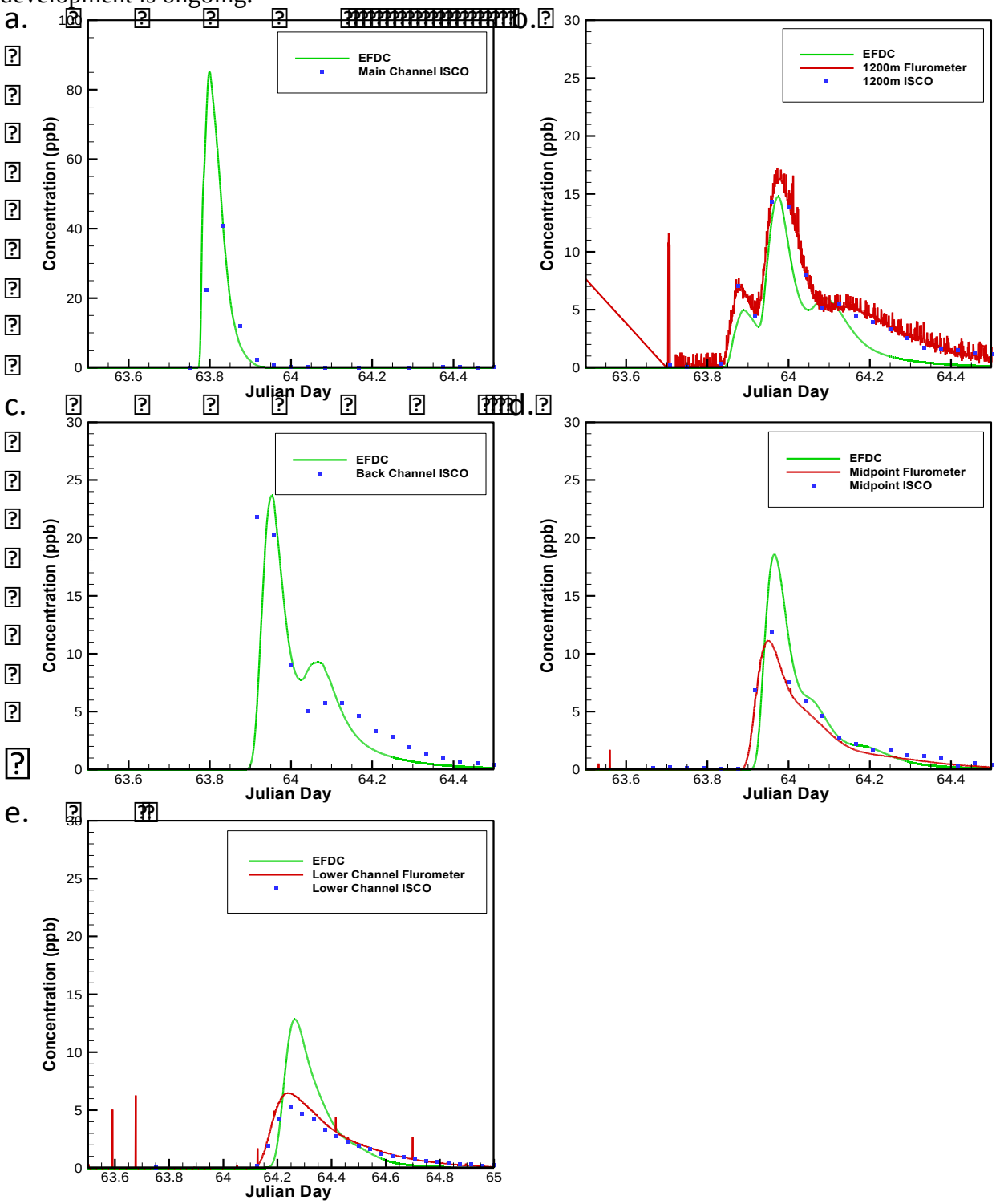

Figure 5.1.13. Comparison between observed (red lines, blue dots) and modeled (green lines) BTCs at five locations on the Silver River. See Figure 5.1.2 for measurement locations. Figures by Yanfeng Zhang.

The uncalibrated model is able to capture some of the major features captured by the dye injection experiment and provides insight in locations where the match is poor. For example, the model recreates the three-peaked BTC observed at the 1,200 m station (Figure 5.1.13b) and two-peaked BTC at the back channel station (Figure 5.1.13c), corroborating our interpretation of flowpaths and incomplete channel mixing. On the other hand, measured data at these stations suggest longer residence times than those simulated in EFDC, which predicts rapid declines in concentration. Upriver in the main channel (Figure 5.1.13a), it is unclear whether EFDC overestimates the BTC peak or the 1-hr sampling resolution was insufficient to capture the peak concentration. The general time of arrival and mean residence times at the mid-point (Figure 5.1.13d) and downstream (Figure 5.1.13e) stations agree fairly well between modeled and measured data, though EFDC overestimates the peak at both stations. Model performance is expected to improve with further calibration.

5.1.4.2 Raz-Rru Experiments

5.1.4.2.1 Raz and Rru Transformation versus Time

For samples with autoclaved soils (see Figure 5.1.14), the added tracer was the only compound assumed present throughout the experiment; concentrations over time were determined using a single calibration for the given tracer to avoid the introduction of error in solving the full set of equations. From the inactivated samples, the decrease of both Raz and Rru concentrations over the incubation period was more pronounced for the Silver River soils. As shown in Figure 5.1.15, this was also the case for live soils where the Raz concentration in Silver River soil decreased by more than 60% over the first 40 minutes of incubation vs the initial 38% change observed in the Jennings Creek sediment. However, the reported increasing Raz trend for the inactive Jennings Creek sediment is not possible and likely the product of signal separation error.

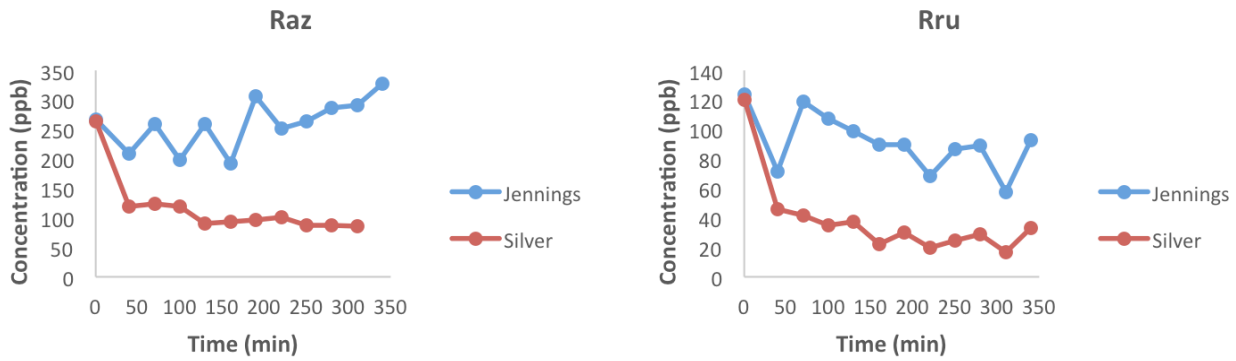

Figure 5.1.14. Adsorption to inactive sediment.

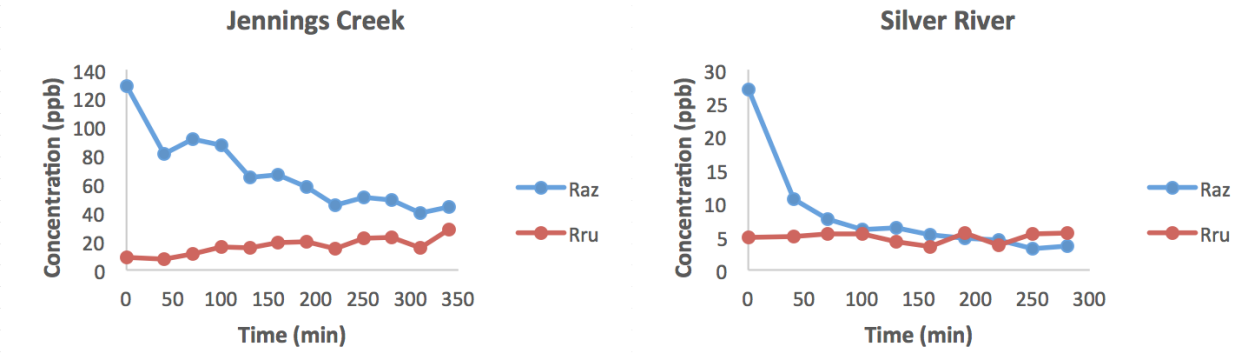

Figure 5.1.15. Combined effects of microbial activity and adsorption to sediment.

5.1.4.2.2 Kinetic Parameters

Tables 5.1.3 and 5.1.4 summarize the sorption and kinetic transformation rates for Raz and Rru determined by fitting the batch experiment data to the set of equations relating bacterial concentration, soil sorption, and overall conversion of Raz to Rru. For both tracers, the Silver River sediment was found to have a higher total adsorption capacity and in both sites, the adsorption capacity for Rru was twice that of Raz. The Silver River sediment was also more biologically active with a relative microbial concentration five times that of the Jennings Creek sediment. In terms of transformation and sorption rates, values were consistently greater for the Silver River, except for Raz conversion. In this organic sediment, adsorption may be the dominant removal mechanism for Raz. The results in Table 5.1.4 are also comparable to kinetic rates and sorption data in other studies (González-Pinzón et al. 2012; Lemke et al. 2013).

Table 5.1.3. Relative sediment sorption capacities.

System	Total Sorption Sites (M)	Total Microbes (M)
Jennings	1	2.2
Silver	5.8	11

Table 5.1.4. Fitted reaction and sorption rates.

Tracer	Kinetic rate (1/M*s)		Adsorption (1/M*s)	
	Jennings	*Silver*	*Jennings*	*Silver*
Raz	$2*10^{-5}$	$8.33*10^{-6}$	$1.67*10^{-6}$	$3.46*10^{-5}$
Rru	$3.33*10^{-5}$	$6.67*10^{-5}$	$1.67*10^{-5}$	$2.97*10^{-5}$

5.1.4.2.3 Advection-Dispersion Modeling

Kinetic transformation and sorption rates were combined as a single decay coefficient for each tracer and utilized in OTIS modeling of Raz and Rru breakthrough curves (BTCs) for simulated stream reaches containing the two sediment types. The Raz and Rru BTCs are presented alongside that of a conservative tracer for both reaches. Hydraulic parameters of the systems are summarized in Table 5.1.5.

Table 2.1.5. Fitted reaction and sorption rates.

Parameter	Modeled Value
Flow (m^3 min^{-1})	0.283
Effective Area (m^2)	0.5
Storage Area (mm^2)	1
Dispersion Coefficient (m^2 min^{-1})	0.003
Exchange Coefficient (1 min^{-1})	0.12

As shown in Figure 5.1.16, a pulse injection of Raz and the conservative tracer fluorescein to a reach with Jennings Creek sediment would likely exhibit peak concentrations of 3.2 and 0.4 ppb Raz and Rru, respectively. This sums to the 3.6 ppb peak for fluorescein as expected. The Rru peak also occurs later due to retention in the transient storage zone. For the same reach with Silver River sediment, the same mean residence time of approximately 80 minutes is observed, however the Raz peak occurs sooner and the conversion of Raz to Rru is more pronounced as would be expected for more organic sediment. All three breakthrough curves also show longer tails than for the Jennings sediment which is likely a product of increased sorption and short-term tracer retention and release from hyporheic zones.

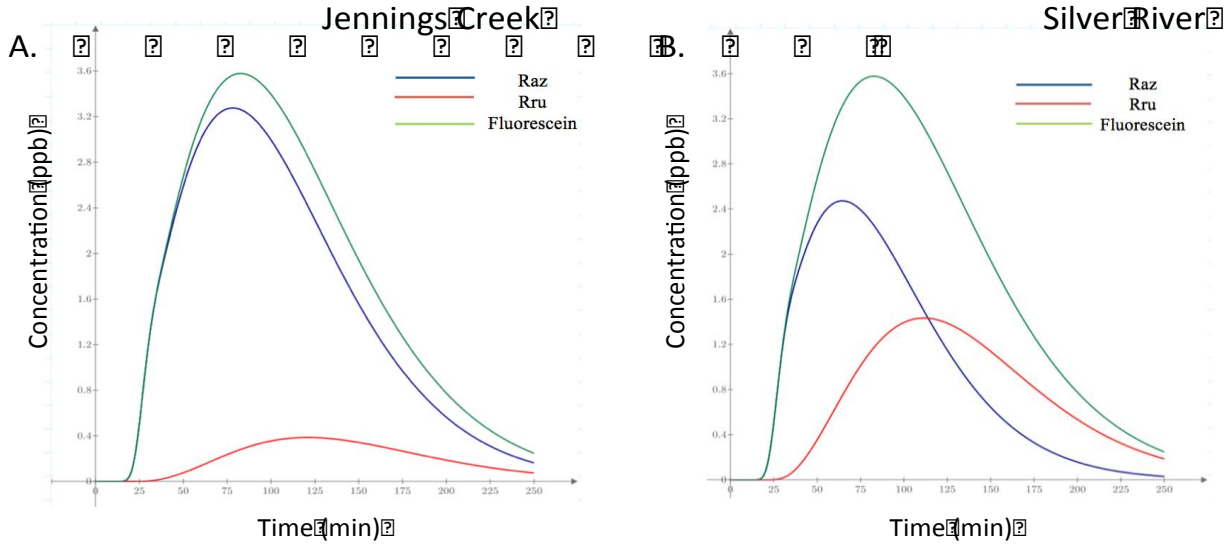

Figure 1. Raz and Rru breakthrough curves using kinetic and transport parameters for Jennings Creek (A) and Silver River (B).

5.1.4.2.4 Raz and Rru Discussion

As shown in Figures 5.1.14 and 5.1.15, measured Raz and Rru concentrations from the batch experiments contained a degree of uncertainty likely introduced by a combination of experimental and calibration error. Experimental issues could include pipetting and volume errors in sample preparation as well as slight photodegradation of the tracers. However, signal separation was likely dominant as preliminary tests of known Raz and Rru concentration mixes consistently produced overestimates of the Rru concentration. This is attributed to the fact that the fluorescence spectra for the two tracers overlap and that Rru is more fluorescent. Depending

on the excitation and emission wavelengths employed, simultaneous measurements of both tracers below 1 ppb are not considered reliable (Lemke et al. 2013). In future laboratory work, calibrations will be performed with a set of wavelengths that will allow for more accurate Raz and Rru separation.

From the kinetic rate and sorption results summarized in Tables 5.1.3 and 5.1.4, the organic sediments of the Silver River were found to be orders of magnitude more active than those of Jennings Creek for some parameters. As Rru sorption was most significant in both systems, it is likely that this could be a major source of concentration detection error in reach scale studies and could make pulse injections infeasible even in small streams. The breakthrough curves shown in Figure 5.1.16 illustrates the predicted breakthrough curves for pulse injection tracer tests in reaches with Jennings Creek and Silver River sediment, respectively. As shown in Figure 5.1.16, Rru concentrations produced in Jennings Creek are below the 1 ppb detection limit for in-stream fluorometers which agrees with previous results in the actual stream (Lemke et al. 2013). For the same reach geometry with Silver River sediment, about 3 times more conversion of Raz to Rru can be expected with increased transient storage retention due to the higher sorption capacity and microbial activity of the system. Overall, fitted parameters from the batch experiments provide an accurate representation of the breakthrough curve trends that would be expected for sandy vs organic sediments.

In terms of the effectiveness of the system in estimating microbial activity for a specific site, the model utilized in this study did predict a microbial concentration for the Silver River that was five times that of Jennings Creek as expected for a more productive system. While full reach scale studies in large, highly organic spring systems may be impractical, this may indicate that for studies of isolated areas within a reach, the Raz-Rru system could provide an estimate of the overall biogeochemical activity given varying hydraulic parameters. However, further work is needed to determine whether this estimate could provide proportions of various reactions (e.g., aerobic respiration versus denitrification).

5.1.5 CONCLUSIONS, RECOMMENDATIONS, AND FUTURE RESEARCH NEEDS

Work to meet the goals of this chapter will continue in project years 2 and 3, at which time overall conclusions and recommendations can be given. In particular, we plan to conduct several additional tracer injection experiments. If possible, injection studies will be performed during periods of low, medium, and high downstream stage (i.e., ~25th, 50th, and 75th percentile water levels at the confluence of the Silver and Ocklawaha Rivers) to develop a relationship between fitted hydraulic parameters at the reach scale and downstream water management. We also propose to continue measurement of BTCs in storage zones (i.e., macrophyte beds) during these experiments to characterize patch-scale flow patterns (i.e., two-layer flow, turbulent mixing) that can strongly affect solute transport. Both reach- and patch-scale BTC measurements will be useful for corroborating ongoing 3-D modeling (EFDC) by providing empirical support for modeled velocities and suggested mixing zones. Analysis of our existing rover data will help guide locations for these measurements during the next injection.

5.1.6 REFERENCES

Briggs, M. A., Lautz, L. K., Hare, D. K., and González-Pinzón, R. (2013). Relating hyporheic fluxes, residence times, and redox-sensitive biogeochemical processes upstream of beaver dams. *Freshwater Science, 32*(2).

Bristow, J. M., and Whitcombe, M. (1971). The role of roots in the nutrition of aquatic vascular plants. *Amer. J. Bot., 58*(1).

Caffrey, J. M., & Kemp W. Michael. (1992). Influence of the submersed plant, *potamogeton perfoliatus,* on nitrogen cycling in estuarine sediments. *Limnol.Oceanogr., 37*(7).

Carignan, R. (1982). An empirical model to estimate the relative importance of roots in phosphorus uptake by aquati macrophytes. *Can.J.Fish.Aquat.Sci, 39.*

Cedergreen, N., and Madsen, T. V. (2002). Nitrogen uptake by the floating macrophyte lemna minor. *New Phytologist, 155*(2), 285-292.

Chapman, R. S., and et al. (1995). *Investigation of wetlands hydraulic and hydrological processes, model development, and application.* (No. Wetlands Research Program Technical Report WRP-CP-6). Washington, D.C.: US Army Corps of Engineers.

González-Pinzón, R., Haggerty, R., and Myrold, D. D. (2012). Measuring aerobic respiration in stream ecosystems using the resazurin-resorufin system. *Journal of Geophysical Research: Biogeosciences, 117*(G3).

Haggerty, R., Argerich, A., and Martí, E. (2008). Development of a "smart" tracer for the assessment of microbiological activity and sediment-water interaction in natural waters: The resazurin-resorufin system.*Water Resources Research, 40.*

Haggerty, R., E. Marti, A. Argerich, D. von Schiller, and N. B. Grimm (2009), Resazurin as a ‘‘smart’’ tracer for quantifying metabolically active transient storage in stream ecosystems, *Journal of Geophysical Research: Biogeosciences*,114: G03014.

Hanson, G. C., Groffman, P. M., and Gold, A. J. (1994). Denitrification in riparian wetlands receiving high and low groundwater nitrate inputs. *Journal of Environmental Quality, 23*(5), 917-922.

Heffernan, J. B., and Cohen, M. J. (2010). Direct and indirect coupling of primary production and diel nitrate dynamics in a subtropical spring-fed river. *Limnology and Oceanography, 55*(2), 677.

Hensley, R. T., and Cohen, M. J. (2012). Controls on solute transport in large spring-fed karst rivers. *Limnology & Oceanography, 57*(4), 912.

Hinkle, S. R., and et al. (2001). Linking hyporheic flow and nitrogen cycling near the willamette river-a large river in oregon, USA. *Journal of Hydrology, 244*(3-4).

Kelleher, C., et al. "Identifiability of transient storage model parameters along a mountain stream." *Water Resources Research* 49.9 (2013): 5290-5306.

Lemke, D., Liao, Z., Wohling, T., Osenbruck, K., and Cirpka, O. A. (2013). Concurrent conservative and reactive tracer tests in a stream undergoing hyporheic exchange. *Water Resources Research, 49,* 1-14.

Lemke, D., Schnegg, P. A., Schwientek, M., Osenbruck, K., and Cirpka, O. A. (2013). On-line fluorometry of multiple reactive and conservative tracers in streams. *Environmental Earth Science, 69,* 349-358.

Lin, Y., Jing, S., Wang, T., and Lee, D. (2002). Effects of macrophytes and external carbon sources on nitrate removal from groundwater in constructed wetlands. *Environmental Pollution, 119*(3).

Madsen, J. D., Chambers, P. A., James, W. F., Koch, E. W., and Westlake, D. F. (2002). The interaction between water movement, sediment dynamics and submersed macrophytes. *Hydrobiologia, 444*(1-3), 71-84. doi:10.1023/A:1017520800568.

Morris, E. P.,and et al. (2008). Interaction between hydrodynamics and seagrass canopy structure: Spatially explicit effects on ammonium uptake rates. *Limnology and Oceanography, 53*(4), 1531–1539.

Mulholland, P., and et al. (2008). Stream denitrification across biomes and its response to anthropogenic nitrate loading. *Nature, 452*.

Mulholland, P.J., H.M. Valett, J.R. Webster, S.A. Thomas, L.N. Cooper, S. Hamilton, and B.J. Peterson. 2004. Stream denitrification and total nitrate uptake rates measured using a field ^{15}N tracer addition approach. Limnology and Oceanography 49:809-820.

Pusch, M., Fiebig, D., Brettar, I., Eisenmann, H., Ellis, B. K., Kaplan, L. A., and Traunspurger, W. (1998). The role of micro- organisms in the ecological connectivity of running waters. *Freshwater Biology, 40*(3), 453-495.

Reddy, K. R. (1983). *Fate of nitrogen and phosphorus in a waste-water retention reservoir containing aquatic Macrophytes1* Retrieved from https://www.agronomy.org/publications/jeq/abstracts/12/1/137

Runkel, R. L. (1998). *One-dimensional transport with inflow and storage (OTIS): A solute transport model for streams and rivers.* (No. 98-4018). Denver, CO: US Geological Survey.

Stapel, J., and et al. (1996). Nutrient uptake by leaves and roots of the seagrass *thalassia hemprichii* in the spermonde archipelago, indonesia. *Marine Ecology Progress Series, 134*

Stream Solute Workshop. (1990). Concepts and methods for assessing solute dynamics in stream ecosystems. *Journal of the North American Benthological Society, 9*(2), 95.

Veraart, A., Bruijne, W. J., Klein, J. M., Peeters, E. H. M., & Scheffer, M. (2011). Effects of aquatic vegetation type on denitrification. *Biogeochemistry, 104*(1-3), 267-274. doi:10.1007/s10533-010-9500-z.

Zarnetske, J. P. (2009). Resazurin as a "smart" tracer for investigating hyporheic biogeochemical processes. *Geological Society of America Abstracts with Programs, 41*(7), 470.

Section 5.2 Critical Velocity/Shear Stress

5.2.1 INTRODUCTION

Section 4 of the RFQ identifies the identification of an upper velocity threshold or event (duration of exceedence) for the presence of filamentous algae or hydrilla as a major question, based on correlated observations of velocity declines and algal expansion. One previous study (King 2012) suggests that inhibitory effects may be present at low velocities (ca.5 cm s^{-1}). Between 1933 and 1997, measured velocity in the Silver River exceeded this level approximately 50% of the time, but in recent years this velocity is exceeded < 5% of the time (Figure 5.2.1), providing correlative support for this hypothesis, however the presence of dense algal mats in areas where this velocity is frequently exceeded highlights a remaining gap in knowledge about the critical bed-shear for algal sloughing. Moreover, we expect that critical velocities or shear stresses for algal sloughing likely exhibit non-linear and density-dependent behavior whereby the clearing of dense algal mats (i.e., via flow increases) requires much greater velocity/shear stress than the prevention of algal accumulation in sparsely colonized reaches. Finally, we note that there are currently no data to support velocity/shear stress thresholds for uprooting of hydrilla.

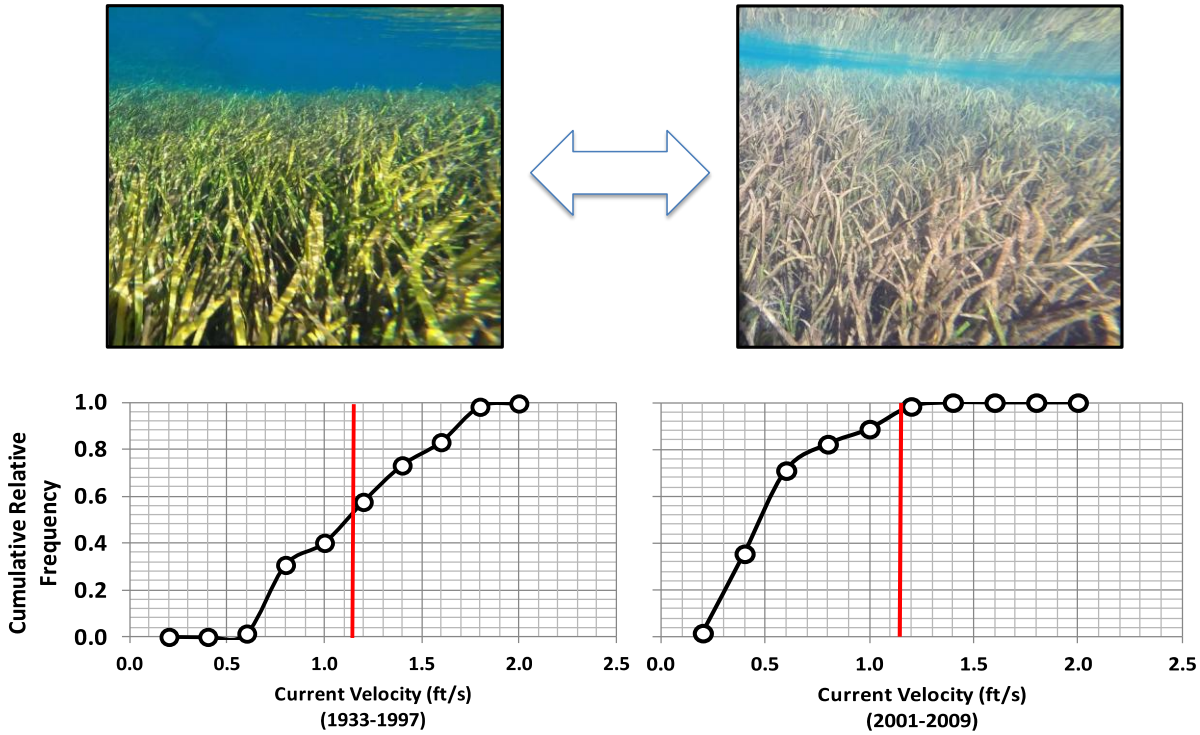

Figure 5.2.1. Algal cover is hypothesized to be controlled strongly by velocity, which has decreased markedly in the Silver River in recent years. Lower figure from Lowe (2014).

5.2.2 MATERIALS AND METHODS

Based on the knowledge gaps summarized above, we propose to use two field efforts to better test the velocity/shear stress-algal cover hypothesis and determined critical thresholds for algal entrainment that can be used as management targets: *in-situ* flow-ways and coupled optical algal and velocity measurements over large areas.

5.2.2.1 Flow-ways

Our primary approach to addressing these knowledge gaps is to perform *in situ* experiments to elevate and exclude flow in order to determine critical shear stresses for the entrainment and sloughing of epiphytic and benthic algae. The application of *in situ* flow-ways deployed across a range of bottom types, vegetation covers, and algal densities will provide a more robust estimation of critical hydraulic variables, which can incorporated into models existing and proposed hydrodynamic models to predict the effect of management actions on attached algae. Adjustable experimental flow-ways may also be used by other groups to test the effects of flow on other ecological components and processes (e.g., grazer density, grazing rate, productivity, autotrophic NO_3-N uptake, etc.).

Flow-ways will be constructed based on a modified design based on both the "Benthos Boxes" proposed for experimental work by the Nitrogen Effects/Dynamics and Trophic Interaction Groups and the experimental design used by King (2012). Flow-ways will be rectangular (ca.1 x 2 m) enclosures that may extend out of the water columns, are open to flow on both ends, and are screened to catch detached algae at the downstream end. An adjustable flange-type opening on the upstream end will allow us to focus or exclude incoming flow to provide a range of flows, velocities, and shear stresses within a single experimental location (Figure 5.2.2).

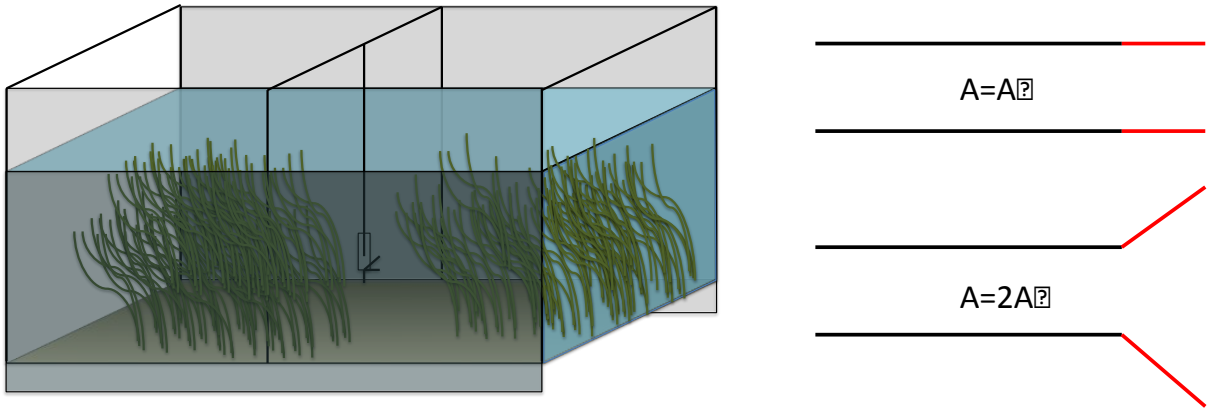

Figure 5.2.2. Proposed flow-way design.

Within each flow-way, velocities will be measured using a Sontek 3-D acoustic Doppler velocimeter (ADV) and velocity profiles will be used to calculate shear stresses under different flow scenarios. Biomass (dry weight) of sloughed algae will be correlated against hydraulic variables (flow, velocity, turbulence, and shear stress). We expect that shear stress will best predict both benthic and epiphytic algae sloughing, but that the proportion of sloughed algae as a function of stress will be density dependent (i.e., more difficult to slough when algal communities are well established and densities are high). We will test this by deploying the flow-ways in locations with a gradient of both benthic and epiphytic algae. Flow-way prototype construction is ongoing, and results from these experiments are not yet available.

5.2.2.2 Optical Methods

The goal of these optical methods are to collect algal cover and velocity data over wide areas to better explore the velocity-algal cover relationship and determined critical velocities more

robustly. Current methods for algal cover characterization (i.e., visual estimation using quadrats) are impractical for acquiring high spatial resolution, spatially distributed data and relies on human estimation, which introduces subjectivity. We seek a rapid, quantitative method to cover large areas using continuous image capture and processing coupled with continuous velocity measurement. We are pursuing two optical techniques for algal cover estimation: average-image color shift and chromaticity (Figure 5.2.3).

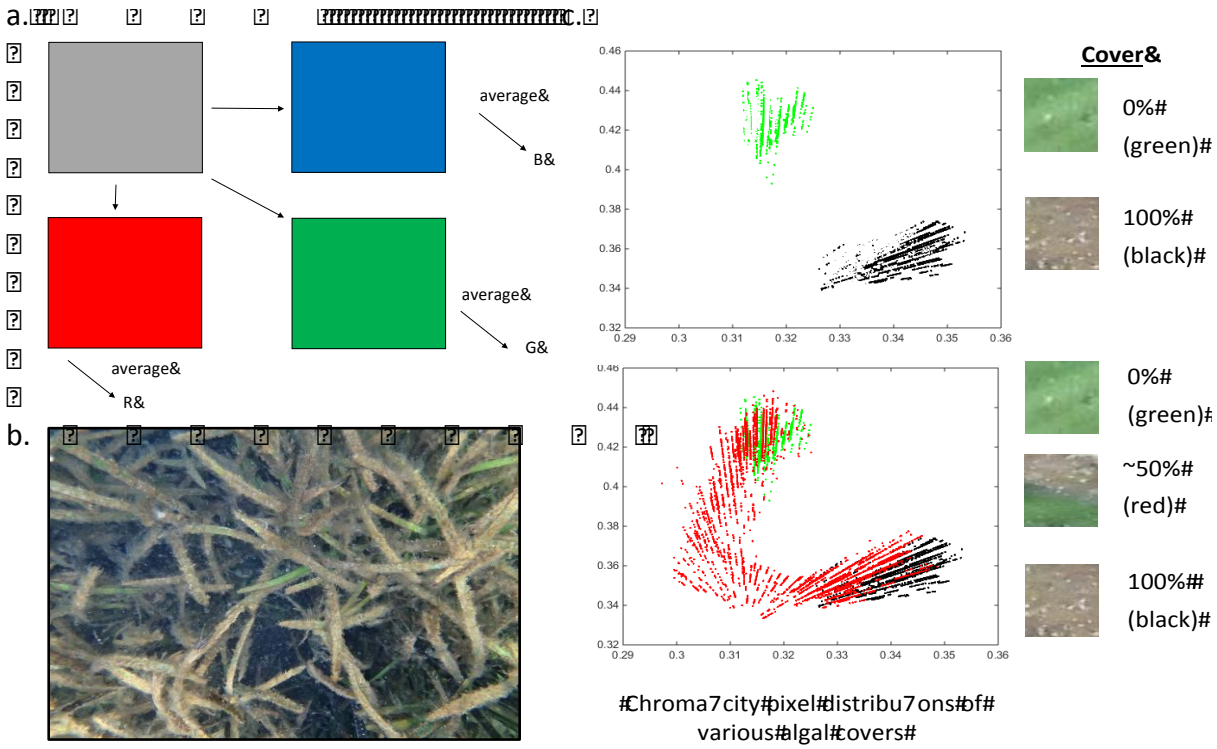

Figure 5.2.3.. Schematic of red-green-blue color separation (a), standard SAV-algae image used to test optical methods (b), and chromaticity distribution of various algal covers (c).

Average-image color shift processes entire images by decomposing color into image-averaged values of the red, blue, and green bands (Figure 5.2.3a). Average image color was then calculated color according to:

$$Color = \log(Band\ 1) - \log(Band\ 2) = \log\left(\frac{Band\ 1}{Band\ 2}\right)$$

$$ColorBG = \log(B) - \log(G) = \log\left(\frac{B}{G}\right)$$

$$ColorGR = \log(G) - \log(R) = \log\left(\frac{G}{R}\right)$$

The photometric color system was calibrated against field measurements of algal cover using a standard SAV image from the Silver River (Figure 5.2.3b) segmented into regions of varying algal cover using both a subjective (i.e., visual) and an objective K-clustering method. We present tests of the algal cover-velocity relationship using cover estimates derived with this method.

For field tests, still and video images were collected using a hand-held or boat mounted GoPro

camera (Figure 5.2.5), and velocity was measured using an electromagnetic flow meter (EFM) (MF Pro Flow Meter, OTT Hydromet Inc., Loveland, CO). Additionally, depth measurements were taken with each image and used to correct image color for depth using a standard relationship developed using a color loss vs. depth relationship.

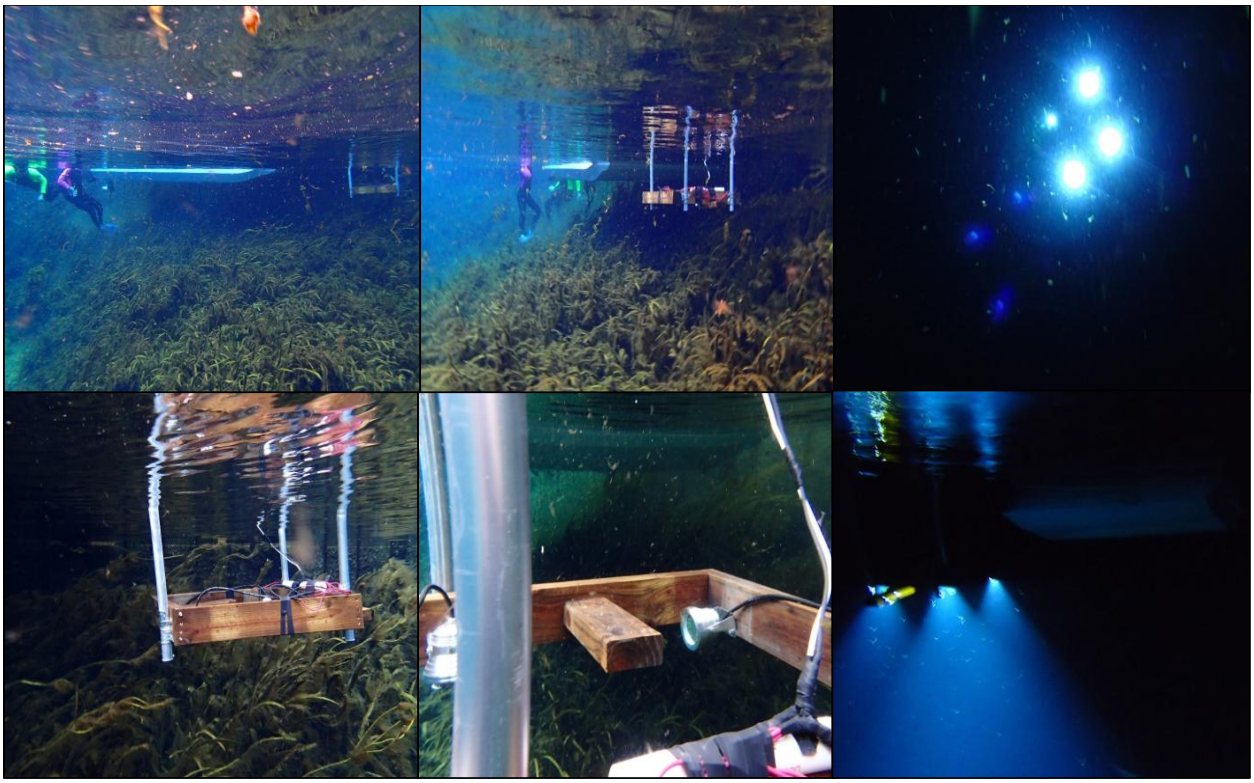

Figure 2. Optical algal cover image collection via GoPro camera mounted to research vessel. Ongoing work seeks to capture images at night using an artificial light source to standardize lighting.

For the chromaticity method, the image is analyzed pixel-by-pixel; since SAV and algae are visually distinct, they can be potentially be identified based on their chromaticity, with total cover being calculated by summing cells the number of pixels that match a training image. While only preliminary test data are available for the chromaticity method (Figure 5.2.3c), the chromaticity pixel distribution of SAV (green points in Figure 5.2.3c) does not overlap with the periphytic algae distribution (black points). Moreover the pixel distribution of 50% algal cover is concentrated in the same locations as a pure SAV or algal image. Taken together, these initial findings show promise and we continue to refine these methods.

5.2.3 RESULTS AND DISCUSSION

Initial results from the average-image color shift show substantial promise for high-resolution, spatially distributed mapping of algal cover (Figure 5.2.4). Both of the integrated images colors (B-G and G-R) are correlated to algal cover, and are more tightly correlated to cover determined by K-clustering method. Moreover, both B-G color and algal cover correlate with flow velocity, suggesting that the B-G color of an algal covered SAV bed can be used as a proxy for algal

cover, perhaps providing a more accurate measure than quadrat methods. This process can be automated to map large areas of SAV beds and provides additional support for the hypothesis that velocity plays some level of control on periphytic algal communities.

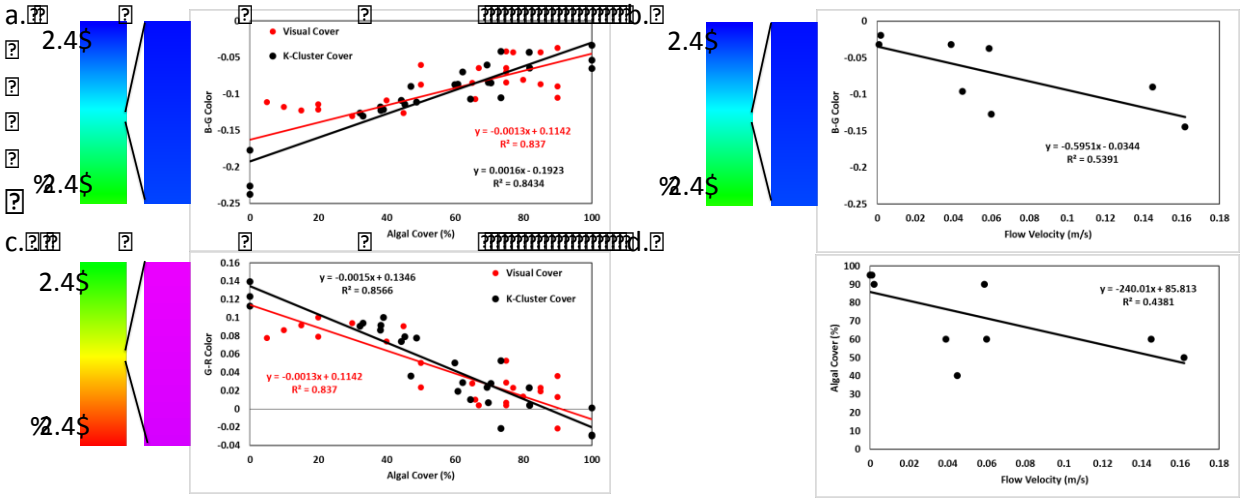

Figure5.2.5. Relationships between integrated images colors (B-G and G-R) and algal cover determined using visual and automated techniques.

5.2.4 CONCLUSIONS, RECOMMENDATIONS, AND FUTURE RESEARCH NEEDS

Work to meet the goals of this chapter will continue in project years 2 and 3, at which time overall conclusions and recommendations can be given. Future work includes field-testing flow-way prototypes, improving image capture and processing techniques (Figure 5.2.5), and integrating the image capture and velocity measurement platform to collect real-time data over large areas.

5.2.5 REFERENCES

Lowe, E. (2014). The Research Component of the Springs Protection Initiative of the St. Johns Water Management District. UF Water Institute Symposium, February 2014, Gainesville, FL.

King, S. A. (2014). Hydrodynamic control of filamentous macroalgae in a sub-tropical spring-fed river in Florida, USA. *Hydrobiologia*, *734*(1), 27-37.

Section 5.3 Additional Links with SJRWMD Modeling Efforts

5.3.1 INTRODUCTION

The aim of this effort is to link study findings (within this work order and from other project components) to ongoing 3-D modeling, with a focus on SAV impacts on velocity, residence times, and effects on stage-discharge relationship. This effort is made up of three primary tasks: 1) velocity validation, 2) reduced complexity modeling, and 3) a water quality modeling assessment.

1. A major objective of EFDC modeling is to generate predictions of horizontal and vertical flow velocities under a variety of boundary conditions and bottom characteristics. In order to validate EFDC results, field measurements of velocity are required, however the use of 4-beam acoustic Doppler current profilers (ADCP) provides limited information in reaches with dense submerged aquatic vegetation. The goals of the velocity validation effort are to provide discrete, point-based velocity data for use in model calibration and validation and to determine when and where ADCP measurements are sufficient to characterize discharge and velocity profiles.

2. The goal of pursuing reduced complexity modeling is to assist the District hydrodynamics/ hydraulics modeling team to synthesize EFDC results based on a smaller number of parameters, with a focus on management relevant interventions (i.e., levers) that can be used to address specific management goals. While this is an existing goal of the work plan, particular attention is required to ensure that the reduced complexity model adequately characterizes the system, is driven by specific actions (water level management, vegetation control, etc.), and is integrated with the proposed "Synthesis Model". Potential simplifications include reach-scale hydraulic parameterization that includes baseline information for channel geometry, slope, and roughness, which can be modified as a function of bottom type, vegetation types and density, season, and discharge. Based on the set of field studies and modeling efforts proposed in the larger work plan, we expect that empirical relationships between these factors can be used to incorporate a basic set of hydraulic variables into the synthesis model. A primary goal of this effort will be to coordinate efforts between working groups to identify the most critical hydraulic variables (e.g., not only for algae sloughing and hyporheic exchange, but also productivity, autotrophic NO_3-N uptake, grazing rates, etc.).

The goal of the water quality modeling assessment is to understand the potential for the field data and modeling work completed in thus study to be useful in future water quality modeling and to serve as a value-added component of this work that can be applied to other locations. For this objective, we propose a *post-hoc* assessment of how the data and models available by the end of the project can be used to achieve further water quality modeling (e.g., QUAL2K, WASP, etc.). Based on this "feasibility" study, we will make recommendations for future work (if any) in the Silver River and propose a general framework for the organization of future studies that aim to model riverine water quality.

In this year 1 report, we present results from the first of these three tasks. Tasks 2 and 3 are schedule for completion in years 2 and 3 after additional field data collection and model development are completed.

5.3.2 MATERIALS AND METHODS

Velocity measurements are needed to validate the EFDC modeling to predict horizontal and vertical flow velocities under a variety of boundary conditions and bottom characteristics. The District will deploy 4-beam acoustic Doppler current profilers (ADCP) for this purpose; however, ADCP profilers provide limited information in reaches with dense submerged aquatic vegetation. As such, UF collected discrete, point-based velocity data for use in model calibration and validation and to aid in determining when and where ADCP measurements are sufficient to characterize discharge and velocity profiles.

To meet this goal, UF worked with the District to develop a set of riverine transects where velocity measurements were made using both a floating ADCP (District-owned) and point-based electromagnetic flow meter (UF-owned). Transect locations were selected to characterize a variety of bottom conditions (bare, sparse and dense macrophyte coverage, benthic algae dominated, etc.). Selected transects corresponded to transects developed for development of the Silver River MFL and include T3, T7, and T10 (Figure 5.3.1).

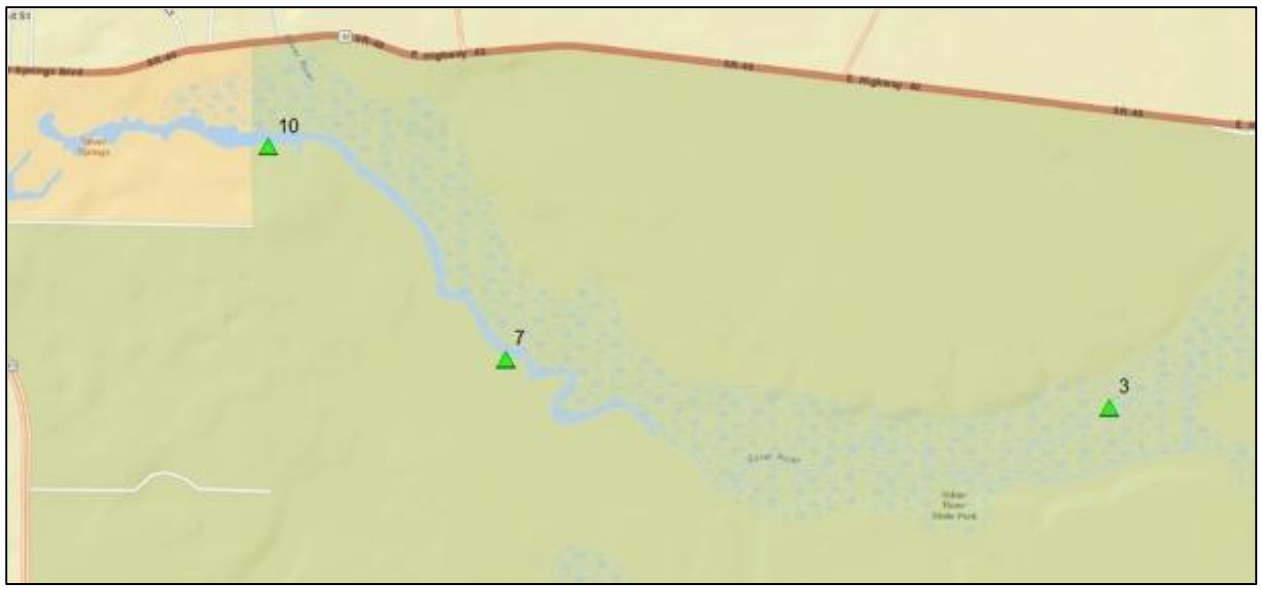

Figure 5.3.1. Velocity validation transect locations.

At each transect, velocity was measured using an electromagnetic flow meter (EFM) (MF Pro Flow Meter, OTT Hydromet Inc., Loveland, CO). The EFM was found to provide reasonable velocity data even in dense vegetation, which the previously proposed acoustic Doppler velocimeter (ADV) was unable to do. The EFM was mounted to a custom-made wading rod (Figure 5.3.2) to allow discrete depth measurements to a depth of 19.7 ft (i.e., 6 m).

Velocity profiles were made by traversing the river with a boat secured on both banks to keep the boat perpendicular to flow. A dedicated transect line marked with meters Figure 5.3.2B) was used to determine distance across the transect. The wading rod was placed so that it rested on the sediment surface, and velocity readings were taken at a minimum of 8 depths at each

measurement location. Horizontal spacing across the transect was every 3.28 ft (1 m) on T3 and every 6.56 ft (2 m). Velocity measurements were not collected on T10 due to glass-bottom boat traffic, which made the placement of transect and boat lines unfeasible.

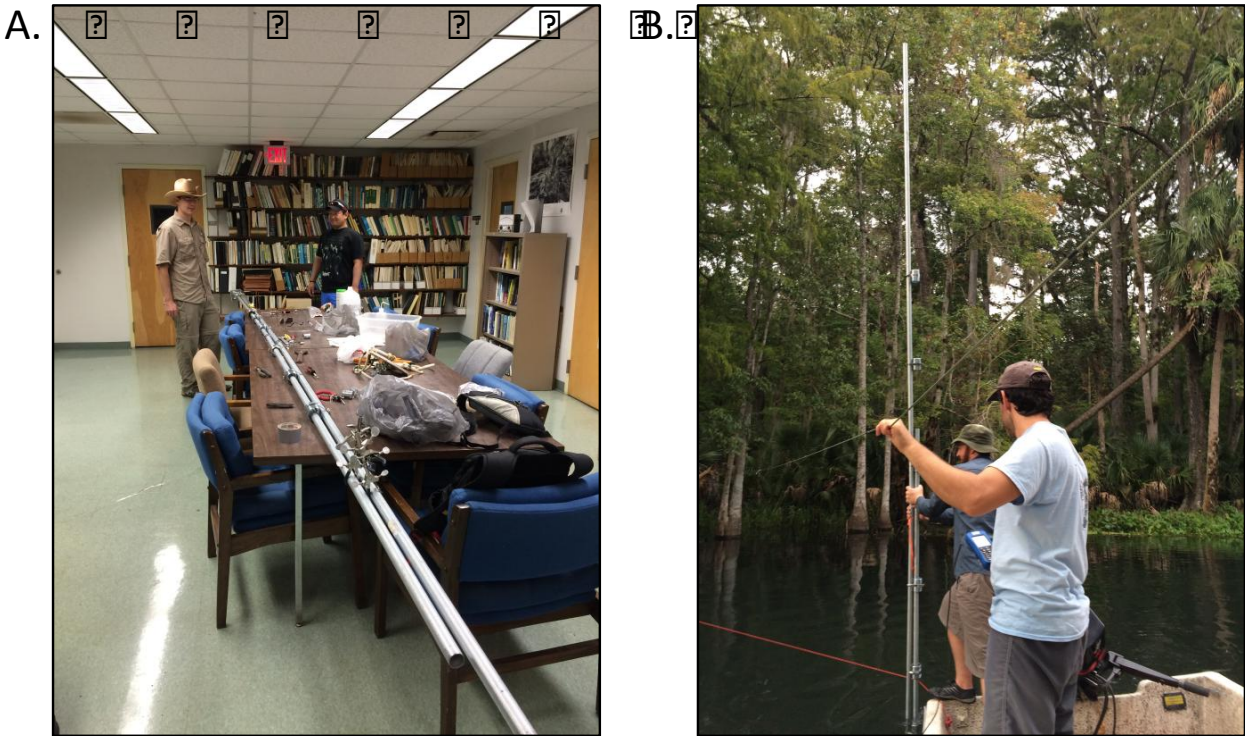

Figure 3. A) Wading rod construction showing full-length extension. B) Taking velocity readings on T3. Note transect line for horizontal spacing and boat line (red) for stability.

The EFM was programmed to output 10-second velocity averages based on 4 Hz data; a minimum of three 10-s average samples were taken for calculation of an average velocity value at each measurement point. Based on the horizontal and vertical spacing described above, a total of 1,131 discrete velocity measurements were taken on 10/3, 10/6, and 10/8/2014 (Appendix 5.3.1). Depth to vegetation was also noted at each distance across the transect where it was visible. Based on the average value at each measurement point, we created velocity contours and surfaces for each transect by ordinary kriging using statistical software (Surfer 11, Golden Software, Golden, CO).

5.3.3 RESULTS AND DISCUSSION

Velocity data are presented in Figures 5.3.3 and 5.3.4. These figures are useful for comparison with ADCP data collected at the same transects. We note that we were able to coordinate with District staff in the field to co-locate ADCP and EFM measurements on T3, but not on T7, so comparability of data collected by ADCP and EFM should be better on T3 (Figure 5.3.5). In general, velocities measured by each method are in the same range, but with several noteworthy exceptions. The ADCP data is clearly more highly resolved and identifies small patches of high-velocity flow that is not captured by the point-based EFM technique due to its lower spatial resolution. On the other hand, the point-based measurements capture velocity data near the

benthic surface in some locations where the ADCP does not provide data. This is also evident in the differences in inferred bathymetry between the EFM and ADCP approaches. Additional analysis of these data and subsequent velocity measurements will quantify "missing" flows from the absence of velocity readings in shallow and vegetated regions.

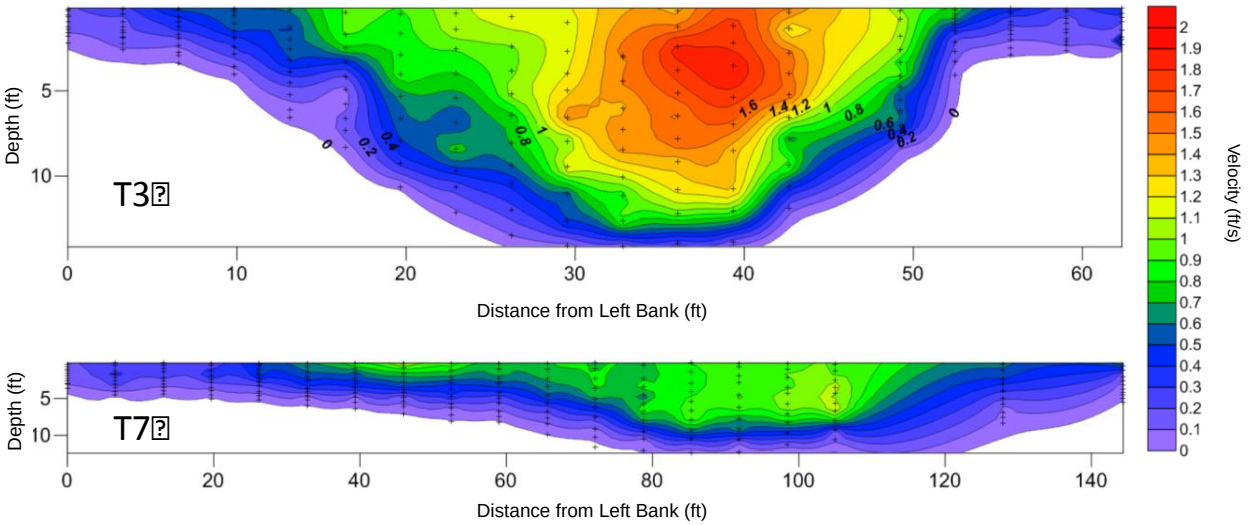

Figure 5.3.3. Velocity transects at T3 (top) and T7 (bottom). Velocity is indicated by a shared color scale, illustrating slower velocities at T7. Point velocity measurement locations are indicated by crosses. X and Y scales are proportional (i.e., 1:1).

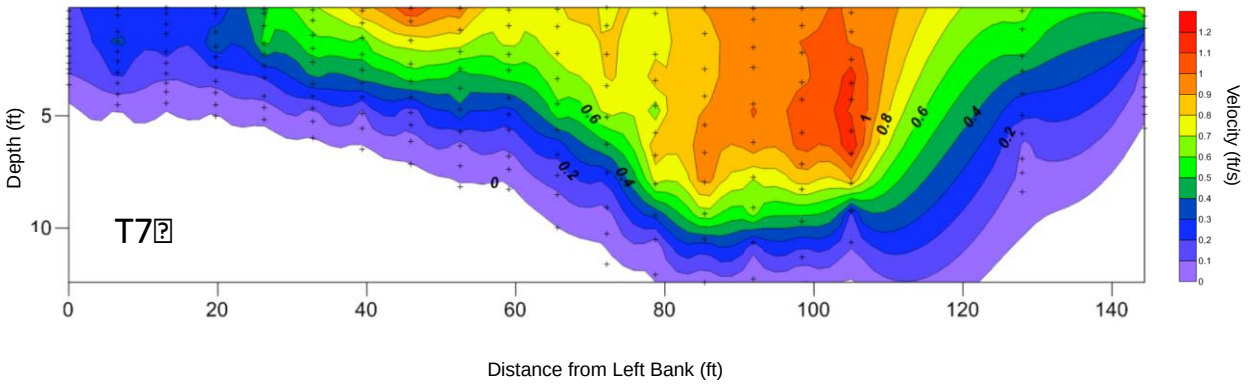

Figure 5.3.4. Rescaled velocity transect at T7. Color scale illustrates full range of measured velocity on T7. The Y scale is exaggerated 3x to make velocity variation with depth more visible.

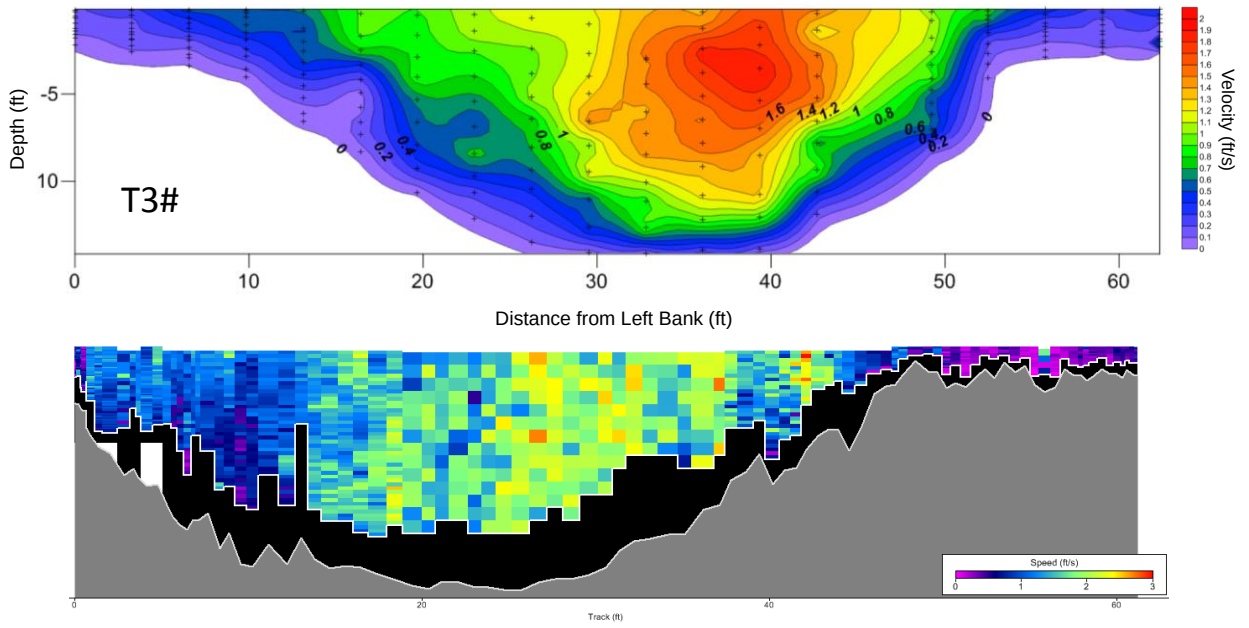

Figure 5.3.5. Comparison of kriged point-based velocity EFM velocity measurements (top) and ADCP velocity measurements (bottom) on T3 (co-located transect). Note different color scales in top and bottom figures.

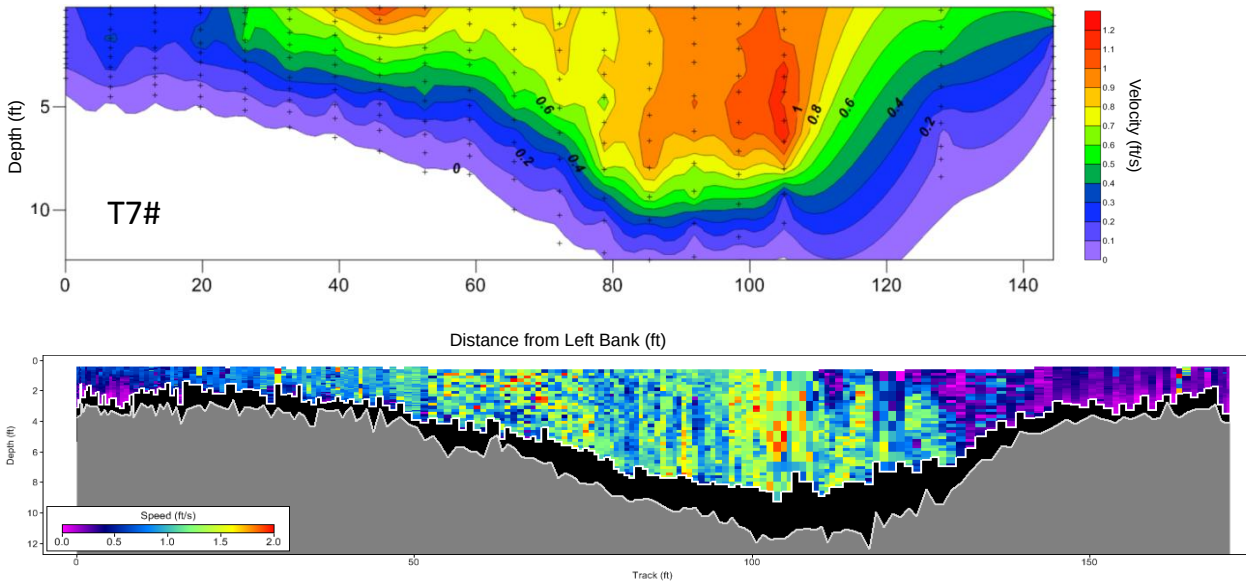

Figure 5.3.6. Comparison of kriged point-based velocity EFM velocity measurements (top) and ADCP velocity measurements (bottom) on T7 (transects NOT co-located). Note different color scales.

Critically, these data also provide a set of reference velocity measurements for calibration and validation of modeled 1-D velocity profiles using EFDC algorithms and an analytical vegetation drag and turbulence closure model (Figure 5.3.6). Initial parameterization of these 1-D velocity profiles showed general agreement with measured velocities on Transects 3 and 7 despite simplified assumptions about vegetation cover characteristics, providing support for their formulation.

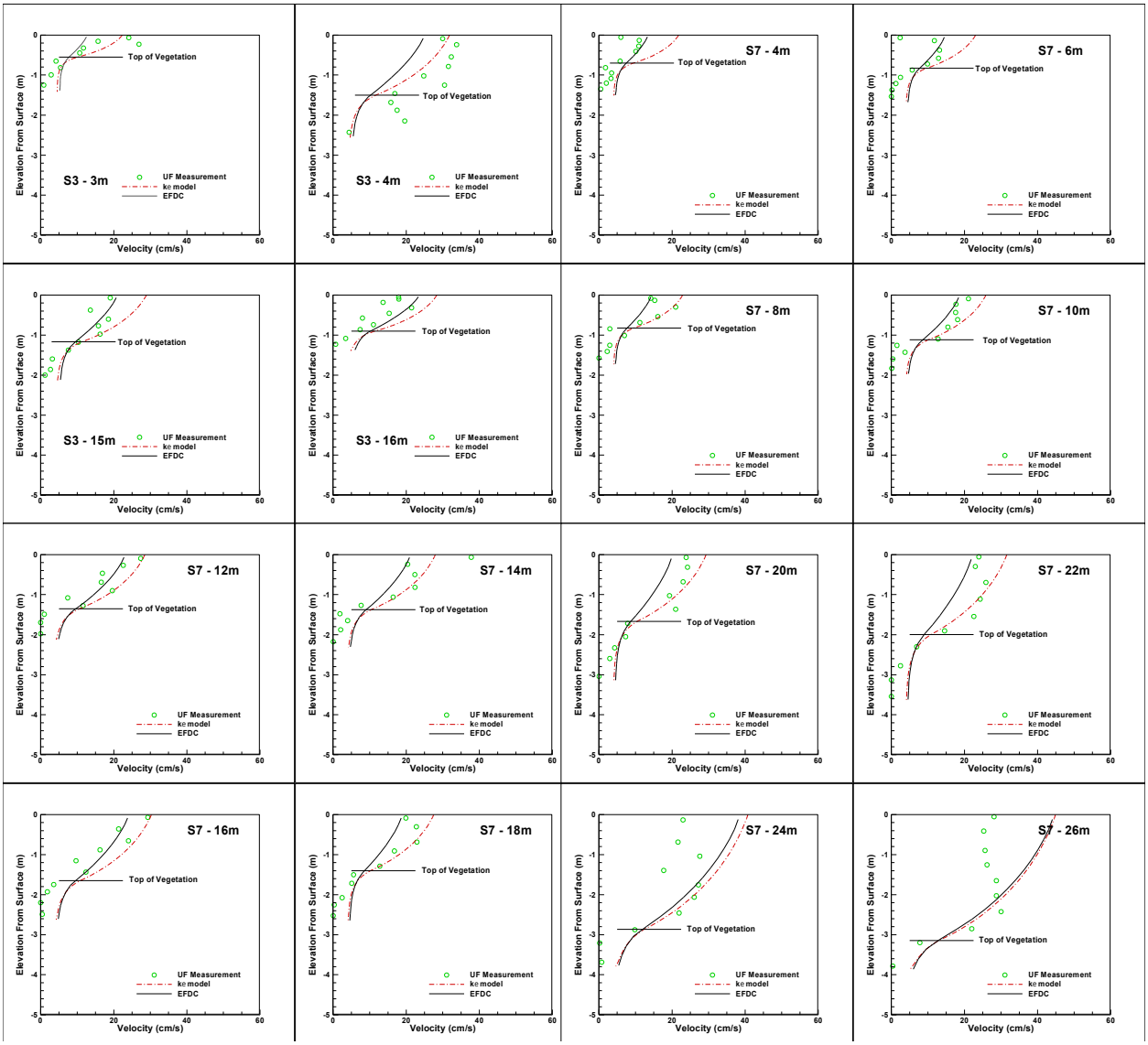

Figure 5.3.7. Comparison of measured velocity profiles at 16 (of >100) locations with velocities simulated by EFDC and modeled with a 1-D turbulence closure model. Figures by Yanfeng Zhang.

5.3.4 CONCLUSIONS, RECOMMENDATIONS, AND FUTURE RESEARCH NEEDS

Work to meet the goals of this chapter will continue in project years 2 and 3, at which time overall conclusions and recommendations can be given. Initial results suggest that ADCP measurements while extremely useful for reach scale characterization, may be insufficient for finer-scale EFDC model calibration and validation. Planned future work includes developing highly spatially and temporally resolved vertical velocity profiles using a fixed 50 Hz ADV to provide improved velocity profiles for comparisons like those in Figure 5.3.7, as well as to calculate turbulence in a variety of morphological settings.

Section 5.4 Hydrodynamic Effects of Vegetation on Velocity and Stage in Silver River

5.4.1 INTRODUCTION

A hydrodynamic analysis of velocity, discharge, and stage in Silver River is needed to meet the overall aim of the CRISPS study to determine whether velocity is an important non-nitrate factor influencing the community structure and function of primary producers in the system. King (2014) suggested that hydrodynamics could contribute to, or even dominate, the control of filamentous macroalgae on and attached to submersed aquatic vegetation in Florida spring runs. Section 5.2 of this report illustrated that much of Silver River falls within a zone of velocity close to King's target threshold for control of filamentous macroalgae.

The role of hydrodynamics in determining the dominant plant communities in streams is well-documented (Biggs 1996; Franklin 2008). Increases in velocity tend to increase growth rates of submersed aquatic vegetation (SAV) by thinning the diffusive boundary layer over the plant surface (Biggs 1996; Biggs et al. 1998). At too high a velocity, however, the plants suffer stress from excessive drag and are ultimately uprooted as velocity increases. In general, SAV in streams require low absolute velocity, low velocity variability and stable substrates (Biggs 1996). Velocity < 30 cm s^{-1} was reported by Biggs (1996) for macrophyte dominance. Hoyer et al. (2004) found unfavorable conditions for both macrophytes and macroalgae in three west Florida springs at velocities exceeding only 25 cm s^{-1}, a threshold similarly reported by King (2014) for macroalgae. Franklin (2008) reported peak vegetative abundance in stable streams occurring in the range of 30 – 50 cm s^{-1}. This optimal range is particularly interesting given that SAV generally is absent when inter-flood velocities exceed 70 cm s^{-1}. An optimum velocity range for SAV in Silver River may be constrained, then, to a fairly narrow velocity range of 25 – 70 cm s^{-1} (0.8 – 2.3 ft s^{-1}), below which the macrophyte beds are subject to invasion by macroalgae, and above which the macrophyte beds cannot withstand the drag forces.

Flow resistance within the river channel, of course, directly effects velocity since greater flow resistance lowers velocity and increases stage and depth of the river for a given discharge. After the year 2000, Silver River experienced a distinct shift in its stage/discharge relationship (Figure 5.4.1) with increased stage for lower discharge. If flow resistance in Silver River was dominated by wall resistance alone, then stage would have decreased with lower discharge. Wall resistance could not, then, be the cause of the change to the stage/discharge relationship. The altered stage/discharge relationship must instead be a result of a change to vegetative drag.

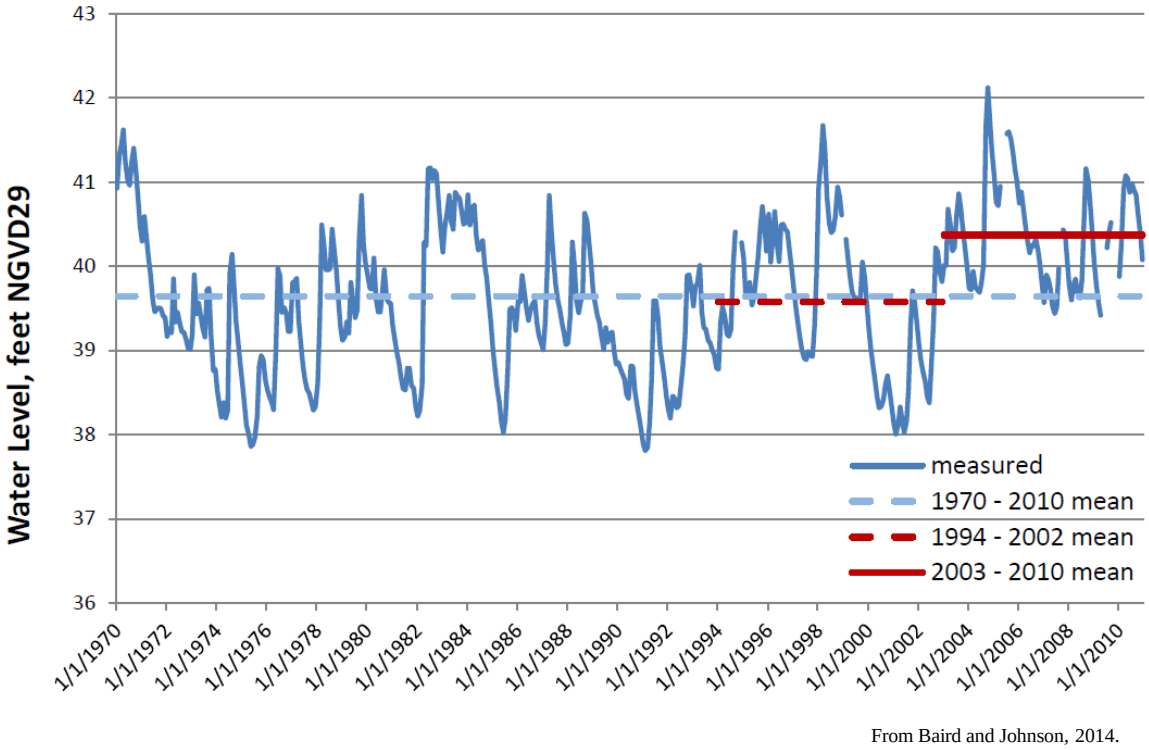

From Baird and Johnson, 2014.

Figure 5.4.1. Monthly mean water level, 1970 to 2010, at the Silver Spring pool (USGS 02239500).

The hydrodynamic analysis required to address the above issues must include mechanisms accounting for vegetative drag, spatial gradients of velocity, turbulent shear stress at the top of macrophyte beds, and turbulence intensity. The range of hydrodynamic mechanisms needed warrants the use of a three-dimensional hydrodynamic model. Numerical turbulence models were first developed to solve the turbulent flow field with incorporation of both form drag and vegetation effects on turbulence. Aquatic vegetation properties of density, height and stem diameter were used as model inputs. Drag coefficients were obtained by comparison with both laboratory experiments and field measurements. After testing, a final turbulence model was then adapted to a three-dimensional hydrodynamics model, Environmental Fluid Dynamics Code (EFDC; Hamrick 1992), to predict unsteady water level, velocity profiles and estimate turbulent shear stress within the heavily vegetated Silver River.

Numerical tests using EFDC illustrate the dominance of vegetative drag on flow resistance, consistent with the general hydrodynamic analysis of Luhar et al. (2008). Numerical tests also illustrate the relative sensitivity of model stage (and hence resistance) to vegetative bed height and the relative insensitivity to stem density. The sensitivity of Silver River stage to bed height points to reconfiguration of vegetation as a possible cause of the altered stage/discharge relationship after the year 2000. Reconfiguration refers to changes in the resistance of vegetation to flow as velocity increases because of greater streamlining at higher velocity (Vogel 1994).

Reconfiguration can result from either a change in frontal area exposed to the flow (caused by plant bending) or streamlining of plant blades allowed by the plant's flexible tissues (Luhar et al. 2013). Reconfiguration, then, is an alternative hypothesis to increased areal coverage and biomass for explaining the unusual shift of stage/discharge relationship as discharge dropped following the 1999–2000 droughts.

Our hydrodynamic analyses and hydrodynamic model development, then, are aimed at understanding the important factors dynamically influencing velocity in Silver River. This understanding will help us determine whether velocity is an important non-nitrate factor influencing the community structure and function of primary producers in Silver River, with an ultimate goal of improving our understanding—and providing management recommendations—on how velocity in this system affects the ecological health and ecosystem services of the river.

5.4.2 REVIEW OF VEGETATIVE FLOW RESISTANCE

Historically the primary purpose of engineering research on the effects of vegetation on flow has been limited to resistance estimation in streams and flood plains (Arcement and Schneider, 1990). These early studies generally assessed vegetation effects using bulk energy loss coefficients, such as Manning *n*, Darcy-Weisbach f or Chezy C, because of their ease of application and demonstrated validity. The effects of flow conditions and vegetation properties are normally incorporated in these coefficients from empirical formulations or other regression techniques. Of these energy loss coefficients, Manning *n* is most frequently used in the computation of open-channel and overland flows.

Guidance for selection of Manning *n* coefficients was provided by Arcement and Schneider (1990) with an emphasis on unsubmerged vegetation on flood plains. For floodplains with nonrigid and unsubmerged vegetation, Manning *n* increases proportionally to the square root of flow depth regardless of tree species, or foliage shape and distribution due to the increase of submerged momentum absorbing area with depth of flow (Fathi-Maghadam and Kouwen 1997). Density of vegetation is always a dominant parameter, then, under nonsubmerged conditions.

Flow resistance by submerged vegetation, in contrast, has a strong dependence on the height of the vegetative bed. For flexible vegetation, bed height is variable, depending on flow conditions, and is defined as the projection of the vegetation in the direction perpendicular to the water flow and often termed "*effective vegetative height*" (Kutija and Hong 1996). The dependence of flow resistance on effective vegetative height often leads to a lowering of friction coefficients at higher flow velocities. This phenomenon is long known from the classical use of empirical *n*-VR curves for estimating flow resistance in vegetated channels (Kouwen 1992) which relate Manning *n* to the product of cross-sectionally averaged velocity and hydraulic radius. Wu (1999) pointed out that, given relatively constant kinematic viscosity, VR is directly related to a Reynolds number with hydraulic radius (often channel depth) the characteristic length. Wu (1999) further noted that Manning *n* decreases with flow depth for flexible submerged vegetation but increases with flow depth for unsubmerged vegetation. Carollo et.al (2005) expanded on this research to develop a flow resistance law for channels with flexible submerged vegetation that depended on a shear Reynolds number, the depth-vegetation height ratio and the degree of

vegetation inflection. The shear Reynolds number is defined for inside the vegetated bed and uses the effective vegetative height as the characteristic length.

Although the Manning Equation with dynamic alteration of Manning *n* can be used to assess the bulk frictional resistance of a vegetated channel, it is difficult to apply as a predictive tool and it does not provide information about either flow structure or turbulence intensity (Nepf 1999) that directly affect transport processes for sediments and nutrients in the water. For this reason, numerous numerical modeling efforts have focused on understanding vegetative effects on velocity profiles and turbulent characteristics (Lopez and Garcia 2001; Choi and Kang 2003; Defina and Bixio 2005; Gao et al. 2011; Dimitris and Panayotis 2011). This modeling focus is a move away from lumped friction parameterizations to physically based laws describing each component contributing to the energy loss source term in the Navier-Stokes equations. Because of the complex nature of the interaction between vegetation and flow, some assumptions and parameterizations are normally made for these conceptual and mathematical models. In general, uniform flow conditions are assumed and vegetation spatial variations are not considered. As the wake turbulence generated by vegetation has a larger effect on vertical than on horizontal mixing, turbulence closure modeling is simplified to a one-dimensional, rather than a fully three-dimensional, model structure. Bottom friction from roughness is often neglected because near-bottom velocities are small in the presence of vegetation and drag force becomes the major contributor to total resistance (Luhar and Nepf 2013).

Two principal one-dimensional model types have been used to describe the flow and turbulence structure within and above a vegetated canopy: two-layer and modified turbulence κ-ε models. A two-layer model determines flow velocity profiles in two separate layers, the bottom vegetated layer and the upper layer above the vegetation. For this model type, the momentum equation is solved in the vegetated layer by mixing length turbulent theory and vegetation drag. In the upper layer, a logarithmic velocity profile is assumed (Defina and Bixio 2005). The parameters of the log law are determined by matching the continuity of velocity and shear stress at the interface. The characteristic length of turbulence is obtained from a semi empirical model (Klopstra et al. 1997; Meijer and van Velzen 1999; Righetti and Armanini 2002; Defina and Bixio 2005). The two-layer model can only be applied to steady state system with uniform vegetation distribution and constant drag coefficient.

A modified turbulence κ-ε model accounts for vegetative drag through both a momentum equation and turbulence equations for κ (turbulent kinetic energy) and ε (dissipation rate) (Lopez and Garcia 2001; Stoesser et al. 2004; Defina and Bixio 2005). The coefficients for drag-related source terms in κ and ε turbulence equations are determined empirically. For a one dimensional κ-ε model, both vegetation density and drag coefficient can vary vertically.

Both the two-layer model and one-dimensional κ-ε model were tested for Silver River as a progression towards a fully three-dimensional model. Both models reasonably reproduced vertical velocity profiles and shear stress obtained from laboratory experiments. (Figure 28 in Section 5.3 shows results from the κ-ε model). These one-dimensional models, however, are not practical for direct application to Silver River for two reasons. First, the pressure gradients required for boundary conditions are generally not available to solve for velocity profiles at a given location. Second, these models cannot account for varying flow patterns caused by

spatially varying shoreline, bathymetry and vegetation characteristics. The methodologies developed from these one-dimensional models were thus incorporated into a fully three-dimensional circulation model EFDC (Environmental Fluid Dynamics Code) to simulate flows and turbulence in the highly vegetated Silver River system.

5.4.3 DESCRIPTION OF STUDY AREA

The study area for the hydrodynamic analysis is the Silver River main-stem, the back channel and boat basin (Figure 5.4.2). Nearly all discharge enters Silver River through a complex of spring vents at the head. USGS monitors discharge just below this complex at the "3,900 ft stage" approximately 1,200 m from the head pool and immediately downstream of the back channel exit. The Silver River enters the Ocklawaha River about 8 km below the head pool. The Ocklawaha River water level at the confluence ranges over 2 m (6.5 ft) and backwater effects are observed in Silver River as far as the head pool.

SJRWMD has monitored water level at ten locations in Silver River (S1 through S10) since June 2007 (Figure 5.4.2). USGS monitors four additional locations with long-term monitoring near the head pool (1947 to present) and at the Hwy 40 Bridge at Conner (1963 to present). These locations are listed as "Pool Stage" and "Ocklawaha Stage, Discharge" in Figure 5.4.2. Silver River discharge at the 3,900-ft station also has a long-term record with daily discharge available from 1933 to present.

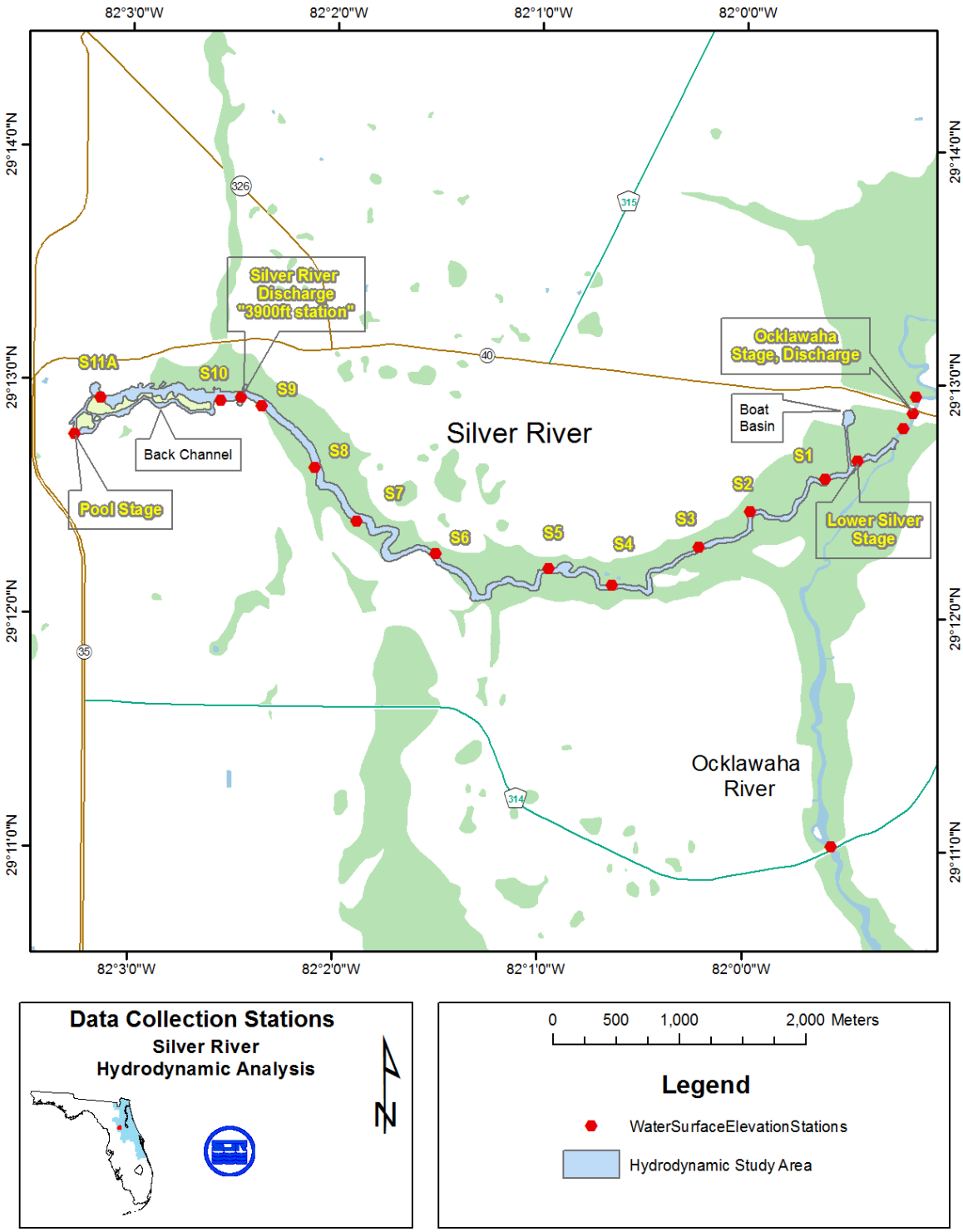

Figure 5.4.2. Study area for the hydrodynamic analysis of Silver River comprising the main river channel, back-channel, and boat basin. SJRWMD collects water surface elevation at ten stations in Silver River (stations S1 through S10). USGS collects water surface elevation at four additional locations denoted "Pool Stage", "3,900 ft station", "Lower Silver Stage", and Ocklawaha Stage, Discharge" in the figure.

5.4.4 MATERIALS AND METHODS

5.4.4.1 Defining the Shoreline

A critical component for a robust model is an accurate representation of the model domain, in this case the shoreline of the mainstem and back channel of the Silver River. Use of aerial imagery for discerning the shoreline suffered from spatial inaccuracies in this relatively small system. The forested canopy that overhangs the river also obscures a significant percentage of the open water surface further compounding the difficulty of using aerial imagery. The District's 1:24,000 GIS Hydrography layer was (likely) developed from 1984 aerials and is not sufficiently accurate for hydrodynamic analysis of the river. We thus developed an alternative shoreline for the study area specifically designed for the hydrodynamic analyses of the river.

The new shoreline coverage was created by first mapping the navigable "open edge" of flow and then using a horizontal offset based on shoreline type to estimate the location of the zero flow boundary (hereafter termed the *flow boundary*). Kayaks with mounted GPS units were used to trace the open edge during June 2014. Any areas too shallow or with too dense of vegetation for passage by kayak generally contribute minimally to total river discharge. A GPS antenna was mounted on a rod tall enough to clear the operator but low enough to avoid overhead obstructions. The GPS antenna was connected to a handheld Trimble Pathfinder. A Garmin 441s was used to collect additional waypoints of features of interest, and a description was noted for each waypoint in a field journal. A shape file was produced from the waypoints. Two kayaks were employed so that both north and south banks could be mapped simultaneously. The kayaks were maneuvered typically within half paddle length (ca.1 m) from the water edge or as far as could be reached along the shoreline to map the open edge of flow.

Shoreline types were categorized into three classes: hardened, abrupt, and gradual. Hardened shorelines with concrete headwalls are found in the head pool and the boat basin at the lower end (Figure 5.4.3). The remainder of the river shoreline is either an abrupt shift to uplands in excavated areas of canals, the back channel, and along the edge of Indian mounds or a gradual transition from open water to forested wetlands (Figure 5.4.4).

Figure 5.4.3. Hardened shoreline in Silver River just downstream of the head pool.

Figure 5.4.4. Gradual shoreline adjacent to forested wetland.

Tree canopy sometimes interfered with the GPS antennae and satellites requiring remapping of affected areas during times of more advantageous satellite geometries. In some areas, floating vegetation mats and logs blocked surface flow, but obviously allowed subsurface flow. For these areas the open edge was extrapolated across to the next good open edge location.

5.4.4.2 Defining Bottom Type

Bottom types were mapped at the spatial scale of the hydrodynamics model grid for two primary purposes: first, to guide the interpretation of remotely-sensed vegetative heights using Sonar, and second, to guide selection of stem density. We are presently collecting Sonar data using a Sontek M9 Acoustic Doppler Current Profiler. This device is assumed to measure depth to the top of vegetation in areas of high vegetative cover. In these areas, the measured depths must be corrected for vegetative bed height. In bare or sparsely vegetated areas no correction to depth is required. Areas with topped out vegetation cannot be measured using Sonar. Estimation of stem density will be based on an established relationship with Braun-Blanquet number (Munch et al. 2006). For this reason, bottom types were established to be consistent with the Braun-Blanquet classification, with allowances for horizontal scale.

Where water clarity was sufficient (primarily the upper half of the river above S-6) visual inspection was made by boat. In the lower river (below S-6), high turbidity obscured the bottom and inspection was made using a GoPro camera mounted on a 10-ft PVC pole.

Bottom types were classified into six categories: bare, patchy, vegetated, heavily vegetated, topped out, and with trees. General category definitions are as follows:

1. ***Bare*** Sandy, rocky, or muddy bottom with less than 5% rooted vegetation. Logs may be present.

2. ***Patchy*** Clumped, thin, or widely spaced vegetation.

3. ***Vegetated*** Continuously vegetated with the bottom mostly obscured; open water above canopy deeper than 1 m.

4. ***Heavily Vegetated*** Continuously vegetated with the bottom mostly obscured; vegetation takes up the majority of the water column.

5. ***Topped Out*** Vegetation reaches completely to the surface; emergent vegetation may be present.

6. ***Trees*** Extensive roots and trunks of cypress and other trees.

5.4.4.3 Model Grid Development

A curvilinear, orthogonal boundary-fitted grid was developed jointly by Jones Edmunds Associates, Janicki Environmental, and SJRWMD. The grid encompassed the open edge and followed the flow boundary as much as was practical for maintaining orthogonality (Figure 5.4.5).

The model grid consists of 13,439 horizontal cells and 8 vertical cells for a total of 107,512 cells. The total surface area of the grid is 108.12 acres, which includes 3.58 acres for the boat basin and 15.0 acres in the back channel. Cell area generally increases from upstream to downstream with an average cell area of 29.4 m^2 in the upper third of the river (Figure 5.4.6, Map A), 30.2 m^2 in the middle third (Figure 5.4.6, Map B), and 41.5m^2 in the lower third (not shown). The average horizontal cell length is 5.8 meters.

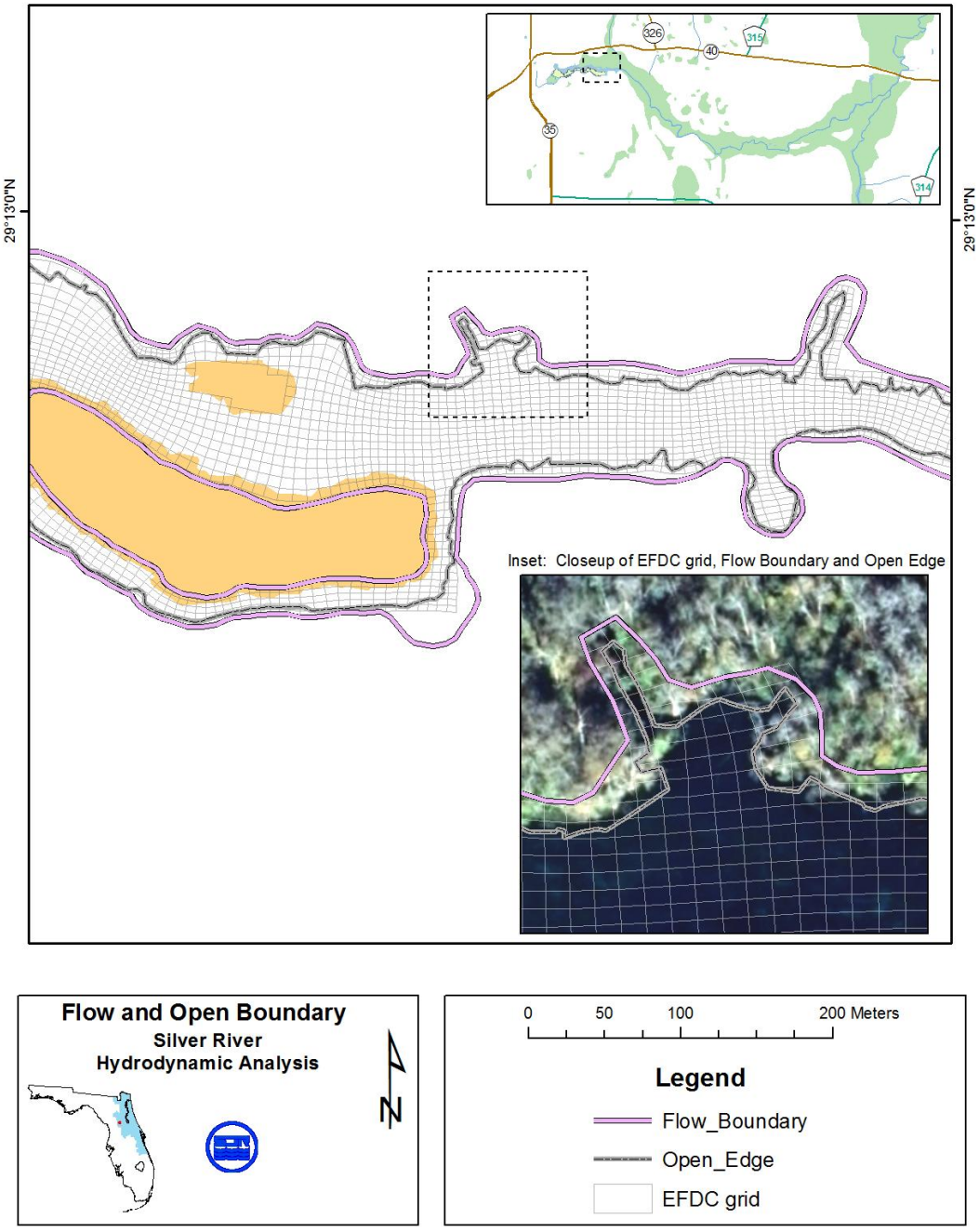

Figure 5.4.5. Model grid detail with open edge boundary and shoreline ("flow boundary") used to guide the gridded area.

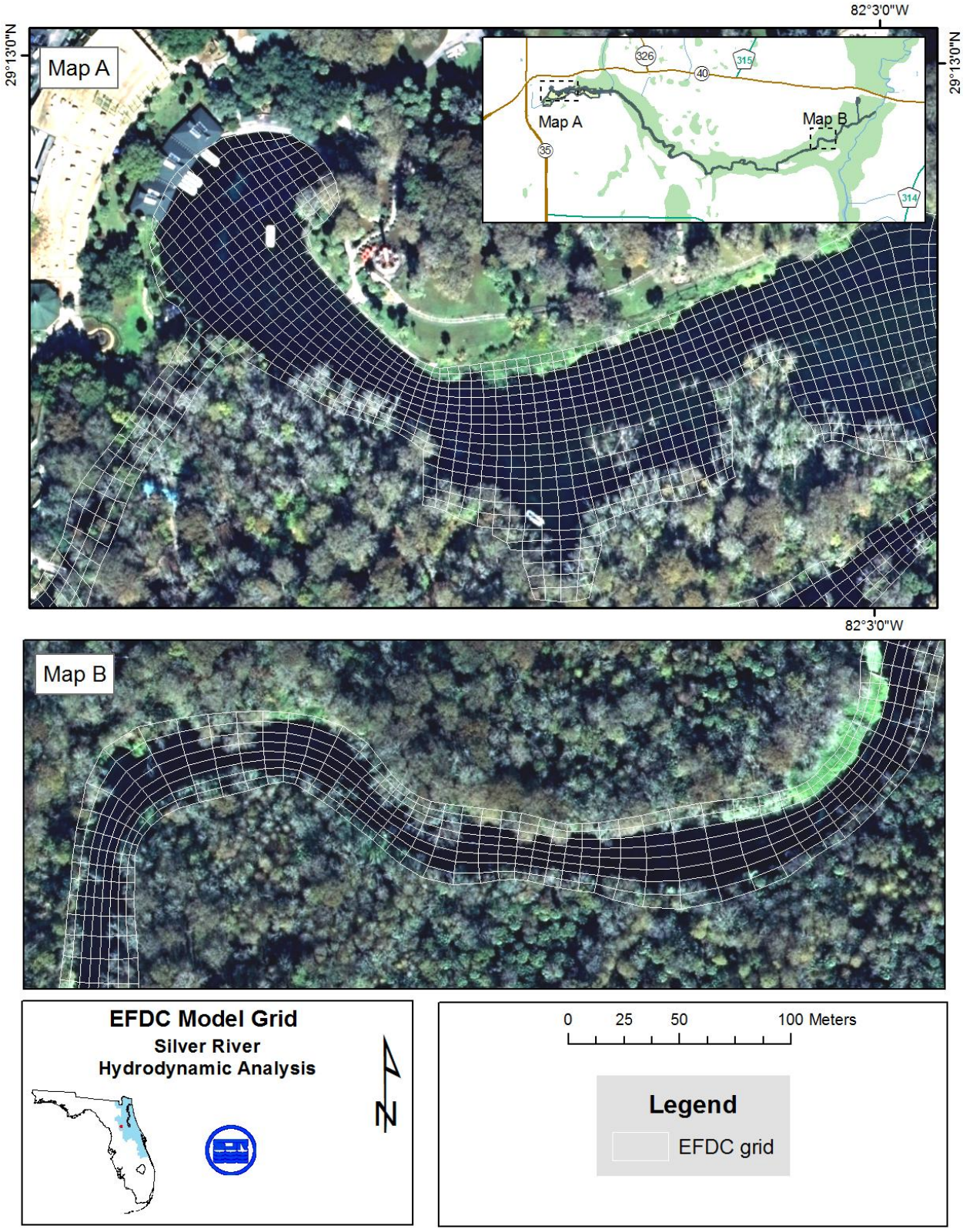

Figure 5.4.6. Final hydrodynamic model grid in head pool (upper plot, Map A) and lower river (lower plot, Map B).

5.4.4.4 Formulation of the Governing Equations for EFDC With Vegetation

The formulation of the governing equations of EFDC is developed for an incompressible, variable density fluid to account for the effects of submersed vegetation on drag and turbulence. In horizontal, the equations are formulated in curvilinear and orthogonal coordinates to accommodate realistic boundaries. In vertical, a time variable mapping or stretching transformation is used to provide uniform vertical resolution with changing depth.

The momentum and continuity equations from Hamrick (1986) are adjusted to incorporate the vegetation effect and can be written in the following form:

$$\partial_t(mHu) + \partial_x\left(m_y Huu\right) + \partial_y(m_x Hvu) + \partial_z(mwu) - \left(mf + v\partial_x m_y - u\partial_y m_x\right)Hv$$
$$= -m_y H\partial_x(g\zeta + p) - m_y(\partial_x h - z\partial_x H)\partial_z p + \partial_z(mH^{-1}A_V\partial_z u) + Q_u - c_t\sqrt{u^2+v^2}umH \quad (1)$$

$$\partial_t(mHv) + \partial_x\left(m_y Huv\right) + \partial_y(m_x Hvv) + \partial_z(mwv) + \left(mf + v\partial_x m_y - u\partial_y m_x\right)Hu$$
$$= -m_x H\partial_y(g\zeta + p) - m_x(\partial_y h - z\partial_y H)\partial_z p + \partial_z(mH^{-1}A_V\partial_z v) + Q_v - c_t\sqrt{u^2+v^2}vmH \quad (2)$$

$$\partial_z p = -gH(\rho - \rho_0)\rho_0^{-1} = -gHb \quad (3)$$

$$\partial_t(m\zeta) + \partial_x\left(m_y Hu\right) + \partial_y(m_x Hv) + \partial_z(mw) = 0 \quad (4)$$

$$\partial_t(m\zeta) + \partial_x\left(m_y H\int_0^1 udz\right) + \partial_y\left(m_x H\int_0^1 vdz\right) = 0 \quad (5)$$

$$\rho = \rho(p,S,T) \quad (6)$$

In these equations, u and v are the horizontal velocity components in the curvilinear, orthogonal coordinates x and y, m_x and m_y are the square roots of the diagonal components of the metric tensor, $m = m_x m_y$ is the Jacobian or square root of the metric tensor determinant. The vertical velocity, with physical units, in the stretched, dimensionless vertical coordinate z is w. H is total depth, ζ is surface elevation, f is the Coriolis parameter, p is the physical pressure in excess of the reference density hydrostatic pressure, $\rho_o gH(1- z)$, divided by the reference density, ρ_o, A_v is vertical eddy viscosity, and Q_u and Q_v are momentum source-sink terms which will be later modeled as subgrid scale horizontal diffusion. The density, ρ is in general a function of temperature, T, and salinity, S. The buoyancy, b, is defined as the normalized deviation of density from the reference value. The continuity equation has been integrated with respect to z over the interval (0, 1) to produce the depth-integrated continuity equation. The total drag coefficient from vegetation is defined as:

$$c_t = \begin{cases} \frac{1}{2} C_D A_z \lambda & z \le h_p \\ 0 & z > h_p \end{cases} \quad (7)$$

Where C_D is form drag coefficient, A_z is frontal plant area per unit depth, λ is the number of stems per unit area, and h_p is plant height.

To provide the vertical turbulent viscosity and diffusivity, the second-moment turbulence closure model developed by Mellor and Yamada (1982) and modified by Galperin et al. (1988) is used. The model relates the vertical turbulent viscosity and diffusivity to the turbulent intensity, qq, a turbulent length scale, l, and a Richardson number R_q by:

$$A_v = \phi_v q l = 0.4\left(1 + 36R_q\right)^{-1}\left(1 + 6R_q\right)^{-1}\left(1 + 8R_q\right) q l \quad (8)$$

$$A_b = \phi_b q l = 0.5\left(1 + 36R_q\right)^{-1} q l \quad (9)$$

$$R_q = \frac{gH\,\partial_z b}{q^2}\frac{l^2}{H^2} \quad (10)$$

where the so-called stability functions ϕ_v and ϕ_b account for reduced and enhanced vertical mixing or transport in stable and unstable vertically density stratified environments, respectively. The turbulence intensity and the turbulence length scale are determined by a pair of transport equations:

$$\partial_t(mHq^2) + \partial_x\left(m_y Huq^2\right) + \partial_y(m_x Hvq^2) + \partial_z(mwq^2) = \partial_z\left(mH^{-1}A_q\partial_z q^2\right) + Q_q$$

$$+2mH^{-1}A_V((\partial_z u)^2 + (\partial_z v)^2) + 2mgA_b\partial_z b - 2mH(B_1 l)^{-1}q^3 + c_{fq}c_t(u^2 + v^2)umH \quad (11)$$

$$\partial_t(mHq^2 l) + \partial_x\left(m_y Huq^2 l\right) + \partial_y(m_x Hvq^2 l) + \partial_z(mwq^2 l) = \partial_z\left(mH^{-1}A_q\partial_z q^2 l\right) + Q_l$$
$$+mH^{-1}E_1 l A_V((\partial_z u)^2 + (\partial_z v)^2) + mgE_1E_3 l A_b\partial_z b - mHB_1^{-1}q^3(1 + E_2(\kappa L)^{-2}l^2) + c_{fl}c_t(u^2 + v^2)umHl \quad (12)$$

with,

$$L^{-1} = H^{-1}(z^{-1} + (1 - z)^{-1}) \quad (13)$$

and where B1, E1, E2, and E3 are empirical constants, and Q_q and Q_l are additional source-sink terms for subgrid scale horizontal diffusion. The vertical diffusivity, A_q, is in general taken equal to the vertical turbulent viscosity, A_v. The last term in equation (11) and (12) account for the presence of vegetation.

5.4.5 RESULTS AND DISCUSSION

5.4.5.1 Bottom Type

Bottom types associated with each hydrodynamic model grid cell are shown in Figure 5.4.7 for two representative areas. The percentage of each bottom type over the entire 108.1 acres contained within the hydrodynamic model grid is 8.5% bare, 17.7 % patchy, 37.6% vegetated, 8.7% heavily vegetated, 14% topped out, and 13.5% trees. The river is highly vegetated; slightly

more than 60% of the model area is completely covered with vegetation and 78% of the area contains at least some submersed aquatic vegetation.

Present day coverage in the upper 1,200 m (¾ mile) near the headspring is similar to that observed by Odum (1957) and Munch et al. (2006). The extensive vegetative cover in the lower river, however, is in stark contrast to the lack of SAV reported in the early 1950s by both Odum (1957) and Whitford (1956).

The large spatial coverage of present day Silver River by aquatic plants is confirmed also by vegetation surveys made along several transects perpendicular to the channel (Figure 5.4.8). Vegetation tends to be absent in deeper areas of the river. The deep thalweg in the lower river, for example, was often bare as were the deep holes near S-1. Odum (1957) noted that *Sagittaria kurtziana* was not found in depths greater than 15 feet (4.5 m). We similarly observed few macrophytes of any kind below 4.5 m and none deeper than 5.5 m (19 ft).

5.4.5.2 Hydrodynamic Model Tests

The EFDC model modified for vegetation effects was tested using observed conditions of 29 May 2014 when discharge was 17 $m^3 s^{-1}$ (605 cfs) and the downstream stage was 10.75 m (35.27 ft) NAVD88 at Conner. Water elevations were observed at ten stations along the river (S1 to S10). In addition to testing EFDC with the added vegetation algorithms, we simulated stage using the original EFDC model formulated with the Manning Equation. A Manning *n* of 0.5 was used to conservatively represent flow resistance by dense, extensive SAV coverage. Although this value of Manning *n* is extreme (five times greater than the largest value suggested by Arcement and Schneider 1990), the original EFDC model could not generate friction sufficient to explain the elevation drop of the river. The observed elevation drop of the river from head to mouth was 1.3 m and the simulated drop using Manning *n* was only 0.5 m. The EFDC model modified to include the effects of SAV drag significantly improved the simulated elevation drop (Figure 5.4.9, black line). The simulated elevation drop using the modified EFDC model was 1.2 m, in close agreement to observations. We note that this is at present an uncalibrated model that should be significantly improved when more realistic bathymetry and spatially varying vegetation characteristics are developed for the CRISPS project.

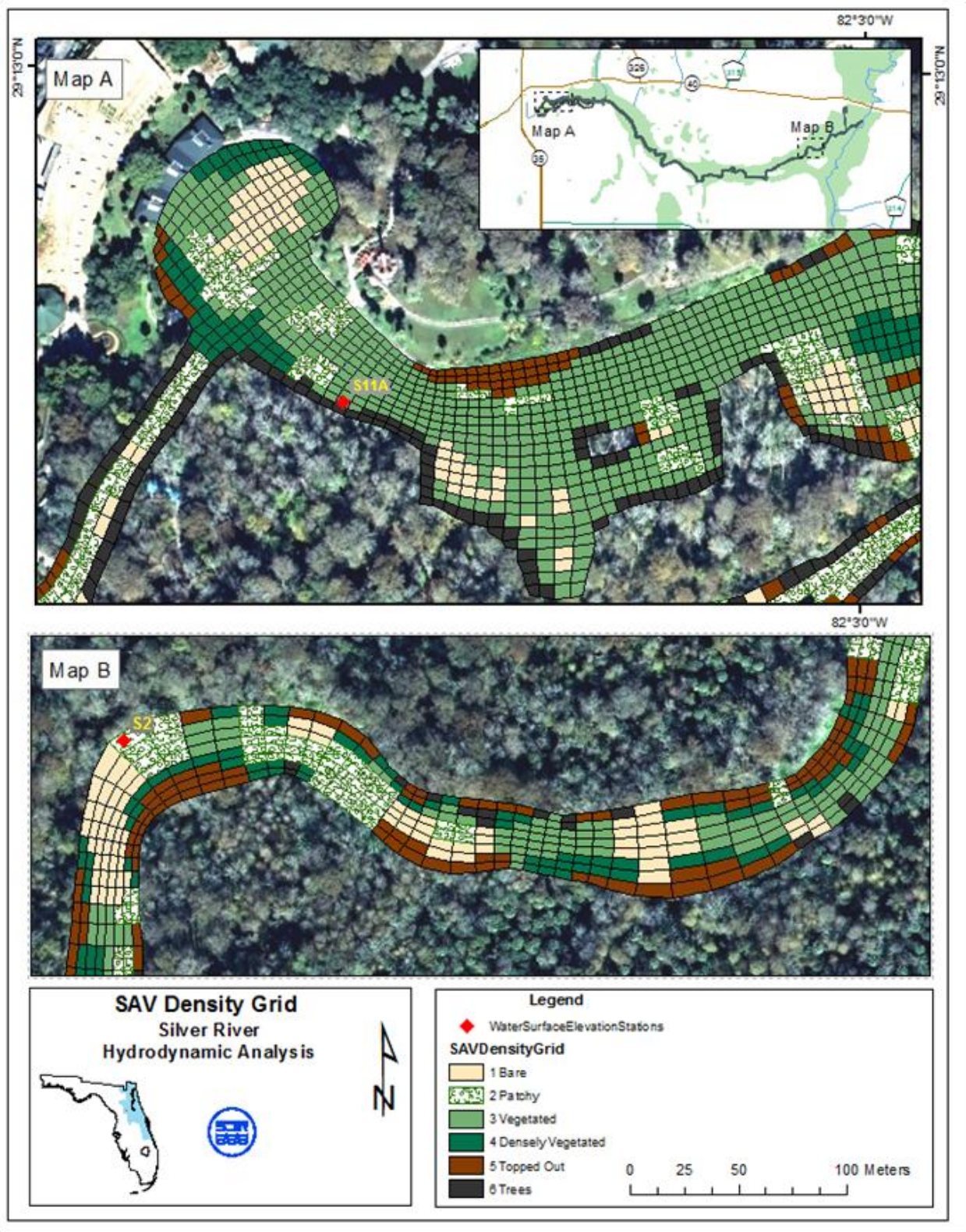

Figure 5.4.7. Bottom type of Silver River assigned to each hydrodynamic model cell.

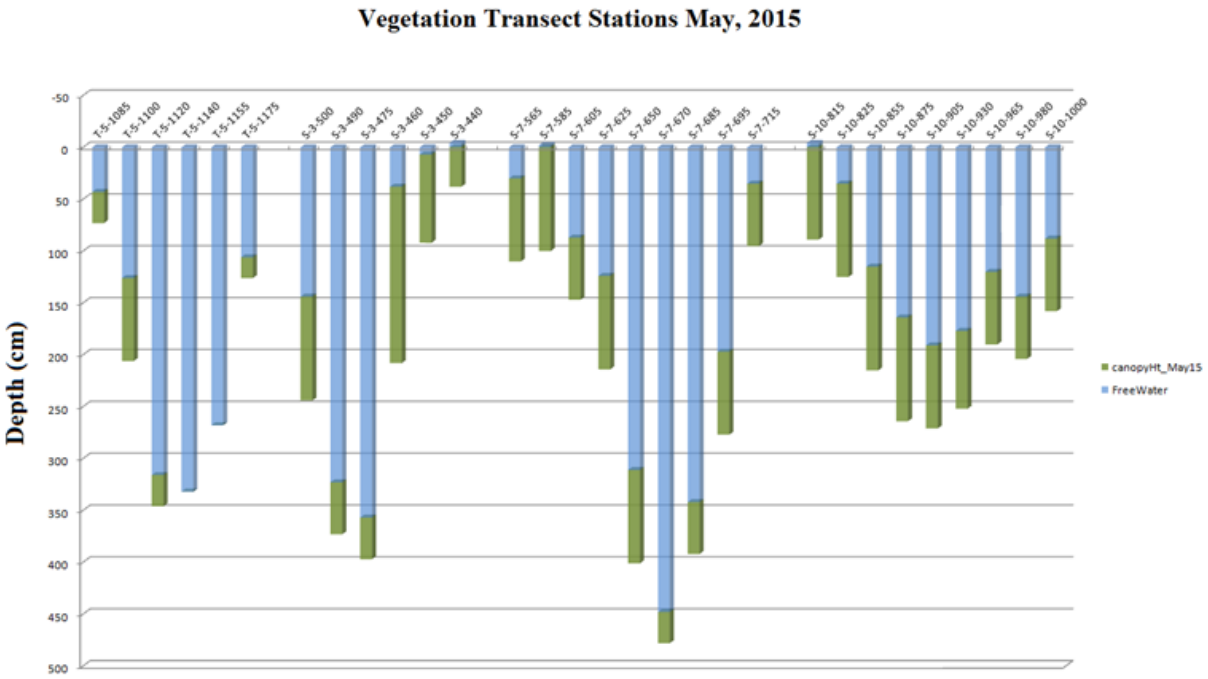

Figure 5.4.8. Fraction of bottom vegetation (green) compared with open water above the canopy (blue) at four transects. Transect T3 is in the Ocklawaha River just downstream of the Silver river mouth. Transects S-3, S-7, and S-10 are in the lower, middle, and upper portions of the Silver River, respectively.

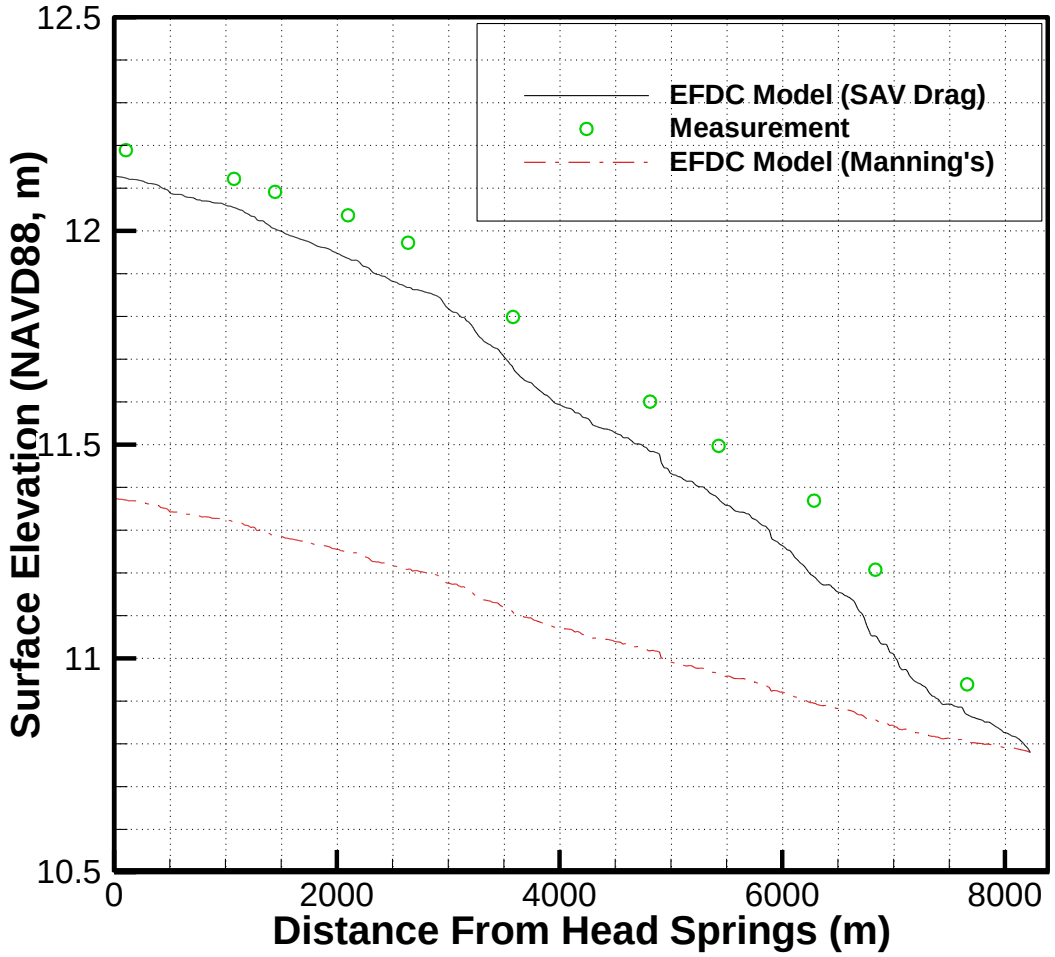

Figure 5.4.9. Comparison of simulated and observed water elevation along Silver River for a discharge of 605 cfs. Green circles are observed water level, dashed red line is simulated water level without submersed vegetation, and the solid black line is with submersed vegetation.

Model sensitivity was tested for two vegetative parameters, effective vegetative height and vegetation density, on water elevation. For context, the sensitivity of water elevation to river discharge was also tested. Values for each of the two vegetative parameters and river discharge were varied ±30%. The results (Figure 5.4.10) imply that for the same percentage change of parameter, the model is more sensitive to effective vegetative height than to vegetative density. Interestingly, altering effective vegetative height had nearly an equivalent effect on water elevation as altering river discharge. These results illustrate the possible importance of reconfiguration for prediction of water elevation in Silver River.

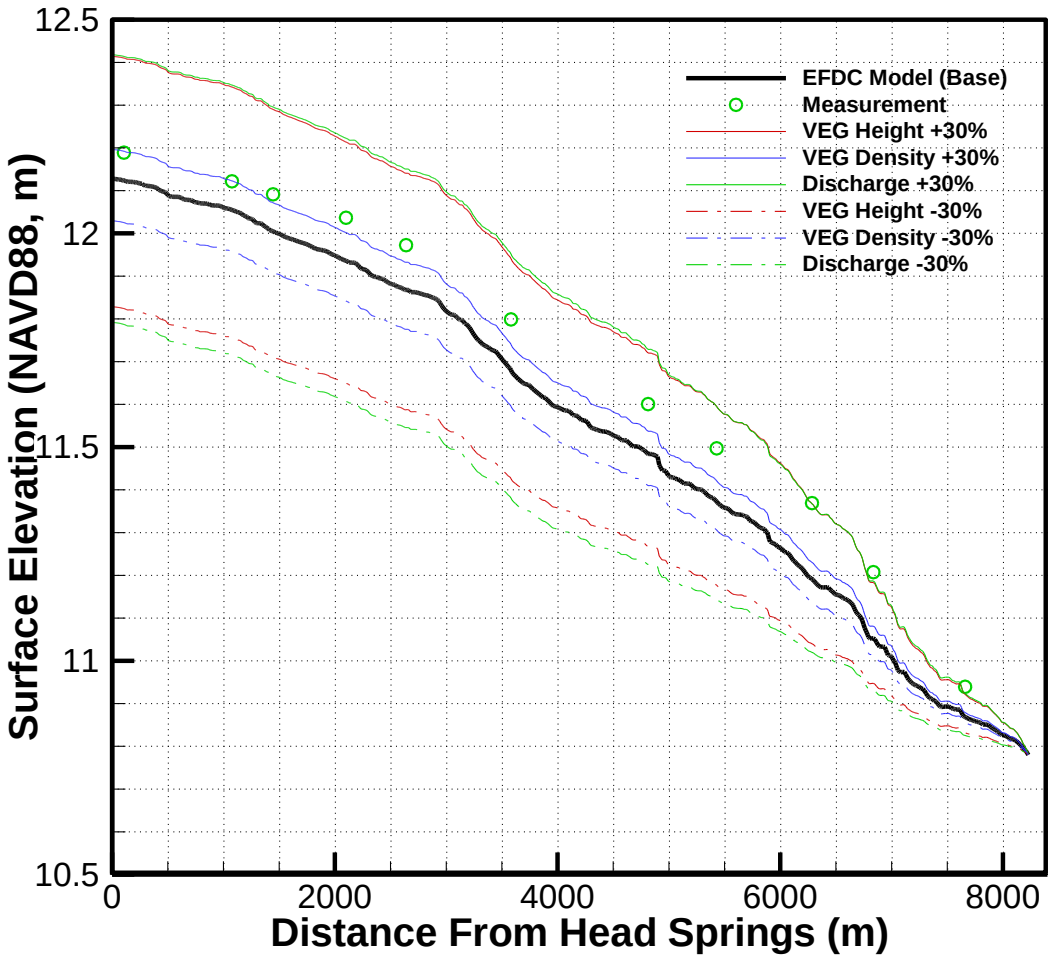

Figure 5.4.10. Sensitivity of simulated water elevation along Silver River to ±30% changes in effective vegetative height, vegetative density and river discharge in comparison to a base test case.

5.4.5.3 Cause of Altered Stage/Discharge Relationship of Silver River

Determining the causes of the altered stage/discharge relationship of Silver River following the year 2000 has practical value since this understanding will allow us to understand how vegetation controls both stage and velocity throughout the river. At present, we have identified three possible causes: (a) expansion of vegetative coverage and/or density, (b) reconfiguration of vegetation under lower velocities, and (c) expansion of hydrilla in the lower Silver River and adjacent Ocklawaha River.

Historic observations of vegetative cover in the lower Silver River are sparse. Only recently have studies addressed the ecosystem structure of the lower Silver River (Wetlands Solutions 2012;

Wetlands Solutions 2014). Little information exists, then, for the lower Silver River prior to 2012 regarding SAV abundance, community structure, vegetative cover presence or absence of vegetation, or even the general structure of the river channel.

Two descriptions, provided verbatim, indicate a distinct absence of SAV in the early 1950s:
Whitford (1956):

> "After the first mile Silver Springs run becomes narrow and the banks heavily wooded. It also receives some brown water down run. Consequently *about 2 ½ miles from the boil flowering plants largely disappear* probably due to reduced light. Mats of Vaucheria with some filamentous blue-green algae, and a few of the usually dominant diatoms, are abundant in the shallows. The deeper channel has *relatively little plant life*."

Odum (1957):

> "Except for its thick bed of rich muck Silver River would be a rushing canal through a pipe of limestone rock. *Further downstream below the study area it is of this nature*"

Odum is describing the substrate underlying *Sagittaria* beds in the head pool region when the total river discharge was about 930 cfs (26.28 $m^3 s^{-1}$) with a velocity of 0.21 m s^{-1} and a cross-sectional area of 125.1 m^2. He concludes the sedimentation rate is balanced by organic matter decomposition and downstream transport. The net sedimentation balance observed by Odum is consistent with Hoyer et al. (2004) who found a gradient of bottom sediment from "mud, mud/sand, sand and rock substrates" over a velocity gradient of 0.08, 0.11, 0.16 and 0.22 m s^{-1}, respectively.

Importantly, they found "little or no SAV" above a velocity of approximately 0.25 m s^{-1}. Velocity in the lower river would easily have exceeded this threshold during the high discharges of the 1950s. Scaling the characteristic velocities shown for the lower river in Table 2 Ch 6.1, for example, results in a characteristic velocity of 0.32 m s^{-1} in the lower river. It seems possible, then, that velocity may play a role in determining vegetative structure and density in portions of Silver River, especially downstream where the typical stream cross-section is smaller producing higher velocity for a given discharge. The absence of vegetation observed by Odum (1957) and Whitford (1956) in the lower river may have been a result of higher stream velocities.

It is tempting, then, to explain the stage/discharge shift about the year 2000 as a sudden expansion of vegetative cover in the lower river as discharge and velocity decreased. Such a supposition is not supported by the limited available data, however. Over a decade prior to 2000, Duarte et al. (1990) observed SAV biomass at four locations throughout the length of Silver River and found macrophytes present throughout the lower river. Vegetation survey data by the Florida Fish & Wildlife Commission (FWC 2014) also indicate a continued presence of macrophytes in the lower river at least since 1990. Finally, it seems uncharacteristic of a river known for its remarkable stability (Odum 1957) to experience a rapid change in its SAV coverage.

A sudden expansion of SAV in the Silver River about the year 2000, then, seems unlikely to be the sole cause of the 2000 stage/discharge shift. There is some evidence that river stage in the

Ocklawaha River has recently been elevated due to blockage by hydrilla, but FWC (2014) data indicates that expansion of hydrilla in the Silver River is a recent phenomenon, perhaps only becoming appreciable since 2011. This observation does not discount the possibility of blockage by hydrilla in the Ocklawaha River. An analysis of stage/discharge at Conner is presently underway to examine this possibility. Preliminary results, however, seem to indicate that flow blockages by hydrilla in the Ocklawaha River are transient and blockages are removed during high discharge events. If this preliminary result holds, the blockage of the Ocklawaha River by hydrilla is unlikely to be more than a secondary factor influencing the stage/discharge of Silver River.

Finally, model results have demonstrated that reconfiguration can have an appreciable effect on stage under lowering discharge as occurred during the prolonged drought of 1999 through 2000. This correlation of events and subsequent continued decline in discharge supports the reconfiguration hypothesis. We expect, though, that each of the three factors may have played a role to some extent. Reconfiguration of vegetation as an important mechanism for predicting stage and velocity changes in Silver River has not been widely discussed, however, and we emphasize it here for the benefit of its proper consideration.

5.4.6 CONCLUSIONS AND RECOMMENDATIONS

Flow resistance in Silver River is dominated by vegetative drag. A three-dimensional hydrodynamic model that accounts for vegetative drag and turbulence was successfully implemented and tested for Silver River. The model provides a methodology for estimating velocity profiles, shear stresses, and dispersion throughout the river, especially for conditions outside of present day observations, and provides a means to test the efficacy of proposed management scenarios.

A distinct shift in discharge-stage relationship in Silver River that occurred about 2000 is likely a result of some alteration to vegetative characteristics. Preliminary analyses show three possible mechanisms, perhaps in combination, could account for this change. These three mechanisms are as follows:

- Increased spatial coverage of submersed aquatic vegetation
- Reconfiguration of vegetation under low discharge conditions
- Expansion of hydrilla in the lower Silver River and Ocklawaha River near Conner.

Work should continue to separate the relative importance of these mechanisms using available hydrologic data over as much of the historic flow record as practical. These results would inform management decisions concerning appropriate baselines, spring flow management, and conceptual project development. Finally, quantification of the relative importance of the highly altered Ocklawaha River flow regime on Silver River stages and velocities can guide potential development of a “designed hydrograph” for this managed system or at least determine the practical limitations to restoration targets or management goals.

5.4.7 REFERENCES

Arcement, G.J., and Schneider, V.R. 1990. *Guide for Selecting Manning's Roughness Coefficients for Natural Channels and Flood Plains*, United States Geological Survey Water-supply Paper 2339.

Baird, S. F, and Johnson, N.T. 2014. Guide to Silver River Hydrologic Data. St. Johns River Water Management District, Palatka, FL. May 2014. 59 pp.

Biggs, B.J.F. 1996. Hydraulic habitat of plants in stream. Regulated Rivers: Research and Management. Vol. 12: 131–144.

Biggs, B.J.F., Goring, D.G., and Nikora, V.I. 1998. Subsidy and stress responses of stream periphyton to gradients in water velocityas a function of community growth form. J. Phycol., 34: 598–607.

Carollo, F.G., Ferro, V., and Termini, D. 2005. Flow resistance law in channels with flexible submerged Vegetation". Journal of Hydraulic Engineering, Vol. 10: 554–564.

Choi, S. and Kang H. 2003. Reynolds stress modeling of vegetated open channels. J. Hydr. Res., Vol. 42(1): 3–11.

Defina, A. and Bixio, A.C. 2005. Mean flow and turbulence in vegetated open channel flow. Water Resources Res., 41: W07006, 12 pp.

Dimitris, S. and Panayotis, P. 2011. Macroscopic turbulence models and their application in turbulent vegetated flows. J. Hydraul. Eng., 137: 315–332.

Fathi-Maghadam, M., and Kouwen, N. 1997. Nonrigid, unsubmerged, vegetative roughness on floodplains". Journal of Hydraulic Engineering, Vol. 123(1): 51–57.

Florida Fish & Wildlife Conservation Commission. 2014. EXCEL spreadsheet containing results of vegetative surveys made within Ocklawaha River and Silver River. Obtained from Jodi Slater, SJRWMD.

Franklin, P., Dunbar, M., Whitehead, P. 2008. Flow controls on lowland river macrophytes: A review. Science of the Total Environment, 400: 369–378.

Galperin, B., L. H. Kantha, S. Hassid, and A. Rosati. 1988. A quasi-equilibrium turbulent energy model for geophysical flows. J. Atmos. Sci., 45: 55–62.

Gao, G., Falconer, R.A., and Lin, B. 2011. Modelling open channel flows with vegetation using a three-dimensional model. J. Water Res. Protection, 3: 114–119.

Hamrick, J.M. 1992. A Three-Dimensional Environmental Fluid Dynamics Computer Code: Theoretical and Computational Aspects. The College of William and Mary, Virginia Institute of Marine Science, 50 pp.

Hoyer, M.V., Frazer, T.K., Notestein, S.K., and Canfield, D.E. 2004. Vegetative characteristics of three low-lying Florida coastal rivers in relation to flow, light, salinity and nutrients. Hydrobiologia, 528: 31–43.

King, S.A. 2014. Hydrodynamic control of filamentous macroalgae in a sub-tropical spring-fed river in Florida, USA. Hydrobiologia, 734: 27–37.

Klopstra, D., Barneveld, H.J., Van Noortwijk, M., and Van Velzen, E.H. 1997. Analytical model for hydraulic roughness of submerged vegetation. In *Managing Water With Scarcity and Abundance, Proceddings IAHR*, pp. 775-780, ASCE, Reston, VA.

Kouwen, N. 1992. Modern approach to design of grassed channels. Journal of Irrigation and Drainage Engineering, 118 (5): 733–743.

Lopez, F. and Garcia, M.H. 2001. Mean flow and turbulence structure of open-channel flow through non-emergent vegetation. J. Hydraul. Eng., 127: 392–402.

Luhar, M., Rominger, J. and Nepf, H. 2008. Interaction between flow, transport and vegetation spatial structure. Eviron. Fluid. Mech., 8: 423–439.

Luhar, M., and Nepf, H. 2013. From the blade scale to the reach scale: A characterization of aquatic vegetative drag. Adv. Water Res., 51: 305–316.

Meijer, D.G. and Van Velzen, E.H. 1999. Prototype-scale flume experiment on hydraulic roughness of submerged vegetation, in Proceedings of XXVII IAHR Congess, Graz, Abstract 221, & pp., Int. Assoc. for Hydraul. Res., Madrid.

Mellor, G. L., and T. Yamada. 1982. Development of a turbulence closure model for geophysical fluid problems. Rev. Geophys. Space Phys., 20: 851–875.

Munch, D.A., D.J. Toth, C. Huang, J.B. Davis, C.M. Fortich, W.L. Osburn, E.J. Phlips, E.L. Quinlan, M.S. Allen, M.J. Woods, P.Cooney, R.L. Knight, R.A. Clarke, and S.L. Knight. 2006. *Fifty-Year Retrospective Study of the Ecology of Silver Springs, Florida.* Special Publication SJ2007-SP4, SJRWMD, Palatka, FL. 314 pp.

Odum, H.T. 1957. Trophic structure and productivity of Silver Springs, Florida. Ecological Monographs. Vol. 27(1): 55–112.

Righetti, M. and Armanini, A. 2002. Flow resistance in open channel flows with sparsely distributed bushes. J. Hydrolog., 269: 55–64.

Stoesser, T, Neary, V., and Wilson, C.A.M.E. 2004. *Modeling Vegetated Channel Flows: Challenges & Opportunities*, WSEAS Conference, Corfu, August 2004.

Vogel, S. 1994. Life in Moving Fluids. Princeton University Press, Princeton, NJ.

Wetlands Solutions, Inc. 2012. Silver River Ecosystem Metabolism (2011-2012). Gainesville, FL. 46 pp.

Wetlands Solutions, Inc. 2014. Silver Springs Ecosystem Study (2012-2013). Gainesville, FL. 39 pp.

Whitford, L.A. 1956. The communities of algae in the springs and spring streams of Florida. Ecology. Vol. 37(3): 433-444.

Wu, F., Shen, W.H., and Chou, Y. 1999. Variation of roughness coefficients for unsubmerged and submerged vegetation". Journal of Hydraulic Engineering, Vol. 125(9): 934–942.

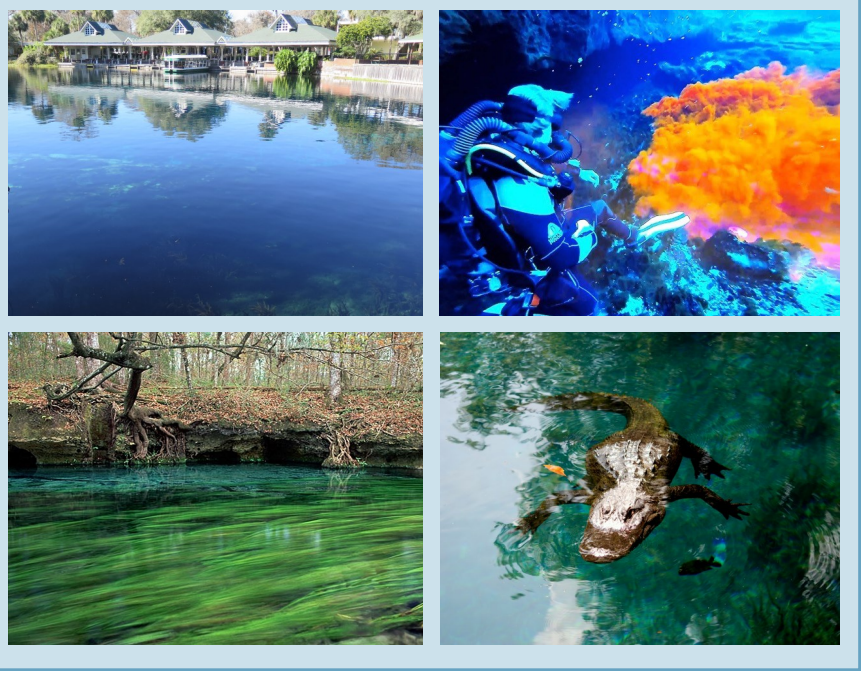

Collaborative Research Initiative on
Sustainability and Protection of Springs [**CRISPS]**

Section 6

[Work Order No: 3]

ANNUAL REPORT

July 2015

submitted to:

St. Johns River Water Management District
Springs Protection Initiative [SPI], UF Contract # 27789

UF | UNIVERSITY of FLORIDA
Water Institute

C R I S P S

Section 6

PHYSICOCHEMISTRY

Nitrogen Dynamics and Metabolism

Annual Report 2015
Work Order No.3: Part 1 of 3

Principal Investigators:

Matthew Cohen, University of Florida
Michael F. Coveney, St. Johns River Water Management District

Project Team

Matthew Cohen, University of Florida
Jennifer McBride, MS Student
Courtney Reijo, PhD Student
Larry Korhnak, Laboratory Manager
Lily Kirk, PhD Student
Sarah Power, Undergraduate Assistant in SFRC
UF Ecohydrology Laboratory

School of Forest Resources and Conservation
University of Florida

Michael F. Coveney
St. Johns River Water Management District

This document reports interim progress of a work order in the first year of a 3-year project in compliance with Agreement between University of Florida (UF) and St. Johns River Water Management District (SJRWMD) UF Contract #27789. It is part of the *UF Collaborative Research Initiative on Springs Protection and Sustainability (CRISPS)* and supports the science component of *the SJRWMD Springs Protection Initiative (SPI).*

6.1 ABSTRACT

Elevated nitrate levels have been invoked to explain increasing algal abundance and declining SAV health across springs. In this research element, we initiated four parallel lines of inquiry to evaluate this hypothesis, emphasizing spatial heterogeneity within springs, and contrasting patterns across two springs with dramatically different nitrate concentrations (Silver River and Alexander Springs Creek). First, we used synoptic spatial sampling of algal and SAV cover along the entire length of the Silver River, along with a suite of hydraulic, edaphic and ecological variables to explore patterns of, and controls on, variation in primary producer community structure. SAV cover was generally high (>75% cover at nearly 90% of our 100 sites) while algal cover was more variable. Spatial variation in algal cover was best explained by SAV cover (negative correlation, suggesting an inhibitory association, the direction of which is unknown) and distance downstream (negative), and surface water velocity (negative). While none of the water chemistry parameters provided significant explanatory power for algal cover, some sediment properties (Ca, P, Mg content) were positively associated with algal cover. SAV cover declined with increasing water column Ca, chloride concentrations (water column and porewater) and sediment clay content. Surveys of Alexander Springs Creek are underway, and will provide useful chemical contrast, and also be used to inform the location of subsequent measurements of SAV growth, and benthic metabolism. Second, working closely with SJRWMD scientists, we have initiated the quantitative interpretation of high resolution time series of pH, dissolved oxygen, nitrate, and phosphate to estimate open-channel ecosystem metabolism and autotroph nutrient use in 4 reaches along the Silver River and 2 reaches along Alexander Springs Creek. Data analysis protocols have been established, and formal analysis of these time series is scheduled to begin in Year 2 of our workplan. Third, we have initiated benthic chamber measurements of ecosystem metabolism. These chambers enable the investigation of nutrient use kinetics at below-ambient concentrations, which is integral for predicting ecosystem behavior as nitrate concentration are reduced. The study consists of 4 co-deployed roving chambers (1 control, 3 nutrient additions, including factorial additions of nitrate, phosphate and iron) with in situ dissolved oxygen sensors for measuring metabolism during week-long deployments; periodic measurements of high resolution nutrient dynamics are also part of our ongoing protocols. Finally, we have initiated SAV growth monitoring at 16 sites in each river spanning the range of benthic conditions observed during our survey (algal cover, sediment properties, physical factors such as light and flow velocity). At each location, we are monitoring SAV growth, morphometric properties (root:shoot ratios) and both water and soil chemistry. Our goal is to understand spatial controls on SAV vigor, and temporal controls on biomass accrual. For details see the report by Cohen et al. (2015).

6.2 INTRODUCTION

The St. Johns River Water Management District (SJRWMD), in partnership with the University of Florida (UF), has initiated the SJRWMD-UF Springs Protection Initiative – Collaborative Research Initiative on Sustainability and Protection of Springs (CRISPS). A detailed background and set of major objectives and questions related to Silver River nitrogen dynamics are presented elsewhere, with a primary goal of predicting how nitrogen enrichment impacts primary producer community structure and function, and whether N reductions alone (to meet the statewide springs TMDL) will be sufficient to restore community structure. The purpose of this annual report is to describe four (4) research elements to address that primary goal, with links explicitly made to other elements of CRISPS: 1) quantify continuous C and N metabolism using in situ sensor data collected by SJRWMD; 2) comprehensive survey of the benthic condition of Silver River, including vegetation composition and abundance, water column and pore water chemistry, and sediment characteristics; 3) in situ pathway-specific nitrogen depletion experiments with factorial investigation of sediment, vegetation and trace nutrient effects; and 4) in situ SAV growth experiments with factorial evaluation of sediment/porewater variation, algal cover, light regime and velocity. A fifth section described in the original workplan (#5: mesocosm measurements of SAV growth under varying experimental controls such as N enrichment, DO depletion, velocity, trace element availability) will be reported on separately.

Silver River is the primary field site for these measurements, and most of the results presented in this report are from that system. However, the next year will include implementations of most of the research components in Alexander Springs Creek to provide a low N site for comparison.
We have divided this report into four main sections, corresponding to the three work elements outlined above. In each section, we describe the rationale, methods, and preliminary results from efforts to date. Where appropriate, we also describe work either already started or proposed to Year 2 of the overall project effort.

6.3 ECOSYSTEM METABOLISM

Ecosystem metabolism is an integrative measure of autotroph and heterotroph activity. Using diel variation in dissolved oxygen concentrations (Figure 6.1; Odum 1957; Munch et al. 2005), it is possible to estimate C fluxes associated with aggregate gross primary production (GPP), and whole system respiration (R_E); based on published estimates of autotroph respiration, it's also possible to estimate the respiration due to microbes and animals. Exploring the temporal and spatial variation in ecosystem metabolism provides an important foundation for understanding specific ecological behaviors. For example, does an increase in biomass correspond to an increase the rate of primary production? Similarly, how does variation in flow, light (seasonal and day-to-day), and chemistry impact metabolic behavior at the ecosystem scale. Recently, sensor advances have enabled an expansion of the method to also include ecosystem N and P dynamics (Heffernan and Cohen 2010; Cohen et al. 2013), from which both autotrophic ($U_{a,N}$, $U_{a,P}$), heterotrophic (U_{den}) and geochemical ($U_{geo,P}$) removal pathways can be determined; note that metabolism measurement nomenclature is summarized in Table 6.1. This advance allows coupling between C, N and P element cycles to be made explicit, and to ask questions about how changes in both time and space in metabolism or ecosystem structure affect the ecosystems capacity to process nitrogen. Given the central role that N and P processing plays in the rationale

for setting statewide water quality standards for springs (especially for N), this coupling is integral to understanding how and why springs change, and for interpreting the responses to ongoing restoration activities.

Table 6.1. Summary of metabolism variables, their associated symbols, and units.

Variable	Symbol	Units
Gross Primary Production	GPP	g O_2 m^{-2} d^{-1}
Net Primary Production	NPP = 0.1875 * GPP	mol C m^{-2} d^{-1}
Ecosystem Respiration	R_E	g O_2 m^{-2} d^{-1}
Net Ecosystem Production	NEP = GPP - R_E	g O_2 m^{-2} d^{-1}
Production:Respiration	P:R	Unitless
Autotroph N assimilation	$U_{a,N}$	mg N m^{-2} d^{-1}
Denitrification	U_{den}	mg N m^{-2} d^{-1}
Autotrophic P assimilation	$U_{a,P}$	mg P m^{-2} d^{-1}
Abiotic P retention	$U_{geo,P}$	mg p m^{-2} d^{-1}
Ecosystem stoichiometry*	NPP:$U_{a,N}$:$U_{a,P}$	Unitless

* - Note that for ecosystem metabolism stoichiometry, the mass flux of autotroph assimilation of P and N is converted to a molar basis using the atomic mass.

Metabolism data are most informative when they are continuous and long term (e.g., Roberts and Mulholland 2007). The SJRWMD is planning to deploy and maintain both dissolved oxygen and nitrate sensors at multiple locations in the Silver River, providing an important opportunity to process those data into estimates of metabolic behavior (GPP, R, $U_{a,N}$, $U_{a,P}$, U_{den}, $U_{geo,P}$). These measurements will serve as a foundation for assessing changes in the river, and for interpreting the finer-scale results from other elements.

6.3.1 Proposed Tasks and Methodology

Using continuous time series (e.g., 15 min sampling resolution) of DO and NO_3-N (Figure 6.1), SRP (Figure 6.2), as well as discharge information and travel times (from Element #1), we will construct daily estimates of GPP, R, $U_{a,N}$, $U_{a,P}$, U_{den} and $U_{geo,P}$ (data for C and N in Figure 6.3) using existing analytical templates developed by Cohen et al. (2013) for spring-fed rivers. Estimates of oxygen reaeration will use published relationships with flow velocity where the nighttime regression (Owens 1973) or peak DO lag (Chapra and DiToro 1992) techniques cannot be validated. An existing 1-D solute transport model parameterized for the Silver River (Hensley and Cohen 2010) coupled with new field measurements of velocity distributions from the hydrodynamics group (D. Kaplan and P. Suscy) will allow us to represent between-station travel times.

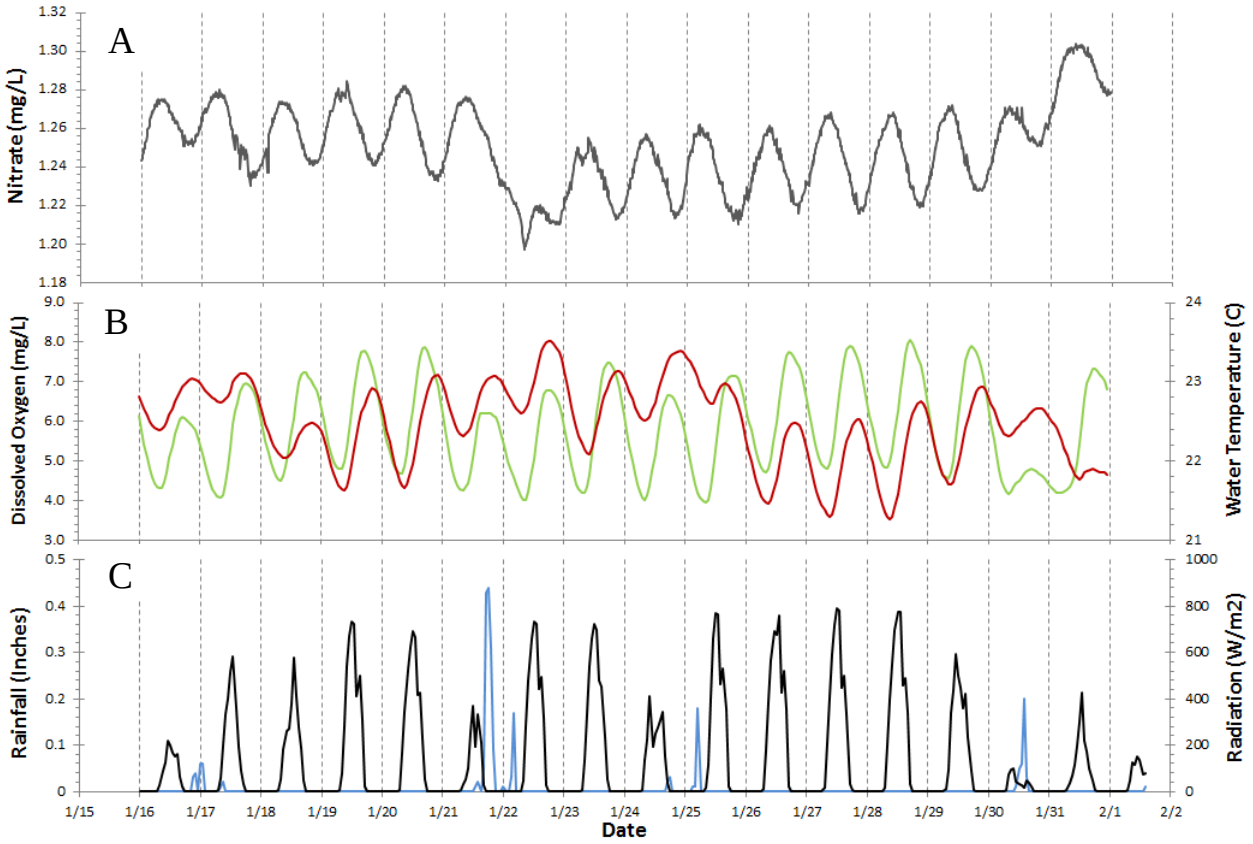

Figure 6.1. Diel variation in nitrate (grey line), dissolved oxygen (green line), water temperature (red line), radiation (black line) and rainfall (blue line) for Silver River during January 2010.

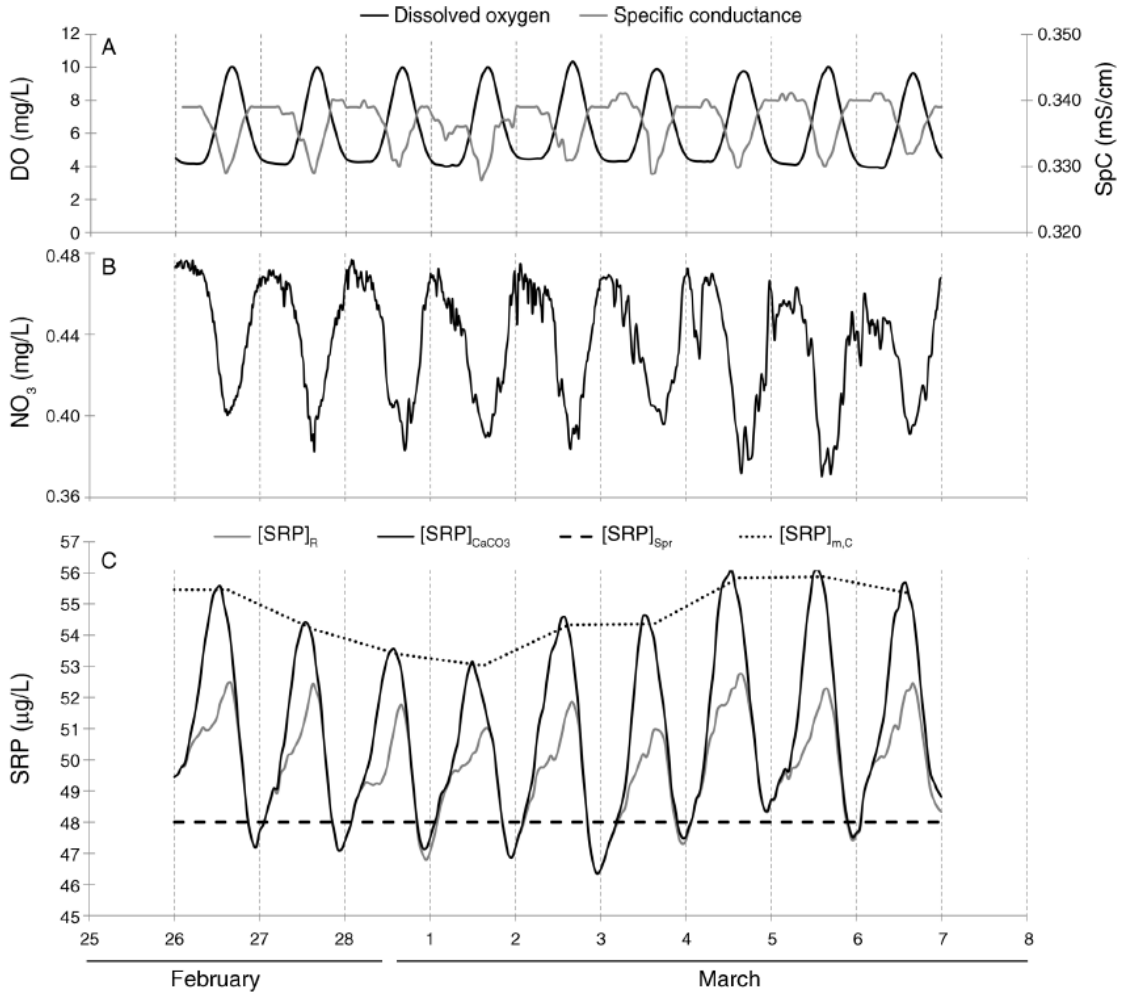

Figure 6.2. Diel variation in dissolved oxygen and specific conductance (a proxy for calcium concentration in solution) (top), nitrate (middle) and soluble reactive P (bottom) for the Ichetucknee River during March 2011 (Cohen et al. 2013). Note that geochemical P retention due to calcite co-precipitation creates the difference between the observed data (grey lines in bottom panel) and imputed SRP values without geologic retention pathways (black line). The horizontal dashed line is the flow-weighted springs inputs, and the stippled line denotes the night-time baseline from which P assimilation ($U_{a,P}$) is computed.

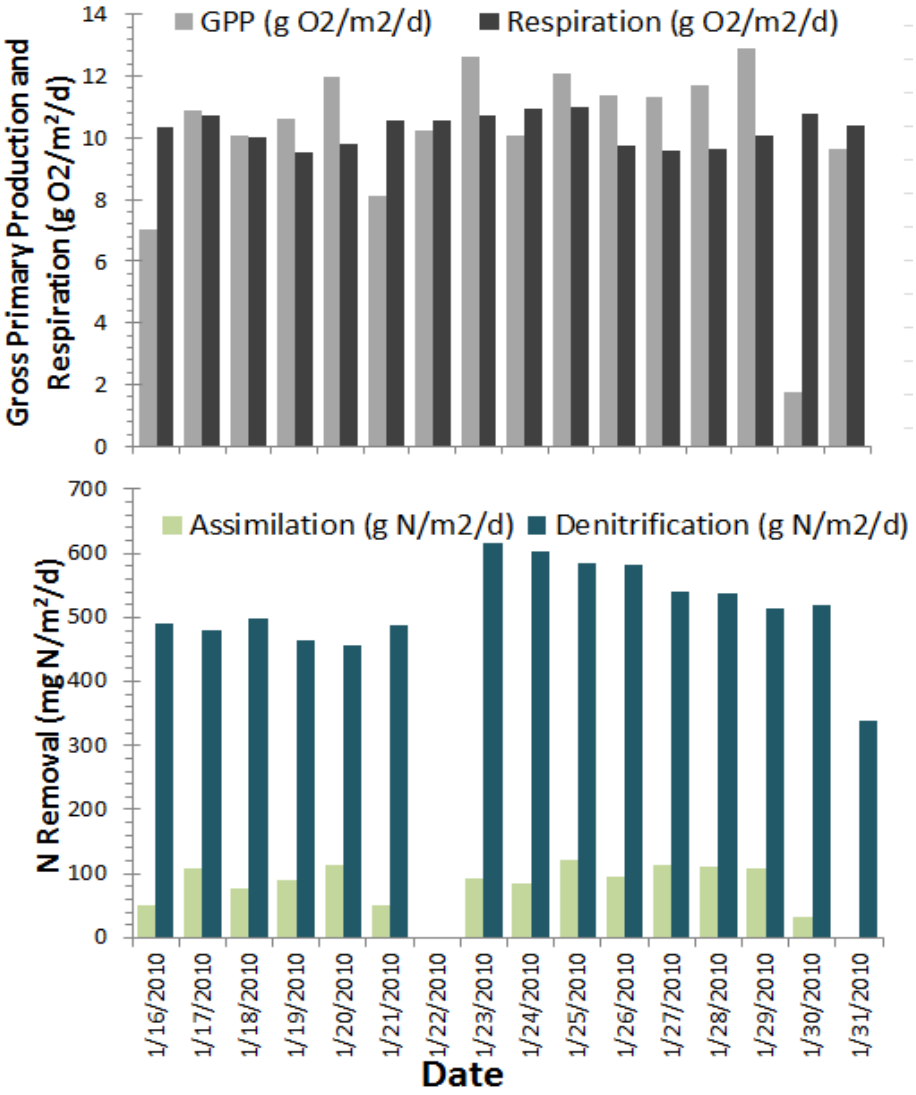

Figure 6.3. Summary of Jan. 2010 deployment at Silver River showing estimates of gross primary production and respiration (top) and assimilatory and dissimilatory N removal (bottom).Carbon and nitrogen metabolism calculations (Element #1) were slated to begin in Year 2 of the CRISPS project. However, we have already been working with SJRWMD to ensure quality and timely delivery of sensor data so we can do these calculations. We have made progress in the following areas:

While this work is nascent, as we waited for sensors to be installed, data QA/QC protocols to be emplaced, and trouble-shooting to occur, we summarize here three elements of our participation in preparation for more comprehensive analyses of the high resolution data streams in Year 2:

1) Sensor locations at Silver River – our field crews have visited all of the sensor locations, and provided important feedback to SJRWMD staff regarding the utility of the selected deployment locations.

2) Data transfer test case – while finalized QA/QC protocols are still being developed, we worked with SJRWMD staff to take delivery of a test data set that has been the focal point for evaluating protocols (data delivery intervals, QA/QC requirements, access mechanisms)

3) Establishing a protocol for data delivery – based on our test case data transfer, we have worked with SJRWMD to streamline the process of data transfer so that UF can perform this Year 2 and 3 task.

6.3.1.1 Sensor Locations at Silver River

SJRWMD has installed EXO, SUNA, and Cycle-P sensors at four continuous monitoring stations on Silver River. From upstream to downstream, they are named SILHEAD, SILBIRD, SILVERRIVERS5, and SILCONN.

While performing other field work on Silver River, we visited each station and evaluated its location, taking into account distance from the river bank, water velocity, and presence of SAV/algae. For ecosystem metabolism calculations to accurately represent the river reach, concentration data MUST be from the advective zone. The SILBIRD and SILVERRIVERS5 are well-placed for this effort, though SILVERRIVERS5 is situated in the obvious plume of a floodplain tributary delivering high turbidity water to the river. At the other two sites (SILHEAD and SILCONN), we made recommendations to SJRWMD to reposition the sensors since both are currently placed in non-flowing areas of the river (i.e., where SAV and channel margin vegetation preclude exchange with the main river advective zone. SJRWMD has informed us that they will move SILCONN; we have not heard about the status of SILHEAD. Because SILHEAD represents the upstream boundary condition for all metabolism calculations, its placement is especially critical to ensure quality data and inferences.

6.3.1.2 Examining a Test Case of Sensor Data

SJRWMD extraced water quality data for the entire period of record for one of the stations (SILVERRIVER5) up until June 14, 2015. Figure 6.4a and 6.4b show all parameters over the latest five days. Most signals behave as expected (i.e., diel signals of plausible magnitude and phase) and show clean signals at high resolution. The nitrate data, however, is truncated due to only logging three significant figures (see Figure 6.4a). Since nitrate uptake is based on the area under concentration curves, this truncation will lead to errors in the nitrate metabolism calculations.

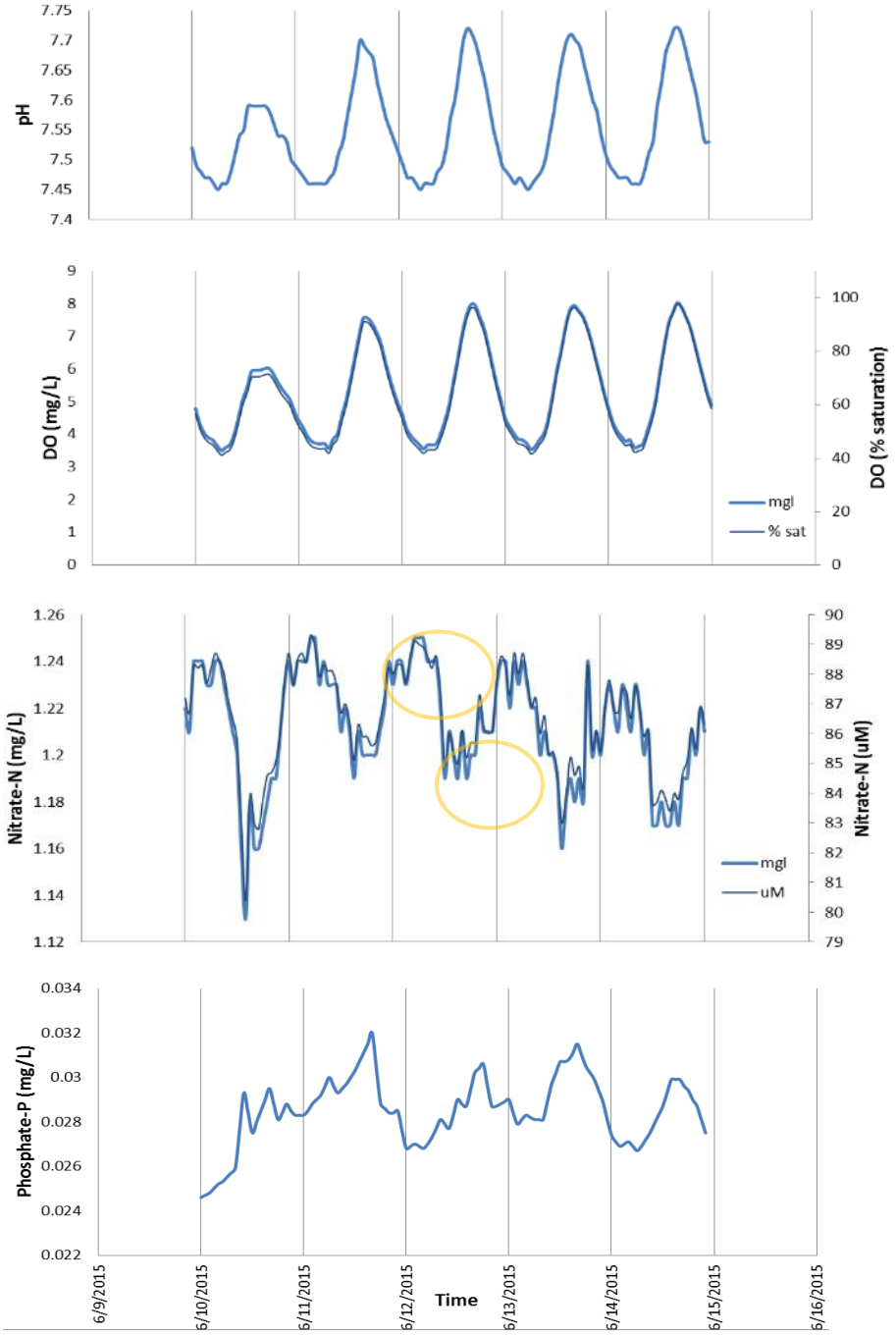

Figure 6.4a. Diel signals at SILVERRIVERS5. Note: Truncated NO_3-N concentrations produce plateaus and excessive wiggling where there a smooth peak and trough are expected (yellow circles). This will likely necessitate the application of smoothing algorithms to obtain $U_{a,N}$. While SRP data looks slightly less diel than other applications, there is clear 24 h periodicity, with a trough at ca. 01:00 each day, as expected from similar data Ichetucknee River. These data are influenced by a storm on June 10, 2015.

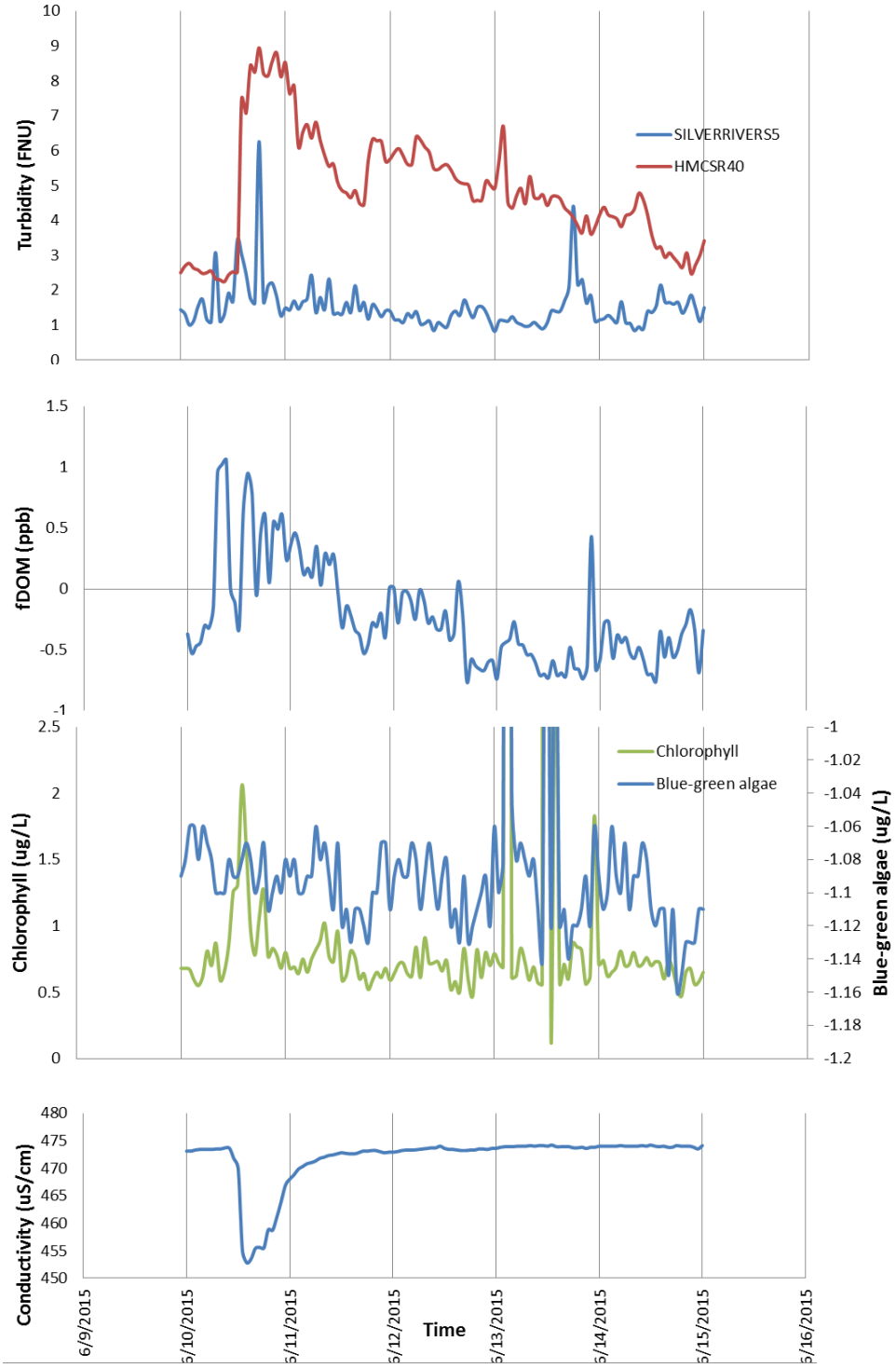

Figure 6.4b. Signals at SILVERRIVERS5, some strongly influenced by a storm event.

6.3.1.3 Data Delivery Protocols

We have been in frequent communication Margaret Guyette at SJRWMD to establish a protocol for delivering sensor data to our lab and delivering metabolism data back to SJRWMD. Currently, we favor an automated, periodic pull of data and email delivery of .csv files (although we have also considered using the CRISPS project FTP site if file sizes are too large for email).

There is apparently no way to flag any changes to the data following quality control, so the primary issue to resolve with data delivery is whether we can receive data only after QA/QC. We noted between 15 to 100 changes between data pulls in a two week period (although many changes may be to quality control codes). It would be redundant to analyze data if they subsequently change. Moreover, the current protocol delivers data for the entire period of record for each station, which is cumbersome to wade through since most will have already been processed. Because SJRWMD has not yet finalized their QA/QC procedure, we have recommended integrating our data delivery into their QA/QC procedure so we can receive data only after quality control.

6.4 SILVER RIVER COMPREHENSIVE SURVEY

Beginning in August 2014 and ending in December 2014, a comprehensive survey was completed to characterize the physical, chemical, and biological components of Silver Springs and Silver River. The survey was used to 1) determine how these characteristics co-vary across the Silver Springs system, and 2) inform site selection for vegetation growth and benthos box experiments. Twenty longitudinal transects were selected based on proximity to MFL locations, proximity to SLVR locations, and overall water depth (Figure 6.5). Across each transect, five quadrat locations with water depths less than 3-meters were selected so free-diving could be used for sample collection. In total, the survey included 100 sample locations (20 longitudinal transects with 5 latitudinal locations within each) where the biological, chemical, and physical components of the river were characterized (see Appendix 6.1 for geographic locations of transects and samples).

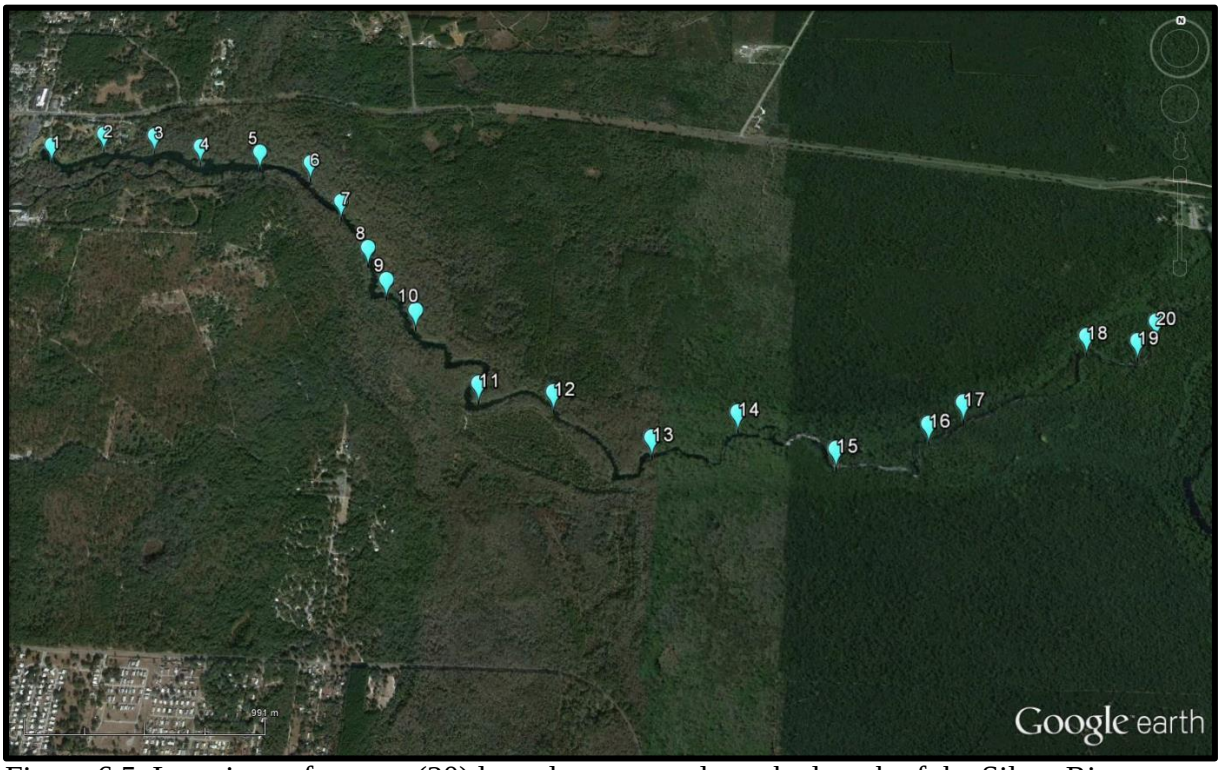

Figure 6.5. Locations of twenty (20) lateral transects along the length of the Silver River at which channel morphology, vegetation, water chemistry and sediment properties were measured. Each transect consisted of 5 locations spanning the width of the river. A similar survey is planned for summer 2015 in Alexander Springs Creek.

6.4.1 Field Methodology

At each location, a 2'x2' vegetation quadrat was placed on the stream bottom (Figure 6.6) and the percent cover of submerged aquatic vegetation (SAV) and algae was characterized by species using the 5-point Braun-Blanquet classification system (described in section 6.5.2). Percent cover of bare substrate was also recorded. The quadrat location was characterized by distance from channel bank and latitude/longitude coordinates. Water depth was taken within the quadrat and surface water velocity and canopy cover measurements were taken above the quadrat. Canopy cover was determined by using a densiometer, determining percent open canopy in the four cardinal directions around the quadrat location, and converting to percent canopy cover. Porewater and water column samples were collected using a peristaltic pump, 0.45 micron filter, and acid preservative. Finally, two plant samples and a sediment grab sample were collected from within the quadrat. All water, sediment, and vegetation samples were placed on ice for transport. Analytes, sample sizes, and preservative per analysis are in Table 6.2.

6.4.2 Laboratory Analyses

Water samples were stored on ice and refrigerated until chemical analyses (Table 6.2) were performed. All water analyte (NO_3-N, NH_4-N SRP, Ca, Cl, Fe, Mn) concentrations were analyzed at the University of Florida Analytical Research Laboratory (UF ARL) according to EPA standard methods. Specifically, NO_3-N, NH_4-N, SRP, and Cl were measured by automated colorimetry (EPA Method 353.2, 350.1, 365.1, and 325.2; respectively) and Ca, Fe, and Mn

concentrations were determined through Inductively Coupled Mass Spectrometry (ICP-MS). Average, minimum, maximum, standard deviation, and variation in soil, water column, and porewater analyte concentrations were calculated.

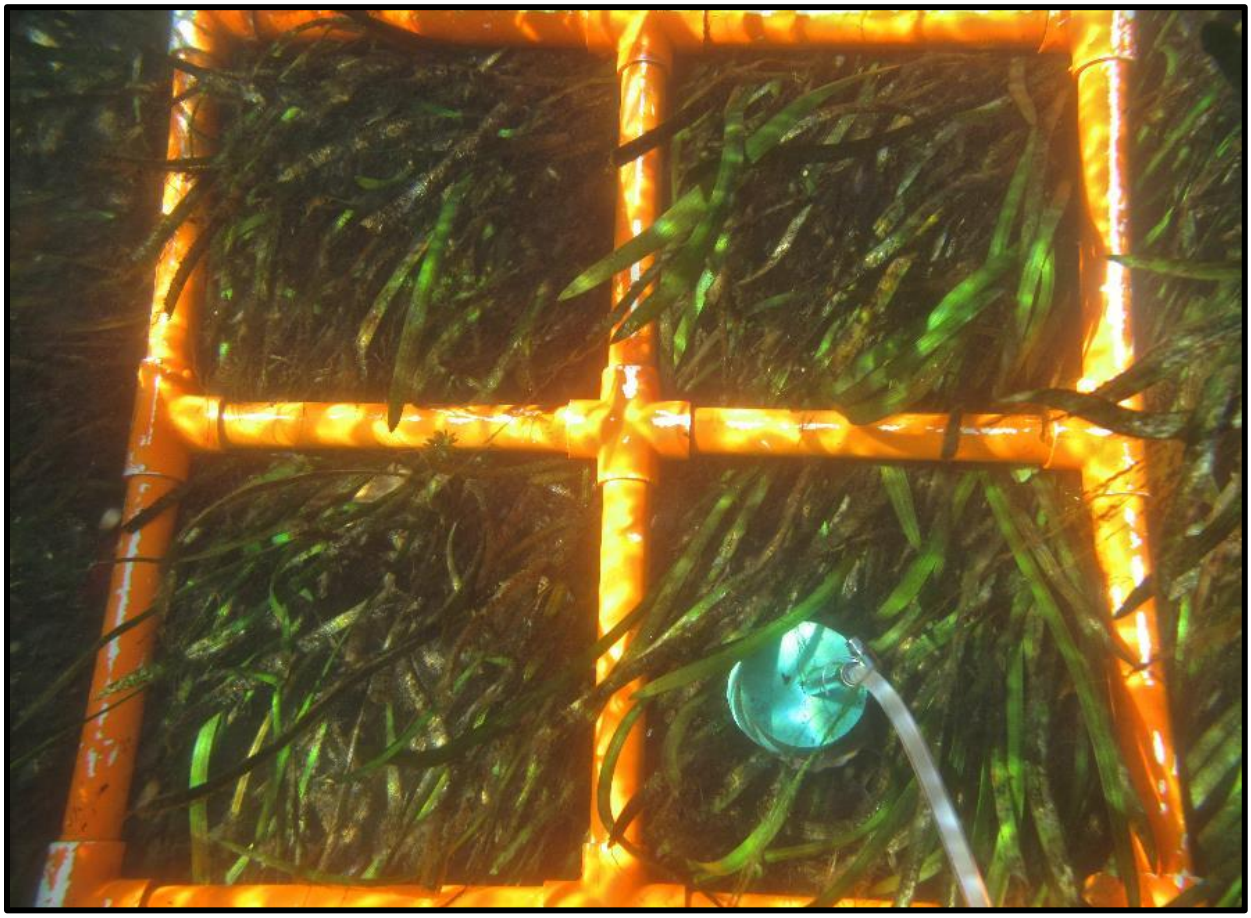

Figure 6.6. Deployment of quadrat for cover and composition measurements, and porewater sampler for collecting water samples. After benthic characterization is complete, a sediment sample is obtained using a modified Ekman sampler, and a water sample from the river is obtained.

Sediment samples were dried at 60°C for 60-72 hours. After drying, the soils were homogenized through grinding by mortar and pestle and sieved with a 2mm mesh (#10) sieve. Approximately 10 g of soil were analyzed for percent carbon, nitrogen, and sulfur (%C, %N, %S) by weight through Light Isotope Mass Spectrometry. The soil metals (P, K, Ca, Mg, Mn, and Fe) were extracted using 5 g of soil and 20 mL Mehlich-1 solution and analyzed on an Inductively Coupled Plasma Spectrometer at the UF ARL (EPA Method 200.7). The Loss on Ignition (LOI) Method was also used to analyze the soil for percent organic matter (%OM). Each sample (1-2 g of soil) was weighed, heated at 450°C for 6 hours, and reweighed where percent organic matter is calculated as the difference between the dried (60°C) and furnace (450°C) weight. Lastly, soil particle size analysis was determined using the hydrometer method which is based on the rate of particle sedimentation when suspended in water (i.e. Stoke's Law).

Table 6.2. Summary of characteristics, sample size, and added preservative by stream sample area.

Sample Area	Analysis	Sample size	Preservative
Porewater and Water Column	NO_3, NH_4	20 mL scintillation	H_2SO_4; pH<2
	SRP, Ca, Cl	20 mL scintillation	No preservative
	Fe, Mn	20 mL scintillation	HNO_3 + HCl
	DOC	40 mL amber glass	HCl
	DIC	40 mL clear glass	$HgCl_2$
Sediment	%C, %N, %S	1-2 g dried soil	N/A
	Fe, Mn, Ca, P, Mg	5 g dried soil	
	%OM	10 g dried soil	
	Texture	50 g dried soil	
Vegetation	%C, %N, %P	Two plant samples measured, weighed, and dried	
	Aboveground biomass		
	Belowground biomass		
	Shoot and root length		
	Number of shoots		

Approximately 50 g of soil was treated with 100 mL of 5% dispersing solution (hexametaphosphate), diluted to 1,000 mL with deionized water, and equilibrated to room temperature overnight. Prior to each reading, the water temperature and density of a blank sample (blank = 100 mL dispersing solution and 880 mL deionized water) was recorded. A plunger was then used to mix the soil sample for 30 seconds and a hydrometer was inserted into the suspension. Hydrometer readings were taken 40 seconds after mixing and 6 hours, 52 minutes after mixing. The difference in sample densities (corrected for temperature and the difference in blank readings) at both time intervals were used to determine % sand, % clay, and % silt distributions, where:

- % clay = corrected hydrometer reading at 6 hours, 52 minutes X 100/weight of sample
- % silt = corrected hydrometer reading at 40 seconds x 100/weight of sample
- % sand = 100% - % silt - % clay

Vegetation samples were stored on ice and triple washed in deionized water within 48 hours of collection to remove epiphytes. Submerged aquatic vegetation samples were separated into above- and belowground live biomass, and shoot and root lengths were measured. All samples were dried at 60°C to constant weight, and above- and belowground biomass (g dry weight) was determined. Aboveground biomass was ground and homogenized for tissue analysis. Foliar carbon and nitrogen concentrations, in %C and %N, were measured using a Carlo Erba NA1500 CNHS elemental analyzer at the UF Light Stable Isotope Mass Spectrometry Laboratory. Total phosphorus was analyzed at the UF ARL according to EPA Method 365.1.

6.5 RESULTS

6.5.1 Physical Controls

Physical and morphological conditions measured during the comprehensive survey were imported into ArcGIS and will be included in the Springs Initiative GIS database. In general, water depth was greater at the upstream transects, canopy cover increased downstream, and surface water velocity was variable across all transects (Figure 6.7). An ANOVA showed that there was significant variation between these three characteristics (p-value <0.001). Water depth explained little variation in surface water velocity ($R^2 = 0.08$; Figure 6.8), which may suggest future work should include measurements made within the water column.

6.5.2 Vegetation Inventory

In total, 207 vegetation samples were collected during the survey. *Sagittaria kurziana* and *Vallisneria americana* composed 80.2% and 17.4% of samples, respectively. Other species identified in the survey include *Ceratophyllum demersum* (Coontail), *Hydrilla verticillata*, *Lyngbya wollei*, *Spirogyra spp*., and *Vaucheria spp*. Our benthic inventory included cover estimates for each taxa, and as guilds (i.e., SAV vs. algae). We used a modified Braun-Blanquet score for characterizing cover with:

- 0 = 0% cover
- 1 = 1 - 5% cover
- 2 = 6 - 25% cover
- 3 = 26 - 50% cover
- 4 = 51 - 75% cover
- 5 = 76 - 100% cover

While there is evidence of significant algal accumulation in the river (40% of sites had algal cover > 50%), the river remains dominated by dense SAV, with almost 75% of sites having SAV cover in excess of 75%.

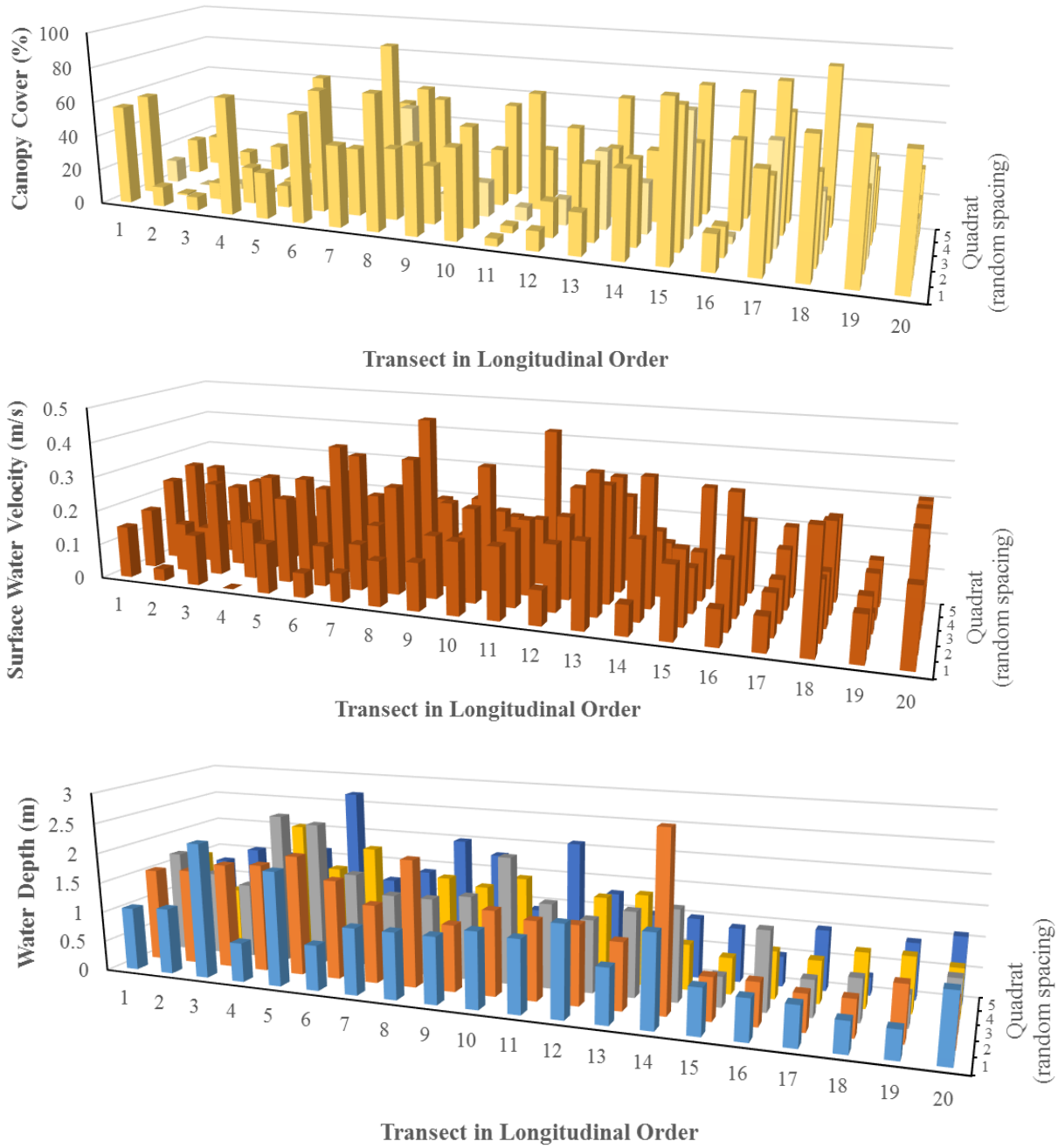

Figure 6.7. Ambient conditions, including percent canopy cover, surface water velocity (m/s), and water depth (m), were measured during the comprehensive survey. Shown are values for each of 5 locations on each of the 20 transects along the river.

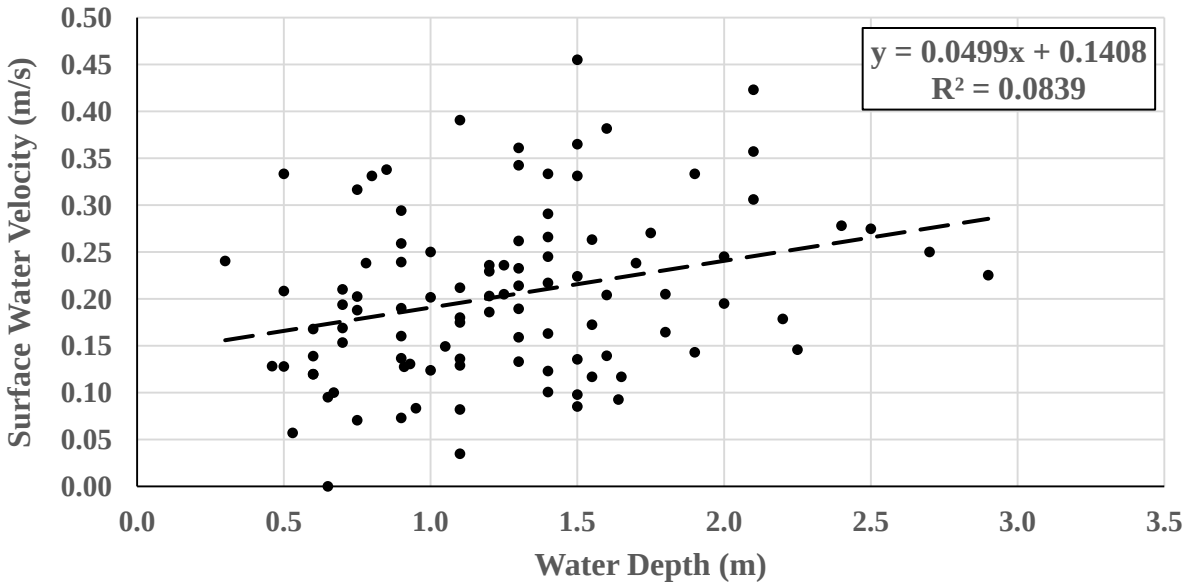

Figure 6.8. Individual water depths (m) and surface water velocity (m s^{-1}) for each location on each transect were measured as part of the comprehensive survey. Water depth explained little variation in surface water velocity.

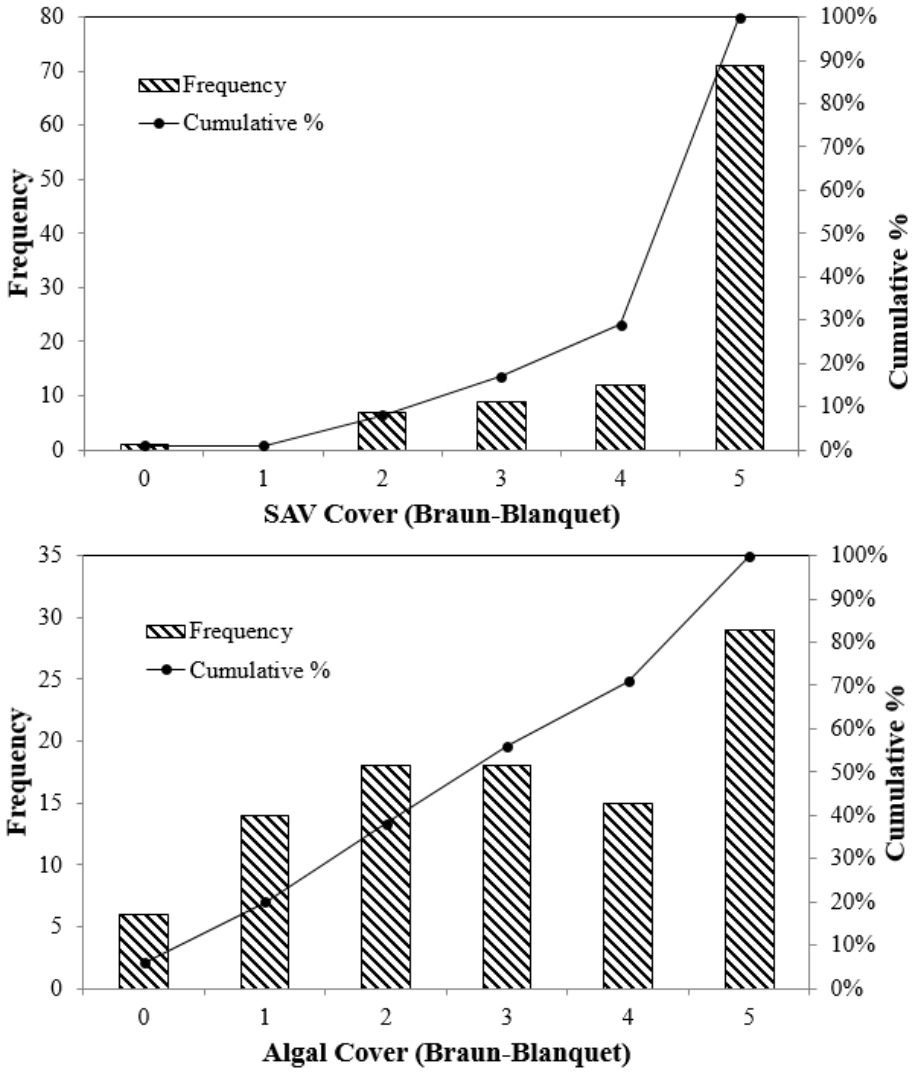

Figure 6.9. Summary of overall river benthic cover of a) SAV and b) algae using the Braun-Blaunquet scale. The survey suggests that most (over 75%) of the river retains dense SAV beds. Algal cover is variable, suggesting important controls on spatial heterogeneity that are the subject of our subsequent work.

One of the key questions about the interaction between SAV and algae has to do with the shape of their competitive interaction. Plausible relationships include:

- Linear exclusion, wherein benthic cover for algae is the complement of benthic cover of SAV.
- Non-linear negative effects, wherein high algae is associated with low SAV (and vice versa), but the effect is not complementary.
- Positive effects, wherein SAV provide a venue for algal attachment, and therefore high algae is only found where there is high SAV.

We found evidence for a non-linear negative effect, with high algal cover associated with variation in SAV cover; that is, at high algal cover, SAV ranges from <5% to over 75% cover, but is always above 50% when algal cover is low (Figure 6.10).

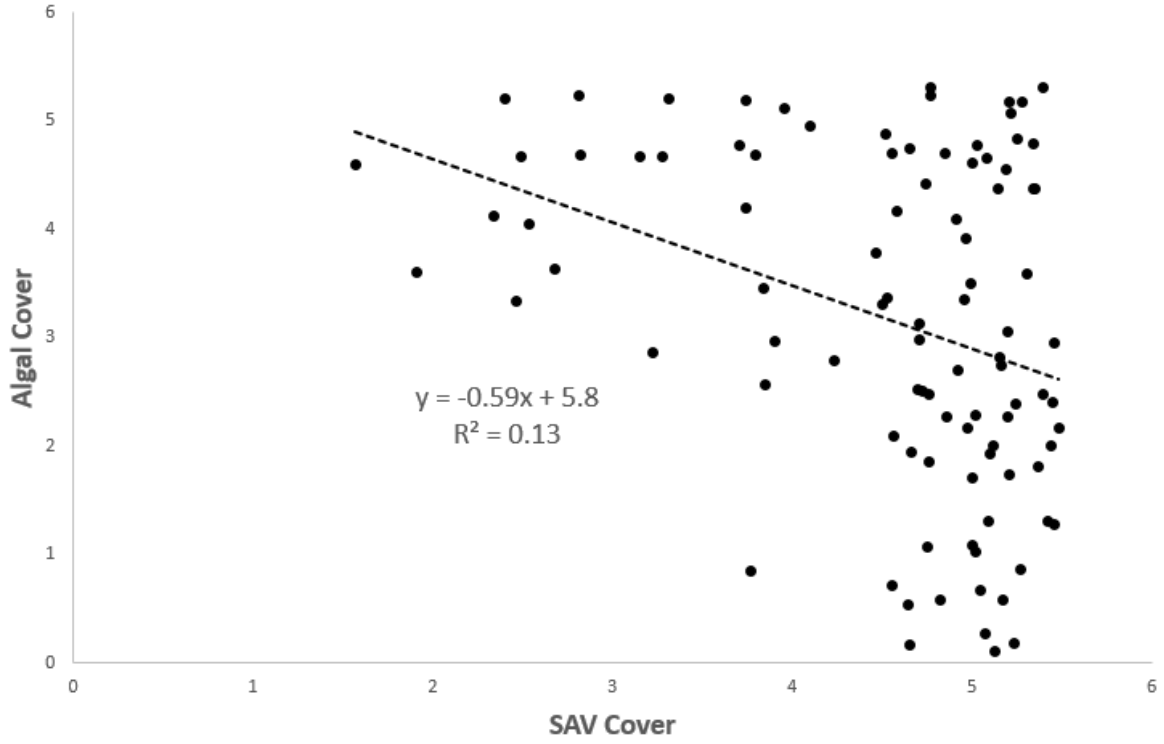

Figure 6.10. Association between benthic algae and SAV cover from individual locations on 20 transects along the Silver River. A non-linear negative association suggests some capacity for SAV and algae to co-exist. However, while the river is uniformly high SAV when algae cover is low, at high algal cover, there is evidence of spatial heterogeneity in SAV cover, associated with potential smothering effects. Random variance has been added to these categorical cover class data to assist visualization of the association; regression results are for unmodified data.

Average shoot length of all *Vallisneria* samples (75.65 cm) exceeded that of *Sagittaria* (65.86 cm), while average *Sagittaria* root length (14.70 cm) was longer than *Vallisneria* root length (11.29 cm). However, despite significant variation in velocity, water depth, water clarity, and sediment properties, there were few systematic trends in any of the vegetation morphometric properties (Figure 6.11). Root:shoot biomass appeared to maximize through the middle part of the river (Transects 11-14), especially for *Sagittaria kurziana*, but that trend was less clear for root:shoot lengths, nor was is clear for *Vallisneria americana*.

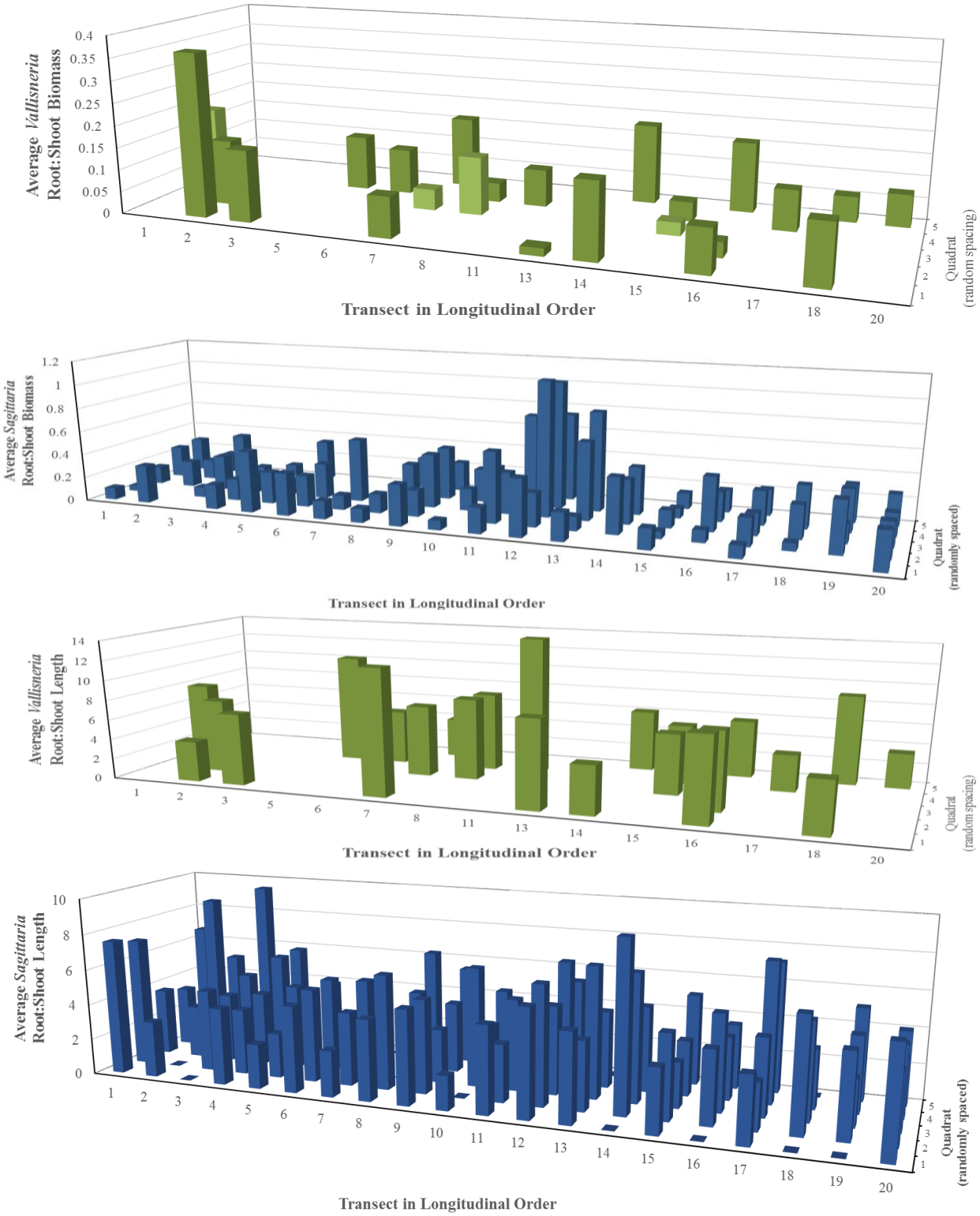

Figure 6.11. Summary of SAV morphologic characterization with distance downstream for each of 5 locations location along each of 20 transects. Locations with no data were where that taxa was not found.

Despite the absence of major vegetative morphologic variation, as would be expected if significant spatial heterogeneity in nutrient availability, or root porewater stresses exist, we did observe significant spatial patterns in benthic cover, both longitudinally (Figure 6.12) and laterally (Figure 6.13). We observed strong evidence for longitudinal declines in algae (to a predicted cover less than 25% by the Ocklawaha confluence) and also evidence that algal cover is most pronounced on the south edge of the transects, suggesting some interaction with direct insolation.

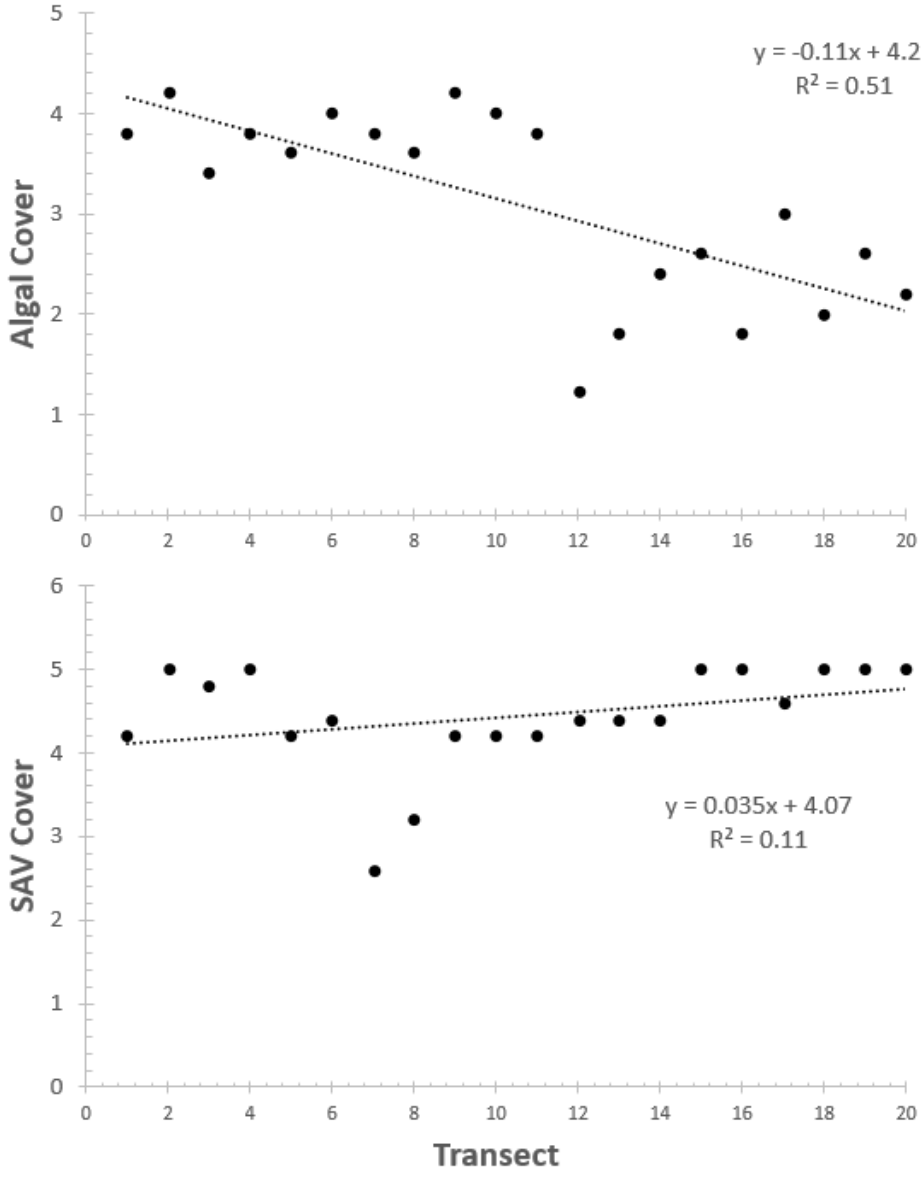

Figure 6.12. Longitudinal patterns in the mean cover of a) algae and b) SAV from each transect from the headspring (at left) to the confluence with the Ocklawaha River (at right). The decline in mean algal cover is statistically significant ($p < 0.001$), as is the increase in SAV cover ($p = 0.02$).

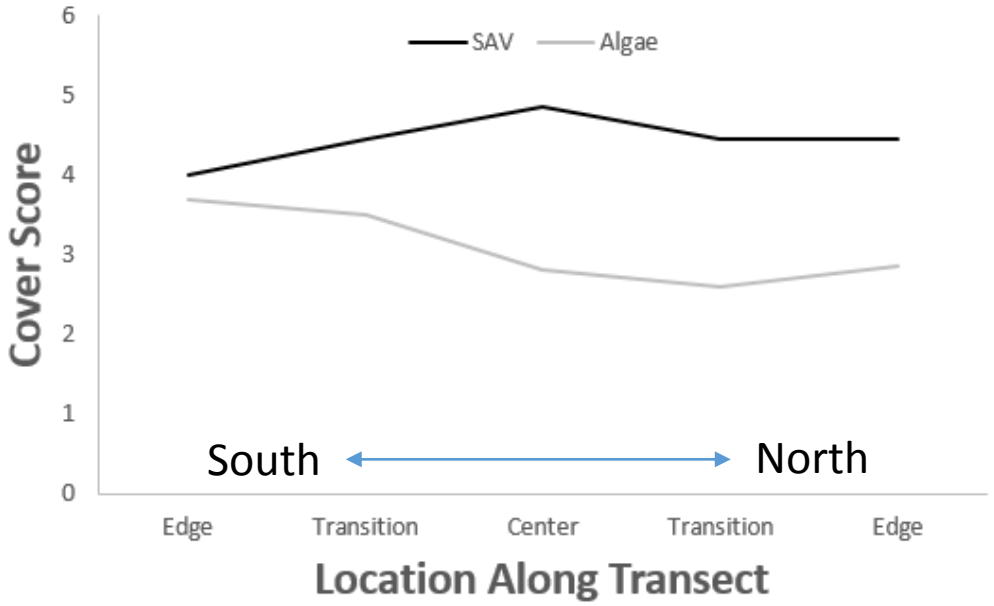

Figure 6.13. Across transects, mean SAV cover was highest in the center of the channel and declined towards the channel margins, while algae was highest at the south edge. Data are pooled across transect for each sampling location perpendicular to river flow.

6.5.2.1 Vegetation Chemistry

Student's t-tests showed no significant difference in average C (p-value = 0.30) and N (p-value = 0.50) tissue percent content between the two dominant SAV species (Figure 6.14).

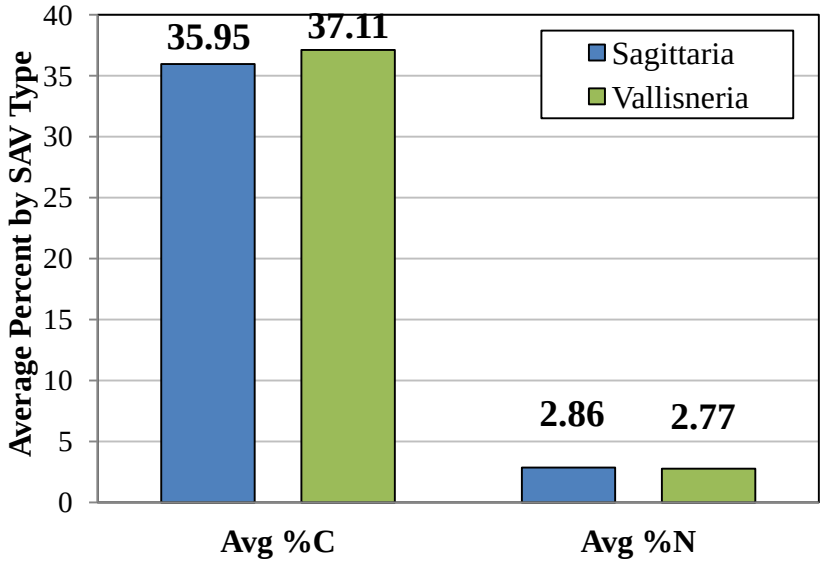

Figure 6.14. No significant difference was found between average % carbon and nitrogen content in two dominant species found in Silver River, *Sagittaria kurziana* and *Vallisneria americana*.

Average tissue C:N for all *Sagittaria* and *Vallisneria* samples was 12.97 and 12.84, respectively. We observed an increase in tissue C:N for both taxa near the confluence with the Ocklawaha River (Figure 6.15). This remains unexplained, and may indicate stoichiometric changes induced by backwater effects from Ocklawaha River flooding. The mangnitude of the downstream increase is large compared to the variation along the rest of the river, or within and across other spring-fed rivers (Nifong et al. 2014).

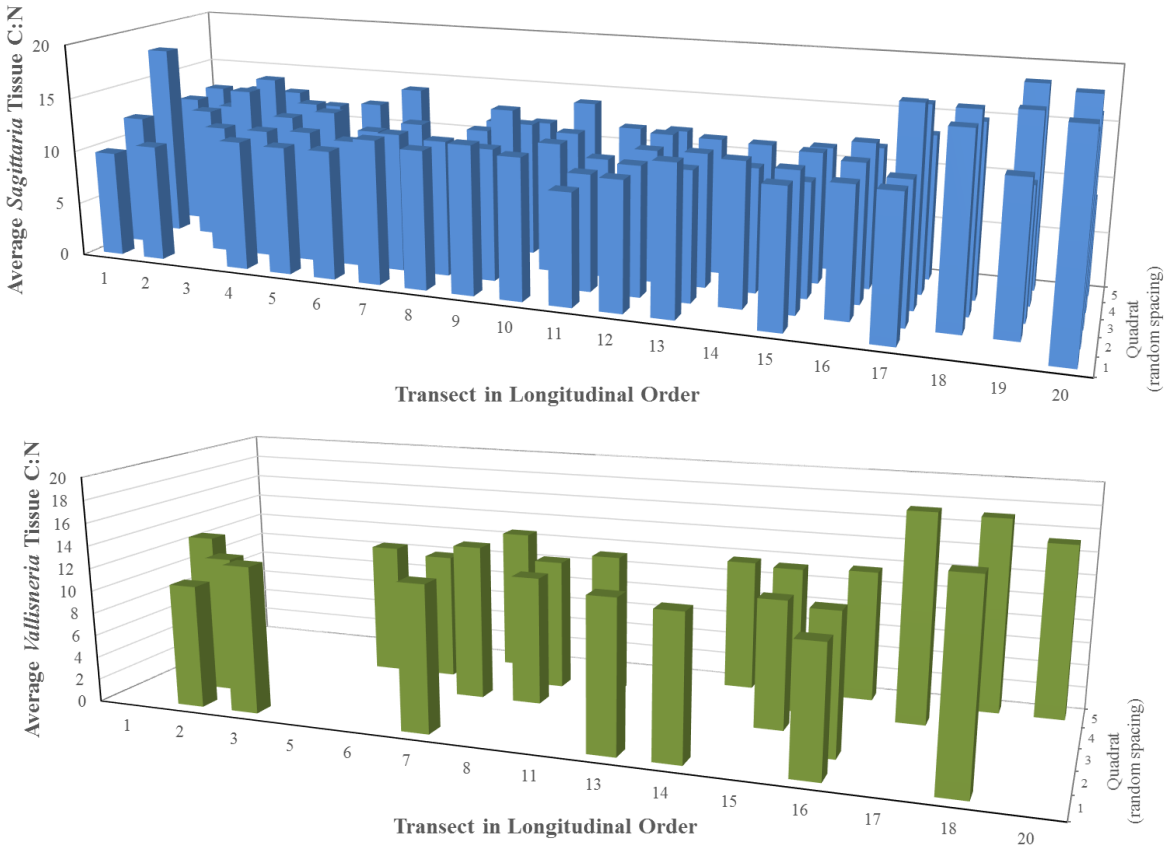

Figure 6.15. Spatial patterns in tissue C:N (molar basis) across the Silver River. We noted a substantial increase in C:N in the lower river, though subsequent measurements (Figure 6.52) do not replicate finding.

6.5.2.2 Water Chemistry

Concentrations in Fe and Mn were below detection limit for every sample collected from the water column and porewater (<0.001 mg L^{-1}); the analytical method employed had a lower detection limit than others used in this report (e.g., Element #2; Dr. Jon Martin), which confirm extremely low levels of both elements, both in the water column and in the shallow porewaters. The other porewater and water column species (NO_3-N, NH_4-N, SRP, Ca, and Cl) were analyze, and exhibited interesting spatial variation. A summary of porewater and water column chemistry across all samples (i.e., pooled both laterally and longitudinally) are shown in Table 6.3. While mean and minima concentrations are as expected, we did obtain some samples that were extremely high concentrations, especially for NH_4 and SRP.

Table 6.3. Summary of porewater, soil and water chemsitry across the Silver River. Note that concentrations for Fe and Mn were consistently below detection limits.

Location	Parameter	Mean	Min	Max	SD
Soil	%OM	23.39	2.40	74.55	12.88
	%C	16.48	7.02	40.52	4.53
	%N	0.90	0.12	2.18	0.37
	C:N	21.79	12.12	91.58	11.96
	Mg (g kg^{-1})	0.31	0.00	1.30	0.18
	P (g kg^{-1})	0.04	0.00	0.28	0.05
	Ca (g kg^{-1})	10.91	2.36	35.96	4.40
Porewater	NO_3-N (mg L^{-1})	0.87	0.01	10.59	1.35
	NH_4-N (mg L^{-1})	4.86	0.06	25.23	6.09
	SRP (mg L^{-1})	0.47	0.00	3.26	0.73
	Ca (mg L^{-1})	88.88	37.54	162.82	27.90
	Cl (mg L^{-1})	12.12	5.71	31.10	4.14
Water Column	NO_3-N (mg L^{-1})	1.45	0.33	24.95	2.42
	NH_4-N (mg/L^{-1})	0.84	0.06	19.92	2.71
	SRP (mg L^{-1})	0.09	0.00	3.48	0.37
	Ca (mg L^{-1})	71.73	30.65	132.99	23.29
	Cl (mg L^{-1})	11.17	4.28	27.39	3.36

We also observed interesting longitudinal trends in many of the analytes, which together suggest that the river is both processing solutes and likely mixing with both shallow groundwater and possibly also surface water from the Ocklawaha River. Figure 6.16 shows the longitudinal trends in the thalweg concentrations (channel center), and fits a trendline where that line was statistically significant ($p < 0.05$). For all analytes except NO_3-N, the trend is significant, with NH4 increasing with distance downstream and SRP, Cl and Ca decreasing. The latter two analytes (Ca and Cl) may suggest that some of the water in the lower river represents a mixture of Silver River and Ocklawaha River water, but this would need to be further verified. Modest enrichment of NH_4 and depletion of SRP with distance may indicate N cycling (i.e., assimilation of nitrate, conversion and export as NH_4), and P retention via both biotic and abiotic pathways. Further work using benthic chambers and open channel measurements will be part of Year 2 activities.

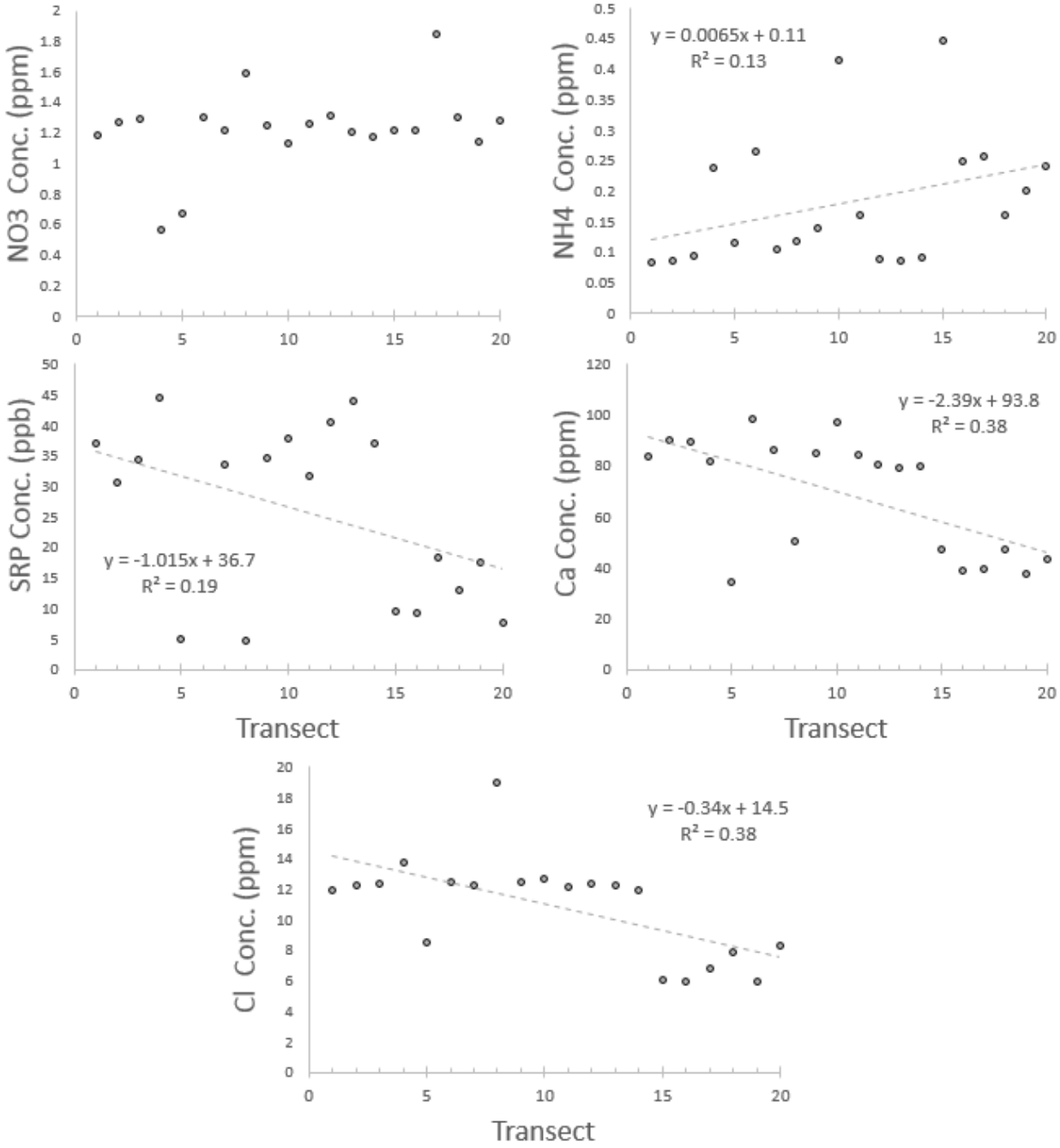

Figure 6.16. Concentrations of key analytes in the thalweg sample along the length of the Silver River. All fitted lines are significant at $p < 0.001$. The nitrate trend was not significant despite repeated measures (Hensley et al. 2014) showing strong depletion trends along the length of the river. Likely this is due to sampling on different days for this relatively low variance analyte.

We also explored whether thalweg samples differed from channel margin samples. We defined the lateral ratio as the ratio of the thalweg samples mean to the channel margin samples mean; values above 1 indicate that thalweg samples are enriched compared to channel margin samples. Results suggest that the thalweg and the channel margin samples are very similar, with modest depletion of NO_3-N in channel margins, and modest enrichment of SRP, NH_4, Ca and Cl.

Despite significant spatial variation, there were no obvious longitudinal trends in this ratio (Figure 6.17).

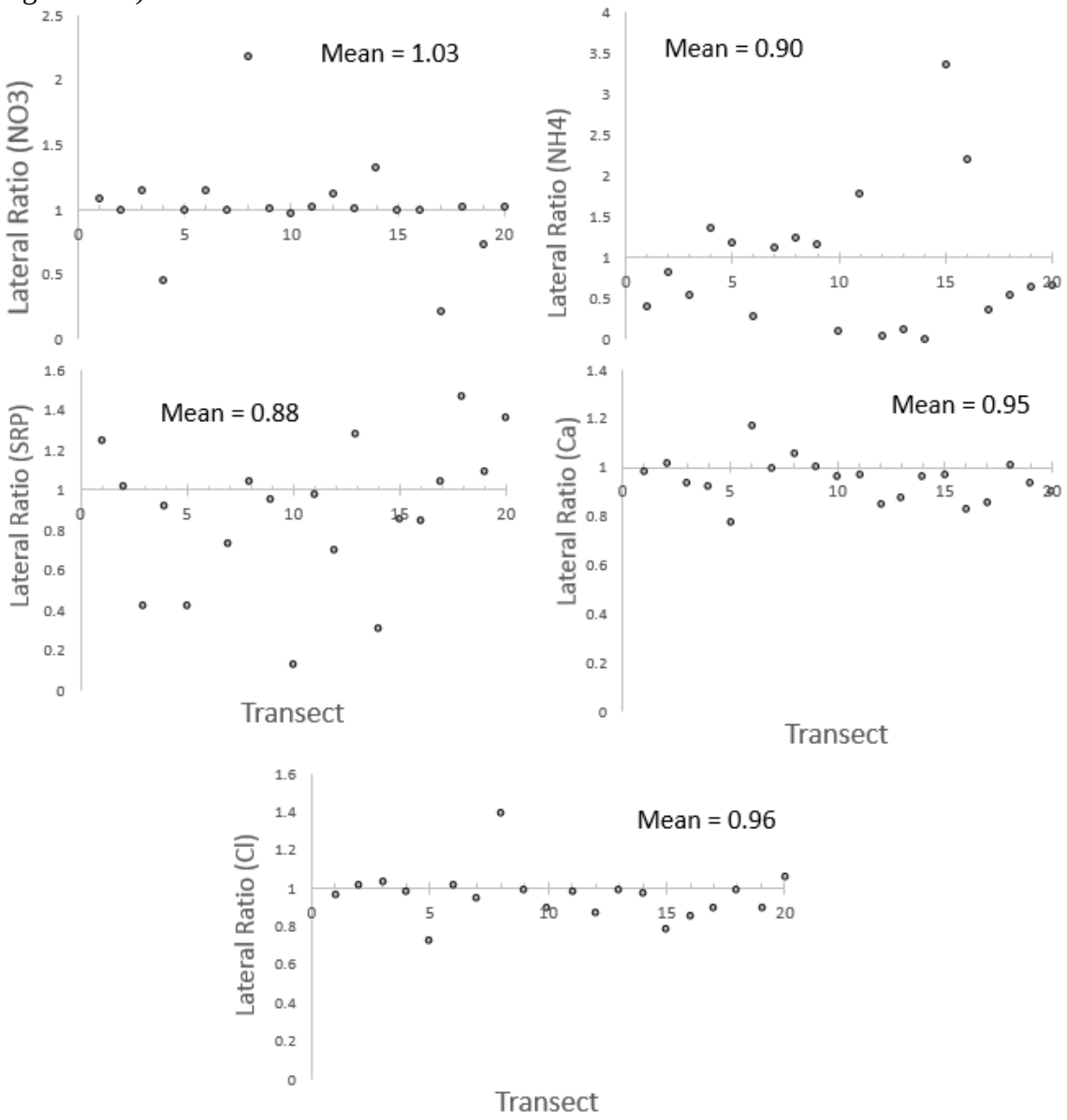

Figure 6.17. Ratios of concentrations for key analytes in the thalweg sample vs. the channel margin samples along the length of the Silver River. Values greater than 1 indicate a solute that is enriched in the thalweg compared with the channel margins, while values less than 1 indicate solutes that are depleted in the thalweg. Mean values for the entire river are shown in each graph, suggesting NO_3-N is slightly enriched in the thalweg vis-à-vis the channel margins, while all other solutes are depleted in the thalweg.

Finally, we evaluate the same ratio, but this time comparing the thalweg samples (the actively mixed part of the river) with the porewater samples for each transect. These results (Figure 6.18) illustrated much more significant variation, with massive depletion of nitrate in the shallow

porewaters vis-à-vis the thalweg, and similarly significant enrichment of SRP and NH_4 in the porewaters. Modest depletion of Ca and Cl in porewaters may suggest other sources of water.

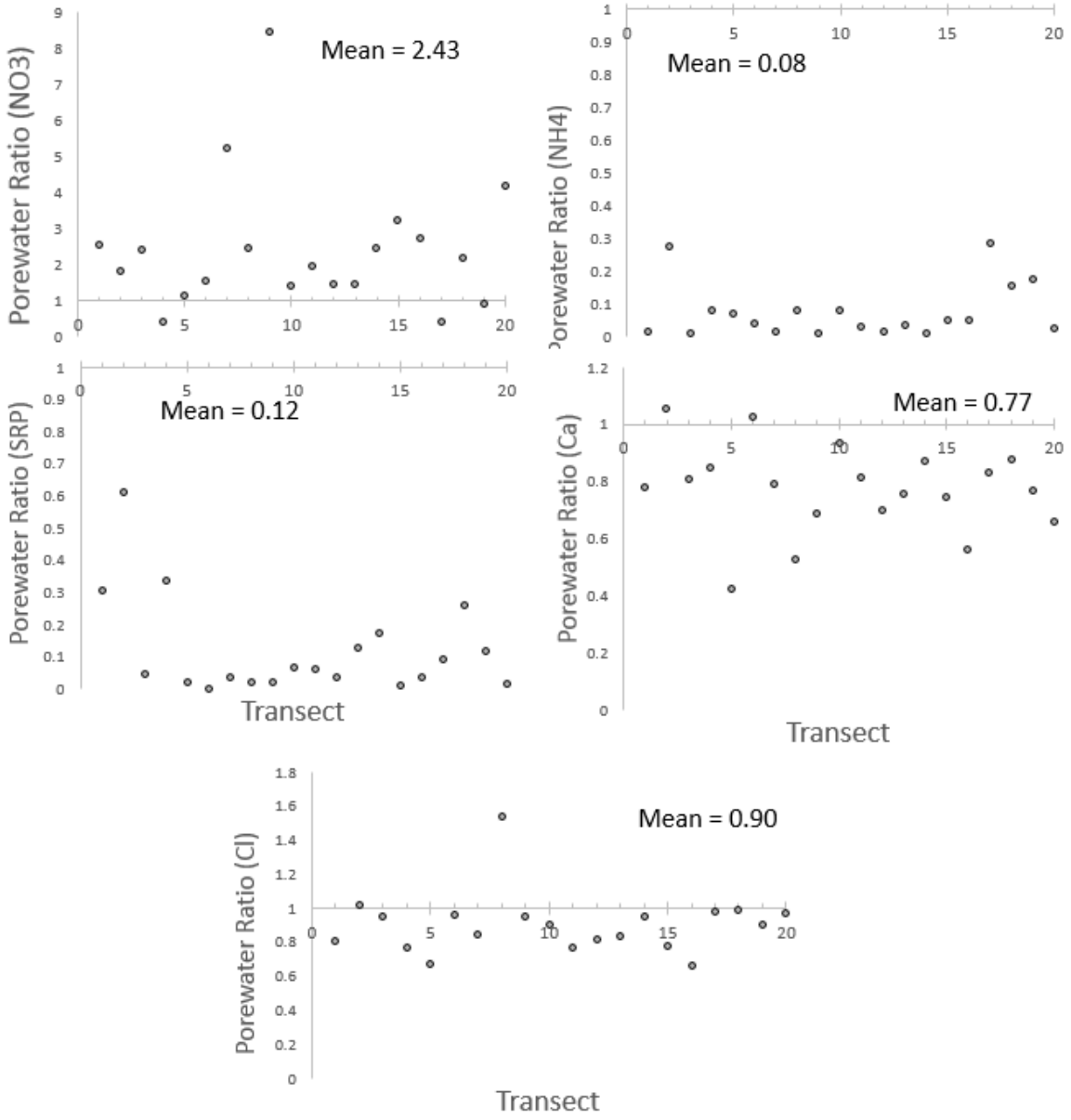

Figure 6.18. Ratios of concentrations for key analytes in the thalweg sample vs. the porewater samples along the length of the Silver River (later. Values greater than 1 indicate a solute that is enriched in the thalweg compared with the porewaters, while values less than 1 indicate solutes that are depleted in the thalweg. Mean values for the entire river are shown in each graph, suggesting NO_3-N is dramatically enriched in the thalweg vis-à-vis the porewaters, while all other solutes are depleted in the thalweg, some greatly so (e.g., NH_4 and SRP).

While NO_3-N and SRP concentrations were not significantly correlated to each other within the water column or porewater (p-value = 0.745 and 0.105, respectively), NH_4-N and SRP concentrations where significantly correlated. Specifically, the porewater SRP and NH_4-N

concentrations were more significantly correlated to each other (R^2 = 0.532; p-value < 0.001) than in the water column (R^2 = 0.153; p-value = <0.001) (Figure 6.19).

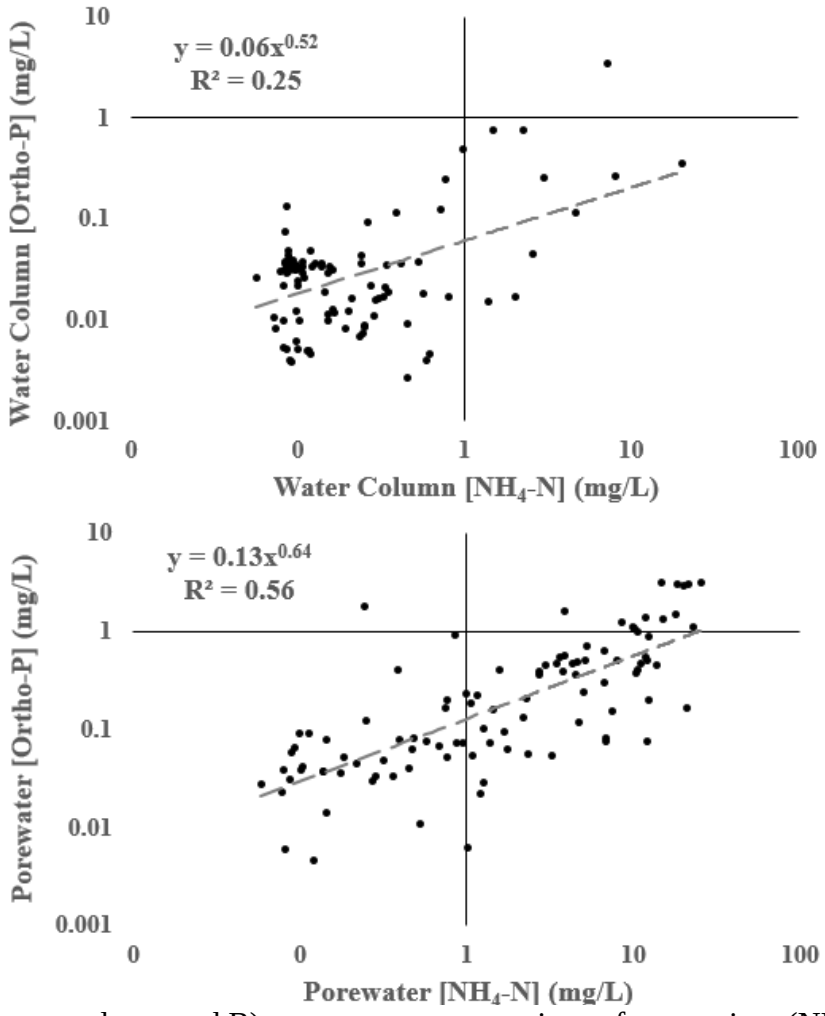

Figure 6.19. A) water column and B) porewater concentrations of ammonium (NH4) and orthophosphate (SRP) showing the range of concentrations, and the covariance patterns, suggestive of regions of significant benthic porewater influences on river water. Note (Figure 6.20) that high concentrations are samples obtained near channel margins in low advection zones.

Finally, we evaluated whether systematic trends existed for water chemistry across transects (Figure 6.20). We note no trend for chloride, a modest center sample enrichment of NO_3-N compared with the channel margins, and massive enrichment of PO_4 and NH_4 in the channel margins compared with the center samples.

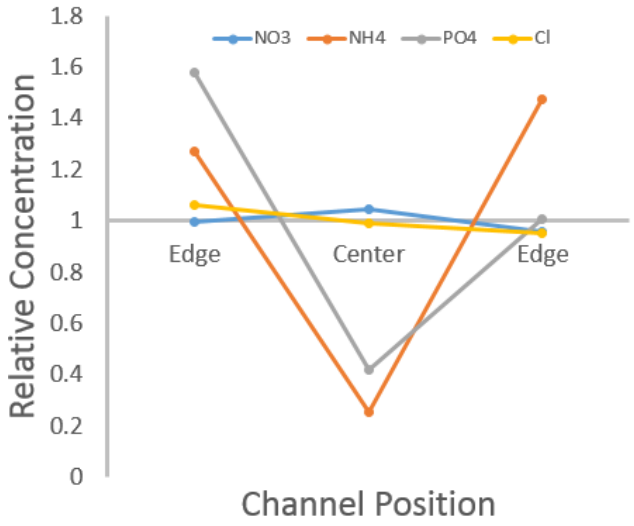

Figure 6.20. Summary of relative water concentrations across each transect, illustrating strong spatial heterogeneity driven by advection rates (high in the center, low at the edges). The clearest trends are for SRP and NH_4, which are significantly enriched in the channel margins, presumably influenced by the porewaters. In the channel center, these concentrations are markedly lower on average (ca. 4-8 times lower), while nitrate concentrations are slightly higher (also consistent with spatial patterns in retention of that solute).

6.5.2.3 Soil Chemistry

We measured a suite of informative analytes in the solid phase of the Silver River sediments, with samples from each location on each of the 20 transects. We observed significant variation in chroma (Figure 6.21) and field-based measures of texture, and these were confirmed with significant variation in soil chemical properties (Figure 6.22).

Figure 6.21. Soil samples collected across one transect prior to drying as well as dried samples from four transects (oriented by column) prior to LOI determination of organic matter content.

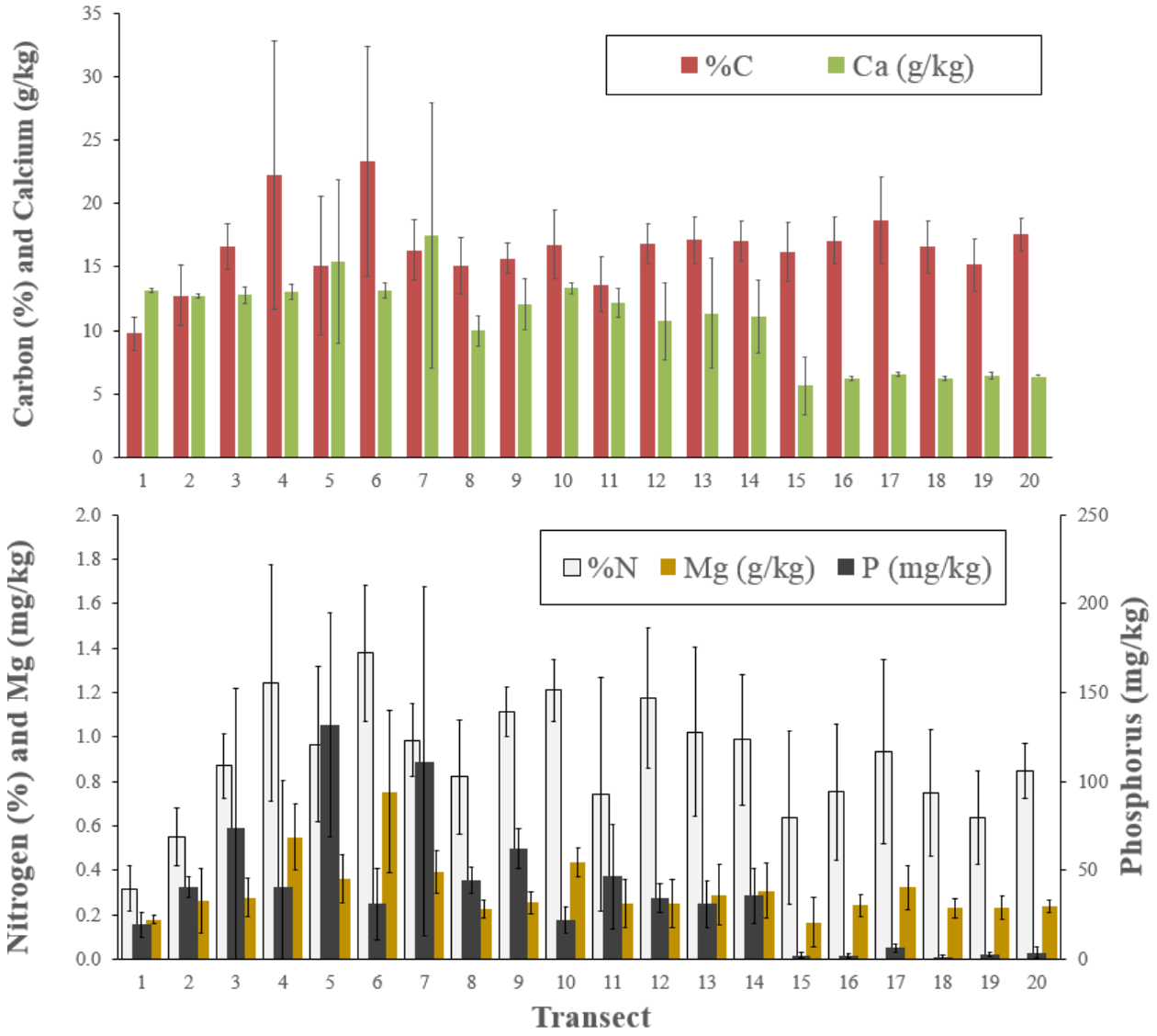

Figure 6.22. Average soil content by analyte by transect. Error bars represent standard deviation.

Of particular note was the strong longitudinal enrichment of sediment C (roughly doubling along the length of the river), and the attendant decline in Ca (declining by 50% along the length of the river). While longitudinal trends in N, Mg and P were less obvious, there were interesting spatial patterns, with the highest concentrations of P and Mg occurring from transect 5 to 7, and declining thereafter. This is coincident with the decline in water column P as well (Figure 6.16). While sediment N content was relatively constant after transect 4, the upper most river had very low N concentrations, likely indicating that fixed N is exported downstream rather than accumulating as sediment storage in the upper river.

Soil % organic matter (% loss on ignition) was explored as a potential explanatory factor in both vegetation and sediment and water chemistry variation. While the abundance of sediment organic matter was generally not a useful predictor of vegetation dynamics, there were interesting patterns present along the river. Specifically, OM was highest in the vicinity of the

confluence with Half Mile Creek, declining thereafter towards the Ocklawaha River (Figure 6.23).

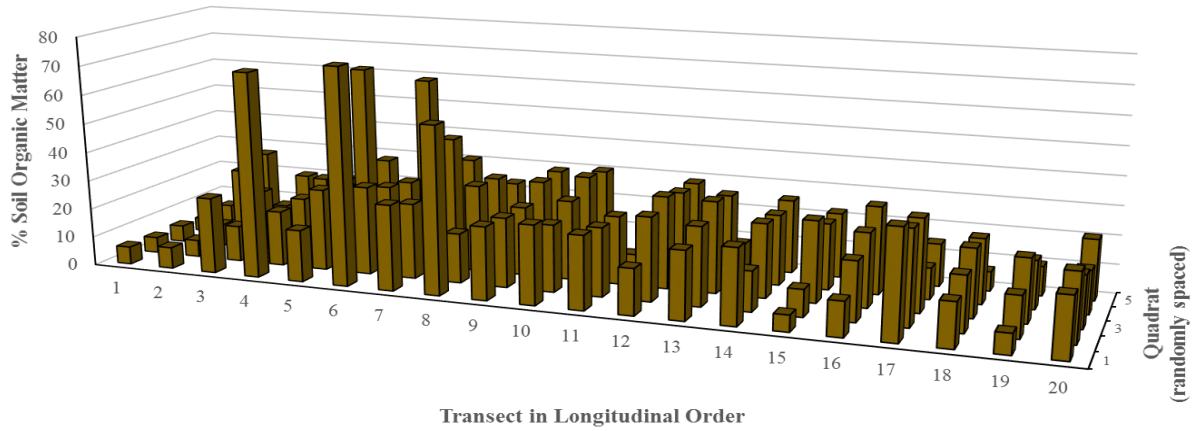

Figure 6.23. Percent (%) soil organic matter was greatest along the upper and middle transects.

Some interesting covariance patterns were observed in the sediment chemistry and water chemistry. Most notably, there was a strong correlation between sediment Ca concentration and porewater Ca concentration (Figure 6.24), suggesting the sediment actively affect the porewater profile. There was an even strong association between soil Ca and the water column, which, while slightly surprising, suggests that water exchange between the advective zone of the river and the porewaters and sediments is sufficient in magnitude to affect the water column chemical composition. Not unsurprisingly, soil C and soil N were strongly correlated (Figure 6.25), suggesting that the vast majority of sediment N is as stored organic matter, and not as a mineral solutes. Finally, we observed a significant correlation found between soil Ca and P content (R^2 = 0.314; p-value < 0. 001) (Figure 6.26)

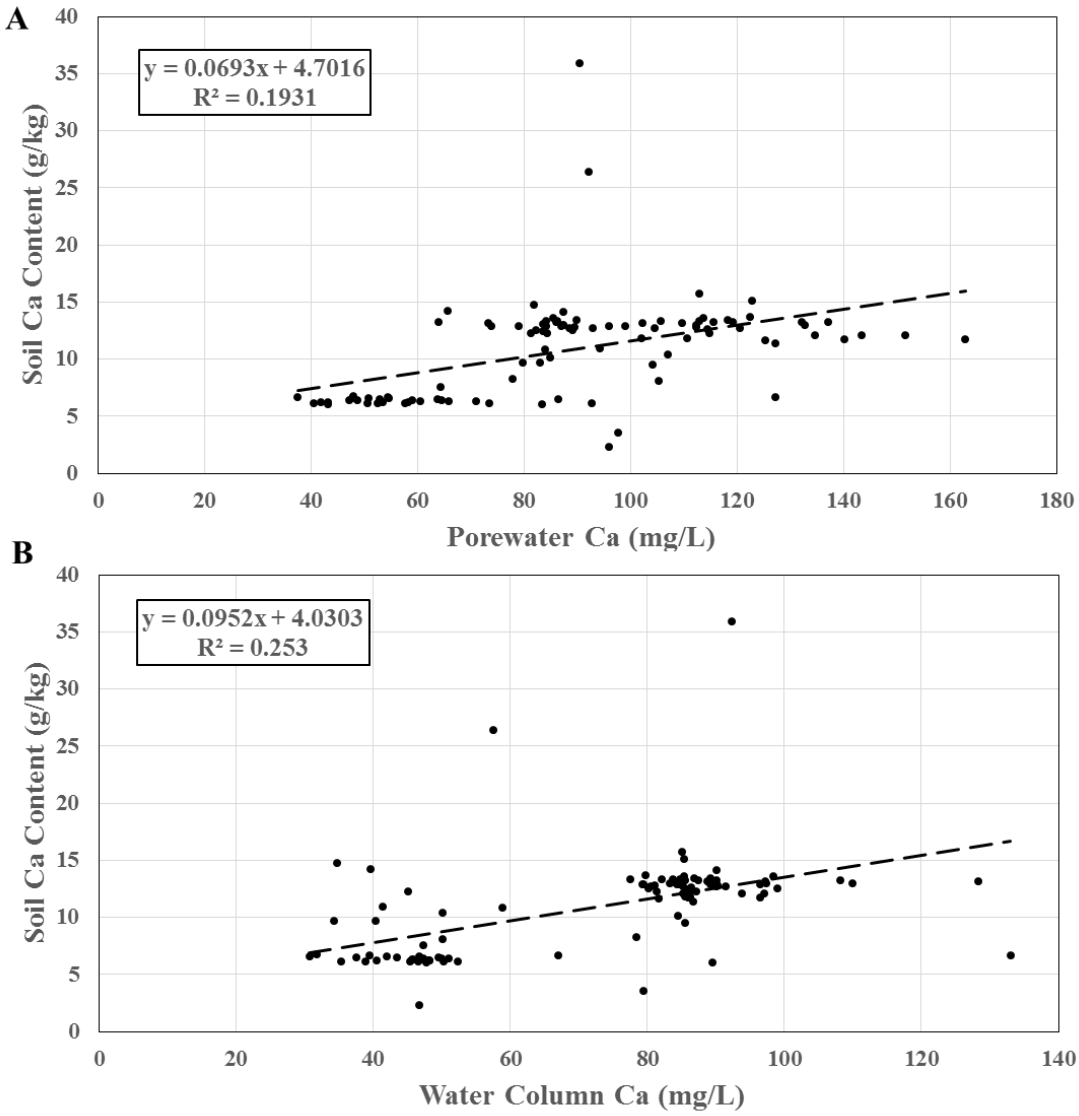

Figure 6.24. Variation in soil calcium content (Ca; g kg^{-1}) was explained by both a) porewater Ca concentrations (mg/L) and b) water column Ca concentrations (mg L^{-1}).

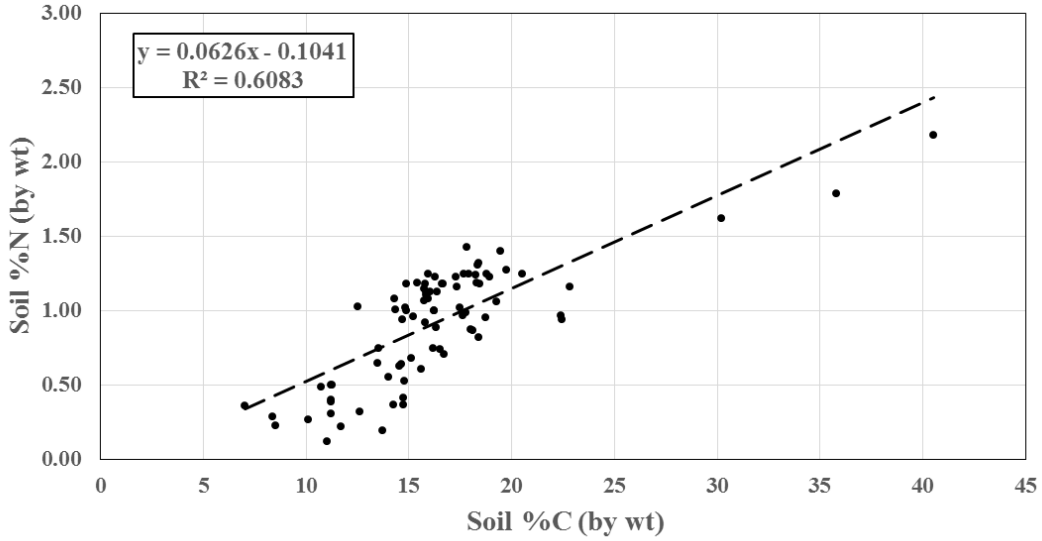

Figure 6.25. Soil %C and %N were significantly correlated to each other. This association was strongly significant ($p < 0.001$).

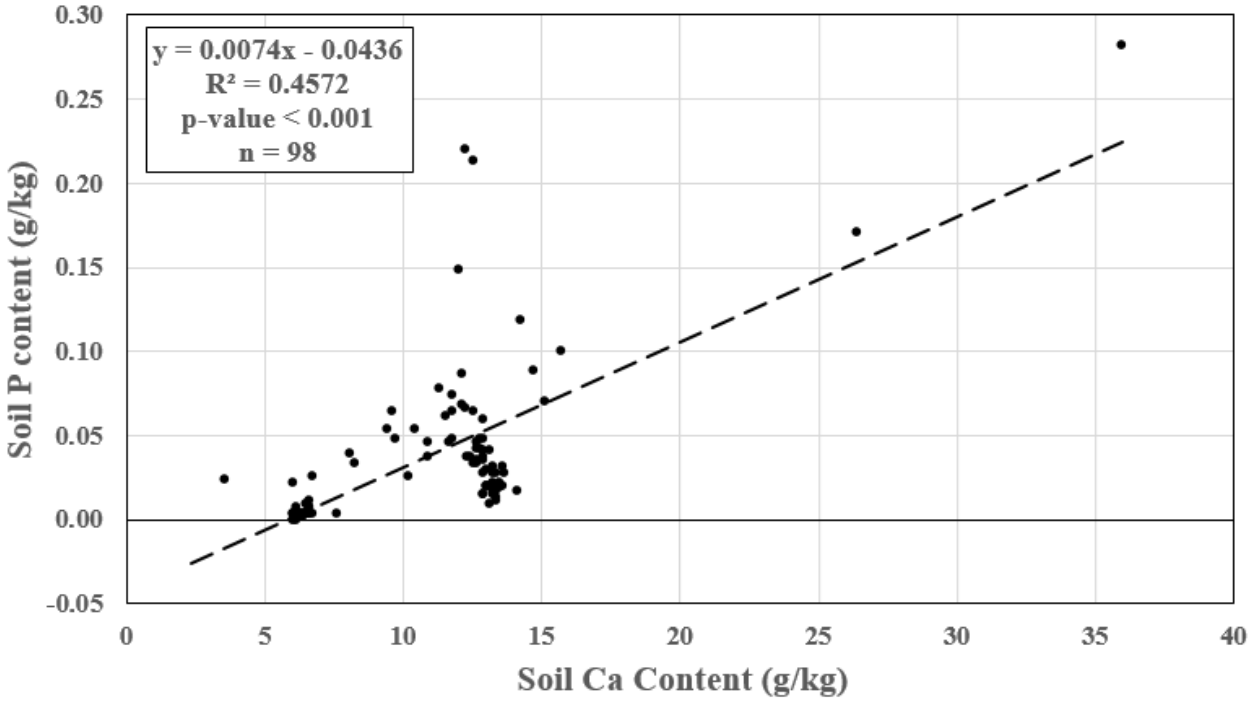

Figure 6.26. Soil Ca and P content were significantly correlated to each other.

6.5.3 Soil Particle Size Distribution

The distribution of soil particle sizes across the upstream transects at Silver showed an initial decrease in percent sand and increase in percent silt and clay (Figure 6.27). Percent clay was highest (15-25%) in the middle transects (transects 5-9), located between the 0.7 Mile Mark and

just below the county dock. The particle size analysis in the last few transects showed similarity in sand and silt distributions (40-50%) and clay remained at approximately 10%.

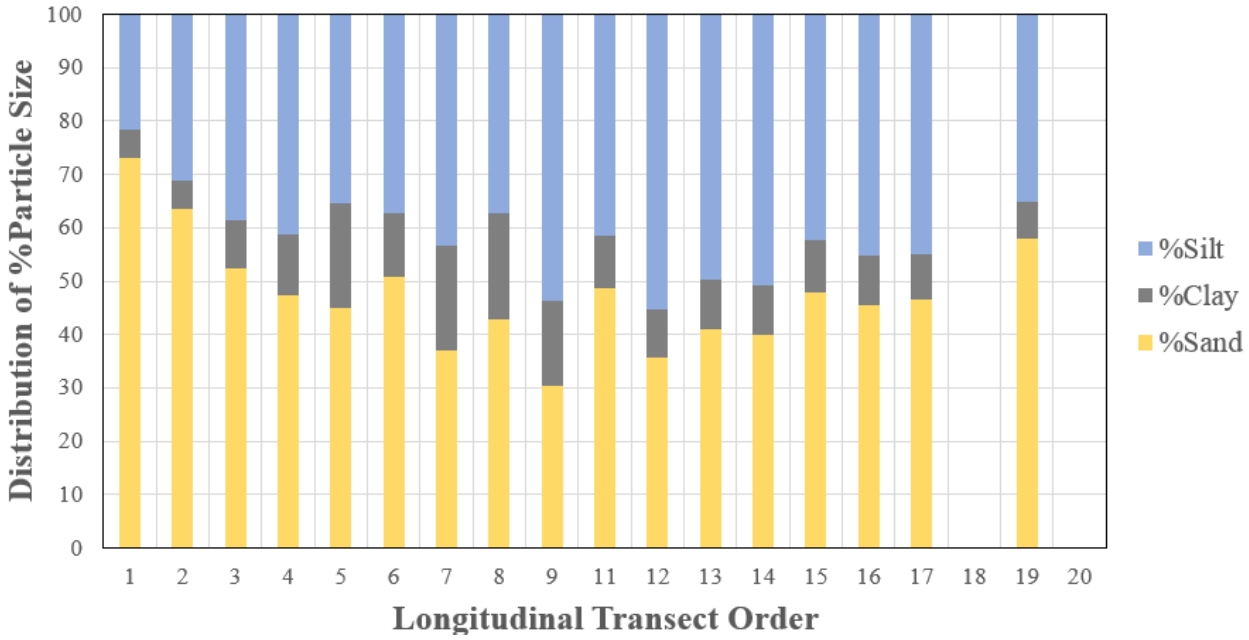

Figure 6.27. Particle size analysis was completed on the upstream transects at Silver and mean values within transects showed and initial decrease in % sand, initial increase in % silt and clay, and stabilization in the last few transects. Note that texture analysis for 2 transects (18 and20) was not yet completed at the time of this report.

The relationships between the soil particle size distributions and other soil and water parameters were analyzed. No significant relationships were found between percent sand or silt and other water and soil parameters. A weak but significant negative relationship (p-value = 0.025, R^2 = 0.0823) was seen in percent clay and percent organic matter (Figure 6.28). Percent clay did explain approximately 19% of the variation in soil phosphorus (p-value < 0.001, R^2 = 0.1937; Figure 6.29) and approximately 12% of variation in soil calcium content (p-value = 0. 006, R^2 = 0.120; Figure 6.30).

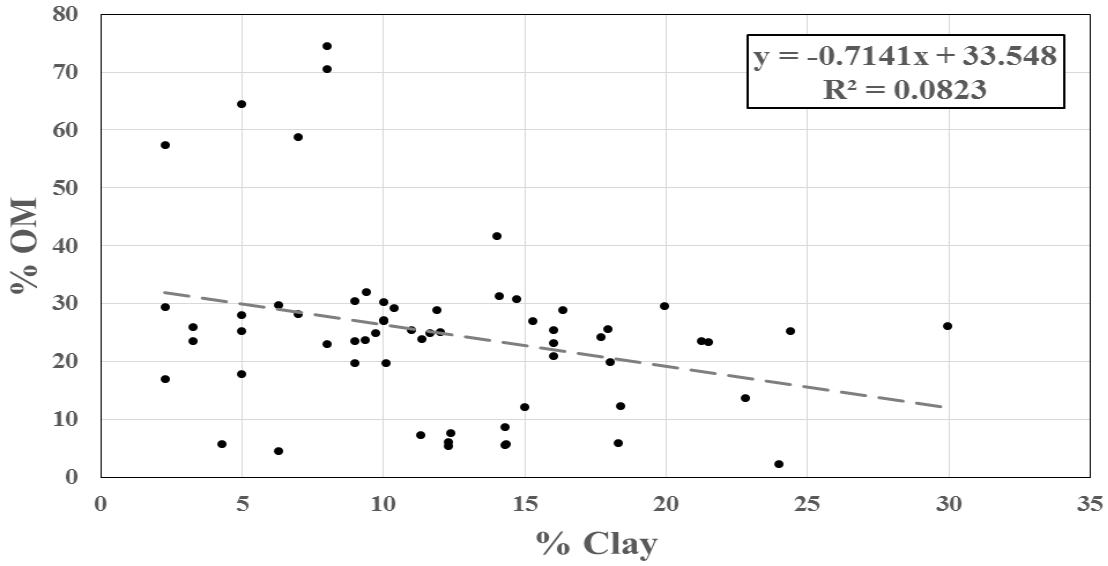

Figure 6.28. Percent clay and percent organic matter were found to have a weak but significant negative relationship (p-value = 0.0249).

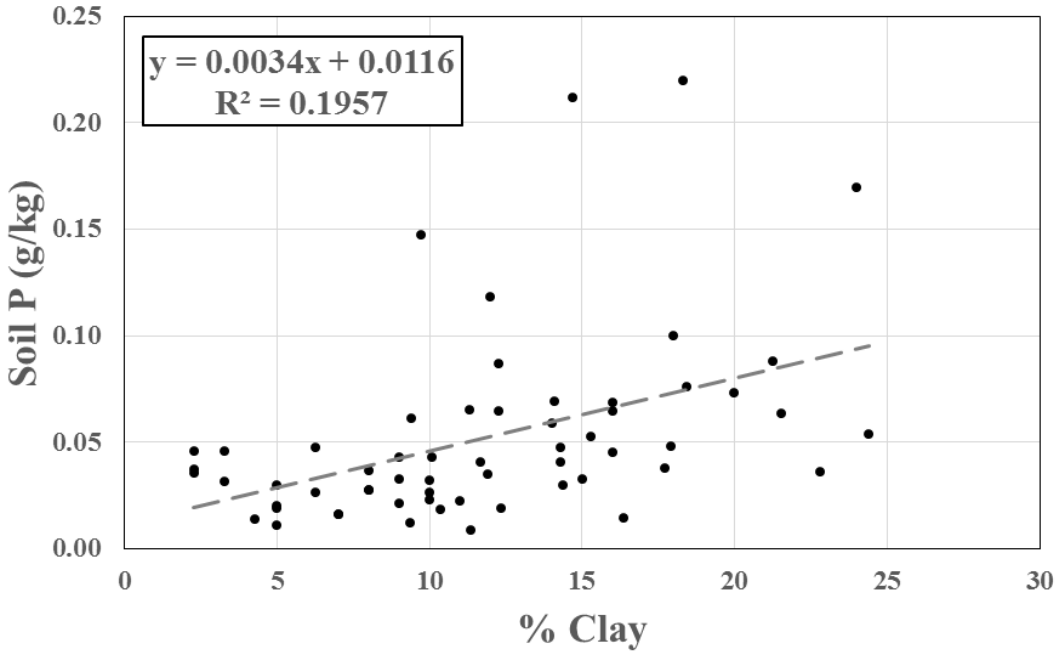

Figure 6.29. Percent clay explained approximately 19% of the variation in soil phosphorus content (g kg^{-1}) over the first 14 transects surveyed at Silver River.

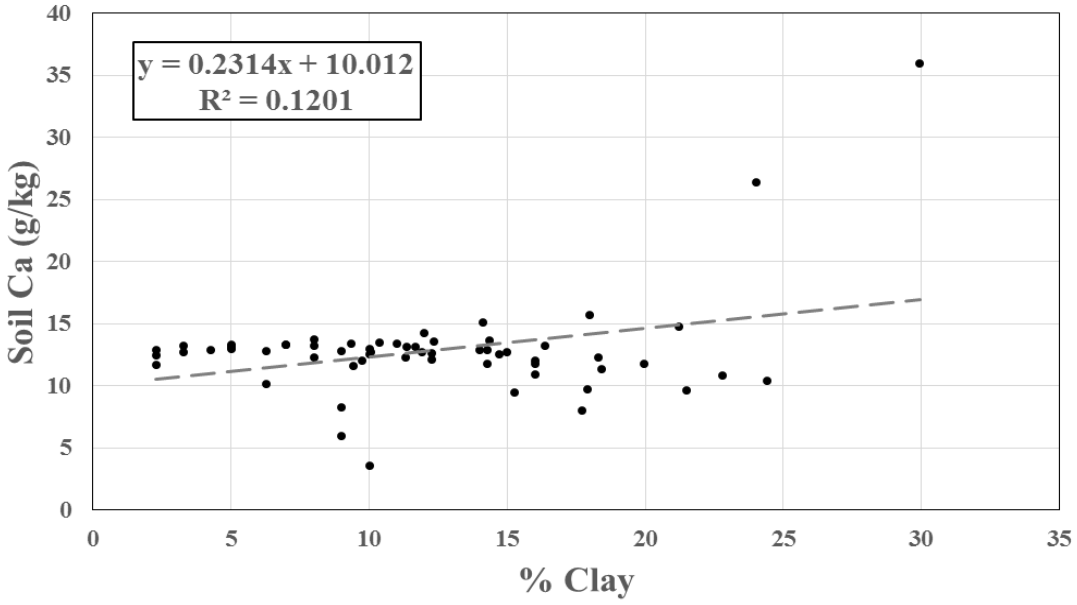

Figure 6.30. Percent clay explained approximately 12% of the variation in soil calcium content (g kg^{-1}) over the first 14 transects surveyed at Silver River.

6.5.3.1 Physical and Chemical Controls on SAV and Algal Abundance

The inventory of benthic conditions on Silver River was principally done to explore spatial covariation patterns. Of particular interest was correlative evidence on the various controls on algal and SAV cover, ranging from physical controls (canopy cover, light) to chemical controls in the sediment, porewater and surface water. Below we summarize the preliminary results of that effort, focusing on both pairwise correlation analysis, and multivariate predictions.

6.5.3.1.1 Physical Controls

The physical controls on algal and SAV cover include canopy cover (%), water depth (m), flow velocity (m/s) and river position (longitudinal transect order). Table 6.4 summarizes the pairwise linear correlations between physical variables. The results suggest that SAV cover and canopy cover significantly increase with distance downstream, while algal cover and water depth significantly decrease. Significant physical controls on SAV cover also include canopy cover (significant negative association) and algal cover (significant negative association), while controls on algal cover also include velocity (significant negative association) and SAV.

The pairwise association between algal cover and velocity (Figure 6.31) indicates the limited explanatory power of that variable alone, but does indicate a promising covariate for more complex predictive models.

Table 6.4. Correlation matrix for physical controls on autotroph cover. Bolded correlations are significant at $p < 0.05$.

	Mean	SD	River Position (Transect)	% Canopy Cover	Water depth (m)	Velocity (m/s)	SAV Cover
River Position (transect)	na	na					
Canopy Cover	37.02	24.96	**0.41**				
Water depth (m)	1.26	0.52	**-0.57**	**-0.49**			
Velocity (m s^{-1})	0.20	0.09	0.11	-0.09	**0.29**		
SAV Cover Class	4.44	1.03	**0.20**	**-0.21**	-0.04	0.16	
Algal Cover Class	3.09	1.61	**-0.40**	-0.17	0.09	**-0.38**	**-0.36**

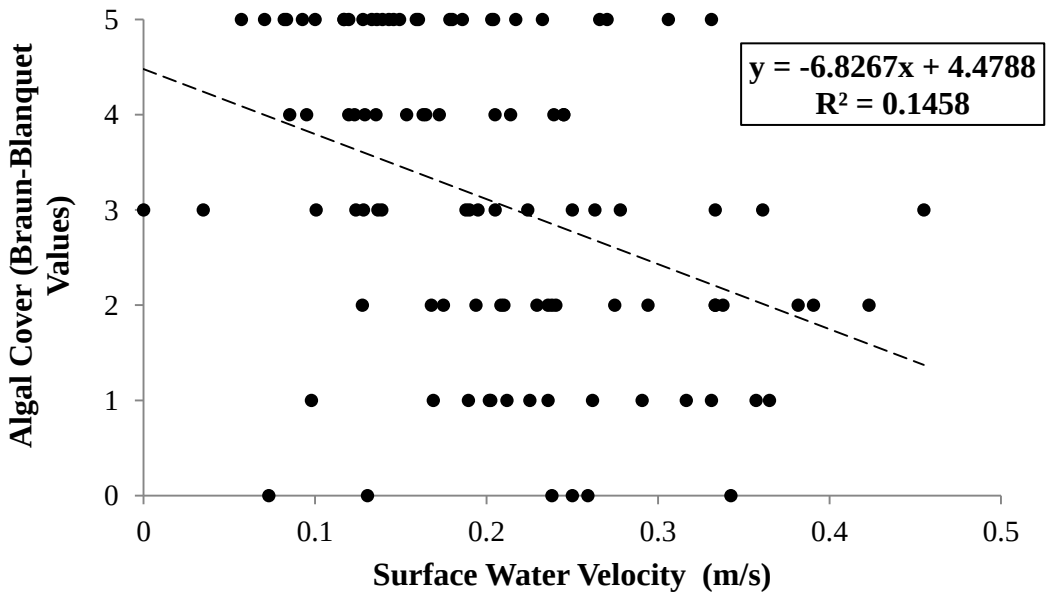

Figure 6.31. Surface water velocity (m s^{-1}) explained some of the variation seen in algae cover (Braun-Blanquet values). The relationship is statistically significant ($p < 0.001$), but suggests that over 80% of the variation in algal cover is not explained by surface velocity variation.

A multivariate model of algal cover based on the 4 physical variables and SAV cover yielded a model with an R^2 of 0.28, and with only two significant predictors: river position (slope =0.36, $p = 0.003$) and velocity (slope = -0.31, $p = 0.001$). That is, the SAV-algal cover association was no long significant when conditioned on other variables, suggesting that the association may arise from covariance with river position or velocity, and not a direct competitive interaction.

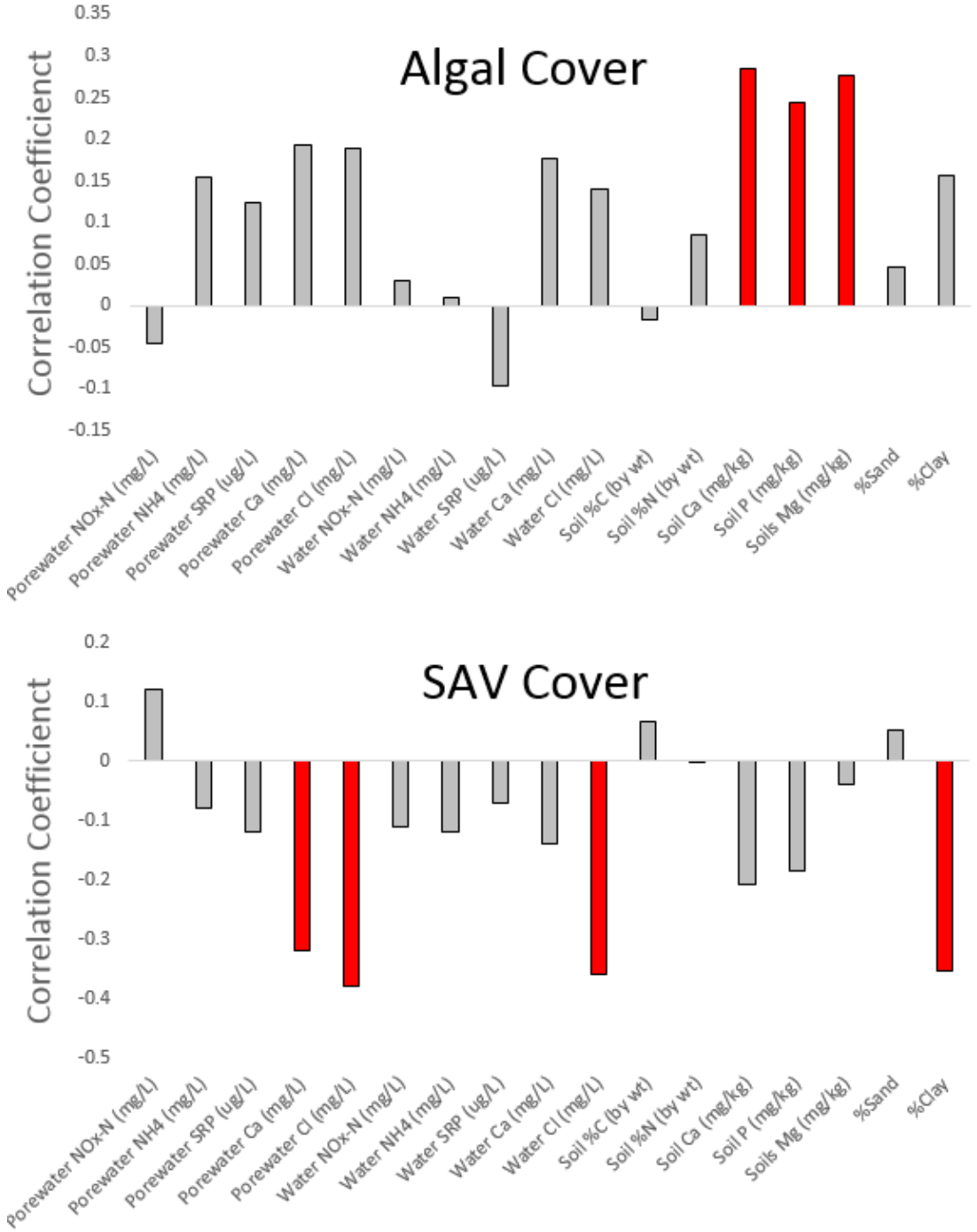

Figure 6.32. Summary of patterns of covariance between solutes in the water column, porewater and some of the soil attributes and algal cover (above) or SAV cover (below). Correlations (y-axis) that are statistically significant are denoted in red.

6.5.3.1.2 Water Chemistry Controls

Despite evidence for significant spatial variation in solutes, both in the porewater and the water column, we observed no significant associations between these chemical attributes and algal cover (summarized in Figure 6.32). Indeed, the main water column drivers (SRP, NH_4, NO_3-N) all had linear correlation coefficients that suggest that these analytes explain less than 2% of the

variation in algal cover. Further evidence on Fe and Mn, which were uniformly below detection, and therefore sufficiently scarce to merit attention as limiting nutrients, is required.

Table 6.5. Summary of correlation coefficients between water chemistry and both SAV and algal cover. Shown are correlations for both water column chemistry and porewater chemistry. Note that while Fe concentrations were analyzed in both water column and porewater samples, all were returned below detection limit. Further attention to analytical precision will allow future analysis to consider this potentially significant analyte. Note that bolded correlations are significant at $p < 0.05$. Variables with a superscript "A" were log-transformed prior to analysis to meet assumptions of normality.

	Mean	SD	Algal Cover	SAV Cover	Porewater NOx-N (mg/L)	Porewater NH4 (mg/L)	Porewater SRP (ug/L)	Porewater Ca (mg/L)	Porewater Cl (mg/L)	Water NOx-N (mg/L)	Water NH4 (mg/L)	Water SRP (ug/L)	Water Ca (mg/L)
Algal Cover	3.09	1.61											
SAV Cover	4.40	1.03	**-0.36**										
Porewater NOx-N (mg L^{-1})^A	0.86	1.34	-0.04	0.12									
Porewater NH4 (mg L^{-1}) ^{A}	4.72	6.05	0.15	-0.08	**-0.25**								
Porewater SRP (µg L^{-1}) ^{A}	466	729	0.12	-0.12	-0.16	**0.73**							
Porewater Ca (mg L^{-1})	88.5	27.9	0.19	**-0.32**	**-0.21**	**0.47**	**0.57**						
Porewater Cl (mg L^{-1})	12.1	4.13	0.20	**-0.38**	-0.14	0.17	**0.24**	**0.78**					
Water NOx-N (mg L^{-1}) ^{A}	1.45	2.40	0.03	-0.11	0.11	-0.07	-0.04	**-0.22**	-0.19				
Water NH4 (mg L^{-1}) ^{A}	0.70	2.28	0.01	-0.12	0.01	**0.30**	0.14	0.06	0.04	-0.05			
Water SRP (µg L^{-1}) ^{A}	93.5	364	-0.10	-0.07	-0.02	0.19	**0.41**	**0.22**	0.19	-0.03	**0.40**		
Water Ca (mg L^{-1})	71.5	23.3	0.18	-0.14	-0.14	0.18	**0.27**	**0.67**	**0.61**	-0.04	**0.22**	**0.42**	
Water Cl (mg L^{-1})	11.1	3.36	0.24	**-0.36**	-0.14	-0.01	0.13	**0.56**	**0.60**	-0.03	0.12	**0.20**	**0.64**

A – Variables log-transformed prior to correlation analysis

The results from the pairwise correlation analysis (Table 6.5) suggest that no aspect of water chemistry in the porewater or water column can provide useful predictive power for algal cover. We further performed a multiple regression analysis using all of the water chemical variables (except Fe, which was below detection at all locations). That model removed all variables from analysis except SRP, which exerted a significant negative effect on algal cover (slope = -0.28, $p = 0.04$); notably, concentrations of NO_3-N in the porewater ($p = 0.84$) and water column ($p = 0.69$) were not significant predictors of algal cover. The overall model R^2 was 0.13, suggesting that the conjoined explanatory power of water chemistry on algal cover is low. Furthermore, we are aware of no mechanism via which P concentrations can inhibit algal cover.

The pairwise correlations for SAV yielded more significant associations (Table 6.5), with porewater calcium and chloride, as well as water column chloride concentrations exerting significant pairwise effects (negative associations for all three variables). A multivariate model

of SAV cover given the suite of chemical analytes yielded a relatively strong model (R^2= 0.29), but with two different significant predictors of cover than were expected from the pairwise analysis: water column nitrate (slope = -0.09, p = 0.02) and water column calcium (slope = 0.02, p = 0.004). These results suggest that SAV are inhibited by high nitrate, and enhanced by high Ca concentrations. It is particularly striking that chloride was not significant (though p = 0.05 for water column Cl) given the strong pairwise association. We note that none of the porewater chemical properties were significant predictors, providing limited support for hypothesis about SAV decline that invoke porewater enrichment of ammonium. Indeed, while porewater NH_4 and NO_3-N concentrations were not significant, their slopes were both positive.

6.5.3.1.3 Soil Chemistry and Texture Controls

Despite the absence of significant predictors of algal cover from porewater and water column chemical properties, we explored covariance patterns of SAV and algae with soil chemical properties, including texture distributions (i.e., %sand, %clay). The results of a pairwise correlation analysis (Table 6.6) are striking, in that two soil chemical variables apparently inhibit SAV cover (soil Ca and %clay), while three variables appear to enhance algal cover (soil Ca, soil P and soil Mg). Moreover, the correlations between variables suggests that there are numerous associations between sediment quality and texture (e.g., %clay impacts soil N, Ca, P and Mg). Since there are strong spatial gradients in soil texture (Figure 6.27), this merits consideration for inclusion in an overall model of SAV and algal abundance.

Table 6.6. Summary of correlation coefficients between soil chemistry and both SAV and algal cover. Bolded correlations are significant at p < 0.05. Note that some differences in mean SAV and algal cover values between this analysis and previous analyses arises because texture results were available for only 18 of 20 transects.

	Mean	SD	SAV Cover	Algal Cover	Soil %C	Soil %N	Soil Ca (mg/kg)	Soil P (mg/kg)	Soils Mg (mg/kg)	%Sand
SAV Cover	4.38	1.07								
Algal Cover	3.17	1.63	**-0.36**							
Soil %C	16.46	4.71	0.07	-0.02						
Soil %N	0.91	0.38	0.00	0.09	**0.77**					
Soil Ca (g kg^{-1})	11.36	4.29	**-0.21**	**0.29**	-0.09	0.08				
Soil P (mg kg^{-1})	41.08	48.47	-0.19	**0.24**	0.13	**0.22**	**0.66**			
Soils Mg (mg kg^{-1})	323.00	177.92	-0.04	**0.28**	**0.69**	**0.61**	**0.36**	**0.23**		
%Sand	46.68	15.32	0.05	0.05	-0.09	**-0.52**	-0.08	-0.03	-0.04	
%Clay	11.15	5.27	**-0.35**	0.16	0.08	**0.31**	**0.40**	**0.58**	**0.21**	**-0.52**

As with other controls, we performed a multivariate regression to assess to conjoined explanatory power of soil properties. Overall, the explanatory power for SAV cover was modest (R^2 = 0.18), with only %clay (slope = -0.12, p < 0.001) emerging as a significant predictor, further suggesting that the correlation of SAV with Ca arises largely because Ca and % clay are

correlated. The fact that dense sediments (i.e., high clay content) inhibits SAV comports with observations of SAV declines in other settings (e.g., Rainbow River) where clay content varies dramatically across the river. The model to predict algal cover yielded two significant predictors in a model that explained 21% of the variation (i.e., $R^2 = 0.21$): soil %C was a significant negative predictor of algal cover (slope = -0.21, p = 0.007), while soil Mg was a positive predictor (slope = 0.005, p = 0.009). All other predictors were not significant. These results are striking in that they depart so dramatically from the pairwise correlations, especially with regard to soil C content. Further exploration of these associations is clearly warranted.

Finally, we combined all of the predictor variables into a stepwise regression analysis where variables were omitted where they failed to meet significance criteria. Starting with all of the physical, water chemical and soil chemical properties, we arrived at overall models of SAV and algal cover. The algal model explains over 30% of the variation in algal cover ($R^2 = 0.30$) based on three selected variables: soil %C (slope = -0.15, $p < 0.001$), soil Mg (slope = 0.005, $p < 0.001$) and water velocity (slope = -0.69, $p < 0.001$). This suggests that the dominant spatial controls on algal density are sediment properties, the mechanisms of action for which are poorly understood, and water velocity. The SAV model has similar explanatory power ($R^2 = 0.32$), and also selected three variables: %clay (slope = -0.06, p = 0.001), % canopy cover (slope -0.014, $p < 0.001$) and porewater chloride concentrations (slope = -0.099, $p < 0.001$). The impacts of clay content and canopy cover would appear relatively clear (rooting inhibition for the former, light limitation for the latter). The mechanism of the strong inhibitory effect of chloride concentrations is less obvious. We note that chloride concentrations were generally relatively low (mean = 12.1 mg L^{-1}) and did not vary substantially across the river (SD = 4.13 mg L^{-1}). It may be that chloride concentrations act as a proxy for other variables, such as DO depletion or Fe concentrations, because direct effects seem unlikely given observed variation. It is also notable that there is a strong decline in chloride concentrations at the downstream end of the river (near the confluence with the Ocklawaha; (Figure 6.16), possibly suggesting mixing waters or diluted porewaters from interactions with the softer water Ocklawaha flow.

6.6 NUTRIENT LIMITATION ASSAYS – METABOLISM AND NUTRIENT DEPLETION

Nutrient concentration is widely invoked as the dominant control on autotroph production in aquatic systems despite increasing evidence that enrichment effects in lotic systems differ from those in lakes (Biggs and Close 1999; Biggs 2000, Dodds et al. 2002; Hilton et al. 2006; King et al. 2014). In flowing water systems, nutrient resupply from upstream mean flux may be more important than concentration in describing nutrient availability to autotrophs (Newbold et al. 1982). To understand the impacts of nutrient enrichment on primary producers requires a description of the kinetics of nutrient assimilation; that is, ***how does nutrient uptake vary with changing supply?*** A variety of studies have suggested that total nutrient retention (i.e., autotrophic uptake plus denitrification) in streams follows Michaelis-Menten (Earl et al. 2007, Covino et al. 2010) or efficiency loss (Mulholland et al. 2008; O'Brien et al. 2011; Hensley et al. 2014) kinetics where nutrient uptake declines with concentration as the system transitions from limitation by that nutrient to limitation by something else (e.g., light, another nutrient). Describing where a lotic system lies on the nutrient kinetic curve is important for understanding impacts of nutrient enrichment and also for setting functional thresholds of nutrient availability.

The underlying kinetics are important (Figure 6.33); where a system exhibits first order kinetics, metabolism and nutrient uptake scale linearly with concentration. Alternatively, where kinetics are zeroth order, uptake will be independent of concentration. Michaelis-Menton (and other similar formulations like the Droop Model) include both first and zeroth order phases of uptake kinetics depending on concentration. Kinetics informs expected primary producer shifts due to nutrient enrichment, which may range from greater biomass to changes in structure.

In addition to understanding how nutrient uptake changes with variation in concentration, we are fundamentally interested in how metabolism (primary production and respiration, GPP and ER) respond to nutrient enrichment. Metabolism is the integral of all ecological energy transformations, and thus represents the gold standard for assessing nutrient limitation. Methods such as periphytometers are useful in this regard, but cannot evaluate the reaction of the actual ecosystem, focusing instead on an artificial subset of the attached algae, separated from sediment nutrient sources. To assess evidence for nutrient limitation, which means, precisely, that nutrients limit primary production OR respiration, we will compare metabolic activity in benthic boxes (described below) is a full factorial experimental nutrient addition experiment focusing on the stimulatory effects of N, P and Fe (iron). The adoption of a control-treatment pair (i.e., no addition vs. some factorial addition of N, P and/or Fe) with replication will allow us to compare metabolic activity under similar benthic and insolation conditions. This will allow us to evaluate the overarching and central question of ***nutrient limitation of primary production in springs***.

Methods for documenting nutrient uptake kinetics in streams have been developed and refined in the last 5 years. Most focus on plateau additions, wherein the nutrient concentration in a stream is increased to a constant level, sustained for an extended period, and then retention rates estimated at the reach scale (Payn et al. 2005; Earl et al. 2007; O'Brien et al. 2011). More recently, applications of pulse injections have been shown to yield total uptake kinetics (i.e., the combination of assimilation and denitrification; Covino et al. 2010). This more recent approach

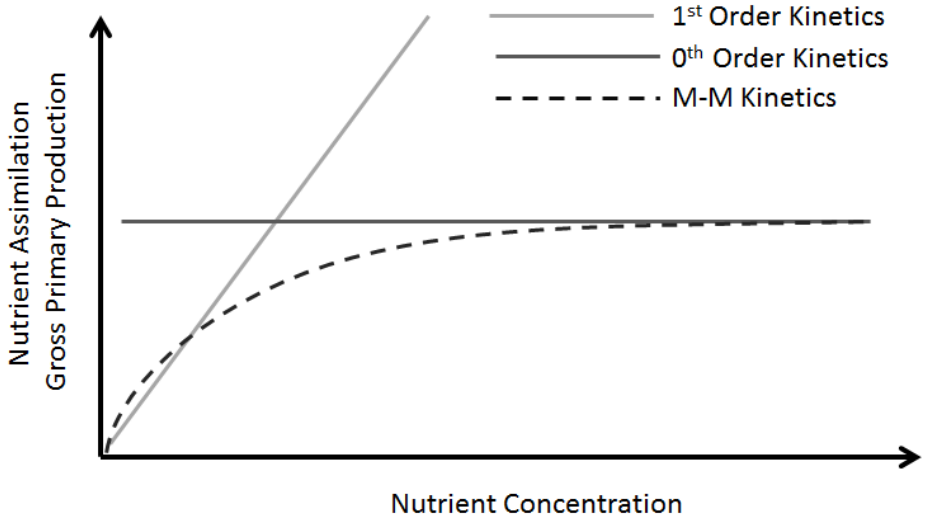

Figure 6.33. Nutrient uptake kinetics, showing assimilation vs. concentration for 3 different kinetic models.

has the advantage of being synoptic and with dramatically reduced logistics. However, all these methods depend on enrichment (with attendant problems; Mulholland et al. 2002) because the reverse (nutrient depletion) is not usually possible. We propose to make central use of a new method to explore nutrient uptake kinetics in spring-fed rivers. This allows us to combine enrichment approaches at reach and point scales with point scale depletion experiments to explore the entire kinetic curve. The approach, described in detail below, facilitates measures of nutrient retention and benthic metabolism; because it is an experimental approach, multiple ancillary factors can also be explored (e.g., shading, vegetation conditions, sediment properties, other nutrients). Most importantly, the approach roughly decomposes retention into autotrophic and heterotrophic pathways, which greatly enhances the utility for understanding primary producer responses to nutrients (Tank and Dodds 2003; Hall and Tank 2003).

The general method involves benthic chambers (clear polycarbonate) sealed into the sediments, which occlude flow and thus nutrient resupply due to flow. Chambers (0.4 x 0.4 m) constructed to date extend above the water column to allow normal gas exchange and light penetration, and are scaled to allow representative benthic communities to be sampled (e.g., algal mats, SAV beds, bare sediments) (Figure 6.34). Future versions for deployment in Silver River and Alexander Springs Creek may be sealed below the water surface for more discrete installations and to minimize reaeration. Regardless of chamber design, which will be evaluated during Year 1 of the project (Q1 in Year 1), the basic inferences from solute concentration dynamics will be the same. After installing each chamber, two sondes will be deployed in the water: 1) a DS5X Hydrolab to measure temperature, pH, dissolved oxygen and specific conductance and 2) a UV nitrate analyzer to measure nitrate (Satlantic SUNA; Heffernan and Cohen 2010).

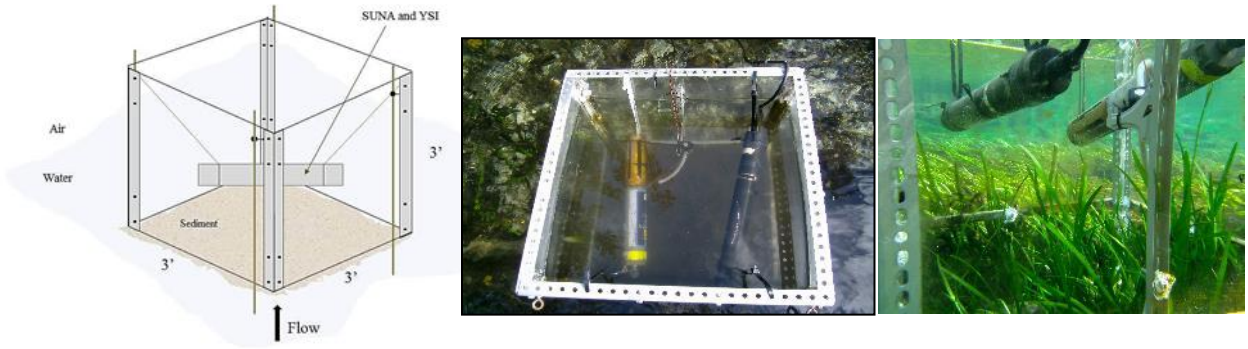

Figure 6.34. Construction of benthic metabolism chambers (left). Current versions of the chambers (right) are open to the atmosphere, but closed chambers will be explored.

In addition, a NaBr salt addition will be added to ensure that chemical changes in the water are not due to hydraulic exchange. The resulting data, concentrations over time, has profiles that look like those presented in Figure 6.4. In short, nitrate depletion with time indicates total uptake. Diel variation in nitrate retention allows us to separate denitrification from assimilation, while variation in the slope in response to changing concentration allows up to populate the kinetic profiles shown in Figure 6.35 and test hypotheses about the behavior of metabolism (from diel DO concentrations) and nutrient uptake as the system approaches nutrient limitation.

While nitrate (and phosphate) depletion rates are the centerpiece of this method, measurements include DO over time to estimate metabolism (given known air-water gas exchange; Odum 1956), and N_2 production and N_2:Ar over time, which can be used to directly estimate denitrification, a measurement also subject to air-water gas exchange. This depletion experiment can be reversed by adding nutrients, alone or in combination, and also adjusting the location of the chamber (vegetation and sediment variation), and the degree of shading (to explore light limitation). This set of measurements is particularly relevant in Alexander Springs Creek where the diel nitrate variation pattern is notably different from other springs (Figure 6.36). We previously hypothesized (Cohen et al. 2013) that the inversion of the diel NO_3-N signal was evidence of nutrient limitation, and the benthic chamber approach allows us to test that by exploring whether nutrient depletion rates behave like other rivers when concentrations are enriched above ambient.

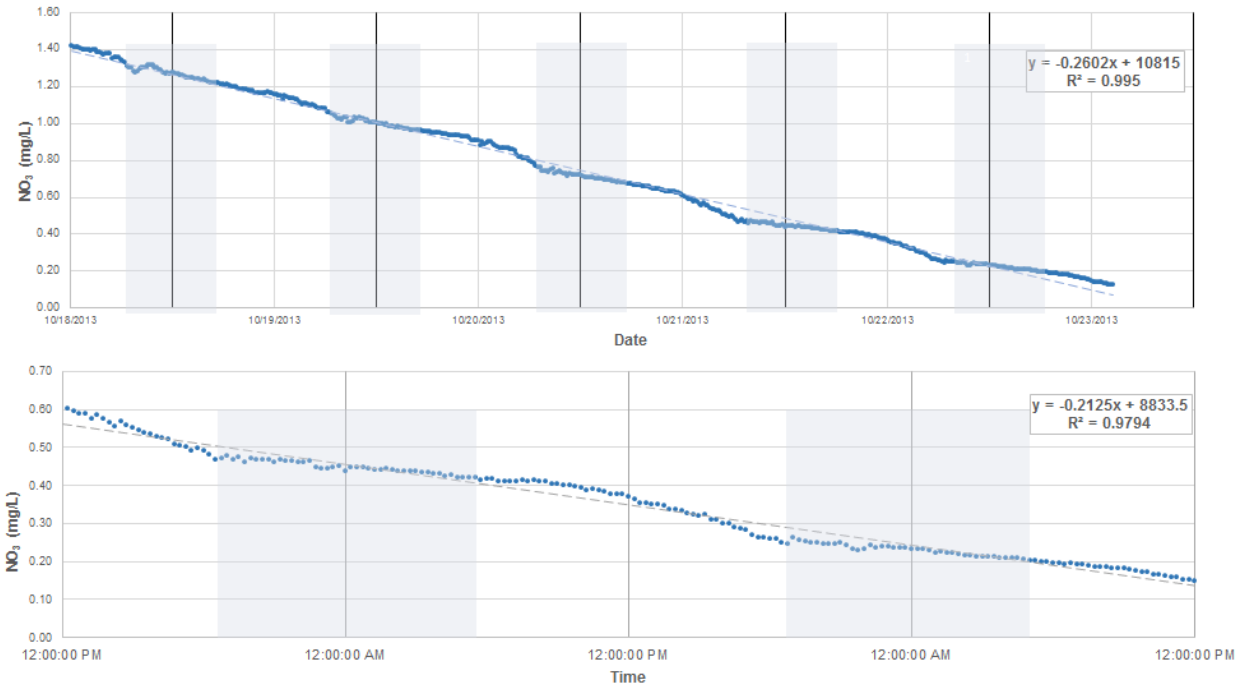

Figure 6.35. Illustration of benthic-box time-series data from Gum Slough (C. Riejo, unpublished data). Day-night variation in nitrate can be used to estimate process rates (uptake, denitrification, primary production) from the time-varying slope of the line. Kinetics (first order, zero order, Michaelis-Menten) can also be directly observed from the geometry of the declining concentration with time. To date, evidence for Michaelis-Menten kinetics exists, with a half-saturation constant near 0.1 mg N L^{-1}. Nutrient depletion tests are the only way to reasonably obtain these crucial ecosystem-scale N use parameters.

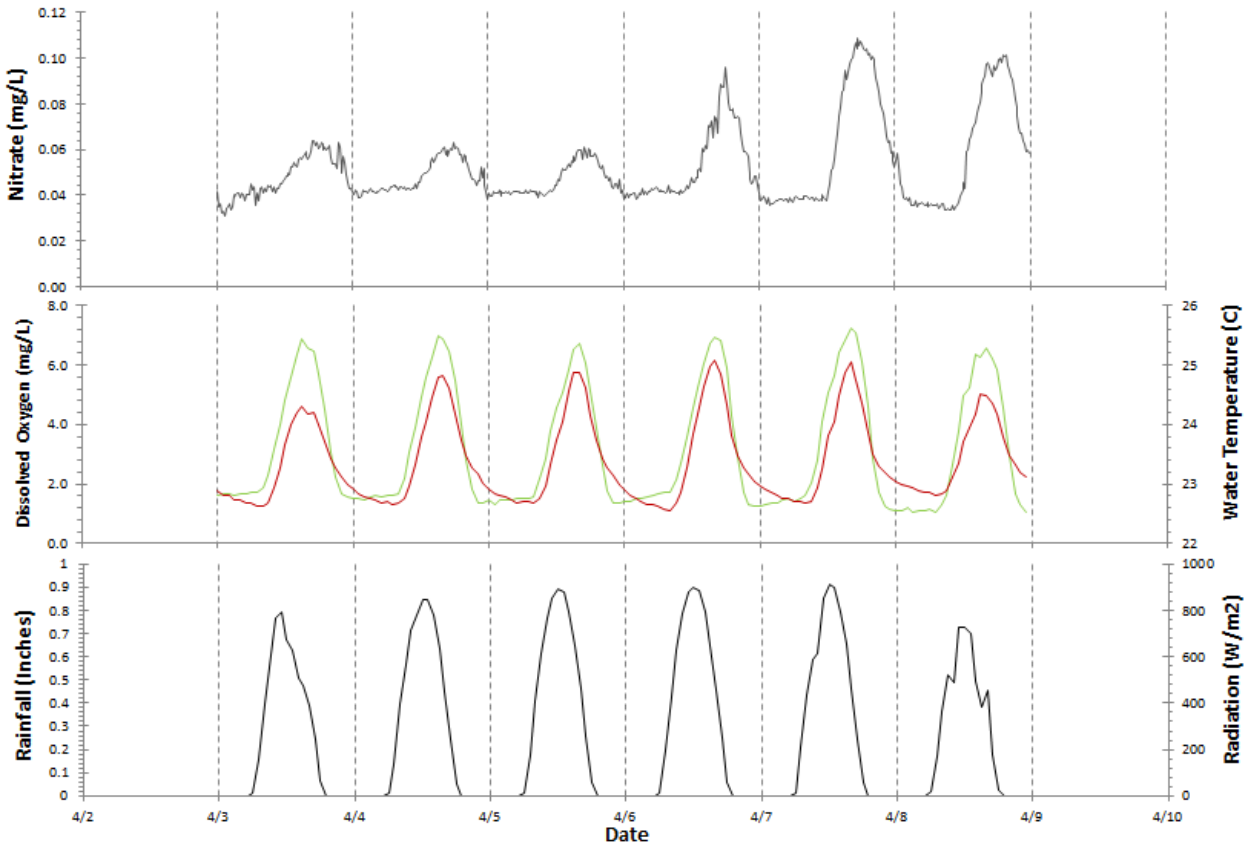

Figure 6.36. Diel variation in nitrate (grey line), dissolved oxygen (green line), water temperature (red line), radiation (black line) and rainfall (blue line) for Alexander Springs Creek during an April 2010 deployment. Vertical dashed lines are at midnight every day. Note the striking departure from patterns in other rivers in nitrate variation which is in phase with DO rather than exactly out of phase elsewhere. The increase in daytime nitrate variation on the last two days is due to massive amounts of detached algal biomass enshrouding the sensor.

In-stream methods exist to characterize nutrient uptake behavior as nutrient concentrations change from ambient to saturation, but no methods exist to estimate these effects at concentrations below ambient levels. To fill this knowledge gap, we developed a chamber-based method which allows characterization of changes in metabolism, water quality, and nutrient utilization as nutrient concentrations are depleted below ambient levels. This method has been tested at Gum Slough Springs and redesigned from an open to closed chamber to specifically use at Silver River which is deeper and more highly used for recreation.

The clear Plexiglass chamber (dimensions of 2’ x 2’ x 3’) blocks flow by insertion into upper sediments but allows light in and sediment-water-vegetation interactions to occur. By stopping flow, the continuous supply of nutrients and materials from upstream sources is also blocked which allows nitrate utilization to be specifically characterized as it is used over time. The chamber was placed within the stream channel at Gum Slough Springs, Florida and *in situ* sensors measured water quality while NO_3 reduced from ambient levels (1.40 mg N L^{-1}) to below regulatory thresholds (ca. 0.20 mg N L^{-1}) within one week (Figure 6.35). The daytime and

nighttime changes in nitrate concentrations were used to calculate areal uptake rate of nitrate (U_{NO3}; mg m^{-2} d^{-1}) over each time period. Using this method, we compared NO_3 uptake rates (U_{NO3}) and gross primary production (GPP) across three vegetative regimes (i.e., submerged aquatic vegetation (SAV), SAV with epiphytic algae, and algae alone). DO and nitrate fluxes were measured using the two-station method (Odum 1956) across a 0.5-mile section of the springrun and combined with a comprehensive vegetation survey to scale GPP estimates from the chamber to reach level. The closed chamber was tested at Gum Slough Springs and is now deployed at Silver River (Figures 6.37 and 6.38).

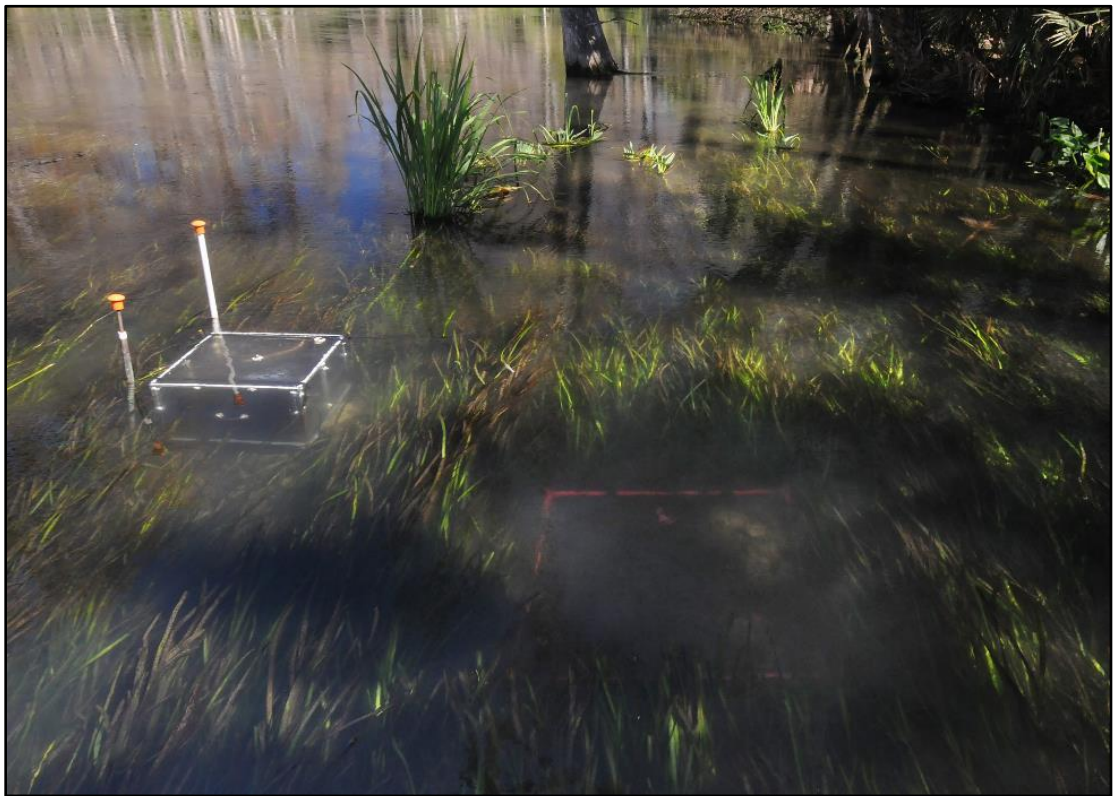

Figure 6.37. Initial SAV growth experiment plot (right) and benthos box (left) deployed and tested downstream of MFL2 in Silver River.

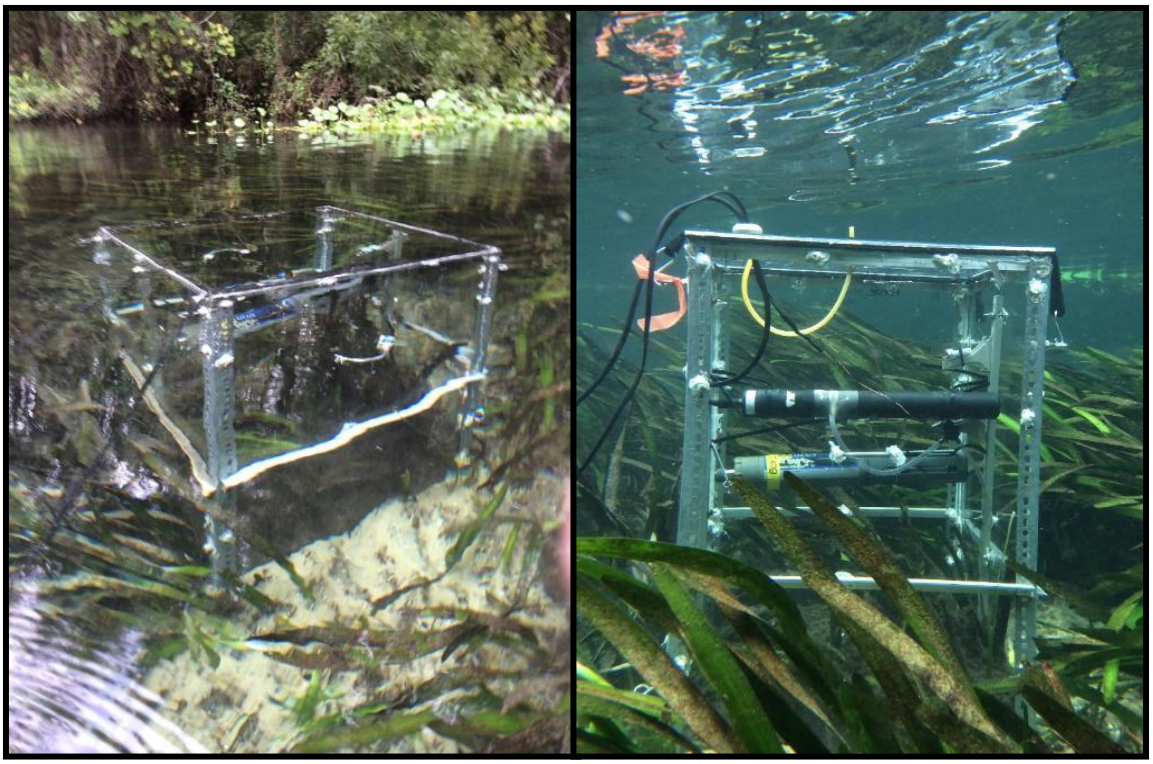

Figure 6.38. Photos of benthos boxes deployed and tested downstream of MFL2 in Silver River.

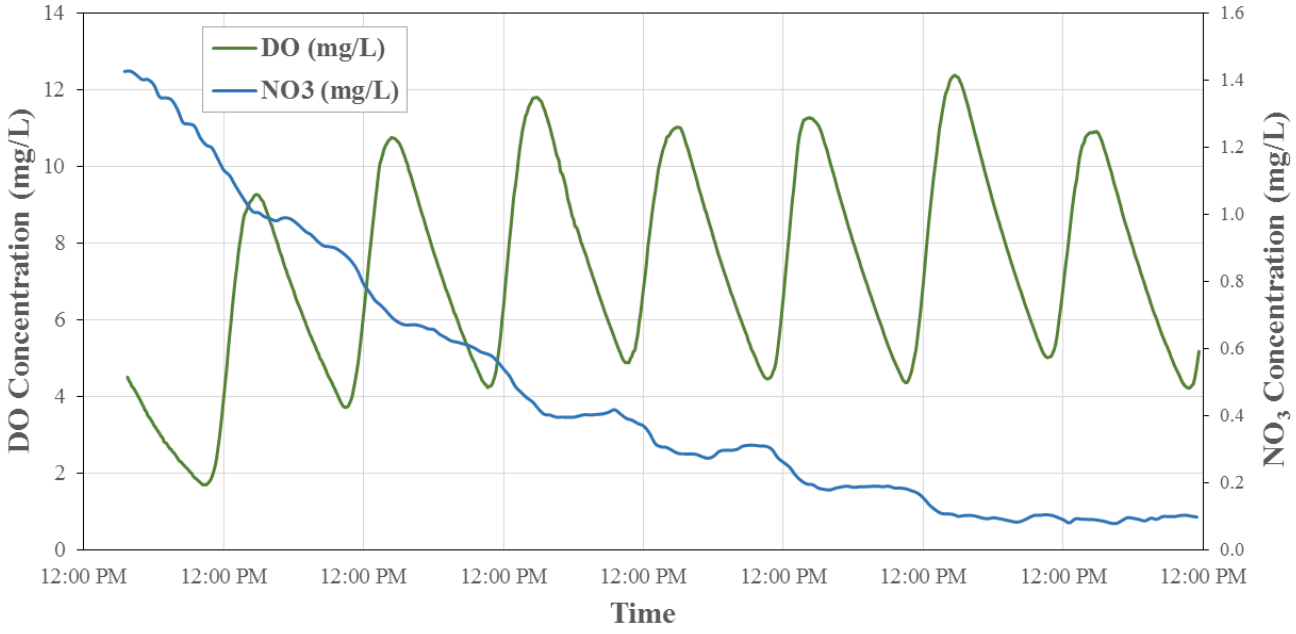

Figure 6.39. The nutrient depletion chambers were tested at Gum Slough Springs across different vegetation types where greatest nitrate uptake and gross primary production occurred in SAV only area.

Results at Gum Slough Springs (Figure 6.39) showed that U_{NO3} and GPP was greatest in SAV, GPP was negatively correlated to NO_3–N concentrations in algae, denitrification rates did not

vary by vegetation type, and chamber GPP (e.g. 6-8 g O_2 m^{-2} d^{-1} in SAV) was comparable to reach-scale estimates (6-12 g O_2 m^{-2} d^{-1}). These results show that primary production did not become limited by low nitrate concentrations, even below regulatory thresholds, and measurements from the chamber were effectively scaled to the reach level, illustrating how this method is an effective tool for assessing stream ecosystem response to reduced nutrient concentrations.

Using these methods, chamber deployments were initiated at Silver River beginning in February 2015 near MFL2. The objectives of future chamber studies at Silver River include using this method to determine how stream ecosystem metabolism responds nutrient enrichment effects.

6.6.1 Initial Chamber Study Results

Several chamber deployments occurred at Silver River near MFL2 between March and May 2015, including dual open and closed chamber tests. Initial deployments showed that the high water level fluctuation at Silver River resulted in the open chamber water exchanging with river water (i.e. flooding) and water within the closed chambers exchanging with the air (i.e. drawdown below box level). From these results, both the open and closed chambers were placed at locations allowing five to 10 inches of river water fluctuation. To account for this fluctuation, the open chamber was placed closer to the river bank and the closed chamber placed within the river thalweg, both areas having less vegetation cover than other surrounding areas and greater amounts of organic matter. During this deployment, sediment entrapment occurred on top of the closed chamber which, in combination with the high organic matter and no reaeration, resulted in eventual septic conditions (Figure 6.40). Although reaeration occurred within the open chamber, little oxygen production was observed (Figure 6.40) which likely maximized denitrification rates, seen in the continuous linear decline in nitrate concentrations over daytime and nighttime periods (Figure 6.40). Likewise, only nighttime nitrate uptake was seen in the closed chamber, resulting in a reversed stair-step pattern from that previously seen at Gum Slough Springs (Figure 6.40).

Results from placing a HOBO light logger within each chamber showed that light availability differed even though the chambers were in close proximity to each other (20 to 30 feet from each other) [Figure 6.41].

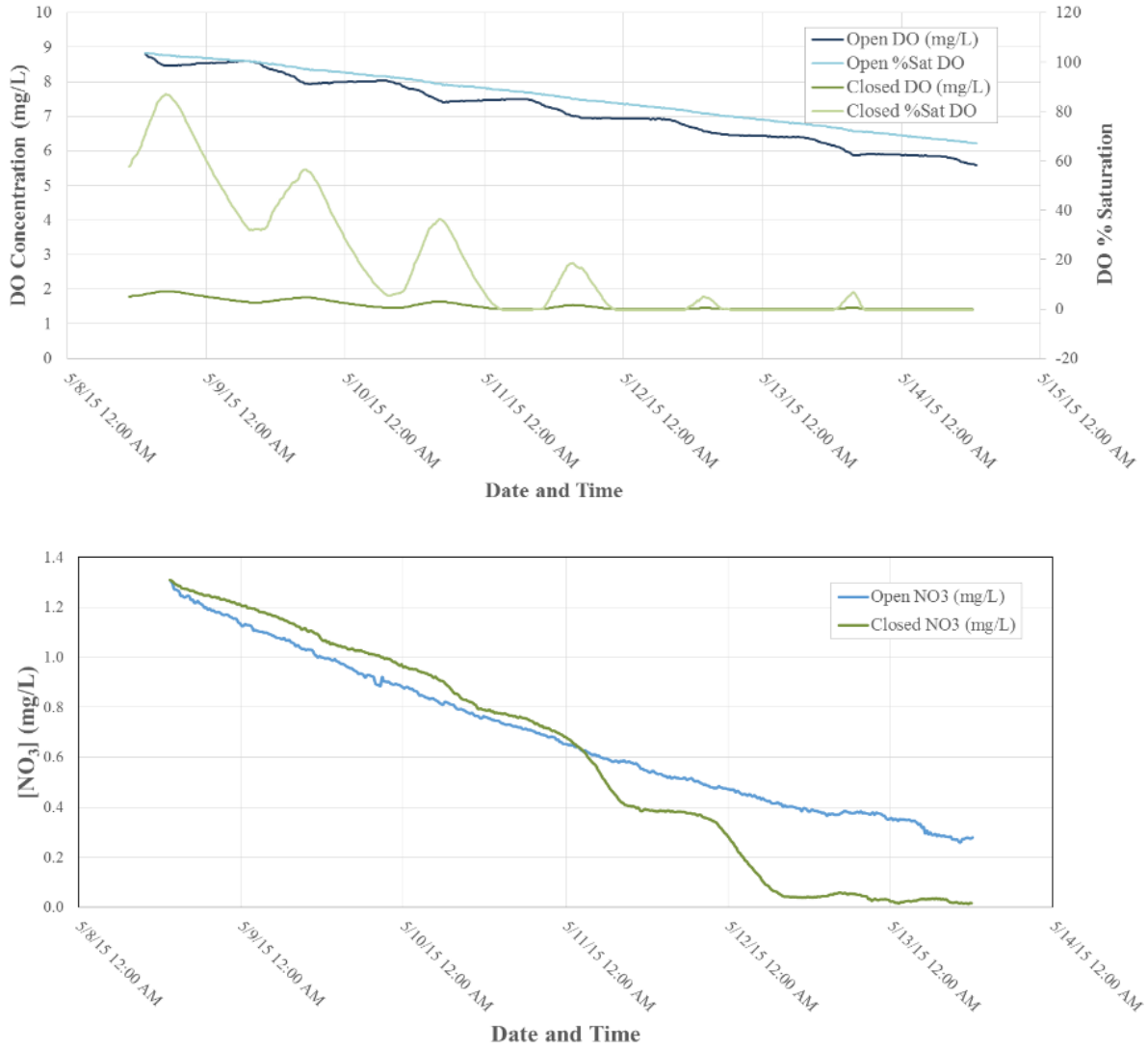

Figure 6.40. (above) Observed dissolved oxygen levels and percent saturation showed resulting septic conditions in the closed chamber and little primary production in either chamber type. (below) Measured nitrate levels in the open and closed chambers showed high nitrate uptake in the open chamber likely due to denitrification only as little oxygen was produced. A reversed stair-step pattern was observed in the closed chamber with highest nitrate uptake occurring during nighttime period and little to no uptake occurring during the day.

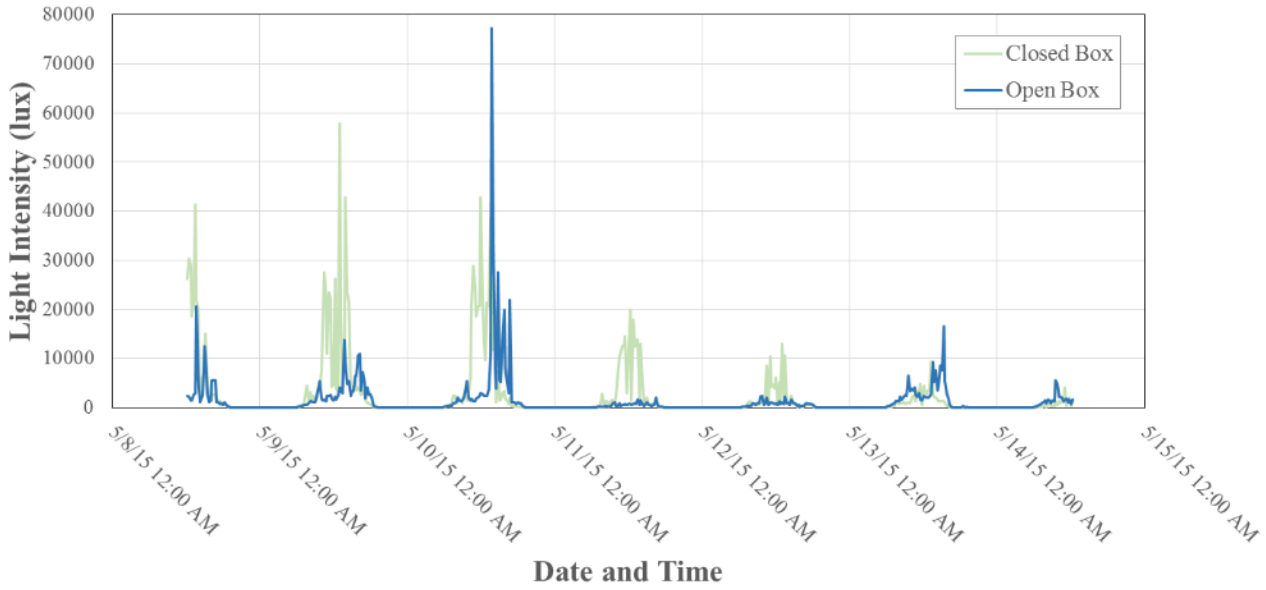

Figure 6.41. Light intensity (in lux), measured using a HOBO Pendant light logger, differed between the chambers when placed 20 to 30 feet apart from each other.

From these results, the closed chamber lid was redesigned from a detachable lid to an attached lid to minimize possibilities of water exchange and sedimentation. Likewise, the height of both the closed and open chambers were adjusted to increase potential site selection. The height of the closed chamber was decreased from three feet to two and a half feet so it can be placed closer to the stream bank and the open chamber height was increased from three feet to four feet so it can be placed farther from the stream bank. With these adjustments, the range of potential site locations and conditions (i.e., light availability, substrate type, velocity, etc.) will be maximized for both chamber types in future studies.

6.6.2 Nutrient Enrichment Effects on Stream Metabolism

Beginning in July 2015, chamber deployments will be used to study the effects of nutrient enrichment on metabolism. This study will 1) determine the effect of added iron, nitrate, and phosphate on metabolism dynamics and 2) simultaneously determine how stream metabolism varies across the ambient physical, chemical, and vegetational gradients present at Silver River. The nutrient bioassay design includes a pair of chambers, one control and one treatment, deployed adjacent to each other for one week at a unique location. Unique chamber locations will span longitudinally across the river and will cover three substrate types: 1) SAV only, 2) SAV with algal cover, and 3) algal cover only. For each deployment, one of seven nutrient combinations will added to the treatment chamber, including nitrate (N), phosphate (P), iron (Fe), nitrate and phosphate (N+P), nitrate and iron (N+Fe), phosphate and iron (P+Fe), and nitrate, phosphate and iron (N+P+Fe). Each treatment (paired with a control) will be tested over the three substrate types, giving a total of 21 treatment/substrate combinations (Figure 6.42). The treatment/substrate combinations will be replicated three times, totaling 63 unique deployments. Three chamber pairs will be deployed per week which will follow a randomized design of treatment/substrate combinations over time.

Note that nutrient depletion assays (where nitrate concentrations are tracked over time) will be deployed in a subset of these nutrient limitation assays. We foresee utilizing two control boxes for assessing nitrate dynamics every third week. In total, there will be 63 unique 1-week deployments (control vs. treatment pairs) of the metabolism experiments, of which ca. 21 control locations will be analyzed for nitrate depletion dynamics. This two-phase (i.e., metabolism as phase 1, nutrient depletion as a subset we refer to as phase 2) design is predicated on the limited availability of the expensive SUNA sensors, and the field logistics of deploying those sensors in the boxes. The expected timeline for starting and completing this comprehensive nutrient limitation study is shown in Figure 6.43.

SAV Only		SAV with Algal Cover		Algal Cover	
Control	N	Control	N	Control	N
Control	P	Control	P	Control	P
Control	Fe	Control	Fe	Control	Fe
Control	N + P	Control	N + P	Control	N + P
Control	N + Fe	Control	N + Fe	Control	N + Fe
Control	P + Fe	Control	P + Fe	Control	P + Fe
Control	N + P + Fe	Control	N + P + Fe	Control	N + P + Fe

Figure 6.42. The nutrient enrichment study will measure the effects of nutrient additions (N, P, Fe; individually and in combination) over three substrate types (SAV only, SAV with algal cover, and algae only). Each treatment/substrate combination will be replicated three times for a total of 63 deployments. Of these, 21 control boxes will be used to evaluate benthic nutrient depletion using nitrate sensors.

During chamber deployment, canopy cover, velocity, and vegetation percent cover will be recorded, and pre-deployment sediment samples collected. Water samples will be collected

following the protocol outlined by the comprehensive survey and will be analyzed for nutrient content pre- and post-deployment. Characterization of ambient, physical and chemical conditions will be used to account for any variation seen between each chamber location, as well as determine overall change in nutrient concentrations over the deployment period. A conservative tracer (chloride as NaCl) will be added to all control and treatment chambers and pre- and post-sampling will verify if any hydrologic loss or exchange occurs. Within each chamber, a HOBO dissolved oxygen sensor, a HOBO Pendant light logger, and an aquatic pump will be deployed. The pump ensures mixing of the chamber and simultaneously simulates flow while the HOBO sondes record changes in oxygen and light levels at 15-minute intervals. Deployment of three chamber pairs per week will begin in July 2015 and continue until February 2016. Overall, this pair-wise nutrient enrichment study will determine how metabolism varies over different substrate types and ambient conditions and will determine the effect of elevated nutrient levels on GPP and GPP efficiency at Silver River.

Table 6.7. Proposed timeline of nutrient enrichment paired chamber deployments at Silver River. Note that similar efforts will start in Spring 2016 in Alexander Springs Creek.

Month	# Box Pairs	Deployment Location
July 2015	2	Between MFL 6 and 7
August 2015	12	Between MFL 1 and 3
September 2015	3	Between MFL 3 and 4
	6	MFL 9 and 10
October 2015	12	MFL 7 and 9
November 2015	3	Downstream of MFL 1
November 2015 – January 2016	12	Between MFL 5 and 7
January 2015	3	Between MFL 4 and 5
February 2016	10	Upstream of MFL 10

6.7 *IN SITU* VEGETATION GROWTH EXPERIMENTS

Submerged aquatic vegetation is an important biological, chemical, and physical component of spring-fed ecosystems, influencing water column chemistry, stabilizing sediments, and providing habitat. The growth and vigor of SAV is an indicator of spring ecosystem health, and growth response is evidence of change in environmental conditions. Nitrogen enrichment, along with dissolved oxygen and grazer abundance, are presumed to impact primary producer community structure as algal proliferation results in macrophyte shading. However, factors exerting direct and indirect control on SAV growth in Florida springs are poorly understood. Potential controls include water column and pore water chemistry, sediment, water velocity, algal cover, and light. Long-term SAV aboveground production data and improved understanding of drivers contributing to growth will inform management strategies and restoration activities.

The SAV growth experiments explore the dynamics of shoot elongation and aboveground productivity over an annual cycle across a gradient of naturally occurring conditions. *In-situ* estimates of leaf blade elongation, aboveground biomass production, and turnover time will be made at 16 sites in both Silver River and Alexander Springs Creek that are selected according to data collected during comprehensive surveys (Table 6.8). The experimental sites are characterized as areas of relatively dense and homogenous SAV beds with depth limited to 1.5m. Parameters for site selection include natural gradients in light regime, water velocity, sediment organic matter, and epiphytic algal cover such that all potential low-high combinations are represented by the 16 sites. Leaf elongation, biomass production, and turnover rates are measured using a modified version of the leaf-clipping technique described by Virnstein (1982) for two dominant SAV species, *Sagittaria kurziana* and *Vallisneria americana*. In May 2015, shoots within each of the sixteen 1 m^2 vegetation quadrats in Silver River were clipped 2cm above the basal sheath to enable regrowth from the basal meristem. Original biomass clipped from 0.25 m^2 of each plot was harvested, separated by species, measured for shoot length and width, weighed for total aboveground biomass, and analyzed for foliar composition (%C, %N, %P). These measurements are useful for understanding variation in SAV shoot morphology and tissue composition under different ambient conditions, as well as calculating productivity and turnover time.

Leaf blade elongation is measured biweekly in the initial two months after clipping, then at monthly intervals throughout the duration of the experiment. Growth rate for each species is calculated by measuring the length of all clipped leaf blades from each site, while aboveground productivity is assessed by weighing dried SAV biomass clipped from a 0.25 m^2 area from each quadrat at specific time intervals. The SAV in the upstream portion of each quadrat will be clipped and collected at one month and three month intervals in order to examine seasonal variability, while the downstream portion of the quadrat will remain unclipped for up to six months in order to assess long-term growth rate, aboveground productivity, and turnover time (Figure 6.43). Surrounding vegetation is clipped such that light penetrating the vegetation quadrat is not obstructed. Canopy cover, water depth, velocity profile, sediment, pore water, and surface water were sampled at each site, and the reattachment of epiphytic algae on clipped leaves will be documented. Methods will be repeated at Alexander Springs Creek as a comparison to establish the role of nitrogen availability in SAV growth and vigor.

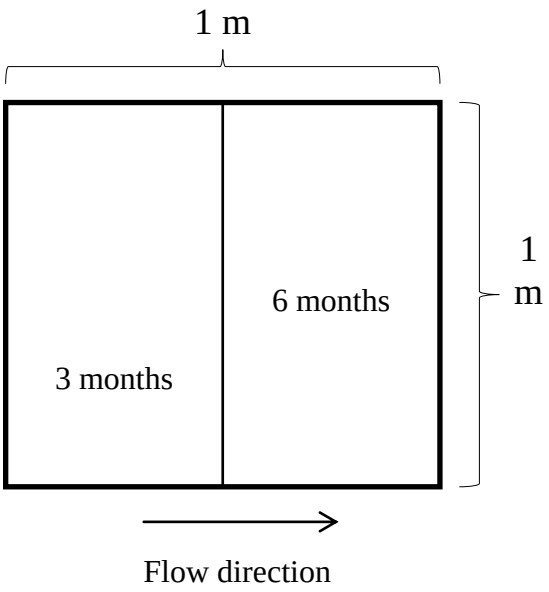

Figure 6.43. Aboveground biomass in the upstream portion of the quadrat will be clipped at one month and three month intervals, and downstream biomass will be clipped biannually to examine growth rate and aboveground production variability.

6.7.1 Experiment Site Selection

Site selection for SAV growth experiments was based on locations that covered gradients of all measured characteristics (i.e. biological, physical, and chemical) with high SAV cover and maximum water depth of 1.5 m. Natural gradients in organic matter, water velocity, algal cover, and light regime will be used to assess variation in shoot elongation, aboveground productivity, and turnover rates in *Vallisneria americana* and *Sagittaria kurziana*. The frequency and distribution of these parameters from the comprehensive survey were used to categorize values as low and high (Table 6.8). Sites were chosen (Table 6.9) based on this quantitative data such that all potential gradient combinations and parameters are represented (Figure 6.44). Most sites are composed of both *Sagittaria kurizana* and *Vallisneria americana*, however some sites contain only *Sagittaria.* Photos of sampling are presented in Figures 6.45-6.48.

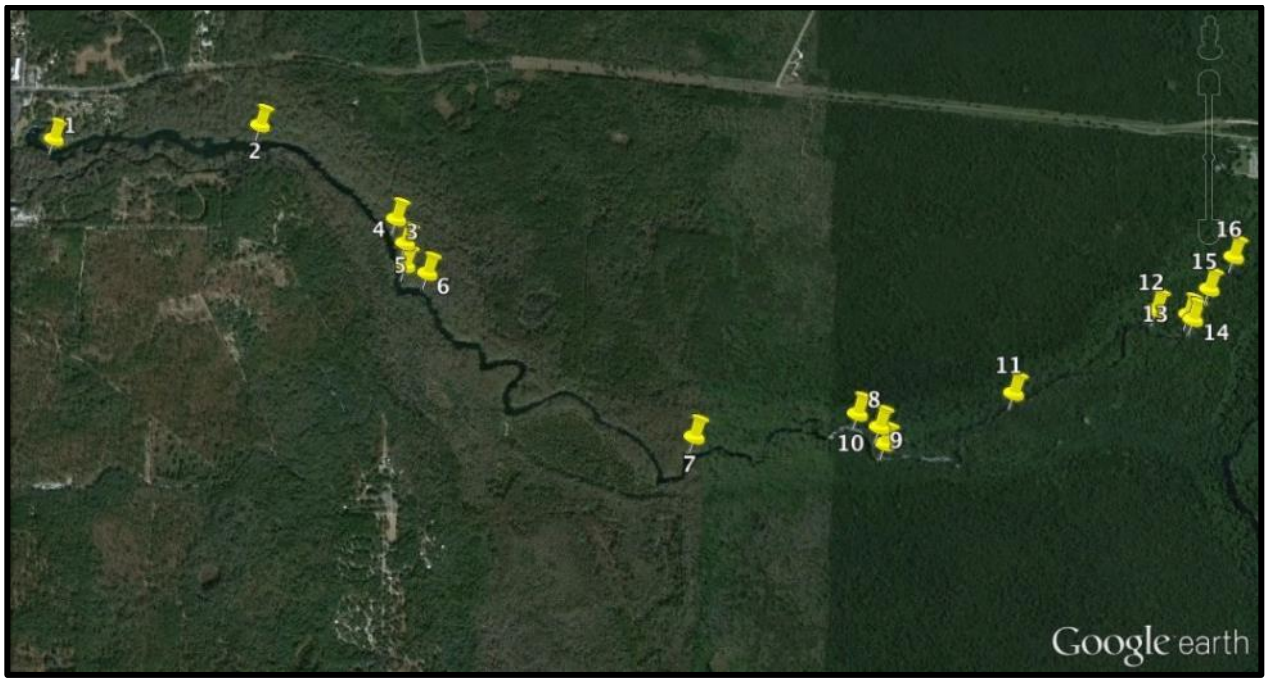

Figure 6.44. Geographic locations of SAV growth experiment sites in Silver River (Google Earth).

Table 6.8. Classification for each parameter used in vegetation growth experiments based on quantitative data collected during the comprehensive survey and installation of SAV experimental sites.

	Low	High
Algal Cover (Braun- Blanquet)	1-2	4-5
Velocity (m s^{-1})	<0.10	>0.20
Canopy Cover (% open)	>50%	<30%
Organic Matter (%)	<15%	>25%

Table 6.9. Algal cover, velocity, canopy cover, and organic matter measurements collected during the installment of the SAV experiment sites, representing all potential combinations of low and high values for each parameter (%OM data incomplete).

Site	Algal Cover (BB)	Maximum Velocity ($m\ s^{-1}$)	Canopy Cover (% open)	Organic Matter (%)
1 (Upstream)	5 (High)	0 (Low)	24.44 (High)	Low
2	1 (Low)	0.25 (High)	50.30 (Low)	High
3	5 (High)	0.252 (High)	55.64 (Low)	Low
4	5 (High)	0.21 (High)	53.94 (Low)	High
5	1 (Low)	0.215 (High)	27.56 (High)	High
6	5 (High)	0.09 (Low)	55.24 (Low)	High
7	1 (Low)	0.39 (High)	22.62 (High)	Low
8	5 (High)	0.09 (Low)	14.82 (High)	High
9	1 (Low)	0.40 (High)	55.12 (Low)	Low
10	1 (Low)	0.1 (Low)	17.68 (High)	Low
11	5 (High)	0.302 (High)	27.04 (High)	High
12	2 (Low)	0.078 (Low)	52.12 (Low)	Low
13	1 (Low)	0.105 (Low)	73.06 (Low)	High
14	4 (High)	0.10 (Low)	91.26 (Low)	Low
15	4 (High)	0.22 (High)	10.14 (High)	Low
16 (Downstream)	1 (Low)	0.075 (Low)	8.06 (High)	High

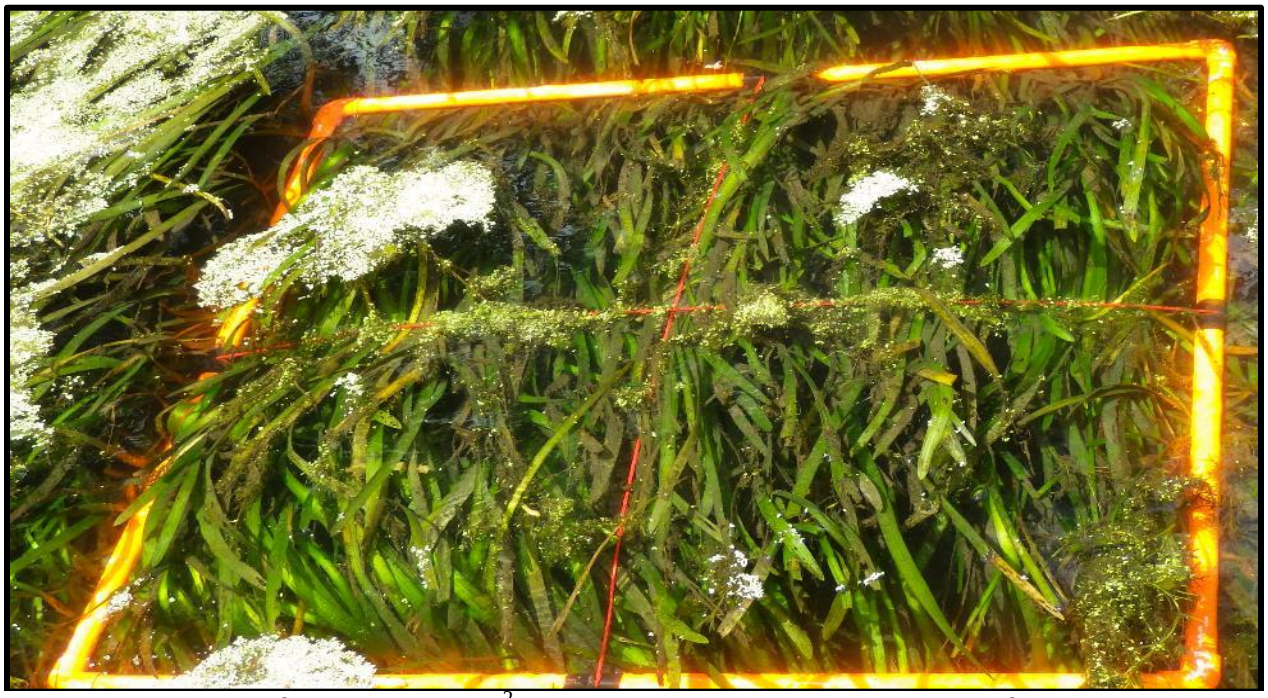

Figure 6.45. Picture of undisturbed 1 m^2 SAV growth experiment site taken before clipping SAV shoots to 2 cm above basal meristem in Silver River.

Figure 6.46. Picture taken after clipping SAV shoots to 2 cm in Silver River. Clipped aboveground biomass from 0.25 m^2 was collected, separated by species, measured for length and width, weighed, and analyzed for %C, N, and P.

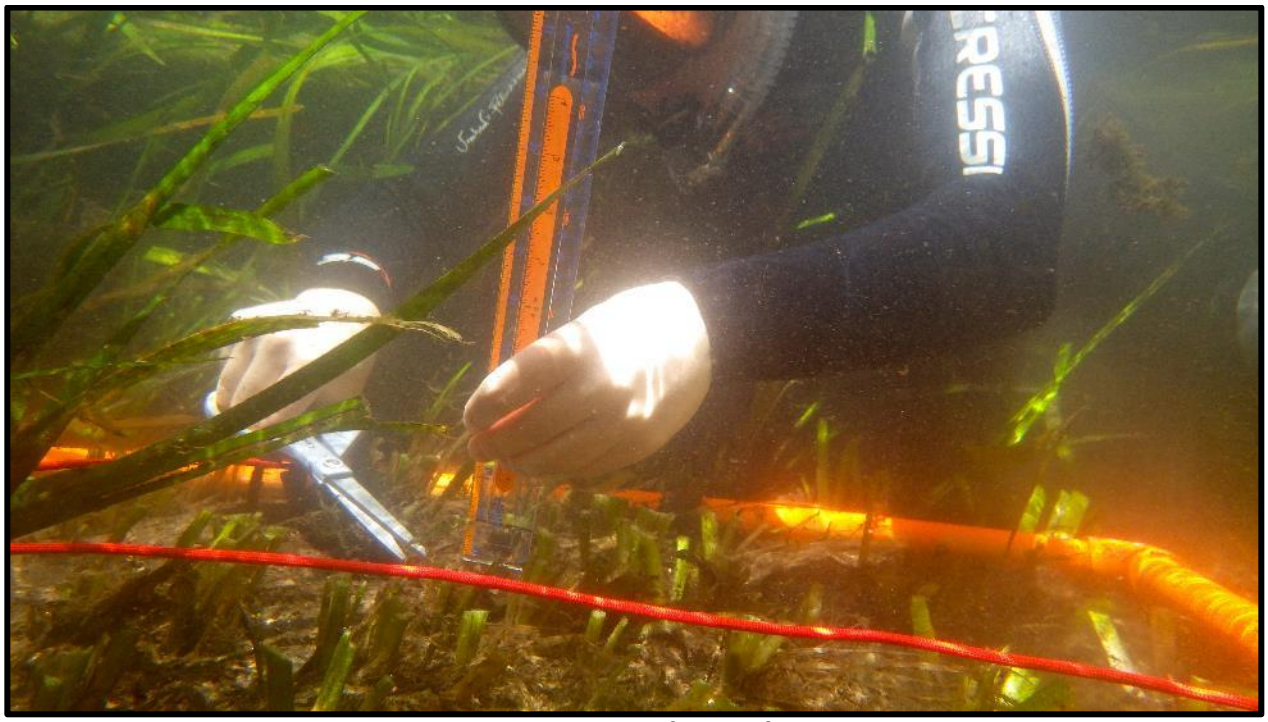

Figure 6.47. SAV growth is measured using a modified leaf-clipping technique described by Virnstein (1982) in which leaf blades are cut to 2 cm above the basal sheath to enable regrowth from the basal meristem.

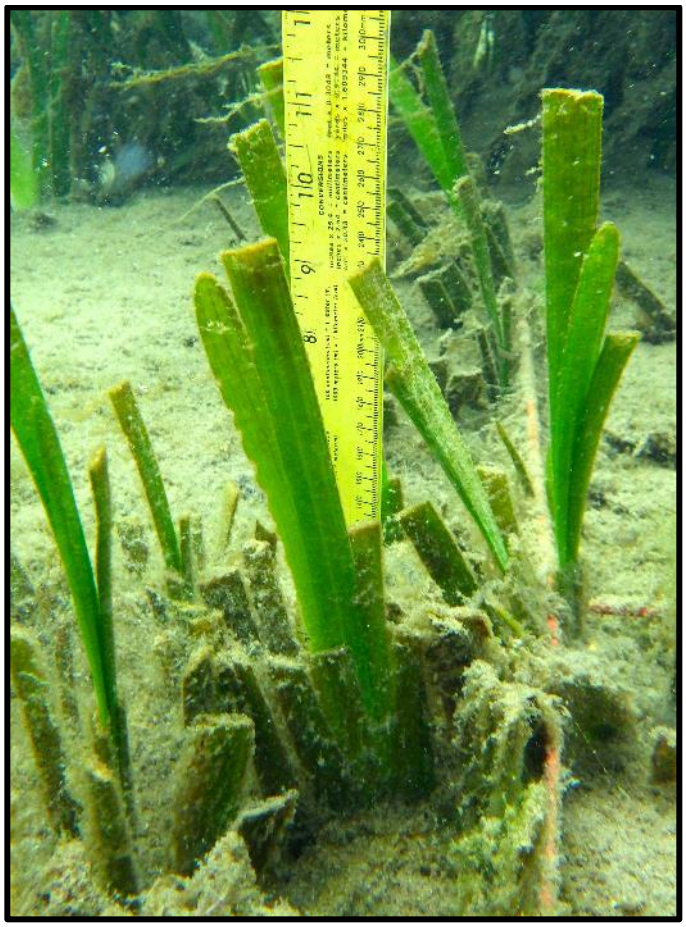

Figure 6.48. Variation in SAV shoot elongation was observed two weeks after initial plot installment and clipping. Twenty shoots from each site were randomly selected and measured for growth. Unclipped leaf blade tips indicate new growth since plot installment.

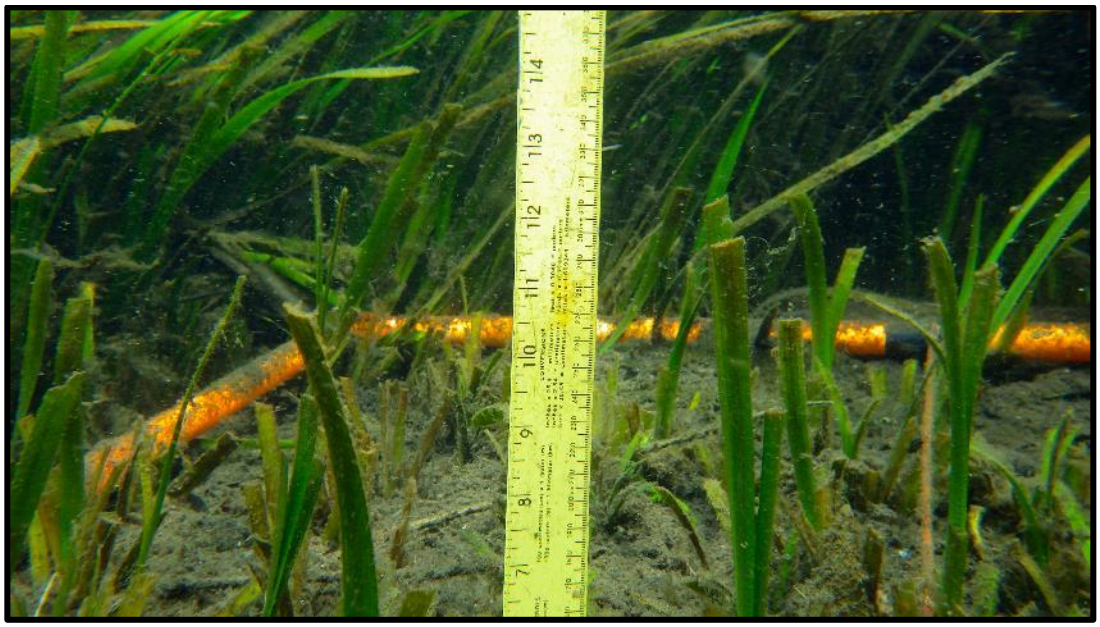

6.7.2 Preliminary Measurements and Observations

Within the first month after installing and clipping the SAV plots in Silver River, preliminary observations and measurements regarding SAV shoot morphology and growth were made. Length and width measurements of harvested shoots from 0.25 m^2 of each plot reveal differences in SAV morphology and growth form. Maximum water velocity is positively correlated to shoot length-to-width ratio for both species, suggesting augmented energetic investment in longer and narrower leaf blades at high water velocity sites to reduce resistance and drag (Figure 6.49). *In situ* measurements after one month reveal variation in growth rates between and within experimental sites, with a modest of canopy cover on Vallisneria growth, but not such effect on Sagittaria growth rates (Figure 6.50). Differences in the length of new and clipped shoots suggest preferential allocation of energy and resources into certain leaves. New, unclipped shoots less than 2cm in length at the time of installing plots and clipped, mature shoots widely vary in length after two weeks. The average growth rate of *Vallisneria americana* exceeds that of *Sagittaria kurziana* at all sites where both species are present. Additionally, a decrease in growth rate was observed for both species with increasing distance from the head spring, requiring further investigation (Figure 6.51). Causal mechanisms may include elevated downstream turbidity resulting in diminished light attenuation, or growth inhibition due to excessive NO_3-N, H_2S, or other undetermined factors.

6.7.3 Future Work

The SAV growth experiment sites installed in Silver River will be monitored, clipped, and measured at specified intervals throughout the project. Harvested shoots will be measured for shoot length, width, and aboveground biomass and analyzed for foliar tissue composition. Average growth rates between species and sites at Silver River will be compared to understand effects of epiphytic algae, velocity, light, and organic matter on SAV growth. Characterization of light regimes will be made at each site by measuring photosynthetically active radiation (PAR) in the water column to quantify light attenuation by submerged aquatic vegetation, as well as understand turbidity and water quality effects on SAV growth. In addition, sediment organic matter, surface water, and pore water chemistry will be analyzed for each site. In August 2015, we will survey at Alexander Springs Creek, using the same methodology, to inform site selection for SAV growth experiments which will be implemented in September 2015. Parameters of interest and their quantitative values in Silver River (Table 6.9) and Alexander Springs Creek will be maintained in order to understand the implications of nitrogen enrichment on SAV growth.

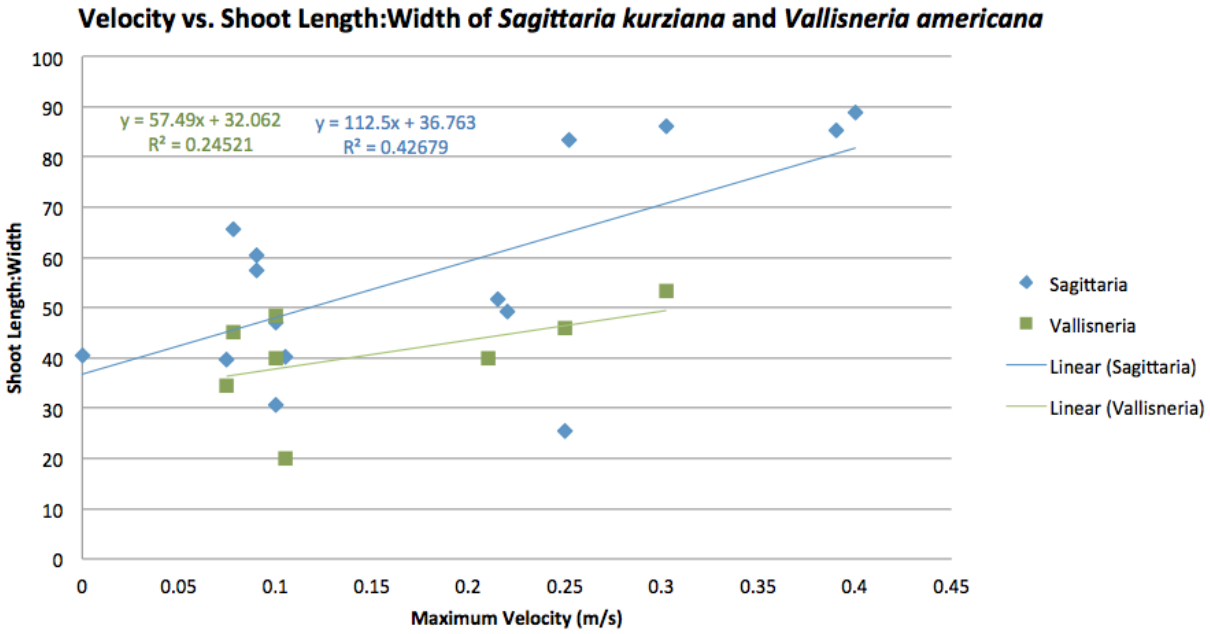

Figure 6.49. Length and width measurements of all intact shoots clipped and harvested from 0.25 m^2 area within each experimental site indicate longer, narrower leaf blades at higher velocities for *Sagittaria kurziana* and *Vallisneria americana*.

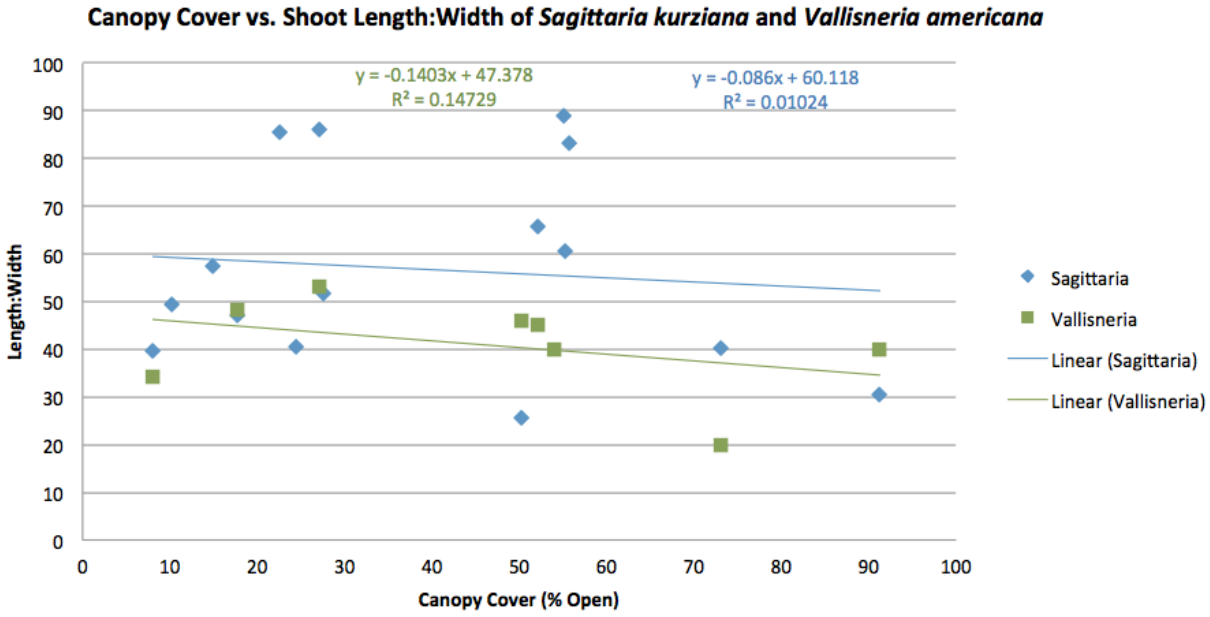

Figure 6.50. Variation in shoot length-to-width ratios for Sagittaria kurziana and Vallisneria americana along a natural gradient in canopy cover at 16 SAV growth experiment sites in Silver River. All shoots from 0.25 m^2 area were separated by species, measured for length and width, and analyzed for foliar composition.

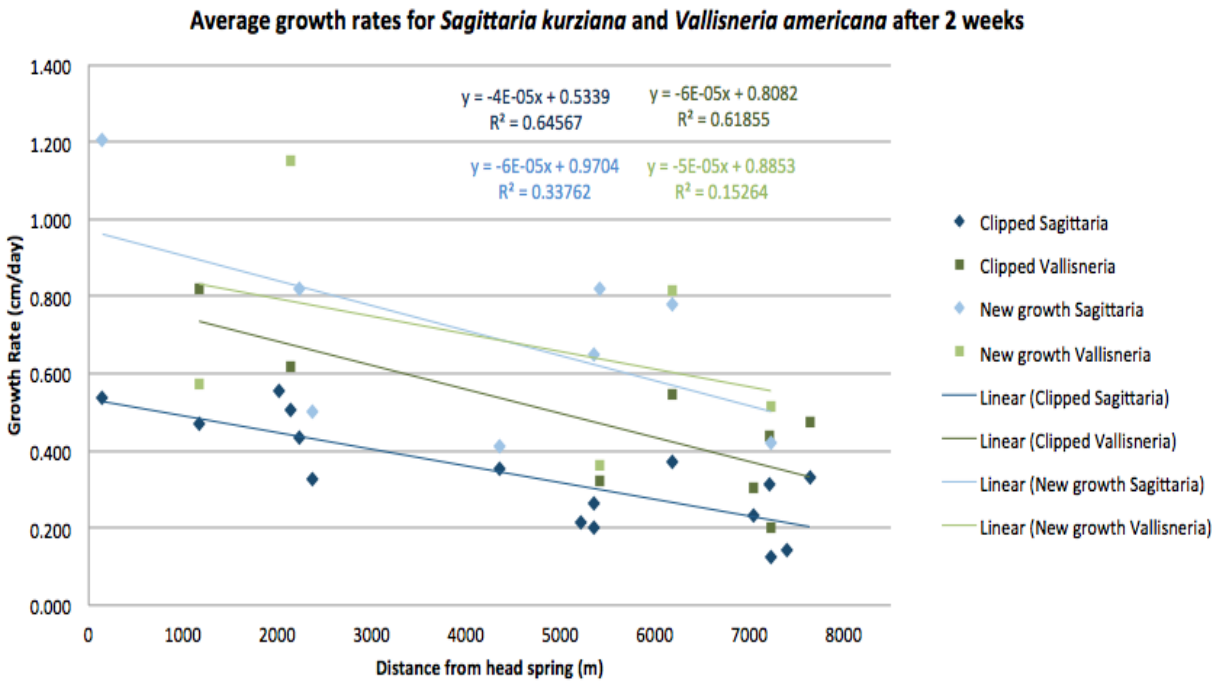

Figure 6.51. Growth rate decreases with increasing distance from the headspring for both species two weeks after the initial clipping at the 16 SAV growth experiment sites in Silver River.

We also evaluated the molar ratio and elemental content of the sampled tissues in the selected SAV growth locations. These are plotted in Figure 6.52, and suggest that tissue stoichiometry and elemental composition are highly consistent along the length of the river, consistent with finding in this and other springs by Nifong et al. (2014), but at odds with observations made during the benthic survey work presented above. The reason for the differences are not clear, but repeated measurements of tissue stoichiometry as part of this SAV growth effort will provide an important venue for better understanding what controls elemental composition in these systems, and the controls on the attendant spatial and temporal variation.

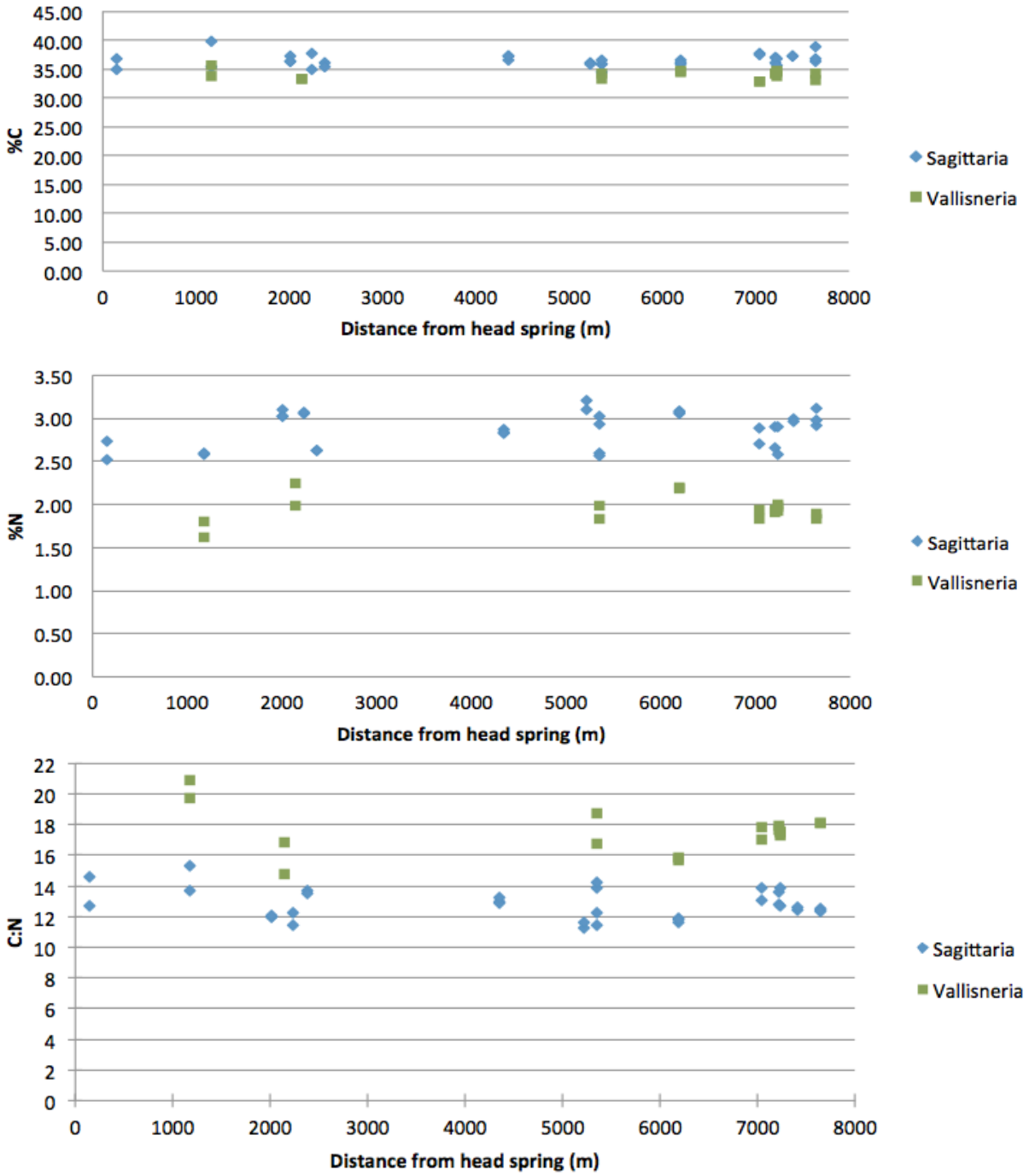

Figure 6.52. Summary of tissue measurements of %C, %N and molar C:N from the samples obtained as part of the SAV growth experiments. No longitudinal variation was observed in either of the target taxa.

Figure 6.53. Mean shoot elongation rates for S. kurziana (above) and V. Americana (below) for sites with high and low algae (left), velocity (center) and canopy cover (right). Error bars are standard deviations of 20 individual leaf measurements. These measurements are for shoot elongation for those shoots that were clipped. Figure 6.50 shows the same data for new emergent shoots.

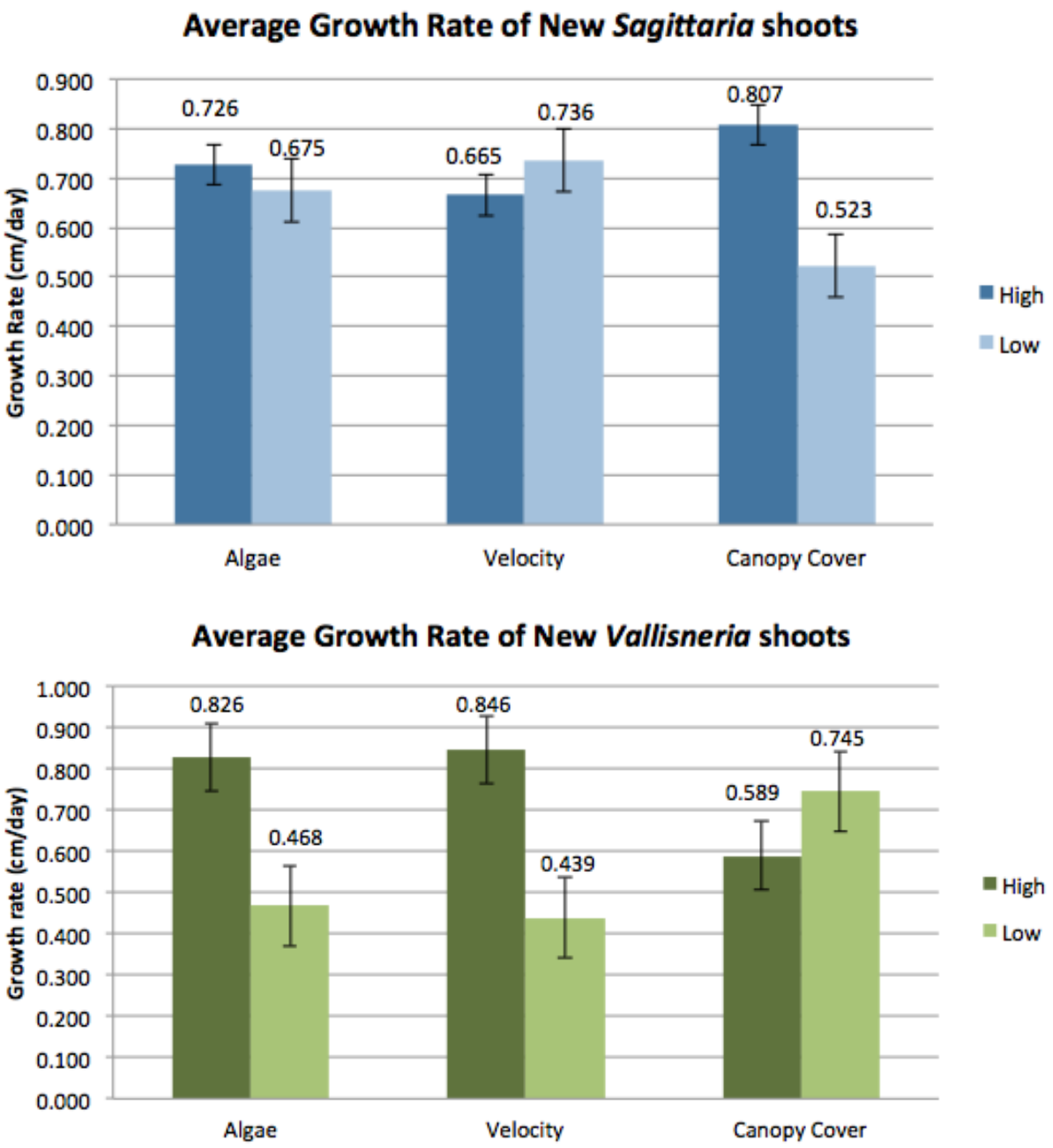

Figure 6.54. Mean shoot elongation rates for S. kurziana (above) and V. Americana (below) for sites with high and low algae (left), velocity (center) and canopy cover (right). Error bars are standard deviations of 20 individual leaf measurements. These measurements are for shoot elongation for new emergent shoots. Figure 6.49 shows the same data for shoots that were clipped.

The controls on growth rates is obviously somewhat preliminary, but we have already observed some important variation worthy of mentioning here. First, we observed significant velocity control on growth of *Sagittaria* clipped leaves (i.e., not new emergent leaves), but no effect of algae or canopy cover (Figure 6.53). This effect was even stronger forVallisneria. For new

leaves, the velocity effect on *Sagittaria* growth disappeared (Figure 6.54), but was retained for *Vallisneria*. An additional significant effect of algal cover (high algal cover increasing *Vallisneria* growth) was observed as well.

A timeline for further SAV growth experiment work is presented in Table 6.10.

Table 6.10. Proposed timeline of SAV growth experiments at Silver River and Alexander Springs Creek.

Proposed Date	Activity
March 2015	Initial SAV clipping for all sites in Silver River
March – May 2015	Seasonal SAV growth measurements in Silver River (Spring)
August 2015	Alexander Springs Creek survey and experiment site selection. Initial SAV clipping for all sites in Alexander Springs Creek
August 2015	Seasonal SAV growth measurements in both rivers (Summer)
September – November 2015	Seasonal SAV growth measurements in both rivers (Fall)
Dec. 2015 – February 2016	Seasonal SAV growth measurements in both rivers (Winter)

6.8 REFERENCES

Bristow, J. M., and Whitcombe, M. (1971). The role of roots in the nutrition of aquatic vascular plants. *Amer. J. Bot., 58*(1).

Burkholder, J.M., K.M. Mason, H.B. Glasgow, Jr. 1992. Water column nitrate enrichment promotes decline of eelgrass *Zostera marina*: evidence from seasonal mesocosm experiments. Marine Ecological Progress Series 81: 163-178.

Caffrey, J. M., and Kemp W. Michael. (1992). Influence of the submersed plant, *Potamogeton perfoliatus,* on nitrogen cycling in estuarine sediments. *Limnol.Oceanogr., 37*(7).

Carignan, R. (1982). An empirical model to estimate the relative importance of roots in phosphorus uptake by aquati macrophytes. *Can.J.Fish.Aquat.Sci, 39.*

Heffernan, J. B., and Cohen, M. J. (2010). Direct and indirect coupling of primary production and diel nitrate dynamics in a subtropical spring-fed river. *Limnology and Oceanography, 55*(2), 677.

Hensley, R.T., M.J. Cohen and L.V. Korhnak. 2014. Inferring nitrogen removal in large rivers from high-resolution longitudinal profiling. *Limnology and Oceanography* 59:1152-1170.

Morris, E. P., E.P. Morris, G. Peralta, F.G. Brun, L. van Duren, T.J. Bouma, and J.L. Perez-Llorens. (2008). Interaction between hydrodynamics and seagrass canopy structure: Spatially explicit effects on ammonium uptake rates. *Limnology and Oceanography, 53*(4), 1531–1539.

Mulholland, P., Mulholland, P.J., A.M. Helton, G.C. Poole, R.O. Hall, Jr., S.K. Hamilton, B.J. Peterson, J.L. Tank, L.R. Ashkenas, L.W. Cooper, C.N. Dahm, W.K. Dodds, S.E.G.

Findlay, S.V. Gregory, N.B. Grimm, S.L. Johnson, W.H. McDowell, J.L. Meyer, H.M. Valett, J.R. Webster, C.P. Arango, J.J. Beaulieu, M.J. Bernot, A.J. Burgin, C.L. Crenshaw, L.T. Johnson, B.R. Niederlehner, J.M. O'Brien, J.D. Potter, R.W. Sheibley, D.J. Sobota, and S.M. Thomas.. (2008). Stream denitrification across biomes and its response to anthropogenic nitrate loading. *Nature, 452.*

Mulholland, P.J., H.M. Valett, J.R. Webster, S.A. Thomas, L.N. Cooper, S. Hamilton, and B.J. Peterson. 2004. Stream denitrification and total nitrate uptake rates measured using a field ^{15}N tracer addition approach. Limnology and Oceanography 49:809-820.

Nifong, R.L., M.J. Cohen and W.P. Cropper. 2014. Homeostasis and nutrient limitation of benthic autotrophs in natural chemostats. Limnology and Oceanography 59: 2101-2111.

Reddy, K. R. (1983). *Fate of nitrogen and phosphorus in a waste-water retention reservoir containing aquatic Macrophytes1* Retrieved from https://www.agronomy.org/publications/jeq/abstracts/12/1/137.

Smolders, A.J., C.D. Hartog, C.B. Gestel, J.G. Roelof. 1996. The effects of ammonium on growth, accumulation of free amino acid and nutritional status of young phosphorus deficient *Stratiotes aloides* plants. Aquatic Botany 53: 85-96.

Smolders, A.J., M.C. van Reil, J.G.M Roelofs. 2000. Accumulation of free amino acids as an early indication for physiological stress (nitrogen overload) due to elevated ammonium levels in vital *Stratiotes aloides* L. stands. Archeif fur Hydrobiologie 150: 169-175.

Smolders, A.J.P, R.J.J. Hendriks, H.M. Campschueur, J.G.M Roelofs. 1997. Nitrate induces iron

Stapel, J., J. Stapel, T.L. Aarts, B.H.M. van Duynhoven, J.D. DeGroot, P.H.W. van den Hoogen and M.A. Hemminga.(1996). Nutrient uptake by leaves and roots of the seagrass *thalassia hemprichii* in the spermonde archipelago, indonesia. *Marine Ecology Progress Series, 134.*

van der Heide, T., E.H. van Nes, M.M. van Ktawijk, M. Scheffer, A.J. Hendriks, A.J.P. Smolders. 2010. Alternative stable states driven by density-dependent toxicity. Ecosystems 13: 841-850.

Van Dijk. H. F. G. & Roelofs, J. G. M. (1988): Effects of excessive ammonium deposition on the nutritional status and condition of pine needles. - Physiologia Plantarum 73: 494-501.

Veraart, A., Bruijne, W. J., Klein, J. M., Peeters, E. H. M., & Scheffer, M. (2011). Effects of aquatic vegetation type on denitrification. *Biogeochemistry, 104*(1-3), 267-274. doi:10.1007/s10533-010-9500-z.

Wang, Y., G. Gao, B. Qin, X. Wang. 2012. Ecophysiological and anatomical responses of *Vallisneria natans* to nitrogen and phosphorus enrichment. Knowledge and Management of Aquatic Ecosystems 405, 05.

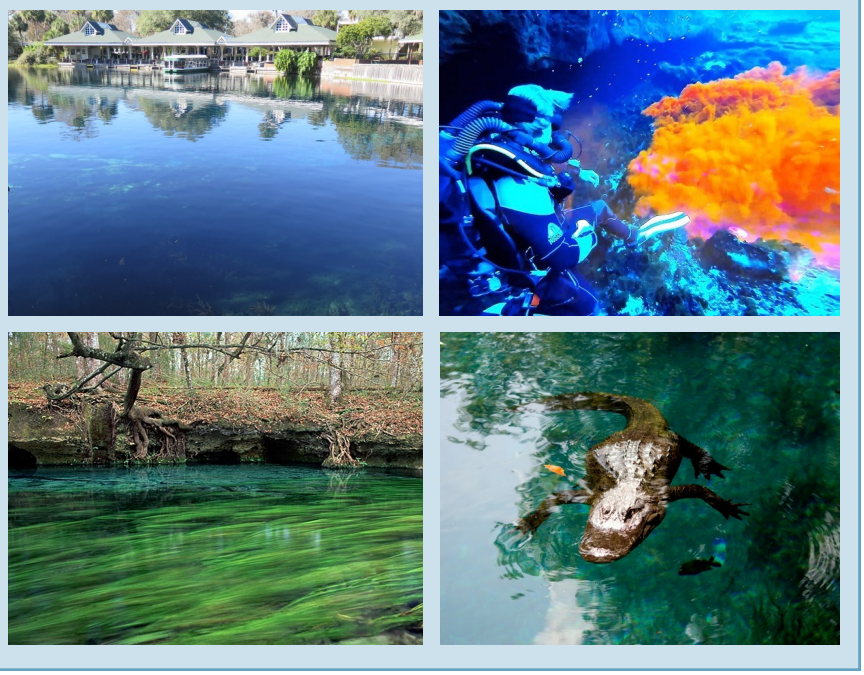

Collaborative Research Initiative on
Sustainability and Protection of Springs [**CRISPS]**

Section 7

[Work Order No: 3]

ANNUAL REPORT

July 2015

submitted to:

St. Johns River Water Management District
Springs Protection Initiative [SPI], UF Contract # 27789

UF | UNIVERSITY of FLORIDA
Water Institute

C R I S P S

Section 7

PHYSICOCHEMISTRY

Nitrate Inhibition of Submerged Aquatic Vegetation: Investigation of the Nitrogen Overload Hypothesis

Annual Report 2015
Work Order No. 3: Part 2 of 3

Principal Investigators:

Todd Z. Osborne, University of Florida
Michael F. Coveney, St. Johns River Water Management District

Project Team:
Todd Z. Osborne
Leah H. Laplaca, MS Student
Tracey B. Schafer, MS Student
Jacob Johansen, Post Doctoral Associate
Whitney Laboratory of Marine for Marine Bioscience
Soil and Water Science Department
University of Florida

Michael F. Coveney
Robert A. Mattson
St. Johns River Water Management District

This document reports interim progress of a work order in the first year of a 3-year project in compliance with Agreement between University of Florida (UF) and St. Johns River Water Management District (SJRWMD) UF Contract #27789. It is part of the *UF Collaborative Research Initiative on Springs Protection and Sustainability (CRISPS)* and supports the science component of *the SJRWMD Springs Protection Initiative (SPI).*

7.i PROLOGUE

In response to observations of declining populations and productivity of submerged aquatic vegetation (SAV) in several Florida springs, an investigation has been initiated to determine the potential role of nitrate/ nitrite (NOx) concentrations in the inhibition of SAV growth. The proposed mechanism of inhibition stems from the hypothesis that two dominant species of SAV, *Vallisneria americana* and *Sagittaria kurziana* have not yet evolved a metabolic mechanism to turn off nitrate reductase, an enzyme that converts readily available nitrate into ammonia. Because ammonia is phyto-toxic at elevated concentrations, it must be utilized rapidly, predominantly in protein synthesis. This process requires energy from photosynthate and under elevated NOx availability, could produce a significant energetic burden on SAV.

Evidence for such a process is expected to be found in several key places. First and foremost, under controlled conditions where NO_3-Nconcentration can be modulated, the root to shoot ratio, leaf blade elongation rate, tissue protein, and abundance of starch storage in tissues of both species would support the hypotheses. Quantitative observations of these characteristics (biometric and tissue chemistry) under several relevant levels of NO_3–N comprise the majority of this investigation where both species of SAV are grown in mesocosms. In addition to this mesocosm work, field assessment of nitrate reductase activity (NRA) across several springs has been initiated to determine the naturally occurring range of this enzyme in SAV tissue to determine if it is regulated by concentration of NO_3-N.

To date, a multiple tank recirculating mesocosm array has been constructed and both species of SAV have been established and are growing under a range of NO_3-N concentrations. At the cessation of the growing season, plants will be harvested and biometry and chemical analyses completed. Further investigations include role of hypoxia on survivorship and proliferation of SAV. Algae shear stress tests will also be performed on plants during the harvest phase of year 1 and 2 to determine the velocity required to remove periphytic algal growth from both species.

An additional investigation into the role of hypoxia on the extirpation of invertebrate herbivores in the Silver River has also been initiated under this work order due in large to the opportunistic availability of respirometry equipment and resident expertise at the Whitney Laboratory for Marine Bioscience where the SAV mesocosms work is taking place. The species of invertebrates tested for hypoxia thresholds to date include

Section 7.1 Direct Effects of Elevated NO_3-N in the Growth of *Vallisneria americana* and *Sagittaria kurziana* in Spring Ecosystems.

7.1.1 ABSTRACT

Current observations of water quality in groundwater discharge from springs in Florida show anthropogenic enrichment of nitrate plus nitrite (NO_3-N) generally attributed to fertilizer application and/or wastewater or manure sources in individual spring sheds. Excessive levels of NO_3-N have been implicated in eutrophication of, and observed changes in, submerged aquatic vegetation (SAV) communities in several spring runs. While the indirect effects of nitrogen (N)

enrichment on aquatic macrophytes are well-documented (i.e, algal productivity resulting in shading of macrophytes), there is considerably less information available concerning direct effects of NO_3-N such as toxicity or inhibition of macrophyte growth.

This ongoing work explores the hypothesis that nitrate may have direct inhibitory effects on SAV growth in Florida springs via analysis of nitrate reductase activity (NRA) and anatomical responses, including quantification of starch grains by assay and visualization and measurement of starch, arenchyma, epidermis and vascular bundles. Ratios of root to shoot biomass, measured at the end of the growing season, will further help determine the effect of NO_3-N on SAV growth.

7.1.2 INTRODUCTION

Phosphorus (P) is often considered the limiting nutrient in freshwater ecosystems, and thus when available in excess, it is implicated as a causative agent in eutrophication. Nitrogen (N), however, has been traditionally viewed by many as a lesser contributor to eutrophication of freshwaters, either because of the overshadowing nature of P issues or due to the ability of many cyanobacteria to fix atmospheric N, a process that significantly reduces perceived N limitation. This prevailing view stems from research conducted to elucidate the role of P in eutrophication (Schindler and Fee 1974; Schindler 1978) following the 1960s chemical industry claims of no effect of increased P in aquatic systems (Barker et al. 2008). More recently, several researchers have reasserted the view that N either alone or in concert with P, may exert ultimate control over algal productivity and subsequently macrophyte productivity in aquatic systems across the globe (Turpin 1991; Talling and Lemoalle 1998; Maberly et al. 2002; Clark and Baldwin 2002; James et al. 2003; James et al. 2005; Sagario et al. 2005; Dzialowski et al. 2005; Weyhenmeyer et al. 2007; Li et al. 2008). The extreme of this viewpoint suggests that N may have been the limiting nutrient in most northern hemisphere lakes and rivers prior to substantial N fertilizer utilization, which precipitated P limitation in enriched systems (Bergstrom and Jansson 2006). A recent meta-analysis of published nutrient limitation studies found the number of N limitation cases to equal those of P limitation (Elser et al. 2007) and a significant number of cases of co-limitation. Moss (1990) contends that co-limitation was the normal condition prior to anthropogenic enrichment of nutrients. Recently, the role of N enrichment in alteration of ecosystem health has received renewed attention in aquatic ecosystems (Porter et al. 2013; Baron et al. 2013).

Countless studies of eutrophication of freshwater ecosystems have observed a catastrophic shift from macrophyte to phytoplankton dominance after anthropogenic increases in available P (Wetzel 2001; Lacoul and Freedman 2005; Reddy and DeLaune 2008). The process involves rapid utilization of excess nutrients by phytoplankton and epiphytic algae, which in turn enables explosive algal growth. The shift in primary productivity is also self- reinforcing, as turbidity increases with algal productivity, light becomes limiting to submerged aquatic vegetation (SAV)(Burkholder et al. 1992; Van den Berg et al. 1999). Death of SAV and decomposition of biomass only exacerbates excessive nutrient conditions.

Often, N and P have a positive synergistic effect on phytoplankton productivity. In a study by Sagarario et al. (2005) N and P additions alone did not show a significant effect, but when

combined, the increase in phytoplankton and epiphytic algal biomass was dramatic. In addition to light attenuation by phytoplankton proliferation, epiphyte biomass burden and subsequent shading can be a primary causal mechanism for SAV mortality under eutrophic conditions (Borum 1985). In many spring runs in Florida, proliferation of epiphytic algae, as well as benthic macroalgae, have been observed concomitantly with declines of SAV communities (Stevenson et al. 2004; Frazer et al. 2006; Pinowska et al. 2007; Stevenson et al. 2007; Quinlan et al. 2008; Brown et al. 2008). Water quality in groundwater discharged from many springs in Florida has shown significant increases in NO_3-N concentration, attributed predominantly to fertilizer application and/or wastewater or manure sources in individual spring sheds (Jones et al. 1996; Katz 2004; Albertin et al. 2012). Odum (1957) reported mean NO_3-N concentration of 0.45 mg L^{-1} for Silver Springs in the 1950s which had risen to over 1 mg L^{-1} by 2005 (Munch et al. 2006; Quinlan et al. 2008). More dramatically, Rainbow River NO_3-N concentrations have increased from 0.08 to 1.22 mg L^{-1} (a 15-fold increase) over last 50 years (Cowell and Dawes 2008). Interestingly, during this period of increasing NO_3-N, P concentrations have remained constant (Maddox et al. 1992; Scott et al. 2004). These observations, while somewhat inconsistent with the common eutrophication paradigm, have prompted several hypotheses as to the role of increased nitrogen availability in the observed loss of SAV in spring systems statewide.

This manuscript reviews these competing hypotheses concerning the relationship between elevated NO_3-N and observed ecological changes, specifically declines in SAV coverage and increases in epiphytic and benthic algae, in regional springs ecosystems. Significant attention is given to potential inhibitory effects of elevated NO_3-N on SAV growth in springs and possible mechanisms for this inhibition are discussed. These mechanisms focus on the assimilative nitrate reduction process, resulting buildup of toxic ammonia (NH_3), and energetic consequences of unregulated NO_3-N uptake on SAV. This discussion concludes with a call for research to clarify the role of elevated NO_3-N in the observed degradation of SAV communities.

7.1.2.1 Competing Hypotheses

The initial hypothesis posited by members of the scientific community, as well as the general public, was that the increase in N availability, observed as NO_3-N concentration in spring waters, alleviated N limitation and therefore was responsible for a shift in primary productivity from SAV to epiphytic algae and benthic macroalgae. While there have been studies to report N utilization by algal mats in Florida springs (Cowell and Botts 1994; Cowell and Dawes 2004; Albertin 2009; Sickman et al. 2009), there have been several observations that contradict the normal eutrophication paradigm, namely the lack of significant increase in other forms of N (Cohen et al. 2007) or P (Maddox et al. 1992; Scott et al. 2004) in spring waters. Brown et al. (2008) concluded that there was insufficient evidence to link nitrate enrichment to changes in algal cover. Heffernan et al. (2010) argue convincingly that studies by Canfield and Hoyer (1988) and Duarte and Canfield (1990) found no relationships between nutrients and total vegetative biomass in spring runs as would be expected under nutrient limitation scenarios, and that recent surveys of algal biomass have not found any significant linkage to N or P concentrations (Stevenson et al. 2004; Stevenson et al. 2007). Further, Heffernan et al. (2010) and Liebowitz (2013) report stronger relationships between dissolved oxygen (DO), grazer populations, and algal abundance than with nutrients.

Heffernan et al. (2010) suggests looking to other drivers of algal proliferation in spring systems, including DO control of invertebrate grazers, resulting in altered trophic structure in springs to favor algal dominance. Liebowitz (2013) reports a significant negative association between algal and gastropod biomass in Florida springs suggesting top down control of algae by invertebrate grazers, a finding supported by several studies of grazer control of algae in other systems (Hildebrand 2002; Heck and Valentine 2007; Gruner et al. 2008; Baum and Worm 2009; Estes et al. 2011). Further, Liebowitz (2013) also found a significant relationship between dissolved oxygen (DO) and gastropod biomass in a survey of 11 springs, suggesting DO has a significant indirect effect on algal biomass via controlling grazer abundance and/or activity. Under low flow or current velocity conditions, nutrient enrichment and subsequent algal growth may outpace grazer pressure resulting in severe light reductions (Harlin and Thorne-Miller 1981). Alternatively, under similar nutrient enrichment and moderate to high flushing or exchange of water (as in lotic or tidally influenced systems), herbivores have been observed to control epiphytic algal biomass (Neckles 1993; Liebowitz (2013) argues that hysteretic responses of grazer populations to disturbances could be responsible for the over abundance of algae in springs where no clear grazer stress is present. For instance, invasive plant control measures utilizing herbicides and copper compounds are widely employed with known negative impacts on grazer populations (Evans 2008). Such a disturbance could enable algal populations to exceed thresholds for grazer control. This gives rise to a second hypothesis that grazer control of algae in springs has been altered by DO in some cases and by episodic or unknown exposures to other stressors.

The presence of herbicides or other agrochemicals that may be inhibitory to either algal grazers or macrophytes themselves supports a third hypothesis which states that a "nitrate cohort" (substance[s] associated with the same mechanisms involved in nitrate increases such as land use or waste disposal) has an inhibitory or toxic effect on SAV. The widespread use of agro-chemicals such as commercial pesticides, fungicides and herbicides increases potential for these compounds to impact spring ecosystems. Several anthropogenic organic compounds have been detected in springs, however, the low levels observed did not elicit alarm (Phelps et al. 2006; Phelps 2004). Recent increases in consumer use of compounds such as atrazine, a herbicidal fertilizer additive, (Ackerman 2007) and triclosan, an antimicrobial agent, (Fulton et al. 2010) suggest these compounds may have deleterious effects on SAV (and/or grazer population dynamics).

A fourth and least well understood hypothesis is that nitrate itself has an inhibitory (direct) effect on SAV growth resulting in a shift to algae dominated system. The accepted view of nitrate and ammonia combined with P to create conditions for algal dominance and subsequent shading out of macrophytes (Mulligan et al. 1976) is that of an indirect effect. However, a direct effect of nutrient enrichment has been suggested as a factor in macrophyte disappearance in aquatic systems undergoing enrichment (Genevieve et al. 1997; Farnsworth and Baker 2000). Several authors (Klotzli 1971; Schroder 1979; Boar et al. 1989) have reported correlation of reed bed disintegration and increases in nitrate loading to lakes in England. Decreases in *Phragmites australis* root and rhizome production was observed in concert with increased nitrate loading (Ulrich and Burton 1985). Ulrich and Burton (1985) also reported that nitrate stimulated growth and overall biomass increased with increased nitrate availability, however, below ground

biomass production (roots and rhizomes) did not increase at concentrations up to 6 mg NO_3-N L^{-1}. These NO_3-N concentrations resulted in significant decreases in below ground to above ground biomass ratios and resulted in an overall decline in health of the reed stands. Nitrate to potassium ratios in surface waters and in tissues are correlated with highest degree of degradation of *Phragmites australis* beds (Boar et al. 1989), however, the causative mechanism is unknown as is the potential for synergistic effects of increased availability of N and K. Because the aforementioned species is an emergent macrophyte, free of algal shading, it serves as a significant indicator of potential inhibitory effects of NO_3-N on plant growth. An in depth review of current literature suggests several authors have observed apparent direct inhibitory effects of NO_3-N on SAV in both marine and freshwater environments. The remainder of this paper will synthesize the available literature and investigate potential causal mechanisms for the observed effects of elevated NO_3-N on SAV.

7.1.2.2 Evidence of Direct Effects of Nitrate on SAV

Opportunistic luxury consumption of nutrients is characteristic of SAV and thus accumulation in tissues is anticipated for macrophytes adapted to limited nutrient availability, such as seagrasses and some freshwater SAV (Wetzel 2001). The prevailing viewpoint is that most macrophytes acquire nitrogen via roots (Cedergreen and Madsen 2003), however, foliar absorption is also a viable mechanism when sediment sources are not available or abundant (Barko and Smart 1986). When ammonium nitrogen (NH_4-N) concentration exceeds 0.1 mg L^{-1}, macrophytes preferentially use NH_4-N (Nichols and Keeny 1976). Hence, the dominant form of N utilized by most SAV is NH_4-N, but under N limitation nitrate is also utilized, predominately from the water column. Due to the abundance of NO_3-N, this is the presumed mechanism for N uptake by SAV in Florida springs. Several researchers have made qualitative observations of SAV inhibition closest to spring vents where NO_3-N concentrations are highest (Munch et al. 2006; Osborne and Mattson unpublished data- Figure 7.1.1). Similarly, several authors suggest observed declines in macrophytes in other systems was a direct effect of increased NO_3-N (Burkholder et al. 1992; Burkholder et al. 1994; Wang et al. 2012), suggesting closer investigation of this phenomenon is warranted.

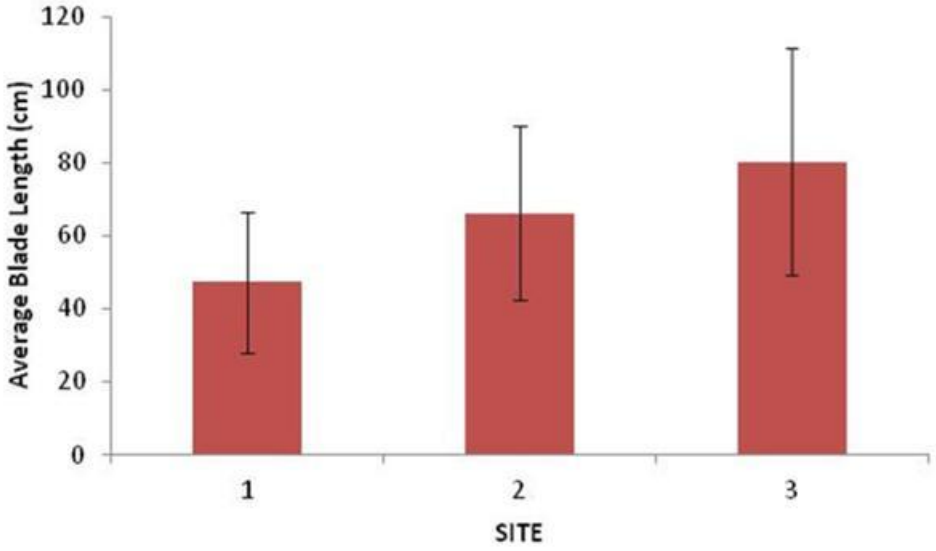

Figure 7.1.1. Average blade length of V. americana along a transect down the Wekiva River (Osborne and Mattson unpublished data). NO_3-N concentration declines downstream from site 1-3 which spans a distance of approximately 9 miles. These findings support the observation of increased vigor in *V. americana* as NO_3-N concentrations decrease.

Burkholder et al. (1992) report that *Zostera marina* (eelgrass) exhibited highly negative physiological effects (even death) when dosed with 0.05, 0.1 and 0.5 mg NO_3-N L^{-1}. Although a marine species, this plant shows extreme sensitivity to increased nitrate evidenced through loss of carbon storage in roots unrelated to shading by algae. The apparent lack of an inhibition or regulation mechanism of nitrate uptake by eelgrass (Roth and Pregnall 1988) was implicated in the observed disruption of internal nutrient ratios, presumably due to carbon expenditure in amino acid synthesis to reduce intracellular ammonia toxicity. Hierarchical partitioning analysis of water quality parameters found NO_3-N exerted the greatest detrimental effect on charophyte occurrence in wetlands of the UK (Lambert and Davy 2011). *In situ* studies of *Chara globularis* showed that it was extremely sensitive to nitrate with maximal relative growth rate observed at 0.5 mg NO_3-N L^{-1} and a linear decline in growth with higher concentrations. At 6 mg NO_3-N L^{-1}, growth was severely limited, similar to results of no NO_3-N treatment (Lambert and Davy 2011). Similarly, biomass accumulation was strongly inhibited by nutrient accumulation (N) in *Potamogeton maackianus* A. Been (Ni 2001). The most definitive observations of inhibition were in the form of shrinkage of arenchyma tissues and disappearance of starches and chloroplasts observed in increased NO_3-N and NH_4-N concentration treatments of *Vallisneria natans* (Wang et al. 2012.)

The paradigm of nitrogen effects on water clarity often overshadows potential direct effects of excess N on SAV. For instance, Sagrario et al. (2005) reported that high N is not directly inhibitory to *Potamogeton pectinatus* L., *Elodea canadensis* and *Nymphea sp*. at 10 mg L^{-1} of total N (TN) due to overpowering effects of increased algal shading. However, closer inspection of the results indicates moderate dosing of 4 mg TN L^{-1} resulted in decreased growth with respect to controls under equal or better water clarity, a noteworthy result that went

unmentioned. Further, summer TN levels declined significantly in mesocosms truncating the duration of exposure for macrophytes, which likely confound interpretation of the results by the authors. In a study by Li et al. (2008), NO_3-N additions were noted to increase *Vallisneria spinulosa* biomass over control at 2.5, 5.0, 7.5 mg L^{-1} concentrations in water column but at 10 mg L^{-1} growth was not significantly different from control (1 mg L^{-1}) suggesting some inhibition of growth. It is unclear why the authors did not conclude that a NO_3-N threshold had been exceeded between 7.5 and 10 mg L^{-1}. This lack of interpretation by some authors is likely due to a strong focus on algal production and subsequent shading, not direct effects of nitrate on SAV (Sturgis and Murray 1997). Further, variability among species with respect to effects of NO_3-N appears to be high (Burkholder et al. 1994). This is exemplified by conflicting reports on potential inhibition of macrophyte growth by excessive water column nitrate (Li et al 2005). Best (1980) reported no inhibition of *Ceratophyllum demersum* at concentrations of up to 105 mg NO_3-N L^{-1} but did observe ammonia toxicity at 45 mg NH_4-N L^{-1}. This finding suggests that *C. demersum* is well suited to luxury uptake of N. Conversely, Lambert and Davy (2011) assert a mean annual concentration limit of 2 mg NO_3-N L^{-1} is necessary to protect charophytes.

Our review of available literature did not find studies of N enrichment with SAV species common in Florida spring systems (*Vallisneria americana, Sagittaria kurziana, Najas* spp., *Potamogeton* spp.*)*. However, the potential mechanisms of inhibition, which likely vary among species, are discussed here in general terms for SAV and are viewed as potential mechanisms until tested on individual species of interest.

7.1.2.3 Potential Mechanisms of Inhibition

Nitrate toxicity has been well documented for vertebrate animals (including humans) (Kim-Shapiro et al. 2005) as well as invertebrates (Mattson et al. 2007). However, the potential of NO_3-N toxicity or inhibition of SAV is not well understood, nor is it intuitive given our understanding of mechanisms of toxicity for higher organisms. Observations coinciding with elevated inorganic N (NO_3-N and or NH_4-N) include stunted growth, iron deficiency, amino acid accumulation, oxidative stress and structural tissue damage (Burkholder et al 1992; Smolders et al. 1997 Smolders et al. 2000; van der Heide et al. 2005; Wang et al. 2012). To better determine potential inhibitory mechanism of NO_3-N, a closer look at the process of assimilation is necessary.

7.1.2.4 Assimilatory Nitrate Reduction

Most aquatic plants absorb nitrate, which is then sequentially converted to nitrite and then ammonium by the nitrate reductase system (Salisbury and Ross 1992). In SAV before nitrate can be utilized by the plants, it must be converted to ammonium by a series of sequential enzyme mediated reactions (Figure 7.1.2) involving nitrate reductase and nitrite reductase (Guerrero et al. 1981). This process is termed assimilatory nitrate reduction (ANR) and results in ammonium being incorporated into amino acids. Genetic or environmental factors, such as light, temperature, depth, pH, and location within vegetated patch (edge versus center) (Roth and Pregnall 1988; van der Heide et al. 2008), can modulate this series of biochemical reactions resulting in a high level of variability among species with respect to nitrate reduction processes and rates (Pate 1980; Guerrero et al. 1981). Water temperature can be problematic for SAV by increasing respiration rates and impairing enzyme function (Zimmerman et al. 1989; Lacoul and

Freedman 2006; Riis et al. 2012), however, SAV in spring runs generally do not experience thermal stress due to the thermal consistency of groundwater (unless exposed in shallow backwaters).

Uptake of NO_3-N is driven primarily by external nitrate concentrations (Marschner 1998) and in aquatic macrophytes, increased water column concentrations of NO_3-N results in significant increases in nitrate reductase activity (NRA) (Cedergreen and Madsen 2003). Studies of *Zostera marina* indicate newer leaves are more active with respect to NRA and rates between individual plants can be variable with a 2-3 fold difference (Roth and Pregnall 1988). It has been suggested that differences between root and shoot NRA depends upon uptake rates of individual species (Gojon et al. 1994)and that location of nitrate reduction (root or shoot) is also species specific (Cedergreen and Madsen 2003). From an energetic standpoint, photosynthetic tissues would be a more advantageous location for NRA to occur (Raven 1985) and this appears to be the case for SAV (Roth and Pregnall 1988).

There is little intracellular space to store nitrate, therefore rapid conversion to ammonia occurs before vacuolar storage. Increasing ammonia requires plants to avoid toxicity by allocating carbon and energy to protein (amino acid) synthesis to alleviate ammonia buildup (Salisbury and Ross 1992). Under normal exposure, ANR uses approximately 25% of the reductant energy produced by photosynthesis and root/shoot respiration (Crawford 1995).

Closer inspection of the biochemical pathways for ANR reveals some significant differences between SAV and filamentous macroalgae, the two competing primary producers in many springs. Assimilatory nitrate reductase activity in green algae and higher plants is dependant upon NAD(P)H for reducing power (Figure 7.1.3A). This first reaction can be inhibited by p-HMB, cyanide, azide, and cyanate. Further, the negative feedback inhibitor of the nitrate reductase enzyme in some species is nitrite, which competitively binds with nitrate reductase. This is not the case for all species as reported by Roth and Pregnall (1988) who documented the inability of *Zostera marina* to "turn off" or regulate nitrate reductase, a very critical observation with respect to the potential for some SAV to moderate this enzyme. Cyanobacteria, on the other hand, cannot utilize reduced pyridine nucleotides as do green algae and higher plants. The alternative electron donor for algal nitrate reductase (Figure 7.1.3B) is ferredoxin (Guerrero et al. 1981). This reaction appears to give cyanobacteria a slight energetic advantage as the ΔG of the reaction is 4.6 Kcal greater per mole for ferredoxin mediated reduction versus NAD(P)H. The second reduction reaction, nitrite reduction to ammonium, is very similar in all photosynthetic organisms and utilizes ferredoxin as the electron donor specifically.

Ferredoxin requires iron in its structural complex, thus increased iron in springs may also give cyanobacteria a competitive advantage over green algae and SAV. This is due to the inability of the latter organisms to utilize ferredoxin in nitrate reduction. Smolders et al. (1997) report iron deficiency in SAV exposed to higher levels of NO_3-N, presumably due to the need for ferredoxin in nitrite reduction. Because NAD(P)H also serves as reducing power for many other metabolic reactions, utilization of NAD(P)H for nitrate reductase results in a decrease of other metabolic

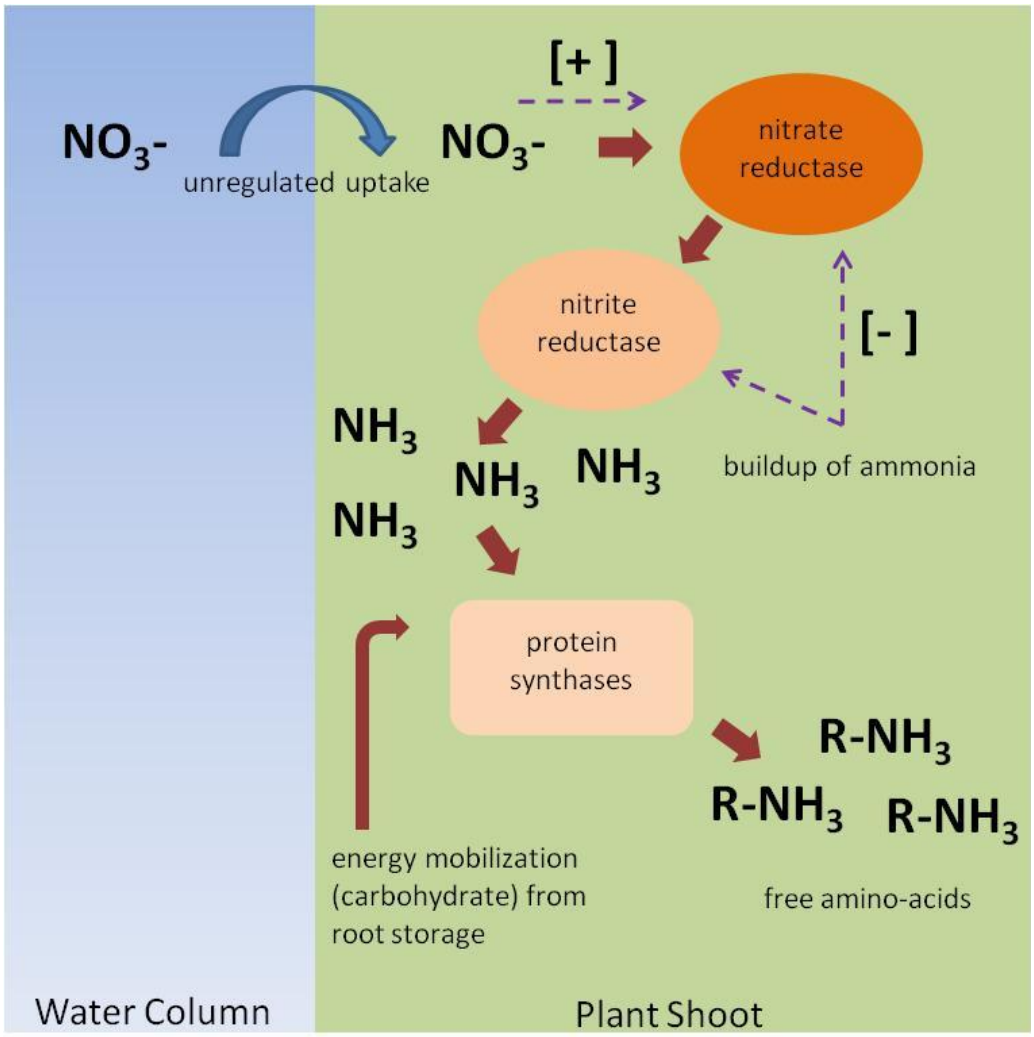

Figure 7.1.2. Conceptual model of nitrate overload hypothesis. Uptake of nitrate is unregulated at the cellular level and presence of nitrate induces nitrate reduction to ammonia. Buildup of ammonia should be a negative feedback[-] for nitrate reduction enzymes; however this process appears not to function in some species. Ammonia can be toxic to plants and therefore is alleviated via protein synthesis, which requires energetic inputs from plant carbohydrate stores. Buildup of free amino acids and depletion of root carbohydrate stores are potential diagnostics of nitrate overload in SAV.

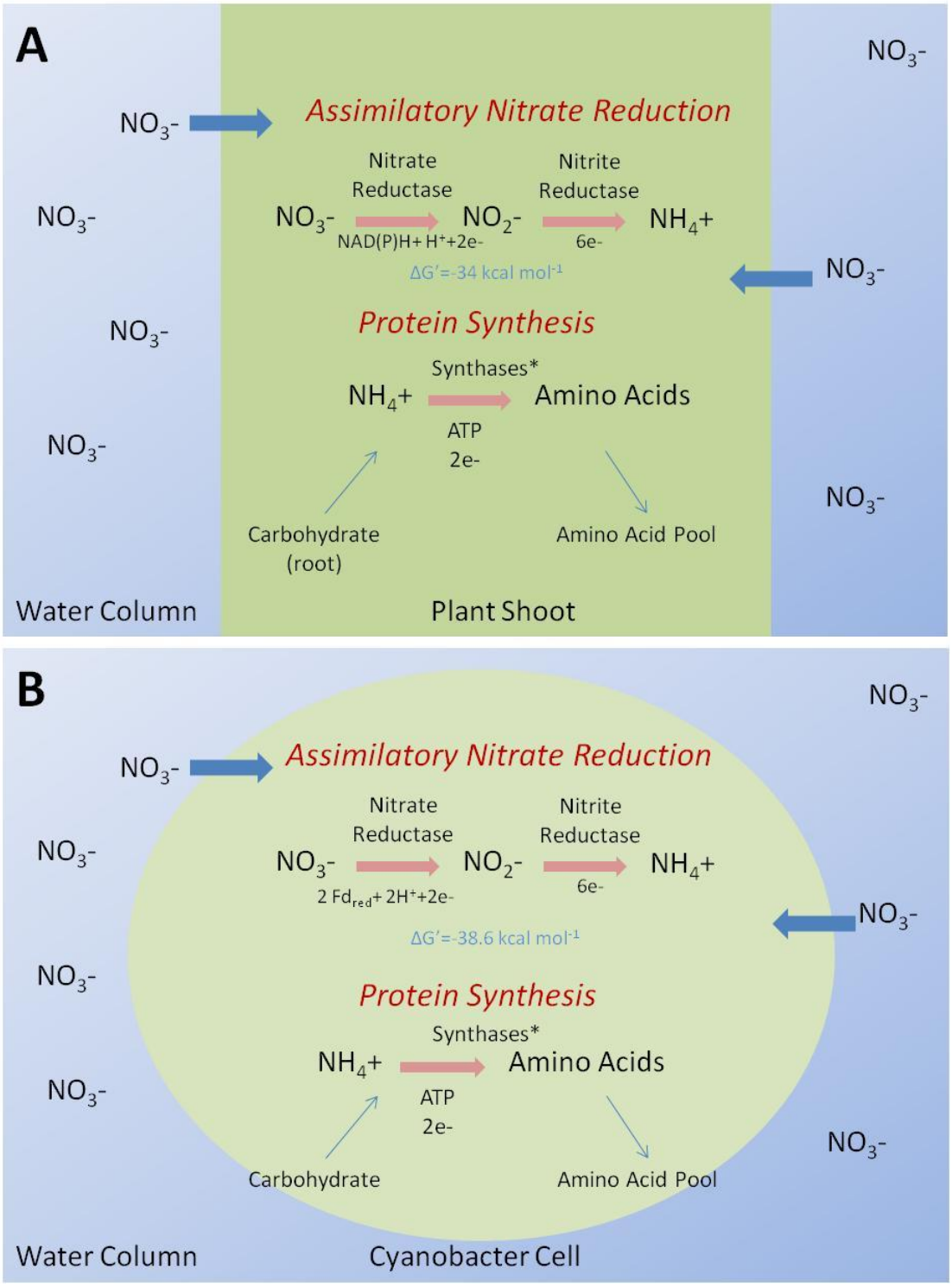

Figure 7.1.3. Assimilatory nitrate reduction in [A] SAV shoot and [B] cyanobacterial cell. Note cyanobacteria cannot utilize NAD(P)H as an electron donor in the reduction of nitrate to nitrite and thus rely solely upon ferrodoxin. Also note a slight energetic advantage [ΔG'] exists for cyanobacteria in the reduction of nitrate to nitrite.

reactions and potential buildup of other metabolites within cells, which is another potential source of toxicity (Lea and Miflin 1979). Of greater concern, the accumulation of ammonia, the end product of ANR, can be extremely detrimental to photosynthetic organisms. Ammonia toxicity represents a primary potential source of toxicity for SAV due to the combined effect of excess nitrate availability and the possibility of poorly regulated ANR, which can result in ammonia buildup in tissues.

7.1.2.5 Ammonium Toxicity

Ammonia toxicity is well documented in terrestrial plants (Salisbury and Ross 1992) as well as seagrasses (Katwijik et al. 1997; Hemminga and Duarte 2000). In most plants, ammonium toxicity is often associated with a decrease in soluble sugars in tissues due to ammonium assimilation and resulting need for protein synthesis (Cramer et al. 1993) or in excessive tissue concentrations that exceed the plants' ability to incorporate into amino acids (Meher and Mohr 1989). Inhibitory effects of high ammonium on SAV have been documented (Best 1980; Smolders et al. 1996) and implicated in succession of freshwater SAV communities (Schuurke et al. 1986; Brouwer et al. 1997; Clarke and Baldwin. 2002). Excessive ammonium can inhibit photosynthesis (Cao et al. 2004) resulting in diminished soluble sugar production and lead to necrosis in some macrophytes (Smolders et al. 1996). Water column ammonia concentrations >1 mg L^{-1} resulted in decreased soluble sugar content in *Potamogeton crispus* and increased soluble amino acids (Cao et al. 2004). Interestingly, in the study by Cao et al. (2004) responses of amino acids and soluble sugar indicators of ammonia stress were dependent upon duration of exposure. Further, activity of ascorbate peroxidase and superoxide dismutase (both anti-oxidant enzymes) were highest at 1 mg L^{-1} ammonium and decreased significantly as ammonium increased (Cao et al. 2004).

To alleviate NH_4-N stress, plants must convert the free ammonium to amino acids via synthesis (Figures 1 and 2). This process has an energetic cost, requiring carbon and energy inputs from the plant. Lambert and Davy (2011) invoke energetic expenditure in regulating ammonia internally as a likely cause of growth decline in *Chara* sp. exposed to NO_3-N in excess of 2 mg L^{-1}. The energetic demand of reducing ammonia toxicity, in concert with unregulated ANR, could represent a very significant stress on SAV (Smolders et al. 2000; Wang et al. 2012).

7.1.2.6 Amino-Acid Synthesis

Ammonia is incorporated into α-amino-acids by way of one or both known pathways (Figure 7.1.2), the glutamate dehydrogenase and the glutamate synthetase-glutamate synthase pathway (Guerrero et al. 1981). Buildup of free amino acids in tissues is considered an indication of "nitrogen overload" or impending toxicity due to excessive nitrogen availability (Smolders et al. 1996; Smolders et al. 2000; Wang et al. 2012). Specific types of amino acids that accumulate (for instance arginine, glutamine, asparagines) are dependant on the stresses involved (toxicity, mineral deficiency, grazer pressure) and the species of SAV (Rabe and Lovatt 1986; Rabe 1990; Marschner 1998; Smolders et al. 2000). Significant evidence of the nitrogen overload hypothesis is presented by Wang et al. (2012) who reported reduction of arenchyma tissue, chloroplasts and starch grains in tissues of *Vallisneria natans* exposed to increased nitrate and ammonia levels. The authors contend that loss of structures and starch content is related to photosynthate required

to reduce nitrate to ammonia and further sequester toxic ammonia in amino acids, a process that requires significant energy expenditure by plants. Due to the high energetic demand, NO_3-N overload may perhaps lead to susceptibility to pathogens. For example, *Zostera marina*, as well as some other angiosperms, are known to decrease production of antimicrobial compounds such as phenolics during times of increased protein synthesis associated with N enrichment (Buchsbaum et al. 1990).

7.1.2.7 Summary of Mechanisms of Inhibition

Review of the current literature concerning NO_3-N effects on SAV is compelling in that the process of ANR is highly variable among species and the potential for unregulated uptake, an adaptation ostensibly stemming from luxury uptake, could induce the "nitrogen overload" condition (Smolders et al. 1996; Smolders et al 2000; Boedeltje et al. 2005; Wang et al. 2012). The resulting accumulation of ammonia, the end product of ANR, can itself be a significant stressor to plants or, by necessitating protein synthesis to alleviate ammonia stress, can cause depletion of SAV carbohydrate stores (Guerrero et al. 1981; Wang et al. 2012). In other ecosystems, potential NO_3-N toxicity may be reduced based upon density of SAV (van der Heide et al. 2010), however, under the unique lotic conditions of springs (increasing nitrate concentrations and constant exposure), this effect is not anticipated. Determining the direct effects of NO_3-N on SAV native to Florida springs will be of primary importance to directing management effort with respect to springs restoration.

7.1.2.8 Ecological Implications

Globally, many aquatic ecosystems have been altered, some seemingly irrevocably, by the anthropogenic addition of excessive nutrients (N and P). For example, in both temperate and tropical lakes receiving nutrient enrichment, catastrophic shifts from macrophyte to phytoplankton dominance have been observed with regularity in the last half century. In Florida, significant effort has been invested in ameliorating these catastrophic shifts on large lakes such as Apopka (Dunne et al. 2012) or Okeechobee (James et al. 2011; Harwell and Sharfstein 2009). This shift in primary productivity has resounding effects throughout the food web. Further, habitat loss and susceptibility to altered environmental conditions (for example: hypoxia, shifts in pH) can have detrimental effects on established flora and fauna. In wetlands such as the Everglades, nutrient enrichment has resulted in marked shifts in the vegetation community from the native *Cladium jamaicense* dominated ridges and *Nymphaea odorata* and *Eleocharis interstincta* dominated sloughs to monotypic stands of *Typha latifolia* (Osborne et al. 2011). This shift in vegetation precipitated significant changes to ecosystem services such as carbon storage, biogeochemical cycling of nutrients, and habitat quality for fauna. Similarly, Florida's springs systems, which have immense ecological, cultural and economic value to the state have undergone significant ecological degradation in recent decades. Therefore, concern exists for determining the relationship between these changes and the observed increase in NO_3-N in springs. Of primary concern is elucidating the role nitrate enrichment has had (whether direct or indirect via synergistic interactions with other stressors) in the observed decline of these systems.

7.1.2.9 Objectives

The objectives of this research are to investigate if SAV native to Florida springs are experiencing any inhibitory effects due to elevated NO_3-N concentrations by one or more of the

proposed mechanisms: 1) unregulated NO_3-N uptake and reduction, 2) NH_3-N toxicity from excess accumulation in vivo, and 3) carbohydrate depletion from intercellular or root storages. The mechanisms will be evaluated in SAV in both mesocosms and in leaf samples collected from selected sites within Silver River, Alexander Springs, and Wekiva River.

7.1.3 MATERIALS AND METHODS

7.1.3.1 Site Description

All experiments were conducted in either controlled growth chambers in the laboratory or in an outdoor mesocosm facility constructed onsite at the University of Florida Whitney Laboratory for Marine Bioscience in St. Augustine, FL.

Mesocosms were constructed of high density polyethylene (HDPE) tanks of approximately 120 gallon volume (72" L x 24"W x 34"H)(Figure 7.1.4). All tanks were plumbed with inert PVC and connected to opaque HDPE 250 gallon drums (water reservoirs) where flow is controlled via submersible pumps. The mesocosm facility is housed at the Whitney Laboratory in St. Augustine. Spring water was pumped from the onsite well at Silver Springs State Park and transported to the mesocosms via tanker truck. Regional well water is transported regularly to maintain water levels in experimental tanks in response to evaporation. Temperature control was initiated midsummer using frozen water bottles and subsequently, electric chiller units.

7.1.3.2 Field Methods

Collection of live plants was conducted along the middle reach of the Silver River in June of 2015 via motorized vessel under Florida Department of Agriculture and Consumer Services (FDACS) permit number 48016783. Suitable collection areas were identified in shallow (< 2 m depth) waters near the banks of the river and site GPS coordinates recorded, however, no site markers were installed. Individual ramets of each species were collected by hand and placed in coolers in the river water and transported back to the laboratory. Care was taken to harvest smaller plants (<20 cm in length) in a highly sustainable way with no more than 2-4 individuals being removed from a square meter. This method allowed harvest without observable denuding of vegetated areas.

Collection of plant material for nitrate reductase activity (NRA) was conducted in several locations by hand and single blades of each species were removed and stored in a 3 L liquid nitrogen dewar (US Solid Cryogenics ®) and returned to the laboratory for analysis.

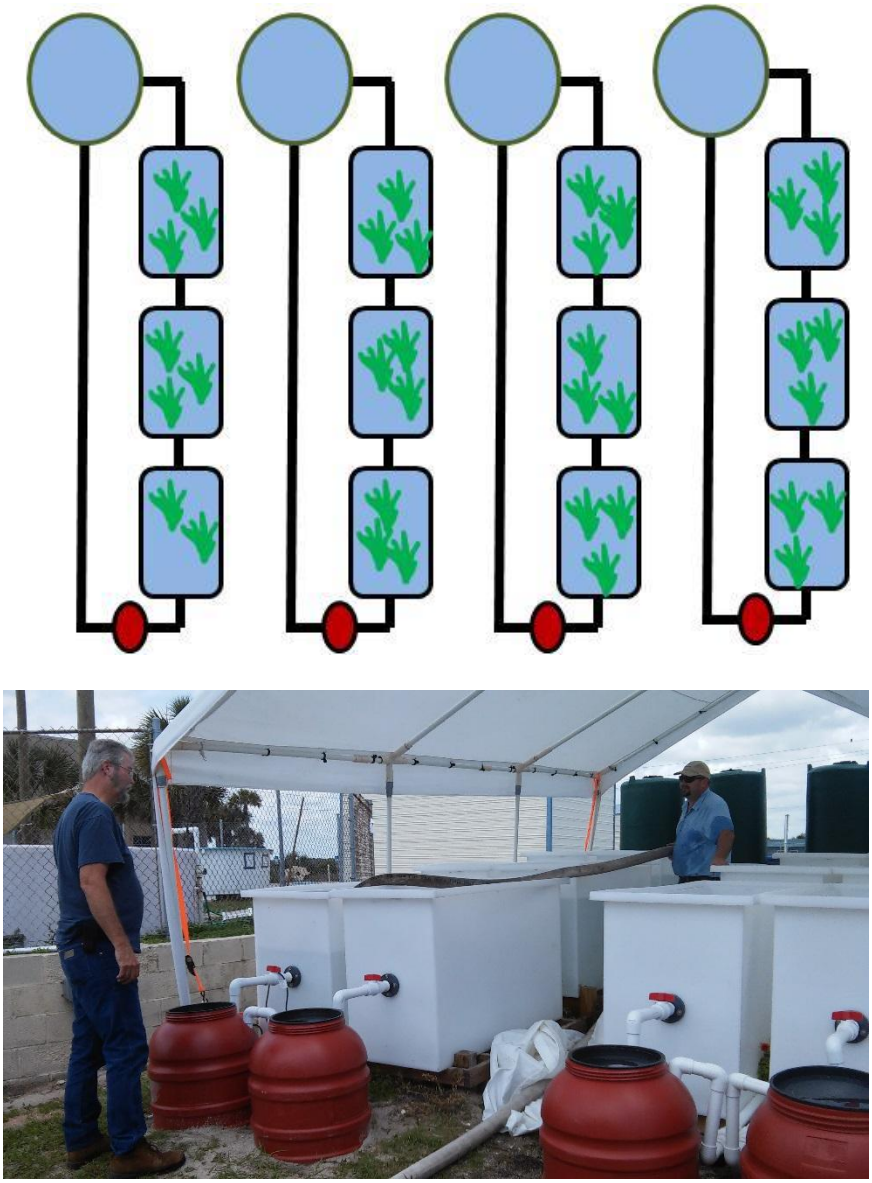

Figure7.1.4. Schematic of mesocosm facility (top) and picture of constructed facility (bottom).

7.1.3.3 Laboratory methods

Mesocosms were maintained at 4 relevant nutrient treatments of 0.1, 0.5, 1.0 and 5.0 mg L^{-1} NO_3-N. NO_3-N concetrations were artificially elevated from background with granular KNO_3 and monitored every 2-3 days with an Orion ® Ion Selective Probe to determine when nutrient additions are necessary. Water levels are also monitored for specific conductance to determine the need of water additions due to evaporative losses.

7.1.3.3.1 Nutrient Analysis of SAV

Total nitrogen TN and total carbon TC will be conducted using a CN analyzer and TP determined using acid digestion of tissue and analyzed using colorimetric procedures (Method

365.4; USEPA, 1993). ^{13}C and ^{15}N stable isotopes signatures will be analyzed using a coupled Costech model 4010 Elemental Analyzer (Costech Analytical Industries, Valencia, CA) and Finnigan Mat Delta XL Isotope Ratio Mass Spectrometry (Thermo Finnigan, San Jose, CA).

7.1.3.3.2 Nitrate Reductase Activity (NRA)

Nitrate reductase activity (NRA) is being measured as maximal nitrate reductase activity (MacKintosh et al. 1995) on SAV, epiphytic and benthic algae from North-Central Florida springs with variable nitrate concentrations and on shoots and roots of SAV cultured in mesocosms. The analysis will be performed according to Cedergreen and Madsen (2003), Corzo and Niell (1991) and Scheible et al. (1997a) using an induction medium of 50mM HEPES, 0.1% 1-propanol, 30 mM KNO_3^-, 10 mM glucose, 1 mM EDTA and 0.1 M phosphate buffer. 5 mL of assay medium in test 15 mL test tubes is then flushed with N_2 gas 2 minutes before and after the addition of 0.16 g of fresh tissue. Test tubes are then sealed with stoppers and incubated in the dark for 1 h in a water bath maintained at 30°C. The NO_2^- produced is determined spectrophotometrically by adding 300µL Sulfanilamide/ N-(1 Naphthyl)ethylenediamine Dihydrochloride solution (Ricca Chemical Company) to 700µL of incubated assay and measuring OD at 540 nm after 20 minutes. Dry weight/ fresh weight ratio of plants was measured on similar SAV for relation in NRA values.

7.1.3.3.3 Quantification of Growth

Root and Shoot Biometrics- At the end of the 8-week culture period analysis of root and shoot biometrics will be conducted. Digital images of the cultured SAV will be taken and analyzed using the software programs RootFly and Easy Leaf Area. Assess 2.0: Image Analysis Software will be used for measurement of leaf area and volume. The image analysis software program RootFly will be used to determine root length, diameter, surface area and volume. RootFly and Easy Leaf Area uses the color ratios of each pixel to distinguish roots, leaves and calibration areas from their background and compares leaf pixel counts. Traditional measurements of leaf blade width, length, and root and shoot mass will also be taken for comparison to concurrent measurements being made by Cohen et al (2007).

7.1.3.3.4 Anatomical Responses

7.1.3.3.4.1 Starch Grain Quantification

SAV samples are ground to <0.5 mm and weighed to 0.2 g. Samples are then transferred to 150 mL flask and stirred while adding 25 mL of DI. The pH is then checked and adjusted to pH 5-7. The mixture is then boiled while continuing to gently stir for 3 minutes and then autoclaved for 1 hour at 135°C. Allow to cool to 60°C then add DI to a total volume of 100 mL. Then pipette 1 mL of Starch Assay Reagent (Sigma Aldrich) and 1 mL of sample into test tubes to be incubated for 15 minutes at 60°C in a shaking water bath. Next, 1.0 mL of glucose assay reagent (Sigma Aldrich) and 100 µL of starch assay. Mix tubes and incubate for 15 minutes at room temperature. The glucose produced is determined spectrophotometrically by measuring OD at 340 nm.

7.1.3.3.4.2 Leaf anatomical Structure Analysis

Microscopic visualization of SAV anatomical structure will be made by fixation, dehydration, paraffin infiltration, sectioning (Institute of Molecular Development 2001) and staining of leaf

and root tissue. 3 cm sections of leaf tissue is fixed in formalin-acetic acid-alcohol (FAA) solution for 3 h. Tissue is then dehydrated in a series of increasing concentrations of t-butyl alcohol (TBA) and decreasing concentrations of ethanol and DI. Leaf tissue is then infiltrated with paraffin overnight and then changed with fresh paraffin every 4 h for 2-3 changes. Tissue is embedded in paraffin wax blocks sectioned to 30 µm using a microtome blade. Analysis of leaf and root anatomical structures (starch grains, arenchyma, vascular bundles, and epidermis) will be made from bright/dark field microphotographs of structures at 100x magnification (similar to methods of Wang et al. 2012).

7.1.4 PRELIMINARY RESULTS AND DISCUSSION

Although mesocosm growth experiments are only partially through the growing season, some preliminary data has been collected on the more robust growing *V. americana* from the four treatments (0.1, 0.5, 1.0 and 5.0 mg NO_3-N L^{-1}) (Figure 7.1.5) and from indoor treatment tanks (0.1 and 2.5 mg NO_3-N L^{-1})(Figure 7.1.6)These results suggest a NO_3-N induced increase in enzyme activity, a condition that could be interpreted as potentially detrimental if exposure is continuous. However, as NO_3-N increases, the increase in NRA is not increasing in proportion. An important consideration is that only one of several sampling periods is represented here, it is yet unknown if this trend is consistent for all sampling intervals.

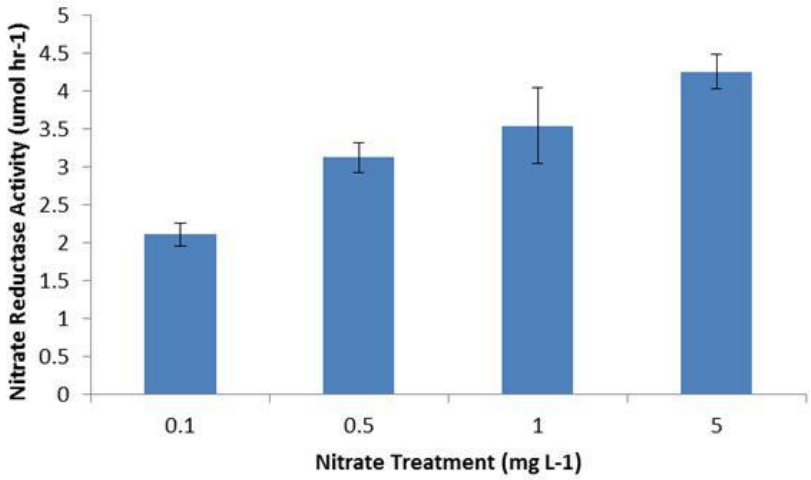

Figure 7.1.5. Two week shoot nitrate reductase activity (µmol h^{-1}) from mesocosm vegetation (*V. americana* under variable water NO_3-N concentrations.

While the ramets were acclimating to the mesocosm conditions, opportunistic sampling of both SAV species in the Alexander Springs were conducted to collect tissue samples for NRA assays. Fine roots, rhizomes, shoots and shoot tips were investigated with NRA assays using 1cm punch disks and whole tissue samples (preliminary methods comparison). Results of the trial assay suggests significant partitioning of NRA activity in the fine roots (Figure 7.1.7). However, when viewed upon a tissue mass basis, this finding supports the assertion that most NO_3-N is derived from the water column via foliar adsorption versus root uptake from sediments as blade biomass is significantly higher than root.

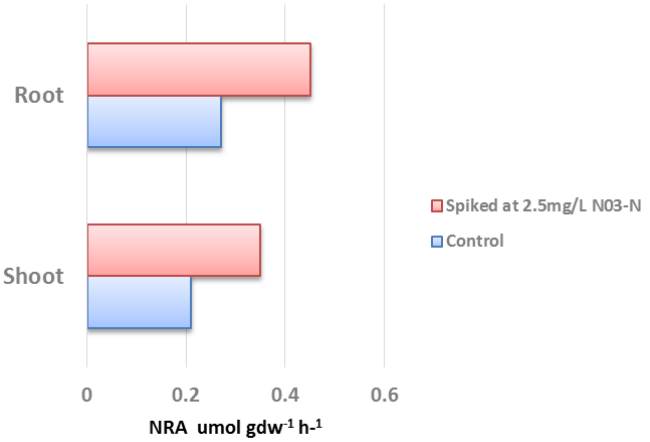

Figure 7.1.6. Root and shoot nitrate reductase activity for *S. kurziana* under 0.1 and 2.5 mg NO_3-N L^{-1})

Although the preliminary data presented here is suggestive of uptake mechanisms, this reporting constitutes only a fraction of the data thus far collected. At the time of reporting, expanded sampling data is undergoing QA/QC measures and initial analysis.

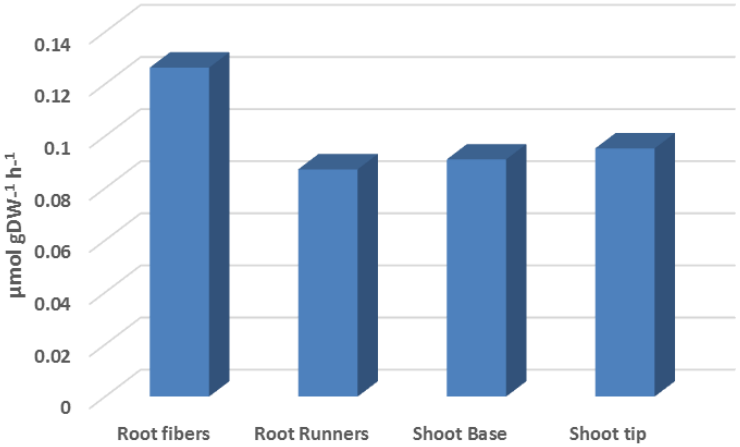

Figure 7.1.7. Nitrate reductase activity from fine roots, roots, mid shoots, and shoot tips of *V. americana* in Alexander Springs

7.1.5 CONCLUSIONS AND RECOMMENDATIONS

As of this reporting, data generated in this first year are undergoing QA/QC and initial data analysis. Therefore, no conclusions or recommendations are yet available.

7.1.6 FUTURE RESEARCH

Task 1. Following the initial NO_3-N inhibition study, the mesocosms will be utilized to investigate flow velocity effects on epiphytic algae (Year 2) and then micronutrient and sediment

type effects on SAV productivity (Year 3). The value of investment in mesocosm infrastructure will be realized in our ability to experimentally verify field measurements and better constrain rate parameters useful for model construction.

Task 2. Utilizing mesocosms constructed for Task 1, a study of velocity effects on algal abundance will be conducted to determine relationships between flow rates and growth/density of epiphytic algae on plants. Similar to the first experiment, potted ramets of *Vallisneria americana* taken from field sites will be subjected to a series of flow velocities representing the range of naturally occurring flows in springs. After 2 weeks of exposure to flow rates, algal biomass will be measured on SAV surfaces. As with the inhibition study, morphometrics will be monitored to determine effects of flow and algal burden on SAV growth. This work directly complements measurements made in other parts of this workplan (e.g., objective #2) and also other elements of the spring ecosystem research effort (e.g., Element #1 led by D. Kaplan and P. Suscy).

*Task 3***.** (Year 2-Year 3) Sediment and micronutrient effects on SAV.Ramets planted in individual containers will be grown under constant flow and light conditions with a series of sediment types and micronutrient additions to determine effects of both factors on SAV growth. Morphometrics and tissue concentrations of micronutrients will be sampled destructively at the termination of 90 day growth trials. This work directly complements measurements to made in other parts of this workplan (e.g., objective #2) and also other elements of the spring ecosystem research effort (e.g., Element #2 led by J. Martin and M. Coveney).

7.1.7 REFERENCES

Ackerman, F. 2007. The economics of atrazine. International Journal of Occupational and Environmental Health. 13:437-445.

Albertin, A.R. 2009. Nutrient dynamics in Florida springs and relationships to algal blooms. Dissertation, University of Florida.

Albertin, A.R., J.O. Sickman, A. Pinowska, R.J. Stevenson. 2012. Identification of nitrogen sources and transformations within karst springs using isotope tracers of nitrogen. Biogeochemistry 108: 219-232.

Barker, T., K. Hatton, M. O'Connor, L. Connor, B. Moss. 2008. Effects of nitrate load on submergedplant biomass and species richness: results of a mesocosm experiment. Fundamental and Applied Limnology 173: 89-100.

Barko J.W. and R. M. Smart. 1986. Sediment-related mechanisms of growth limitation in submersed macrophytes *Ecology* 67: 1328-1340.

Baron, J.S., E.K. Hall, B.T. Nolan, J.C. Finlay, E.S. Bernhardt, J.A. Harrison, F. Chan, E.W. Boyer. 2013.Theinteractive effects of excess reactive nitrogen and climate change on aquatic ecosystems and water resources of the United States. Biogeochemistry 114: 71-92.

Baum, J. K., and B. Worm. 2009. Cascading top-down effects of changing oceanic predator abundances. Journal of Animal Ecology 78:699–714.

Bergstrom, A.K., and M. Jansson. 2006. Atmospheric nitrogen deposition has caused nitrogenenrichment and eutrophication of lakes in the northern hemisphere. Global Change Biology 12: 635-643.

van den Berg, M.S., M. sheffer, E. van Nes, H. Coops. 1999. Dynamics and stability of *Chara sp*. And *Potamogeton pectinaus* in a shallow lake changing in eutrophication level. Hydrobiologia 408: 335-342.

Best, E.P.H. 1980. Effects of nitrogen on the growth and nitrogenous compounds of *Ceratophyllum demersum*. Aquatic Botany 8: 197-206.

Boar, R.R., C.E. Crook, B. Moss. 1989. Regression of *Phragmites ausitralis* reed swamps and recent changes if water chemistry in the Norfolk Broadland, England. Aquatic Botany 35: 41-55.

Boedeltje, G., A.J. Alfons, J.P. Smolders, J.G.M. Roelofs. 2005. Combined effects of water column Nitrate enrichment, sediment type and irradiance on growth and foliar nutrient concentrations of *Potamogeton alpines*. Freshwater Biology 50: 1537-1547.

Borum, J. 1985. Development of epiphytic communities on eelgrass (*Zostera marina*) along a nutrient gradient in a Danish estuary. Marine Biology 87: 211-218.

Brouwer, E., R. Bobbink, F. Meeuwsen, J.G.M. Roelofs. 1997. Recovery from acidification in aquatic mesocosms after reducing ammonium and sulfate deposition. Aquatic Botany 56: 119-130.

Brown, M.T., K. Chinner-Reiss, M.J. Cohen, J.M. Evans, K.R. Reddy, P.W. Inglett, K.S. Inglett, T. K. Frazer, C.A Jacoby, E.J. Philips, R. L. Knight, S. K. Notestein, K.A. McKee. 2008. Summary and synthesis of the available literature on the effectsof nutrients on springs organisms and systems. Final Report. Florida Department of Environmental Protection, Tallahassee FL.

Buchsbaum, R.N., F.T. Short, D.P. Cheney. 1990. Phenolic-nitrogen interactions in eelgrass (*Zostera marina* L.): possible implications of disease resistance. Aquatic Botany 37: 291-297.

Burkholder, J.M., K.M. Mason, H.B. Glasgow, Jr. 1992. Water column nitrate enrichment promotes decline of eelgrass *Zostera marina*: evidence from seasonal mesocosm experiments. Marine Ecological Progress Series 81: 163-178.

Burkholder, J.M., H.B. Glasgow, J.E. Cooke. 1994. Comparative effects of water column nitrate enrichment on eelgrass *Zostera marina*, shoal grass *Halodule wrightii* and widgeongrass *Ruppia maritime*. Marine Ecological Progress Series 105:121-138.

Canfield, H.E.,and M.V. Hoyer. 1988. Influence of nutrient enrichment and light availability on the abundance of aquatic macrophytes in Florida streams. Canadian Journal of Fisheries and Aquatic Sciences 45: 1467-1472.

Cao, T., L. Ni, P. Xie. 2004. Acute biochemical responses of a submersed macrophyte, *Potamogeton crispus L*., to high ammonium in an aquarium experiment. Journal of Freshwater Ecology 19: 279-284.

Cedergreen, N. and T.V. Madsen. 2003. Nitrate reductase activity in roots and shoots of aquatic macrophytes. Aquatic Botany 76: 203-212.

Clarke, E. and H.A. Baldwin. 2002. Responses of wetland plants to ammonia and water level. Ecological Engineering 18: 257-264.

Cohen, M.J., S. Lamsal and L.V. Korhnak. 2007. Sources, Transport and Transformations of Nitrate-N in the Florida Environment. St. Johns River Water Management District

SJ2007-SP10. 125 pp. Palatka, FL.
Cowell, B.C. and P.S. Botts. 1994. Factors influnceing the distribution, abundance, and growth of *Lyngbya wollei* in Central Florida. Aquatic Botany 49: 1-17.
Cowell, B.C. and C.J. Dawes. 2004. Growth and nitrate nitrogen uptake by the cyanobacterium *Lyngbya wollei*. Journal of Aquatic Plant Management. 42: 69-71.
Cowell, B.C., C.J. Davis. 2008. Seasonal comparisons of the phytoplankton and decline in water transparency in spring-fed rainbow River, Florida. Journal of Freshwater Ecology 23: 169-177.
Cramer, M.D., O.A. M. Lewis. 1993. The influence of NO_3 and NH_4 nutrition on carbon and nitrogen partitioning characteristics of wheat (*Triticum aestivum*) and maize (*Zea maize*) plants. Plant and Soil 154: 289-300.
Crawford, N.M. 1995. Nitrate: nutrient signal for plant growth . The Plant Cell 7:859-868.
De Brabandere, L., T.K. Frazer, J.P. Montoya. 2007. Stable isotope ratios of macrophytes and associated periphyton along a nitrate gradient in two subtropical, spring fed streams. Freshwater Biology 52: 1564-1575.
Duarte, C.M. and D.E. Canfield, Jr. 1990. Macrophyte standing crop and primary productivityin some Florida spring-runs. Water Resources Bulletin 26(6): 927-934.
Dunne, E.J., M.F Coveney, E.R. Marzolf, V.R. Hogue, R. Conrow, R. Naleway, E.F. Lowe, L.E. Battoe. 2012. Efficacy of a large-scale constrcutied wetland to remove phosphorus and suspended solids from Lake Apopka, Florida. Ecological Engeineering 42: 90-100.
Dzialowski, A.R., S.H. Wang, N.C. Lim, W.W. Spotts. 2005. Nutrient limitation of phytoplankton growth in central plains reservoirs, USA. Journal of Plankton Research 27: 587-595.
Elser, J.J., M.E.S. Bracken, E.E. Cleland, D.S. Gruner, W.S. Harpole, H. Hillebrand, J.T. Ngai, E.W. Seabloom, J.B. Shurin, J.E. Smith. 2007. Global analysis of nitrogen and phosphorus limitation of primary producers in freshwater, marine , and terrestrial systems. Ecological Letters 10: 1135-1142.
Evans, J. 2008. Ecosystem implications of invasive aquatic plants and aquatic plant control in Florida Springs. P 249-270 In: M.T. Brown, Ed. Summary and synthesis of available literature on the effects of nutrients on springs organisms and systems. Florida Department of Environmental Protection. Tallahassee, FL.
Estes, J. a, J. Terborgh, J. S. Brashares, M. E. Power, J. Berger, W. J. Bond, S. R. Carpenter, T.E. Essington,R. D. Holt, J. B. C. Jackson, R. J. Marquis, L. Oksanen, T. Oksanen, R. T. Paine, E. K. Pikitch, W. J. Ripple, S. a Sandin, M. Scheffer, T. W. Schoener, J. B. Shurin, A. R. E. Sinclair, M. E. Soulé, R. Virtanen, and D. Wardle. 2011. Trophic downgrading of planet Earth. Science 333:301–6.
Farnswoth, L., and L.A. Baker. 2000. Conceptual model of aquatic plant decay and ammonium toxicity for shallow lakes. Journal of Environmental Engineering. 126: 199-207.
Frazer, T.K., S.K. Notestein, W.E. Pine. 2006. Changes in the physical, chemical and vegetative characteristics of the Homosassa, Chassahowitzka and Weeki Wachee rivers. Final Report. Southwest Florida Water Mangement District, Brooksville, FL.
Fulton, B.A., R. A. Brain, S. Usenko, J.A. Back, B.W. Brooks. 2010. Exploring *Lemna gibba* thresholdsto nutrient and chemical stressors: differential effects of triclosan on internal stoichiometry and nitrate uptake across a nitrogen: phosphorus gradient. Environmental Toxicology and Chemistry 29:2363-2370.

Genevieve, M.C, H.C Duthie, W.D. Taylor. 1997. Models of aquatic plant productivity: a review of the factors that influence growth. Aquatic Botany 59: 195-215.

Gojon, A., C. Plassard, C. Bussi. 1994. Root/shoot distribution of NO_3- assimilation in herbaceous and woody species. In: Roy, J. and E. Garnier (Eds.) A Whole Plant Perspective on Carbon – Nitrogen Interactions. SPB Academic Publishing, Hague, pp 131-148.

Gruner, D. S., J. E. Smith, E. W. Seabloom, J. T. Ngai, S. Sandin, H. Hillebrand, W. S. Harpole, J. J. Elser, E. E. Cleland, M. E. S. Bracken, E. T. Borer, and B. Bolker. 2008. A cross system synthesis of consumer and nutrient resource control on producer biomass. Ecology Letters 11:740–755.

Guerrero, M.G., J.M. Vega, M. Losada. 1981. The assimilatory nitrate reducing system and its regulation. Annual Reviews of Plant Physiology 32: 169-204.

Harlin, M.M., and B. Thorne-Miller. 1981. Nutrient enrichment of seagrass beds in a Rhode Island coastal lagoon. Marine Biology. 65: 221-229.

Harwell, M. C., B. Sharfstein. 2009. Submerged aquatic vegetation and bulrush in Lake Okeechobee as indicators of greater Everglades ecosystem restoration. Ecological Indicators 9: S46-S55.

Heck, K. L. J., and J. F. Valentine. 2007. The primacy of top-down effects in shallow benthic ecosystems. Estuaries and Coasts 30:371–381.

Heffernan, J. B., D. M. Liebowitz, T. K. Frazer, J. M. Evans,and M. J. Cohen. 2010. Algal blooms and the nitrogen enrichment hypothesis in Florida springs: evidence, alternatives, and adaptive management. Ecological Applications 20:816–829.

van der Heide, T., E.H. van Nes, M.M. van Ktawijk, M. Scheffer, A.J. Hendriks, A.J.P. Smolders. 2010. Alternative stable states driven by density-dependent toxicity. Ecosystems 13: 841-850.

Hemminga, M.A., and C.M. Duarte. 2000. Seagrass Ecology. Cambridge University Press, Cambridge UK. 298 pp.

Hillebrand, H. 2002. Top-down versus bottom-up control of autotrophic biomass—a meta analysis on experiments with periphyton. Journal of the North American Benthological Society 21:349–369.

James,C., J. Fisher, B. Moss. 2003. Nitrogen driven lakes: the Shropshire and Cheshire Meres. Archif fur Hydrobiologia 164: 249-266.

James, C., J. Fisher, V. Russell, S. Collings, B. Moss. 2005. Nitrate avilabliity and hydrophyte species richness in shallow lakes. Freshwater Biology 50:1049-1063.

James, R.T., W.S. Gardner, M.J. McCarthy, S.A. Carini. 2011. Nitrogen dynamics in Lake Okeechobee: forms, functions, and changes. Hydrobiologia 669: 199-212.

Jones, G.W., S.B. Upchurch, K.M. Champion. 1996. Origin of nitrate in ground water discharging from Rainbow Springs, Marion County, Florida. Southwest Florida Water Management District, Brooksville, FL.

Katwijik, M.M.V., L.H.T. Vergeer, G.H.W. Schmitz, J.G.M. Reolofs. 1997. Ammonium toxicity in Eelgrass *Zostera marina*. Marine Ecology Progress Series 157: 159-173.

Katz, B.G. 2004. Sources of nitrate contamination and age of water in large karstic springs in Florida. Environmental Geology 46:689-706.

Kim-Shapiro, D.B., M.T. Gladwin, R.P. Patel, N. Hogg. 2005. The reaction between nitrite and hemoglobin: the role of nitrite in hemoglobin mediated hypoxic vasodilation. Journal of Inorganic Biochemistry 99: 237-246.

Klotzli, F. 1971. Biogenous influence on aquatic macrophytes especially *Phragmites communus*. Hydrobiologia 12: 107-111.

Lacoul, P., and B. Freedman. 2006. Environmental influences on aquatic plants in freshwater ecosystems. Environmental Reviews 14: 89-136.

Lambert, S. J., and A.J. Davy. 2011. Water quality as a threat to aquatic plants: discriminating between the effects of nitrate, phosphate, boron and heavy metals on Charophytes. New Phytologist 189: 1051-1059.

Lea, P.J., and B.J. Miflin. 1979. Photosyntheitc ammonia assimilation. *In:* Encyclopedia of Plant Physiology. Eds. M. Gibbs, E. Latzko. Springer, Berlin 578 pp.

Li, W., Z. Zhang, and E. Jeppesen. 2008. The response of *Vallisneria spinulosa* (Hydrocharitaceae) to different loadings of ammonia and nitrate at moderate phosphorus concentration: a mesocosm approach. Freshwater Biology 53: 2321-2330.

Liebowitz, D.M. 2013. Environmentally mediated consumer control of algae proliferation in Florida springs. Doctoral Dissertation, University of Florida, Gainesville, FL.

Liebowitz, D.M., M.J. Cohen, J.B. Heffernan, T.K. Frazer, L.V. Korhnak. (In review) Environmentally mediated consumer control of algae proliferation in Florida springs.

Maberly, S.C., L. King, M.M. Dent, R.I Jones, C.E. Gibson. 2002. Nutrient limitation of phytoplankton And periphyton growth in upland lakes. Freshwater Biology 47: 2136-2152.

Maddox, G.L., J.M. Lloyd, T.M. Scott, B. Upchurch, R. Copeland. 1992. Florida's groundwater quality monitoring program, background geochemistry. Florida Geological Survey, Tallahassee, FL.

Marschner, H. 1998. Mineral Nutrition of Higher Plants. Academic Press, London, pp. 232-242.

Mattson, R.A. 2013. Personal Communication.

Mattson, R.A., M. Lehmensiek, E.F. Lowe. 2007. Nitrate toxicity in Florida springs and spring-run streams: a review of the literature and its implications. Professional Paper SJ2007-PP1. St. Johns River Water Management District, Palatka, FL.

Mehrer, I., and H. Mohr. 1989. Ammonium toxicity: description of the syndrome in Sinapis alba and search for its causation. Physiologia Plantarum 77: 54554,

Moss, B. 1990. Engineering and biological approaches to restoration from eutrophication of shallow lakes in which aquatic plant communities are important components. Hydrobiologia 200: 367-377.

Mulligan, H.F., A. Baranowsky, R. Johnson. 1976. Nitrogen and phosphorus fertilization of aquatic vascular plants and algae in replicated ponds. Initial responses to fertilization. Hydrobiologia 48: 109-116.

Munch, D.A., D.J. Toth. C. Huang, J.B. Davis, C.M. Fortich, W.L. Osburn, E.J. Phlips, E.L Quinlan,M.S. Allen, M.J. Woods, P.Cooney, R.L Knight, R.A. Clarke, S.L. Knight. 2006. Fifty year retrospective study of the ecology of Silver springs, Florida. Special Publication SJ2007-SPA. St. John's River Water Management District, Palatka.

Neckles, H.A., R.L. Wetzel, R.J. Orth. 1993. Effects of nutrient enrichment and grazing on epiphyte-macrophyte (Zostera marina L.) dynamics. Oecologia 93: 285-295.

Ni, L. 2001. Effects of water column nutrient enrichment on the growth of *Potamogeton maackianus* A. Been. Journal of Aquatic Plant Management 39: 83-87.

Nichols, D.S. and D.R. Keeney. 1976. Nitrogen nutrition of Microphyllum spicatum: uptake and translocation of ^{15}N by ramets and roots. Freshwater Biology 6: 145-154.

Odum, H.T. 1957. The Ecology of Silver Springs. Ecological Monographs.

Osborne, T.Z., S. Newman, P. Kalla, D.J. Scheidt, G.L. Bruland, M.J. Cohen, L.J. Scinto, and L.R. Ellis. 2011. Landscape patterns of significant soil nutrients and contaminants in the Greater Everglades Ecosystem: Past, Present, and Future. Crit. Rev. Environ. Sci. Technol. 41:6 121-148

Pate, J.S. 1980. Transport and partitioning of nitrogenous solutes. Annual Review of Plant Physiology 31: 313-340.

Phelps, G. G. 2004. Chemistry of Ground Water in the Silver Springs Basin, Florida, with an Emphasis on Nitrate. U.S. Geological Survey Scientific Investigations Report 2004-5144. vi, 54 pp.

Phelps, G.G., S.J. walsh, R.M. Gerwig, W.B. Tate. 2006. Characterization of the hydrology, water chemistry, and aquatic communities of selected springs in the St. Johns river Water Management District, Florida, 2004. Open-file report 2006-1107. USGS Reston, VA.

Pinowska, A., R.J. Stevenson, J.O. Sickman, M. Anderson. 2007. Integrated interpretation of survey for determining nutrient thresholds for macroalgae in Floirda springs: macroalgal relationships to water, sediment, nutrients, diatom indicators, and land use. Florida Department of environmental Protection, Tallhalssee, FL.

Porter, E.M., W. D. Bowman, C.M. lark, J.E. Compton, L.H. Pardo, J.L Soong. 2013. Interactive effects Of anthropogenic nitrogen enrichment and clomate change on terrestrial and aquatic biodiversity. Biogeochemistry 114: 93-12.

Quinlan, E.L., E.J. Phlips, K.A. Donnelly, C.H. Jett, P. Sleszynski, S. Keller. 2008. Primary producers And nutrient loading in Silver Springs, FL, USA. Aquatic Botany 88: 247-255.

Rabe, E. 1990. Stress physiology: the functional significance of the accumulation of nitrogen containing compounds. Journal of Horticultural Science. 65: 231-243.

Rabe, E., and C.J. Lovatt. 1986. Increased arginine biosynthesis during P deficiency. Plant Physiology 81: 774-779.

Raven, J.A. 1985. Regulation of pH and generation of osmolarity in vascular plants: a cost-benefit analysis in relation to efficiency of use of energy, nitrogen, and water. New Phytologist 101: 25-77.

Reddy, K.R and R.L. DeLaune. 2008. Biogeochemistry of Wetlands: Science and Applications. CRC Press Boca Raton. 774 pp.

Riis, T., B. Olesen, J.S. Clayton, C. Lambertini, H. Brix, B.K. Sorrell. 2012. Growth and morphology in relation to temperature and light availability during the establishment of three invasive aquatic plant species. Aquatic Botany 102: 56-64.

Roth, N.C and A.M. Pregnall. 1988. Nitrate reductase activity in Zostera marina. Marine Biology 99: 457-463.

Sagrario, M.A.G.; E. Jeppesen, J. Goma, M. Sondergaard, J.P. Jensen, T. Lauridsen, F. Landkildehus. 2005. Does high nitrogen loading prevent clear-water conditions in shallow lakes at moderately high phosphorus concentrations? Freshwater Biology 50: 27-41.

Schindler, D.W. 1978. Factors regulating phytoplankton production and standing crop in the world's freshwaters. Limnology and Oceanography 23: 478-486.

Schindler, D.W., and E.J. Fee. 1974. Experimental lakes area: whole lake experiments in eutrophication. Journal of Fisheries Research Board Canada 32:937-953.

Schroder, R. 1979. Decline of reedswamps in Lake Constance. Symp. Biol. Hung. 19: 43-48.

Schuurkes, J.A., C.J. Kok, C.D. Hartog. 1986. Ammonium and nitrate uptake by aqutic plants from poorly buffered and acidified waters. Aquatic botany 24: 131-146.

Scott, T., G. Means, R. Meagan, R. Means, S. Upchurch, R. Copeland, R. Jones, A. Willet. 2004. Springs of Florida. Bulletin No. 66 Florida Geological Survey, Tallahassee, FL.

Sickman, J.O. A.R. Albertin, M.W. Anderson, A Pinowska and R.J. Stevenson. 2009. A comparison of internal and external supply of nutrients to algal mats in two first magnitude springs in Florida. Journal of Aquatic Plant Management. 47: 135-144.

Smolders, A.J., C.D. Hartog, C.B. Gestel, J.G. Roelof. 1996. The effects of ammonium on growth, accumulation of free amino acid and nutritional status of young phosphorus deficient *Stratiotes aloides* plants. Aquatic Botany 53: 85-96.

Smolders, A.J., M.C. van Reil, J.G.M Roelofs. 2000. Accumulation of free amino acids as an early indication for physiological stress (nitrogen overload) due to elevated ammonium levels in vital *Stratiotes aloides* L. stands. Archeif fur Hydrobiologie 150: 169-175.

Smolders, A.J.P, R.J.J. Hendriks, H.M. Campschueur, J.G.M Roelofs. 1997. Nitrate induces iron deficiency chlorosis in J*uncus acutiflorus*. Plant and Soil 196: 37-45.

Stevenson, R.J., A. Pinowska, Y. Wang. 2004. Ecological condition of algae and nutrients in Florida Springs. Florida Department of Environmental Protection, Tallahassee, FL.

Stevenson, R.J., A. Pinowska, A. R. Albertin, J.O. Sickman. 2007. Ecological condition of algae and nutrients in Florida springs the synthesis report. Florida Department of Environmental Protection, Tallahassee, FL.

Sturgis, R.B., L. Murray. 1997. Scaling of nutrient inputs to submersed plant communities: temporal and spatial variations. Marine Ecological Progress Series 152: 89-102.

Talling, J.F. and J. Lemoalle. 1998. Ecological Dynamics of Tropical Waters. Cambridge University Press. Cambridge UK 455 pp.

Ulrich, K.E. and T.M. Burton. 1985. The effect of nitrate, phosphate, and potassium fertilization on growth and nutrient uptake patterns of Phragmites australis (Cav.) Trin. Ex Steudel. Aquatic Botany 21:53-62.

Wang, Y., G. Gao, B. Qin, X. Wang. 2012. Ecophysiological and anatomical responses of *Vallisneria natans* to nitrogen and phosphorus enrichment. Knowledge and Management of Aquatic Ecosystems 405, 05.

Wetzel, R.G. 2001. Limnology: Lake and River Ecosystems 3rd Ed. Academic Press, San Diego. 1006 pp.

Weyhenmeyer, G.A., E. Jeppesen, R. Adrian, L. Arvola, T. Blenckner, T. Jankowski, E. Jennings, D. Straile. 2007. Nitrate depleted conditions on the increase in shallow northern European lakes. Limnology Oceanography 52: 13346-1353.

Zimmerman, R.C., R.D. Smith, R.S. Alberte. 1989. Thermal acclimation and whole-plant carbon balance in *Zostera marina* L. (eelgrass). Journal of Experimental Marine Biology and Ecology 130: 93-109.

7.1.8 PUBLICATIONS AND PRODUCTS

Osborne, T.Z., R.A. Mattson, M.F. Coveney. IN PRESS. Potential for Direct Nitrate-Nitrite Inhibition of Submerged Aquatic Vegetation (SAV) in Florida Springs: A Review and Synthesis of Current Literature. *Water*.

7.1.8.1 Theses

In Progress: LaPlaca, L.H. 201X. The role of NOx in submerged aquatic vegetation growth and proliferation in spring ecosystems. MS Thesis, University of Florida.

7.1.8.2 Presentations

Osborne, T.Z. 2014. Freshwater springs: environmental and cultural treasures of Florida. REU lecture- Whitney Laboratory for Marine Bioscience, July 2014.

Osborne, T.Z. 2015. Evolution of Florida's aquatic ecosystems. REU lecture- Whitney Laboratory for Marine Bioscience, June 2015.

Section 7.2. Declining Oxygen as a Mechanism for Extirpation of Invertebrate Herbivores in Silver Springs- a Respirometry Study of *Viviparus georgianus, Elimia floridensis, Micromenteus floridensis* and *Palaemonetes paludosus*

7.2.1 ABSTRACT

Dissolved oxygen stress has been suggested in recent studies to be a significant causal mechanism in population declines of aquatic herbivores in spring ecosystems. The decline of invertebrate grazers is suspected to have significant ecological effects (ie trophic cascade), such as a lapse of top-down control on the proliferation of algae in many springs across the state of Florida. This research is being conducted to better our understanding of the relationships among water quality, grazers and algal community dynamics in spring ecosystems. Dissolved oxygen respiration requirements and survivorship thresholds for several key gastropod grazer species (*Viviparus georgianus*, *Elimia floridensis*, *Micromenteus floridensis)* and one decapod (*Palaemonetes paludosus*-Ghost Shrimp) from Silver River have been experimentally determined utilizing closed chamber respirometry methods in controlled laboratory conditions. Preliminary results suggest that at least one of the four species tested experiences hypoxic stress below 4 mg L^{-1} O_2. While data analysis is ongoing at this time for the initial thresholds investigation, cursory review of the data suggests that thresholds of tolerance were reached for all 4 species tested. Further analysis will reveal the exact levels of hypoxia stress that these organisms can survive.

7.2.2 INTRODUCTION

Hypoxia is emerging as one of the most significant stressors to biota in the estuarine and freshwater ecosystems worldwide due to the resulting impacts of mortality and food web alteration (Vaquer-Sunyer and Duarte 2008; Levin et al. 2009; Keeling et al. 2010). Recent reviews of the subject highlight the need for a multi-level approach to understanding the ecological consequences of consumer stressors, such as hypoxia, in aquatic systems (Diaz and Rosenberg 1995; Rabalais et al. 2002; Wu et al. 2002).

To better understand how stressors in the aquatic environment of Florida springs may result in the uncontrolled proliferation of algae, a review of the ecological drivers and controls of algal productivity is warranted. Aquatic communities and food web structure can be regulated by resource availability (bottom up forces)(Smith 2006; Carpenter et al. 2001; Rosemond et al. 1993) as well as, predation, herbivory, and physical characteristics of the environment such as flow velocity (top down forces)(King 2012; Liboriussen et al. 2005; Feminella and Hawkins 1995; Power 1992; Carpenter et al. 1987). In the case of Florida's spring ecosystems, resource availability refers to both water column nutrients (nitrogen and phosphorus) and sunlight. These resources directly affect the production of algal biomass and are thus considered bottom-up controls. Alternatively, herbivore (predation) by algal grazers and the sheer stress associated with flow velocity acts to reduce or control the standing population of algae and is termed top-down control (Figure 7.2.1).

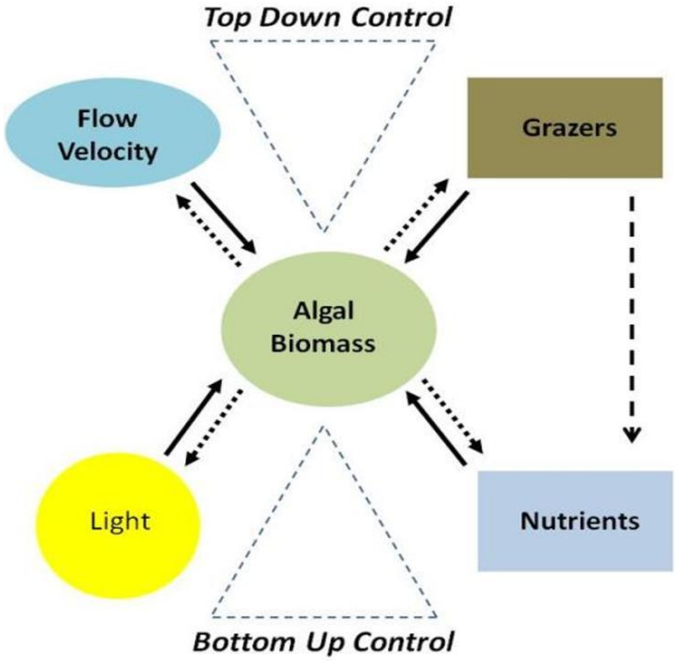

Figure 7.2.1. Conceptual model of top down versus bottom up control of primary production in Florida Springs. Note bottom up control mechanisms limit production while top down control mechanisms limit standing biomass. Solid lines indicate direct influence of drivers and dotted lines represent feedbacks. Figure adapted from Osborne et al. (2013).

7.2.2.1 Bottom Up Control of Algal Productivity

With respect to bottom up control mechanisms (those that exert control over the production of algal biomass), nutrients are by far the most well studied and therefore became the first priority in determining the drivers of algal proliferation in springs. Recent observations of increasing NO_3-N concentrations in Florida springs have garnered much attention by ecosystem managers (Munch et al. 2006; Quinlan et al. 2008; Heffernan et al. 2010). Contrary to expectation of a direct relationship between nutrients and algal biomass (Smith 2006; Smith 1982), the increase in nitrogen availability has not been shown to have any positive correlation with algal productivity (Canfield and Hoyer 1988; Duarte and Canfield 1990; Stevenson et al. 2004; Stevenson et al. 2007; Brown et al. 2008; Heffernan et al. 2010). While there have been studies to report N utilization by algal mats in Florida springs (Cowell and Botts 1994; Cowell and Dawes 2004; Albertin 2009; Sickman et al. 2009), there have been several observations that contradict the normal eutrophication paradigm, namely the lack of significant increase in other forms of N (Cohen et al. 2007; Hensley and Cohen 2012) or P (Maddox et al. 1992; Scott et al. 2004) in spring waters. Therefore, focus on nutrient catalyzed algal proliferation is somewhat unwarranted Brown et al. 2008; Heffernan et al. 2010.

A second bottom up control mechanisms of algal population common to all systems is that of light availability (Biggs 1996; Wetzel 2001). Light availability in spring systems is directly related to vegetative canopy cover of the spring run and turbidity of water. Recent investigations

by Szafraniec (2014) report preferential use of different portions of the red and blue spectra by SAV in spring runs. This has been documented in the seagrass literature (Dennison et al. 1993; Kirk 1994; Anastasiou 2009; Gallegos et al. 2009) but is a new finding with respect to spring ecosystem functions. Similarly, algae exhibit preferential usage of available light spectra, with nuisance algae such as *Lyngbya*, readily utilizing most spectra available (Szfraniec 2014). This additional finding suggests great adaptability of *Lyngbya* and other blue green algae to reduced light conditions.

7.2.2.2 Top Down Control of Algal Biomass

The effects of flow on attached algae in lotic systems (e.g. rivers, streams), are well known and include influencing nutrient availability and standing biomass. Increased flow can reduce the diffusive boundary layer above algae and increase advective flux of nutrients through the water column effectively increasing the exposure of algae to nutrients and aiding growth in situations where nutrients are limited (Stevenson and Glover 1993; Stevenson 1996; Biggs et al 1989). Alternatively, higher flow velocities can also limit algal biomass by creating sheer stress on algal communities that scours algal biomass (an abiotic top down control mechanism). This observation can be confounded as flow velocities that limit algal biomass can also limit grazer accessibility to algae when flow velocity is high (Poff and Ward 1995; Opsahl et al. 2003). Spring runs, much like other lotic systems, experience a variety of flow velocities due to the influence of rainfall and groundwater withdrawls on spring vent discharge (Copeland et al. 2009). Similarly, the positive relationship between flow and nutrient availability observed in lotic systems (Stevenson 1996) would predict potential nutrient limitation if flow were reduced significantly. As the nutrient enrichment relationship with algae in Florida springs has not been established, and very few springs are nutrient limited, it is likely that the observed decrease in flow is not exacerbating nutrient availability. This assertion is support by King (2012) who tested the nutrient spiraling hypothesis (Newbold et al. 1981; Newbold et al 1982) with respect to flow on a Florida spring run and found no N limitation in *Lyngbya wolle*i at flow velocities above 5 cm s^{-1} (a velocity well below the average for most Florida springs).

More relevant to the discussion of flow mediated control of algae in springs is the inhibitory effect of flow velocity on algal biomass. For example, local flow velocities and the intensity and frequency of flood events have been shown to limit the amount of algal biomass in a given area (Biggs and Close 1989; Biggs 1996; Biggs et al. 1998) by physically scouring (via increased sheer stress) periphyton from surfaces. This sheer stress is directly proportional to flow velocity and has been shown to have a negative effect on algal biomass at velocities from 5-35 cm s^{-1} with flows above 35 cm s^{-1} dramatically decreasing filamentous algal biomass (King 2012). Decrease in discharge and thus flow velocity has the potential to contribute to proliferation of algae in several Florida springs.

Perhaps the most important form of top down control of algal biomass is grazing by herbivores (Figure 7.2.1). Top down control by grazers is a critical feedback to primary productivity (Altieri et al 2013) and is often termed density mediated control. Herbivory is an interactive process involving a primary producer that produces organic matter and a consumer that ingests this material (Mulholland et al. 1989). Capacity of primary producers to generate biomass may significantly influence herbivore interactions and vice-versa (Crawley 1983; Mulholland et al.

1989). Attached algae, also known as periphyton or epiphyton, is the main focus of grazing in springs. Periphyton is a complex assemblage of algae and bacteria living on the surfaces of benthic substrata or macrophytes (Vermaat 2005; Burkholder and Wetzel 1989). A significant body of research reports periphyton abundance to be negatively correlated with grazer population (e.g. ciliates, metazoans, aquatic insects, gastropods) (Tarkowska-Kukuryk and Mieczan 2012; Mulholland 1991; Liboriussen et al. 2005; Wetzel 2001; Cuker 1983; Hill et al. 1992; Rosemond et al. 1993).

Grazers may show high specificity of forage by focusing on highly edible and nutritious algae (Jones et al. 1998; Jones and Sayer 2003). In a study conducted by Bronmark et al. (1992), snails preferred to feed on periphyton composed of filamentous algae and large stalked diatoms over filamentous blue-green algae (*Gloeotrichia*) and small adnate diatoms that came to dominate the highly grazed treatments. Grazing on inert substrate was observed to have greater effect on epiphytic algae than on macrophytes suggesting some nutrient source in aquatic macrophytes (Mulholland et al 1991). In addition to location of periphyton, other physical characteristics of aquatic systems may influence grazing activity. In a recent study by Liboriussen et al. (2005), top down control by grazers was more pronounced in clear lakes and was dominated by snails while in turbid lakes, grazing was dominated by chironomids and ostracods. Mulholland et al. (1989) report that algal productivity outpaced consumer control (<15 % of biomass consumed at high irradiance while >90% was consumed at low irradiance conditions in experimental streams. Rosemond (1993) found that light, nutrients, and grazer activity, simultaneously limited algal productivity and community structure. Relationship between ciliates, metazoan and chironomid grazer activity was found to be significantly related to NO_3-N, temperature, Secchi and DO (Tarkowska-Kukuryk and Mieczan 2012).

Grazing on algae may be significant enough to offset the effects of increased algal productivity (Jacoby et al. 2008; Hauxwell et al. 1998; Duarte 1995), however, any perturbation to grazer population could cause a dramatic shift in algal production. Recent work by Libowitz et al. (in press) suggests an escape threshold exists at which point algal productivity outpaces grazer control. The mechanisms are not clear as to what causes algal production to reach that threshold, but the current view is that it may be due to several factors acting in concert similar to multiple drivers of algal growth.

7.2.2.3 Controls on Grazers

Established ecological theory predicts top down controls of grazers could be an alternative explanation for algal dominance in spring systems when bottom up controls and the abiotic top down controls of algae growth appear to be unrestrictive (Liebowitz et al. in press)(Figure 7.2.2). Top down control of grazers by fish can alter grazer population dynamics, and indirectly promote algal productivity (Mazumder et al. 1989; Power 1990; Brönmark et al. 1992; Liboriussen et al 2005; Korpinen et al. 2007). A study by Beklioglu et al. (2003) supports top down control of fish to promote grazers and thus promote algae control.

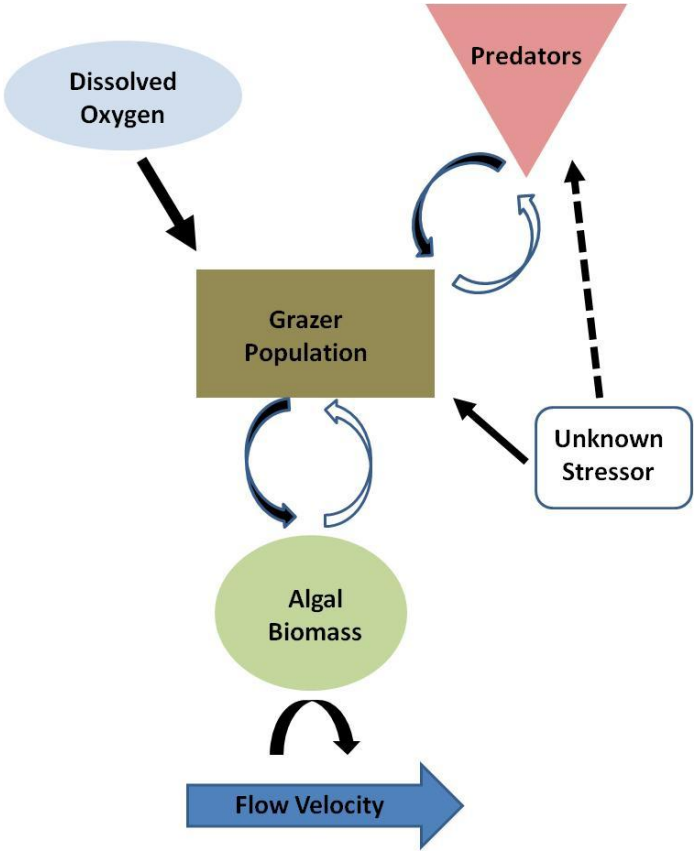

Figure 7.2.2. Conceptual model of drivers of grazer population. The unknown stressor could be any compound or condition that negatively impacts grazer population leading to population decline or episodic extirpation.

Changes in biotic populations often signal anthropogenic stress and impending ecosystem change (van Boclaer et al. 2012). Anecdotal evidence suggests a decline in grazer populations in many Florida springs, unfortunately, little biological data exists to support the assertion that grazer control of algae has lapsed. Many springs do not have any biological monitoring in place, hence the few existing reports highly influence the current expectation on the grazer communities. Historic studies of Silver Springs by Odum (1957) lend some guidance in grazer community structure and populations. Review of that seminal work indicates that approximately 44% of the grazer biomass in Silver Springs was made up of grazing gastropods (*Pomacea, Oxytrema, and Viviparus*)(Figure 7.2.3). Grass shrimp (*Palaemonetes*) make up the next largest group of grazers by biomass (42%). All other invertebrate grazers, including aquatic insects, make up the remaining 14% of grazer biomass, hence the study of trophic interactions should rightfully focus on herbivorous snails and shrimp.

Because quantitative scientific observations of pristine spring ecosystem components are very rare. The work of Odum (1957) in Silver Springs provides a baseline from which change can be assessed in springs. Of significant interest for springs restoration is the type and distribution of algal grazers (snails and shrimp) in Florida springs prior to the shift in primary productivity that is commonly observed today. The largest group of taxa by biomass is that of Gastropods.

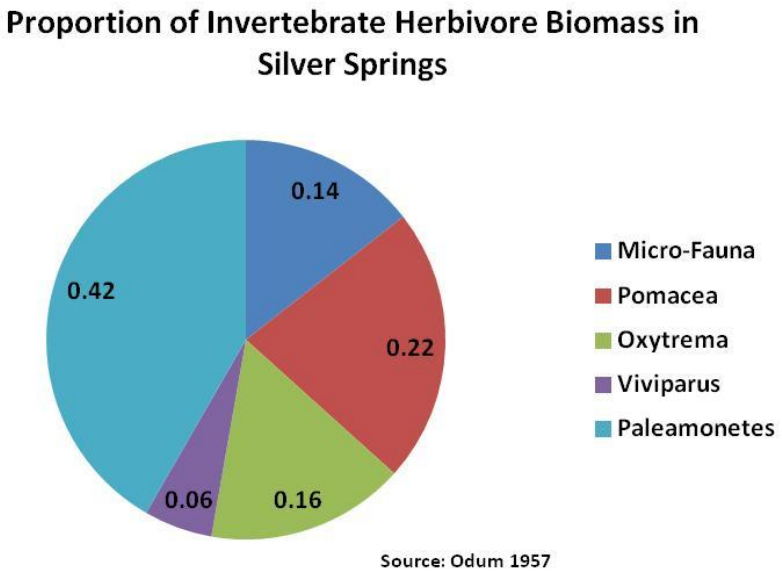

Figure 7.2.3. Proportion of invertebrate herbivore biomass in Silver Springs. The micro-fauna category consists of several sub-groups each representing a very small portion of overall herbivore biomass including Hydrobiidae (mud snails), Oligochetes, gammarids (amphipods), midges, copepods, ostracods, flatworms, Hydroptera (caddisflies), Elophila (moths) and Arcella (testate amoebae). Pomacea (Apple snails), Oxytrema (spiral stream snails), and Viviparus (river snail) are all gastropods. Paleomonetes is a freshwater decapod (grass shrimp). (Adapted from Odum 1957).

7.2.2.4 Gastropoda

The effect of snail herbivory on aquatic primary productivity has been supported in the current literature. Mulholland et al. (1991) reported that nutrient reduction did not have a significant effect on algae in test streams, however, herbivory by snails reduced biomass, carbon fixation and reduced taxonomic diversity of periphyton. Sheldon (1987) found that macrophyte diversity increased with decreased snail population and increased snail grazing resulted in lowered macrophyte diversity by species least preferred by herbivorous snails. Bronmark (1990) however, discounted the simple association of snails and macrophytes citing several studies (among them his own) that show greater macrophyte herbivory by aquatic insects and decapods (crayfish) over aquatic snails. The relationship between snail abundance and macrophyte diversity, according to Bronmark (1990) is due to complex chemical and biological interactions, not simply snail herbivory. Studies of grazing activities of snails indicates they have a significant effect on epiphytic algal biomass, productivity and species composition (Marks and Lowe, 1989; Atalha et al. 2007; Li et al. 2008; Zhu et al. 2013). Grazing by snails has also been shown to have a significant indirect effect on macrophytes by reducing the adverse effects of epiphyton such as shading and nutrient competition (Bronmark 1989; Li et al. 2008). Wojdak and Mittelbach (2007) report that microcosms with multiple snail species had greater final biomass, less epiphytic algae, and less total organic matter at the end of experiment than did microcosms with

a single species. This study strongly suggests that niche overlap among grazers has an additive effect on control of periphyton biomass.

Gastropods of the family *Pleuroceridae* have 12 genera found in North America but only one (Elimia) in the state of Florida (Thompson 2004).The Goblin Elimia (Elimia vanhayningiana) described by Goodrich (1921) is confined to springs and smaller streams of the St. Johns River basin in peninsular Florida and is amed after O.C. Van Hyning the founder Florida Museum of Natural History. Grazer densities of *Elimia clavaeformis* can reach 1000 individuals m^{-2} under normal conditions (Mulholland et al. 1991) with 250 snails m^{-2} or 5 g m^{-2} (dry mass) considered a moderate consumer population (Lamberti et al. 1987; Steinman et al 1987; Mulholland et al. 1989). These populations sizes suggest potential for significant effect on physicochemical properties of water and on algal community structure. (Zhu et al. 2013; Rosemond 1993). Further, benthic snail feeding activity can enhance microbial growth and nutrient cycling via mixing of surface sediments and processing of detritus Covich et al. 1999; Arango et al. 2009; Zheng et al. 2011).

Pulmonate snails (especially of the family Physidae) can tolerate low DO and are often observed in moderately to highly eutrophic systems receiving municipal wastewater (Giovanelli et al. 2005; Cui et al. 2008; Varnosfaderany et al. 2010; Cloherty and Rachlin 2011). Respiration of *Pleuroceridae* is strictly aquatic via internal gills (*ctenidium*) while several other families of gastropods utilize a pseudo "lung" or pulmonary cavity, an airfilled, highly vascualrized cavity portion of the mantle cavity that holds air and allows gas exchange. Requires exchange with atmosphere for refreshing of oxygen supply. Some gilled snails such as Amnicola limnosa can talerate DO below 3-4 mg L^{-1}, as can some species of Planorbidae, Physidae, Hydrobiidae, and Lymnaeidae (Cloherty and Rachlin 2011). This level of DO may not be lethal to some species, however, chronic low DO may inhibit reproduction and encourage extirpation (Korpinen et al. 2006). Other environmental stressors such as pesticides, herbicides, and fungicides can have significant negative effect on grazers (snails) resulting in increased algal production (McMahon et al. 2012).

7.2.2.5 Decapoda

The genus Palaemonetes, commonly known as the grass shrimp or ghost shrimp, is a group of caridean shrimp consisting of over 35 species worldwide. This genus occupies predominately freshwater but has been found in brackish (Tabb and Manning 1961; Rouse 1969) and salt waters (St. Amant and Hulquist 1969). Noted survival in laboratory studies at 30 ppt suggests a large tolerance range for environmental conditions (Dobkin and Manning 1964). In Florida springs, *Palaemonetes paludosus* (Gibbes) predominately feed on algae, however, they are omnivourous and also ingest vascular plants, aquatic insects, and detritus (Beck and Cowell, 1976; Wessell et al. 2001). In Silver Springs, *P. paludosus* represented 42% of the grazer population by biomass (Odum 1957). Longevity of these shrimp is confined to 1 year, with post spawning mortality occurring from April- October in FL. Fecundity can be variable with 8-85 eggs per female (Beck and Cowell 1976).Grass shrimp have been observed in habitats with a range of DO tolerances from 2.8-6.0 mg L^{-1} (Wessell et al. 2001) suggesting significant tolerance of low DO. Brown-Peterson et al. (2008) report that *Palemonetes pugio*, an estuarine grass shrimp, exposed to cyclic hypoxis (3 days at 1.5 mg L^{-1}) showed reduced number of broods and eggs. Both cyclic and

chronic (77 day) hypoxia resulted in decreased population growth indicative of population level impacts. These shrimp are especially abundant in central and South Florida marshes (Kushlan and Kushlan 1980) associated with vegetation communities providing cover and likely occupy similar niche in spring systems.

7.2.2.6 Hypotheses

Nitrate reduction in the Upper Florida Aquifer, the source of water in springs across the state, is linked to observations of reduced DO in spring vents and runs (Heffernan et al. 2012). Heffernan et al. (2010) suggests Top down control of invertebrate grazers via altered DO has resulted in altered trophic structure in springs to favor algal dominance. Liebowitz (2013) reports a significant negative association between algal and gastropod biomass in Florida springs suggesting top down control of algae by invertebrate grazers, a finding supported by several studies of grazer control of algae in other systems (Hildebrand 2002; Heck and Valentine 2007; Gruner et al. 2008; Baum and Worm 2009; Estes et al. 2011). Further, Liebowitz (2013) also found a significant relationship between dissolved oxygen (DO) and gastropod biomass in a survey of 11 springs, suggesting DO has a significant indirect effect on algal biomass via controlling grazer abundance and/or activity. Under low flow or current velocity conditions, nutrient enrichment and subsequent algal growth may outpace grazer pressure resulting in severe light reductions (Harlin and Thorne-Miller 1981). Alternatively, under similar nutrient enrichment and moderate to high flushing or exchange of water (as in lotic or tidally influenced systems), herbivores have been observed to control epiphytic algal biomass (Neckles 1993). Liebowitz (2013) argues that hysteretic responses of grazer populations to disturbances could be responsible for the over abundance of algae in springs where no clear grazer stress is present. For instance, invasive plant control measures utilizing herbicides and copper compounds are widely employed with known negative impacts on grazer populations (Evans 2008). Such a disturbance could enable algal populations to exceed thresholds for grazer control.

Based upon the available scientific literature, several hypotheses as to the causal mechanisms behind algal proliferation in springs are currently supported. The following hypotheses have foundations in the principles of top down control and trophic cascade theory. The commonality of all of these hypotheses is that alteration of top down control of grazers (be it predation or environmental stress) results in a cascading effect to the primary producer population, namely the epiphytic algal community in spring systems.

H_1- Declining DO levels have created chronic hypoxic stress on grazer communities resulting in lowered fecundity and grazing pressure (consumer stressor hypothesis 1)

H_2- Episodic hypoxia has extirpated invertebrate grazers resulting in loss of top down control of algal biomass (consumer stressor hypothesis 2)

H_3-Some combination of drivers/ stressors such as elevated NO_3 and hypoxia, working synergistically have caused dramatic declines in grazer communities (multiple stressor hypothesis)

7.2.2.7 Objectives

The objectives of this work are two-fold. First, we experimentally determine the necessary dissolved oxygen levels required for normal respiration, as well as, critical oxygen saturation thresholds for survival of hypoxic conditions. Secondly, once those experiments are complete, we will raise a second generation of test organisms under ambient, medium and high NO_3-N concentrations and test for NO_3-N effects on both respiration and critical oxygen saturation requirements for these four organisms to determine if there is any compound effect of NO_3-N on the already present oxygen stress.

7.2.3 MATERIALS AND METHODS

7.2.3.1 Field Collection

All test organisms were collected from Silver River and Alexander Springs Run in March and April of 2015. The gastropods (*Viviparus georgianus*, *Elimia floridensis*, *Micromenteus floridensis*) and decapods (*Palaemonetes paludosus)*(Figure 7.2.4) were returned to the Whitney Laboratory at ambient temperatures where they were then cultured in aquaria utilizing algal pellets as a primary food source. Spawning of gastropods was induced by the temperature change, resulting in large populations of snails of each species. These populations were allowed to grow unhindered until experimental phase began in which a majority of the population was moved to the mesocosm tanks to aid in algal control. The remaining specimens (approximately 25 of each species) were retained in the laboratory aquaria for testing.

Figure 7.2.4. Algal grazers utilized in respirometry experiments (clockwise from top left), *Palaemonetes paludosus* (decapoda); *Elimia floridensis* (gastropoda); *Viviparus georgianus* (gastropoda); *Micromenteus floridensis* (gastropoda).

7.2.3.2 Laboratory Analyses

The experimental respiration manipulations were conducted in a closed system consisting of an experimental aquarium (20 L aquarium) and a 100 L sump. Water in this closed system was circulated from the sump to the experimental aquarium using a brushless DC pump, before overflowing through a drain back into the sump. To minimise bacterial respiration, water was continuously circulated through a UV sterilization system (9 Watt Clarity +). The system was placed in a temperature controlled room which maintained the water temperature at 22.2 $\pm$ 0.1 °C, equivalent to the natural temperature experienced by this species in the wild.

Four identical 20 mL respirometry setups were placed in the aquarium side by side. Each respirometry set up consisted of a sealed 20 mL glass vial chamber connected to a recirculating pump (which mixed water inside the respirometer) and a flushing pump (which pumped water from the aquarium in and out of the chamber) (Steffensen, 1989; Clark et al., 2013; Svendsen et al. 2015). Dissolved oxygen concentration in the chamber was measured and logged using a FireSting fibre-optic oxygen meter (Pyroscience, Germany). The sensor was mounted in the recirculation loop, to ensure that flow was sufficient for a fast response time of the sensor. (Figure 7.2.5).

7.2.3.3 Settling Period

Snails were starved for a minimum of 16 hours prior to experimentation to ensure they were in a post-absorptive state (Niimi and Beamish 1974). A test subject (*E. floridensis*, wet mass = 0.85 $\pm$ 0.05 g, wet volume = 0.32 $\pm$ 0.08 ml, mean $\pm$ SE; n = 12) was randomly selected and placed into one of the respirometry chambers 12-15 h prior to the experimental period in order to allow the test subjects to settle in and acclimate to the experimental setup. Oxygen uptake rate (MO_2) was estimated using intermittent-flow respirometry, with a 180 s flush, 30 s wait and 690 s measurement period (controlled using a Titan Controls, Hades 2 ® timer). During the 690 s measurement period, the respirometry chamber was sealed to prevent water exchange between the chamber and surrounding aquarium. The length of the measuring period ensured that the snail reduced the oxygen saturation in the chamber by 3-5 % during each measurement period. After measurement phases were complete, snails were weighed whole in the shell and then without the shell.

7.2.3.4 Hypoxia Treatment

Following the overnight settling period, the oxygen saturation of the water in the system was systematically reduced by bubbling nitrogen through air stones into the experimental sump. The rate of nitrogen bubbling was manually controlled by monitoring the oxygen saturation in the sump using an YSI dissolved probe (oxygen EcoSense DO200A). This allowed MO_2 to be measured at 100, 70, 60, 50, 40, 30, 20 and 10% oxygen saturation for each snail (for detailed methodology, see Domenici et al. 2000). Three MO_2 determinations were carried out at each oxygen saturation level. Time between the oxygen saturation levels ranged between 45 to 60 minutes, for a total experimental duration of approximately 8 hours.

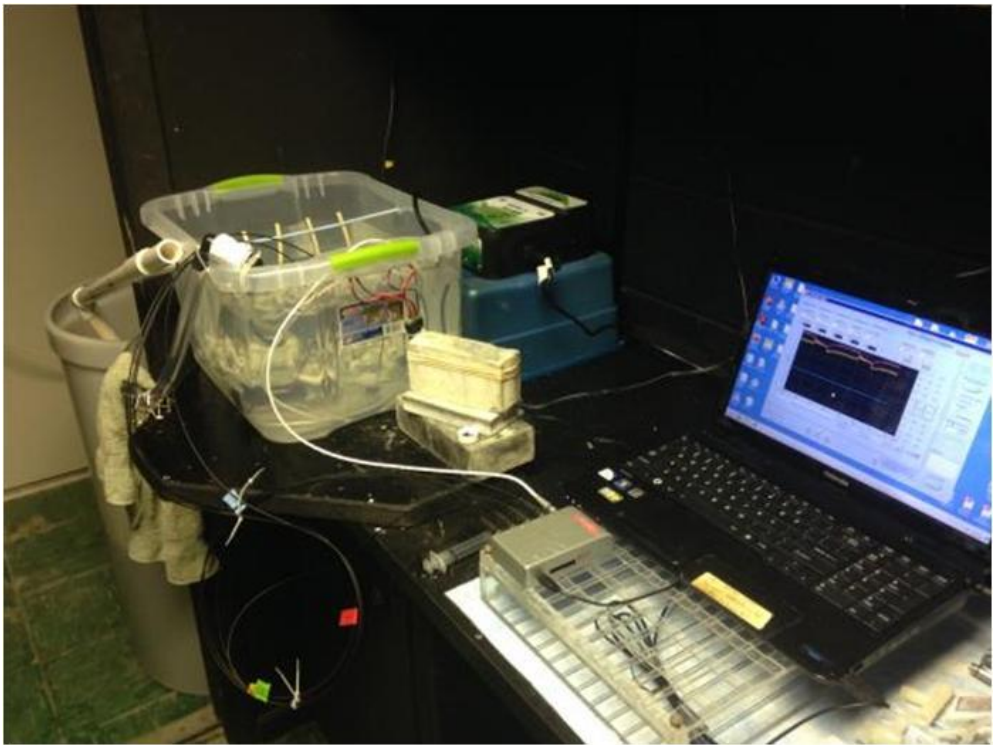

Figure 7.2.5. Photograph of respirometry experimental array with 20 liter holding tank fitted with test cells and timer switch, multi-plexer, and computer in foreground and 100L sump in background.

7.2.4 RESULTS AND DISCUSSION

Data generated from respirometry requires extensive post processing (10-12 h for each run of 4 individuals). As this work is ongoing, the selected data from a trial with *E. floridensis* is presented as provisional only (Figure 7.2.6). The trace depicted in Figure 7.2.6 shows a relatively stable MO_2 over time, until the end of the hypoxia experiment where oxygen saturation levels are experimentally reduced from 100% to 70, 60, 50, 40, 30, 20 and finally 10%. This decline in oxygen consumption at approximately 20% saturation indicates an inability of *E. floridensis* to adequately respire at its normal metabolic rate. While this experiment did not determine point of death for the test organisms, this will be determined experimentally in the coming months.

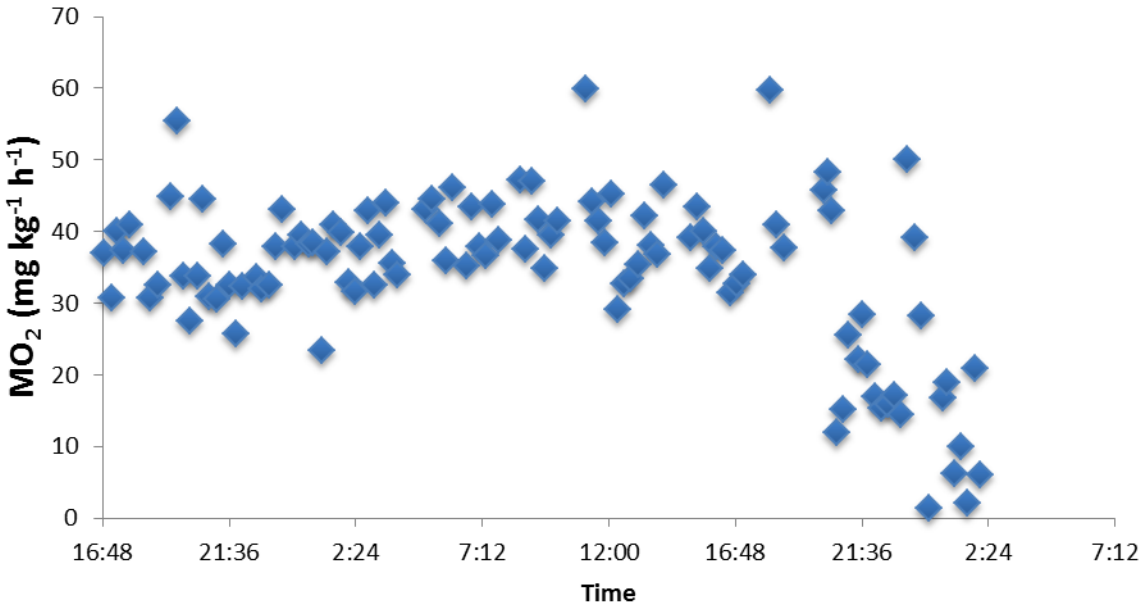

Figure 7.2.6: Raw data trace for one snail (*E. floridensis*) showing oxygen consumption in mgO_2 per kg snail per hour (MO_2) as a function of time.

While little work has been done in spring systems to determine the DO thresholds of algal grazers, current research on *Elimia floridensis* in Florida springs by Liebowitz et al. (In press) suggests strong relationship between DO and snail grazing efficiency. Although hypoxic conditions were not tested in that investigation, other research suggests a wide range of tolerances similar to those observed in other invertebrate groups. For example, there was no observed negative effects of *Bellamya sp*. in high density algae experiments where DO averaged below 2 mg L^{-1} over 30 days (Zhu et al 2013). This assertion does not appear to hold true for *E. floridensis* in experimental trials (Figure 7.2.7).

The horizontal linear regression demonstrates the standard metabolic rate (SMR) equivalent to 35.6 ± 0.7 mg O_2 kg^{-1} h^{-1} (mean ± S.E.). The linear regression intersecting with 0.0 shows the oxygen consumption of the snail under hypoxic conditions. The intersect between the two regression lines depicts the critical oxygen saturation level (O_2 crit), below which the snail can no longer extract adequate oxygen from the water to maintain it's SMR. For these individuals (n=4) O_2 crit = 4.9 mg O_2 L^{-1}, which is well above observed low DO saturation in dark hours in both Silver River and Alexander Springs. This finding suggests that snails in both ecosystems are significantly stressed in the dark hours when DO often falls below 3 mg L^{-1} and perhaps remain in a low grade stressed condition at all times that DO falls below the O_2 crit.

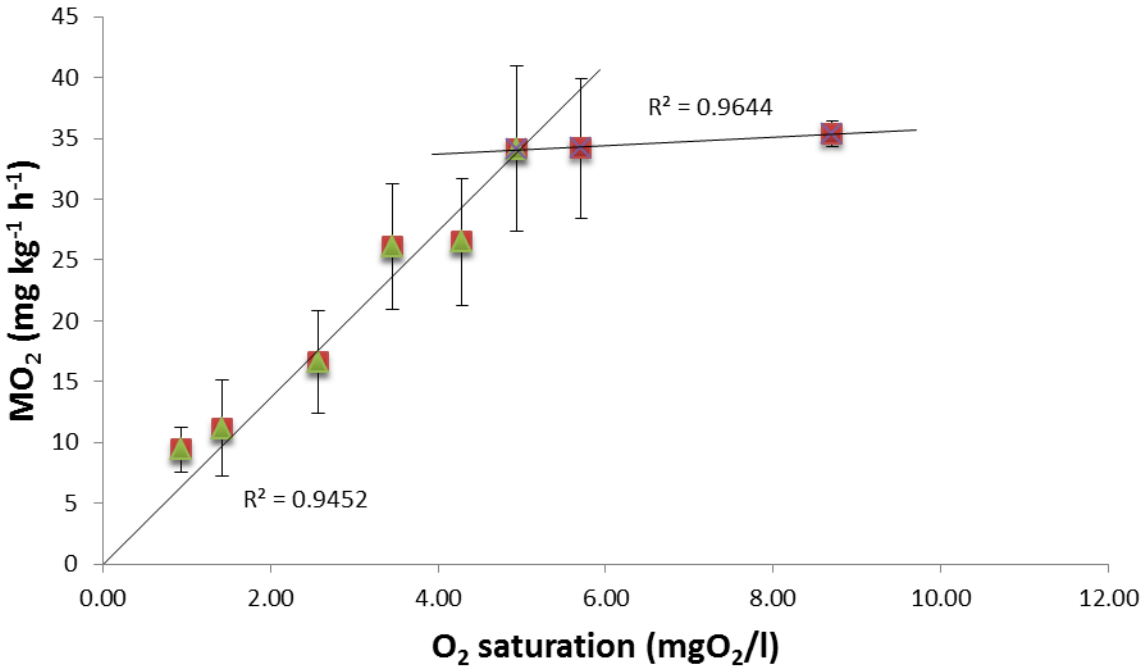

Figure 7.2.7. Metabolic rate of *E. floridensis* relative to oxygen saturation. Metabolic rate (MO_2) is described in mgO_2 per kg of snail per hour. Oxygen saturation is in mg O_2 per litre of water.

7.2.4.1 Chronic and Episodic Hypoxia

Oxygen saturated, or normoxic, conditions are considered optimal for aquatic systems and thus DO may range from 5-14 mg L^{-1} depending on water temperature and barometric pressure. However, many organisms are adapted to tolerate much lower DO conditions. Hypoxia, or low oxygen stress, is by convention, considered to be below 2.0-2.8 mg L^{-1}(Joyner-Matos et al. 2011). There has been significant efforts to study hypoxia in marine systems where many studies identifiy hypoxia at 2.0 mg L^{-1} with higher values (up to 4.0 mg L^{-1}) reported (Paerl 2006; Li et al. 2011). Ecological responses to hypoxia in marine systems include mass mortality, reduction of biomass and secondary production, and changes to community structure *sensu lato* elimination of sensitive species and proliferation of tolerant ones (Liu et al. 2011; Weisberg et al. 2008; Riedel et al. 2008; Wu 2002; Dauer 1993). Extinction or extirpation of local foundation species by hypoxic events has been well documented in estuarine and freshwater literature as well with many reports of effects of high BOD effluents altering structure of biotic communities in receiving waters (Altieri and Witman 2006; Wu 1982).

In some cases, low DO is advantageous to some invertebrates as it can serve as refugia from predators such as fish (Chapman 2007; Chapman et al. 2004). Commonly, low DO forces invertebrates, especially insects, into areas with higher current and less cover, ostensibly to increase respiratory efficiency, however, this increases risk of predation by fish (Lowell et al. 2000). Perhaps more importantly, DO can be a stressor in itself or compound the affects of other stressors such as heavy metal toxicity (Irving et al. 2008). Oxygen availability can influence distribution of species of invertebrates and fishes alike (Parson 1991; Osborne et al. 2001; Chapman 2007). In many aquatic systems where hypoxia is prevalent, invertebrate communities

are often dominated by physically small organisms (Chapman 2007). Too much oxygen can also be detrimental as organisms must repair damage from free radical exposure (Joyner-Matos et al. 2007).

Looking to the extensive aquatic insect (and other invertebrate) literature, interspecies variability in tolerances and responses to hypoxia by aquatic invertebrate grazers can be great (Merritt et al. 2008; Thorp and Covich 1991). For example, Munro Fox et al (1936) reported that for two species of Ephemoroptera (*Cloeon* and *Baetis*) responses to low oxygen were dramatically different with *Cloeon* reducing oxygen consumption only when levels reached 20% saturation while *Baetis* reduced consumption linearly with decreases in O_2 availability. Similarly, DO below 5mg L^{-1} reduced feeding by *Baetis tricaudatus* (Ephemeroptera) by 80% and after two weeks of exposure , 60-90% mortality was observed compared to high DO experimental streams (11 mg L^{-1} DO) (Lowell and Culp 1999). Further, similar species variability in oxygen consumption depends significantly on environmental conditions during growth (fast versus slow flowing water), a finding that suggests phenotypic plasticity in some aquatic insects with respect to adaptations to oxygen conditions. Invertebrates that utilize hemoglobin appear to have greater toleranes for hypoxia versus hemocyanin. Most FL gastropods use hemocyanin with the exception of the *Planorbidae* (Pennak 1989).

Many invertebrates can evade oxygen stress events with myriad adaptations for low oxygen survival. Some examples for highly mobile species includes drifting with current (downstream emigration)(Connolly and Pearson 2007) to evade oxygen depleted waters or seeking surface films where oxygen diffusion is more rapid and thus DO more available (Apodaca and Chapman 2004). Estuarine fishes and crustaceans practice avoidance or escape behaviors when subjected hypoxic conditions (Wannamaker and Rice 2000; Wu et al. 2002; Bell and Eggelston 2005) and may still suffer reductions in growth (Eby et al. 2005; Stierhoff et al. 2006). Physiological oxygen transport mechanisms have been documented in some organisms (McMahon 2001; Paul et al. 2004).Other avoidance mechanisms include decreasing activity, O_2 uptake capacity, or anaerobic metabolism (Grieshaber et al. 1994; Diaz and Rosenberg; Hochachka and Somero 2002; Wu et al. 2002). Eriksen (1963) describes respiratory adjustment as a phenomenon where aquatic insects reduce their oxygen consumption when oxygen availability is reduced (*Ephemera simulans* can survive oxygen concentrations down to 1.0 mg L^{-1} using this mechanism), however, not all species are capable.

Invertebrates show great adaptation in respiratory modes from atmospheric breathing to tracheal gill breathing allowing for dispersal in low DO habitats (Chapman et al. 2004; Chapman 2007). Some invertebrates have been documented to survive hypoxia and anoxia better if acclimated to cooler water tempetures (Nagell and Fagerstrom 1978). A study of stream invertebrates in tropical African aquatic systems with variable oxygen stress found low levels of gastropod grazers (<5% relative abundance) in streams with DO averaging 7 mg L^{-1} while an adjacent swamp with average DO of 2 mg L^{-1} had a relative abundance >25% (Osborne et al. 2001) In the same study, insect grazers such as tricopterans and ephemeropterans were reported in greater abundance in streams with DO 5 mg L^{-1} than in high DO rivers or low DO swamps indicating adaptation and potential advantage of predator evasion under low DO.

As this work progresses, the metabolic costs of existence in a low DO environment will be examined and other ongoing work, such as grazer feeding trials being conducted by Frazer et al. (will be discussed in context of DO and compared with results found in this experimental manipulation of DO.

7.2.5 CONCLUSIONS AND RECOMMENDATIONS

As of this reporting, data generated in this first year are undergoing QA/QC and initial data analysis. Therefore, no conclusions or recommendations are yet available.

7.2.6 FUTURE RESEARCH

The work conducted thus far suggests that hypoxia stress may be a factor in grazer population dynamics in spring ecosystems. The next step in the research process will be to culture the same four test organisms under variable levels of NO_3-N and repeat similar respirometry testing to determine if NO_3-N has a synergistic effect on hypoxia in these organisms. This will address both H_2 and H_3. This work will be completed in year 2 and 3 of the project.

7.2.7 REFERENCES

Albertin, A.R. 2009. Nutrient dynamics in Florida springs and relationships to algal blooms. Dissertation, University of Florida.

Altieri, A.H., J.D. Witman. 2006. Local extinction of a foundation species in a hypoxic estuary: integrating individuals to ecosystems. Ecology 87: 717-730.

Altieri, A.H., M.D. Bertness, T.C. Coverdale, E.E. Axelman, N.C. Herrmann, P.L. Szathmary. 2013.Feedbacks underlie the resilience of salt marshes and rapid reversal of consumer driven die-off. Ecology 94(7): 1647-1657.

Anastasiou, C. 2009. Characterization of the underwater light environment and its relevance to seagrass recovery and sustainability in Tampa Bay, Florida. PhD Dissertation. University of South Florida.

Apodaca, C.K. and L.J. Chapman. 2004. Larval damselflies in extreme environments: Behavioral and physiological response to hypoxic stress. Journal of Insect Phyisology 50:767-775.

Arango, CP, LA Riley, JL Tank, RO Hall. 2009. Herbivory by an invasive snail increases nitrogen fixation in a nitrogen-limited stream. Can. J. Fish. Aquat. Sci. 66: 1309-1317.

Atalah, J., MJ Anderson, MJ Costello. 2007. Temporal variability and intensity of grazing: a mesocosm experiment. Marine Ecology Progress Series 341: 15-24.

Baum, J. K., and B. Worm. 2009. Cascading top-down effects of changing oceanic predator abundances. Journal of Animal Ecology 78:699–714.

Beck, JT, BC Cowell. 1976. Life history and ecology of the freshwater Caridean shrimp, *Palaemonetes paludosus* (Gibbes). Ameican Midland naturalist 96(1): 52-65.

Beklioglu, M., O Ince, I Tuzun. 2003.. Restoration of the eutrophic Lake Eymir, Turkey, by biomanipulation after a major external control. Hydrobiologia 489: 93-105.

Bell, GW, DB Eggleston, TG Wolcott. 2003. Behavioral responses of free-ranging blue crabs to episodic hypoxia. I. Movement. Marine Ecological Progress Series 259: 215-225.

Biggs, B. J. F. and M. E. Close. 1989. Periphyton biomass dynamics in gravel bed rivers: the relative effects of flows and nutrients. Freshwater Biology 22:209-231.

Biggs, B. J. F., D. G. Goring and V. I. Nikora. 1998. Subsidy and stress responses of stream periphyton togradients in water velocity as a function of community growth form. Journal of Phycology 34:598-607.

Bluzat, R., J. Segue. 1983. Chronic intoxication by an herbicide 2,4,5-Trichlorophenoxyacetic acid in the pond snail Lymnaea stagnalis L. Environmental Research 31: 440-447.

van Boclaer,B., R. Shultheis, P. Plisnier, C. Albrecht. 2012. Does the decline of gastropods in deep water herald ecosystem change in lakes Malawi and Tanganyika? Freshwater Biology : 57:1733-1744.

Bothwell, ML. 1985. Phosphorus limitation of lotic periphyton growth rates: an intersite comparison using continuos flow troughs (Thompson River system, British Columbia). Limnology and Oceanography 30: 527-542.

Bronmark, C. 1989. Interactions between epiphytes, macrophytes, and freshwater snails: A review. Journal of Molluscan Studies 55: 299-311.

Bronmark, C. 1990. Do herbivorous freshwater snails affect macrophytes?- A comment. Ecology 71(3): 1212-1215.

Bronmark, C, SP Klosiewski, RA Stein. 1992. Indirect effects of predation in a freshwater, benthic food chain. Ecology 73(5): 1662-1674.

Brown, M.T., K. Chinner-Reiss, M.J. Cohen, J.M. Evans, K.R. Reddy, P.W. Inglett, K.S. Inglett, T. K. Frazer, C.A Jacoby, E.J. Philips, R. L. Knight, S. K. Notestein, K.A. McKee. 2008. Summary and synthesis of the available literature on the effects of nutrients on springs organisms and systems. Final Report. Florida Department of Environmental Protection, Tallahassee FL.

Brown-Peterson, NJ, CS Manning, V Patel, N Denslow, M. Brouwer. 2008. Effects of cyclic hypoxia on gene expression and reproduction in a grass shrimp, *Palaemonetes pugio*. Biological Bulletin 214: 6-16.

Burkholder J.M. and Wetzel R.G. 1989. Epiphytic microalgae on natural substrata in a hardwater lake: Seasonal dynamics of community structure, biomass and ATP content. Archiv für Hydrobiologie, Suppl. 83: 1–56.

Canfield, H.E.,and M.V. Hoyer. 1988. Influence of nutrient enrichment and light availability on the abundance of aquatic macrophytes in Florida streams. Canadian Journal of Fisheries and Aquatic Sciences 45: 1467-1472.

Carpetner, SR, JF Kitchell, JR Jodgeson, PA Cochran, JJ Elser, MM Elser, DM Lodge, D. Kretchmer, X. He, CN Vonende. 1987. Regulation of lake primary productivity by food web structure. Ecology 68(6): 1863-1876.

Carpenter, SR, JJ Cole, JR Hodgeson, JF Kitchell, ML Pace, D. Blade, KL Cottingham, TE Essington, JN Houser, DE Schlindler. 2001. Trophic cascades, nutrients, and lake productivity: whole lake experiments. Ecological Monographs 71(2): 163-186.

Carpenter, S.R., J.F. Kitchell. 1988. Consumer control of lake productivity. Bioscience 38: 764-769.

Chapman, L.J., K. Schneider, C.K. Apodaca, and C.A. Chapman. 2004. Respiratory ecology of macroinvertebrates in a swamp-river system of East Africa. Biotropica 36: 572-585.

Chapman, L.J. 2007. Morpho-physiological divergence across oxygen gradients in fishes. Invited book chapter. Pp. 14-29. In: M.N. Fernandes, F.T. Rantin, M.L. Glass, and B.G. Kapoor (editors). Fish Respiration and the Environment. Science Publisher, Inc., Enfield, NH.

Clark, Timothy D., Sandblom, Erik, and Fredrik Jutfelt, 2013. Aerobic scope measurements of fishes in an era of climate change: respirometry, relevance and recommendations. The Journal of Experimental Biology 216: 2771-2782.

Cloherty, T.M., J.W. Rachlin. 2011. Physico-chemical and shoreline development factors affecting lake littoral benthic macroinvertebrates. Journal of Freshwater Ecology. 26: 517-525.

Cohen, M.J., S. Lamsal and L.V. Korhnak. 2007. Sources, Transport and Transformations of Nitrate-N inthe Florida Environment. St. Johns River Water Management District SJ2007-SP10. 125 pp. Palatka, FL.

Cohen, M.J., J.B. Heffernan, A. Albertin, J.B. Martin. 2012. Inference of riverine nitrogen processing from longitudinal and diel variation in dual nitrate isotopes. Journal of Geophysical Research 117: 1-17.

Connolly, N.M, R.G. Pearson. 2007. The effect of fine sedimentation on tropical stream macroinvertebrate assemblages: a comparison using flow-through artificial stream channels and recirculating mesocosms. Hydrobiologia 592: 423-438.

Copeland, R. 2003. Florida spring classification system and spring glossary. Special Publication No. 52. Florida Geological Survey, Tallahassee, Florida, USA.

Copeland, R., N. A. Doran, A. J. White and S. B. Upchurch. 2009. Regional and statewide trends in Florida's spring and well groundwater quality (1991-2003). Bulletin No. 69. Florida Geological Survey, Tallahassee, Florida, USA.

Covich, AP, MA Palmer, TA Crowl. 1999. The role of benthic invertebrate species in freshwater ecosystems: zoobenthic species influence energy flows and nutrient cycling. BioScience 49: 119-127.

Cowell, B.C. and P.S. Botts. 1994. Factors influnceing the distribution, abundance, and growth of *Lyngbya wollei* in Central Florida. Aquatic Botany 49: 1-17.

Cowell, B.C. and C.J. Dawes. 2004. Growth and nitrate nitrogen uptake by the cyanobacterium *Lyngbya wollei*. Journal of Aquatic Plant Management. 42: 69-71.

Crawley, M.J. 1983. Herbivory: the dynamics of animal-plant interactions. University of California Press, Berkely CA USA.

Cui, Y., X Liu, H. Wang. 2008. Macrozoobenthic community of Fuxian Lake, the deepest lake of southwest China. Limnologica 38: 116-125.

Cuker B.E. 1983. Competition and coexistence among the grazing snail Lymnaea, chironomidae, and microcrustacea in an arctic epilithic lacustrine community. Ecology 64_1_: 10–15.

Dauer, D.M. 1993. Biological criteria, environmental health and estuarine macrobenthic community structure. Marine Pollution Bulletin 26: 249-257.

Dennison, W., C. and others 1993. Assessing water quality with submersed aquatic vegetation. BioScience **43:** 86-94.

Diaz, R.J., R. Rosenberg. 1995. Marine Benthic hypoxia: a review of its ecological effects and the behavioral responses of benthic macrofauna. Oceanography and Marine Biology Annual Review 33: 245-303.

Dobkin, S., R.B. Manning. 1964. Osmoregulation in two species of *Palaemonetes monetes* (Crustacea: Decapoda) from Florida. Bull. Mar. Sci. Gulf. Caribb. 14: 149-157.

Domenici, P, Steffensen, JF, and RS Batty, 2000. The effect of progressive hypoxia on swimming activity and schooling in Atlantic herring. Journal of Fish Biology 57: 6, 1526-1538.

Duarte, C.M. 1995. Submerged aquatic vegetation in relation to different nutrient regimes. Ophelia 41: 87–112.

Duarte, C.M. and D.E. Canfield, Jr. 1990. Macrophyte standing crop and primary productivity in some Florida spring-runs. Water Resources Bulletin 26(6): 927-934.

Eby, LA, LB Crowder, CM McClellan, CH Peterson, and MJ Powers. 2005. Habitat degradation from intermittent hypoxia: impacts on demersal fishes. Marine Ecological Progress Series 291: 249-261.

Eriksen, C.H. 1963. Respiratory regulation in Ephemera simulans Walker and Hexagenia limbata (Serville) (Ephemeratopera). Journal of Experimental Biology 40: 455-467.

Estes, J. a, J. Terborgh, J. S. Brashares, M. E. Power, J. Berger, W. J. Bond, S. R. Carpenter, T.E. Essington, R. D. Holt, J. B. C. Jackson, R. J. Marquis, L. Oksanen, T. Oksanen, R. T.Paine, E. K. Pikitch, W. J. Ripple, S. a Sandin, M. Scheffer, T. W. Schoener, J. B. Shurin,A. R. E. Sinclair, M. E. Soulé, R. Virtanen, and D. Wardle. 2011. Trophic downgrading ofplanet Earth. Science 333:301–306.

Farwick, F. Schröder, A. Thienemann. 1909 Bericht über die botanischen und zoologischen Exkursionen nach dem Weißenstein bei Hohenlimburg und nach der Glörtalsperre am 25. -- S.-B. naturhist. Ver. preuß. Rheinl. Westf., E 1909: 94-101.

Feminella JW, Power ME, Resh VH (1989) Periphyton responses to invertebrate grazing and riparian canopy in three northern California coastal streams. Freshwater Biol 22:445-457.

Feminella, J.W., C.P Hawkins. 1995. Interactions between stream herbivores and periphyton: a quantitative analysis of past experiments. J. North American Benthological Society 14(4): 465-509.

Gallegos, C. L., W. J. Kenworthy, P. D. Biber, B. S. Wolfe. 2009. Underwater spectral energy distribution and seagrass depth limits along an optical water quality gradient. Smithsonian Contributions to the Marine Sciences 38: 359-367.

Gilliom, RJ, JE Barbash, CG Crawford, PA Hamilton, JD Martin, N Nakagaki. 2007. Th equality of our nations waters: pesticides in the nations streams and ground water, 1992-2001. US Department of Interior, US Geological Survey, http://www.usgs.gov/pubprod. Accessed 8/7/2013.

Giovanelli, A., CL da Silva; GB Leal, DF Baptista. 2005. Habitat preference of freshwater snails in relation to environmental factors and presence of the competitor snail Melanoides tuberculatus (Muller 1774). Memorias do Instituto Oswald Cruz, Rio de Janeiro 100: 169-176.

Giudice, B.D., T.M. Young. 2010. The antimicrobial triclocarban stimulates embryo production in the freshwater mudsnail Potamopyrgus antipodarum. Environmental Toxicology and Chemistry 29(4): 966-970.

Goodrich, C. 1942. The Pleuroceridae of the Atlantic Coastal Plain. Occasional Papers of the Museum of Zoology, University of Michigan, (456): 1-6.

Grieshaber, M.K., I. Hartwig, U. Kreutzer, and H.O. Portner. 1994. Physiological and metabolic response to hypoxia in invertebrates. Reviews in Physiology, biochemistry, and Pharmacology 125: 43-147.

Gruner, D. S., J. E. Smith, E. W. Seabloom, J. T. Ngai, S. Sandin, H. Hillebrand, W. S. Harpole,

J. J. Elser, E. E. Cleland, M. E. S. Bracken, E. T. Borer, and B. Bolker. 2008. A cross system synthesis of consumer and nutrient resource control on producer biomass. EcologyLetters 11:740–755.

Hart DD, Robinson CT (1990) Resource limitation in a stream community: phosphorus enrichment effects on periphyton and grazers. Ecology 71:1494-1502.

Hauxwell, J., J. McClelland, P.J. Behr and I. Valiela. 1998. Relative importance of grazing and nutrient controls of macroalgal biomass in three temperate shallow estuaries. Estuaries 21: 347–360.

Heck, K. L. J., and J. F. Valentine. 2007. The primacy of top-down effects in shallow benthic ecosystems. Estuaries and Coasts 30:371–381.

Heffernan, J. B., D. M. Liebowitz, T. K. Frazer, J. M. Evans,and M. J. Cohen. 2010. Algal blooms and the nitrogen enrichment hypothesis in Florida springs: evidence, alternatives, and adaptive management. Ecological Applications 20:816–829.

Heffernan, J.B., A.R. Albertin, M.L. Fork, B.G. Kats, M.J. Cohen. 2012. Denitrification and inference of nitrogen sources in the karstic Floridan Aquifer. Biogeosciences 9: 1671-1690

Hensley, R.T., M.J. cohen. 2012. Controls on solute transport in large spring fed karst rivers. Limnology and Oceanography 57(4): 912-924.

Hill WR, Knight AW (1987) Experimental analysis of the grazing interaction between a mayfly and stream algae. Ecology 68: 1955-1965.

Hill WR, Harvey BC (1990) Periphyton responses to higher trophic levels and light in a shaded stream. Can J Fish Aquat Sci 47: 2307-2314.

Hill W.R., Boston H.L. and Steinman A.D. 1992. Grazers and nutrients simultaneously limits lotic primary productivity. Canadian Journal of Fisheries and Aquatic Sciences 49: 504–512.

Hillebrand, H. 2002. Top-down versus bottom-up control of autotrophic biomass—a metaanalysis on experiments with periphyton. Journal of the North American BenthologicalSociety 21:349–369.

Hochachka, P.W., G.N. Somero. 2002. Biochemical adaptation: mechanism and process in physiological evolution. Oxford University Press, New York.

Irving, EC, RB Lowell, JM Culp, K Liber, Q Xie, R. Kerrich. 2008. Effects of arsenic speciation and low dissolved oxygen condition on the toxicity of arsenic to a lotic mayfly. Environmental Toxicology and Chemistry 27: 583-590.

Jacoby, C., T.K Frazer, E.J. Phlips. 2008. Nutrient effects on springs flora and fauna. Pgs 179-230. In Brown et al. Summary and Synthesis of the Available Literature on the Effects of Nutrients on Spring Organisms and Systems. Final Report to Florida Department of Environmental Protection Tallahassee, FL.

Jones, J.I., B. Moss, J.O. Young. 1998. The interactions between periphyton, non-moluscan invertebrates and fish in standing freshwaters. P.69-90. In E. Jeppesen, M. Sondergaard, M. Sondergaard, K. Christophersen (Eds.) The structuring Role of Submerged Macrophytes in Lakes. Springer-Verlag, New York, USA.

Jones, J.I. and C.D. Sayer. 2003. Does the fish-invertebrate –periphyton cascade precipitate plant loss in shallow lakes? Ecology 84: 2155-2167.

Joyner-Matos, J., L.J. Chapman, C.A. Downs, T. Hofer, C. Leeuwenburgh, and D. Julian. 2007. Population distribution and stress response of a freshwater clam along a natural oxygen gradient. Functional Ecology 21:344-355.

Joyner-Matos, J., H. Richardson, T. Sammeli, and L.J. Chapman. 2011. A fingernail clam shows higher fitness in hypoxic waters. Canadian Journal of Zoology 89:161-168.

Joyner-Matos, J., L.J. Chapman, C.A. Downs, T. hofer, C. Leeuwenburgh, D. Julian. 2007. Stress response of a freshwater clam along an abiotic gradient: too much oxygen may limit distribution. Functional Ecology 21: 344-355.

Karevia, P.M., J.G. Kingsolver, R.B. Huey. 1993. Biotic interaction and global change. Sinauer Associates, Sunderland, Massachusetts, USA.

Keeling, R.F., A. Kortzinger, N. Gruber. 2010. Ocean deoxygenation in a warming world. Annual Review of Marine Science 2: 199-229.

King, S.A. 2012. Effects of flow on filamentous algae and nutrient limitation in lotic systems. Dissertation, University of Florida, Gainesville, FL.

Kirk, J. T. O. 1994. Light and photosynthesis in aquatic ecosystems, Second Edition Cambridge University Press.

Korpinen, S., V. Jormalainen, T. Honkanen. 2007. Bottom-up and cascading top-down control of macroalgae along a depth gradient. Journal of Experimental Marine Biology and Ecology 343: 52-63.

Korpinen, S., M. Karjalainen, M. Viitasalo. 2006. Effects of cyanobacteria on survival and repordcutionof the littoral crustacean Gammarus zaddachi (Amphopoda). Hydrobiologia 559: 285-295.

Lamberti GA, Resh VH (1983) Stream periphyton and insect herbivores: an experimental study of grazing by a caddis fly population. Ecology 64:1124-1135.

Lamberti, G.A., J.W. Feminella, V.H. Resh. 1987. Herbivory and intraspecific competition in a stream caddisfly population. Oecologia 73: 75-81.

Lamberti, G.A., S.V. Gregory, L.R. Ashkenas, A.D. Steinman, C.D. McIntire. 1989. Prodcutive capacity of periphyton as a determinant of plant-herbivore interactions in streams. Ecology 70: 1840-1856.

Lawler, JJ, JE Aukema, JB Grant, BS Halpern, P Kareiva, CR Nelson. 2006. Conservation science: a 20 year report card. Frontiers in Ecology and the Environment 4: 473-480.

Lawton, J.H. 2000. Community ecology in a changing world. Ecology Institute, Oldendorf/ luhe, Germany.

Levin, L.A., W. Ekau, A.J. Gooday, F. Jorissen, J.J.Middleburg, S.W.A. Naqvi, C. Neira, N.N. rabalais, J. Zhang. 2009. Effects of natural and human induced hypoxia on coastal benthos. Biosciences 6(10): 2063-2098.

Li, KY, ZW Liu, BH Gu. 2008. Persistence of clear water in a nutrient impacted region of Lake Taihu: the role of periphyton grazing by snails. Fundamental and Applied Limnology 173(1): 15-20.

Liboriussen, L., E. Jeppesen, M.E. Bramm, M.F. Lassen. 2005. Periphyton-macroinvertebrate interactions in light and fish manipulated enclosures in a clear and a turbid shallow lake. Aquatic Ecology 39:23-39.

Liebowitz, DM, MJ Cohen, JB Heffernan, TK Frazer, LV Korhnak. 201X. Environmentally mediated consumer control of algae proliferation in Florida springs. In Press.

Liu, C.C., J.M.Y. Chiu, L. Li, P.K.S. Shin, S.G. Cheung. 2011. Physiological response of two sublittoral nassariid gastropods to hypoxia. Marine Ecological Progress Series 429: 75-85.

Lowell, RB, JM Culp. 1999. Cumulative effects of multiple effluent and low dissolved oxygen stressors on mayflies at cold temperatures. Canadian Journal of Fisheries and Aquatic Sciences. 56: 1624-1630.

Lowell, RB, JM Culp, MG Dube. 2000. A weight-of-evidence approach for northern river risk assessment: Integrating the effects of multiple stressors. Environmental Toxicology and Chemistry 19: 1182-1190.

Maddox, G.L., J.M. Lloyd, T.M. Scott, B. Upchurch, R. Copeland. 1992. Florida's groundwater quality monitoring program, background geochemistry. Florida Geological Survey, Tallahassee, FL.

Marks, JC, RL Lowe. 1989. The independent and interactive effects of snail grazing and nutrient enrichment on structuring periphyton communities. Hydrobiologia 185: 9-17.

McMahon, BR. 2001. Respiratory and circulatory compensation to hypoxia in crustaceans. Respiration Physiology 128: 349-364.

McMahon, TA, NT Halstead, S Johnson, TR Raffel, JM Romansic, PW Crumrine, JR Rohr. 2012. Fungicide induced declines in freshwater biodiversity modify ecosystem functions and services. Ecology Letters 15: 714-722.

Merrit, R.W., K.W. Cummins, M.B. Berg. 2008. An Introduction to the Aquatic Insects of North America 4th ed. Kendal Hunt Publishing Co. Dubuque IA USA. 1157 pp.

Mulholland, P.J., A.D. Steinman, A.V. Palumbo, J.W. Elwood. 1991. Role of nutrients cycling on herbivory in regulating periphyton communities in laboratory streams. Ecology 72: 966-982.

Munch, D.A., D.J. Toth. C. Huang, J.B. Davis, C.M. Fortich, W.L. Osburn, E.J. Phlips, E.L Quinlan, M.S. Allen, M.J. Woods, P.Cooney, R.L Knight, R.A. Clarke, S.L. Knight. 2006. Fifty year retrospective study of the ecology of Silver springs, Florida. Special Publication SJ2007-SPA. St. John's River Water Management District, Palatka.

Munro-Fox, H., CA Wingfield, BG Simmons. 1936. The oxygen Consumption of Ephemerid nymphs from flowing and from still waters in relation to the concentration of oxygen in the water. Journal of Experimental Biology 13: 210-218.

Munro-Fox, H., CA Wingfield, BG Simmons. 1936. Oxygen consumption of mayfly nymphs in relation to oxygen availability. Nature 134: 1015.

Nagell, B., T. Fagerstrom. 1978. Adaptations and resistance to anoxia in *Cloen dipterum* (Ephemeroptera) and *Nemoura cinera* (Plecoptera). Oikos 30: 95-99.

Newbold, J. D., J. W. Elwood, R. V. O'Neill and W. Van Winkle. 1981. Measuring nutrient spiralling in streams. Canadian Journal of Fisheries and Aquatic Sciences 38:860-863.

Newbold, J. D., R. V. O'Neill, J. W. Elwood and W. Van Winkle. 1982. Nutrient spiralling in streams: implications for nutrient limitation and invertebrate activity. The American Naturalist 120:628-652.

Niimi, A.J., and F.W.H. Beamish, 1974. Bioenergetics and Growth of Largemouth Bass (*Micropterus- salmoides*) in Relation to Body-Weight and Temperature. Canadian Journal of Zoology 52: 4, 447-456.

Opsahl, R W., T. Wellnitz and N. L. Poff. 2003. Current velocity and invertebrate grazing regulate stream algae: results of an in situ electrical exclusion. Hydrobiologia 499:135-145.

Osborne, T.Z., L.J. Chapman, C.A. Chapman, T.L. Crisman, J. Prenger, S. Nyguen, and E. Stecker. 2001. Invertebrate community structure and oxygen availability in an intermittent stream/wetland system of the Uganda uplands. Verhandlungen Internationale Vereinigung Limnologie 27:3599-3603.

Paerl, H.W. 2006. Assessing and managing nutrient-enhanced eutrophication in estuarine and coastal waters: interactive effects of human and climatic perturbations. Ecological Engineering 26: 40-54.

Parsons, P.A. 1991. Evolutionary rates: stress and species boundaries. *Annual Review of Ecology and Systematics* **22**, 1–18.

Paul, RJ, B. Zeis, T. Lamkemeyer, M. Seidl, R. Pirow. 2004. Control of oxygen transport in the microcrustacean Daphnia: regulation of haemoglobin expression as central mechanism of adaptation to different oxygen and temperature conditions. Acta Physiol. Scand. 182: 259-275.

Pearson, R.G., N.M. Connolly. 2000. Nutrient enhancement, food quality and community dynamics in a tropical rainforest stream. Freshwater Biology 43: 31-42.

Pennak, R.W. 1989. Fresh-water invertebrates of the United States, 3rd Ed. Protozoa to Mollusca. John Wiley and Sons. New York. 628 p.

Pimentel, D., C.A. Edwards. 1982. Pesticides and ecosystems. Bioscience 32(7): 595-600.

Poff, N. L. and J. V. Ward. 1995. Herbivory under different flow regimes: a field experiment and test of a model with a benthic stream insect. Oikos 72:179-188.

Power ME, Stewart A J, Matthews WJ (1988) Grazer control of algae in an Ozark mountain stream: effects of short-term exclusion. Ecology 69:1894-1898.

Power M.E. 1990. Effects of Fish in River Food Webs. Science 250: 811–814.

Power M. 1992. Top-down and bottom-up forces in food webs: Do plants have primacy? Ecology 73_3_: 733–746.

Pringle CM 1987. Effects of water and substratum nutrient supplies on lotic periphyton growth: an integrated bioassay. Can J Fish Aquati Sci 44:619-629.

Quinlan, E.L., E.J. Phlips, K.A. Donnelly, C.H. Jett, P. Sleszynski, S. Keller. 2008. Primary producers and nutrient loading in Silver Springs, FL, USA. Aquatic Botany 88: 247-255.

Riedel, B., M. Zushin, A. Haselmair, M. Stachowitsch. 2008. Oxygen depletion under glass: behavioral responses of benthic macrofauna to induced anoxia in the Northern Adriatic. Journal of experimental Marine Biology and Ecology 367: 17-27.

Rabalais, N.N., R.E. Turner, W.J. Wiseman. 2002. Gulf of Mexico hypoxia, aka "the dead zone". Annual Review of Ecology and Systematics 33: 235-263.

Rosemond, A.D., P. Mulholland, J.W. Elwood. 1993. Top-down and bottom-up control of stream periphyton: effects of nutrients and herbivores. Ecology 74: 1264-1280.

Rosemond, A. D. 1993. Interactions among irradiance, nutrients, and herbivores constrain a stream algal community. Oecologia 94: 585-596.

Rouse, W.L. 1969. Littoral crusatcea from southwest Florida. Q. J. Fla. Acad. Sci. 32: 127-152

Scott, T., G. Means, R. Meagan, R. Means, S. Upchurch, R. Copeland, R. Jones, A. Willet. 2004. Springs of Florida. Bulletin No. 66 Florida Geological Survey, Tallahassee, FL.

Sheeb, N.H., I. Flores, T. Kurobe, B. Franze, A. Ranganthan, B.D. Hammock, S.J. The. 2011. Bioconcentration, metabolism, and excretionof triclocarban in larval Qurt Medaka (Oryzias latipes). Aquatic Toxicology 105: 448-454.

Sheldon, SP. 1987. The effects of herbivorous snails on submerged communities in Minnesota lakes. Ecology 68: 1920-1931.

Sickman, J.O. A.R. Albertin, M.W. Anderson, A Pinowska and R.J. Stevenson. 2009.A comparison of internal and external supply of nutrients to algal mats in two first magnitude springs in Florida. Journal of Aquatic Plant Management. 47: 135-144.

Smith, V.H. 2006. Response of estuarine and coastal marinephytoplankton to nitrogen and phosphorus enrichment. Limnology and Oceanography 51(1): 377-384.

Smith, V.H. 1982. The nitrogen and phosphorus dependence of algal biomass in lakes: an empirical and theoretical analysis. Limnology and Oceanography 27(6): 1101-1111.

St. Amant, J.A., R.G. Hulquist. 1969. *Palaemonetes paludosus* collected in the Rio Hardy and Colorado River, Baja California. Calif. Fish game 55: 252.

Steinman, A.D., C.D. McIntire, S.V. Gregory, G.A. Lamberti, L.R. Ashkenas. 1987. Effects of herbivore type and density on taxanomic structure and physiognomy of algal assemblages in laboratory streams. Journal of the North American Benthological Society 6: 175-188.

Steinman AD (1992) Does an increase in irradiance influence periphyton in a heavily-grazed woodland stream? Oecologia 91: 163-170.

Steinman AD, McIntire CD (1987) Effects of irradiance on the community structure and biomass of algal assemblages in laboratory streams. Can J Fish Aquat Sci 44:1640 1648.

Steffensen, John Fleng, 1989. Some errors in respirometry of aquatic breathers: how to avoid and correct for them. Fish Physology and Biochemistry 6:1, 49-59.

Stevenson, R.J., A. Pinowska, Y. Wang. 2004. Ecological condition of algae and nutrients in Florida Springs. Florida Department of Environmental Protection, Tallahassee, FL.

Stevenson, R.J., A. Pinowska, A. R. Albertin, J.O. Sickman. 2007. Ecological condition of algae and nutrients in Florida springs: the synthesis report. Florida Department of Environmental Protection, Tallahassee, FL.

Stevenson, R. J. 1996. The stimulation and drag of current. Pages 321-340 in R.J. Stevenson, M.L. Bothwell and R.L. Lowe (editors). Algal ecology: freshwater benthic ecosystems. Academic Press, Inc., San Diego, CA, USA.

Stevenson, R. J. and R. Glover. 1993. Effects of algal density and current on ion transport through periphyton communities. Limnology and Oceanography 38:1276-1281.

Stierhoff, KL, TE Targett, K Miller. 2006. Ecophsiological responses of juvenile summer and winter flounder to hypoxia: experimental and modeling analyses of effects on estuarine nursery quality. Marine Ecological Progress Series 325: 255-266.

Svendsen, J.C., Tirsgaard, B., Cordero, G.A., and J.E. Steffenson, 2015. Intraspecific variation in aerobic and anaerobic locomotion: gilthead sea bream (*Sparus aurata*) and Trinidadian guppy (*Poecilia reticulate*) do not exhibit a trade-off between maximum sustained swimming speed and minimum cost of transport. Frontiers in Physiology 6:43. DOI < 10.3389/fphys.2015.00043>.

Szafraniec, M.L. 2014. Spectral distribution of light in Florida spring ecosystems: the quantity and quality of light available for primary producers. Doctoral Dissertation, University of Florida, Gainesville, FL.

Tabb, D. RB Manning. 1961. A checklist of the flora and fauna of northern Florida Bay and adjacent brackish waters of the Florida mainland collected during the period July a957 through September 1960. Bulletin Mar. Sci. Gulf. Caribbean 11: 554-649.

Tarkowska-Kukuryk, M., T. Mieczan. 2012. Effect of substrate on periphyton communities and relationships among food web components in shallow hypertrophic lake. Journal of Limnology 71(2): 279-290.

Thompson, F.G. 2004. An identification manual for the freshwater snails of Florida. The Florida Museum of Natural History. http://www.flmnh.ufl.edu/malacology/fl-snail/snails1.htm Last accessed 7/31/2013.

Thorp, JH , AP Covich. 1991. Ecology and Classification of North American Freshwater Invertebrates. Academic Press, San Diego CA, USA. 911 pp.

Varnosfaderany, M.N., E. Ebrahimi, N. Mirghaffary, A. Safyanian. 2010. Biological assessment of Zayandeh Rud River, Iran, using benthic macroinvertebrates. Limnologica 40: 226-232.

Vermaat, J.E. 2005. Periphyton dynamics and influencing factors. P. 35-49 In: M.E. Azim, M. Verdegem, A. van Dam, M. Beveridge (Eds.) Periphyton: Ecology, Exploitation, and Management. CABI Publishing, London UK.

Vitousek, P.M. 1994. Beyond global warming: ecology and global change. Ecology 75: 1861-1876

Wannamaker, CM, JA Rice. 2000. Effects of hypoxia on movements and behavior of estuarine organisms from the southeastern United States. Journal of Experimental Marine Biology and Ecology 249: 145-163.

Warren, G. L., D. A. Hohlt, C. E. Cichra, and D. VanGenechten. 2000. Fish and Aquatic Invertebrate Communities of the Wekiva and Little Wekiva Rivers: A Baseline Evaluation in the Context of Florida's Minimum Flows and Levels Statutes. St. Johns River Water Management District Special Publication SJ2000-SP4. Pp. variously numbered.

Weisberg, SB, B. Thompson, J.A. Ranasinghe, D.E. Montagne. 2008. The level of agreement among experts applying best professional judgement to assess the condition of benthic infaunal communities. Ecological Indicators 8: 389-394.

Werner, E. E. 1998. Ecological experiments and a research program in community ecology. Pages 3–26 *in* W. J. J. Resetarits and J. Bernardo, editors. Experimental ecology: issues and perspectives. Oxford University Press, Oxford, UK.

Wessell, KJ, RW Merritt, KW Cummins. 2001. Distribution, diel movement, and growth of grass shrimp Palaemonetes paludosus in the Kissimmee River-floodplain ecosystem, Florida. Ann. Limnol. 37: 85-95.

Wetzel, R.G. 2001. 2001. Lake and River Ecosystems 3rd Ed. Academic Press, San Diego CA USA. 1006 pp.

Wilcove, DS, LL Master. 2005. How many endangered species are there in the United States? Frontiers of Ecology and Environment 3: 414-420.

Woin, P., C. Bronmark. 1992. Effect of DDT and MCPA (4-Chloro-2-Methylphenoxyacetic acid) on reproduction of the pond snail, Lymnaea stagnalis L. Bulletin of Environmental Contamination and Toxicology 48: 7-13.

Wojdak, JM, GG Mittelbach. 2007. Consequences of niche overlap for ecosystem functioning: an experimental test with pond grazers. Ecology 88(8): 2072-2083.

Wu, R.S.S. 2002. Hypoxia: from molecular responses to ecosystem responses. Marine Pollution Bulletin 45:35-45.

Wu, RSS, PKS Lam, KL Wan. 2002. Tolerance to, and avoidance of, hypoxia by the peniad shrimp (*Metapenaeus ensis*). Environmental Pollution 118: 351-355.

Zheng, ZM, J Lv, KH Lu, CH Jin, JY Zhu, XS Liu. 2011. The impact of snail (Bellamya aeruginosa) bioturbation on sediment characteristics and organic carbon fluxes in an eutrophic pond. Clean Soil, Air, Water 39: 566-571.

Zhu, J., K. Lu, X. Liu. 2013. Can the freshwater sanil Bellamya aeruginosa (Mollusca) affect phytoplankton community and water quality? Hydrobiologia 707: 147-157.

7.2.8 PUBLICATIONS AND PRODUCTS

Osborne, T.Z., R.A. Mattson, M.F. Coveney. 201X. Macroinvertebrate grazers, dissolved oxygen, and the loss of top-down control of algae in Florida spring ecosystems: a review. Submitted to *Oecologia* June 2015

7.2.8.1 Theses

N/A

7.2.8.2 Presentations

N/A

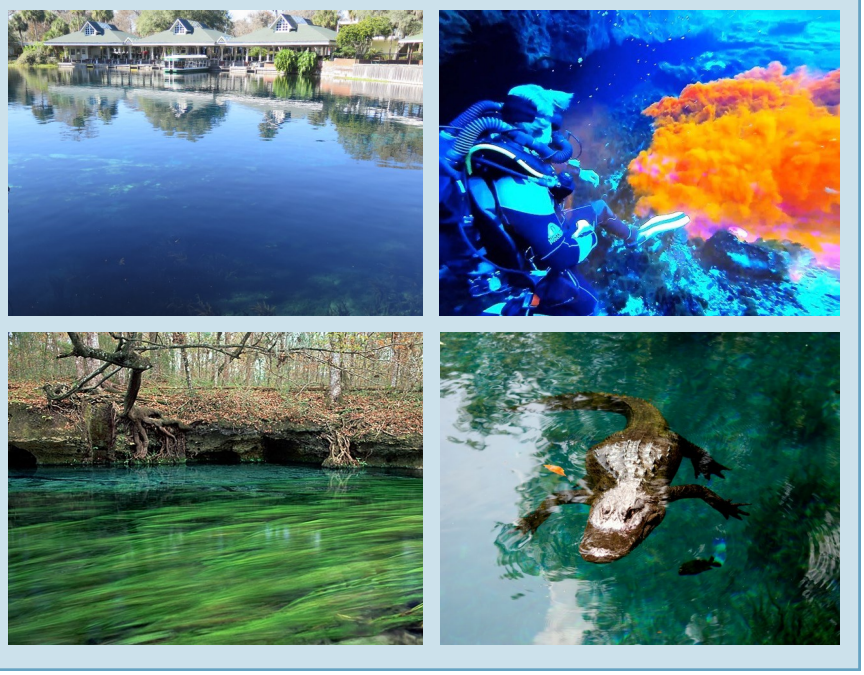

Collaborative Research Initiative on
Sustainability and Protection of Springs [**CRISPS]**

Section 8

[Work Order No: 3]

ANNUAL REPORT

July 2015

submitted to:

St. Johns River Water Management District
Springs Protection Initiative [SPI], UF Contract # 27789

UF | UNIVERSITY of FLORIDA
Water Institute

C R I S P S

Section 8

PHYSICOCHEMISTRY

Benthic Sources and Sinks of Nutrients

Annual Report 2015
Work Order 3: Part 3 of 3

Principal Investigators:

Jonathan B. Martin, University of Florida
Michael F. Coveney, St. Johns River Water Management District

Project Team
Jonathan B. Martin
Mitra B. Khadka,
Department of Geological Sciences, University of Florida
Michael F. Coveney
St. Johns River Water Management District

Other Collaborators
Junbing Pu, Robin Treilles, John Ezell
Department of Geological Sciences, University of Florida

This document reports interim progress of a work order in the first year of a 3-year project in compliance with Agreement between University of Florida (UF) and St. Johns River Water Management District (SJRWMD) UF Contract #27789. It is part of the *UF Collaborative Research Initiative on Springs Protection and Sustainability (CRISPS)* and supports the science component of *the SJRWMD Springs Protection Initiative (SPI).*

8.1 ABSTRACT

Bottom sediments of streams act as biogeochemical reactors that alter chemical compositions of pore water from the compositions of the overlying stream water. Biogeochemical reactions could thus provide an important source of solutes to stream water and affect benthic and lotic ecosystems, depending on the magnitude of fluxes of pore water and solutes. In support of the primary objective of the CRISP project (prediction of impacts of nitrogen enrichment on Silver River ecosystem and efficacy of N reduction for remediation), the goals of this work are to (1) evaluate bottom sediment distributions and chemical compositions, (2) measure physical and hydraulic characteristics of the sediment, (3) assess the biogeochemical reactions in the sediment and their impacts on pore water compositions, and (4) estimate potential impacts of fluxes of solutes between bottom sediment and the river. Our preliminary results indicate that bottom sediment are ubiquitous and in places greater than 6 m thick. They originate from erosion of highlands to the west and may have been deposited in flowing water or a lake. The sediments contain interbedded shell hash layers and organic carbon-rich fine grained deposits. The sediments appear to retain N based on smaller C:N ratios than expected from terrestrial organic matter, and have mineral sources of P (apatite and metal oxides) in addition to organic P. The shell layers have high hydraulic conductivities, and depending on their continuity (unknown at this time) may channelize horizontal flow to the river thalweg. Hydraulic heads in the shell hash layers are elevated above river water levels, suggesting water may flow from this sediment to the river. Remineralization of sedimentary organic carbon alters electron acceptor concentrations, decreasing NO_3-N, and increasing DIC, NH_4, PO_4, Fe, and Mn concentrations. Concentration gradients reflect the energetics of the redox ladder, but rates of the redox reactions may be spatially variable downstream. Concentration gradients cause solutes to diffuse between the river and sediment. The magnitude and rates of solute fluxes will be refined as additional information is collected in the remaining years of this project.

8.2 INTRODUCTION

Assessment of transport and cycling of reactive solutes to and within streams is critical for understanding the controls of water quality, ecological health and ecosystem services of stream systems (Stream Solute Workshop 1990; Jones and Mulholland 2000). The fate of reactive solutes in streams is determined by several distinct physical and biogeochemical processes including sorption/desorption on particulate matter, biological uptake, and exchange of stream water with pore water of the benthic sediment (Runkel and Bencala 1995; Worman et al. 2002). The exchange between surface and pore waters, which occurs in a region of bed sediments known as the hyporheic zone (e.g., see recent review by Cardenas 2015), is characterized by sharp gradients in physical, chemical and biological characteristics. As a result, the exchange processes of stream water with hyporheic zone water regulate fluxes of ecologically relevant substances including nutrients, carbon, and trace metals across the sediment-water interface (Kurz et al. 2015). The exchange process is responsible for transporting dissolved oxygen, nutrients and organic matter into the stream sediments, where active biofilms carry out microbially mediated transformation of pore water compositions and influences the biogeochemical characteristics of both surface and subsurface waters (Jones and Mulholland 2000; Packman and Salehin 2003; Boulton and Hancock 2006). Exchange between the stream and pore water may thus alter the stream water chemistry as water travels downstream (Findlay

1995; Boulton et al. 1998; Kurz et al. 2015). The presence and rate of each biogeochemical process depend on the rate of water exchange, solute content and residence time in contact with benthic sediments.

Remineralization of OC drives a sequence of oxidation-reduction reactions along the well-known "redox ladder" of elements (Figure 8.1), including in order of energy yield (Froelich et al., 1979): oxygen, NO_3 and Mn-oxides, Fe-oxides, SO_4, and CO_2 (i.e., methanogenesis). Reduction of NO_3–N acts as a sink for reactive N as it converts to N_2 gas and volatizes from the system. Reduction of Fe-Mn oxides acts as sources of these elements to pore water because they are transformed from the solid Fe(III) and Mn(IV) oxidation states as mineral and amorphous phases to soluble Fe(II) and Mn(II). Reduction of SO_4 to H_2S or HS^-, which depends on the pH of the system, may provide toxic environments for rhizomes of benthic SAV (Terrados et al. 1999). Remineralization of organic carbon also releases NH_4 and soluble reactive phosphorous (SRP), which may develop concentrations elevated by many times over the value of the overlying water column (Cohen et al. 2013; Kurz et al. 2015). Assessments of fluxes of these solutes from bottom sediment to the river and their effects on riverine ecosystems require measurements of the redox conditions and changes in solute concentrations in the pore water of the sediment.

Pore water solutes may be transported from bottom sediment to the over lying water column by two physical mechanisms: diffusion and advection. Advection can dominate solute exchange across the sediment-water interface in sediments with elevated permeability (Harvey and Bencala 1993; Packman and Brooks 2001; Worman et al. 2002). Advective fluxes may include bi-directional exchange of water between the hyporheic zone and water column or by unidirectional flow from the underlying aquifer. Hyporheic exchange results from pressure differences as water flow across bedforms, meander bends, and other perturbations in the stream channel, while unidirectional flow from the aquifer depends on head gradients between aquifers

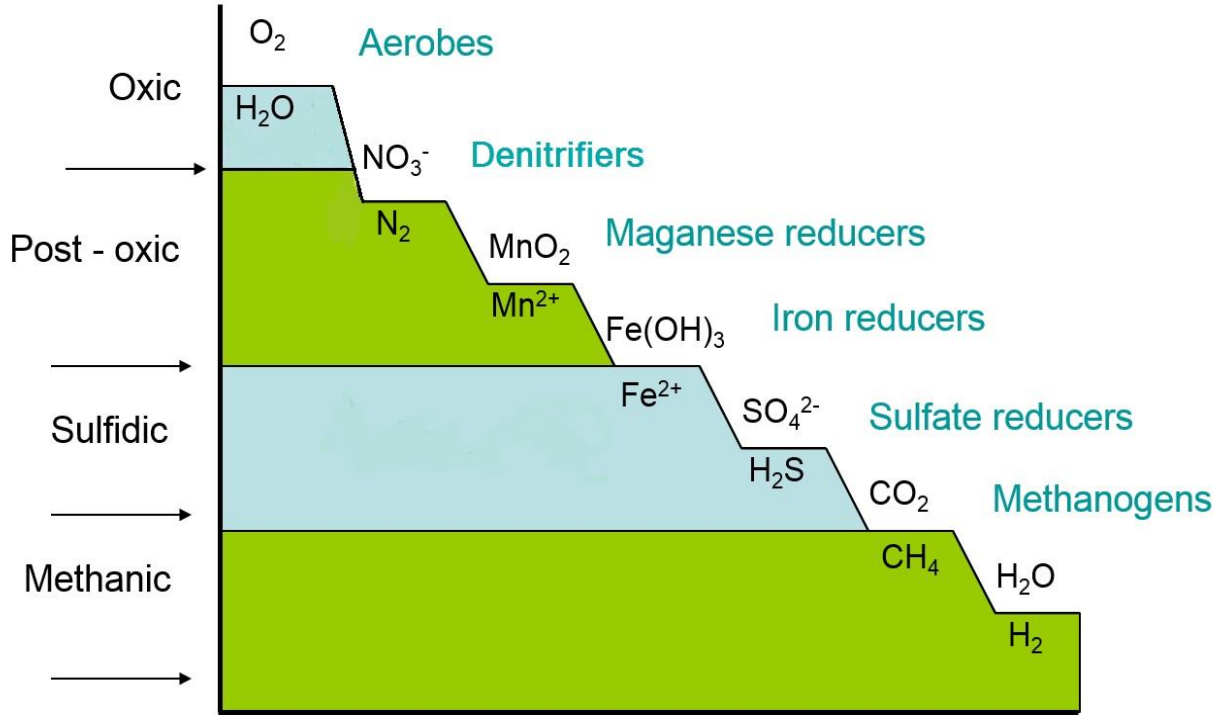

Figure 8.1. Redox reactions catalyzed by microbes in benthic sediments (Adapted after Gao et al. 2003).

and the overlying water column of the river. These head gradients may change through time depending on the river water elevation and the amount of recharge to the aquifer.

Diffusive fluxes of solutes depend on the concentration gradients between the sediment and the overlying water column and these concentration gradients may be oriented into or out of the sediment. For example NO_3, which is expected to be lost in the sediment through denitrification, should have concentration gradients oriented into the sediment, but NH_4 and SRP, which will be sourced from remineralization of organic matter, is expected to have gradients oriented toward the river. Diffusive fluxes could be particularly significant in streams, where fine-grained sediments, low turbulence, and planar bedforms minimize advective exchange and allow development of steep concentration gradients between pore water and the overlying stream water (Kasahara and Wondzell 2003; Cardenas et al. 2004; O'Conner and Harvey 2008; Kurz et al. 2015). Separating and quantifying diffusive and advective transportation mechanisms, the primary objective of this project, is critical for understanding solute supplies to streams, particularly for redox-sensitive nutrients and trace metals.

8.2.1 Project Objectives

A primary goal of the CRISP project is to predict how nitrogen enrichment impacts primary producer community structure and function, and whether N reduction alone will be sufficient to restore community structure in Silver River. Our portion of this goal is to assess the potential nutrient fluxes to and from Silver River through reactions in its bottom sediment. To meet this goal, we are working on four research objectives that will address the exchange of solutes, particularly nutrients, between river water, ecosystems and the river-bottom sediments:

1) map distribution and thickness of bottom sediment within the Silver River channel,

2) assess the physical properties of the sediment to estimate potential for flow through the sediment and from the sediment to the river,

3) identify biogeochemical transformations of pore water compositions with particular emphasis on N dynamics, alteration of SRP, and reductive dissolution of Fe-Mn oxide mineral phases, and

4) estimate the potential for and magnitudes of diffusive and advective fluxes of these solutes from the sediment to the overlying water column.

8.3 SITE DESCRIPTION

Silver River is a 9.7-km spring-fed river in central Florida. Its head water is the Silver Spring group, which is sourced from the Upper Floridan aquifer, a thick sequence of carbonate rocks of Eocene to early Miocene age (Faulkner 1973). The river flows east from the springs with an

annual mean discharge of 21.7 $m^3 s^{-1}$ (Knowles et al. 2010) before discharging to the Ocklawaha River (Figure 8.2).

The Silver Springs ground water basin (i.e., springshed), as delineated on the basis of the potentiometric surfaces of the Upper Floridan aquifer, covers about 3,100 km^2 in north-central Florida (Figure 8.2). Land surface altitude in the basin ranges from about 65 ft to 180 ft above mean sea level and decreases in elevation from west to east. Faulkner (1973) has suggested that the area to the east of springshed is controlled by faulting that structurally lowered the land surface. Knowles et al. (2010) instead suggested that the highly karstic nature of the top of the limestone can give the appearance of displacement and that an erosional unconformity has lowered the area east of the springshed (Figure 8.3). Regardless of the mechanism, low-permeability sediments overlie the limestone aquifer east of the river; the source of these sediments is erosion of older rocks from the west, including the Miocene Hawthorn Gp. The Hawthorn Gp is composed primarily of fine-grained sedimentary rocks with common phosphate-bearing minerals and carbonate stringers of the Intermediate aquifer. Where present, the Hawthorn Gp serves as a confining unit to the Upper Floridan aquifer. Erosional processes of the strata west of the springs has placed low-permeability beds in position to block eastward flow

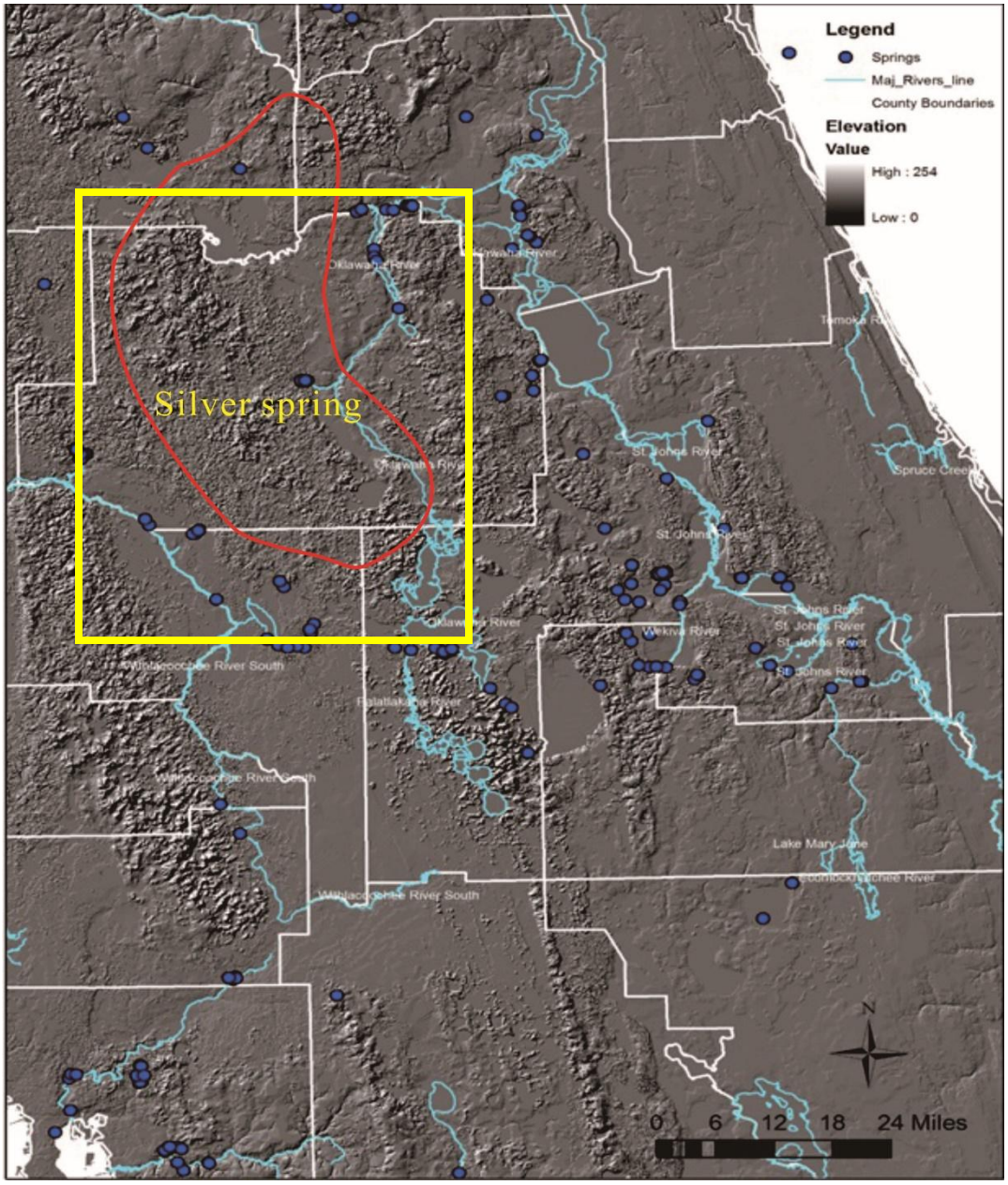

Figure 8.2. DEM of the St. John River Water Management District area showing the location of Silver Springs and other major springs (not labelled on figure). The red line indicates the Silver Spring ground water basin from Knowles et al. (2010). Yellow box outlines the area shown in

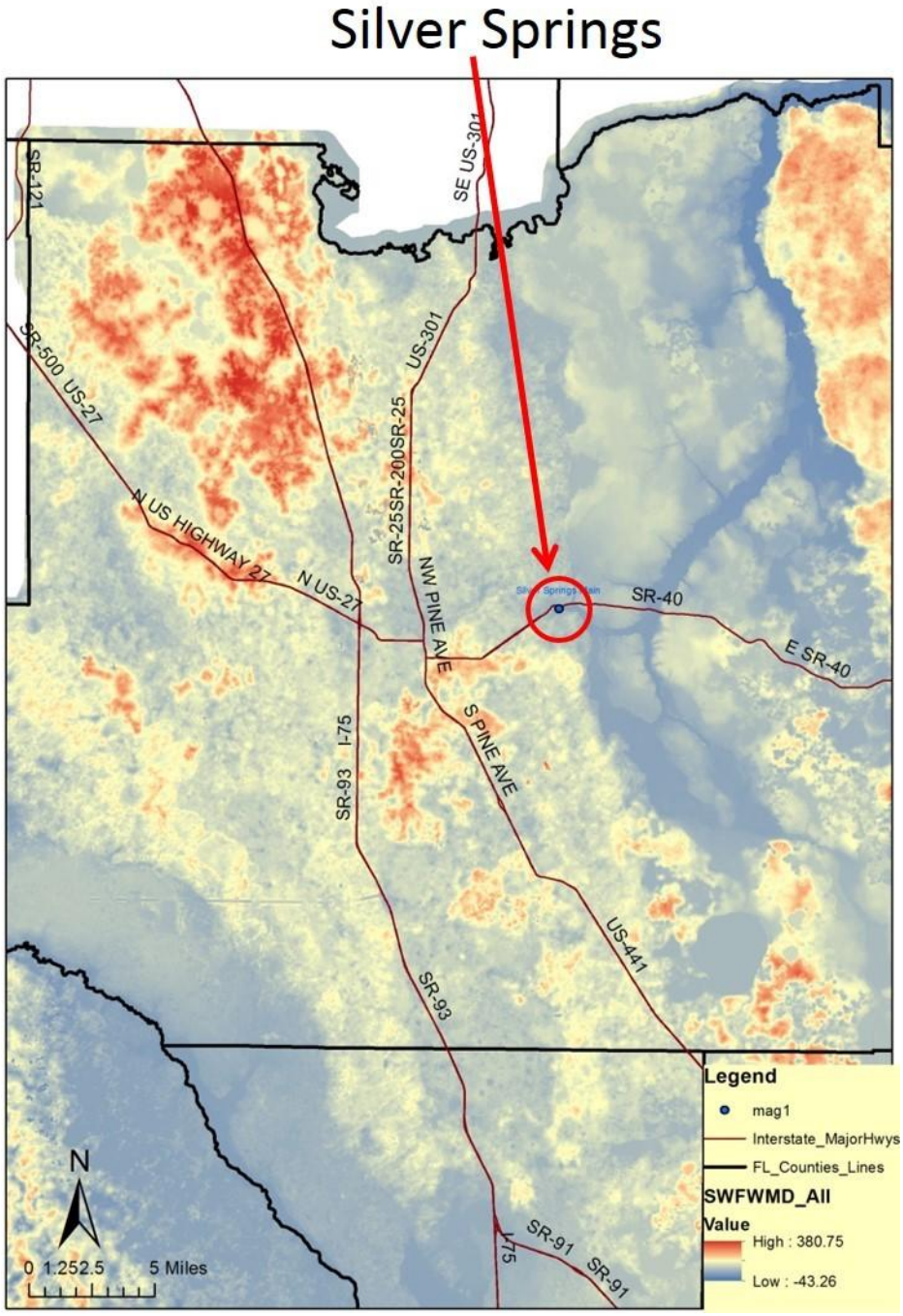

Figure 8.3. LIDAR image of area surrounding Silver Springs. Image provided by Harley Means, FGS.

.

in the Upper Floridan aquifer, thus maintaining a high enough potentiometric surface to cause discharge from open limestone caverns and sinkholes that source the Silver Spring group (Knowles et al. 2010).

8.4 MATERIALS AND METHODS

To accomplish our goals for this project, field sampling at the Silver River and laboratory analyses have been undertaken to assess physical properties and to determine chemical compositions and biogeochemical reactions occurring in the bottom sediment of the Silver River. The specific tasks include measuring sediment thicknesses, distributions, chemical compositions, and hydraulic conductivity, measuring river elevations relative to the groundwater head, sampling of pore water at various spatial scales, and measuring the chemical compositions of the pore water. Rainfall data were downloaded from the Florida Automated Weather Network (FAWN; http://fawn.ifas.ufl.edu/) at its Ocklawaha station located approximately 23 km south of Silver Springs. All of these results will be used ultimately to assess fluxes of solutes to the river with an emphasis on nutrients.

8.4.1 Sediment Mapping, Core Collection and Analysis

Fifteen transects of water depths and sediment thicknesses were measured by inserting a tile probe (6-m long, thin diameter metal rod) to refusal or to the maximum length of the rod at five stations at each transect (Figure 8.4). Water depth was measured at each sediment probe site using a hand-held depth sounder and their locations were recorded using hand-held Garmin GPS. Where water plus sediment thickness is greater than 6 m, the measured depth to refusal is a minimum value. Our transects are co-located with transects developed for minimum flows and level (MFL) studies, as well as at the USGS gauging station near the headwaters (USGS station 02239501 at river mile 0.7). Based on the distribution and thickness of the sediment, four transects were selected for more detailed observations and analyses along the length of the river (Figure 8.4). These transects are named for other studies occurring at the locations; three are co-located at the MFL transects (MFL3, MFL6, MFL7) and the fourth at the USGS gauging station (RM0.7).

The initial sampling included collection of five piston cores at the four transects, one each at RM0.7, MFL6 and MFL7 and two on opposite banks of the river at MFL3 (Figure 8.5). Two cores were collected from MFL3 because the core could not penetrate beyond about 0.5 m below the sediment-water interface on the right bank. All of the other cores penetrated nearly the entire sediment column, i.e., to the depth of refusal by tile probe, suggesting the full sedimentary section was collected (Figure 8.5). Except for the short core at MFL3, the other cores ranged in length from 2.1 to 4.2 m. All cores were returned to laboratory intact and were stored at 4ºC in a refrigerated cold room until further analysis.

Bulk densities of the whole round cores were measured with a Geotek Multi-sensor core logger at a resolution of 1 cm (Figure 8.6). Cores were split vertically and digital photographs were taken after opening by the core logger from the fresh core surface. The cores were divided into a working half for sampling and an archived half. The working half of the cores were subsampled at 5 cm intervals in the upper 50 cm and at 10 cm intervals at depths below 50 cm

Figure 8.4. Google earth view of the Silver River with the location of sediment transects showing the spatial distribution of sediment thickness and water depth. The red stars indicate the four transects where detailed sampling and observations are being carried out.

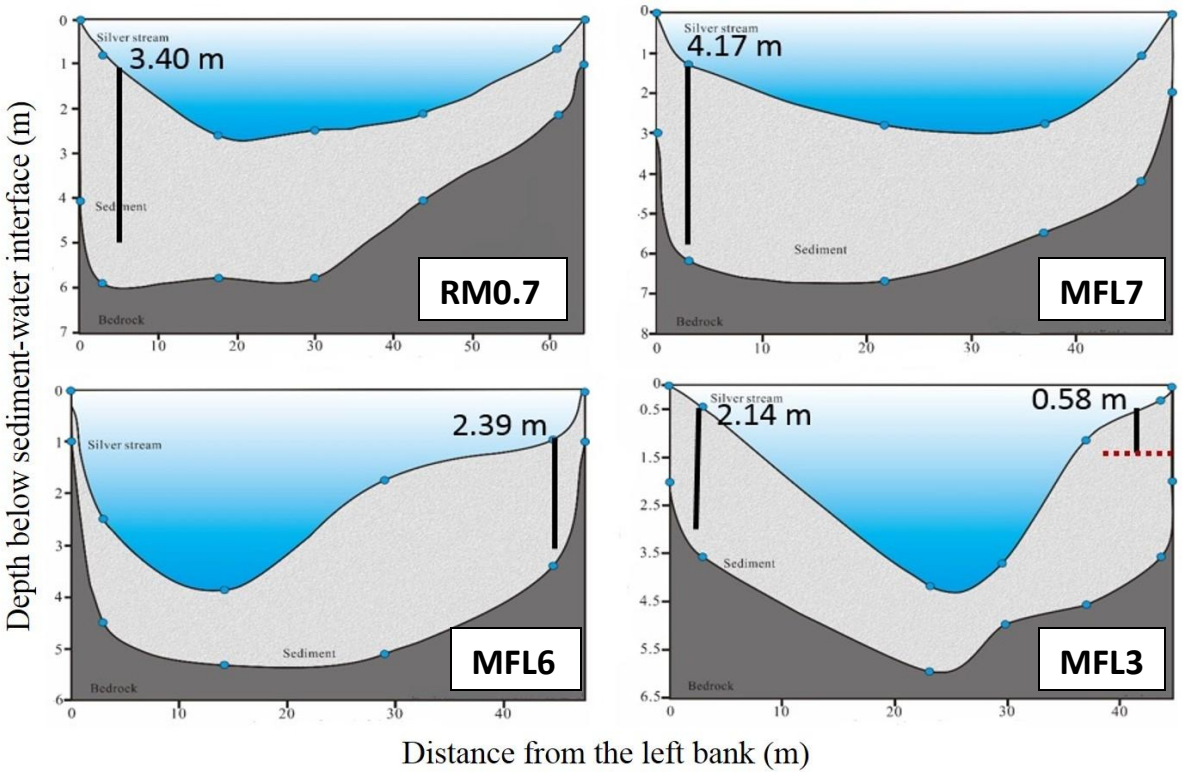

Figure 8.5. Four transects selected for core collection, pore water sampling and CTDs installation. The transects show the location and depth of cores relative to the sediment thickness.

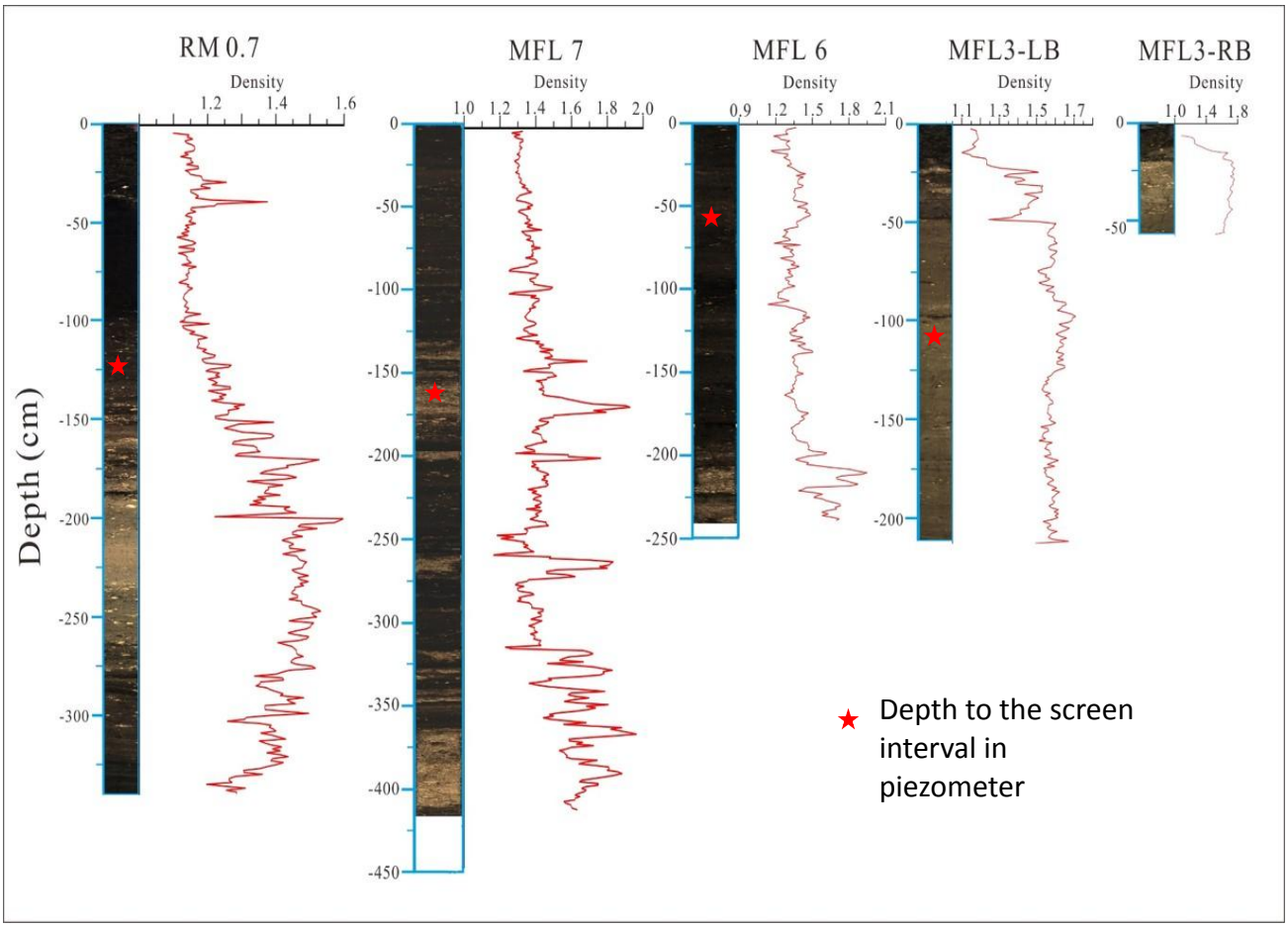

Figure 8.6. Sediment core image and distribution of bulk sediment density with depth. The dark colors indicate finer grained and higher organic carbon contents and the light colors indicate greater amounts of sandy and shelly layers.

for analysis of porosity, inorganic and organic carbon content, total nitrogen (TN), total phosphorous (TP), and trace metal content. Weighed samples were freeze dried for a week and reweighed after drying to determine the water content, from which sediment porosity was calculated. The freeze dried samples were then crushed and homogenized for further analysis. Total carbon (TC) and TN contents were measured using a Carla-Erba NA1500 CNS elemental analyzer. The total inorganic carbon (TIC) contents were measured using an automated UIC (Coulometrics) 5011 CO_2 coulometer. Total organic carbon (TOC) contents were estimated by subtracting TIC from TC. The TP contents of sediment were determined on a Seal Auto-Analyzer III after potassium persulfate digestion method (Schelske et al. 1986). Reproducibility of replicate measurements was better than 5%. Trace metal content are currently being measured with XRF.

8.4.2 Hydraulic Head Gradients and Conductivity

Conductivity, temperature, depth (CTD) loggers have been mounted in piezometers at all four transects (Table 8.1). The piezometers were installed by pushing, or pounding, 1.25-in diameter PVC piezometers into the sediment, with 13-64 cm long screened (125 µm slot) intervals at the bottom of the piezometers (Table 8.1). The screened interval was installed in course-grained

sediment on the assumption these horizons would conduct most flow. After the piezometers were installed, they were developed by jetting water into the screened interval. The CTDs were set to log at 15 minute intervals and hung at a known distance from the top of the piezometers using non-stretch nylon line. At the time of installation and at two subsequent times when data were downloaded from the CTDs, water surface elevations inside and outside of the piezometers were measured with a sounding tape to directly measure the elevation differences between the pore water and river water. At MFL6, a second stilling well was installed in the river and instrumented with two additional CTDs, one above the water level to measure barometric pressure, and one below the water surface to measure the river elevation. The other sites have river levels monitored by the either St. John River Water Management District or the USGS. Published sensor accuracy and resolution are ±0.5 and 0.2% (cm H_2O) for pressure, ±0.1 and 0.01% (°C) for temperature, and ±1% and 0.1% (µS cm^{-1}) for conductivity. The paired CTDs were intercalibrated prior to the installation.

We carried out slug tests to calculate the horizontal hydraulic conductivity of sediment at each of the piezometer in which CTDs were installed. The falling head method as described by Hvorslev (1951) was used by filling the piezometers with river water and measuring the drop in the water elevation through time with the CTDs set to make pressure measurements at a rate of 1 Hz. At least four slug tests were run on each piezometer and the hydraulic conductivity was calculated from these data using four applications of two methods. The first method is based on Hvorsley (1951) in which hydraulic conductivity, K is estimated from

$$K = -\frac{A*S}{C} \tag{1}$$

Where A is the natural log of the slope of the change in water height, i.e., A = $\ln\left(\frac{H(t)}{H_0}\right)$, S is the cross sectional area of the piezometer, and C is the shape factor given by

$$\frac{C}{D} = \frac{2\pi*(L/D)}{ln(L/D+\sqrt{(L/D)^2+1})} \tag{2}$$

where L is the length of the screened interval and D is the diameter of the piezometer. The second method, referred to as the time ratio lag method, uses:

$$-\frac{C*K}{S} * t = \ln\left(\frac{H(t)}{H_0}\right) \tag{3}$$

from which a new variable T, the basic time lag, is defined:

$$T = \frac{S}{C*K} \tag{4}$$

Substituting T (eq. 4) into equation 3 gives

$$-\frac{t}{T} = \ln\left(\frac{H(t)}{H_0}\right) \leftrightarrow \frac{H(t)}{H_0} = e^{\frac{-t}{T}} \tag{5}$$

where $\frac{t}{T}$ is called the time ratio lag. When t=T, equation 5 can be rewritten to be

$$\frac{H(T)}{H_0} = e^{\frac{-T}{T}} = \frac{1}{e} \approx 0.37 \quad (6)$$

The basic time lag T can be estimated by plotting and measuring the time required for $\frac{H(T)}{H_0}$ to equal 0.37. Hydraulic conductivity can then be estimated from T and the dimensions of the piezometer by:

$$K = \frac{R^2 * \ln(L/R)}{2 * L * T} \quad (7)$$

(Freeze and Cherry 1979) where R is the radius of the piezometer. The value of T is found by fitting curves to plots of $H(t)/H_0$ versus t using

$$\frac{H(t)}{H_0} = A * e^{-B*t} \quad (8)$$

where A and B are fitted coefficients. We use three possible scenarios to fit the data where: (1) A and B are free parameters, (2) A = 1 and only B is fitted, and (3) A and B are fit to satisfy equation 6.

8.4.3 Pore Water Chemistry

Although pore water sampling was originally planned to be initiated in year 2 of the project, we began sample collections at the end of the first year as a means to test pore water sampling tools and to estimate the potential range of chemical compositions of the pore water. To date, partial sampling has occurred at two sites (RM0.7 and MFL3) and selected analyses of the water have included nutrients (NO_3, SRP, NH_4), carbon (DIC, DOC), sulfide, trace metals (Fe, Mn), major ion concentrations, and $\delta^{13}C$ values. We used two methods for pore water sampling, which include the vapor probe method (Charette and Allen 2006) for deep pore waters and a whole core squeezing method (Jahnke 1988) for high resolution sampling of pore waters at depths < 35 cm below the sediment-water interface. The vapor probe technique has been able to extract water only from the shell hash layers and therefore this technique provides a low vertical resolution. The whole core squeezer produces samples from fine grained sediment and thus has higher resolution than the vapor probe, but is limited in the depth of collection. Our initial sampling was done every 2 cm in the upper 14 cm and every 3 cm below that depth. To date, we have collected low resolution deep pore water from RM0.7 and MFL3 and high resolution shallow samples from RM0.7. At the time of pore water sampling, we also collected samples from the river.

Prior to collecting deep pore water and river water samples, dissolved oxygen (DO), specific conductivity, temperature and pH were monitored constantly using a calibrated YSI ProPlus multisensor probe until these parameters stabilized to ensure collection of pristine samples. All samples were filtered through 0.45 μm pore size in-line, trace-metal grade, canister filters and collected in HDPE plastic bottles for NO_3, NH_4 and SRP measurement. Samples collected for cation and metal concentrations were preserved with concentrated trace metal-grade HNO_3, samples for sulfide measurements were preserved with zinc acetate, and no preservative was added to the samples collected for alkalinity and anions. Samples for DIC concentrations and

$\delta^{13}C$ values were collected in glass vials and preserved with saturated $HgCl_2$ solution to prevent microbial activity. Samples for DOC concentrations were collected in 40 ml amber glass vials with septa caps and preserved with HCl to a pH~3. Samples were kept on ice and delivered to the lab where nutrients were kept frozen until analyzed and all other samples were kept chilled at 4°C until analyzed.

We have completed the analyses of samples for alkalinity, major ions, trace metals, nutrients, and DIC concentrations and $\delta^{13}C$ values from MFL3 and for sulfide and DIC concentrations from RM0.7. Alkalinity was measured by titration within 24 h of the sampling using the Gran method (Drever 1997). Concentrations of major cations (Ca, Na, K, Mg) were measured using an automated Dionex model ICS1600 ion chromatograph and concentrations of anions (Cl, F, SO_4) were measured using an automated Dionex model ICS2100 ion chromatograph. The relative standard deviation of internal standards measured along with the samples had a precision of <3%. DIC concentrations were measured on CO_2 extracted by acidifying samples using an AutoMate Prep Device coupled with a UIC (Coulometrics) 5011 carbon coulometer. The method was standardized with dissolved $KHCO_3$. Data accuracy was better than ± 0.04 μg L^{-1} for all runs. The $\delta^{13}C$ values were analyzed using a Thermo Finnigan GasBench II coupled with Thermo Finnigan DeltaPlus XL isotope ratio mass spectrometer and reported in standard delta notation relative to Vienna Peedee Belemnite (VPDB) with analytical precision of ±0.09‰. We measured total dissolved Mn and Fe concentrations with an HR ICP-MS Element 2 (Thermo-Finnigan, Bremen, Germany). We measured sulfide following the methylene blue method (Cline 1969). Nitrate, NH_4 and SRP concentrations in water were measured with a Seal Analytical Autoanalyzer III (AA3). Precision of all analyses was <5%, based on replicate analysis of internal standards.

8.5 RESULTS

8.5.1 Sediment Stratigraphy

The Silver River contains thick layers of sediments ranging up to >5 m that are present in each of the probe locations (Figure 8.4). We did not find bare rock exposed anywhere at the bottom of the river channel. Spatial distribution of the sediments appears to be homogeneous with no systematic variations in thickness with distance downstream or across the channel. In general, sediments near the sediment-water interface are mostly black, organic carbon rich mud (Figure 8.6). Except at RM0.7 where the sediments near the bottom of the core are also muddy, sediments gradually become coarser and lighter in color with depth as a result of increasing carbonate sand content with sporadic stringers of coarse shell hash (Figure 8.7). These shell hash layers have course grained carbonate minerals, with occasional intact fossils. The abundance of course grained layers decreases downstream, with sediments containing more uniform sandy sediments and fewer fine grained organic carbon-rich layers than at the upstream sites. The bulk density of the sediment ranges from 1.1 to 2.0 gm cm^{-3} with course grained layers having elevated bulk density (Figure 8.6). Porosity of the sediments ranges from 26 to 63% and decreases with depth. Porosity exhibits a strong negative correlation with the sediment bulk density (Figure 8.8).

8.5.2 Chemical Compositions of the Sediment

The chemical compositions of the Silver River sediments vary widely between cores and with depth in individual cores (Figure 8.9). In the upper reaches of the channel, the sediment tends toward higher organic carbon (OC) contents than the lower reaches, with sediment containing nearly 50% (by weight) organic carbon between about 50 and 100 cm below the sediment-water interface at RM0.7. The higher organic carbon content is reflected in lower inorganic carbon mineral phases (assumed to be calcite). In contrast, the farthest downstream core (MFL3) contains less organic carbon, with a maximum of around 20 wt % at the sediment-water interface that decreases in the upper 25 cm to $\leq$ 5 wt %. Variations with depth in total nitrogen (TN) in individual cores and with distance downstream are similar to the organic carbon concentrations, resulting in good positive correlations for each core ($0.87 < r^2 < 0.99$) between these two variables (Figure 8.10). The slope of the correlations for MFL3, MFL6 and MFL7 are similar, ranging from 12.7 to 14.4. RM0.7, which has the greatest scatter and thus the lowest r^2 value, has a steeper slope than the other cores of around 17. These slope values represent the average C:N weight ratios for each core, which indicate the average C:N molar ratio of the RM0.7 is around 20 while the average molar C:N ratios of the other cores range from around 15 to 17.

Total phosphorous (TP) contents in the sediments by weight percent are more variable with depth and distances downstream than the TOC and TN contents. The TP content ranges from about 0 to 1% (Figure 8.9). The lowest contents occur in core RM0.7 and the highest content in MFL7. At MFL3, the top 25 cm contains elevated TP and below this depth the values are almost constant. However, at other sites, TP concentrations are highly variable and don't show any clear trend with depth. Because of the variable TP contents in the cores, the correlations between TOC and TP are poor and the relationships are variable between the cores (Figure 8.11). Core RM0.7 has the highest TOC relative to TP content, while core MFL7 has the lowest TOC relative to TP content of all the cores.

8.5.3 Hydrological Variables

The results of slug tests conducted at all sites indicate the horizontal hydraulic conductivity of the Silver River bottom sediments is high, ranging from 1×10^{-3} to 5.2×10^{-5} m s^{-1} (Table 8.2). Two of the techniques used to estimate hydraulic gradients, one based on equation 1 and the other based on equation 7, scenario 3 are more closely constrained by the data than the other two methods and consequently we focus on the hydraulic conductivity estimated from these methods, which range from 2.6×10^{-4} to 5.2×10^{-5} m s^{-1}. These hydraulic conductivities are high as would be expected from the sandy layers in which the CTDs are installed, but are unlikely to reflect the range of hydraulic conductivities possible in these sediments because no measurements have been made in the fine grained sediments (Figure 8.7).

CTD data at MFL6 from February 2015 to April 2015 showed that the ground water level was always higher than river water level by approximately 4 cm (Figure 8.12), a value that is greater than when the difference was measured directly in the field, which was typically $\leq$ 1 cm at all of the sites, including MFL6. We are uncertain of the cause in the difference between the directly measured and in situ measured values, and we plan to re-measure the CTD elevations during future field excursions to resolve this uncertainty. All of the hydraulic gradients are oriented from the sediments toward the river whether measured in situ using CTDs or directly in the field with a sounding tape. Although we currently do not have river stage data from the other three sites (RM 0.7, MFL3 and MFL7) to determine the direction of hydraulic gradients through time

at those locations, our occasional field measurements show groundwater heads are consistently higher than river water elevations there as well. Figure 8.12 also shows that both the river water and groundwater elevations decreased over the two months of record although several rainfall events occurred during this time, with the highest rainfall around 2 cm d^{-1}. The river water and groundwater elevations show several short-lived maxima during the overall downward trend, but the maxima do not appear to correspond to the rainfall events.

8.5.4 Pore Water Chemistry

We currently have analyzed only limited pore water compositions since the time line scheduled these analyses for years 2 and 3 of the project. Nonetheless, the preliminary results show steep chemical gradients of the selected solutes measured to date (Figures 8.13 and 8.14). At MFL3, NH_4 and SRP concentrations in pore water increase steadily with depth from river values < 5 μg L^{-1} to values of around 500 and 350 μg L^{-1}, respectively, indicating chemical gradients oriented toward the river (Figure 8.13). In contrast, NO_3-N concentrations decreased with depth from river values of > 400 μg L^{-1} to values below the detections limit at depths 100 cm below the sediment-water interface. Both DIC concentrations and $\delta^{13}C$ values pass through maxima of around 175 mg L^{-1} and –9‰ at depths less than around 40 cm below the sediment-water interface. The Fe and Mn concentrations also exhibit maxima of around 30 ppb at depths of around 150 cm below the sediment-water interface, approximately 110 cm below the maxima shown by the DIC concentrations and $\delta^{13}C$ values (Figure 8.13).

The high resolution sampling shows maxima in both the DIC and sulfide concentrations at RM0.7 (Figure 8.14). The depths of the maxima differ, with the DIC maximum occurring at depths ranging from around 5 to 20 cm below the sediment-water interface, while the sulfide maximum occurs at depths of between about 15 and 30 cm below the sediment-water interface. The DIC concentrations increase from river values of around 40 mg L^{-1} to around 105 mg L^{-1} at the maximum. The DIC concentrations are slightly below those in the river in the deep pore waters between 150 and 275 cm below the sediment-water interface. Sulfide concentrations are below the detection limit in the river while their maximum value is around 0.92 mM (Figure 8.14). Unlike the DIC concentration the sulfide concentrations remain elevated above the river values at depth, decreasing to around 0.5 mM at in the deepest pore waters.

Table 8.1. Location and information of the CTDs deployment

Site	GPS Location		Serial no.	Measured Parameters	Screen Length (cm)	Top of screen (cm below S-W interface)	CTD depth (cm below S-W interface)	CTD cable length (cm)
	Latitude	Longitude						
RM0.7	N29°12.946'	W82°02.487'	R6313	GW level,temp, SpC,	64	125	160	369
MFL7	N29°12.429'	W82°01.902'	R6318	GW level,temp, SpC,	31	160	160	332
MFL6	N29°12.257'	W82°01.526'	R6288	GW level,temp, SpC,	13	53	60	229
			P4461	River water level, temp, SpC				219
			K0868	Atmospheric pressure				
MFL3	N29°12.296'	W82°00.227'	R7702	GW level,temp, SpC,	30	105	110	245

GW: ground water, SpC: specific conductivity, S-W: sediment-water

Table 8.2. Hydraulic conductivity values (m s^{-1})

Site	Eq. 1	Eq. 7, scenario 1	Eq. 7, scenario 2	Eq. 7, scenario 3
RM 0,7	9.82E-05	3.08E-04	8.70E-05	2.60E-04
MFL7	6.82E-05	3.08E-04	8.70E-05	2.60E-04
MFL3	5.23E-05	-1.46E-04	7.10E-05	2.82E-04
MFL6	6.65E-04	1.00E-03	7.09E-04	5.06E-04

Red highlight has $r^2 < 0.7$, yellow highlight has $0.7 < r^2 > 0.8$. All others $r^2 > 0.8$.

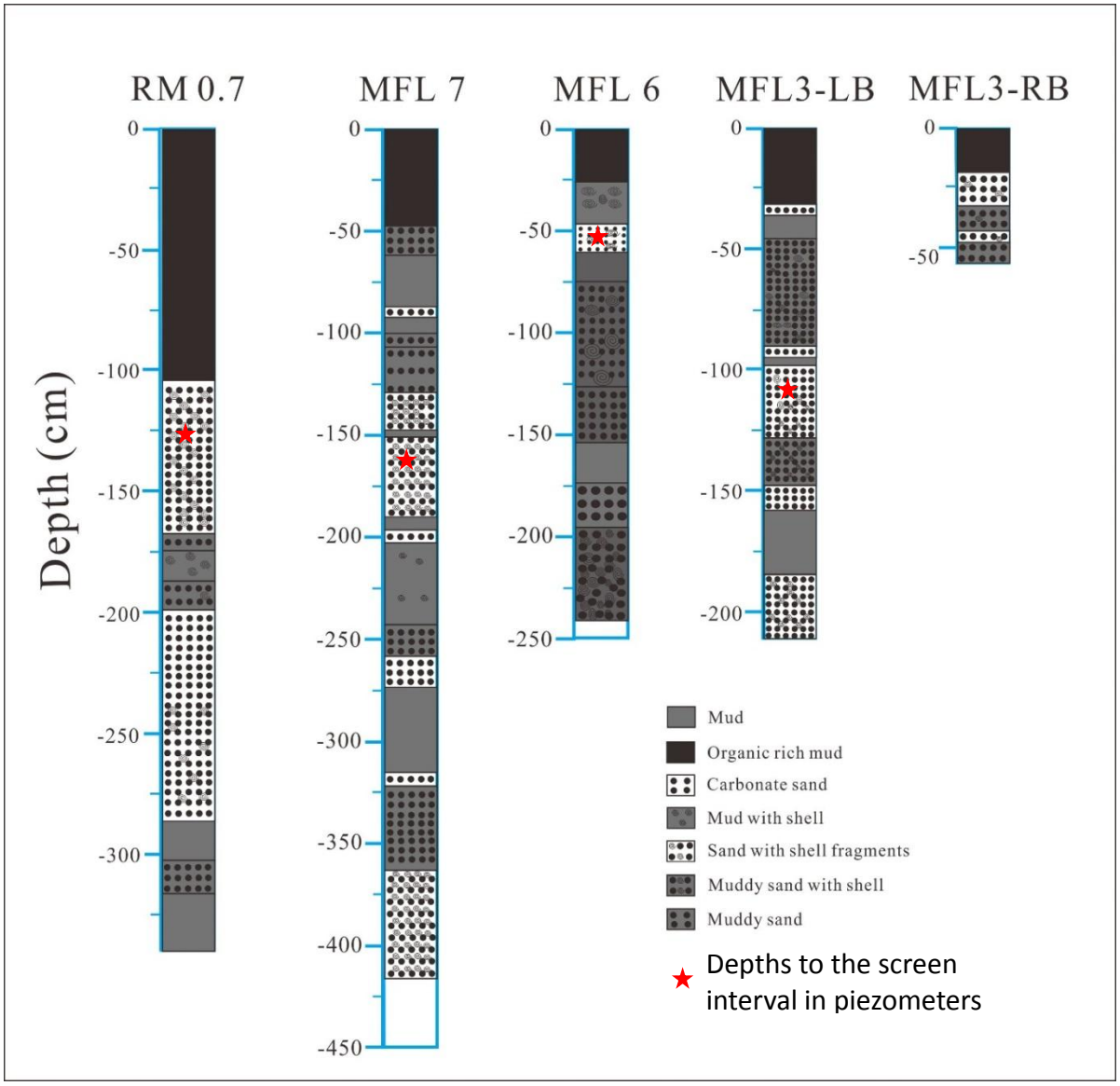

Figure 8.7. Sediment stratigraphy showing the distribution of different sediment types based in visible core inspections.

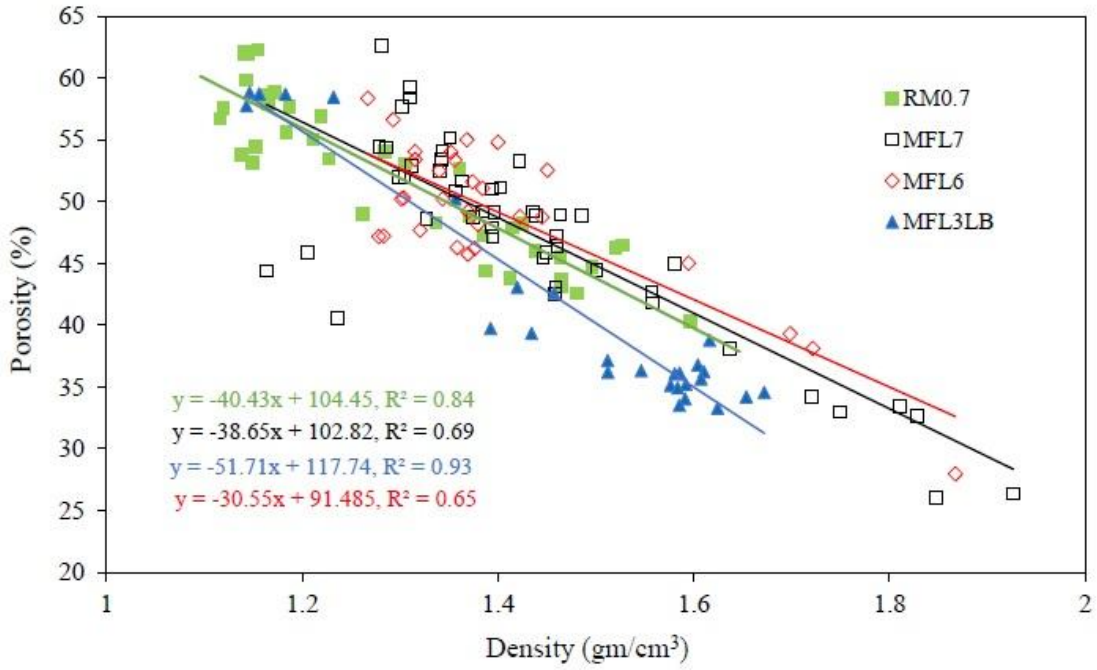

Figure 8.8. Correlation between sediment bulk density and sediment porosity.

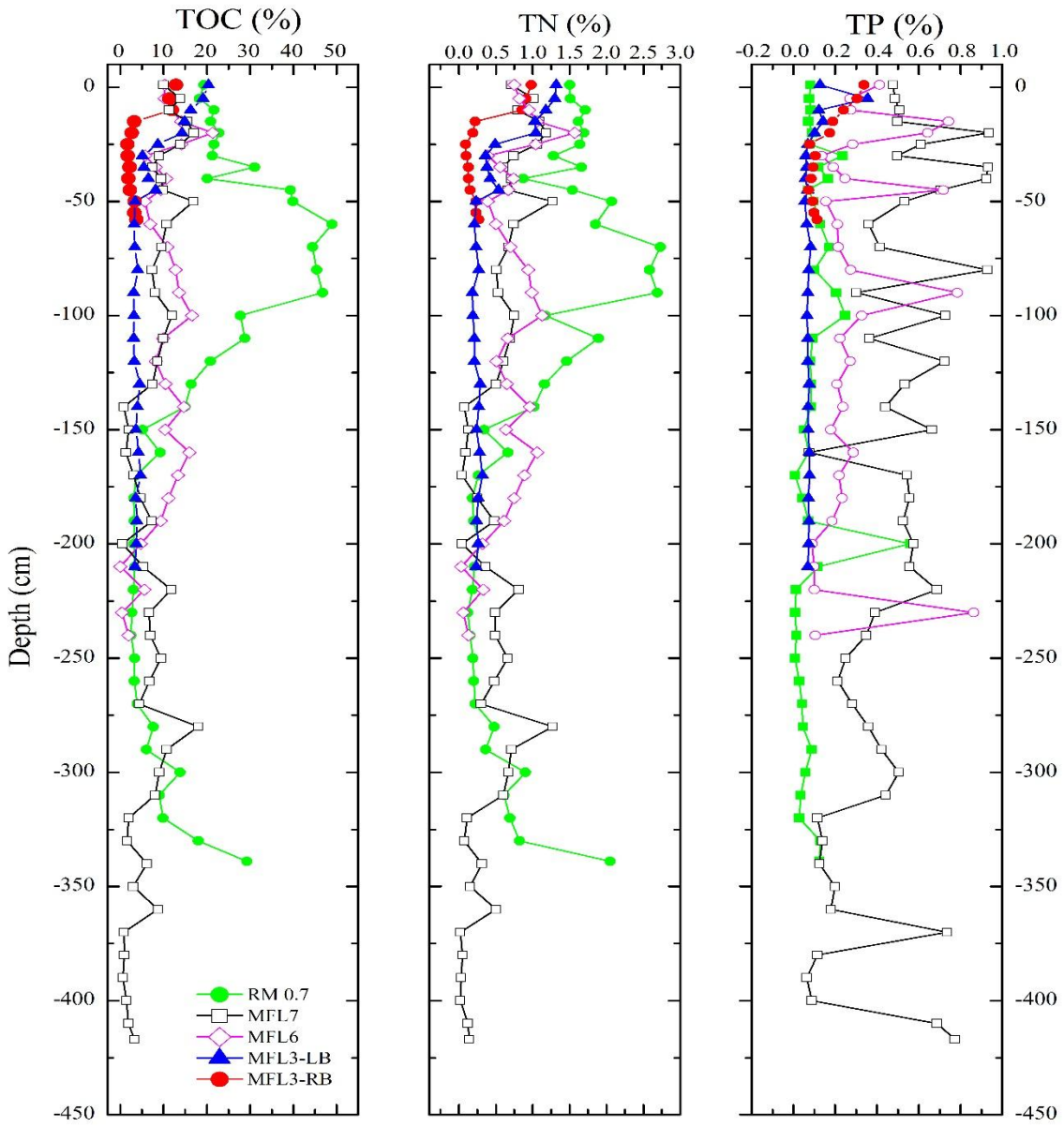

Figure 8.9. Variation in the composition of the five cores (by weight) collected from Silver River including TOC (left), TN (middle) and TP (right).

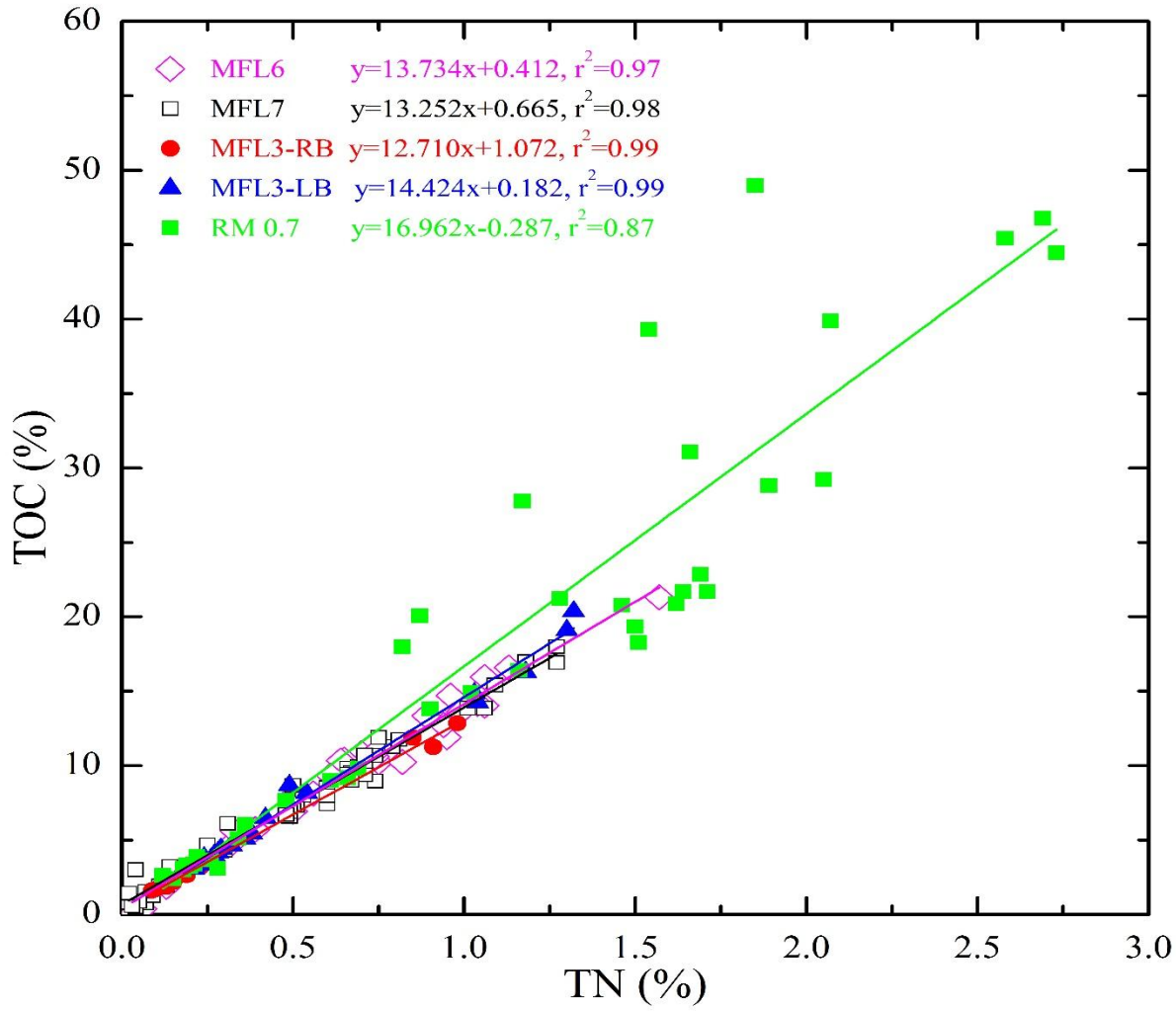

Figure 8.10. Correlation between total organic carbon (TOC) and total nitrogen (TN). Linear regressions are shown for each core.

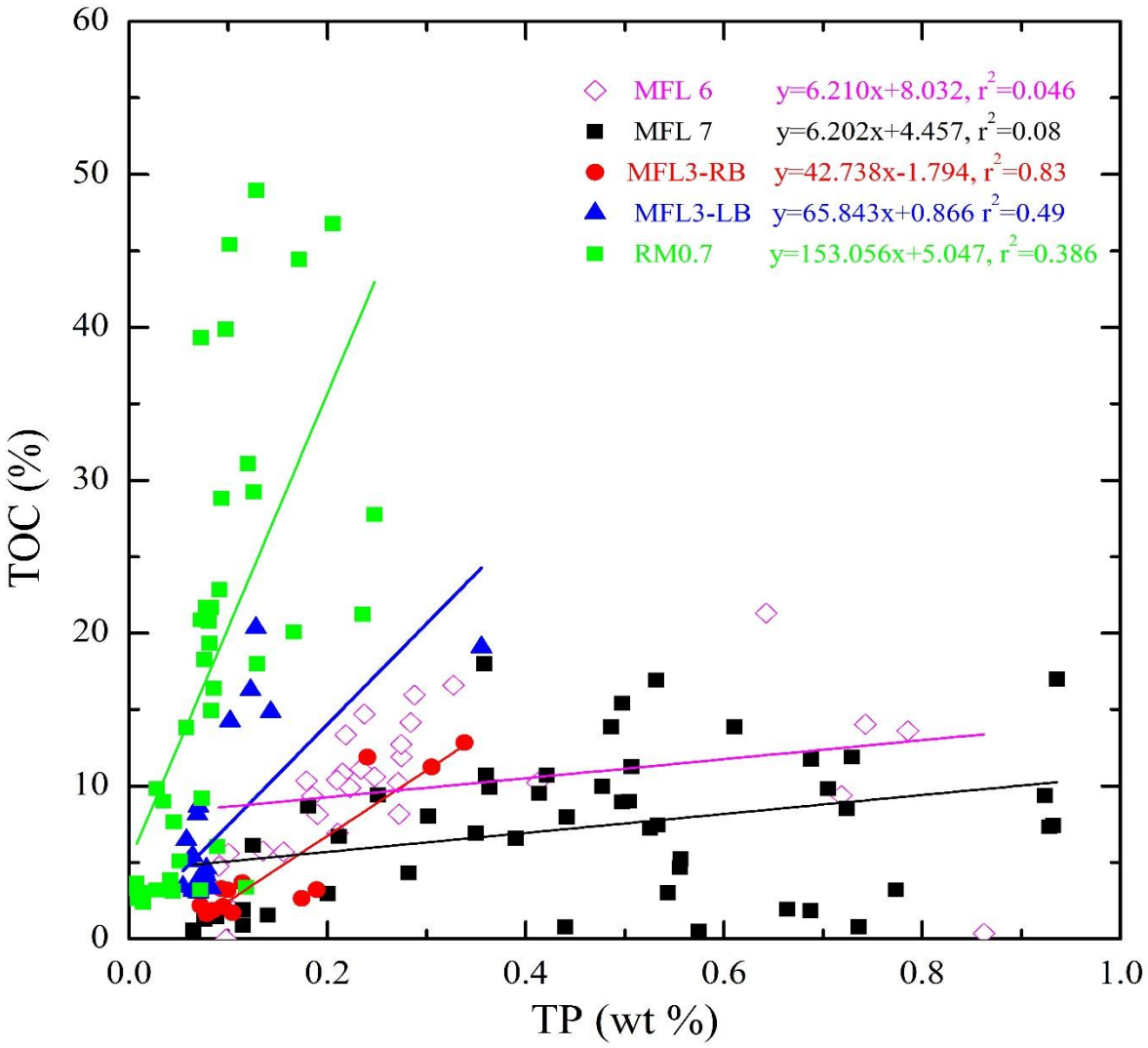

Figure 8.11. Correlation between total organic carbon (TOC) and total nitrogen (TP) in the Silver River bottom sediments. Linear regressions are shown for each core.

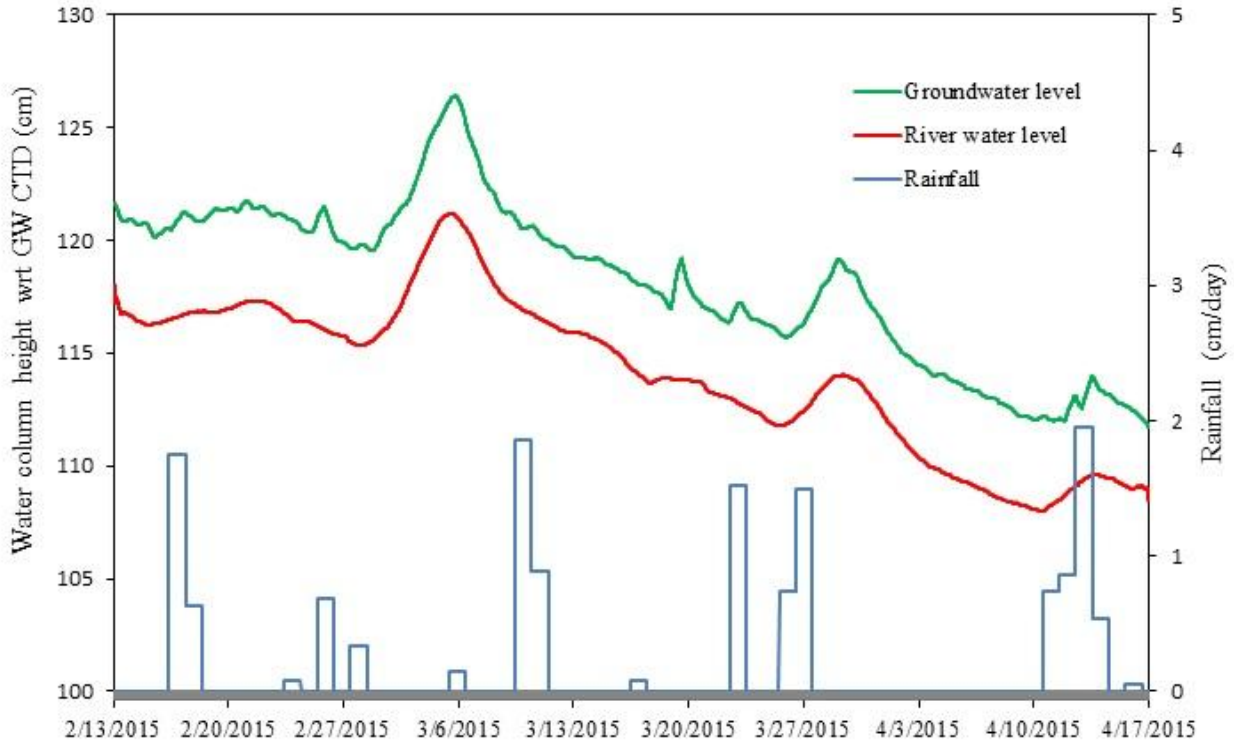

Figure 8.12. River elevation, groundwater hydraulic head and rainfall data for February through April 2015 at MFL6. The hydraulic head data were measured at 15 minute intervals and smoothed with a 24-hr window. Rainfall data are total daily values.

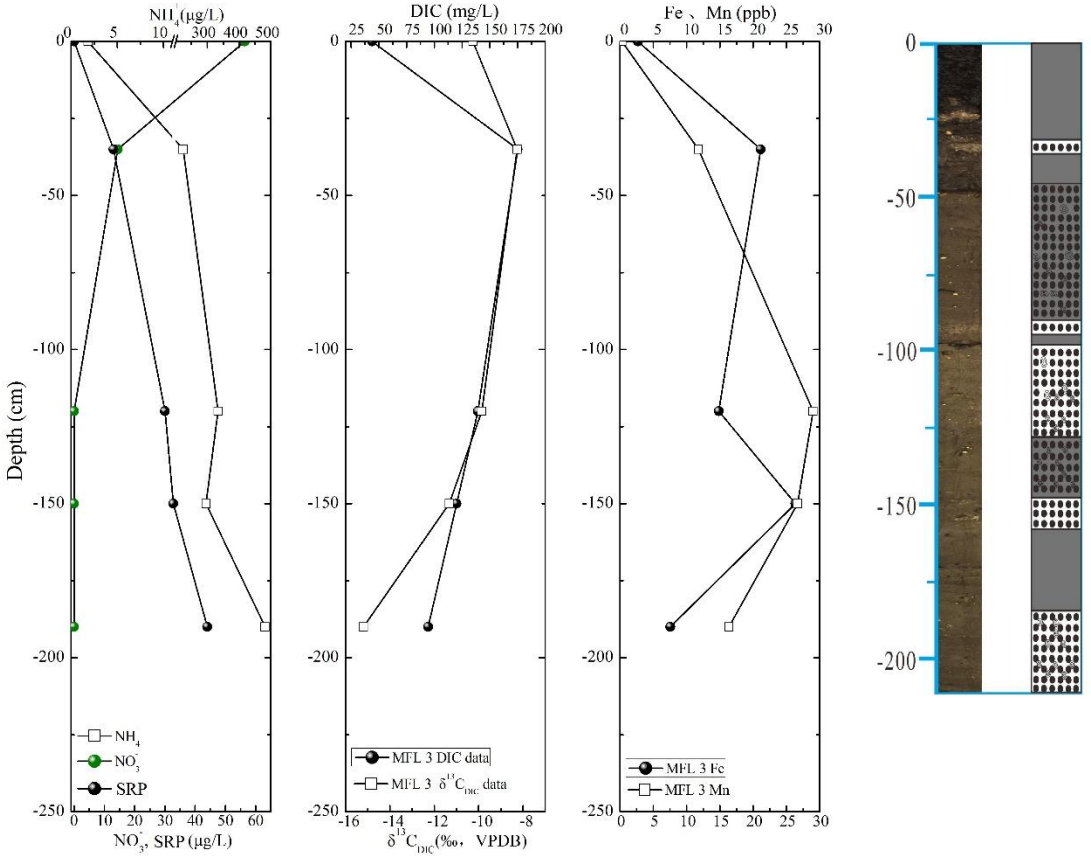

Figure 8.13. Deep pore water concentrations from MFL3. Left panel: Pore water profile of nutrient (NO_3, NH_4 and SRP) concentrations. Middle left panel: Pore water concentrations of DIC concentrations and $\delta^{13}C$ values of the DIC. Middle right panel: Pore water profiles of Fe and Mn concentrations. River water concentrations are plotted at 0 cm depth. Right panel: digital core image and stratigraphy interpreted based on visual core analysis from Figures 8.6 and 8.7.

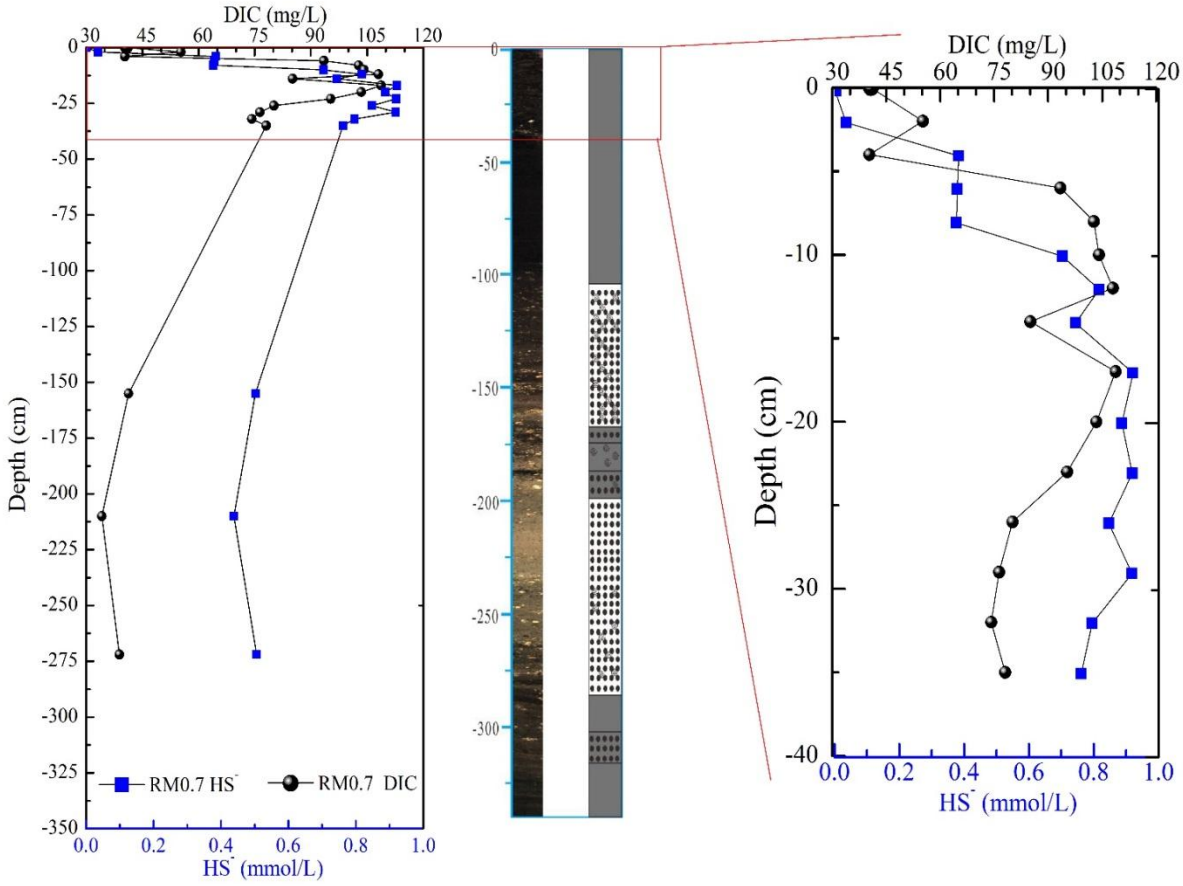

Figure 8.14. Depth profiles of DIC and sulfide concentrations from RM0.7. The left panel combines solute concentrations from the deep pore waters (collected by vapor probe) and high-resolution sampling at the sediment-water interface using the whole-core squeezer. The right panel is an expanded view of the whole core squeezer data. River water concentrations are plotted at 0 cm depth. The middle panel shows the digital core image and stratigraphy interpreted based on visual core analysis shown in Figures 8.6 and 8.7.

8.6 DISCUSSION

Preliminary analyses of our results are described below. We stress here that these analyses are preliminary because our sampling and sample analyses are incomplete at this time and thus on-going work may change our interpretations. Nonetheless, we provide our analyses here to guide future field sampling, laboratory-based measurements, and data modeling. The analyses provided below are divided into three areas including (1) the characteristics of the bottom sediments, (2) the potential for flow through the sediments, and (3) biogeochemical reactions with emphasis on the potential for solute fluxes to the river.

8.6.1 Distributions, Compositions, and Possible Origins of Bottom Sediments

The physiography of the Silver Springs springshed and surrounding area support inferences from Phelps (1994; 2004) and Knowles et al. (2010) that the Silver River flows across a region which has been lowered relative to highlands to the west and east of the springshed (Figure 8.3). Regions to the east and south of Silver River are exceptionally flat and have elevations similar to extant lakes and rivers in the region (Figure 8.3), suggesting that the river may flow across an old lake bed (Harley Means, FGS, email communication). The uniform thickness and widespread sediments within the river basin support this inference. The interlayering of fine grained and organic carbon-rich sediment (Figures 8.6 and 8.7) suggest that these sediments could have been deposited in alternatingly quiescent and flowing water. Alternatively, the course grained shell hash layers could also reflect localized deposition of carbonate-producing organisms within a lake. The origin of these layers could control their continuity (i.e., either isolated lenses or as broadly deposited strata) and thus may control the ability for water to flow through the river bottom sediments and the locations of that flow. The distribution of the course shell layers could be determined by additional coring that would allow stratigraphic correlations between the layers.

The correlations between TOC and TN contents and relatively uniform C:N ratios in the sediments suggest that the N is largely contained within the sedimentary organic matter (Figure 8.10). The molar C:N ratios of all the cores are less than ratios of 50 to 200 expected from vascular plants, but could represent mixtures with plankton, bacteria, and fungi which have molar C:N ratios of between 4 and 10 (Hedges et al. 1986; 1997; McGroddy et al. 2004). The elevated TOC and TN contents, elevated C:N ratio and largest scatter in C:N ratios at RM0.7 (Figure 8.10) suggest that organic matter at RM0.7 may represent a C:N ratio closer to unaltered organic matter compositions. If true, the lower C:N ratios at MFL3, MFL6, and MFL 7 than at RM0.7, and a similar ratio at RM0.7 for its low TOC content sediments, suggest that the N in the sediment may have been enriched relative to the C during alteration of the organic matter. Alternatively, sediment with elevated organic carbon contents at RM0.7 may originate from a different source than the other cores. Enrichment of N could reflect preferential diagenetic removal of C from the sediments or retention of the N within the sediments. Retention could occur in sediments if NH_4 produced during organic matter remineralization is sequestered during exchange with clay interlayer sites, while the CO_2 produced remains dissolved in the pore water or flushed from the sediments. Sequestration of NH_4 in clay interlayer sites might be assessed based on slopes of the depth profiles of the NH_4 concentrations relative to other solutes involved in organic matter remineralization such as DIC concentrations as they become available from all the sites.

The poor correlation between TOC and TP in the sediment suggests several sources of P exist in the sediments (Figure 8.11). One source of P is from organic matter deposited in the sediment. P may also be contained within apatite ($Ca_5(PO_4)(OH,F,Cl)$), a mineral that is common to the Hawthorn Gp. This source of P would be expected assuming the bottom sediments originated from erosion of Hawthorn Gp rocks with their redeposition as modern sediments, either in the flowing river channel or as lake bottom sediments. P can also be sequestered in solid Fe and Mn-oxide phases, and the precipitation and reductive dissolution of these phases as the sediments are buried through variable redox zones could cause co-precipitation and release to the pore water. Regardless of the source of P, the elevated contents in the sediments indicate they may be an

important source of P to the river, similar to results found in the Ichetucknee River (Kurz et al. 2015).

8.6.2 Potential for Flow from Sediments

Although hydraulic conductivity values measured at each of the transects vary by about one and half orders of magnitude, this variation is small for possible hydraulic conductivity in sediments, which range from 8×10^{-13} to 3×10^{-2} m s^{-1} (Schwartz and Zhang 2003). The values we measured in the Silver River bottom sediments (Table 8.2) are at the upper end of the scale and are at the upper end of the range for gravel and sandy sediments, which vary between around 2×10^{-7} to 3×10^{-2} m s^{-1}. One cause for our measured high hydraulic conductivity values could be an artifact resulting from the high porosity and water content of the sediment (Figure 8.8), which may allow the sediment to be mobilized during the slug tests because of the elevated pressure caused by the falling head permeability test. We plan to repeat the slug test as the project continues, but rather than using a falling head we will use a rising head by pumping water from the piezometers and monitoring the rate of increase. This method will limit sediment mobilization, and if it provides a similar value of hydraulic conductivity to the falling head test, we will assume the values shown in Table 8.2 are correct. Regardless of this potential artifact, the measured values could be close to the true values considering that the piezometer screens were located in coarse-grained sand layers that include large shell fragments (Figure 8.7), which could have hydraulic conductivity values similar to those of gravel aquifers (e.g., Schwartz and Zhang 2003).

The head gradients between groundwater and river water through time (Figure 8.12) as well as measured directly at the piezometers during field excursions indicate that water flows from the bottom sediment to the river. The high hydraulic conductivity values suggests that these flows could be large, but calculations of their rates require first understanding the cause of the discrepancy between the gradients measured in situ with the CTDs and those measured by hand during field excursions. In addition, the interbedded layers of course-grained sediment with high hydraulic conductivity and fine grained sediment, which would be expected to have low hydraulic conductivity, suggests that most of the flow would be horizontal through the sediments rather than vertical with discharge occurring across the entire river bed. Horizontal flow could still discharge to the river, but would at seepage points along the banks of the channels where the shell hash layers would crop out at the edge of the thalweg (e.g., Figure 8.4).

The rate of horizontal flow would also depend on the continuity of the sandy-shell hash layers. If these layers are discontinuous, e.g., are deposited as lenses, for example within a lake bed, the flow rates would be limited by low hydraulic conductivity of any fine-grained sediment that surrounds the course sediment lenses. Alternatively, if the course layers found in the cores are continuous, their high hydraulic conductivity would act as a preferential flow path and allow flow from source to the river. The distribution of these lenses could be mapped through additional coring in transects from the banks to the channel, and possibly into the surround wetlands, and using these data to develop stratigraphic correlations of the course grained sediments between the cores. Regardless of the current uncertainties in the potential flow rates through the sediments, the head gradients (Figure 8.12) and the estimated hydraulic conductivities (Table 8.2) suggest that water flows from the sediment to the river. The

importance of that flow for solute fluxes will depend on the flow rates as well as the chemical compositions of the water.

8.6.3 Origins of Pore Water Compositions and Potential Diffusive Fluxes

Pore water compositions are controlled largely by changes in redox state caused by the oxidation of organic matter consuming electron acceptors through sulfate (Figure 8.1)[1]. The source of DIC controls $\delta^{13}C_{DIC}$ values; if DIC originates from carbonate dissolution, the $\delta^{13}C_{DIC}$ would be approximately 0‰ and if from oxidation of organic carbon, it should be around -22 to -25‰. The $\delta^{13}C_{DIC}$ value in the pore water at MFL3 (Figure 8.13) suggests that the DIC is a mixture of these two end-members but that the DIC originates largely from organic carbon remineralization with increasing depth in the sediment.

Organic carbon remineralization is reflected in the continuously increasing values of the NH_4 and SRP concentrations (Figure 8.13). If these two solutes were sourced solely from organic matter, then they should reflect the N:P ratio of the organic matter. Terrestrial organic matter exhibits N:P molar ratios that can vary from around 5 to as high as 30 in tropical forests, but tend to concentration around 5 to 15 (Güsewell 2004; McGoddy et al. 2004). If the organic matter in sediment of Silver River had these ratios and provided the sole source of N and P to the pore water, the ratio of NH_4 and SRP concentrations should increase at this rate. The NH_4:SRP weight ratio in the pore water at MFL3 is approximately 10 (Figure 8.13), reflecting a molar ratio of around 52, or slightly higher than expected for pristine terrestrial organic matter (e.g., Güsewell 2004; McGoddy et al. 2004). This high ratio is somewhat of a surprise considering the elevated P contents in the sediment relative to the TOC contents (Figure 8.11). Although P could have numerous sources in the sediment, it appears that these sources are not mobilized and have limited effects on the pore water SRP concentrations. The NH_4:SRP ratios in the pore water could also be increased by retention of NH_4 in the sediment, as indicated by the lower sedimentary C:N ratios than expected from terrestrial organic matter (Figure 8.10). The apparent lack of mobilization of mineral P suggests that the primary source of P to the river would be through organic matter oxidation, and thus would not constitute a flux of new mineral P to the river, but rather recycling of the organic P. This question could be addressed through separation of P sources in the sediment through sequential leaching experiments (e.g., Ruttenberg 1992).

Comparison of the limited pore water compositions currently available from RM0.7 and MFL3 indicate that the redox conditions vary both with depth in the sediment as well as spatially along the river. Although depth resolution sampling is limited at MFL3 because only deep pore water has been collected, these results show the maximum in DIC concentrations occurs near the base of the rapid decrease in the NO_3-N concentrations (Figure 8.13). Similarly, the low NO_3 and elevated DIC concentrations occur approximately 100 cm higher in the sediments than the Fe and Mn maxima. These different depths are expected based on the energy yield available to

[1] We have also measured the methane concentration in the pore waters and river, which suggests that CO_2 reduction occurs as well. These data are not shown or discussed further because they are not an integral part of the primary goal of this project of assessing the role of N in changing ecosystems of the river. Nonetheless, these data may ultimately be useful in understanding exchange of water between the sediments and the river, and if so, will be included in future reports.

microbes during the oxidation of organic carbon (Figure 8.1), but this conclusion is poorly constrained because of the large spacing depths between samples. High resolution sampling near the sediment-water interface using whole core squeezers, which is to be completed as the project continues, should provide additional information on the depths where the different electron acceptors are utilized to remineralize organic carbon. These data will provide information on the production rates and magnitudes of nutrients from the organic matter and thus the potential for fluxes of nutrients to the river.

Whole core squeezing at RM0.7 provides an example of how high resolution sampling may provide additional information, even though not all solute concentrations have been measured (Figure 8.14). At this site, the DIC maximum occurs at depths of only 10 cm below the sediment-water interface, or about 20 cm higher in the sediment than at MFL3 (Figure 8.13). The difference in the depth of the DIC maximum could be an artifact of the lack of high resolution sampling at MFL3. Alternatively, if the differences in the two maxima are real, it would suggest that pore water at RM0.7 becomes reducing more rapidly that that at MFL3. Such rapid reduction would be expected at RM0.7 because of the elevated TOC contents there (Figure 8.9) and because the organic matter has the highest C:N ratios expected from less altered, and potentially more labile, organic matter (Figure 8.10). The pore water at RM0.7 also shows a maximum in sulfide concentrations at 30 cm below the sediment-water interface, indicating that most of the energetically favored electron acceptors have been reduced (e.g., Figure 8.1). These sorts of comparisons from all four sites, including analyses of all of the redox sensitive elements, which will be accomplished during the remainder of the project, should provide important information on the distribution of the reduction reactions in the sediment and thus the potential for nutrient production in the pore water. Coupling these observations with estimates of flow and observations of the gradients will allow estimates of solute fluxes to the river.

Although limited, the concentration profiles suggest NH_4 and SRP have strong diffusive fluxes from sediment at MFL3 (Figure 8.13). Similarly, the decrease in the NO_3–N concentration in the sediment indicates that NO_3 diffuses from the river to the sediment. The maxima in Fe and Mn concentrations reflect reductive dissolution of the metal oxides, but since the concentration gradients are oriented away from maxima, their diffusive fluxes would be both into the river as well as into deeper pore water. Similar gradients have been observed in Ichetucknee River pore waters (Kurz et al. 2015) but the fluxes to the river of each solute depends on its reactivity as it passes through the sediment-water interface. The Fe fluxes are limited by re-precipitation of Fe-oxides as Fe diffuses from the sediment to the oxic river, but P fluxes are not limited by re-precipitation and consequently are an important source of P to the river (Kurz et al. 2015). In addition to these nutrient fluxes, the increase in sulfide concentrations within the pore water could also be an important factor for the benthic ecosystems of the river depending on the toxic effects of the sulfide on the rhizomes of the subaquatic vegetation. Reducing environments have been shown to limit growth in some seagrasses (Terrados et al. 1999), and similar effects may occur in the Silver River.

In addition to diffusive fluxes, the elevated concentrations of redox sensitive solutes will flow to the river along with the water. These fluxes will depend both on the rate of flow, which is unknown at this time because of the necessity of refining the hydraulic conductivity and head gradient measurements and the concentrations of the pore water solute concentrations relative to

the river water concentrations. Based on the limited data available now, NH_4 and SRP could have important advective fluxes because their concentrations in the pore water are several hundred times higher than in the river water, and they should not be sequestered at the sediment-water interface similar to Fe. The relative importance of transportation mechanism, either advection or diffusion, will be assessed as the project proceeds and additional information on concentration gradients are obtained.

8.7 CONCLUSIONS AND RECOMMENDATIONS

Our preliminary conclusions, including brief discussions of future plans are listed below. These conclusions address the primary goals of the project, but we emphasize again here that these conclusions may change as additional information becomes available.

(1) Thick sedimentary deposits underlie all of the Silver River and may have been deposited in quiescent lake settings and/or by flowing water. Their origins are from erosion of highlands to the west, and they act as a barrier to flow from the underlying Upper Floridan aquifer to the river. They are composed of interbedded shell hash and sandy layers with fine grained and organic carbon-rich layers. The sediments exhibit C:N ratios that reflect an organic N source enriched in the sediment relative to the C contents. These sediments also have variable C:P ratios that suggest the presence of mineral P in apatite and Fe-Mn oxides in addition to organic P.

(2) Hydraulic conductivity of the sediments range from between 10^{-5} and 10^{-4} m s^{-1}, which are values expected from gravel beds. These high values may be an artifact of using falling head techniques that may have mobilized the sediment, but since they were measured in the shell hash layers, could be an accurate estimate of the hydraulic conductivity. Hydraulic conductivity is likely to be lower in the fine grained layers than the sandy shell layers and the bedding in the sediments suggests flow may be channelize to seepage discharge points to the thalweg. Flow from the sediment is likely considering that all measured head gradients are oriented from the sediments to the river. Estimating magnitudes of the flow requires refinements of the hydraulic conductivity and head gradient analyses.

(3) Biogeochemical reactions in the sediment are dominated by redox reactions and preliminary profiles at limited sites indicate that the redox state extends to sulfate reduction (and methanogenesis, data not shown), but that the gradients differ between sites. These reactions create concentration gradients to maximum concentrations of solutes that can be more than 100 times greater than the concentrations in the river. Solutes produced by these reactions may be important sources to the river, depending on reactions at the sediment-water interface as they discharge from the sediment to the river.

(4) Concentration gradients created by the biogeochemical reactions should be sufficient to drive diffusional fluxes from the sediments to the river. In addition, the measured hydraulic conductivity and head gradients indicate that flow will also provide an additional mechanism to transport solutes to the river. At the moment we have refrained from speculating on the relative importance of these two mechanisms because of the preliminary nature of the data collection and analyses. This assessment will occur as the project moves forward.

8.7.1 Future Research Needs

We have made good progress on the project as outline in the original timeline and are on track to complete all tasks by the end of the project. Our preliminary results have raised additional questions concerning linkages between Silver River and pore water of its bottom sediment that could not be developed until we understood more about the sediment characteristics. Consequently, we believe a better understanding of potential fluxes of nutrients to the river and controls on those fluxes could be developed with a few additional tasks. Specifically:

(1) Additional coring would allow stratigraphic mapping of the course shell layers that would assess the three dimensional nature of these high permeability flow paths. This coring should occur at least as transects from the banks of river to the thalweg. Additional coring/drilling may be required from the uplands and wetlands surrounding the river. This three dimensional mapping would reflect potential drainage paths for interflow from the wetlands to the river.

(2) Our preliminary results indicate that Silver River bottom sediments are widespread, covering the entire river bottom, and thick. Development of additional sites for expanded detailed measurements of sediment pore water compositions would provide a refined assessment of the true heterogeneity of the sediment, biogeochemical reactions within the sediment, and the total loading of nutrients and other solutes from the pore waters.

(3) Methane concentrations and isotope ratios would further refine the redox states of the sediments to estimate the magnitude of organic carbon remineralization and the amount of nutrients provided by these reactions. In addition elevated methane concentrations could provide a natural tracer for flow of solutes from the sediments to the river (Cable et al. 1996a). These methane concentrations could be coupled with measurements of ^{222}Rn activities, which also may provide natural tracers for seepage (Cable et al. 1996b).

(4) The multiple potential sources of P available within the bottom sediments (e.g., Figure 8.11) could be determined through sequential leaching experiments on the sediments (Ruttenberg 1992). These experiments would be able to separate the P content of loosely sorbed P; Fe-bound P, apatite-bearing P (although both authigenic and detrital apatite can be separated, in Silver River most apatite is likely to be detrital), and organic P. Separating these different P-bearing components would allow a better assessment of the potential magnitudes of P fluxes from sediments to the river, a source that is critical for P dynamics in Ichetucknee River (Kurz et al. 2015).

8.8 REFERENCES

Boulton, A. J., and Hancock, P. J. (2006). Rivers as groundwater-dependent ecosystems: a review of degrees of dependency, riverine processes and management implications. *Australian Journal of Botany*, 54(2), 133-144.

Boulton, A. J., Findlay, S., Marmonier, P., Stanley, E. H., and Valett, H. M. (1998). The functional significance of the hyporheic zone in streams and rivers. *Annual Review of Ecology and Systematics*, 59-81.

Cable, J.E., Bugna, G.C., Burnett, W.C., Chanton, J.P. (1996a). Application of ^{222}Rn and CH_4 for assessment of ground water discharge to the coastal ocean. *Limnology and Oceanography*, 41(6): 1347-1353.

Cable, J.E., Burnett, W.C., Chanton, J.P., Weatherly, G.L. (1996b). Estimating groundwater discharge into the northeastern Gulf of Mexico using radon-222. *Earth Planet. Sci. Lett*., 144: 591-604.

Cardenas, M. B., Wilson, J. L., and Zlotnik, V. A. (2004). Impact of heterogeneity, bed forms, and stream curvature on subchannel hyporheic exchange. *Water Resources Research*, 40(8).

Cardenas, M.B. (2015). Hyporheic zone hydrologic science: A historical account of its emergence and a prospectus. *Water Resources Research*, 51(5): 3601-3616.

Charette, M.A., Allen, M.C. (2006). Precision ground water sampling in coastal aquifers using a direct-push, shielded-screen well-point system. *Ground Water Monitoring and Remediation*, 26: 87-93.

Cline, J. D. (1969). Spectrophotometric determination of hydrogen sulfide in natural waters. *Limnology and Oceanography*, 14(3), 454-458.

Cohen, M. J., Kurz, M. J., Heffernan, J. B., Martin, J. B., Douglass, R. L., Foster, C. R., and Thomas, R. G. (2013). Diel phosphorus variation and the stoichiometry of ecosystem metabolism in a large spring-fed river. *Ecological Monographs*, 83(2), 155-176.

Drever, J. I. (1997). The Geochemistry of Natural Waters: Surface and Groundwater Environments, third ed. Prentice Hall, Englewood Cliffs, New Jersey, pp. 436.

Faulkner, G. L. (1973). Geohydrology of the cross-Florida barge canal area with special reference to the Ocala vicinity. US Geol. Surv. Water-Resour. Inves. Rep. 1-73, 117 pp.

Freeze, R. A. and Cherry, J.A. (1977). Groundwater, Prentice-Hall.

Findlay, S. (1995). Importance of surface-subsurface exchange in stream ecosystems: The hyporheic zone. *Limnology and oceanography*, 40(1), 159-164.

Froelich, P., Klinkhammer, G. P., Bender, M. A. A., Luedtke, N. A., Heath, G. R., Cullen, D., ... and Maynard, V. (1979). Early oxidation of organic matter in pelagic sediments of the eastern equatorial Atlantic: suboxic diagenesis. *Geochimica et Cosmochimica Acta*, 43(7), 1075-1090.

Gao, S., Tanji, K. K., and Scardaci, S. C. (2003). Incorporating straw may induce sulfide toxicity in paddy rice. *California Agriculture*, 57(2), 55-59.

Güsewell, S. (2004). N: P ratios in terrestrial plants: variation and functional significance. *New phytologist* **164**(2): 243-266.

Harvey, J. W., and Bencala, K. E. (1993). The effect of streambed topography on surface-subsurface water exchange in mountain catchments. *Water Resources Research*, 29(1), 89-98.

Hedges, J. I., et al. (1986). Compositions and fluxes of particulate organic material in the Amazon River1. *Limnology and Oceanography*, 31(4): 717-738.

Hedges, J. I., et al. (1997). What happens to terrestrial organic matter in the ocean? *Organic Geochemistry*, 27(5–6): 195-212.

Hvorslev, M. J. (1951). Time lag and soil permeability in groundwater observations. Bulletin 36. U.S. Waterways Experimental Station, US Army Corps of Engineers, Vicksburg, Mississippi.

Jahnke, R.A. (1988). A simple, reliable, and inexpensive pore-water sampler. *Limnology and Oceanography*, 33(3): 483-487.

Jones, J. B., and Mulholland, P. J. (1999). Streams and ground waters. Academic Press.

Kasahara, T., and Wondzell, S. M. (2003). Geomorphic controls on hyporheic exchange flow in mountain streams. *Water Resources Research*, 39(1), SBH-3.

Knowles Jr, L., Katz, B. G., and Toth, D. J. (2010). Using multiple chemical indicators to characterize and determine the age of groundwater from selected vents of the Silver Springs Group, central Florida, USA. *Hydrogeology journal*, 18(8), 1825-1838.

Kurz, M. J., Martin, J. B., Cohen, M. J., and Hensley, R. T. (2015). Diffusion and seepage-driven element fluxes from the hyporheic zone of a karst river. *Freshwater Science*, 34(1), 206-221.

McGroddy, M. E., et al. (2004). Scaling of C:N:P stoichiometry in forests worldwide: Implication of terrestrial Redfield-type ratios. *Ecology*, 85(9): 2390-2401.

O'Connor, B. L., and Harvey, J. W. (2008). Scaling hyporheic exchange and its influence on biogeochemical reactions in aquatic ecosystems. *Water Resources Research*, 44(12).

Packman, A. I., and Brooks, N. H. (2001). Hyporheic exchange of solutes and colloids with moving bed forms. *Water Resources Research*, 37(10), 2591-2605.

Packman, A. I., and Salehin, M. (2003). Relative roles of stream flow and sedimentary conditions in controlling hyporheic exchange. In The Interactions between Sediments and Water (pp. 291-297). Springer Netherlands.

Phelps, G.G. (1994). Hydrogeology, water quality, and potential for contamination of the Upper Floridan aquifer in the Silver Springs ground-water basin, central Marion County, Florida. 92-4159.

Phelps, G.G. (2004). Chemistry of Ground Water in the Silver springs Basin, Florida, with an Emphasis on Nitrate, US Geological Survey Scientific investigations Report 2004-5144, 54 p.

Runkel, R. L., and Bencala, K. E. (1995). Transport of reacting solutes in rivers and streams. In Environmental hydrology (pp. 137-164). Springer Netherlands.

Ruttenberg, K.C., 1992. Development of a sequential extraction method for different forms of phosphorus in marine sediments. *Limnology and Oceanography*, 37(7): 1460-1482.

Schelske, C. L., Conley, D. J., Stoermer, E. F., Newberry, T. L., and Campbell, C. D. (1986). Biogenic silica and phosphorus accumulation in sediments as indices of eutrophication in the Laurentian Great Lakes. *Hydrobiologia*, 143, 79–86.

Schwartz, F.W., Zhang, H. (2003). Fundamentals of ground water. Wiley New York.

Stream Solute Workshop (1990). Concepts and methods for assessing solute dynamics in stream ecosystems. *Journal of the North American Benthological Society*, 95-119.

Terrados, J., et al. (1999). Are seagrass growth and survival constrained by the reducing conditions of the sediment? *Aquatic Botany*, 65(1–4): 175-197.

Wörman, A., Packman, A. I., Johansson, H., and Jonsson, K. (2002). Effect of flow-induced exchange in hyporheic zones on longitudinal transport of solutes in streams and rivers. *Water Resources Research*, 38(1), 2-1.

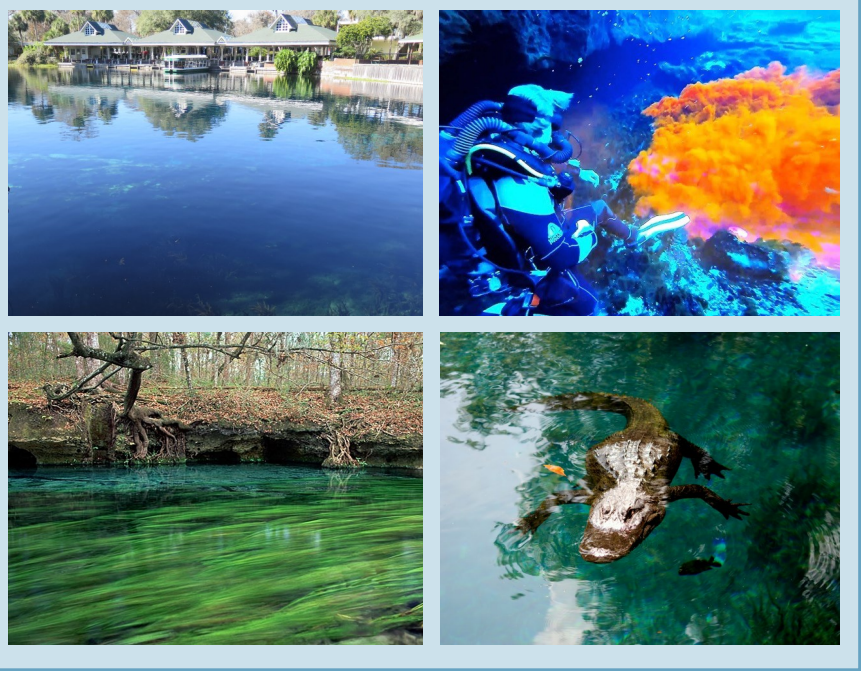

Collaborative Research Initiative on
Sustainability and Protection of Springs [**CRISPS]**

Section 9

[Work Order No: 5]

ANNUAL REPORT

July 2015

submitted to:

St. Johns River Water Management District
Springs Protection Initiative [SPI], UF Contract # 27789

UF | UNIVERSITY of FLORIDA
Water Institute

C R I S P S

Section 9

BIOLOGY

Trophic Interactions

Annual Report 2015
Work Order No. 5

Principal Investigators:

Thomas K. Frazer, University of Florida
Robert A. Mattson, St. Johns River Water Management District

Project Team:

Thomas K. Frazer, School of Natural Resources and Environment
and School of Forest Resources and Conservation
James Nifong, School of Forest Resources and Conservation
Camilo Mojica, School of Forest Resources and Conservation
University of Florida

Robert A. Mattson
St. Johns River Water Management District

This document reports interim progress of a work order in the first year of a 3-year project in compliance with Agreement between University of Florida (UF) and St. Johns River Water Management District (SJRWMD) UF Contract #27789. It is part of the *UF Collaborative Research Initiative on Springs Protection and Sustainability (CRISPS)* and supports the science component of *the SJRWMD Springs Protection Initiative (SPI).*

9.1 ABSTRACT

Natural abundance measures of stable carbon and nitrogen isotopes ($\delta^{13}C$ and $\delta^{15}N$) were employed as natural tracers to identify pathways of energy flow and material transport in Silver River. Of particular importance was the potential use of stable isotope signatures to discriminate among primary producers supporting the Silver River food web and to determine also the fate of filamentous benthic algae that are considered nuisance species in this system and other spring-fed systems throughout the region. Data generated to date indicate clearly that rooted macrophytes and their epiphytes fuel much of the secondary production that, in turn, supports a diverse assemblage of organisms that occupy higher trophic levels. A key finding thus far is that benthic algae (comprised largely of nuisance filamentous species) do not appear to contribute substantially to the production of higher-level organisms in the aquatic food web. Herbivorous insects, however, do appear to use these algae as food. Because algal production is consumed by chironomids and trichopterans (emergent insects), it is likely that much of this algal production is exported to the terrestrial environment. In essence, benthic algal mats in Silver River, and likely other spring systems, may be largely decoupled from the broader food web. With regard to secondary consumers in the Silver River, stable isotope analysis coupled with other diet information indicates clearly that redear sunfish and kinosternid turtles are primary predators on gastropods that are known to have the potential to exert control on production by nuisance algae. These predator prey interactions to date have received little attention, but merit further study to understand more fully the strength of the relationships as they are likely to have a profound influence on ecosystem function. Finally, we note that alligators in the Silver River rely heavily on gastropods and crustaceans to support metabolism and growth. This finding has profound implications for any effort to model the Silver River food web. Previous food web models have considered alligators to be top/apex predators which mainly consume fish and other vertebrates occupying higher trophic levels. In other ecosystems alligators are known to both directly and indirectly affect key ecosystem processes through their interactions with prey and the environment. Integration of these novel data and insights into spring food webs will help to refine our understanding of predation and top-down pressures in influencing community dynamics within these complex ecosystems.

9.2 INTRODUCTION

The artesian springs of Florida, and the spring-run streams to which they give rise (e.g., Silver River, Rainbow River, and Ichetucknee River), have been long recognized as unique aquatic ecosystems. Exceptionally clear water and relatively stable physical-chemical conditions create what H.T. Odum termed "a giant constant temperature laboratory" (Odum 1957). Spring ecosystems are well suited for the study of biotic interactions due to the stable conditions, as suggested decades ago by Sanders (1969) in his "stability-time hypothesis." The clear water allows for the development of extensive beds of submerged aquatic vegetation (SAV) with an associated epiphytic algal community that is a source of high in-stream (autochthonous) primary production (Odum 1957, Wetland Solutions Inc. 2010). Measurements of primary production and available photosynthetically active radiation (PAR) indicate that spring ecosystems are highly efficient at converting light energy into organic carbon (Wetland Solutions Inc. 2010). Because the occurrence of relatively large springs and their associated spring-run streams is somewhat unique to Florida and only a few other places on earth, the Florida Natural Areas

Inventory has designated these ecosystems "G2/S2", meaning "imperiled globally (G) and statewide (S) due to rarity" (www.fnai.org).

Florida's spring systems are subject to a variety of stresses, both natural and anthropogenic in nature, ranging from declining flows to physical disturbance from heavy recreational use. Elevated concentrations of nitrate (measured as Nitrate-Nitrite N or NO_3-N) in the springs and downstream receiving waters are of particular concern given the potential for eutrophication and the associated negative impacts. Increased nitrate concentrations have, in fact, been implicated as the cause of increased filamentous algae (primarily taxa in the Cyanobacteria, Chlorophyta, and Xanthophyta) in many Florida springs (Figure 9.1; Cowell and Dawes 2004; Stevenson et al. 2007; Sickman et al. 2009) and reduction in nitrate levels continues to be a management priority. Recent evidence suggests, however, that increased nitrate loading cannot explain fully the proliferation of algae (Heffernan et al. 2010a) and other factors have been invoked as causal agents. Changes in the abundance of key grazers, for example, may be responsible, in part, for the documented increases in algae. In support of this hypothesis, Dormsjo (2008) and Liebowitz et al. (2014) provide compelling evidence that algal grazers can and do exert controls on algal abundance in Florida spring ecosystems. Further investigation of food web linkages and interactions among taxa are clearly warranted.

The Objectives of the Trophic Interactions component of the CRISPS study effort are:

1. Identify the major algal grazers and their consumers. Collect samples of vegetation (algae and macrophytes), dominant/common invertebrate species, dominant/common fish species, turtles and alligators. Analyze stable isotope composition of the collected material to delineate food webs.

2. Determine algal growth and grazing rates of small grazer species. Based on the results of Objective 1, samples of the dominant algal and grazer species will be collected live and maintained in laboratory mesocosms to evaluate algal growth rates and grazing rates.

3. Assess the potential for top-down (consumer) control of key grazers in the ecosystem that were identified as part of Objectives 1 and 2. Manipulative experiments will be performed in the field to further assess grazing effects on algal populations and also to assess the influence of predators on those rates.

The focus of this annual report is Objective 1. Natural abundance measures of stable carbon and nitrogen isotope ratios, $\delta^{13}C$ and $\delta^{15}N$, were employed in combination with stomach content and scat analyses to characterize pathways of energy flow and material transport in the Silver River. Primary goals were to (1) assess the potential for stable isotopes to discriminate among primary producers in the system; (2) identify key algal grazers; and (3) identify their potential predators.

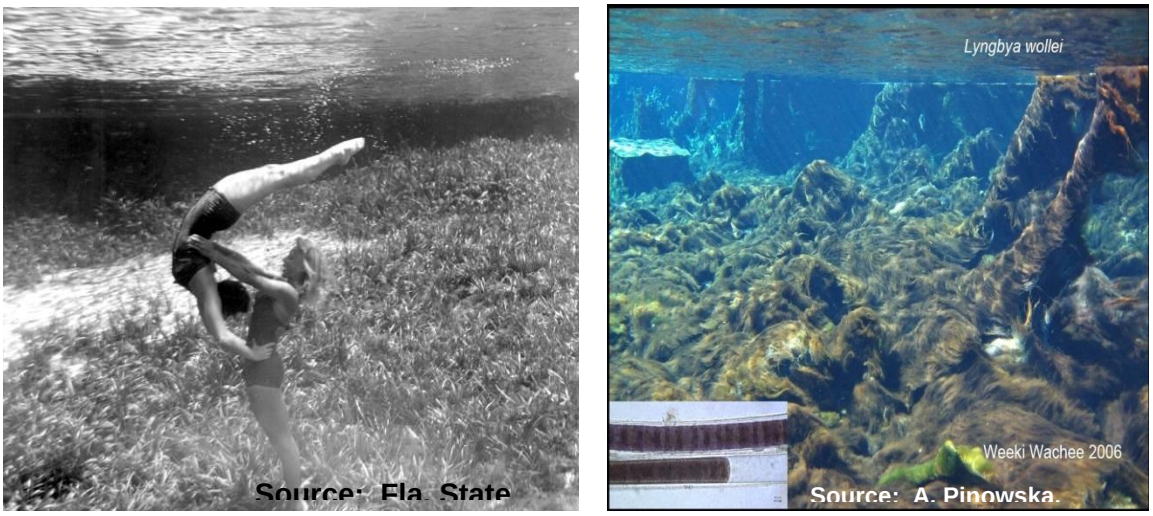

Figure 9.1. Photos of Weeki Wachee Spring in 1951 (left) and 2006 (right), showing shift in primary producer community, from rooted vascualr plants to filamentous algae.

9.3 STUDY SITE DESCRIPTION

The main CRISPS study area is the Silver River, including its headsprings (Figure 9.2). This stream is located in central Marion County, just east of the City of Ocala. The Silver River system (defined as the river itself and its associated headsprings) is located in the Ocklawaha River sub-basin of the St. Johns River drainage. Silver River is a tributary of the Ocklawaha River and runs 5.2 miles (8.4 km), from the headspring to the confluence with the Ocklawaha. Silver Springs is defined as a "spring group" (Copeland 2003), consisting of 30 known springs with numerous spring vents, all located in the upper 1,200 m of the river system. It is the largest spring system in the St. Johns River drainage (in terms of mean annual discharge), and historically was the largest inland freshwater spring in Florida. Silver Springs has been a destination for tourists/site seers for over a century; steamboats from Palatka began ferrying tourists to the spring in the late 1800s. The headspring and surrounding land were leased by W.M. Ray and W.C. Davidson in the 1920s and developed into a tourist attraction, with glass-bottom boats, a reptile show, and other exhibits and amenities. At one point Silver Springs was the premier tourist destination in Florida. The headsprings and river are now part of Silver Springs State Park and managed accordingly by the Florida Park Service.

The Silver River originates at a main headspring, known as Mammoth Spring or Silver Spring. An additional 29 springs (many named, such as Catfish Reception Hall Spring, Blue Grotto Spring, Ladies Parlor Spring, etc.) contribute groundwater discharge to the river system. The water source for the Silver Springs group is the Floridan Aquifer. The Silver Springs group is a first magnitude spring system (defined as >100 cfs mean annual discharge), one of four in the St. Johns River Drainage. Historically, the combined flow of the spring group was listed as 820 cfs (Rosenau et al. 1977). Based on current period-of-record, the mean annual flow of the spring group is currently listed at 704 cfs (U.S. Geological Survey gauging station 02239501: access at http://waterdata.usgs.gov/fl/nwis/current/?type=flow& group_ key= basin_cd).

Silver Springs is characterized as a "calcium bicarbonate" system based on the dissolved solids composition of the discharged groundwater (Woodruff 1993). Basic water quality characteristics are summarized in Table 9.1. The principal water quality issue now affecting Silver Springs is a significant increase in concentrations of nitrate (measured as Nitrate-Nitrite N or NO_3-N) over the past several decades (Figure 9.3). Natural background concentrations of NO_3-N in the Floridan Aquifer are circa 0.05 mg L^{-1} (Scott et al. 2004), and Silver Springs/Mammoth Springs was at this level in the early 1900s (Collins and Howard 1928, Munch et al. 2006). The Florida Department of Environmental Protection has adopted a Total Maximum Daily Load for nitrate for Silver Springs/upper Silver River based on the recently adopted NO_3-N criterion of 0.35 mg L^{-1} for springs (Hicks and Holland 2012).

Table 9.1. Summary of water quality characteristics of the Silver Springs group. Summary statistics are for the period-of-record, which varied by analyte. Source: SJRWMD unpublished and Munch et al. (2006).

Analyte	Mean	Min	Max	Stand. Dev.
Basic Physical				
Alkalinity (mg L^{-1} as CaCO3)	177.3	140	214	17.6
Conductivity (μmhos cm^{-1})	430.7	350	499	32.0
Total dissolved solids (mg L^{-1})	270.8	229	318	16.3
pH (units)	7.4	5.7	8.1	0.4
Dissolved oxygen (mg L^{-1})	1.9	1.0	5.7	0.9
Transparency				
Color (PCU)	3.0	0	5	1.7
Turbidity (NTU)	0.2	0.1	0.5	0.1
Horizontal secchi length (m)	73	24	96	---
Nutrients				
Total ammonia (mg L^{-1}; dissolved)	0.01	0	0.04	0.01
Nitrate-Nitrite N (mg L^{-1}; dissolved)	0.92	0.07	1.28	0.27
Total Kjeldahl N (mg L^{-1}; total)	0.10	0.02	0.90	0.15
Total Phosphorus (mg L^{-1}; total)	0.04	0.01	0.07	0.01
Orthophosphate (mg L^{-1}; dissolved)	0.04	0.02	0.07	0.01

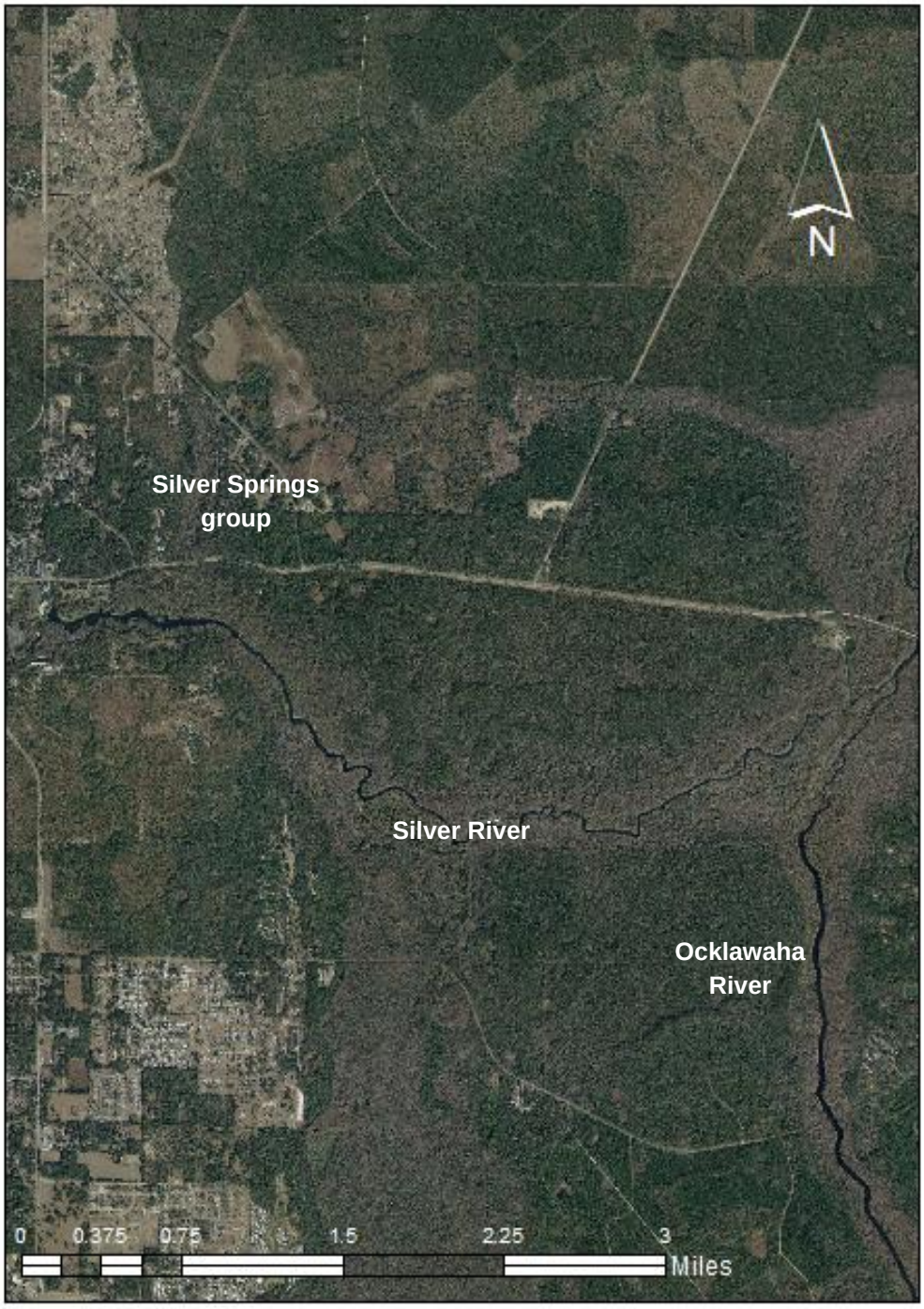

Figure 9.2. Aerial imagery of the Silver River system.

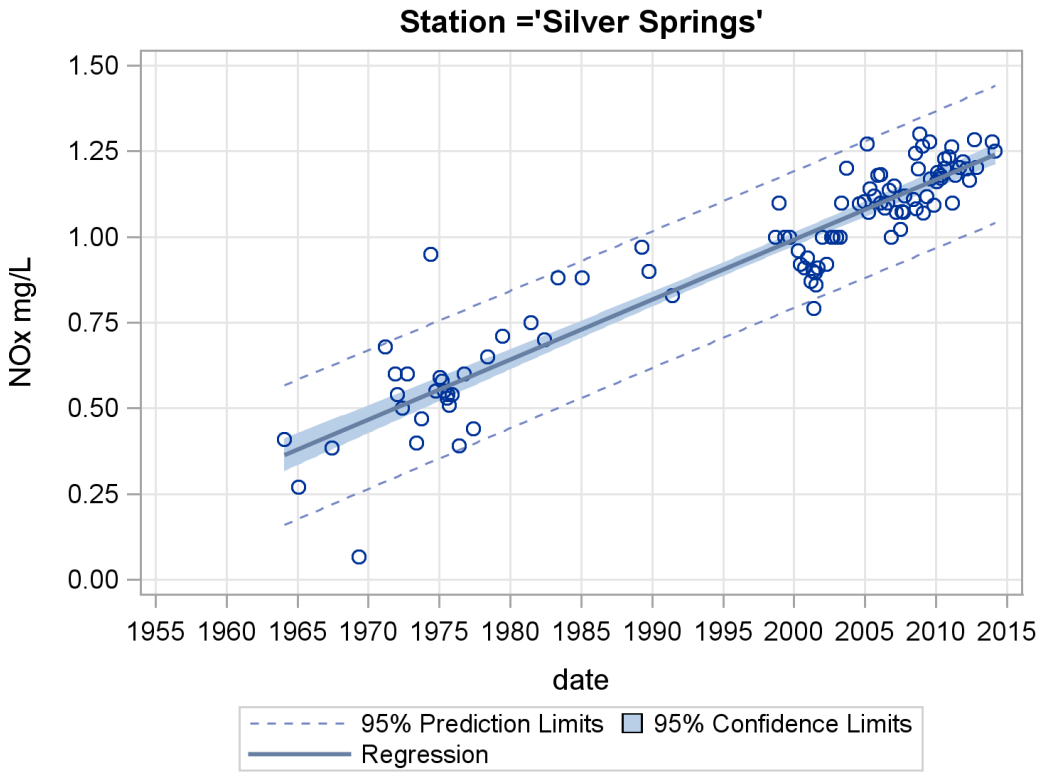

Figure 9.3. Temporal trend in Nitrate-Nitrite N (NO_3-N) concentration in Silver Springs.

As with many spring-run streams, Silver River supports extensive beds of SAV. Dominant macrophytes include spring-tape (*Sagittaria kurziana*), eelgrass (*Vallisneria americana*), southern naiad (*Najas guadalupensis*), coontail (*Ceratophyllum demersum*) and hydrilla (*Hydrilla verticillata*). Total SAV cover in many areas of the riverbed is on the order of 75-100 % (SJRWMD unpublished data). The assemblage of benthic macroinvertebrates appears to be typical assemblages in other stream ecosystems in north-central Florida; i.e., dominated by various larval and adult aquatic insects (Ephemeroptera, Odonata, Chironomidae and other Diptera, Coleoptera, Trichoptera, and Hemiptera). Other major freshwater benthic invertebrate groups are mollusks (snails, calms, and mussels), oligochaetes, and crustaceans (amphipods, isopods, grass shrimp, and crayfish). The river is known to harbor 47 species of fish. Dominant groups (by taxa richness and abundance) are Centrarchidae (sunfish and bass), Cyprinidae (minnows and shiners), and Ictaluridae (catfish and madtoms). Marine species such as striped mullet and Atlantic needlefish are also common, along with gizzard shad.

A second study area in the CRISPS effort is Alexander Springs Creek, located in Lake County (Figure 9.4). The creek begins at Alexander Spring, located in a public recreation area in the Ocala National Forest. Alexander Spring is a first magnitude spring with a mean annual flow of 118 cfs (Scott et al. 2002). The spring-run stream runs 11.9 miles (19.1 km) from the headspring to a confluence with the St. Johns River in Lakes Dexter and Woodruff. Alexander Spring is classified as a "mixed" spring in terms of its dissolved solids composition (Woodruff 1993), primarily due to higher sodium and chloride levels. Thus, it is a "saltier" spring than the Silver Springs group. However, nitrate concentrations (as NO_3-N) in the spring approximate

background, generally running less than 0.1 mg L^{-1} NO_3-N. Therefore, we sampled this system as a "reference" stream in terms of water quality.

Like the Silver River, Alexander Springs Creek supports extensive beds of SAV. A mapping effort conducted in the creek in 2008 identified 113.35 total acres (Dial, Cordy and Assoc. 2008). Dominant taxa are, in general, similar to those observed in Silver River: eelgrass (dominant), southern naiad, and coontail. Spring-tape was not found in this system. SAV cover is slightly more variable, ranging from 50-100 % in much of the stream channel, but 75-100 % in many reaches (SJRWMD unpublished data). The benthic invertebrate community of Alexander Springs Creek has received little attention. Some fish community sampling has been conducted, with 40 species observed in the creek. Fish community composition appears similar to that of Silver River, and is dominated by centrarchids and cyprinids. Mullet, needlefish and possibly other marine taxa also occupy Alexander Springs Creek.

9.4 METHODS

9.4.1 Sample Collection and Processing

In July 2014, we established six sampling segments in the main channel of the Silver River (each 200 m in length) classified into three river regions (upper, mid, lower) based on relative distance to the main spring boil (Figure 9.5). All sampling sites were in close proximity to established SJRWMD vegetation monitoring stations. During initial sampling we collected a broad suite of plants and animals to capture the full range of isotopic variation present in the food web. Targeted sampling of particular taxa provided additional insights into the observed isotopic variation. Larger-bodied consumers such as *Alligator mississippiensis* (American alligator), snakes, turtles, and highly mobile fish were opportunistically sampled throughout the study area and capture locations recorded using handheld GPS (Model 60 CSx, Garmin International, Inc., Olathe, Kansas). Data from opportunistically captured taxa were subsequently assigned to nearest river region for subsequent analyses.

9.4.2 Primary Producers

Vascular plants and algae were hand-collected from a boat, by snorkeling, or using SCUBA. Along sampling transects with each river segment, we collected live healthy leaf material from 10 to 15 macrophytes and pooled like samples for subsequent analysis. Composite samples of epiphytic macroalgae and diatoms consisted of epiphyton removed from 10 to 15 macrophyte leaves, samples of benthic algal growth forms were pooled from 5 to 10 locations within and among individual mats (dependent on abundance), and samples of unattached filamentous algae were comprised of bulk material collected from 5-10 individual algal patches. All of the aforementioned samples were stored in clean Ziploc bags, placed on ice at the time of collection, and frozen at -10°C until further processing.

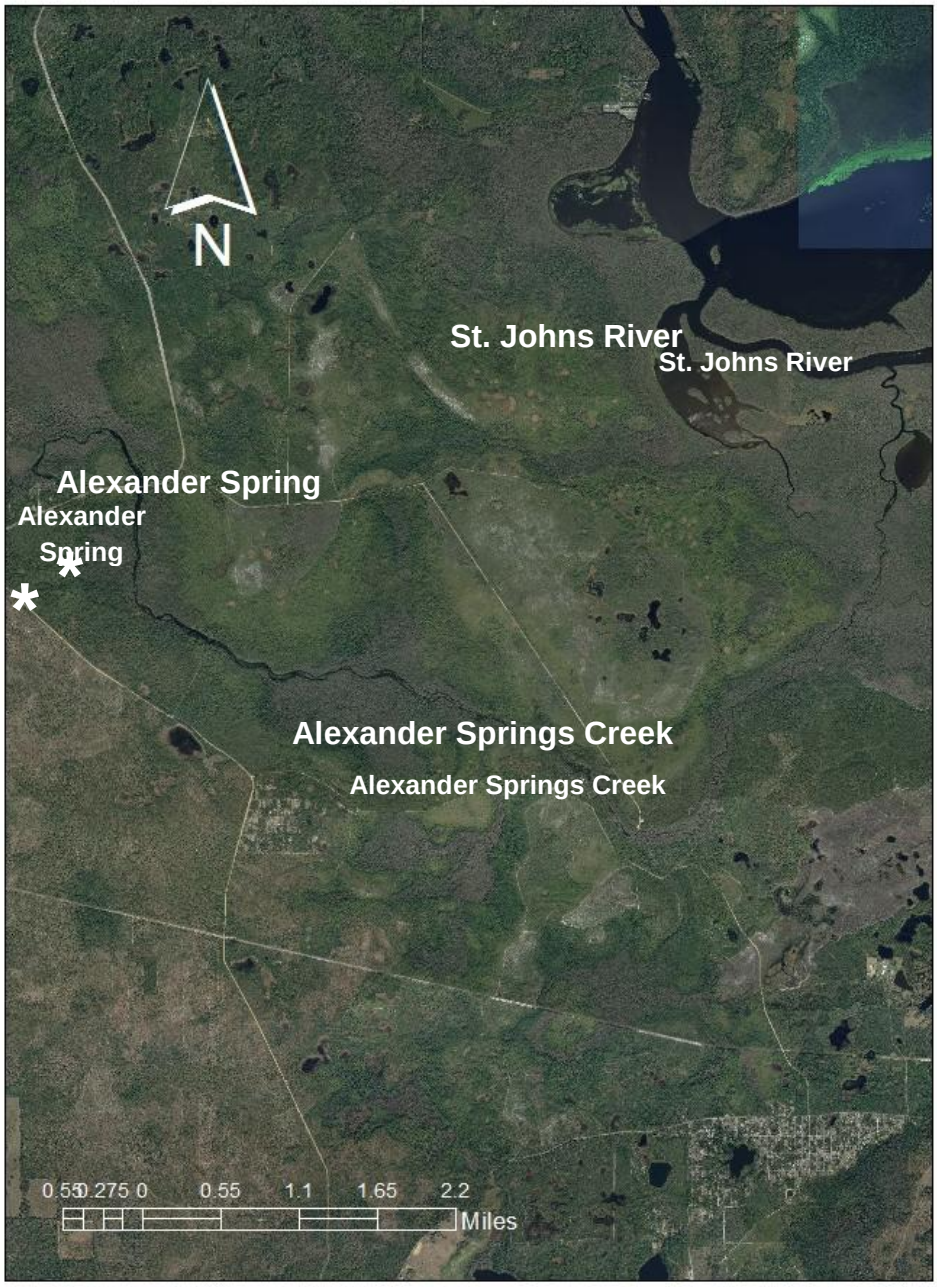

Figure 9.4. Aerial imagery of Alexander Springs Creek.

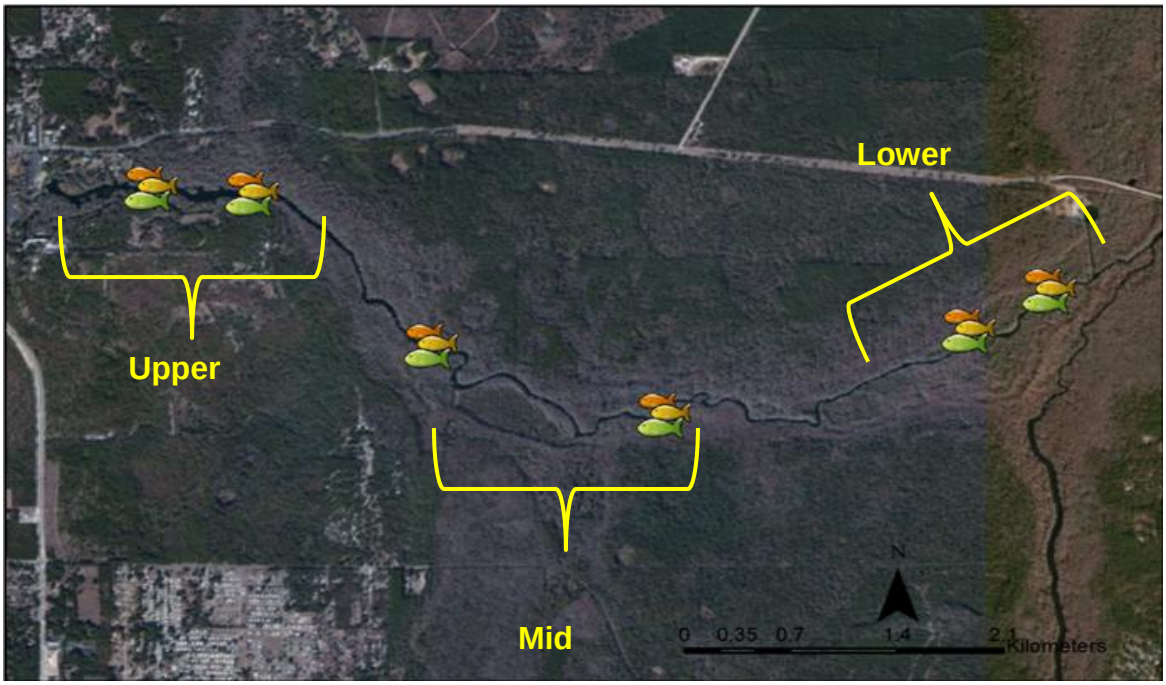

Figure 9.5. Map of Silver River with stable isotope sampling areas identified for the upper, mid and lower river reaches. Symbols denote center of 200 m sampling segment.

In the laboratory, samples were thawed and washed with deionized water. Macrophytes were thoroughly scraped/rubbed free of all epiphytic material using a sterile razor blade (material retained for subsampling of epiphytic algae), and examined with the aid of a dissecting scope and/or microscope (10-45X) to identify to least taxonomic subdivision possible and remove macroinvertebrates as well as any remaining debris (i.e., minerals, detritus, etc.). Samples were then dried to a constant weight at 60°C and homogenized to fine powder scissors and/or mortar and pestle.

9.4.3 Consumers

Consumers were collected with a variety of gear types that depended on microhabitat conditions and body size. Macroinvertebrates and small fish (total length-TL < 5 cm) were collected from submerged and emergent macrophytes using dip-nets or removed from macrophytes and algae during processing. Larger fish were collected via electrofishing. Turtles, snakes, and alligators were captured using standard capture techniques (i.e., by hand, tongs, snare, snag hook). For the majority of macroinvertebrate taxa (i.e., larval and adult insects), composite samples comprised 10-20 whole individuals. For larger specimens (i.e., grass shrimp and crayfish) and those with calcareous shells (i.e., gastropods, bivalves) bulk muscle tissue was removed from 1-5 individuals of similar size and combined into one sample. Fish tissues were obtained through a combination of non-invasive fin clipping and dorsal muscle sampling. For small fish, we collected whole individuals then clipped the entire dorsal portion of the caudal fin and removed a small section of dorsal muscle using sterile dissection scissors and/or scalpel. Tissues from 10-15 individuals were combined to yield one composite sample for each tissue type. In the case of larger fish, single individuals were sampled by removing approximately 1 cm^2 of caudal fin tissue using sterile dissection scissors. A subset of larger fish were sacrificed for stomach content

analysis; from these specimens we removed 1 cm^3 of dorsal muscle tissue to compare isotope values of fin and dorsal muscle tissue (Sanderson et al. 2009). From turtles we collected a 6-mm diameter section of keratinized scute tissue from the plastron using a sterile biopsy punch. Alligators were subject to collection of keratinized skin tissue from the caudal scute whirl and blood. Excluding blood collected from alligators all tissue samples were stored in sterile containers/bags, immediately placed on ice at the time of collection, and frozen at -10°C until further processing. Before freezing, alligator blood samples were centrifuged at 3,000 rpm for 5 minutes to separate the red blood cell and plasma fractions.

Prior to stable isotope analysis whole specimens and sampled tissues were thawed, thoroughly cleaned of debris (i.e., epiphytic algae, detritus, and other foreign materials) using deionized water, dried at 60°C to constant weight, and homogenized into a fine powder. In the case of alligator scute tissue, thawed samples were cleaned and the keratinous epidermal layer of the alligator scute separated from dermal collagen layer using NaOH digestion prior to drying and homogenizing (Radloff et al. 2012).

9.4.4 Stable Isotope and Elemental Analyses

All tissue samples were analyzed for stable carbon and nitrogen isotope composition ($\delta^{13}C$ and $\delta^{15}N$). In addition, elemental ratios (C:N) was measured for all primary producer samples and certain consumer samples (e.g., macroinvertebrates) with variable elemental composition which could potentially influence the interpretation of stable isotope data and require adjustment/normalization (i.e., lipid content, Post et al. 2007). Approximately 500 to 800 µg of homogenized consumer tissues or 1 to 3 mg of primary producer tissues was weighed and loaded into 9 mm × 5 mm tin capsules for stable isotope analysis at the University of Florida Geology Stable Isotope Laboratory, Gainesville, Florida. Analyses were performed using one of two systems: either a Finnigan DeltaPlus XL isotope mass spectrometer with ConFlo III interface linked to a Costech ECS 4010 Elemental Combustion System (elemental analyzer) or Finnigan-MAT 252 isotope ratio mass spectrometer coupled with a ConFlo II interface linked to a Carlo Erba NA 1500 CNS Elemental Analyzer. Stable isotope values are expressed in standard per mil notation δX (‰): $\delta X\ (‰) = [R_{sample}/R_{standard} - 1] \times 1000$, where X is the element of interest and R is the ratio of heavy to light isotopes ($^{13}C/^{12}C$ or $^{15}N/^{14}N$) of the sample and standard (Vienna Pee Dee Belemnite used for $\delta^{13}C$ and Atmospheric Nitrogen-AIR for $\delta^{15}N$). Machine accuracy was measured and data adjusted for during each sample run (max 42 samples per run), using four to seven measures of in-lab standard USGS-40 (L-glutamic acid, $\delta^{13}C$ = -26.39 and $\delta^{15}N = -4.52$). Across all runs analytical machine error for USGS-40 was 0.16‰ ± 0.05 for $\delta^{15}N$ and 0.14‰ ± 0.07 $\delta^{13}C$ (n = 21).

9.4.5 Stomach Content Analysis

For the majority of fish species, stomach contents were collected from live individuals by gastric lavage following momentary immobilization by electrofishing. Smaller fish (TL<10 cm) and those species whose anatomy limits the success of gastric lavage (e.g., striped mullet [*Mugil cephalus*], gizzard shad [*Dorosoma cepedianum*], gar [*Lepisosteus* spp.]) were sacrificed and the entire stomach removed. Similar to large fish, stomach contents were collected from alligators using a modified form of gastric lavage known as the hose-Heimlich technique developed for crocodilians (Fitzgerald 1989). Once removed, stomach contents were sieved using 300-µm mesh, preserved in 10% formalin, and transferred to 70% ethanol for storage. Contents were

visually inspected under a dissecting and/or microscope scope to separate prey and non-prey items; prey items were identified to least taxonomic subdivisions possible (family in most cases) and the minimal number of identifiable individuals counted. For fish, stomach content fractions (i.e., prey item, non-prey material) were dehydrated at 60°C and dry mass measured to the nearest 0.0001 g. Due to the large size of some prey remains in alligator stomach contents, wet mass was measured to the nearest 0.01 g using after gently blotting material to remove excess water and preservative.

Diets of species and/or species subgroupings were quantified using three measures: frequency of occurrence (%FO, proportion of stomachs containing one or more prey from a prey category divided by the number of stomachs), numerical abundance (%N, total number of prey items that belong to a prey category divided by the total number of prey), and gravimetric abundance (%M, total mass of a given prey category divided by the total mass of all prey recovered).

9.4.6 Turtles, Gastropods, and Herbivorous/Omnivorous Fish

Since gastric lavage of live specimens is rarely successful on turtles, we employed non-invasive fecal material analysis (i.e., scat analysis). Following capture, body measurements, and tissue collection, individual turtles were placed into appropriately sized plastic storage containers containing a few inches of ambient water free of particulates and/or small organisms and held overnight for approximately 12 hours. Following this time period the water and any scat passed by each individual was sieved using 300 μm mesh, preserved in 10% buffered formalin, and transferred to 70% ethanol for storage. All individuals were subsequently released at the site of capture. Due to the nature of scat analysis, we only quantified turtle diets using frequency of occurrence (%FO).

We removed the contents from the intestinal tract of gastropods and stomach of herbivorous/omnivorous fish from sacrificed individuals, preserved collected material, and examined for presence and absence of primary producer groups (macroalgae, diatoms, macrophytes). Diet for these consumer taxa were quantified using frequency of occurrence (%FO).

9.4.7 Statistical Methods

To examine differences in stable isotope values among primary producers, we first grouped data from all river regions into three broad categories (algae, emergent macrophytes, and submerged macrophytes) representing the dominant resource pools available to primary consumers. The isotopic data from less common and/or unique taxa that were excluded from broad autotroph groupings are discussed separately. To draw more in-depth comparisons and determine how to delineate resource pools for use in isotopic mixing model analyses, we further categorized autotrophs based on river region, taxonomy, and growth form. To assess the potential effects of these factors on isotopic and elemental composition we performed separate one- or two-way ANOVAs for each dependent variable of interest (i.e., $\delta^{15}N$, $\delta^{13}C$, and C:N) and tested for interactions among predictor variables. If significant effects were detected, we performed post-hoc pairwise comparisons (Tukey HSD, $\alpha = 0.05$) to further examine significant differences among the groups being compared. Relationships between body size of consumers and isotope composition were assessed using Pearson's correlation test. All significant differences were

evaluated at $\alpha = 0.05$. All statistical analyses were performed in R 3.1.1 (R Core Team 2014). Stable isotope values are presented as mean ± 1 standard deviation (SD) unless otherwise noted.

9.5 RESULTS

9.5.1 Stable Isotope ($\delta^{13}C$ & $\delta^{15}N$) and Elemental C (C:N) of Primary Producers

To date, we have conducted 19 field expeditions to Silver River and two to Alexander Spring Creek from 08-06-2014 to 06-11-2015 to collect tissue samples from resident primary producers. Although we have collected and processed a total of 154 composite samples from approximately 42 autotroph taxa (this includes some broader classifications and mixed species groups), the data here represent preliminary results from 139 samples analyzed from Silver River (Appendix 9.1).

In general, $\delta^{13}C$ values in algal taxa (n = 76, -37.3‰ ± 6.2) were lower in comparison to submerged (n = 33, -34.7‰ ± 3.7) and emergent macrophytes (n = 30, -30.3‰ ± 2.0) (Figure 9.6). Mean $\delta^{13}C$ values of broad autotroph groups significantly differed from one another ($F_{2,130}$ = 20.8, p-value < 0.001), but were not significantly influenced by river region ($F_{2,130}$ = 1.6, p-value = 0.19). There was no significant interaction between group and river region ($F_{4,130}$ = 0.7, p-value = 0.57). Post-hoc analysis indicated mean $\delta^{13}C$ values between all autotroph groups were significantly different from one another.

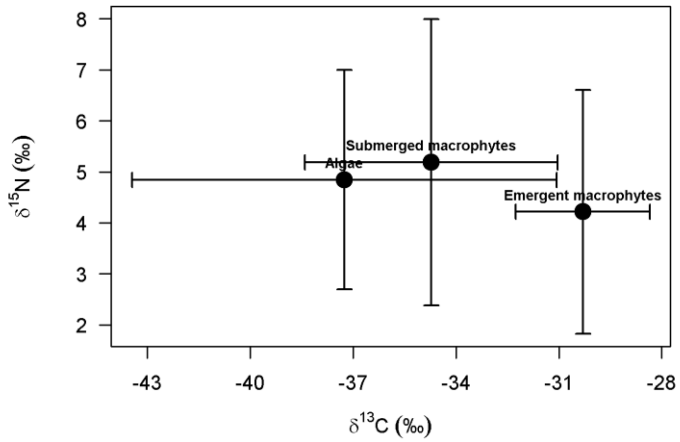

Figure 9.6. Stable carbon and nitrogen isotope composition of dominant autotroph groups. Points are means and error bars are ± 1 standard deviation (SD).

This general pattern in $\delta^{13}C$ values held relatively well across the three river regions with the exception of mid-river, wherein $\delta^{13}C$ values of algae were slightly more positive and closer to those of submerged macrophytes than in the upper and lower river (Table 9.2 and Figure 9.7). The range in mean $\delta^{15}N$ values was narrower than for $\delta^{13}C$ values, ranging from 4.2‰ ± 2.4 for emergent macrophytes to 5.2‰ ± 2.6 for submerged macrophytes. We found $\delta^{15}N$ values were not significantly influenced by autotroph group ($F_{2,130}$ = 1.7, p-value = 0.19), but were significantly affected by river region ($F_{2,130}$ = 13.7, p-value < 0.001) with no significant interaction between group and river region ($F_{4,130}$ = 2.1, p-value = 0.09). Overall, $\delta^{15}N$ values

increased with distance from the main spring boil, but were only found to be significantly different between the upper and lower river.

We found mean C:N ratios of autotrophs differed significantly among groups ($F_{2,130}$ = 52.1, p-value < 0.001), and were not affected by river region ($F_{2,130}$ = 0.18, p-value = 0.83), with no significant interaction between groups and river region ($F_{4,130}$ = 1.5, p-value = 0.09). Post-hoc analysis indicated mean C:N significantly differed among all autotroph groups. Tissue C:N was highest for emergent macrophytes, slightly lower for submerged macrophytes, and lowest for algal taxa (Table 9.2).

Table 9.2. Stable isotope composition ($\delta^{15}N$ and $\delta^{13}C$) and elemental ratios (C:N) of broadly characterized primary producer groups from Silver River as a function of river region. For each group the bold numbers are overall values averaged across river regions, i.e. upper, mid and lower.

		$\delta^{15}N$ (‰)		$\delta^{13}C$ (‰)		C:N	
Autotroph group	**n**	**mean**	**SD**	**mean**	**SD**	**mean**	**SD**
Algae	**76**	**4.8**	**2.1**	**-37.3**	**6.2**	**9.0**	**1.5**
Upper	42	4.0	2.0	-37.3	6.2	8.7	0.8
Mid	21	5.1	1.9	-35.5	6.9	9.4	2.0
Lower	13	7.2	1.0	-39.8	4.1	8.8	1.2
Submerged macrophytes	**33**	**5.2**	**2.8**	**-34.7**	**3.7**	**13.2**	**3.3**
Upper	20	4.3	2.9	-34.8	4.4	13.9	3.6
Mid	8	5.5	1.9	-34.4	2.4	11.5	1.7
Lower	5	8.2	0.9	-35.1	2.7	13.1	3.4
Emergent macrophytes	**30**	**4.2**	**2.4**	**-30.3**	**2.0**	**14.4**	**3.7**
Upper	13	4.1	2.6	-30.5	2.5	13.4	3.0
Mid	13	4.5	2.4	-30.4	1.5	15.5	4.4
Lower	4	3.7	2.1	-29.4	1.3	13.9	2.9

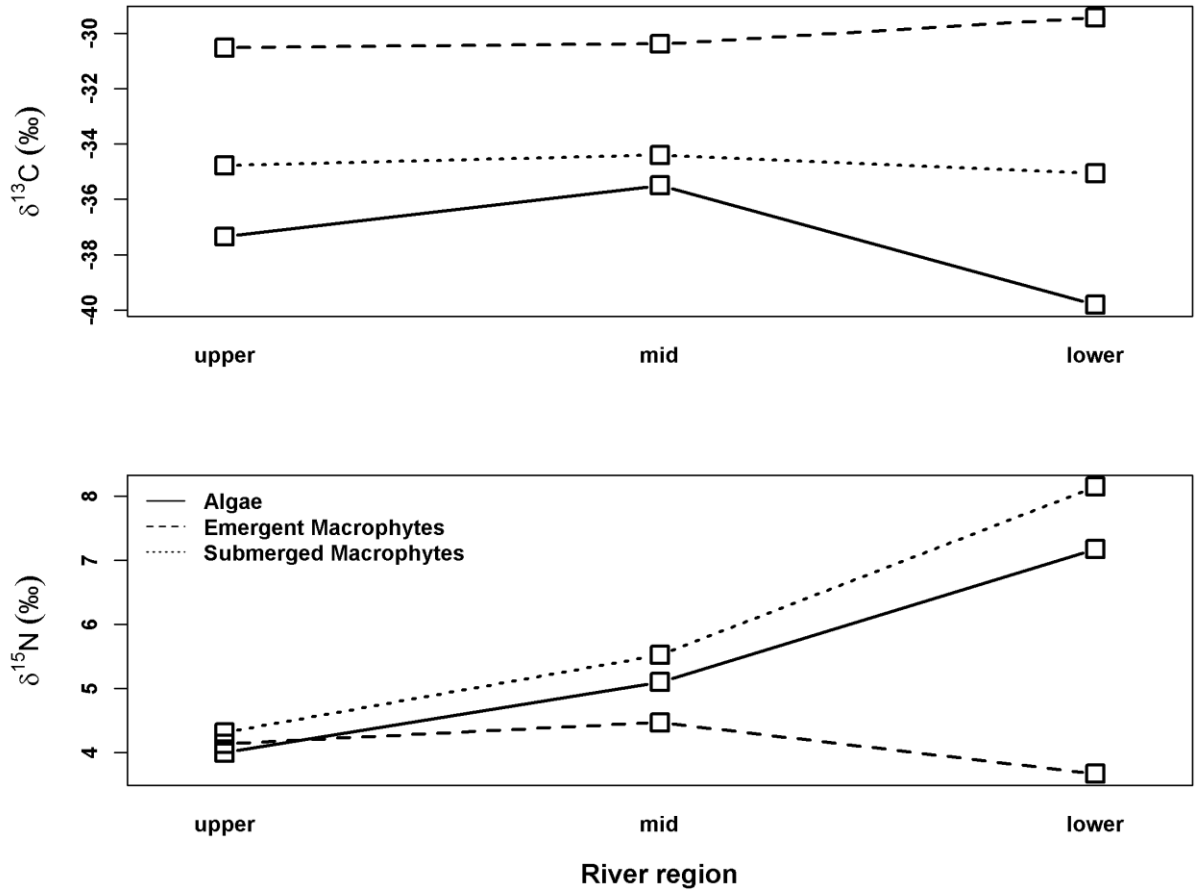

Figure 9.7. Interaction plots of the combined effects of group and river region on $\delta^{13}C$ (top panel) and $\delta^{15}N$ (bottom panel) values of dominant autotrophs. Symbols represent mean values.

Within our broad autotroph groups we further investigated the effects of taxonomy and growth form to gain insight into the potential drivers of isotopic variation within each resource pool. Algae within Silver River is represented by a diverse assemblage of organisms including diatoms, cyanobacteria, chlorophytes (green algae), rhodophytes (red algae), and xanthophytes (yellow-green algae). We separated algae data based on growth form as follows: epiphytic (found attached to surface of submerged macrophytes), benthic (found growing directly from or resting on the benthic substrate), or unattached (found free in the water column or gently resting on macrophytes). The most commonly observed benthic algae were *Vaucheria* (Xanthophyta) and *Lyngbya* (cyanobacteria); other filamentous taxa such as *Dichotomosiphon* (Chlorophyta) and *Compsopogon* (Rhodophyta) were found on occasion in benthic algal mats in the upper and mid river. The most commonly encountered unattached algae were chlorophytes including *Spirogyra*, *Ulothrix*, and *Rhizoclonium*. The epiphyton community included a variety of chlorophytes (e.g., *Cladophora*, *Mougeotia*, *Stigeoclonium*, *Ulothrix*), the rhodophyte *Compsopogon*, and numerous pennate and centric diatoms (for detailed list of diatom genera and other algal taxa present at Silver River see Odum 1957 and Quinlan et al. 2008). It should be noted that all samples of filamentous algae likely contained a marginal amount of diatoms and microscopic bacteria in addition to the dominant filamentous taxa present in the composite

sample. In addition to the presence of diatoms, benthic and epiphytic algae samples often contained two or more filamentous algal taxa (Jacoby et al. 2007).

Among primary producers, algal taxa demonstrated the greatest range in stable carbon isotope composition. We found $\delta^{13}C$ values measured in individual algae samples ranged widely, -45.9‰ in the benthic algae *Vaucheria* to -15.3‰ in the epiphytic algae *Cladophora* (Appendix 9.1). $\delta^{13}C$ and $\delta^{15}N$ values of algae were significantly affected by growth form ($F_{2,67} = 19.1$, p-value < 0.001 and $F_{2,67} = 10.9$, p-value < 0.001, for $\delta^{13}C$ and $\delta^{15}N$, respectively), while only $\delta^{15}N$ values were affected by river region ($F_{2,67} = 2.3$, p-value = 0.10 and $F_{2,67} = 21.4$, p-value < 0.001, for $\delta^{13}C$ and $\delta^{15}N$, respectively) with no significant interactions detected ($F_{4,67} = 2.1$, p-value = 0.09; $F_{4,67} = 1.1$, p-value = 0.34, for $\delta^{13}C$ and $\delta^{15}N$, respectively). Post-hoc analysis indicated that stable carbon isotope composition of epiphytic algae was significantly different from both benthic and unattached algae, which were more negative similarly more negative, but similar to one another. $\delta^{15}N$ values were significantly greater for unattached algae than in benthic and epiphytic forms (Table 9.3 and Figure 9.8). Similar to the overall trend across autotrophs, $\delta^{15}N$ values measured in algae increased with distance down river (Figure 9.9).

Table 9.3. Stable isotope composition ($\delta^{15}N$ and $\delta^{13}C$) and elemental ratios (C:N) of algal growth forms from Silver River.

Growth form	n	$\delta^{15}N$ (‰)		$\delta^{13}C$ (‰)		C:N	
		mean	SD	mean	SD	mean	SD
Benthic	24	4.5	2.2	-41.7	5.3	8.0	0.5
Epiphytic	35	4.3	2.0	-33.7	5.6	9.3	1.5
Unattached	17	6.4	1.6	-38.3	3.6	9.5	1.7

We found mean C:N of algae was significantly affected by growth form ($F_{2,67} = 3.4$, p-value = 0.04), but not affected by river region ($F_{2,67} = 0.1$, p-value = 0.86). There was no statistically significant interaction between growth form and region ($F_{4,67} = 0.6$, p-value = 0.69). Post-hoc analysis indicated no significant differences between mean C:N of epiphytic and unattached algae or benthic and unattached algae, however, C:N of epiphytic algae was found to be significantly greater than for benthic algae (Table 9.3).

By far the most abundant submerged macrophyte in Silver River is *Sagittaria kurziana* (springtape); however, a number of other taxa were frequently encountered throughout the study area (Appendix 9.1). While our sample sizes were small, we found a significant effect of taxon on submerged macrophyte $\delta^{13}C$ values ($F_{4,28} = 7.5$, p-value < 0.001) and C:N ratios ($F_{4,28} = 4.8$, p-value = 0.005). Post-hoc analysis revealed $\delta^{13}C$ values *S. kurziana* were significantly greater than *Ceratophyllum demersum* and *Hydrilla verticillata*, all other pair-wise differences were non-significant. Qualitatively, $\delta^{13}C$ values of submerged macrophytes seemed to fall into two major groupings with *S. kurziana* and *Vallisneria americana* (eelgrass) having more similar values to each other than to *Hydrilla*, *Najas guadalupensis*, or *C. demersum* (Figure 9.10).

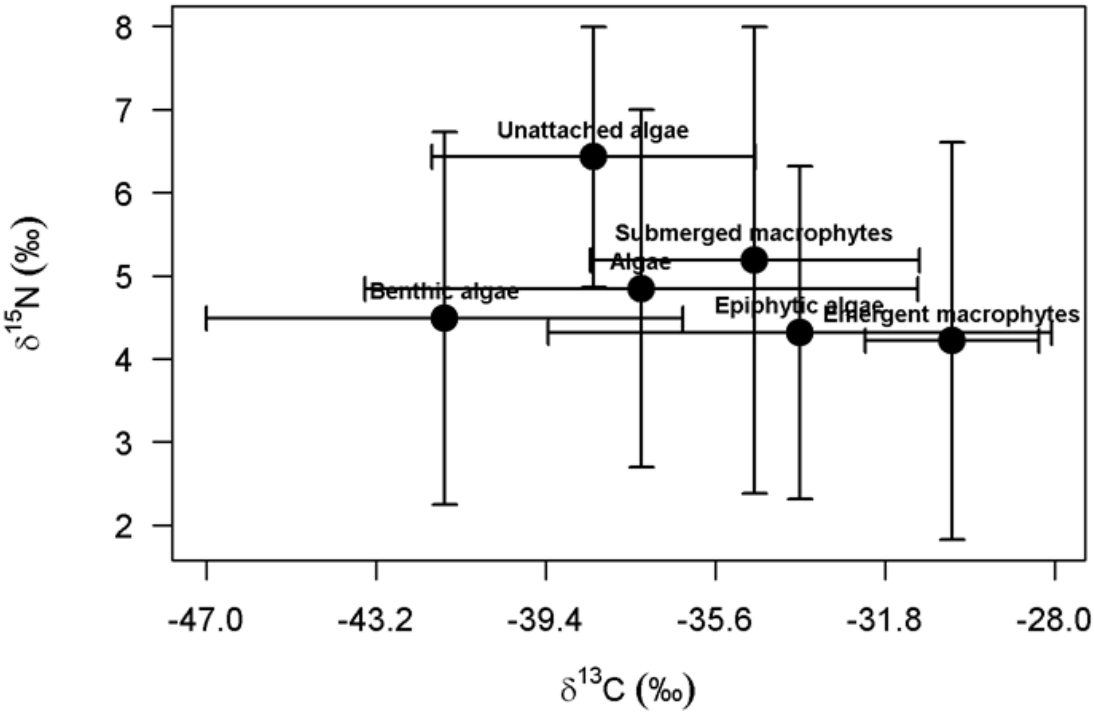

Figure 9.8. Carbon and nitrogen isotope composition of dominant autotroph groups and algal growth forms. Points are means and error bars are ± 1 standard deviation (SD).

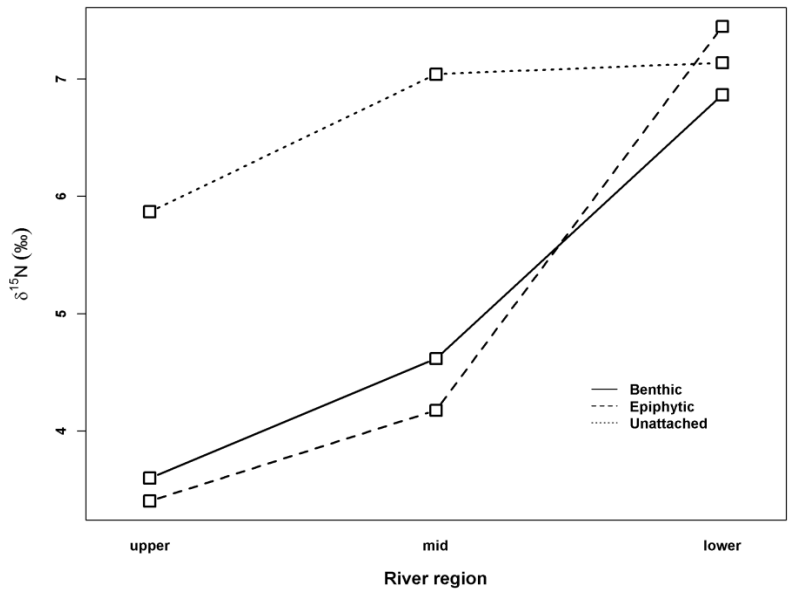

Figure 9.9. Interaction plots of the combined effects of growth form and river region on $\delta^{13}C$ (top panel) and $\delta^{15}N$ (bottom panel) values of algal taxa. Symbols represent mean values.

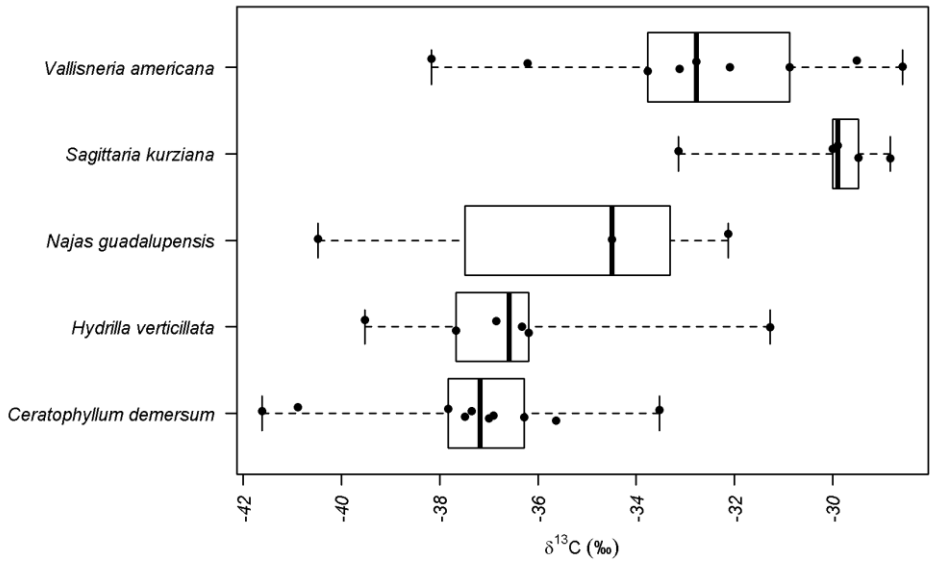

Figure 9.10. Box plot of $\delta^{13}C$ values measured in submerged macrophyte taxa. Center bars denote the median, box constrains the first and third quartiles, whiskers extend to data extremes, and points are individual sample values.

Stable nitrogen isotope composition did not significantly vary among submerged macrophytes ($F_{4,28}$ = 2.2, p-value = 0.09). C:N ratios, however, were found to significantly differ among taxa ($F_{4,28}$ = 4.8, p-value = 0.005). Post-hoc analysis indicated C:N of *C. demersum* was significantly lower than *V. americana* (p-value = 0.002) and all other pair-wise differences were not statistically significant.

The emergent autotroph assemblage present at Silver River is comprised of numerous species ranging from small plants such as duckweed (*Lemna* spp.) and floating fern (*Salvinia* spp.) to dense stands of large rooted plants, chiefly *Nuphar advena* (spatterdock) and *Pontederia cordata* (pickerel weed). In general, the $\delta^{13}C$ values of emergent autotrophs were more positive than submerged macrophytes and algae, values ranged from -35.7‰ to -26.8 ‰, measured in *Nasturtium floridanus* (watercress) and *N. advena*, respectively. $\delta^{15}N$ values were also variable and ranged from 0‰ to 8.6‰, measured in *N. floridanus* and *P. cordata*, respectively. While we measured the stable isotope composition of a variety of emergent and floating autotrophs (Appendix 9.1), for the purposes of this study we concentrated on isotopic composition of the dominant taxa *N. advena* and *P. cordata* since these species comprised the majority of emergent autotroph biomass and structure. Stable carbon isotope composition of *N. advena* (-28.5‰ ± 1.7) and *P. cordata* (-29.3‰ ± 0.7) were similarly positive and did not significantly differ (Welch t-test: t = 1.17, df = 9.7, p-value = 0.26). However, mean $\delta^{15}N$ of *P. cordata* (6.3‰ ± 1.4) was found to be significantly greater than *N. advena* (2.8‰ ± 1.5) (t = -4.6, df = 11.4, p-value < 0.001).

9.5.2 Stable Composition of Less Common and Unique Autotroph Taxa

To assess the potential for terrestrial leaf litter deposition to be incorporated into the detrital resources we measured the isotopic composition of the dominant tree species along the river margins, *Taxodium distichum* (Bald cypress). The stable isotope composition of *T. distichum* was similar to that of emergent macrophytes; $\delta^{13}C$ measured for *T. distichum* was -29.6‰ ± 0.2 and $\delta^{15}N$ was 1.8‰ ± 1.6 (n = 2). We measured also the stable isotopic composition of a number unique autotroph taxa that could potentially contribute to basal resource pools including *Tillandsia usneoides* (Spanish moss), *Utricularia* sp. (bladderwort), *Fontinalis* sp. (water moss), and lichen. The isotopic composition of *T. usneoides* was quite distinctive in that $\delta^{15}N$ values measured for this plant were extremely negative (-9.5‰) and $\delta^{13}C$ values (-17.2‰) were considerably higher than the majority of autotrophs. Bladderwort, water moss, and lichen were found to have similar $\delta^{13}C$ and $\delta^{15}N$ values to algal taxa. $\delta^{13}C$ values for these taxa ranged from -41.0 to -36.0 ‰, measured in water moss and bladderwort, respectively. $\delta^{15}N$ values for these taxa ranged from 3.5 to 7.0‰, measured in lichen and water moss, respectively.

9.5.3 Stable Isotope Composition of Consumers

To date we have analyzed a total 713 samples from 56 taxa for stable carbon and nitrogen isotope composition (Appendix 9.2 and 9.3). Samples analyzed thus far include 195 macroinvertebrates, 430 fish, 39 turtles, and 49 alligators. Analyses are ongoing. Here we summarize available data in an effort to determine the efficacy of stable isotopes as a tool to delineate food webs and characterize energy flow in springs and spring-fed rivers.

In general, we found the stable isotope composition of consumers to follow well known patterns of isotopic discrimination within food webs (Figure 9.11). Specifically, we found enrichment of both ^{13}C and ^{15}N with increasing trophic position (i.e., primary producers to top predators); however, there was substantial variation in isotopic composition among taxa with similar trophic ecology (i.e., primary consumer, predator, etc.), within taxa due to body size and life history stage, and also among river regions.

9.5.4 Primary Consumers and Omnivores

Florida springs are home to a diverse assemblage of primary consumers and omnivores which have the potential to directly utilize algal and macrophyte production. Species range in size from minute insect larvae such as chironomids (non-biting midges) to large-bodied fish (e.g., striped mullet, lake chubsucker [*Erimyzon sucetta*]). The gastropod assemblage present in springs and spring-fed rivers was of particular interest as these organisms can be remarkably abundant, comprising the majority of macroinvertebrate biomass in macrophytes beds and benthic algae mats (Heffernan et al. 2010b, Liebowitz 2013). The gastropod assemblage present in Florida springs is comprised of taxa from six families, Ampullariidae, Hydrobiidae, Physidae, Planorbidae, Pleuroceridae and Viviparidae.

The largest gastropod present in Silver River is the ampullarid *Pomacea paludosa* (Florida apple snail), whereas the smallest are various species of hydrobiids and physids. The most frequently encountered gastropods in submerged macrophytes beds were the pleurocerid *Elimia floridensis* (Rasp elimia), various planorbids, and the viviparid *Viviparus georgianus* (banded mystery snail).

The stable carbon isotope signatures of gastropods ranged widely, i.e. -39.1‰ to -20.0‰, whereas the stable nitrogen isotope signatures exhibited less variation, i.e. 5.0‰ to 9.7‰. To assess taxon specific differences in gastropods, isotopic data from smaller gastropods (i.e., Hydrobiidae, Planorbidae, Physidae) were aggregated and all other gastropods grouped by family. The stable carbon isotope composition of ampullariids (-33.3‰ ± 4.1), represented by the single species *P. paludosa*, was on average similar to pleurocerids and viviparids, however there was a considerable amount of variation across our limited sample size (n = 7). Small gastropods were found to be enriched in ^{13}C relative to other gastropods and displayed the most variability (Table 9.4). We found no significant effect of taxon ($F_{3,32}$ = 1.9, p-value= 0.15) or river region ($F_{2,32}$ = 1.3, p-value = 0.28) as well as a no significant interaction ($F_{6,32}$ = 1.3, p-value = 0.31) among these factors on gastropod $\delta^{13}C$ values (Figure 9.12).

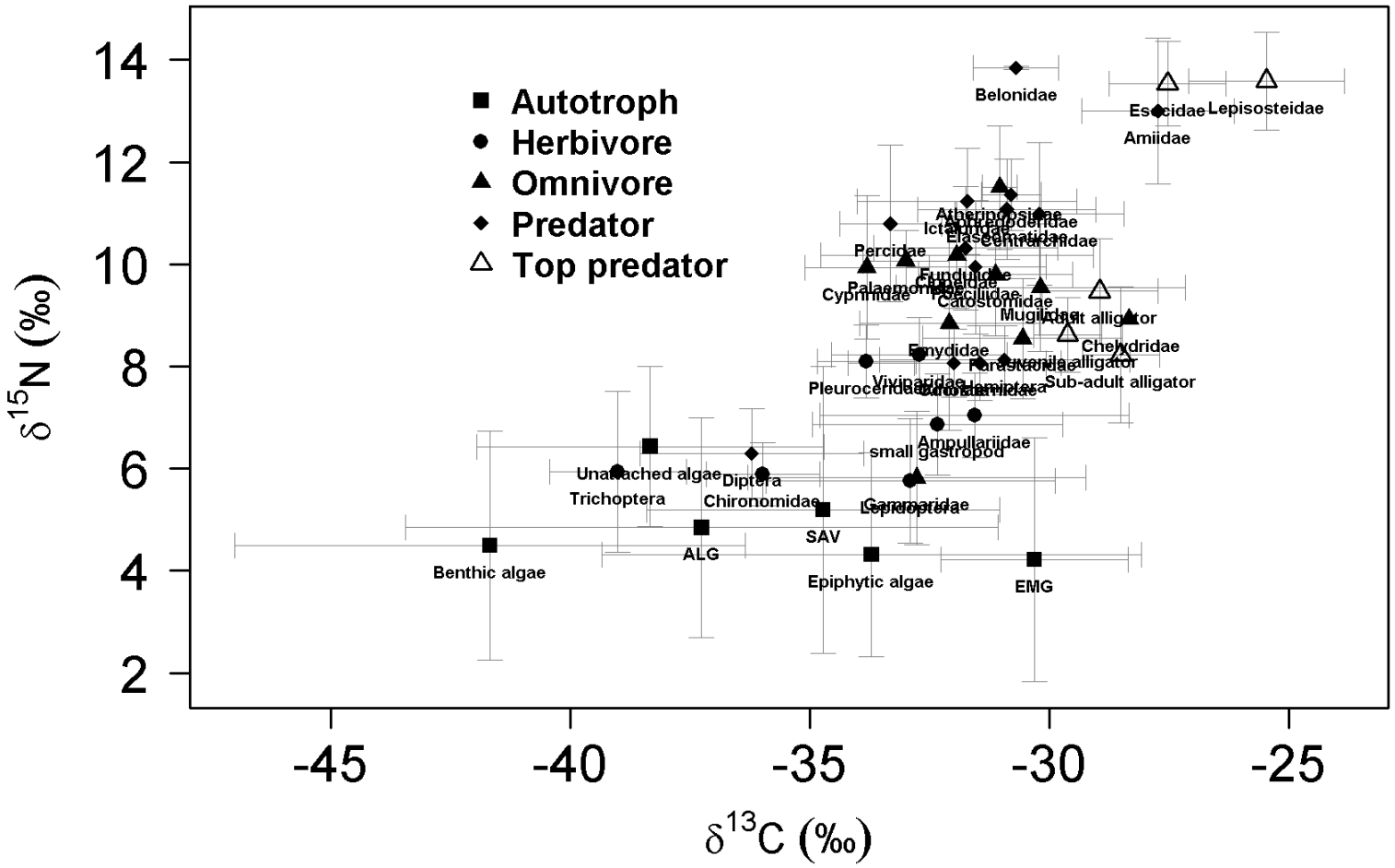

Figure 9.11. Scatter plot of $\delta^{13}C$ and $\delta^{15}N$ values measured in all food web constituents. Symbols represent means and error bars are ± 1 standard deviation (SD). Resource group and consumer taxon are labeled under each symbol.

Table 9.4. Stable isotope composition ($\delta^{15}N$ and $\delta^{13}C$) of gastropods.

Taxa	n	$\delta^{15}N$ (‰)		$\delta^{13}C$ (‰)	
		mean	SD	mean	SD
Ampullariidae	7	6.6	1.0	-33.3	4.1
Pleuroceridae	14	8.1	0.7	-33.8	1.0
Small gastropods	10	6.7	1.1	-31.1	4.6
Viviparidae	13	7.7	1.2	-33.2	1.8

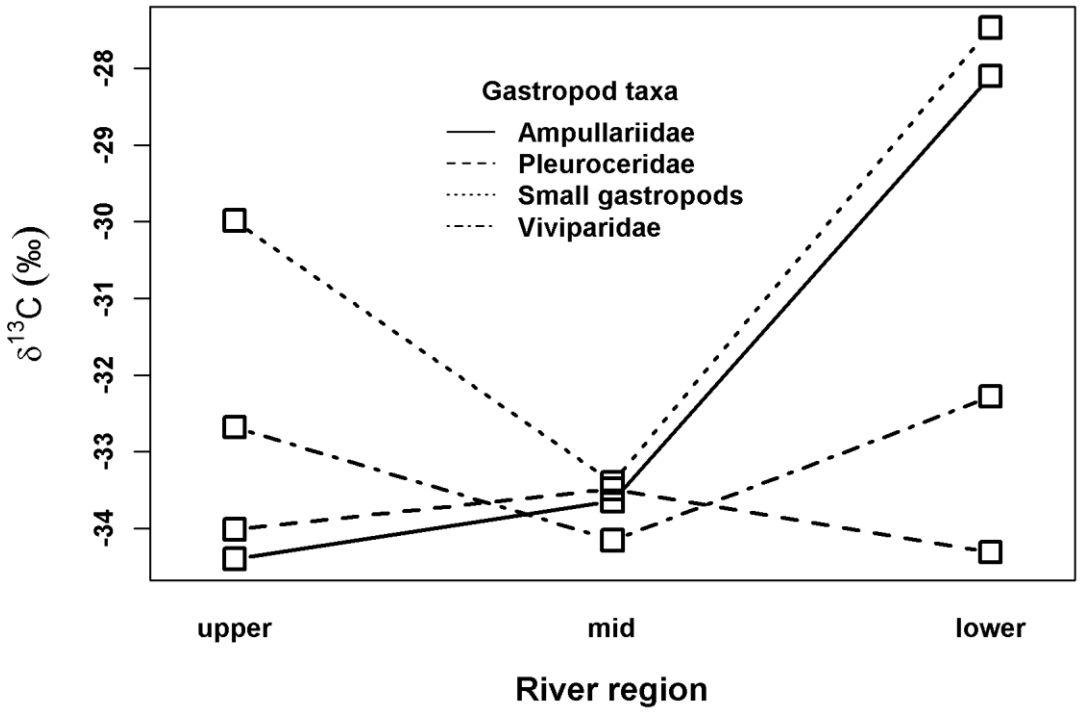

Figure 9.12. Interaction plot of the combined effects of taxon and river region on $\delta^{13}C$ values of gastropod taxa. Symbols represent mean values.

The stable nitrogen isotope composition of gastropods was significantly affected by taxon ($F_{3,32}$ = 6.8, p-value = 0.001) and river region ($F_{2,32}$ = 5.9, p-value = 0.006), but no significant interaction between taxon and region was detected ($F_{6,32}$ = 0.6, p-value = 0.70). $\delta^{15}N$ values measured in viviparids and pleurocerids were significantly greater than ampullariids and small gastropod taxa (Figure 9.13). As expected from patterns observed for primary producers, $\delta^{15}N$ values of gastropods were significantly elevated in the lower river relative to the mid- (p-value = 0.02) and upper regions (p-value = 0.04, Figure 9.14).

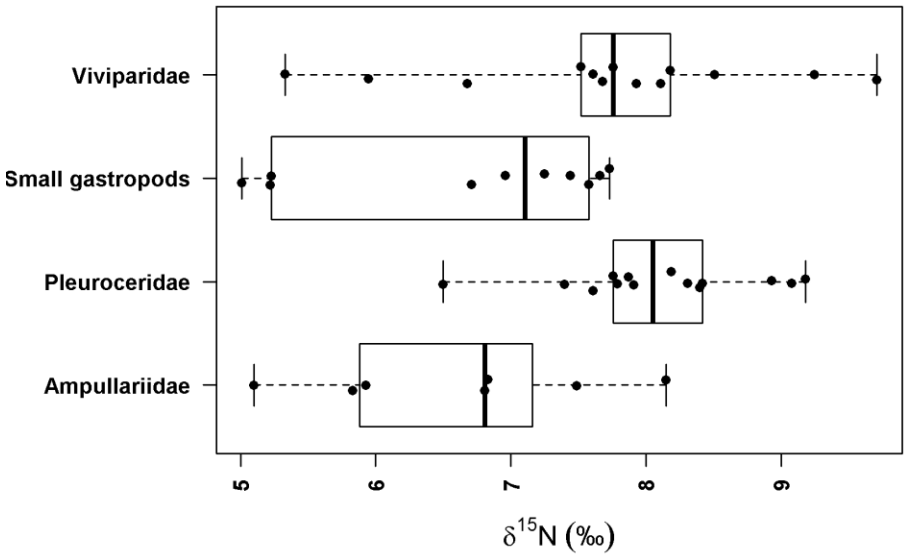

Figure 9.13. Box plot of $\delta^{15}N$ values measured for gastropods. Center bars denote the median, box constrains the first and third quartiles, whiskers extend to data extremes, and points are individual sample values.

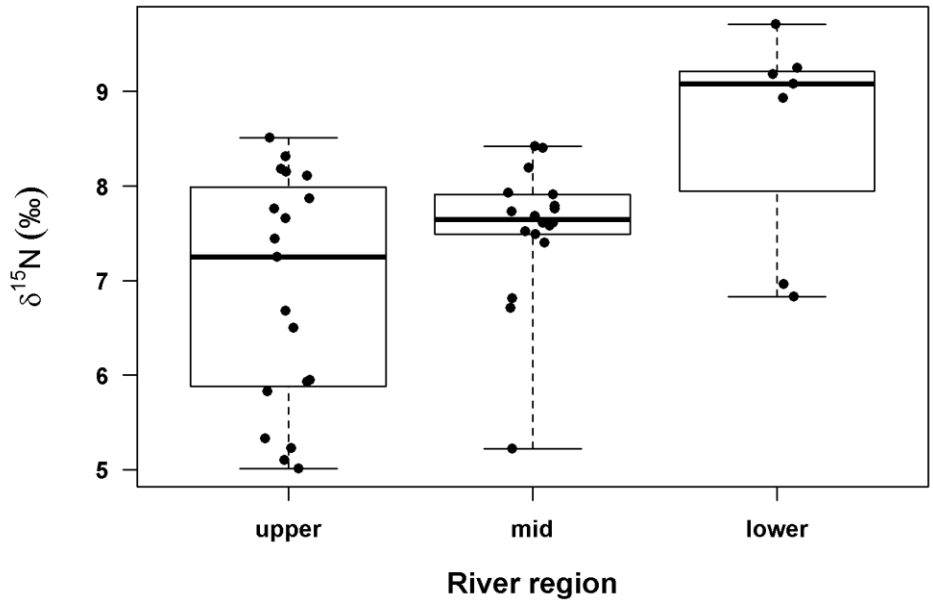

Figure 9.14. Box plot of $\delta^{15}N$ values measured for gastropods from different river regions. Center bars denote the median, box constrains the first and third quartiles, whiskers extend to data extremes, and points are individual sample values.

Many bivalves are long-lived, non-mobile filter feeders and their $\delta^{15}N$ values are often used as baselines for the estimation of trophic position of higher order consumers in aquatic ecosystems (Post 2002). In springs, unionid mussels provide an integrated representation of the isotopic composition of particulate organic matter (POM) and planktonic organisms. Along the entire length of Silver River the $\delta^{13}C$ and $\delta^{15}N$ values of unionid mussels showed little variation (n = 9, $\delta^{15}N$ = 8.3‰ ± 0.6 and $\delta^{13}C$ = -32.9‰ ± 0.5).

In addition to gastropods and bivalves, the macroinvertebrate community inhabiting Silver River includes aquatic insects (larvae and adults) and crustaceans. The feeding habits of larval insects can vary tremendously even by species, thus we acknowledge isotopic variation within broad taxonomic groups may be driven largely by interspecific differences in foraging ecology. For herbivorous aquatic insects, we found significant effects of taxon ($F_{2,48}$ = 27.3, p-value < 0.001) and river region ($F_{2,48}$ = 2.8, p-value = 0.07) on $\delta^{13}C$ values; however, the interaction of taxon and river region was not significant ($F_{3,48}$ = 0.5, p-value = 0.65). Post-hoc analysis indicated $\delta^{13}C$ significantly differed among the groups of herbivorous insects identified (Figure 9.15).

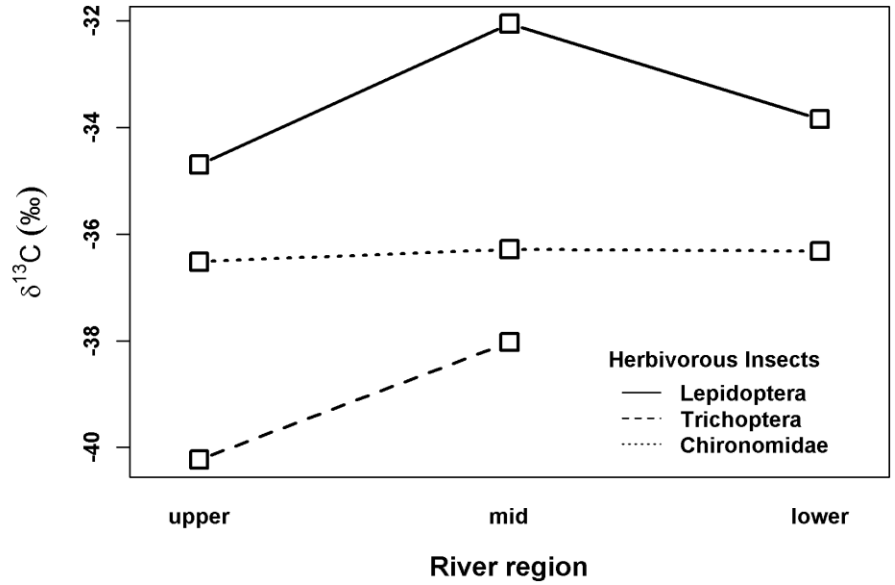

Figure 9.15. Interaction plot of the combined effects of taxon and river region on $\delta^{13}C$ values of aquatic herbivorous insects. Symbols represent mean values.

$\delta^{15}N$ values of herbivorous insects were not found to be significantly affected by taxa ($F_{2,48}$ = 0.03, p-value = 0.96), but the main effect of river region was significant ($F_{2,48}$ = 16.8, p-value < 0.001) and the interaction of taxon and river region also was significant ($F_{3,48}$ = 3.4, p-value = 0.02, Figure 9.16).

Trichopteran larvae (caddisflies), predominantly hydroptilids (purse caddisflies), were commonly encountered on submerged macrophytes and in macroalgae. $\delta^{13}C$ values measured in trichopterans (-39.5‰ ± 2.4) were the most negative of any primary consumer or omnivore taxa. $\delta^{15}N$ values of trichopterans were low (5.7‰ ± 1.5) in the upper river relative to the mid-river (data from lower river sites are forthcoming). Larval chironomids were highly abundant in the epiphyton as well as benthic algal mats. While more negative than most primary consumers, $\delta^{13}C$ values measured in chironomids (-36.4‰ ± 2.6) were highly variable. $\delta^{15}N$ values were less variable and consistently low (5.6‰ ± 0.7). Isotopic composition of other more omnivorous

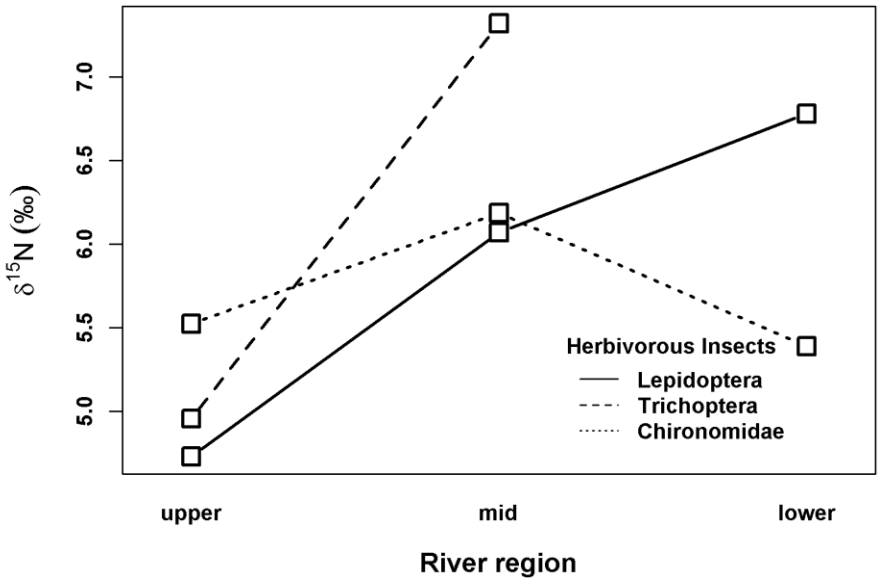

Figure 9.16. Interaction plot of the combined effects of taxon and river region on $\delta^{15}N$ values of aquatic herbivorous insect taxa. Symbols represent mean values.

dipteran larvae (i.e., Athericidiae, Stratiomyidae) was highly variable among taxon (n = 4, range $\delta^{13}C$ = -35.5 to -28.4‰; range $\delta^{15}N$ = 6.0 to 9.0‰). Larvae of multiple crambid and pyralid species (Lepidoptera; aquatic moths) were abundant on submerged macrophyte blades. Mean $\delta^{13}C$ values of crambids and pyralids (-33.2‰ ± 2.9) were more positive than other aquatic insects; however, there was a considerable range among individual samples (n = 20, range $\delta^{13}C$ = -35.5 to -26.6‰). Overall $\delta^{15}N$ values of crambids and pyralids were low (5.7‰ ± 1.5), despite $\delta^{15}N$ values increasing from upper to lower river sites.

We measured stable isotope composition in species from three crustacean families, Gammaridae (amphipods), Palaemonidae (grass shrimp), and Parastacidae (crayfish). The stable carbon isotope composition of crustaceans was found to be significantly affected by taxon ($F_{2,35}$ = 8.5, p-value < 0.001) and were not found to be affected by river region ($F_{2,35}$ = 2.7, p-value = 0.08) nor was the interaction of taxon and region significant ($F_{4,35}$ = 0.9, p-value = 0.50). Post-hoc analysis indicated $\delta^{13}C$ values measured in crayfish (-30.5‰ ± 2.1) were significantly heavier than grass shrimp (p-value = 0.01) and amphipods (p-value = 0.001, Figure 9.17). Stable nitrogen isotope composition of omnivorous crustaceans was only found to be significantly affected by taxon ($F_{2,31}$ = 49.4, p-value < 0.001). Post-hoc analysis indicated $\delta^{15}N$ values of all taxa were significantly different from one another. $\delta^{15}N$ values were lowest in amphipods (5.8‰ ± 1.3), higher in crayfish (8.5‰ ± 1.2) and highest in grass shrimp (10.1‰ ± 0.6).

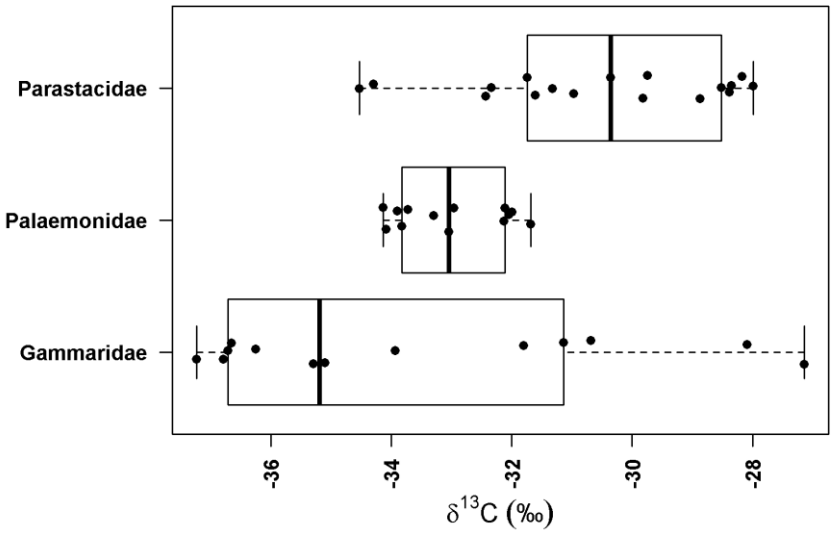

Figure 9.17. Boxplot of $\delta^{13}C$ values measured in omnivorous crustaceans. Center bars denote the median, box constrains the first and third quartiles, whiskers extend to data extremes, and points are individual sample values.

There are a number of fishes that are potentially important consumers of algal production in Florida springs and spring-fed rivers. While historically reported as one of the most abundant herbivorous fish in Silver River, striped mullet are still present, albeit in lower numbers (Odum 1957). Both stable carbon and nitrogen isotope composition of striped mullet fin tissue were highly variable. From the 17 striped mullet samples analyzed thus far $\delta^{13}C$ values ranged from -35.3 to -26.6‰ and $\delta^{15}N$ values from 7.7 to 11.6‰. Other omnivorous fish sampled included 4 families; silver sides (Atherniodidae), suckers (Catostomidae), shad (Clupeidae), and shiners (Cyprinidae). Mean $\delta^{13}C$ values measured in omnivorous fish ranged from -34.3 to -31.0‰ and mean $\delta^{15}N$ from 8.8 to 11.3‰. While groups differed in the amount of variation in mean $\delta^{13}C$, values of silver sides (*Menidia* sp.), striped mullet, gizzard shad (*Dorosoma cepedianum*), and lake chubsucker (*Erimyzon sucetta*) were around -31‰, while mean $\delta^{13}C$ of shiners (*Notemigonus crysoleucas*, golden shiner, *Notropis petersoni*, coastal shiner, and *Pteronotropis hypselopterus*, sailfin shiner) were more negative (n = 39,-33.8‰ ± 1.3, Figure 9.18). Mean $\delta^{15}N$ values were lowest for lake chubsucker (9.8‰ ± 1.2) and highest in silver sides (11.3‰ ± 1.3, Figure 9.19). For the two species that were encountered in all river regions (*E. sucetta* and *N. petersoni*), river region did not significantly affect $\delta^{13}C$ values ($F_{1,50}$ = 1.89, p-value = 0.16). However, $\delta^{15}N$ values of these two species were found to affected by river region ($F_{2,50}$ = 31.4, p-value < 0.001) and were significantly higher in the lower river compared to mid- and upper (Figure 9.20).

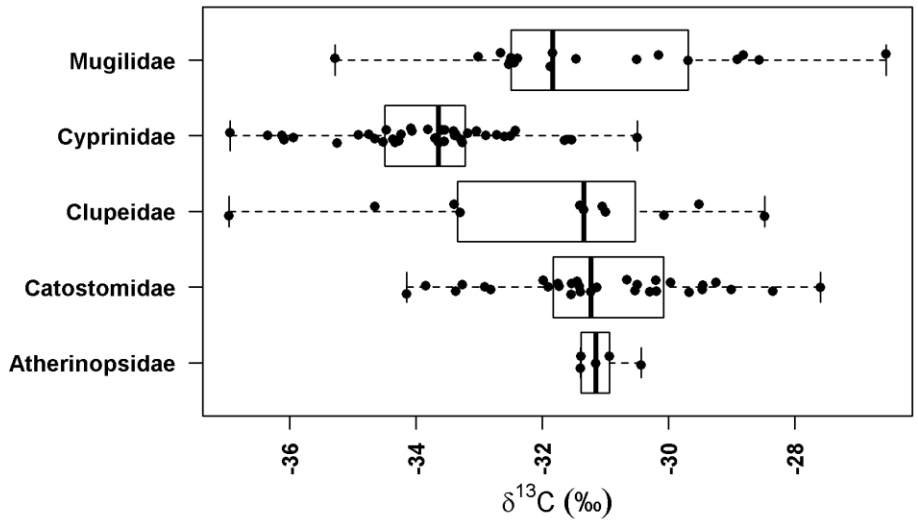

Figure 9.18. Boxplot of $\delta^{13}C$ values measured in families of herbivorous and omnivorous fish. Center bars denote the median, box constrains the first and third quartiles, whiskers extend to data extremes, and points are individual sample values.

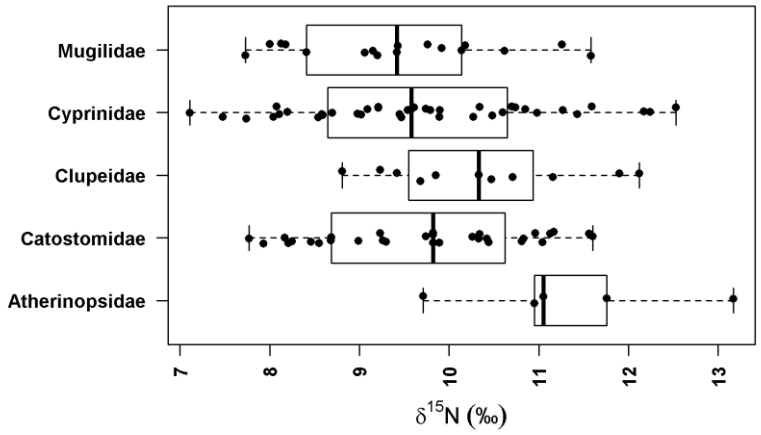

Figure 9.19. Boxplot of $\delta^{15}N$ values measured in families of herbivorous and omnivorous fish. Center bars denote the median, box constrains the first and third quartiles, whiskers extend to data extremes, and points are individual sample values.

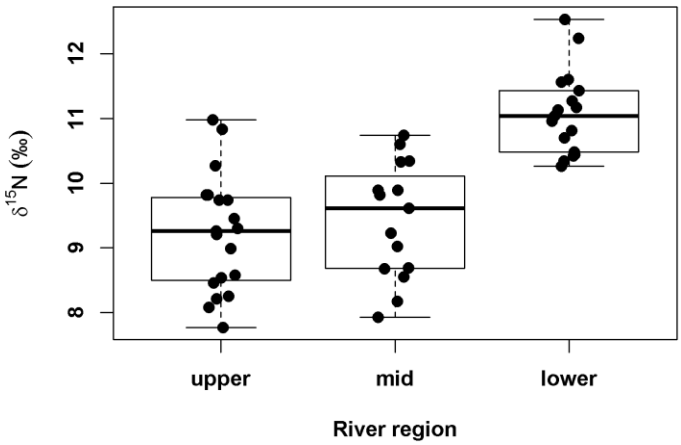

Figure 9.20. Boxplot of $\delta^{15}N$ values measured in omnivorous fish across river regions. Center bars denote the median, box constrains the first and third quartiles, whiskers extend to data extremes, and points are individual sample values.

Florida springs and associated rivers are home to a number of different turtle species. Turtles within the genus *Pseudemys* (River cooters) and the common snapping turtle (*Chelydra serpentina*) are known to consume SAV and macroalgae as well as infaunal organisms and carrion (Aresco et al. 2015). We have obtained tissue samples from 39 individuals across four species, *Pseudemys nelsoni* (n = 13, Florida redbelly cooter), *P. peninsularis* (n = 9, Peninsular cooter), *P. suwanniensis* (n = 13, Suwannee cooter), and *C. serpentina* (n = 4) in Silver River. To date, stable isotope analysis has been performed on 15 of these samples. $\delta^{13}C$ values measured in these species ranged from -35.1‰ to -28.2‰; measured in *P. peninsularis* and *P. suwanniensis*, respectively. Likewise, the stable nitrogen isotope composition spanned a 7‰ range, from 5.9‰ measured in *P. suwanniensis* to 13.2‰ measured in *P. nelsoni*.

9.5.5 Secondary Consumers

Secondary consumers in Florida springs include larval and adult predaceous insects (i.e., hemiptera, odonota, diptera), snakes, turtles, and numerous predatory fishes. To date, we have analyzed a robust set of predatory fish samples (n = 272); however, we have analyzed only a relatively small sample set of predaceous insects (n = 25) and while we have collected samples from two species of carnivorous turtles (n = 20) and three snake species (n = 5) we have not received isotopic data from all these individuals at this time.

The stable isotope composition of predaceous insects was highly variable and taxon dependent. Hemipterans (true bugs,) and odonate larvae (damselflies and dragon flies) were found to have more positive $\delta^{13}C$ values (-30.1‰ ± 2.6 and -32.0‰ ± 2.2, for hemipterans and odonates, respectively) than dipterans (-36.2 ‰ ± 2.3). $\delta^{15}N$ values of hemipterans (8.1‰ ± 0.7) and odonates (8.1‰ ± 0.7) were more positive than dipterans (6.3‰ ± 0.9).

We were able to collect stable isotope samples from 9 families of predatory fish ranging from small poeciliids (livebearers) to multiple centrarchids (sunfish) and large amiids (bowfin)

(Appendix 9.2). Mean stable carbon isotope composition of predatory fish families ranged from -33.3 to -27.7‰ measured for Percidae (darters) and Amiidae, respectively (Figure 9.21). Mean $\delta^{15}N$ values of predatory fish families ranged from 9.9 to 12.9‰, measured in Poeciliidae and Amiidae, respectively (Figure 9.22). For the predatory fish families that were sampled in all river regions we found significant differences among mean $\delta^{13}C$ and $\delta^{15}N$ values ($F_{6,242}$ = 23.9, p-value < 0.001; $F_{6,242}$ = 18.5, p-value < 0.001, for $\delta^{13}C$ and $\delta^{15}N$, respectively), river regions ($F_{2,242}$ = 5.5, p-value = 0.004; $F_{2,242}$ = 32.4, p-value < 0.001; Figure 9.23), and the interaction between family and river region was significant for $\delta^{15}N$ ($F_{12,242}$ = 2.3, p-value = 0.01). Post-hoc analysis indicated 10 significant pair-wise differences in $\delta^{13}C$ values among predatory fish families and 9 significant pair-wise differences in $\delta^{15}N$ values. We found significant positive correlation between both $\delta^{13}C$ and $\delta^{15}N$ values and body size (TL) of predatory fish (r = 0.62, p-value < 0.001 for $\delta^{13}C$ and r =0.63, p-value < 0.001 for $\delta^{15}N$; Figure 9.24).

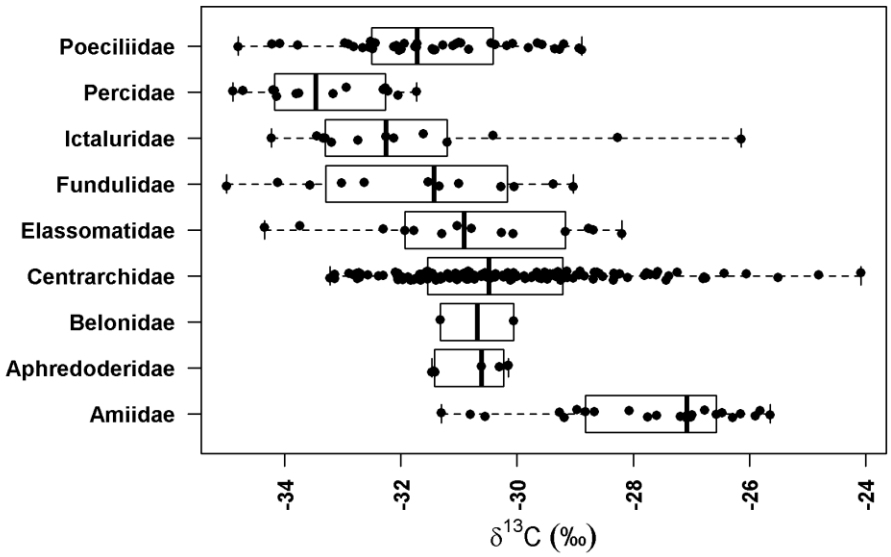

Figure 9.21. Boxplot of $\delta^{13}C$ values measured in families of predatory fish. Center bars denote the median, box constrains the first and third quartiles, whiskers extend to data extremes, and points are individual sample values.

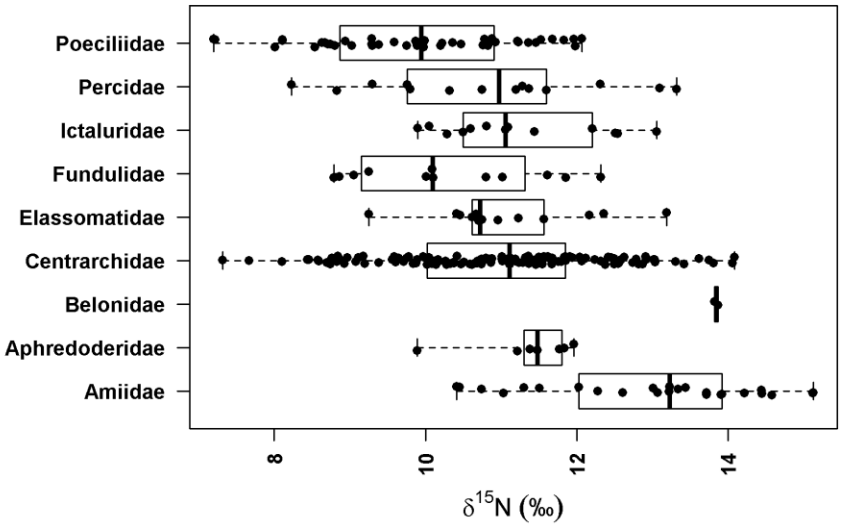

Figure 9.22. Boxplot of $\delta^{15}N$ values measured in families of predatory fish. Center bars denote the median, box constrains the first and third quartiles, whiskers extend to data extremes, and points are individual sample values.

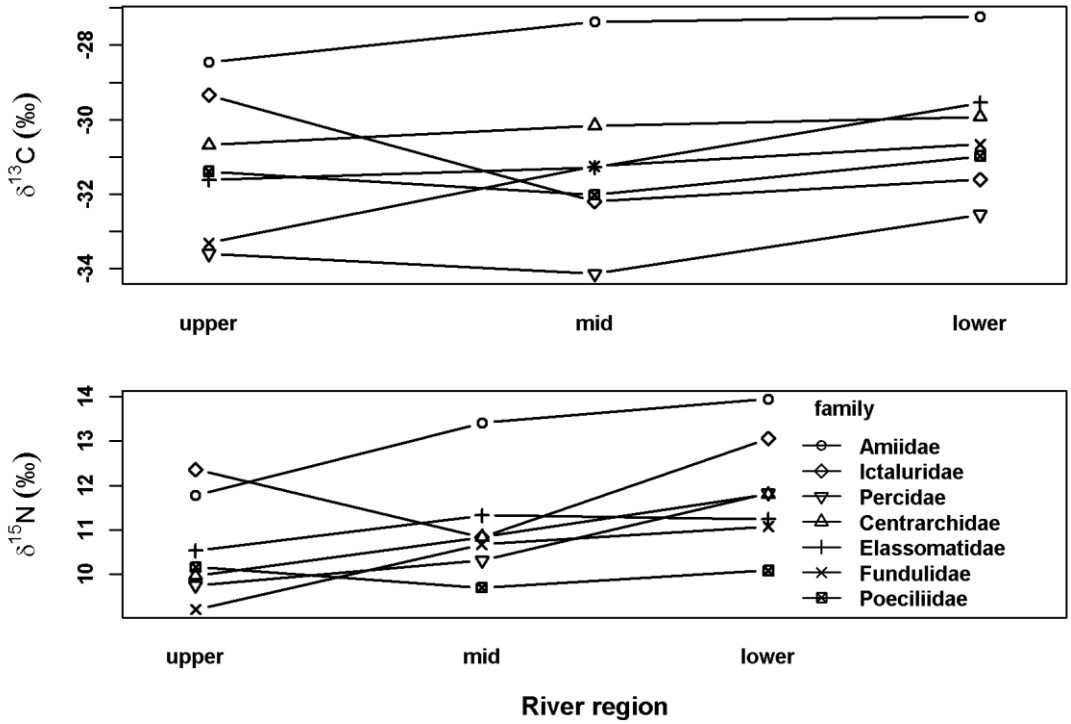

Figure 9.23. Interaction plot of the combined effects of taxon and river region on predatory fish isotopic composition. Top panel $\delta^{13}C$ values and bottom panel $\delta^{15}N$ values. Symbols represent mean values.

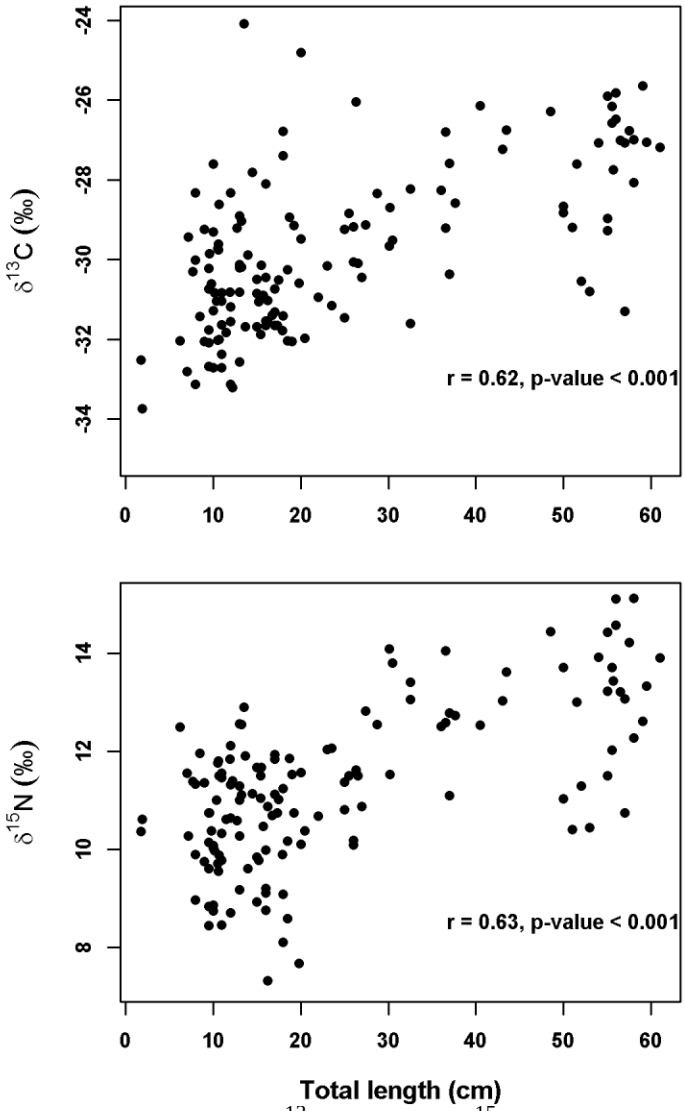

Figure 9.24. Scatterplots of predatory fish $\delta^{13}C$ (top) and $\delta^{15}N$ (bottom) values as a function of total length (cm).

9.5.6 Comments on Parasitic Organisms (leeches and water mites)

Consumers in spring ecosystems are host to a variety of parasitic organisms. We measured the stable isotope composition of two types of organisms, leeches (subclass: Hirudinea) and aquatic mites (order: Trombidiformes), known to parasitize gastropod hosts. Since parasites are often host specific the isotopic composition of parasitic organisms may provide insight into the host's dietary patterns. $\delta^{13}C$ values measured in leeches (n = 2, -35.5 ‰ ±1.7) and water mites (n = 3, -35.4‰ ± 0.8) were slightly more negative than their gastropod hosts/prey (see Table 9.4). Parasite $\delta^{15}N$ values (8.1‰ ±1.2 for leeches and 7.6‰ ± 0.5 for water mites) were similar to viviparid and pleurocerid snails and slightly higher than small gastropods and apple snails.

9.5.7 Top/Apex Predators

The top predator assemblage in Florida springs and spring-fed rivers is presumed to be comprised of large predatory fish and alligators. Florida springs are, in fact, home to multiple species of predatory fish that can attain large body sizes (TL > 40 cm) and can be considered top predators as they are known to specialize on fish prey. We analyzed a total of 21 individuals from two families pickerel (Esocidae) and gar (Lepisosteidae). $\delta^{13}C$ values (-26 ‰ ± 1.8) of large predatory fish were the most positive of any consumer species. Likewise $\delta^{15}N$ values (13.6 ‰ ± 0.9) were uniformly high. The maximum $\delta^{13}C$ and $\delta^{15}N$ values found in this study (-24.8 ‰ and 14.1 ‰) were measured in fin tissues of a 129.5 cm TL *Lepisosteus osseus* (longnose gar).

We captured 56 *Alligator mississippiensis* (American alligator) ranging from in size from 26.5 to 261.5 cm TL, representing the full range in *A. mississippiensis* size/age classes from young juveniles to dominant adult males and females (Figure 9.25). Despite extreme values contributing to the moderately large range in $\delta^{13}C$ (range = -31.0 to -26.3‰) and $\delta^{15}N$ (range = 3.7 to 10.8 ‰) values, overall we found low variation in both stable carbon and nitrogen isotope composition (n = 49, $\delta^{13}C_{SD}$ = 0.99 ‰ and $\delta^{15}N_{SD}$ = 1.15 ‰). Excluding values of individuals captured from a single pod of yearlings (n = 13) and two individuals of undetermined sex, we tested for significant effects of sex and size class (juvenile: TL < 75 cm, sub-adult: 75 cm < TL < 175, adult: TL > 175 cm) on alligator $\delta^{13}C$ and $\delta^{15}N$ values. Carbon isotope composition was found to be unaffected by sex ($F_{1,27}$ = 0.01, p-value = 0.93) or size class ($F_{2,27}$ = 0.69, p-value = 0.51). Stable isotopes of nitrogen, however, were found to be significantly affected by size class ($F_{2,27}$ = 4.9, p-value = 0.01), but not by sex ($F_{1,27}$ = 0.45, p-value = 0.51). Post-hoc analysis indicated $\delta^{15}N$ values of adults were significantly greater than sub-adult and juvenile size classes (Figure 9.26).

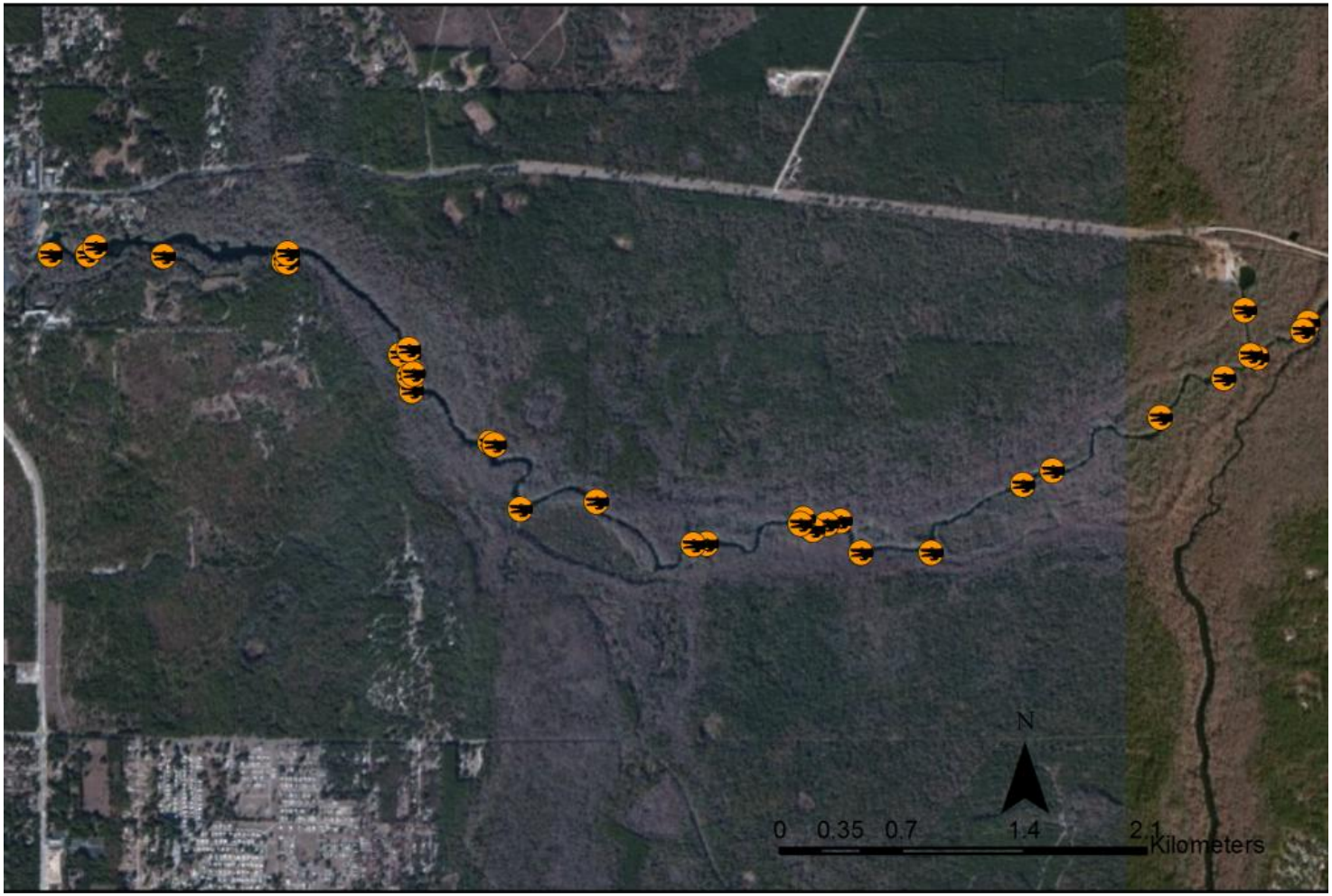

Figure 9.25. Map of American alligator capture locations. Symbols are individual capture locations.

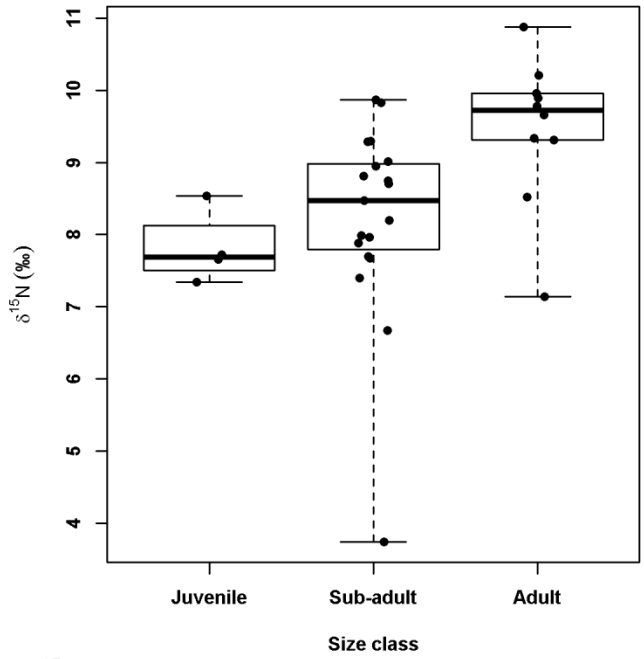

Figure 9.26. Boxplot of $\delta^{15}N$ value measured in American alligator size classes. Center bars denote the median, box constrains the first and third quartiles, whiskers extend to data extremes, and points are individual sample values.

9.5.8 Stomach Content and Scat Analysis

To date, stomach contents have been analyzed from 49 individual American alligators ranging in size (TL) from 59.1 to 248.0 cm. Thus far, we have found that the diet of alligators consists of macroinvertebrates (gastropods and decopods), reptiles (turtles and snakes), fish, birds, and mammals. The most frequently encountered prey items have been apple snails (*Pomacea paludosa*, %FO = 80%) and decopod crustaceans (grass shrimp and crayfish combined, %FO = 97%). Turtles (chiefly kinosternids) were found in 34% of the stomach contents analyzed. Fish and mammals occurred in similar frequencies (26%). Birds and snakes were found least often, each only occurring in 11% of the individuals analyzed.

While stomach content analysis of fish is ongoing, we have collected samples from all species that were subject to stable isotope analysis. In total, we have collected 392 stomach content samples. From samples analyzed thus far there are a number of interesting observatoins. First, decopod crustaceans (crayfish and grass shrimp) are highly important prey species for predatory fish (both juvenile and adult life stages), occurring in very high frequency in the stomach contents of numerous species including multiple centrarchids (sunfish) and *Amia calva* (bowfin). The main predator of small gastropods (i.e., planorbids, physids, and hydrobids) and viviparid snails in Silver River appears to be *Lepomis microlophus* (redear sunfish). Other sunfish species such as *L. macrochirus* (bluegill) and *L. punctatus* (spotted sunfish) chiefly consume larval insects and crustaceans (amphipods and decopods).

To date, scat has been collected from 46 turtles comprised of six species (Table 9.5). From samples analyzed thus far and observations at the time of sample collection there is a clear demarcation of dietary preferences across taxa. River cooters (*Pseudemys* spp.) largely consume submerged macrophytes and macroalgae while the scat of two species of kinosternids (*Stenotherous minor* and *S. odoratus*) contained large numbers of smaller bodied gastropods including planorbids, physids, hydrobids, and juvenile pleurocerids, and also small crustaceans (i.e., amphipods and juvenile crayfish). Common snapping turtle (*Chelydra serpentina*) scat was found to be a mix of submerged macrophytes, detritus including coarse woody debris, and crayfish.

Table 9.5. Number of individuals and species of turtle subject to stable isotope and scat analyses.

Taxon	n
Chelydridae	**4**
Chelydra serpentina (common snapping)	4
Emydidae	**35**
Pseudemys nelsoni (Florida redbelly cooter)	13
Pseudemys peninsularis (Peninsula cooter)	9
Pseudemys suwanniensis (Suwannee cooter)	13
Kinosternidae	**20**
Sternotherus minor (Loggerhead musk)	17
Sternotherus odoratus (common musk)	3

9.6 DISCUSSION

Overall, results from preliminary stable isotope analyses indicate a functional and diverse food web in Silver River (Figure 9.11). We detected significant differences in stable carbon isotope composition among broad primary producer groups and within algae due to growth form (Figure 9.8). The discriminatory ability of isotopic mixing models (SIAR and IsoWeb) to delineate resource use patterns hinges on sufficient differences in the isotopic composition of resource pools used as end-members in the model parametrization (Phillips et al. 2014). Given the position of consumers compared to primary producer groups and expected diet to tissue isotopic discrimination, it appears that the majority of energy transferred within the aquatic food web originates from epiphytic algae and macrophyte production. Benthic filamentous algae production, on the other hand, is likely exported to the terrestrial food web by emergent insects and transferred to a lesser degree to the aquatic food web.

We found the isotopic values of consumers to vary both among and within taxa due to location and body size/life history stage. More in-depth analyses of taxon-level differences in isotopic composition will provide inference to the ecological relevance of this variation. Through longitudinal sampling of the Silver River, from the main spring boil to the confluence with the Ocklawaha River, we found evidence of increasing $\delta^{15}N$ values throughout the food web. Downstream enrichment of ^{15}N is indicative of upstream nitrogen uptake and removal processes in lotic systems (Brabandere et al. 2007) and important to consider when establishing isotopic baselines in food web models and when estimating trophic position (Post 2002). Furthermore,

developing an understanding of how the isotopic composition of major resource pools varies spatially helps to increase model accuracy.

The isotopic differences among primary producers, consumers, and along the spatial extent of the system should allow for key inferences to be drawn regarding food web and energy-flow using isotopic mixing model analyses. Our target objective is to develop of a fully parameterized food web model by estimating the trophic interaction strengths of dominant consumers. Coupled with stomach content and scat data, isotopic mixing model analyses should enable us to develop a detailed depiction of food web interactions in spring ecosystems. Until further analyses are completed, however, we can only qualitatively assess resource use patterns and trophic status by assessing the relative position of consumer isotope values in iso-space (i.e., the bivariate space created by a $\delta^{13}C$-$\delta^{15}N$ bi-plot of consumer and resource values).

9.6.1 Dominant Herbivores and Omnivores

Data collected and analyzed to date suggest that few herbivore species exclusively exploit benthic algal production and the majority of species likely rely heavily upon epiphytic algae and macrophyte resources. The isotopic composition of larval trichoptera (caddisfly) and chironomids (non-biting midges) were the most suggestive of a diet with strict reliance on benthic algal resources. Other herbivorous and omnivorous aquatic insects varied in their position within isotopic space from what appears to be diets heavily reliant on benthic and epiphytic algal resources (e.g., diptera) to those more reliant on submerged and emergent macrophytes (e.g., lepidoptera).

Isotopic variation within the gastropod assemblage suggests a wide range in dietary preferences among taxa. Given what is known of the dietary preferences and distribution of the pleurcerid, *Elimia flordensis* and viviparid snails their isotope values are indicative of similar foraging patterns, both likely relying chiefly on epiphytic algal resources. On the other hand, small gastropods (i.e., hydrobids, physids, and planorbids) appeared to be more closely associated with macrophyte-derived detrital resources. The isotope composition of the ampullariid, *Pomacea paludosa* (apple snail) was highly variable, suggesting a greater degree of diet variability among individuals. Crustaceans also displayed stark differentiation among groups in isotope values. Amphipods showed a large amount of variation in both stable carbon and nitrogen isotope composition suggesting a wide range of assimilated food items, while palaemonids (grass shrimp) showed little variation and are likely more specialized foragers (Figure 9.17). The isotopic composition of parastacids (crayfish) was somewhat variable, but more indicative of a stronger reliance on macrophyte-derived detritus as opposed to algal resources. The carbon composition of some omnivorous fish (shiners) is suggestive of the assimilation of epiphytic algal resources either through direct ingestion or predation of small macroinvertebrate grazers. Other omnivorous fish such as *Mugil cephalus* (striped mullet), *Dorosoma cepedianum* (gizzard shad) and *Erimyzon sucetta* (lake chubsucker) showed substantial variation in their isotopic signatures which may be a product of larger foraging areas or more generalized foraging behaviors. Stable isotope data and observations from scat analysis indicate turtles within the genus *Pseudemys* are important grazers of submerged macrophytes and epiphytic algae.

9.6.2 Secondary Consumers and Top Predators

The isotopic values of secondary consumers varied markedly among taxa and within a particular taxon due, in large part, to differences in body size and life history stage. One interesting finding was the location of American alligators in iso-space relative to other top predators such as gar and pickerel. Stomach contents of alligators indicate that all life-history stages heavily rely on crayfish and apple snail prey. The phenomena of a large-bodied predator foraging on small-bodied organisms from low trophic levels truncates food webs and should be considered when modeling energy-flow in this system. Through stomach content analysis we identified two major predators of gastropods, the redear sunfish and kinosternid turtles. Furthermore, we found a large amount of isotopic variation within predatory fish families; in particular both $\delta^{13}C$ and $\delta^{15}N$ values measured in species of Centrarchidae were highly variable and indicative of dietary specialization among species.

9.6.3 Future Research Directions

Using isotope data collected thus far and data from samples currently being analyzed we plan to move forward in incorporating these data into isotopic mixing model analyses to provide more quantitative assessment of food web structure and energy-flow in Silver River. In addition, it will be necessary to concentrate future isotope sampling efforts on taxa with a high degree of variation in isotope composition (e.g., striped mullet, apple snail) to identify sources of variation such as body size or habitat type. In addition, two primary resource categories that have yet to be sampled thoroughly are benthic mats of diatoms and detritus. Future sampling will include these two categories. In addition, we plan to expand our sampling of Alexander Springs (less intensive) to allow for comparisons with Silver River and other spring systems in an effort to generalize our findings.

Findings thus far provide ample evidence to move forward in pursuing objectives 2 and 3 as outlined in Work Order # 5:

Objective 2 Determine algal growth and grazing rates of small grazer species. Based on the results of Objective 1, samples of the dominant algal and grazer species will be collected live and maintained in mesocosms in the laboratory to evaluate algal growth rates and grazing rates.

Objective 3 Assess the potential for top-down (consumer) control of key grazers in the ecosystem which were identified in Objectives 1 and 2. Manipulative experiments will be performed in the field to further assess grazing effects on algal populations and also to assess the influence of predators on those rates.

With regard to Objective 2, we will focus our laboratory studies on the following taxa: *Pomacea paludosa* (Ampullariidae, apple snail), *Elimia floridensis* (rasp elimia), and *Viviparus georgianus* (banded mystery snails), grass shrimp (*Palaemonetes* sp.), and crayfish (*Procambarus speculifer*). We are interested specifically in quantifying the grazing rates of these organisms on benthic filamentous algae considered to be nuisance species, *Lyngbya* and *Vaucheria*, the unattached algae *Spirogyra*, and the epiphytic algae *Cladophora*. Given results of these trials we intend to perform a suite of experiments to assess foraging preferences. For Objective 3, we will, in the short-term, explore the feasibility of using a combination of enclosure and exclusion mesocosms to assess experimentally the direct and indirect effects of predators on herbivores and algae.

9.7 CONCLUSIONS AND RECOMMENDATIONS

Natural abundance measures of stable carbon and nitrogen isotopes provide new and important insights into energy flow and material transport in the Silver River ecosystem. With regard to primary producers in the Silver River, $\delta^{13}C$ and $\delta^{15}N$ values indicate clearly that rooted macrophytes and their epiphytes fuel much of the secondary production that, in turn, supports a diverse assemblage of organisms that occupy higher trophic levels. Of particular importance is the finding that benthic algae (comprised largely of nuisance filamentous species) do not contribute substantially to the diet of key consumers such as snails. Instead, it appears that only herbivorous insects heavily exploit these algae as a food source. Because algal production is consumed by chironomids and trichopterans (emergent insects), it is likely that much of this algal production is exported to the terrestrial environment. In essence, benthic algal mats in Silver River, and likely other spring systems, may be largely decoupled from the broader food web. This is a dynamic that merits further investigation as it may fundamentally impact energy flow and material transport at the watershed scale. Such an effort is, however, beyond the scope, of this investigation.

Stable isotope analysis coupled with other diet information indicates clearly that redear sunfish and kinosternid turtles are primary predators on gastropods that have the potential to exert control on production by nuisance algae (Dormsjo 2008; Liebowitz et al. 2014). These predator prey interactions to date have received little attention, but merit further study to understand more fully the strength of the relationships as they are likely to have a profound influence on ecosystem function.

Finally, we note that alligators in the Silver River rely heavily on gastropods and crustaceans to support metabolism and growth. This finding has profound implications for any effort to model the Silver River food web. Previous food web models have considered alligators to be top/apex predators which mainly consume fish and other vertebrates occupying higher trophic levels. In other ecosystems alligators are known to both directly and indirectly affect key ecosystem processes through their interactions with prey and the environment (Nifong and Silliman 2013, Rosenblatt et al. 2013). Integration of this novel data into spring food webs will help to refine our understanding of predation and top-down pressures in influencing community dynamics within these complex ecosystems.

9.8 REFERENCES

Aresco, M. J., J. Travis, and P. S. D. MacRae. 2015. Trophic Interactions of Turtles in a North Florida Lake Food Web: Prevalence of Omnivory. Copeia 103:343–356.

Brabandere, L. D., T. K. Frazer, and J. P. Montoya. 2007. Stable nitrogen isotope ratios of macrophytes and associated periphyton along a nitrate gradient in two subtropical, spring-fed streams. Freshwater Biology 52:1564–1575.

Collins, W.D. and C.S. Howard. 1928. Chemical Character of Waters of Florida. U.S. Geological Survey Water-Supply Paper 596-G. 60 pp

Copeland, R. 2003. Florida Spring Classification System and Spring Glossary. Florida Geological Survey Special Publication No. 52, Tallahassee, FL. vi, 18 pp.

Cowell, B. C. and C. J. Dawes. 2004. Growth and nitrate-nitrogen uptake by the cyanobacterium *Lyngbya wollei*. J. Aquatic Plant Management 42: 69-71.

Dial, Cordy & Associates. 2008. Submerged Aquatic Vegetation Communities in Selected Springs and Spring Runs in the Middle St. Johns River Basin. Report submitted to the St. Johns River Water Management District, Palatka, FL. iii, 13 pp., Appendices.

Dormsjo, K. 2008. Oxygen mediated grazing impacts in Florida springs. M.S. Thesis. University of Florida, Gainesville, FL. 69 pp.

Fitzgerald, L. A. 1989. An evaluation of stomach flushing techniques for crocodilians. Journal of Herpetology 23:170–172.

Heffernan, J.B., D.M. Liebowitz, T.K. Frazer, J.M. Evans,and M.J. Cohen. 2010. Algal blooms and the nitrogen enrichment hypothesis in Florida springs: evidence, alternatives, and adaptive management. Ecological Applications 20: 816–829.

Heffernan, J. B., M. J. Cohen, T. K. Frazer, R. G. Thomas, T. J. Rayfield, J. Gulley, J. B. Martin, J. J. Delfino, and W. D. Graham. 2010. Hydrologic and biotic influences on nitrate removal in a subtropical spring-fed river. Limnology and Oceanography 55:249–263.

Hicks, R. and K. Holland. 2012. Nutrient TMDL for Silver Springs, Silver Springs Group, and Upper Silver River (WBIDs 2772A, 2772C, and 2772E). Division of Environmental Assessment and Restoration, Florida Department of Environmental Protection, Tallahassee, FL. 112 pp.

Jacoby, C.A., T.K. Frazer, R.A. Swett, S.R. Keller and S.K. Notestein. 2007. Kings Bay vegetation evaluation. Final Report. Southwest Florida Water Management District, Brooksville, Florida. 166 p.

Liebowitz, D. M. 2013. Environmentally mediated consumer control of algae proliferation in Florida springs. University of Florida.

Liebowitz, D.M., M.J. Cohen, J.B. Heffernan, L.V. Korhnak, and T.K. Frazer. 2014. Environmentally-mediated consumer control of algal proliferation in Florida springs. Freshwater Biology 59: 2009-2023.

Munch, D. A., E. J. Phlips, M. S. Allen, and R. L. Knight, et al. 2006. Fifty-Year Retrospective Study of the Ecology of Silver Springs, Florida. St. Johns River Water Management District Special Publication SJ2007-SP4. pp. variously numbered. Appendices.

Nifong J, Silliman B (2013) Impacts of a large-bodied, apex predator (Alligator mississippiensis Daudin 1801) on salt marsh food webs. Journal of Experimental Marine Biology and Ecology 440:185–191.

Odum, H. 1957. Trophic structure and productivity of Silver Springs, Florida. Ecological monographs 27:55–112.

Post, D., C. Layman, D. Arrington, G. Takimoto, J. Quattrochi, and C. G. Montana. 2007. Getting to the fat of the matter: models, methods and assumptions for dealing with lipids in stable isotope analyses. Oecologia 152:179–189.

Post, D. M. 2002. Using stable isotopes to estimate trophic position: models, methods, and assumptions. Ecology 83:703–718.

Quinlan, E. L., E. J. Phlips, K. a. Donnelly, C. H. Jett, P. Sleszynski, and S. Keller. 2008. Primary producers and nutrient loading in Silver Springs, FL, USA. Aquatic Botany 88:247–255.

Radloff, F. G. T., K. A. Hobson, and A. J. Leslie. 2012. Characterising ontogenetic niche shifts in Nile crocodile using stable isotope ($\delta^{13}C$, $\delta^{15}N$) analyses of scute keratin. Isotopes in Environmental and Health Studies 48:439–56.

Rosenau, J. C., G. L. Faulkner, C. W. Hendry, Jr., and R. W. Hull. 1977. Springs of Florida. Florida Department of Natural Resources Bureau of Geology Bulletin No. 31 (Revised). 461 pp.

Rosenblatt, A. E., and M. R. Heithaus. 2013. Slow isotope turnover rates and low discrimination values in the american alligator: implications for interpretation of ectotherm stable isotope data. Physiological and Biochemical Zoology 86:137–48.

Sanders, H.L. 1969. Benthic marine diversity and the stability-time hypothesis. Pp. 71-81 IN: Diversity and Stability in Ecological Systems, Brookhaven Symposia in Biology, No. 22. Brookhaven National Laboratory, Upton, NY.

Sanderson, B. L., C. D. Tran, H. J. Coe, V. Pelekis, E. A. Steel, and W. L. Reichert. 2009. Nonlethal Sampling of Fish Caudal Fins Yields Valuable Stable Isotope Data for Threatened and Endangered Fishes. Transactions of the American Fisheries Society 138:1166–1177.

Scott, T. M., G. H. Means, R. C. Means, and R. P. Meegan. 2002. First Magnitude Springs of Florida. Florida Geological Survey Open File Report No. 85. 138 pp.

Scott, T. M., G. H. Means, R. P. Meegan, R. C. Means, S. B. Upchurch, R. E. Copeland, et al. 2004. Springs of Florida. Florida Geological Survey Bulletin No. 66. 377 pp, CD.

Sickman, J. O., A. Albertin, M. W. Anderson, A. Pinowska, and R. J. Stevenson. 2009. A comparison of internal and external supply of nutrients to algal mats in two first magnitude springs in Florida. J. Aquatic Plant Manage 47: 135-144.

Stevenson, R., A. Pinowska, A. Albertin, and J. Sickman. 2007. Ecological condition of algae and nutrients in Florida springs: The synthesis report. Tallahassee, FL.

Wetland Solutions, Inc. 2010. An Ecosystem-Level Study of Florida's Springs. FWC Project Agreement No. 08010. Report submitted to the Florida Fish and Wildlife Conservation Commission, Tallahassee, FL. Pp. variously numbered.

Woodruff, A. 1993. Florida Springs Chemical Classification and Aquatic Biological Communities. M.S. Thesis. University of Florida, Gainesville, FL. 117 pp.

APPENDICES

Appendix 5.1.1. BTC data.

Location	Date and Time	Rhodmaine Concentration Adjusted Concentration (ppb)
Spring Bowl ISCO	3/4/15 18:00	-0.061630859
Spring Bowl ISCO	3/4/15 18:30	93.15714589
Spring Bowl ISCO	3/4/15 19:00	66.21165902
Spring Bowl ISCO	3/4/15 19:30	26.85093745
Spring Bowl ISCO	3/4/15 20:00	10.41305477
Spring Bowl ISCO	3/4/15 20:30	4.09104542
Spring Bowl ISCO	3/4/15 21:00	1.406536894
Spring Bowl ISCO	3/4/15 21:30	0.639534458
Spring Bowl ISCO	3/4/15 22:00	0.219822825
Spring Bowl ISCO	3/4/15 22:30	0.073335235
Spring Bowl ISCO	3/4/15 23:00	-0.023774515
Spring Bowl ISCO	3/4/15 23:30	-0.028712299
Spring Bowl ISCO	3/5/15 0:00	-0.055047147
Spring Bowl ISCO	3/5/15 0:30	-0.028712299
Spring Bowl ISCO	3/5/15 1:00	-0.06821457
Spring Bowl ISCO	3/5/15 1:30	-0.058339003
Spring Bowl ISCO	3/5/15 2:00	-0.027066371
Spring Bowl ISCO	3/5/15 2:30	-0.046817507
Spring Bowl ISCO	3/5/15 3:00	-0.09290349
Spring Bowl ISCO	3/5/15 3:30	-0.114300554
Spring Bowl ISCO	3/5/15 4:00	-0.12582205
Spring Bowl ISCO	3/5/15 4:30	-0.134051689
Spring Bowl ISCO	3/5/15 5:00	-0.051755291
Spring Bowl ISCO	3/5/15 5:30	-0.035296011
Main Channel ISCO	3/4/15 18:00	0.03712482
Main Channel ISCO	3/4/15 19:00	22.35426222
Main Channel ISCO	3/4/15 20:00	40.84132523
Main Channel ISCO	3/4/15 21:00	11.97174856
Main Channel ISCO	3/4/15 22:00	2.32825656
Main Channel ISCO	3/4/15 23:00	0.567113628
Main Channel ISCO	3/5/15 0:00	0.213239113
Main Channel ISCO	3/5/15 1:00	0.068397451
Main Channel ISCO	3/5/15 2:00	0.033832964
Main Channel ISCO	3/5/15 3:00	-0.107716842
Main Channel ISCO	3/5/15 4:00	0.02066554
Main Channel ISCO	3/5/15 5:00	-0.036941939
Main Channel ISCO	3/5/15 6:00	-0.035296011
Main Channel ISCO	3/5/15 7:00	0.00420626
Main Channel ISCO	3/5/15 8:00	-0.041879723
Main Channel ISCO	3/5/15 9:00	0.130942714
Main Channel ISCO	3/5/15 10:00	0.107899723
Main Channel ISCO	3/5/15 11:00	0.030541108
Main Channel ISCO	3/5/15 12:00	0.070043379
Back Channel ISCO	3/4/15 18:00	-0.097841274

Location	Date and Time	Rhodmaine Concentration Adjusted Concentration (ppb)
Back Channel ISCO	3/4/15 19:00	-0.104424986
Back Channel ISCO	3/4/15 20:00	-0.173553961
Back Channel ISCO	3/4/15 21:00	-0.163678393
Back Channel ISCO	3/4/15 22:00	21.83744084
Back Channel ISCO	3/4/15 23:00	20.21290993
Back Channel ISCO	3/5/15 0:00	8.972867792
Back Channel ISCO	3/5/15 1:00	5.063788853
Back Channel ISCO	3/5/15 2:00	5.717222259
Back Channel ISCO	3/5/15 3:00	5.743557106
Back Channel ISCO	3/5/15 4:00	4.642431292
Back Channel ISCO	3/5/15 5:00	3.325688912
Back Channel ISCO	3/5/15 6:00	2.825326808
Back Channel ISCO	3/5/15 7:00	1.956276838
Back Channel ISCO	3/5/15 8:00	1.27980044
Back Channel ISCO	3/5/15 9:00	1.004930469
Back Channel ISCO	3/5/15 10:00	0.624721107
Back Channel ISCO	3/5/15 11:00	0.51608986
Back Channel ISCO	3/5/15 12:00	0.433793462
Back Channel ISCO	3/5/15 13:00	0.170444986
1200 m Sattion Flurometer	3/4/15 8:08	1.297
1200 m Sattion Flurometer	3/4/15 8:09	1.585
1200 m Sattion Flurometer	3/4/15 8:10	1.257
1200 m Sattion Flurometer	3/4/15 8:11	1.33
1200 m Sattion Flurometer	3/4/15 8:12	1.364
1200 m Sattion Flurometer	3/4/15 8:13	1.449
1200 m Sattion Flurometer	3/4/15 8:14	1.19
1200 m Sattion Flurometer	3/4/15 8:15	1.467
1200 m Sattion Flurometer	3/4/15 8:16	1.105
1200 m Sattion Flurometer	3/4/15 9:06	11.9
1200 m Sattion Flurometer	3/4/15 9:07	12.26
1200 m Sattion Flurometer	3/4/15 16:48	-0.017
1200 m Sattion Flurometer	3/4/15 16:49	0.411
1200 m Sattion Flurometer	3/4/15 16:50	-0.143
1200 m Sattion Flurometer	3/4/15 16:51	-0.449
1200 m Sattion Flurometer	3/4/15 16:52	-0.39
1200 m Sattion Flurometer	3/4/15 16:53	10.8
1200 m Sattion Flurometer	3/4/15 16:54	10.44
1200 m Sattion Flurometer	3/4/15 16:55	11.58
1200 m Sattion Flurometer	3/4/15 16:56	11.18
1200 m Sattion Flurometer	3/4/15 16:57	10.72
1200 m Sattion Flurometer	3/4/15 16:58	10.59
1200 m Sattion Flurometer	3/4/15 16:59	0.167
1200 m Sattion Flurometer	3/4/15 17:00	-0.39
1200 m Sattion Flurometer	3/4/15 17:01	0.004
1200 m Sattion Flurometer	3/4/15 17:02	-0.401
1200 m Sattion Flurometer	3/4/15 17:03	0.097

Location	Date and Time	Rhodmaine Concentration Adjusted Concentration (ppb)
1200 m Sattion Flurometer	3/4/15 17:04	-0.364
1200 m Sattion Flurometer	3/4/15 17:05	-0.353
1200 m Sattion Flurometer	3/4/15 17:06	-0.209
1200 m Sattion Flurometer	3/4/15 17:07	-0.231
1200 m Sattion Flurometer	3/4/15 17:08	-0.523
1200 m Sattion Flurometer	3/4/15 17:09	-0.505
1200 m Sattion Flurometer	3/4/15 17:10	-0.143
1200 m Sattion Flurometer	3/4/15 17:11	-0.095
1200 m Sattion Flurometer	3/4/15 17:12	-0.091
1200 m Sattion Flurometer	3/4/15 17:13	-0.024
1200 m Sattion Flurometer	3/4/15 17:14	-0.261
1200 m Sattion Flurometer	3/4/15 17:15	-0.161
1200 m Sattion Flurometer	3/4/15 17:16	-0.157
1200 m Sattion Flurometer	3/4/15 17:17	-0.486
1200 m Sattion Flurometer	3/4/15 17:18	-0.375
1200 m Sattion Flurometer	3/4/15 17:19	-0.364
1200 m Sattion Flurometer	3/4/15 17:20	1.142
1200 m Sattion Flurometer	3/4/15 17:21	-0.106
1200 m Sattion Flurometer	3/4/15 17:22	0.115
1200 m Sattion Flurometer	3/4/15 17:23	-0.257
1200 m Sattion Flurometer	3/4/15 17:24	0.954
1200 m Sattion Flurometer	3/4/15 17:25	-0.198
1200 m Sattion Flurometer	3/4/15 17:26	1.039
1200 m Sattion Flurometer	3/4/15 17:27	0.093
1200 m Sattion Flurometer	3/4/15 17:28	-0.013
1200 m Sattion Flurometer	3/4/15 17:29	-0.076
1200 m Sattion Flurometer	3/4/15 17:30	-0.128
1200 m Sattion Flurometer	3/4/15 17:31	0.085
1200 m Sattion Flurometer	3/4/15 17:32	0.824
1200 m Sattion Flurometer	3/4/15 17:33	0.943
1200 m Sattion Flurometer	3/4/15 17:34	0.1
1200 m Sattion Flurometer	3/4/15 17:35	0.946
1200 m Sattion Flurometer	3/4/15 17:36	1.29
1200 m Sattion Flurometer	3/4/15 17:37	-0.021
1200 m Sattion Flurometer	3/4/15 17:38	0.133
1200 m Sattion Flurometer	3/4/15 17:39	1.028
1200 m Sattion Flurometer	3/4/15 17:40	-0.265
1200 m Sattion Flurometer	3/4/15 17:41	0.052
1200 m Sattion Flurometer	3/4/15 17:42	1.29
1200 m Sattion Flurometer	3/4/15 17:43	-0.132
1200 m Sattion Flurometer	3/4/15 17:44	0.684
1200 m Sattion Flurometer	3/4/15 17:45	0.152
1200 m Sattion Flurometer	3/4/15 17:46	-0.054
1200 m Sattion Flurometer	3/4/15 17:47	1.031
1200 m Sattion Flurometer	3/4/15 17:48	-0.42
1200 m Sattion Flurometer	3/4/15 17:49	-0.039

Location	Date and Time	Rhodmaine Concentration Adjusted Concentration (ppb)
1200 m Sattion Flurometer	3/4/15 17:50	-0.084
1200 m Sattion Flurometer	3/4/15 17:51	0.019
1200 m Sattion Flurometer	3/4/15 17:52	0.241
1200 m Sattion Flurometer	3/4/15 17:53	0.019
1200 m Sattion Flurometer	3/4/15 17:54	0.289
1200 m Sattion Flurometer	3/4/15 17:55	0.994
1200 m Sattion Flurometer	3/4/15 17:56	-0.146
1200 m Sattion Flurometer	3/4/15 17:57	0.226
1200 m Sattion Flurometer	3/4/15 17:58	0.048
1200 m Sattion Flurometer	3/4/15 17:59	0.156
1200 m Sattion Flurometer	3/4/15 18:00	0.215
1200 m Sattion Flurometer	3/4/15 18:01	0.004
1200 m Sattion Flurometer	3/4/15 18:02	-0.231
1200 m Sattion Flurometer	3/4/15 18:03	0.163
1200 m Sattion Flurometer	3/4/15 18:04	0.285
1200 m Sattion Flurometer	3/4/15 18:05	0.928
1200 m Sattion Flurometer	3/4/15 18:06	-0.013
1200 m Sattion Flurometer	3/4/15 18:07	0.928
1200 m Sattion Flurometer	3/4/15 18:08	0.496
1200 m Sattion Flurometer	3/4/15 18:09	0.015
1200 m Sattion Flurometer	3/4/15 18:10	-0.165
1200 m Sattion Flurometer	3/4/15 18:11	-0.261
1200 m Sattion Flurometer	3/4/15 18:12	0.078
1200 m Sattion Flurometer	3/4/15 18:13	0.034
1200 m Sattion Flurometer	3/4/15 18:14	0.137
1200 m Sattion Flurometer	3/4/15 18:15	-0.076
1200 m Sattion Flurometer	3/4/15 18:16	-0.065
1200 m Sattion Flurometer	3/4/15 18:17	0.366
1200 m Sattion Flurometer	3/4/15 18:18	-0.168
1200 m Sattion Flurometer	3/4/15 18:19	0.048
1200 m Sattion Flurometer	3/4/15 18:20	-0.12
1200 m Sattion Flurometer	3/4/15 18:21	0.115
1200 m Sattion Flurometer	3/4/15 18:22	1.172
1200 m Sattion Flurometer	3/4/15 18:23	0.211
1200 m Sattion Flurometer	3/4/15 18:24	0.167
1200 m Sattion Flurometer	3/4/15 18:25	-0.124
1200 m Sattion Flurometer	3/4/15 18:26	0.045
1200 m Sattion Flurometer	3/4/15 18:27	0.126
1200 m Sattion Flurometer	3/4/15 18:28	0.259
1200 m Sattion Flurometer	3/4/15 18:29	0.111
1200 m Sattion Flurometer	3/4/15 18:30	-0.128
1200 m Sattion Flurometer	3/4/15 18:31	0.189
1200 m Sattion Flurometer	3/4/15 18:32	1.057
1200 m Sattion Flurometer	3/4/15 18:33	-0.043
1200 m Sattion Flurometer	3/4/15 18:34	-0.098
1200 m Sattion Flurometer	3/4/15 18:35	1.227

Location	Date and Time	Rhodmaine Concentration Adjusted Concentration (ppb)
1200 m Sattion Flurometer	3/4/15 18:36	-0.338
1200 m Sattion Flurometer	3/4/15 18:37	0.041
1200 m Sattion Flurometer	3/4/15 18:38	-0.047
1200 m Sattion Flurometer	3/4/15 18:39	0.085
1200 m Sattion Flurometer	3/4/15 18:40	-0.106
1200 m Sattion Flurometer	3/4/15 18:41	0.333
1200 m Sattion Flurometer	3/4/15 18:42	0.159
1200 m Sattion Flurometer	3/4/15 18:43	0.636
1200 m Sattion Flurometer	3/4/15 18:44	0.484
1200 m Sattion Flurometer	3/4/15 18:45	0.252
1200 m Sattion Flurometer	3/4/15 18:46	0.259
1200 m Sattion Flurometer	3/4/15 18:47	0.222
1200 m Sattion Flurometer	3/4/15 18:48	0.093
1200 m Sattion Flurometer	3/4/15 18:49	0.082
1200 m Sattion Flurometer	3/4/15 18:50	1.016
1200 m Sattion Flurometer	3/4/15 18:51	1.216
1200 m Sattion Flurometer	3/4/15 18:52	-0.006
1200 m Sattion Flurometer	3/4/15 18:53	0.263
1200 m Sattion Flurometer	3/4/15 18:54	0.097
1200 m Sattion Flurometer	3/4/15 18:55	0.233
1200 m Sattion Flurometer	3/4/15 18:56	0.296
1200 m Sattion Flurometer	3/4/15 18:57	0.374
1200 m Sattion Flurometer	3/4/15 18:58	-0.01
1200 m Sattion Flurometer	3/4/15 18:59	-0.065
1200 m Sattion Flurometer	3/4/15 19:00	0.133
1200 m Sattion Flurometer	3/4/15 19:01	0.88
1200 m Sattion Flurometer	3/4/15 19:02	-0.165
1200 m Sattion Flurometer	3/4/15 19:03	0.159
1200 m Sattion Flurometer	3/4/15 19:04	0.163
1200 m Sattion Flurometer	3/4/15 19:05	-0.087
1200 m Sattion Flurometer	3/4/15 19:06	0.222
1200 m Sattion Flurometer	3/4/15 19:07	-0.006
1200 m Sattion Flurometer	3/4/15 19:08	1.186
1200 m Sattion Flurometer	3/4/15 19:09	-0.209
1200 m Sattion Flurometer	3/4/15 19:10	-0.028
1200 m Sattion Flurometer	3/4/15 19:11	-0.154
1200 m Sattion Flurometer	3/4/15 19:12	-0.024
1200 m Sattion Flurometer	3/4/15 19:13	1.286
1200 m Sattion Flurometer	3/4/15 19:14	0.444
1200 m Sattion Flurometer	3/4/15 19:15	0.233
1200 m Sattion Flurometer	3/4/15 19:16	0.041
1200 m Sattion Flurometer	3/4/15 19:17	0.322
1200 m Sattion Flurometer	3/4/15 19:18	0.108
1200 m Sattion Flurometer	3/4/15 19:19	-0.102
1200 m Sattion Flurometer	3/4/15 19:20	0.902
1200 m Sattion Flurometer	3/4/15 19:21	-0.157

Location	Date and Time	Rhodmaine Concentration Adjusted Concentration (ppb)
1200 m Sattion Flurometer	3/4/15 19:22	-0.076
1200 m Sattion Flurometer	3/4/15 19:23	0.355
1200 m Sattion Flurometer	3/4/15 19:24	0.266
1200 m Sattion Flurometer	3/4/15 19:25	0.418
1200 m Sattion Flurometer	3/4/15 19:26	0.111
1200 m Sattion Flurometer	3/4/15 19:27	-0.072
1200 m Sattion Flurometer	3/4/15 19:28	0.063
1200 m Sattion Flurometer	3/4/15 19:29	0.207
1200 m Sattion Flurometer	3/4/15 19:30	1.279
1200 m Sattion Flurometer	3/4/15 19:31	-0.05
1200 m Sattion Flurometer	3/4/15 19:32	-0.183
1200 m Sattion Flurometer	3/4/15 19:33	0.34
1200 m Sattion Flurometer	3/4/15 19:34	0.082
1200 m Sattion Flurometer	3/4/15 19:35	0.13
1200 m Sattion Flurometer	3/4/15 19:36	1.216
1200 m Sattion Flurometer	3/4/15 19:37	0.2
1200 m Sattion Flurometer	3/4/15 19:38	1.094
1200 m Sattion Flurometer	3/4/15 19:39	0.337
1200 m Sattion Flurometer	3/4/15 19:40	0.913
1200 m Sattion Flurometer	3/4/15 19:41	-0.021
1200 m Sattion Flurometer	3/4/15 19:42	1.257
1200 m Sattion Flurometer	3/4/15 19:43	0.089
1200 m Sattion Flurometer	3/4/15 19:44	0.163
1200 m Sattion Flurometer	3/4/15 19:45	-0.028
1200 m Sattion Flurometer	3/4/15 19:46	0.266
1200 m Sattion Flurometer	3/4/15 19:47	0.137
1200 m Sattion Flurometer	3/4/15 19:48	0.263
1200 m Sattion Flurometer	3/4/15 19:49	-0.242
1200 m Sattion Flurometer	3/4/15 19:50	0.074
1200 m Sattion Flurometer	3/4/15 19:51	0.078
1200 m Sattion Flurometer	3/4/15 19:52	0.097
1200 m Sattion Flurometer	3/4/15 19:53	-0.12
1200 m Sattion Flurometer	3/4/15 19:54	0.174
1200 m Sattion Flurometer	3/4/15 19:55	-0.198
1200 m Sattion Flurometer	3/4/15 19:56	0.976
1200 m Sattion Flurometer	3/4/15 19:57	1.253
1200 m Sattion Flurometer	3/4/15 19:58	0.2
1200 m Sattion Flurometer	3/4/15 19:59	0.133
1200 m Sattion Flurometer	3/4/15 20:00	0.979
1200 m Sattion Flurometer	3/4/15 20:01	0.152
1200 m Sattion Flurometer	3/4/15 20:02	-0.087
1200 m Sattion Flurometer	3/4/15 20:03	0.008
1200 m Sattion Flurometer	3/4/15 20:04	0.163
1200 m Sattion Flurometer	3/4/15 20:05	0.226
1200 m Sattion Flurometer	3/4/15 20:06	0.473
1200 m Sattion Flurometer	3/4/15 20:07	0.617

Location	Date and Time	Rhodmaine Concentration Adjusted Concentration (ppb)
1200 m Sattion Flurometer	3/4/15 20:08	0.558
1200 m Sattion Flurometer	3/4/15 20:09	0.322
1200 m Sattion Flurometer	3/4/15 20:10	0.329
1200 m Sattion Flurometer	3/4/15 20:11	0.854
1200 m Sattion Flurometer	3/4/15 20:12	0.266
1200 m Sattion Flurometer	3/4/15 20:13	0.717
1200 m Sattion Flurometer	3/4/15 20:14	0.832
1200 m Sattion Flurometer	3/4/15 20:15	1.142
1200 m Sattion Flurometer	3/4/15 20:16	1.375
1200 m Sattion Flurometer	3/4/15 20:17	0.883
1200 m Sattion Flurometer	3/4/15 20:18	1.264
1200 m Sattion Flurometer	3/4/15 20:19	1.5
1200 m Sattion Flurometer	3/4/15 20:20	2.771
1200 m Sattion Flurometer	3/4/15 20:21	1.53
1200 m Sattion Flurometer	3/4/15 20:22	1.737
1200 m Sattion Flurometer	3/4/15 20:23	1.844
1200 m Sattion Flurometer	3/4/15 20:24	2.121
1200 m Sattion Flurometer	3/4/15 20:25	2.128
1200 m Sattion Flurometer	3/4/15 20:26	2.527
1200 m Sattion Flurometer	3/4/15 20:27	3.248
1200 m Sattion Flurometer	3/4/15 20:28	3.163
1200 m Sattion Flurometer	3/4/15 20:29	2.934
1200 m Sattion Flurometer	3/4/15 20:30	3.307
1200 m Sattion Flurometer	3/4/15 20:31	4.109
1200 m Sattion Flurometer	3/4/15 20:32	2.834
1200 m Sattion Flurometer	3/4/15 20:33	4.057
1200 m Sattion Flurometer	3/4/15 20:34	3.543
1200 m Sattion Flurometer	3/4/15 20:35	4.944
1200 m Sattion Flurometer	3/4/15 20:36	3.806
1200 m Sattion Flurometer	3/4/15 20:37	4.131
1200 m Sattion Flurometer	3/4/15 20:38	3.998
1200 m Sattion Flurometer	3/4/15 20:39	4.508
1200 m Sattion Flurometer	3/4/15 20:40	4.404
1200 m Sattion Flurometer	3/4/15 20:41	4.973
1200 m Sattion Flurometer	3/4/15 20:42	4.674
1200 m Sattion Flurometer	3/4/15 20:43	5.113
1200 m Sattion Flurometer	3/4/15 20:44	5.394
1200 m Sattion Flurometer	3/4/15 20:45	4.822
1200 m Sattion Flurometer	3/4/15 20:46	4.633
1200 m Sattion Flurometer	3/4/15 20:47	5.173
1200 m Sattion Flurometer	3/4/15 20:48	5.627
1200 m Sattion Flurometer	3/4/15 20:49	6.636
1200 m Sattion Flurometer	3/4/15 20:50	5.945
1200 m Sattion Flurometer	3/4/15 20:51	6.019
1200 m Sattion Flurometer	3/4/15 20:52	6.347
1200 m Sattion Flurometer	3/4/15 20:53	6.159

Location	Date and Time	Rhodmaine Concentration Adjusted Concentration (ppb)
1200 m Sattion Flurometer	3/4/15 20:54	7.615
1200 m Sattion Flurometer	3/4/15 20:55	6.735
1200 m Sattion Flurometer	3/4/15 20:56	6.684
1200 m Sattion Flurometer	3/4/15 20:57	6.791
1200 m Sattion Flurometer	3/4/15 20:58	6.466
1200 m Sattion Flurometer	3/4/15 20:59	6.624
1200 m Sattion Flurometer	3/4/15 21:00	6.728
1200 m Sattion Flurometer	3/4/15 21:01	6.868
1200 m Sattion Flurometer	3/4/15 21:02	6.676
1200 m Sattion Flurometer	3/4/15 21:03	7.777
1200 m Sattion Flurometer	3/4/15 21:04	6.728
1200 m Sattion Flurometer	3/4/15 21:05	6.979
1200 m Sattion Flurometer	3/4/15 21:06	6.687
1200 m Sattion Flurometer	3/4/15 21:07	6.695
1200 m Sattion Flurometer	3/4/15 21:08	6.621
1200 m Sattion Flurometer	3/4/15 21:09	6.691
1200 m Sattion Flurometer	3/4/15 21:10	6.857
1200 m Sattion Flurometer	3/4/15 21:11	7.06
1200 m Sattion Flurometer	3/4/15 21:12	6.961
1200 m Sattion Flurometer	3/4/15 21:13	7.223
1200 m Sattion Flurometer	3/4/15 21:14	6.868
1200 m Sattion Flurometer	3/4/15 21:15	7.101
1200 m Sattion Flurometer	3/4/15 21:16	6.562
1200 m Sattion Flurometer	3/4/15 21:17	6.95
1200 m Sattion Flurometer	3/4/15 21:18	5.952
1200 m Sattion Flurometer	3/4/15 21:19	6.865
1200 m Sattion Flurometer	3/4/15 21:20	6.669
1200 m Sattion Flurometer	3/4/15 21:21	6.092
1200 m Sattion Flurometer	3/4/15 21:22	6.658
1200 m Sattion Flurometer	3/4/15 21:23	6.639
1200 m Sattion Flurometer	3/4/15 21:24	6.251
1200 m Sattion Flurometer	3/4/15 21:25	6.606
1200 m Sattion Flurometer	3/4/15 21:26	6.351
1200 m Sattion Flurometer	3/4/15 21:27	6.307
1200 m Sattion Flurometer	3/4/15 21:28	6.358
1200 m Sattion Flurometer	3/4/15 21:29	6.111
1200 m Sattion Flurometer	3/4/15 21:30	6.052
1200 m Sattion Flurometer	3/4/15 21:31	6.381
1200 m Sattion Flurometer	3/4/15 21:32	5.974
1200 m Sattion Flurometer	3/4/15 21:33	5.982
1200 m Sattion Flurometer	3/4/15 21:34	6.288
1200 m Sattion Flurometer	3/4/15 21:35	6
1200 m Sattion Flurometer	3/4/15 21:36	5.993
1200 m Sattion Flurometer	3/4/15 21:37	5.686
1200 m Sattion Flurometer	3/4/15 21:38	6.17
1200 m Sattion Flurometer	3/4/15 21:39	6.044

Location	Date and Time	Rhodmaine Concentration Adjusted Concentration (ppb)
1200 m Sattion Flurometer	3/4/15 21:40	5.535
1200 m Sattion Flurometer	3/4/15 21:41	5.727
1200 m Sattion Flurometer	3/4/15 21:42	5.657
1200 m Sattion Flurometer	3/4/15 21:43	5.402
1200 m Sattion Flurometer	3/4/15 21:44	6.222
1200 m Sattion Flurometer	3/4/15 21:45	5.206
1200 m Sattion Flurometer	3/4/15 21:46	5.139
1200 m Sattion Flurometer	3/4/15 21:47	5.405
1200 m Sattion Flurometer	3/4/15 21:48	4.98
1200 m Sattion Flurometer	3/4/15 21:49	5.317
1200 m Sattion Flurometer	3/4/15 21:50	4.984
1200 m Sattion Flurometer	3/4/15 21:51	5.228
1200 m Sattion Flurometer	3/4/15 21:52	6.37
1200 m Sattion Flurometer	3/4/15 21:53	5.054
1200 m Sattion Flurometer	3/4/15 21:54	5.025
1200 m Sattion Flurometer	3/4/15 21:55	5.232
1200 m Sattion Flurometer	3/4/15 21:56	4.87
1200 m Sattion Flurometer	3/4/15 21:57	4.744
1200 m Sattion Flurometer	3/4/15 21:58	4.674
1200 m Sattion Flurometer	3/4/15 21:59	4.836
1200 m Sattion Flurometer	3/4/15 22:00	5.801
1200 m Sattion Flurometer	3/4/15 22:01	5.479
1200 m Sattion Flurometer	3/4/15 22:02	4.907
1200 m Sattion Flurometer	3/4/15 22:03	4.415
1200 m Sattion Flurometer	3/4/15 22:04	4.744
1200 m Sattion Flurometer	3/4/15 22:05	5.734
1200 m Sattion Flurometer	3/4/15 22:06	4.537
1200 m Sattion Flurometer	3/4/15 22:07	4.537
1200 m Sattion Flurometer	3/4/15 22:08	4.519
1200 m Sattion Flurometer	3/4/15 22:09	5.971
1200 m Sattion Flurometer	3/4/15 22:10	4.593
1200 m Sattion Flurometer	3/4/15 22:11	5.043
1200 m Sattion Flurometer	3/4/15 22:12	4.497
1200 m Sattion Flurometer	3/4/15 22:13	5.069
1200 m Sattion Flurometer	3/4/15 22:14	6.536
1200 m Sattion Flurometer	3/4/15 22:15	5.102
1200 m Sattion Flurometer	3/4/15 22:16	5.298
1200 m Sattion Flurometer	3/4/15 22:17	5.387
1200 m Sattion Flurometer	3/4/15 22:18	5.756
1200 m Sattion Flurometer	3/4/15 22:19	5.886
1200 m Sattion Flurometer	3/4/15 22:20	5.778
1200 m Sattion Flurometer	3/4/15 22:21	5.778
1200 m Sattion Flurometer	3/4/15 22:22	6.144
1200 m Sattion Flurometer	3/4/15 22:23	5.908
1200 m Sattion Flurometer	3/4/15 22:24	6.817
1200 m Sattion Flurometer	3/4/15 22:25	7.204

Location	Date and Time	Rhodmaine Concentration Adjusted Concentration (ppb)
1200 m Sattion Flurometer	3/4/15 22:26	6.761
1200 m Sattion Flurometer	3/4/15 22:27	6.894
1200 m Sattion Flurometer	3/4/15 22:28	7.389
1200 m Sattion Flurometer	3/4/15 22:29	7.567
1200 m Sattion Flurometer	3/4/15 22:30	8.56
1200 m Sattion Flurometer	3/4/15 22:31	7.94
1200 m Sattion Flurometer	3/4/15 22:32	8.715
1200 m Sattion Flurometer	3/4/15 22:33	8.335
1200 m Sattion Flurometer	3/4/15 22:34	8.723
1200 m Sattion Flurometer	3/4/15 22:35	9.007
1200 m Sattion Flurometer	3/4/15 22:36	9.007
1200 m Sattion Flurometer	3/4/15 22:37	9.066
1200 m Sattion Flurometer	3/4/15 22:38	10.4
1200 m Sattion Flurometer	3/4/15 22:39	9.879
1200 m Sattion Flurometer	3/4/15 22:40	9.861
1200 m Sattion Flurometer	3/4/15 22:41	10.44
1200 m Sattion Flurometer	3/4/15 22:42	11.78
1200 m Sattion Flurometer	3/4/15 22:43	10.83
1200 m Sattion Flurometer	3/4/15 22:44	10.6
1200 m Sattion Flurometer	3/4/15 22:45	11.03
1200 m Sattion Flurometer	3/4/15 22:46	11.92
1200 m Sattion Flurometer	3/4/15 22:47	11.96
1200 m Sattion Flurometer	3/4/15 22:48	12.32
1200 m Sattion Flurometer	3/4/15 22:49	12.69
1200 m Sattion Flurometer	3/4/15 22:50	12.21
1200 m Sattion Flurometer	3/4/15 22:51	13.81
1200 m Sattion Flurometer	3/4/15 22:52	12.47
1200 m Sattion Flurometer	3/4/15 22:53	12.95
1200 m Sattion Flurometer	3/4/15 22:54	13.21
1200 m Sattion Flurometer	3/4/15 22:55	13.46
1200 m Sattion Flurometer	3/4/15 22:56	13.56
1200 m Sattion Flurometer	3/4/15 22:57	14.21
1200 m Sattion Flurometer	3/4/15 22:58	14.86
1200 m Sattion Flurometer	3/4/15 22:59	13.94
1200 m Sattion Flurometer	3/4/15 23:00	14.48
1200 m Sattion Flurometer	3/4/15 23:01	14.31
1200 m Sattion Flurometer	3/4/15 23:02	14.58
1200 m Sattion Flurometer	3/4/15 23:03	14.65
1200 m Sattion Flurometer	3/4/15 23:04	14.73
1200 m Sattion Flurometer	3/4/15 23:05	15.94
1200 m Sattion Flurometer	3/4/15 23:06	15.32
1200 m Sattion Flurometer	3/4/15 23:07	15.71
1200 m Sattion Flurometer	3/4/15 23:08	15.01
1200 m Sattion Flurometer	3/4/15 23:09	16.22
1200 m Sattion Flurometer	3/4/15 23:10	16.69
1200 m Sattion Flurometer	3/4/15 23:11	15.62

Location	Date and Time	Rhodmaine Concentration Adjusted Concentration (ppb)
1200 m Sattion Flurometer	3/4/15 23:12	16.06
1200 m Sattion Flurometer	3/4/15 23:13	15.97
1200 m Sattion Flurometer	3/4/15 23:14	17.05
1200 m Sattion Flurometer	3/4/15 23:15	15.87
1200 m Sattion Flurometer	3/4/15 23:16	16.01
1200 m Sattion Flurometer	3/4/15 23:17	16.07
1200 m Sattion Flurometer	3/4/15 23:18	16.3
1200 m Sattion Flurometer	3/4/15 23:19	15.96
1200 m Sattion Flurometer	3/4/15 23:20	17.27
1200 m Sattion Flurometer	3/4/15 23:21	15.88
1200 m Sattion Flurometer	3/4/15 23:22	16.28
1200 m Sattion Flurometer	3/4/15 23:23	16.09
1200 m Sattion Flurometer	3/4/15 23:24	16.27
1200 m Sattion Flurometer	3/4/15 23:25	16.12
1200 m Sattion Flurometer	3/4/15 23:26	16.14
1200 m Sattion Flurometer	3/4/15 23:27	16.33
1200 m Sattion Flurometer	3/4/15 23:28	16.24
1200 m Sattion Flurometer	3/4/15 23:29	16.36
1200 m Sattion Flurometer	3/4/15 23:30	16.18
1200 m Sattion Flurometer	3/4/15 23:31	16.38
1200 m Sattion Flurometer	3/4/15 23:32	16.31
1200 m Sattion Flurometer	3/4/15 23:33	17.09
1200 m Sattion Flurometer	3/4/15 23:34	16.28
1200 m Sattion Flurometer	3/4/15 23:35	16.06
1200 m Sattion Flurometer	3/4/15 23:36	16.06
1200 m Sattion Flurometer	3/4/15 23:37	16.11
1200 m Sattion Flurometer	3/4/15 23:38	15.82
1200 m Sattion Flurometer	3/4/15 23:39	16.09
1200 m Sattion Flurometer	3/4/15 23:40	15.83
1200 m Sattion Flurometer	3/4/15 23:41	16.69
1200 m Sattion Flurometer	3/4/15 23:42	16.1
1200 m Sattion Flurometer	3/4/15 23:43	15.66
1200 m Sattion Flurometer	3/4/15 23:44	15.07
1200 m Sattion Flurometer	3/4/15 23:45	16.75
1200 m Sattion Flurometer	3/4/15 23:46	15.29
1200 m Sattion Flurometer	3/4/15 23:47	15.34
1200 m Sattion Flurometer	3/4/15 23:48	15.27
1200 m Sattion Flurometer	3/4/15 23:49	14.97
1200 m Sattion Flurometer	3/4/15 23:50	14.77
1200 m Sattion Flurometer	3/4/15 23:51	14.73
1200 m Sattion Flurometer	3/4/15 23:52	16.68
1200 m Sattion Flurometer	3/4/15 23:53	14.74
1200 m Sattion Flurometer	3/4/15 23:54	15.13
1200 m Sattion Flurometer	3/4/15 23:55	14.61
1200 m Sattion Flurometer	3/4/15 23:56	14.36
1200 m Sattion Flurometer	3/4/15 23:57	14.57

Location	Date and Time	Rhodmaine Concentration Adjusted Concentration (ppb)
1200 m Sattion Flurometer	3/4/15 23:58	14.28
1200 m Sattion Flurometer	3/4/15 23:59	14.29
1200 m Sattion Flurometer	3/5/15 0:00	14.02
1200 m Sattion Flurometer	3/5/15 0:01	13.86
1200 m Sattion Flurometer	3/5/15 0:02	15.32
1200 m Sattion Flurometer	3/5/15 0:03	14.23
1200 m Sattion Flurometer	3/5/15 0:04	15.04
1200 m Sattion Flurometer	3/5/15 0:05	13.95
1200 m Sattion Flurometer	3/5/15 0:06	13.65
1200 m Sattion Flurometer	3/5/15 0:07	13.49
1200 m Sattion Flurometer	3/5/15 0:08	13.19
1200 m Sattion Flurometer	3/5/15 0:09	13.62
1200 m Sattion Flurometer	3/5/15 0:10	13.53
1200 m Sattion Flurometer	3/5/15 0:11	13.62
1200 m Sattion Flurometer	3/5/15 0:12	15.92
1200 m Sattion Flurometer	3/5/15 0:13	13.07
1200 m Sattion Flurometer	3/5/15 0:14	12.92
1200 m Sattion Flurometer	3/5/15 0:15	12.4
1200 m Sattion Flurometer	3/5/15 0:16	16.58
1200 m Sattion Flurometer	3/5/15 0:17	12.73
1200 m Sattion Flurometer	3/5/15 0:18	12.56
1200 m Sattion Flurometer	3/5/15 0:19	12.39
1200 m Sattion Flurometer	3/5/15 0:20	13.33
1200 m Sattion Flurometer	3/5/15 0:21	12.37
1200 m Sattion Flurometer	3/5/15 0:22	11.82
1200 m Sattion Flurometer	3/5/15 0:23	13.19
1200 m Sattion Flurometer	3/5/15 0:24	11.95
1200 m Sattion Flurometer	3/5/15 0:25	12.22
1200 m Sattion Flurometer	3/5/15 0:26	11.61
1200 m Sattion Flurometer	3/5/15 0:27	11.81
1200 m Sattion Flurometer	3/5/15 0:28	11.25
1200 m Sattion Flurometer	3/5/15 0:29	11.31
1200 m Sattion Flurometer	3/5/15 0:30	11.67
1200 m Sattion Flurometer	3/5/15 0:31	13.87
1200 m Sattion Flurometer	3/5/15 0:32	11.93
1200 m Sattion Flurometer	3/5/15 0:33	13.68
1200 m Sattion Flurometer	3/5/15 0:34	11.71
1200 m Sattion Flurometer	3/5/15 0:35	10.24
1200 m Sattion Flurometer	3/5/15 0:36	11.47
1200 m Sattion Flurometer	3/5/15 0:37	10.58
1200 m Sattion Flurometer	3/5/15 0:38	10.72
1200 m Sattion Flurometer	3/5/15 0:39	10.4
1200 m Sattion Flurometer	3/5/15 0:40	10.21
1200 m Sattion Flurometer	3/5/15 0:41	10.13
1200 m Sattion Flurometer	3/5/15 0:42	10.17
1200 m Sattion Flurometer	3/5/15 0:43	10.19

Location	Date and Time	Rhodmaine Concentration Adjusted Concentration (ppb)
1200 m Sattion Flurometer	3/5/15 0:44	10.98
1200 m Sattion Flurometer	3/5/15 0:45	9.007
1200 m Sattion Flurometer	3/5/15 0:46	10.31
1200 m Sattion Flurometer	3/5/15 0:47	9.078
1200 m Sattion Flurometer	3/5/15 0:48	8.882
1200 m Sattion Flurometer	3/5/15 0:49	9.011
1200 m Sattion Flurometer	3/5/15 0:50	8.608
1200 m Sattion Flurometer	3/5/15 0:51	8.66
1200 m Sattion Flurometer	3/5/15 0:52	9.731
1200 m Sattion Flurometer	3/5/15 0:53	8.605
1200 m Sattion Flurometer	3/5/15 0:54	9.654
1200 m Sattion Flurometer	3/5/15 0:55	8.339
1200 m Sattion Flurometer	3/5/15 0:56	8.468
1200 m Sattion Flurometer	3/5/15 0:57	7.991
1200 m Sattion Flurometer	3/5/15 0:58	8.276
1200 m Sattion Flurometer	3/5/15 0:59	8.361
1200 m Sattion Flurometer	3/5/15 1:00	8.232
1200 m Sattion Flurometer	3/5/15 1:01	8.132
1200 m Sattion Flurometer	3/5/15 1:02	7.607
1200 m Sattion Flurometer	3/5/15 1:03	8.697
1200 m Sattion Flurometer	3/5/15 1:04	7.729
1200 m Sattion Flurometer	3/5/15 1:05	7.999
1200 m Sattion Flurometer	3/5/15 1:06	7.504
1200 m Sattion Flurometer	3/5/15 1:07	8.254
1200 m Sattion Flurometer	3/5/15 1:08	8.416
1200 m Sattion Flurometer	3/5/15 1:09	7.315
1200 m Sattion Flurometer	3/5/15 1:10	7.171
1200 m Sattion Flurometer	3/5/15 1:11	7.116
1200 m Sattion Flurometer	3/5/15 1:12	7.149
1200 m Sattion Flurometer	3/5/15 1:13	6.961
1200 m Sattion Flurometer	3/5/15 1:14	6.828
1200 m Sattion Flurometer	3/5/15 1:15	7.991
1200 m Sattion Flurometer	3/5/15 1:16	6.82
1200 m Sattion Flurometer	3/5/15 1:17	6.95
1200 m Sattion Flurometer	3/5/15 1:18	7.903
1200 m Sattion Flurometer	3/5/15 1:19	7.393
1200 m Sattion Flurometer	3/5/15 1:20	6.721
1200 m Sattion Flurometer	3/5/15 1:21	6.528
1200 m Sattion Flurometer	3/5/15 1:22	6.495
1200 m Sattion Flurometer	3/5/15 1:23	6.307
1200 m Sattion Flurometer	3/5/15 1:24	6.388
1200 m Sattion Flurometer	3/5/15 1:25	6.447
1200 m Sattion Flurometer	3/5/15 1:26	7.204
1200 m Sattion Flurometer	3/5/15 1:27	7.005
1200 m Sattion Flurometer	3/5/15 1:28	5.908
1200 m Sattion Flurometer	3/5/15 1:29	6.384

Location	Date and Time	Rhodmaine Concentration Adjusted Concentration (ppb)
1200 m Sattion Flurometer	3/5/15 1:30	5.967
1200 m Sattion Flurometer	3/5/15 1:31	5.996
1200 m Sattion Flurometer	3/5/15 1:32	5.974
1200 m Sattion Flurometer	3/5/15 1:33	6.118
1200 m Sattion Flurometer	3/5/15 1:34	5.93
1200 m Sattion Flurometer	3/5/15 1:35	5.664
1200 m Sattion Flurometer	3/5/15 1:36	6.673
1200 m Sattion Flurometer	3/5/15 1:37	5.856
1200 m Sattion Flurometer	3/5/15 1:38	5.886
1200 m Sattion Flurometer	3/5/15 1:39	5.793
1200 m Sattion Flurometer	3/5/15 1:40	5.645
1200 m Sattion Flurometer	3/5/15 1:41	5.908
1200 m Sattion Flurometer	3/5/15 1:42	6.602
1200 m Sattion Flurometer	3/5/15 1:43	5.416
1200 m Sattion Flurometer	3/5/15 1:44	5.505
1200 m Sattion Flurometer	3/5/15 1:45	6.569
1200 m Sattion Flurometer	3/5/15 1:46	6.499
1200 m Sattion Flurometer	3/5/15 1:47	5.383
1200 m Sattion Flurometer	3/5/15 1:48	5.627
1200 m Sattion Flurometer	3/5/15 1:49	5.032
1200 m Sattion Flurometer	3/5/15 1:50	6.628
1200 m Sattion Flurometer	3/5/15 1:51	5.235
1200 m Sattion Flurometer	3/5/15 1:52	6.554
1200 m Sattion Flurometer	3/5/15 1:53	6.58
1200 m Sattion Flurometer	3/5/15 1:54	5.128
1200 m Sattion Flurometer	3/5/15 1:55	5.125
1200 m Sattion Flurometer	3/5/15 1:56	5.287
1200 m Sattion Flurometer	3/5/15 1:57	5.427
1200 m Sattion Flurometer	3/5/15 1:58	6.281
1200 m Sattion Flurometer	3/5/15 1:59	5.298
1200 m Sattion Flurometer	3/5/15 2:00	5.52
1200 m Sattion Flurometer	3/5/15 2:01	5.498
1200 m Sattion Flurometer	3/5/15 2:02	5.029
1200 m Sattion Flurometer	3/5/15 2:03	5.335
1200 m Sattion Flurometer	3/5/15 2:04	4.803
1200 m Sattion Flurometer	3/5/15 2:05	6.096
1200 m Sattion Flurometer	3/5/15 2:06	5.435
1200 m Sattion Flurometer	3/5/15 2:07	6.362
1200 m Sattion Flurometer	3/5/15 2:08	5.102
1200 m Sattion Flurometer	3/5/15 2:09	5.431
1200 m Sattion Flurometer	3/5/15 2:10	4.992
1200 m Sattion Flurometer	3/5/15 2:11	5.125
1200 m Sattion Flurometer	3/5/15 2:12	5.354
1200 m Sattion Flurometer	3/5/15 2:13	6.137
1200 m Sattion Flurometer	3/5/15 2:14	5.309
1200 m Sattion Flurometer	3/5/15 2:15	5.213

Location	Date and Time	Rhodmaine Concentration Adjusted Concentration (ppb)
1200 m Sattion Flurometer	3/5/15 2:16	5.254
1200 m Sattion Flurometer	3/5/15 2:17	5.25
1200 m Sattion Flurometer	3/5/15 2:18	4.918
1200 m Sattion Flurometer	3/5/15 2:19	5.464
1200 m Sattion Flurometer	3/5/15 2:20	5.143
1200 m Sattion Flurometer	3/5/15 2:21	5.099
1200 m Sattion Flurometer	3/5/15 2:22	4.884
1200 m Sattion Flurometer	3/5/15 2:23	5.457
1200 m Sattion Flurometer	3/5/15 2:24	5.043
1200 m Sattion Flurometer	3/5/15 2:25	6.237
1200 m Sattion Flurometer	3/5/15 2:26	5.165
1200 m Sattion Flurometer	3/5/15 2:27	5.11
1200 m Sattion Flurometer	3/5/15 2:28	5.317
1200 m Sattion Flurometer	3/5/15 2:29	4.814
1200 m Sattion Flurometer	3/5/15 2:30	5.136
1200 m Sattion Flurometer	3/5/15 2:31	5.217
1200 m Sattion Flurometer	3/5/15 2:32	5.642
1200 m Sattion Flurometer	3/5/15 2:33	4.774
1200 m Sattion Flurometer	3/5/15 2:34	4.929
1200 m Sattion Flurometer	3/5/15 2:35	5.572
1200 m Sattion Flurometer	3/5/15 2:36	4.951
1200 m Sattion Flurometer	3/5/15 2:37	5.446
1200 m Sattion Flurometer	3/5/15 2:38	5.158
1200 m Sattion Flurometer	3/5/15 2:39	5.15
1200 m Sattion Flurometer	3/5/15 2:40	5.535
1200 m Sattion Flurometer	3/5/15 2:41	4.984
1200 m Sattion Flurometer	3/5/15 2:42	5.302
1200 m Sattion Flurometer	3/5/15 2:43	5.287
1200 m Sattion Flurometer	3/5/15 2:44	4.977
1200 m Sattion Flurometer	3/5/15 2:45	6.244
1200 m Sattion Flurometer	3/5/15 2:46	6.081
1200 m Sattion Flurometer	3/5/15 2:47	5.531
1200 m Sattion Flurometer	3/5/15 2:48	5.243
1200 m Sattion Flurometer	3/5/15 2:49	5.427
1200 m Sattion Flurometer	3/5/15 2:50	5.176
1200 m Sattion Flurometer	3/5/15 2:51	5.239
1200 m Sattion Flurometer	3/5/15 2:52	6.31
1200 m Sattion Flurometer	3/5/15 2:53	5.258
1200 m Sattion Flurometer	3/5/15 2:54	6.288
1200 m Sattion Flurometer	3/5/15 2:55	5.128
1200 m Sattion Flurometer	3/5/15 2:56	4.881
1200 m Sattion Flurometer	3/5/15 2:57	5.195
1200 m Sattion Flurometer	3/5/15 2:58	5.239
1200 m Sattion Flurometer	3/5/15 2:59	5.195
1200 m Sattion Flurometer	3/5/15 3:00	5.184
1200 m Sattion Flurometer	3/5/15 3:01	5.165

Location	Date and Time	Rhodmaine Concentration Adjusted Concentration (ppb)
1200 m Sattion Flurometer	3/5/15 3:02	5.088
1200 m Sattion Flurometer	3/5/15 3:03	6.27
1200 m Sattion Flurometer	3/5/15 3:04	4.999
1200 m Sattion Flurometer	3/5/15 3:05	5.287
1200 m Sattion Flurometer	3/5/15 3:06	5.021
1200 m Sattion Flurometer	3/5/15 3:07	5.117
1200 m Sattion Flurometer	3/5/15 3:08	5.121
1200 m Sattion Flurometer	3/5/15 3:09	4.903
1200 m Sattion Flurometer	3/5/15 3:10	5.368
1200 m Sattion Flurometer	3/5/15 3:11	5.335
1200 m Sattion Flurometer	3/5/15 3:12	5.258
1200 m Sattion Flurometer	3/5/15 3:13	4.77
1200 m Sattion Flurometer	3/5/15 3:14	5.121
1200 m Sattion Flurometer	3/5/15 3:15	5.276
1200 m Sattion Flurometer	3/5/15 3:16	5.671
1200 m Sattion Flurometer	3/5/15 3:17	4.921
1200 m Sattion Flurometer	3/5/15 3:18	5.235
1200 m Sattion Flurometer	3/5/15 3:19	5.221
1200 m Sattion Flurometer	3/5/15 3:20	5.306
1200 m Sattion Flurometer	3/5/15 3:21	5.154
1200 m Sattion Flurometer	3/5/15 3:22	5.335
1200 m Sattion Flurometer	3/5/15 3:23	5.154
1200 m Sattion Flurometer	3/5/15 3:24	5.394
1200 m Sattion Flurometer	3/5/15 3:25	6.362
1200 m Sattion Flurometer	3/5/15 3:26	5.25
1200 m Sattion Flurometer	3/5/15 3:27	5.206
1200 m Sattion Flurometer	3/5/15 3:28	5.254
1200 m Sattion Flurometer	3/5/15 3:29	5.187
1200 m Sattion Flurometer	3/5/15 3:30	5.125
1200 m Sattion Flurometer	3/5/15 3:31	6.288
1200 m Sattion Flurometer	3/5/15 3:32	5.176
1200 m Sattion Flurometer	3/5/15 3:33	5.616
1200 m Sattion Flurometer	3/5/15 3:34	5.354
1200 m Sattion Flurometer	3/5/15 3:35	5.494
1200 m Sattion Flurometer	3/5/15 3:36	4.921
1200 m Sattion Flurometer	3/5/15 3:37	5.265
1200 m Sattion Flurometer	3/5/15 3:38	5.176
1200 m Sattion Flurometer	3/5/15 3:39	6.181
1200 m Sattion Flurometer	3/5/15 3:40	5.512
1200 m Sattion Flurometer	3/5/15 3:41	5.069
1200 m Sattion Flurometer	3/5/15 3:42	4.995
1200 m Sattion Flurometer	3/5/15 3:43	5.136
1200 m Sattion Flurometer	3/5/15 3:44	4.98
1200 m Sattion Flurometer	3/5/15 3:45	5.213
1200 m Sattion Flurometer	3/5/15 3:46	5.162
1200 m Sattion Flurometer	3/5/15 3:47	5.062

Location	Date and Time	Rhodmaine Concentration Adjusted Concentration (ppb)
1200 m Sattion Flurometer	3/5/15 3:48	6.129
1200 m Sattion Flurometer	3/5/15 3:49	5.091
1200 m Sattion Flurometer	3/5/15 3:50	5.017
1200 m Sattion Flurometer	3/5/15 3:51	5.239
1200 m Sattion Flurometer	3/5/15 3:52	4.914
1200 m Sattion Flurometer	3/5/15 3:53	4.951
1200 m Sattion Flurometer	3/5/15 3:54	4.792
1200 m Sattion Flurometer	3/5/15 3:55	5.52
1200 m Sattion Flurometer	3/5/15 3:56	4.955
1200 m Sattion Flurometer	3/5/15 3:57	5.043
1200 m Sattion Flurometer	3/5/15 3:58	4.94
1200 m Sattion Flurometer	3/5/15 3:59	5.989
1200 m Sattion Flurometer	3/5/15 4:00	5.017
1200 m Sattion Flurometer	3/5/15 4:01	5.213
1200 m Sattion Flurometer	3/5/15 4:02	5.014
1200 m Sattion Flurometer	3/5/15 4:03	5.948
1200 m Sattion Flurometer	3/5/15 4:04	4.881
1200 m Sattion Flurometer	3/5/15 4:05	4.932
1200 m Sattion Flurometer	3/5/15 4:06	5.014
1200 m Sattion Flurometer	3/5/15 4:07	4.98
1200 m Sattion Flurometer	3/5/15 4:08	4.977
1200 m Sattion Flurometer	3/5/15 4:09	5.106
1200 m Sattion Flurometer	3/5/15 4:10	4.955
1200 m Sattion Flurometer	3/5/15 4:11	4.785
1200 m Sattion Flurometer	3/5/15 4:12	5.069
1200 m Sattion Flurometer	3/5/15 4:13	4.94
1200 m Sattion Flurometer	3/5/15 4:14	5.915
1200 m Sattion Flurometer	3/5/15 4:15	6.011
1200 m Sattion Flurometer	3/5/15 4:16	4.833
1200 m Sattion Flurometer	3/5/15 4:17	4.777
1200 m Sattion Flurometer	3/5/15 4:18	4.892
1200 m Sattion Flurometer	3/5/15 4:19	4.836
1200 m Sattion Flurometer	3/5/15 4:20	4.733
1200 m Sattion Flurometer	3/5/15 4:21	4.711
1200 m Sattion Flurometer	3/5/15 4:22	4.792
1200 m Sattion Flurometer	3/5/15 4:23	4.718
1200 m Sattion Flurometer	3/5/15 4:24	4.596
1200 m Sattion Flurometer	3/5/15 4:25	4.585
1200 m Sattion Flurometer	3/5/15 4:26	4.589
1200 m Sattion Flurometer	3/5/15 4:27	4.559
1200 m Sattion Flurometer	3/5/15 4:28	4.988
1200 m Sattion Flurometer	3/5/15 4:29	4.884
1200 m Sattion Flurometer	3/5/15 4:30	4.729
1200 m Sattion Flurometer	3/5/15 4:31	4.282
1200 m Sattion Flurometer	3/5/15 4:32	4.493
1200 m Sattion Flurometer	3/5/15 4:33	4.511

Location	Date and Time	Rhodmaine Concentration Adjusted Concentration (ppb)
1200 m Sattion Flurometer	3/5/15 4:34	5.797
1200 m Sattion Flurometer	3/5/15 4:35	4.526
1200 m Sattion Flurometer	3/5/15 4:36	5.671
1200 m Sattion Flurometer	3/5/15 4:37	4.201
1200 m Sattion Flurometer	3/5/15 4:38	4.615
1200 m Sattion Flurometer	3/5/15 4:39	4.493
1200 m Sattion Flurometer	3/5/15 4:40	4.478
1200 m Sattion Flurometer	3/5/15 4:41	4.515
1200 m Sattion Flurometer	3/5/15 4:42	5.391
1200 m Sattion Flurometer	3/5/15 4:43	4.596
1200 m Sattion Flurometer	3/5/15 4:44	5.427
1200 m Sattion Flurometer	3/5/15 4:45	4.467
1200 m Sattion Flurometer	3/5/15 4:46	4.714
1200 m Sattion Flurometer	3/5/15 4:47	4.448
1200 m Sattion Flurometer	3/5/15 4:48	4.607
1200 m Sattion Flurometer	3/5/15 4:49	4.371
1200 m Sattion Flurometer	3/5/15 4:50	4.319
1200 m Sattion Flurometer	3/5/15 4:51	4.63
1200 m Sattion Flurometer	3/5/15 4:52	4.315
1200 m Sattion Flurometer	3/5/15 4:53	4.386
1200 m Sattion Flurometer	3/5/15 4:54	4.482
1200 m Sattion Flurometer	3/5/15 4:55	4.415
1200 m Sattion Flurometer	3/5/15 4:56	4.423
1200 m Sattion Flurometer	3/5/15 4:57	4.389
1200 m Sattion Flurometer	3/5/15 4:58	4.36
1200 m Sattion Flurometer	3/5/15 4:59	4.637
1200 m Sattion Flurometer	3/5/15 5:00	4.452
1200 m Sattion Flurometer	3/5/15 5:01	4.426
1200 m Sattion Flurometer	3/5/15 5:02	5.18
1200 m Sattion Flurometer	3/5/15 5:03	4.253
1200 m Sattion Flurometer	3/5/15 5:04	5.56
1200 m Sattion Flurometer	3/5/15 5:05	4.179
1200 m Sattion Flurometer	3/5/15 5:06	5.147
1200 m Sattion Flurometer	3/5/15 5:07	4.112
1200 m Sattion Flurometer	3/5/15 5:08	4.471
1200 m Sattion Flurometer	3/5/15 5:09	4.264
1200 m Sattion Flurometer	3/5/15 5:10	3.691
1200 m Sattion Flurometer	3/5/15 5:11	3.88
1200 m Sattion Flurometer	3/5/15 5:12	4.079
1200 m Sattion Flurometer	3/5/15 5:13	4.168
1200 m Sattion Flurometer	3/5/15 5:14	4.168
1200 m Sattion Flurometer	3/5/15 5:15	5.191
1200 m Sattion Flurometer	3/5/15 5:16	4.12
1200 m Sattion Flurometer	3/5/15 5:17	3.88
1200 m Sattion Flurometer	3/5/15 5:18	4.267
1200 m Sattion Flurometer	3/5/15 5:19	3.983

Location	Date and Time	Rhodmaine Concentration Adjusted Concentration (ppb)
1200 m Sattion Flurometer	3/5/15 5:20	3.998
1200 m Sattion Flurometer	3/5/15 5:21	4.027
1200 m Sattion Flurometer	3/5/15 5:22	4.146
1200 m Sattion Flurometer	3/5/15 5:23	3.983
1200 m Sattion Flurometer	3/5/15 5:24	4.072
1200 m Sattion Flurometer	3/5/15 5:25	3.983
1200 m Sattion Flurometer	3/5/15 5:26	3.961
1200 m Sattion Flurometer	3/5/15 5:27	3.754
1200 m Sattion Flurometer	3/5/15 5:28	5.051
1200 m Sattion Flurometer	3/5/15 5:29	4.87
1200 m Sattion Flurometer	3/5/15 5:30	3.902
1200 m Sattion Flurometer	3/5/15 5:31	3.946
1200 m Sattion Flurometer	3/5/15 5:32	4.349
1200 m Sattion Flurometer	3/5/15 5:33	3.887
1200 m Sattion Flurometer	3/5/15 5:34	3.935
1200 m Sattion Flurometer	3/5/15 5:35	3.536
1200 m Sattion Flurometer	3/5/15 5:36	3.761
1200 m Sattion Flurometer	3/5/15 5:37	3.591
1200 m Sattion Flurometer	3/5/15 5:38	4.652
1200 m Sattion Flurometer	3/5/15 5:39	3.772
1200 m Sattion Flurometer	3/5/15 5:40	4.707
1200 m Sattion Flurometer	3/5/15 5:41	3.75
1200 m Sattion Flurometer	3/5/15 5:42	4.622
1200 m Sattion Flurometer	3/5/15 5:43	3.676
1200 m Sattion Flurometer	3/5/15 5:44	3.965
1200 m Sattion Flurometer	3/5/15 5:45	4.086
1200 m Sattion Flurometer	3/5/15 5:46	4.596
1200 m Sattion Flurometer	3/5/15 5:47	3.931
1200 m Sattion Flurometer	3/5/15 5:48	3.917
1200 m Sattion Flurometer	3/5/15 5:49	3.458
1200 m Sattion Flurometer	3/5/15 5:50	3.61
1200 m Sattion Flurometer	3/5/15 5:51	3.602
1200 m Sattion Flurometer	3/5/15 5:52	3.894
1200 m Sattion Flurometer	3/5/15 5:53	3.499
1200 m Sattion Flurometer	3/5/15 5:54	3.658
1200 m Sattion Flurometer	3/5/15 5:55	4.474
1200 m Sattion Flurometer	3/5/15 5:56	3.54
1200 m Sattion Flurometer	3/5/15 5:57	3.133
1200 m Sattion Flurometer	3/5/15 5:58	3.599
1200 m Sattion Flurometer	3/5/15 5:59	3.58
1200 m Sattion Flurometer	3/5/15 6:00	3.529
1200 m Sattion Flurometer	3/5/15 6:01	3.17
1200 m Sattion Flurometer	3/5/15 6:02	3.532
1200 m Sattion Flurometer	3/5/15 6:03	3.503
1200 m Sattion Flurometer	3/5/15 6:04	3.606
1200 m Sattion Flurometer	3/5/15 6:05	2.993

Location	Date and Time	Rhodmaine Concentration Adjusted Concentration (ppb)
1200 m Sattion Flurometer	3/5/15 6:06	3.226
1200 m Sattion Flurometer	3/5/15 6:07	3.732
1200 m Sattion Flurometer	3/5/15 6:08	4.763
1200 m Sattion Flurometer	3/5/15 6:09	3.2
1200 m Sattion Flurometer	3/5/15 6:10	3.418
1200 m Sattion Flurometer	3/5/15 6:11	3.333
1200 m Sattion Flurometer	3/5/15 6:12	3.181
1200 m Sattion Flurometer	3/5/15 6:13	3.44
1200 m Sattion Flurometer	3/5/15 6:14	4.157
1200 m Sattion Flurometer	3/5/15 6:15	3.255
1200 m Sattion Flurometer	3/5/15 6:16	3.318
1200 m Sattion Flurometer	3/5/15 6:17	3.602
1200 m Sattion Flurometer	3/5/15 6:18	3.089
1200 m Sattion Flurometer	3/5/15 6:19	3.185
1200 m Sattion Flurometer	3/5/15 6:20	3.115
1200 m Sattion Flurometer	3/5/15 6:21	3.425
1200 m Sattion Flurometer	3/5/15 6:22	3.518
1200 m Sattion Flurometer	3/5/15 6:23	3.056
1200 m Sattion Flurometer	3/5/15 6:24	3.233
1200 m Sattion Flurometer	3/5/15 6:25	3.115
1200 m Sattion Flurometer	3/5/15 6:26	2.963
1200 m Sattion Flurometer	3/5/15 6:27	4.057
1200 m Sattion Flurometer	3/5/15 6:28	3.192
1200 m Sattion Flurometer	3/5/15 6:29	2.827
1200 m Sattion Flurometer	3/5/15 6:30	4.16
1200 m Sattion Flurometer	3/5/15 6:31	2.771
1200 m Sattion Flurometer	3/5/15 6:32	3.022
1200 m Sattion Flurometer	3/5/15 6:33	3.126
1200 m Sattion Flurometer	3/5/15 6:34	2.882
1200 m Sattion Flurometer	3/5/15 6:35	3.252
1200 m Sattion Flurometer	3/5/15 6:36	4.075
1200 m Sattion Flurometer	3/5/15 6:37	3.296
1200 m Sattion Flurometer	3/5/15 6:38	3.019
1200 m Sattion Flurometer	3/5/15 6:39	4.19
1200 m Sattion Flurometer	3/5/15 6:40	2.93
1200 m Sattion Flurometer	3/5/15 6:41	3.174
1200 m Sattion Flurometer	3/5/15 6:42	3.566
1200 m Sattion Flurometer	3/5/15 6:43	3.03
1200 m Sattion Flurometer	3/5/15 6:44	2.753
1200 m Sattion Flurometer	3/5/15 6:45	2.889
1200 m Sattion Flurometer	3/5/15 6:46	2.967
1200 m Sattion Flurometer	3/5/15 6:47	3.133
1200 m Sattion Flurometer	3/5/15 6:48	3.026
1200 m Sattion Flurometer	3/5/15 6:49	2.723
1200 m Sattion Flurometer	3/5/15 6:50	2.635
1200 m Sattion Flurometer	3/5/15 6:51	2.779

Location	Date and Time	Rhodmaine Concentration Adjusted Concentration (ppb)
1200 m Sattion Flurometer	3/5/15 6:52	2.635
1200 m Sattion Flurometer	3/5/15 6:53	2.749
1200 m Sattion Flurometer	3/5/15 6:54	2.997
1200 m Sattion Flurometer	3/5/15 6:55	2.997
1200 m Sattion Flurometer	3/5/15 6:56	2.683
1200 m Sattion Flurometer	3/5/15 6:57	2.705
1200 m Sattion Flurometer	3/5/15 6:58	2.823
1200 m Sattion Flurometer	3/5/15 6:59	2.812
1200 m Sattion Flurometer	3/5/15 7:00	2.893
1200 m Sattion Flurometer	3/5/15 7:01	3.787
1200 m Sattion Flurometer	3/5/15 7:02	2.557
1200 m Sattion Flurometer	3/5/15 7:03	2.853
1200 m Sattion Flurometer	3/5/15 7:04	2.546
1200 m Sattion Flurometer	3/5/15 7:05	2.723
1200 m Sattion Flurometer	3/5/15 7:06	2.723
1200 m Sattion Flurometer	3/5/15 7:07	2.768
1200 m Sattion Flurometer	3/5/15 7:08	2.793
1200 m Sattion Flurometer	3/5/15 7:09	2.967
1200 m Sattion Flurometer	3/5/15 7:10	2.816
1200 m Sattion Flurometer	3/5/15 7:11	2.531
1200 m Sattion Flurometer	3/5/15 7:12	2.775
1200 m Sattion Flurometer	3/5/15 7:13	3.795
1200 m Sattion Flurometer	3/5/15 7:14	2.668
1200 m Sattion Flurometer	3/5/15 7:15	2.716
1200 m Sattion Flurometer	3/5/15 7:16	2.745
1200 m Sattion Flurometer	3/5/15 7:17	2.224
1200 m Sattion Flurometer	3/5/15 7:18	2.756
1200 m Sattion Flurometer	3/5/15 7:19	2.45
1200 m Sattion Flurometer	3/5/15 7:20	2.86
1200 m Sattion Flurometer	3/5/15 7:21	2.72
1200 m Sattion Flurometer	3/5/15 7:22	2.668
1200 m Sattion Flurometer	3/5/15 7:23	2.413
1200 m Sattion Flurometer	3/5/15 7:24	2.45
1200 m Sattion Flurometer	3/5/15 7:25	2.465
1200 m Sattion Flurometer	3/5/15 7:26	2.398
1200 m Sattion Flurometer	3/5/15 7:27	3.359
1200 m Sattion Flurometer	3/5/15 7:28	2.79
1200 m Sattion Flurometer	3/5/15 7:29	3.44
1200 m Sattion Flurometer	3/5/15 7:30	2.306
1200 m Sattion Flurometer	3/5/15 7:31	2.779
1200 m Sattion Flurometer	3/5/15 7:32	2.413
1200 m Sattion Flurometer	3/5/15 7:33	2.738
1200 m Sattion Flurometer	3/5/15 7:34	4.005
1200 m Sattion Flurometer	3/5/15 7:35	3.843
1200 m Sattion Flurometer	3/5/15 7:36	2.731
1200 m Sattion Flurometer	3/5/15 7:37	3.894

Location	Date and Time	Rhodmaine Concentration Adjusted Concentration (ppb)
1200 m Sattion Flurometer	3/5/15 7:38	2.646
1200 m Sattion Flurometer	3/5/15 7:39	2.298
1200 m Sattion Flurometer	3/5/15 7:40	2.454
1200 m Sattion Flurometer	3/5/15 7:41	2.59
1200 m Sattion Flurometer	3/5/15 7:42	2.723
1200 m Sattion Flurometer	3/5/15 7:43	2.609
1200 m Sattion Flurometer	3/5/15 7:44	2.494
1200 m Sattion Flurometer	3/5/15 7:45	3.639
1200 m Sattion Flurometer	3/5/15 7:46	2.413
1200 m Sattion Flurometer	3/5/15 7:47	2.723
1200 m Sattion Flurometer	3/5/15 7:48	1.947
1200 m Sattion Flurometer	3/5/15 7:49	2.461
1200 m Sattion Flurometer	3/5/15 7:50	3.665
1200 m Sattion Flurometer	3/5/15 7:51	2.816
1200 m Sattion Flurometer	3/5/15 7:52	2.579
1200 m Sattion Flurometer	3/5/15 7:53	2.317
1200 m Sattion Flurometer	3/5/15 7:54	2.114
1200 m Sattion Flurometer	3/5/15 7:55	2.531
1200 m Sattion Flurometer	3/5/15 7:56	2.535
1200 m Sattion Flurometer	3/5/15 7:57	2.498
1200 m Sattion Flurometer	3/5/15 7:58	2.465
1200 m Sattion Flurometer	3/5/15 7:59	3.928
1200 m Sattion Flurometer	3/5/15 8:00	3.093
1200 m Sattion Flurometer	3/5/15 8:01	2.516
1200 m Sattion Flurometer	3/5/15 8:02	2.114
1200 m Sattion Flurometer	3/5/15 8:03	2.424
1200 m Sattion Flurometer	3/5/15 8:04	2.114
1200 m Sattion Flurometer	3/5/15 8:05	2.11
1200 m Sattion Flurometer	3/5/15 8:06	1.888
1200 m Sattion Flurometer	3/5/15 8:07	2.158
1200 m Sattion Flurometer	3/5/15 8:08	2.003
1200 m Sattion Flurometer	3/5/15 8:09	2.062
1200 m Sattion Flurometer	3/5/15 8:10	2.169
1200 m Sattion Flurometer	3/5/15 8:11	3.019
1200 m Sattion Flurometer	3/5/15 8:12	2.176
1200 m Sattion Flurometer	3/5/15 8:13	1.822
1200 m Sattion Flurometer	3/5/15 8:14	2.439
1200 m Sattion Flurometer	3/5/15 8:15	2.066
1200 m Sattion Flurometer	3/5/15 8:16	2.066
1200 m Sattion Flurometer	3/5/15 8:17	2.069
1200 m Sattion Flurometer	3/5/15 8:18	2.062
1200 m Sattion Flurometer	3/5/15 8:19	1.999
1200 m Sattion Flurometer	3/5/15 8:20	1.733
1200 m Sattion Flurometer	3/5/15 8:21	2.284
1200 m Sattion Flurometer	3/5/15 8:22	2.088
1200 m Sattion Flurometer	3/5/15 8:23	1.8

Location	Date and Time	Rhodmaine Concentration Adjusted Concentration (ppb)
1200 m Sattion Flurometer	3/5/15 8:24	1.984
1200 m Sattion Flurometer	3/5/15 8:25	2.945
1200 m Sattion Flurometer	3/5/15 8:26	1.825
1200 m Sattion Flurometer	3/5/15 8:27	2.014
1200 m Sattion Flurometer	3/5/15 8:28	1.91
1200 m Sattion Flurometer	3/5/15 8:29	3.026
1200 m Sattion Flurometer	3/5/15 8:30	2.088
1200 m Sattion Flurometer	3/5/15 8:31	1.855
1200 m Sattion Flurometer	3/5/15 8:32	2.457
1200 m Sattion Flurometer	3/5/15 8:33	1.981
1200 m Sattion Flurometer	3/5/15 8:34	1.936
1200 m Sattion Flurometer	3/5/15 8:35	1.94
1200 m Sattion Flurometer	3/5/15 8:36	2.04
1200 m Sattion Flurometer	3/5/15 8:37	1.648
1200 m Sattion Flurometer	3/5/15 8:38	2.121
1200 m Sattion Flurometer	3/5/15 8:39	1.984
1200 m Sattion Flurometer	3/5/15 8:40	1.323
1200 m Sattion Flurometer	3/5/15 8:41	2.568
1200 m Sattion Flurometer	3/5/15 8:42	1.567
1200 m Sattion Flurometer	3/5/15 8:43	1.829
1200 m Sattion Flurometer	3/5/15 8:44	2.671
1200 m Sattion Flurometer	3/5/15 8:45	1.519
1200 m Sattion Flurometer	3/5/15 8:46	1.637
1200 m Sattion Flurometer	3/5/15 8:47	2.679
1200 m Sattion Flurometer	3/5/15 8:48	1.888
1200 m Sattion Flurometer	3/5/15 8:49	1.678
1200 m Sattion Flurometer	3/5/15 8:50	1.962
1200 m Sattion Flurometer	3/5/15 8:51	1.744
1200 m Sattion Flurometer	3/5/15 8:52	1.77
1200 m Sattion Flurometer	3/5/15 8:53	1.885
1200 m Sattion Flurometer	3/5/15 8:54	1.885
1200 m Sattion Flurometer	3/5/15 8:55	1.829
1200 m Sattion Flurometer	3/5/15 8:56	1.777
1200 m Sattion Flurometer	3/5/15 8:57	1.678
1200 m Sattion Flurometer	3/5/15 8:58	3.004
1200 m Sattion Flurometer	3/5/15 8:59	1.209
1200 m Sattion Flurometer	3/5/15 9:00	1.585
1200 m Sattion Flurometer	3/5/15 9:01	2.564
1200 m Sattion Flurometer	3/5/15 9:02	1.859
1200 m Sattion Flurometer	3/5/15 9:03	1.486
1200 m Sattion Flurometer	3/5/15 9:04	1.781
1200 m Sattion Flurometer	3/5/15 9:05	1.763
1200 m Sattion Flurometer	3/5/15 9:06	1.733
1200 m Sattion Flurometer	3/5/15 9:07	1.692
1200 m Sattion Flurometer	3/5/15 9:08	1.364
1200 m Sattion Flurometer	3/5/15 9:09	1.523

Location	Date and Time	Rhodmaine Concentration Adjusted Concentration (ppb)
1200 m Sattion Flurometer	3/5/15 9:10	1.755
1200 m Sattion Flurometer	3/5/15 9:11	1.504
1200 m Sattion Flurometer	3/5/15 9:12	2.594
1200 m Sattion Flurometer	3/5/15 9:13	1.766
1200 m Sattion Flurometer	3/5/15 9:14	1.622
1200 m Sattion Flurometer	3/5/15 9:15	1.323
1200 m Sattion Flurometer	3/5/15 9:16	1.09
1200 m Sattion Flurometer	3/5/15 9:17	1.796
1200 m Sattion Flurometer	3/5/15 9:18	1.467
1200 m Sattion Flurometer	3/5/15 9:19	2.066
1200 m Sattion Flurometer	3/5/15 9:20	1.704
1200 m Sattion Flurometer	3/5/15 9:21	1.19
1200 m Sattion Flurometer	3/5/15 9:22	2.731
1200 m Sattion Flurometer	3/5/15 9:23	1.345
1200 m Sattion Flurometer	3/5/15 9:24	1.611
1200 m Sattion Flurometer	3/5/15 9:25	1.364
1200 m Sattion Flurometer	3/5/15 9:26	2.498
1200 m Sattion Flurometer	3/5/15 9:27	1.818
1200 m Sattion Flurometer	3/5/15 9:28	2.21
1200 m Sattion Flurometer	3/5/15 9:29	1.641
1200 m Sattion Flurometer	3/5/15 9:30	1.548
1200 m Sattion Flurometer	3/5/15 9:31	1.227
1200 m Sattion Flurometer	3/5/15 9:32	1.692
1200 m Sattion Flurometer	3/5/15 9:33	1.523
1200 m Sattion Flurometer	3/5/15 9:34	1.305
1200 m Sattion Flurometer	3/5/15 9:35	1.364
1200 m Sattion Flurometer	3/5/15 9:36	1.563
1200 m Sattion Flurometer	3/5/15 9:37	1.452
1200 m Sattion Flurometer	3/5/15 9:38	1.205
1200 m Sattion Flurometer	3/5/15 9:39	1.681
1200 m Sattion Flurometer	3/5/15 9:40	1.644
1200 m Sattion Flurometer	3/5/15 9:41	1.526
1200 m Sattion Flurometer	3/5/15 9:42	1.415
1200 m Sattion Flurometer	3/5/15 9:43	1.386
1200 m Sattion Flurometer	3/5/15 9:44	1.467
1200 m Sattion Flurometer	3/5/15 9:45	1.5
1200 m Sattion Flurometer	3/5/15 9:46	1.257
1200 m Sattion Flurometer	3/5/15 9:47	1.353
1200 m Sattion Flurometer	3/5/15 9:48	1.334
1200 m Sattion Flurometer	3/5/15 9:49	1.039
1200 m Sattion Flurometer	3/5/15 9:50	1.877
1200 m Sattion Flurometer	3/5/15 9:51	1.415
1200 m Sattion Flurometer	3/5/15 9:52	0.946
1200 m Sattion Flurometer	3/5/15 9:53	1.404
1200 m Sattion Flurometer	3/5/15 9:54	1.489
1200 m Sattion Flurometer	3/5/15 9:55	1.231

Location	Date and Time	Rhodmaine Concentration Adjusted Concentration (ppb)
1200 m Sattion Flurometer	3/5/15 9:56	1.131
1200 m Sattion Flurometer	3/5/15 9:57	1.696
1200 m Sattion Flurometer	3/5/15 9:58	1.475
1200 m Sattion Flurometer	3/5/15 9:59	0.909
1200 m Sattion Flurometer	3/5/15 10:00	1.172
1200 m Sattion Flurometer	3/5/15 10:01	1.234
1200 m Sattion Flurometer	3/5/15 10:02	1.482
1200 m Sattion Flurometer	3/5/15 10:03	1.072
1200 m Sattion Flurometer	3/5/15 10:04	1.297
1200 m Sattion Flurometer	3/5/15 10:05	2.04
1200 m Sattion Flurometer	3/5/15 10:06	1.253
1200 m Sattion Flurometer	3/5/15 10:07	1.571
1200 m Sattion Flurometer	3/5/15 10:08	1.282
1200 m Sattion Flurometer	3/5/15 10:09	0.972
1200 m Sattion Flurometer	3/5/15 10:10	1.105
1200 m Sattion Flurometer	3/5/15 10:11	2.202
1200 m Sattion Flurometer	3/5/15 10:12	0.843
1200 m Sattion Flurometer	3/5/15 10:13	2.487
1200 m Sattion Flurometer	3/5/15 10:14	0.577
1200 m Sattion Flurometer	3/5/15 10:15	1.556
1200 m Sattion Flurometer	3/5/15 10:16	2.28
1200 m Sattion Flurometer	3/5/15 10:17	1.186
1200 m Sattion Flurometer	3/5/15 10:18	0.791
1200 m Sattion Flurometer	3/5/15 10:19	1.903
1200 m Sattion Flurometer	3/5/15 10:20	1.408
1200 m Sattion Flurometer	3/5/15 10:21	1.393
1200 m Sattion Flurometer	3/5/15 10:22	0.968
1200 m Sattion Flurometer	3/5/15 10:23	1.386
1200 m Sattion Flurometer	3/5/15 10:24	1.29
1200 m Sattion Flurometer	3/5/15 10:25	1.367
1200 m Sattion Flurometer	3/5/15 10:26	1.375
1200 m Sattion Flurometer	3/5/15 10:27	1.161
1200 m Sattion Flurometer	3/5/15 10:28	0.972
1200 m Sattion Flurometer	3/5/15 10:29	0.887
1200 m Sattion Flurometer	3/5/15 10:30	1.249
1200 m Sattion Flurometer	3/5/15 10:31	0.979
1200 m Sattion Flurometer	3/5/15 10:32	1.076
1200 m Sattion Flurometer	3/5/15 10:33	1.112
1200 m Sattion Flurometer	3/5/15 10:34	1.009
1200 m Sattion Flurometer	3/5/15 10:35	0.987
1200 m Sattion Flurometer	3/5/15 10:36	1.744
1200 m Sattion Flurometer	3/5/15 10:37	1.36
1200 m Sattion Flurometer	3/5/15 10:38	2.232
1200 m Sattion Flurometer	3/5/15 10:39	2.176
1200 m Sattion Flurometer	3/5/15 10:40	0.769
1200 m Sattion Flurometer	3/5/15 10:41	1.316

Location	Date and Time	Rhodmaine Concentration Adjusted Concentration (ppb)
1200 m Sattion Flurometer	3/5/15 10:42	1.057
1200 m Sattion Flurometer	3/5/15 10:43	1.024
1200 m Sattion Flurometer	3/5/15 10:44	0.839
1200 m Sattion Flurometer	3/5/15 10:45	0.577
1200 m Sattion Flurometer	3/5/15 10:46	0.769
1200 m Sattion Flurometer	3/5/15 10:47	0.846
1200 m Sattion Flurometer	3/5/15 10:48	0.902
1200 m Sattion Flurometer	3/5/15 10:49	1.33
1200 m Sattion Flurometer	3/5/15 10:50	0.75
1200 m Sattion Flurometer	3/5/15 10:51	1.024
1200 m Sattion Flurometer	3/5/15 10:52	1.083
1200 m Sattion Flurometer	3/5/15 10:53	1.316
1200 m Sattion Flurometer	3/5/15 10:54	1.209
1200 m Sattion Flurometer	3/5/15 10:55	2.025
1200 m Sattion Flurometer	3/5/15 10:56	1.434
1200 m Sattion Flurometer	3/5/15 10:57	0.994
1200 m Sattion Flurometer	3/5/15 10:58	1.238
1200 m Sattion Flurometer	3/5/15 10:59	1.035
1200 m Sattion Flurometer	3/5/15 11:00	1.046
1200 m Sattion Flurometer	3/5/15 11:01	1.079
1200 m Sattion Flurometer	3/5/15 11:02	1.083
1200 m Sattion Flurometer	3/5/15 11:03	0.651
1200 m Sattion Flurometer	3/5/15 11:04	1.175
1200 m Sattion Flurometer	3/5/15 11:05	1.042
1200 m Sattion Flurometer	3/5/15 11:06	1.02
1200 m Sattion Flurometer	3/5/15 11:07	0.617
1200 m Sattion Flurometer	3/5/15 11:08	0.961
1200 m Sattion Flurometer	3/5/15 11:09	0.643
1200 m Sattion Flurometer	3/5/15 11:10	0.865
1200 m Sattion Flurometer	3/5/15 11:11	0.802
1200 m Sattion Flurometer	3/5/15 11:12	2.058
1200 m Sattion Flurometer	3/5/15 11:13	0.754
1200 m Sattion Flurometer	3/5/15 11:14	1.231
1200 m Sattion Flurometer	3/5/15 11:15	0.351
1200 m Sattion Flurometer	3/5/15 11:16	0.946
1200 m Sattion Flurometer	3/5/15 11:17	0.887
1200 m Sattion Flurometer	3/5/15 11:18	2.243
1200 m Sattion Flurometer	3/5/15 11:19	0.854
1200 m Sattion Flurometer	3/5/15 11:20	0.769
1200 m Sattion Flurometer	3/5/15 11:21	1.914
1200 m Sattion Flurometer	3/5/15 11:22	0.928
1200 m Sattion Flurometer	3/5/15 11:23	1.009
1200 m Sattion Flurometer	3/5/15 11:24	2.047
1200 m Sattion Flurometer	3/5/15 11:25	0.991
1200 m Sattion Flurometer	3/5/15 11:26	1.715
1200 m Sattion Flurometer	3/5/15 11:27	1.874

Location	Date and Time	Rhodmaine Concentration Adjusted Concentration (ppb)
1200 m Sattion Flurometer	3/5/15 11:28	1.951
1200 m Sattion Flurometer	3/5/15 11:29	1.781
1200 m Sattion Flurometer	3/5/15 11:30	1.881
1200 m Sattion Flurometer	3/5/15 11:31	1.789
1200 m Sattion Flurometer	3/5/15 11:32	1.722
1200 m Sattion Flurometer	3/5/15 11:33	0.828
1200 m Sattion Flurometer	3/5/15 11:34	0.909
1200 m Sattion Flurometer	3/5/15 11:35	0.529
1200 m Sattion Flurometer	3/5/15 11:36	1.918
1200 m Sattion Flurometer	3/5/15 11:37	0.994
1200 m Sattion Flurometer	3/5/15 11:38	0.858
1200 m Sattion Flurometer	3/5/15 11:39	1.094
1200 m Sattion Flurometer	3/5/15 11:40	1.984
1200 m Sattion Flurometer	3/5/15 11:41	0.562
1200 m Sattion Flurometer	3/5/15 11:42	0.88
1200 m Sattion Flurometer	3/5/15 11:43	0.544
1200 m Sattion Flurometer	3/5/15 11:44	1.164
1200 m Sattion Flurometer	3/5/15 11:45	0.943
1200 m Sattion Flurometer	3/5/15 11:46	0.858
1200 m Sattion Flurometer	3/5/15 11:47	0.924
1200 m Sattion Flurometer	3/5/15 11:48	0.762
1200 m Sattion Flurometer	3/5/15 11:49	0.673
1200 m Sattion Flurometer	3/5/15 11:50	0.429
1200 m Sattion Flurometer	3/5/15 11:51	0.765
1200 m Sattion Flurometer	3/5/15 11:52	0.972
1200 m Sattion Flurometer	3/5/15 11:53	0.584
1200 m Sattion Flurometer	3/5/15 11:54	0.695
1200 m Sattion Flurometer	3/5/15 11:55	0.78
1200 m Sattion Flurometer	3/5/15 11:56	0.946
1200 m Sattion Flurometer	3/5/15 11:57	0.525
1200 m Sattion Flurometer	3/5/15 11:58	1.792
1200 m Sattion Flurometer	3/5/15 11:59	0.473
1200 m Sattion Flurometer	3/5/15 12:00	1.752
1200 m Sattion Flurometer	3/5/15 12:01	1.153
1200 m Sattion Flurometer	3/5/15 12:02	0.854
1200 m Sattion Flurometer	3/5/15 12:03	1.161
1200 m Sattion Flurometer	3/5/15 12:04	0.954
1200 m Sattion Flurometer	3/5/15 12:05	0.895
1200 m Sattion Flurometer	3/5/15 12:06	0.813
1200 m Sattion Flurometer	3/5/15 12:07	1.042
1200 m Sattion Flurometer	3/5/15 12:08	1.862
1200 m Sattion Flurometer	3/5/15 12:09	1.637
1200 m Sattion Flurometer	3/5/15 12:10	0.518
1200 m Sattion Flurometer	3/5/15 12:11	1.153
1200 m Sattion Flurometer	3/5/15 12:12	1.5
1200 m Sattion Flurometer	3/5/15 12:13	0.821

Location	Date and Time	Rhodmaine Concentration Adjusted Concentration (ppb)
1200 m Sattion Flurometer	3/5/15 12:14	0.311
1200 m Sattion Flurometer	3/5/15 12:15	0.167
1200 m Sattion Flurometer	3/5/15 12:16	0.606
1200 m Sattion Flurometer	3/5/15 12:17	1.741
1200 m Sattion Flurometer	3/5/15 12:18	0.455
1200 m Sattion Flurometer	3/5/15 12:19	0.61
1200 m Sattion Flurometer	3/5/15 12:20	1.789
1200 m Sattion Flurometer	3/5/15 12:21	0.791
1200 m Sattion Flurometer	3/5/15 12:22	1.615
1200 m Sattion Flurometer	3/5/15 12:23	1.46
1200 m Sattion Flurometer	3/5/15 12:24	1.364
1200 m Sattion Flurometer	3/5/15 12:25	0.647
1200 m Sattion Flurometer	3/5/15 12:26	0.883
1200 m Sattion Flurometer	3/5/15 12:27	0.532
1200 m Sattion Flurometer	3/5/15 12:28	1.016
1200 m Sattion Flurometer	3/5/15 12:29	0.795
1200 m Sattion Flurometer	3/5/15 12:30	1.811
1200 m Sattion Flurometer	3/5/15 12:31	0.566
1200 m Sattion Flurometer	3/5/15 12:32	0.872
1200 m Sattion Flurometer	3/5/15 12:33	0.651
1200 m Sattion Flurometer	3/5/15 12:34	1.6
1200 m Sattion Flurometer	3/5/15 12:35	0.422
1200 m Sattion Flurometer	3/5/15 12:36	0.355
1200 m Sattion Flurometer	3/5/15 12:37	0.58
1200 m Sattion Flurometer	3/5/15 12:38	1.53
1200 m Sattion Flurometer	3/5/15 12:39	0.555
1200 m Sattion Flurometer	3/5/15 12:40	0.266
1200 m Sattion Flurometer	3/5/15 12:41	0.318
1200 m Sattion Flurometer	3/5/15 12:42	0.363
1200 m Sattion Flurometer	3/5/15 12:43	1.478
1200 m Sattion Flurometer	3/5/15 12:44	0.684
1200 m Sattion Flurometer	3/5/15 12:45	1.77
1200 m Sattion Flurometer	3/5/15 12:46	1.707
1200 m Sattion Flurometer	3/5/15 12:47	0.595
1200 m Sattion Flurometer	3/5/15 12:48	0.58
1200 m Sattion Flurometer	3/5/15 12:49	0.425
1200 m Sattion Flurometer	3/5/15 12:50	0.473
1200 m Sattion Flurometer	3/5/15 12:51	0.311
1200 m Sattion Flurometer	3/5/15 12:52	0.252
1200 m Sattion Flurometer	3/5/15 12:53	0.422
1200 m Sattion Flurometer	3/5/15 12:54	0.27
1200 m Sattion Flurometer	3/5/15 12:55	0.507
1200 m Sattion Flurometer	3/5/15 12:56	0.758
1200 m Sattion Flurometer	3/5/15 12:57	0.736
1200 m Sattion Flurometer	3/5/15 12:58	1.076
1200 m Sattion Flurometer	3/5/15 12:59	0.381

Location	Date and Time	Rhodmaine Concentration Adjusted Concentration (ppb)
1200 m Sattion Flurometer	3/5/15 13:00	1.039
1200 m Sattion Flurometer	3/5/15 13:01	0.163
1200 m Sattion Flurometer	3/5/15 13:02	0.817
1200 m Sattion Flurometer	3/5/15 13:03	0.089
1200 m Sattion Flurometer	3/5/15 13:04	0.307
1200 m Sattion Flurometer	3/5/15 13:05	1.641
1200 m Sattion Flurometer	3/5/15 13:06	0.739
1200 m Sattion Flurometer	3/5/15 13:07	0.562
1200 m Sattion Flurometer	3/5/15 13:08	0.152
1200 m Sattion Flurometer	3/5/15 13:09	0.717
1200 m Sattion Flurometer	3/5/15 13:10	0.614
1200 m Sattion Flurometer	3/5/15 13:11	1.696
1200 m Sattion Flurometer	3/5/15 13:12	0.126
1200 m Sattion Flurometer	3/5/15 13:13	0.333
1200 m Sattion Flurometer	3/5/15 13:14	0.23
1200 m Sattion Flurometer	3/5/15 13:15	0.281
1200 m Sattion Flurometer	3/5/15 13:16	0.965
1200 m Sattion Flurometer	3/5/15 13:17	0.189
1200 m Sattion Flurometer	3/5/15 13:18	0.529
1200 m Sattion Flurometer	3/5/15 13:19	0.326
1200 m Sattion Flurometer	3/5/15 13:20	1.404
1200 m Sattion Flurometer	3/5/15 13:21	0.632
1200 m Sattion Flurometer	3/5/15 13:22	0.359
1200 m Sattion Flurometer	3/5/15 13:23	0.392
1200 m Sattion Flurometer	3/5/15 13:24	1.585
1200 m Sattion Flurometer	3/5/15 13:25	1.401
1200 m Sattion Flurometer	3/5/15 13:26	0.425
1200 m Sattion Flurometer	3/5/15 13:27	0.303
1200 m Sattion Flurometer	3/5/15 13:28	0.193
1200 m Sattion Flurometer	3/5/15 13:29	1.345
1200 m Sattion Flurometer	3/5/15 13:30	0.484
1200 m Sattion Flurometer	3/5/15 13:31	0.669
1200 m Sattion Flurometer	3/5/15 13:32	0.414
1200 m Sattion Flurometer	3/5/15 13:33	0.292
1200 m Sattion Flurometer	3/5/15 13:34	0.555
1200 m Sattion Flurometer	3/5/15 13:35	0.344
1200 m Sattion Flurometer	3/5/15 13:36	0.266
1200 m Sattion Flurometer	3/5/15 13:37	0.702
1200 m Sattion Flurometer	3/5/15 13:38	1.231
1200 m Sattion Flurometer	3/5/15 13:39	0.303
1200 m Sattion Flurometer	3/5/15 13:40	0.913
1200 m Sattion Flurometer	3/5/15 13:41	1.567
1200 m Sattion Flurometer	3/5/15 13:42	0.403
1200 m Sattion Flurometer	3/5/15 13:43	0
1200 m Sattion Flurometer	3/5/15 13:44	0.414
1200 m Sattion Flurometer	3/5/15 13:45	0.241

Location	Date and Time	Rhodmaine Concentration Adjusted Concentration (ppb)
1200 m Sattion Flurometer	3/5/15 13:46	0.64
1200 m Sattion Flurometer	3/5/15 13:47	7.707
1200 m Sattion Flurometer	3/5/15 16:13	13.72
1200 m ISCO	3/4/15 17:00	0.259325096
1200 m ISCO	3/4/15 18:00	0.058521884
1200 m ISCO	3/4/15 19:00	-0.007315235
1200 m ISCO	3/4/15 20:00	0.29718144
1200 m ISCO	3/4/15 21:00	7.083342477
1200 m ISCO	3/4/15 22:00	4.449857719
1200 m ISCO	3/4/15 23:00	14.30238257
1200 m ISCO	3/5/15 0:00	13.81847975
1200 m ISCO	3/5/15 1:00	8.052794054
1200 m ISCO	3/5/15 2:00	5.081894061
1200 m ISCO	3/5/15 3:00	5.470333063
1200 m ISCO	3/5/15 4:00	4.51404891
1200 m ISCO	3/5/15 5:00	3.901763703
1200 m ISCO	3/5/15 6:00	3.332272624
1200 m ISCO	3/5/15 7:00	2.558686476
1200 m ISCO	3/5/15 8:00	1.71103357
1200 m ISCO	3/5/15 9:00	1.66988537
1200 m ISCO	3/5/15 10:00	1.500354789
1200 m ISCO	3/5/15 11:00	1.233714457
1200 m ISCO	3/5/15 12:00	1.156355842
1200 m ISCO	3/5/15 13:00	0.868318447
Mid Point Flurometer	3/4/2015 9:01	0
Mid Point Flurometer	3/4/2015 9:02	0
Mid Point Flurometer	3/4/2015 9:03	0
Mid Point Flurometer	3/4/2015 9:04	0
Mid Point Flurometer	3/4/2015 9:05	0
Mid Point Flurometer	3/4/2015 9:06	0
Mid Point Flurometer	3/4/2015 9:07	0
Mid Point Flurometer	3/4/2015 9:08	0
Mid Point Flurometer	3/4/2015 9:09	0
Mid Point Flurometer	3/4/2015 9:10	0
Mid Point Flurometer	3/4/2015 9:11	0
Mid Point Flurometer	3/4/2015 9:12	0
Mid Point Flurometer	3/4/2015 9:13	0
Mid Point Flurometer	3/4/2015 9:14	0
Mid Point Flurometer	3/4/2015 9:15	0
Mid Point Flurometer	3/4/2015 9:16	0
Mid Point Flurometer	3/4/2015 9:17	0
Mid Point Flurometer	3/4/2015 9:18	0
Mid Point Flurometer	3/4/2015 9:19	0
Mid Point Flurometer	3/4/2015 9:20	0
Mid Point Flurometer	3/4/2015 9:21	0
Mid Point Flurometer	3/4/2015 9:22	0

Location	Date and Time	Rhodmaine Concentration Adjusted Concentration (ppb)
Mid Point Flurometer	3/4/2015 9:23	0
Mid Point Flurometer	3/4/2015 9:24	0
Mid Point Flurometer	3/4/2015 9:25	0
Mid Point Flurometer	3/4/2015 9:26	0
Mid Point Flurometer	3/4/2015 9:27	0
Mid Point Flurometer	3/4/2015 9:28	0
Mid Point Flurometer	3/4/2015 9:29	0
Mid Point Flurometer	3/4/2015 9:30	0
Mid Point Flurometer	3/4/2015 9:31	0
Mid Point Flurometer	3/4/2015 9:32	0
Mid Point Flurometer	3/4/2015 9:33	0
Mid Point Flurometer	3/4/2015 9:34	0
Mid Point Flurometer	3/4/2015 9:35	0
Mid Point Flurometer	3/4/2015 9:36	0
Mid Point Flurometer	3/4/2015 9:37	0
Mid Point Flurometer	3/4/2015 9:38	0
Mid Point Flurometer	3/4/2015 9:39	0
Mid Point Flurometer	3/4/2015 9:40	0
Mid Point Flurometer	3/4/2015 9:41	0
Mid Point Flurometer	3/4/2015 9:42	0
Mid Point Flurometer	3/4/2015 9:43	0
Mid Point Flurometer	3/4/2015 9:44	0
Mid Point Flurometer	3/4/2015 9:45	0
Mid Point Flurometer	3/4/2015 9:46	0
Mid Point Flurometer	3/4/2015 9:47	0
Mid Point Flurometer	3/4/2015 9:48	0
Mid Point Flurometer	3/4/2015 9:49	0
Mid Point Flurometer	3/4/2015 9:50	0
Mid Point Flurometer	3/4/2015 9:51	0
Mid Point Flurometer	3/4/2015 9:52	0
Mid Point Flurometer	3/4/2015 9:53	0
Mid Point Flurometer	3/4/2015 9:54	0
Mid Point Flurometer	3/4/2015 9:55	0
Mid Point Flurometer	3/4/2015 9:56	0
Mid Point Flurometer	3/4/2015 9:57	0
Mid Point Flurometer	3/4/2015 9:58	0
Mid Point Flurometer	3/4/2015 9:59	0
Mid Point Flurometer	3/4/2015 10:00	0
Mid Point Flurometer	3/4/2015 10:01	0
Mid Point Flurometer	3/4/2015 10:02	0
Mid Point Flurometer	3/4/2015 10:03	0
Mid Point Flurometer	3/4/2015 10:04	0
Mid Point Flurometer	3/4/2015 10:05	0
Mid Point Flurometer	3/4/2015 10:06	0
Mid Point Flurometer	3/4/2015 10:07	0
Mid Point Flurometer	3/4/2015 10:08	0

Location	Date and Time	Rhodmaine Concentration Adjusted Concentration (ppb)
Mid Point Flurometer	3/4/2015 10:09	0
Mid Point Flurometer	3/4/2015 10:10	0
Mid Point Flurometer	3/4/2015 10:11	0
Mid Point Flurometer	3/4/2015 10:12	0
Mid Point Flurometer	3/4/2015 10:13	0
Mid Point Flurometer	3/4/2015 10:14	0
Mid Point Flurometer	3/4/2015 10:15	0
Mid Point Flurometer	3/4/2015 10:16	0
Mid Point Flurometer	3/4/2015 10:17	0
Mid Point Flurometer	3/4/2015 10:18	0
Mid Point Flurometer	3/4/2015 10:19	0
Mid Point Flurometer	3/4/2015 10:20	0
Mid Point Flurometer	3/4/2015 10:21	0
Mid Point Flurometer	3/4/2015 10:22	0
Mid Point Flurometer	3/4/2015 10:23	0
Mid Point Flurometer	3/4/2015 10:24	0
Mid Point Flurometer	3/4/2015 10:25	0
Mid Point Flurometer	3/4/2015 10:26	0
Mid Point Flurometer	3/4/2015 10:27	0
Mid Point Flurometer	3/4/2015 10:28	0
Mid Point Flurometer	3/4/2015 10:29	0
Mid Point Flurometer	3/4/2015 10:30	0
Mid Point Flurometer	3/4/2015 10:31	0
Mid Point Flurometer	3/4/2015 10:32	0
Mid Point Flurometer	3/4/2015 10:33	0
Mid Point Flurometer	3/4/2015 10:34	0
Mid Point Flurometer	3/4/2015 10:35	0
Mid Point Flurometer	3/4/2015 10:36	0
Mid Point Flurometer	3/4/2015 10:37	0
Mid Point Flurometer	3/4/2015 10:38	0
Mid Point Flurometer	3/4/2015 10:39	0
Mid Point Flurometer	3/4/2015 10:40	0
Mid Point Flurometer	3/4/2015 10:41	0
Mid Point Flurometer	3/4/2015 10:42	0
Mid Point Flurometer	3/4/2015 10:43	0
Mid Point Flurometer	3/4/2015 10:44	0
Mid Point Flurometer	3/4/2015 10:45	0
Mid Point Flurometer	3/4/2015 10:46	0
Mid Point Flurometer	3/4/2015 10:47	0
Mid Point Flurometer	3/4/2015 10:48	0
Mid Point Flurometer	3/4/2015 10:49	0
Mid Point Flurometer	3/4/2015 10:50	0
Mid Point Flurometer	3/4/2015 10:51	0
Mid Point Flurometer	3/4/2015 10:52	0
Mid Point Flurometer	3/4/2015 10:53	0
Mid Point Flurometer	3/4/2015 10:54	0

Location	Date and Time	Rhodmaine Concentration Adjusted Concentration (ppb)
Mid Point Flurometer	3/4/2015 10:55	0
Mid Point Flurometer	3/4/2015 10:56	0
Mid Point Flurometer	3/4/2015 10:57	0
Mid Point Flurometer	3/4/2015 10:58	0
Mid Point Flurometer	3/4/2015 10:59	0
Mid Point Flurometer	3/4/2015 11:00	0
Mid Point Flurometer	3/4/2015 11:01	0
Mid Point Flurometer	3/4/2015 11:02	0
Mid Point Flurometer	3/4/2015 11:03	0
Mid Point Flurometer	3/4/2015 11:04	0
Mid Point Flurometer	3/4/2015 11:05	0
Mid Point Flurometer	3/4/2015 11:06	0
Mid Point Flurometer	3/4/2015 11:07	0
Mid Point Flurometer	3/4/2015 11:08	0
Mid Point Flurometer	3/4/2015 11:09	0
Mid Point Flurometer	3/4/2015 11:10	0
Mid Point Flurometer	3/4/2015 11:11	0
Mid Point Flurometer	3/4/2015 11:12	0
Mid Point Flurometer	3/4/2015 11:13	0
Mid Point Flurometer	3/4/2015 11:14	0
Mid Point Flurometer	3/4/2015 11:15	0
Mid Point Flurometer	3/4/2015 11:16	0
Mid Point Flurometer	3/4/2015 11:17	0
Mid Point Flurometer	3/4/2015 11:18	0
Mid Point Flurometer	3/4/2015 11:19	0
Mid Point Flurometer	3/4/2015 11:20	0
Mid Point Flurometer	3/4/2015 11:21	0
Mid Point Flurometer	3/4/2015 11:22	0
Mid Point Flurometer	3/4/2015 11:23	0
Mid Point Flurometer	3/4/2015 11:24	0
Mid Point Flurometer	3/4/2015 11:25	0
Mid Point Flurometer	3/4/2015 11:26	0
Mid Point Flurometer	3/4/2015 11:27	0
Mid Point Flurometer	3/4/2015 11:28	0
Mid Point Flurometer	3/4/2015 11:29	0
Mid Point Flurometer	3/4/2015 11:30	0
Mid Point Flurometer	3/4/2015 11:31	0
Mid Point Flurometer	3/4/2015 11:32	0
Mid Point Flurometer	3/4/2015 11:33	0
Mid Point Flurometer	3/4/2015 11:34	0
Mid Point Flurometer	3/4/2015 11:35	0
Mid Point Flurometer	3/4/2015 11:36	0
Mid Point Flurometer	3/4/2015 11:37	0
Mid Point Flurometer	3/4/2015 11:38	0
Mid Point Flurometer	3/4/2015 11:39	0
Mid Point Flurometer	3/4/2015 11:40	0

Location	Date and Time	Rhodmaine Concentration Adjusted Concentration (ppb)
Mid Point Flurometer	3/4/2015 11:41	0
Mid Point Flurometer	3/4/2015 11:42	0
Mid Point Flurometer	3/4/2015 11:43	0
Mid Point Flurometer	3/4/2015 11:44	0
Mid Point Flurometer	3/4/2015 11:45	0
Mid Point Flurometer	3/4/2015 11:46	0
Mid Point Flurometer	3/4/2015 11:47	0
Mid Point Flurometer	3/4/2015 11:48	0
Mid Point Flurometer	3/4/2015 11:49	0
Mid Point Flurometer	3/4/2015 11:50	0
Mid Point Flurometer	3/4/2015 11:51	0
Mid Point Flurometer	3/4/2015 11:52	0
Mid Point Flurometer	3/4/2015 11:53	0
Mid Point Flurometer	3/4/2015 11:54	0
Mid Point Flurometer	3/4/2015 11:55	0
Mid Point Flurometer	3/4/2015 11:56	0
Mid Point Flurometer	3/4/2015 11:57	0
Mid Point Flurometer	3/4/2015 11:58	0
Mid Point Flurometer	3/4/2015 11:59	0
Mid Point Flurometer	3/4/2015 12:00	0
Mid Point Flurometer	3/4/2015 12:01	0
Mid Point Flurometer	3/4/2015 12:02	0
Mid Point Flurometer	3/4/2015 12:03	0
Mid Point Flurometer	3/4/2015 12:04	0
Mid Point Flurometer	3/4/2015 12:05	0
Mid Point Flurometer	3/4/2015 12:06	0
Mid Point Flurometer	3/4/2015 12:07	0
Mid Point Flurometer	3/4/2015 12:08	0
Mid Point Flurometer	3/4/2015 12:09	0
Mid Point Flurometer	3/4/2015 12:10	0
Mid Point Flurometer	3/4/2015 12:11	0
Mid Point Flurometer	3/4/2015 12:12	0
Mid Point Flurometer	3/4/2015 12:13	0
Mid Point Flurometer	3/4/2015 12:14	0
Mid Point Flurometer	3/4/2015 12:15	0
Mid Point Flurometer	3/4/2015 12:16	0
Mid Point Flurometer	3/4/2015 12:17	0
Mid Point Flurometer	3/4/2015 12:18	0
Mid Point Flurometer	3/4/2015 12:19	0
Mid Point Flurometer	3/4/2015 12:20	0
Mid Point Flurometer	3/4/2015 12:21	0
Mid Point Flurometer	3/4/2015 12:22	0
Mid Point Flurometer	3/4/2015 12:23	0
Mid Point Flurometer	3/4/2015 12:24	0
Mid Point Flurometer	3/4/2015 12:25	0
Mid Point Flurometer	3/4/2015 12:26	0

Location	Date and Time	Rhodmaine Concentration Adjusted Concentration (ppb)
Mid Point Flurometer	3/4/2015 12:27	0
Mid Point Flurometer	3/4/2015 12:28	0
Mid Point Flurometer	3/4/2015 12:29	0
Mid Point Flurometer	3/4/2015 12:30	0
Mid Point Flurometer	3/4/2015 12:31	0
Mid Point Flurometer	3/4/2015 12:32	0
Mid Point Flurometer	3/4/2015 12:33	0
Mid Point Flurometer	3/4/2015 12:34	0
Mid Point Flurometer	3/4/2015 12:35	0
Mid Point Flurometer	3/4/2015 12:36	0
Mid Point Flurometer	3/4/2015 12:37	0
Mid Point Flurometer	3/4/2015 12:38	0
Mid Point Flurometer	3/4/2015 12:39	0
Mid Point Flurometer	3/4/2015 12:40	0
Mid Point Flurometer	3/4/2015 12:41	0
Mid Point Flurometer	3/4/2015 12:42	0
Mid Point Flurometer	3/4/2015 12:43	0
Mid Point Flurometer	3/4/2015 12:44	0
Mid Point Flurometer	3/4/2015 12:45	0
Mid Point Flurometer	3/4/2015 12:46	0.52
Mid Point Flurometer	3/4/2015 12:47	0
Mid Point Flurometer	3/4/2015 12:48	0
Mid Point Flurometer	3/4/2015 12:49	0
Mid Point Flurometer	3/4/2015 12:50	0
Mid Point Flurometer	3/4/2015 12:51	0
Mid Point Flurometer	3/4/2015 12:52	0
Mid Point Flurometer	3/4/2015 12:53	0
Mid Point Flurometer	3/4/2015 12:54	0
Mid Point Flurometer	3/4/2015 12:55	0
Mid Point Flurometer	3/4/2015 12:56	0
Mid Point Flurometer	3/4/2015 12:57	0
Mid Point Flurometer	3/4/2015 12:58	0
Mid Point Flurometer	3/4/2015 12:59	0
Mid Point Flurometer	3/4/2015 13:00	0
Mid Point Flurometer	3/4/2015 13:01	0
Mid Point Flurometer	3/4/2015 13:02	0
Mid Point Flurometer	3/4/2015 13:03	0
Mid Point Flurometer	3/4/2015 13:04	0
Mid Point Flurometer	3/4/2015 13:05	0
Mid Point Flurometer	3/4/2015 13:06	0
Mid Point Flurometer	3/4/2015 13:07	0
Mid Point Flurometer	3/4/2015 13:08	0
Mid Point Flurometer	3/4/2015 13:09	0
Mid Point Flurometer	3/4/2015 13:10	0
Mid Point Flurometer	3/4/2015 13:11	0
Mid Point Flurometer	3/4/2015 13:12	0

Location	Date and Time	Rhodmaine Concentration Adjusted Concentration (ppb)
Mid Point Flurometer	3/4/2015 13:13	0
Mid Point Flurometer	3/4/2015 13:14	0
Mid Point Flurometer	3/4/2015 13:15	0
Mid Point Flurometer	3/4/2015 13:16	0
Mid Point Flurometer	3/4/2015 13:17	0
Mid Point Flurometer	3/4/2015 13:18	0
Mid Point Flurometer	3/4/2015 13:19	0
Mid Point Flurometer	3/4/2015 13:20	0
Mid Point Flurometer	3/4/2015 13:21	0
Mid Point Flurometer	3/4/2015 13:22	0
Mid Point Flurometer	3/4/2015 13:23	0
Mid Point Flurometer	3/4/2015 13:24	0
Mid Point Flurometer	3/4/2015 13:25	0
Mid Point Flurometer	3/4/2015 13:26	1.7
Mid Point Flurometer	3/4/2015 13:27	0.03
Mid Point Flurometer	3/4/2015 13:28	0
Mid Point Flurometer	3/4/2015 13:29	0
Mid Point Flurometer	3/4/2015 13:30	0
Mid Point Flurometer	3/4/2015 13:31	0
Mid Point Flurometer	3/4/2015 13:32	0
Mid Point Flurometer	3/4/2015 13:33	0
Mid Point Flurometer	3/4/2015 13:34	0
Mid Point Flurometer	3/4/2015 13:35	0
Mid Point Flurometer	3/4/2015 13:36	0
Mid Point Flurometer	3/4/2015 13:37	0
Mid Point Flurometer	3/4/2015 13:38	0
Mid Point Flurometer	3/4/2015 13:39	0
Mid Point Flurometer	3/4/2015 13:40	0
Mid Point Flurometer	3/4/2015 13:41	0
Mid Point Flurometer	3/4/2015 13:42	0
Mid Point Flurometer	3/4/2015 13:43	0
Mid Point Flurometer	3/4/2015 13:44	0
Mid Point Flurometer	3/4/2015 13:45	0
Mid Point Flurometer	3/4/2015 13:46	0
Mid Point Flurometer	3/4/2015 13:47	0
Mid Point Flurometer	3/4/2015 13:48	0
Mid Point Flurometer	3/4/2015 13:49	0
Mid Point Flurometer	3/4/2015 13:50	0
Mid Point Flurometer	3/4/2015 13:51	0
Mid Point Flurometer	3/4/2015 13:52	0
Mid Point Flurometer	3/4/2015 13:53	0
Mid Point Flurometer	3/4/2015 13:54	0
Mid Point Flurometer	3/4/2015 13:55	0
Mid Point Flurometer	3/4/2015 13:56	0
Mid Point Flurometer	3/4/2015 13:57	0
Mid Point Flurometer	3/4/2015 13:58	0

Location	Date and Time	Rhodmaine Concentration Adjusted Concentration (ppb)
Mid Point Flurometer	3/4/2015 13:59	0
Mid Point Flurometer	3/4/2015 14:00	0
Mid Point Flurometer	3/4/2015 14:01	0
Mid Point Flurometer	3/4/2015 14:02	0
Mid Point Flurometer	3/4/2015 14:03	0
Mid Point Flurometer	3/4/2015 14:04	0
Mid Point Flurometer	3/4/2015 14:05	0
Mid Point Flurometer	3/4/2015 14:06	0
Mid Point Flurometer	3/4/2015 14:07	0
Mid Point Flurometer	3/4/2015 14:08	0
Mid Point Flurometer	3/4/2015 14:09	0
Mid Point Flurometer	3/4/2015 14:10	0
Mid Point Flurometer	3/4/2015 14:11	0
Mid Point Flurometer	3/4/2015 14:12	0
Mid Point Flurometer	3/4/2015 14:13	0
Mid Point Flurometer	3/4/2015 14:14	0.02
Mid Point Flurometer	3/4/2015 14:15	0
Mid Point Flurometer	3/4/2015 14:16	0
Mid Point Flurometer	3/4/2015 14:17	0
Mid Point Flurometer	3/4/2015 14:18	0
Mid Point Flurometer	3/4/2015 14:19	0
Mid Point Flurometer	3/4/2015 14:20	0
Mid Point Flurometer	3/4/2015 14:21	0
Mid Point Flurometer	3/4/2015 14:22	0
Mid Point Flurometer	3/4/2015 14:23	0
Mid Point Flurometer	3/4/2015 14:24	0
Mid Point Flurometer	3/4/2015 14:25	0
Mid Point Flurometer	3/4/2015 14:26	0
Mid Point Flurometer	3/4/2015 14:27	0
Mid Point Flurometer	3/4/2015 14:28	0
Mid Point Flurometer	3/4/2015 14:29	0
Mid Point Flurometer	3/4/2015 14:30	0
Mid Point Flurometer	3/4/2015 14:31	0
Mid Point Flurometer	3/4/2015 14:32	0
Mid Point Flurometer	3/4/2015 14:33	0
Mid Point Flurometer	3/4/2015 14:34	0
Mid Point Flurometer	3/4/2015 14:35	0
Mid Point Flurometer	3/4/2015 14:36	0
Mid Point Flurometer	3/4/2015 14:37	0
Mid Point Flurometer	3/4/2015 14:38	0
Mid Point Flurometer	3/4/2015 14:39	0
Mid Point Flurometer	3/4/2015 14:40	0
Mid Point Flurometer	3/4/2015 14:41	0
Mid Point Flurometer	3/4/2015 14:42	0
Mid Point Flurometer	3/4/2015 14:43	0
Mid Point Flurometer	3/4/2015 14:44	0

Location	Date and Time	Rhodmaine Concentration Adjusted Concentration (ppb)
Mid Point Flurometer	3/4/2015 14:45	0
Mid Point Flurometer	3/4/2015 14:46	0
Mid Point Flurometer	3/4/2015 14:47	0
Mid Point Flurometer	3/4/2015 14:48	0
Mid Point Flurometer	3/4/2015 14:49	0
Mid Point Flurometer	3/4/2015 14:50	0
Mid Point Flurometer	3/4/2015 14:51	0
Mid Point Flurometer	3/4/2015 14:52	0
Mid Point Flurometer	3/4/2015 14:53	0
Mid Point Flurometer	3/4/2015 14:54	0
Mid Point Flurometer	3/4/2015 14:55	0
Mid Point Flurometer	3/4/2015 14:56	0
Mid Point Flurometer	3/4/2015 14:57	0
Mid Point Flurometer	3/4/2015 14:58	0
Mid Point Flurometer	3/4/2015 14:59	0
Mid Point Flurometer	3/4/2015 15:00	0
Mid Point Flurometer	3/4/2015 15:01	0
Mid Point Flurometer	3/4/2015 15:02	0
Mid Point Flurometer	3/4/2015 15:03	0
Mid Point Flurometer	3/4/2015 15:04	0
Mid Point Flurometer	3/4/2015 15:05	0
Mid Point Flurometer	3/4/2015 15:06	0
Mid Point Flurometer	3/4/2015 15:07	0
Mid Point Flurometer	3/4/2015 15:08	0
Mid Point Flurometer	3/4/2015 15:09	0
Mid Point Flurometer	3/4/2015 15:10	0
Mid Point Flurometer	3/4/2015 15:11	0
Mid Point Flurometer	3/4/2015 15:12	0
Mid Point Flurometer	3/4/2015 15:13	0
Mid Point Flurometer	3/4/2015 15:14	0
Mid Point Flurometer	3/4/2015 15:15	0
Mid Point Flurometer	3/4/2015 15:16	0
Mid Point Flurometer	3/4/2015 15:17	0
Mid Point Flurometer	3/4/2015 15:18	0
Mid Point Flurometer	3/4/2015 15:19	0.04
Mid Point Flurometer	3/4/2015 15:20	0
Mid Point Flurometer	3/4/2015 15:21	0
Mid Point Flurometer	3/4/2015 15:22	0
Mid Point Flurometer	3/4/2015 15:23	0
Mid Point Flurometer	3/4/2015 15:24	0
Mid Point Flurometer	3/4/2015 15:25	0
Mid Point Flurometer	3/4/2015 15:26	0
Mid Point Flurometer	3/4/2015 15:27	0
Mid Point Flurometer	3/4/2015 15:28	0
Mid Point Flurometer	3/4/2015 15:29	0
Mid Point Flurometer	3/4/2015 15:30	0

Location	Date and Time	Rhodmaine Concentration Adjusted Concentration (ppb)
Mid Point Flurometer	3/4/2015 15:31	0
Mid Point Flurometer	3/4/2015 15:32	0
Mid Point Flurometer	3/4/2015 15:33	0
Mid Point Flurometer	3/4/2015 15:34	0
Mid Point Flurometer	3/4/2015 15:35	0
Mid Point Flurometer	3/4/2015 15:36	0
Mid Point Flurometer	3/4/2015 15:37	0
Mid Point Flurometer	3/4/2015 15:38	0
Mid Point Flurometer	3/4/2015 15:39	0
Mid Point Flurometer	3/4/2015 15:40	0
Mid Point Flurometer	3/4/2015 15:41	0
Mid Point Flurometer	3/4/2015 15:42	0
Mid Point Flurometer	3/4/2015 15:43	0
Mid Point Flurometer	3/4/2015 15:44	0
Mid Point Flurometer	3/4/2015 15:45	0
Mid Point Flurometer	3/4/2015 15:46	0
Mid Point Flurometer	3/4/2015 15:47	0
Mid Point Flurometer	3/4/2015 15:48	0
Mid Point Flurometer	3/4/2015 15:49	0
Mid Point Flurometer	3/4/2015 15:50	0
Mid Point Flurometer	3/4/2015 15:51	0
Mid Point Flurometer	3/4/2015 15:52	0
Mid Point Flurometer	3/4/2015 15:53	0
Mid Point Flurometer	3/4/2015 15:54	0
Mid Point Flurometer	3/4/2015 15:55	0
Mid Point Flurometer	3/4/2015 15:56	0
Mid Point Flurometer	3/4/2015 15:57	0
Mid Point Flurometer	3/4/2015 15:58	0
Mid Point Flurometer	3/4/2015 15:59	0
Mid Point Flurometer	3/4/2015 16:00	0
Mid Point Flurometer	3/4/2015 16:01	0
Mid Point Flurometer	3/4/2015 16:02	0
Mid Point Flurometer	3/4/2015 16:03	0
Mid Point Flurometer	3/4/2015 16:04	0
Mid Point Flurometer	3/4/2015 16:05	0
Mid Point Flurometer	3/4/2015 16:06	0
Mid Point Flurometer	3/4/2015 16:07	0
Mid Point Flurometer	3/4/2015 16:08	0
Mid Point Flurometer	3/4/2015 16:09	0
Mid Point Flurometer	3/4/2015 16:10	0
Mid Point Flurometer	3/4/2015 16:11	0
Mid Point Flurometer	3/4/2015 16:12	0
Mid Point Flurometer	3/4/2015 16:13	0
Mid Point Flurometer	3/4/2015 16:14	0
Mid Point Flurometer	3/4/2015 16:15	0
Mid Point Flurometer	3/4/2015 16:16	0

Location	Date and Time	Rhodmaine Concentration Adjusted Concentration (ppb)
Mid Point Flurometer	3/4/2015 16:17	0
Mid Point Flurometer	3/4/2015 16:18	0
Mid Point Flurometer	3/4/2015 16:19	0
Mid Point Flurometer	3/4/2015 16:20	0
Mid Point Flurometer	3/4/2015 16:21	0
Mid Point Flurometer	3/4/2015 16:22	0
Mid Point Flurometer	3/4/2015 16:23	0
Mid Point Flurometer	3/4/2015 16:24	0
Mid Point Flurometer	3/4/2015 16:25	0
Mid Point Flurometer	3/4/2015 16:26	0
Mid Point Flurometer	3/4/2015 16:27	0
Mid Point Flurometer	3/4/2015 16:28	0
Mid Point Flurometer	3/4/2015 16:29	0
Mid Point Flurometer	3/4/2015 16:30	0
Mid Point Flurometer	3/4/2015 16:31	0
Mid Point Flurometer	3/4/2015 16:32	0
Mid Point Flurometer	3/4/2015 16:33	0
Mid Point Flurometer	3/4/2015 16:34	0
Mid Point Flurometer	3/4/2015 16:35	0
Mid Point Flurometer	3/4/2015 16:36	0
Mid Point Flurometer	3/4/2015 16:37	0
Mid Point Flurometer	3/4/2015 16:38	0
Mid Point Flurometer	3/4/2015 16:39	0
Mid Point Flurometer	3/4/2015 16:40	0
Mid Point Flurometer	3/4/2015 16:41	0
Mid Point Flurometer	3/4/2015 16:42	0
Mid Point Flurometer	3/4/2015 16:43	0
Mid Point Flurometer	3/4/2015 16:44	0
Mid Point Flurometer	3/4/2015 16:45	0
Mid Point Flurometer	3/4/2015 16:46	0
Mid Point Flurometer	3/4/2015 16:47	0
Mid Point Flurometer	3/4/2015 16:48	0
Mid Point Flurometer	3/4/2015 16:49	0.17
Mid Point Flurometer	3/4/2015 16:50	0
Mid Point Flurometer	3/4/2015 16:51	0
Mid Point Flurometer	3/4/2015 16:52	0
Mid Point Flurometer	3/4/2015 16:53	0
Mid Point Flurometer	3/4/2015 16:54	0
Mid Point Flurometer	3/4/2015 16:55	0
Mid Point Flurometer	3/4/2015 16:56	0
Mid Point Flurometer	3/4/2015 16:57	0
Mid Point Flurometer	3/4/2015 16:58	0
Mid Point Flurometer	3/4/2015 16:59	0
Mid Point Flurometer	3/4/2015 17:00	0
Mid Point Flurometer	3/4/2015 17:01	0
Mid Point Flurometer	3/4/2015 17:02	0

Location	Date and Time	Rhodmaine Concentration Adjusted Concentration (ppb)
Mid Point Flurometer	3/4/2015 17:03	0
Mid Point Flurometer	3/4/2015 17:04	0
Mid Point Flurometer	3/4/2015 17:05	0
Mid Point Flurometer	3/4/2015 17:06	0
Mid Point Flurometer	3/4/2015 17:07	0
Mid Point Flurometer	3/4/2015 17:08	0
Mid Point Flurometer	3/4/2015 17:09	0
Mid Point Flurometer	3/4/2015 17:10	0
Mid Point Flurometer	3/4/2015 17:11	0
Mid Point Flurometer	3/4/2015 17:12	0
Mid Point Flurometer	3/4/2015 17:13	0
Mid Point Flurometer	3/4/2015 17:14	0
Mid Point Flurometer	3/4/2015 17:15	0
Mid Point Flurometer	3/4/2015 17:16	0
Mid Point Flurometer	3/4/2015 17:17	0
Mid Point Flurometer	3/4/2015 17:18	0
Mid Point Flurometer	3/4/2015 17:19	0
Mid Point Flurometer	3/4/2015 17:20	0
Mid Point Flurometer	3/4/2015 17:21	0
Mid Point Flurometer	3/4/2015 17:22	0
Mid Point Flurometer	3/4/2015 17:23	0
Mid Point Flurometer	3/4/2015 17:24	0
Mid Point Flurometer	3/4/2015 17:25	0
Mid Point Flurometer	3/4/2015 17:26	0
Mid Point Flurometer	3/4/2015 17:27	0
Mid Point Flurometer	3/4/2015 17:28	0
Mid Point Flurometer	3/4/2015 17:29	0
Mid Point Flurometer	3/4/2015 17:30	0
Mid Point Flurometer	3/4/2015 17:31	0
Mid Point Flurometer	3/4/2015 17:32	0
Mid Point Flurometer	3/4/2015 17:33	0
Mid Point Flurometer	3/4/2015 17:34	0
Mid Point Flurometer	3/4/2015 17:35	0
Mid Point Flurometer	3/4/2015 17:36	0
Mid Point Flurometer	3/4/2015 17:37	0
Mid Point Flurometer	3/4/2015 17:38	0
Mid Point Flurometer	3/4/2015 17:39	0
Mid Point Flurometer	3/4/2015 17:40	0
Mid Point Flurometer	3/4/2015 17:41	0
Mid Point Flurometer	3/4/2015 17:42	0
Mid Point Flurometer	3/4/2015 17:43	0
Mid Point Flurometer	3/4/2015 17:44	0
Mid Point Flurometer	3/4/2015 17:45	0
Mid Point Flurometer	3/4/2015 17:46	0
Mid Point Flurometer	3/4/2015 17:47	0
Mid Point Flurometer	3/4/2015 17:48	0

Location	Date and Time	Rhodmaine Concentration Adjusted Concentration (ppb)
Mid Point Flurometer	3/4/2015 17:49	0
Mid Point Flurometer	3/4/2015 17:50	0
Mid Point Flurometer	3/4/2015 17:51	0
Mid Point Flurometer	3/4/2015 17:52	0
Mid Point Flurometer	3/4/2015 17:53	0
Mid Point Flurometer	3/4/2015 17:54	0
Mid Point Flurometer	3/4/2015 17:55	0
Mid Point Flurometer	3/4/2015 17:56	0
Mid Point Flurometer	3/4/2015 17:57	0
Mid Point Flurometer	3/4/2015 17:58	0
Mid Point Flurometer	3/4/2015 17:59	0
Mid Point Flurometer	3/4/2015 18:00	0
Mid Point Flurometer	3/4/2015 18:01	0
Mid Point Flurometer	3/4/2015 18:02	0
Mid Point Flurometer	3/4/2015 18:03	0
Mid Point Flurometer	3/4/2015 18:04	0
Mid Point Flurometer	3/4/2015 18:05	0
Mid Point Flurometer	3/4/2015 18:06	0
Mid Point Flurometer	3/4/2015 18:07	0
Mid Point Flurometer	3/4/2015 18:08	0
Mid Point Flurometer	3/4/2015 18:09	0
Mid Point Flurometer	3/4/2015 18:10	0
Mid Point Flurometer	3/4/2015 18:11	0
Mid Point Flurometer	3/4/2015 18:12	0
Mid Point Flurometer	3/4/2015 18:13	0
Mid Point Flurometer	3/4/2015 18:14	0.12
Mid Point Flurometer	3/4/2015 18:15	0
Mid Point Flurometer	3/4/2015 18:16	0
Mid Point Flurometer	3/4/2015 18:17	0
Mid Point Flurometer	3/4/2015 18:18	0
Mid Point Flurometer	3/4/2015 18:19	0
Mid Point Flurometer	3/4/2015 18:20	0
Mid Point Flurometer	3/4/2015 18:21	0
Mid Point Flurometer	3/4/2015 18:22	0
Mid Point Flurometer	3/4/2015 18:23	0
Mid Point Flurometer	3/4/2015 18:24	0
Mid Point Flurometer	3/4/2015 18:25	0
Mid Point Flurometer	3/4/2015 18:26	0
Mid Point Flurometer	3/4/2015 18:27	0
Mid Point Flurometer	3/4/2015 18:28	0
Mid Point Flurometer	3/4/2015 18:29	0
Mid Point Flurometer	3/4/2015 18:30	0
Mid Point Flurometer	3/4/2015 18:31	0
Mid Point Flurometer	3/4/2015 18:32	0
Mid Point Flurometer	3/4/2015 18:33	0
Mid Point Flurometer	3/4/2015 18:34	0.01

Location	Date and Time	Rhodmaine Concentration Adjusted Concentration (ppb)
Mid Point Flurometer	3/4/2015 18:35	0
Mid Point Flurometer	3/4/2015 18:36	0
Mid Point Flurometer	3/4/2015 18:37	0
Mid Point Flurometer	3/4/2015 18:38	0
Mid Point Flurometer	3/4/2015 18:39	0
Mid Point Flurometer	3/4/2015 18:40	0
Mid Point Flurometer	3/4/2015 18:41	0
Mid Point Flurometer	3/4/2015 18:42	0
Mid Point Flurometer	3/4/2015 18:43	0
Mid Point Flurometer	3/4/2015 18:44	0
Mid Point Flurometer	3/4/2015 18:45	0
Mid Point Flurometer	3/4/2015 18:46	0
Mid Point Flurometer	3/4/2015 18:47	0
Mid Point Flurometer	3/4/2015 18:48	0
Mid Point Flurometer	3/4/2015 18:49	0
Mid Point Flurometer	3/4/2015 18:50	0
Mid Point Flurometer	3/4/2015 18:51	0
Mid Point Flurometer	3/4/2015 18:52	0
Mid Point Flurometer	3/4/2015 18:53	0
Mid Point Flurometer	3/4/2015 18:54	0
Mid Point Flurometer	3/4/2015 18:55	0
Mid Point Flurometer	3/4/2015 18:56	0
Mid Point Flurometer	3/4/2015 18:57	0
Mid Point Flurometer	3/4/2015 18:58	0
Mid Point Flurometer	3/4/2015 18:59	0
Mid Point Flurometer	3/4/2015 19:00	0
Mid Point Flurometer	3/4/2015 19:01	0
Mid Point Flurometer	3/4/2015 19:02	0
Mid Point Flurometer	3/4/2015 19:03	0
Mid Point Flurometer	3/4/2015 19:04	0
Mid Point Flurometer	3/4/2015 19:05	0
Mid Point Flurometer	3/4/2015 19:06	0
Mid Point Flurometer	3/4/2015 19:07	0
Mid Point Flurometer	3/4/2015 19:08	0
Mid Point Flurometer	3/4/2015 19:09	0
Mid Point Flurometer	3/4/2015 19:10	0
Mid Point Flurometer	3/4/2015 19:11	0
Mid Point Flurometer	3/4/2015 19:12	0
Mid Point Flurometer	3/4/2015 19:13	0
Mid Point Flurometer	3/4/2015 19:14	0
Mid Point Flurometer	3/4/2015 19:15	0
Mid Point Flurometer	3/4/2015 19:16	0
Mid Point Flurometer	3/4/2015 19:17	0
Mid Point Flurometer	3/4/2015 19:18	0
Mid Point Flurometer	3/4/2015 19:19	0
Mid Point Flurometer	3/4/2015 19:20	0

Location	Date and Time	Rhodmaine Concentration Adjusted Concentration (ppb)
Mid Point Flurometer	3/4/2015 19:21	0
Mid Point Flurometer	3/4/2015 19:22	0
Mid Point Flurometer	3/4/2015 19:23	0
Mid Point Flurometer	3/4/2015 19:24	0
Mid Point Flurometer	3/4/2015 19:25	0
Mid Point Flurometer	3/4/2015 19:26	0
Mid Point Flurometer	3/4/2015 19:27	0
Mid Point Flurometer	3/4/2015 19:28	0
Mid Point Flurometer	3/4/2015 19:29	0
Mid Point Flurometer	3/4/2015 19:30	0
Mid Point Flurometer	3/4/2015 19:31	0
Mid Point Flurometer	3/4/2015 19:32	0
Mid Point Flurometer	3/4/2015 19:33	0
Mid Point Flurometer	3/4/2015 19:34	0
Mid Point Flurometer	3/4/2015 19:35	0
Mid Point Flurometer	3/4/2015 19:36	0
Mid Point Flurometer	3/4/2015 19:37	0
Mid Point Flurometer	3/4/2015 19:38	0
Mid Point Flurometer	3/4/2015 19:39	0
Mid Point Flurometer	3/4/2015 19:40	0
Mid Point Flurometer	3/4/2015 19:41	0
Mid Point Flurometer	3/4/2015 19:42	0
Mid Point Flurometer	3/4/2015 19:43	0
Mid Point Flurometer	3/4/2015 19:44	0
Mid Point Flurometer	3/4/2015 19:45	0
Mid Point Flurometer	3/4/2015 19:46	0
Mid Point Flurometer	3/4/2015 19:47	0
Mid Point Flurometer	3/4/2015 19:48	0
Mid Point Flurometer	3/4/2015 19:49	0
Mid Point Flurometer	3/4/2015 19:50	0
Mid Point Flurometer	3/4/2015 19:51	0
Mid Point Flurometer	3/4/2015 19:52	0
Mid Point Flurometer	3/4/2015 19:53	0
Mid Point Flurometer	3/4/2015 19:54	0
Mid Point Flurometer	3/4/2015 19:55	0
Mid Point Flurometer	3/4/2015 19:56	0
Mid Point Flurometer	3/4/2015 19:57	0
Mid Point Flurometer	3/4/2015 19:58	0
Mid Point Flurometer	3/4/2015 19:59	0
Mid Point Flurometer	3/4/2015 20:00	0
Mid Point Flurometer	3/4/2015 20:01	0
Mid Point Flurometer	3/4/2015 20:02	0
Mid Point Flurometer	3/4/2015 20:03	0
Mid Point Flurometer	3/4/2015 20:04	0
Mid Point Flurometer	3/4/2015 20:05	0
Mid Point Flurometer	3/4/2015 20:06	0

Location	Date and Time	Rhodmaine Concentration Adjusted Concentration (ppb)
Mid Point Flurometer	3/4/2015 20:07	0
Mid Point Flurometer	3/4/2015 20:08	0
Mid Point Flurometer	3/4/2015 20:09	0
Mid Point Flurometer	3/4/2015 20:10	0
Mid Point Flurometer	3/4/2015 20:11	0
Mid Point Flurometer	3/4/2015 20:12	0
Mid Point Flurometer	3/4/2015 20:13	0
Mid Point Flurometer	3/4/2015 20:14	0
Mid Point Flurometer	3/4/2015 20:15	0
Mid Point Flurometer	3/4/2015 20:16	0
Mid Point Flurometer	3/4/2015 20:17	0.03
Mid Point Flurometer	3/4/2015 20:18	0
Mid Point Flurometer	3/4/2015 20:19	0
Mid Point Flurometer	3/4/2015 20:20	0
Mid Point Flurometer	3/4/2015 20:21	0
Mid Point Flurometer	3/4/2015 20:22	0
Mid Point Flurometer	3/4/2015 20:23	0
Mid Point Flurometer	3/4/2015 20:24	0
Mid Point Flurometer	3/4/2015 20:25	0
Mid Point Flurometer	3/4/2015 20:26	0
Mid Point Flurometer	3/4/2015 20:27	0
Mid Point Flurometer	3/4/2015 20:28	0
Mid Point Flurometer	3/4/2015 20:29	0
Mid Point Flurometer	3/4/2015 20:30	0
Mid Point Flurometer	3/4/2015 20:31	0
Mid Point Flurometer	3/4/2015 20:32	0
Mid Point Flurometer	3/4/2015 20:33	0
Mid Point Flurometer	3/4/2015 20:34	0
Mid Point Flurometer	3/4/2015 20:35	0
Mid Point Flurometer	3/4/2015 20:36	0
Mid Point Flurometer	3/4/2015 20:37	0
Mid Point Flurometer	3/4/2015 20:38	0
Mid Point Flurometer	3/4/2015 20:39	0
Mid Point Flurometer	3/4/2015 20:40	0
Mid Point Flurometer	3/4/2015 20:41	0
Mid Point Flurometer	3/4/2015 20:42	0
Mid Point Flurometer	3/4/2015 20:43	0
Mid Point Flurometer	3/4/2015 20:44	0
Mid Point Flurometer	3/4/2015 20:45	0
Mid Point Flurometer	3/4/2015 20:46	0
Mid Point Flurometer	3/4/2015 20:47	0
Mid Point Flurometer	3/4/2015 20:48	0
Mid Point Flurometer	3/4/2015 20:49	0
Mid Point Flurometer	3/4/2015 20:50	0
Mid Point Flurometer	3/4/2015 20:51	0
Mid Point Flurometer	3/4/2015 20:52	0

Location	Date and Time	Rhodmaine Concentration Adjusted Concentration (ppb)
Mid Point Flurometer	3/4/2015 20:53	0
Mid Point Flurometer	3/4/2015 20:54	0
Mid Point Flurometer	3/4/2015 20:55	0
Mid Point Flurometer	3/4/2015 20:56	0
Mid Point Flurometer	3/4/2015 20:57	0
Mid Point Flurometer	3/4/2015 20:58	0
Mid Point Flurometer	3/4/2015 20:59	0
Mid Point Flurometer	3/4/2015 21:00	0
Mid Point Flurometer	3/4/2015 21:01	0
Mid Point Flurometer	3/4/2015 21:02	0
Mid Point Flurometer	3/4/2015 21:03	0
Mid Point Flurometer	3/4/2015 21:04	0
Mid Point Flurometer	3/4/2015 21:05	0
Mid Point Flurometer	3/4/2015 21:06	0
Mid Point Flurometer	3/4/2015 21:07	0
Mid Point Flurometer	3/4/2015 21:08	0
Mid Point Flurometer	3/4/2015 21:09	0
Mid Point Flurometer	3/4/2015 21:10	0
Mid Point Flurometer	3/4/2015 21:11	0
Mid Point Flurometer	3/4/2015 21:12	0
Mid Point Flurometer	3/4/2015 21:13	0
Mid Point Flurometer	3/4/2015 21:14	0
Mid Point Flurometer	3/4/2015 21:15	0.03
Mid Point Flurometer	3/4/2015 21:16	0.03
Mid Point Flurometer	3/4/2015 21:17	0.05
Mid Point Flurometer	3/4/2015 21:18	0.07
Mid Point Flurometer	3/4/2015 21:19	0.09
Mid Point Flurometer	3/4/2015 21:20	0.17
Mid Point Flurometer	3/4/2015 21:21	0.16
Mid Point Flurometer	3/4/2015 21:22	0.2
Mid Point Flurometer	3/4/2015 21:23	0.24
Mid Point Flurometer	3/4/2015 21:24	0.27
Mid Point Flurometer	3/4/2015 21:25	0.36
Mid Point Flurometer	3/4/2015 21:26	0.39
Mid Point Flurometer	3/4/2015 21:27	0.48
Mid Point Flurometer	3/4/2015 21:28	0.55
Mid Point Flurometer	3/4/2015 21:29	0.57
Mid Point Flurometer	3/4/2015 21:30	0.66
Mid Point Flurometer	3/4/2015 21:31	0.8
Mid Point Flurometer	3/4/2015 21:32	0.86
Mid Point Flurometer	3/4/2015 21:33	1.01
Mid Point Flurometer	3/4/2015 21:34	1.07
Mid Point Flurometer	3/4/2015 21:35	1.12
Mid Point Flurometer	3/4/2015 21:36	1.22
Mid Point Flurometer	3/4/2015 21:37	1.38
Mid Point Flurometer	3/4/2015 21:38	1.48

Location	Date and Time	Rhodmaine Concentration Adjusted Concentration (ppb)
Mid Point Flurometer	3/4/2015 21:39	1.59
Mid Point Flurometer	3/4/2015 21:40	1.73
Mid Point Flurometer	3/4/2015 21:41	1.95
Mid Point Flurometer	3/4/2015 21:42	1.96
Mid Point Flurometer	3/4/2015 21:43	2.15
Mid Point Flurometer	3/4/2015 21:44	2.24
Mid Point Flurometer	3/4/2015 21:45	2.41
Mid Point Flurometer	3/4/2015 21:46	2.75
Mid Point Flurometer	3/4/2015 21:47	3.02
Mid Point Flurometer	3/4/2015 21:48	3.18
Mid Point Flurometer	3/4/2015 21:49	3.16
Mid Point Flurometer	3/4/2015 21:50	3.51
Mid Point Flurometer	3/4/2015 21:51	3.69
Mid Point Flurometer	3/4/2015 21:52	3.74
Mid Point Flurometer	3/4/2015 21:53	4.01
Mid Point Flurometer	3/4/2015 21:54	4.19
Mid Point Flurometer	3/4/2015 21:55	4.46
Mid Point Flurometer	3/4/2015 21:56	4.62
Mid Point Flurometer	3/4/2015 21:57	4.98
Mid Point Flurometer	3/4/2015 21:58	5.25
Mid Point Flurometer	3/4/2015 21:59	5.47
Mid Point Flurometer	3/4/2015 22:00	5.42
Mid Point Flurometer	3/4/2015 22:01	6.03
Mid Point Flurometer	3/4/2015 22:02	6.13
Mid Point Flurometer	3/4/2015 22:03	6.32
Mid Point Flurometer	3/4/2015 22:04	6.41
Mid Point Flurometer	3/4/2015 22:05	6.43
Mid Point Flurometer	3/4/2015 22:06	6.52
Mid Point Flurometer	3/4/2015 22:07	6.74
Mid Point Flurometer	3/4/2015 22:08	6.97
Mid Point Flurometer	3/4/2015 22:09	7.19
Mid Point Flurometer	3/4/2015 22:10	7.47
Mid Point Flurometer	3/4/2015 22:11	7.77
Mid Point Flurometer	3/4/2015 22:12	7.98
Mid Point Flurometer	3/4/2015 22:13	8.06
Mid Point Flurometer	3/4/2015 22:14	8.33
Mid Point Flurometer	3/4/2015 22:15	8.47
Mid Point Flurometer	3/4/2015 22:16	8.56
Mid Point Flurometer	3/4/2015 22:17	8.46
Mid Point Flurometer	3/4/2015 22:18	8.69
Mid Point Flurometer	3/4/2015 22:19	9.02
Mid Point Flurometer	3/4/2015 22:20	9.32
Mid Point Flurometer	3/4/2015 22:21	9.47
Mid Point Flurometer	3/4/2015 22:22	9.57
Mid Point Flurometer	3/4/2015 22:23	9.61
Mid Point Flurometer	3/4/2015 22:24	9.73

Location	Date and Time	Rhodmaine Concentration Adjusted Concentration (ppb)
Mid Point Flurometer	3/4/2015 22:25	9.7
Mid Point Flurometer	3/4/2015 22:26	9.99
Mid Point Flurometer	3/4/2015 22:27	10.15
Mid Point Flurometer	3/4/2015 22:28	10.27
Mid Point Flurometer	3/4/2015 22:29	10.3
Mid Point Flurometer	3/4/2015 22:30	10.26
Mid Point Flurometer	3/4/2015 22:31	10.55
Mid Point Flurometer	3/4/2015 22:32	10.68
Mid Point Flurometer	3/4/2015 22:33	10.7
Mid Point Flurometer	3/4/2015 22:34	10.52
Mid Point Flurometer	3/4/2015 22:35	10.61
Mid Point Flurometer	3/4/2015 22:36	10.73
Mid Point Flurometer	3/4/2015 22:37	10.87
Mid Point Flurometer	3/4/2015 22:38	10.93
Mid Point Flurometer	3/4/2015 22:39	10.95
Mid Point Flurometer	3/4/2015 22:40	11.01
Mid Point Flurometer	3/4/2015 22:41	10.99
Mid Point Flurometer	3/4/2015 22:42	11.03
Mid Point Flurometer	3/4/2015 22:43	11.06
Mid Point Flurometer	3/4/2015 22:44	11.1
Mid Point Flurometer	3/4/2015 22:45	11.13
Mid Point Flurometer	3/4/2015 22:46	11.12
Mid Point Flurometer	3/4/2015 22:47	11.12
Mid Point Flurometer	3/4/2015 22:48	11.15
Mid Point Flurometer	3/4/2015 22:49	11.11
Mid Point Flurometer	3/4/2015 22:50	11.15
Mid Point Flurometer	3/4/2015 22:51	11.12
Mid Point Flurometer	3/4/2015 22:52	11.1
Mid Point Flurometer	3/4/2015 22:53	11.1
Mid Point Flurometer	3/4/2015 22:54	11.05
Mid Point Flurometer	3/4/2015 22:55	11.05
Mid Point Flurometer	3/4/2015 22:56	11.01
Mid Point Flurometer	3/4/2015 22:57	10.97
Mid Point Flurometer	3/4/2015 22:58	10.91
Mid Point Flurometer	3/4/2015 22:59	10.91
Mid Point Flurometer	3/4/2015 23:00	10.9
Mid Point Flurometer	3/4/2015 23:01	10.87
Mid Point Flurometer	3/4/2015 23:02	10.81
Mid Point Flurometer	3/4/2015 23:03	10.74
Mid Point Flurometer	3/4/2015 23:04	10.7
Mid Point Flurometer	3/4/2015 23:05	10.63
Mid Point Flurometer	3/4/2015 23:06	10.57
Mid Point Flurometer	3/4/2015 23:07	10.51
Mid Point Flurometer	3/4/2015 23:08	10.45
Mid Point Flurometer	3/4/2015 23:09	10.41
Mid Point Flurometer	3/4/2015 23:10	10.34

Location	Date and Time	Rhodmaine Concentration Adjusted Concentration (ppb)
Mid Point Flurometer	3/4/2015 23:11	10.33
Mid Point Flurometer	3/4/2015 23:12	10.22
Mid Point Flurometer	3/4/2015 23:13	10.16
Mid Point Flurometer	3/4/2015 23:14	10.18
Mid Point Flurometer	3/4/2015 23:15	10.05
Mid Point Flurometer	3/4/2015 23:16	10.02
Mid Point Flurometer	3/4/2015 23:17	9.88
Mid Point Flurometer	3/4/2015 23:18	9.78
Mid Point Flurometer	3/4/2015 23:19	9.73
Mid Point Flurometer	3/4/2015 23:20	9.63
Mid Point Flurometer	3/4/2015 23:21	9.57
Mid Point Flurometer	3/4/2015 23:22	9.51
Mid Point Flurometer	3/4/2015 23:23	9.54
Mid Point Flurometer	3/4/2015 23:24	9.4
Mid Point Flurometer	3/4/2015 23:25	9.27
Mid Point Flurometer	3/4/2015 23:26	9.15
Mid Point Flurometer	3/4/2015 23:27	9.16
Mid Point Flurometer	3/4/2015 23:28	9.08
Mid Point Flurometer	3/4/2015 23:29	8.97
Mid Point Flurometer	3/4/2015 23:30	8.9
Mid Point Flurometer	3/4/2015 23:31	8.87
Mid Point Flurometer	3/4/2015 23:32	8.82
Mid Point Flurometer	3/4/2015 23:33	8.76
Mid Point Flurometer	3/4/2015 23:34	8.67
Mid Point Flurometer	3/4/2015 23:35	8.52
Mid Point Flurometer	3/4/2015 23:36	8.5
Mid Point Flurometer	3/4/2015 23:37	8.42
Mid Point Flurometer	3/4/2015 23:38	8.33
Mid Point Flurometer	3/4/2015 23:39	8.2
Mid Point Flurometer	3/4/2015 23:40	8.14
Mid Point Flurometer	3/4/2015 23:41	8.1
Mid Point Flurometer	3/4/2015 23:42	8.06
Mid Point Flurometer	3/4/2015 23:43	8.02
Mid Point Flurometer	3/4/2015 23:44	7.99
Mid Point Flurometer	3/4/2015 23:45	7.87
Mid Point Flurometer	3/4/2015 23:46	7.8
Mid Point Flurometer	3/4/2015 23:47	7.83
Mid Point Flurometer	3/4/2015 23:48	7.71
Mid Point Flurometer	3/4/2015 23:49	7.7
Mid Point Flurometer	3/4/2015 23:50	7.5
Mid Point Flurometer	3/4/2015 23:51	7.51
Mid Point Flurometer	3/4/2015 23:52	7.46
Mid Point Flurometer	3/4/2015 23:53	7.38
Mid Point Flurometer	3/4/2015 23:54	7.33
Mid Point Flurometer	3/4/2015 23:55	7.24
Mid Point Flurometer	3/4/2015 23:56	7.19

Location	Date and Time	Rhodmaine Concentration Adjusted Concentration (ppb)
Mid Point Flurometer	3/4/2015 23:57	7.1
Mid Point Flurometer	3/4/2015 23:58	7.06
Mid Point Flurometer	3/4/2015 23:59	7.01
Mid Point Flurometer	3/5/2015 0:00	6.94
Mid Point Flurometer	3/5/2015 0:01	6.91
Mid Point Flurometer	3/5/2015 0:02	6.85
Mid Point Flurometer	3/5/2015 0:03	6.78
Mid Point Flurometer	3/5/2015 0:04	6.72
Mid Point Flurometer	3/5/2015 0:05	6.7
Mid Point Flurometer	3/5/2015 0:06	6.7
Mid Point Flurometer	3/5/2015 0:07	7.02
Mid Point Flurometer	3/5/2015 0:08	6.51
Mid Point Flurometer	3/5/2015 0:09	6.49
Mid Point Flurometer	3/5/2015 0:10	6.49
Mid Point Flurometer	3/5/2015 0:11	6.46
Mid Point Flurometer	3/5/2015 0:12	6.41
Mid Point Flurometer	3/5/2015 0:13	6.33
Mid Point Flurometer	3/5/2015 0:14	6.32
Mid Point Flurometer	3/5/2015 0:15	6.3
Mid Point Flurometer	3/5/2015 0:16	6.18
Mid Point Flurometer	3/5/2015 0:17	6.19
Mid Point Flurometer	3/5/2015 0:18	6.15
Mid Point Flurometer	3/5/2015 0:19	6.15
Mid Point Flurometer	3/5/2015 0:20	6.08
Mid Point Flurometer	3/5/2015 0:21	6.11
Mid Point Flurometer	3/5/2015 0:22	6.09
Mid Point Flurometer	3/5/2015 0:23	6.05
Mid Point Flurometer	3/5/2015 0:24	5.98
Mid Point Flurometer	3/5/2015 0:25	5.96
Mid Point Flurometer	3/5/2015 0:26	5.88
Mid Point Flurometer	3/5/2015 0:27	5.88
Mid Point Flurometer	3/5/2015 0:28	5.83
Mid Point Flurometer	3/5/2015 0:29	5.82
Mid Point Flurometer	3/5/2015 0:30	5.77
Mid Point Flurometer	3/5/2015 0:31	5.77
Mid Point Flurometer	3/5/2015 0:32	5.75
Mid Point Flurometer	3/5/2015 0:33	5.69
Mid Point Flurometer	3/5/2015 0:34	5.69
Mid Point Flurometer	3/5/2015 0:35	5.65
Mid Point Flurometer	3/5/2015 0:36	5.63
Mid Point Flurometer	3/5/2015 0:37	5.63
Mid Point Flurometer	3/5/2015 0:38	5.61
Mid Point Flurometer	3/5/2015 0:39	5.59
Mid Point Flurometer	3/5/2015 0:40	5.55
Mid Point Flurometer	3/5/2015 0:41	5.53
Mid Point Flurometer	3/5/2015 0:42	5.5

Location	Date and Time	Rhodmaine Concentration Adjusted Concentration (ppb)
Mid Point Flurometer	3/5/2015 0:43	5.48
Mid Point Flurometer	3/5/2015 0:44	5.45
Mid Point Flurometer	3/5/2015 0:45	5.45
Mid Point Flurometer	3/5/2015 0:46	5.39
Mid Point Flurometer	3/5/2015 0:47	5.37
Mid Point Flurometer	3/5/2015 0:48	5.35
Mid Point Flurometer	3/5/2015 0:49	5.35
Mid Point Flurometer	3/5/2015 0:50	5.29
Mid Point Flurometer	3/5/2015 0:51	5.29
Mid Point Flurometer	3/5/2015 0:52	5.3
Mid Point Flurometer	3/5/2015 0:53	5.29
Mid Point Flurometer	3/5/2015 0:54	5.2
Mid Point Flurometer	3/5/2015 0:55	5.23
Mid Point Flurometer	3/5/2015 0:56	5.19
Mid Point Flurometer	3/5/2015 0:57	5.19
Mid Point Flurometer	3/5/2015 0:58	5.1
Mid Point Flurometer	3/5/2015 0:59	5.1
Mid Point Flurometer	3/5/2015 1:00	5.06
Mid Point Flurometer	3/5/2015 1:01	5.07
Mid Point Flurometer	3/5/2015 1:02	5.07
Mid Point Flurometer	3/5/2015 1:03	5.05
Mid Point Flurometer	3/5/2015 1:04	5.03
Mid Point Flurometer	3/5/2015 1:05	5.02
Mid Point Flurometer	3/5/2015 1:06	4.98
Mid Point Flurometer	3/5/2015 1:07	4.98
Mid Point Flurometer	3/5/2015 1:08	4.93
Mid Point Flurometer	3/5/2015 1:09	4.91
Mid Point Flurometer	3/5/2015 1:10	4.9
Mid Point Flurometer	3/5/2015 1:11	4.86
Mid Point Flurometer	3/5/2015 1:12	4.87
Mid Point Flurometer	3/5/2015 1:13	4.83
Mid Point Flurometer	3/5/2015 1:14	4.78
Mid Point Flurometer	3/5/2015 1:15	4.76
Mid Point Flurometer	3/5/2015 1:16	4.74
Mid Point Flurometer	3/5/2015 1:17	4.73
Mid Point Flurometer	3/5/2015 1:18	4.71
Mid Point Flurometer	3/5/2015 1:19	4.67
Mid Point Flurometer	3/5/2015 1:20	4.65
Mid Point Flurometer	3/5/2015 1:21	4.65
Mid Point Flurometer	3/5/2015 1:22	4.62
Mid Point Flurometer	3/5/2015 1:23	4.64
Mid Point Flurometer	3/5/2015 1:24	4.59
Mid Point Flurometer	3/5/2015 1:25	4.56
Mid Point Flurometer	3/5/2015 1:26	4.53
Mid Point Flurometer	3/5/2015 1:27	4.5
Mid Point Flurometer	3/5/2015 1:28	4.49

Location	Date and Time	Rhodmaine Concentration Adjusted Concentration (ppb)
Mid Point Flurometer	3/5/2015 1:29	4.46
Mid Point Flurometer	3/5/2015 1:30	4.44
Mid Point Flurometer	3/5/2015 1:31	4.41
Mid Point Flurometer	3/5/2015 1:32	4.41
Mid Point Flurometer	3/5/2015 1:33	4.37
Mid Point Flurometer	3/5/2015 1:34	4.34
Mid Point Flurometer	3/5/2015 1:35	4.33
Mid Point Flurometer	3/5/2015 1:36	4.29
Mid Point Flurometer	3/5/2015 1:37	4.27
Mid Point Flurometer	3/5/2015 1:38	4.27
Mid Point Flurometer	3/5/2015 1:39	4.21
Mid Point Flurometer	3/5/2015 1:40	4.21
Mid Point Flurometer	3/5/2015 1:41	4.19
Mid Point Flurometer	3/5/2015 1:42	4.16
Mid Point Flurometer	3/5/2015 1:43	4.14
Mid Point Flurometer	3/5/2015 1:44	4.11
Mid Point Flurometer	3/5/2015 1:45	4.07
Mid Point Flurometer	3/5/2015 1:46	4.07
Mid Point Flurometer	3/5/2015 1:47	4.03
Mid Point Flurometer	3/5/2015 1:48	4.04
Mid Point Flurometer	3/5/2015 1:49	4.01
Mid Point Flurometer	3/5/2015 1:50	3.97
Mid Point Flurometer	3/5/2015 1:51	3.96
Mid Point Flurometer	3/5/2015 1:52	3.94
Mid Point Flurometer	3/5/2015 1:53	3.93
Mid Point Flurometer	3/5/2015 1:54	3.91
Mid Point Flurometer	3/5/2015 1:55	3.88
Mid Point Flurometer	3/5/2015 1:56	3.86
Mid Point Flurometer	3/5/2015 1:57	3.87
Mid Point Flurometer	3/5/2015 1:58	3.82
Mid Point Flurometer	3/5/2015 1:59	3.78
Mid Point Flurometer	3/5/2015 2:00	3.76
Mid Point Flurometer	3/5/2015 2:01	3.71
Mid Point Flurometer	3/5/2015 2:02	3.72
Mid Point Flurometer	3/5/2015 2:03	3.67
Mid Point Flurometer	3/5/2015 2:04	3.67
Mid Point Flurometer	3/5/2015 2:05	3.65
Mid Point Flurometer	3/5/2015 2:06	3.64
Mid Point Flurometer	3/5/2015 2:07	3.59
Mid Point Flurometer	3/5/2015 2:08	3.54
Mid Point Flurometer	3/5/2015 2:09	3.52
Mid Point Flurometer	3/5/2015 2:10	3.53
Mid Point Flurometer	3/5/2015 2:11	3.5
Mid Point Flurometer	3/5/2015 2:12	3.5
Mid Point Flurometer	3/5/2015 2:13	3.46
Mid Point Flurometer	3/5/2015 2:14	3.4

Location	Date and Time	Rhodmaine Concentration Adjusted Concentration (ppb)
Mid Point Flurometer	3/5/2015 2:15	3.4
Mid Point Flurometer	3/5/2015 2:16	3.36
Mid Point Flurometer	3/5/2015 2:17	3.35
Mid Point Flurometer	3/5/2015 2:18	3.34
Mid Point Flurometer	3/5/2015 2:19	3.33
Mid Point Flurometer	3/5/2015 2:20	3.32
Mid Point Flurometer	3/5/2015 2:21	3.28
Mid Point Flurometer	3/5/2015 2:22	3.23
Mid Point Flurometer	3/5/2015 2:23	3.22
Mid Point Flurometer	3/5/2015 2:24	3.19
Mid Point Flurometer	3/5/2015 2:25	3.17
Mid Point Flurometer	3/5/2015 2:26	3.19
Mid Point Flurometer	3/5/2015 2:27	3.16
Mid Point Flurometer	3/5/2015 2:28	3.11
Mid Point Flurometer	3/5/2015 2:29	3.08
Mid Point Flurometer	3/5/2015 2:30	3.05
Mid Point Flurometer	3/5/2015 2:31	3.04
Mid Point Flurometer	3/5/2015 2:32	3.01
Mid Point Flurometer	3/5/2015 2:33	2.99
Mid Point Flurometer	3/5/2015 2:34	2.98
Mid Point Flurometer	3/5/2015 2:35	2.92
Mid Point Flurometer	3/5/2015 2:36	2.92
Mid Point Flurometer	3/5/2015 2:37	2.89
Mid Point Flurometer	3/5/2015 2:38	2.87
Mid Point Flurometer	3/5/2015 2:39	2.85
Mid Point Flurometer	3/5/2015 2:40	2.83
Mid Point Flurometer	3/5/2015 2:41	2.81
Mid Point Flurometer	3/5/2015 2:42	2.78
Mid Point Flurometer	3/5/2015 2:43	2.83
Mid Point Flurometer	3/5/2015 2:44	2.76
Mid Point Flurometer	3/5/2015 2:45	2.71
Mid Point Flurometer	3/5/2015 2:46	2.7
Mid Point Flurometer	3/5/2015 2:47	2.7
Mid Point Flurometer	3/5/2015 2:48	2.66
Mid Point Flurometer	3/5/2015 2:49	2.67
Mid Point Flurometer	3/5/2015 2:50	2.61
Mid Point Flurometer	3/5/2015 2:51	2.6
Mid Point Flurometer	3/5/2015 2:52	2.57
Mid Point Flurometer	3/5/2015 2:53	2.58
Mid Point Flurometer	3/5/2015 2:54	2.55
Mid Point Flurometer	3/5/2015 2:55	2.53
Mid Point Flurometer	3/5/2015 2:56	2.52
Mid Point Flurometer	3/5/2015 2:57	2.5
Mid Point Flurometer	3/5/2015 2:58	2.47
Mid Point Flurometer	3/5/2015 2:59	2.46
Mid Point Flurometer	3/5/2015 3:00	2.44

Location	Date and Time	Rhodmaine Concentration Adjusted Concentration (ppb)
Mid Point Flurometer	3/5/2015 3:01	2.41
Mid Point Flurometer	3/5/2015 3:02	2.4
Mid Point Flurometer	3/5/2015 3:03	2.4
Mid Point Flurometer	3/5/2015 3:04	2.38
Mid Point Flurometer	3/5/2015 3:05	2.36
Mid Point Flurometer	3/5/2015 3:06	2.44
Mid Point Flurometer	3/5/2015 3:07	2.31
Mid Point Flurometer	3/5/2015 3:08	2.3
Mid Point Flurometer	3/5/2015 3:09	2.31
Mid Point Flurometer	3/5/2015 3:10	2.28
Mid Point Flurometer	3/5/2015 3:11	2.25
Mid Point Flurometer	3/5/2015 3:12	2.22
Mid Point Flurometer	3/5/2015 3:13	2.21
Mid Point Flurometer	3/5/2015 3:14	2.21
Mid Point Flurometer	3/5/2015 3:15	2.19
Mid Point Flurometer	3/5/2015 3:16	2.15
Mid Point Flurometer	3/5/2015 3:17	2.13
Mid Point Flurometer	3/5/2015 3:18	2.12
Mid Point Flurometer	3/5/2015 3:19	2.13
Mid Point Flurometer	3/5/2015 3:20	2.13
Mid Point Flurometer	3/5/2015 3:21	2.09
Mid Point Flurometer	3/5/2015 3:22	2.1
Mid Point Flurometer	3/5/2015 3:23	2.08
Mid Point Flurometer	3/5/2015 3:24	2.06
Mid Point Flurometer	3/5/2015 3:25	2.05
Mid Point Flurometer	3/5/2015 3:26	2.02
Mid Point Flurometer	3/5/2015 3:27	2.03
Mid Point Flurometer	3/5/2015 3:28	2.01
Mid Point Flurometer	3/5/2015 3:29	1.99
Mid Point Flurometer	3/5/2015 3:30	2.01
Mid Point Flurometer	3/5/2015 3:31	1.97
Mid Point Flurometer	3/5/2015 3:32	1.97
Mid Point Flurometer	3/5/2015 3:33	1.94
Mid Point Flurometer	3/5/2015 3:34	1.9
Mid Point Flurometer	3/5/2015 3:35	1.91
Mid Point Flurometer	3/5/2015 3:36	1.92
Mid Point Flurometer	3/5/2015 3:37	1.89
Mid Point Flurometer	3/5/2015 3:38	1.91
Mid Point Flurometer	3/5/2015 3:39	1.86
Mid Point Flurometer	3/5/2015 3:40	1.84
Mid Point Flurometer	3/5/2015 3:41	1.82
Mid Point Flurometer	3/5/2015 3:42	1.83
Mid Point Flurometer	3/5/2015 3:43	1.84
Mid Point Flurometer	3/5/2015 3:44	1.79
Mid Point Flurometer	3/5/2015 3:45	1.79
Mid Point Flurometer	3/5/2015 3:46	1.77

Location	Date and Time	Rhodmaine Concentration Adjusted Concentration (ppb)
Mid Point Flurometer	3/5/2015 3:47	1.77
Mid Point Flurometer	3/5/2015 3:48	1.78
Mid Point Flurometer	3/5/2015 3:49	1.75
Mid Point Flurometer	3/5/2015 3:50	1.77
Mid Point Flurometer	3/5/2015 3:51	1.73
Mid Point Flurometer	3/5/2015 3:52	1.72
Mid Point Flurometer	3/5/2015 3:53	1.7
Mid Point Flurometer	3/5/2015 3:54	1.7
Mid Point Flurometer	3/5/2015 3:55	1.69
Mid Point Flurometer	3/5/2015 3:56	1.7
Mid Point Flurometer	3/5/2015 3:57	1.7
Mid Point Flurometer	3/5/2015 3:58	1.67
Mid Point Flurometer	3/5/2015 3:59	1.67
Mid Point Flurometer	3/5/2015 4:00	1.65
Mid Point Flurometer	3/5/2015 4:01	1.64
Mid Point Flurometer	3/5/2015 4:02	1.65
Mid Point Flurometer	3/5/2015 4:03	1.63
Mid Point Flurometer	3/5/2015 4:04	1.63
Mid Point Flurometer	3/5/2015 4:05	1.62
Mid Point Flurometer	3/5/2015 4:06	1.6
Mid Point Flurometer	3/5/2015 4:07	1.6
Mid Point Flurometer	3/5/2015 4:08	1.58
Mid Point Flurometer	3/5/2015 4:09	1.59
Mid Point Flurometer	3/5/2015 4:10	1.59
Mid Point Flurometer	3/5/2015 4:11	1.58
Mid Point Flurometer	3/5/2015 4:12	1.56
Mid Point Flurometer	3/5/2015 4:13	1.56
Mid Point Flurometer	3/5/2015 4:14	1.53
Mid Point Flurometer	3/5/2015 4:15	1.53
Mid Point Flurometer	3/5/2015 4:16	1.55
Mid Point Flurometer	3/5/2015 4:17	1.53
Mid Point Flurometer	3/5/2015 4:18	1.53
Mid Point Flurometer	3/5/2015 4:19	1.51
Mid Point Flurometer	3/5/2015 4:20	1.5
Mid Point Flurometer	3/5/2015 4:21	1.55
Mid Point Flurometer	3/5/2015 4:22	1.51
Mid Point Flurometer	3/5/2015 4:23	1.5
Mid Point Flurometer	3/5/2015 4:24	1.51
Mid Point Flurometer	3/5/2015 4:25	1.47
Mid Point Flurometer	3/5/2015 4:26	1.47
Mid Point Flurometer	3/5/2015 4:27	1.47
Mid Point Flurometer	3/5/2015 4:28	1.46
Mid Point Flurometer	3/5/2015 4:29	1.46
Mid Point Flurometer	3/5/2015 4:30	1.47
Mid Point Flurometer	3/5/2015 4:31	1.47
Mid Point Flurometer	3/5/2015 4:32	1.43

Location	Date and Time	Rhodmaine Concentration Adjusted Concentration (ppb)
Mid Point Flurometer	3/5/2015 4:33	1.52
Mid Point Flurometer	3/5/2015 4:34	1.43
Mid Point Flurometer	3/5/2015 4:35	1.42
Mid Point Flurometer	3/5/2015 4:36	1.43
Mid Point Flurometer	3/5/2015 4:37	1.42
Mid Point Flurometer	3/5/2015 4:38	1.42
Mid Point Flurometer	3/5/2015 4:39	1.4
Mid Point Flurometer	3/5/2015 4:40	1.41
Mid Point Flurometer	3/5/2015 4:41	1.43
Mid Point Flurometer	3/5/2015 4:42	1.4
Mid Point Flurometer	3/5/2015 4:43	1.4
Mid Point Flurometer	3/5/2015 4:44	1.37
Mid Point Flurometer	3/5/2015 4:45	1.38
Mid Point Flurometer	3/5/2015 4:46	1.39
Mid Point Flurometer	3/5/2015 4:47	1.38
Mid Point Flurometer	3/5/2015 4:48	1.36
Mid Point Flurometer	3/5/2015 4:49	1.37
Mid Point Flurometer	3/5/2015 4:50	1.35
Mid Point Flurometer	3/5/2015 4:51	1.36
Mid Point Flurometer	3/5/2015 4:52	1.35
Mid Point Flurometer	3/5/2015 4:53	1.35
Mid Point Flurometer	3/5/2015 4:54	1.35
Mid Point Flurometer	3/5/2015 4:55	1.33
Mid Point Flurometer	3/5/2015 4:56	1.34
Mid Point Flurometer	3/5/2015 4:57	1.29
Mid Point Flurometer	3/5/2015 4:58	1.34
Mid Point Flurometer	3/5/2015 4:59	1.3
Mid Point Flurometer	3/5/2015 5:00	1.34
Mid Point Flurometer	3/5/2015 5:01	1.3
Mid Point Flurometer	3/5/2015 5:02	1.29
Mid Point Flurometer	3/5/2015 5:03	1.31
Mid Point Flurometer	3/5/2015 5:04	1.3
Mid Point Flurometer	3/5/2015 5:05	1.29
Mid Point Flurometer	3/5/2015 5:06	1.3
Mid Point Flurometer	3/5/2015 5:07	1.28
Mid Point Flurometer	3/5/2015 5:08	1.27
Mid Point Flurometer	3/5/2015 5:09	1.3
Mid Point Flurometer	3/5/2015 5:10	1.27
Mid Point Flurometer	3/5/2015 5:11	1.29
Mid Point Flurometer	3/5/2015 5:12	1.27
Mid Point Flurometer	3/5/2015 5:13	1.25
Mid Point Flurometer	3/5/2015 5:14	1.24
Mid Point Flurometer	3/5/2015 5:15	1.24
Mid Point Flurometer	3/5/2015 5:16	1.25
Mid Point Flurometer	3/5/2015 5:17	1.26
Mid Point Flurometer	3/5/2015 5:18	1.22

Location	Date and Time	Rhodmaine Concentration Adjusted Concentration (ppb)
Mid Point Flurometer	3/5/2015 5:19	1.22
Mid Point Flurometer	3/5/2015 5:20	1.24
Mid Point Flurometer	3/5/2015 5:21	1.22
Mid Point Flurometer	3/5/2015 5:22	1.23
Mid Point Flurometer	3/5/2015 5:23	1.24
Mid Point Flurometer	3/5/2015 5:24	1.21
Mid Point Flurometer	3/5/2015 5:25	1.22
Mid Point Flurometer	3/5/2015 5:26	1.21
Mid Point Flurometer	3/5/2015 5:27	1.23
Mid Point Flurometer	3/5/2015 5:28	1.19
Mid Point Flurometer	3/5/2015 5:29	1.19
Mid Point Flurometer	3/5/2015 5:30	1.19
Mid Point Flurometer	3/5/2015 5:31	1.21
Mid Point Flurometer	3/5/2015 5:32	1.24
Mid Point Flurometer	3/5/2015 5:33	1.18
Mid Point Flurometer	3/5/2015 5:34	1.2
Mid Point Flurometer	3/5/2015 5:35	1.18
Mid Point Flurometer	3/5/2015 5:36	1.19
Mid Point Flurometer	3/5/2015 5:37	1.15
Mid Point Flurometer	3/5/2015 5:38	1.16
Mid Point Flurometer	3/5/2015 5:39	1.16
Mid Point Flurometer	3/5/2015 5:40	1.17
Mid Point Flurometer	3/5/2015 5:41	1.16
Mid Point Flurometer	3/5/2015 5:42	1.15
Mid Point Flurometer	3/5/2015 5:43	1.15
Mid Point Flurometer	3/5/2015 5:44	1.14
Mid Point Flurometer	3/5/2015 5:45	1.15
Mid Point Flurometer	3/5/2015 5:46	1.13
Mid Point Flurometer	3/5/2015 5:47	1.14
Mid Point Flurometer	3/5/2015 5:48	1.12
Mid Point Flurometer	3/5/2015 5:49	1.14
Mid Point Flurometer	3/5/2015 5:50	1.16
Mid Point Flurometer	3/5/2015 5:51	1.13
Mid Point Flurometer	3/5/2015 5:52	1.13
Mid Point Flurometer	3/5/2015 5:53	1.13
Mid Point Flurometer	3/5/2015 5:54	1.11
Mid Point Flurometer	3/5/2015 5:55	1.12
Mid Point Flurometer	3/5/2015 5:56	1.1
Mid Point Flurometer	3/5/2015 5:57	1.11
Mid Point Flurometer	3/5/2015 5:58	1.14
Mid Point Flurometer	3/5/2015 5:59	1.12
Mid Point Flurometer	3/5/2015 6:00	1.09
Mid Point Flurometer	3/5/2015 6:01	1.11
Mid Point Flurometer	3/5/2015 6:02	1.17
Mid Point Flurometer	3/5/2015 6:03	1.11
Mid Point Flurometer	3/5/2015 6:04	1.08

Location	Date and Time	Rhodmaine Concentration Adjusted Concentration (ppb)
Mid Point Flurometer	3/5/2015 6:05	1.16
Mid Point Flurometer	3/5/2015 6:06	1.07
Mid Point Flurometer	3/5/2015 6:07	1.07
Mid Point Flurometer	3/5/2015 6:08	1.13
Mid Point Flurometer	3/5/2015 6:09	1.07
Mid Point Flurometer	3/5/2015 6:10	1.06
Mid Point Flurometer	3/5/2015 6:11	1.06
Mid Point Flurometer	3/5/2015 6:12	1.05
Mid Point Flurometer	3/5/2015 6:13	1.04
Mid Point Flurometer	3/5/2015 6:14	1.04
Mid Point Flurometer	3/5/2015 6:15	1.04
Mid Point Flurometer	3/5/2015 6:16	1.04
Mid Point Flurometer	3/5/2015 6:17	1.04
Mid Point Flurometer	3/5/2015 6:18	1.03
Mid Point Flurometer	3/5/2015 6:19	1.13
Mid Point Flurometer	3/5/2015 6:20	1.05
Mid Point Flurometer	3/5/2015 6:21	1.04
Mid Point Flurometer	3/5/2015 6:22	1.03
Mid Point Flurometer	3/5/2015 6:23	1.01
Mid Point Flurometer	3/5/2015 6:24	1.03
Mid Point Flurometer	3/5/2015 6:25	1.04
Mid Point Flurometer	3/5/2015 6:26	1.03
Mid Point Flurometer	3/5/2015 6:27	1
Mid Point Flurometer	3/5/2015 6:28	1
Mid Point Flurometer	3/5/2015 6:29	1.03
Mid Point Flurometer	3/5/2015 6:30	1.01
Mid Point Flurometer	3/5/2015 6:31	1
Mid Point Flurometer	3/5/2015 6:32	1
Mid Point Flurometer	3/5/2015 6:33	1.03
Mid Point Flurometer	3/5/2015 6:34	0.99
Mid Point Flurometer	3/5/2015 6:35	0.98
Mid Point Flurometer	3/5/2015 6:36	0.98
Mid Point Flurometer	3/5/2015 6:37	0.97
Mid Point Flurometer	3/5/2015 6:38	0.99
Mid Point Flurometer	3/5/2015 6:39	0.99
Mid Point Flurometer	3/5/2015 6:40	0.99
Mid Point Flurometer	3/5/2015 6:41	0.95
Mid Point Flurometer	3/5/2015 6:42	0.98
Mid Point Flurometer	3/5/2015 6:43	0.98
Mid Point Flurometer	3/5/2015 6:44	0.94
Mid Point Flurometer	3/5/2015 6:45	0.96
Mid Point Flurometer	3/5/2015 6:46	0.93
Mid Point Flurometer	3/5/2015 6:47	0.93
Mid Point Flurometer	3/5/2015 6:48	0.93
Mid Point Flurometer	3/5/2015 6:49	0.94
Mid Point Flurometer	3/5/2015 6:50	0.93

Location	Date and Time	Rhodmaine Concentration Adjusted Concentration (ppb)
Mid Point Flurometer	3/5/2015 6:51	0.93
Mid Point Flurometer	3/5/2015 6:52	0.99
Mid Point Flurometer	3/5/2015 6:53	0.92
Mid Point Flurometer	3/5/2015 6:54	0.91
Mid Point Flurometer	3/5/2015 6:55	0.9
Mid Point Flurometer	3/5/2015 6:56	0.92
Mid Point Flurometer	3/5/2015 6:57	0.91
Mid Point Flurometer	3/5/2015 6:58	0.92
Mid Point Flurometer	3/5/2015 6:59	0.91
Mid Point Flurometer	3/5/2015 7:00	0.94
Mid Point Flurometer	3/5/2015 7:01	0.91
Mid Point Flurometer	3/5/2015 7:02	0.91
Mid Point Flurometer	3/5/2015 7:03	0.9
Mid Point Flurometer	3/5/2015 7:04	0.9
Mid Point Flurometer	3/5/2015 7:05	0.88
Mid Point Flurometer	3/5/2015 7:06	0.88
Mid Point Flurometer	3/5/2015 7:07	0.89
Mid Point Flurometer	3/5/2015 7:08	0.89
Mid Point Flurometer	3/5/2015 7:09	0.9
Mid Point Flurometer	3/5/2015 7:10	0.89
Mid Point Flurometer	3/5/2015 7:11	0.88
Mid Point Flurometer	3/5/2015 7:12	0.87
Mid Point Flurometer	3/5/2015 7:13	0.86
Mid Point Flurometer	3/5/2015 7:14	0.87
Mid Point Flurometer	3/5/2015 7:15	0.91
Mid Point Flurometer	3/5/2015 7:16	0.87
Mid Point Flurometer	3/5/2015 7:17	0.84
Mid Point Flurometer	3/5/2015 7:18	0.85
Mid Point Flurometer	3/5/2015 7:19	0.86
Mid Point Flurometer	3/5/2015 7:20	0.82
Mid Point Flurometer	3/5/2015 7:21	0.84
Mid Point Flurometer	3/5/2015 7:22	0.87
Mid Point Flurometer	3/5/2015 7:23	0.85
Mid Point Flurometer	3/5/2015 7:24	0.84
Mid Point Flurometer	3/5/2015 7:25	0.81
Mid Point Flurometer	3/5/2015 7:26	0.83
Mid Point Flurometer	3/5/2015 7:27	0.81
Mid Point Flurometer	3/5/2015 7:28	0.82
Mid Point Flurometer	3/5/2015 7:29	0.83
Mid Point Flurometer	3/5/2015 7:30	0.81
Mid Point Flurometer	3/5/2015 7:31	0.82
Mid Point Flurometer	3/5/2015 7:32	0.82
Mid Point Flurometer	3/5/2015 7:33	0.79
Mid Point Flurometer	3/5/2015 7:34	0.79
Mid Point Flurometer	3/5/2015 7:35	0.75
Mid Point Flurometer	3/5/2015 7:36	0.83

Location	Date and Time	Rhodmaine Concentration Adjusted Concentration (ppb)
Mid Point Flurometer	3/5/2015 7:37	0.81
Mid Point Flurometer	3/5/2015 7:38	0.81
Mid Point Flurometer	3/5/2015 7:39	0.79
Mid Point Flurometer	3/5/2015 7:40	0.78
Mid Point Flurometer	3/5/2015 7:41	0.83
Mid Point Flurometer	3/5/2015 7:42	0.79
Mid Point Flurometer	3/5/2015 7:43	0.76
Mid Point Flurometer	3/5/2015 7:44	0.73
Mid Point Flurometer	3/5/2015 7:45	0.75
Mid Point Flurometer	3/5/2015 7:46	0.8
Mid Point Flurometer	3/5/2015 7:47	0.74
Mid Point Flurometer	3/5/2015 7:48	0.76
Mid Point Flurometer	3/5/2015 7:49	0.74
Mid Point Flurometer	3/5/2015 7:50	0.73
Mid Point Flurometer	3/5/2015 7:51	0.78
Mid Point Flurometer	3/5/2015 7:52	0.73
Mid Point Flurometer	3/5/2015 7:53	0.71
Mid Point Flurometer	3/5/2015 7:54	0.73
Mid Point Flurometer	3/5/2015 7:55	0.7
Mid Point Flurometer	3/5/2015 7:56	0.69
Mid Point Flurometer	3/5/2015 7:57	0.71
Mid Point Flurometer	3/5/2015 7:58	0.73
Mid Point Flurometer	3/5/2015 7:59	0.7
Mid Point Flurometer	3/5/2015 8:00	0.71
Mid Point Flurometer	3/5/2015 8:01	0.72
Mid Point Flurometer	3/5/2015 8:02	0.75
Mid Point Flurometer	3/5/2015 8:03	0.7
Mid Point Flurometer	3/5/2015 8:04	0.68
Mid Point Flurometer	3/5/2015 8:05	0.68
Mid Point Flurometer	3/5/2015 8:06	0.67
Mid Point Flurometer	3/5/2015 8:07	0.67
Mid Point Flurometer	3/5/2015 8:08	0.7
Mid Point Flurometer	3/5/2015 8:09	0.68
Mid Point Flurometer	3/5/2015 8:10	0.71
Mid Point Flurometer	3/5/2015 8:11	0.67
Mid Point Flurometer	3/5/2015 8:12	0.7
Mid Point Flurometer	3/5/2015 8:13	0.69
Mid Point Flurometer	3/5/2015 8:14	0.66
Mid Point Flurometer	3/5/2015 8:15	0.67
Mid Point Flurometer	3/5/2015 8:16	0.65
Mid Point Flurometer	3/5/2015 8:17	0.68
Mid Point Flurometer	3/5/2015 8:18	0.66
Mid Point Flurometer	3/5/2015 8:19	0.66
Mid Point Flurometer	3/5/2015 8:20	0.69
Mid Point Flurometer	3/5/2015 8:21	0.66
Mid Point Flurometer	3/5/2015 8:22	0.63

Location	Date and Time	Rhodmaine Concentration Adjusted Concentration (ppb)
Mid Point Flurometer	3/5/2015 8:23	0.64
Mid Point Flurometer	3/5/2015 8:24	0.62
Mid Point Flurometer	3/5/2015 8:25	0.62
Mid Point Flurometer	3/5/2015 8:26	0.61
Mid Point Flurometer	3/5/2015 8:27	0.61
Mid Point Flurometer	3/5/2015 8:28	0.63
Mid Point Flurometer	3/5/2015 8:29	0.63
Mid Point Flurometer	3/5/2015 8:30	0.6
Mid Point Flurometer	3/5/2015 8:31	0.61
Mid Point Flurometer	3/5/2015 8:32	0.64
Mid Point Flurometer	3/5/2015 8:33	0.61
Mid Point Flurometer	3/5/2015 8:34	0.6
Mid Point Flurometer	3/5/2015 8:35	0.59
Mid Point Flurometer	3/5/2015 8:36	0.61
Mid Point Flurometer	3/5/2015 8:37	0.62
Mid Point Flurometer	3/5/2015 8:38	0.59
Mid Point Flurometer	3/5/2015 8:39	0.59
Mid Point Flurometer	3/5/2015 8:40	0.63
Mid Point Flurometer	3/5/2015 8:41	0.6
Mid Point Flurometer	3/5/2015 8:42	0.57
Mid Point Flurometer	3/5/2015 8:43	0.58
Mid Point Flurometer	3/5/2015 8:44	0.57
Mid Point Flurometer	3/5/2015 8:45	0.6
Mid Point Flurometer	3/5/2015 8:46	0.59
Mid Point Flurometer	3/5/2015 8:47	0.58
Mid Point Flurometer	3/5/2015 8:48	0.56
Mid Point Flurometer	3/5/2015 8:49	0.58
Mid Point Flurometer	3/5/2015 8:50	0.55
Mid Point Flurometer	3/5/2015 8:51	0.57
Mid Point Flurometer	3/5/2015 8:52	0.55
Mid Point Flurometer	3/5/2015 8:53	0.56
Mid Point Flurometer	3/5/2015 8:54	0.54
Mid Point Flurometer	3/5/2015 8:55	0.56
Mid Point Flurometer	3/5/2015 8:56	0.57
Mid Point Flurometer	3/5/2015 8:57	0.56
Mid Point Flurometer	3/5/2015 8:58	0.52
Mid Point Flurometer	3/5/2015 8:59	0.54
Mid Point Flurometer	3/5/2015 9:00	0.54
Mid Point Flurometer	3/5/2015 9:01	0.56
Mid Point Flurometer	3/5/2015 9:02	0.54
Mid Point Flurometer	3/5/2015 9:03	0.53
Mid Point Flurometer	3/5/2015 9:04	0.5
Mid Point Flurometer	3/5/2015 9:05	0.54
Mid Point Flurometer	3/5/2015 9:06	0.54
Mid Point Flurometer	3/5/2015 9:07	0.5
Mid Point Flurometer	3/5/2015 9:08	0.52

Location	Date and Time	Rhodmaine Concentration Adjusted Concentration (ppb)
Mid Point Flurometer	3/5/2015 9:09	0.48
Mid Point Flurometer	3/5/2015 9:10	0.54
Mid Point Flurometer	3/5/2015 9:11	0.52
Mid Point Flurometer	3/5/2015 9:12	0.5
Mid Point Flurometer	3/5/2015 9:13	0.51
Mid Point Flurometer	3/5/2015 9:14	0.5
Mid Point Flurometer	3/5/2015 9:15	0.48
Mid Point Flurometer	3/5/2015 9:16	0.5
Mid Point Flurometer	3/5/2015 9:17	0.49
Mid Point Flurometer	3/5/2015 9:18	0.5
Mid Point Flurometer	3/5/2015 9:19	0.49
Mid Point Flurometer	3/5/2015 9:20	0.5
Mid Point Flurometer	3/5/2015 9:21	0.47
Mid Point Flurometer	3/5/2015 9:22	0.45
Mid Point Flurometer	3/5/2015 9:23	0.46
Mid Point Flurometer	3/5/2015 9:24	0.47
Mid Point Flurometer	3/5/2015 9:25	0.46
Mid Point Flurometer	3/5/2015 9:26	0.47
Mid Point Flurometer	3/5/2015 9:27	0.48
Mid Point Flurometer	3/5/2015 9:28	0.44
Mid Point Flurometer	3/5/2015 9:29	0.45
Mid Point Flurometer	3/5/2015 9:30	0.47
Mid Point Flurometer	3/5/2015 9:31	0.48
Mid Point Flurometer	3/5/2015 9:32	0.48
Mid Point Flurometer	3/5/2015 9:33	0.42
Mid Point Flurometer	3/5/2015 9:34	0.43
Mid Point Flurometer	3/5/2015 9:35	0.43
Mid Point Flurometer	3/5/2015 9:36	0.43
Mid Point Flurometer	3/5/2015 9:37	0.44
Mid Point Flurometer	3/5/2015 9:38	0.46
Mid Point Flurometer	3/5/2015 9:39	0.46
Mid Point Flurometer	3/5/2015 9:40	0.43
Mid Point Flurometer	3/5/2015 9:41	0.52
Mid Point Flurometer	3/5/2015 9:42	0.47
Mid Point Flurometer	3/5/2015 9:43	0.4
Mid Point Flurometer	3/5/2015 9:44	0.41
Mid Point Flurometer	3/5/2015 9:45	0.41
Mid Point Flurometer	3/5/2015 9:46	0.41
Mid Point Flurometer	3/5/2015 9:47	0.38
Mid Point Flurometer	3/5/2015 9:48	0.41
Mid Point Flurometer	3/5/2015 9:49	0.37
Mid Point Flurometer	3/5/2015 9:50	0.46
Mid Point Flurometer	3/5/2015 9:51	0.4
Mid Point Flurometer	3/5/2015 9:52	0.4
Mid Point Flurometer	3/5/2015 9:53	0.42
Mid Point Flurometer	3/5/2015 9:54	0.43

Location	Date and Time	Rhodmaine Concentration Adjusted Concentration (ppb)
Mid Point Flurometer	3/5/2015 9:55	0.4
Mid Point Flurometer	3/5/2015 9:56	0.43
Mid Point Flurometer	3/5/2015 9:57	0.38
Mid Point Flurometer	3/5/2015 9:58	0.39
Mid Point Flurometer	3/5/2015 9:59	0.39
Mid Point Flurometer	3/5/2015 10:00	0.43
Mid Point Flurometer	3/5/2015 10:01	0.38
Mid Point Flurometer	3/5/2015 10:02	0.41
Mid Point Flurometer	3/5/2015 10:03	0.47
Mid Point Flurometer	3/5/2015 10:04	0.36
Mid Point Flurometer	3/5/2015 10:05	0.38
Mid Point Flurometer	3/5/2015 10:06	0.39
Mid Point Flurometer	3/5/2015 10:07	0.38
Mid Point Flurometer	3/5/2015 10:08	0.37
Mid Point Flurometer	3/5/2015 10:09	0.36
Mid Point Flurometer	3/5/2015 10:10	0.37
Mid Point Flurometer	3/5/2015 10:11	0.37
Mid Point Flurometer	3/5/2015 10:12	0.35
Mid Point Flurometer	3/5/2015 10:13	0.38
Mid Point Flurometer	3/5/2015 10:14	0.33
Mid Point Flurometer	3/5/2015 10:15	0.35
Mid Point Flurometer	3/5/2015 10:16	0.37
Mid Point Flurometer	3/5/2015 10:17	0.33
Mid Point Flurometer	3/5/2015 10:18	0.33
Mid Point Flurometer	3/5/2015 10:19	0.37
Mid Point Flurometer	3/5/2015 10:20	0.38
Mid Point Flurometer	3/5/2015 10:21	0.36
Mid Point Flurometer	3/5/2015 10:22	0.34
Mid Point Flurometer	3/5/2015 10:23	0.32
Mid Point Flurometer	3/5/2015 10:24	0.34
Mid Point Flurometer	3/5/2015 10:25	0.34
Mid Point Flurometer	3/5/2015 10:26	0.34
Mid Point Flurometer	3/5/2015 10:27	0.34
Mid Point Flurometer	3/5/2015 10:28	0.32
Mid Point Flurometer	3/5/2015 10:29	0.35
Mid Point Flurometer	3/5/2015 10:30	0.33
Mid Point Flurometer	3/5/2015 10:31	0.36
Mid Point Flurometer	3/5/2015 10:32	0.29
Mid Point Flurometer	3/5/2015 10:33	0.35
Mid Point Flurometer	3/5/2015 10:34	0.34
Mid Point Flurometer	3/5/2015 10:35	0.31
Mid Point Flurometer	3/5/2015 10:36	0.31
Mid Point Flurometer	3/5/2015 10:37	0.34
Mid Point Flurometer	3/5/2015 10:38	0.3
Mid Point Flurometer	3/5/2015 10:39	0.33
Mid Point Flurometer	3/5/2015 10:40	0.3

Location	Date and Time	Rhodmaine Concentration Adjusted Concentration (ppb)
Mid Point Flurometer	3/5/2015 10:41	0.31
Mid Point Flurometer	3/5/2015 10:42	0.32
Mid Point Flurometer	3/5/2015 10:43	0.32
Mid Point Flurometer	3/5/2015 10:44	0.28
Mid Point Flurometer	3/5/2015 10:45	0.31
Mid Point Flurometer	3/5/2015 10:46	0.28
Mid Point Flurometer	3/5/2015 10:47	0.31
Mid Point Flurometer	3/5/2015 10:48	0.26
Mid Point Flurometer	3/5/2015 10:49	0.27
Mid Point Flurometer	3/5/2015 10:50	0.32
Mid Point Flurometer	3/5/2015 10:51	0.3
Mid Point Flurometer	3/5/2015 10:52	0.28
Mid Point Flurometer	3/5/2015 10:53	0.3
Mid Point Flurometer	3/5/2015 10:54	0.28
Mid Point Flurometer	3/5/2015 10:55	0.29
Mid Point Flurometer	3/5/2015 10:56	0.26
Mid Point Flurometer	3/5/2015 10:57	0.31
Mid Point Flurometer	3/5/2015 10:58	0.29
Mid Point Flurometer	3/5/2015 10:59	0.34
Mid Point Flurometer	3/5/2015 11:00	0.32
Mid Point Flurometer	3/5/2015 11:01	0.29
Mid Point Flurometer	3/5/2015 11:02	0.28
Mid Point Flurometer	3/5/2015 11:03	0.36
Mid Point Flurometer	3/5/2015 11:04	0.26
Mid Point Flurometer	3/5/2015 11:05	0.29
Mid Point Flurometer	3/5/2015 11:06	0.27
Mid Point Flurometer	3/5/2015 11:07	0.25
Mid Point Flurometer	3/5/2015 11:08	0.25
Mid Point Flurometer	3/5/2015 11:09	0.25
Mid Point Flurometer	3/5/2015 11:10	0.27
Mid Point Flurometer	3/5/2015 11:11	0.28
Mid Point Flurometer	3/5/2015 11:12	0.24
Mid Point Flurometer	3/5/2015 11:13	0.31
Mid Point Flurometer	3/5/2015 11:14	0.26
Mid Point Flurometer	3/5/2015 11:15	0.25
Mid Point Flurometer	3/5/2015 11:16	0.25
Mid Point Flurometer	3/5/2015 11:17	0.25
Mid Point Flurometer	3/5/2015 11:18	0.24
Mid Point Flurometer	3/5/2015 11:19	0.25
Mid Point Flurometer	3/5/2015 11:20	0.24
Mid Point Flurometer	3/5/2015 11:21	0.28
Mid Point Flurometer	3/5/2015 11:22	0.25
Mid Point Flurometer	3/5/2015 11:23	0.24
Mid Point Flurometer	3/5/2015 11:24	0.26
Mid Point Flurometer	3/5/2015 11:25	0.26
Mid Point Flurometer	3/5/2015 11:26	0.21

Location	Date and Time	Rhodmaine Concentration Adjusted Concentration (ppb)
Mid Point Flurometer	3/5/2015 11:27	0.28
Mid Point Flurometer	3/5/2015 11:28	0.22
Mid Point Flurometer	3/5/2015 11:29	0.23
Mid Point Flurometer	3/5/2015 11:30	0.23
Mid Point Flurometer	3/5/2015 11:31	0.27
Mid Point Flurometer	3/5/2015 11:32	0.23
Mid Point Flurometer	3/5/2015 11:33	0.19
Mid Point Flurometer	3/5/2015 11:34	0.3
Mid Point Flurometer	3/5/2015 11:35	0.22
Mid Point Flurometer	3/5/2015 11:36	0.19
Mid Point Flurometer	3/5/2015 11:37	0.22
Mid Point Flurometer	3/5/2015 11:38	0.23
Mid Point Flurometer	3/5/2015 11:39	0.24
Mid Point Flurometer	3/5/2015 11:40	0.2
Mid Point Flurometer	3/5/2015 11:41	0.2
Mid Point Flurometer	3/5/2015 11:42	0.2
Mid Point Flurometer	3/5/2015 11:43	0.24
Mid Point Flurometer	3/5/2015 11:44	0.24
Mid Point Flurometer	3/5/2015 11:45	0.19
Mid Point Flurometer	3/5/2015 11:46	0.25
Mid Point Flurometer	3/5/2015 11:47	0.22
Mid Point Flurometer	3/5/2015 11:48	0.19
Mid Point Flurometer	3/5/2015 11:49	0.2
Mid Point Flurometer	3/5/2015 11:50	0.21
Mid Point Flurometer	3/5/2015 11:51	0.21
Mid Point Flurometer	3/5/2015 11:52	0.17
Mid Point Flurometer	3/5/2015 11:53	0.21
Mid Point Flurometer	3/5/2015 11:54	0.22
Mid Point Flurometer	3/5/2015 11:55	0.2
Mid Point Flurometer	3/5/2015 11:56	0.23
Mid Point Flurometer	3/5/2015 11:57	0.2
Mid Point Flurometer	3/5/2015 11:58	0.26
Mid Point Flurometer	3/5/2015 11:59	0.2
Mid Point Flurometer	3/5/2015 12:00	0.18
Mid Point Flurometer	3/5/2015 12:01	0.18
Mid Point Flurometer	3/5/2015 12:02	0.18
Mid Point Flurometer	3/5/2015 12:03	0.18
Mid Point Flurometer	3/5/2015 12:04	0.19
Mid Point Flurometer	3/5/2015 12:05	0.15
Mid Point Flurometer	3/5/2015 12:06	0.22
Mid Point Flurometer	3/5/2015 12:07	0.18
Mid Point Flurometer	3/5/2015 12:08	0.17
Mid Point Flurometer	3/5/2015 12:09	0.16
Mid Point Flurometer	3/5/2015 12:10	0.17
Mid Point Flurometer	3/5/2015 12:11	0.17
Mid Point Flurometer	3/5/2015 12:12	0.2

Location	Date and Time	Rhodmaine Concentration Adjusted Concentration (ppb)
Mid Point Flurometer	3/5/2015 12:13	0.18
Mid Point Flurometer	3/5/2015 12:14	0.17
Mid Point Flurometer	3/5/2015 12:15	0.19
Mid Point Flurometer	3/5/2015 12:16	0.2
Mid Point Flurometer	3/5/2015 12:17	0.15
Mid Point Flurometer	3/5/2015 12:18	0.2
Mid Point Flurometer	3/5/2015 12:19	0.16
Mid Point Flurometer	3/5/2015 12:20	0.17
Mid Point Flurometer	3/5/2015 12:21	0.19
Mid Point Flurometer	3/5/2015 12:22	0.16
Mid Point Flurometer	3/5/2015 12:23	0.19
Mid Point Flurometer	3/5/2015 12:24	0.17
Mid Point Flurometer	3/5/2015 12:25	0.14
Mid Point Flurometer	3/5/2015 12:26	0.18
Mid Point Flurometer	3/5/2015 12:27	0.15
Mid Point Flurometer	3/5/2015 12:28	0.16
Mid Point Flurometer	3/5/2015 12:29	0.18
Mid Point Flurometer	3/5/2015 12:30	0.13
Mid Point Flurometer	3/5/2015 12:31	0.15
Mid Point Flurometer	3/5/2015 12:32	0.16
Mid Point Flurometer	3/5/2015 12:33	0.16
Mid Point Flurometer	3/5/2015 12:34	0.12
Mid Point Flurometer	3/5/2015 12:35	0.19
Mid Point Flurometer	3/5/2015 12:36	0.13
Mid Point Flurometer	3/5/2015 12:37	0.13
Mid Point Flurometer	3/5/2015 12:38	0.16
Mid Point Flurometer	3/5/2015 12:39	0.15
Mid Point Flurometer	3/5/2015 12:40	0.12
Mid Point Flurometer	3/5/2015 12:41	0.13
Mid Point Flurometer	3/5/2015 12:42	0.13
Mid Point Flurometer	3/5/2015 12:43	0.15
Mid Point Flurometer	3/5/2015 12:44	0.15
Mid Point Flurometer	3/5/2015 12:45	0.61
Mid Point Flurometer	3/5/2015 12:46	0.13
Mid Point Flurometer	3/5/2015 12:47	0.17
Mid Point Flurometer	3/5/2015 12:48	0.11
Mid Point Flurometer	3/5/2015 12:49	0.13
Mid Point Flurometer	3/5/2015 12:50	0.12
Mid Point Flurometer	3/5/2015 12:51	0.14
Mid Point Flurometer	3/5/2015 12:52	0.11
Mid Point Flurometer	3/5/2015 12:53	0.13
Mid Point Flurometer	3/5/2015 12:54	0.14
Mid Point Flurometer	3/5/2015 12:55	0.13
Mid Point Flurometer	3/5/2015 12:56	0.16
Mid Point Flurometer	3/5/2015 12:57	0.13
Mid Point Flurometer	3/5/2015 12:58	0.14

Location	Date and Time	Rhodmaine Concentration Adjusted Concentration (ppb)
Mid Point Flurometer	3/5/2015 12:59	0.11
Mid Point Flurometer	3/5/2015 13:00	0.14
Mid Point Flurometer	3/5/2015 13:01	0.16
Mid Point Flurometer	3/5/2015 13:02	0.16
Mid Point Flurometer	3/5/2015 13:03	0.12
Mid Point Flurometer	3/5/2015 13:04	0.14
Mid Point Flurometer	3/5/2015 13:05	0.12
Mid Point Flurometer	3/5/2015 13:06	0.11
Mid Point Flurometer	3/5/2015 13:07	0.1
Mid Point Flurometer	3/5/2015 13:08	0.16
Mid Point Flurometer	3/5/2015 13:09	0.12
Mid Point Flurometer	3/5/2015 13:10	0.12
Mid Point Flurometer	3/5/2015 13:11	0.13
Mid Point Flurometer	3/5/2015 13:12	0.11
Mid Point Flurometer	3/5/2015 13:13	0.39
Mid Point Flurometer	3/5/2015 13:14	0.12
Mid Point Flurometer	3/5/2015 13:15	0.1
Mid Point Flurometer	3/5/2015 13:16	0.11
Mid Point Flurometer	3/5/2015 13:17	0.13
Mid Point Flurometer	3/5/2015 13:18	0.14
Mid Point Flurometer	3/5/2015 13:19	0.13
Mid Point Flurometer	3/5/2015 13:20	0.24
Mid Point Flurometer	3/5/2015 13:21	0.11
Mid Point Flurometer	3/5/2015 13:22	0.1
Mid Point Flurometer	3/5/2015 13:23	0.15
Mid Point Flurometer	3/5/2015 13:24	0.12
Mid Point Flurometer	3/5/2015 13:25	0.31
Mid Point Flurometer	3/5/2015 13:26	0.1
Mid Point Flurometer	3/5/2015 13:27	0.13
Mid Point Flurometer	3/5/2015 13:28	0.1
Mid Point Flurometer	3/5/2015 13:29	0.12
Mid Point Flurometer	3/5/2015 13:30	0.14
Mid Point Flurometer	3/5/2015 13:31	0.1
Mid Point Flurometer	3/5/2015 13:32	0.1
Mid Point Flurometer	3/5/2015 13:33	0.13
Mid Point Flurometer	3/5/2015 13:34	0.16
Mid Point Flurometer	3/5/2015 13:35	0.13
Mid Point Flurometer	3/5/2015 13:36	0.11
Mid Point Flurometer	3/5/2015 13:37	0.14
Mid Point Flurometer	3/5/2015 13:38	0.14
Mid Point Flurometer	3/5/2015 13:39	0.08
Mid Point Flurometer	3/5/2015 13:40	0.16
Mid Point Flurometer	3/5/2015 13:41	0.07
Mid Point Flurometer	3/5/2015 13:42	0.09
Mid Point Flurometer	3/5/2015 13:43	0.08
Mid Point Flurometer	3/5/2015 13:44	0.1

Location	Date and Time	Rhodmaine Concentration Adjusted Concentration (ppb)
Mid Point Flurometer	3/5/2015 13:45	0.19
Mid Point Flurometer	3/5/2015 13:46	0.09
Mid Point Flurometer	3/5/2015 13:47	0.09
Mid Point Flurometer	3/5/2015 13:48	0.11
Mid Point Flurometer	3/5/2015 13:49	0.15
Mid Point Flurometer	3/5/2015 13:50	0.09
Mid Point Flurometer	3/5/2015 13:51	0.17
Mid Point Flurometer	3/5/2015 13:52	0.09
Mid Point Flurometer	3/5/2015 13:53	0.08
Mid Point Flurometer	3/5/2015 13:54	0.08
Mid Point Flurometer	3/5/2015 13:55	0.18
Mid Point Flurometer	3/5/2015 13:56	0.07
Mid Point Flurometer	3/5/2015 13:57	0.12
Mid Point Flurometer	3/5/2015 13:58	0.09
Mid Point Flurometer	3/5/2015 13:59	0.11
Mid Point Flurometer	3/5/2015 14:00	0.08
Mid Point Flurometer	3/5/2015 14:01	0.07
Mid Point Flurometer	3/5/2015 14:02	0.07
Mid Point Flurometer	3/5/2015 14:03	0.09
Mid Point Flurometer	3/5/2015 14:04	0.05
Mid Point Flurometer	3/5/2015 14:05	0.07
Mid Point Flurometer	3/5/2015 14:06	0.06
Mid Point Flurometer	3/5/2015 14:07	0.07
Mid Point Flurometer	3/5/2015 14:08	0.09
Mid Point Flurometer	3/5/2015 14:09	0.07
Mid Point Flurometer	3/5/2015 14:10	0.16
Mid Point Flurometer	3/5/2015 14:11	0.28
Mid Point Flurometer	3/5/2015 14:12	0.11
Mid Point Flurometer	3/5/2015 14:13	0.09
Mid Point Flurometer	3/5/2015 14:14	0.05
Mid Point Flurometer	3/5/2015 14:15	0.17
Mid Point Flurometer	3/5/2015 14:16	0.08
Mid Point Flurometer	3/5/2015 14:17	0.07
Mid Point Flurometer	3/5/2015 14:18	0.1
Mid Point Flurometer	3/5/2015 14:19	0.08
Mid Point Flurometer	3/5/2015 14:20	0.07
Mid Point Flurometer	3/5/2015 14:21	0.06
Mid Point Flurometer	3/5/2015 14:22	0.1
Mid Point Flurometer	3/5/2015 14:23	0.04
Mid Point Flurometer	3/5/2015 14:24	0.07
Mid Point Flurometer	3/5/2015 14:25	0.05
Mid Point Flurometer	3/5/2015 14:26	0.06
Mid Point Flurometer	3/5/2015 14:27	0.18
Mid Point Flurometer	3/5/2015 14:28	0.06
Mid Point Flurometer	3/5/2015 14:29	0.07
Mid Point Flurometer	3/5/2015 14:30	0.07

Location	Date and Time	Rhodmaine Concentration Adjusted Concentration (ppb)
Mid Point Flurometer	3/5/2015 14:31	0.05
Mid Point Flurometer	3/5/2015 14:32	0.09
Mid Point Flurometer	3/5/2015 14:33	0.06
Mid Point Flurometer	3/5/2015 14:34	0.05
Mid Point Flurometer	3/5/2015 14:35	0.04
Mid Point Flurometer	3/5/2015 14:36	0.05
Mid Point Flurometer	3/5/2015 14:37	0.05
Mid Point Flurometer	3/5/2015 14:38	0.03
Mid Point Flurometer	3/5/2015 14:39	0.04
Mid Point Flurometer	3/5/2015 14:40	0.05
Mid Point Flurometer	3/5/2015 14:41	0.06
Mid Point Flurometer	3/5/2015 14:42	0.04
Mid Point Flurometer	3/5/2015 14:43	0.06
Mid Point Flurometer	3/5/2015 14:44	0.08
Mid Point Flurometer	3/5/2015 14:45	0.02
Mid Point Flurometer	3/5/2015 14:46	0.04
Mid Point Flurometer	3/5/2015 14:47	0.96
Mid Point Flurometer	3/5/2015 14:48	0.02
Mid Point Flurometer	3/5/2015 14:49	0.05
Mid Point Flurometer	3/5/2015 14:50	0.03
Mid Point Flurometer	3/5/2015 14:51	0.08
Mid Point Flurometer	3/5/2015 14:52	0.09
Mid Point Flurometer	3/5/2015 14:53	0.07
Mid Point Flurometer	3/5/2015 14:54	0.03
Mid Point Flurometer	3/5/2015 14:55	0.02
Mid Point Flurometer	3/5/2015 14:56	0.04
Mid Point Flurometer	3/5/2015 14:57	0.04
Mid Point Flurometer	3/5/2015 14:58	0.05
Mid Point Flurometer	3/5/2015 14:59	0.06
Mid Point Flurometer	3/5/2015 15:00	0.01
Mid Point Flurometer	3/5/2015 15:01	0.06
Mid Point Flurometer	3/5/2015 15:02	0.04
Mid Point Flurometer	3/5/2015 15:03	0.07
Mid Point Flurometer	3/5/2015 15:04	0.08
Mid Point Flurometer	3/5/2015 15:05	0.03
Mid Point Flurometer	3/5/2015 15:06	0.04
Mid Point Flurometer	3/5/2015 15:07	0.03
Mid Point Flurometer	3/5/2015 15:08	0.06
Mid Point Flurometer	3/5/2015 15:09	0.04
Mid Point Flurometer	3/5/2015 15:10	0.06
Mid Point Flurometer	3/5/2015 15:11	0.04
Mid Point Flurometer	3/5/2015 15:12	0.04
Mid Point Flurometer	3/5/2015 15:13	0.06
Mid Point Flurometer	3/5/2015 15:14	0.04
Mid Point Flurometer	3/5/2015 15:15	0.03
Mid Point Flurometer	3/5/2015 15:16	0.03

Location	Date and Time	Rhodmaine Concentration Adjusted Concentration (ppb)
Mid Point Flurometer	3/5/2015 15:17	0.02
Mid Point Flurometer	3/5/2015 15:18	0.05
Mid Point Flurometer	3/5/2015 15:19	0.1
Mid Point Flurometer	3/5/2015 15:20	0.06
Mid Point Flurometer	3/5/2015 15:21	0.04
Mid Point Flurometer	3/5/2015 15:22	0.07
Mid Point Flurometer	3/5/2015 15:23	0.06
Mid Point Flurometer	3/5/2015 15:24	0.13
Mid Point Flurometer	3/5/2015 15:25	0.09
Mid Point Flurometer	3/5/2015 15:26	0.07
Mid Point Flurometer	3/5/2015 15:27	0.09
Mid Point Flurometer	3/5/2015 15:28	0.1
Mid Point Flurometer	3/5/2015 15:29	0.07
Mid Point Flurometer	3/5/2015 15:30	0.12
Mid Point Flurometer	3/5/2015 15:31	0.02
Mid Point Flurometer	3/5/2015 15:32	0.01
Mid Point Flurometer	3/5/2015 15:33	0.04
Mid Point Flurometer	3/5/2015 15:34	0.03
Mid Point Flurometer	3/5/2015 15:35	0.11
Mid Point Flurometer	3/5/2015 15:36	0.03
Mid Point Flurometer	3/5/2015 15:37	0.05
Mid Point Flurometer	3/5/2015 15:38	0.03
Mid Point Flurometer	3/5/2015 15:39	0.04
Mid Point Flurometer	3/5/2015 15:40	0.04
Mid Point Flurometer	3/5/2015 15:41	0.03
Mid Point Flurometer	3/5/2015 15:42	0.02
Mid Point Flurometer	3/5/2015 15:43	0.13
Mid Point Flurometer	3/5/2015 15:44	0.04
Mid Point Flurometer	3/5/2015 15:45	0.03
Mid Point Flurometer	3/5/2015 15:46	0.01
Mid Point Flurometer	3/5/2015 15:47	0.04
Mid Point Flurometer	3/5/2015 15:48	0.02
Mid Point Flurometer	3/5/2015 15:49	0.02
Mid Point Flurometer	3/5/2015 15:50	0.04
Mid Point Flurometer	3/5/2015 15:51	0.03
Mid Point Flurometer	3/5/2015 15:52	0.1
Mid Point Flurometer	3/5/2015 15:53	0.04
Mid Point Flurometer	3/5/2015 15:54	0.04
Mid Point Flurometer	3/5/2015 15:55	0.03
Mid Point Flurometer	3/5/2015 15:56	0
Mid Point Flurometer	3/5/2015 15:57	0.02
Mid Point Flurometer	3/5/2015 15:58	0.02
Mid Point Flurometer	3/5/2015 15:59	0.04
Mid Point Flurometer	3/5/2015 16:00	0.02
Mid Point Flurometer	3/5/2015 16:01	0.05
Mid Point Flurometer	3/5/2015 16:02	0.02

Location	Date and Time	Rhodmaine Concentration Adjusted Concentration (ppb)
Mid Point Flurometer	3/5/2015 16:03	0.05
Mid Point Flurometer	3/5/2015 16:04	0.04
Mid Point Flurometer	3/5/2015 16:05	3.85
Mid Point Flurometer	3/5/2015 16:06	0.34
Mid Point Flurometer	3/5/2015 16:07	0.06
Mid Point Flurometer	3/5/2015 16:08	0
Mid Point Flurometer	3/5/2015 16:09	0.15
Mid Point Flurometer	3/5/2015 16:10	0.07
Mid Point Flurometer	3/5/2015 16:11	1.14
Mid Point Flurometer	3/5/2015 16:12	0.24
Mid Point Flurometer	3/5/2015 16:13	0.2
Mid Point Flurometer	3/5/2015 16:14	0.11
Mid Point Flurometer	3/5/2015 16:15	1.76
Mid Point Flurometer	3/5/2015 16:16	0.97
Mid Point Flurometer	3/5/2015 16:17	0.07
Mid Point Flurometer	3/5/2015 16:18	0.03
Mid Point Flurometer	3/5/2015 16:19	0.12
Mid Point Flurometer	3/5/2015 16:20	2.42
Mid Point Flurometer	3/5/2015 16:21	0.03
Mid Point Flurometer	3/5/2015 16:22	1.72
Mid Point Flurometer	3/5/2015 16:23	0.12
Mid Point Flurometer	3/5/2015 16:24	4.87
Mid Point Flurometer	3/5/2015 16:25	0.04
Mid Point Flurometer	3/5/2015 16:26	0.4
Mid Point Flurometer	3/5/2015 16:27	0.98
Mid Point Flurometer	3/5/2015 16:28	0.04
Mid Point Flurometer	3/5/2015 16:29	0.32
Mid Point Flurometer	3/5/2015 16:30	0.12
Mid Point Flurometer	3/5/2015 16:31	0.1
Mid Point Flurometer	3/5/2015 16:32	0.35
Mid Point Flurometer	3/5/2015 16:33	0.08
Mid Point Flurometer	3/5/2015 16:34	0.06
Mid Point Flurometer	3/5/2015 16:35	0.07
Mid Point Flurometer	3/5/2015 16:36	0.35
Mid Point Flurometer	3/5/2015 16:37	0.12
Mid Point Flurometer	3/5/2015 16:38	0.21
Mid Point Flurometer	3/5/2015 16:39	0.21
Mid Point Flurometer	3/5/2015 16:40	0.11
Mid Point Flurometer	3/5/2015 16:41	0.02
Mid Point Flurometer	3/5/2015 16:42	3.76
Mid Point Flurometer	3/5/2015 16:43	0.86
Mid Point Flurometer	3/5/2015 16:44	0.44
Mid Point Flurometer	3/5/2015 16:45	0.04
Mid Point Flurometer	3/5/2015 16:46	0.32
Mid Point Flurometer	3/5/2015 16:47	0.07
Mid Point Flurometer	3/5/2015 16:48	1.51

Location	Date and Time	Rhodmaine Concentration Adjusted Concentration (ppb)
Mid Point Flurometer	3/5/2015 16:49	0.02
Mid Point Flurometer	3/5/2015 16:50	0.26
Mid Point Flurometer	3/5/2015 16:51	0.07
Mid Point Flurometer	3/5/2015 16:52	0.23
Mid Point Flurometer	3/5/2015 16:53	0.7
Mid Point Flurometer	3/5/2015 16:54	1.81
Mid Point Flurometer	3/5/2015 16:55	0.23
Mid Point Flurometer	3/5/2015 16:56	0.53
Mid Point Flurometer	3/5/2015 16:57	0.02
Mid Point Flurometer	3/5/2015 16:58	0.06
Mid Point Flurometer	3/5/2015 16:59	0.44
Mid Point Flurometer	3/5/2015 17:00	0.51
Mid Point Flurometer	3/5/2015 17:01	0.28
Mid Point Flurometer	3/5/2015 17:02	0.05
Mid Point Flurometer	3/5/2015 17:03	0.04
Mid Point Flurometer	3/5/2015 17:04	2.54
Mid Point Flurometer	3/5/2015 17:05	0.21
Mid Point Flurometer	3/5/2015 17:06	0.15
Mid Point Flurometer	3/5/2015 17:07	0.17
Mid Point Flurometer	3/5/2015 17:08	0.32
Mid Point Flurometer	3/5/2015 17:09	0.09
Mid Point Flurometer	3/5/2015 17:10	0.29
Mid Point Flurometer	3/5/2015 17:11	0
Mid Point Flurometer	3/5/2015 17:12	1.11
Mid Point Flurometer	3/5/2015 17:13	0.03
Mid Point Flurometer	3/5/2015 17:14	0.09
Mid Point Flurometer	3/5/2015 17:15	0.06
Mid Point Flurometer	3/5/2015 17:16	2.14
Mid Point Flurometer	3/5/2015 17:17	0
Mid Point Flurometer	3/5/2015 17:18	1.51
Mid Point Flurometer	3/5/2015 17:19	0.87
Mid Point Flurometer	3/5/2015 17:20	2.48
Mid Point Flurometer	3/5/2015 17:21	1.68
Mid Point Flurometer	3/5/2015 17:22	0.08
Mid Point Flurometer	3/5/2015 17:23	1.66
Mid Point Flurometer	3/5/2015 17:24	0.54
Mid Point Flurometer	3/5/2015 17:25	0.87
Mid Point Flurometer	3/5/2015 17:26	0.09
Mid Point Flurometer	3/5/2015 17:27	0.08
Mid Point Flurometer	3/5/2015 17:28	0.26
Mid Point Flurometer	3/5/2015 17:29	0.65
Mid Point Flurometer	3/5/2015 17:30	0.22
Mid Point Flurometer	3/5/2015 17:31	3.78
Mid Point Flurometer	3/5/2015 17:32	0.06
Mid Point Flurometer	3/5/2015 17:33	0.21
Mid Point Flurometer	3/5/2015 17:34	0.03

Location	Date and Time	Rhodmaine Concentration Adjusted Concentration (ppb)
Mid Point Flurometer	3/5/2015 17:35	0.07
Mid Point Flurometer	3/5/2015 17:36	0.07
Mid Point Flurometer	3/5/2015 17:37	2.49
Mid Point Flurometer	3/5/2015 17:38	1.27
Mid Point Flurometer	3/5/2015 17:39	0.15
Mid Point Flurometer	3/5/2015 17:40	0.11
Mid Point Flurometer	3/5/2015 17:41	3.95
Mid Point Flurometer	3/5/2015 17:42	0.06
Mid Point Flurometer	3/5/2015 17:43	0.08
Mid Point Flurometer	3/5/2015 17:44	0.75
Mid Point Flurometer	3/5/2015 17:45	0.07
Mid Point Flurometer	3/5/2015 17:46	2.96
Mid Point Flurometer	3/5/2015 17:47	0.05
Mid Point Flurometer	3/5/2015 17:48	0.14
Mid Point Flurometer	3/5/2015 17:49	0.48
Mid Point Flurometer	3/5/2015 17:50	0.66
Mid Point Flurometer	3/5/2015 17:51	0.02
Mid Point Flurometer	3/5/2015 17:52	0.14
Mid Point Flurometer	3/5/2015 17:53	0.25
Mid Point Flurometer	3/5/2015 17:54	0.12
Mid Point Flurometer	3/5/2015 17:55	0.6
Mid Point Flurometer	3/5/2015 17:56	0.22
Mid Point Flurometer	3/5/2015 17:57	2.58
Mid Point Flurometer	3/5/2015 17:58	3.75
Mid Point Flurometer	3/5/2015 17:59	0.07
Mid Point Flurometer	3/5/2015 18:00	0.03
Mid Point Flurometer	3/5/2015 18:01	0.06
Mid Point Flurometer	3/5/2015 18:02	0.07
Mid Point Flurometer	3/5/2015 18:03	0.02
Mid Point Flurometer	3/5/2015 18:04	0.13
Mid Point Flurometer	3/5/2015 18:05	0.02
Mid Point Flurometer	3/5/2015 18:06	7.56
Mid Point Flurometer	3/5/2015 18:07	0.08
Mid Point Flurometer	3/5/2015 18:08	0.05
Mid Point Flurometer	3/5/2015 18:09	0.02
Mid Point Flurometer	3/5/2015 18:10	0.12
Mid Point Flurometer	3/5/2015 18:11	0.27
Mid Point Flurometer	3/5/2015 18:12	0.09
Mid Point Flurometer	3/5/2015 18:13	0.26
Mid Point Flurometer	3/5/2015 18:14	0.03
Mid Point Flurometer	3/5/2015 18:15	1
Mid Point Flurometer	3/5/2015 18:16	0.11
Mid Point Flurometer	3/5/2015 18:17	0.53
Mid Point Flurometer	3/5/2015 18:18	0.2
Mid Point Flurometer	3/5/2015 18:19	1.13
Mid Point Flurometer	3/5/2015 18:20	0.06

Location	Date and Time	Rhodmaine Concentration Adjusted Concentration (ppb)
Mid Point Flurometer	3/5/2015 18:21	0.38
Mid Point Flurometer	3/5/2015 18:22	1.39
Mid Point Flurometer	3/5/2015 18:23	0.03
Mid Point Flurometer	3/5/2015 18:24	0.05
Mid Point Flurometer	3/5/2015 18:25	0.2
Mid Point Flurometer	3/5/2015 18:26	0.11
Mid Point Flurometer	3/5/2015 18:27	0.04
Mid Point Flurometer	3/5/2015 18:28	0.45
Mid Point Flurometer	3/5/2015 18:29	1.97
Mid Point Flurometer	3/5/2015 18:30	0.82
Mid Point Flurometer	3/5/2015 18:31	0.08
Mid Point Flurometer	3/5/2015 18:32	0.16
Mid Point Flurometer	3/5/2015 18:33	2.88
Mid Point Flurometer	3/5/2015 18:34	0.05
Mid Point Flurometer	3/5/2015 18:35	0.01
Mid Point Flurometer	3/5/2015 18:36	0.84
Mid Point Flurometer	3/5/2015 18:37	0.49
Mid Point Flurometer	3/5/2015 18:38	0.14
Mid Point Flurometer	3/5/2015 18:39	0.81
Mid Point Flurometer	3/5/2015 18:40	0.1
Mid Point Flurometer	3/5/2015 18:41	0.11
Mid Point Flurometer	3/5/2015 18:42	0.11
Mid Point Flurometer	3/5/2015 18:43	0.07
Mid Point Flurometer	3/5/2015 18:44	0.47
Mid Point Flurometer	3/5/2015 18:45	0.79
Mid Point Flurometer	3/5/2015 18:46	0.1
Mid Point Flurometer	3/5/2015 18:47	0.04
Mid Point Flurometer	3/5/2015 18:48	5.31
Mid Point Flurometer	3/5/2015 18:49	0.11
Mid Point Flurometer	3/5/2015 18:50	1.87
Mid Point Flurometer	3/5/2015 18:51	0.93
Mid Point Flurometer	3/5/2015 18:52	0.76
Mid Point Flurometer	3/5/2015 18:53	0.3
Mid Point Flurometer	3/5/2015 18:54	0.13
Mid Point Flurometer	3/5/2015 18:55	0.07
Mid Point Flurometer	3/5/2015 18:56	0.05
Mid Point Flurometer	3/5/2015 18:57	0.11
Mid Point Flurometer	3/5/2015 18:58	4.15
Mid Point Flurometer	3/5/2015 18:59	0.26
Mid Point Flurometer	3/5/2015 19:00	0.37
Mid Point Flurometer	3/5/2015 19:01	0.24
Mid Point Flurometer	3/5/2015 19:02	0.13
Mid Point Flurometer	3/5/2015 19:03	2.65
Mid Point Flurometer	3/5/2015 19:04	0.43
Mid Point Flurometer	3/5/2015 19:05	0.24
Mid Point Flurometer	3/5/2015 19:06	1.01

Location	Date and Time	Rhodmaine Concentration Adjusted Concentration (ppb)
Mid Point Flurometer	3/5/2015 19:07	3.25
Mid Point Flurometer	3/5/2015 19:08	0.47
Mid Point Flurometer	3/5/2015 19:09	0.12
Mid Point Flurometer	3/5/2015 19:10	0.16
Mid Point Flurometer	3/5/2015 19:11	0.1
Mid Point Flurometer	3/5/2015 19:12	0.09
Mid Point Flurometer	3/5/2015 19:13	0.13
Mid Point Flurometer	3/5/2015 19:14	0.09
Mid Point Flurometer	3/5/2015 19:15	2.6
Mid Point Flurometer	3/5/2015 19:16	0.06
Mid Point Flurometer	3/5/2015 19:17	0.56
Mid Point Flurometer	3/5/2015 19:18	0.76
Mid Point Flurometer	3/5/2015 19:19	0.89
Mid Point Flurometer	3/5/2015 19:20	0.05
Mid Point Flurometer	3/5/2015 19:21	0
Mid Point Flurometer	3/5/2015 19:22	0.1
Mid Point Flurometer	3/5/2015 19:23	0.02
Mid Point Flurometer	3/5/2015 19:24	0.11
Mid Point Flurometer	3/5/2015 19:25	0.15
Mid Point Flurometer	3/5/2015 19:26	1.26
Mid Point Flurometer	3/5/2015 19:27	0.03
Mid Point Flurometer	3/5/2015 19:28	0.08
Mid Point Flurometer	3/5/2015 19:29	3.02
Mid Point Flurometer	3/5/2015 19:30	0.05
Mid Point Flurometer	3/5/2015 19:31	0.35
Mid Point Flurometer	3/5/2015 19:32	0.05
Mid Point Flurometer	3/5/2015 19:33	0
Mid Point Flurometer	3/5/2015 19:34	0.32
Mid Point Flurometer	3/5/2015 19:35	0.02
Mid Point Flurometer	3/5/2015 19:36	0.05
Mid Point Flurometer	3/5/2015 19:37	2.51
Mid Point Flurometer	3/5/2015 19:38	0.02
Mid Point Flurometer	3/5/2015 19:39	8.46
Mid Point Flurometer	3/5/2015 19:40	0.11
Mid Point Flurometer	3/5/2015 19:41	0
Mid Point Flurometer	3/5/2015 19:42	0.05
Mid Point Flurometer	3/5/2015 19:43	0.19
Mid Point Flurometer	3/5/2015 19:44	0.15
Mid Point Flurometer	3/5/2015 19:45	0.01
Mid Point Flurometer	3/5/2015 19:46	0.12
Mid Point Flurometer	3/5/2015 19:47	0.23
Mid Point Flurometer	3/5/2015 19:48	0.56
Mid Point Flurometer	3/5/2015 19:49	0.41
Mid Point Flurometer	3/5/2015 19:50	0.01
Mid Point Flurometer	3/5/2015 19:51	0.02
Mid Point Flurometer	3/5/2015 19:52	0.05

Location	Date and Time	Rhodmaine Concentration Adjusted Concentration (ppb)
Mid Point Flurometer	3/5/2015 19:53	1.21
Mid Point Flurometer	3/5/2015 19:54	0.15
Mid Point Flurometer	3/5/2015 19:55	4.9
Mid Point Flurometer	3/5/2015 19:56	0.45
Mid Point Flurometer	3/5/2015 19:57	0.35
Mid Point Flurometer	3/5/2015 19:58	0.03
Mid Point Flurometer	3/5/2015 19:59	0.05
Mid Point Flurometer	3/5/2015 20:00	0.77
Mid Point Flurometer	3/5/2015 20:01	0.93
Mid Point Flurometer	3/5/2015 20:02	0.12
Mid Point Flurometer	3/5/2015 20:03	0.11
Mid Point Flurometer	3/5/2015 20:04	0.41
Mid Point Flurometer	3/5/2015 20:05	0.69
Mid Point Flurometer	3/5/2015 20:06	0.06
Mid Point Flurometer	3/5/2015 20:07	0.08
Mid Point Flurometer	3/5/2015 20:08	0.12
Mid Point Flurometer	3/5/2015 20:09	4.57
Mid Point Flurometer	3/5/2015 20:10	0.41
Mid Point Flurometer	3/5/2015 20:11	0.04
Mid Point Flurometer	3/5/2015 20:12	1.45
Mid Point Flurometer	3/5/2015 20:13	0.02
Mid Point Flurometer	3/5/2015 20:14	0.04
Mid Point Flurometer	3/5/2015 20:15	0.12
Mid Point Flurometer	3/5/2015 20:16	0.16
Mid Point Flurometer	3/5/2015 20:17	0.31
Mid Point Flurometer	3/5/2015 20:18	7.26
Mid Point Flurometer	3/5/2015 20:19	2.91
Mid Point Flurometer	3/5/2015 20:20	0.61
Mid Point Flurometer	3/5/2015 20:21	0.1
Mid Point Flurometer	3/5/2015 20:22	0.91
Mid Point Flurometer	3/5/2015 20:23	1.23
Mid Point Flurometer	3/5/2015 20:24	1.08
Mid Point Flurometer	3/5/2015 20:25	0.17
Mid Point Flurometer	3/5/2015 20:26	0.05
Mid Point Flurometer	3/5/2015 20:27	0.75
Mid Point Flurometer	3/5/2015 20:28	0.06
Mid Point Flurometer	3/5/2015 20:29	0.23
Mid Point Flurometer	3/5/2015 20:30	0.09
Mid Point Flurometer	3/5/2015 20:31	1.35
Mid Point Flurometer	3/5/2015 20:32	0.06
Mid Point Flurometer	3/5/2015 20:33	0.25
Mid Point Flurometer	3/5/2015 20:34	3.39
Mid Point Flurometer	3/5/2015 20:35	0.04
Mid Point Flurometer	3/5/2015 20:36	0.31
Mid Point Flurometer	3/5/2015 20:37	0.08
Mid Point Flurometer	3/5/2015 20:38	1.61

Location	Date and Time	Rhodmaine Concentration Adjusted Concentration (ppb)
Mid Point Flurometer	3/5/2015 20:39	2.01
Mid Point Flurometer	3/5/2015 20:40	0
Mid Point Flurometer	3/5/2015 20:41	0.22
Mid Point Flurometer	3/5/2015 20:42	0.74
Mid Point Flurometer	3/5/2015 20:43	0.05
Mid Point Flurometer	3/5/2015 20:44	0.1
Mid Point Flurometer	3/5/2015 20:45	0.16
Mid Point Flurometer	3/5/2015 20:46	0.05
Mid Point Flurometer	3/5/2015 20:47	0.03
Mid Point Flurometer	3/5/2015 20:48	0.26
Mid Point Flurometer	3/5/2015 20:49	0.02
Mid Point Flurometer	3/5/2015 20:50	0.05
Mid Point Flurometer	3/5/2015 20:51	1.95
Mid Point Flurometer	3/5/2015 20:52	2.4
Mid Point Flurometer	3/5/2015 20:53	0.26
Mid Point Flurometer	3/5/2015 20:54	0.35
Mid Point Flurometer	3/5/2015 20:55	1.21
Mid Point Flurometer	3/5/2015 20:56	0.92
Mid Point Flurometer	3/5/2015 20:57	0.08
Mid Point Flurometer	3/5/2015 20:58	0.14
Mid Point Flurometer	3/5/2015 20:59	0.24
Mid Point Flurometer	3/5/2015 21:00	0.16
Mid Point Flurometer	3/5/2015 21:01	1.59
Mid Point Flurometer	3/5/2015 21:02	0.02
Mid Point Flurometer	3/5/2015 21:03	0.19
Mid Point Flurometer	3/5/2015 21:04	0.3
Mid Point Flurometer	3/5/2015 21:05	0.18
Mid Point Flurometer	3/5/2015 21:06	0.08
Mid Point Flurometer	3/5/2015 21:07	0.08
Mid Point Flurometer	3/5/2015 21:08	0.39
Mid Point Flurometer	3/5/2015 21:09	0.15
Mid Point Flurometer	3/5/2015 21:10	0.03
Mid Point Flurometer	3/5/2015 21:11	0.07
Mid Point Flurometer	3/5/2015 21:12	0.25
Mid Point Flurometer	3/5/2015 21:13	0
Mid Point Flurometer	3/5/2015 21:14	2
Mid Point Flurometer	3/5/2015 21:15	0.07
Mid Point Flurometer	3/5/2015 21:16	0.12
Mid Point Flurometer	3/5/2015 21:17	0.06
Mid Point Flurometer	3/5/2015 21:18	0.09
Mid Point Flurometer	3/5/2015 21:19	0.04
Mid Point Flurometer	3/5/2015 21:20	2.57
Mid Point Flurometer	3/5/2015 21:21	0.49
Mid Point Flurometer	3/5/2015 21:22	0.03
Mid Point Flurometer	3/5/2015 21:23	0.1
Mid Point Flurometer	3/5/2015 21:24	0.11

Location	Date and Time	Rhodmaine Concentration Adjusted Concentration (ppb)
Mid Point Flurometer	3/5/2015 21:25	0.27
Mid Point Flurometer	3/5/2015 21:26	0.09
Mid Point Flurometer	3/5/2015 21:27	0.12
Mid Point Flurometer	3/5/2015 21:28	4.49
Mid Point Flurometer	3/5/2015 21:29	0.36
Mid Point Flurometer	3/5/2015 21:30	0.11
Mid Point Flurometer	3/5/2015 21:31	0.66
Mid Point Flurometer	3/5/2015 21:32	1.07
Mid Point Flurometer	3/5/2015 21:33	1.03
Mid Point Flurometer	3/5/2015 21:34	1.53
Mid Point Flurometer	3/5/2015 21:35	0.02
Mid Point Flurometer	3/5/2015 21:36	1
Mid Point Flurometer	3/5/2015 21:37	0.04
Mid Point Flurometer	3/5/2015 21:38	0.32
Mid Point Flurometer	3/5/2015 21:39	0.2
Mid Point Flurometer	3/5/2015 21:40	0.15
Mid Point Flurometer	3/5/2015 21:41	0.88
Mid Point Flurometer	3/5/2015 21:42	0.03
Mid Point Flurometer	3/5/2015 21:43	1.1
Mid Point Flurometer	3/5/2015 21:44	0.04
Mid Point Flurometer	3/5/2015 21:45	0.35
Mid Point Flurometer	3/5/2015 21:46	0.17
Mid Point Flurometer	3/5/2015 21:47	2.03
Mid Point Flurometer	3/5/2015 21:48	0
Mid Point Flurometer	3/5/2015 21:49	0.09
Mid Point Flurometer	3/5/2015 21:50	0.1
Mid Point Flurometer	3/5/2015 21:51	1.24
Mid Point Flurometer	3/5/2015 21:52	0.11
Mid Point Flurometer	3/5/2015 21:53	0.49
Mid Point Flurometer	3/5/2015 21:54	0.07
Mid Point Flurometer	3/5/2015 21:55	0.4
Mid Point Flurometer	3/5/2015 21:56	0.13
Mid Point Flurometer	3/5/2015 21:57	2.09
Mid Point Flurometer	3/5/2015 21:58	0.09
Mid Point Flurometer	3/5/2015 21:59	0.03
Mid Point Flurometer	3/5/2015 22:00	0.01
Mid Point Flurometer	3/5/2015 22:01	0.14
Mid Point Flurometer	3/5/2015 22:02	0.81
Mid Point Flurometer	3/5/2015 22:03	0.21
Mid Point Flurometer	3/5/2015 22:04	0.14
Mid Point Flurometer	3/5/2015 22:05	0.82
Mid Point Flurometer	3/5/2015 22:06	0.96
Mid Point Flurometer	3/5/2015 22:07	1.81
Mid Point Flurometer	3/5/2015 22:08	0.1
Mid Point Flurometer	3/5/2015 22:09	0.41
Mid Point Flurometer	3/5/2015 22:10	0.15

Location	Date and Time	Rhodmaine Concentration Adjusted Concentration (ppb)
Mid Point Flurometer	3/5/2015 22:11	0.59
Mid Point Flurometer	3/5/2015 22:12	2.7
Mid Point Flurometer	3/5/2015 22:13	1.35
Mid Point Flurometer	3/5/2015 22:14	0.06
Mid Point Flurometer	3/5/2015 22:15	0.1
Mid Point Flurometer	3/5/2015 22:16	0
Mid Point Flurometer	3/5/2015 22:17	0.3
Mid Point Flurometer	3/5/2015 22:18	0.02
Mid Point Flurometer	3/5/2015 22:19	0.6
Mid Point Flurometer	3/5/2015 22:20	0.67
Mid Point Flurometer	3/5/2015 22:21	1.01
Mid Point Flurometer	3/5/2015 22:22	1.4
Mid Point Flurometer	3/5/2015 22:23	0.35
Mid Point Flurometer	3/5/2015 22:24	0.12
Mid Point Flurometer	3/5/2015 22:25	0.09
Mid Point Flurometer	3/5/2015 22:26	1.64
Mid Point Flurometer	3/5/2015 22:27	1.48
Mid Point Flurometer	3/5/2015 22:28	2.08
Mid Point Flurometer	3/5/2015 22:29	0.09
Mid Point Flurometer	3/5/2015 22:30	0.27
Mid Point Flurometer	3/5/2015 22:31	0.01
Mid Point Flurometer	3/5/2015 22:32	0
Mid Point Flurometer	3/5/2015 22:33	2.74
Mid Point Flurometer	3/5/2015 22:34	0.12
Mid Point Flurometer	3/5/2015 22:35	0.18
Mid Point Flurometer	3/5/2015 22:36	0.1
Mid Point Flurometer	3/5/2015 22:37	0.74
Mid Point Flurometer	3/5/2015 22:38	0.15
Mid Point Flurometer	3/5/2015 22:39	0.69
Mid Point Flurometer	3/5/2015 22:40	0
Mid Point Flurometer	3/5/2015 22:41	0.13
Mid Point Flurometer	3/5/2015 22:42	0.04
Mid Point Flurometer	3/5/2015 22:43	1.85
Mid Point Flurometer	3/5/2015 22:44	0.51
Mid Point Flurometer	3/5/2015 22:45	0.16
Mid Point Flurometer	3/5/2015 22:46	0
Mid Point Flurometer	3/5/2015 22:47	0.01
Mid Point Flurometer	3/5/2015 22:48	0.05
Mid Point Flurometer	3/5/2015 22:49	0.02
Mid Point Flurometer	3/5/2015 22:50	0.02
Mid Point Flurometer	3/5/2015 22:51	1.03
Mid Point Flurometer	3/5/2015 22:52	0.03
Mid Point Flurometer	3/5/2015 22:53	0.5
Mid Point Flurometer	3/5/2015 22:54	0.2
Mid Point Flurometer	3/5/2015 22:55	1.32
Mid Point Flurometer	3/5/2015 22:56	1.66

Location	Date and Time	Rhodmaine Concentration Adjusted Concentration (ppb)
Mid Point Flurometer	3/5/2015 22:57	0.27
Mid Point Flurometer	3/5/2015 22:58	0.16
Mid Point Flurometer	3/5/2015 22:59	0.14
Mid Point Flurometer	3/5/2015 23:00	0.28
Mid Point Flurometer	3/5/2015 23:01	0.1
Mid Point Flurometer	3/5/2015 23:02	0.62
Mid Point Flurometer	3/5/2015 23:03	0.61
Mid Point Flurometer	3/5/2015 23:04	0.16
Mid Point Flurometer	3/5/2015 23:05	0.18
Mid Point Flurometer	3/5/2015 23:06	0.82
Mid Point Flurometer	3/5/2015 23:07	0
Mid Point Flurometer	3/5/2015 23:08	0.02
Mid Point Flurometer	3/5/2015 23:09	0.01
Mid Point Flurometer	3/5/2015 23:10	0.3
Mid Point Flurometer	3/5/2015 23:11	1.06
Mid Point Flurometer	3/5/2015 23:12	1.71
Mid Point Flurometer	3/5/2015 23:13	0.08
Mid Point Flurometer	3/5/2015 23:14	0.1
Mid Point Flurometer	3/5/2015 23:15	0.01
Mid Point Flurometer	3/5/2015 23:16	0.23
Mid Point Flurometer	3/5/2015 23:17	0.04
Mid Point Flurometer	3/5/2015 23:18	1.38
Mid Point Flurometer	3/5/2015 23:19	0.1
Mid Point Flurometer	3/5/2015 23:20	0.02
Mid Point Flurometer	3/5/2015 23:21	0.93
Mid Point Flurometer	3/5/2015 23:22	0.09
Mid Point Flurometer	3/5/2015 23:23	1.2
Mid Point Flurometer	3/5/2015 23:24	4.6
Mid Point Flurometer	3/5/2015 23:25	0.42
Mid Point Flurometer	3/5/2015 23:26	3.07
Mid Point Flurometer	3/5/2015 23:27	0.19
Mid Point Flurometer	3/5/2015 23:28	0.05
Mid Point Flurometer	3/5/2015 23:29	0
Mid Point Flurometer	3/5/2015 23:30	0.9
Mid Point Flurometer	3/5/2015 23:31	0.74
Mid Point Flurometer	3/5/2015 23:32	0.06
Mid Point Flurometer	3/5/2015 23:33	3.27
Mid Point Flurometer	3/5/2015 23:34	0.09
Mid Point Flurometer	3/5/2015 23:35	0.12
Mid Point Flurometer	3/5/2015 23:36	0.41
Mid Point Flurometer	3/5/2015 23:37	0.1
Mid Point Flurometer	3/5/2015 23:38	0.09
Mid Point Flurometer	3/5/2015 23:39	0.06
Mid Point Flurometer	3/5/2015 23:40	2.4
Mid Point Flurometer	3/5/2015 23:41	0.38
Mid Point Flurometer	3/5/2015 23:42	0.1

Location	Date and Time	Rhodmaine Concentration Adjusted Concentration (ppb)
Mid Point Flurometer	3/5/2015 23:43	0.56
Mid Point Flurometer	3/5/2015 23:44	1.4
Mid Point Flurometer	3/5/2015 23:45	1.64
Mid Point Flurometer	3/5/2015 23:46	0.07
Mid Point Flurometer	3/5/2015 23:47	0.08
Mid Point Flurometer	3/5/2015 23:48	0.06
Mid Point Flurometer	3/5/2015 23:49	0.02
Mid Point Flurometer	3/5/2015 23:50	0.51
Mid Point Flurometer	3/5/2015 23:51	0.05
Mid Point Flurometer	3/5/2015 23:52	0.05
Mid Point Flurometer	3/5/2015 23:53	2.85
Mid Point Flurometer	3/5/2015 23:54	0.07
Mid Point Flurometer	3/5/2015 23:55	0.11
Mid Point Flurometer	3/5/2015 23:56	0.12
Mid Point Flurometer	3/5/2015 23:57	0.03
Mid Point Flurometer	3/5/2015 23:58	0.06
Mid Point Flurometer	3/5/2015 23:59	0
Mid Point Flurometer	3/6/2015 0:00	0.42
Mid Point Flurometer	3/6/2015 0:01	1.74
Mid Point Flurometer	3/6/2015 0:02	0.13
Mid Point Flurometer	3/6/2015 0:03	1.23
Mid Point Flurometer	3/6/2015 0:04	0.12
Mid Point Flurometer	3/6/2015 0:05	0.38
Mid Point Flurometer	3/6/2015 0:06	6.31
Mid Point Flurometer	3/6/2015 0:07	0.06
Mid Point Flurometer	3/6/2015 0:08	0.02
Mid Point Flurometer	3/6/2015 0:09	1.09
Mid Point Flurometer	3/6/2015 0:10	0
Mid Point Flurometer	3/6/2015 0:11	0.48
Mid Point Flurometer	3/6/2015 0:12	0.01
Mid Point Flurometer	3/6/2015 0:13	0.35
Mid Point Flurometer	3/6/2015 0:14	0
Mid Point Flurometer	3/6/2015 0:15	0.18
Mid Point Flurometer	3/6/2015 0:16	0.02
Mid Point Flurometer	3/6/2015 0:17	0.12
Mid Point Flurometer	3/6/2015 0:18	0.07
Mid Point Flurometer	3/6/2015 0:19	0.08
Mid Point Flurometer	3/6/2015 0:20	0.25
Mid Point Flurometer	3/6/2015 0:21	0.05
Mid Point Flurometer	3/6/2015 0:22	0.03
Mid Point Flurometer	3/6/2015 0:23	3.5
Mid Point Flurometer	3/6/2015 0:24	0.05
Mid Point Flurometer	3/6/2015 0:25	6.32
Mid Point Flurometer	3/6/2015 0:26	0.35
Mid Point Flurometer	3/6/2015 0:27	0.04
Mid Point Flurometer	3/6/2015 0:28	0.2

Location	Date and Time	Rhodmaine Concentration Adjusted Concentration (ppb)
Mid Point Flurometer	3/6/2015 0:29	0
Mid Point Flurometer	3/6/2015 0:30	0.18
Mid Point Flurometer	3/6/2015 0:31	0.03
Mid Point Flurometer	3/6/2015 0:32	0.05
Mid Point Flurometer	3/6/2015 0:33	1.41
Mid Point Flurometer	3/6/2015 0:34	0.06
Mid Point Flurometer	3/6/2015 0:35	0.08
Mid Point Flurometer	3/6/2015 0:36	0.28
Mid Point Flurometer	3/6/2015 0:37	3.5
Mid Point Flurometer	3/6/2015 0:38	0.14
Mid Point Flurometer	3/6/2015 0:39	1.51
Mid Point Flurometer	3/6/2015 0:40	0.24
Mid Point Flurometer	3/6/2015 0:41	0.28
Mid Point Flurometer	3/6/2015 0:42	0.03
Mid Point Flurometer	3/6/2015 0:43	0.1
Mid Point Flurometer	3/6/2015 0:44	0.36
Mid Point Flurometer	3/6/2015 0:45	1.25
Mid Point Flurometer	3/6/2015 0:46	0.12
Mid Point Flurometer	3/6/2015 0:47	0.05
Mid Point Flurometer	3/6/2015 0:48	0.1
Mid Point Flurometer	3/6/2015 0:49	0.43
Mid Point Flurometer	3/6/2015 0:50	0.04
Mid Point Flurometer	3/6/2015 0:51	0.77
Mid Point Flurometer	3/6/2015 0:52	0.1
Mid Point Flurometer	3/6/2015 0:53	0.02
Mid Point Flurometer	3/6/2015 0:54	0.91
Mid Point Flurometer	3/6/2015 0:55	0.02
Mid Point Flurometer	3/6/2015 0:56	0.06
Mid Point Flurometer	3/6/2015 0:57	0.04
Mid Point Flurometer	3/6/2015 0:58	1.86
Mid Point Flurometer	3/6/2015 0:59	0.16
Mid Point Flurometer	3/6/2015 1:00	0.42
Mid Point Flurometer	3/6/2015 1:01	0.11
Mid Point Flurometer	3/6/2015 1:02	8.36
Mid Point Flurometer	3/6/2015 1:03	0.11
Mid Point Flurometer	3/6/2015 1:04	0.67
Mid Point Flurometer	3/6/2015 1:05	0
Mid Point Flurometer	3/6/2015 1:06	0.67
Mid Point Flurometer	3/6/2015 1:07	1.27
Mid Point Flurometer	3/6/2015 1:08	0.03
Mid Point Flurometer	3/6/2015 1:09	0.11
Mid Point Flurometer	3/6/2015 1:10	0.11
Mid Point Flurometer	3/6/2015 1:11	0.1
Mid Point Flurometer	3/6/2015 1:12	0.03
Mid Point Flurometer	3/6/2015 1:13	0
Mid Point Flurometer	3/6/2015 1:14	0.12

Location	Date and Time	Rhodmaine Concentration Adjusted Concentration (ppb)
Mid Point Flurometer	3/6/2015 1:15	0.23
Mid Point Flurometer	3/6/2015 1:16	1.51
Mid Point Flurometer	3/6/2015 1:17	0.05
Mid Point Flurometer	3/6/2015 1:18	0.05
Mid Point Flurometer	3/6/2015 1:19	1.6
Mid Point Flurometer	3/6/2015 1:20	0.2
Mid Point Flurometer	3/6/2015 1:21	0.02
Mid Point Flurometer	3/6/2015 1:22	0.01
Mid Point Flurometer	3/6/2015 1:23	0.04
Mid Point Flurometer	3/6/2015 1:24	0.65
Mid Point Flurometer	3/6/2015 1:25	0.08
Mid Point Flurometer	3/6/2015 1:26	0.32
Mid Point Flurometer	3/6/2015 1:27	1.71
Mid Point Flurometer	3/6/2015 1:28	0.12
Mid Point Flurometer	3/6/2015 1:29	0
Mid Point Flurometer	3/6/2015 1:30	0.15
Mid Point Flurometer	3/6/2015 1:31	0.14
Mid Point Flurometer	3/6/2015 1:32	0.3
Mid Point Flurometer	3/6/2015 1:33	0.05
Mid Point Flurometer	3/6/2015 1:34	0.06
Mid Point Flurometer	3/6/2015 1:35	0.09
Mid Point Flurometer	3/6/2015 1:36	0.05
Mid Point Flurometer	3/6/2015 1:37	0.45
Mid Point Flurometer	3/6/2015 1:38	0.05
Mid Point Flurometer	3/6/2015 1:39	0.09
Mid Point Flurometer	3/6/2015 1:40	0.12
Mid Point Flurometer	3/6/2015 1:41	0.02
Mid Point Flurometer	3/6/2015 1:42	0.02
Mid Point Flurometer	3/6/2015 1:43	0.07
Mid Point Flurometer	3/6/2015 1:44	0.32
Mid Point Flurometer	3/6/2015 1:45	0.04
Mid Point Flurometer	3/6/2015 1:46	0.11
Mid Point Flurometer	3/6/2015 1:47	0.05
Mid Point Flurometer	3/6/2015 1:48	0.21
Mid Point Flurometer	3/6/2015 1:49	0.03
Mid Point Flurometer	3/6/2015 1:50	0.14
Mid Point Flurometer	3/6/2015 1:51	1
Mid Point Flurometer	3/6/2015 1:52	0.01
Mid Point Flurometer	3/6/2015 1:53	0.14
Mid Point Flurometer	3/6/2015 1:54	0.05
Mid Point Flurometer	3/6/2015 1:55	0
Mid Point Flurometer	3/6/2015 1:56	0.08
Mid Point Flurometer	3/6/2015 1:57	0.07
Mid Point Flurometer	3/6/2015 1:58	0.12
Mid Point Flurometer	3/6/2015 1:59	0.02
Mid Point Flurometer	3/6/2015 2:00	0.02

Location	Date and Time	Rhodmaine Concentration Adjusted Concentration (ppb)
Mid Point Flurometer	3/6/2015 2:01	0.04
Mid Point Flurometer	3/6/2015 2:02	0.03
Mid Point Flurometer	3/6/2015 2:03	0.13
Mid Point Flurometer	3/6/2015 2:04	0.1
Mid Point Flurometer	3/6/2015 2:05	0.01
Mid Point Flurometer	3/6/2015 2:06	0.06
Mid Point Flurometer	3/6/2015 2:07	0.01
Mid Point Flurometer	3/6/2015 2:08	0.01
Mid Point Flurometer	3/6/2015 2:09	0.04
Mid Point Flurometer	3/6/2015 2:10	0.02
Mid Point Flurometer	3/6/2015 2:11	0.01
Mid Point Flurometer	3/6/2015 2:12	0.05
Mid Point Flurometer	3/6/2015 2:13	0.09
Mid Point Flurometer	3/6/2015 2:14	0.07
Mid Point Flurometer	3/6/2015 2:15	0.02
Mid Point Flurometer	3/6/2015 2:16	0
Mid Point Flurometer	3/6/2015 2:17	0.2
Mid Point Flurometer	3/6/2015 2:18	0.41
Mid Point Flurometer	3/6/2015 2:19	0.01
Mid Point Flurometer	3/6/2015 2:20	0.14
Mid Point Flurometer	3/6/2015 2:21	0
Mid Point Flurometer	3/6/2015 2:22	0.16
Mid Point Flurometer	3/6/2015 2:23	0.02
Mid Point Flurometer	3/6/2015 2:24	0.1
Mid Point Flurometer	3/6/2015 2:25	0.04
Mid Point Flurometer	3/6/2015 2:26	0.01
Mid Point Flurometer	3/6/2015 2:27	0.1
Mid Point Flurometer	3/6/2015 2:28	0.06
Mid Point Flurometer	3/6/2015 2:29	0.04
Mid Point Flurometer	3/6/2015 2:30	0.07
Mid Point Flurometer	3/6/2015 2:31	0
Mid Point Flurometer	3/6/2015 2:32	0.37
Mid Point Flurometer	3/6/2015 2:33	0.08
Mid Point Flurometer	3/6/2015 2:34	0.19
Mid Point Flurometer	3/6/2015 2:35	0.03
Mid Point Flurometer	3/6/2015 2:36	0.05
Mid Point Flurometer	3/6/2015 2:37	0.04
Mid Point Flurometer	3/6/2015 2:38	2.49
Mid Point Flurometer	3/6/2015 2:39	0
Mid Point Flurometer	3/6/2015 2:40	0.04
Mid Point Flurometer	3/6/2015 2:41	0.05
Mid Point Flurometer	3/6/2015 2:42	0.26
Mid Point Flurometer	3/6/2015 2:43	0.29
Mid Point Flurometer	3/6/2015 2:44	0.07
Mid Point Flurometer	3/6/2015 2:45	0.04
Mid Point Flurometer	3/6/2015 2:46	0.16

Location	Date and Time	Rhodmaine Concentration Adjusted Concentration (ppb)
Mid Point Flurometer	3/6/2015 2:47	0.02
Mid Point Flurometer	3/6/2015 2:48	0.09
Mid Point Flurometer	3/6/2015 2:49	0.11
Mid Point Flurometer	3/6/2015 2:50	0.03
Mid Point Flurometer	3/6/2015 2:51	1.14
Mid Point Flurometer	3/6/2015 2:52	0
Mid Point Flurometer	3/6/2015 2:53	0.04
Mid Point Flurometer	3/6/2015 2:54	0.15
Mid Point Flurometer	3/6/2015 2:55	0.25
Mid Point Flurometer	3/6/2015 2:56	0.05
Mid Point Flurometer	3/6/2015 2:57	0
Mid Point Flurometer	3/6/2015 2:58	0
Mid Point Flurometer	3/6/2015 2:59	0.09
Mid Point Flurometer	3/6/2015 3:00	0.02
Mid Point Flurometer	3/6/2015 3:01	0.03
Mid Point Flurometer	3/6/2015 3:02	0.01
Mid Point Flurometer	3/6/2015 3:03	0.03
Mid Point Flurometer	3/6/2015 3:04	0.06
Mid Point Flurometer	3/6/2015 3:05	1.58
Mid Point Flurometer	3/6/2015 3:06	0.03
Mid Point Flurometer	3/6/2015 3:07	0.06
Mid Point Flurometer	3/6/2015 3:08	0.17
Mid Point Flurometer	3/6/2015 3:09	0.1
Mid Point Flurometer	3/6/2015 3:10	0.06
Mid Point Flurometer	3/6/2015 3:11	0.18
Mid Point Flurometer	3/6/2015 3:12	0.05
Mid Point Flurometer	3/6/2015 3:13	2.37
Mid Point Flurometer	3/6/2015 3:14	0.07
Mid Point Flurometer	3/6/2015 3:15	0.05
Mid Point Flurometer	3/6/2015 3:16	0.07
Mid Point Flurometer	3/6/2015 3:17	0
Mid Point Flurometer	3/6/2015 3:18	0.63
Mid Point Flurometer	3/6/2015 3:19	0.04
Mid Point Flurometer	3/6/2015 3:20	0.1
Mid Point Flurometer	3/6/2015 3:21	0.16
Mid Point Flurometer	3/6/2015 3:22	0.05
Mid Point Flurometer	3/6/2015 3:23	0.03
Mid Point Flurometer	3/6/2015 3:24	0.05
Mid Point Flurometer	3/6/2015 3:25	0.08
Mid Point Flurometer	3/6/2015 3:26	0.1
Mid Point Flurometer	3/6/2015 3:27	0.08
Mid Point Flurometer	3/6/2015 3:28	0.04
Mid Point Flurometer	3/6/2015 3:29	0.06
Mid Point Flurometer	3/6/2015 3:30	1.08
Mid Point Flurometer	3/6/2015 3:31	0
Mid Point Flurometer	3/6/2015 3:32	0.28

Location	Date and Time	Rhodmaine Concentration Adjusted Concentration (ppb)
Mid Point Flurometer	3/6/2015 3:33	0.72
Mid Point Flurometer	3/6/2015 3:34	0.19
Mid Point Flurometer	3/6/2015 3:35	0.12
Mid Point Flurometer	3/6/2015 3:36	0.07
Mid Point Flurometer	3/6/2015 3:37	0.12
Mid Point Flurometer	3/6/2015 3:38	0.12
Mid Point Flurometer	3/6/2015 3:39	0.17
Mid Point Flurometer	3/6/2015 3:40	0.2
Mid Point Flurometer	3/6/2015 3:41	0.04
Mid Point Flurometer	3/6/2015 3:42	0.01
Mid Point Flurometer	3/6/2015 3:43	0.03
Mid Point Flurometer	3/6/2015 3:44	0.09
Mid Point Flurometer	3/6/2015 3:45	0.07
Mid Point Flurometer	3/6/2015 3:46	0.03
Mid Point Flurometer	3/6/2015 3:47	0.03
Mid Point Flurometer	3/6/2015 3:48	0.09
Mid Point Flurometer	3/6/2015 3:49	0.05
Mid Point Flurometer	3/6/2015 3:50	0.07
Mid Point Flurometer	3/6/2015 3:51	0.08
Mid Point Flurometer	3/6/2015 3:52	0.05
Mid Point Flurometer	3/6/2015 3:53	0.18
Mid Point Flurometer	3/6/2015 3:54	0.12
Mid Point Flurometer	3/6/2015 3:55	0.04
Mid Point Flurometer	3/6/2015 3:56	0.35
Mid Point Flurometer	3/6/2015 3:57	0.09
Mid Point Flurometer	3/6/2015 3:58	0.07
Mid Point Flurometer	3/6/2015 3:59	0.04
Mid Point Flurometer	3/6/2015 4:00	0.56
Mid Point Flurometer	3/6/2015 4:01	0.07
Mid Point Flurometer	3/6/2015 4:02	0.07
Mid Point Flurometer	3/6/2015 4:03	0.21
Mid Point Flurometer	3/6/2015 4:04	3.33
Mid Point Flurometer	3/6/2015 4:05	0.12
Mid Point Flurometer	3/6/2015 4:06	0.01
Mid Point Flurometer	3/6/2015 4:07	0.01
Mid Point Flurometer	3/6/2015 4:08	0.05
Mid Point Flurometer	3/6/2015 4:09	0.26
Mid Point Flurometer	3/6/2015 4:10	0.06
Mid Point Flurometer	3/6/2015 4:11	0.04
Mid Point Flurometer	3/6/2015 4:12	0
Mid Point Flurometer	3/6/2015 4:13	0.01
Mid Point Flurometer	3/6/2015 4:14	0.54
Mid Point Flurometer	3/6/2015 4:15	0.11
Mid Point Flurometer	3/6/2015 4:16	0.06
Mid Point Flurometer	3/6/2015 4:17	0.11
Mid Point Flurometer	3/6/2015 4:18	0.02

Location	Date and Time	Rhodmaine Concentration Adjusted Concentration (ppb)
Mid Point Flurometer	3/6/2015 4:19	0.2
Mid Point Flurometer	3/6/2015 4:20	0.1
Mid Point Flurometer	3/6/2015 4:21	0.05
Mid Point Flurometer	3/6/2015 4:22	2.69
Mid Point Flurometer	3/6/2015 4:23	0.14
Mid Point Flurometer	3/6/2015 4:24	0.14
Mid Point Flurometer	3/6/2015 4:25	0.12
Mid Point Flurometer	3/6/2015 4:26	0
Mid Point Flurometer	3/6/2015 4:27	0.5
Mid Point Flurometer	3/6/2015 4:28	0.04
Mid Point Flurometer	3/6/2015 4:29	0
Mid Point Flurometer	3/6/2015 4:30	0.1
Mid Point Flurometer	3/6/2015 4:31	0.04
Mid Point Flurometer	3/6/2015 4:32	0.15
Mid Point Flurometer	3/6/2015 4:33	0.12
Mid Point Flurometer	3/6/2015 4:34	0.09
Mid Point Flurometer	3/6/2015 4:35	0.09
Mid Point Flurometer	3/6/2015 4:36	0.04
Mid Point Flurometer	3/6/2015 4:37	0.03
Mid Point Flurometer	3/6/2015 4:38	0.09
Mid Point Flurometer	3/6/2015 4:39	0.13
Mid Point Flurometer	3/6/2015 4:40	0.1
Mid Point Flurometer	3/6/2015 4:41	0.06
Mid Point Flurometer	3/6/2015 4:42	0.14
Mid Point Flurometer	3/6/2015 4:43	0.73
Mid Point Flurometer	3/6/2015 4:44	0.06
Mid Point Flurometer	3/6/2015 4:45	0.04
Mid Point Flurometer	3/6/2015 4:46	1.01
Mid Point Flurometer	3/6/2015 4:47	0.06
Mid Point Flurometer	3/6/2015 4:48	0.71
Mid Point Flurometer	3/6/2015 4:49	0.1
Mid Point Flurometer	3/6/2015 4:50	0.02
Mid Point Flurometer	3/6/2015 4:51	0.05
Mid Point Flurometer	3/6/2015 4:52	0.12
Mid Point Flurometer	3/6/2015 4:53	0.09
Mid Point Flurometer	3/6/2015 4:54	0.06
Mid Point Flurometer	3/6/2015 4:55	0.16
Mid Point Flurometer	3/6/2015 4:56	0.08
Mid Point Flurometer	3/6/2015 4:57	0.04
Mid Point Flurometer	3/6/2015 4:58	0.01
Mid Point Flurometer	3/6/2015 4:59	0.05
Mid Point Flurometer	3/6/2015 5:00	0.05
Mid Point Flurometer	3/6/2015 5:01	0.04
Mid Point Flurometer	3/6/2015 5:02	8.21
Mid Point Flurometer	3/6/2015 5:03	0.13
Mid Point Flurometer	3/6/2015 5:04	0.02

Location	Date and Time	Rhodmaine Concentration Adjusted Concentration (ppb)
Mid Point Flurometer	3/6/2015 5:05	0.12
Mid Point Flurometer	3/6/2015 5:06	0.07
Mid Point Flurometer	3/6/2015 5:07	0.13
Mid Point Flurometer	3/6/2015 5:08	0.03
Mid Point Flurometer	3/6/2015 5:09	0.14
Mid Point Flurometer	3/6/2015 5:10	0.06
Mid Point Flurometer	3/6/2015 5:11	0.03
Mid Point Flurometer	3/6/2015 5:12	0.1
Mid Point Flurometer	3/6/2015 5:13	0.1
Mid Point Flurometer	3/6/2015 5:14	0
Mid Point Flurometer	3/6/2015 5:15	0.05
Mid Point Flurometer	3/6/2015 5:16	0.09
Mid Point Flurometer	3/6/2015 5:17	0.02
Mid Point Flurometer	3/6/2015 5:18	0.13
Mid Point Flurometer	3/6/2015 5:19	0.13
Mid Point Flurometer	3/6/2015 5:20	0.09
Mid Point Flurometer	3/6/2015 5:21	0.07
Mid Point Flurometer	3/6/2015 5:22	0.71
Mid Point Flurometer	3/6/2015 5:23	0.11
Mid Point Flurometer	3/6/2015 5:24	0.09
Mid Point Flurometer	3/6/2015 5:25	0.96
Mid Point Flurometer	3/6/2015 5:26	0.41
Mid Point Flurometer	3/6/2015 5:27	0.06
Mid Point Flurometer	3/6/2015 5:28	1.68
Mid Point Flurometer	3/6/2015 5:29	0.04
Mid Point Flurometer	3/6/2015 5:30	0.09
Mid Point Flurometer	3/6/2015 5:31	0
Mid Point Flurometer	3/6/2015 5:32	0.2
Mid Point Flurometer	3/6/2015 5:33	0.09
Mid Point Flurometer	3/6/2015 5:34	0.08
Mid Point Flurometer	3/6/2015 5:35	0.07
Mid Point Flurometer	3/6/2015 5:36	0.07
Mid Point Flurometer	3/6/2015 5:37	0.15
Mid Point Flurometer	3/6/2015 5:38	0.12
Mid Point Flurometer	3/6/2015 5:39	0.08
Mid Point Flurometer	3/6/2015 5:40	0.34
Mid Point Flurometer	3/6/2015 5:41	0.3
Mid Point Flurometer	3/6/2015 5:42	0.24
Mid Point Flurometer	3/6/2015 5:43	0.18
Mid Point Flurometer	3/6/2015 5:44	0.06
Mid Point Flurometer	3/6/2015 5:45	0.06
Mid Point Flurometer	3/6/2015 5:46	0.13
Mid Point Flurometer	3/6/2015 5:47	0.11
Mid Point Flurometer	3/6/2015 5:48	0
Mid Point Flurometer	3/6/2015 5:49	0.19
Mid Point Flurometer	3/6/2015 5:50	0.22

Location	Date and Time	Rhodmaine Concentration Adjusted Concentration (ppb)
Mid Point Flurometer	3/6/2015 5:51	0.3
Mid Point Flurometer	3/6/2015 5:52	0.07
Mid Point Flurometer	3/6/2015 5:53	0.1
Mid Point Flurometer	3/6/2015 5:54	0.31
Mid Point Flurometer	3/6/2015 5:55	0.09
Mid Point Flurometer	3/6/2015 5:56	0.48
Mid Point Flurometer	3/6/2015 5:57	0.19
Mid Point Flurometer	3/6/2015 5:58	0.04
Mid Point Flurometer	3/6/2015 5:59	0.04
Mid Point Flurometer	3/6/2015 6:00	8.42
Mid Point Flurometer	3/6/2015 6:01	0.09
Mid Point Flurometer	3/6/2015 6:02	0.07
Mid Point Flurometer	3/6/2015 6:03	0.1
Mid Point Flurometer	3/6/2015 6:04	0.08
Mid Point Flurometer	3/6/2015 6:05	0.08
Mid Point Flurometer	3/6/2015 6:06	0.09
Mid Point Flurometer	3/6/2015 6:07	0.08
Mid Point Flurometer	3/6/2015 6:08	0.04
Mid Point Flurometer	3/6/2015 6:09	0.38
Mid Point Flurometer	3/6/2015 6:10	0.25
Mid Point Flurometer	3/6/2015 6:11	0.17
Mid Point Flurometer	3/6/2015 6:12	0.11
Mid Point Flurometer	3/6/2015 6:13	0.02
Mid Point Flurometer	3/6/2015 6:14	0.11
Mid Point Flurometer	3/6/2015 6:15	0.09
Mid Point Flurometer	3/6/2015 6:16	0.18
Mid Point Flurometer	3/6/2015 6:17	0.08
Mid Point Flurometer	3/6/2015 6:18	0.17
Mid Point Flurometer	3/6/2015 6:19	0.13
Mid Point Flurometer	3/6/2015 6:20	0.07
Mid Point Flurometer	3/6/2015 6:21	0.16
Mid Point Flurometer	3/6/2015 6:22	0.13
Mid Point Flurometer	3/6/2015 6:23	0.19
Mid Point Flurometer	3/6/2015 6:24	0.23
Mid Point Flurometer	3/6/2015 6:25	0.01
Mid Point Flurometer	3/6/2015 6:26	0.07
Mid Point Flurometer	3/6/2015 6:27	0.12
Mid Point Flurometer	3/6/2015 6:28	0.15
Mid Point Flurometer	3/6/2015 6:29	0.17
Mid Point Flurometer	3/6/2015 6:30	0.95
Mid Point Flurometer	3/6/2015 6:31	0.18
Mid Point Flurometer	3/6/2015 6:32	0.82
Mid Point Flurometer	3/6/2015 6:33	0.43
Mid Point Flurometer	3/6/2015 6:34	0.17
Mid Point Flurometer	3/6/2015 6:35	0.09
Mid Point Flurometer	3/6/2015 6:36	0.08

Location	Date and Time	Rhodmaine Concentration Adjusted Concentration (ppb)
Mid Point Flurometer	3/6/2015 6:37	0.24
Mid Point Flurometer	3/6/2015 6:38	0.27
Mid Point Flurometer	3/6/2015 6:39	0.03
Mid Point Flurometer	3/6/2015 6:40	0.09
Mid Point Flurometer	3/6/2015 6:41	0.19
Mid Point Flurometer	3/6/2015 6:42	0.07
Mid Point Flurometer	3/6/2015 6:43	0.1
Mid Point Flurometer	3/6/2015 6:44	0.06
Mid Point Flurometer	3/6/2015 6:45	0.24
Mid Point Flurometer	3/6/2015 6:46	0.31
Mid Point Flurometer	3/6/2015 6:47	0.81
Mid Point Flurometer	3/6/2015 6:48	0.03
Mid Point Flurometer	3/6/2015 6:49	0.12
Mid Point Flurometer	3/6/2015 6:50	0.13
Mid Point Flurometer	3/6/2015 6:51	0.13
Mid Point Flurometer	3/6/2015 6:52	0.15
Mid Point Flurometer	3/6/2015 6:53	0.19
Mid Point Flurometer	3/6/2015 6:54	2.25
Mid Point Flurometer	3/6/2015 6:55	0.15
Mid Point Flurometer	3/6/2015 6:56	0.11
Mid Point Flurometer	3/6/2015 6:57	0.05
Mid Point Flurometer	3/6/2015 6:58	0.3
Mid Point Flurometer	3/6/2015 6:59	0.1
Mid Point Flurometer	3/6/2015 7:00	0.12
Mid Point Flurometer	3/6/2015 7:01	0.13
Mid Point Flurometer	3/6/2015 7:02	0.17
Mid Point Flurometer	3/6/2015 7:03	0.16
Mid Point Flurometer	3/6/2015 7:04	0.08
Mid Point Flurometer	3/6/2015 7:05	0.14
Mid Point Flurometer	3/6/2015 7:06	1.81
Mid Point Flurometer	3/6/2015 7:07	0.34
Mid Point Flurometer	3/6/2015 7:08	0.25
Mid Point Flurometer	3/6/2015 7:09	0.19
Mid Point Flurometer	3/6/2015 7:10	0.59
Mid Point Flurometer	3/6/2015 7:11	0.42
Mid Point Flurometer	3/6/2015 7:12	0.08
Mid Point Flurometer	3/6/2015 7:13	0.19
Mid Point Flurometer	3/6/2015 7:14	0.11
Mid Point Flurometer	3/6/2015 7:15	0.87
Mid Point Flurometer	3/6/2015 7:16	0.04
Mid Point Flurometer	3/6/2015 7:17	0.1
Mid Point Flurometer	3/6/2015 7:18	0.12
Mid Point Flurometer	3/6/2015 7:19	0.42
Mid Point Flurometer	3/6/2015 7:20	0
Mid Point Flurometer	3/6/2015 7:21	0
Mid Point Flurometer	3/6/2015 7:22	0

Location	Date and Time	Rhodmaine Concentration Adjusted Concentration (ppb)
Mid Point Flurometer	3/6/2015 7:23	0
Mid Point Flurometer	3/6/2015 7:24	0
Mid Point Flurometer	3/6/2015 7:25	0
Mid Point Flurometer	3/6/2015 7:26	0.04
Mid Point Flurometer	3/6/2015 7:27	1.37
Mid Point Flurometer	3/6/2015 7:28	0
Mid Point Flurometer	3/6/2015 7:29	0
Mid Point Flurometer	3/6/2015 7:30	0
Mid Point Flurometer	3/6/2015 7:31	0
Mid Point Flurometer	3/6/2015 7:32	0
Mid Point Flurometer	3/6/2015 7:33	0
Mid Point Flurometer	3/6/2015 7:34	0
Mid Point Flurometer	3/6/2015 7:35	0
Mid Point Flurometer	3/6/2015 7:36	0
Mid Point Flurometer	3/6/2015 7:37	0
Mid Point Flurometer	3/6/2015 7:38	0
Mid Point Flurometer	3/6/2015 7:39	0.01
Mid Point Flurometer	3/6/2015 7:40	0.01
Mid Point Flurometer	3/6/2015 7:41	0.03
Mid Point Flurometer	3/6/2015 7:42	0.03
Mid Point Flurometer	3/6/2015 7:43	0
Mid Point Flurometer	3/6/2015 7:44	0
Mid Point Flurometer	3/6/2015 7:45	0
Mid Point Flurometer	3/6/2015 7:46	0.05
Mid Point Flurometer	3/6/2015 7:47	0
Mid Point Flurometer	3/6/2015 7:48	0
Mid Point Flurometer	3/6/2015 7:49	0.01
Mid Point Flurometer	3/6/2015 7:50	0
Mid Point Flurometer	3/6/2015 7:51	0.03
Mid Point Flurometer	3/6/2015 7:52	0
Mid Point Flurometer	3/6/2015 7:53	0.03
Mid Point Flurometer	3/6/2015 7:54	0.03
Mid Point Flurometer	3/6/2015 7:55	0.04
Mid Point Flurometer	3/6/2015 7:56	0.09
Mid Point Flurometer	3/6/2015 7:57	0.01
Mid Point Flurometer	3/6/2015 7:58	0
Mid Point Flurometer	3/6/2015 7:59	0.05
Mid Point Flurometer	3/6/2015 8:00	0.05
Mid Point Flurometer	3/6/2015 8:01	0
Mid Point Flurometer	3/6/2015 8:02	0
Mid Point Flurometer	3/6/2015 8:03	0
Mid Point Flurometer	3/6/2015 8:04	0.07
Mid Point Flurometer	3/6/2015 8:05	0
Mid Point Flurometer	3/6/2015 8:06	0
Mid Point Flurometer	3/6/2015 8:07	0
Mid Point Flurometer	3/6/2015 8:08	0.02

Location	Date and Time	Rhodmaine Concentration Adjusted Concentration (ppb)
Mid Point Flurometer	3/6/2015 8:09	0
Mid Point Flurometer	3/6/2015 8:10	0.06
Mid Point Flurometer	3/6/2015 8:11	0.01
Mid Point Flurometer	3/6/2015 8:12	0
Mid Point Flurometer	3/6/2015 8:13	0
Mid Point Flurometer	3/6/2015 8:14	0
Mid Point Flurometer	3/6/2015 8:15	0.18
Mid Point Flurometer	3/6/2015 8:16	0.04
Mid Point Flurometer	3/6/2015 8:17	0.06
Mid Point Flurometer	3/6/2015 8:18	0
Mid Point Flurometer	3/6/2015 8:19	0.05
Mid Point Flurometer	3/6/2015 8:20	0
Mid Point Flurometer	3/6/2015 8:21	0.01
Mid Point Flurometer	3/6/2015 8:22	0.03
Mid Point Flurometer	3/6/2015 8:23	0.11
Mid Point Flurometer	3/6/2015 8:24	0.06
Mid Point Flurometer	3/6/2015 8:25	0
Mid Point Flurometer	3/6/2015 8:26	0
Mid Point Flurometer	3/6/2015 8:27	0
Mid Point Flurometer	3/6/2015 8:28	0
Mid Point Flurometer	3/6/2015 8:29	0
Mid Point Flurometer	3/6/2015 8:30	0
Mid Point Flurometer	3/6/2015 8:31	0
Mid Point Flurometer	3/6/2015 8:32	0
Mid Point Flurometer	3/6/2015 8:33	0.27
Mid Point Flurometer	3/6/2015 8:34	0
Mid Point Flurometer	3/6/2015 8:35	0
Mid Point Flurometer	3/6/2015 8:36	0
Mid Point Flurometer	3/6/2015 8:37	0
Mid Point Flurometer	3/6/2015 8:38	0.03
Mid Point Flurometer	3/6/2015 8:39	0
Mid Point Flurometer	3/6/2015 8:40	0
Mid Point Flurometer	3/6/2015 8:41	0
Mid Point Flurometer	3/6/2015 8:42	0.01
Mid Point Flurometer	3/6/2015 8:43	0.46
Mid Point Flurometer	3/6/2015 8:44	0.01
Mid Point Flurometer	3/6/2015 8:45	0
Mid Point Flurometer	3/6/2015 8:46	0.09
Mid Point Flurometer	3/6/2015 8:47	0
Mid Point Flurometer	3/6/2015 8:48	0.04
Mid Point Flurometer	3/6/2015 8:49	0
Mid Point Flurometer	3/6/2015 8:50	0.15
Mid Point Flurometer	3/6/2015 8:51	0.01
Mid Point Flurometer	3/6/2015 8:52	0.26
Mid Point Flurometer	3/6/2015 8:53	0.02
Mid Point Flurometer	3/6/2015 8:54	0.05

Location	Date and Time	Rhodmaine Concentration Adjusted Concentration (ppb)
Mid Point Flurometer	3/6/2015 8:55	0
Mid Point Flurometer	3/6/2015 8:56	0
Mid Point Flurometer	3/6/2015 8:57	0.07
Mid Point Flurometer	3/6/2015 8:58	0.71
Mid Point Flurometer	3/6/2015 8:59	0.03
Mid Point Flurometer	3/6/2015 9:00	0
Mid Point Flurometer	3/6/2015 9:01	0
Mid Point Flurometer	3/6/2015 9:02	0
Mid Point Flurometer	3/6/2015 9:03	0.07
Mid Point Flurometer	3/6/2015 9:04	0
Mid Point Flurometer	3/6/2015 9:05	0
Mid Point Flurometer	3/6/2015 9:06	0
Mid Point Flurometer	3/6/2015 9:07	0
Mid Point Flurometer	3/6/2015 9:08	0
Mid Point Flurometer	3/6/2015 9:09	0
Mid Point Flurometer	3/6/2015 9:10	0.01
Mid Point Flurometer	3/6/2015 9:11	0
Mid Point Flurometer	3/6/2015 9:12	0
Mid Point Flurometer	3/6/2015 9:13	0.1
Mid Point Flurometer	3/6/2015 9:14	0.02
Mid Point Flurometer	3/6/2015 9:15	0
Mid Point Flurometer	3/6/2015 9:16	0.02
Mid Point Flurometer	3/6/2015 9:17	0
Mid Point Flurometer	3/6/2015 9:18	0
Mid Point Flurometer	3/6/2015 9:19	0.02
Mid Point Flurometer	3/6/2015 9:20	0
Mid Point Flurometer	3/6/2015 9:21	0.06
Mid Point Flurometer	3/6/2015 9:22	0
Mid Point Flurometer	3/6/2015 9:23	0
Mid Point Flurometer	3/6/2015 9:24	0
Mid Point Flurometer	3/6/2015 9:25	0
Mid Point Flurometer	3/6/2015 9:26	0.24
Mid Point Flurometer	3/6/2015 9:27	0
Mid Point Flurometer	3/6/2015 9:28	0
Mid Point Flurometer	3/6/2015 9:29	0
Mid Point Flurometer	3/6/2015 9:30	0
Mid Point Flurometer	3/6/2015 9:31	0
Mid Point Flurometer	3/6/2015 9:32	0
Mid Point Flurometer	3/6/2015 9:33	0.09
Mid Point Flurometer	3/6/2015 9:34	0.02
Mid Point Flurometer	3/6/2015 9:35	0.3
Mid Point Flurometer	3/6/2015 9:36	0
Mid Point Flurometer	3/6/2015 9:37	0
Mid Point Flurometer	3/6/2015 9:38	0
Mid Point Flurometer	3/6/2015 9:39	0
Mid Point Flurometer	3/6/2015 9:40	0.04

Location	Date and Time	Rhodmaine Concentration Adjusted Concentration (ppb)
Mid Point Flurometer	3/6/2015 9:41	0.03
Mid Point Flurometer	3/6/2015 9:42	0.06
Mid Point Flurometer	3/6/2015 9:43	0.02
Mid Point Flurometer	3/6/2015 9:44	0
Mid Point Flurometer	3/6/2015 9:45	0
Mid Point Flurometer	3/6/2015 9:46	0
Mid Point Flurometer	3/6/2015 9:47	0.07
Mid Point Flurometer	3/6/2015 9:48	0
Mid Point Flurometer	3/6/2015 9:49	0
Mid Point Flurometer	3/6/2015 9:50	0.06
Mid Point Flurometer	3/6/2015 9:51	0
Mid Point Flurometer	3/6/2015 9:52	0.03
Mid Point Flurometer	3/6/2015 9:53	0.01
Mid Point Flurometer	3/6/2015 9:54	0.05
Mid Point Flurometer	3/6/2015 9:55	0
Mid Point Flurometer	3/6/2015 9:56	0
Mid Point Flurometer	3/6/2015 9:57	0
Mid Point Flurometer	3/6/2015 9:58	0
Mid Point Flurometer	3/6/2015 9:59	0
Mid Point Flurometer	3/6/2015 10:00	0.15
Mid Point Flurometer	3/6/2015 10:01	0
Mid Point Flurometer	3/6/2015 10:02	0.1
Mid Point Flurometer	3/6/2015 10:03	0.01
Mid Point Flurometer	3/6/2015 10:04	0
Mid Point Flurometer	3/6/2015 10:05	0
Mid Point Flurometer	3/6/2015 10:06	0.01
Mid Point Flurometer	3/6/2015 10:07	0
Mid Point Flurometer	3/6/2015 10:08	0
Mid Point Flurometer	3/6/2015 10:09	0
Mid Point Flurometer	3/6/2015 10:10	0.05
Mid Point Flurometer	3/6/2015 10:11	0
Mid Point Flurometer	3/6/2015 10:12	0
Mid Point Flurometer	3/6/2015 10:13	0.05
Mid Point Flurometer	3/6/2015 10:14	0.1
Mid Point Flurometer	3/6/2015 10:15	0.05
Mid Point Flurometer	3/6/2015 10:16	0
Mid Point Flurometer	3/6/2015 10:17	0
Mid Point Flurometer	3/6/2015 10:18	0.06
Mid Point Flurometer	3/6/2015 10:19	0
Mid Point Flurometer	3/6/2015 10:20	0
Mid Point Flurometer	3/6/2015 10:21	0
Mid Point Flurometer	3/6/2015 10:22	0.04
Mid Point Flurometer	3/6/2015 10:23	0
Mid Point Flurometer	3/6/2015 10:24	0
Mid Point Flurometer	3/6/2015 10:25	0
Mid Point Flurometer	3/6/2015 10:26	0.32

Location	Date and Time	Rhodmaine Concentration Adjusted Concentration (ppb)
Mid Point Flurometer	3/6/2015 10:27	0
Mid Point Flurometer	3/6/2015 10:28	0
Mid Point Flurometer	3/6/2015 10:29	0
Mid Point Flurometer	3/6/2015 10:30	0.02
Mid Point Flurometer	3/6/2015 10:31	0.01
Mid Point Flurometer	3/6/2015 10:32	0.06
Mid Point Flurometer	3/6/2015 10:33	0
Mid Point Flurometer	3/6/2015 10:34	0
Mid Point Flurometer	3/6/2015 10:35	0.04
Mid Point Flurometer	3/6/2015 10:36	0.05
Mid Point Flurometer	3/6/2015 10:37	0.21
Mid Point Flurometer	3/6/2015 10:38	0.03
Mid Point Flurometer	3/6/2015 10:39	0.09
Mid Point Flurometer	3/6/2015 10:40	0.09
Mid Point Flurometer	3/6/2015 10:41	0.04
Mid Point Flurometer	3/6/2015 10:42	0.01
Mid Point Flurometer	3/6/2015 10:43	0
Mid Point Flurometer	3/6/2015 10:44	0
Mid Point Flurometer	3/6/2015 10:45	0
Mid Point Flurometer	3/6/2015 10:46	0
Mid Point Flurometer	3/6/2015 10:47	0
Mid Point Flurometer	3/6/2015 10:48	0.07
Mid Point Flurometer	3/6/2015 10:49	0
Mid Point Flurometer	3/6/2015 10:50	0
Mid Point Flurometer	3/6/2015 10:51	0
Mid Point Flurometer	3/6/2015 10:52	0.01
Mid Point Flurometer	3/6/2015 10:53	0
Mid Point Flurometer	3/6/2015 10:54	0
Mid Point Flurometer	3/6/2015 10:55	0
Mid Point Flurometer	3/6/2015 10:56	0
Mid Point Flurometer	3/6/2015 10:57	0
Mid Point Flurometer	3/6/2015 10:58	0.01
Mid Point Flurometer	3/6/2015 10:59	0
Mid Point Flurometer	3/6/2015 11:00	0
Mid Point Flurometer	3/6/2015 11:01	0
Mid Point Flurometer	3/6/2015 11:02	0.09
Mid Point Flurometer	3/6/2015 11:03	0.01
Mid Point Flurometer	3/6/2015 11:04	0
Mid Point Flurometer	3/6/2015 11:05	0.04
Mid Point Flurometer	3/6/2015 11:06	0.01
Mid Point Flurometer	3/6/2015 11:07	0
Mid Point Flurometer	3/6/2015 11:08	0
Mid Point Flurometer	3/6/2015 11:09	0.05
Mid Point Flurometer	3/6/2015 11:10	0.05
Mid Point Flurometer	3/6/2015 11:11	0
Mid Point Flurometer	3/6/2015 11:12	0

Location	Date and Time	Rhodmaine Concentration Adjusted Concentration (ppb)
Mid Point Flurometer	3/6/2015 11:13	0.02
Mid Point Flurometer	3/6/2015 11:14	0
Mid Point Flurometer	3/6/2015 11:15	0.04
Mid Point Flurometer	3/6/2015 11:16	0
Mid Point Flurometer	3/6/2015 11:17	0
Mid Point Flurometer	3/6/2015 11:18	0.01
Mid Point Flurometer	3/6/2015 11:19	0.05
Mid Point Flurometer	3/6/2015 11:20	0
Mid Point Flurometer	3/6/2015 11:21	0.01
Mid Point Flurometer	3/6/2015 11:22	0
Mid Point Flurometer	3/6/2015 11:23	0
Mid Point Flurometer	3/6/2015 11:24	0
Mid Point Flurometer	3/6/2015 11:25	0
Mid Point Flurometer	3/6/2015 11:26	0
Mid Point Flurometer	3/6/2015 11:27	0.11
Mid Point Flurometer	3/6/2015 11:28	0.02
Mid Point Flurometer	3/6/2015 11:29	0.01
Mid Point Flurometer	3/6/2015 11:30	0.03
Mid Point Flurometer	3/6/2015 11:31	0
Mid Point Flurometer	3/6/2015 11:32	0.02
Mid Point Flurometer	3/6/2015 11:33	0
Mid Point Flurometer	3/6/2015 11:34	0.06
Mid Point Flurometer	3/6/2015 11:35	0
Mid Point Flurometer	3/6/2015 11:36	0.06
Mid Point Flurometer	3/6/2015 11:37	0.01
Mid Point Flurometer	3/6/2015 11:38	0
Mid Point Flurometer	3/6/2015 11:39	0
Mid Point Flurometer	3/6/2015 11:40	0
Mid Point Flurometer	3/6/2015 11:41	0
Mid Point Flurometer	3/6/2015 11:42	0
Mid Point Flurometer	3/6/2015 11:43	0
Mid Point Flurometer	3/6/2015 11:44	0
Mid Point Flurometer	3/6/2015 11:45	0
Mid Point Flurometer	3/6/2015 11:46	0
Mid Point Flurometer	3/6/2015 11:47	0
Mid Point Flurometer	3/6/2015 11:48	0
Mid Point Flurometer	3/6/2015 11:49	0.01
Mid Point Flurometer	3/6/2015 11:50	0.03
Mid Point Flurometer	3/6/2015 11:51	0.02
Mid Point Flurometer	3/6/2015 11:52	0
Mid Point Flurometer	3/6/2015 11:53	0
Mid Point Flurometer	3/6/2015 11:54	0
Mid Point Flurometer	3/6/2015 11:55	0.01
Mid Point Flurometer	3/6/2015 11:56	0
Mid Point Flurometer	3/6/2015 11:57	0.02
Mid Point Flurometer	3/6/2015 11:58	0.06

Location	Date and Time	Rhodmaine Concentration Adjusted Concentration (ppb)
Mid Point Flurometer	3/6/2015 11:59	0.11
Mid Point Flurometer	3/6/2015 12:00	0
Mid Point Flurometer	3/6/2015 12:01	0
Mid Point Flurometer	3/6/2015 12:02	0.02
Mid Point Flurometer	3/6/2015 12:03	0.02
Mid Point Flurometer	3/6/2015 12:04	0
Mid Point Flurometer	3/6/2015 12:05	0.04
Mid Point Flurometer	3/6/2015 12:06	0
Mid Point Flurometer	3/6/2015 12:07	0.51
Mid Point Flurometer	3/6/2015 12:08	0.1
Mid Point Flurometer	3/6/2015 12:09	0.17
Mid Point Flurometer	3/6/2015 12:10	0.11
Mid Point Flurometer	3/6/2015 12:11	0
Mid Point Flurometer	3/6/2015 12:12	0.18
Mid Point Flurometer	3/6/2015 12:13	0.12
Mid Point Flurometer	3/6/2015 12:14	0.18
Mid Point Flurometer	3/6/2015 12:15	0
Mid Point Flurometer	3/6/2015 12:16	0.07
Mid Point Flurometer	3/6/2015 12:17	0
Mid Point Flurometer	3/6/2015 12:18	0.03
Mid Point Flurometer	3/6/2015 12:19	0.06
Mid Point Flurometer	3/6/2015 12:20	0.08
Mid Point Flurometer	3/6/2015 12:21	0.11
Mid Point Flurometer	3/6/2015 12:22	0.03
Mid Point Flurometer	3/6/2015 12:23	0.17
Mid Point Flurometer	3/6/2015 12:24	0.1
Mid Point Flurometer	3/6/2015 12:25	0.03
Mid Point Flurometer	3/6/2015 12:26	0
Mid Point Flurometer	3/6/2015 12:27	0.02
Mid Point Flurometer	3/6/2015 12:28	0.08
Mid Point Flurometer	3/6/2015 12:29	0.18
Mid Point Flurometer	3/6/2015 12:30	0.06
Mid Point Flurometer	3/6/2015 12:31	0.08
Mid Point Flurometer	3/6/2015 12:32	0.1
Mid Point Flurometer	3/6/2015 12:33	0.22
Mid Point Flurometer	3/6/2015 12:34	0.1
Mid Point Flurometer	3/6/2015 12:35	0.14
Mid Point Flurometer	3/6/2015 12:36	0.01
Mid Point Flurometer	3/6/2015 12:37	0.58
Mid Point Flurometer	3/6/2015 12:38	0.04
Mid Point Flurometer	3/6/2015 12:39	0.17
Mid Point Flurometer	3/6/2015 12:40	0.03
Mid Point Flurometer	3/6/2015 12:41	0.26
Mid Point Flurometer	3/6/2015 12:42	0
Mid Point Flurometer	3/6/2015 12:43	0.18
Mid Point Flurometer	3/6/2015 12:44	0.11

Location	Date and Time	Rhodmaine Concentration Adjusted Concentration (ppb)
Mid Point Flurometer	3/6/2015 12:45	0.01
Mid Point Flurometer	3/6/2015 12:46	0.05
Mid Point Flurometer	3/6/2015 12:47	0
Mid Point Flurometer	3/6/2015 12:48	0.11
Mid Point Flurometer	3/6/2015 12:49	0
Mid Point Flurometer	3/6/2015 12:50	0.09
Mid Point Flurometer	3/6/2015 12:51	0.04
Mid Point Flurometer	3/6/2015 12:52	0.1
Mid Point Flurometer	3/6/2015 12:53	0.01
Mid Point Flurometer	3/6/2015 12:54	0.02
Mid Point Flurometer	3/6/2015 12:55	0.01
Mid Point Flurometer	3/6/2015 12:56	0
Mid Point Flurometer	3/6/2015 12:57	0.04
Mid Point Flurometer	3/6/2015 12:58	0.01
Mid Point Flurometer	3/6/2015 12:59	0.05
Mid Point Flurometer	3/6/2015 13:00	0
Mid Point Flurometer	3/6/2015 13:01	0.02
Mid Point Flurometer	3/6/2015 13:02	0.04
Mid Point Flurometer	3/6/2015 13:03	0.22
Mid Point Flurometer	3/6/2015 13:04	0.1
Mid Point Flurometer	3/6/2015 13:05	0
Mid Point Flurometer	3/6/2015 13:06	0.07
Mid Point Flurometer	3/6/2015 13:07	0.27
Mid Point Flurometer	3/6/2015 13:08	0.04
Mid Point Flurometer	3/6/2015 13:09	0
Mid Point Flurometer	3/6/2015 13:10	0
Mid Point Flurometer	3/6/2015 13:11	0
Mid Point Flurometer	3/6/2015 13:12	0.05
Mid Point Flurometer	3/6/2015 13:13	0
Mid Point Flurometer	3/6/2015 13:14	0.19
Mid Point Flurometer	3/6/2015 13:15	0
Mid Point Flurometer	3/6/2015 13:16	0.04
Mid Point Flurometer	3/6/2015 13:17	0.04
Mid Point Flurometer	3/6/2015 13:18	0.04
Mid Point Flurometer	3/6/2015 13:19	0.03
Mid Point Flurometer	3/6/2015 13:20	0.09
Mid Point Flurometer	3/6/2015 13:21	0.27
Mid Point Flurometer	3/6/2015 13:22	0.5
Mid Point Flurometer	3/6/2015 13:23	0.36
Mid Point Flurometer	3/6/2015 13:24	0.22
Mid Point Flurometer	3/6/2015 13:25	0.14
Mid Point Flurometer	3/6/2015 13:26	0.08
Mid Point Flurometer	3/6/2015 13:27	0
Mid Point Flurometer	3/6/2015 13:28	0.06
Mid Point Flurometer	3/6/2015 13:29	0
Mid Point Flurometer	3/6/2015 13:30	0

Location	Date and Time	Rhodmaine Concentration Adjusted Concentration (ppb)
Mid Point Flurometer	3/6/2015 13:31	0
Mid Point Flurometer	3/6/2015 13:32	0
Mid Point Flurometer	3/6/2015 13:33	0
Mid Point Flurometer	3/6/2015 13:34	0
Mid Point Flurometer	3/6/2015 13:35	0
Mid Point Flurometer	3/6/2015 13:36	0
Mid Point Flurometer	3/6/2015 13:37	0
Mid Point Flurometer	3/6/2015 13:38	0
Mid Point Flurometer	3/6/2015 13:39	0
Mid Point Flurometer	3/6/2015 13:40	0
Mid Point Flurometer	3/6/2015 13:41	0
Mid Point Flurometer	3/6/2015 13:42	0
Mid Point Flurometer	3/6/2015 13:43	0
Mid Point Flurometer	3/6/2015 13:44	0
Mid Point Flurometer	3/6/2015 13:45	0
Mid Point Flurometer	3/6/2015 13:46	0
Mid Point Flurometer	3/6/2015 13:47	0
Mid Point Flurometer	3/6/2015 13:48	0
Mid Point Flurometer	3/6/2015 13:49	0
Mid Point Flurometer	3/6/2015 13:50	0
Mid Point Flurometer	3/6/2015 13:51	0
Mid Point Flurometer	3/6/2015 13:52	0
Mid Point Flurometer	3/6/2015 13:53	0
Mid Point Flurometer	3/6/2015 13:54	0
Mid Point Flurometer	3/6/2015 13:55	0
Mid Point Flurometer	3/6/2015 13:56	0
Mid Point Flurometer	3/6/2015 13:57	0
Mid Point Flurometer	3/6/2015 13:58	0
Mid Point Flurometer	3/6/2015 13:59	0
Mid Point Flurometer	3/6/2015 14:00	0
Mid Point Flurometer	3/6/2015 14:01	0
Mid Point Flurometer	3/6/2015 14:02	0
Mid Point Flurometer	3/6/2015 14:03	0
Mid Point Flurometer	3/6/2015 14:04	0
Mid Point Flurometer	3/6/2015 14:05	0
Mid Point Flurometer	3/6/2015 14:06	0
Mid Point Flurometer	3/6/2015 14:07	0
Mid Point Flurometer	3/6/2015 14:08	0
Mid Point Flurometer	3/6/2015 14:09	0
Mid Point Flurometer	3/6/2015 14:10	0
Mid Point Flurometer	3/6/2015 14:11	0
Mid Point Flurometer	3/6/2015 14:12	0
Mid Point Flurometer	3/6/2015 14:13	0
Mid Point Flurometer	3/6/2015 14:14	0
Mid Point Flurometer	3/6/2015 14:15	0
Mid Point Flurometer	3/6/2015 14:16	0

Location	Date and Time	Rhodmaine Concentration Adjusted Concentration (ppb)
Mid Point Flurometer	3/6/2015 14:17	0
Mid Point Flurometer	3/6/2015 14:18	0
Mid Point Flurometer	3/6/2015 14:19	0
Mid Point Flurometer	3/6/2015 14:20	0
Mid Point Flurometer	3/6/2015 14:21	0
Mid Point Flurometer	3/6/2015 14:22	0
Mid Point Flurometer	3/6/2015 14:23	0
Mid Point Flurometer	3/6/2015 14:24	0
Mid Point Flurometer	3/6/2015 14:25	0
Mid Point Flurometer	3/6/2015 14:26	0
Mid Point Flurometer	3/6/2015 14:27	0
Mid Point Flurometer	3/6/2015 14:28	0
Mid Point Flurometer	3/6/2015 14:29	0
Mid Point Flurometer	3/6/2015 14:30	0
Mid Point Flurometer	3/6/2015 14:31	0
Mid Point Flurometer	3/6/2015 14:32	0
Mid Point Flurometer	3/6/2015 14:33	0
Mid Point Flurometer	3/6/2015 14:34	0
Mid Point Flurometer	3/6/2015 14:35	0
Mid Point Flurometer	3/6/2015 14:36	0
Mid Point Flurometer	3/6/2015 14:37	0
Mid Point Flurometer	3/6/2015 14:38	0
Mid Point Flurometer	3/6/2015 14:39	0
Mid Point Flurometer	3/6/2015 14:40	0
Mid Point Flurometer	3/6/2015 14:41	0
Mid Point Flurometer	3/6/2015 14:42	0
Mid Point Flurometer	3/6/2015 14:43	0
Mid Point Flurometer	3/6/2015 14:44	0
Mid Point Flurometer	3/6/2015 14:45	0
Mid Point Flurometer	3/6/2015 14:46	0
Mid Point Flurometer	3/6/2015 14:47	0
Mid Point Flurometer	3/6/2015 14:48	0
Mid Point Flurometer	3/6/2015 14:49	0
Mid Point Flurometer	3/6/2015 14:50	0
Mid Point Flurometer	3/6/2015 14:51	0
Mid Point Flurometer	3/6/2015 14:52	0
Mid Point Flurometer	3/6/2015 14:53	0
Mid Point Flurometer	3/6/2015 14:54	0
Mid Point Flurometer	3/6/2015 14:55	0
Mid Point Flurometer	3/6/2015 14:56	0
Mid Point Flurometer	3/6/2015 14:57	0
Mid Point Flurometer	3/6/2015 14:58	0
Mid Point Flurometer	3/6/2015 14:59	0
Mid Point Flurometer	3/6/2015 15:00	0
Mid Point Flurometer	3/6/2015 15:01	0
Mid Point Flurometer	3/6/2015 15:02	0

Location	Date and Time	Rhodmaine Concentration Adjusted Concentration (ppb)
Mid Point Flurometer	3/6/2015 15:03	0
Mid Point Flurometer	3/6/2015 15:04	0
Mid Point Flurometer	3/6/2015 15:05	0
Mid Point Flurometer	3/6/2015 15:06	0
Mid Point Flurometer	3/6/2015 15:07	0
Mid Point Flurometer	3/6/2015 15:08	0
Mid Point Flurometer	3/6/2015 15:09	0
Mid Point Flurometer	3/6/2015 15:10	0
Mid Point Flurometer	3/6/2015 15:11	0
Mid Point Flurometer	3/6/2015 15:12	0
Mid Point Flurometer	3/6/2015 15:13	0
Mid Point Flurometer	3/6/2015 15:14	0
Mid Point Flurometer	3/6/2015 15:15	0
Mid Point Flurometer	3/6/2015 15:16	0
Mid Point Flurometer	3/6/2015 15:17	0
Mid Point Flurometer	3/6/2015 15:18	0
Mid Point Flurometer	3/6/2015 15:19	0
Mid Point Flurometer	3/6/2015 15:20	0
Mid Point Flurometer	3/6/2015 15:21	0
Mid Point Flurometer	3/6/2015 15:22	0
Mid Point Flurometer	3/6/2015 15:23	0
Mid Point Flurometer	3/6/2015 15:24	0
Mid Point Flurometer	3/6/2015 15:25	0
Mid Point Flurometer	3/6/2015 15:26	0
Mid Point Flurometer	3/6/2015 15:27	0
Mid Point Flurometer	3/6/2015 15:28	0
Mid Point Flurometer	3/6/2015 15:29	0
Mid Point Flurometer	3/6/2015 15:30	0
Mid Point Flurometer	3/6/2015 15:31	0
Mid Point Flurometer	3/6/2015 15:32	0
Mid Point Flurometer	3/6/2015 15:33	0
Mid Point Flurometer	3/6/2015 15:34	0
Mid Point Flurometer	3/6/2015 15:35	0
Mid Point Flurometer	3/6/2015 15:36	0
Mid Point Flurometer	3/6/2015 15:37	0
Mid Point Flurometer	3/6/2015 15:38	0
Mid Point Flurometer	3/6/2015 15:39	0
Mid Point Flurometer	3/6/2015 15:40	0
Mid Point Flurometer	3/6/2015 15:41	0
Mid Point Flurometer	3/6/2015 15:42	0
Mid Point Flurometer	3/6/2015 15:43	0
Mid Point Flurometer	3/6/2015 15:44	0
Mid Point Flurometer	3/6/2015 15:45	0
Mid Point Flurometer	3/6/2015 15:46	0
Mid Point Flurometer	3/6/2015 15:47	0
Mid Point Flurometer	3/6/2015 15:48	0

Location	Date and Time	Rhodmaine Concentration Adjusted Concentration (ppb)
Mid Point Flurometer	3/6/2015 15:49	0
Mid Point Flurometer	3/6/2015 15:50	0
Mid Point Flurometer	3/6/2015 15:51	0
Mid Point Flurometer	3/6/2015 15:52	0
Mid Point Flurometer	3/6/2015 15:53	0
Mid Point Flurometer	3/6/2015 15:54	0
Mid Point Flurometer	3/6/2015 15:55	0
Mid Point Flurometer	3/6/2015 15:56	0
Mid Point ISCO	3/4/15 16:00	0.162215346
Mid Point ISCO	3/4/15 17:00	0.224760609
Mid Point ISCO	3/4/15 18:00	0.117775291
Mid Point ISCO	3/4/15 19:00	0.145756066
Mid Point ISCO	3/4/15 20:00	0.048646316
Mid Point ISCO	3/4/15 21:00	0.068397451
Mid Point ISCO	3/4/15 22:00	6.823285857
Mid Point ISCO	3/4/15 23:00	11.86970103
Mid Point ISCO	3/5/15 0:00	7.511283751
Mid Point ISCO	3/5/15 1:00	5.957527743
Mid Point ISCO	3/5/15 2:00	4.621034228
Mid Point ISCO	3/5/15 3:00	2.715049634
Mid Point ISCO	3/5/15 4:00	2.204811962
Mid Point ISCO	3/5/15 5:00	1.714325426
Mid Point ISCO	3/5/15 6:00	1.66988537
Mid Point ISCO	3/5/15 7:00	1.269924873
Mid Point ISCO	3/5/15 8:00	1.15800177
Mid Point ISCO	3/5/15 9:00	0.937447422
Mid Point ISCO	3/5/15 10:00	0.371248199
Mid Point ISCO	3/5/15 11:00	0.51608986
Mid Point ISCO	3/5/15 12:00	0.420626038
Mid Point ISCO	3/5/15 13:00	0.221468753
Mid Point ISCO	3/5/15 14:00	0.311994792
Lower Flurometer	3/4/2015 9:53	0.44
Lower Flurometer	3/4/2015 9:54	0.37
Lower Flurometer	3/4/2015 9:55	0.35
Lower Flurometer	3/4/2015 9:56	0.4
Lower Flurometer	3/4/2015 9:57	0.38
Lower Flurometer	3/4/2015 9:58	0.43
Lower Flurometer	3/4/2015 9:59	0.31
Lower Flurometer	3/4/2015 10:00	0.39
Lower Flurometer	3/4/2015 10:01	0.43
Lower Flurometer	3/4/2015 10:02	0.39
Lower Flurometer	3/4/2015 10:03	0.43
Lower Flurometer	3/4/2015 10:04	0.37
Lower Flurometer	3/4/2015 10:05	0.43
Lower Flurometer	3/4/2015 10:06	0.38
Lower Flurometer	3/4/2015 10:07	0.37

Location	Date and Time	Rhodmaine Concentration Adjusted Concentration (ppb)
Lower Flurometer	3/4/2015 10:08	0.45
Lower Flurometer	3/4/2015 10:09	0.41
Lower Flurometer	3/4/2015 10:10	0.38
Lower Flurometer	3/4/2015 10:11	0.32
Lower Flurometer	3/4/2015 10:12	0.34
Lower Flurometer	3/4/2015 10:13	0.38
Lower Flurometer	3/4/2015 10:14	0.38
Lower Flurometer	3/4/2015 10:15	0.41
Lower Flurometer	3/4/2015 10:16	0.34
Lower Flurometer	3/4/2015 10:17	0.43
Lower Flurometer	3/4/2015 10:18	0.38
Lower Flurometer	3/4/2015 10:19	0.34
Lower Flurometer	3/4/2015 10:20	0.39
Lower Flurometer	3/4/2015 10:21	0.36
Lower Flurometer	3/4/2015 10:22	0.33
Lower Flurometer	3/4/2015 10:23	0.44
Lower Flurometer	3/4/2015 10:24	0.38
Lower Flurometer	3/4/2015 10:25	0.36
Lower Flurometer	3/4/2015 10:26	0.42
Lower Flurometer	3/4/2015 10:27	0.42
Lower Flurometer	3/4/2015 10:28	0.35
Lower Flurometer	3/4/2015 10:29	0.4
Lower Flurometer	3/4/2015 10:30	0.4
Lower Flurometer	3/4/2015 10:31	0.39
Lower Flurometer	3/4/2015 10:32	0.42
Lower Flurometer	3/4/2015 10:33	0.34
Lower Flurometer	3/4/2015 10:34	0.43
Lower Flurometer	3/4/2015 10:35	0.45
Lower Flurometer	3/4/2015 10:36	0.39
Lower Flurometer	3/4/2015 10:37	0.33
Lower Flurometer	3/4/2015 10:38	0.39
Lower Flurometer	3/4/2015 10:39	0.39
Lower Flurometer	3/4/2015 10:40	0.43
Lower Flurometer	3/4/2015 10:41	0.37
Lower Flurometer	3/4/2015 10:42	0.35
Lower Flurometer	3/4/2015 10:43	0.41
Lower Flurometer	3/4/2015 10:44	0.46
Lower Flurometer	3/4/2015 10:45	0.38
Lower Flurometer	3/4/2015 10:46	0.44
Lower Flurometer	3/4/2015 10:47	0.35
Lower Flurometer	3/4/2015 10:48	0.39
Lower Flurometer	3/4/2015 10:49	0.44
Lower Flurometer	3/4/2015 10:50	0.44
Lower Flurometer	3/4/2015 10:51	0.45
Lower Flurometer	3/4/2015 10:52	0.42
Lower Flurometer	3/4/2015 10:53	0.4

Location	Date and Time	Rhodmaine Concentration Adjusted Concentration (ppb)
Lower Flurometer	3/4/2015 10:54	0.34
Lower Flurometer	3/4/2015 10:55	0.34
Lower Flurometer	3/4/2015 10:56	0.38
Lower Flurometer	3/4/2015 10:57	0.31
Lower Flurometer	3/4/2015 10:58	0.34
Lower Flurometer	3/4/2015 10:59	0.34
Lower Flurometer	3/4/2015 11:00	0.45
Lower Flurometer	3/4/2015 11:01	0.44
Lower Flurometer	3/4/2015 11:02	0.34
Lower Flurometer	3/4/2015 11:03	0.38
Lower Flurometer	3/4/2015 11:04	0.43
Lower Flurometer	3/4/2015 11:05	0.31
Lower Flurometer	3/4/2015 11:06	0.43
Lower Flurometer	3/4/2015 11:07	0.34
Lower Flurometer	3/4/2015 11:08	0.36
Lower Flurometer	3/4/2015 11:09	0.33
Lower Flurometer	3/4/2015 11:10	0.39
Lower Flurometer	3/4/2015 11:11	0.33
Lower Flurometer	3/4/2015 11:12	0.38
Lower Flurometer	3/4/2015 11:13	0.4
Lower Flurometer	3/4/2015 11:14	0.44
Lower Flurometer	3/4/2015 11:15	0.4
Lower Flurometer	3/4/2015 11:16	0.37
Lower Flurometer	3/4/2015 11:17	0.37
Lower Flurometer	3/4/2015 11:18	0.44
Lower Flurometer	3/4/2015 11:19	0.35
Lower Flurometer	3/4/2015 11:20	0.33
Lower Flurometer	3/4/2015 11:21	0.33
Lower Flurometer	3/4/2015 11:22	0.43
Lower Flurometer	3/4/2015 11:23	0.43
Lower Flurometer	3/4/2015 11:24	0.35
Lower Flurometer	3/4/2015 11:25	0.36
Lower Flurometer	3/4/2015 11:26	0.43
Lower Flurometer	3/4/2015 11:27	0.35
Lower Flurometer	3/4/2015 11:28	0.37
Lower Flurometer	3/4/2015 11:29	0.36
Lower Flurometer	3/4/2015 11:30	0.36
Lower Flurometer	3/4/2015 11:31	0.36
Lower Flurometer	3/4/2015 11:32	0.38
Lower Flurometer	3/4/2015 11:33	0.35
Lower Flurometer	3/4/2015 11:34	0.4
Lower Flurometer	3/4/2015 11:35	0.43
Lower Flurometer	3/4/2015 11:36	0.34
Lower Flurometer	3/4/2015 11:37	0.36
Lower Flurometer	3/4/2015 11:38	0.33
Lower Flurometer	3/4/2015 11:39	0.36

Location	Date and Time	Rhodmaine Concentration Adjusted Concentration (ppb)
Lower Flurometer	3/4/2015 11:40	0.41
Lower Flurometer	3/4/2015 11:41	0.33
Lower Flurometer	3/4/2015 11:42	0.33
Lower Flurometer	3/4/2015 11:43	0.35
Lower Flurometer	3/4/2015 11:44	0.33
Lower Flurometer	3/4/2015 11:45	0.32
Lower Flurometer	3/4/2015 11:46	0.27
Lower Flurometer	3/4/2015 11:47	0.3
Lower Flurometer	3/4/2015 11:48	0.27
Lower Flurometer	3/4/2015 11:49	0.35
Lower Flurometer	3/4/2015 11:50	0.33
Lower Flurometer	3/4/2015 11:51	0.25
Lower Flurometer	3/4/2015 11:52	0.21
Lower Flurometer	3/4/2015 11:53	0.26
Lower Flurometer	3/4/2015 11:54	0.26
Lower Flurometer	3/4/2015 11:55	0.26
Lower Flurometer	3/4/2015 11:56	0.27
Lower Flurometer	3/4/2015 11:57	0.25
Lower Flurometer	3/4/2015 11:58	0.24
Lower Flurometer	3/4/2015 11:59	0.34
Lower Flurometer	3/4/2015 12:00	0.29
Lower Flurometer	3/4/2015 12:01	0
Lower Flurometer	3/4/2015 12:02	0.29
Lower Flurometer	3/4/2015 12:03	0.33
Lower Flurometer	3/4/2015 12:04	0.31
Lower Flurometer	3/4/2015 12:05	0
Lower Flurometer	3/4/2015 12:06	0
Lower Flurometer	3/4/2015 12:07	0
Lower Flurometer	3/4/2015 12:08	0
Lower Flurometer	3/4/2015 12:09	0
Lower Flurometer	3/4/2015 12:10	0
Lower Flurometer	3/4/2015 12:11	0
Lower Flurometer	3/4/2015 12:12	0
Lower Flurometer	3/4/2015 12:13	0
Lower Flurometer	3/4/2015 12:14	0
Lower Flurometer	3/4/2015 12:15	0
Lower Flurometer	3/4/2015 12:16	0
Lower Flurometer	3/4/2015 12:17	0
Lower Flurometer	3/4/2015 12:18	0
Lower Flurometer	3/4/2015 12:19	0
Lower Flurometer	3/4/2015 12:20	0
Lower Flurometer	3/4/2015 12:21	0
Lower Flurometer	3/4/2015 12:22	0
Lower Flurometer	3/4/2015 12:23	0
Lower Flurometer	3/4/2015 12:24	0
Lower Flurometer	3/4/2015 12:25	0

Location	Date and Time	Rhodmaine Concentration Adjusted Concentration (ppb)
Lower Flurometer	3/4/2015 12:26	0
Lower Flurometer	3/4/2015 12:27	0
Lower Flurometer	3/4/2015 12:28	0
Lower Flurometer	3/4/2015 12:29	0
Lower Flurometer	3/4/2015 12:30	0
Lower Flurometer	3/4/2015 12:31	0
Lower Flurometer	3/4/2015 12:32	0
Lower Flurometer	3/4/2015 12:33	0
Lower Flurometer	3/4/2015 12:34	0
Lower Flurometer	3/4/2015 12:35	0
Lower Flurometer	3/4/2015 12:36	0
Lower Flurometer	3/4/2015 12:37	0
Lower Flurometer	3/4/2015 12:38	0
Lower Flurometer	3/4/2015 12:39	0
Lower Flurometer	3/4/2015 12:40	0
Lower Flurometer	3/4/2015 12:41	0
Lower Flurometer	3/4/2015 12:42	0
Lower Flurometer	3/4/2015 12:43	0
Lower Flurometer	3/4/2015 12:44	0
Lower Flurometer	3/4/2015 12:45	0
Lower Flurometer	3/4/2015 12:46	0
Lower Flurometer	3/4/2015 12:47	0
Lower Flurometer	3/4/2015 12:48	0
Lower Flurometer	3/4/2015 12:49	0
Lower Flurometer	3/4/2015 12:50	0
Lower Flurometer	3/4/2015 12:51	0
Lower Flurometer	3/4/2015 12:52	0
Lower Flurometer	3/4/2015 12:53	0
Lower Flurometer	3/4/2015 12:54	0
Lower Flurometer	3/4/2015 12:55	0
Lower Flurometer	3/4/2015 12:56	0
Lower Flurometer	3/4/2015 12:57	0
Lower Flurometer	3/4/2015 12:58	0
Lower Flurometer	3/4/2015 12:59	0
Lower Flurometer	3/4/2015 13:00	0
Lower Flurometer	3/4/2015 13:01	0
Lower Flurometer	3/4/2015 13:02	0
Lower Flurometer	3/4/2015 13:03	0
Lower Flurometer	3/4/2015 13:04	0
Lower Flurometer	3/4/2015 13:05	0
Lower Flurometer	3/4/2015 13:06	0
Lower Flurometer	3/4/2015 13:07	0
Lower Flurometer	3/4/2015 13:08	0
Lower Flurometer	3/4/2015 13:09	0
Lower Flurometer	3/4/2015 13:10	0
Lower Flurometer	3/4/2015 13:11	0

Location	Date and Time	Rhodmaine Concentration Adjusted Concentration (ppb)
Lower Flurometer	3/4/2015 13:12	0
Lower Flurometer	3/4/2015 13:13	0
Lower Flurometer	3/4/2015 13:14	0
Lower Flurometer	3/4/2015 13:15	0
Lower Flurometer	3/4/2015 13:16	0
Lower Flurometer	3/4/2015 13:17	0
Lower Flurometer	3/4/2015 13:18	0
Lower Flurometer	3/4/2015 13:19	0
Lower Flurometer	3/4/2015 13:20	0
Lower Flurometer	3/4/2015 13:21	0
Lower Flurometer	3/4/2015 13:22	0
Lower Flurometer	3/4/2015 13:23	0
Lower Flurometer	3/4/2015 13:24	0
Lower Flurometer	3/4/2015 13:25	0.05
Lower Flurometer	3/4/2015 13:26	0
Lower Flurometer	3/4/2015 13:27	0
Lower Flurometer	3/4/2015 13:28	0
Lower Flurometer	3/4/2015 13:29	0
Lower Flurometer	3/4/2015 13:30	0
Lower Flurometer	3/4/2015 13:31	0
Lower Flurometer	3/4/2015 13:32	0
Lower Flurometer	3/4/2015 13:33	0
Lower Flurometer	3/4/2015 13:34	0
Lower Flurometer	3/4/2015 13:35	0
Lower Flurometer	3/4/2015 13:36	0
Lower Flurometer	3/4/2015 13:37	0
Lower Flurometer	3/4/2015 13:38	0
Lower Flurometer	3/4/2015 13:39	0
Lower Flurometer	3/4/2015 13:40	0
Lower Flurometer	3/4/2015 13:41	0
Lower Flurometer	3/4/2015 13:42	0
Lower Flurometer	3/4/2015 13:43	0
Lower Flurometer	3/4/2015 13:44	0
Lower Flurometer	3/4/2015 13:45	0
Lower Flurometer	3/4/2015 13:46	0
Lower Flurometer	3/4/2015 13:47	0
Lower Flurometer	3/4/2015 13:48	0
Lower Flurometer	3/4/2015 13:49	0
Lower Flurometer	3/4/2015 13:50	0
Lower Flurometer	3/4/2015 13:51	0
Lower Flurometer	3/4/2015 13:52	0
Lower Flurometer	3/4/2015 13:53	0
Lower Flurometer	3/4/2015 13:54	0
Lower Flurometer	3/4/2015 13:55	0
Lower Flurometer	3/4/2015 13:56	0
Lower Flurometer	3/4/2015 13:57	0

Location	Date and Time	Rhodmaine Concentration Adjusted Concentration (ppb)
Lower Flurometer	3/4/2015 13:58	0
Lower Flurometer	3/4/2015 13:59	0
Lower Flurometer	3/4/2015 14:00	0
Lower Flurometer	3/4/2015 14:01	0
Lower Flurometer	3/4/2015 14:02	0
Lower Flurometer	3/4/2015 14:03	0
Lower Flurometer	3/4/2015 14:04	0
Lower Flurometer	3/4/2015 14:05	0
Lower Flurometer	3/4/2015 14:06	0
Lower Flurometer	3/4/2015 14:07	0
Lower Flurometer	3/4/2015 14:08	0
Lower Flurometer	3/4/2015 14:09	0
Lower Flurometer	3/4/2015 14:10	5.04
Lower Flurometer	3/4/2015 14:11	0
Lower Flurometer	3/4/2015 14:12	0
Lower Flurometer	3/4/2015 14:13	0
Lower Flurometer	3/4/2015 14:14	0
Lower Flurometer	3/4/2015 14:15	0
Lower Flurometer	3/4/2015 14:16	0
Lower Flurometer	3/4/2015 14:17	0
Lower Flurometer	3/4/2015 14:18	0
Lower Flurometer	3/4/2015 14:19	0
Lower Flurometer	3/4/2015 14:20	0
Lower Flurometer	3/4/2015 14:21	0
Lower Flurometer	3/4/2015 14:22	0
Lower Flurometer	3/4/2015 14:23	0
Lower Flurometer	3/4/2015 14:24	0
Lower Flurometer	3/4/2015 14:25	0
Lower Flurometer	3/4/2015 14:26	0
Lower Flurometer	3/4/2015 14:27	0
Lower Flurometer	3/4/2015 14:28	0
Lower Flurometer	3/4/2015 14:29	0
Lower Flurometer	3/4/2015 14:30	0
Lower Flurometer	3/4/2015 14:31	0
Lower Flurometer	3/4/2015 14:32	0
Lower Flurometer	3/4/2015 14:33	0
Lower Flurometer	3/4/2015 14:34	0
Lower Flurometer	3/4/2015 14:35	0
Lower Flurometer	3/4/2015 14:36	0
Lower Flurometer	3/4/2015 14:37	0
Lower Flurometer	3/4/2015 14:38	0
Lower Flurometer	3/4/2015 14:39	0
Lower Flurometer	3/4/2015 14:40	0
Lower Flurometer	3/4/2015 14:41	0
Lower Flurometer	3/4/2015 14:42	0
Lower Flurometer	3/4/2015 14:43	0

Location	Date and Time	Rhodmaine Concentration Adjusted Concentration (ppb)
Lower Flurometer	3/4/2015 14:44	0
Lower Flurometer	3/4/2015 14:45	0
Lower Flurometer	3/4/2015 14:46	0
Lower Flurometer	3/4/2015 14:47	0
Lower Flurometer	3/4/2015 14:48	0
Lower Flurometer	3/4/2015 14:49	0
Lower Flurometer	3/4/2015 14:50	0
Lower Flurometer	3/4/2015 14:51	0
Lower Flurometer	3/4/2015 14:52	0
Lower Flurometer	3/4/2015 14:53	0
Lower Flurometer	3/4/2015 14:54	0
Lower Flurometer	3/4/2015 14:55	0
Lower Flurometer	3/4/2015 14:56	0
Lower Flurometer	3/4/2015 14:57	0
Lower Flurometer	3/4/2015 14:58	0
Lower Flurometer	3/4/2015 14:59	0
Lower Flurometer	3/4/2015 15:00	0
Lower Flurometer	3/4/2015 15:01	0
Lower Flurometer	3/4/2015 15:02	0
Lower Flurometer	3/4/2015 15:03	0
Lower Flurometer	3/4/2015 15:04	0
Lower Flurometer	3/4/2015 15:05	0
Lower Flurometer	3/4/2015 15:06	0
Lower Flurometer	3/4/2015 15:07	0
Lower Flurometer	3/4/2015 15:08	0
Lower Flurometer	3/4/2015 15:09	0
Lower Flurometer	3/4/2015 15:10	0
Lower Flurometer	3/4/2015 15:11	0
Lower Flurometer	3/4/2015 15:12	0
Lower Flurometer	3/4/2015 15:13	0
Lower Flurometer	3/4/2015 15:14	0
Lower Flurometer	3/4/2015 15:15	0
Lower Flurometer	3/4/2015 15:16	0
Lower Flurometer	3/4/2015 15:17	0
Lower Flurometer	3/4/2015 15:18	0
Lower Flurometer	3/4/2015 15:19	0
Lower Flurometer	3/4/2015 15:20	0
Lower Flurometer	3/4/2015 15:21	0
Lower Flurometer	3/4/2015 15:22	0
Lower Flurometer	3/4/2015 15:23	0
Lower Flurometer	3/4/2015 15:24	0
Lower Flurometer	3/4/2015 15:25	0
Lower Flurometer	3/4/2015 15:26	0
Lower Flurometer	3/4/2015 15:27	0
Lower Flurometer	3/4/2015 15:28	0
Lower Flurometer	3/4/2015 15:29	0

Location	Date and Time	Rhodmaine Concentration Adjusted Concentration (ppb)
Lower Flurometer	3/4/2015 15:30	0
Lower Flurometer	3/4/2015 15:31	0
Lower Flurometer	3/4/2015 15:32	0
Lower Flurometer	3/4/2015 15:33	0
Lower Flurometer	3/4/2015 15:34	0
Lower Flurometer	3/4/2015 15:35	0
Lower Flurometer	3/4/2015 15:36	0
Lower Flurometer	3/4/2015 15:37	0
Lower Flurometer	3/4/2015 15:38	0
Lower Flurometer	3/4/2015 15:39	0
Lower Flurometer	3/4/2015 15:40	0
Lower Flurometer	3/4/2015 15:41	0
Lower Flurometer	3/4/2015 15:42	0
Lower Flurometer	3/4/2015 15:43	0
Lower Flurometer	3/4/2015 15:44	0
Lower Flurometer	3/4/2015 15:45	0
Lower Flurometer	3/4/2015 15:46	0
Lower Flurometer	3/4/2015 15:47	0
Lower Flurometer	3/4/2015 15:48	0
Lower Flurometer	3/4/2015 15:49	0
Lower Flurometer	3/4/2015 15:50	0
Lower Flurometer	3/4/2015 15:51	0
Lower Flurometer	3/4/2015 15:52	0
Lower Flurometer	3/4/2015 15:53	0
Lower Flurometer	3/4/2015 15:54	0
Lower Flurometer	3/4/2015 15:55	0
Lower Flurometer	3/4/2015 15:56	0.03
Lower Flurometer	3/4/2015 15:57	0
Lower Flurometer	3/4/2015 15:58	0
Lower Flurometer	3/4/2015 15:59	0
Lower Flurometer	3/4/2015 16:00	0
Lower Flurometer	3/4/2015 16:01	0
Lower Flurometer	3/4/2015 16:02	0
Lower Flurometer	3/4/2015 16:03	0
Lower Flurometer	3/4/2015 16:04	0
Lower Flurometer	3/4/2015 16:05	0
Lower Flurometer	3/4/2015 16:06	0
Lower Flurometer	3/4/2015 16:07	0
Lower Flurometer	3/4/2015 16:08	0
Lower Flurometer	3/4/2015 16:09	0
Lower Flurometer	3/4/2015 16:10	0
Lower Flurometer	3/4/2015 16:11	0
Lower Flurometer	3/4/2015 16:12	0
Lower Flurometer	3/4/2015 16:13	0
Lower Flurometer	3/4/2015 16:14	6.27
Lower Flurometer	3/4/2015 16:15	0

Location	Date and Time	Rhodmaine Concentration Adjusted Concentration (ppb)
Lower Flurometer	3/4/2015 16:16	0
Lower Flurometer	3/4/2015 16:17	0
Lower Flurometer	3/4/2015 16:18	0
Lower Flurometer	3/4/2015 16:19	0
Lower Flurometer	3/4/2015 16:20	0
Lower Flurometer	3/4/2015 16:21	0
Lower Flurometer	3/4/2015 16:22	0
Lower Flurometer	3/4/2015 16:23	0
Lower Flurometer	3/4/2015 16:24	0
Lower Flurometer	3/4/2015 16:25	0
Lower Flurometer	3/4/2015 16:26	0
Lower Flurometer	3/4/2015 16:27	0
Lower Flurometer	3/4/2015 16:28	0
Lower Flurometer	3/4/2015 16:29	0
Lower Flurometer	3/4/2015 16:30	0
Lower Flurometer	3/4/2015 16:31	0
Lower Flurometer	3/4/2015 16:32	0
Lower Flurometer	3/4/2015 16:33	0
Lower Flurometer	3/4/2015 16:34	0
Lower Flurometer	3/4/2015 16:35	0
Lower Flurometer	3/4/2015 16:36	0
Lower Flurometer	3/4/2015 16:37	0
Lower Flurometer	3/4/2015 16:38	0
Lower Flurometer	3/4/2015 16:39	0
Lower Flurometer	3/4/2015 16:40	0
Lower Flurometer	3/4/2015 16:41	0
Lower Flurometer	3/4/2015 16:42	0
Lower Flurometer	3/4/2015 16:43	0
Lower Flurometer	3/4/2015 16:44	0
Lower Flurometer	3/4/2015 16:45	0
Lower Flurometer	3/4/2015 16:46	0
Lower Flurometer	3/4/2015 16:47	0
Lower Flurometer	3/4/2015 16:48	0
Lower Flurometer	3/4/2015 16:49	0
Lower Flurometer	3/4/2015 16:50	0
Lower Flurometer	3/4/2015 16:51	0
Lower Flurometer	3/4/2015 16:52	0
Lower Flurometer	3/4/2015 16:53	0
Lower Flurometer	3/4/2015 16:54	0
Lower Flurometer	3/4/2015 16:55	0
Lower Flurometer	3/4/2015 16:56	0
Lower Flurometer	3/4/2015 16:57	0
Lower Flurometer	3/4/2015 16:58	0
Lower Flurometer	3/4/2015 16:59	0
Lower Flurometer	3/4/2015 17:00	0
Lower Flurometer	3/4/2015 17:01	0

Location	Date and Time	Rhodmaine Concentration Adjusted Concentration (ppb)
Lower Flurometer	3/4/2015 17:02	0
Lower Flurometer	3/4/2015 17:03	0
Lower Flurometer	3/4/2015 17:04	0
Lower Flurometer	3/4/2015 17:05	0
Lower Flurometer	3/4/2015 17:06	0
Lower Flurometer	3/4/2015 17:07	0
Lower Flurometer	3/4/2015 17:08	0
Lower Flurometer	3/4/2015 17:09	0
Lower Flurometer	3/4/2015 17:10	0
Lower Flurometer	3/4/2015 17:11	0
Lower Flurometer	3/4/2015 17:12	0
Lower Flurometer	3/4/2015 17:13	0
Lower Flurometer	3/4/2015 17:14	0
Lower Flurometer	3/4/2015 17:15	0
Lower Flurometer	3/4/2015 17:16	0
Lower Flurometer	3/4/2015 17:17	0
Lower Flurometer	3/4/2015 17:18	0
Lower Flurometer	3/4/2015 17:19	0
Lower Flurometer	3/4/2015 17:20	0
Lower Flurometer	3/4/2015 17:21	0
Lower Flurometer	3/4/2015 17:22	0
Lower Flurometer	3/4/2015 17:23	0
Lower Flurometer	3/4/2015 17:24	0
Lower Flurometer	3/4/2015 17:25	0
Lower Flurometer	3/4/2015 17:26	0
Lower Flurometer	3/4/2015 17:27	0
Lower Flurometer	3/4/2015 17:28	0
Lower Flurometer	3/4/2015 17:29	0
Lower Flurometer	3/4/2015 17:30	0
Lower Flurometer	3/4/2015 17:31	0
Lower Flurometer	3/4/2015 17:32	0
Lower Flurometer	3/4/2015 17:33	0
Lower Flurometer	3/4/2015 17:34	0
Lower Flurometer	3/4/2015 17:35	0
Lower Flurometer	3/4/2015 17:36	0
Lower Flurometer	3/4/2015 17:37	0
Lower Flurometer	3/4/2015 17:38	0
Lower Flurometer	3/4/2015 17:39	0
Lower Flurometer	3/4/2015 17:40	0
Lower Flurometer	3/4/2015 17:41	0
Lower Flurometer	3/4/2015 17:42	0
Lower Flurometer	3/4/2015 17:43	0
Lower Flurometer	3/4/2015 17:44	0
Lower Flurometer	3/4/2015 17:45	0
Lower Flurometer	3/4/2015 17:46	0
Lower Flurometer	3/4/2015 17:47	0

Location	Date and Time	Rhodmaine Concentration Adjusted Concentration (ppb)
Lower Flurometer	3/4/2015 17:48	0
Lower Flurometer	3/4/2015 17:49	0
Lower Flurometer	3/4/2015 17:50	0
Lower Flurometer	3/4/2015 17:51	0
Lower Flurometer	3/4/2015 17:52	0
Lower Flurometer	3/4/2015 17:53	0
Lower Flurometer	3/4/2015 17:54	0
Lower Flurometer	3/4/2015 17:55	0
Lower Flurometer	3/4/2015 17:56	0
Lower Flurometer	3/4/2015 17:57	0
Lower Flurometer	3/4/2015 17:58	0
Lower Flurometer	3/4/2015 17:59	0
Lower Flurometer	3/4/2015 18:00	0
Lower Flurometer	3/4/2015 18:01	0
Lower Flurometer	3/4/2015 18:02	0
Lower Flurometer	3/4/2015 18:03	0
Lower Flurometer	3/4/2015 18:04	0
Lower Flurometer	3/4/2015 18:05	0
Lower Flurometer	3/4/2015 18:06	0
Lower Flurometer	3/4/2015 18:07	0
Lower Flurometer	3/4/2015 18:08	0
Lower Flurometer	3/4/2015 18:09	0
Lower Flurometer	3/4/2015 18:10	0
Lower Flurometer	3/4/2015 18:11	0
Lower Flurometer	3/4/2015 18:12	0
Lower Flurometer	3/4/2015 18:13	0
Lower Flurometer	3/4/2015 18:14	0
Lower Flurometer	3/4/2015 18:15	0
Lower Flurometer	3/4/2015 18:16	0
Lower Flurometer	3/4/2015 18:17	0
Lower Flurometer	3/4/2015 18:18	0
Lower Flurometer	3/4/2015 18:19	0
Lower Flurometer	3/4/2015 18:20	0
Lower Flurometer	3/4/2015 18:21	0
Lower Flurometer	3/4/2015 18:22	0
Lower Flurometer	3/4/2015 18:23	0
Lower Flurometer	3/4/2015 18:24	0
Lower Flurometer	3/4/2015 18:25	0
Lower Flurometer	3/4/2015 18:26	0
Lower Flurometer	3/4/2015 18:27	0
Lower Flurometer	3/4/2015 18:28	0
Lower Flurometer	3/4/2015 18:29	0
Lower Flurometer	3/4/2015 18:30	0
Lower Flurometer	3/4/2015 18:31	0
Lower Flurometer	3/4/2015 18:32	0
Lower Flurometer	3/4/2015 18:33	0

Location	Date and Time	Rhodmaine Concentration Adjusted Concentration (ppb)
Lower Flurometer	3/4/2015 18:34	0
Lower Flurometer	3/4/2015 18:35	0
Lower Flurometer	3/4/2015 18:36	0
Lower Flurometer	3/4/2015 18:37	0
Lower Flurometer	3/4/2015 18:38	0
Lower Flurometer	3/4/2015 18:39	0
Lower Flurometer	3/4/2015 18:40	0
Lower Flurometer	3/4/2015 18:41	0
Lower Flurometer	3/4/2015 18:42	0
Lower Flurometer	3/4/2015 18:43	0
Lower Flurometer	3/4/2015 18:44	0
Lower Flurometer	3/4/2015 18:45	0
Lower Flurometer	3/4/2015 18:46	0
Lower Flurometer	3/4/2015 18:47	0
Lower Flurometer	3/4/2015 18:48	0
Lower Flurometer	3/4/2015 18:49	0
Lower Flurometer	3/4/2015 18:50	0
Lower Flurometer	3/4/2015 18:51	0
Lower Flurometer	3/4/2015 18:52	0
Lower Flurometer	3/4/2015 18:53	0
Lower Flurometer	3/4/2015 18:54	0
Lower Flurometer	3/4/2015 18:55	0
Lower Flurometer	3/4/2015 18:56	0
Lower Flurometer	3/4/2015 18:57	0
Lower Flurometer	3/4/2015 18:58	0
Lower Flurometer	3/4/2015 18:59	0
Lower Flurometer	3/4/2015 19:00	0
Lower Flurometer	3/4/2015 19:01	0
Lower Flurometer	3/4/2015 19:02	0
Lower Flurometer	3/4/2015 19:03	0
Lower Flurometer	3/4/2015 19:04	0
Lower Flurometer	3/4/2015 19:05	0
Lower Flurometer	3/4/2015 19:06	0
Lower Flurometer	3/4/2015 19:07	0
Lower Flurometer	3/4/2015 19:08	0
Lower Flurometer	3/4/2015 19:09	0
Lower Flurometer	3/4/2015 19:10	0
Lower Flurometer	3/4/2015 19:11	0
Lower Flurometer	3/4/2015 19:12	0
Lower Flurometer	3/4/2015 19:13	0
Lower Flurometer	3/4/2015 19:14	0
Lower Flurometer	3/4/2015 19:15	0
Lower Flurometer	3/4/2015 19:16	0
Lower Flurometer	3/4/2015 19:17	0
Lower Flurometer	3/4/2015 19:18	0
Lower Flurometer	3/4/2015 19:19	0

Location	Date and Time	Rhodmaine Concentration Adjusted Concentration (ppb)
Lower Flurometer	3/4/2015 19:20	0
Lower Flurometer	3/4/2015 19:21	0
Lower Flurometer	3/4/2015 19:22	0
Lower Flurometer	3/4/2015 19:23	0
Lower Flurometer	3/4/2015 19:24	0
Lower Flurometer	3/4/2015 19:25	0
Lower Flurometer	3/4/2015 19:26	0
Lower Flurometer	3/4/2015 19:27	0
Lower Flurometer	3/4/2015 19:28	0
Lower Flurometer	3/4/2015 19:29	0
Lower Flurometer	3/4/2015 19:30	0
Lower Flurometer	3/4/2015 19:31	0
Lower Flurometer	3/4/2015 19:32	0
Lower Flurometer	3/4/2015 19:33	0
Lower Flurometer	3/4/2015 19:34	0
Lower Flurometer	3/4/2015 19:35	0
Lower Flurometer	3/4/2015 19:36	0
Lower Flurometer	3/4/2015 19:37	0
Lower Flurometer	3/4/2015 19:38	0
Lower Flurometer	3/4/2015 19:39	0
Lower Flurometer	3/4/2015 19:40	0
Lower Flurometer	3/4/2015 19:41	0
Lower Flurometer	3/4/2015 19:42	0
Lower Flurometer	3/4/2015 19:43	0
Lower Flurometer	3/4/2015 19:44	0
Lower Flurometer	3/4/2015 19:45	0
Lower Flurometer	3/4/2015 19:46	0
Lower Flurometer	3/4/2015 19:47	0
Lower Flurometer	3/4/2015 19:48	0
Lower Flurometer	3/4/2015 19:49	0
Lower Flurometer	3/4/2015 19:50	0
Lower Flurometer	3/4/2015 19:51	0
Lower Flurometer	3/4/2015 19:52	0
Lower Flurometer	3/4/2015 19:53	0
Lower Flurometer	3/4/2015 19:54	0
Lower Flurometer	3/4/2015 19:55	0
Lower Flurometer	3/4/2015 19:56	0
Lower Flurometer	3/4/2015 19:57	0
Lower Flurometer	3/4/2015 19:58	0
Lower Flurometer	3/4/2015 19:59	0
Lower Flurometer	3/4/2015 20:00	0
Lower Flurometer	3/4/2015 20:01	0
Lower Flurometer	3/4/2015 20:02	0
Lower Flurometer	3/4/2015 20:03	0
Lower Flurometer	3/4/2015 20:04	0
Lower Flurometer	3/4/2015 20:05	0

Location	Date and Time	Rhodmaine Concentration Adjusted Concentration (ppb)
Lower Flurometer	3/4/2015 20:06	0
Lower Flurometer	3/4/2015 20:07	0
Lower Flurometer	3/4/2015 20:08	0
Lower Flurometer	3/4/2015 20:09	0
Lower Flurometer	3/4/2015 20:10	0
Lower Flurometer	3/4/2015 20:11	0
Lower Flurometer	3/4/2015 20:12	0
Lower Flurometer	3/4/2015 20:13	0
Lower Flurometer	3/4/2015 20:14	0
Lower Flurometer	3/4/2015 20:15	0
Lower Flurometer	3/4/2015 20:16	0
Lower Flurometer	3/4/2015 20:17	0
Lower Flurometer	3/4/2015 20:18	0
Lower Flurometer	3/4/2015 20:19	0
Lower Flurometer	3/4/2015 20:20	0
Lower Flurometer	3/4/2015 20:21	0
Lower Flurometer	3/4/2015 20:22	0
Lower Flurometer	3/4/2015 20:23	0
Lower Flurometer	3/4/2015 20:24	0
Lower Flurometer	3/4/2015 20:25	0
Lower Flurometer	3/4/2015 20:26	0
Lower Flurometer	3/4/2015 20:27	0
Lower Flurometer	3/4/2015 20:28	0
Lower Flurometer	3/4/2015 20:29	0
Lower Flurometer	3/4/2015 20:30	0
Lower Flurometer	3/4/2015 20:31	0
Lower Flurometer	3/4/2015 20:32	0
Lower Flurometer	3/4/2015 20:33	0
Lower Flurometer	3/4/2015 20:34	0
Lower Flurometer	3/4/2015 20:35	0
Lower Flurometer	3/4/2015 20:36	0
Lower Flurometer	3/4/2015 20:37	0
Lower Flurometer	3/4/2015 20:38	0
Lower Flurometer	3/4/2015 20:39	0
Lower Flurometer	3/4/2015 20:40	0
Lower Flurometer	3/4/2015 20:41	0
Lower Flurometer	3/4/2015 20:42	0
Lower Flurometer	3/4/2015 20:43	0
Lower Flurometer	3/4/2015 20:44	0
Lower Flurometer	3/4/2015 20:45	0
Lower Flurometer	3/4/2015 20:46	0
Lower Flurometer	3/4/2015 20:47	0
Lower Flurometer	3/4/2015 20:48	0
Lower Flurometer	3/4/2015 20:49	0
Lower Flurometer	3/4/2015 20:50	0
Lower Flurometer	3/4/2015 20:51	0

Location	Date and Time	Rhodmaine Concentration Adjusted Concentration (ppb)
Lower Flurometer	3/4/2015 20:52	0
Lower Flurometer	3/4/2015 20:53	0
Lower Flurometer	3/4/2015 20:54	0
Lower Flurometer	3/4/2015 20:55	0
Lower Flurometer	3/4/2015 20:56	0
Lower Flurometer	3/4/2015 20:57	0
Lower Flurometer	3/4/2015 20:58	0
Lower Flurometer	3/4/2015 20:59	0
Lower Flurometer	3/4/2015 21:00	0
Lower Flurometer	3/4/2015 21:01	0
Lower Flurometer	3/4/2015 21:02	0
Lower Flurometer	3/4/2015 21:03	0
Lower Flurometer	3/4/2015 21:04	0
Lower Flurometer	3/4/2015 21:05	0
Lower Flurometer	3/4/2015 21:06	0
Lower Flurometer	3/4/2015 21:07	0
Lower Flurometer	3/4/2015 21:08	0
Lower Flurometer	3/4/2015 21:09	0
Lower Flurometer	3/4/2015 21:10	0
Lower Flurometer	3/4/2015 21:11	0
Lower Flurometer	3/4/2015 21:12	0
Lower Flurometer	3/4/2015 21:13	0
Lower Flurometer	3/4/2015 21:14	0
Lower Flurometer	3/4/2015 21:15	0
Lower Flurometer	3/4/2015 21:16	0
Lower Flurometer	3/4/2015 21:17	0
Lower Flurometer	3/4/2015 21:18	0
Lower Flurometer	3/4/2015 21:19	0
Lower Flurometer	3/4/2015 21:20	0
Lower Flurometer	3/4/2015 21:21	0
Lower Flurometer	3/4/2015 21:22	0
Lower Flurometer	3/4/2015 21:23	0
Lower Flurometer	3/4/2015 21:24	0
Lower Flurometer	3/4/2015 21:25	0
Lower Flurometer	3/4/2015 21:26	0.1
Lower Flurometer	3/4/2015 21:27	0
Lower Flurometer	3/4/2015 21:28	0
Lower Flurometer	3/4/2015 21:29	0
Lower Flurometer	3/4/2015 21:30	0
Lower Flurometer	3/4/2015 21:31	0
Lower Flurometer	3/4/2015 21:32	0
Lower Flurometer	3/4/2015 21:33	0
Lower Flurometer	3/4/2015 21:34	0
Lower Flurometer	3/4/2015 21:35	0
Lower Flurometer	3/4/2015 21:36	0
Lower Flurometer	3/4/2015 21:37	0

Location	Date and Time	Rhodmaine Concentration Adjusted Concentration (ppb)
Lower Flurometer	3/4/2015 21:38	0
Lower Flurometer	3/4/2015 21:39	0
Lower Flurometer	3/4/2015 21:40	0
Lower Flurometer	3/4/2015 21:41	0
Lower Flurometer	3/4/2015 21:42	0
Lower Flurometer	3/4/2015 21:43	0
Lower Flurometer	3/4/2015 21:44	0
Lower Flurometer	3/4/2015 21:45	0
Lower Flurometer	3/4/2015 21:46	0
Lower Flurometer	3/4/2015 21:47	0
Lower Flurometer	3/4/2015 21:48	0
Lower Flurometer	3/4/2015 21:49	0
Lower Flurometer	3/4/2015 21:50	0
Lower Flurometer	3/4/2015 21:51	0
Lower Flurometer	3/4/2015 21:52	0
Lower Flurometer	3/4/2015 21:53	0
Lower Flurometer	3/4/2015 21:54	0
Lower Flurometer	3/4/2015 21:55	0
Lower Flurometer	3/4/2015 21:56	0
Lower Flurometer	3/4/2015 21:57	0
Lower Flurometer	3/4/2015 21:58	0
Lower Flurometer	3/4/2015 21:59	0
Lower Flurometer	3/4/2015 22:00	0
Lower Flurometer	3/4/2015 22:01	0
Lower Flurometer	3/4/2015 22:02	0
Lower Flurometer	3/4/2015 22:03	0
Lower Flurometer	3/4/2015 22:04	0
Lower Flurometer	3/4/2015 22:05	0
Lower Flurometer	3/4/2015 22:06	0
Lower Flurometer	3/4/2015 22:07	0
Lower Flurometer	3/4/2015 22:08	0
Lower Flurometer	3/4/2015 22:09	0
Lower Flurometer	3/4/2015 22:10	0
Lower Flurometer	3/4/2015 22:11	0
Lower Flurometer	3/4/2015 22:12	0
Lower Flurometer	3/4/2015 22:13	0
Lower Flurometer	3/4/2015 22:14	0
Lower Flurometer	3/4/2015 22:15	0
Lower Flurometer	3/4/2015 22:16	0
Lower Flurometer	3/4/2015 22:17	0
Lower Flurometer	3/4/2015 22:18	0
Lower Flurometer	3/4/2015 22:19	0
Lower Flurometer	3/4/2015 22:20	0
Lower Flurometer	3/4/2015 22:21	0
Lower Flurometer	3/4/2015 22:22	0
Lower Flurometer	3/4/2015 22:23	0

Location	Date and Time	Rhodmaine Concentration Adjusted Concentration (ppb)
Lower Flurometer	3/4/2015 22:24	0
Lower Flurometer	3/4/2015 22:25	0
Lower Flurometer	3/4/2015 22:26	0
Lower Flurometer	3/4/2015 22:27	0
Lower Flurometer	3/4/2015 22:28	0
Lower Flurometer	3/4/2015 22:29	0
Lower Flurometer	3/4/2015 22:30	0
Lower Flurometer	3/4/2015 22:31	0
Lower Flurometer	3/4/2015 22:32	0
Lower Flurometer	3/4/2015 22:33	0
Lower Flurometer	3/4/2015 22:34	0
Lower Flurometer	3/4/2015 22:35	0
Lower Flurometer	3/4/2015 22:36	0
Lower Flurometer	3/4/2015 22:37	0
Lower Flurometer	3/4/2015 22:38	0
Lower Flurometer	3/4/2015 22:39	0
Lower Flurometer	3/4/2015 22:40	0
Lower Flurometer	3/4/2015 22:41	0
Lower Flurometer	3/4/2015 22:42	0
Lower Flurometer	3/4/2015 22:43	0
Lower Flurometer	3/4/2015 22:44	0
Lower Flurometer	3/4/2015 22:45	0
Lower Flurometer	3/4/2015 22:46	0
Lower Flurometer	3/4/2015 22:47	0
Lower Flurometer	3/4/2015 22:48	0
Lower Flurometer	3/4/2015 22:49	0
Lower Flurometer	3/4/2015 22:50	0
Lower Flurometer	3/4/2015 22:51	0
Lower Flurometer	3/4/2015 22:52	0
Lower Flurometer	3/4/2015 22:53	0
Lower Flurometer	3/4/2015 22:54	0
Lower Flurometer	3/4/2015 22:55	0
Lower Flurometer	3/4/2015 22:56	0
Lower Flurometer	3/4/2015 22:57	0
Lower Flurometer	3/4/2015 22:58	0
Lower Flurometer	3/4/2015 22:59	0
Lower Flurometer	3/4/2015 23:00	0
Lower Flurometer	3/4/2015 23:01	0
Lower Flurometer	3/4/2015 23:02	0
Lower Flurometer	3/4/2015 23:03	0
Lower Flurometer	3/4/2015 23:04	0
Lower Flurometer	3/4/2015 23:05	0
Lower Flurometer	3/4/2015 23:06	0
Lower Flurometer	3/4/2015 23:07	0
Lower Flurometer	3/4/2015 23:08	0
Lower Flurometer	3/4/2015 23:09	0

Location	Date and Time	Rhodmaine Concentration Adjusted Concentration (ppb)
Lower Flurometer	3/4/2015 23:10	0
Lower Flurometer	3/4/2015 23:11	0
Lower Flurometer	3/4/2015 23:12	0
Lower Flurometer	3/4/2015 23:13	0
Lower Flurometer	3/4/2015 23:14	0
Lower Flurometer	3/4/2015 23:15	0
Lower Flurometer	3/4/2015 23:16	0
Lower Flurometer	3/4/2015 23:17	0
Lower Flurometer	3/4/2015 23:18	0
Lower Flurometer	3/4/2015 23:19	0
Lower Flurometer	3/4/2015 23:20	0
Lower Flurometer	3/4/2015 23:21	0
Lower Flurometer	3/4/2015 23:22	0
Lower Flurometer	3/4/2015 23:23	0
Lower Flurometer	3/4/2015 23:24	0
Lower Flurometer	3/4/2015 23:25	0
Lower Flurometer	3/4/2015 23:26	0
Lower Flurometer	3/4/2015 23:27	0
Lower Flurometer	3/4/2015 23:28	0
Lower Flurometer	3/4/2015 23:29	0
Lower Flurometer	3/4/2015 23:30	0
Lower Flurometer	3/4/2015 23:31	0
Lower Flurometer	3/4/2015 23:32	0
Lower Flurometer	3/4/2015 23:33	0
Lower Flurometer	3/4/2015 23:34	0
Lower Flurometer	3/4/2015 23:35	0
Lower Flurometer	3/4/2015 23:36	0
Lower Flurometer	3/4/2015 23:37	0
Lower Flurometer	3/4/2015 23:38	0
Lower Flurometer	3/4/2015 23:39	0
Lower Flurometer	3/4/2015 23:40	0
Lower Flurometer	3/4/2015 23:41	0
Lower Flurometer	3/4/2015 23:42	0
Lower Flurometer	3/4/2015 23:43	0
Lower Flurometer	3/4/2015 23:44	0
Lower Flurometer	3/4/2015 23:45	0
Lower Flurometer	3/4/2015 23:46	0
Lower Flurometer	3/4/2015 23:47	0
Lower Flurometer	3/4/2015 23:48	0
Lower Flurometer	3/4/2015 23:49	0
Lower Flurometer	3/4/2015 23:50	0
Lower Flurometer	3/4/2015 23:51	0
Lower Flurometer	3/4/2015 23:52	0
Lower Flurometer	3/4/2015 23:53	0
Lower Flurometer	3/4/2015 23:54	0
Lower Flurometer	3/4/2015 23:55	0

Location	Date and Time	Rhodmaine Concentration Adjusted Concentration (ppb)
Lower Flurometer	3/4/2015 23:56	0
Lower Flurometer	3/4/2015 23:57	0
Lower Flurometer	3/4/2015 23:58	0
Lower Flurometer	3/4/2015 23:59	0
Lower Flurometer	3/5/2015 0:00	0
Lower Flurometer	3/5/2015 0:01	0
Lower Flurometer	3/5/2015 0:02	0
Lower Flurometer	3/5/2015 0:03	0
Lower Flurometer	3/5/2015 0:04	0
Lower Flurometer	3/5/2015 0:05	0
Lower Flurometer	3/5/2015 0:06	0
Lower Flurometer	3/5/2015 0:07	0
Lower Flurometer	3/5/2015 0:08	0
Lower Flurometer	3/5/2015 0:09	0
Lower Flurometer	3/5/2015 0:10	0
Lower Flurometer	3/5/2015 0:11	0
Lower Flurometer	3/5/2015 0:12	0
Lower Flurometer	3/5/2015 0:13	0
Lower Flurometer	3/5/2015 0:14	0
Lower Flurometer	3/5/2015 0:15	0
Lower Flurometer	3/5/2015 0:16	0
Lower Flurometer	3/5/2015 0:17	0
Lower Flurometer	3/5/2015 0:18	0
Lower Flurometer	3/5/2015 0:19	0
Lower Flurometer	3/5/2015 0:20	0
Lower Flurometer	3/5/2015 0:21	0
Lower Flurometer	3/5/2015 0:22	0
Lower Flurometer	3/5/2015 0:23	0
Lower Flurometer	3/5/2015 0:24	0
Lower Flurometer	3/5/2015 0:25	0
Lower Flurometer	3/5/2015 0:26	0
Lower Flurometer	3/5/2015 0:27	0
Lower Flurometer	3/5/2015 0:28	0
Lower Flurometer	3/5/2015 0:29	0
Lower Flurometer	3/5/2015 0:30	0
Lower Flurometer	3/5/2015 0:31	0
Lower Flurometer	3/5/2015 0:32	0
Lower Flurometer	3/5/2015 0:33	0
Lower Flurometer	3/5/2015 0:34	0
Lower Flurometer	3/5/2015 0:35	0
Lower Flurometer	3/5/2015 0:36	0
Lower Flurometer	3/5/2015 0:37	0
Lower Flurometer	3/5/2015 0:38	0
Lower Flurometer	3/5/2015 0:39	0
Lower Flurometer	3/5/2015 0:40	0
Lower Flurometer	3/5/2015 0:41	0

Location	Date and Time	Rhodmaine Concentration Adjusted Concentration (ppb)
Lower Flurometer	3/5/2015 0:42	0
Lower Flurometer	3/5/2015 0:43	0
Lower Flurometer	3/5/2015 0:44	0
Lower Flurometer	3/5/2015 0:45	0
Lower Flurometer	3/5/2015 0:46	0
Lower Flurometer	3/5/2015 0:47	0
Lower Flurometer	3/5/2015 0:48	0
Lower Flurometer	3/5/2015 0:49	0
Lower Flurometer	3/5/2015 0:50	0
Lower Flurometer	3/5/2015 0:51	0
Lower Flurometer	3/5/2015 0:52	0
Lower Flurometer	3/5/2015 0:53	0
Lower Flurometer	3/5/2015 0:54	0
Lower Flurometer	3/5/2015 0:55	0
Lower Flurometer	3/5/2015 0:56	0
Lower Flurometer	3/5/2015 0:57	0
Lower Flurometer	3/5/2015 0:58	0
Lower Flurometer	3/5/2015 0:59	0
Lower Flurometer	3/5/2015 1:00	0
Lower Flurometer	3/5/2015 1:01	0
Lower Flurometer	3/5/2015 1:02	0
Lower Flurometer	3/5/2015 1:03	0
Lower Flurometer	3/5/2015 1:04	0
Lower Flurometer	3/5/2015 1:05	0
Lower Flurometer	3/5/2015 1:06	0
Lower Flurometer	3/5/2015 1:07	0
Lower Flurometer	3/5/2015 1:08	0
Lower Flurometer	3/5/2015 1:09	0
Lower Flurometer	3/5/2015 1:10	0
Lower Flurometer	3/5/2015 1:11	0
Lower Flurometer	3/5/2015 1:12	0
Lower Flurometer	3/5/2015 1:13	0.21
Lower Flurometer	3/5/2015 1:14	0
Lower Flurometer	3/5/2015 1:15	0
Lower Flurometer	3/5/2015 1:16	0
Lower Flurometer	3/5/2015 1:17	0
Lower Flurometer	3/5/2015 1:18	0
Lower Flurometer	3/5/2015 1:19	0
Lower Flurometer	3/5/2015 1:20	0
Lower Flurometer	3/5/2015 1:21	0
Lower Flurometer	3/5/2015 1:22	0
Lower Flurometer	3/5/2015 1:23	0
Lower Flurometer	3/5/2015 1:24	0
Lower Flurometer	3/5/2015 1:25	0
Lower Flurometer	3/5/2015 1:26	0
Lower Flurometer	3/5/2015 1:27	0

Location	Date and Time	Rhodmaine Concentration Adjusted Concentration (ppb)
Lower Flurometer	3/5/2015 1:28	0
Lower Flurometer	3/5/2015 1:29	0
Lower Flurometer	3/5/2015 1:30	0
Lower Flurometer	3/5/2015 1:31	0
Lower Flurometer	3/5/2015 1:32	0
Lower Flurometer	3/5/2015 1:33	0
Lower Flurometer	3/5/2015 1:34	0
Lower Flurometer	3/5/2015 1:35	0
Lower Flurometer	3/5/2015 1:36	0
Lower Flurometer	3/5/2015 1:37	0
Lower Flurometer	3/5/2015 1:38	0
Lower Flurometer	3/5/2015 1:39	0
Lower Flurometer	3/5/2015 1:40	0
Lower Flurometer	3/5/2015 1:41	0
Lower Flurometer	3/5/2015 1:42	0
Lower Flurometer	3/5/2015 1:43	0
Lower Flurometer	3/5/2015 1:44	0
Lower Flurometer	3/5/2015 1:45	0
Lower Flurometer	3/5/2015 1:46	0
Lower Flurometer	3/5/2015 1:47	0
Lower Flurometer	3/5/2015 1:48	0
Lower Flurometer	3/5/2015 1:49	0
Lower Flurometer	3/5/2015 1:50	0
Lower Flurometer	3/5/2015 1:51	0
Lower Flurometer	3/5/2015 1:52	0
Lower Flurometer	3/5/2015 1:53	0
Lower Flurometer	3/5/2015 1:54	0
Lower Flurometer	3/5/2015 1:55	0
Lower Flurometer	3/5/2015 1:56	0
Lower Flurometer	3/5/2015 1:57	0
Lower Flurometer	3/5/2015 1:58	0
Lower Flurometer	3/5/2015 1:59	0
Lower Flurometer	3/5/2015 2:00	0
Lower Flurometer	3/5/2015 2:01	0
Lower Flurometer	3/5/2015 2:02	0
Lower Flurometer	3/5/2015 2:03	0
Lower Flurometer	3/5/2015 2:04	0
Lower Flurometer	3/5/2015 2:05	0
Lower Flurometer	3/5/2015 2:06	0
Lower Flurometer	3/5/2015 2:07	0
Lower Flurometer	3/5/2015 2:08	0
Lower Flurometer	3/5/2015 2:09	0
Lower Flurometer	3/5/2015 2:10	0
Lower Flurometer	3/5/2015 2:11	0
Lower Flurometer	3/5/2015 2:12	0
Lower Flurometer	3/5/2015 2:13	0

Location	Date and Time	Rhodmaine Concentration Adjusted Concentration (ppb)
Lower Flurometer	3/5/2015 2:14	0
Lower Flurometer	3/5/2015 2:15	0
Lower Flurometer	3/5/2015 2:16	0
Lower Flurometer	3/5/2015 2:17	0
Lower Flurometer	3/5/2015 2:18	0
Lower Flurometer	3/5/2015 2:19	0
Lower Flurometer	3/5/2015 2:20	0
Lower Flurometer	3/5/2015 2:21	0
Lower Flurometer	3/5/2015 2:22	0
Lower Flurometer	3/5/2015 2:23	0
Lower Flurometer	3/5/2015 2:24	0
Lower Flurometer	3/5/2015 2:25	0
Lower Flurometer	3/5/2015 2:26	0
Lower Flurometer	3/5/2015 2:27	0
Lower Flurometer	3/5/2015 2:28	0
Lower Flurometer	3/5/2015 2:29	0
Lower Flurometer	3/5/2015 2:30	0
Lower Flurometer	3/5/2015 2:31	0
Lower Flurometer	3/5/2015 2:32	0
Lower Flurometer	3/5/2015 2:33	0
Lower Flurometer	3/5/2015 2:34	0
Lower Flurometer	3/5/2015 2:35	0
Lower Flurometer	3/5/2015 2:36	0
Lower Flurometer	3/5/2015 2:37	0
Lower Flurometer	3/5/2015 2:38	0
Lower Flurometer	3/5/2015 2:39	0
Lower Flurometer	3/5/2015 2:40	0
Lower Flurometer	3/5/2015 2:41	0
Lower Flurometer	3/5/2015 2:42	0
Lower Flurometer	3/5/2015 2:43	0
Lower Flurometer	3/5/2015 2:44	0
Lower Flurometer	3/5/2015 2:45	0
Lower Flurometer	3/5/2015 2:46	0
Lower Flurometer	3/5/2015 2:47	0
Lower Flurometer	3/5/2015 2:48	0.07
Lower Flurometer	3/5/2015 2:49	0
Lower Flurometer	3/5/2015 2:50	0.04
Lower Flurometer	3/5/2015 2:51	0
Lower Flurometer	3/5/2015 2:52	0.04
Lower Flurometer	3/5/2015 2:53	0.06
Lower Flurometer	3/5/2015 2:54	0.1
Lower Flurometer	3/5/2015 2:55	0.08
Lower Flurometer	3/5/2015 2:56	0.06
Lower Flurometer	3/5/2015 2:57	0.08
Lower Flurometer	3/5/2015 2:58	0.12
Lower Flurometer	3/5/2015 2:59	0.16

Location	Date and Time	Rhodmaine Concentration Adjusted Concentration (ppb)
Lower Flurometer	3/5/2015 3:00	0.15
Lower Flurometer	3/5/2015 3:01	0.15
Lower Flurometer	3/5/2015 3:02	1.69
Lower Flurometer	3/5/2015 3:03	0.23
Lower Flurometer	3/5/2015 3:04	0.2
Lower Flurometer	3/5/2015 3:05	0.19
Lower Flurometer	3/5/2015 3:06	0.28
Lower Flurometer	3/5/2015 3:07	0.3
Lower Flurometer	3/5/2015 3:08	0.3
Lower Flurometer	3/5/2015 3:09	0.39
Lower Flurometer	3/5/2015 3:10	0.42
Lower Flurometer	3/5/2015 3:11	0.41
Lower Flurometer	3/5/2015 3:12	0.43
Lower Flurometer	3/5/2015 3:13	0.46
Lower Flurometer	3/5/2015 3:14	0.45
Lower Flurometer	3/5/2015 3:15	0.52
Lower Flurometer	3/5/2015 3:16	0.6
Lower Flurometer	3/5/2015 3:17	0.57
Lower Flurometer	3/5/2015 3:18	0.62
Lower Flurometer	3/5/2015 3:19	0.62
Lower Flurometer	3/5/2015 3:20	0.7
Lower Flurometer	3/5/2015 3:21	0.7
Lower Flurometer	3/5/2015 3:22	0.76
Lower Flurometer	3/5/2015 3:23	0.77
Lower Flurometer	3/5/2015 3:24	0.77
Lower Flurometer	3/5/2015 3:25	0.83
Lower Flurometer	3/5/2015 3:26	0.84
Lower Flurometer	3/5/2015 3:27	0.92
Lower Flurometer	3/5/2015 3:28	1.02
Lower Flurometer	3/5/2015 3:29	1.07
Lower Flurometer	3/5/2015 3:30	1.11
Lower Flurometer	3/5/2015 3:31	1.11
Lower Flurometer	3/5/2015 3:32	1.14
Lower Flurometer	3/5/2015 3:33	1.29
Lower Flurometer	3/5/2015 3:34	1.16
Lower Flurometer	3/5/2015 3:35	1.28
Lower Flurometer	3/5/2015 3:36	1.26
Lower Flurometer	3/5/2015 3:37	1.35
Lower Flurometer	3/5/2015 3:38	1.46
Lower Flurometer	3/5/2015 3:39	1.49
Lower Flurometer	3/5/2015 3:40	1.48
Lower Flurometer	3/5/2015 3:41	1.56
Lower Flurometer	3/5/2015 3:42	1.56
Lower Flurometer	3/5/2015 3:43	1.6
Lower Flurometer	3/5/2015 3:44	1.79
Lower Flurometer	3/5/2015 3:45	1.77

Location	Date and Time	Rhodmaine Concentration Adjusted Concentration (ppb)
Lower Flurometer	3/5/2015 3:46	1.92
Lower Flurometer	3/5/2015 3:47	1.87
Lower Flurometer	3/5/2015 3:48	2.01
Lower Flurometer	3/5/2015 3:49	2.01
Lower Flurometer	3/5/2015 3:50	2.08
Lower Flurometer	3/5/2015 3:51	2.14
Lower Flurometer	3/5/2015 3:52	2.24
Lower Flurometer	3/5/2015 3:53	2.3
Lower Flurometer	3/5/2015 3:54	2.31
Lower Flurometer	3/5/2015 3:55	2.29
Lower Flurometer	3/5/2015 3:56	2.37
Lower Flurometer	3/5/2015 3:57	2.56
Lower Flurometer	3/5/2015 3:58	2.56
Lower Flurometer	3/5/2015 3:59	2.59
Lower Flurometer	3/5/2015 4:00	2.64
Lower Flurometer	3/5/2015 4:01	2.64
Lower Flurometer	3/5/2015 4:02	2.73
Lower Flurometer	3/5/2015 4:03	2.85
Lower Flurometer	3/5/2015 4:04	2.98
Lower Flurometer	3/5/2015 4:05	2.96
Lower Flurometer	3/5/2015 4:06	3.02
Lower Flurometer	3/5/2015 4:07	3.02
Lower Flurometer	3/5/2015 4:08	3.16
Lower Flurometer	3/5/2015 4:09	3.2
Lower Flurometer	3/5/2015 4:10	3.28
Lower Flurometer	3/5/2015 4:11	3.3
Lower Flurometer	3/5/2015 4:12	3.41
Lower Flurometer	3/5/2015 4:13	3.45
Lower Flurometer	3/5/2015 4:14	3.5
Lower Flurometer	3/5/2015 4:15	3.49
Lower Flurometer	3/5/2015 4:16	3.68
Lower Flurometer	3/5/2015 4:17	3.66
Lower Flurometer	3/5/2015 4:18	3.81
Lower Flurometer	3/5/2015 4:19	3.89
Lower Flurometer	3/5/2015 4:20	3.96
Lower Flurometer	3/5/2015 4:21	3.96
Lower Flurometer	3/5/2015 4:22	4.09
Lower Flurometer	3/5/2015 4:23	4.06
Lower Flurometer	3/5/2015 4:24	4.09
Lower Flurometer	3/5/2015 4:25	4.16
Lower Flurometer	3/5/2015 4:26	4.24
Lower Flurometer	3/5/2015 4:27	4.31
Lower Flurometer	3/5/2015 4:28	4.31
Lower Flurometer	3/5/2015 4:29	4.35
Lower Flurometer	3/5/2015 4:30	4.37
Lower Flurometer	3/5/2015 4:31	4.5

Location	Date and Time	Rhodmaine Concentration Adjusted Concentration (ppb)
Lower Flurometer	3/5/2015 4:32	4.95
Lower Flurometer	3/5/2015 4:33	4.57
Lower Flurometer	3/5/2015 4:34	4.63
Lower Flurometer	3/5/2015 4:35	4.79
Lower Flurometer	3/5/2015 4:36	4.79
Lower Flurometer	3/5/2015 4:37	4.87
Lower Flurometer	3/5/2015 4:38	4.93
Lower Flurometer	3/5/2015 4:39	4.97
Lower Flurometer	3/5/2015 4:40	5.05
Lower Flurometer	3/5/2015 4:41	4.98
Lower Flurometer	3/5/2015 4:42	5
Lower Flurometer	3/5/2015 4:43	5.12
Lower Flurometer	3/5/2015 4:44	5.15
Lower Flurometer	3/5/2015 4:45	5.27
Lower Flurometer	3/5/2015 4:46	5.33
Lower Flurometer	3/5/2015 4:47	5.26
Lower Flurometer	3/5/2015 4:48	5.29
Lower Flurometer	3/5/2015 4:49	5.3
Lower Flurometer	3/5/2015 4:50	5.33
Lower Flurometer	3/5/2015 4:51	5.4
Lower Flurometer	3/5/2015 4:52	5.52
Lower Flurometer	3/5/2015 4:53	5.59
Lower Flurometer	3/5/2015 4:54	5.62
Lower Flurometer	3/5/2015 4:55	5.56
Lower Flurometer	3/5/2015 4:56	5.6
Lower Flurometer	3/5/2015 4:57	5.69
Lower Flurometer	3/5/2015 4:58	5.65
Lower Flurometer	3/5/2015 4:59	5.67
Lower Flurometer	3/5/2015 5:00	5.76
Lower Flurometer	3/5/2015 5:01	5.73
Lower Flurometer	3/5/2015 5:02	5.75
Lower Flurometer	3/5/2015 5:03	5.79
Lower Flurometer	3/5/2015 5:04	5.88
Lower Flurometer	3/5/2015 5:05	5.96
Lower Flurometer	3/5/2015 5:06	5.9
Lower Flurometer	3/5/2015 5:07	6.03
Lower Flurometer	3/5/2015 5:08	6.06
Lower Flurometer	3/5/2015 5:09	6.07
Lower Flurometer	3/5/2015 5:10	6.02
Lower Flurometer	3/5/2015 5:11	6.11
Lower Flurometer	3/5/2015 5:12	6.1
Lower Flurometer	3/5/2015 5:13	6.12
Lower Flurometer	3/5/2015 5:14	6.14
Lower Flurometer	3/5/2015 5:15	6.19
Lower Flurometer	3/5/2015 5:16	6.25
Lower Flurometer	3/5/2015 5:17	6.19

Location	Date and Time	Rhodmaine Concentration Adjusted Concentration (ppb)
Lower Flurometer	3/5/2015 5:18	6.23
Lower Flurometer	3/5/2015 5:19	6.25
Lower Flurometer	3/5/2015 5:20	6.27
Lower Flurometer	3/5/2015 5:21	6.28
Lower Flurometer	3/5/2015 5:22	6.35
Lower Flurometer	3/5/2015 5:23	6.3
Lower Flurometer	3/5/2015 5:24	6.36
Lower Flurometer	3/5/2015 5:25	6.36
Lower Flurometer	3/5/2015 5:26	6.36
Lower Flurometer	3/5/2015 5:27	6.36
Lower Flurometer	3/5/2015 5:28	6.42
Lower Flurometer	3/5/2015 5:29	6.43
Lower Flurometer	3/5/2015 5:30	6.39
Lower Flurometer	3/5/2015 5:31	6.4
Lower Flurometer	3/5/2015 5:32	6.45
Lower Flurometer	3/5/2015 5:33	6.44
Lower Flurometer	3/5/2015 5:34	6.46
Lower Flurometer	3/5/2015 5:35	6.41
Lower Flurometer	3/5/2015 5:36	6.45
Lower Flurometer	3/5/2015 5:37	6.48
Lower Flurometer	3/5/2015 5:38	6.4
Lower Flurometer	3/5/2015 5:39	6.43
Lower Flurometer	3/5/2015 5:40	6.46
Lower Flurometer	3/5/2015 5:41	6.5
Lower Flurometer	3/5/2015 5:42	6.43
Lower Flurometer	3/5/2015 5:43	6.46
Lower Flurometer	3/5/2015 5:44	6.49
Lower Flurometer	3/5/2015 5:45	6.53
Lower Flurometer	3/5/2015 5:46	6.47
Lower Flurometer	3/5/2015 5:47	6.45
Lower Flurometer	3/5/2015 5:48	6.5
Lower Flurometer	3/5/2015 5:49	6.46
Lower Flurometer	3/5/2015 5:50	6.43
Lower Flurometer	3/5/2015 5:51	6.48
Lower Flurometer	3/5/2015 5:52	6.41
Lower Flurometer	3/5/2015 5:53	6.44
Lower Flurometer	3/5/2015 5:54	6.44
Lower Flurometer	3/5/2015 5:55	6.45
Lower Flurometer	3/5/2015 5:56	6.45
Lower Flurometer	3/5/2015 5:57	6.46
Lower Flurometer	3/5/2015 5:58	6.44
Lower Flurometer	3/5/2015 5:59	6.41
Lower Flurometer	3/5/2015 6:00	6.41
Lower Flurometer	3/5/2015 6:01	6.45
Lower Flurometer	3/5/2015 6:02	6.39
Lower Flurometer	3/5/2015 6:03	6.39

Location	Date and Time	Rhodmaine Concentration Adjusted Concentration (ppb)
Lower Flurometer	3/5/2015 6:04	6.39
Lower Flurometer	3/5/2015 6:05	6.4
Lower Flurometer	3/5/2015 6:06	6.36
Lower Flurometer	3/5/2015 6:07	6.39
Lower Flurometer	3/5/2015 6:08	6.34
Lower Flurometer	3/5/2015 6:09	6.4
Lower Flurometer	3/5/2015 6:10	6.36
Lower Flurometer	3/5/2015 6:11	6.32
Lower Flurometer	3/5/2015 6:12	6.34
Lower Flurometer	3/5/2015 6:13	6.3
Lower Flurometer	3/5/2015 6:14	6.33
Lower Flurometer	3/5/2015 6:15	6.25
Lower Flurometer	3/5/2015 6:16	6.26
Lower Flurometer	3/5/2015 6:17	6.25
Lower Flurometer	3/5/2015 6:18	6.23
Lower Flurometer	3/5/2015 6:19	6.28
Lower Flurometer	3/5/2015 6:20	6.2
Lower Flurometer	3/5/2015 6:21	6.22
Lower Flurometer	3/5/2015 6:22	6.26
Lower Flurometer	3/5/2015 6:23	6.18
Lower Flurometer	3/5/2015 6:24	6.19
Lower Flurometer	3/5/2015 6:25	6.24
Lower Flurometer	3/5/2015 6:26	6.19
Lower Flurometer	3/5/2015 6:27	6.2
Lower Flurometer	3/5/2015 6:28	6.12
Lower Flurometer	3/5/2015 6:29	6.14
Lower Flurometer	3/5/2015 6:30	6.11
Lower Flurometer	3/5/2015 6:31	6.12
Lower Flurometer	3/5/2015 6:32	6.09
Lower Flurometer	3/5/2015 6:33	6.1
Lower Flurometer	3/5/2015 6:34	6.05
Lower Flurometer	3/5/2015 6:35	6.06
Lower Flurometer	3/5/2015 6:36	6.05
Lower Flurometer	3/5/2015 6:37	6.06
Lower Flurometer	3/5/2015 6:38	6.06
Lower Flurometer	3/5/2015 6:39	5.97
Lower Flurometer	3/5/2015 6:40	6.08
Lower Flurometer	3/5/2015 6:41	6.04
Lower Flurometer	3/5/2015 6:42	5.97
Lower Flurometer	3/5/2015 6:43	5.91
Lower Flurometer	3/5/2015 6:44	5.94
Lower Flurometer	3/5/2015 6:45	5.92
Lower Flurometer	3/5/2015 6:46	5.9
Lower Flurometer	3/5/2015 6:47	5.9
Lower Flurometer	3/5/2015 6:48	5.86
Lower Flurometer	3/5/2015 6:49	5.87

Location	Date and Time	Rhodmaine Concentration Adjusted Concentration (ppb)
Lower Flurometer	3/5/2015 6:50	5.86
Lower Flurometer	3/5/2015 6:51	5.81
Lower Flurometer	3/5/2015 6:52	5.87
Lower Flurometer	3/5/2015 6:53	5.83
Lower Flurometer	3/5/2015 6:54	5.82
Lower Flurometer	3/5/2015 6:55	5.81
Lower Flurometer	3/5/2015 6:56	5.7
Lower Flurometer	3/5/2015 6:57	5.75
Lower Flurometer	3/5/2015 6:58	5.75
Lower Flurometer	3/5/2015 6:59	5.73
Lower Flurometer	3/5/2015 7:00	5.75
Lower Flurometer	3/5/2015 7:01	5.72
Lower Flurometer	3/5/2015 7:02	5.7
Lower Flurometer	3/5/2015 7:03	5.67
Lower Flurometer	3/5/2015 7:04	5.65
Lower Flurometer	3/5/2015 7:05	5.56
Lower Flurometer	3/5/2015 7:06	5.61
Lower Flurometer	3/5/2015 7:07	5.61
Lower Flurometer	3/5/2015 7:08	5.57
Lower Flurometer	3/5/2015 7:09	5.6
Lower Flurometer	3/5/2015 7:10	5.56
Lower Flurometer	3/5/2015 7:11	5.6
Lower Flurometer	3/5/2015 7:12	5.52
Lower Flurometer	3/5/2015 7:13	5.52
Lower Flurometer	3/5/2015 7:14	5.5
Lower Flurometer	3/5/2015 7:15	5.52
Lower Flurometer	3/5/2015 7:16	5.45
Lower Flurometer	3/5/2015 7:17	5.49
Lower Flurometer	3/5/2015 7:18	5.38
Lower Flurometer	3/5/2015 7:19	5.49
Lower Flurometer	3/5/2015 7:20	5.36
Lower Flurometer	3/5/2015 7:21	5.43
Lower Flurometer	3/5/2015 7:22	5.38
Lower Flurometer	3/5/2015 7:23	5.33
Lower Flurometer	3/5/2015 7:24	5.37
Lower Flurometer	3/5/2015 7:25	5.37
Lower Flurometer	3/5/2015 7:26	5.31
Lower Flurometer	3/5/2015 7:27	5.31
Lower Flurometer	3/5/2015 7:28	5.34
Lower Flurometer	3/5/2015 7:29	5.3
Lower Flurometer	3/5/2015 7:30	5.28
Lower Flurometer	3/5/2015 7:31	5.2
Lower Flurometer	3/5/2015 7:32	5.25
Lower Flurometer	3/5/2015 7:33	5.16
Lower Flurometer	3/5/2015 7:34	5.18
Lower Flurometer	3/5/2015 7:35	5.2

Location	Date and Time	Rhodmaine Concentration Adjusted Concentration (ppb)
Lower Flurometer	3/5/2015 7:36	5.12
Lower Flurometer	3/5/2015 7:37	5.13
Lower Flurometer	3/5/2015 7:38	5.12
Lower Flurometer	3/5/2015 7:39	5.14
Lower Flurometer	3/5/2015 7:40	5.13
Lower Flurometer	3/5/2015 7:41	5.12
Lower Flurometer	3/5/2015 7:42	5.09
Lower Flurometer	3/5/2015 7:43	5.03
Lower Flurometer	3/5/2015 7:44	5
Lower Flurometer	3/5/2015 7:45	5
Lower Flurometer	3/5/2015 7:46	5.03
Lower Flurometer	3/5/2015 7:47	4.97
Lower Flurometer	3/5/2015 7:48	4.95
Lower Flurometer	3/5/2015 7:49	4.99
Lower Flurometer	3/5/2015 7:50	5.01
Lower Flurometer	3/5/2015 7:51	4.95
Lower Flurometer	3/5/2015 7:52	4.99
Lower Flurometer	3/5/2015 7:53	4.89
Lower Flurometer	3/5/2015 7:54	4.88
Lower Flurometer	3/5/2015 7:55	4.86
Lower Flurometer	3/5/2015 7:56	4.89
Lower Flurometer	3/5/2015 7:57	4.84
Lower Flurometer	3/5/2015 7:58	4.82
Lower Flurometer	3/5/2015 7:59	4.82
Lower Flurometer	3/5/2015 8:00	4.8
Lower Flurometer	3/5/2015 8:01	4.87
Lower Flurometer	3/5/2015 8:02	4.73
Lower Flurometer	3/5/2015 8:03	4.77
Lower Flurometer	3/5/2015 8:04	4.75
Lower Flurometer	3/5/2015 8:05	4.74
Lower Flurometer	3/5/2015 8:06	4.71
Lower Flurometer	3/5/2015 8:07	4.69
Lower Flurometer	3/5/2015 8:08	4.6
Lower Flurometer	3/5/2015 8:09	4.63
Lower Flurometer	3/5/2015 8:10	4.65
Lower Flurometer	3/5/2015 8:11	4.62
Lower Flurometer	3/5/2015 8:12	4.59
Lower Flurometer	3/5/2015 8:13	4.59
Lower Flurometer	3/5/2015 8:14	4.65
Lower Flurometer	3/5/2015 8:15	4.57
Lower Flurometer	3/5/2015 8:16	4.52
Lower Flurometer	3/5/2015 8:17	4.55
Lower Flurometer	3/5/2015 8:18	4.63
Lower Flurometer	3/5/2015 8:19	4.51
Lower Flurometer	3/5/2015 8:20	4.49
Lower Flurometer	3/5/2015 8:21	4.47

Location	Date and Time	Rhodmaine Concentration Adjusted Concentration (ppb)
Lower Flurometer	3/5/2015 8:22	4.45
Lower Flurometer	3/5/2015 8:23	4.45
Lower Flurometer	3/5/2015 8:24	4.39
Lower Flurometer	3/5/2015 8:25	4.44
Lower Flurometer	3/5/2015 8:26	4.39
Lower Flurometer	3/5/2015 8:27	4.36
Lower Flurometer	3/5/2015 8:28	4.39
Lower Flurometer	3/5/2015 8:29	4.35
Lower Flurometer	3/5/2015 8:30	4.31
Lower Flurometer	3/5/2015 8:31	4.31
Lower Flurometer	3/5/2015 8:32	4.29
Lower Flurometer	3/5/2015 8:33	4.33
Lower Flurometer	3/5/2015 8:34	4.28
Lower Flurometer	3/5/2015 8:35	4.24
Lower Flurometer	3/5/2015 8:36	4.22
Lower Flurometer	3/5/2015 8:37	4.2
Lower Flurometer	3/5/2015 8:38	4.18
Lower Flurometer	3/5/2015 8:39	4.2
Lower Flurometer	3/5/2015 8:40	4.14
Lower Flurometer	3/5/2015 8:41	4.18
Lower Flurometer	3/5/2015 8:42	4.19
Lower Flurometer	3/5/2015 8:43	4.12
Lower Flurometer	3/5/2015 8:44	4.09
Lower Flurometer	3/5/2015 8:45	4.08
Lower Flurometer	3/5/2015 8:46	4.07
Lower Flurometer	3/5/2015 8:47	4.1
Lower Flurometer	3/5/2015 8:48	4.07
Lower Flurometer	3/5/2015 8:49	4.06
Lower Flurometer	3/5/2015 8:50	3.99
Lower Flurometer	3/5/2015 8:51	4
Lower Flurometer	3/5/2015 8:52	3.96
Lower Flurometer	3/5/2015 8:53	4.01
Lower Flurometer	3/5/2015 8:54	3.98
Lower Flurometer	3/5/2015 8:55	3.91
Lower Flurometer	3/5/2015 8:56	3.93
Lower Flurometer	3/5/2015 8:57	3.92
Lower Flurometer	3/5/2015 8:58	3.87
Lower Flurometer	3/5/2015 8:59	3.86
Lower Flurometer	3/5/2015 9:00	3.92
Lower Flurometer	3/5/2015 9:01	3.89
Lower Flurometer	3/5/2015 9:02	3.88
Lower Flurometer	3/5/2015 9:03	3.83
Lower Flurometer	3/5/2015 9:04	3.77
Lower Flurometer	3/5/2015 9:05	3.79
Lower Flurometer	3/5/2015 9:06	3.77
Lower Flurometer	3/5/2015 9:07	3.74

Location	Date and Time	Rhodmaine Concentration Adjusted Concentration (ppb)
Lower Flurometer	3/5/2015 9:08	3.77
Lower Flurometer	3/5/2015 9:09	3.76
Lower Flurometer	3/5/2015 9:10	3.75
Lower Flurometer	3/5/2015 9:11	3.7
Lower Flurometer	3/5/2015 9:12	3.75
Lower Flurometer	3/5/2015 9:13	3.78
Lower Flurometer	3/5/2015 9:14	3.64
Lower Flurometer	3/5/2015 9:15	3.65
Lower Flurometer	3/5/2015 9:16	3.58
Lower Flurometer	3/5/2015 9:17	3.64
Lower Flurometer	3/5/2015 9:18	3.64
Lower Flurometer	3/5/2015 9:19	3.56
Lower Flurometer	3/5/2015 9:20	3.6
Lower Flurometer	3/5/2015 9:21	3.54
Lower Flurometer	3/5/2015 9:22	3.52
Lower Flurometer	3/5/2015 9:23	3.56
Lower Flurometer	3/5/2015 9:24	3.54
Lower Flurometer	3/5/2015 9:25	3.56
Lower Flurometer	3/5/2015 9:26	3.55
Lower Flurometer	3/5/2015 9:27	3.49
Lower Flurometer	3/5/2015 9:28	3.5
Lower Flurometer	3/5/2015 9:29	3.43
Lower Flurometer	3/5/2015 9:30	3.44
Lower Flurometer	3/5/2015 9:31	3.46
Lower Flurometer	3/5/2015 9:32	3.44
Lower Flurometer	3/5/2015 9:33	3.45
Lower Flurometer	3/5/2015 9:34	3.43
Lower Flurometer	3/5/2015 9:35	3.38
Lower Flurometer	3/5/2015 9:36	3.38
Lower Flurometer	3/5/2015 9:37	3.39
Lower Flurometer	3/5/2015 9:38	3.36
Lower Flurometer	3/5/2015 9:39	3.33
Lower Flurometer	3/5/2015 9:40	3.35
Lower Flurometer	3/5/2015 9:41	3.34
Lower Flurometer	3/5/2015 9:42	3.32
Lower Flurometer	3/5/2015 9:43	3.29
Lower Flurometer	3/5/2015 9:44	3.3
Lower Flurometer	3/5/2015 9:45	3.3
Lower Flurometer	3/5/2015 9:46	3.27
Lower Flurometer	3/5/2015 9:47	3.26
Lower Flurometer	3/5/2015 9:48	3.25
Lower Flurometer	3/5/2015 9:49	3.25
Lower Flurometer	3/5/2015 9:50	3.22
Lower Flurometer	3/5/2015 9:51	3.2
Lower Flurometer	3/5/2015 9:52	3.21
Lower Flurometer	3/5/2015 9:53	3.16

Location	Date and Time	Rhodmaine Concentration Adjusted Concentration (ppb)
Lower Flurometer	3/5/2015 9:54	3.15
Lower Flurometer	3/5/2015 9:55	3.18
Lower Flurometer	3/5/2015 9:56	3.14
Lower Flurometer	3/5/2015 9:57	3.19
Lower Flurometer	3/5/2015 9:58	4.4
Lower Flurometer	3/5/2015 9:59	3.17
Lower Flurometer	3/5/2015 10:00	3.11
Lower Flurometer	3/5/2015 10:01	3.06
Lower Flurometer	3/5/2015 10:02	3.08
Lower Flurometer	3/5/2015 10:03	3.02
Lower Flurometer	3/5/2015 10:04	3.07
Lower Flurometer	3/5/2015 10:05	3.02
Lower Flurometer	3/5/2015 10:06	3.06
Lower Flurometer	3/5/2015 10:07	3
Lower Flurometer	3/5/2015 10:08	3.06
Lower Flurometer	3/5/2015 10:09	3.01
Lower Flurometer	3/5/2015 10:10	3
Lower Flurometer	3/5/2015 10:11	2.98
Lower Flurometer	3/5/2015 10:12	2.97
Lower Flurometer	3/5/2015 10:13	2.99
Lower Flurometer	3/5/2015 10:14	2.9
Lower Flurometer	3/5/2015 10:15	2.91
Lower Flurometer	3/5/2015 10:16	2.96
Lower Flurometer	3/5/2015 10:17	2.89
Lower Flurometer	3/5/2015 10:18	2.85
Lower Flurometer	3/5/2015 10:19	2.9
Lower Flurometer	3/5/2015 10:20	2.94
Lower Flurometer	3/5/2015 10:21	2.82
Lower Flurometer	3/5/2015 10:22	2.89
Lower Flurometer	3/5/2015 10:23	2.84
Lower Flurometer	3/5/2015 10:24	2.83
Lower Flurometer	3/5/2015 10:25	2.81
Lower Flurometer	3/5/2015 10:26	2.83
Lower Flurometer	3/5/2015 10:27	2.79
Lower Flurometer	3/5/2015 10:28	2.81
Lower Flurometer	3/5/2015 10:29	2.79
Lower Flurometer	3/5/2015 10:30	2.79
Lower Flurometer	3/5/2015 10:31	2.76
Lower Flurometer	3/5/2015 10:32	2.77
Lower Flurometer	3/5/2015 10:33	2.74
Lower Flurometer	3/5/2015 10:34	2.75
Lower Flurometer	3/5/2015 10:35	2.78
Lower Flurometer	3/5/2015 10:36	2.72
Lower Flurometer	3/5/2015 10:37	2.73
Lower Flurometer	3/5/2015 10:38	2.77
Lower Flurometer	3/5/2015 10:39	2.66

Location	Date and Time	Rhodmaine Concentration Adjusted Concentration (ppb)
Lower Flurometer	3/5/2015 10:40	2.79
Lower Flurometer	3/5/2015 10:41	2.75
Lower Flurometer	3/5/2015 10:42	2.69
Lower Flurometer	3/5/2015 10:43	2.69
Lower Flurometer	3/5/2015 10:44	2.67
Lower Flurometer	3/5/2015 10:45	2.66
Lower Flurometer	3/5/2015 10:46	2.69
Lower Flurometer	3/5/2015 10:47	2.66
Lower Flurometer	3/5/2015 10:48	2.65
Lower Flurometer	3/5/2015 10:49	2.61
Lower Flurometer	3/5/2015 10:50	2.65
Lower Flurometer	3/5/2015 10:51	2.62
Lower Flurometer	3/5/2015 10:52	2.6
Lower Flurometer	3/5/2015 10:53	2.56
Lower Flurometer	3/5/2015 10:54	2.58
Lower Flurometer	3/5/2015 10:55	2.57
Lower Flurometer	3/5/2015 10:56	2.51
Lower Flurometer	3/5/2015 10:57	2.5
Lower Flurometer	3/5/2015 10:58	2.52
Lower Flurometer	3/5/2015 10:59	2.5
Lower Flurometer	3/5/2015 11:00	2.52
Lower Flurometer	3/5/2015 11:01	2.47
Lower Flurometer	3/5/2015 11:02	2.52
Lower Flurometer	3/5/2015 11:03	2.63
Lower Flurometer	3/5/2015 11:04	2.5
Lower Flurometer	3/5/2015 11:05	2.47
Lower Flurometer	3/5/2015 11:06	2.46
Lower Flurometer	3/5/2015 11:07	2.48
Lower Flurometer	3/5/2015 11:08	2.48
Lower Flurometer	3/5/2015 11:09	2.46
Lower Flurometer	3/5/2015 11:10	2.45
Lower Flurometer	3/5/2015 11:11	2.42
Lower Flurometer	3/5/2015 11:12	2.46
Lower Flurometer	3/5/2015 11:13	2.43
Lower Flurometer	3/5/2015 11:14	2.39
Lower Flurometer	3/5/2015 11:15	2.37
Lower Flurometer	3/5/2015 11:16	2.39
Lower Flurometer	3/5/2015 11:17	2.36
Lower Flurometer	3/5/2015 11:18	2.33
Lower Flurometer	3/5/2015 11:19	2.38
Lower Flurometer	3/5/2015 11:20	2.38
Lower Flurometer	3/5/2015 11:21	2.37
Lower Flurometer	3/5/2015 11:22	2.38
Lower Flurometer	3/5/2015 11:23	2.34
Lower Flurometer	3/5/2015 11:24	2.33
Lower Flurometer	3/5/2015 11:25	2.36

Location	Date and Time	Rhodmaine Concentration Adjusted Concentration (ppb)
Lower Flurometer	3/5/2015 11:26	2.36
Lower Flurometer	3/5/2015 11:27	2.29
Lower Flurometer	3/5/2015 11:28	2.35
Lower Flurometer	3/5/2015 11:29	2.28
Lower Flurometer	3/5/2015 11:30	2.3
Lower Flurometer	3/5/2015 11:31	2.24
Lower Flurometer	3/5/2015 11:32	2.34
Lower Flurometer	3/5/2015 11:33	2.29
Lower Flurometer	3/5/2015 11:34	2.24
Lower Flurometer	3/5/2015 11:35	2.22
Lower Flurometer	3/5/2015 11:36	2.23
Lower Flurometer	3/5/2015 11:37	2.34
Lower Flurometer	3/5/2015 11:38	2.2
Lower Flurometer	3/5/2015 11:39	2.3
Lower Flurometer	3/5/2015 11:40	2.2
Lower Flurometer	3/5/2015 11:41	2.19
Lower Flurometer	3/5/2015 11:42	2.21
Lower Flurometer	3/5/2015 11:43	2.18
Lower Flurometer	3/5/2015 11:44	2.17
Lower Flurometer	3/5/2015 11:45	2.22
Lower Flurometer	3/5/2015 11:46	2.17
Lower Flurometer	3/5/2015 11:47	2.14
Lower Flurometer	3/5/2015 11:48	2.12
Lower Flurometer	3/5/2015 11:49	2.2
Lower Flurometer	3/5/2015 11:50	2.12
Lower Flurometer	3/5/2015 11:51	2.17
Lower Flurometer	3/5/2015 11:52	2.21
Lower Flurometer	3/5/2015 11:53	2.12
Lower Flurometer	3/5/2015 11:54	2.12
Lower Flurometer	3/5/2015 11:55	2.16
Lower Flurometer	3/5/2015 11:56	2.09
Lower Flurometer	3/5/2015 11:57	2.13
Lower Flurometer	3/5/2015 11:58	2.12
Lower Flurometer	3/5/2015 11:59	2.09
Lower Flurometer	3/5/2015 12:00	2.09
Lower Flurometer	3/5/2015 12:01	2.09
Lower Flurometer	3/5/2015 12:02	2.11
Lower Flurometer	3/5/2015 12:03	2.09
Lower Flurometer	3/5/2015 12:04	2.07
Lower Flurometer	3/5/2015 12:05	2.08
Lower Flurometer	3/5/2015 12:06	2.08
Lower Flurometer	3/5/2015 12:07	2.06
Lower Flurometer	3/5/2015 12:08	2.03
Lower Flurometer	3/5/2015 12:09	2.05
Lower Flurometer	3/5/2015 12:10	2.05
Lower Flurometer	3/5/2015 12:11	2.05

Location	Date and Time	Rhodmaine Concentration Adjusted Concentration (ppb)
Lower Flurometer	3/5/2015 12:12	2.05
Lower Flurometer	3/5/2015 12:13	2.01
Lower Flurometer	3/5/2015 12:14	1.99
Lower Flurometer	3/5/2015 12:15	2.04
Lower Flurometer	3/5/2015 12:16	2.03
Lower Flurometer	3/5/2015 12:17	1.93
Lower Flurometer	3/5/2015 12:18	2.02
Lower Flurometer	3/5/2015 12:19	1.97
Lower Flurometer	3/5/2015 12:20	2.09
Lower Flurometer	3/5/2015 12:21	1.99
Lower Flurometer	3/5/2015 12:22	1.99
Lower Flurometer	3/5/2015 12:23	1.96
Lower Flurometer	3/5/2015 12:24	1.95
Lower Flurometer	3/5/2015 12:25	1.91
Lower Flurometer	3/5/2015 12:26	1.9
Lower Flurometer	3/5/2015 12:27	1.95
Lower Flurometer	3/5/2015 12:28	1.95
Lower Flurometer	3/5/2015 12:29	1.9
Lower Flurometer	3/5/2015 12:30	1.88
Lower Flurometer	3/5/2015 12:31	1.88
Lower Flurometer	3/5/2015 12:32	1.86
Lower Flurometer	3/5/2015 12:33	1.89
Lower Flurometer	3/5/2015 12:34	1.88
Lower Flurometer	3/5/2015 12:35	1.89
Lower Flurometer	3/5/2015 12:36	1.9
Lower Flurometer	3/5/2015 12:37	1.88
Lower Flurometer	3/5/2015 12:38	1.88
Lower Flurometer	3/5/2015 12:39	1.89
Lower Flurometer	3/5/2015 12:40	1.85
Lower Flurometer	3/5/2015 12:41	1.88
Lower Flurometer	3/5/2015 12:42	1.85
Lower Flurometer	3/5/2015 12:43	1.81
Lower Flurometer	3/5/2015 12:44	1.83
Lower Flurometer	3/5/2015 12:45	1.79
Lower Flurometer	3/5/2015 12:46	1.8
Lower Flurometer	3/5/2015 12:47	1.82
Lower Flurometer	3/5/2015 12:48	1.87
Lower Flurometer	3/5/2015 12:49	1.82
Lower Flurometer	3/5/2015 12:50	1.77
Lower Flurometer	3/5/2015 12:51	1.78
Lower Flurometer	3/5/2015 12:52	1.81
Lower Flurometer	3/5/2015 12:53	1.77
Lower Flurometer	3/5/2015 12:54	1.79
Lower Flurometer	3/5/2015 12:55	1.79
Lower Flurometer	3/5/2015 12:56	1.78
Lower Flurometer	3/5/2015 12:57	1.78

Location	Date and Time	Rhodmaine Concentration Adjusted Concentration (ppb)
Lower Flurometer	3/5/2015 12:58	1.72
Lower Flurometer	3/5/2015 12:59	1.76
Lower Flurometer	3/5/2015 13:00	1.74
Lower Flurometer	3/5/2015 13:01	1.75
Lower Flurometer	3/5/2015 13:02	1.71
Lower Flurometer	3/5/2015 13:03	1.73
Lower Flurometer	3/5/2015 13:04	1.7
Lower Flurometer	3/5/2015 13:05	1.73
Lower Flurometer	3/5/2015 13:06	1.67
Lower Flurometer	3/5/2015 13:07	1.69
Lower Flurometer	3/5/2015 13:08	1.7
Lower Flurometer	3/5/2015 13:09	1.7
Lower Flurometer	3/5/2015 13:10	1.65
Lower Flurometer	3/5/2015 13:11	1.69
Lower Flurometer	3/5/2015 13:12	1.67
Lower Flurometer	3/5/2015 13:13	1.65
Lower Flurometer	3/5/2015 13:14	1.7
Lower Flurometer	3/5/2015 13:15	1.63
Lower Flurometer	3/5/2015 13:16	1.65
Lower Flurometer	3/5/2015 13:17	1.67
Lower Flurometer	3/5/2015 13:18	1.66
Lower Flurometer	3/5/2015 13:19	1.62
Lower Flurometer	3/5/2015 13:20	1.58
Lower Flurometer	3/5/2015 13:21	1.62
Lower Flurometer	3/5/2015 13:22	1.64
Lower Flurometer	3/5/2015 13:23	1.62
Lower Flurometer	3/5/2015 13:24	1.58
Lower Flurometer	3/5/2015 13:25	1.62
Lower Flurometer	3/5/2015 13:26	1.57
Lower Flurometer	3/5/2015 13:27	1.57
Lower Flurometer	3/5/2015 13:28	1.61
Lower Flurometer	3/5/2015 13:29	1.62
Lower Flurometer	3/5/2015 13:30	1.63
Lower Flurometer	3/5/2015 13:31	1.55
Lower Flurometer	3/5/2015 13:32	1.54
Lower Flurometer	3/5/2015 13:33	1.62
Lower Flurometer	3/5/2015 13:34	1.57
Lower Flurometer	3/5/2015 13:35	1.6
Lower Flurometer	3/5/2015 13:36	1.5
Lower Flurometer	3/5/2015 13:37	1.51
Lower Flurometer	3/5/2015 13:38	1.54
Lower Flurometer	3/5/2015 13:39	1.49
Lower Flurometer	3/5/2015 13:40	1.48
Lower Flurometer	3/5/2015 13:41	1.54
Lower Flurometer	3/5/2015 13:42	1.51
Lower Flurometer	3/5/2015 13:43	1.51

Location	Date and Time	Rhodmaine Concentration Adjusted Concentration (ppb)
Lower Flurometer	3/5/2015 13:44	1.48
Lower Flurometer	3/5/2015 13:45	1.52
Lower Flurometer	3/5/2015 13:46	1.49
Lower Flurometer	3/5/2015 13:47	1.5
Lower Flurometer	3/5/2015 13:48	1.51
Lower Flurometer	3/5/2015 13:49	1.47
Lower Flurometer	3/5/2015 13:50	1.51
Lower Flurometer	3/5/2015 13:51	1.51
Lower Flurometer	3/5/2015 13:52	1.47
Lower Flurometer	3/5/2015 13:53	1.47
Lower Flurometer	3/5/2015 13:54	1.52
Lower Flurometer	3/5/2015 13:55	1.43
Lower Flurometer	3/5/2015 13:56	1.47
Lower Flurometer	3/5/2015 13:57	1.52
Lower Flurometer	3/5/2015 13:58	1.39
Lower Flurometer	3/5/2015 13:59	1.45
Lower Flurometer	3/5/2015 14:00	1.46
Lower Flurometer	3/5/2015 14:01	1.43
Lower Flurometer	3/5/2015 14:02	1.39
Lower Flurometer	3/5/2015 14:03	1.43
Lower Flurometer	3/5/2015 14:04	1.4
Lower Flurometer	3/5/2015 14:05	1.38
Lower Flurometer	3/5/2015 14:06	1.39
Lower Flurometer	3/5/2015 14:07	1.33
Lower Flurometer	3/5/2015 14:08	1.33
Lower Flurometer	3/5/2015 14:09	1.35
Lower Flurometer	3/5/2015 14:10	1.36
Lower Flurometer	3/5/2015 14:11	1.36
Lower Flurometer	3/5/2015 14:12	1.32
Lower Flurometer	3/5/2015 14:13	1.35
Lower Flurometer	3/5/2015 14:14	1.32
Lower Flurometer	3/5/2015 14:15	1.33
Lower Flurometer	3/5/2015 14:16	1.38
Lower Flurometer	3/5/2015 14:17	1.33
Lower Flurometer	3/5/2015 14:18	1.35
Lower Flurometer	3/5/2015 14:19	1.32
Lower Flurometer	3/5/2015 14:20	1.39
Lower Flurometer	3/5/2015 14:21	1.31
Lower Flurometer	3/5/2015 14:22	1.36
Lower Flurometer	3/5/2015 14:23	1.31
Lower Flurometer	3/5/2015 14:24	1.32
Lower Flurometer	3/5/2015 14:25	1.28
Lower Flurometer	3/5/2015 14:26	1.3
Lower Flurometer	3/5/2015 14:27	1.27
Lower Flurometer	3/5/2015 14:28	1.27
Lower Flurometer	3/5/2015 14:29	1.27

Location	Date and Time	Rhodmaine Concentration Adjusted Concentration (ppb)
Lower Flurometer	3/5/2015 14:30	1.26
Lower Flurometer	3/5/2015 14:31	1.23
Lower Flurometer	3/5/2015 14:32	1.29
Lower Flurometer	3/5/2015 14:33	1.28
Lower Flurometer	3/5/2015 14:34	1.24
Lower Flurometer	3/5/2015 14:35	1.26
Lower Flurometer	3/5/2015 14:36	1.23
Lower Flurometer	3/5/2015 14:37	1.26
Lower Flurometer	3/5/2015 14:38	1.29
Lower Flurometer	3/5/2015 14:39	1.24
Lower Flurometer	3/5/2015 14:40	1.23
Lower Flurometer	3/5/2015 14:41	1.24
Lower Flurometer	3/5/2015 14:42	1.22
Lower Flurometer	3/5/2015 14:43	1.23
Lower Flurometer	3/5/2015 14:44	1.24
Lower Flurometer	3/5/2015 14:45	1.23
Lower Flurometer	3/5/2015 14:46	1.25
Lower Flurometer	3/5/2015 14:47	1.23
Lower Flurometer	3/5/2015 14:48	1.19
Lower Flurometer	3/5/2015 14:49	1.18
Lower Flurometer	3/5/2015 14:50	1.22
Lower Flurometer	3/5/2015 14:51	1.2
Lower Flurometer	3/5/2015 14:52	1.19
Lower Flurometer	3/5/2015 14:53	1.16
Lower Flurometer	3/5/2015 14:54	1.19
Lower Flurometer	3/5/2015 14:55	1.18
Lower Flurometer	3/5/2015 14:56	1.16
Lower Flurometer	3/5/2015 14:57	1.13
Lower Flurometer	3/5/2015 14:58	1.14
Lower Flurometer	3/5/2015 14:59	1.09
Lower Flurometer	3/5/2015 15:00	1.15
Lower Flurometer	3/5/2015 15:01	1.18
Lower Flurometer	3/5/2015 15:02	1.11
Lower Flurometer	3/5/2015 15:03	1.14
Lower Flurometer	3/5/2015 15:04	1.09
Lower Flurometer	3/5/2015 15:05	1.12
Lower Flurometer	3/5/2015 15:06	1.07
Lower Flurometer	3/5/2015 15:07	1.11
Lower Flurometer	3/5/2015 15:08	1.12
Lower Flurometer	3/5/2015 15:09	1.15
Lower Flurometer	3/5/2015 15:10	1.12
Lower Flurometer	3/5/2015 15:11	1.12
Lower Flurometer	3/5/2015 15:12	1.11
Lower Flurometer	3/5/2015 15:13	1.12
Lower Flurometer	3/5/2015 15:14	1.12
Lower Flurometer	3/5/2015 15:15	1.1

Location	Date and Time	Rhodmaine Concentration Adjusted Concentration (ppb)
Lower Flurometer	3/5/2015 15:16	1.07
Lower Flurometer	3/5/2015 15:17	1.11
Lower Flurometer	3/5/2015 15:18	1.02
Lower Flurometer	3/5/2015 15:19	1.05
Lower Flurometer	3/5/2015 15:20	1.06
Lower Flurometer	3/5/2015 15:21	1.06
Lower Flurometer	3/5/2015 15:22	1.06
Lower Flurometer	3/5/2015 15:23	1.02
Lower Flurometer	3/5/2015 15:24	1.01
Lower Flurometer	3/5/2015 15:25	1.04
Lower Flurometer	3/5/2015 15:26	1.05
Lower Flurometer	3/5/2015 15:27	1.02
Lower Flurometer	3/5/2015 15:28	1.01
Lower Flurometer	3/5/2015 15:29	1.03
Lower Flurometer	3/5/2015 15:30	1.03
Lower Flurometer	3/5/2015 15:31	1.02
Lower Flurometer	3/5/2015 15:32	1.01
Lower Flurometer	3/5/2015 15:33	1.03
Lower Flurometer	3/5/2015 15:34	1
Lower Flurometer	3/5/2015 15:35	0.98
Lower Flurometer	3/5/2015 15:36	1
Lower Flurometer	3/5/2015 15:37	0.99
Lower Flurometer	3/5/2015 15:38	1.02
Lower Flurometer	3/5/2015 15:39	1
Lower Flurometer	3/5/2015 15:40	0.99
Lower Flurometer	3/5/2015 15:41	0.97
Lower Flurometer	3/5/2015 15:42	0.99
Lower Flurometer	3/5/2015 15:43	0.93
Lower Flurometer	3/5/2015 15:44	0.98
Lower Flurometer	3/5/2015 15:45	0.98
Lower Flurometer	3/5/2015 15:46	0.97
Lower Flurometer	3/5/2015 15:47	0.97
Lower Flurometer	3/5/2015 15:48	0.92
Lower Flurometer	3/5/2015 15:49	0.97
Lower Flurometer	3/5/2015 15:50	0.95
Lower Flurometer	3/5/2015 15:51	1.05
Lower Flurometer	3/5/2015 15:52	0.94
Lower Flurometer	3/5/2015 15:53	0.94
Lower Flurometer	3/5/2015 15:54	0.94
Lower Flurometer	3/5/2015 15:55	0.98
Lower Flurometer	3/5/2015 15:56	0.89
Lower Flurometer	3/5/2015 15:57	0.95
Lower Flurometer	3/5/2015 15:58	0.91
Lower Flurometer	3/5/2015 15:59	0.93
Lower Flurometer	3/5/2015 16:00	0.88
Lower Flurometer	3/5/2015 16:01	0.97

Location	Date and Time	Rhodmaine Concentration Adjusted Concentration (ppb)
Lower Flurometer	3/5/2015 16:02	0.87
Lower Flurometer	3/5/2015 16:03	0.98
Lower Flurometer	3/5/2015 16:04	0.89
Lower Flurometer	3/5/2015 16:05	0.91
Lower Flurometer	3/5/2015 16:06	0.92
Lower Flurometer	3/5/2015 16:07	0.89
Lower Flurometer	3/5/2015 16:08	0.88
Lower Flurometer	3/5/2015 16:09	0.88
Lower Flurometer	3/5/2015 16:10	0.87
Lower Flurometer	3/5/2015 16:11	0.87
Lower Flurometer	3/5/2015 16:12	0.9
Lower Flurometer	3/5/2015 16:13	0.84
Lower Flurometer	3/5/2015 16:14	0.86
Lower Flurometer	3/5/2015 16:15	0.88
Lower Flurometer	3/5/2015 16:16	0.9
Lower Flurometer	3/5/2015 16:17	0.87
Lower Flurometer	3/5/2015 16:18	0.87
Lower Flurometer	3/5/2015 16:19	0.84
Lower Flurometer	3/5/2015 16:20	0.85
Lower Flurometer	3/5/2015 16:21	0.82
Lower Flurometer	3/5/2015 16:22	0.82
Lower Flurometer	3/5/2015 16:23	0.8
Lower Flurometer	3/5/2015 16:24	0.8
Lower Flurometer	3/5/2015 16:25	0.79
Lower Flurometer	3/5/2015 16:26	0.83
Lower Flurometer	3/5/2015 16:27	0.81
Lower Flurometer	3/5/2015 16:28	0.84
Lower Flurometer	3/5/2015 16:29	0.82
Lower Flurometer	3/5/2015 16:30	0.78
Lower Flurometer	3/5/2015 16:31	0.79
Lower Flurometer	3/5/2015 16:32	0.78
Lower Flurometer	3/5/2015 16:33	0.76
Lower Flurometer	3/5/2015 16:34	0.84
Lower Flurometer	3/5/2015 16:35	0.79
Lower Flurometer	3/5/2015 16:36	0.79
Lower Flurometer	3/5/2015 16:37	0.8
Lower Flurometer	3/5/2015 16:38	0.79
Lower Flurometer	3/5/2015 16:39	0.77
Lower Flurometer	3/5/2015 16:40	0.85
Lower Flurometer	3/5/2015 16:41	0.84
Lower Flurometer	3/5/2015 16:42	0.8
Lower Flurometer	3/5/2015 16:43	0.75
Lower Flurometer	3/5/2015 16:44	0.73
Lower Flurometer	3/5/2015 16:45	0.78
Lower Flurometer	3/5/2015 16:46	0.72
Lower Flurometer	3/5/2015 16:47	2.68

Location	Date and Time	Rhodmaine Concentration Adjusted Concentration (ppb)
Lower Flurometer	3/5/2015 16:48	0.76
Lower Flurometer	3/5/2015 16:49	0.79
Lower Flurometer	3/5/2015 16:50	0.72
Lower Flurometer	3/5/2015 16:51	0.75
Lower Flurometer	3/5/2015 16:52	0.7
Lower Flurometer	3/5/2015 16:53	0.72
Lower Flurometer	3/5/2015 16:54	0.78
Lower Flurometer	3/5/2015 16:55	0.74
Lower Flurometer	3/5/2015 16:56	0.79
Lower Flurometer	3/5/2015 16:57	0.69
Lower Flurometer	3/5/2015 16:58	0.72
Lower Flurometer	3/5/2015 16:59	0.71
Lower Flurometer	3/5/2015 17:00	0.75
Lower Flurometer	3/5/2015 17:01	0.73
Lower Flurometer	3/5/2015 17:02	0.68
Lower Flurometer	3/5/2015 17:03	0.72
Lower Flurometer	3/5/2015 17:04	0.74
Lower Flurometer	3/5/2015 17:05	0.7
Lower Flurometer	3/5/2015 17:06	0.7
Lower Flurometer	3/5/2015 17:07	0.71
Lower Flurometer	3/5/2015 17:08	0.67
Lower Flurometer	3/5/2015 17:09	0.69
Lower Flurometer	3/5/2015 17:10	0.72
Lower Flurometer	3/5/2015 17:11	0.66
Lower Flurometer	3/5/2015 17:12	0.67
Lower Flurometer	3/5/2015 17:13	0.66
Lower Flurometer	3/5/2015 17:14	0.66
Lower Flurometer	3/5/2015 17:15	0.69
Lower Flurometer	3/5/2015 17:16	0.67
Lower Flurometer	3/5/2015 17:17	0.7
Lower Flurometer	3/5/2015 17:18	0.71
Lower Flurometer	3/5/2015 17:19	0.66
Lower Flurometer	3/5/2015 17:20	0.66
Lower Flurometer	3/5/2015 17:21	0.65
Lower Flurometer	3/5/2015 17:22	0.68
Lower Flurometer	3/5/2015 17:23	0.65
Lower Flurometer	3/5/2015 17:24	0.66
Lower Flurometer	3/5/2015 17:25	0.65
Lower Flurometer	3/5/2015 17:26	0.64
Lower Flurometer	3/5/2015 17:27	0.66
Lower Flurometer	3/5/2015 17:28	0.62
Lower Flurometer	3/5/2015 17:29	0.64
Lower Flurometer	3/5/2015 17:30	0.62
Lower Flurometer	3/5/2015 17:31	0.65
Lower Flurometer	3/5/2015 17:32	0.64
Lower Flurometer	3/5/2015 17:33	0.59

Location	Date and Time	Rhodmaine Concentration Adjusted Concentration (ppb)
Lower Flurometer	3/5/2015 17:34	0.62
Lower Flurometer	3/5/2015 17:35	0.63
Lower Flurometer	3/5/2015 17:36	0.63
Lower Flurometer	3/5/2015 17:37	0.59
Lower Flurometer	3/5/2015 17:38	0.59
Lower Flurometer	3/5/2015 17:39	0.64
Lower Flurometer	3/5/2015 17:40	0.58
Lower Flurometer	3/5/2015 17:41	0.61
Lower Flurometer	3/5/2015 17:42	0.64
Lower Flurometer	3/5/2015 17:43	0.58
Lower Flurometer	3/5/2015 17:44	0.57
Lower Flurometer	3/5/2015 17:45	0.64
Lower Flurometer	3/5/2015 17:46	0.61
Lower Flurometer	3/5/2015 17:47	0.62
Lower Flurometer	3/5/2015 17:48	0.59
Lower Flurometer	3/5/2015 17:49	0.6
Lower Flurometer	3/5/2015 17:50	0.59
Lower Flurometer	3/5/2015 17:51	0.58
Lower Flurometer	3/5/2015 17:52	0.57
Lower Flurometer	3/5/2015 17:53	0.56
Lower Flurometer	3/5/2015 17:54	0.57
Lower Flurometer	3/5/2015 17:55	0.58
Lower Flurometer	3/5/2015 17:56	0.56
Lower Flurometer	3/5/2015 17:57	0.53
Lower Flurometer	3/5/2015 17:58	0.54
Lower Flurometer	3/5/2015 17:59	0.58
Lower Flurometer	3/5/2015 18:00	0.56
Lower Flurometer	3/5/2015 18:01	0.56
Lower Flurometer	3/5/2015 18:02	0.54
Lower Flurometer	3/5/2015 18:03	0.57
Lower Flurometer	3/5/2015 18:04	0.54
Lower Flurometer	3/5/2015 18:05	0.57
Lower Flurometer	3/5/2015 18:06	0.57
Lower Flurometer	3/5/2015 18:07	0.56
Lower Flurometer	3/5/2015 18:08	0.54
Lower Flurometer	3/5/2015 18:09	0.57
Lower Flurometer	3/5/2015 18:10	0.53
Lower Flurometer	3/5/2015 18:11	0.52
Lower Flurometer	3/5/2015 18:12	0.54
Lower Flurometer	3/5/2015 18:13	0.51
Lower Flurometer	3/5/2015 18:14	0.51
Lower Flurometer	3/5/2015 18:15	0.5
Lower Flurometer	3/5/2015 18:16	0.55
Lower Flurometer	3/5/2015 18:17	0.56
Lower Flurometer	3/5/2015 18:18	0.53
Lower Flurometer	3/5/2015 18:19	0.54

Location	Date and Time	Rhodmaine Concentration Adjusted Concentration (ppb)
Lower Flurometer	3/5/2015 18:20	0.52
Lower Flurometer	3/5/2015 18:21	0.49
Lower Flurometer	3/5/2015 18:22	0.55
Lower Flurometer	3/5/2015 18:23	0.52
Lower Flurometer	3/5/2015 18:24	0.54
Lower Flurometer	3/5/2015 18:25	0.49
Lower Flurometer	3/5/2015 18:26	0.49
Lower Flurometer	3/5/2015 18:27	0.49
Lower Flurometer	3/5/2015 18:28	0.45
Lower Flurometer	3/5/2015 18:29	0.58
Lower Flurometer	3/5/2015 18:30	0.5
Lower Flurometer	3/5/2015 18:31	0.49
Lower Flurometer	3/5/2015 18:32	0.48
Lower Flurometer	3/5/2015 18:33	0.52
Lower Flurometer	3/5/2015 18:34	0.51
Lower Flurometer	3/5/2015 18:35	0.53
Lower Flurometer	3/5/2015 18:36	0.47
Lower Flurometer	3/5/2015 18:37	0.5
Lower Flurometer	3/5/2015 18:38	0.5
Lower Flurometer	3/5/2015 18:39	0.5
Lower Flurometer	3/5/2015 18:40	0.46
Lower Flurometer	3/5/2015 18:41	0.45
Lower Flurometer	3/5/2015 18:42	0.48
Lower Flurometer	3/5/2015 18:43	0.55
Lower Flurometer	3/5/2015 18:44	0.44
Lower Flurometer	3/5/2015 18:45	0.44
Lower Flurometer	3/5/2015 18:46	0.48
Lower Flurometer	3/5/2015 18:47	0.44
Lower Flurometer	3/5/2015 18:48	0.45
Lower Flurometer	3/5/2015 18:49	0.46
Lower Flurometer	3/5/2015 18:50	0.43
Lower Flurometer	3/5/2015 18:51	0.44
Lower Flurometer	3/5/2015 18:52	0.42
Lower Flurometer	3/5/2015 18:53	0.47
Lower Flurometer	3/5/2015 18:54	0.45
Lower Flurometer	3/5/2015 18:55	0.44
Lower Flurometer	3/5/2015 18:56	0.43
Lower Flurometer	3/5/2015 18:57	0.43
Lower Flurometer	3/5/2015 18:58	0.44
Lower Flurometer	3/5/2015 18:59	0.42
Lower Flurometer	3/5/2015 19:00	0.44
Lower Flurometer	3/5/2015 19:01	0.45
Lower Flurometer	3/5/2015 19:02	0.45
Lower Flurometer	3/5/2015 19:03	0.45
Lower Flurometer	3/5/2015 19:04	0.4
Lower Flurometer	3/5/2015 19:05	0.44

Location	Date and Time	Rhodmaine Concentration Adjusted Concentration (ppb)
Lower Flurometer	3/5/2015 19:06	0.44
Lower Flurometer	3/5/2015 19:07	0.46
Lower Flurometer	3/5/2015 19:08	0.4
Lower Flurometer	3/5/2015 19:09	0.46
Lower Flurometer	3/5/2015 19:10	0.44
Lower Flurometer	3/5/2015 19:11	0.43
Lower Flurometer	3/5/2015 19:12	0.39
Lower Flurometer	3/5/2015 19:13	0.44
Lower Flurometer	3/5/2015 19:14	0.4
Lower Flurometer	3/5/2015 19:15	0.45
Lower Flurometer	3/5/2015 19:16	0.39
Lower Flurometer	3/5/2015 19:17	0.41
Lower Flurometer	3/5/2015 19:18	0.39
Lower Flurometer	3/5/2015 19:19	0.38
Lower Flurometer	3/5/2015 19:20	0.4
Lower Flurometer	3/5/2015 19:21	0.37
Lower Flurometer	3/5/2015 19:22	0.42
Lower Flurometer	3/5/2015 19:23	0.39
Lower Flurometer	3/5/2015 19:24	0.44
Lower Flurometer	3/5/2015 19:25	0.38
Lower Flurometer	3/5/2015 19:26	0.49
Lower Flurometer	3/5/2015 19:27	0.42
Lower Flurometer	3/5/2015 19:28	0.38
Lower Flurometer	3/5/2015 19:29	0.41
Lower Flurometer	3/5/2015 19:30	0.37
Lower Flurometer	3/5/2015 19:31	0.37
Lower Flurometer	3/5/2015 19:32	0.42
Lower Flurometer	3/5/2015 19:33	0.37
Lower Flurometer	3/5/2015 19:34	0.36
Lower Flurometer	3/5/2015 19:35	0.36
Lower Flurometer	3/5/2015 19:36	0.4
Lower Flurometer	3/5/2015 19:37	0.36
Lower Flurometer	3/5/2015 19:38	0.36
Lower Flurometer	3/5/2015 19:39	0.4
Lower Flurometer	3/5/2015 19:40	0.37
Lower Flurometer	3/5/2015 19:41	0.36
Lower Flurometer	3/5/2015 19:42	0.38
Lower Flurometer	3/5/2015 19:43	0.36
Lower Flurometer	3/5/2015 19:44	0.37
Lower Flurometer	3/5/2015 19:45	0.39
Lower Flurometer	3/5/2015 19:46	0.37
Lower Flurometer	3/5/2015 19:47	0.38
Lower Flurometer	3/5/2015 19:48	0.37
Lower Flurometer	3/5/2015 19:49	0.41
Lower Flurometer	3/5/2015 19:50	0.39
Lower Flurometer	3/5/2015 19:51	0.38

Location	Date and Time	Rhodmaine Concentration Adjusted Concentration (ppb)
Lower Flurometer	3/5/2015 19:52	0.37
Lower Flurometer	3/5/2015 19:53	0.33
Lower Flurometer	3/5/2015 19:54	0.37
Lower Flurometer	3/5/2015 19:55	0.36
Lower Flurometer	3/5/2015 19:56	0.32
Lower Flurometer	3/5/2015 19:57	0.3
Lower Flurometer	3/5/2015 19:58	0.33
Lower Flurometer	3/5/2015 19:59	0.37
Lower Flurometer	3/5/2015 20:00	0.35
Lower Flurometer	3/5/2015 20:01	0.35
Lower Flurometer	3/5/2015 20:02	0.36
Lower Flurometer	3/5/2015 20:03	0.31
Lower Flurometer	3/5/2015 20:04	0.35
Lower Flurometer	3/5/2015 20:05	0.35
Lower Flurometer	3/5/2015 20:06	0.33
Lower Flurometer	3/5/2015 20:07	0.33
Lower Flurometer	3/5/2015 20:08	0.35
Lower Flurometer	3/5/2015 20:09	0.29
Lower Flurometer	3/5/2015 20:10	0.36
Lower Flurometer	3/5/2015 20:11	0.3
Lower Flurometer	3/5/2015 20:12	0.33
Lower Flurometer	3/5/2015 20:13	0.31
Lower Flurometer	3/5/2015 20:14	0.31
Lower Flurometer	3/5/2015 20:15	0.3
Lower Flurometer	3/5/2015 20:16	0.33
Lower Flurometer	3/5/2015 20:17	0.31
Lower Flurometer	3/5/2015 20:18	0.29
Lower Flurometer	3/5/2015 20:19	0.32
Lower Flurometer	3/5/2015 20:20	0.32
Lower Flurometer	3/5/2015 20:21	0.29
Lower Flurometer	3/5/2015 20:22	0.29
Lower Flurometer	3/5/2015 20:23	0.28
Lower Flurometer	3/5/2015 20:24	0.3
Lower Flurometer	3/5/2015 20:25	0.3
Lower Flurometer	3/5/2015 20:26	0.3
Lower Flurometer	3/5/2015 20:27	0.28
Lower Flurometer	3/5/2015 20:28	0.32
Lower Flurometer	3/5/2015 20:29	0.28
Lower Flurometer	3/5/2015 20:30	0.27
Lower Flurometer	3/5/2015 20:31	0.27
Lower Flurometer	3/5/2015 20:32	0.29
Lower Flurometer	3/5/2015 20:33	0.27
Lower Flurometer	3/5/2015 20:34	0.29
Lower Flurometer	3/5/2015 20:35	0.27
Lower Flurometer	3/5/2015 20:36	0.26
Lower Flurometer	3/5/2015 20:37	0.31

Location	Date and Time	Rhodmaine Concentration Adjusted Concentration (ppb)
Lower Flurometer	3/5/2015 20:38	0.33
Lower Flurometer	3/5/2015 20:39	0.31
Lower Flurometer	3/5/2015 20:40	0.32
Lower Flurometer	3/5/2015 20:41	0.29
Lower Flurometer	3/5/2015 20:42	0.25
Lower Flurometer	3/5/2015 20:43	0.3
Lower Flurometer	3/5/2015 20:44	0.26
Lower Flurometer	3/5/2015 20:45	0.26
Lower Flurometer	3/5/2015 20:46	0.26
Lower Flurometer	3/5/2015 20:47	0.29
Lower Flurometer	3/5/2015 20:48	0.28
Lower Flurometer	3/5/2015 20:49	0.25
Lower Flurometer	3/5/2015 20:50	0.26
Lower Flurometer	3/5/2015 20:51	0.25
Lower Flurometer	3/5/2015 20:52	0.26
Lower Flurometer	3/5/2015 20:53	0.29
Lower Flurometer	3/5/2015 20:54	0.29
Lower Flurometer	3/5/2015 20:55	0.28
Lower Flurometer	3/5/2015 20:56	0.27
Lower Flurometer	3/5/2015 20:57	0.23
Lower Flurometer	3/5/2015 20:58	0.29
Lower Flurometer	3/5/2015 20:59	0.28
Lower Flurometer	3/5/2015 21:00	0.25
Lower Flurometer	3/5/2015 21:01	0.25
Lower Flurometer	3/5/2015 21:02	0.22
Lower Flurometer	3/5/2015 21:03	0.27
Lower Flurometer	3/5/2015 21:04	0.28
Lower Flurometer	3/5/2015 21:05	0.27
Lower Flurometer	3/5/2015 21:06	0.21
Lower Flurometer	3/5/2015 21:07	0.26
Lower Flurometer	3/5/2015 21:08	0.27
Lower Flurometer	3/5/2015 21:09	0.23
Lower Flurometer	3/5/2015 21:10	0.27
Lower Flurometer	3/5/2015 21:11	0.23
Lower Flurometer	3/5/2015 21:12	0.23
Lower Flurometer	3/5/2015 21:13	0.24
Lower Flurometer	3/5/2015 21:14	0.22
Lower Flurometer	3/5/2015 21:15	0.21
Lower Flurometer	3/5/2015 21:16	0.22
Lower Flurometer	3/5/2015 21:17	0.25
Lower Flurometer	3/5/2015 21:18	0.25
Lower Flurometer	3/5/2015 21:19	0.25
Lower Flurometer	3/5/2015 21:20	0.22
Lower Flurometer	3/5/2015 21:21	0.22
Lower Flurometer	3/5/2015 21:22	0.2
Lower Flurometer	3/5/2015 21:23	0.19

Location	Date and Time	Rhodmaine Concentration Adjusted Concentration (ppb)
Lower Flurometer	3/5/2015 21:24	0.25
Lower Flurometer	3/5/2015 21:25	0.24
Lower Flurometer	3/5/2015 21:26	0.19
Lower Flurometer	3/5/2015 21:27	0.24
Lower Flurometer	3/5/2015 21:28	0.19
Lower Flurometer	3/5/2015 21:29	0.2
Lower Flurometer	3/5/2015 21:30	0.38
Lower Flurometer	3/5/2015 21:31	0.2
Lower Flurometer	3/5/2015 21:32	0.25
Lower Flurometer	3/5/2015 21:33	0.22
Lower Flurometer	3/5/2015 21:34	0.27
Lower Flurometer	3/5/2015 21:35	0.22
Lower Flurometer	3/5/2015 21:36	0.24
Lower Flurometer	3/5/2015 21:37	0.24
Lower Flurometer	3/5/2015 21:38	0.24
Lower Flurometer	3/5/2015 21:39	0.24
Lower Flurometer	3/5/2015 21:40	0.24
Lower Flurometer	3/5/2015 21:41	0.21
Lower Flurometer	3/5/2015 21:42	0.21
Lower Flurometer	3/5/2015 21:43	0.2
Lower Flurometer	3/5/2015 21:44	0.2
Lower Flurometer	3/5/2015 21:45	0.19
Lower Flurometer	3/5/2015 21:46	0.21
Lower Flurometer	3/5/2015 21:47	0.2
Lower Flurometer	3/5/2015 21:48	0.22
Lower Flurometer	3/5/2015 21:49	0.23
Lower Flurometer	3/5/2015 21:50	0.21
Lower Flurometer	3/5/2015 21:51	0.19
Lower Flurometer	3/5/2015 21:52	0.22
Lower Flurometer	3/5/2015 21:53	0.17
Lower Flurometer	3/5/2015 21:54	0.17
Lower Flurometer	3/5/2015 21:55	0.2
Lower Flurometer	3/5/2015 21:56	0.17
Lower Flurometer	3/5/2015 21:57	0.17
Lower Flurometer	3/5/2015 21:58	0.17
Lower Flurometer	3/5/2015 21:59	0.22
Lower Flurometer	3/5/2015 22:00	0.17
Lower Flurometer	3/5/2015 22:01	0.19
Lower Flurometer	3/5/2015 22:02	0.16
Lower Flurometer	3/5/2015 22:03	0.18
Lower Flurometer	3/5/2015 22:04	0.22
Lower Flurometer	3/5/2015 22:05	0.22
Lower Flurometer	3/5/2015 22:06	0.16
Lower Flurometer	3/5/2015 22:07	0.21
Lower Flurometer	3/5/2015 22:08	0.19
Lower Flurometer	3/5/2015 22:09	0.19

Location	Date and Time	Rhodmaine Concentration Adjusted Concentration (ppb)
Lower Flurometer	3/5/2015 22:10	0.16
Lower Flurometer	3/5/2015 22:11	0.19
Lower Flurometer	3/5/2015 22:12	0.19
Lower Flurometer	3/5/2015 22:13	0.18
Lower Flurometer	3/5/2015 22:14	0.18
Lower Flurometer	3/5/2015 22:15	0.17
Lower Flurometer	3/5/2015 22:16	0.17
Lower Flurometer	3/5/2015 22:17	0.21
Lower Flurometer	3/5/2015 22:18	0.19
Lower Flurometer	3/5/2015 22:19	0.19
Lower Flurometer	3/5/2015 22:20	0.18
Lower Flurometer	3/5/2015 22:21	0.19
Lower Flurometer	3/5/2015 22:22	0.15
Lower Flurometer	3/5/2015 22:23	0.15
Lower Flurometer	3/5/2015 22:24	0.18
Lower Flurometer	3/5/2015 22:25	0.15
Lower Flurometer	3/5/2015 22:26	0.14
Lower Flurometer	3/5/2015 22:27	0.13
Lower Flurometer	3/5/2015 22:28	0.19
Lower Flurometer	3/5/2015 22:29	0.17
Lower Flurometer	3/5/2015 22:30	0.15
Lower Flurometer	3/5/2015 22:31	0.14
Lower Flurometer	3/5/2015 22:32	0.13
Lower Flurometer	3/5/2015 22:33	0.15
Lower Flurometer	3/5/2015 22:34	0.17
Lower Flurometer	3/5/2015 22:35	0.15
Lower Flurometer	3/5/2015 22:36	0.22
Lower Flurometer	3/5/2015 22:37	0.12
Lower Flurometer	3/5/2015 22:38	0.17
Lower Flurometer	3/5/2015 22:39	0.13
Lower Flurometer	3/5/2015 22:40	0.17
Lower Flurometer	3/5/2015 22:41	0.13
Lower Flurometer	3/5/2015 22:42	0.13
Lower Flurometer	3/5/2015 22:43	0.14
Lower Flurometer	3/5/2015 22:44	0.15
Lower Flurometer	3/5/2015 22:45	0.12
Lower Flurometer	3/5/2015 22:46	0.13
Lower Flurometer	3/5/2015 22:47	0.17
Lower Flurometer	3/5/2015 22:48	0.14
Lower Flurometer	3/5/2015 22:49	0.11
Lower Flurometer	3/5/2015 22:50	0.17
Lower Flurometer	3/5/2015 22:51	0.13
Lower Flurometer	3/5/2015 22:52	0.13
Lower Flurometer	3/5/2015 22:53	0.11
Lower Flurometer	3/5/2015 22:54	0.13
Lower Flurometer	3/5/2015 22:55	0.12

Location	Date and Time	Rhodmaine Concentration Adjusted Concentration (ppb)
Lower Flurometer	3/5/2015 22:56	0.16
Lower Flurometer	3/5/2015 22:57	0.13
Lower Flurometer	3/5/2015 22:58	0.16
Lower Flurometer	3/5/2015 22:59	0.11
Lower Flurometer	3/5/2015 23:00	0.17
Lower Flurometer	3/5/2015 23:01	0.13
Lower Flurometer	3/5/2015 23:02	0.12
Lower Flurometer	3/5/2015 23:03	0.13
Lower Flurometer	3/5/2015 23:04	0.11
Lower Flurometer	3/5/2015 23:05	0.15
Lower Flurometer	3/5/2015 23:06	0.12
Lower Flurometer	3/5/2015 23:07	0.15
Lower Flurometer	3/5/2015 23:08	0.12
Lower Flurometer	3/5/2015 23:09	0.18
Lower Flurometer	3/5/2015 23:10	0.12
Lower Flurometer	3/5/2015 23:11	0.14
Lower Flurometer	3/5/2015 23:12	0.12
Lower Flurometer	3/5/2015 23:13	0.14
Lower Flurometer	3/5/2015 23:14	0.1
Lower Flurometer	3/5/2015 23:15	0.16
Lower Flurometer	3/5/2015 23:16	0.11
Lower Flurometer	3/5/2015 23:17	0.1
Lower Flurometer	3/5/2015 23:18	0.12
Lower Flurometer	3/5/2015 23:19	0.11
Lower Flurometer	3/5/2015 23:20	0.09
Lower Flurometer	3/5/2015 23:21	0.14
Lower Flurometer	3/5/2015 23:22	0.13
Lower Flurometer	3/5/2015 23:23	0.13
Lower Flurometer	3/5/2015 23:24	0.12
Lower Flurometer	3/5/2015 23:25	0.11
Lower Flurometer	3/5/2015 23:26	0.09
Lower Flurometer	3/5/2015 23:27	0.1
Lower Flurometer	3/5/2015 23:28	0.09
Lower Flurometer	3/5/2015 23:29	0.13
Lower Flurometer	3/5/2015 23:30	0.14
Lower Flurometer	3/5/2015 23:31	0.08
Lower Flurometer	3/5/2015 23:32	0.09
Lower Flurometer	3/5/2015 23:33	0.13
Lower Flurometer	3/5/2015 23:34	0.11
Lower Flurometer	3/5/2015 23:35	0.12
Lower Flurometer	3/5/2015 23:36	0.14
Lower Flurometer	3/5/2015 23:37	0.09
Lower Flurometer	3/5/2015 23:38	0.12
Lower Flurometer	3/5/2015 23:39	0.1
Lower Flurometer	3/5/2015 23:40	0.11
Lower Flurometer	3/5/2015 23:41	0.09

Location	Date and Time	Rhodmaine Concentration Adjusted Concentration (ppb)
Lower Flurometer	3/5/2015 23:42	0.11
Lower Flurometer	3/5/2015 23:43	0.09
Lower Flurometer	3/5/2015 23:44	0.09
Lower Flurometer	3/5/2015 23:45	0.13
Lower Flurometer	3/5/2015 23:46	0.1
Lower Flurometer	3/5/2015 23:47	0.12
Lower Flurometer	3/5/2015 23:48	0.12
Lower Flurometer	3/5/2015 23:49	0.12
Lower Flurometer	3/5/2015 23:50	0.1
Lower Flurometer	3/5/2015 23:51	0.12
Lower Flurometer	3/5/2015 23:52	0.09
Lower Flurometer	3/5/2015 23:53	0.07
Lower Flurometer	3/5/2015 23:54	0.09
Lower Flurometer	3/5/2015 23:55	0.07
Lower Flurometer	3/5/2015 23:56	0.08
Lower Flurometer	3/5/2015 23:57	0.12
Lower Flurometer	3/5/2015 23:58	0.07
Lower Flurometer	3/5/2015 23:59	0.11
Lower Flurometer	3/6/2015 0:00	0.1
Lower Flurometer	3/6/2015 0:01	0.12
Lower Flurometer	3/6/2015 0:02	0.08
Lower Flurometer	3/6/2015 0:03	0.1
Lower Flurometer	3/6/2015 0:04	0.09
Lower Flurometer	3/6/2015 0:05	0.09
Lower Flurometer	3/6/2015 0:06	0.1
Lower Flurometer	3/6/2015 0:07	0.07
Lower Flurometer	3/6/2015 0:08	0.09
Lower Flurometer	3/6/2015 0:09	0.11
Lower Flurometer	3/6/2015 0:10	0.08
Lower Flurometer	3/6/2015 0:11	0.07
Lower Flurometer	3/6/2015 0:12	0.08
Lower Flurometer	3/6/2015 0:13	0.1
Lower Flurometer	3/6/2015 0:14	0.11
Lower Flurometer	3/6/2015 0:15	0.06
Lower Flurometer	3/6/2015 0:16	0.15
Lower Flurometer	3/6/2015 0:17	0.06
Lower Flurometer	3/6/2015 0:18	0.12
Lower Flurometer	3/6/2015 0:19	0.06
Lower Flurometer	3/6/2015 0:20	0.06
Lower Flurometer	3/6/2015 0:21	0.07
Lower Flurometer	3/6/2015 0:22	0.08
Lower Flurometer	3/6/2015 0:23	0.1
Lower Flurometer	3/6/2015 0:24	0.1
Lower Flurometer	3/6/2015 0:25	0.09
Lower Flurometer	3/6/2015 0:26	0.07
Lower Flurometer	3/6/2015 0:27	0.08

Location	Date and Time	Rhodmaine Concentration Adjusted Concentration (ppb)
Lower Flurometer	3/6/2015 0:28	0.05
Lower Flurometer	3/6/2015 0:29	0.07
Lower Flurometer	3/6/2015 0:30	0.1
Lower Flurometer	3/6/2015 0:31	0.09
Lower Flurometer	3/6/2015 0:32	0.06
Lower Flurometer	3/6/2015 0:33	0.09
Lower Flurometer	3/6/2015 0:34	0.04
Lower Flurometer	3/6/2015 0:35	0.05
Lower Flurometer	3/6/2015 0:36	0.04
Lower Flurometer	3/6/2015 0:37	0.08
Lower Flurometer	3/6/2015 0:38	0.07
Lower Flurometer	3/6/2015 0:39	0.06
Lower Flurometer	3/6/2015 0:40	0.08
Lower Flurometer	3/6/2015 0:41	0.04
Lower Flurometer	3/6/2015 0:42	0.09
Lower Flurometer	3/6/2015 0:43	0.09
Lower Flurometer	3/6/2015 0:44	0.08
Lower Flurometer	3/6/2015 0:45	0.04
Lower Flurometer	3/6/2015 0:46	0.05
Lower Flurometer	3/6/2015 0:47	0.04
Lower Flurometer	3/6/2015 0:48	0.06
Lower Flurometer	3/6/2015 0:49	0.09
Lower Flurometer	3/6/2015 0:50	0.07
Lower Flurometer	3/6/2015 0:51	0.04
Lower Flurometer	3/6/2015 0:52	0.11
Lower Flurometer	3/6/2015 0:53	0.04
Lower Flurometer	3/6/2015 0:54	0.05
Lower Flurometer	3/6/2015 0:55	0.05
Lower Flurometer	3/6/2015 0:56	0.03
Lower Flurometer	3/6/2015 0:57	0.09
Lower Flurometer	3/6/2015 0:58	0.05
Lower Flurometer	3/6/2015 0:59	0.06
Lower Flurometer	3/6/2015 1:00	0.03
Lower Flurometer	3/6/2015 1:01	0.07
Lower Flurometer	3/6/2015 1:02	0.07
Lower Flurometer	3/6/2015 1:03	0.06
Lower Flurometer	3/6/2015 1:04	0.07
Lower Flurometer	3/6/2015 1:05	0.04
Lower Flurometer	3/6/2015 1:06	0.07
Lower Flurometer	3/6/2015 1:07	0.03
Lower Flurometer	3/6/2015 1:08	0.05
Lower Flurometer	3/6/2015 1:09	0.09
Lower Flurometer	3/6/2015 1:10	0.04
Lower Flurometer	3/6/2015 1:11	0.07
Lower Flurometer	3/6/2015 1:12	0.08
Lower Flurometer	3/6/2015 1:13	0.03

Location	Date and Time	Rhodmaine Concentration Adjusted Concentration (ppb)
Lower Flurometer	3/6/2015 1:14	0.05
Lower Flurometer	3/6/2015 1:15	0.04
Lower Flurometer	3/6/2015 1:16	0.02
Lower Flurometer	3/6/2015 1:17	0.05
Lower Flurometer	3/6/2015 1:18	0.06
Lower Flurometer	3/6/2015 1:19	0.05
Lower Flurometer	3/6/2015 1:20	0.04
Lower Flurometer	3/6/2015 1:21	0.06
Lower Flurometer	3/6/2015 1:22	0.03
Lower Flurometer	3/6/2015 1:23	0.06
Lower Flurometer	3/6/2015 1:24	0.06
Lower Flurometer	3/6/2015 1:25	0.06
Lower Flurometer	3/6/2015 1:26	0.05
Lower Flurometer	3/6/2015 1:27	0.06
Lower Flurometer	3/6/2015 1:28	0.07
Lower Flurometer	3/6/2015 1:29	0.08
Lower Flurometer	3/6/2015 1:30	0.15
Lower Flurometer	3/6/2015 1:31	0.04
Lower Flurometer	3/6/2015 1:32	0.03
Lower Flurometer	3/6/2015 1:33	0.02
Lower Flurometer	3/6/2015 1:34	0.03
Lower Flurometer	3/6/2015 1:35	0.02
Lower Flurometer	3/6/2015 1:36	0.03
Lower Flurometer	3/6/2015 1:37	0.05
Lower Flurometer	3/6/2015 1:38	0.03
Lower Flurometer	3/6/2015 1:39	0.07
Lower Flurometer	3/6/2015 1:40	0.02
Lower Flurometer	3/6/2015 1:41	0.07
Lower Flurometer	3/6/2015 1:42	0.05
Lower Flurometer	3/6/2015 1:43	0.04
Lower Flurometer	3/6/2015 1:44	0.07
Lower Flurometer	3/6/2015 1:45	0.04
Lower Flurometer	3/6/2015 1:46	0.01
Lower Flurometer	3/6/2015 1:47	0.06
Lower Flurometer	3/6/2015 1:48	0
Lower Flurometer	3/6/2015 1:49	0.01
Lower Flurometer	3/6/2015 1:50	0.06
Lower Flurometer	3/6/2015 1:51	0.05
Lower Flurometer	3/6/2015 1:52	0.04
Lower Flurometer	3/6/2015 1:53	0.04
Lower Flurometer	3/6/2015 1:54	0.04
Lower Flurometer	3/6/2015 1:55	0.04
Lower Flurometer	3/6/2015 1:56	0.03
Lower Flurometer	3/6/2015 1:57	0.03
Lower Flurometer	3/6/2015 1:58	0.03
Lower Flurometer	3/6/2015 1:59	0

Location	Date and Time	Rhodmaine Concentration Adjusted Concentration (ppb)
Lower Flurometer	3/6/2015 2:00	0.02
Lower Flurometer	3/6/2015 2:01	0.04
Lower Flurometer	3/6/2015 2:02	0.03
Lower Flurometer	3/6/2015 2:03	0.03
Lower Flurometer	3/6/2015 2:04	0.05
Lower Flurometer	3/6/2015 2:05	0.02
Lower Flurometer	3/6/2015 2:06	0.03
Lower Flurometer	3/6/2015 2:07	0.01
Lower Flurometer	3/6/2015 2:08	0.05
Lower Flurometer	3/6/2015 2:09	0.04
Lower Flurometer	3/6/2015 2:10	0
Lower Flurometer	3/6/2015 2:11	0.04
Lower Flurometer	3/6/2015 2:12	0
Lower Flurometer	3/6/2015 2:13	0.01
Lower Flurometer	3/6/2015 2:14	0.01
Lower Flurometer	3/6/2015 2:15	0.04
Lower Flurometer	3/6/2015 2:16	0.04
Lower Flurometer	3/6/2015 2:17	0.02
Lower Flurometer	3/6/2015 2:18	0
Lower Flurometer	3/6/2015 2:19	0.04
Lower Flurometer	3/6/2015 2:20	0.09
Lower Flurometer	3/6/2015 2:21	0
Lower Flurometer	3/6/2015 2:22	0.05
Lower Flurometer	3/6/2015 2:23	0.03
Lower Flurometer	3/6/2015 2:24	0.04
Lower Flurometer	3/6/2015 2:25	0
Lower Flurometer	3/6/2015 2:26	0.02
Lower Flurometer	3/6/2015 2:27	0
Lower Flurometer	3/6/2015 2:28	0.01
Lower Flurometer	3/6/2015 2:29	0.01
Lower Flurometer	3/6/2015 2:30	0.01
Lower Flurometer	3/6/2015 2:31	0
Lower Flurometer	3/6/2015 2:32	0.05
Lower Flurometer	3/6/2015 2:33	0.19
Lower Flurometer	3/6/2015 2:34	0.04
Lower Flurometer	3/6/2015 2:35	0.03
Lower Flurometer	3/6/2015 2:36	0.04
Lower Flurometer	3/6/2015 2:37	0.04
Lower Flurometer	3/6/2015 2:38	0.03
Lower Flurometer	3/6/2015 2:39	0.04
Lower Flurometer	3/6/2015 2:40	0.04
Lower Flurometer	3/6/2015 2:41	0
Lower Flurometer	3/6/2015 2:42	0.04
Lower Flurometer	3/6/2015 2:43	0.01
Lower Flurometer	3/6/2015 2:44	0
Lower Flurometer	3/6/2015 2:45	0

Location	Date and Time	Rhodmaine Concentration Adjusted Concentration (ppb)
Lower Flurometer	3/6/2015 2:46	0.03
Lower Flurometer	3/6/2015 2:47	0.05
Lower Flurometer	3/6/2015 2:48	0
Lower Flurometer	3/6/2015 2:49	0
Lower Flurometer	3/6/2015 2:50	0.07
Lower Flurometer	3/6/2015 2:51	0.04
Lower Flurometer	3/6/2015 2:52	0
Lower Flurometer	3/6/2015 2:53	0.03
Lower Flurometer	3/6/2015 2:54	0
Lower Flurometer	3/6/2015 2:55	0.03
Lower Flurometer	3/6/2015 2:56	0
Lower Flurometer	3/6/2015 2:57	0.04
Lower Flurometer	3/6/2015 2:58	0
Lower Flurometer	3/6/2015 2:59	0.01
Lower Flurometer	3/6/2015 3:00	0.02
Lower Flurometer	3/6/2015 3:01	0.05
Lower Flurometer	3/6/2015 3:02	0
Lower Flurometer	3/6/2015 3:03	0.01
Lower Flurometer	3/6/2015 3:04	0
Lower Flurometer	3/6/2015 3:05	0
Lower Flurometer	3/6/2015 3:06	0
Lower Flurometer	3/6/2015 3:07	0.01
Lower Flurometer	3/6/2015 3:08	0.06
Lower Flurometer	3/6/2015 3:09	0.02
Lower Flurometer	3/6/2015 3:10	0.02
Lower Flurometer	3/6/2015 3:11	0
Lower Flurometer	3/6/2015 3:12	0.03
Lower Flurometer	3/6/2015 3:13	0.02
Lower Flurometer	3/6/2015 3:14	0.05
Lower Flurometer	3/6/2015 3:15	0.03
Lower Flurometer	3/6/2015 3:16	0
Lower Flurometer	3/6/2015 3:17	0
Lower Flurometer	3/6/2015 3:18	0.01
Lower Flurometer	3/6/2015 3:19	0
Lower Flurometer	3/6/2015 3:20	0
Lower Flurometer	3/6/2015 3:21	0
Lower Flurometer	3/6/2015 3:22	0
Lower Flurometer	3/6/2015 3:23	0.01
Lower Flurometer	3/6/2015 3:24	0.03
Lower Flurometer	3/6/2015 3:25	0
Lower Flurometer	3/6/2015 3:26	0
Lower Flurometer	3/6/2015 3:27	0
Lower Flurometer	3/6/2015 3:28	0.01
Lower Flurometer	3/6/2015 3:29	0
Lower Flurometer	3/6/2015 3:30	0
Lower Flurometer	3/6/2015 3:31	0.02

Location	Date and Time	Rhodmaine Concentration Adjusted Concentration (ppb)
Lower Flurometer	3/6/2015 3:32	0
Lower Flurometer	3/6/2015 3:33	0
Lower Flurometer	3/6/2015 3:34	0.01
Lower Flurometer	3/6/2015 3:35	0.01
Lower Flurometer	3/6/2015 3:36	0
Lower Flurometer	3/6/2015 3:37	0.04
Lower Flurometer	3/6/2015 3:38	0.02
Lower Flurometer	3/6/2015 3:39	0
Lower Flurometer	3/6/2015 3:40	0
Lower Flurometer	3/6/2015 3:41	0
Lower Flurometer	3/6/2015 3:42	0
Lower Flurometer	3/6/2015 3:43	0.02
Lower Flurometer	3/6/2015 3:44	0.01
Lower Flurometer	3/6/2015 3:45	0.36
Lower Flurometer	3/6/2015 3:46	0.03
Lower Flurometer	3/6/2015 3:47	0.01
Lower Flurometer	3/6/2015 3:48	0.01
Lower Flurometer	3/6/2015 3:49	0
Lower Flurometer	3/6/2015 3:50	0
Lower Flurometer	3/6/2015 3:51	0
Lower Flurometer	3/6/2015 3:52	0
Lower Flurometer	3/6/2015 3:53	0.01
Lower Flurometer	3/6/2015 3:54	0
Lower Flurometer	3/6/2015 3:55	0
Lower Flurometer	3/6/2015 3:56	0.03
Lower Flurometer	3/6/2015 3:57	0
Lower Flurometer	3/6/2015 3:58	0
Lower Flurometer	3/6/2015 3:59	0
Lower Flurometer	3/6/2015 4:00	0
Lower Flurometer	3/6/2015 4:01	0
Lower Flurometer	3/6/2015 4:02	0.01
Lower Flurometer	3/6/2015 4:03	0.01
Lower Flurometer	3/6/2015 4:04	0.03
Lower Flurometer	3/6/2015 4:05	0
Lower Flurometer	3/6/2015 4:06	0
Lower Flurometer	3/6/2015 4:07	0
Lower Flurometer	3/6/2015 4:08	0
Lower Flurometer	3/6/2015 4:09	0.02
Lower Flurometer	3/6/2015 4:10	0
Lower Flurometer	3/6/2015 4:11	0.01
Lower Flurometer	3/6/2015 4:12	0
Lower Flurometer	3/6/2015 4:13	0.02
Lower Flurometer	3/6/2015 4:14	0.01
Lower Flurometer	3/6/2015 4:15	0
Lower Flurometer	3/6/2015 4:16	0
Lower Flurometer	3/6/2015 4:17	0.01

Location	Date and Time	Rhodmaine Concentration Adjusted Concentration (ppb)
Lower Flurometer	3/6/2015 4:18	0
Lower Flurometer	3/6/2015 4:19	0
Lower Flurometer	3/6/2015 4:20	0
Lower Flurometer	3/6/2015 4:21	0
Lower Flurometer	3/6/2015 4:22	0
Lower Flurometer	3/6/2015 4:23	0
Lower Flurometer	3/6/2015 4:24	0
Lower Flurometer	3/6/2015 4:25	0
Lower Flurometer	3/6/2015 4:26	0
Lower Flurometer	3/6/2015 4:27	0
Lower Flurometer	3/6/2015 4:28	0.02
Lower Flurometer	3/6/2015 4:29	0
Lower Flurometer	3/6/2015 4:30	0
Lower Flurometer	3/6/2015 4:31	0
Lower Flurometer	3/6/2015 4:32	0
Lower Flurometer	3/6/2015 4:33	0
Lower Flurometer	3/6/2015 4:34	0.01
Lower Flurometer	3/6/2015 4:35	0
Lower Flurometer	3/6/2015 4:36	0
Lower Flurometer	3/6/2015 4:37	0
Lower Flurometer	3/6/2015 4:38	0.02
Lower Flurometer	3/6/2015 4:39	0
Lower Flurometer	3/6/2015 4:40	0
Lower Flurometer	3/6/2015 4:41	0
Lower Flurometer	3/6/2015 4:42	0
Lower Flurometer	3/6/2015 4:43	0.01
Lower Flurometer	3/6/2015 4:44	0
Lower Flurometer	3/6/2015 4:45	0
Lower Flurometer	3/6/2015 4:46	0
Lower Flurometer	3/6/2015 4:47	0
Lower Flurometer	3/6/2015 4:48	0
Lower Flurometer	3/6/2015 4:49	0
Lower Flurometer	3/6/2015 4:50	0
Lower Flurometer	3/6/2015 4:51	0
Lower Flurometer	3/6/2015 4:52	0
Lower Flurometer	3/6/2015 4:53	0
Lower Flurometer	3/6/2015 4:54	0
Lower Flurometer	3/6/2015 4:55	0
Lower Flurometer	3/6/2015 4:56	0
Lower Flurometer	3/6/2015 4:57	0
Lower Flurometer	3/6/2015 4:58	0
Lower Flurometer	3/6/2015 4:59	0
Lower Flurometer	3/6/2015 5:00	0
Lower Flurometer	3/6/2015 5:01	0
Lower Flurometer	3/6/2015 5:02	0
Lower Flurometer	3/6/2015 5:03	0

Location	Date and Time	Rhodmaine Concentration Adjusted Concentration (ppb)
Lower Flurometer	3/6/2015 5:04	0
Lower Flurometer	3/6/2015 5:05	0
Lower Flurometer	3/6/2015 5:06	0
Lower Flurometer	3/6/2015 5:07	0
Lower Flurometer	3/6/2015 5:08	0
Lower Flurometer	3/6/2015 5:09	0
Lower Flurometer	3/6/2015 5:10	0
Lower Flurometer	3/6/2015 5:11	0
Lower Flurometer	3/6/2015 5:12	0
Lower Flurometer	3/6/2015 5:13	0
Lower Flurometer	3/6/2015 5:14	0
Lower Flurometer	3/6/2015 5:15	0
Lower Flurometer	3/6/2015 5:16	0
Lower Flurometer	3/6/2015 5:17	0
Lower Flurometer	3/6/2015 5:18	0
Lower Flurometer	3/6/2015 5:19	0
Lower Flurometer	3/6/2015 5:20	0
Lower Flurometer	3/6/2015 5:21	0
Lower Flurometer	3/6/2015 5:22	0
Lower Flurometer	3/6/2015 5:23	0
Lower Flurometer	3/6/2015 5:24	0
Lower Flurometer	3/6/2015 5:25	0
Lower Flurometer	3/6/2015 5:26	0
Lower Flurometer	3/6/2015 5:27	0.12
Lower Flurometer	3/6/2015 5:28	0
Lower Flurometer	3/6/2015 5:29	0
Lower Flurometer	3/6/2015 5:30	0
Lower Flurometer	3/6/2015 5:31	0
Lower Flurometer	3/6/2015 5:32	0
Lower Flurometer	3/6/2015 5:33	0
Lower Flurometer	3/6/2015 5:34	0
Lower Flurometer	3/6/2015 5:35	0
Lower Flurometer	3/6/2015 5:36	0
Lower Flurometer	3/6/2015 5:37	0
Lower Flurometer	3/6/2015 5:38	0.01
Lower Flurometer	3/6/2015 5:39	0
Lower Flurometer	3/6/2015 5:40	0
Lower Flurometer	3/6/2015 5:41	0
Lower Flurometer	3/6/2015 5:42	0
Lower Flurometer	3/6/2015 5:43	0
Lower Flurometer	3/6/2015 5:44	0
Lower Flurometer	3/6/2015 5:45	0
Lower Flurometer	3/6/2015 5:46	0
Lower Flurometer	3/6/2015 5:47	0
Lower Flurometer	3/6/2015 5:48	0
Lower Flurometer	3/6/2015 5:49	0

Location	Date and Time	Rhodmaine Concentration Adjusted Concentration (ppb)
Lower Flurometer	3/6/2015 5:50	0
Lower Flurometer	3/6/2015 5:51	0.02
Lower Flurometer	3/6/2015 5:52	0
Lower Flurometer	3/6/2015 5:53	0
Lower Flurometer	3/6/2015 5:54	0
Lower Flurometer	3/6/2015 5:55	0
Lower Flurometer	3/6/2015 5:56	0
Lower Flurometer	3/6/2015 5:57	0
Lower Flurometer	3/6/2015 5:58	0
Lower Flurometer	3/6/2015 5:59	0
Lower Flurometer	3/6/2015 6:00	0
Lower Flurometer	3/6/2015 6:01	0
Lower Flurometer	3/6/2015 6:02	0
Lower Flurometer	3/6/2015 6:03	0
Lower Flurometer	3/6/2015 6:04	0
Lower Flurometer	3/6/2015 6:05	0
Lower Flurometer	3/6/2015 6:06	0
Lower Flurometer	3/6/2015 6:07	0
Lower Flurometer	3/6/2015 6:08	0
Lower Flurometer	3/6/2015 6:09	0
Lower Flurometer	3/6/2015 6:10	0
Lower Flurometer	3/6/2015 6:11	0
Lower Flurometer	3/6/2015 6:12	0
Lower Flurometer	3/6/2015 6:13	0
Lower Flurometer	3/6/2015 6:14	0
Lower Flurometer	3/6/2015 6:15	0
Lower Flurometer	3/6/2015 6:16	0
Lower Flurometer	3/6/2015 6:17	0
Lower Flurometer	3/6/2015 6:18	0
Lower Flurometer	3/6/2015 6:19	0
Lower Flurometer	3/6/2015 6:20	0
Lower Flurometer	3/6/2015 6:21	0
Lower Flurometer	3/6/2015 6:22	0
Lower Flurometer	3/6/2015 6:23	0.01
Lower Flurometer	3/6/2015 6:24	0
Lower Flurometer	3/6/2015 6:25	0
Lower Flurometer	3/6/2015 6:26	0
Lower Flurometer	3/6/2015 6:27	0
Lower Flurometer	3/6/2015 6:28	0
Lower Flurometer	3/6/2015 6:29	0
Lower Flurometer	3/6/2015 6:30	0
Lower Flurometer	3/6/2015 6:31	0
Lower Flurometer	3/6/2015 6:32	0
Lower Flurometer	3/6/2015 6:33	0
Lower Flurometer	3/6/2015 6:34	0
Lower Flurometer	3/6/2015 6:35	0

Location	Date and Time	Rhodmaine Concentration Adjusted Concentration (ppb)
Lower Flurometer	3/6/2015 6:36	0
Lower Flurometer	3/6/2015 6:37	0
Lower Flurometer	3/6/2015 6:38	0
Lower Flurometer	3/6/2015 6:39	0
Lower Flurometer	3/6/2015 6:40	0
Lower Flurometer	3/6/2015 6:41	0
Lower Flurometer	3/6/2015 6:42	0
Lower Flurometer	3/6/2015 6:43	0
Lower Flurometer	3/6/2015 6:44	0
Lower Flurometer	3/6/2015 6:45	0
Lower Flurometer	3/6/2015 6:46	0
Lower Flurometer	3/6/2015 6:47	0
Lower Flurometer	3/6/2015 6:48	0.02
Lower Flurometer	3/6/2015 6:49	0
Lower Flurometer	3/6/2015 6:50	0
Lower Flurometer	3/6/2015 6:51	0
Lower Flurometer	3/6/2015 6:52	0
Lower Flurometer	3/6/2015 6:53	0
Lower Flurometer	3/6/2015 6:54	0
Lower Flurometer	3/6/2015 6:55	0
Lower Flurometer	3/6/2015 6:56	0
Lower Flurometer	3/6/2015 6:57	0
Lower Flurometer	3/6/2015 6:58	0
Lower Flurometer	3/6/2015 6:59	0
Lower Flurometer	3/6/2015 7:00	0
Lower Flurometer	3/6/2015 7:01	0
Lower Flurometer	3/6/2015 7:02	0
Lower Flurometer	3/6/2015 7:03	0
Lower Flurometer	3/6/2015 7:04	0
Lower Flurometer	3/6/2015 7:05	0
Lower Flurometer	3/6/2015 7:06	0
Lower Flurometer	3/6/2015 7:07	0.02
Lower Flurometer	3/6/2015 7:08	0
Lower Flurometer	3/6/2015 7:09	0
Lower Flurometer	3/6/2015 7:10	0
Lower Flurometer	3/6/2015 7:11	0
Lower Flurometer	3/6/2015 7:12	0
Lower Flurometer	3/6/2015 7:13	0
Lower Flurometer	3/6/2015 7:14	0
Lower Flurometer	3/6/2015 7:15	0
Lower Flurometer	3/6/2015 7:16	0
Lower Flurometer	3/6/2015 7:17	0
Lower Flurometer	3/6/2015 7:18	0
Lower Flurometer	3/6/2015 7:19	0
Lower Flurometer	3/6/2015 7:20	0
Lower Flurometer	3/6/2015 7:21	0

Location	Date and Time	Rhodmaine Concentration Adjusted Concentration (ppb)
Lower Flurometer	3/6/2015 7:22	0.23
Lower Flurometer	3/6/2015 7:23	0
Lower Flurometer	3/6/2015 7:24	0
Lower Flurometer	3/6/2015 7:25	0
Lower Flurometer	3/6/2015 7:26	0
Lower Flurometer	3/6/2015 7:27	0
Lower Flurometer	3/6/2015 7:28	0
Lower Flurometer	3/6/2015 7:29	0
Lower Flurometer	3/6/2015 7:30	0
Lower Flurometer	3/6/2015 7:31	0
Lower Flurometer	3/6/2015 7:32	0
Lower Flurometer	3/6/2015 7:33	0
Lower Flurometer	3/6/2015 7:34	0
Lower Flurometer	3/6/2015 7:35	0
Lower Flurometer	3/6/2015 7:36	0
Lower Flurometer	3/6/2015 7:37	0
Lower Flurometer	3/6/2015 7:38	0
Lower Flurometer	3/6/2015 7:39	0
Lower Flurometer	3/6/2015 7:40	0
Lower Flurometer	3/6/2015 7:41	0
Lower Flurometer	3/6/2015 7:42	0
Lower Flurometer	3/6/2015 7:43	0
Lower Flurometer	3/6/2015 7:44	0
Lower Flurometer	3/6/2015 7:45	0
Lower Flurometer	3/6/2015 7:46	0
Lower Flurometer	3/6/2015 7:47	0
Lower Flurometer	3/6/2015 7:48	0
Lower Flurometer	3/6/2015 7:49	0
Lower Flurometer	3/6/2015 7:50	0
Lower Flurometer	3/6/2015 7:51	0
Lower Flurometer	3/6/2015 7:52	0
Lower Flurometer	3/6/2015 7:53	0
Lower Flurometer	3/6/2015 7:54	0
Lower Flurometer	3/6/2015 7:55	0
Lower Flurometer	3/6/2015 7:56	0
Lower Flurometer	3/6/2015 7:57	0
Lower Flurometer	3/6/2015 7:58	0
Lower Flurometer	3/6/2015 7:59	0.02
Lower Flurometer	3/6/2015 8:00	0
Lower Flurometer	3/6/2015 8:01	0
Lower Flurometer	3/6/2015 8:02	0
Lower Flurometer	3/6/2015 8:03	0
Lower Flurometer	3/6/2015 8:04	0
Lower Flurometer	3/6/2015 8:05	0
Lower Flurometer	3/6/2015 8:06	0.06
Lower Flurometer	3/6/2015 8:07	0

Location	Date and Time	Rhodmaine Concentration Adjusted Concentration (ppb)
Lower Flurometer	3/6/2015 8:08	0
Lower Flurometer	3/6/2015 8:09	0.05
Lower Flurometer	3/6/2015 8:10	0
Lower Flurometer	3/6/2015 8:11	0
Lower Flurometer	3/6/2015 8:12	0
Lower Flurometer	3/6/2015 8:13	0
Lower Flurometer	3/6/2015 8:14	0
Lower Flurometer	3/6/2015 8:15	0
Lower Flurometer	3/6/2015 8:16	0
Lower Flurometer	3/6/2015 8:17	0
Lower Flurometer	3/6/2015 8:18	0
Lower Flurometer	3/6/2015 8:19	0
Lower Flurometer	3/6/2015 8:20	0
Lower Flurometer	3/6/2015 8:21	0
Lower Flurometer	3/6/2015 8:22	0.03
Lower Flurometer	3/6/2015 8:23	0
Lower Flurometer	3/6/2015 8:24	0
Lower Flurometer	3/6/2015 8:25	0
Lower Flurometer	3/6/2015 8:26	0
Lower Flurometer	3/6/2015 8:27	0
Lower Flurometer	3/6/2015 8:28	0.12
Lower Flurometer	3/6/2015 8:29	0
Lower Flurometer	3/6/2015 8:30	0
Lower Flurometer	3/6/2015 8:31	0
Lower Flurometer	3/6/2015 8:32	0
Lower Flurometer	3/6/2015 8:33	0
Lower Flurometer	3/6/2015 8:34	0
Lower Flurometer	3/6/2015 8:35	0
Lower Flurometer	3/6/2015 8:36	0
Lower Flurometer	3/6/2015 8:37	0
Lower Flurometer	3/6/2015 8:38	0
Lower Flurometer	3/6/2015 8:39	0
Lower Flurometer	3/6/2015 8:40	0
Lower Flurometer	3/6/2015 8:41	0
Lower Flurometer	3/6/2015 8:42	0
Lower Flurometer	3/6/2015 8:43	0
Lower Flurometer	3/6/2015 8:44	0
Lower Flurometer	3/6/2015 8:45	0
Lower Flurometer	3/6/2015 8:46	0
Lower Flurometer	3/6/2015 8:47	0
Lower Flurometer	3/6/2015 8:48	0
Lower Flurometer	3/6/2015 8:49	0
Lower Flurometer	3/6/2015 8:50	0
Lower Flurometer	3/6/2015 8:51	0
Lower Flurometer	3/6/2015 8:52	0.13
Lower Flurometer	3/6/2015 8:53	0

Location	Date and Time	Rhodmaine Concentration Adjusted Concentration (ppb)
Lower Flurometer	3/6/2015 8:54	0
Lower Flurometer	3/6/2015 8:55	0
Lower Flurometer	3/6/2015 8:56	0
Lower Flurometer	3/6/2015 8:57	0
Lower Flurometer	3/6/2015 8:58	0
Lower Flurometer	3/6/2015 8:59	0
Lower Flurometer	3/6/2015 9:00	0
Lower Flurometer	3/6/2015 9:01	0
Lower Flurometer	3/6/2015 9:02	0
Lower Flurometer	3/6/2015 9:03	0
Lower Flurometer	3/6/2015 9:04	0.08
Lower Flurometer	3/6/2015 9:05	0
Lower Flurometer	3/6/2015 9:06	0
Lower Flurometer	3/6/2015 9:07	0
Lower Flurometer	3/6/2015 9:08	0.36
Lower Flurometer	3/6/2015 9:09	0
Lower Flurometer	3/6/2015 9:10	0
Lower Flurometer	3/6/2015 9:11	0
Lower Flurometer	3/6/2015 9:12	0
Lower Flurometer	3/6/2015 9:13	0
Lower Flurometer	3/6/2015 9:14	0
Lower Flurometer	3/6/2015 9:15	0
Lower Flurometer	3/6/2015 9:16	0
Lower Flurometer	3/6/2015 9:17	0
Lower Flurometer	3/6/2015 9:18	0
Lower Flurometer	3/6/2015 9:19	0
Lower Flurometer	3/6/2015 9:20	0.1
Lower Flurometer	3/6/2015 9:21	0.03
Lower Flurometer	3/6/2015 9:22	0
Lower Flurometer	3/6/2015 9:23	0
Lower Flurometer	3/6/2015 9:24	0.12
Lower Flurometer	3/6/2015 9:25	0
Lower Flurometer	3/6/2015 9:26	0.01
Lower Flurometer	3/6/2015 9:27	0
Lower Flurometer	3/6/2015 9:28	0
Lower Flurometer	3/6/2015 9:29	0
Lower Flurometer	3/6/2015 9:30	0
Lower Flurometer	3/6/2015 9:31	0
Lower Flurometer	3/6/2015 9:32	0
Lower Flurometer	3/6/2015 9:33	0
Lower Flurometer	3/6/2015 9:34	0
Lower Flurometer	3/6/2015 9:35	0
Lower Flurometer	3/6/2015 9:36	0
Lower Flurometer	3/6/2015 9:37	0
Lower Flurometer	3/6/2015 9:38	0
Lower Flurometer	3/6/2015 9:39	0

Location	Date and Time	Rhodmaine Concentration Adjusted Concentration (ppb)
Lower Flurometer	3/6/2015 9:40	0
Lower Flurometer	3/6/2015 9:41	0
Lower Flurometer	3/6/2015 9:42	0
Lower Flurometer	3/6/2015 9:43	0
Lower Flurometer	3/6/2015 9:44	0
Lower Flurometer	3/6/2015 9:45	0
Lower Flurometer	3/6/2015 9:46	0
Lower Flurometer	3/6/2015 9:47	0.01
Lower Flurometer	3/6/2015 9:48	0
Lower Flurometer	3/6/2015 9:49	0
Lower Flurometer	3/6/2015 9:50	0
Lower Flurometer	3/6/2015 9:51	0
Lower Flurometer	3/6/2015 9:52	0
Lower Flurometer	3/6/2015 9:53	0
Lower Flurometer	3/6/2015 9:54	0
Lower Flurometer	3/6/2015 9:55	0
Lower Flurometer	3/6/2015 9:56	0
Lower Flurometer	3/6/2015 9:57	0
Lower Flurometer	3/6/2015 9:58	0
Lower Flurometer	3/6/2015 9:59	0
Lower Flurometer	3/6/2015 10:00	0
Lower Flurometer	3/6/2015 10:01	0
Lower Flurometer	3/6/2015 10:02	0
Lower Flurometer	3/6/2015 10:03	0.01
Lower Flurometer	3/6/2015 10:04	0
Lower Flurometer	3/6/2015 10:05	0
Lower Flurometer	3/6/2015 10:06	0
Lower Flurometer	3/6/2015 10:07	0
Lower Flurometer	3/6/2015 10:08	0
Lower Flurometer	3/6/2015 10:09	0
Lower Flurometer	3/6/2015 10:10	0
Lower Flurometer	3/6/2015 10:11	0
Lower Flurometer	3/6/2015 10:12	0
Lower Flurometer	3/6/2015 10:13	0
Lower Flurometer	3/6/2015 10:14	0
Lower Flurometer	3/6/2015 10:15	0.01
Lower Flurometer	3/6/2015 10:16	0
Lower Flurometer	3/6/2015 10:17	0
Lower Flurometer	3/6/2015 10:18	0
Lower Flurometer	3/6/2015 10:19	0
Lower Flurometer	3/6/2015 10:20	0
Lower Flurometer	3/6/2015 10:21	0
Lower Flurometer	3/6/2015 10:22	0
Lower Flurometer	3/6/2015 10:23	0
Lower Flurometer	3/6/2015 10:24	0
Lower Flurometer	3/6/2015 10:25	0

Location	Date and Time	Rhodmaine Concentration Adjusted Concentration (ppb)
Lower Flurometer	3/6/2015 10:26	0.02
Lower Flurometer	3/6/2015 10:27	0
Lower Flurometer	3/6/2015 10:28	0
Lower Flurometer	3/6/2015 10:29	0
Lower Flurometer	3/6/2015 10:30	0
Lower Flurometer	3/6/2015 10:31	0
Lower Flurometer	3/6/2015 10:32	0
Lower Flurometer	3/6/2015 10:33	0
Lower Flurometer	3/6/2015 10:34	0
Lower Flurometer	3/6/2015 10:35	0
Lower Flurometer	3/6/2015 10:36	0
Lower Flurometer	3/6/2015 10:37	0
Lower Flurometer	3/6/2015 10:38	0
Lower Flurometer	3/6/2015 10:39	0
Lower Flurometer	3/6/2015 10:40	0
Lower Flurometer	3/6/2015 10:41	0
Lower Flurometer	3/6/2015 10:42	0
Lower Flurometer	3/6/2015 10:43	0
Lower Flurometer	3/6/2015 10:44	0
Lower Flurometer	3/6/2015 10:45	0
Lower Flurometer	3/6/2015 10:46	0
Lower Flurometer	3/6/2015 10:47	0
Lower Flurometer	3/6/2015 10:48	0
Lower Flurometer	3/6/2015 10:49	0
Lower Flurometer	3/6/2015 10:50	0.01
Lower Flurometer	3/6/2015 10:51	0
Lower Flurometer	3/6/2015 10:52	0
Lower Flurometer	3/6/2015 10:53	0
Lower Flurometer	3/6/2015 10:54	0
Lower Flurometer	3/6/2015 10:55	0
Lower Flurometer	3/6/2015 10:56	0
Lower Flurometer	3/6/2015 10:57	0
Lower Flurometer	3/6/2015 10:58	0
Lower Flurometer	3/6/2015 10:59	0
Lower Flurometer	3/6/2015 11:00	0
Lower Flurometer	3/6/2015 11:01	0
Lower Flurometer	3/6/2015 11:02	0
Lower Flurometer	3/6/2015 11:03	0
Lower Flurometer	3/6/2015 11:04	0
Lower Flurometer	3/6/2015 11:05	0
Lower Flurometer	3/6/2015 11:06	0
Lower Flurometer	3/6/2015 11:07	0
Lower Flurometer	3/6/2015 11:08	0
Lower Flurometer	3/6/2015 11:09	0
Lower Flurometer	3/6/2015 11:10	0
Lower Flurometer	3/6/2015 11:11	0

Location	Date and Time	Rhodmaine Concentration Adjusted Concentration (ppb)
Lower Flurometer	3/6/2015 11:12	0
Lower Flurometer	3/6/2015 11:13	0
Lower Flurometer	3/6/2015 11:14	0
Lower Flurometer	3/6/2015 11:15	0
Lower Flurometer	3/6/2015 11:16	0
Lower Flurometer	3/6/2015 11:17	0
Lower Flurometer	3/6/2015 11:18	0
Lower Flurometer	3/6/2015 11:19	0
Lower Flurometer	3/6/2015 11:20	0
Lower Flurometer	3/6/2015 11:21	0
Lower Flurometer	3/6/2015 11:22	0
Lower Flurometer	3/6/2015 11:23	0
Lower Flurometer	3/6/2015 11:24	0
Lower Flurometer	3/6/2015 11:25	0
Lower Flurometer	3/6/2015 11:26	0
Lower Flurometer	3/6/2015 11:27	0
Lower Flurometer	3/6/2015 11:28	0
Lower Flurometer	3/6/2015 11:29	0.01
Lower Flurometer	3/6/2015 11:30	0
Lower Flurometer	3/6/2015 11:31	0
Lower Flurometer	3/6/2015 11:32	0
Lower Flurometer	3/6/2015 11:33	0
Lower Flurometer	3/6/2015 11:34	0
Lower Flurometer	3/6/2015 11:35	0
Lower Flurometer	3/6/2015 11:36	0
Lower Flurometer	3/6/2015 11:37	0
Lower Flurometer	3/6/2015 11:38	0
Lower Flurometer	3/6/2015 11:39	0
Lower Flurometer	3/6/2015 11:40	0
Lower Flurometer	3/6/2015 11:41	0
Lower Flurometer	3/6/2015 11:42	0
Lower Flurometer	3/6/2015 11:43	0
Lower Flurometer	3/6/2015 11:44	0
Lower Flurometer	3/6/2015 11:45	0
Lower Flurometer	3/6/2015 11:46	0
Lower Flurometer	3/6/2015 11:47	0
Lower Flurometer	3/6/2015 11:48	0
Lower Flurometer	3/6/2015 11:49	0
Lower Flurometer	3/6/2015 11:50	0
Lower Flurometer	3/6/2015 11:51	0
Lower Flurometer	3/6/2015 11:52	0
Lower Flurometer	3/6/2015 11:53	0
Lower Flurometer	3/6/2015 11:54	0
Lower Flurometer	3/6/2015 11:55	0
Lower Flurometer	3/6/2015 11:56	0
Lower Flurometer	3/6/2015 11:57	0

Location	Date and Time	Rhodmaine Concentration Adjusted Concentration (ppb)
Lower Flurometer	3/6/2015 11:58	0
Lower Flurometer	3/6/2015 11:59	0
Lower Flurometer	3/6/2015 12:00	0
Lower Flurometer	3/6/2015 12:01	0
Lower Flurometer	3/6/2015 12:02	0
Lower Flurometer	3/6/2015 12:03	0
Lower Flurometer	3/6/2015 12:04	0
Lower Flurometer	3/6/2015 12:05	0
Lower Flurometer	3/6/2015 12:06	0
Lower Flurometer	3/6/2015 12:07	0
Lower Flurometer	3/6/2015 12:08	0
Lower Flurometer	3/6/2015 12:09	0
Lower Flurometer	3/6/2015 12:10	0
Lower Flurometer	3/6/2015 12:11	0
Lower Flurometer	3/6/2015 12:12	0
Lower Flurometer	3/6/2015 12:13	0
Lower Flurometer	3/6/2015 12:14	0
Lower Flurometer	3/6/2015 12:15	0
Lower Flurometer	3/6/2015 12:16	0
Lower Flurometer	3/6/2015 12:17	0.04
Lower Flurometer	3/6/2015 12:18	0
Lower Flurometer	3/6/2015 12:19	0.21
Lower Flurometer	3/6/2015 12:20	0
Lower Flurometer	3/6/2015 12:21	0
Lower Flurometer	3/6/2015 12:22	0
Lower Flurometer	3/6/2015 12:23	0
Lower Flurometer	3/6/2015 12:24	0
Lower Flurometer	3/6/2015 12:25	0.04
Lower Flurometer	3/6/2015 12:26	0
Lower Flurometer	3/6/2015 12:27	0
Lower Flurometer	3/6/2015 12:28	0
Lower Flurometer	3/6/2015 12:29	0
Lower Flurometer	3/6/2015 12:30	0
Lower Flurometer	3/6/2015 12:31	0
Lower Flurometer	3/6/2015 12:32	0
Lower Flurometer	3/6/2015 12:33	0
Lower Flurometer	3/6/2015 12:34	0
Lower Flurometer	3/6/2015 12:35	0
Lower Flurometer	3/6/2015 12:36	0
Lower Flurometer	3/6/2015 12:37	0.02
Lower Flurometer	3/6/2015 12:38	0
Lower Flurometer	3/6/2015 12:39	0
Lower Flurometer	3/6/2015 12:40	0
Lower Flurometer	3/6/2015 12:41	0
Lower Flurometer	3/6/2015 12:42	0
Lower Flurometer	3/6/2015 12:43	0

Location	Date and Time	Rhodmaine Concentration Adjusted Concentration (ppb)
Lower Flurometer	3/6/2015 12:44	0
Lower Flurometer	3/6/2015 12:45	0
Lower Flurometer	3/6/2015 12:46	0
Lower Flurometer	3/6/2015 12:47	0
Lower Flurometer	3/6/2015 12:48	0
Lower Flurometer	3/6/2015 12:49	0
Lower Flurometer	3/6/2015 12:50	0
Lower Flurometer	3/6/2015 12:51	0
Lower Flurometer	3/6/2015 12:52	0.04
Lower Flurometer	3/6/2015 12:53	0
Lower Flurometer	3/6/2015 12:54	0.04
Lower Flurometer	3/6/2015 12:55	0
Lower Flurometer	3/6/2015 12:56	0
Lower Flurometer	3/6/2015 12:57	0
Lower Flurometer	3/6/2015 12:58	0
Lower Flurometer	3/6/2015 12:59	0
Lower Flurometer	3/6/2015 13:00	0
Lower Flurometer	3/6/2015 13:01	0
Lower Flurometer	3/6/2015 13:02	0.1
Lower Flurometer	3/6/2015 13:03	0
Lower Flurometer	3/6/2015 13:04	0
Lower Flurometer	3/6/2015 13:05	0
Lower Flurometer	3/6/2015 13:06	0
Lower Flurometer	3/6/2015 13:07	0
Lower Flurometer	3/6/2015 13:08	0
Lower Flurometer	3/6/2015 13:09	0
Lower Flurometer	3/6/2015 13:10	0
Lower Flurometer	3/6/2015 13:11	0.02
Lower Flurometer	3/6/2015 13:12	0
Lower Flurometer	3/6/2015 13:13	0
Lower Flurometer	3/6/2015 13:14	0
Lower Flurometer	3/6/2015 13:15	0.04
Lower Flurometer	3/6/2015 13:16	0
Lower Flurometer	3/6/2015 13:17	0
Lower Flurometer	3/6/2015 13:18	0
Lower Flurometer	3/6/2015 13:19	0.02
Lower Flurometer	3/6/2015 13:20	0
Lower Flurometer	3/6/2015 13:21	0
Lower Flurometer	3/6/2015 13:22	0
Lower Flurometer	3/6/2015 13:23	0
Lower Flurometer	3/6/2015 13:24	0
Lower Flurometer	3/6/2015 13:25	0
Lower Flurometer	3/6/2015 13:26	0
Lower Flurometer	3/6/2015 13:27	0
Lower Flurometer	3/6/2015 13:28	0
Lower Flurometer	3/6/2015 13:29	0.06

Location	Date and Time	Rhodmaine Concentration Adjusted Concentration (ppb)
Lower Flurometer	3/6/2015 13:30	0
Lower Flurometer	3/6/2015 13:31	0
Lower Flurometer	3/6/2015 13:32	0
Lower Flurometer	3/6/2015 13:33	0
Lower Flurometer	3/6/2015 13:34	0
Lower Flurometer	3/6/2015 13:35	0
Lower Flurometer	3/6/2015 13:36	0
Lower Flurometer	3/6/2015 13:37	0
Lower Flurometer	3/6/2015 13:38	0
Lower Flurometer	3/6/2015 13:39	0.02
Lower Flurometer	3/6/2015 13:40	0
Lower Flurometer	3/6/2015 13:41	0
Lower Flurometer	3/6/2015 13:42	0
Lower Flurometer	3/6/2015 13:43	0.02
Lower Flurometer	3/6/2015 13:44	0
Lower Flurometer	3/6/2015 13:45	0.13
Lower Flurometer	3/6/2015 13:46	0
Lower Flurometer	3/6/2015 13:47	0
Lower Flurometer	3/6/2015 13:48	0
Lower Flurometer	3/6/2015 13:49	0
Lower Flurometer	3/6/2015 13:50	0
Lower Flurometer	3/6/2015 13:51	0
Lower Flurometer	3/6/2015 13:52	0
Lower Flurometer	3/6/2015 13:53	0
Lower Flurometer	3/6/2015 13:54	0
Lower Flurometer	3/6/2015 13:55	0
Lower Flurometer	3/6/2015 13:56	0
Lower Flurometer	3/6/2015 13:57	0
Lower Flurometer	3/6/2015 13:58	0
Lower Flurometer	3/6/2015 13:59	0
Lower Flurometer	3/6/2015 14:00	0
Lower Flurometer	3/6/2015 14:01	0
Lower Flurometer	3/6/2015 14:02	0
Lower Flurometer	3/6/2015 14:03	0
Lower Flurometer	3/6/2015 14:04	0
Lower Flurometer	3/6/2015 14:05	0
Lower Flurometer	3/6/2015 14:06	0
Lower Flurometer	3/6/2015 14:07	0
Lower Flurometer	3/6/2015 14:08	0
Lower Flurometer	3/6/2015 14:09	0
Lower Flurometer	3/6/2015 14:10	0
Lower Flurometer	3/6/2015 14:11	0
Lower Flurometer	3/6/2015 14:12	0
Lower Flurometer	3/6/2015 14:13	0
Lower Flurometer	3/6/2015 14:14	0
Lower Flurometer	3/6/2015 14:15	0

Location	Date and Time	Rhodmaine Concentration Adjusted Concentration (ppb)
Lower Flurometer	3/6/2015 14:16	0
Lower Flurometer	3/6/2015 14:17	0.01
Lower Flurometer	3/6/2015 14:18	0
Lower Flurometer	3/6/2015 14:19	0
Lower Flurometer	3/6/2015 14:20	0
Lower Flurometer	3/6/2015 14:21	0
Lower Flurometer	3/6/2015 14:22	0
Lower Flurometer	3/6/2015 14:23	0.04
Lower Flurometer	3/6/2015 14:24	0.09
Lower Flurometer	3/6/2015 14:25	0.09
Lower Flurometer	3/6/2015 14:26	0.04
Lower Flurometer	3/6/2015 14:27	0.08
Lower Flurometer	3/6/2015 14:28	0.04
Lower Flurometer	3/6/2015 14:29	0
Lower Flurometer	3/6/2015 14:30	0.12
Lower Flurometer	3/6/2015 14:31	0.11
Lower Flurometer	3/6/2015 14:32	0.04
Lower Flurometer	3/6/2015 14:33	0.13
Lower Flurometer	3/6/2015 14:34	0.13
Lower Flurometer	3/6/2015 14:35	0.11
Lower Flurometer	3/6/2015 14:36	0.1
Lower Flurometer	3/6/2015 14:37	0.12
Lower Flurometer	3/6/2015 14:38	0.13
Lower Flurometer	3/6/2015 14:39	0.14
Lower Flurometer	3/6/2015 14:40	0.1
Lower Flurometer	3/6/2015 14:41	0.1
Lower Flurometer	3/6/2015 14:42	0.14
Lower Flurometer	3/6/2015 14:43	0.12
Lower Flurometer	3/6/2015 14:44	0.1
Lower Flurometer	3/6/2015 14:45	0.18
Lower Flurometer	3/6/2015 14:46	0.12
Lower Flurometer	3/6/2015 14:47	0.13
Lower Flurometer	3/6/2015 14:48	0.14
Lower Flurometer	3/6/2015 14:49	0.16
Lower Flurometer	3/6/2015 14:50	0.19
Lower Flurometer	3/6/2015 14:51	0.16
Lower Flurometer	3/6/2015 14:52	0.1
Lower Flurometer	3/6/2015 14:53	0.18
Lower Flurometer	3/6/2015 14:54	0.18
Lower Flurometer	3/6/2015 14:55	0.1
Lower Flurometer	3/6/2015 14:56	0.18
Lower Flurometer	3/6/2015 14:57	0.13
Lower Flurometer	3/6/2015 14:58	0.1
Lower Flurometer	3/6/2015 14:59	0.14
Lower Flurometer	3/6/2015 15:00	0.1
Lower Flurometer	3/6/2015 15:01	0.1

Location	Date and Time	Rhodmaine Concentration Adjusted Concentration (ppb)
Lower Flurometer	3/6/2015 15:02	0.18
Lower Flurometer	3/6/2015 15:03	0.17
Lower Flurometer	3/6/2015 15:04	0.15
Lower Flurometer	3/6/2015 15:05	0.08
Lower Flurometer	3/6/2015 15:06	0.17
Lower Flurometer	3/6/2015 15:07	0.12
Lower Flurometer	3/6/2015 15:08	0.15
Lower Flurometer	3/6/2015 15:09	0.09
Lower Flurometer	3/6/2015 15:10	0.1
Lower Flurometer	3/6/2015 15:11	0.14
Lower Flurometer	3/6/2015 15:12	0.1
Lower Flurometer	3/6/2015 15:13	0.12
Lower Flurometer	3/6/2015 15:14	0.17
Lower Flurometer	3/6/2015 15:15	0.17
Lower Flurometer	3/6/2015 15:16	0.1
Lower Flurometer	3/6/2015 15:17	0.15
Lower Flurometer	3/6/2015 15:18	0.07
Lower Flurometer	3/6/2015 15:19	0.17
Lower Flurometer	3/6/2015 15:20	0.14
Lower Flurometer	3/6/2015 15:21	0.13
Lower Flurometer	3/6/2015 15:22	0.1
Lower Flurometer	3/6/2015 15:23	0.11
Lower Flurometer	3/6/2015 15:24	0.09
Lower Flurometer	3/6/2015 15:25	0.1
Lower Flurometer	3/6/2015 15:26	0.12
Lower Flurometer	3/6/2015 15:27	0.09
Lower Flurometer	3/6/2015 15:28	0.14
Lower Flurometer	3/6/2015 15:29	0.08
Lower Flurometer	3/6/2015 15:30	0.13
Lower Flurometer	3/6/2015 15:31	0.13
Lower Flurometer	3/6/2015 15:32	0.08
Lower Flurometer	3/6/2015 15:33	0.1
Lower Flurometer	3/6/2015 15:34	0.08
Lower Flurometer	3/6/2015 15:35	0.06
Lower Flurometer	3/6/2015 15:36	0.13
Lower Flurometer	3/6/2015 15:37	0.07
Lower Flurometer	3/6/2015 15:38	0.14
Lower Flurometer	3/6/2015 15:39	0.14
Lower Flurometer	3/6/2015 15:40	0.06
Lower Flurometer	3/6/2015 15:41	0.12
Lower Flurometer	3/6/2015 15:42	0.13
Lower Flurometer	3/6/2015 15:43	0.04
Lower Flurometer	3/6/2015 15:44	0.08
Lower Flurometer	3/6/2015 15:45	0.04
Lower Flurometer	3/6/2015 15:46	0.05
Lower Flurometer	3/6/2015 15:47	0.11

Location	Date and Time	Rhodmaine Concentration Adjusted Concentration (ppb)
Lower Flurometer	3/6/2015 15:48	0.09
Lower Flurometer	3/6/2015 15:49	0.06
Lower Flurometer	3/6/2015 15:50	0.1
Lower Flurometer	3/6/2015 15:51	0.03
Lower Flurometer	3/6/2015 15:52	0.02
Lower Flurometer	3/6/2015 15:53	0.03
Lower Flurometer	3/6/2015 15:54	0
Lower Flurometer	3/6/2015 15:55	0.01
Lower Flurometer	3/6/2015 15:56	0.1
Lower Flurometer	3/6/2015 15:57	0.02
Lower Flurometer	3/6/2015 15:58	0.06
Lower Flurometer	3/6/2015 15:59	0
Lower Flurometer	3/6/2015 16:00	0.01
Lower Flurometer	3/6/2015 16:01	0.06
Lower Flurometer	3/6/2015 16:02	0.02
Lower ISCO	3/4/15 16:00	-0.091257562
Lower ISCO	3/4/15 17:00	-0.043525651
Lower ISCO	3/4/15 18:00	0.04535446
Lower ISCO	3/4/15 19:00	-0.11759241
Lower ISCO	3/4/15 20:00	-0.12582205
Lower ISCO	3/4/15 21:00	-0.143927257
Lower ISCO	3/4/15 22:00	-0.073152354
Lower ISCO	3/4/15 23:00	-0.048463435
Lower ISCO	3/5/15 0:00	-0.083027922
Lower ISCO	3/5/15 1:00	-0.06821457
Lower ISCO	3/5/15 2:00	-0.061630859
Lower ISCO	3/5/15 3:00	0.173736842
Lower ISCO	3/5/15 4:00	1.901961215
Lower ISCO	3/5/15 5:00	4.273743425
Lower ISCO	3/5/15 6:00	5.317261761
Lower ISCO	3/5/15 7:00	4.668766139
Lower ISCO	3/5/15 8:00	4.168404035
Lower ISCO	3/5/15 9:00	3.312521489
Lower ISCO	3/5/15 10:00	2.746322265
Lower ISCO	3/5/15 11:00	2.254189801
Lower ISCO	3/5/15 12:00	1.905253071
Lower ISCO	3/5/15 13:00	1.633674955
Lower ISCO	3/5/15 14:00	1.227130745
Lower ISCO	3/5/15 15:00	1.046078668
Lower ISCO	3/5/15 16:00	0.968720053
Lower ISCO	3/5/15 17:00	0.838691743
Lower ISCO	3/5/15 18:00	0.621429251
Lower ISCO	3/5/15 19:00	0.519381716
Lower ISCO	3/5/15 20:00	0.433793462
Lower ISCO	3/5/15 21:00	0.307057008
Lower ISCO	3/5/15 22:00	0.29718144

Location	Date and Time	Rhodmaine Concentration Adjusted Concentration (ppb)
Lower ISCO	3/5/15 23:00	0.213239113
Lower ISCO	3/6/15 0:00	0.224760609
Lower ISCO	3/6/15 1:00	0.137526426
Lower ISCO	3/6/15 2:00	0.160569418
Lower ISCO	3/6/15 3:00	0.157277562
Lower ISCO	3/6/15 4:00	0.260971024
Lower ISCO	3/6/15 5:00	0.114483435
Lower ISCO	3/6/15 6:00	0.096378227
Lower ISCO	3/6/15 7:00	0.060167812
Lower ISCO	3/6/15 8:00	0.084856731
Lower ISCO	3/6/15 9:00	0.035478892
Lower ISCO	3/6/15 10:00	0.009144044
Lower ISCO	3/6/15 11:00	0.047000388
Lower ISCO	3/6/15 12:00	0.02066554
Lower ISCO	3/6/15 13:00	-0.018836731
Lower ISCO	3/6/15 14:00	0.027249252

Appendix 5.3.1. Discrete velocity measurements were taken on 10/3, 10/6, and 10/8/2014.

Date	Transect	Distance from Left Bank (m)	Depth (m)	Velocity ($m\ s^{-1}$) (up to 4 repeated measures)					Depth to top of Vegetation (m)
				1	2	3	4	Avg.	
10/3/2014	3	0	0.690	0.010				0.010	n/a
10/3/2014	3	0	0.610	0.240				0.240	n/a
10/3/2014	3	0	0.560	0.060				0.060	n/a
10/3/2014	3	0	0.440	0.020				0.020	n/a
10/3/2014	3	0	0.290	0.080	0.070			0.075	n/a
10/3/2014	3	0	0.210	0.090	0.070			0.080	n/a
10/3/2014	3	0	0.140	0.090	0.080	0.140		0.103	n/a
10/3/2014	3	0	0.050	0.120	0.090	0.140		0.117	n/a
10/3/2014	3	1	0.800	0.000	0.000	0.000		0.000	n/a
10/3/2014	3	1	0.690	0.000	0.070	0.050		0.040	n/a
10/3/2014	3	1	0.640	0.070	0.060	0.060		0.063	n/a
10/3/2014	3	1	0.590	0.090	0.040	0.060		0.063	n/a
10/3/2014	3	1	0.480	0.060	0.060	0.060		0.060	n/a
10/3/2014	3	1	0.420	0.050	0.060	0.070		0.060	n/a
10/3/2014	3	1	0.320	0.070	0.070	0.060		0.067	n/a
10/3/2014	3	1	0.220	0.040	0.040	0.050		0.043	n/a
10/3/2014	3	1	0.100	0.040	0.040	0.050		0.043	n/a
10/3/2014	3	1	0.070	0.100	0.090	0.070		0.087	n/a
10/3/2014	3	2	0.880	0.000	0.000	0.000		0.000	0.05
10/3/2014	3	2	0.760	0.030	0.020	0.030		0.027	0.05
10/3/2014	3	2	0.610	0.020	0.030	0.020		0.023	0.05
10/3/2014	3	2	0.520	0.060	0.060	0.050		0.057	0.05
10/3/2014	3	2	0.440	0.040	0.030	0.040		0.037	0.05
10/3/2014	3	2	0.340	0.050	0.150	0.100		0.100	0.05
10/3/2014	3	2	0.280	0.050	0.050	0.040		0.047	0.05
10/3/2014	3	2	0.140	0.110	0.100	0.110		0.107	0.05
10/3/2014	3	2	0.040	0.080	0.220	0.130	0.170	0.150	0.05
10/3/2014	3	3	1.250	0.008	0.008	0.010		0.009	0.298
10/3/2014	3	3	0.995	0.024	0.026	0.036		0.029	0.298
10/3/2014	3	3	0.813	0.063	0.041	0.059		0.054	0.298
10/3/2014	3	3	0.651	0.050	0.029	0.047		0.042	0.298
10/3/2014	3	3	0.447	0.041	0.069	0.228	0.090	0.107	0.298
10/3/2014	3	3	0.325	0.141	0.150	0.060		0.117	0.298
10/3/2014	3	3	0.230	0.191	0.308	0.308		0.269	0.298
10/3/2014	3	3	0.156	0.100	0.209	0.162		0.157	0.298
10/3/2014	3	3	0.067	0.178	0.266	0.279		0.241	0.298
10/3/2014	3	4	2.429	0.040	0.033	0.058		0.044	1.5
10/3/2014	3	4	2.146	0.154	0.204	0.230		0.196	1.5
10/3/2014	3	4	1.878	0.196	0.079	0.221	0.204	0.175	1.5
10/3/2014	3	4	1.683	0.144	0.132	0.198		0.158	1.5
10/3/2014	3	4	1.461	0.194	0.127	0.186		0.169	1.5
10/3/2014	3	4	1.251	0.310	0.345	0.259		0.305	1.5
10/3/2014	3	4	1.020	0.233	0.275	0.236		0.248	1.5

Date	Transect	Distance from Left Bank (m)	Depth (m)	Velocity (m s^{-1}) (up to 4 repeated measures)					Depth to top of Vegetation (m)
				1	2	3	4	Avg.	
10/3/2014	3	4	0.785	0.259	0.213	0.362	0.428	0.316	1.5
10/3/2014	3	4	0.545	0.280	0.315	0.375		0.323	1.5
10/3/2014	3	4	0.241	0.337	0.391	0.285		0.338	1.5
10/3/2014	3	4	0.090	0.251	0.295	0.353		0.300	1.5
10/6/2014	3	6	3.628	0.052	0.019	0.049		0.040	n/a
10/6/2014	3	6	3.237	0.188	0.140	0.067		0.132	n/a
10/6/2014	3	6	2.849	0.331	0.257	0.298		0.295	n/a
10/6/2014	3	6	2.380	0.252	0.204	0.133		0.196	n/a
10/6/2014	3	6	2.010	0.337	0.342	0.367		0.349	n/a
10/6/2014	3	6	1.594	0.498	0.432	0.527		0.486	n/a
10/6/2014	3	6	1.220	0.526	0.375	0.483		0.461	n/a
10/6/2014	3	6	0.853	0.565	0.449	0.409		0.474	n/a
10/6/2014	3	6	0.413	0.345	0.339	0.371		0.352	n/a
10/6/2014	3	6	0.125	0.451	0.505	0.433		0.463	n/a
10/3/2014	3	7	4.240	0.048	0.028	0.023		0.033	n/a
10/3/2014	3	7	3.674	0.347	0.303	0.229		0.293	n/a
10/3/2014	3	7	3.286	0.407	0.442	0.371		0.407	n/a
10/3/2014	3	7	2.600	0.394	0.390	0.423		0.402	n/a
10/3/2014	3	7	2.121	0.560	0.430	0.462		0.484	n/a
10/3/2014	3	7	1.645	0.555	0.482	0.560		0.532	n/a
10/3/2014	3	7	1.076	0.597	0.568	0.586		0.584	n/a
10/3/2014	3	7	0.660	0.515	0.522	0.547		0.528	n/a
10/3/2014	3	7	0.365	0.494	0.532	0.578		0.535	n/a
10/6/2014	3	8	4.250	0.085	0.018	0.089		0.064	n/a
10/6/2014	3	8	3.725	0.228	0.297	0.366		0.297	n/a
10/6/2014	3	8	3.301	0.387	0.362	0.376		0.375	n/a
10/6/2014	3	8	2.795	0.298	0.470	0.445		0.404	n/a
10/6/2014	3	8	2.381	0.515	0.478	0.489		0.494	n/a
10/6/2014	3	8	1.970	0.411	0.469	0.468		0.449	n/a
10/6/2014	3	8	1.565	0.512	0.507	0.490		0.503	n/a
10/6/2014	3	8	1.155	0.469	0.561	0.562		0.531	n/a
10/6/2014	3	8	0.722	0.635	0.546	0.535		0.572	n/a
10/6/2014	3	8	0.375	0.447	0.459	0.467		0.458	n/a
10/6/2014	3	8	0.095	0.455	0.335	0.452		0.414	n/a
10/6/2014	3	9	4.320	0.016	0.020	0.016		0.017	n/a
10/6/2014	3	9	3.864	0.319	0.264	0.284		0.289	n/a
10/6/2014	3	9	3.407	0.227	0.265	0.269		0.254	n/a
10/6/2014	3	9	3.072	0.378	0.344	0.286		0.336	n/a
10/6/2014	3	9	2.585	0.356	0.483	0.476		0.438	n/a
10/6/2014	3	9	2.218	0.394	0.435	0.517		0.449	n/a
10/6/2014	3	9	1.842	0.341	0.441	0.460		0.414	n/a
10/6/2014	3	9	1.343	0.401	0.494	0.494		0.463	n/a
10/6/2014	3	9	0.922	0.441	0.432	0.449		0.441	n/a
10/6/2014	3	9	0.900	0.518	0.491	0.417		0.475	n/a
10/6/2014	3	10	4.300	0.016	0.005	0.011		0.011	n/a
10/6/2014	3	10	3.863	0.209	0.133	0.134		0.159	n/a

Date	Transect	Distance from Left Bank (m)	Depth (m)	Velocity (m s^{-1}) (up to 4 repeated measures)					Depth to top of Vegetation (m)
				1	2	3	4	Avg.	
10/6/2014	3	10	3.364	0.219	0.195	0.091		0.168	n/a
10/6/2014	3	10	2.888	0.295	0.394	0.430		0.373	n/a
10/6/2014	3	10	2.435	0.248	0.345	0.282		0.292	n/a
10/6/2014	3	10	2.002	0.409	0.480	0.459		0.449	n/a
10/6/2014	3	10	1.523	0.442	0.358	0.355		0.385	n/a
10/6/2014	3	10	1.219	0.380	0.380	0.337		0.366	n/a
10/6/2014	3	10	0.818	0.370	0.333	0.356		0.353	n/a
10/6/2014	3	10	0.297	0.359	0.346	0.337		0.347	n/a
10/6/2014	3	11	4.112	0.034	0.046	0.014		0.031	n/a
10/6/2014	3	11	3.664	0.033	0.120	0.087		0.080	n/a
10/6/2014	3	11	3.184	0.113	0.115	0.152		0.127	n/a
10/6/2014	3	11	2.849	0.190	0.189	0.175		0.185	n/a
10/6/2014	3	11	2.462	0.181	0.296	0.168		0.215	n/a
10/6/2014	3	11	1.955	0.193	0.179	0.303		0.225	n/a
10/6/2014	3	11	1.572	0.286	0.303	0.396		0.328	n/a
10/6/2014	3	11	1.163	0.316	0.226	0.343		0.295	n/a
10/6/2014	3	11	0.729	0.290	0.296	0.309		0.298	n/a
10/6/2014	3	11	0.202	0.344	0.351	0.394		0.363	n/a
10/6/2014	3	12	3.702	0.020	0.015	0.046		0.027	n/a
10/6/2014	3	12	3.243	0.057	0.090	0.071		0.073	n/a
10/6/2014	3	12	2.963	0.129	0.128	0.136		0.131	n/a
10/6/2014	3	12	2.571	0.273	0.264	0.194		0.244	n/a
10/6/2014	3	12	2.101	0.121	0.105	0.208		0.145	n/a
10/6/2014	3	12	1.647	0.204	0.234	0.158		0.199	n/a
10/6/2014	3	12	1.207	0.297	0.246	0.189		0.244	n/a
10/6/2014	3	12	0.773	0.251	0.293	0.277		0.274	n/a
10/6/2014	3	12	0.416	0.339	0.360	0.307		0.335	n/a
10/6/2014	3	12	0.132	0.309	0.340	0.307		0.319	n/a
10/6/2014	3	13	3.243	0.003	0.002	0.002		0.002	n/a
10/6/2014	3	13	2.825	0.073	0.115	0.131		0.106	n/a
10/6/2014	3	13	2.417	0.112	0.125	0.221		0.153	n/a
10/6/2014	3	13	2.025	0.191	0.171	0.163		0.175	n/a
10/6/2014	3	13	1.622	0.156	0.198	0.217		0.190	n/a
10/6/2014	3	13	1.228	0.256	0.298	0.275		0.276	n/a
10/6/2014	3	13	0.881	0.177	0.284	0.272		0.244	n/a
10/6/2014	3	13	0.499	0.233	0.287	0.280		0.267	n/a
10/6/2014	3	13	0.153	0.277	0.280	0.238		0.265	n/a
10/6/2014	3	14	2.530	0.005	0.011	0.021		0.012	n/a
10/6/2014	3	14	2.225	0.056	0.063	0.031		0.050	n/a
10/6/2014	3	14	2.021	0.044	0.048	0.047		0.046	n/a
10/6/2014	3	14	1.758	0.012	0.016	0.021		0.016	n/a
10/6/2014	3	14	1.503	0.023	0.023	0.009		0.018	n/a
10/6/2014	3	14	1.273	0.052	0.015	0.096		0.054	n/a
10/6/2014	3	14	1.010	0.130	0.109	0.128		0.122	n/a
10/6/2014	3	14	0.752	0.214	0.210	0.343		0.256	n/a
10/6/2014	3	14	0.514	0.286	0.252	0.302		0.280	n/a

Date	Transect	Distance from Left Bank (m)	Depth (m)	Velocity (m s^{-1}) (up to 4 repeated measures)					Depth to top of Vegetation (m)
				1	2	3	4	Avg.	
10/6/2014	3	14	0.112	0.369	0.270	0.193		0.277	n/a
10/6/2014	3	15	2.001	0.008	0.013	0.015		0.012	1.17
10/6/2014	3	15	1.860	0.038	0.033	0.010		0.027	1.17
10/6/2014	3	15	1.597	0.038	0.020	0.038		0.032	1.17
10/6/2014	3	15	1.376	0.155	0.024	0.048		0.076	1.17
10/6/2014	3	15	1.178	0.072	0.154	0.084		0.103	1.17
10/6/2014	3	15	0.977	0.154	0.181	0.153		0.163	1.17
10/6/2014	3	15	0.771	0.101	0.178	0.195		0.158	1.17
10/6/2014	3	15	0.603	0.249	0.159	0.148		0.185	1.17
10/6/2014	3	15	0.377	0.063	0.163	0.182		0.136	1.17
10/6/2014	3	15	0.070	0.134	0.242	0.195		0.190	1.17
10/6/2014	3	16	1.230	0.016	0.000	0.005		0.007	0.902
10/6/2014	3	16	1.085	0.020	0.034	0.049		0.034	0.902
10/6/2014	3	16	0.863	0.157	0.051	0.014		0.074	0.902
10/6/2014	3	16	0.741	0.082	0.086	0.163		0.110	0.902
10/6/2014	3	16	0.575	0.092	0.038	0.111		0.080	0.902
10/6/2014	3	16	0.456	0.166	0.115	0.179		0.153	0.902
10/6/2014	3	16	0.318	0.271	0.201	0.172		0.215	0.902
10/6/2014	3	16	0.185	0.222	0.098	0.090		0.137	0.902
10/6/2014	3	16	0.101	0.136	0.202	0.201		0.180	0.902
10/6/2014	3	16	0.051	0.236	0.254	0.048		0.179	0.902
10/6/2014	3	17	1.035	0.002	0.000	0.000		0.001	0.692
10/6/2014	3	17	0.897	0.001	0.017	0.001		0.006	0.692
10/6/2014	3	17	0.826	0.014	0.039	0.013		0.022	0.692
10/6/2014	3	17	0.706	0.030	0.037	0.014		0.027	0.692
10/6/2014	3	17	0.583	0.078	0.038	0.033		0.050	0.692
10/6/2014	3	17	0.515	0.006	0.098	0.141		0.082	0.692
10/6/2014	3	17	0.373	0.132	0.100	0.102		0.111	0.692
10/6/2014	3	17	0.293	0.104	0.116	0.083		0.101	0.692
10/6/2014	3	17	0.189	0.095	0.113	0.128		0.112	0.692
10/6/2014	3	17	0.062	0.128	0.277	0.111		0.172	0.692
10/6/2014	3	18	0.780	0.015	0.027	0.020		0.021	n/a
10/6/2014	3	18	0.681	0.037	0.063	0.053		0.051	n/a
10/6/2014	3	18	0.575	0.121	0.076	0.001		0.066	n/a
10/6/2014	3	18	0.555	0.054	0.002	0.067		0.041	n/a
10/6/2014	3	18	0.481	0.071	0.092	0.063		0.075	n/a
10/6/2014	3	18	0.435	0.007	0.033	0.035		0.025	n/a
10/6/2014	3	18	0.381	0.079	0.066	0.056		0.067	n/a
10/6/2014	3	18	0.286	0.059	0.039	0.069		0.056	n/a
10/6/2014	3	18	0.148	0.055	0.017	0.069		0.047	n/a
10/6/2014	3	18	0.058	0.068	0.094	0.110		0.091	n/a
10/6/2014	3	19	0.670	0.006	0.006	0.005		0.006	n/a
10/6/2014	3	19	0.537	0.011	0.032	0.032		0.025	n/a
10/6/2014	3	19	0.479	0.040	0.008	0.028		0.025	n/a
10/6/2014	3	19	0.415	0.046	0.034	0.042		0.041	n/a
10/6/2014	3	19	0.378	0.054	0.031	0.045		0.043	n/a

Date	Transect	Distance from Left Bank (m)	Depth (m)	Velocity (m s^{-1}) (up to 4 repeated measures)					Depth to top of Vegetation (m)
				1	2	3	4	Avg.	
10/6/2014	3	19	0.280	0.027	0.063	0.069		0.053	n/a
10/6/2014	3	19	0.202	0.027	0.060	0.043		0.043	n/a
10/6/2014	3	19	0.165	0.023	0.047	0.070		0.047	n/a
10/6/2014	3	19	0.091	0.091	0.050	0.060		0.067	n/a
10/6/2014	3	19	0.062	0.046	0.061	0.048		0.052	n/a
10/8/2015	7	0	1.105	0.003	0.001	0.005		0.003	n/a
10/8/2015	7	0	0.951	0.035	0.035	0.035		0.035	n/a
10/8/2015	7	0	0.895	0.029	0.038	0.042		0.036	n/a
10/8/2015	7	0	0.805	0.067	0.067	0.061		0.065	n/a
10/8/2015	7	0	0.710	0.059	0.057	0.057		0.058	n/a
10/8/2015	7	0	0.609	0.071	0.068	0.068		0.069	n/a
10/8/2015	7	0	0.502	0.060	0.058	0.058		0.059	n/a
10/8/2015	7	0	0.403	0.063	0.063	0.063		0.063	n/a
10/8/2015	7	0	0.307	0.056	0.070	0.070		0.065	n/a
10/8/2015	7	0	0.209	0.048	0.051	0.051		0.050	n/a
10/8/2015	7	0	0.105	0.052	0.046	0.046		0.048	n/a
10/8/2015	7	2	1.372	0.000	0.000	0.000		0.000	0.570
10/8/2015	7	2	1.230	0.000	0.000	0.000		0.000	0.570
10/8/2015	7	2	1.086	0.061	0.061	0.063		0.062	0.570
10/8/2015	7	2	0.936	0.065	0.084	0.084		0.078	0.570
10/8/2015	7	2	0.783	0.087	0.086	0.086		0.086	0.570
10/8/2015	7	2	0.654	0.088	0.088	0.088		0.088	0.570
10/8/2015	7	2	0.516	0.114	0.114	0.114		0.114	0.570
10/8/2015	7	2	0.384	0.096	0.096	0.100		0.097	0.570
10/8/2015	7	2	0.156	0.102	0.102	0.119		0.108	0.570
10/8/2015	7	2	0.059	0.054	0.054	0.054		0.054	0.570
10/8/2015	7	4	1.348	0.004	0.000	0.011		0.005	0.702
10/8/2015	7	4	1.201	0.026	0.026	0.009		0.020	0.702
10/8/2015	7	4	1.084	0.039	0.030	0.030		0.033	0.702
10/8/2015	7	4	0.948	0.044	0.030	0.030		0.035	0.702
10/8/2015	7	4	0.815	0.018	0.018	0.018		0.018	0.702
10/8/2015	7	4	0.653	0.059	0.059	0.056		0.058	0.702
10/8/2015	7	4	0.409	0.098	0.098	0.107		0.101	0.702
10/8/2015	7	4	0.277	0.109	0.109	0.109		0.109	0.702
10/8/2015	7	4	0.133	0.134	0.098	0.098		0.110	0.702
10/8/2015	7	4	0.057	0.060	0.060	0.060		0.060	0.702
10/8/2015	7	6	1.535	0.000	0.000	0.000		0.000	0.830
10/8/2015	7	6	1.372	0.005	0.000	0.000		0.002	0.830
10/8/2015	7	6	1.211	0.013	0.012	0.012		0.012	0.830
10/8/2015	7	6	1.057	0.025	0.025	0.025		0.025	0.830
10/8/2015	7	6	0.874	0.057	0.057	0.057		0.057	0.830
10/8/2015	7	6	0.723	0.099	0.099	0.099		0.099	0.830
10/8/2015	7	6	0.580	0.131	0.131	0.125		0.129	0.830
10/8/2015	7	6	0.378	0.141	0.127	0.127		0.132	0.830
10/8/2015	7	6	0.140	0.109	0.122	0.122		0.118	0.830
10/8/2015	7	6	0.067	0.024	0.024	0.024		0.024	0.830

Date	Transect	Distance from Left Bank (m)	Depth (m)	Velocity (m s^{-1}) (up to 4 repeated measures)					Depth to top of Vegetation (m)
				1	2	3	4	Avg.	
10/8/2015	7	8	1.574	0.000	0.000	0.000		0.000	0.825
10/8/2015	7	8	1.410	0.030	0.030	0.008		0.023	0.825
10/8/2015	7	8	1.254	0.031	0.031	0.027		0.030	0.825
10/8/2015	7	8	1.012	0.070	0.070	0.070		0.070	0.825
10/8/2015	7	8	0.844	0.030	0.030	0.030		0.030	0.825
10/8/2015	7	8	0.687	0.112	0.112	0.112		0.112	0.825
10/8/2015	7	8	0.539	0.160	0.160	0.164		0.161	0.825
10/8/2015	7	8	0.302	0.210	0.210	0.210		0.210	0.825
10/8/2015	7	8	0.133	0.150	0.154	0.154		0.153	0.825
10/8/2015	7	8	0.081	0.000	0.213	0.213		0.142	0.825
10/8/2015	7	10	1.830	0.001	0.001	0.001		0.001	1.118
10/8/2015	7	10	1.596	0.004	0.004	0.004		0.004	1.118
10/8/2015	7	10	1.430	0.068	0.022	0.022		0.037	1.118
10/8/2015	7	10	1.257	0.008	0.008	0.030		0.015	1.118
10/8/2015	7	10	1.097	0.157	0.157	0.069		0.128	1.118
10/8/2015	7	10	0.801	0.165	0.165	0.134		0.155	1.118
10/8/2015	7	10	0.614	0.180	0.182	0.182		0.181	1.118
10/8/2015	7	10	0.435	0.176	0.176	0.176		0.176	1.118
10/8/2015	7	10	0.232	0.158	0.186	0.186		0.177	1.118
10/8/2015	7	10	0.092	0.211	0.211	0.211		0.211	1.118
10/8/2015	7	12	1.979	0.000	0.000	0.000		0.000	1.155
10/8/2015	7	12	1.696	0.000	0.000	0.000		0.000	1.155
10/8/2015	7	12	1.490	0.012	0.009	0.009		0.010	1.155
10/8/2015	7	12	1.276	0.116	0.116	0.116		0.116	1.155
10/8/2015	7	12	1.080	0.074	0.074	0.074		0.074	1.155
10/8/2015	7	12	0.901	0.196	0.196	0.196		0.196	1.155
10/8/2015	7	12	0.690	0.159	0.169	0.169		0.166	1.155
10/8/2015	7	12	0.466	0.195	0.156	0.156		0.169	1.155
10/8/2015	7	12	0.268	0.226	0.226	0.226		0.226	1.155
10/8/2015	7	12	0.095	0.301	0.301	0.219		0.274	1.155
10/8/2015	7	14	2.175	0.001	0.000	0.000		0.000	0.976
10/8/2015	7	14	1.877	0.025	0.025	0.012		0.021	0.976
10/8/2015	7	14	1.650	0.035	0.042	0.042		0.040	0.976
10/8/2015	7	14	1.478	0.017	0.017	0.022		0.019	0.976
10/8/2015	7	14	1.268	0.056	0.087	0.087		0.077	0.976
10/8/2015	7	14	1.062	0.177	0.158	0.158		0.164	0.976
10/8/2015	7	14	0.818	0.258	0.207	0.207		0.224	0.976
10/8/2015	7	14	0.500	0.225	0.225	0.221		0.224	0.976
10/8/2015	7	14	0.242	0.212	0.200	0.200		0.204	0.976
10/8/2015	7	14	0.067	0.389	0.389	0.356		0.378	0.976
10/8/2015	7	16	2.490	0.001	0.006	0.006		0.004	1.416
10/8/2015	7	16	2.200	0.000	0.000	0.000		0.000	1.416
10/8/2015	7	16	1.928	0.017	0.019	0.019		0.018	1.416
10/8/2015	7	16	1.748	0.027	0.040	0.040		0.036	1.416
10/8/2015	7	16	1.436	0.157	0.157	0.057		0.124	1.416
10/8/2015	7	16	1.153	0.036	0.127	0.127		0.097	1.416

Date	Transect	Distance from Left Bank (m)	Depth (m)	Velocity (m s^{-1}) (up to 4 repeated measures)					Depth to top of Vegetation (m)
				1	2	3	4	Avg.	
10/8/2015	7	16	0.881	0.055	0.216	0.216		0.162	1.416
10/8/2015	7	16	0.654	0.288	0.216	0.216		0.240	1.416
10/8/2015	7	16	0.358	0.202	0.219	0.219		0.213	1.416
10/8/2015	7	16	0.069	0.293	0.293	0.293		0.293	1.416
10/8/2015	7	18	2.525	0.001	0.000	0.000		0.000	1.260
10/8/2015	7	18	2.254	0.004	0.004	0.001		0.003	1.260
10/8/2015	7	18	2.076	0.019	0.019	0.036		0.025	1.260
10/8/2015	7	18	1.716	0.051	0.051	0.051		0.051	1.260
10/8/2015	7	18	1.503	0.047	0.047	0.074		0.056	1.260
10/8/2015	7	18	1.288	0.145	0.145	0.093		0.128	1.260
10/8/2015	7	18	0.909	0.172	0.172	0.159		0.168	1.260
10/8/2015	7	18	0.687	0.233	0.233	0.222		0.229	1.260
10/8/2015	7	18	0.304	0.209	0.237	0.237		0.228	1.260
10/8/2015	7	18	0.087	0.199	0.199	0.199		0.199	1.260
10/8/2015	7	20	3.041	0.000	0.000	0.000		0.000	1.667
10/8/2015	7	20	2.596	0.032	0.032	0.025		0.030	1.667
10/8/2015	7	20	2.329	0.043	0.043	0.043		0.043	1.667
10/8/2015	7	20	2.051	0.067	0.067	0.085		0.073	1.667
10/8/2015	7	20	1.720	0.145	0.055	0.036		0.079	1.667
10/8/2015	7	20	1.365	0.168	0.231	0.231		0.210	1.667
10/8/2015	7	20	1.025	0.193	0.193	0.193		0.193	1.667
10/8/2015	7	20	0.680	0.232	0.232	0.227		0.230	1.667
10/8/2015	7	20	0.315	0.265	0.231	0.231		0.242	1.667
10/8/2015	7	20	0.071	0.218	0.218	0.280		0.239	1.667
10/8/2015	7	22	3.541	0.000	0.000	0.000		0.000	1.997
10/8/2015	7	22	3.130	0.000	0.000	0.000		0.000	1.997
10/8/2015	7	22	2.777	0.039	0.018	0.018		0.025	1.997
10/8/2015	7	22	2.301	0.027	0.106	0.075		0.069	1.997
10/8/2015	7	22	1.905	0.099	0.157	0.181		0.146	1.997
10/8/2015	7	22	1.545	0.239	0.231	0.207		0.226	1.997
10/8/2015	7	22	1.112	0.249	0.243	0.237		0.243	1.997
10/8/2015	7	22	0.695	0.279	0.266	0.231		0.259	1.997
10/8/2015	7	22	0.298	0.263	0.220	0.206		0.230	1.997
10/8/2015	7	22	0.056	0.206	0.289	0.223		0.239	1.997
10/8/2015	7	24	3.687	0.008	0.008	0.007		0.008	2.865
10/8/2015	7	24	3.209	0.002	0.002	0.002		0.002	2.865
10/8/2015	7	24	2.876	0.051	0.122	0.122		0.098	2.865
10/8/2015	7	24	2.458	0.194	0.232	0.232		0.219	2.865
10/8/2015	7	24	2.063	0.268	0.257	0.257		0.261	2.865
10/8/2015	7	24	1.755	0.284	0.276	0.257		0.272	2.865
10/8/2015	7	24	1.394	0.210	0.161	0.161		0.177	2.865
10/8/2015	7	24	1.040	0.276	0.276	0.276		0.276	2.865
10/8/2015	7	24	0.686	0.257	0.196	0.196		0.216	2.865
10/8/2015	7	24	0.134	0.230	0.230	0.230		0.230	2.865
10/8/2015	7	26	3.785	0.005	0.003	0.003		0.004	3.144
10/8/2015	7	26	3.199	0.046	0.094	0.094		0.078	3.144

Date	Transect	Distance from Left Bank (m)	Depth (m)	Velocity (m s^{-1}) (up to 4 repeated measures)					Depth to top of Vegetation (m)
				1	2	3	4	Avg.	
10/8/2015	7	26	2.852	0.220	0.220	0.220		0.220	3.144
10/8/2015	7	26	2.425	0.313	0.294	0.294		0.300	3.144
10/8/2015	7	26	2.027	0.332	0.265	0.265		0.287	3.144
10/8/2015	7	26	1.650	0.301	0.301	0.260		0.287	3.144
10/8/2015	7	26	1.255	0.277	0.254	0.254		0.262	3.144
10/8/2015	7	26	0.896	0.257	0.257	0.255		0.256	3.144
10/8/2015	7	26	0.412	0.250	0.250	0.258		0.253	3.144
10/8/2015	7	26	0.055	0.281	0.281	0.281		0.281	3.144
10/8/2015	7	28	3.738	0.000	0.007	0.007		0.005	2.900
10/8/2015	7	28	3.246	0.034	0.034	0.061		0.043	2.900
10/8/2015	7	28	2.776	0.266	0.266	0.144		0.225	2.900
10/8/2015	7	28	2.357	0.174	0.174	0.287		0.212	2.900
10/8/2015	7	28	1.880	0.321	0.292	0.292		0.302	2.900
10/8/2015	7	28	1.367	0.279	0.322	0.322		0.308	2.900
10/8/2015	7	28	0.868	0.272	0.267	0.267		0.269	2.900
10/8/2015	7	28	0.600	0.310	0.310	0.277		0.299	2.900
10/8/2015	7	28	0.215	0.278	0.278	0.272		0.276	2.900
10/8/2015	7	28	0.063	0.316	0.316	0.231		0.288	2.900
10/8/2015	7	30	3.440	0.024	0.024	0.041		0.030	3.018
10/8/2015	7	30	2.960	0.129	0.129	0.161		0.140	3.018
10/8/2015	7	30	2.527	0.204	0.221	0.221		0.215	3.018
10/8/2015	7	30	2.175	0.305	0.342	0.342		0.330	3.018
10/8/2015	7	30	1.755	0.291	0.318	0.318		0.309	3.018
10/8/2015	7	30	1.305	0.359	0.322	0.322		0.334	3.018
10/8/2015	7	30	1.068	0.275	0.275	0.249		0.266	3.018
10/8/2015	7	30	0.670	0.295	0.352	0.352		0.333	3.018
10/8/2015	7	30	0.302	0.283	0.283	0.273		0.280	3.018
10/8/2015	7	30	0.067	0.255	0.255	0.311		0.274	3.018
10/8/2015	7	32	3.245	0.023	0.023	0.063		0.036	3.140
10/8/2015	7	32	2.816	0.014	0.014	0.140		0.056	3.140
10/8/2015	7	32	2.440	0.247	0.247	0.300		0.265	3.140
10/8/2015	7	32	2.040	0.347	0.347	0.347		0.347	3.140
10/8/2015	7	32	1.733	0.406	0.406	0.352		0.388	3.140
10/8/2015	7	32	1.308	0.289	0.289	0.325		0.301	3.140
10/8/2015	7	32	1.081	0.379	0.379	0.354		0.371	3.140
10/8/2015	7	32	0.764	0.304	0.304	0.279		0.296	3.140
10/8/2015	7	32	0.386	0.327	0.327	0.260		0.305	3.140
10/8/2015	7	32	0.123	0.372	0.265	0.265		0.301	3.140
10/8/2015	7	39	2.560	0.023	0.023	0.023		0.023	1.680
10/8/2015	7	39	2.297	0.038	0.038	0.033		0.036	1.680
10/8/2015	7	39	2.107	0.015	0.010	0.010		0.012	1.680
10/8/2015	7	39	1.772	0.035	0.035	0.023		0.031	1.680
10/8/2015	7	39	1.518	0.084	0.084	0.099		0.089	1.680
10/8/2015	7	39	1.219	0.054	0.039	0.039		0.044	1.680
10/8/2015	7	39	0.920	0.113	0.113	0.180		0.135	1.680
10/8/2015	7	39	0.719	0.201	0.189	0.189		0.193	1.680

Date	Transect	Distance from Left Bank (m)	Depth (m)	Velocity (m s^{-1}) (up to 4 repeated measures)					Depth to top of Vegetation (m)
				1	2	3	4	Avg.	
10/8/2015	7	39	0.344	0.173	0.173	0.141		0.162	1.680
10/8/2015	7	39	0.101	0.096	0.235	0.235		0.189	1.680
10/8/2015	7	44	1.698	0.000	0.000	0.000		0.000	1.240
10/8/2015	7	44	1.505	0.000	0.000	0.000		0.000	1.240
10/8/2015	7	44	1.397	0.010	0.010	0.000		0.007	1.240
10/8/2015	7	44	1.275	0.044	0.044	0.033		0.040	1.240
10/8/2015	7	44	1.137	0.008	0.008	0.008		0.008	1.240
10/8/2015	7	44	0.962	0.018	0.018	0.012		0.016	1.240
10/8/2015	7	44	0.787	0.066	0.066	0.061		0.064	1.240
10/8/2015	7	44	0.629	0.039	0.034	0.034		0.036	1.240
10/8/2015	7	44	0.336	0.069	0.069	0.069		0.069	1.240
10/8/2015	7	44	0.175	0.020	0.020	0.630		0.223	1.240

Appendix 6.1. Coordinates and image of the 100 locations at Silver River which were surveyed for biological, physical, and chemical characteristics (image by GoogleEarth).

Silver River Transect and Quadrat Locations				
Transect	**Quadrat**	**Latitude (ºN)**	**Longitude (ºW)**	**Location**
1	1	29.215300	82.052526	
1	2	29.215380	82.052547	
1	3	29.215435	82.052450	SLV2
1	4	29.215483	82.052351	
1	5	29.215525	82.052302	
2	1	29.216003	82.049914	
2	2	29.215940	82.049896	
2	3	29.215730	82.049819	SLV4
2	4	29.215626	82.049764	
2	5	29.215321	82.049632	
3	1	29.216020	82.047194	
3	2	29.215956	82.047210	
3	3	29.215785	82.047146	SLV5
3	4	29.215732	82.047119	
3	5	29.215644	82.047041	
4	1	29.215500	82.044612	
4	2	29.215419	82.044616	
4	3	29.215209	82.044542	SLV6
4	4	29.215230	82.044463	
4	5	29.215086	82.044488	
5	1	29.215296	82.041390	
5	2	29.215400	82.041376	
5	3	29.215488	82.041380	0.7 Mile Mark
5	4	29.215695	82.041381	
5	5	29.215657	82.041320	
6	1	29.214822	82.038617	
6	2	29.214748	82.038613	
6	3	29.214805	82.038948	Downstream of MFL 9
6	4	29.214809	82.039073	
6	5	29.214746	82.039115	

Silver River Transect and Quadrat Locations				
Transect	**Quadrat**	**Latitude (ºN)**	**Longitude (ºW)**	**Location**
7	1	29.212811	82.036668	Between MFL 8 and 9
7	2	29.212938	82.036677	
7	3	29.212942	82.036687	
7	4	29.213115	82.036450	
7	5	29.213132	82.036479	
8	1	29.210460	82.034865	MFL8
8	2	29.210490	82.034836	
8	3	29.210402	82.034526	
8	4	29.210417	82.034537	
8	5	29.210423	82.034625	
9	1	29.208899	82.033751	SLV8; downstream of county dock
9	2	29.208974	82.033680	
9	3	29.208999	82.033694	
9	4	29.209259	82.033596	
9	5	29.209227	82.033591	
10	1	29.207468	82.032093	Upstream of MFL7
10	2	29.207468	82.032199	
10	3	29.207472	82.032207	
10	4	29.207104	82.032094	
10	5	29.207059	82.032131	
11	1	29.204168	82.028625	2 Mile Mark
11	2	29.204148	82.028620	
11	3	29.204101	82.028583	
11	4	29.203927	82.028566	
11	5	29.203922	82.028557	
12	1	29.203905	82.025002	MFL6
12	2	29.203951	82.025028	
12	3	29.203930	82.024986	
12	4	29.204012	82.024999	
12	5	29.203922	82.024904	
13	1	29.202055	82.020238	Between MFL5 and 6
13	2	29.202152	82.020236	
13	3	29.202187	82.020258	
13	4	29.202296	82.019921	
13	5	29.202340	82.020029	

Silver River Transect and Quadrat Locations				
Transect	**Quadrat**	**Latitude (ºN)**	**Longitude (ºW)**	**Location**
14	1	29.203311	82.016184	Upstream of MFL5
14	2	29.203319	82.016184	
14	3	29.203252	82.016064	
14	4	29.203203	82.016035	
14	5	29.203206	82.016022	
15	1	29.201867	82.011600	Upstream of MFL4
15	2	29.201933	82.011400	
15	3	29.202150	82.011450	
15	4	29.202116	82.011466	
15	5	29.202066	82.011433	
16	1	29.203116	82.007166	Between MFL3 and 4
16	2	29.203166	82.007100	
16	3	29.203233	82.007116	
16	4	29.203333	82.006866	
16	5	29.203183	82.007000	
17	1	29.204134	82.005429	Between MFL3 and 4
17	2	29.204178	82.005539	
17	3	29.204119	82.005395	
17	4	29.204090	82.005209	
17	5	29.204142	82.005230	
18	1	29.207416	81.999083	Downstream of MFL2
18	2	29.207366	81.999016	
18	3	29.207383	81.999050	
18	4	29.207483	81.999066	
18	5	29.207600	81.999150	
19	1	29.207269	81.996624	Mile Marker 4.7
19	2	29.207260	81.996587	
19	3	29.206934	81.996901	
19	4	29.206948	81.996841	
19	5	29.207053	81.996848	
20	1	29.208233	81.995550	Between MFL1 and 2
20	2	29.208250	81.995533	
20	3	29.208300	81.995600	
20	4	29.208283	81.995616	
20	5	29.208183	81.995866	

Appendix 9.1

Taxa	n	$\delta^{15}N$ (‰)		$\delta^{13}C$ (‰)		C:N	
		Mean	SD	Mean	SD	Mean	SD
Angiosperm	57	4.6	3.2	-32.0	4.0	15.8	10.6
Emergent	22	4.3	2.6	-30.0	2.1	13.8	3.9
Cicuta mexicana (water hemlock)	1	7.3	-	-31.3	-	11.2	-
Nasturtium floridanum (water cress)	3	3.0	4.4	-32.9	2.6	10.4	0.2
Nuphar advena (spatterdock)	8	2.8	1.5	-28.5	1.7	11.3	1.6
Pontederia cordata (pickerel weed)	6	6.4	1.4	-29.3	0.7	16.9	2.0
Sagittaria lancifolia (duck potato)	2	3.0	3.2	-31.0	0.2	13.2	1.2
Zizania aquatica (wild rice)	1	7.7	-	-33.3	-	23.9	-
Floating	8	3.9	1.6	-31.1	1.1	16.0	2.6
Hydrocotyle (dollarweed)	3	3.1	0.7	-30.6	1.1	14.7	2.5
Pistia stratiotes (Water lettuce)	5	4.1	2.1	-31.7	0.9	15.9	2.1
Salvinia (floating fern)	1	5.4	-	-30.0	-	20.0	-
Submerged	33	5.2	2.8	-34.7	3.7	13.2	3.3
Ceratophyllum demersum (coontail)	10	3.6	3.3	-37.4	2.4	10.9	1.8
Hydrilla verticillata (Hydrilla)	6	6.6	2.6	-36.3	2.8	12.7	2.9
Naja guadalupensis (southern waternymph)	3	7.2	4.2	-35.7	4.3	11.6	2.6
Sagittaria kurziana (strap-leaf sagittaria)	5	4.2	1.9	-30.3	1.7	14.2	1.3
Vallisneria americana (eel grass)	9	6.0	1.3	-32.8	3.1	16.0	3.7
Terrestrial	3	-1.9	6.6	-25.5	7.2	55.5	17.4
Taxodium distichum (bald cypress)	2	1.9	1.6	-29.7	0.2	45.6	3.9
Tillandsia usneoides (spanish moss)	1	-9.5	-	-17.2	-	75.3	-
Bacillariophyta (epiphytic diatoms)	8	4.4	1.1	-28.7	5.6	9.4	1.4
Bryophyta (*Fontinalis*, water moss)	2	6.1	1.3	-42.6	2.2	19.9	7.1

Taxa	n	$\delta^{15}N$ (‰)		$\delta^{13}C$ (‰)		C:N	
		Mean	SD	Mean	SD	Mean	SD
Chlorophyta	26	5.6	1.9	-36.5	5.4	9.6	1.7
Benthic	4	3.6	0.7	-42.4	2.9	9.9	2.0
Dichotomosiphon	4	3.6	0.7	-42.4	2.9	9.9	2.0
Epiphytic	18	4.2	2.2	-35.0	5.9	9.6	1.9
Cladophora	7	5.6	2.3	-33.7	8.2	10.4	1.9
Unknown branched	3	3.7	1.4	-35.9	4.9	8.6	1.5
Unknown filamentous+Diatoms	1	2.6	-	-31.9	-	8.6	-
Unknown filamentous	6	2.8	1.9	-36.4	4.3	9.7	1.8
Unknown branched+Diatoms	1	4.9	-	-36.8	-	6.6	-
Unattached	17	6.4	1.6	-38.3	3.6	9.6	2.1
Rhizoclonium (green filamentous)	4	6.5	0.8	-36.9	3.2	8.3	0.5
Spirogyra (green filamentous)	9	6.4	1.5	-38.5	3.7	10.1	2.1
Unknown (green filamentous)	2	4.7	2.8	-41.2	3.1	9.0	0.2
Ulothrix (green filamentous)	2	8.0	0.8	-37.6	5.8	10.3	4.5
Cyanobacteria	4	4.7	2.6	-33.6	9.9	7.8	1.5
Lyngbya (benthic cyanobacteria)	4	4.7	2.6	-33.6	9.9	7.8	1.5
Lentibulariaceae (Utricularia, blatterwort)	1	5.5	-	-35.9	-	11.3	-
Xanthophycea	11	4.3	2.4	-43.3	1.0	8.2	0.8
Vaucheria (benthic yellow algae)	11	4.3	2.4	-43.3	1.0	8.2	0.8
Multiple Algal	14	4.9	2.4	-38.5	4.4	8.2	0.7
Benthic	5	5.5	2.6	-43.9	1.3	7.7	0.4
Vaucheria	1	6.4	-	-43.9	-	7.5	-
Vaucheria+Lyngbya	3	5.1	3.5	-44.0	1.8	7.9	0.5
Vaucheria+Cladophora	1	5.7	-	-43.6	-	7.5	-
Epiphytic	9	4.5	2.3	-35.5	1.5	8.5	0.6

Taxa	n	$\delta^{15}N$ (‰)		$\delta^{13}C$ (‰)		C:N	
		Mean	SD	Mean	SD	Mean	SD
Unknown branched and filamentous+Spyrogira+Diatoms	1	5.7	-	-36.5	-	8.5	-
Cladophora+Vaucheria+Diatoms	2	2.5	0.4	-34.1	1.7	8.7	0.6
Cladophora+Unknown filamentous+Diatoms	1	2.3	-	-35.3	-	8.9	-
Unknown filamentous+Diatoms	1	4.5	-	-35.1	-	8.2	-
Unknown branched+Diatoms	2	5.8	3.9	-36.0	2.8	7.6	0.2
Unknown branched+Unknown filamentous+ Vaucheria+Diatoms	1	3.9	-	-35.2	-	9.2	-
Unknown filamentous+Vaucheria	1	7.6	-	-37.2	-	8.9	-
Lichen	1	3.5	-	-38.3	-	10.3	-

Appendix 9.2

Trophic status	Taxa	n	$\delta^{15}N$ (‰)		$\delta^{13}C$ (‰)	
			Mean	SD	Mean	SD
Filter feeder						
	Unionidae (*Elliptio buckleyi*, Florida shiny spike)	4	8.8	0.6	-32.5	0.4
Herbivore						
	Hydrobiidae	5	6.6	1.4	-31.2	6.2
	Ampullariidae (*Pomacea paludosa*)	7	6.6	1.0	-33.3	4.1
	Physidae + Hydrobiidae	1	7.7	-	-34.1	-
	Physidae + Planorbidae	1	5.2	-	-35.5	-
	Planorbidae	3	7.0	0.3	-29.9	2.2
	Pleuroceridae (*Elimia floridensis*, rasp elimia)	14	8.1	0.7	-33.8	1.0
	Viviparidae (*Viviparus georgianus*, banded mysterysnail)	13	7.7	1.2	-33.2	1.8
	Coleoptera	2	5.7	1.7	-35.0	1.8
	Diptera (Chironomidae)	18	5.7	0.7	-36.5	2.6
	Ephemeroptera	1	5.5	-	-35.9	-
	Lepidoptera	20	5.7	1.2	-33.2	2.9
	Trichoptera	18	5.7	1.5	-39.5	2.4
Omnivore						
	Coleoptera	1	6.1	-	-32.3	-
	Diptera (Athericidae)	4	7.4	1.1	-31.5	3.8
	Diptera (Stratiomyidae)	2	7.0	0.0	-28.4	2.0
	Diptera (Unknown)	1	6.7	-	-35.5	-
	Amphipoda (Gammaridae)	14	5.3	1.4	-33.8	3.4
	Palaemonidae (*Palaemonetes* sp.)	13	10.1	0.6	-33.0	0.9
	Parastacidae (*Procambarus speculifer*)	17	8.5	1.2	-30.6	2.1

Trophic status	Taxa	n	$\delta^{15}N$ (‰)		$\delta^{13}C$ (‰)	
			Mean	SD	Mean	SD
Parasite						
	Trombidiformes	4	6.3	2.7	-37.0	3.4
	Clitellata	2	8.2	1.2	-35.5	1.7
Predator						
	Insecta	25	7.7	1.0	-32.4	3.1
	Diptera (Rhagionidae)	6	6.3	0.8	-36.1	2.1
	Hemiptera	10	8.1	0.7	-30.9	2.6
	Belostomidae	5	7.7	0.6	-29.3	1.2
	Gerridae	3	8.3	0.5	-33.6	2.6
	Naucoridae	1	8.3	-	-29.2	-
	Nepidae	1	9.3	-	-32.7	-
	Odonata	10	8.1	0.7	-32.0	2.2

Appendix 9.3

Trophic status	Taxa	n	$\delta^{15}N$ (‰)		$\delta^{13}C$ (‰)	
			Mean	SD	Mean	SD
omnivore						
	Atherinopsidae (*Menidia* sp., silver side)	6	11.5	1.2	-31.0	0.4
	Catostomidae (*Erimyzon sucetta*, lake chubsucker)	31	9.7	1.1	-31.0	1.6
	Clupeidae (*Dorosoma cepedianum*, gizzard shad)	11	10.3	1.1	-31.9	2.5
	Cyprinidae	46	9.9	1.4	-33.8	1.3
	Notemigonus crysoleucas (Golden Shiner)	20	10.2	1.2	-33.7	0.9
	Notropis petersoni (Coastal Shiner)	24	10.4	1.2	-33.6	0.9
	Pteronotropis hypselopterus (Sailfin Shiner)	4	10.5	0.9	-33.1	0.5
	Mugilidae (*Mugil cephalus*, striped mullet)	17	9.4	1.1	-31.1	2.1
	Chelydridae (*Chelydra serpentina*, common snapping turtle)	1	8.9	-	-28.3	-
	Emydidae	14	8.8	2.1	-32.1	1.9
	Pseudemys nelsoni (Florida redbelly)	8	9.8	2.1	-31.8	1.5
	Pseudemys peninsularis (Peninsular cooter)	4	8.2	1.1	-31.3	2.2
	Pseudemys suwanniensis (Suwannee cooter)	2	6.4	0.6	-34.7	0.7

Trophic status	Taxa	n	$\delta^{15}N$ (‰)		$\delta^{13}C$ (‰)	
			Mean	SD	Mean	SD
Secondary consumer						
	Amiidae (*Amia calva*, bowfin)	25	13.0	1.4	-27.7	1.6
	Aphredoderidae (*Aphredoderus sayanus*, pirate perch)	7	11.4	0.7	-30.8	0.6
	Belonidae (Strongylura marina, Atlantic needlefish)	2	13.8	0.0	-30.7	0.9
	Centrarchidae	145	11.0	1.4	-30.2	1.8
	Lepomis auritus (redbreast sunfish)	8	10.1	1.4	-30.8	2.9
	Lepomis gulosus (warmouth)	8	11.2	0.7	-30.5	1.6
	Lepomis macrochirus (bluegill)	32	10.3	1.2	-30.5	1.6
	Lepomis marginatus (dollar sunfish)	2	11.8	0.9	-28.3	0.9
	Lepomis microlophus (redear sunfish)	22	10.5	1.6	-29.7	1.9
	Lepomis punctatus (spotted sunfish)	28	10.4	1.1	-31.1	1.4
	Micropterus salmoides (largemouth bass)	42	12.1	0.9	-29.6	1.7
	Pomoxis nigromaculatus (black crappie)	3	13.7	0.2	-29.4	1.1
	Elassomatidae (*Elassoma zonatum*, Banded Pygmy Sunfish)	8	10.6	0.6	-31.1	2.2
	Fundulidae (*Lucania goodei*, bluefin killifish)	7	10.0	1.1	-31.5	1.7
	Ictaluridae (catfish)	8	11.5	1.1	-31.2	2.6
	Ameriurus sp. (juvenile catfish)	2	10.6	0.4	-32.2	0.1
	Ameriurus natalis (yellow bullhead catfish)	4	11.9	1.0	-31.1	3.4

Trophic status	Taxa	n	$\delta^{15}N$ (‰)		$\delta^{13}C$ (‰)	
			Mean	SD	Mean	SD
	Ameriurus nebulosus (brown bullhead catfish)	1	12.5	-	-28.3	-
	Noturus leptacanthus (speckled madtom)	1	10.5	-	-32.7	-
	Percidae (*Percina* sp., darter)	12	11.0	1.4	-33.2	1.1
	Poeciliidae	26	9.8	1.2	-31.3	1.3
	Gambusia affinus (mosquitofish)	13	10.1	0.9	-31.2	1.3
	Heterandia formosa (least killifish)	5	10.7	1.1	-31.1	1.7
	Poecilia latipinna (sailfin molly)	8	9.1	1.3	-31.9	1.1
	Kinosternidae	9	8.1	0.7	-31.4	1.4
	Sternotherus minor (loggerhead musk turtle)	7	8.2	0.6	-31.3	1.2
	Sternotherus odoratus (common musk turtle)	2	7.6	1.4	-32.1	2.3
top predator						
	Esocidae (*Esox niger*, Chain pickerel)	8	13.4	0.8	-27.6	1.2
	Lepisosteidae	19	13.6	0.9	-25.7	1.5
	Lepisosteus osseus (Longnose Gar)	1	14.1	-	-24.8	-
	Lepisosteus platyrhincus (Florida Gar)	18	13.6	0.9	-25.8	1.6
	Alligatoridae (*Alligator mississippiensis*, American alligator)	49	8.6	1.1	-29.0	1.0
	Juvenile	19	8.6	0.7	-29.6	0.7
	Sub-adult	20	8.2	1.3	-28.5	0.8
	Adult	10	9.5	1.0	-28.9	1.2